5th Asia-Pacific Symposium on Radiochemistry

APSORC 13

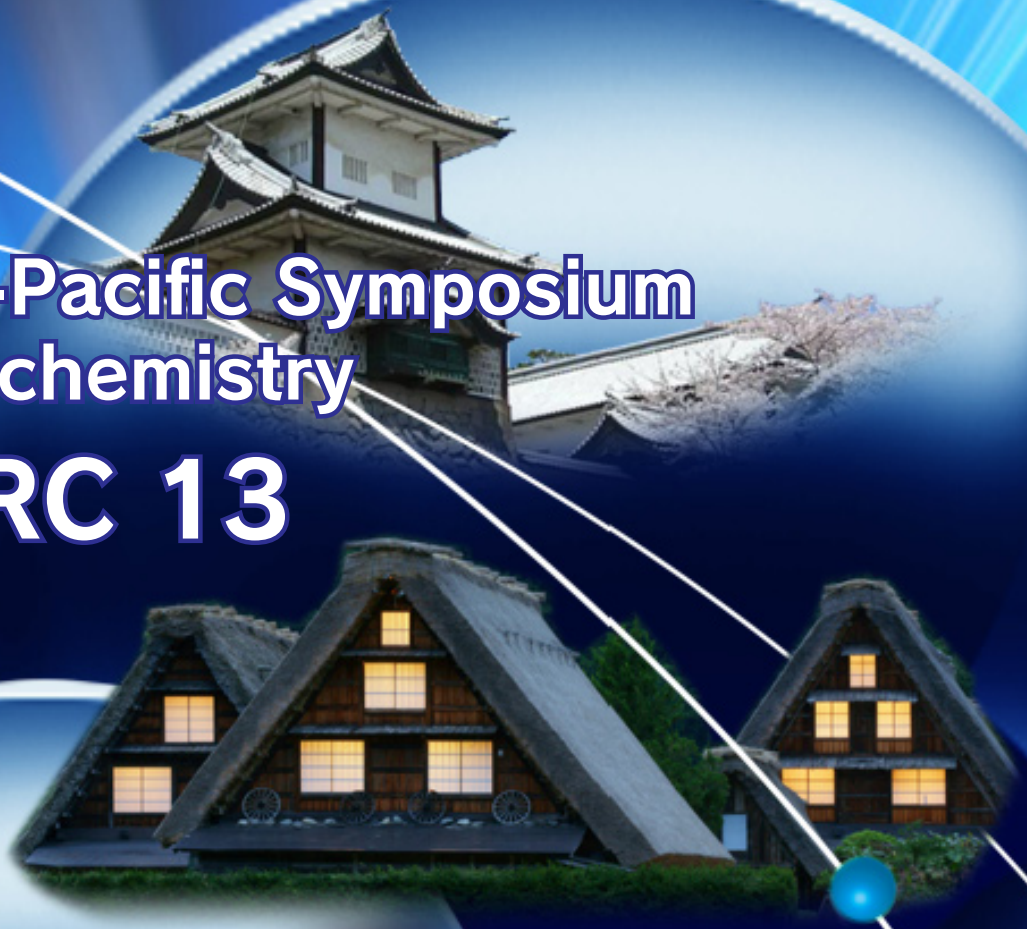

Kanazawa

APSORC 13

JAPAN

JNRS

22-27 September 2013
Kanazawa, Japan

5th Asia Pacific Symposium on Radiochemistry

APSORC 13

Kanazawa, JAPAN

September 22 – 27, 2013

Book of Abstracts

Organizing Committee

Co-chairpersons

Y. Nagame (Tokai, JAEA)
M. Yamamoto (Kanazawa, Kanazawa University)

Secretaries

A. Yokoyama (Kanazawa, Kanazawa University)
M. Watanabe (Tokai, JAEA)

Members of the Organizing Committee

R. Amano (Kanazawa, Kanazawa University), M. Ebihara (Tokyo, Tokyo Metropolitan University), M. K. Kubo (Tokyo, International Christian University), N. Momoshima (Fukuoka, Kyushu University), S. Nagao (Kanazawa, Kanazawa University), W. Sato (Kanazawa, Kanazawa University), A. Shinohara (Osaka, Osaka University), Y. Yamada (Kanazawa, Hokuriku University)

Kanazawa Symposium Committee

T. Nakanishi (Kanazawa, Kanazawa University), M. Inoue (Kanazawa, Kanazawa University), Y. Hamajima (Kanazawa, Kanazawa University), K. Washiyama (Kanazawa, Kanazawa University), K. Yasuike (Kanazawa, Hokuriku University)

International Advisory Committee (IAC)

J. Bennett (Australia), N. Beresford (UK), P. Bode (The Netherlands), Y. H. Chung (Korea), S. B. Clark (USA), S. Dmitriev (Russia), C. E. Düllmann (Germany), M. Ebihara (Japan), E. A. De Nadai Fernandes (Brazil), H. Geckeis (Germany), K. A. Higley (USA), Q. Hua (Australia), J. John (Czech Republic), V. Kolotov (Russia), S. Lahiri (India), M. Garcia-Leon (Spain), D. Moir (Canada), N. Momoshima (Japan), A. Mutalib (Indonesia), S. -I. Nakayama (Japan), Y. Nagame (Japan), H. Nitsche (USA), Y. Ohkubo (Japan), A. V. R. Reddy (India), Z. Révay (Hungary), E. Simoni (France), K. S. Song (Korea), A. Türler (Switzerland), J. H. Wang (China), M. Yamamoto (Japan), S. D. Zhang (China), Y. L. Zhao (China)

Program Chairperson

N. Momoshima (Fukuoka, Kyushu University)

Scientific Topics (Abbrev.)

1. Fukushima issues (FK)
2. Education in nuclear and radiochemistry (ED)
3. Nuclear forensics (NF)
4. Nuclear energy chemistry (NE)
5. Nuclear chemistry (NC)
6. Actinide chemistry (AC)
7. Environmental radiochemistry (EN)
8. Radiopharmaceutical chemistry and Nuclear medicine (RP)
9. Nuclear probes for materials science (NP)
10. Activation analysis (AA)
11. Application of nuclear and radiochemical techniques (AP)

Sunday, 22 September		Monday, 23 September					Tuesday, 24 September				
Time	Robby		Hall		Meeting Room			Hall		Meeting Room	
09:00-09:10		9:00	Arrangement for presentation				9:00	PL-03	**Plenary**		
09:10-09:20									A. Tuerler		
09:20-09:30											
09:30-09:40		9:30	Opening Ceremony				9:30	PL-04	**Plenary**		
09:40-09:50									S. Nagao		
09:50-10:00											
10:00-10:10		10:00	**Hevesy Award Ceremony**				10:00	**Coffee Break**			
10:10-10:20			R. S. Dybczyński								
10:20-10:30							10:20	ENI-01	**Invited**	NCI-01	**Invited**
10:30-10:40									H. Foerstendorf		S. Dmitriev
10:40-10:50							10:50	ENO-01	General	NCI-02	**Invited**
10:50-11:00									Z.J. Guo		
11:00-11:10		11:00	**Coffee Break**				11:10	ENO-02	General		Ch.E. Duellmann
11:10-11:20		11:10	PL-01	**Plenary**					H. Tuovinen	NCI-03	**Invited**
11:20-11:30							11:30	ENO-03	General		
11:30-11:40				M. Yamamoto					M.-C. Wu		H. Haba
11:40-11:50		11:40	PL-02	**Plenary**			11:50	ENO-04	General	NCO-06	General
11:50-12:00									T. Ohnuki		V. Pershina
12:00-12:10				I. McKinley							
12:10-13:20		12:10	**Lunch Time**				12:10	**Lunch Time**			
13:20-13:30		13:20	FKI-01	**Invited**	API-01	**Invited**	13:20	ENO-05	General	NCO-07	General
13:30-13:40									S. Sachs		D. Rudolph
13:40-13:50				H. Tsuruta		H. Harada	13:40	ENO-06	General	NCO-08	General
13:50-14:00		13:50	FKI-02	**Invited**	API-02	**Invited**			Y. Iwahana		A. Yakushev
14:00-14:10							14:00	ENO-07	General	NCO-09	General
14:10-14:20				Y. Takahashi (388)		Y.L. Zhao			J. Krmela		J. Even
14:20-14:30		14:20	FKI-03	**Invited**	APO-01	General	14:20	ENO-08	General	NCO-10	General
14:30-14:40						T. M. Nakanishi			K. Masumoto		H. Nitsche
14:40-14:50				M. Aoyama	APO-02	General	14:40	ENO-09	General	NCO-11	General
14:50-15:00		14:50	FKI-04	**Invited**		S.H. Jung			H.W. Gaeggeler		R. Eichler
15:00-15:10					APO-03	General	15:00	ENO-10	General	NCO-12	General
15:10-15:20				B. Grambow		M. Anvia			A. Sakaguchi		T.K. Sato
15:20-15:30		15:20	**Coffee Break**				15:20	**Coffee Break**			
15:30-15:40											
15:40-15:50		15:40	FKO-01	General	NCO-01	General	15:40	ENI-02	**Invited**	NEI-01	**Invited**
15:50-16:00				A. Shimada		Z. Qin					
16:00-16:10	**Registration Desk OPEN**	16:00	FKO-02	General	NCO-02	General			J.V. Krtaz		Z.F. Chai
16:10-16:20				Y. Miyake		W.M. Kerlin	16:10	ENO-11	General	NEI-02	**Invited**
16:20-16:30		16:20	FKO-03	General	NCO-03	General			J.H. Park		
16:30-16:40				T. Ohta		Y.K. Ha	16:30	ENO-12	General		A. Goswami
16:40-16:50		16:40	FKO-04	General	NCO-04	General			J. Zheng	NEO-01	General
16:50-17:00				Y. Muramatsu		I. Laszak	16:50	ENO-13	General		E. Loefstroem-Engdahl
17:00-17:10		17:00	FKO-05	General	NCO-05	General			I. Milanovic	NEO-02	General
17:10-17:20				Y. Satou		Y. Xu	17:10	FKI-05	**Invited**		Y. Tomobuchi
17:20-17:30		17:20	FKO-06	General	NFO-01	General				NEO-03	General
17:30-17:40				M. C. Honda		Y. Miyamoto			K. Minato		F. Poineau
17:40-17:50		17:40	FKO-07	General	NFO-02	General	17:40	FKO-09	General	NEO-04	General
17:50-18:00	**Welcome Reception**			Z.J. Zhang		N. Gharibyan			Y. Oura		A. Braatz
18:00-18:10		18:00	FKO-08	General	NFO-03	General	18:00	FKO-10	General	NEO-05	General
18:10-18:20				D.R. Neville		R. Sudowe			K. Hirose		R. Chen
18:20-18:30											
18:30-18:40											
18:40-18:50											
18:50-19:00		18:50	**Poster Session**				18:50	**Poster Session**			
19:00-19:20											
19:20-19:40											
19:40-20:00											
20:00-		20:00					20:00				

Wednesday, 25 September					Thursday, 26 September				Friday, 27 September		Time
	Hall		Meeting Room			Hall		Meeting Room		Meeting Room	
9:00	PL-05	**Plenary**			9:00	PL-07	**Plenary**		9:00	AAI-01 **Invited**	09:00-09:10
		M. A. Denecke					S. B. Clark			A. Chatt	09:20-09:30
9:30	PL-06	**Plenary**			9:30	PL-08	**Plenary**		9:30	AAI-02 **Invited**	09:30-09:40
		J. Hatazawa					H. Ueno			T. Miura	09:50-10:00
10:00	**Coffee Break**				10:00	**Coffee Break**			10:00	**Coffee Break**	10:00-10:10
											10:10-10:20
10:20	RPI-01	**Invited**	ACI-01	**Invited**	10:20	NPI-01	**Invited**	EDI-01 **Invited**	10:20	AAO-01 General	10:20-10:30
		D. S. Wilbur		J. Li			W. Sato	J. John		J.H. Moon	10:30-10:40
10:50	RPI-02	**Invited**	ACI-02	**Invited**	10:50	NPO-01	General	EDI-02 **Invited**	10:40	AAO-02 General	10:40-10:50
		S. Lahiri		Y. Kitatsuji			K. Nomura			Y. Toh	10:50-11:00
11:20	RPO-01	General	ACO-01	General	11:10	NPO-02	General	W. Wu	11:00	AAO-03 General	11:00-11:10
		E. Aneheim		A. Kirishima			J. Wang	EDI-03 **Invited**		K. Ninomiya	11:10-11:20
11:40	RPO-02	General	ACO-02	General	11:30	NPO-03	General		11:20	AAO-04 General	11:20-11:30
		Y. Hatsukawa		H. Hayashi			S. Nakashima	A. Yokoyama		M. Fukushima	11:30-11:40
12:00	**Group Photo (Hall)**				11:50	NPO-04	General	EDO-01 General	11:40	AAO-05 General	11:40-11:50
	Lunch Time						G. Yoshida	S. B. Sarmani		N. Shirai	11:50-12:00
13:20					12:10	**Lunch Time**			12:00	**Lunch Time**	12:00-12:10
					13:00						12:10-13:20
13:40	**JNRS General Assembly (For Member of JNRS))**								13:20	API-03 **Invited**	13:20-13:30
14:00											13:30-13:40
14:20	**JNRS Meeting**									Y. Hamajima	13:40-13:50
14:40									13:50	APO-04 General	13:50-14:00
15:00										C. Gautier	14:00-14:10
15:20	**Coffee Break**								14:10	APO-05 General	14:10-14:20
										T.Yoshimura	14:20-14:30
15:40	RPO-03	General	ACO-03	General					14:30	APO-06 General	14:30-14:40
		L. Safavi-Tehrani		T.H. Park						J.D. Despotopulos	14:40-14:50
16:00	FKO-11	General	ACO-04	General					14:50	**Coffee Break**	14:50-15:00
		E. Rasmussen		N. Aoyagi							15:00-15:10
16:20	FKO-12	General	NCO-13	General					15:10	**Closing Ceremony**	15:10-15:20
		K. Minami		A. Toyoshima							15:20-15:30
16:40	FKO-13	General	NCO-14	General							15:30-15:40
		T. Kawamoto		P. Steinegger							15:40-15:50
17:00	FKO-14	General	NCO-15	General							15:50-16:00
		D. Parajuli		R. Tripathi							16:00-16:10
17:20	**Coffee Break**										16:10-16:20
											16:20-16:30
17:50	**JNRS Award Presentation (Open Session) T. Kimura**										16:30-16:40
											16:40-16:50
18:30											16:50-17:00
					17:00						17:00-17:10
18:50	**Poster Session**										17:10-17:20
											17:20-17:30
											17:30-17:40
20:00											17:40-17:50
											17:50-18:00
											18:00-18:10
											18:10-18:20
											18:20-18:30
											18:30-18:40
											18:40-18:50
											18:50-19:00
					19:00						19:00-19:20
											19:20-19:40
						Banquet					19:40-20:00
											20:00-

PROGRAM OF APSORC13

Sunday, 22 September 2013

Lobby, Kanazawa Bunka Hall

15:00-	**Registration**
17:30-18:30	**Welcome reception**

Monday, 23 September 2013

Hall & Meeting Room, Kanazawa Bunka Hall

09:00-		**Registration (continued)**
09:30-10:00		**Opening Ceremony - Welcome address**
Hall		**Y. Nagame**, APSORC13 co-chair, *Japan Atomic Energy Agency, Japan* **T. Kishikawa**, APSORC chair, *Kumamoto University, Japan*
10:00-11:00		**Hevesy Medal Award Ceremony**
Hall		Chair : **A. Chatt**
	HMA-01	**R. S. Dybczyński**, *Institute of Nuclear Chemistry and Technology, Poland* 50 years of adventures with neutron activation analysis with the special emphasis on radiochemical separations
11:00-11:10		**Coffee Break**
11:10-12:10		**Plenary Session**
Hall		**Fukushima issues** Chairs : **N. Momoshima and H. Nitsche**
11:10-11:40	**PL-01**	**M. Yamamoto,** *LLRL, Kanazawa University, Japan* Overview of the Fukushima Dai-ichi nuclear power plant (FDNPP) accident with amounts and nuclear compositions of the released radionuclides
11:40-12:10	**PL-02**	**I. McKinley,** *MCM Consulting, Switzerland* Fukushima challenges in perspective
12:10-13:20		**Lunch**
13:20-18:20		**Parallel session**
Hall		**Fukushima issues (continued)** Chairs : **S. Nagao and I. McKinley**
13:20-13:50	**FKI-01**	**H. Tsuruta,** M. Takigawa, T. Nakajima, *The University of Tokyo, Japan, Japan Agency for Marine-Earth Science and Technology, Japan* Atmospheric transport of radioiodine and radiocesium released in the early

phase by the Fukushima Daiichi Nuclear Power Plant accident from field measurements and a simulation model

13:50-14:20	FKI-02	**Y. Takahashi,** Q. Fan, Y. Togo, A. Sakaguchi, K. Tanaka, *Hiroshima University, Japan, National Institute of Advanced Industrial Science & Technology, Japan* Migration of radiocesium and radioiodine released by FDNPP accident in the terrestrial environment and its interpretation by their speciation analyses
14:20-14:50	FKI-03	**M. Aoyama,** Y. Hamajima, *Meteorological Research Institute, Japan, Kanazawa University, Japan* Oceanic and coastal dispersion of ^{134}Cs and ^{137}Cs released from the TEPCO Fukushima NPP1 accident: past present and prediction
14:50-15:20	FKI-04	**B. Grambow,** *Université de Nantes, France* Interactions between nuclear fuel and water at the Fukushima Daiichi Reactors
15:20-15:40		**Coffee Break**

Hall — **Fukushima issues (continued)**
Chairs : **M. Yamamoto and B. Grambow**

15:40-16:00	FKO-01	**A. Shimada,** K. Sakatani, Y. Kameo, K. Takahashi, *Japan Atomic Energy Agency, Japan* Determination of ^{129}I in the accumulated radioactive water and processing water of Fukushima Daiichi Nuclear Power Plant
16:00-16:20	FKO-02	**Y. Miyake,** H. Matsuzaki, T. Fujiwara, T. Saito, T. Yamagata, M. Honda, *The University of Tokyo, Japan, Nihon University, Japan* Measurement of Iodine-129 in surface soil collected near the Fukushima Daiichi Nuclear Power Plant accident site
16:20-16:40	FKO-03	**T. Ohta,** T. Kutoba, Y. Mahara, H. Matsuzaki, T. Igarashi, *Hokkaido University, Japan, Kyoto University, Japan, The University of Tokyo, Japan* Speciation of ^{137}Cs and ^{129}I in surface soil in Kanto loam layer after the Fukushima NPP accident
16:40-17:00	FKO-04	**Y. Muramatsu,** T. Ohno, N. Inagawa, K. Oda, M. Sato, H. Matsuzaki, *Gakushuin University, Japan, Fukushima Agricultural Technology Centre, Japan, The University of Tokyo, Japan* Transfer of radiocesium and radioiodine in the environment following the Fukushima nuclear accident
17:00-17:20	FKO-05	**Y. Satou,** K. Sueki, K. Sasa, J. Kitagawa, S. Ikarashi, *University of Tsukuba, Japan, High Energy Accelerator Research Organization and J-PARC Center, Japan* States of existence of the cesium and silver radionuclides at the sandy beach in Iwaki city, Fukushima
17:20-17:40	FKO-06	**M. C. Honda,** H. Kawakami, S. Watanabe, T. Saino, S. Nagao, K. Buesseler, C. German, S. Manganini, *Japan Agency for Marine-Earth Science and Technology, Japan, Kanazawa University, Japan, Woods Hole Oceanographic Institution, USA* Vertical transport of FNPP1-derived radiocesium by settling particles in the Western North Pacific
17:40-18:00	FKO-07	**Z. J. Zhang,** S. Kakitani, K. Ninomiya, N. Takahashi, Y. Yamaguchi, T. Yoshimura, T. Saito, K. Kita, H. Tsruta, S. Higaki, A. Shinohara, *Osaka University, Japan, Shokei Gakuin University, Japan, Ibaraki University, Japan, The University of Tokyo, Japan* Strontium-90 determination in air dust filter using solid phase extraction after the accident of FD-NPS

18:00-18:20	FKO-08	**D. R. Neville,** A. J. Phillips, K. A. Higley, *Oregon State University, USA* Dosimetric implications of the Fukushima release for Pacific albacore in the Northern California Current
18:20-18:50		**Mounting of posters**
18:50-20:00		**Poster session 1**

13:20-18:20		**Parallel session**
Meeting Room		**Application of nuclear and radiochemical techniques** Chairs : **T. Yoshimura and C. Gautier**
13:20-13:50	API-01	**H. Harada,** *Japan Atomic Energy Agency, Japan* ANNRI at J-PARC
13:50-14:20	API-02	**Y. L. Zhao,** W. Q. Shi, L. Y. Yuan, Z. F. Chai, *Institute of High Energy Physics, China, National Center for Nanosciences and Technology, Chaina* Nanomaterial and nanotechnology in nuclear energy chemistry
14:20-14:40	APO-01	**T. M. Nakanishi,** N. I. Kobayashi, A. Hirose, T. Saito, R. Sugita, H. Suzuki, R. Iwata, K. Tanoi, *The University of Tokyo, Japan, National Institute of Radiological Sciences, Japan, Tohoku University, Japan* Development of real-time radioisotope imaging system to study plant nutrition
14:40-15:00	APO-02	**S. H. Jung,** J. G. Park, J. B. Kim, J. H. Moon, C. H. Kim, *Korea Atomic Energy Research Institute, Korea, Hanyang Universuty, Korea* MCNP study on the development of industrial SPECT in terms of a radiation measurement design and void influence in multiphase media
15:00-15:20	APO-03	**M. Anvia,** S. A. Brown, *Australian Nuclear Science and Technology Organization Minerals and The University of Sydney, Australia, The University of Sydney, Australia* Tracking the deportment of uranium chain daughters during alkaline leaching of an Australian monazite
15:20-15:40		**Coffee Break**
Meeting Room		**Nuclear chemistry** Chairs : **A. Yokoyama and Z. F. Chai**
15:40-16:00	NCO-01	**Z. Qin**, F.-L. Fan, Y. Wang, F.-Y. Fan, X.-L. Wu, J. Bai, X.-J. Yin, L.-L. Tian, W. Tian, Z. Li, C.-M. Tan, *Institute of Modern Physics, China* Nuclear chemistry and radiochemistry studies at IMP
16:00-16:20	NCO-02	**W. M. Kerlin,** F. Poineau, P. M. Forster, A. P. Sattelberger, K. R. Czerwinski, *University of Nevada Las Vegas, USA, Argonne National Laboratory, USA* Preparation of low valent technetium metal-metal bonded species via solvothermal reduction of pertechnetate salts
16:20-16:40	NCO-03	**Y.-K. Ha,** S.-D. Park, Y.-S. Park, J.-S. Kim, K. Song, *Korean Atomic Energy Research Institute, Korea* The status of chemical characterization of a spent nuclear fuel
16:40-17:00	NCO-04	**I. Laszak,** J. P. Degros, C. Gautier, P. Fichet, F. Goutelard, J. N. Saas, A. Vian, J. F. Valéry, *CEA Saclay, France, AREVA, France* Determination of ^{93}Zr from intermediate level radioactive effluent

17:00-17:20	NCO-05	**Y. L. Xu**, S. Y. Kim, T. Ito, H. Tokuda, T. Tada, K. Hitomi, K. Ishii, *Tohoku University, Japan* Selective separation of cesium from simulated high level liquid waste using a silica-based (Calix[4] + Dodecanol)/SiO_2-P adsorbent
Meeting Room		**Nuclear forensics** Chairs : **A. Yokoyama and Z. F. Chai**
17:20-17:40	NFO-01	**Y. Miyamoto,** F. Esaka, D. Suzuki, M. Magara, *Japan Atomic Energy Agency, Japan* Age determination of a single Pu and Pu/U mixed oxide particle
17:40-18:00	NFO-02	**N. Gharibyan,** K. J. Moody, T. A. Brown, J. D. Despotopulos, J. M. Gostic, R. A. Henderson, E. Tereshatov, S. J. Tumey, D. A. Shaughnessy, *Lawrence Livermore National Laboratory, USA, Air Force Technical Applications Center, USA* Radiochemical measurement of 10-15 MeV proton induced fission yields for U-238
18:00-18:20	NFO-03	**R. Sudowe,** E. M. Bond, A. R. Dailey, D. R. Mclain, A. R. Roman, *University of Nevada Las Vegas, USA, Los Alamos National Laboratory, USA* Effect of interferences on actinide and strontium separations in unusual matrices
18:20-18:50		**Mounting of posters**
18:50-20:00		**Poster session 1**

Tuesday, 24 September 2013

Hall & Meeting Room, Kanazawa Bunka Hall

09:00-10:00		**Plenary Session**
Hall		**Nuclear chemistry (continued) & Environmental radiochemistry** Chairs : **Y. Muramatsu and M. Schädel**
09:00-09:30	**PL-03**	**A. Türler,** *Paul Scherrer Institut & University of Bern, Switzerland* Advances in the production and chemistry of the heaviest elements
09:30-10:00	**PL-04**	**S. Nagao,** *Kanazawa University, Japan* Study on transport of particulate organic matter in river and coastal marine systems using radiocarbon
10:00-10:20		**Coffee Break**
10:20-18:30		**Parallel session**
Hall		**Environmental radiochemistry (continued)** Chairs : **H. Tsuruta and W. S. Wu**
10:20-10:50	**ENI-01**	**H. Foerstendorf,** K. Gückel, N.Jordan, A. Rossberg, V. Brendler, *Helmholtz-Zentrum Dresden-Rossendorf, Germany, Rossendorf Beamline at the European Synchrotron Radiation Facility (ESRF), France* Surface speciation of dissolved radionuclides on mineral phases – A vibrational and X-ray absorption spectroscopic study
10:50-11:10	**ENO-01**	**Z. J. Guo,** Z. Y. Chen, Q. Jin, W. S. Wu, *Lanzhou University, China* Adsorption of Eu(III) and Am(III) on granite
11:10-11:30	**ENO-02**	**H. Tuovinen**, E. Pohjolainen, D. Vesterbacka, C. Kirk, D. Read, D. Solatie, J. Lehto, *University of Helsinki, Finland, Geological Survey of Finland, Loughborough University, UK, Finnish Radiation and Nuclear Safety Authority, Finland* Behaviour of radionuclides and secondary mineral formation in the Talvivaara mining process
11:30-11:50	**ENO-03**	C.-P. Lee, **M.-C. Wu**, C.-Y. Liu, C.-H. Pan, T.-L. Tsai, H.-J. Wei, L.-C. Men, *National Cheng Kung University, Tainan, National Central University, Taiwan, Institute of Nuclear Energy Research, Taiwan* Evaluation of HTO and selenium diffusion behavior in compacted bentonite with different lenghths
11:50-12:10	**ENO-04**	**T. Ohnuki**, N. Kozai, F. Sakamoto, *Japan Atomic Energy Agency, Japan* Sorption behavior of Dy(III) and Np(V) on microbial consortia
12:10-13:20		**Lunch**
Hall		**Environmental radiochemistry (continued)** Chairs : **M. Aoyama and H. Foerstendorf**
13:20-13:40	**ENO-05**	**S. Sachs,** A. Heller, G. Bernhard, *Helmholtz-Zentrum Dresden-Rossendorf, Germany* Interaction of Eu(III) with mammalian cells as a function of Eu(III) concentration and nutrient composition
13:40-14:00	**ENO-06**	**Y. Iwahana,** Y. Koike, M. Kitano, T. Nakamura, *Meiji University, Japan* Monitoring and elution characteristics of radioactive Cs in incinerator fly ashes of municipal solid waste

14:00-14:20	ENO-07	**J. Krmela,** *Ústav Jaderného Výzkumu Řež a.s., The Czech Republic* The issue of separation of uranium from drinking water in the Czech Republic
14:20-14:40	ENO-08	**K. Masumoto**, A. Toyoda, H. Matsumura, T. Kunifuda, *High Energy Accelerator Research Organization, Japan, Tokyo Nuclear Service, Japan* Air-born contamination caused in a high-energy proton accelerator room
14:40-15:00	ENO-09	**H. W. Gäggeler,** L. Tobler, M. Schwikowski, *Paul Scherrer Institut, Switzerland* Application of ^{210}Pb in Glaciology
15:00-15:20	ENO-10	**A. Sakaguchi,** A. Kadokura, P. Steier, Y. Takahashi, K. Shizuma, T. Nakakuki, M. Yamamoto, *Hiroshima University, Japan, University of Vienna, Austria, Kanazawa University, Japan* Depth distributions of uranium-236 and cesium-137 in the Japan Sea; toward the potential use as a new oceanic circulation tracer
15:20-15:40		**Coffee Break**
Hall		**Environmental radiochemistry & Fukushima issues (continued)** Chairs : **S. Nakayama and R. Sudowe**
15:40-16:10	ENI-02	**J. V. Kratz,** *Johannes Gutenberg-University of Mainz, Germany* Ultratrace Analysis of Long-lived Radionuclides by Resonance Ionization Mass Spectrometry (RIMS)
16:10-16:30	ENO-11	**J.-H. Park,** S. Lee, Y.-G. Ha, S. A Lee, K. Jeong, K. Song, *Korea Atomic Energy Research Institute, Korea* The bulk analysis with TIMS measurements preformed in KAERI for nuclear safeguards
16:30-16:50	ENO-12	W. Bu, **J. Zheng,** Q. Guo, T. Aono, K. Tagami, S. Uchida, *Peking University, China, National Institute of Radiological Sciences, Japan* Determination of plutonium isotopes at ultratrace level in seawater samples by sector-field ICP-MS combined with chromatographic separation
16:50-17:10	ENO-13	**I. Milanović,** Ž. Grahek, *Ruđer Bošković Institute, Croatia* Semi-automated procedure for the determination of ^{89,90}Sr in environmental samples by Cherenkov counting
17:10-17:40	FKI-04	**K. Minato,** *Japan Atomic Energy Agency, Japan* Research and development towards decommissioning of Fukushima Daiichi Nuclear Power Plants
17:40-18:00	FKO-09	**Y. Oura,** M. Ebihara, H. Tsuruta, T. Nakajima, T. Ohara, M. Ishimoto, Y. Katsumura, *Tokyo Metropolitan University, Japan, The University of Tokyo, Japan, National Institute for Environmental Studies, Japan* Determination of atmospheric radiocesium on filter tapes used at automated SPM monitoring stations for estimation of transport pathways of radionuclides from Fukushima Daiichi Nuclear Power Plant
18:00-18:20	FKO-10	**K. Hirose,** *Sophia University, Japan* Two-years trend of monthly Cs-137 deposition observed within 300 km of the Fukushima Dai-ichi Nuclear Power Plant
18:20-18:50		**Mounting of posters**
18:50-20:00		**Poster session 2**

10:20-15:20	**Parallel session**

Meeting Room		Nuclear chemistry (continued) Chairs : **H. Kudo and H. W. Gäggeler**
10:20-10:50	NCI-01	**S. Dmitriev,** *The Flerov Laboratory of Nuclear Reactions, Russia* Synthesis and study of properties of superheavy elements: status, problems, and prospects
10:50-11:20	NCI-02	**Ch. E. Düllmann,** *Johannes Gutenberg University of Mainz, Germany* The search for new chemical elements and the possibilities to synthesize transactinide "chemistry" isotopes
11:20-11:50	NCI-03	**H. Haba,** *RIKEN, Japan* Production and decay studies of transactinide nuclides with GARIS at RIKEN
11:50-12:10	NCO-06	**V. Pershina,** *GSI Helmholtzzentrum für Schwerionenforschung, Germany* Theoretical predictions of the electronic structure and properties of the heaviest elements
12:10-13:20		**Lunch**

Meeting Room		Nuclear chemistry (continued) Chairs : **Y. Nagame and S. Dmitriev**
13:20-13:40	NCO-07	**D. Rudolph,** U. Forsberg, P. Golubev, L. G. Sarmiento, A. Yakushev, L.-L. Andersson, Ch. E. Düllmann, J. M. Gates, K. E. Gregorich, F. P. Heßberger, R.-D. Herzberg, J. Khuyagbaatar, J. V. Kratz, K. Rykaczewski, M. Schädel, S. Åberg, D. Ackermann, M. Block, H. Brand, B. G. Carlsson, D. Cox, X. Derkx, A. Di Nitto, K. Eberhardt, J. Even, C. Fahlander, J. Gerl, C. J. Gross, E. Jäger, B. Kindler, J. Krier, I. Kojouharov, N. Kurz, B. Lommel, A. Mistry, C. Mokry, H. Nitsche, J. P. Omtvedt, P. Papadakis, I. Ragnarsson, J. Runke, H. Schaffner, B. Schausten, P. Thörle-Pospiech, T. Torres, A. Türler, A. Ward, D. Ward, N. Wiehl, *Lund University, Sweden, GSI Helmholtzzentrum für Schwerionenforschung, Germany, Helmholtz Institute Mainz, Germany, Johannes Gutenberg-University of Mainz, Germany, Lawrence Berkeley National Laboratory, USA, University of Liverpool, Oak Ridge National Laboratory, USA, Japan Atomic Energy Agency, Japan, Paul Scherrer Institut, Switzerland* Spectroscopy of element 115 decay chains
13:40-14:00	NCO-08	**A. Yakushev,** *GSI Helmholtzzentrum für Schwerionenforschung, Germany* Chemistry at one-atom-per-week level
14:00-14:20	NCO-09	**J. Even,** A. Yakushev, Ch. E. Düllmann, H. Haba, M. Asai, T. Sato, H. Brand, A. Di Nitto, R. Eichler, F. Fangli, W. Hartmann, M. Huang, E. Jäger, D. Kaji, J. Kanaya, Y. Kaneya, J. Khuyagbaatar, B. Kindler, J. V. Kratz, J. Krier, Y. Kudou, N. Kurz, B. Lommel, S. Miyashita, K. Morimoto, K. Morita, Y. Nagame, H. Nitsche, K. Ooe, M. Schädel, J. Steiner, T. Sumita, K. Tanaka, A. Toyoshima, K. Tsukada, A. Türler, I. Usoltsev, Y. Wakabayashi, Y. Wang, N. Wiehl1, S. Yamaki, Q. Zhi, *Helmhotz-Institut Mainz, Germany, GSI Helmholtzzentrum für Schwerionenforschung, Germany, Johannes Gutenberg-University of Mainz, Germany, RIKEN, Japan, Japan Atomic Energy Agency, Japan, University of Bern, Switzerland, Paul Scherrer Institut, Switzerland, Institute of Modern Physics, China, University of California, USA, Lawrence Berkeley National Laboratory, USA, Niigata University, Japan, Saitama University, Japan* $Sg(CO)_6$ - The first organometallic transactinde complex opening a window to a new compound class
14:20-14:40	NCO-10	**H. Nitsche**, G. K. Pang, J. M. Gates, K. E. Gregorich N. E. Esker, O. R, Gothe, *University of California, USA, Lawrence Berkeley National Laboratory , USA* Superheavy element Z and A measurements at the Berkeley Gas-Filled

Separator

14:40-15:00	NCO-11	**R. Eichler**, I. Usoltsev, J. P. Omtvedt, O. V. Petrushkin, D. Piguet, A. V. Sabel'nikov, A. Türler, G. K. Vostokin, A. V. Yeremin, *Paul Scherrer Institute, Switzerland, University of Bern, Switzerland, The Flerov Laboratory of Nuclear Reactions, Russia, University of Oslo, Norway* Intermetallic actinide compounds for SHE production targets
15:00-15:20	NCO-12	**T. K. Sato**, M. Asai, N. Sato, Y. Kaneya, K. Tsukada, A. Toyoshima, S. Miyashita, Y. Nagame, M. Schädel, A. Osa, S. Ichikawa, K. Ooe, T. Stora, J. V. Kratz, *Japan Atomic Energy Agency, Japan, Ibaraki University, Japan, RIKEN, Japan, Niigata University, Japan, ISOLDE, CERN, Switzerland, Johannes Gutenberg-University of Mainz, Germany* The first successful observation of mass-separated lawrencium (Lr, Z = 103) ions with ISOL technique
15:20-15:40		**Coffee Break**
Meeting Room		**Nuclear energy chemistry** Chairs : **Z. Yoshida and S. Clark**
15:40-16:10	NEI-01	**Z. F. Chai,** *Institute of High Energy Physics, China* Nuclear energy chemistry in China: present status and future perspectives
16:10-16:40	NEI-02	**A. Goswami,** *Bhabha Atomic Research Centre, India* Evaluation of new extractants relevant to the back-end of nuclear fuel cycle
16:40-17:00	NEO-01	**E. Löfström-Engdahl,** E. Aneheim, C. Ekberg, H. Elfversson, G. Skarnemark, *Chalmers University of Technology, Sweden* Hexanoic acid as alternative diluent in a GANEX process based on TBP and CyMe4-BTBP
17:00-17:20	NEO-02	**Y. Tomobuchi,** Y. Tachibana, M. Nomura, T. Suzuki, *Nagaoka University of Technology, Japan, Tokyo Institute of Technology, Japan* Effect of alcohols on separation behavior of rare earth elements using benzimidazole-type anion-exchange resin in nitric acid solutions
17:20-17:40	NEO-03	**F. Poineau,** P. Weck, B. P. Burton-Pye, A. Maruk, G. Kirakosyan, I. Denden, D.. B. Rego, E. V. Johnstone, W. Kerlin, E. Kim, M. Ferrier, A. P. Sattelberger, W. Lukens, M. Fattahi, L. C. Francesconi, K. E. German, K. R. Czerwinski, *University of Nevada Las Vegas, USA, Sandia National Laboratories, USA, Hunter college of the City University of New York, USA, A. N. Frumkin Institute of Physical Chemistry and Electrochemistry, Russia, Ecoles des Mines de Nantes, France, Argonne National Laboratory, USA, Lawrence Berkeley National Laboratory, USA* Speciation and reactivity of heptavalent technetium in concentrated acids
17:40-18:00	NEO-04	**A. Braatz,** M. Nilsson, *University of California, Irvine, USA* Fluorescence studies of complex stoichiometry of metal ions in extraction systems combining dibutyl phosphoric acid and tri-n-butyl phosphate
18:00-18:20	NEO-05	**R. Chen,** H. Tanaka, M. Asai, C. Fukushima, T. Kawamoto, M. Ishizaki, M. Kurihara, M. Arisaka, T. Nankawa M. Watanabe, *National Institute of Advanced Industrial Science and Technology, Japan, Yamagata University, Japan, Japan Atomic Energy Agency, Japan* Column study on electrochemical separation of cesium ions from wastewater using copper hexacyanoferrate film
18:20-18:50		**Mounting of posters**
18:50-20:00		**Poster session 2**

Wednesday, 25 September 2013

Hall & Meeting Room, Kanazawa Bunka Hall

09:00-10:00		**Plenary Session**
Hall		**Actinide chemistry & Radiopharmaceutical chemistry and Nuclear medicine** Chairs : **T. Yaita and E. Simoni**
09:00-09:30	**PL-05**	**M. A. Denecke,** *University of Manchester, UK* Actinide speciation using synchrotron-based methods
09:30-10:00	**PL-06**	**J. Hatazawa,** *Osaka University, Japan* Radionuclides in diagnostic nuclear medicine
10:00-10:20		**Coffee Break**
10:20-12:00		**Parallel session**
Hall		**Radiopharmaceutical chemistry and Nuclear medicine (continued)** Chairs : **J. Hatazawa and A. Türler**
10:20-10:50	**RPI-01**	**D. S. Wilbur,** D. K. Hamlin, M.-K. Chyan, E. Balkin, J. M. Pagel, O. W. Press, B. M. Sandmaier, *University of Washington, USA, Fred Hutchinson Cancer Research Center, USA* Addressing challenges in preparation of ^{211}At-labeled biomolecules for use in targeted alpha therapy
10:50-11:20	**RPI-02**	M. Maiti, **S. Lahiri,** *Indian Institute of Technology Roorkee, India, Saha Institute of Nuclear Physics, India* Generation of nuclear data for the production of ^{97}Ru from ^{12}C + ^{89}Y reaction
11:20-11:40	**RPO-01**	**E. Aneheim,** S. Lindegren1, H. Jensen, Sahlgrenska Academy at Gothenburg University, Sweden, Cyclotron and PET Unit, Denmark Towards an automatic procedure for the production of astatinated antibodies
11:40-12:00	**RPO-02**	**Y. Hatsukawa,** K. Hashimoto, K. Tsukada, T. Sato, M. Asai, A. Toyoshima, Y. Nagai, T. Tanimori, S. Sonoda, S. Kabuki, H, Saji, H. Kimura, *Japan Atomic Energy Agency, Japan, Kyoto University, Japan, Tokai University, Japan* Production of ^{95m}Tc for compton camera imaging
12:00-13:20		**Group photo (Hall) and Lunch**
10:20-12:00		**Parallel session**
Meeting Room		**Actinide chemistry (continued)** Chairs : **M. Watanabe and A. Goswami**
10:20-10:50	**ACI-01**	J. Su, **J. Li,** *Tsinghua University, China* Relativistic quantum chemical studies on electronic structures and photoelectron spectra of actinide complexes
10:50-11:20	**ACI-02**	**Y. Kitatsuji,** *Japan Atomic Energy Agency, Japan* Flow electrolysis of actinide ions utilizing electrocatalysis
11:20-11:40	**ACO-01**	**A. Kirishima,** N. Sato, *Tohoku University, Japan* Determination of the thermodynamic quantities of U(VI) complexation with "aliphatic" and "aromatic" di-carboxylic acids by calorimetry
11:40-12:00	**ACO-02**	**H. Hayashi,** M. Akabori, K. Minato, *Japan Atomic Energy Agency, Japan* Electrochemical behavior of americium in NaCl-2CsCl melt

12:10-13:20		**Group photo (Hall) and Lunch**
13:20-15:20 **Hall**		**Japan Society of Nuclear and Radiochemical Sciences (JNRS) General Assembly for Member of JNRS**
13:20-14:20		**JNRS General Assembly**
14:20-15:20		**JNRS Meeting**
15:20-15:40		**Coffee Break**
15:40-17:20 **Hall**		**Parallel session** **Radiopharmaceutical chemistry and Nuclear medicine & Fukushima issues (continued)** Chairs : **T. Ohnuki and D. S. Wilbur**
15:40-16:00	**RPO-03**	**L. Safavi-Tehrani,** G. E. Miller, M. Nilsson, *University of California Irvine, USA* Production of high specific activity radiolanthanides for medical purposes using the UC Irvine TRIGA Reactor
16:00-16:20	**FKO-11**	S. LaZar, **E. Rasmussen,** P. Stamets, *Department of Energy (DOE), USA, San Diego State University, USA, Fungi Perfecti Research Laboratories, USA* Mycoremediation: fungus-based soil remediation of radioisotope contamination
16:20-16:40	**FKO-12**	**K. Minami,** T. Funabashi, R. Kamimura, T. Yasutaka, H. Tanaka, A. Kitajima, H. Ogawa, T. Kawamoto, *National Institute of Advanced Industrial Science and Technology, Japan, Tokyo Power Technology Ltd., Japan* Automatic Cs-uptake device for radioactive-Cs evaluation in environmental water
16:40-17:00	**FKO-13**	K. Minami, H. Ogawa, H. Tanaka, A. Takahashi, T. Uchida, A. Kitajima, D. Parajuli, **T. Kawamoto,** M. Yamaguchi, M. Osada, N. Otake, S. Sato, R. Kamimura, Y. Hakuta, *The National Institute of Advanced Industrial Science and Technology, Japan, Tokyo Power Technology Ltd., Japan* Pilot plant for volume reduction of Cs-contaminated combustible materials
17:00-17:20	**FKO-14**	**D. Parajuli,** H. Tanaka, S. Fukuda, R. Kamimura, T. Kawamoto, *The National Institute of Advanced Industrial Science and Technology, Japan, Tokyo Power Technology Ltd., Japan* Decontamination of radioactive cesium from ash and soil
15:40-17:20 **Meeting Room**		**Parallel session** **Actinide chemistry & Nuclear chemistry (continued)** Chairs : **H. Haba and Ch. E. Düllmann**
15:40-16:00	**ACO-03**	**T.-H. Park,** Y. S. Choi, J.-H. Park, J.-Y. Kim, S.-E. Bae, Y.-H. Cho, J.-W. Yeon, K. Song, *Korea Atomic Energy Research Institute, Korea* Rapid radioanalytical determination of U, Pu, and Am in radioactive wastes via extraction chromatography, alpha spectrometry, and thermal ionization mass spectrometry
16:00-16:20	**ACO-04**	**N. Aoyagi,** M. Watanabe, A. Kirishima, N. Sato, T. Kimura, *Japan Atomic Energy Agency, Japan, Tohoku University, Japan* Luminescence spectroscopy of uranium complexes in non-aqueous media

16:20-16:40	**NCO-13**	**A. Toyoshima,** S. Miyashita, M. Asai, T. K. Sato, Y. Kaneya, K. Tsukada, Y. Kitatsuji, Y. Nagame, M. Schädel, H. V. Lerum, J. P. Omtvedt, Y. Oshimi, K. Ooe, Y. Kitayama, A. Yokoyama, A. Wada, Y. Oura, H. Haba, J. Kanaya, M. Huang, Y. Komori, T. Yokokita, Y. Kasamatsu, A. Shinohara, V. Pershina, J. V. Kratz, *Japan Atomic Energy Agency, Japan, University of Oslo, Norway, Niigata University, Japan, Kanazawa University, Japan, Tokyo Metropolitan University, Japan, RIKEN, Japan, Osaka University, GSI Helmholtzzentrum für Schwerionenforschung, Germany, Johannes Gutenberg-University of Mainz, Germany* Chemical studies of Mo and W in preparation of a seabogrium (Sg) reduction experiment using MDG, FEC, and SISAK
16:40-17:00	**NCO-14**	**P. Steinegger,** R. Dressler, R. Eichler, A. Türler, *Paul Scherrer Institute, Switzerland* , *University of Bern, Switzerland* Diamond detectors for isothermal vacuum chromatography
17:00-17:20	**NCO-15**	**R. Tripathi,** S. Sodaye, K. Mahata, P. K. Pujari, *Bhabha Atomic Research Centre, India* Angular distribution of projectile like fragments in $^{16}O + {}^{89}Y$ reaction
17:20-17:50		**Coffee Break**
17:50-18:30		**Plenary session**
Hall	**JNRS-Award**	**JNRS Award Presentation (Open session)** Chair : **T. Sasaki**
17:50-18:30		**T. Kimura,** *Japan Atomic Energy Agency, Japan* Studies on solution chemistry of actinides and lanthanides by time-resolved laser-induced fluorescence spectroscopy
18:30-18:50		**Mounting of posters**
18:50-20:00		**Poster session 3**

Thursday, 26 September 2013

Hall & Meeting Room, Kanazawa Bunka Hall

09:00-10:00		**Plenary Session**
Hall		**Education in nuclear and radiochemistry & Nuclear probes for material science** Chairs : **K. Kubo and J. John**
09:00-09:30	**PL-07**	**S. B. Clark,** *Washington State University, USA* Preparing the next generation of radiochemists for global challenges
09:30-10:00	**PL-08**	**H. Ueno,** *RIKEN, Japan* Researches with stopped radioisotopes at the RIKEN RIBF facility
10:00-10:20		**Coffee Break**
10:20-12:10		**Parallel session**
Hall		**Nuclear probes for material science (continued)** Chairs : **Y. Yamada and Y. Kobayashi**
10:20-10:50	**NPI-01**	**W. Sato,** S. Komatsuda, Y. Yamada, Y. Ohkubo, *Kanazawa University, Japan, Tokyo University of Science, Japan, Kyoto University, Japan* Local structure at the In impurity site in ZnO probed by the TDPAC technique
10:50-11:10	**NPO-01**	**K. Nomura,** P. de Souza, S. Hirai, N. Kojima, *The University of Tokyo, Japan, University of Tasmania, Australia, Tokyo Toshi University, Japan* Mössbauer analysis of iron ore and rapidly reduced iron ore by micro-discharge
11:10-11:30	**NPO-02**	**J. Wang,** A. I. Rykov, K. Nomura, *Dalian Institute of Chemical Physics, China, The University of Tokyo, Japan* Three ways to fix Cs in prussian blues
11:30-11:50	**NPO-03**	M. Kaneko, H. Dote, **S. Nakashima**, *Hiroshima University, Japan* Theoretical study on Mössbauer parameters of iron assembled complexes
11:50-12:10	**NPO-04**	**G. Yoshida,** K. Ninomiya, M. Inagaki, T. U. Ito, W. Higemoto, T. Nagatomo, P. Strasser, N. Kawamura, K. Shimomura, Y. Miyake, T. Miura, M. K. Kubo, A. Shinohara, *Osaka University, Japan, Japan Atomic Energy Agency, Japan, High Energy Accelerator Research Organization, Japan, International Christianity University, Japan* Study on muon capture process for gaseous molecules containing C and O atoms
12:10-13:00		**Lunch**
10:20-12:10		**Parallel session**
Meeting Room		**Education in nuclear and radiochemistry (continued)** Chairs : **A. Shinohara and Y. H. Chung**
10:20-10:50	**EDI-01**	**J. John,** V. Čuba, M. Němec, T. Retegan, C. Ekberg, G. Skarnemark, J. Lehto, T. Koivula, P. J. Scully, C. Walther, J.-W. Vahlbruch, N. Evans, D. Read, E. Ansoborlo, B. Hanson, L. Skipperud, B. Salbu, J. P. Omtvedt, *Czech Technical University in Prague, Czech Republic, Chalmers University of Technology, Sweden, University of Helsinki, Finland, University of Hanover, Germany, Loughborough University, Great Britain, Commissariat à l'énergie atomique et aux énergies alternatives, France, Leeds University, UK, Norwegian*

		University of Life Sciences, Norway, University of Oslo, Norway CINCH-II Project - Next step in the coordination of education in nuclear and radiochemistry in Europe
10:50-11:20	EDI-02	**W. S. Wu**, Z. F. Chai, *Lanzhou University, China, Institute of High Energy Physics, China* Fostering of personnel for nuclear and radiochemistry according to China's NPP prospects after Fukushima Daiichi accident
11:20-11:50	EDI-03	**A. Yokoyama,** *Kanazawa University, Japan* Post-Fukushima situation on radiation awareness activities and nuclear and radiochemistry education in Japan
11:50-12:10	EDO-01	**S. B. Sarmani,** R. B. Yahaya, M. S. Yasir, A. Ab. Majid, K. S. Khoo, I. A. Rahman, F. Mohamed, *Universiti Kebangsaan, Malaysia* Radiochemistry course in the undergraduate nuclear science program at Universiti Kebangsaan Malaysia
12:10-13:00		**Lunch**
13:00-17:30		**Excursion : Shirakawa-go**
19:00-21:00		**Banquet at Kanazawa Excel Hotel Tokyu**

Friday, 27 September 2013

Meeting Room, Kanazawa Bunka Hall

09:00-10:00

Meeting Room — **Activation analysis**
Chairs : **M. Ebihara and J. H. Moon**

09:00-09:30 **AAI-01** W. M. Sanchez, Y. Shi, **A. Chatt,** *Dalhousie University, Canada*
Simultaneous analysis for As, Sb, and Se species in water by chemical separation and neutron activation

09:30-10:00 **AAI-02** **T. Miura,** R. Okumura, Y. Iinuma, S. Sekimoto, K. Takamiya, M. Ohata, A. Hioki, *National Metrology Institute of Japan, Japan, Kyoto University Research Reactor Institute, Japan*
Precise determination of bromine in PP resin pellet by instrumental neutron activation analysis using internal standardization

10:00-10:20 **Coffee Break**

10:20-12:00

Meeting Room — **Activation analysis (continued)**
Chairs : **T. Miura and A. Chatt**

10:20-10:40 **AAO-01** **J. H. Moon,** B. F. Ni, R. M. Theresia, N. A. Abd. Salim, B. Arporn, C. D. Vu, *Korea Atomic Energy Research Institute, Korea, China Institute of Atomic Energy, China, National Nuclear Energy Agency, Indonesia, Malaysian Nuclear Agency, Malaysia, Thailand Institute of Nuclear Technology, Thailand, Vietnam Atomic Energy Agency, Vietnam*
Analysis of most popular and/or consumed fish species by neutron activation analysis in six Asian countries

10:40-11:00 **AAO-02** **Y. Toh,** M. Ebihara, K. Hara, A. Kimura, H. Harada, S. Nakamura, M. Koizumi, K. Furutaka, F. Kitatani, *Japan Atomic Energy Agency, Japan, Tokyo Metropolitan University, Japan*
Current status and future perspective on time-of-flight prompt gamma-ray analysis combined with gamma-ray coincidence technique development

11:00-11:20 **AAO-03** **K. Ninomiya,** M. K. Kubo, T. Nagatomo, G. Yoshida, M. Inagaki, A. Shinohara, T. Suzuki, N. Kawamura, P. Strasser, K. Shimomura, Y. Miyake, Y. Kobayashi, K. Ishida, W. Higemoto, S. Sakamoto, T. Saito, *Osaka University, Japan, International Christianity University, Japan, High Energy Accelerator Research Organization, Japan, RIKEN, Japan, Japan Atomic Energy Agency, Japan, National Museum of Japanese History, Japan*
Simultaneous and multielemental analysis by muonic X-rays for inside Japanese bronze and gold coin

11:20-11:40 **AAO-04** **M. Fukushima,** A. Chatt, Y. Nakamura, M. Haga, S. Hoshi, T. Sakata, *Ishinomaki Senshu University, Japan, Dalhousie University, Canada, Meiji Co., Ltd., Japan, Shokei Gakuin University, Japan*
Rapid analysis for selenium in urine samples using the 17.4-s neutron activation product ^{77m}Se

11:40-12:00 **AAO-05** **N. Shirai,** Y. Hidaka, S. Sekimoto, M. Ebihara, H. Kojima, *Tokyo Metropolitan University, Japan, Kyoto University Research Reactor Institute, Japan, National Institute of Polar Research, Japan, Graduate University for Advanced Sciences, Japan*

		Neutron activation analysis of iron meteorite
12:00-13:20		**Lunch**
Meeting Room		**Application of nuclear and radiochemical techniques (continued)** Chairs : **W. Sato and Y. L. Zhao**
13:20-13:50	**API-03**	**Y. Hamajima,** *Kanazawa University, Japan* What has been revealed in the low-level radioactivity measurement? - low level gamma-ray counting in Ogoya underground laboratory
13:50-14:10	**APO-04**	**C. Gautier,** M. Coppo, C. Caussignac, I. Laszak, P. Fichet, F. Goutelard, *CEA Saclay, France* Zr and U determination at trace level in simulated deep groundwater by Q ICP-MS using TRU-based and TODGA-based extraction chromatography
14:10-14:30	**APO-05**	**T. Yoshimura,** H. Ikeda, A. Ito, E. Sakuda, N. Kitamura, T. Takayama T. Sekine, A. Shinohara, *Osaka University, Japan, Hokkaido University, Japan, Daido University, Japan, Tohoku University, Japan* Photoluminescence of five- and six-coordinate tetracyanidonitridotechnetium (V) and -rhenium (V) complexes
14:30-14:50	**APO-06**	**J. D. Despotopulos,** N. Gharibyan, R. A. Henderson, W. Kerlin, K. J. Moody, D. A. Shaughnessy, E. Tereshatov, R. Sudowe, *Lawrence Livermore National Laboratory, USA, University of Nevada Las Vegas, USA* Studies of flerovium and element 115 homologs with macrocyclic extractants
14:50-15:10		**Coffee Break**
15:10-15:30		**Closing Ceremony**
Meeting Room		**M. Yamamoto**, APSORC13 co-chair, *Kanazawa University, Japan* Student Poster Award

Monday, 23 September 2013, Poster Session

23-FKP-01 **^{137}Cs accumulation enhanced by potassium starvation in lotus japonicus**
J. Furukawa[1], H. Noda[2], R. Sugita[3], K. Tanoi[3], T. M. Nakanishi[3], S. Satoh[1]
[1]*Faculty of Life and Environmental Sciences, University of Tsukuba,* [2]*Graduate School of Life and Environmental Sciences, University of Tsukuba,* [3]*Graduate School of Agricultural and Life Sciences, The University of Tokyo*

23-FKP-02 **Decontamination of the contaminated water on severe nuclear accidents by titanium oxide adsorption**
Y. Takahatake[1], M. Nakamura[1], A. Shibata[1], K. Nomura[1], Y. Koma[1], Y. Nakajima[1]
[1]*Japan Atomic Energy Agency*

23-FKP-03 **Iodine-129 in the aquatic environment adjacent to a spent nuclear fuel reprocessing plant, Rokkasho, Japan**
S. Ueda[1], H. Kakiuchi[1], H. Hasegawa[1] N. Akata[1], H. Kawamura[2], S. Hisamatsu[1]
[1]*Department of Radioecology, Institute for Environmental Sciences, Japan,* [2]*Kyushu Environmental Evaluation Association, Japan*

23-FKP-04 **Specific activity and time dependence of radionuclides in soils affected by the accident of the Fukushima Dai-ichi nuclear power plant (Part 2).**
T. Shimasaki[1], Y. Shiraishi[1], O. Kawahara[1], K. Goto[1], M. Shimamoto[1], A. Kojima[1], S. Okada[2]
[1]*Institute of Source Development and Analysis, Kumamoto University,* [2]*Center for AIDS Research, Kumamoto University*

23-FKP-05 **Differences between year 2011 and 2012 in Cs-137 concentration in brown rice grown in Fukushima Prefecture**
S. Fujimura[1,2], Y. Sakuma[1], T. Yamauchi[1], K. Niitsuma[1], N. Sato[3], M. Sato[1], T. Saito[1], K. Yoshioka[1]
[1]*Fukushima Agricultural Technology Centre,* [2]*NARO Tohoku Agricultural Research Center,* [3]*Inawashiro Town, Japan*

23-FKP-06 **Size-distribution of airborne radioactive particles from the Fukushima accident**
H. Muramatsu[1], K. Kawasumi[1], T. Kondo[1], and K. Matsuo[2]
[1]*Department of Chemistry, Faculty of Education, Shinshu University, Japan,* [2]*Graduate School of Education, Shinshu University, Japan*

23-FKP-07 **Long-term effects of radionuclides originating from the Fukushima nuclear power plant accident in airborne particulate matters in Kawasaki**
K. Nakamachi[1], H. Matsuno[1], T. Honda[1], Y. Kikawada[2]
[1]*Graduate School of Engineering, Tokyo City University,* [2]*Faculty of Science and Technology, Sophia University*

23-FKP-08 **Measurement of Iodine-129 concentration in water samples in relation with Fukushima Daiichi Nuclear Power Plant accident**
H. Matsuzaki[1], H. Tokuyama[1], Y. Miyake[1], M. Honda[2], T. Yamagata[3], Y. Muramatsu[4]
[1]*Department of Nuclear Engineering and Management, School of Engineering, The University of Tokyo, Japan,* [2]*Graduate School of Integrated Basic Sciences, Nihon University, Japan,* [3]*College of Humanities and Sciences, Nihon University, Japan,* [4]*Department of Chemistry, Gakushuin University, Japan*

23-FKP-09 **Observed radioactivities and activity ratios in aerosols from April 2011 at the geological survey of Japan, Tsukuba, Japan**
Y. KANAI[1]
[1]*Geological Survey of Japan, National Institute of Advanced Industrial and Technology*

23-FKP-10 **Chemical forms of radioactive Cs in soils originated from Fukushima Dai-ichi nuclear power plant accident, as studied by extraction experiments**
M. Hirose[1], Y. Kikawada[1], A. Tsukamoto[2], T. Oi[1], T. Honda[2], K. Hirose[1], H. Takahashi[3]
[1]*Faculty of Science and Technology, Sophia University,* [2]*Graduate School of Engineering, Tokyo City University,* [3]*Graduate School of Engineering, Tohoku University*

23-FKP-11 **Thermal Oxidation of Cesium Loaded Prussian Blue as a Precaution for Exothermic Phase Change in Extreme Conditions**

D. Parajuli, H. Tanaka, A. Takahashi, T. Kawamoto
Nanosystem Research Institute, AIST, Japan

23-FKP-12 **Analysis of ^{134}Cs and ^{137}Cs distribution in soil of Fukushima prefecture and their specific adsorption on clay minerals**

A. Maekawa[1], N. Momoshima[2], S. Sugihara[2], R. Ohzawa[1], A. Nakama[1]
[1]*Graduate School of Sciences, Kyushu University, Japan,* [2]*Radioisotope Center, Kyushu University, Japan*

23-FKP-13 **Distribution of radionuclides in seabed sediments off Ibaraki coast after the Fukushima Daiichi Nuclear Power Plant accident**

M. Nagaoka[1], H. Yokoyama[1], H. Fujita[1], M. Nakano[1], H. Watanabe[1], S. Sumiya[1]
[1]*Nuclear Fuel Cycle Engineering Laboratories, Japan Atomic Energy Agency*

23-FKP-14 **Radiocesium concentration change in tree leaves before and after defoliation**

S. Uchida[1], K. Tagami
[1]*Office of Biospheric Assessments for Waste Disposal, National Institute of Radiological Sciences*

23-FKP-15 **Distributions and concentrations of radionuclides in giant butterbur after the Fukushima Nuclear Power Plant Accident**

K. Tagami[1], S. Uchida[1]
[1]*Office of Biospheric Assessment for Waste Disposal, National Institute of Radiological Sciences, Japan*

23-FKP-16 **The Behavior of Cs adsorption of microcapsule beads nano-prussian blue**

A. Kitajima[1], H. Ogawa[1], K. Yoshino[2], M. Takasaki[2], H. Tanaka[1], T. kawamoto[1]
[1]*Nanosystem Research Institute, Japan,* [2]*Kanto Chemical Company Inc., Japan*

23-FKP-17 **Transfer of radiocesium from soil to cut flowers**

Y. Suzuki[1,2], H. Munakata[1], Y. Yajima[1], Y. Tooyama[3], H. Suzuki[1], H. Tsukada[4], K. Inubushi[2]
[1]*Fukushima Agricultural Technology Centre,* [2]*Graduate School of Horticulture, Chiba University,* [3]*Ken-poku District Agriculture and Forestry Office, Japan,* [4]*Fukushima University*

23-FKP-18 **CLEVASOL, a novel radiation hard cation exchanger suitable for treatment of liquid radioactive waste with high salinity**

A. Yakushev[1], A. Türler[2], Z. Dvorakova[3], K. von Bremen[2]
[1]*GSI Helmholtzzentrum für Schwerionenforschung GmbH,* [2]*University of Bern,* [3]*Neplachova 17, 37004 Ceske Budejovice*

23-FKP-19 **Estimation of I-131/I-129 ratios and vertical distribution of radioiodine in soil collected from Fukushima Prefecture**

N.Inagawa[1], Y. Muramatsu[1], T. Ohno[1], T. Toyama[1], C. Satou[2], M. Outsuki[3], T. Matsuzaki[4]
[1]*Gakushuin University,* [2]*Fukushima Agricultural Technology Centre,* [3]*Tohoku University,* [4]*University of Tokyo*

23-FKP-20 **Effects of soil types on the transfer of radiocesium to plant**

K. Oda[1], Y. Muramatsu[1], T. Ohno[1], T. Kobayashi[2], S. Fujimura[2]
[1]*Gakushuin University,* [2]*Fukushima Agricultural Technology Centre*

23-FKP-21 **Temporal distribution of plutonium isotopes in marine sediments off Fukushima and Ibaraki after the Fukushima Dai-ichi Nuclear Power Plant accident**

W. Bu[1,2], J. Zheng*[2], T. Aono[2], S. Otosaka[3], K. Tagami[2], Q. Guo[1], S. Uchida[2]
[1]*School of Physics, Peking University,* [2]*National Institute of Radiological Sciences, Japan,* [3]*Japan Atomic Energy Agency*

23-FKP-22 **Evaluation of Iodine-129 mobility and deposition amount in the soil contaminated by the Fukushima Daiichi nuclear power plant accident**

M. Honda[1], H. Matsuzaki[2], T. Yamagata [3], Y. (S.) Tuchiya[2], C. Nakano[2], Y. Matsushi[4], Y. Maejima[5], H. Nagai[3]
[1]*Graduate School of Integrated Basic Sciences, Nihon university, Japan,* [2]*Department of Nuclear Engineering and Management, School of Engineering, The University of Tokyo, Japan,* [3]*College Humanities and Sciences, Nihon University, Japan,* [4]*Disaster Prevention Research Institute, Kyoto University, Japan,* [5]*National Institute for Agro-Environmental Sciences, Japan*

23-FKP-23 **Vertical distribution of the Fukushima-derived radiocesium in the western North Pacific in January and February 2011**

Y. Kumamoto[1], A. Murata[1], T. Kawano[1], M. Aoyama[2]
[1]*Japan Agency for Marine-Earth Science and Technology, Japan,* [2]*Meteorological Research Institute, Japan*

23-FKP-24 **Effect of application timing of potassium fertilizer on root uptake of ^{137}Cs in brown rice**

T. Saito[1], K. Takahashi[1], T. Makino[2], H. Tsukada[3,4], M. Sato[1], K. Yoshioka[1]
[1]*Fukushima Agricultural Technology Centre,* [2]*National Institute for Agro-Environmental Sciences,* [3]*Institute for Environmental Sciences,* [4]*Fukushima University*

23-FKP-25 **Low levels of ^{134}Cs and ^{137}Cs in bottom sediments along the Japanese archipelago side of the Sea of Japan after the Fukushima Dai-ichi NPP accident**

M. Inoue[1,*], S. Ochiai[1], T. Murakami[1], S. Oikawa[2], M. Yamamoto[1], S. Nagao[1], Y. Hamajima[1], H. Kofuji[1], J. Misonoo[2]
[1]*Low Level Radioactivity Laboratory, Kanazawa University,* [2]*Marine Ecology Research Institute, Japan*

23-NCP-01 **The heavy-ion reactions ^{238}U + ^{238}U and ^{238}U + ^{248}Cm and actinide production close to the barrier revisited**

J.V. Kratz[1a], M. Schädel[1b], H.W. Gäggeler[1c]
[1]*Gesellschaft für Schwerionenforschung mbH,* [a]*currently at Institut für Kernchemie, Johannes Gutenberg-Universität, Germany,* [b]*currently at Advanced Science Research Center, Japan Atomic Energy Agency, Japan,* [c]*currently at Paul Scherrer Institute, Switzerland*

23-NCP-02 **Mechanism of Mo-99 adsorption and Tc-99m elution from zirconium-based material in Mo-99/Tc-99m generator column using neutron-irradiated natural molybdenum**

R. Awaludin[1], A. H. Gunawan[1], H. Lubis[1], Sriyono[1], Herlina[1], A. Mutalib[1], A. Kimura[2], K. Tsuchiya[2], M. Tanase[3], M. Ishihara[2]
[1]*Center for Radioisotope and Radiopharmaceutical, National Nuclear Energy Agency of Indonesia,* [2]*Neutron Irradiation and Testing Reactor Center, Oarai Research and Development Center, Japan Atomic Energy Agency,* [3]*Chiyoda Technol Corporation, Japan*

23-NCP-03 **Startup of a new gas-filled recoil separator GARIS-II**

D. Kaji[1], K. Morimoto[1], H. Haba[1], Y. Wakabayashi[1], Y. Kudou[1], M. Huang[1], S. Goto[2], M. Murakami[2], N. Goto[2], T. Koyama[2], N. Tamura[2], S. Tsuto[2], T. Sumita[3], K. Tanaka[3], M. Takeyama[4], S. Yamaki[5], K. Morita[1]
[1]*Nishina Center for Accelerator Based Science, RIKEN,* [2]*Niigata University, Japan,* [3]*Tokyo University of Science, Japan,* [4]*Yamagata University,* [5]*Saitama University, Japan*

23-NCP-04 **Purification of scintillation cocktails containing the alpha emitters americium and plutonium**

E. Löfström-Engdahl*, G. Skarnemark, K. El Tayara, J. Eriksson, N. Halldin, J. Halleröd, M. Malmberg, J. Mattiasson Bjugren
Nuclear chemistry, Department of Chemical and Biological Engineering, Chalmers University of Technology, Sweden

23-NCP-05 **Formation and stability of sulfides of the superheavy elements Cn and Fl**

N.M. Chiera[1,2], R. Eichler[1,2*], A. Türler [1,2]
[1]*Department of Chemistry & Biochemistry, University of Berne, Switzerland,* [2]*Laboratory for Radiochemistry and Environmental Chemistry, Paul Scherrer Institute, Switzerland*

23-NCP-06 **Development of a batch-type solid-liquid extraction apparatus for repetitive extraction experiment of element 104, Rf**

Y. Kasamatsu[1], T. Yokokita[1], A. Kino[1], K. Nakamura[1], K. Toyomura[1], Y. Komori[1], N. Takahashi[1], H. Haba[2], J. Kanaya[2], M. Huang[2], Y. Kudou[2], T. Yoshimura[3], A. Shinohara[1]
[1]*Graduate School of Science, Osaka University,* [2]*Nishina Center for Accelerator-Based Science, RIKEN,* [3]*Radioisotope Research Center, Osaka University*

23-NCP-07 **Coprecipitation of Zr, Hf and Th with Sm hydroxide for chemical study of Rf**

K. Toyomura[1], Y. Kasamatsu[1], N. Shiohara[1], T. Yokokita[1], Y. Komori[1], K. Nakamura[1], N. Takahashi[1], T. Yoshimura[2], H. Haba[3], Y. Kudou[3], H. Kikunaga[4], T. Ohtsuki[4], K. Takamiya[5], T. Mitsugashira[6], and A. Shinohara[1]
[1]*Graduate School of Science, Osaka University,* [2]*Radioisotope Research Center, Osaka University,* [3]*Nishina Center for Accelerator-Based Science,* [4]*Research Center for Electron Photon Science, Tohoku University,* [5]*Research Reactor Institute, Kyoto University,* [6]*International Research Center for Nuclear Materials Science,*

Institute for Material Research, Tohoku University

23-NCP-08 **Development of modified epoxy paint films to reduce the volatile iodine source term in the containments of LWRs during severe nuclear accidents**

S. Tietze[1]
[1]*Severe Nuclear Accident Chemistry, Nuclear Chemistry Department, Department of Chemical and Biological Engineering, Chalmers University of Technology, Sweden*

23-NCP-09 **New insights into the formation and stability of molybdenum carbonyl compounds**

I. Usoltsev[1,2], Wang Yang[3], R. Eichler[1,2], A. Türler[1,2], Qin Zhi[3]
[1]*Department of Chemistry & Biochemistry, University of Berne, Switzerland,* [2]*Laboratory for Radiochemistry and Environmental Chemistry, Paul Scherrer Institut, Switzerland,* [3]*Institute of Modern Physics Lanzhou; Chinese Academy of Sciences, China*

23-NCP-10 **Adsorption behavior of super-heavy elements (Z ≥ 112) on metal and inert surfaces**

J. Anton[1], T. Jacob[1], V. Pershina[2]
[1]*Institut für Elektrochemie, Universität Ulm, Germany,* [2]*Gesellschaft für Schwerionenforschung, Germany*

23-ACP-01 **Structural studies of the Eu(III) and U(VI) interactions with pentapeptides**

A. Jeanson[1], J. Roques[1], S. Safi[1], E. Simoni[1], D. Aitken[2]
[1]*IPN Orsay UMR 8608 - Université Paris Sud, France,* [2]*ICMMO - Université Paris Sud, France*

23-ACP-02 **Solubility of amorphous UO_2 and NpO_2 in nitrate media containing platinum catalyst**

A. Kitamura[1], S. Shimoda[2]
[1]*Japan Atomic Energy Agency,* [2]*Mitsubishi Materials Corporation, Japan*

23-ACP-03 **Apparent formation constants of actinide complexes with humic substances determined by solvent extraction**

T. Sasaki[1], Y. M. Kulyako[2], K. Müller[3], T. Kobayashi[1], M. Samsonov[2], B. F. Myasoedov[2]
[1]*Department of Nuclear Engineering, Kyoto University, Japan,* [2]*V.I.Vernadsky Institute of Geochemistry and Analytical Chemistry, Russia,* [3]*Helmholtz-Zentrum Dresden-Rossendorf e.V., Institute of Resource Ecology, Germany*

23-ACP-04 **The solubility of Np(IV) under alkaline and anoxic conditions**

G. Källvenius[1], S. Allard[2], C. Ekberg[2]
[1]*AB SVAFO, SE-611 23 Nyköping, Sweden,* [2]*Chalmers University of Technology, Nuclear Chemistry, Sweden*

23-ACP-05 **Separation of Am and Cm by using TODGA and DOODA(C8) adsorbents with hydrophilic ligand-nitric acid solution**

S. Usuda[1], K. Yamanishi[1], H. Mimura[1], Y. Sasaki[2], A. Kirishima[3], N. Sato[3], Y. Niibori[1]
[1]*Department of Quantum Science and Energy Engineering, Graduate School of Engineering, Tohoku University,* [2]*Research Group for Aqueous Separation Chemistry, Japan Atomic Energy Agency,* [3]*Institute of Multidisciplinary Research for Advanced Materials, Tohoku University*

23-ACP-06 **Growth of uranyl hydroxide nanowires and nanotubes with electrodeposition method**

L. Wang, L.-Y. Yuan, Z.-F. Chai, W.-Q. Shi*
Key Laboratory of Nuclear Analysis Techniques, Institute of High Energy Physics, Chinese Academy of Sciences, China

23-ACP-07 **Adsorption behavior of neptunium ions on pyridine resin in hydrochloric acid solutions**

Y. Tachibana[1], Y. Tomobuchi[1], M. Inaki[1], Y. Yamazaki[1], T. Suzuki[1], T. Yamamura[2]
[1]*Department of Nuclear System Engineering, Nagaoka University of Technology,* [2]*Institute of Material Research, Tohoku University*

23-ACP-08 **A method for ^{237}Np determination with liquid scintillation counting in the experiment of neptunium sorption onto bentonite**

L. Ping, L. Zhi, G. Zhijun, W. Wangsuo*
Radiochemistry Laboratory, School of Nuclear Science and Technology, Lanzhou University, China

23-ACP-09 **Determination of stability constants for the thorium iminodiacetic acid complexes**

D. Rama Mohana Rao, R. M. Sawant, B. S. Tomar.
Radioanalytical Chemistry Division, Bhabha Atomic Research Centre, India

25-ACP-03 **Time-resolved laser fluorescence spectroscopy combined with parallel factor analysis: a robust speciation technique for UO_2^{2+}**
T. Saito[1], N. Aoyagi[2], T. Kimura[2]
[1]*Nuclear Professional School, School of Engineering, The University of Tokyo,* [2]*Nuclear Science and Engineering Directorate, Japan Atomic Energy Agency*

23-ENP-01 **Determination of ^{55}Fe and ^{89,90}Sr in liquid samples using Sr and/or Pb resins for the mutual separation of Fe and Sr**
M. Nodilo, I. Milanović, Ž. Grahek
Division for marine and environmental research, Rudjer Bošković Institute, Croatia

23-ENP-02 **Implementation of dry cow dung powder for biosorption of ^{90}Sr(II) from simulated radioactive waste**
R. P. Khilnani, H. K. Bagla
Department of Nuclear and Radiochemistry, K. C. College, India

23-ENP-03 **Application of simplified desorption method to sorption study: (1) sorption of americium (III) on bentonite and its major components**
N. Kozai[1], T. Ohnuki[1]
[1]*Japan Atomic Energy Agency, Japan*

23-ENP-04 **Effect of aging on availability of iodine in grassland soil collected in Rokkasho, Japan**
A. Takeda, H. Tsukada, Y. Takaku, S. Hisamatsu
Department of Radioecology, Institute for Environmental Sciences

23-ENP-05 **Study on ^{14}C spatial distribution around Qinshan nuclear power plant in China**
Z. Wang[1], D. Hu[2], Q. Guo[1]
[1]*State Key Laboratory of Nuclear Physics and Technology, Peking University, China,* [2]*Radiation Monitoring Technical Center of Ministry of Environmental Protection, China*

23-ENP-06 **Atmospheric deposition of radionuclides (^{7}Be,^{210}Pb,^{134}Cs, and ^{40}K) during 2000–2012 at Rokkasho, Japan, and impact of the Fukushima Dai-ichi Nuclear Power Plant accident**
N. Akata[1], H. Hasegawa[1], H. Kawabata[1], H. Kakiuchi[1], Y. Chikuchi[2], N. Shima[3], T. Suzuki[4], S. Hisamatsu[1]
[1]*Institute for Environmental Sciences, Japan,* [2]*Aomori JGC PLANTECH, Japan,* [3]*Fukushima University, Japan,* [4]*Yamagata University, Japan*

23-ENP-07 **Effect of aging on water extractability of radioactive iodine and cesium from soil**
H. Tsukada, A. Takeda, S. Hisamatsu
Department of Radioecology, Institute for Environmental Sciences, Japan

23-ENP-08 **Background internal dose rates of earthworm and arthropod species in the forests of Aomori, Japan**
Y. Ohtsuka, Y. Takaku, S. Hisamatsu
Department of Radioecology, Institute for Environmental Sciences, Japan

23-ENP-09 **An EXAFS study on the effect of natural organic matter and mineralogy composition on cesium mobility in environment**
Q. Fan, M. Tanaka, Y. Takahashi
Department of Earth and Planetary Systems Science, Graduate School of Science, Hiroshima University

23-ENP-10 **Using factorial design to the robustness analysis of the classic sample preparation method for ^{90}Sr determination in tea leaf**
C.-C. Liu[1*], W.-H. Tsai[1], M.-C. Horng[1], C.-C. Huang[1], Y.-W. Wu[2]
[1]*Radiation Monitoring Center, AEC, Taiwan, ROC,* [2]*Department of Chemical Engineering, I-Shou University, Taiwan, ROC*

23-ENP-11 **A simple method for dehydrogenase assay of soil microorganisms to evaluate the biospheric behavior of C-14 originated in transuranic waste**
K. Iwata, N. Ishii, K. Tagami, S. Uchida
Office of Biospheric Assessment for Waste Disposal, National Institute of Radiological Sciences

23-ENP-12 **Effect of humic acid on the sorption of selenium (VI) on ferric oxide hydrate**
N. Guo, Z. L. Niu, Y. L. Ye, R. Zhang, Z. J. Guo
School of nuclear science and technology, Lanzhou University, China

23-ENP-13 **Uranyl ions adsorption to Na-GMZ and interactions with FA adsorption: experiments and modeling**
Y. Yuanlv, G. Zhijun*, W. Wangsuo
Radiochemistry Laboratory, School of Nuclear Science and Technology, Lanzhou University, China

23-ENP-14 **Foliar uptake and translocation of stable cesium and iodine by radish**
H. Hasegawa[1], H. Tsukada[1], H. Kawabata[1], Y. Takaku[1], S. Hisamatsu[1]
[1]*Institute for Environmental Sciences, Japan*

23-ENP-15 **The rapid determination of radiostrontium from large amount of seawater (within 72hrs) for the emergency situation**
H. Kim[1*], K.-H. Chung[1], H.-K. Park[1], J.-M. Lim[1], M.-J. Kang[1]
[1]*Environmental Radioactivity Assessment Team, Korea Atomic Energy Research Institute, Korea*

23-ENP-16 **Peak tailing correction in measurement of $^{222}Rn/^{220}Rn$ activity concentration with α spectrum method**
L. Zhang[1], Q. Guo[2], R. Ma[2], L. Guo[2]
[1]*Solid Dosimetric Detector and Method Laboratory, China,* [2]*State Key Laboratory of Nuclear Physics and Technology, School of Physics, Peking University, China*

23-ENP-17 **Underwater analysis of sediment chemistry using an autonomous platform**
J. Breen[1], P. de Souza[1,2,3], G. Timms[3], R. Ollington[1]
[1]*School of Computing and Information Systems, University of Tasmania, Australia,* [2]*Vale Institute of Technology, Brazil,* [3]*Intelligent Sensing and Systems Laboratory, ICT Centre, CSIRO, Australia*

23-RPP-01 **Development of the in-line multiple elution cartridge-based radioisotope concentrator device for increasing ^{99m}Tc and ^{188}Re concentration of commercial radionuclide generator eluates**
Van S. Le [1,2*]; N. Morcos,[1] J. McBrayer[1], Z. Bogulski[1], C. Buttigieg[1], G. Phillips[1]
[1]*CYCLOPHARM Ltd, Australia,* [2]*MEDISOTEC, Australia*

23-RPP-02 **Production and preclinical evaluation of diagnostic and therapeutic radionuclides in tumor-bearing mice: recent developments at Paul Scherrer Institute**
A. Türler[1,2], M. Behe[3], M. Bunka[1,2], H. Dorrer[1,2], A. Hohn[3], K. Johnston[4], U. Köster[5], C. Müller[3], J. Reber[3], R. Schibli[3], N.T. van der Walt[6], K. Zhernosekov[1,2]
[1]*Laboratory of Radiochemistry and Environmental Chemistry, Paul Scherrer Institute, Switzerland,* [2]*Laboratory of Radiochemistry and Environmental Chemistry, University of Bern, Switzerland,* [3]*Center for Radiopharmaceutical Sciences ETH-PSI-USZ, Paul Scherrer Institute, Switzerland,* [4]*Physics Department, ISOLDE/CERN, Switzerland,* [5]*Institut Laue-Langevin, France,* [6]*Faculty of Applied Sciences, Cape Peninsula University of Technology, South Africa*

23-RPP-03 **^{99}Mo production by $^{100}Mo(n,2n)^{99}Mo$ using accelerator neutrons**
N. Sato[1], M. Kawabata[1], Y. Nagai[1], K. Hashimoto[1], Y. Hatsukawa[1], H. Saeki[1], S. Motoishi[1], T. Kin[2], C. Konno[3], K. Ochiai[3], K. Takakura[3], F. Minato[4], O. Iwamoto[4], N. Iwamoto[4], S. Hashimoto[4]
[1]*Nuclear Engineering Research Collaboration Center, Japan Atomic Energy Agency,* [2]*Faculty of Engineering Sciences, Kyushu University,* [3]*Fusion Research and Development Directorate, Japan Atomic Energy Agency,* [4]*Nuclear Science and Engineering Directorate, Japan Atomic Energy Agency*

23-RPP-04 **Production and separation of ^{64}Cu and ^{67}Cu using 14 MeV neutrons**
M. Kawabata[1], K. Hashimoto[1], H. Saeki[1], N. Sato[1], S. Motoishi[1], K. Takakura[2], C. Konno[2] and Y. Nagai[1]
[1]*Nuclear Engineering Research Collaboration Centre, Japan,* [2]*Fusion Research and Development Directorate, Japan Atomic Energy Agency*

23-RPP-05 **Novel radiochemical separation of arsenic from selenium for $^{72}Se/^{72}As$ generator.**
E. Chajduk[1], H. Polkowska-Motrenko[1], A.Bilewicz[1]
[1]*Institute of Nuclear Chemistry and Technology, Poland*

23-RPP-06 **Training program of synthesizing a radiopharmaceutical in KAERI**
S. Yang[1], Y. H. Chung[2]
[1]*Advanced Radiation Technology Institute, Korea Atomic Research Institute, Korea,* [2]*Department of*

Chemistry, Hallym University, Korea

23-RPP-07 **Synthesis of ^{64}Cu-labeled MARSGL peptide as an imaging probe for HER2/neu overexpressing tumors**
Y. Sugo, I. Sasaki, S. Watanabe, Y. Ohshima, N. S. Ishioka
Quantum Beam Science Directorate, Japan Atomic Energy Agency

23-RPP-08 **Molybdenum isotope fractionation in ion exchange reaction by using anion exchange chromatography**
M. Inaki[1], Y. Tachibana[1], M. Nomura[2] T. Suzuki[1]
[1]*Department of Nuclear System Safety Engineering, Nagaoka University of Technology,* [2]*Reserch Laboratory for Nuclear Reactors, Tokyo Institute of Technology*

23-APP-01 **The mechanism of oxidized multi-walled carbon nanotubes across placental barrier and its effects on pregnany**
Q. Wei[1], B. Juanjuan[1], W. Jing[1], L.Zhan[2], L. Peng[1], W. Wangsuo[1*]
[1]*Radiochemical Laboratory, Lanzhou University, China,* [2]*Institute of Modern Physics, Chinese Academy of Sciences, Lanzhou, China*

23-APP-02 **Prompt gamma test of a large volume lanthanum bromide detector**
A. A. Naqvi*[1], M. A. Gondal[1], M. Raashid[1], Khateeb-ur-Rehman[1], M. Dastegeer[1]
[1]*Department of Physics, King Fahd University of Petroleum and Minerals, Saudi Arabia*

23-APP-03 **Radiation-induced reactions in D, L-α-alanine adsorbed in solid surfaces**
E. Aguilar, A. Negrón-Mendoza, C. Camargo
Instituto de Ciencias Nucleares, Universidad Nacional Autonoma de Mexico, Mexico

23-APP-04 **^{36}Cl determination in steel radioactive waste**
F. Goutelard[1], P. Perret[1], C. Hamon[1], R. Brennetot[1], C. Andrieu[2]
[1]*Operator Support Analyses Laboratory, Atomic Energy Commission, CEA Saclay, DEN/DANS/DPC/SEARS/LASE, France,* [2]*Electricité de France, EDF – CIDEN / Département Etudes - Division Déconstruction/Groupe Inventaire et Agréments, France*

23-APP-05 **Naturally occurring radioactive materials (NORM) in malaysian oil sludge samples**
B.A. Teiara Mohamed[1], S. B. Sarmani[2]
[1]*Department of Physics, University of Al-Zaituna, Tarhruna, Libya,* [2]*School of Chemical Sciences and Food Technology, Faculty of Science and Technology, Universiti Kebangsaan, Malaysia*

23-APP-06 **On the use of ^{233}U and ^{237}Np as radiotracers for redox potential measurements**
S. Holgersson
Chalmers University of Technology, Department of Chemical and Biological Engineering, Nuclear Chemistry, Sweden

23-APP-07 **Analysis of ^{129}I/^{127}I ratios from underground fluids collected in Japan**
N. Okabe[1], Y. Muramatsu[1], M. Arai[1], H. Matsuzaki[2], M. Takahashi[3], K. Kazahaya[3]
[1]*Gakushuin University, Japan,* [2]*University of Tokyo,* [3]*AIST, Japan*

23-APP-08 **Radiocarbon dating of ancient Japanese calligraphy sheets: checks with ancient documents of known age and its application to kohitsugire calligraphies**
H. Oda[1], K. Ikeda[2], H.i Yasu[3], S. Sakamoto[4]
[1]*Center for Chronological Research, Nagoya University,* [2]*Faculty of Letters, Chuo University,* [3]*Taga High School,* [4]*Degital Archives Research Center, Ryukoku University*

23-APP-09 **μ-XRF study on Wiangkalong pottery**
K. Won-in[1], S. Tancharakorn[2], W. Tanthanuch[2], P. Dararutana[3]
[1]*Department of Earth Sciences, Faculty of Science, Kasetsart University, Thailand,* [2]*Synchrotron Light Research Institute, Thailand,* [3]*The Royal Thai Army Chemical School of the Royal Thai Army Chemical Department, Thailand*

Tuesday, 24 September 2013, Poster Session

24-FKP-01 **Determination of short-lived ^{241}Pu in environmental samples by inductively coupled plasma mass spectrometry**
Jian Zheng*, Keiko Tagami, Shigeo Uchida
Office of Biospheric Assessment for Waste Disposal, National Institute of Radiological Sciences

24-FKP-02 **Numerical evaluation of Cs adsorption in PB column by extended Langmuir formula and one-dimensional adsorption model**
Hiroshi Ogawa, Akiko Kitajima, Hisashi Tanaka, and Tohru Kawamoto
Nanosystem Research Institute, Advanced Industrial Science and Technology (AIST), Tsukuba, 305-8568, Japan

24-FKP-03 **Secular distribution of radioactive concentration in the atmosphere at Fukushima, Hitachi and Marumori**
ZiJian Zhang[1], Shunsuke Kakitani[1], Kazuhiko Ninomiya[1], Naruto Takahashi[1], Yoshiaki Yamaguchi[2], Takashi Yoshimura[2], Kazuyuki Kita[3], Akira Watanabe[4], Atsushi Shinohara[1]
[1]*Graduate School of Science, Osaka University*, [2]*Radioisotope Research Center, Osaka University*, [3]*Faculty of Symbiotic Systems Science, Fukushima University*, [4]*College of Science, Ibaraki University*

24-FKP-04 **Concentration of ^{137}Cs in atmospheric coarse and fine particles collected in Fukushima**
Kyo Kitayama[1], Hirofumi Tsukada[1], Kenji Ohse[1], Chika Suzuki[1], Akira Kanno[1], Kencho Kawatsu[1],
[1]*Fukushima University Future Center for Regional Revitalization*

24-FKP-05 **Electrochemical cesium sorption under coexisting other ions using nanoparticle film of copper hexacyanoferrate**
Hisashi Tanaka[1], Rongzhi Chen[1], Miyuki Asai[1], Chikako Fukushima[1], Tohru Kawamoto[1], Manabu Ishizaki[2], Masato Kurihara[1,2], Makoto Arisaka[3], Takuya Nankawa[3] and Masayuki Watanabe[3]
[1]*Nanosystem Research Institute, AIST, Japan*, [2]*Department of Material and Biological Chemistry, Yamagata University, Japan*, [3]*Japan Atomic Energy Agency, Japan*

24-FKP-06 **Determination of ^{129}I in Fukushima soil samples by ICP-MS**
Takeshi Ohno[1], Yasuyuki Muramatsu[1], Hiroyuki Matsuzaki[2]
[1]*Faculty of Science, Gakushuin University*, [2]*School of Engineering, The University of Tokyo*

24-FKP-07 **Measurement of soil-to-crop transfer factor of tellurium for estimation of potential radiotellurium ingestion from crops**
Guosheng Yang, Keiko Tagami*, Jian Zheng, Shigeo Uchida
Office of Biospheric Assessment for Waste Disposal, National Institute of Radiological Sciences

24-FKP-08 **Retention of radiocesium incorporated in tree leaves contaminated by fallout of the radionuclides emitted from the Fukushima Daiichi Nuclear Power Plant**
Kazuya Tanaka[1], Hokuto Iwatani[2], Aya Sakaguchi[2], Yoshio Takahashi[2], Yuichi Onda[3]
[1]*Institute for Sustainable Sciences and Development, Hiroshima University, Japan*, [2]*Department of Earth and Planetary Systems Science, Hiroshima University, Japan*, [3]*Graduate School of Life and Environmental Sciences, University of Tsukuba, Japan*

24-FKP-09 **Decontamination of radioactive cesium in the soil**
Makoto Yanaga, Ayumi Oishi
Department of Chemistry, Graduate School of Science, Shizuoka University, Japan

24-FKP-10 **Altitude distribution of radioactive cesium at Mt. Fuji due to Fukushima No.1 nuclear power plant accident**
T. Saito[1], Y. Kurihara[2], Y. Koike[2], I. Tanihata[3], M. Fujiwara[3], H. Sakaguchi[3], A. Shinohara[4], H. Yamamoto[5]
[1]*Faculty of Comprehensive Human Sciences, Shokei Gakuin University*, [2]*School of Science and Technology, Meiji University*
[3]*Research Center for Nuclear Physics, Osaka University*, [4]*Graduate School of Science, Osaka University*, [5]*Department for the Administration of Safety and Hygiene, Osaka University*

24-FKP-11 **Isotope compositions of strontium in environmental samples in Fukushima Prefecture**
Y. Shibahara[1], S. Fukutani[1], T. Fujii[1], T. Kubota[1], M. Yoshikawa[2], T. Shibata[2], T. Ohta[3], K. Takamiya[1], N. Sato[1], M. Tanigaki[1], Y. Kobayashi[1], R. Okumura[1], H. Yoshinaga[1], H. Yoshino[1], A. Uehara[1], S. Mizuno[4], T.

Takahashi[1], and H. Yamana[1]
[1]*Research Reactor Institute, Kyoto University*, [2]*Institute for Geothermal Sciences, Kyoto University*, [3]*Faculty of Engineering, Hokkaido University*, [4]*Nuclear Power Safety Division, Fukushima Prefectural Government*

24-FKP-12 **Distribution of radioactive caesium in the North Pacific one year and a half after the Fukushima Dai-ichi Nuclear Power Plant accident**
K. Tsujita[1], A. Hasegawa[1], N. Harada[2], T. Yamagata[2], H. Nagai[2], M. Aoyama[3]
[1]*Graduate School of integrated Basic Sciences, Nihon University*, [2]*College of Humanities and Sciences, Nihon University*, [3]*Geochemical Research Department, Meteorological Research Institute, Japan*

24-FKP-13 **Image analysis for the study of radiocesium distribution in coniferous trees: two years after the Fukushima Daiichi Nuclear Power Plant accident**
Haruka Minowa
Radioisotope Research Facility, The Tokyo Jikei University School of Medicine, Japan

24-FKP-14 **Distribution of Iodine-129 in off Fukushima and the North Pacific one year and a half after the Fukushima Dai-ichi Nuclear Power Plant accident**
A. Hasegawa[1], T. Yamagata[2], H. Nagai[2], M. Aoyama[3], H. Matsuzaki[4]
[1]*Graduate School of integrated Basic Sciences, Nihon University*, [2]*College of Humanities and Sciences, Nihon University,* [3]*Geochemical Research Department, Meteorological Research Institute*, [4]*School of Engineering, The University of Tokyo*

24-FKP-15 **Agricultural implications for Fukushima nuclear accident**
Tomoko M. Nakanishi
Graduate School of Agricultural and Life Sciences, The University of Tokyo

24-FKP-16 **Concentration of radiocesium in rice, vegetables, and fruits cultivated in evacuation area at Okuma town, Fukushima**
Kenji Ohse[1], Kyo Kitayama[1], Seiich Suenaga[2], Kiyoyuki Matsumoto[2], Akira Kanno[1], Chika Suzuki[1], Kencho Kawatsu[1], Hirofumi Tsukada[1]
[1]*Fukushima Future Center for Regional Revitalization, Fukushima University*, [2]*Okuma Government Office, Japan*

24-FKP-17 **Isotopic U, Pu, Am and Cm signatures in environmental samples from the Fukusima Dai-ichi Nuclear Power Plant accident**
Masayoshi Yamamoto[1], Aya Sakaguchi[2], Shinya Ochiai[1],Takahiro Takada[1], Seiya Nagao[1], Peter Steier[3]
[1]*Low Level Radioactivity Laboratory, Kanazawa University, Japan*, [2]*Graduate School of Science, Hiroshima University, Japan*, [3]*VERA-Laboratory, University of Vienna, Austria*

24-FKP-18 **Influence of the Fukushima Daiichi nuclear disaster on the tritium concentration in the precipitation of Kanazawa city**
Yoshimune Yamada[1], Kaeko Yasuike[1], Toshiyuki Kawabata[2], Akihiro Fujii[2], Hitoshi Kakimoto[2]
[1]*Faculty of Pharmaceutical Sciences, Hokuriku University, Japan*, [2]*Ishikawa Prefectural Institute of Public Health and Environmental Science, Japan*

24-FKP-19 **Sediment transport processes in reservoir-catchment system inferred from sediment trap observation and fallout radionuclides**
Shinya Ochiai[1], Seiya Nagao[1], Masayoshi Yamamoto[1], Taeko Itono[2], Kenji Kashiwaya[3]
[1]*Low Level Radioactivity Laboratory, Institute of Nature and Environmental Technology, Kanazawa University, Japan*, [2]*Graduate School of Natural Science & Technology, Kanazawa University, Japan*, [3]*Institute of Nature and Environmental Technology, Kanazawa University, Japan*

24-FKP-20 **Transfer of radiocesium to crops cultivated in Fukushima**
Shinji Sugihara[1], Toshio Hara[2], Akihiro Maekawa[3], Noriyuki Momoshima[1]
[1]*Radioisotope Center, Kyushu University, Japan*, [2]*Molecular Engineering Institute, Kinki University, Japan*, [3]*Graduate School of Sciences, Kyushu University, Japan*

24-FKP-21 **Dynamics of radiocesium in bamboo forests after the accident of Fukushima Daiichi nuclear power plant**
Tsutomu Kanasashi, Mitsutoshi Umemura, Yuki Sugiura , Chisato Takenaka
Graduate School of Bioagricultural Sciences, Nagoya University, Japan

24-FKP-22 **Reaction behavior of uranium and zirconium oxides in oxidative and reductive conditions**
Nobuaki Sato, Kohei Fukuda and Akira Kirishima
Institute of Multidisciplinary Research for Advanced Materials, Tohoku University, Japan

24-FKP-23 **Radiocesium in zooplankton in seawaters off Miyagi, Fukushima, and Ibaraki Prefectures**
H. Takata[1], M. Kusakabe[2], S. Oikawa[1]
[1]*Central Laboratory, Marine Ecology Research Institute*, [2]*Head Office, Marine Ecology Research Institute*

24-FKP-24 **Plutonium isotopes and ^{241}Am in surface sediments off the coast of the Japanese islands after the Fukushima accident**
S. Oikawa[1], T. Watabe[2], H. Takata[1], J. Misonoo[2], M. Kusakabe[2]
[1]*Central Laboratory, Marine Ecology Research Institute*, [2]*Head Office, Marine Ecology Research Institute*

24-NEP-01 **A theoretical study of actinide and lanthanide extraction with carbamoylmethylphosphine oxide ligands**
Cong-Zhi Wang , Jian-Hui Lan , Yu-Liang Zhao , Zhi-Fang Chai , Wei-Qun Shi*
Nuclear Energy Nano-Chemistry Group, Key Laboratory of Nuclear Analytical Techniques and Key Laboratory For Biomedical Effects of Nanomaterials and Nanosafety, Institute of High Energy Physics, Chinese Academy of Sciences, China

24-NEP-02 **The role of microorganisms during the wet nuclear fuel storage in Slovak Republic**
Martin Pipíška[1], Lenka Tišáková[2], Miroslav Horník[1], Jozef Augustín[1]
[1]*Department of Ecochemistry and Radioecology, University of SS Cyril and Methodius, Slovak Republic*, [2]*Institute of Molecular Biology, Slovak Academy of Sciences, Slovak Republic*

24-NEP-03 **Single centrifugal contactor test of a proposed group actinide extraction process for partitioning and transmutation purposes**
Emma Aneheim[1,2], Christian Ekberg[1], Giuseppe Modolo[3], Andreas Wilden[3]
[1]*Nuclear Chemistry, Department of Chemical- and Biological Engineering, Chalmers University of Technology, Sweden*, [2]*Targeted Alpha Therapy group, Department of Radiation Physics, Sahlgrenska Academy at Gothenburg University, Sweden*, [3]*Forschungszentrum Jülich GmbH (FZJ), Institut für Energie- und Klimaforschung, Nukleare Entsorgung und Reaktorsicherheit (IEK-6), Germany*

24-NEP-04 **Application of flow analytical methods for determination of radionuclides in cooling water and wastes from nuclear plants**
Anna Bojanowska-Czajka[1], Kamila Kołacińska[1], Marek Trojanowicz[1]
[1]*Institut of Nuclear Chemistry and Technology, Poland*

24-NEP-05 **Determination of low level ^{99}Tc in the primary coolant water by ICP-MS. Analysis of potential interferences**
Ewelina Chajduk[1], Sylwia Witman-Zając[1], Halina Polkowska-Motrenko[1]
[1]*Institute of Nuclear Chemistry and Technology, Poland*

24-NCP-01 **Extraction of homologous elements of dubnium and seaborgium from HCl solution**
T. Yokokita[1], K. Nakamura[1], A. Kino[1], Y. Komori[1], K. Toyomura[1], Y. Kasamatsu[1], N. Takahashi[1], T. Yoshimura[2], K. Ooe[3], Y. Kudou[4], K. Takamiya[5], A. Shinohara[1]
[1]*Graduate School of Science, Osaka University*, [2]*Radioisotope Research Center, Osaka University*, [3]*Faculty of Science, Niigata University*, [4]*Nishina Center for Accelerator Based Science, RIKEN*, [5]*Research Reactor Institute, Kyoto University*

24-NCP-02 **Evaluation of stopping powers of superheavy ions in Al and U**
Y. H. Chung
Department of Chemistry, Hallym University, Korea

24-NCP-03 **Separation of tungsten from LEU fission-produced ^{99}Mo solution to improve technological performance in both the processes of ^{99}Mo and ^{99m}Tc generator production**
Van So Le[1] , Cong Duc Nguyen[2]
[1]*Medisotec, NSW, Australia*, [2]*ChoRay Hospital, HCM, Vietnam*

24-NCP-04 **Effecting separation of fission products from the actinides by direct reaction with diketones**
Daniel B. Rego, Paul M. Forster, Kenneth R. Czerwinski
University of Nevada, Las Vegas, USA

24-NCP-05 **Muonic atom formation by muon transfer process in C_6H_6 / C_6H_{12} + CCl_4 mixtures**

M. Inagaki[1], K. Fujihara[1], G. Yoshida[1], K. Ninomiya[1], Y. Kasamatsu[1], A. Shinohara[1], M. K. Kubo[2], W. Higemoto[3], Y. Miyake[4], T. Miura[5]
[1]*Graduate School of Science, Osaka University*, [2]*Colleage of Liberal Arts, International Christian University*, [3]*Advanced Science Research Center, Japan Atomic Energy Agency*, [4]*Institute of Materials Structure Science, High Energy Accelerator Research Organization (KEK)*, [5]*Radiation Science Center, High Energy Accelerator Research Organization (KEK)*

24-NCP-06 **Research for fusion reaction mechanisms with deformed nuclei**

S. Ueno[1], K. Toda[1], A. Asano[1], N. Takahashi[2], Y. Kasamatsu[2], T. Yokokita[2], A. Yokoyama[3],
[1]*Graduate School of Natural Science and Technology, Kanazawa Univ.*, [2]*Graduate School of Science, Osaka Univ.*
[3]*Institute of Science and Engineering, Kanazawa Univ.*

24-NCP-07 **Extraction behavior of Nb and Ta in HF solutions with tributyl phosphate**

M. Murakami[1,2], S. Tsuto[1], K. Ooe[1], H. Haba[2], J. Kanaya[2], S. Goto[1], and H. Kudo[1]
[1]*Department of Chemistry, Faculty of Science, Niigata University, Japan*, [2]*Nishina Center for Accelerator-Based Science, RIKEN, Japan*

24-NCP-08 **A modified method for synthesis of [γ-32P] labeled adenosine triphosphate**

Wira Y Rahman[1]*, Endang Sarmini[1], Herlina[1], Triyanto[1], Rien Ritawidya[1], Abdul Mutalib[1] and Santi Nurbaiti[2]
[1]*Center for Radioisotope and Radiopharmaceuticals (PRR) - BATAN*, [2]*Biochemistry Research Division, faculty of Mathematics and Natural Sciences, Institut Teknologi Bandung, Indonesia*

24-NCP-09 **Production of ^{88}Nb and ^{170}Ta for chemical studies of element 105 Db using the GARIS gas-jet system**

M. Huang,[1] M. Asai,[2] H. Haba,[1] D. Kaji,[1] J. Kanaya,[1] Y. Kasamatsu,[3] H. Kikunaga,[4] Y. Kikutani,[3] Y. Komori,[3] H. Kudo,[5] Y. Kudou,[1] K. Morimoto,[1] K. Morita,[1] M. Murakami,[5] K. Nakamura,[3] K. Ozeki,[1] R. Sakai,[1] A. Shinohara,[3] T. Sumita,[1] K. Tanaka,[1] A. Toyoshima,[2] K. Tsukada,[2] Y. Wakabayashi[1] and A. Yoneda[2]
[1]*Nishina Center for Accelerator-Based Science, RIKEN*, [2]*Advanced Science Research Center, JAEA*, [3]*Graduate School of Science, Osaka University*, [4]*Research Center for Electron Photon Science, Tohoku University*, [5]*Department of Chemistry, Niigata University*

24-NCP-10 **Half-life measurement of ^{7}Be in several materials**

T. Ohtsuki
Research Center for Electron Photon Science, Tohoku University, Japan

24-ENP-01 **Verification of anticlockwise gyre in the semi-closed water area of Lake Nakaumi, southwest Japan, by using ^{224}Ra/^{228}Ra activity ratios**

Ritsuo Nomura[1],* Mutsuo Inoue[2], Hisaki Kofuji[3] and Shota Ikeda[1]
[1]*Foraminiferal Laboratory, Faculty of Education, Shimane University, Japan*, [2]*Institute of Nature and Environmental Technology, Kanazawa University, Japan*, [3]*Mutsu Marine Laboratory, Japan Marine Science Foundation*

24-ENP-02 **Effect of hydroxylated fullerene on U(VI) adsorption onto oxidized multi-walled carbon nanotubes**

Jing Wang[1], Zhan Li[2], Peng Liu[1], Wei Qi[1], Juanjuan Bi[1], Wangsuo Wu[1]*
[1]*Radiochemistry Laboratory, School of Nuclear Science and Technology, Lanzhou University, China*, [2]*Institute of Modern Physics, Chinese Academy of Sciences, China*

24-ENP-03 **Corrosion of copper in water and colloid formation under intense radiation field**

Kotaro Bessho[1], Yuichi Oki[2], Naoya Akimune[3], Hiroshi Matsumura[1], Kazuyoshi Masumoto[1], Shun Sekimoto[2], Naoyuki Osada[4], Norikazu Kinoshita[5], Hideaki Monjushiro[1], Seiichi Shibata[2]
[1]*Radiation Science Center, High Energy Accelerator Research Organization (KEK)*, [2]*Research Reactor Institute, Kyoto University (KURRI)*, [3]*Graduate School of Engineering, Kyoto University*, [4]*Graduate School of Engineering, Tohoku University*, [5]*Institute of Technology, Shimizu Corporation, Japan*

24-ENP-04 **Study on unattached fraction of radon progeny and its environmental influence factors**

Lu Guo[1], Lei Zhang[2], Qiuju Guo[1]
[1]*State Key Laboratory of Nuclear Physics and Technology, Peking University, China*, [2]*Solid Dosimetric Detector and Method Laboratory, China*

24-ENP-05 **Preliminary study on measuring radon progeny concentration using alpha/beta spectroscopic method**

Abdumomin Kadir[1], Lei Zhang[2], Qiuju Guo[1], and Juncheng Liang[3]
[1]*State Key Laboratory of Nuclear Physics and Technology, School of Physics, Peking University, China*, [2]*Solid Dosimetric Detector and Method Laboratory, China*, [3]*Ionizing Radiation and Medical Science, National Institute of Metrology, China*

24-ENP-06 **The measurement comparability of ^{134}Cs and ^{137}Cs in foodstuff samples in Japan - result of inter-laboratory experiment for certification of certified reference material**

Tsutomu Miura[1], Yoshitaka Minai[2], Shoji Hirai[3], Hiroshi Iwamoto[4], Chushiro Yonezawa[5], Yoshinobu Uematsu[6], Akira Okada[7], Masami Shibukawa[8], Koichi Chiba[1], Kiyoshi Kitamura[9], Takahiro Yamada[10], Kazutoshi Kakita[11], Isao Kojima[11], [1]*National Metrology Institute of Japan, AIST*, [2]*Musashi University*, [3]*Tokyo City University*, [4]*Environmental Technology Service Co, Ltd.*, [5]*Japan Institute of International Affairs*, [6]*Japan Accreditation Board*, [7]*TERM*, [8]*Saitama University*, [9]*Japan Chemical Analysis Center*, [10]*Japan Radioisotope Association*, [11]*The Japan Society for Analytical Chemistry*

24-ENP-07 **Synthesis and Characterization of Volatile Technetium Compound**

Bradley C. Childs[1], Frederic Poineau[2], Ken R. Czerwinski[2]
[1]*University of Nevada Las Vegas, Las Vegas, Nevada 89154, USA*

24-ENP-08 **Time variation of concentrations of radioactive cesium-134, 137 and iodine-129 in the Ohori River, Chiba Prefecture, Japan**

Nao Shibayama[1], Keisuke Sueki[2], Kimikazu Sasa[2,3], Yukihiko Satou[1], Tsutomu Takahashi[3], Masumi Matsumura[3], Hiroyuki Matsuzaki[4], Michio Murakami[5], Rey Yamashita[6], Mahua Saha[6], Hideshige Takada[6], Yukio Koibuchi[7], Soulichan Lamxay[7], Taikan Oki[8]
[1]*Graduate School of Pure and Applied Sciences, Univ. of Tsukuba*, [2]*Faculty of Pure and Applied Sciences, Univ. of Tsukuba,* [3]*Research Facility Center for Science and Technology, Univ. of Tsukuba*, [4]*MALT, The Univ. of Tokyo*, [5]*"Wisdom of Water"(Suntory), The Univ. of Tokyo*, [6]*Tokyo Univ. of Agri. & Tech.*, [7]*Graduate School of Frontier Sciences, The Univ. of Tokyo,* [8]*Insitute of Industrial Science, The Univ. of Tokyo*

24-ENP-09 **Ra isotopes in Na-Cl type groundwater in Japan**

Junpei Tomita[1,a], Takahiro Takada[1], Seiya Nagao[1], Masayoshi Yamamoto[1]
[1]*Low Level Radioactivity Laboratory, Institute of Nature and Environmental Technology, Kanazawa University, Japan*, [a]*Department of Radiation Protection, Nuclear Science Research Institute, Japan Atomic Energy Agency, Japan*

24-ENP-10 **A new method to estimate $^{210}Po/^{210}Pb$ activity ratio in atmospheric aerosol by alpha spectrometry**

N. Momoshima[1], S. Nishio[2], K. Hibino[2], S. Sugihara[1]
[1]*Radioisotope Center, Kyushu University, Japan*, [2]*Graduate School of Science and Technology, Kumamoto University, Japan*

24-ENP-11 **Sedimentary environment inferred from sedimentation rates by ^{210}Pb and ^{137}Cs and their inventories in Mutsu Bay, Japan**

Kazuhito Hamataka[1], Seiya Nagao[1], Michio Kato[2], Isao Kudo[3], Masayoshi Yamamoto[1]
[1]*Low Level Radioactivity Laboratory, KINET, Kanazawa University, Japan*, [2]*Graduate School of Science, Kanazawa University, Japan*, [3]*Graduate School of Fisheries Sciences, Hokkaido University, Japan*

24-ENP-12 **Distribution of radiocarbon in Japanese agricultural soils**

Nobuyoshi Ishii, Keiko Tagami, Shigeo Uchida
Office of Biospheric Assessment for Waste Disposal, National Institute of Radiological Sciences

24-ENP-13 **Lateral distributions of $^{228}Th/^{228}Ra$ and $^{228}Ra/^{226}Ra$ ratios in surface waters of the Sea of Japan and their physical implications**

Y. Furusawa[1], M. Inoue[1], S. Nagao[1], M. Yamamoto[1], Y. Hamajima[1], H. Kofuji[1], K. Yoshida[1], Y. Nakano[1], K. Fujimoto[2], A. Morimoto[3], T. Takikawa[4], Y. Isoda[5]
[1]*Low Level Radioactivity Laboratory, Kanazawa University*, [2]*Fisheries Research Agency, National Research Institute of Fisheries Science*, [3]*Hydrospheric Atmospheric Research Center, Nagoya University*, [4]*National Fisheries University*, [5]*Graduate School of Fisheries Sciences, Hokkaido University*

24-ENP-14 **Vertical profiles of ^{228}Ra and ^{226}Ra activities in the Sea of Japan and their implications for water circulation**

M. Inoue[1], M. Minakawa[2,*], K. Yoshida[1], Y. Nakano[1], H. Kofuji[1], S. Nagao[1], M. Yamamoto[1], Y. Hamajima[1]
[1]*Low Level Radioactivity Laboratory, Kanazawa University*, [2]*Fisheries Research Agency, National Research*

Institute of Fisheries Science

24-ENP-15 **Induced radioactivity in air and water at medical accelerators**
K. Masumoto[1], K. Takahashi[1], H. Nakamura[1], A. Toyoda[1], K. Iijima[1], K. Kosako[2], K. Oishi[2], F. Nobuhara[3]
[1]*High Energy Accelerator Research Organization (KEK)*, [2]*Shimizu Co., Japan*, [3]*Tokyo Nuclear Service Co., Japan*

24-ENP-16 **Radioactivity determination of ^{14}C and ^{3}H in solid waste samples by liquid scintillation counter**
Jong-Myoung Lim[1*], Mun-Ja Kang[1], Kun-Ho Chung[1], Chang-Jong Kim[1], Geun-Sik Choi[1]
[1]*Environmental Radioactivity Assessment Team, Korea Atomic Energy Research Institute, Korea*

24-ENP-17 **Preparation of pure TiO_2 sorption material**
Irena Špendlíková, Jakub Raindl, Mojmír Němec
Czech Technical University in Prague, Department of Nuclear Chemistry, Czech Republic

24-NPP-01 **Mössbauer study of iron carbide nanoparticles produced by sonochemical synthesis**
R. Miyatani[1], Y. Yamada[1], Y. Kobayashi[2,3]
[1]*Department of Chemistry, Tokyo University of Science*, [2]*Department of Engineering Science, The University of Electro-Communications*, [3]*RIKEN*

24-NPP-02 **Mössbauer study of iron fluoride films produced by pulsed laser deposition**
K. Shiga[1], Y. Yamada[1], Y. Kobayashi[2,3]
[1]*Department of Chemistry, Tokyo University of Science*, [2]*Department of Engineering Science, The University of Electro-Communications*, [3]*RIKEN*

24-NPP-03 **Iron sulfide particles synthesized in liquid phase**
R. Shimizu[1], Y. Yamada[1], Y. Kobayashi[2,3]
[1]*Department of Chemistry, Tokyo University of Science*, [2]*Department of Engineering Science, The University of Electro-Communications*, [3]*RIKEN, Japan*

24-NPP-04 **Mössbauer and XRD studies of NiCuZn ferrites by Sol-Gel auto-combustion**
Chenglong Lei[1], Qing Lin[1,2]*, Haifu Huang[3], Hui Zhang[1], Yun He[1]
[1]*College of Physics and Technology, Guangxi Normal University, China*, [2]*Department of Information Technology, Hainan Medical College, China*, [3]*Nanjing National Laboratory of Microstructures and Jiangsu Provincial Laboratory for NanoTechnology,,Department of Physics, Nanjing University, China*

24-NPP-05 **Thermal stability of locally-associated Al and In impurities in zinc oxide**
S. Komatsuda[1], W. Sato[1,2], and Y. Ohkubo[3]
[1]*Graduate School of Natural Science and Technology, Kanazawa University*, [2]*Institute of Science and Engineering, Kanazawa University*, [3]*Research Reactor Institute, Kyoto University*

24-NPP-06 **Structure and antimony-121 Mössbauer spectra of hypervalent antimony compounds with an antimony–gold bond in equatorial position**
Masashi Takahashi, Asumi Sato, Shiro Matsukawa
Department of Chemistry, Toho University, Japan

24-NPP-07 **Local structure of $^{57}Mn/^{57}Fe$ implanted into lithium hydride**
Jun Miyazaki[1], Takashi Nagatomo[2], Yoshio Kobayashi[3, 4], Michael K. Kubo[5], Yasuhiro Yamada[6], Mototsugu Mihara[7], Wataru Sato[8], Kazuya Mae[5], Shinji Sato[9], Atsushi Kitagawa[9]
[1]*College of Industrial Technology, Nihon University*, [2]*J-PARC Center, High Energy Accelerator Research Organization,* [3]*Department of Engineering Science, The University of Electro-Communications*, [4]*RIKEN Nishina Center for Accelerator-Based Science, RIKEN*, [5]*The Division of Arts and Sciences, International Christian University*, [6]*Department of Chemistry, Tokyo University of Science*, [7]*Department of Physics, Osaka University*, [8]*Institute of Science and Engineering, Kanazawa University*, [9]*Department of Accelerator and Medical Physics, National Institute of Radiological Sciences*

24-NPP-08 **Evaluation of vacancy-type defects in ZnO by the positron annihilation lifetime spectroscopy**
R. Ono[1], T. Togimitsu[1], and W. Sato[1,2]
[1]*Graduate School of Natural Science and Technology, Kanazawa University*, [2]*Institute of Science and Engineering, Kanazawa University*

24-AAP-01 **Determination of ultratrace-levels of ^{99}Tc using ICP-QMS in the low level radioactive waste samples**
Te-Yen Su, Tsuey-Lin Tsai, Hsin-Chieh Wu, Lee-Chung Men
Chemistry Division, Institute of Nuclear Energy Research, Taiwan, R.O.C.

24-AAP-02 **Development of an automatic prompt gamma-ray activation analysis system**
Takahito Osawa[1]
[1]*Neutron Imaging and Quantum Beam Analysis Group, Quantum Beam Science Directorate, Japan Atomic Energy Agency*

24-AAP-03 **Concentration of heavy metal elements in Chinese medicine by INAA**
S. Ishihara[1], E. Furuta[2], N. Iwasaki[1], Y. Yoshihara[3], R.Okumura[4], Y.Iinuma[4]
[1]*Ochanomizu University, Facility of Sciences*, [2]*Ochanomizu University, Graduate School of Humanities and Sciences*, [3]*Ochanomizu University, Facility of Human Life and Environmental Sciences*, [4]*Kyoto University, Research Reactor Institute*

24-AAP-04 **Application of instrumental neutron activation analysis to assess dietary intake of selenium in Korean adults from meat and eggs**
Jong-Hwa Moon[1], Sun-Ha Kim[1], Yong-Sam Chung[1], Ok-Hee Lee[2]
[1]*Korea Atomic Energy Research Institute, Korea*, [2]*Dept of Food Science and Nutrition, Yongin University, Korea*

24-AAP-05 **Evaluation of hypoxia at dredged trenches in Tokyo Bay by determination of redox sensitive elements in the sediments**
T. Yamagata[1], K. Shozugawa[1], R. Okumura[2], K. Takamiya[2], M. Matsuo[1]
[1]*Graduate School of Arts and Sciences, The Univ. of Tokyo*, [2]*Research Reactor Institute, Kyoto Univ.*

24-AAP-06 **Determination of ultra trace amounts of Mn in iron meteorites by preconcentration neutron activation analysis**
Y. Tanaka[1], Y. Arai[1], T. Imamura[1], Y. Oura[1]
[1]*Department of Chemistry, Tokyo Metropolitan University*

24-AAP-07 **Instrumental photon activation analysis of geological and cosmochemical samples**
Naoki Shirai[1], Shun Sekimoto[2], Mitsuru Ebihara[1]
[1]*Tokyo Metropolitan University*, [2]*Kyoto University Research Reactor Institute*

24-AAP-08 **Monte carlo calculation of chloride diffusion in concrete**
A. A. Naqvi[1], Khateeb-ur-Rehman[1], M. Maslehuddin[2], O.S.B. Al-Amoudi[3] and M. Raashid[1]
[1]*Department of Physics*, [2]*Center for Engineering Research*, and [3]*Department of Civil and Environmental Engineering King Fahd University of Petroleum and Minerals, Dhahran, Saudi Arabia*

24-APP-01 **Catalysis induced by radiation in fatty acids adsorbed on clay minerals**
A. Negron-Mendoza[1]*, S. Ramos-Bernal[1], M. Colin-Garcia[2] and F.G. Mosqueira[3]
[1]*Instituto de Ciencias Nucleares, Universidad Nacional Autonoma de Mexico, México*, [2]*Instituto de Geología, Universidad Nacional Autonoma de Mexico, México*, [3]*Dirección General de Divulgación de la Ciencia, Universidad Nacional Autonoma de Mexico, México*

24-APP-02 **Preliminary study for highly sensitive airborne radioiodine monitor**
Yoshimune Ogata[1], Tadashi Yamasaki[2], Ryuji Hanafusa[3]
[1]*Nagoya University*, [2]*CEPCO, Japan*, [3]*Fuji Electric, Japan*

24-APP-03 **Radiation synthesis and cesium removal of cellulose microsphere based hybrid adsorbent**
Long Zhao[1*], Yanliang Chen[1], Yuezhou Wei[1]
[1]*School of Nuclear Science and Engineering, Shanghai Jiao Tong University, China*

24-APP-04 **Study about separation mechanism of endohedral metallofullerenes with Lewis acid**
K. Chiba[1], T. Hamano[1], E. Takeuchi[1], K. Akiyama[1], S. Kubuki[1], and H. Shinohara[2]
[1]*Department of Chemistry, Tokyo Metropolitan University, Japan*, [2]*Graduate School of Science, Nagoya University, Japan*

24-APP-05 **Crystal structure and spin state of mixed-crystals of $Fe(NCS)_x(NCBH_3)_{2-x}(bpp)_2$ (bpp = 1,3-bis(4-Pyridyl)Propane)**

Haruka Dote[1], Hiroki Yasuhara[1], Satoru Nakashima[2]
[1]*Graduate School of Science, Hiroshima University*, [2]*Natural Science Center for Basic Research and Development (N-BARD), Hiroshima University*

24-APP-06 **Analysis of fragments of a roman mask using Mössbauer spectroscopy**

Paulo de Souza[1,2], G. Klingelhöfer[3], P Gütlich[3], M. Egg[4]
[1]*University of Tasmania, Australia*, [2]*Commonwealth Scientific and Industrial Research Organisation, Australia*, [3]*Johannes Gutenberg-Universität Mainz, Germany*, [4]*Römisch-Germanisches Zentralmuseum, Germany*

24-APP-07 **Synthesis of ^{14}C labeled C_{60} with higher specific activity**

T. Tadai[1], K. Akiyama[1], H. Aoshima[2], R. Ibuki[2], S. Kubuki[1]
[1]*Department of Chemistry, Tokyo Metropolitan University, Japan*, [2]*Vitamin C_{60} BioResearch Corporation, Japan*

24-APP-08 **Adsorption behavior of Zr and Hf to TTA-resin in microcolumn for determining the forming ability of Rf monofluoride complex**

Y. Kitayama[1], Y. Shigeyoshi[1], A. Yokoyama[2], A. Toyoshima[3], K. Tsukada[3], K. Ooe[4], E. Maeda[1], H. Kimura[1], H. Kikunaga[5], Y. Kudou[6], J. Kanaya[6], M. Huang[6], and H. Haba[6]
[1] *Graduate School of Natural Science and Technology, Kanazawa University,* [2] *Institute of Science and Engineering, Kanazawa University,* [3] *Japan Atomic Energy Research Institute,* [4] *Institute of Science and Technology, Niigata University,* [5] *Research Center for Electron Photon Science, Tohoku University,* [6] *Nishina Center for Accelerator-Based Sience, RIKEN*

Wednesday, 25 September 2013, Poster Session

25-FKP-01 **$^{235}U/^{238}U$ isotopic ratio in environmental samples at the Fukushima area**
Y. Shibahara[1], T. Fujii[1], S. Fukutani[1], T. Kubota[1], R. Okumura[1], T. Ohta[2], K. Takamiya[1], N. Sato[1], M. Tanigaki[1], Y. Kobayashi[1], H. Yoshinaga[1], H. Yoshino[1], A. Uehara[1], S. Mizuno[3], T. Takahashi[1], and H. Yamana[1]
[1]*Research Reactor Institute, Kyoto University,* [2]*Faculty of Engineering, Hokkaido University,* [3]*Nuclear Power Safety Division, Fukushima Prefectural Government*

25-FKP-02 **Particulates of Ag and Pu radioisotopes released from Fukushima Daiichi nuclear power plants**
H. Kimura[1], M. Uesugi[2], A. Muneda[2], R. Watanabe[1], A. Yokoyama[3], T. Nakanishi[4]
[1]*Grad. School Nat. Sci. Tech., Kanazawa Univ.,* [2]*Col. Sci. Eng., Kanazawa Univ.,* [3]*Inst. Sci. Eng., Kanazawa Univ.,* [4]*Adv. Sci. Res. Cent., Kanazawa Univ.*

25-FKP-03 **The measurement of $^{14}C/^{12}C$ ratios in Japanese plant samples affected by anthropogenic sources**
R. Hashimoto[1], A. Inoue[1], Y. Muramatsu[1], H. Matsuzaki[2]
[1]*Depertment of Chemistry, Gakushuin University,* [2]*School of Engineering, The University of Tokyo*

25-FKP-04 **Radiocesium and stable cesium in edible wild plants (Sansai) collected from forests in Fukushima Prefecture**
M. Sugiyama[1], Y. Muramatsu[1], T.Ohno[1], M. Sato [2]
[1]*Gakushuin University, Japan,* [2]*Fukushima Agricultural Technology Center*

25-FKP-05 **Annual variation of radioactivity in marine biota in the Pacific off Fukushima after TEPCO's Fukushima Daiichi Nuclear Power Station accident**
T. Aono [1], S. Yoshida[1], T. Saotome [2],T. Mizuno [2], Y. Ito[3], J. Kanda[3], T. Ishimaru [3]
[1]*National Institute of Radiological Sciences,* [2]*Fukushima prefecture fisheries experimental station,* [3]*Tokyo University of Marine Science and Technology*

25-FKP-06 **Migration behavior of ^{134}Cs and ^{137}Cs in the Niida River water in Fukushima Prefecture, Japan during 2011-2012**
S. Nagao[1], M. Kanamori[2], S. Ochiai[1], M. Yamamoto[1]
[1]*Low Level Radioactivity Laboratory, Kanazawa University,* [2]*Graduate School of Natural Science and Technology, Kanazawa University*

25-FKP-07 **Migration behavior of radiocesium released from Fukushima Daiichi Nuclear Power Plant accident**
T. Ohnuki[1], N. Kozai[1], F. Sakamoto[1]
[1]*Japan Atomic Energy Agency, Japan*

25-FKP-08 **Research on atmospheric radionuclides from the Fukushima Nuclear Accident at the MRI, Japan**
Y. Igarashi[1], K. Adachi [1], T. Tanaka[1], M. Kajino[1], T. Sekiyama[1], T. Maki[1], Y. Zaizen[1], M. Mikami[1]
[1]*Meteorological Research Institute, Japan*

25-FKP-09 **Presuming techniques of radioactive cesium concentration in muscle for beef cattle**
T. Ohtsuki[1], F. Koga[2], M. Uchida[2], Y. Ishikawa[2], T. Takase[3], K. Kawatsu[3], M. Mogi[4] S. Murayama[4], Y. Izumi[4], H. Kikunaga[1], T. Tachiya[5], Y. Shiraishi[2], K. Endo[2]
[1]*Research Center for Electron Photon Science, Tohoku University,* [2]*Fukushima Agricultural Technology Center Livestock Industry Research Center, Fukushima Prefecture,* [3]*Faculty of Symbiotic System Science, Fukushima University,* [4]*Japan Environment Research Co., LTD,* [5]*Comtec Eng. Co., LTD, Fukushima*

25-FKP-10 **Spatio-temporal distribution of atmospheric radiocesium at monitoring stations for suspended particulate matter in Fukushima area released from the TEPCO Fukushima Daiichi Nuclear Power Plant accident**
H. Tsuruta[1], Y. Oura[2], M. Ebihara[2], M. Ishimoto[3], Y. Katsumura[3], T. Ohara[4], T. Nakajima[1]
[1]*Atmosphere and Ocean Research Institute, The University of Tokyo, Japan,* [2]*Department of Chemistry, Tokyo Metropolitan University, Japan,* [3]*Center for Regional Environmental Research, National Institute for Environmental Studies,* [4]*Nuclear Professional School, The University of Tokyo, Japan*

25-EDP-01 **Education of nuclear and radiochemistry in Hallym University, Korea**
Y. H. Chung
Department of Chemistry, Hallym University, Korea

25-EDP-02 **Use of small $^{68}Ge/^{68}Ga$ generators in experiments for the education of radioisotope-related fields as well as of**

natural and social sciences in general
T. Nozaki,[1] K. Ogawa[2]
[1]*School of Sciences, Kitasato University,* [2]*School of Allied Health Sciences, Kitasato University, Japan*

25-NFP-01 **Application of alpha spectrometry to the measurement of a single plutonium particle for nuclear safeguards**
K. Yasuda, D. Suzuki, F. Esaka and M. Magara
Research group for analytical chemistry, Japan Atomic Energy Agency

25-NEP-01 **High LET radiolytic degradation studies of separation processes for spent nuclear fuel**
J. Pearson and M. Nilsson
University of California – Irvine, USA, Department of Chemical Engineering and Materials Science

25-NEP-02 **Effects of helium retention and lithium depletion on tritium behaviors in Li_2TiO_3**
M. Kobayashi[1], H. Uchimura[1], K. Toda[1], M. Sato[1], K. Tatunuma[2], Y. Oya[1] and K. Okuno[1]
[1]*Radioscience Research Laboratory, Faculty of Science, Shizuoka University, Japan,* [2]*Kaken Co. Ltd., Japan*

25-NEP-03 **Adsorptivity of various metal ions onto benzo-18-crown-6 and dibenzo-18-crown-6 resins**
M. Nogami[1], T. Haratani[1], Y. Tachibana[2], T. Kaneshiki[3], M. Nomura[3], T. Suzuki[2]
[1]*Department of Electric and Electronic Engineering, Kinki University,* [2]*Department of Nuclear System Safety Engineering, Nagaoka University of Technology,* [3]*Research Laboratories for Nuclear Reactors, Tokyo Institute of Technology*

25-NEP-04 **Cesium adsorption ability and stability of metal hexacyanoferrate irradiated with gamma-rays**
M. Arisaka[1], M. Watanabe[1], M. Ishizaki[2], M. Kurihara[2], R. Chen[3], H. Tanaka[3]
[1]*Research Group for Radiochemistry, Nuclear Science and Engineering Directorate, Japan Atomic Energy Agency,* [2]*Department of Material and Biological Chemistry, Faculty of Science, Yamagata University,* [3]*Nanosystem Research Institute, National Institute of Advanced Industrial Science and Technology, Japan*

25-NEP-05 **Residual actinides separation from the DIAMEX/SANEX secondary waste and decontamination of the spent DIAMEX solvent from the "difficult-to-strip" elements**
J. John, F. Šebesta, K. V. Mareš, F. Klimek, M. Vlk
Czech Technical University in Prague, Department of Nuclear Chemistry, Czech Republic

25-NEP-06 **Thorium based molten salt fuel cycle**
Q.-N. Li*, L. Zhang, W.-X. Li, G.-Z. Wu
Shanghai Institute of applied physics, Chinese Academy of Sciences, China

25-NEP-07 **Study on electrochemical behaviors of rare earth elements in FLINAK eutectic salt**
L.-F. Tian, W. Huang, F. Jiang, C.-F. She, H.-Y. Zheng, D.-W. Long*, Q.-N. Li
Shanghai Institute of applied physics, Chinese Academy of Sciences, China

25-NCP-01 **Measurement of cosmogenic nuclides in meteorites by well-type Ge detector in Ogoya Underground Laboratory - correction of coincidence sum effect for Al-26,Co-56,Na-22 and Co-60 -**
Y. Hamajima
LLRL, Kanazawa Univ., Japan

25-NCP-02 **Development of multipurpose neutron irradiation apparatus at KUR**
K. Takamiya[1], Y. Yoshida[2], H. Tanaka[1], T. Fujii[1], S. Fukutani[1], T. Sano[1], H. Yoshino[1], Y. Iinuma[1], R. Okumura[1], S. Shibata[1]
[1]*Research Reactor Institute, Kyoto University,* [2]*Graduate School of Engineering, Kyoto University*

25-NCP-03 **Development of a new continuous dissolution apparatus with a hydrophobic membrane for superheavy element chemistry**
K. Ooe[1,2], K. Tsukada[2],M. Asai[2], T. K. Sato[2], A. Toyoshima[2], S. Miyashita[2], Y. Nagame[2], M. Schädel[2], Y. Kaneya[3], H. V. Lerum[4], J. P. Omtvedt[4], J. V. Kratz[5], H. Haba[6], A. Wada[7], Y. Kitayama[8]
[1]*Institute of Science and Technology, Niigata University,* [2]*Japan Atomic Energy Agency,* [3]*Graduate School of Science and Engineering, Ibaraki University,* [4]*Department of Chemistry, University of Oslo,* [5]*Institut für Kernchemie, Universität Mainz,* [6]*Nishina Center for Accelerator-Based Science, RIKEN,* [7]*Department of Chemistry, Tokyo Metropolitan University,* [8]*Graduate School of Natural Science and Technology, Kanazawa University*

25-NCP-04 **Cross-section measurements of high energy neutron-induced reactions for Cu and Nb**

K. Ninomiya[1], T. Omoto[1], R. Nakagaki[1], N. Takahashi[1], Y. Kasamatsu[1], A. Shinohara[1], S. Sekimoto[2], H. Yashima[2], S. Shibata[2], T. Shima[3], H. Matsumura[4], M. Hagiwara[4], Y. Iwamoto[5], D. Satoh[5], M. W. Caffee[6], K. Nishiizumi[7]
[1]*Graduate School of Science, Osaka University,* [2]*Research Reactor Institute, Kyoto University,* [3]*Research Center of Nuclear Physics, Osaka University,* [4]*Radiation Research Center, High Energy Accelerator Organization,* [5]*Nuclear Science and Engineering Directorate, Japan Atomic Energy Agency,* [6]*Department of Physics, Purdue University,* [7]*Space Sciences Laboratory, University of California*

25-NCP-05 **Development of a rapid solvent extraction technique with flow injection analysis for superheavy element chemistry**

T. Koyama[1], N. Goto[1], M. Murakami[1,2], K. Ooe[1], H. Haba[2], J. Kaneya[2], S. Goto[1], and H. Kudo[1]
[1]*Department of Chemistry, Faculty of Science, Niigata University, Japan,* [2]*Nishina Center for Accelerator-Based Science, RIKEN, Japan*

25-NCP-06 **Solid-liquid extraction of Mo and W by Aliquat 336 from HF and HCl solutions towards extraction chromatography experiments of Sg**

Y. Komori[1], T. Yokokita[1], K. Toyomura[1], K. Nakamura[1], Y. Kasamatsu[1], H. Haba[2], J. Kanaya[2], M. Huang[2], Y. Kudou[2], A. Toyoshima[3], N. Takahashi[1], A. Shinohara[1]
[1]*Graduate School of Science, Osaka University,* [2]*Nishina Center for Accelerator-Based Science, RIKEN,* [3]*Advanced Science Research Center, Japan Atomic Energy Agency*

25-NCP-07 **Off-line isothermal gas chromatography of Zr and Hf compounds**

Y. Oshimi, S. Goto, T. Taguchi, T. Tomitsuka, K. Ooe, H. Kudo
Department of Chemistry, Faculty of Science, Niigata University, Japan

25-NCP-08 **Chemical studies of Rf and Db in liquid-phases using automated rapid chemical separation apparatuses at JAEA**

K. Tsukada[1], A. Toyoshima[1], M. Asai[1], Y. Kasamatsu[2], Z. J. Li[3], Y. Ishii[1], H. Haba[4], T. K. Sato[1], Y. Nagame[1], M. Schädel[1]
[1]*Japan Atomic Energy Agency,* [2]*Graduate School of Science, Osaka University,* [3]*Institute of High Energy Physics, Chinese Academy of Science, China,* [4]*Nishina Center for Accelerator Based Science, RIKEN, Japan*

25-NCP-09 **Solvent extraction of hexavalent Mo and W using 4-isopropyltropolone (Hinokitiol) for Seaborgium (Sg) reduction experiment**

S. Miyashita[1], A. Toyoshima[1], K. Ooe[2], M. Asai[1], T. K. Sato[1], K. Tsukada[1], Y. Nagame[1], M. Schädel[1], Y. Kaneya[3], H. Haba[4], J. Kanaya[4], M. Huang[4], Y. Kitayama[5], A. Yokoyama[5], A. Wada[6], Y. Oura[6] J. V. Kratz[7], H. V. Lerum[8] and J. P. Omtvedt[8]
[1]*Advanced Science Research Center, Japan Atomic Energy Agency,* [2]*Institute of Science and Technology, Niigata University,* [3]*Graduate School of Science and Engineering, Ibaraki University,* [4]*Nishina Center for Accelerator-Based Science, RIKEN,* [5]*College and Institute of Science and Engineering, Kanazawa University,* [6]*Graduate School of Science and Engineering, Tokyo Metropolitan University,* [7]*Institut für Kernchemie, Universität Mainz, Germany,* [8]*Department of Chemistry, University of Oslo, Norway*

25-NCP-10 **Development of surface ionization ion-source for determination of the first ionization potentials of heavy actinides**

Y. Kaneya[1,2], T. K. Sato[2], M. Asai[2], K. Tsukada[2], A. Toyoshima[2], S. Miyashita[2], Y. Nagame[1,2], M. Schädel[2], N. Sato[3], K. Ooe[4], A. Osa[5], S. Ichikawa[2,6], T. Stora[7], J. V. Kratz[8]
[1]*Graduate School of Science and Engineering, Ibaraki University, Japan,* [2]*Advanced Science Research Center, Japan Atomic Energy Agency,* [3]*Nuclear Science and Engineering Directorate, Japan Atomic Energy Agency,* [4]*Institute of Science and Technology, Niigata University, Japan,* [5]*Department of Research Reactor and Tandem Accelerator, Japan Atomic Energy Agency,* [6]*Nishina Center for Accelerator Based Science, RIKEN, Japan,* [7]*ISOLDE, CERN, Switzerland,* [8]*Institut für Kernchemie, Universität Mainz, Germany*

25-NCP-11 **Comparison of the decay constants of ^{51}Cr with various valence states**

H. Kikunaga[1], K. Takamiya[2], K. Hirose[1*], T. Otsuki[1]
[1]*Research Center for Electron Photon Science, Tohoku University,* [2]*Research Reactor Institute, Kyoto University,* [*]*Present address: Advanced Science Research Center, Japan Atomic Energy Agency*

25-NCP-12 **Selective separation of strontium (II) from nitric acid solution by a macroporous silica-based $DtBuCH_{18}C_6$ adsorbent modified with surfactants**

Y. Wu, Z. Chen, Y. Wei*

School of Nuclear Science and Engineering, Shanghai Jiao Tong University, China

25-NCP-13 **Exploring the synthesis and characterization of binary technetium chlorides and bromides**
E. Johnstone[1], F. Poineau[1], P. M. Forster[1], P. Weck,[2] C. D. Malliakas[3], E. Kim[4], M. G. Kanatzidis[3], B. L. Scott[5], A. P. Sattelberger[6], and K. R. Czerwinski[1]
[1]*Department of Chemistry, University of Nevada Las Vegas, Las Vegas, USA,* [2]*Sandia National Laboratories, USA,* [3]*Department of Chemistry, Northwestern University, USA,* [4]*Department of Physics and Astronomy, University of Nevada, USA,* [5]*Materials Physics and Applications Division, Los Alamos National Laboratory, USA,* [6]*Energy Engineering and Systems Analysis Directorate, Argonne National Laboratory, USA*

25-ACP-01 **Solvent extraction of americium(III) and europium(III) using hydroxyoctanoic acid and n-heteroaromatic compound**
M. Seike[1], M. Eguchi[1], A. Shinohara[1], T. Yoshimura[2]
[1]*Graduate School of Science, Osaka University,* [2]*Radioisotope Research Center, Osaka University*

25-ACP-02 **Stability of uranyl peroxo-carbonato complex ions in the presence of metal oxide in carbonate media**
D.-Y. Chung[1], M.-S. Park[1], K.-Y. Lee[1], H.-B. Yang[1], E.-H. Lee[1], K.-W. Kim[1], J.-K. Moon[1]
[1]*Korea Atomic Energy Research Institute, Korea*

25-ACP-04 **Raman spectroscopic study on uranyl and neptunyl complexes in highly concentrated calcium chloride**
T. Fujii[1], A. Uehara[1], Y. Kitatsuji[2], and H. Yamana[1]
[1]*Division of Nuclear Engineering Science, Research Reactor Institute, Kyoto University,* [2]*Nuclear Science and Engineering Directorate, Japan Atomic Energy Agency*

25-ACP-05 **Electrode reaction of actinide ions in a weak acidic solution**
Y. Kitatsuji[1], H. Otobe[1], T. Kimura[1]
[1]*Nuclear Science and Engineering Directorate, Japan Atomic Energy Agency*

25-ACP-06 **Biomineralization of uraninite and uranyl phosphate controlled by organic acids**
Y. Suzuki[1], N. Kozai[2], T. Ohnuki[2]
[1]*Graduate School of Bionics, Tokyo University of Technology, Japan,* [2]*Advanced Science Research Center, Japan Atomic Energy Agency, Japan*

25-ACP-07 **Comparison of the spectroscopic characteristics of uranium species when U(III) in a LiCl-KCl molten salt is leached out with water and ionic liquid**
H.-J. Im, K. Song
Nuclear Chemistry Research Division, Korea Atomic Energy Research Institute, Korea

25-ACP-08 **Distribution of Neptunium in PUREX streams**
N. Rawat, A. Kar, M.A. Mahajan, N.B. Khedekar, R.M. Sawant, B. S. Tomar and K. L. Ramakumar
Radioanalytical Chemistry Division, Bhabha Atomic Research Centre, India

25-ACP-09 **α-radiation effect on solvent extraction of minor actinide**
Y. Sugo[1], Y. Sasaki[2], M. Taguchi[1], N. S. Ishioka[1]
[1]*Quantum Beam Science Directorate, Japan Atomic Energy Agency,* [2]*Nuclear Science and Engineering Directorate, Japan Atomic Energy Agency*

25-ENP-01 **Retardation and release study of U(VI) on phlogopite at conditions relevant to uranium contamination in environment**
D. Pan[1,2], Z. Wang[2], W. S. Wu[1]
[1]*Radiochemistry Laboratory, Lanzhou University, China,* [2]*Pacific Northwest National Laboratory, USA*

25-ENP-02 **Application of simplified desorption method to sorption study: (2) sorption of neptunium (V) on montmorillonite-based mixtures**
N. Kozai[1], T. Ohnuki[1]
[1]*Japan Atomic Energy Agency, Japan*

25-ENP-03 **Continuous measurement of radon exhalation rate of soil in Beijing**
L. Zhang[1,2], K. S.[2], Q. Guo[2]
[1]*Solid Dosimetric Detector and Method Laboratory, China,* [2]*State Key Laboratory of Nuclear Physics and Technology, School of Physics, Peking University, China*

25-ENP-04 **Dosimetric evaluation of thoron exposure in three typical rural indoor environments in China**
L. Zhang[1], Q. Guo[2], S. Wang[1]
[1]*Solid Dosimetric Detector and Method Laboratory, China,* [2]*State Key Laboratory of Nuclear Physics and Technology, School of Physics, Peking University, China*

25-ENP-05 **Binary technetium phosphide synthesis at low temperature conditions**
B. C. Childs[1], W. M. Kerlin[1], K. R. Czerwinski[1]
[1]*University of Nevada Las Vegas, USA*

25-ENP-06 **Dissolution behavior of ^{137}Cs absorbed on the green tea leaves**
Y. Oya[1], H. Uchimura[1], K. Toda[1], T. Ikka[2], A. Morita[2], K. Okuno[1]
[1]*Graduate School of Science, Shizuoka University,* [2]*Graduate School of Agriculture, Shizuoka University*

25-ENP-07 **Characterization on the radioactive aerosols dispersed during plasma arc cutting of radioactive metal piping**
T. Shimada[1], T. Tanaka[1]
[1]*Nuclear Safety Research Center, Japan Atomic Energy Agency, Japan*

25-ENP-08 **A passive collection method for whole size fractions of suspended river materials**
T. Matsunaga[1], T. Nakanishi[1], M. Atarashi-Andoh[1], E. Takeuchi[1], K. Tsuduki[1], S. Nishimura[1], J. Koarashi[1], S. Otosaka[1], T. Sato[2], S. Nagao[3]
[1]*Nuclear Science and Engineering Directorate, Japan Atomic Energy Agency,* [2]*Division of Sustainable Resources Engineering, Graduate School of Engineering, Hokkaido University, Japan,* [3]*Low Level Radioactivity Laboratory, Institute of Nature and Environmental Technology, Kanazawa University, Japan*

25-ENP-09 **Study of factors controlling organic pollution in Lake Kiba**
Y. Kawano[1], S. Nagao[1], S. Ochiai[1], M. Yamamoto[1]
[1]*Low Level Radioactivity Laboratory, Kanazawa Univ., Japan*

25-ENP-10 **Rapid monitoring particulate radiocesium with nonwoven fabric cartridge filter and application to field monitoring**
H. Tsuji[1], Y. Kondo[2], S. Kawashima[2], T. Yasutaka[1]
[1]*National Institute of Advanced Industrial Science and Technology,* [2] *Japan Vilene Company. Ltd.*

25-ENP-11 **In-situ measurement of ^{134}Cs and ^{137}Cs in seabed by underwater γ-spectrometry systems and application for the survey to the Fukushima Dai-ichi NPP accident**
H. Kofuji
Japan Marine Science Foundation, Japan

25-ENP-12 **Radiocarbon dating of molluscan shells and its application**
Y. Miyata[1, 2, 3], H. Matsuzaki[2]
[1]*The Low Level Radioactivity Laboratory (LLRL), Institute of Nature and Environmental Technology, Kanazawa University, Japan,* [2]*The College of Liberal Arts, International Christian University, Japan,* [3]*National Museum of Japanese History, Japan,* [4]*Department of Nuclear Engineering and Management, School of Engineering (MALT), The University of Tokyo, Japan*

25-ENP-13 **Concentration of uranium on TiO-PAN and NaTiO-PAN composite absorbers**
A. Motl, F. Šebesta, J. John, I. Špendlíková, M. Němec
Czech Technical University in Prague, Department of Nuclear Chemistry, Czech Republic

25-ENP-14 **Use of radon to characterise surface water recharge to groundwater**
N Hermanspahn,[1] M Close,[1] M Matthews,[1] L Burbery,[1] P Abraham,[1]
[1]*Institute of Environmental Science and Research (ESR), Christchurch, New Zealand*

25-RPP-01 **Production and utilization of radioactive astatine isotopes in the ^{7}Li + ^{nat}Pb reaction**
I. Nishinaka[1], A. Yokoyama[2], K. Washiyama[2], R. Amano[2], E. Maeda[2], N. Yamada[2], H. Makii[1], A. Toyoshima[1], S. Watanabe[1], N. S. Ishioka[1], K. Hashimoto[1]
[1]*Japan Atomic Energy Agency (JAEA),* [2]*Kanazawa University*

25-RPP-02 **Production of actinium-225 from natural thorium irradiated with protons**
A. N. Vasiliev[1], V. S. Ostapenko[1], R. A. Aliev[1], S. N. Kalmykov[1], E. V. Lapshina[2], S. V. Ermolaev[2] and B. L.

Zhuikov[2]
[1]*Chemisrtry Department, Lomonosov Moscow State University, Russia,* [2]*Institute for Nuclear Research of Russian Academy of Sciences, Russia*

25-RPP-03 **Development of ^{99}Mo-^{99m}Tc domestic production with high-density MoO_3 pellets by (n, γ) reaction**
K. Tsuchiya[1], M. Tanase[2], T. Shiina[2], A. Ohta[2], M. Kobayashi[3], A. Yamamoto[3], Y. Morikawa[3], M. Kaminaga[1], H. Kawamura[1]
[1]*Japan Atomic Energy Agency,* [2]*Chiyoda Technol Corporation, Japan,* [3]*FUJIFILM RI Pharma Co. Ltd., Japan*

25-RPP-04 **Preparation of ^{99}Mo–^{99m}Tc by using spallation neutron**
Y. Hayashi*[1], N. Takahashi[1], K.Nakai[1], H. Ikeda[2], G. Horitsugi[2], T. Watabe[2], Y. Kanai[2], H. Watabe[2], E. Shimosegawa[2], Y. Miyake[2], J. Hatazawa[2], M. Fukuda[3], K. Hatanaka[3], K. Takamiya[4], S. Yamamoto[5], Y. Kasamatsu[1], A. Shinohara[1]
[1]*Graduate School of Science, Osaka University,* [2]*Graduate School of Medicine, Osaka University,* [3]*Research Center for Nuclear Physics, Osaka University,* [4]*Kyoto University Research Reactor Institute,* [5]*Graduate School of Medicine, Nagoya University*

25-RPP-05 **Development of automated measurement system for radioactive intensities of sealed small radiation sources (Iodine-125 seed source) for brachytherapy**
M. Sakama,[1] H. Ikushima,[2] T. Saze,[3] Y. Nagano,[4] T. Yamada,[5] T. Ichiraku,[5] H. Takai,[5] Y. Kuwahara,[6] S. Nakayama[7]
[1]*Department of Radiological Science (also Advanced Radio-Analytical Chemistry, Division of Biomedical Information Sciences, Institute of Health Biosciences, The University of Tokushima, Japan,* [2]*Department of Radiation Therapy Technology, Division of Biomedical Information Sciences, Institute of Health Biosciences, The University of Tokushima,* [3]*Otsuka Pharmaceutical Factory, Japan,* [4]*Department of Radiological Science, Division of Biomedical Information Sciences, Institute of Health Biosciences, The University of Tokushima,* [5]*Dairyu Co. Ltd., Japan,* [6]*Radioisotope Center, The University of Tokushima,* [7]*Department of Nuclear Science, Institute of Socio-Arts and Sciences, The University of Tokushima, Japan*

25-RPP-06 **Extraction of astatine isotopes for development of radiopharmaceuticals**
E. Maeda[1], A.Yokoyama[2], T. Taniguchi[1], K. Washiyama[3] I. Nishinaka[4]
[1]*Grad. School Nat. Sci., Tech. Kanazawa Univ.,* [2]*Inst. Sci. Eng., Kanazawa Univ.,* [3]*Sch. of Health Sci., College of Med., Pharma. Health Sci., Kanazawa Univ.,* [4]*ASRC, Japan Atomic Energy Agency*

25-RPP-07 **Lutetium-177 complexation of DOTA and DTPA in the presence of competing metals**
S. Watanabe[1], K. Hashimoto[1], N. S Ishioka[1]
[1]*Medical Radioisotope Application Group, Quantum Beam Science Directorate, Japan Atomic Energy Agency*

25-NPP-01 **Hyperfine fields at ^{140}Ce in He-doped Fe**
Y. Ohkubo[1], A. Taniguchi[1], Q. Xu[1], M. Tanigaki[1], K. Sato[1] and M. Tsuneyama[2]
[1]*Research Reactor Institute, Kyoto University,* [2]*Grauduate School of Science, Kyoto University*

25-NPP-02 **Mössbauer studies of lanthanum doped $Ni_{0.4}Cu_{0.2}Zn_{0.4}Fe_2O_4$ ferrites by sol-gel autocombustion**
Q. Lin[1,2], C. Lei[1]*, H. Huang[3], H. Zhang[1], Y. He[1]
[1]*College of Physics and Technology, Guangxi Normal University, China,* [2]*Department of Information Technology, Hainan Medical College,China,* [3]*Nanjing National Laboratory of Microstructures and Jiangsu Provincial Laboratory for NanoTechnology, Department of Physics, Nanjing University, China*

25-NPP-03 **Analysis of corrosion products formed on anti-weather steel**
M. Oyabu[1], R. Satoh[1], K. Nomura[2]
[1]*Math & Science Division, Kanazawa Institute of Technology, Japan,* [2]*The University of Tokyo*

25-NPP-04 **Study of the spin-crossover phenomena in 1D coordination polymers, $[FeII(NH_2\text{-triazole})_3](C_nH_{2n+1}SO_3)_2$, by Fe-K edge XAFS and ^{57}Fe Mössbauer spectroscopy**
H. Kamebuchi[1], A. Nakamoto[1], M. Enomoto[2], T. Yokoyama[3], N. Kojima[1]
[1]*Graduate School of Arts and Sciences, The University of Tokyo,* [2]*Department of Chemistry, Tokyo University of Science,* [3]*Department of Materials Molecular Science, Institute for Molecular Science, Japan*

25-NPP-05 **Mössbauer spectroscopic and powder X-ray diffraction studies on incorporation of gaseous organic molecules into intermolecular nano-voids of mixed-valence trinuclear iron pentafluorobenzoate complex**
Y. Sakai[1], S. Onaka[1], R. Ogiso[1], M. Takahashi[2], T. Nakamoto[3], and T. Takayama[1]

[1]*DaidoUniversity,Japan,* [2]*Toho University, Japan,* [3]*Toray Research Center, Japan*

25-NPP-06 **Dynamic perturbation to $^{111}Cd(\leftarrow{}^{111}Ag)$ doped in AgI nanoparticles**

W. Sato[1,2], R. Mizuuchi[2], N. Irioka[3], S. Komatsuda[2], S. Kawata[4], A. Taoka[1,2], and Y. Ohkubo[5]
[1]*Institute of Science and Engineering, Kanazawa University,* [2]*Graduate School of Natural Science and Technology, Kanazawa University,* [3]*School of Chemistry, Kanazawa University,* [4]*Department of Chemistry, Faculty of Science, Fukuoka University,* [5]*Research Reactor Institute, Kyoto University*

25-AAP-01 **A prototype of a simple collection system for the determination of ^{14}C**

T.-H. Chuang, T. –L. Tsai, H. –J. Wei, L. –C. Men
Chemistry Division, Institute of Nuclear Energy Research, Taiwan, ROC

25-AAP-02 **Elemental analysis of Korean adult toenail using of instrumental neutron activation analysis**

S. –H. Kim[1], J. –H. Moon[1], Y. –S. Chung[1], O.-H. Lee[2]
[1]*Korea Atomic Energy Research Institute,* [2]*Dept of Food Science and Nutrition, Yongin University, Korea*

25-AAP-03 **Determination of vanadium at ppb levels in relatively high-salt biological materials without chemical separation and using neutron activation coupled to compton suppression gamma-ray spectrometry**

W. Zhang and A. Chatt
Trace Analysis Research Centre, Department of Chemistry, Dalhousie University, Canada

25-AAP-04 **Radiochemical neutron activation analysis of halogens (Cl, Br and I) in geological and cosmochemical samples**

M. Ebihara[1] and S. Sekimoto[2]
[1]*Tokyo Metropolitan University,* [2]*Kyoto University Research Reactor Institute*

25-AAP-05 **Multielement analysis of KIGAM reference samples by INAA, ICP-AES and ICP-MS**

N. Shirai[1], M. Toktaganov[2], H. Takahashi[1], Y. Yokozuka[1], S. Sekimoto[3], M. Ebihara[1]
[1]*Tokyo Metropolitan University,* [2]*National Nuclear Center Republic of Kazakhstan Institute of Atomic Energy*
[3]*Kyoto University Research Reactor Institute*

25-AAP-06 **Comparison of calculated results with NTD measured data for establishment of burned core model for monte carlo simulation of HANARO reactor**

D.-K. Cho and M.-S. Kim
Korea Atomic Energy Research Institute, Korea

25-AAP-07 **Neutron activation analysis of JCFA-1, JCu-1 and JZn-1**

S. Sekimoto[1], Y. Homura[1], R. Okumura[1], N. Shirai[2]
[1]*Kyoto University Research Reactor Institute,* [2]*Tokyo Metropolitan University*

25-AAP-08 **Prompt gamma-ray analysis of chloride concentration in blended cement concretes**

A. A. Naqvi[1*], M. Maslehuddin[2], O.S.B. Al-Amoudi[3], Khateeb-ur-Rehman[1], M. Raashid[1]
[1]*Department of Physics,* [2]*Center for Engineering Research, and* [3]*Department of Civil and Environmental Engineering, King Fahd University of Petroleum and Minerals, Saudi Arabia*

25-AAP-09 **Cold neutron and thermal neutron PGAA facilities at The HANARO research reactor**

G.M. Sun[1], E.J. Lee[1], B.G. Park[1], J.H. Moon[1]
[1]*Neutron Utilization Technology Division, Korea Atomic Energy Research Institute, Korea*

25-AAP-10 **Exposing dogs to uranium contained in commercial diets**

Camila Elias,[1] Elisabete A. De Nadai Fernandes,[1] Márcio A. Bacchi,[1] Peter Bode[2]
[1] *University of São Paulo, Nuclear Energy Center for Agriculture, Brazil*
[2] *Reactor Institute Delft, Delft University of Technology, The Netherlands*

Oral Presentations

Monday, 23 September 2013

Hall & Meeting Room, Kanazawa Bunka Hall

		Monday, 23 September			
Time		Hall		Meeting Room	
09:00-09:10	9:00	Arrangement for presentation			
09:10-09:20					
09:20-09:30					
09:30-09:40	9:30	Opening Ceremony			
09:40-09:50					
09:50-10:00					
10:00-10:10	10:00	**Hevesy Award Ceremony** R. S. Dybczyński			
10:10-10:20					
10:20-10:30					
10:30-10:40					
10:40-10:50					
10:50-11:00					
11:00-11:10	11:00	**Coffee Break**			
11:10-11:20	11:10	PL-01	**Plenary**		
11:20-11:30					
11:30-11:40			M. Yamamoto		
11:40-11:50	11:40	PL-02	**Plenary**		
11:50-12:00					
12:00-12:10			I. McKinley		
12:10-13:20	12:10	**Lunch Time**			
13:20-13:30	13:20	FKI-01	**Invited**	API-01	**Invited**
13:30-13:40					
13:40-13:50			H. Tsuruta		H. Harada
13:50-14:00	13:50	FKI-02	**Invited**	API-02	**Invited**
14:00-14:10					
14:10-14:20			Y. Takahashi		Y.L. Zhao
14:20-14:30	14:20	FKI-03	**Invited**	APO-01	General
14:30-14:40					T. M. Nakanishi
14:40-14:50			M. Aoyama	APO-02	General
14:50-15:00	14:50	FKI-04	**Invited**		S.H. Jung
15:00-15:10				APO-03	General
15:10-15:20			B. Grambow		M. Anvia
15:20-15:30	15:20	**Coffee Break**			
15:30-15:40					
15:40-15:50	15:40	FKO-01	General	NCO-01	General
15:50-16:00			A. Shimada		Z. Qin
16:00-16:10	16:00	FKO-02	General	NCO-02	General
16:10-16:20			Y. Miyake		W.M. Kerlin
16:20-16:30	16:20	FKO-03	General	NCO-03	General
16:30-16:40			T. Ohta		Y.K. Ha
16:40-16:50	16:40	FKO-04	General	NCO-04	General
16:50-17:00			Y. Muramatsu		I. Laszak
17:00-17:10	17:00	FKO-05	General	NCO-05	General
17:10-17:20			Y. Satou		Y. Xu
17:20-17:30	17:20	FKO-06	General	NFO-01	General
17:30-17:40			M. C. Honda		Y. Miyamoto
17:40-17:50	17:40	FKO-07	General	NFO-02	General
17:50-18:00			Z.J. Zhang		N. Gharibyan
18:00-18:10	18:00	FKO-08	General	NFO-03	General
18:10-18:20			D.R. Neville		R. Sudowe
18:20-18:30					
18:30-18:40					
18:40-18:50					
18:50-19:00	18:50	**Poster Session**			
19:00-19:20					
19:20-19:40					
19:40-20:00					
20:00-	20:00				

50 Years of Adventures with Neutron Activation Analysis with the Special Emphasis on Radiochemical Separations

Rajmund S. Dybczyński
Laboratory of Nuclear Analytical Techniques, Institute of Nuclear Chemistry and Technology, 03-195 Warszawa, POLAND
r.dybczynski@ichtj.waw.pl

Radiochemical separations are the key element of analytical methods based on radiochemical neutron activation analysis (RNAA). At the same time, the work in this area is the best reference to the heritage of George Hevesy who received Nobel Prize in Chemistry 1943 *"for his work on the use of isotopes as tracers in the study of chemical processes"*. In this paper author's activities in devising new systems for the separation of inorganic ions, determination of trace elements by RNAA, but also purely instrumental NAA (INAA), are reviewed. In the early years of atomic era, only non-selective radiation detectors such as Geiger-Müller or proportional counters were available, so except of some special cases , the analysis had to rely on chemical separations. Radiochemical separation retained much of its significance even with the advent of scintillation spectrometry. After Ge(Li) and HPGe detectors became available, most of analyses were done by γ-ray spectrometry (INAA) but in several instances group separation was necessary. There were always two philosophies in radiochemical separations intended for RNAA. First, relied on addition of inactive carriers for the radionuclides to be quantified, isolation of a portion of an element in the state of sufficient radiochemical purity, followed by radioactivity measurement and determination of chemical yield. Second, assumed that sufficiently selective and practically quantitative separation of radionuclides into groups or individual species can be attained by properly designed and tested chromatographic procedures , thus obviating the need for the determination of chemical yield. This second approach was mostly used in author's laboratory. New anion exchange system for the separation of rare earth elements (REE) as complexes with EDTA was devised and used for the determination of traces of Lu, Ho and Dy in Er_2O_3 as well as La in Pr_6O_{11}. Fundamental study performed on the effect of temperature and resin cross-linking was helpful in optimization of the separation procedure. Ion exchange behavior of several elements in the system: Dowex50WX2[H^+] – HBr was studied and was the basis for selective separation and determination of La,Sc, Ga and Hf by NaI(Tl) spectrometry in refractory materials. Complex separation schemes involving some cation and anion exchange columns were devised for the determination of impurities in platinum and rhodium metals by RNAA. Traces of cesium in mineral salts (down to $8x10^{-9}$%) were determined by pre-irradiation isolating cesium on phenolsulfonic resin followed by post-irradiation purification and measurement of short-lived ^{134m}Cs with very thin NaI(Tl) crystal. Pre-irradiation separation together with post-irradiation purification and γ-ray spectrometry was used for the determination of noble metals in geological materials as well as all lanthanides in biological materials. The uses of INAA included *inter alia* analysis of meteorites, human hair (for forensic, environmental and biomedical purposes), analysis of fly ashes (together with investigation of leaching of trace elements by water and acid rain), study on homogeneity of certified reference materials (CRMs), and contribution to the certification of new CRMs. The idea of "definitive methods" by RNAA was proposed, the essence of which is the combination of neutron activation with selective and quantitative post-irradiation separation of the desired radionuclide by column chromatography followed by γ-ray spectrometric measurement. A set of rules which should be observed when constructing definitive methods , as well as criteria which must be fulfilled to acknowledge the analytical result as obtained by definitive method, were formulated. The methods elaborated by us , e.g. those for the determination of Co, Se or Fe in biological materials , with their expanded uncertainties of 2.7-3.4% are comparable to those by ID-MS. Definitive methods by RNAA are the only methods of such class, possible for monoisotopic elements. In accordance with the ISO/IEC Guide 99:2007, definitive methods by RNAA may be termed: Ratio primary reference measurement procedures (RPRMPs). Such methods are intended for verification of accuracy of other methods of trace analysis and certification of the candidate reference materials.

APSORC'13 - 5th Asia-Pacific Symposium on Radiochemistry
Kanazawa, Japan, 22-27 September 2013

Overview of the Fukushima Dai-ichi nuclear power plant (FDNPP) accident, with amounts and nuclear compositions of the released radionuclides

Masayoshi Yamamoto
Low Level Radioactivity Laboratory, KINET, Kanazawa University, Nomi, Ishikawa 923-1224, Japan

Since release of artificial radionuclide into the environment was first initiated in 1945 at Alamogordo, New Mexico, the emission developed through the World War II of Hiroshima and Nagasaki, and continued with nuclear weapons testings, which finished in 1980. Furthermore, accidental releases of radioactivities have occurred through the events such as the fall of nuclear-fueled satellites, and accident in nuclear power plants and the related facilities (Windscale (Sellafield), Three Mile Island, Chernobly, etc.). The Japanese also experienced tragedies of the Fifth Fukuryu-Maru accident at Bikini atoll (1954) and the JCO criticality accident at Tokai-mura (1999).

This time, as widely recognized, the *M 9.0* earthquake off the Pacific coast of Japan on 11 March 2011 and the subsequent tsunami induced an accident in the FDNPP. Total loss of electric power happed and the cooling systems of some of the reactor units 1-3 failed, resulting in hydrogen explosion in the reactor buildings and venting of gases, with significant releases of radionuclides into the atmosphere. In addition, highly contaminated water with large amounts of radionuclides was directly leaked or discharged into the North Pacific. Public health actions to reduce the negative consequence of this event were taken by government; a 20-km evacuation zone was put in place around the site, with a sheltering zone between 20 and 30 km. The Japanese Government and various prefectural governments started emergency monitoring of radioactivity to assess the environmental and human effects by the FDNPP accident. The details of the FDNPP accident have been already opened in a report by the Japanese Government to the IAEA (IAEA 2011, NISA, 2011, Japanese Government 2011). The Fukushima accident was classified on the INES (International Nuclear and Radiological Event Scale) scale at the maximum level of 7, being the same as that of the Chernobyl nuclear power plant (CNPP) accident (April 26, 1986). Compared to the CNPP accident, the FDNPP accident presents a much more difficult situation, since various reactor cores and spent fuel pools may have contributed to the emissions.

Several atmospheric radionuclide releases occurred mainly during the periods from March 12 through March 23, 2011. The air contaminated by the released radionuclides, especially noble gas (^{133}Xe, etc.) and volatile nuclides such as ^{131}I, ^{134}Cs and ^{137}Cs, eventually spread over large distances, and were observed at monitoring stations (IMS by CTBTO) throughout the world. In Japan, the radionuclide fallout resulted in a track of contaminated land that expanded approximately 50 km to the northwest of the FDNPP and later in a larger, lower level area of contamination mostly to the south and southwest. Total estimated atmospheric releases of ^{131}I and ^{137}Cs by government are around 160 and 15 PBq, respectively, although exact amount of radionuclides emitted are still being argued. These levels are lower for ^{131}I and ^{137}Cs by about a factor of 12 and 7, respectively, compared with those of the CNPP accident. More than 70% of the released radionuclides into the atmosphere were deposited over the North Pacific. Thus, by broad survey and early investigations, whole picture about levels and spreading areas of contaminants, especially ^{134}Cs and ^{137}Cs, has been becoming clear, together with the situation of the plant. For radioiodine released, this nuclide consists of gaseous and particulate forms, therefore, its behavior seems to be very difficult, resulting in large variation of ^{131}I/^{137}Cs ratios measured in air and soil. Since ^{131}1 is a short half-life (8 d), its reconstruction in the initial stage by ^{129}I is attempted to evaluate the impact of human health from radioiodine. For other possible released radionuclides, radiostrontium (^{89}Sr and ^{90}Sr) and transuranic nuclides, which have attracted much scientific and potential radiological concern, are poorly investigated, mainly because of the difficulties of analyzing and measuring these beta- and alpha-emitting radionuclides. These nuclides are much less volatile than other fission products such as cesium and iodine isotopes. TEPCO published a ^{90}Sr/^{137}Cs ratio in soils 10^{-3}. Actual environmental measurements showed variability in the ^{90}Sr/^{137}Cs ratios for different locations, ranging of 10^{-2}-10^{-4} in surface soils within the 50 km area from the FNPP. On the other hand, in addition to the limited data of Pu isotopes in soil and litter samples, ^{236}U, Pu isotopes (^{238}Pu, ^{239}Pu and ^{240}Pu), ^{241}Am and Cm isotopes (^{242}Cm and ^{243,244}Cm) have been measured by us for roadside dust collected at the Fukushima areas heavily contaminated. When the ratios among these nuclides measured are compared with those of fuel compositions in the FDNPP estimated by Nishihara et al (2012) of the JAEA group, fairly good agreement was found, indicating that traces of U and transuranic nuclides, probably with forms of fine particles, were released into the environment without their large fractionation. In any event, such measurements may allow us to give information (burn-up, conditions of fuel during the release phase, etc.) on the on-site situation, which may be difficult to receive otherwise.

In this presentation, I have two main objectives as follows: first, I will show the overview of the accident, second, I want to present the amounts and isotopic signatures of the released radionuclides, especially transuranic nuclides. We hope that this special session on Fukushima accident promotes further investigations about radiological impact of the accident and transport dynamics.

PL-02

Fukushima Challenges in Perspective

Ian G. McKinley[1], Susie M. L. Hardie[1], Elizaveta Klein[1]
[1]MCM Consulting, Täfernstrasse 11, 5405 Baden-Dättwil, Switzerland

Keywords – Fukushima, decontamination, radioactive waste, knowledge transfer, communication

The accident at the Fukushima Dai-ichi nuclear power plant was undoubtedly a local industrial disaster that has had a global impact on the "nuclear renaissance", which was beginning to blossom in 2011. Nevertheless, from a purely radiochemical perspective, the environmental consequences of the core meltdowns were significantly less than a worst case scenario and much can be learnt from this. A key factor was containment of most of the radioactivity from the fuel melt within the reactor buildings, releases being limited to volatile elements, which were either vented to the atmosphere or picked up by cooling waters. This will make decommissioning of the heavily contaminated parts of units 1-4 tricky, but the overall situation is certainly less problematic than Chernobyl.

The most significant radionuclides off-site were isotopes of I and Cs, possibly the best understood of all environmental radionuclides due to the huge knowledge base built up since the middle of the last century [1]. Evacuation, issue of iodine tablets and limitation of consumption of contaminated foodstuffs has ensured that radiological risks to the general public have been negligible. Subsequent remediation actions will complement decay and "self-cleaning" to ensure that most of the evacuated populations can safely return home and resume normal lifestyles in the near future. Nevertheless, a huge volume of radioactive waste will result, which needs to be managed in a safe and efficient manner.

For the international community, there are two issues to be considered – how can experience from other locations be utilised to support recovery in Fukushima and how can the experience gained from this incident be taken over to reduce the risk of something similar happening elsewhere and also to increase the effectiveness of any similar large-scale clean-up operations, for example in military legacy sites? Here modern "knowledge management" technology can facilitate the process of capture and transfer of such experience.

Apart from such technical considerations, a special challenge after the accident was communicating information on extent of contamination and progress with cleanup to the general public. This is an international concern and is complicated by campaigns of disinformation by nuclear opponents and the tone of reporting by a generally critical mass media. The nuclear industry, government organisations and professional bodies have all performed poorly here - the response to public concerns being virtually non-existent. This indicates that, despite the pervasive nature of background radiation and the widespread use of radionuclides in medicine, industry and research, radiochemists need to take a more active role in public education, to help replace non-technical audiences' visceral fear of anything radioactive with a real understanding of the issues involved.

REFERENCES

[1] McKinley, I.G., Grogan, H.A., McKinley, L.E., Fukushima: Overview of relevant international experience. J. Nuclear Fuel Cycle and Environment, **18**, 89-99 (2011)

Atmospheric transport of radioiodine and radiocesium released in the early phase by the Fukushima Daiichi Nuclear Power Plant accident from field measurements and a simulation model

Haruo Tsuruta[1], Masayuki Takigawa[2], Teruyuki Nakajima[1]
[1]Atmosphere and Ocean Research Institute, The University of Tokyo, Kashiwa, Chiba 277-8568, Japan
[2]Japan Agency for Marine-Earth Science and Technology, Yokohama, Kanagawa 236-0001, Japan

Abstracts – The continuous measurements of atmospheric concentration of ^{131}I and ^{137}Cs at ten stations in the Kanto area located 120km south from Fukushima, showed that $^{131}I/^{137}Cs$ and the ratio of particulate ^{131}I to the sum of particulate ^{131}I and gaseous ^{131}I significantly changed in the periods when the polluted air masses were transported, compared with those in the other periods. A numerical model well simulated the transport of the polluted air masses to the Kanto and Fukushima area, while any field data did not suggest the transport to Fukushima on March 20-21due to no precipitation.

Keywords – FD1NPP accident, gaseous and particulate ^{131}I, ^{137}Cs, $^{131}I/^{137}Cs$, atmospheric concentration

I. INTRODUCTION

A large amount of radioactive materials was released into the atmosphere after the accident of the Fukushima Daiichi Nuclear Power Plant (FD1NPP) caused by the Tohoku Earthquake and Tsunami on March 11, 2011, and was transported and deposited to the land surface in a regional scale. Many datasets have been opened such as the routine monitoring of radiation dose rate and fallout by MEXT, and the regional map of radionuclides deposited to the land surface by MEXT, and by aircraft monitoring by MEXT and DOE. In contrast, continuous monitoring of atmospheric radionuclides in an early phase after the accident, was made only in the Kanto area located more than 120km south from the Fukushima prefecture, although it is critical for evaluation of the internal exposure dose, reconstruction of time-dependent release rate of radionuclides, and for validation of numerical simulations by atmospheric transport models. The purpose of this paper is to summarize new findings on atmospheric ^{131}I and ^{137}Cs from the field measurements, and to discuss the results of transport pathways by a numerical model.

II. MATERIALS AND METHODS

In the Kanto area, ten research groups independently measured radionuclides in the atmosphere just after the accident, and their results and/or datasets were already reported, and most of them have been summarized elsewhere[1]. Furthermore, gaseous ^{131}Ig and particulate ^{131}Ia were separately measured at a few stations. The datasets were used for an analysis of time series of atmospheric concentration of ^{131}I and ^{137}Cs, $^{131}I/^{137}Cs$ (=R1), and $^{131}Ia/(^{131}Ia+^{131}Ig)$ (=R2). A numerical simulation of radioactive materials in the atmosphere was performed by using an atmospheric transport model for radionuclides based on a regional chemical transport model of WRF/Chem[2]. In the model, the radionuclide of ^{131}I and ^{137}Cs was taken into account, and their release rates were based on the estimate by Katata et al.[3].

III. RESULTS AND DISCUSSION

According to the field measurements in the Kanto area, high concentrations of ^{131}I and ^{137}Cs (>100 Bq m^{-3}) were measured during March 15-16 (the first period) and March 20-23 (the second period), and ^{131}I was much higher than ^{137}Cs. A numerical simulation by the atmospheric transport model showed that the polluted air masses with high ^{131}I and ^{137}Cs were directly transported to the Kanto area from the FD1NPP in the morning of both periods by northeasterly wind, in good agreement with the results of the field measurements. The model also simulated the transport of the polluted air masses to the Fukushima area in the afternoon to the midnight in both periods. The radiation dose rates and deposition rates in the Fukushima area increased only in the first period with precipitation, supporting the transport. On the contrary, they did not show any increase in the second period due to no precipitation. The recent analysis for stored filters on which atmospheric aerosols in the early phase were collected, revealed the high concentration of ^{137}Cs in both periods[4,5], validating the calculated transport of the polluted air masses by the model.

The time series of R1 at all the stations showed that R1 was around or less than 10 when the plume with high radionuclides from the FD1NPP was transported in the Kanto area, which was almost equal to the ratio in a calculated core inventory on March 11, 2011[6]. In contrast, R1 was around 100 in the other periods. On the morning of March 22 when the polluted air masses were also transported to the Kanto area, R1 increased to around 100, much higher than that in the previous day, suggesting the possible change in the release condition in the reactor units. The ratio of R2 was 0.4-0.8 when the plume was directly transported, while it was 0.1-0.3 in the other periods. Hence, the ratio of R1 and R2 at the time when the radionuclides were released into the atmosphere possibly suggests any change in conditions of the reactor units.

[1] Tsuruta et al. (2012), Proceedings of the 1st NIRS Symposium on Reconstruction of Early Internal Dose in the TEPCO Fukushima Daiichi Nuclear Power station accident, Chiba, Japan
[2] Takigawa (2012), Proceedings of 92nd American Meteorological Society, New Orleans, US.
[3] Katata et al. (2012), J. Environ. Radioactiv., 109, 103-113.
[4] Oura et al. (2013), A paper in the APSORC'2013.
[5] Tsuruta et al. (2013). A paper in the APSORC'2013.
[6] Nishihara et al. (2012), Transactions of Atomic Energy Society of Japan, 12, 13-19.

APSORC'13 - 5th Asia-Pacific Symposium on Radiochemistry
Kanazawa, Japan, 22-27 September 2013

Migration of Radiocesium and Radioiodine released by FDNPP accident in the terrestrial environment and its interpretation by their speciation analyses

Yoshio Takahashi,[1] Qiaohui Fan,[1] Yoko S. Togo,[2] Aya Sakaguchi,[1] and Kazuya Tanaka[1]
[1]Graduate School of Science, Hiroshima University, Higashi-Hiroshima, 739-8526, Japan
[2]National Institute of Advanced Industrial Science & Technology (AIST), Tsukuba, Ibaraki 305-8567, Japan

Abstract – Distribution of radiocesium and radioiodine such as vertical profile in soil layer, particulate matter-water distribution in river water, and size distributions in sediments were studied to understand their migration in the terrestrial environment in Fukushima area. In addition, speciation studies on cesium and iodine focusing on (i) the surface complex structure of cesium on clay minerals and (ii) formation of organoiodine in soil have been conducted, which can clearly explain the possible chemical processes that control the behavior of these radionuclides in the terrestrial environment.

Keywords – FDNPP accident, radiocesium, radioiodine, clay mineral, humic substances, X-ray absorption fine structure

I. INTRODUCTION

Radionuclides such as radiocesium and radioiodine were emitted from the Fukushima Daiichi Nuclear Power Plant (FDNPP) accident caused by the Great East Japan Earthquake and Tsunami on March 11, 2011. Highly contaminated areas spread in the northwest direction from FDNNP in Fukushima Prefecture, which mainly resulted from the distribution of the wet deposition on March 15 [1]. After the deposition, they have migrated in the terrestrial environment depending on their chemical properties and interactions with various components in the soil, sediment, and water. In this presentation, we report our results on the distributions of radiocesium and radioiodine in soil, river water, and sediments in Fukushima coupled with speciation studies of cesium and iodine in the systems that should be important to understand their behaviors in the terrestrial environment.

II. EXPERIMENTAL

Distributions of radiocesium in the soil layer, river water, and river sediments mainly in Fukushima Prefecture were determined. Vertical profile in soil was also obtained for radioiodine. Sequential extraction studies have been also conducted for radiocesium and radioiodine to estimate main chemical species of the radionuclides. On the other hand, interactions of radiocesium with various clay minerals in the absence and presence of humic acid were examined by X-ray absorption fine structure (XAFS) to interpret the behavior of radiocesium in the soil-water and river water-sediment systems. Formation of organoiodine species were also examined using XAFS in laboratory and natural systems.

III. RESULTS AND DISCUSSION

After the deposition of radiocesium and radioiodine, their vertical profiles in soil in Fukushima showed that more than 90% of radiocesium and radioiodine have been retained within 5 cm from the surface [2]. Leaching experiment of the soil sample showed that radiocesium is strongly bound to soil particles. Size distribution analyses for particulate matters and sediment particles in rivers in the region showed that radiocesium is enriched in finer particle fractions. These results suggested that radiocesium has a high affinity for soil particles, in particular for clay minerals. Thus, XAFS spectroscopy has been used to characterize structure of surface complex of cesium to solid phase [3]. It was found that cesium forms inner-sphere complex to 2:1 phyllosilicate with medium interlayer distance such as vermiculite and weathered illite. In the presence of humic substances, however, formation of inner-sphere complex was inhibited because of the blocking effect of humic substances on the adsorption of cesium into the interlayer. This result also showed that direct complexation between radiocesium and humic substances is not important. These results are consistent with sequential extraction analysis of soil samples and clay mineral-humic substances hybrid containing cesium.

As for radioiodine, about 30% of radioiodine leached by NaOH solution (pH 10.5) from the soil collected one month after the accident [2]. When the extracted solution was acidified, more than 60% of radioiodine was precipitated possibly with humic materials that can bind iodine in the polyorganic structure. This leaching-precipitation behavior suggests that a part of iodine is in the organic form in the soil, which can be a reason for the retention of radioiodine in the soil surface. The formation of organic iodine in natural soil has been suggested by XAFS using X-ray microbeam [4], which can proceed in a relatively short period, such as within a week or a month. Thus, the formation of organoiodine is likely for radioiodine in the soil.

As seen above, speciation studies of cesium and iodine can explain the chemical processes controlling migration behaviors of radiocesium and radioiodine in Fukushima area.

[1] N. Yoshida and Y. Takahashi, Elements 8 (1012) 201.
[2] K. Tanaka et al., Geochem. J. 46 (2012) 73.
[3] Q. Fan et al., submitted to Geochim. Cosmochim. Acta.
[4] Y. Shimamoto et al., Environ. Sci. Technol. 45 (2011) 2086.

Oceanic and coastal dispersion of ^{134}Cs and ^{137}Cs released from the TEPCO Fukushima NPP1 accident: past, present and prediction

Michio AOYAMA[1], Yasunori HAMAJIMA[2]
1Meteorological Research Institute, Tsukuba, 305-0052 Japan
2 Low Level Radioactivity Laboratory,Kanazawa University, Nomi, Ishikawa 923-1224, Japan

Abstract: The bulk of the anthropogenic radionuclide ^{137}Cs present in the oceans today was injected about five decades ago from atmospheric nuclear weapons tests. In the North Pacific Ocean ^{137}Cs inventory was 290 ± 30 PBq in 1970 and it was 69 PBq just before the TEPCO Fukushima Dai-ichi Nuclear Power Plant (FNPP1) accident. An impact of FNPPP1 accident to the North Pacific Ocean in terms of inventory was estimated to be 10 – 13 PBq by atmospheric deposition and 3.5 ± 0.7 PBq by direct discharge, therefore the total ^{137}Cs inventory in the North Pacific Ocean increased by up to 20 – 23%.Fukushima released radiocaesium already subducted in 2011/2012 winter and formed subsurface maximum at a densities of Central Mode Water (CMW), and Subtropical Mode Water (STMW).

Key words: *^{137}Cs, Pacific Ocean, inventory, subduction, radioactive plume*

I. INTRODUCTION

On 11 March 2011, an extraordinary earthquake of magnitude 9.0 centered about 130 km off the Pacific coast of Japan's main island, at 38.3 ºN, 142.4 ºE, was followed by a huge tsunami with waves reaching up to 40 m height in Iwate region and about 10 m in Fukushima region. The station blackout developed into a disaster that left three of the six FNPP1 reactors heavily damaged, meltdown of core, and caused radionuclides to be discharged into the air and ocean[1, 2].

II. SAMPLING AND METHODS

We collected 2 litre surface seawater samples at more than 300 stations. The samples were treated by an improved ammonium phosphomolybdate, AMP, procedure [3, 4].

III.RESULTS

^{134}Cs and ^{137}Cs activities in surface water at Hasaki, a coastal station 180 km south of the Fukushima Dai-ichi Nuclear Power Plant (FNPP1) accident site, were observed in April to December 2011 [5]. The maximum in radiocaesium activity at Hasaki was observed in June 2011, representing a delay of two months from the corresponding maximum in April 2011 at FNPP1. Directly discharged ^{134}Cs and ^{137}Cs were transported dominantly southward along the coastline of north eastern Honshu, at least in May and June 2011.

Before the FNPP1 accident, ^{137}Cs was already exist which was originated from the nuclear weapon tests conducted in the late 1950s and in the early 1960s [4, 6]. In the western North Pacific Ocean, ^{90}Sr and ^{137}Cs activities in surface water was 10 – 100 Bq m^{-3} in the late 1950s and in the early 1960s, then it decreased gradually and the ^{137}Cs activity in surface water decreased to around a few Bq m^{-3} just before FNPP1 accident as shown in Figure 1[6, 7].

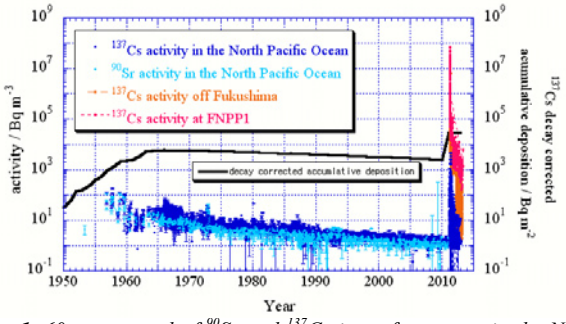

Figure1. *60 years trend of ^{90}Sr and ^{137}Cs in surface water in the North Pacific Ocean and decay corrected accumulative deposition in Tokyo/Tsukuba, Japan.*

The ^{137}Cs inventory in the North Pacific Ocean was 290 ± 30 PBq in January 1970 based on 10 º by 10 º mesh data of the ^{137}Cs deposition [7]. In 2003, ^{137}Cs inventory in the North Pacific Ocean was 86 PBq by the model study [8] and 85 PBq by the observation [9], then it decreased to 69 PBq in 2011 because due to decay [9].

The horizontal distribution of FNPP1 derived ^{134}Cs in the western North Pacific Ocean except just in front of the FNPP1 site showed that the high concentration area located close to the FNPP1 accident site which might have received both atmospheric deposition – showing good consistency with previous atmospheric transport model study [10] – and direct discharge [2] from the FNPP1 site. During the winter between 2011/2012, Fukushima derived radiocaesium subducted and formed subsurface maximum at a densities of Central Mode Water (CMW) of which depth is about 400 meters depths and Subtropical Mode Water (STMW) of which depth is about 150 meters depths due to cooling at sea surface. This implies that a speed of main body of Fukushima derived radiocaesium will be decreased much because of less wind driven force at subsurface layers rather than those at surface layers which was 8 cm s-1 as the average speed of radioactive plume at sea surface stated previously. [6]

REFERENCES

1. Chino, M., et al., Journal of Nuclear Science and Technology, **48**(7), p. 1129-1134, 2011.
2. Tsumune, D., et al., J Environ Radioact, **111**, p. 100-108, 2012.
3. Hirose, K., et al., Journal of Radioanalytical and Nuclear Chemistry, **263**(2), p. 349-353, 2005.
4. Aoyama, M. and K. Hirose, *Radiometric determination of anthropogenic radionuclides in seawater*, in *Radioactivity in the Environment*, P.P. Pavel, Editor. 2008, Elsevier. p. 137-162.
5. Aoyama, M., et al., Geochem. J, **46**, p. 321-325, 2012.
6. Aoyama, M., et al., Progress In Oceanography, **89**(1-4), p. 7-16, 2011.
7. Aoyama, M., K. Hirose, and Y. Igarashi, Journal of Environmental Monitoring, **8**(4), p. 431-8, 2006.
8. Tsumune, D., et al., Progress In Oceanography, **89**(1-4), p. 38-48, 2011.
9. Aoyama, M., D. Tsumune, and Y. Hamajima, Journal of Radioanalytical and Nuclear Chemistry, p. 1-5, 2012.
10. Honda, M.C., et al., Geochem. J, **46**, p. e1-e9, 2012.

FKI-04

Interactions between nuclear fuel and water at the Fukushima Daiichi Reactors

Bernd Grambow[1]
[1] SUBATECH (Ecole des Mines de Nantes, University of Nantes, IN2P3-CNRS)
4 rue Alfred Kastler, 44307 Nantes, France,
Grambow@subatech.in2p3.fr

The rapid increase in temperature in the cores of the Fukushima reactors was caused by the loss of coolant in the aftermath of the damage from the tsunami. High temperatures caused partial melting of not only the UO_2 in the fuel but also the zircaloy cladding and steel, forming a quenched melt, termed corium. Substantial amounts of volatile fission products, such as Xe, Cs and I, were released during melting, but the less volatile fission products and the actinides (probably >99.9%) were incorporated into the corium as the melt cooled and was quenched. The corium still contains these radionuclides, which leads to a very large long-term radiotoxicity of the molten reactor core. Access by water to the core may constitute an important vector for transfer of radioactivity. The challenge for radiochemists is to assess the long-term interactions between water and the mixture of corium and potentially still-existing unmelted fuel, particularly if the molten reactor core is left in place and covered with a sarcophagus for hundreds of years. Part of the answer to this question can be found in the knowledge that has been gained from research into the disposal of spent nuclear fuel in a geologic repository.

Comparison of radionuclide release during the accident from the reactors with the radionuclide inventories remaining in the reactor and estimation of corium–water interaction from known spent fuel–water interaction provide important insight for developing assessment and management strategies for the molten fuel in the reactor cores. Furthermore, analyzing the radiochemical analyses of the temporal evolution of the radioactive elements in the cooling water of the accidental reactors provide valuable information on the chemical state of the corium and potential phase separations. Models for corium stability and for radionuclide release from corium upon contact with water will have to be developed based on (1) analyses of radionuclide activities in actual cooling waters, (2) chemical modeling of the analytical results in the context of the kinetics and thermodynamics of actinide and fission product release (solubility constraints, redox states, etc.), and (3) comparison with spent fuel behavior and experimental corium databases. Such models may be very useful in developing appropriate corium management strategies.

Determination of ^{129}I in the Accumulated radioactive water and processing water of Fukushima Daiichi Nuclear Power Plant

Asako Shimada[1,2], Keiichi Sakatani[1], Yutaka Kameo[1,2], Kuniaki Takahashi[1]
[1] Nuclear Cycle Backend Directorate, Japan Atomic Energy Agency
[2]Fukushima Project Team, Japan Atomic Energy Agency

Abstract – Accumulated radioactive water (AW) and processing water (PW) were sampled from some positions of the Accumulated Radioactive Water Processing Facility (ARWPF) at Fukushima Daiichi Nuclear Power Plant (FDNPP) to estimate the radioactivity of the secondary waste such as zeolite and sludge which adsorbed radioactive material. Separation method of I^- from the radionuclides using solid phase extractant, Anion-SR, was developed. After the chemical separation, the concentration of ^{129}I in the sampled water was determined by Inductively Coupled Plasma Mass Spectrometry with dynamic reaction cell (DRC-ICP-MS).

Keywords – ^{129}I, Accumulated radioactive water, Fukushima Daiichi Nuclear Power Plant, Anion-SR

I. INTRODUCTION

In the early stage of the handling to cool down the reactor core of FDNPP, seawater was poured in the severely damaged reactor buildings. Highly contaminated water was leaked and accumulated in the reactor and turbine buildings. The ARWPF were installed to decontaminate the radioactive materials and to desalinate. Highly contaminated sludge was generated from these apparatus as the secondary waste. To estimate the radioactivity of the waste, AW and PW were sampled from the inflow and outflow of the apparatus.

Because of the long half-life, ^{129}I is one of the important nuclide to assess the safety of radioactive waste disposal. The present study focuses the development of separation method of I^- and determination of ^{129}I in the sampled water. Separation method of I^- with Anion-SR was optimized to improve the detection limit of ^{129}I and to reduce radioactivity of the analyte. After separation, the ratio of ^{127}I and ^{129}I were determined by DRC-ICP-MS to reduce the influence of ^{129}Xe.

II. EXPERIMENTAL

Samples

The AW and PW were sampled at ①reactor/turbine building, ②, ③outflow of Cs adsorption apparatus, ④ outflow of decontamination instruments, ⑤outflow of Cs adsorption apparatus, ⑥outflow of desalination apparatus, ⑦concentrated sea water tank, ⑧processed water tank ⑨ outflow of evaporative concentration apparatus, as shown in Fig.1.

Separation of I with Anion-SR

Anion-SR disk was assembled suction filtration apparatus. The disk was conditioned by passing solutions as follows; 1. 10 ml acetone, 2. 10 ml methanol, 3. 5 ml ultrapure water, 4. 5 ml of 1 M HNO_3, 5. 10 ml ultrapure water, 6. 15 ml of 1 M NaOH (ultrapure), 7. 3 times of 15 ml ultrapure water. After then, sample solution was passed through the disk and the disk was washed with ultrapure water. The extracted I^- was recovered with 9.5 ml of 1 M HNO_3 in the 10 ml measuring flask, and 50 µl NaClO was added to oxidize I^- to IO_3^-. Finally, 1 ml of 1 M HNO_3 was added untill the total volume became 10 ml. The ratio of ^{127}I and ^{129}I was determined by DRC-ICP-MS.

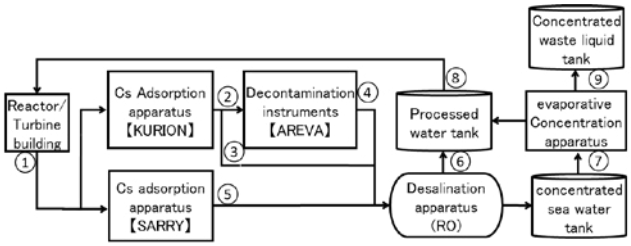

Fig.1 Sampling point of the AW and PW

III. RESULTS AND DISCUSSION

Because sample volume of the AW and PW was 0.1 ml, they were needed to be diluted by appropriate solution to carry out the separation of I^- with Anion-SR. Before analysis of the water samples, the dilutant was optimized. Five ml of 3 M NaOH (ultrpure), 3 M NaOH (97%), 2.7 M tetramethyl ammonium hydroxide (TMAH, ultrapure), and 3 M Na_2CO_3 (99.8%) solutions were examined as the diluent to obtain high recovery of I^- and low contamination for the DRC-ICP-MS measurement. Approximately 90% recovery was accomplished by all the examined dilutant, whereas the lowest back ground count from blank operation was obtained for ultrapure 3 M NaOH solution. Therefore, it was used for the analysis of AW and PW samples.

Iodide in AW and PW solution was analyzed with and without known amount of ^{127}I spike, and the concentration was calculated with the ratio of ^{127}I and ^{129}I. Table 1 shows the concentration of ^{129}I in the AW and PW samples. It was found that ^{129}I was decontaminated by desalination and evaporation apparatus. Results of periodically measurements and development of analysis of IO_3^- with I^- will be delivered on the presentation.

Table 1 Concentration of ^{129}I in the AW and PW samples

Concentration of ^{129}I /Bq· g^{-1}		
① 0.25±0.002	④ 0.085±0.001	⑦ 0.18±0.002
② 0.083±0.002	⑤ 0.13±0.001	⑧ <0.021
③ 0.27±0.003	⑥ <0.021	⑨ 1.3±0.03

Measurement of Iodine-129 in surface soil collected near the Fukushima Daiichi nuclear power plant accident site

Yasuto Miyake[1], Hiroyuki Matsuzaki[1], Takeshi Fujiwara[2], Takumi Saito[2], Takeyasu Yamagata[3] and Maki Honda[3]

[1]Department of Nuclear Engineering and Management, School of Engineering, The University of Tokyo, Japan
[2] Nuclear Professional School, School of Engineering, The University of Tokyo, Japan
[3]Nihon University, Japan

Abstract – Iodine-129 in soil around Fukushima Daiichi nuclear power plant were measured by Accelerator Mass Spectrometry and isotopic ratio of radioiodine was estimated. Surface deposition amount of Iodine-129 resulted in 6.7 to 5500mBq/m^2. The mean isotopic ratio between Iodine-129 and Iodine-131 at the accident was estimated that $^{129}I/^{131}I = 26 \pm 6$ as of March 11 2011. This result was compared to the calculation result of ORIGEN2 code to test the validity of this estimation.

Keywords – FDNPP accident, Iodine-129, Accelerator Mass Spectrometry, soil, isotopic ratio

I. INTRODUCTION

A lot of radioactive materials were released into the environment owing to the Fukushima Daiichi nuclear power plant (FDNPP) accident. Among them, Iodine-131 has already decayed out and cannot be detected now. On the other hand, Iodine-129, which is the isotope of Iodine-131, has long half-life and can be measured by Accelerator Mass Spectrometry. If isotopic ratio of radioactive iodine ($^{129}I/^{131}I$) at the initial stage at the accident is obtained, distribution of Iodine-131 at the accident can be reconstructed by measuring Iodine-129 in soil. In this study, Iodine-129 was measured in soils, which were collected within 60km distance from FDNPP on April 2011.

II. METHOD

50 soil samples were collected within 60km distance from FDNPP on April 20, 2011. Sampling strategy was shown in other paper [1]. Iodine-131 and other radionuclides have already been determined by gamma ray measurement [1]. In order to extract Iodine from soil, homogenization, combustion, solvent extraction, and back extraction were conducted [2]. After making AgI precipitation, samples were pressed into a cathode for AMS and ^{129}I was measured at MALT (Micro Analysis Laboratory, Tandem accelerator), The University of Tokyo. Iodine-127 in soil was measured by ICP-MS at the University of Tokyo.

III. RESULTS AND DISCUSSION

Surface deposition amount of Iodine-129 resulted in between 6.7 to 5500mBq/m^2 within the area 60km distant from FDNPP. These values were corresponding to Iodine-129 concentration between 7.8E7 to 5.9E10atoms/g. Iodine-127 concentration was distributed from 1 to 16ppm. The mean isotopic ratio of $^{129}I/^{131}I$ =26 ± 6 on March 11, 2011 was obtained.

In order to check the validity of analytical result, it was compared to the calculation result of ORIGEN2 code [3]. In Fig. 1, $^{134}Cs/^{137}C$ data were plotted against $^{129}I/^{131}I$ data. Each of nuclides was decay-corrected as of March 11, 2011. Not only observation results but also calculation data of isotopic ratio of Unit 1, Unit 2, and Unit 3 were shown here.

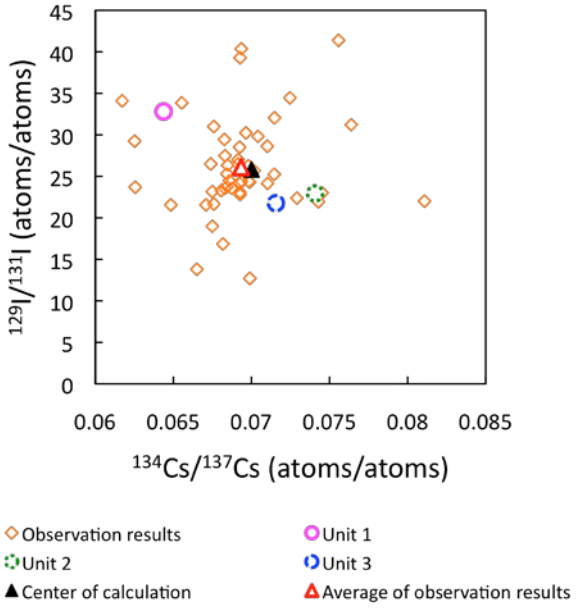

Fig. 1. Comparison of isotopic ratio of radioiodine and radio cesium between observation results and calculation result of ORIGEN2 code

In Fig. 1, average of observation results is located close to center of calculation and this average seems to be affected by Unit 1. This suggests contribution of Unit 1 might be larger than expected or there are other reasons. Problems are still under debate.

IV. REFERENCE

[1] Fujiwara et al., J. Environ. Radioact., 113, 37 – 44 (2012).
[2] Miyake et al., Geochemical Journal, vol. 46, 327 – 333 (2012).
[3] Nishihara et al., JAEA-Data/Code, 2012-018 (2012).

APSORC'13 - 5th Asia-Pacific Symposium on Radiochemistry
Kanazawa, Japan, 22-27 September 2013

Speciation of ^{137}Cs and ^{129}I in surface soil in Kanto loam layer after the Fukushima NPP accident

Tomoko Ohta[1], Takumi Kutoba[2], Yasunori Mahara[3], Hiroyuki Matsuzaki[4], Toshifumi Igarashi[1]

[1] Faculty of Engineering, Hokkaido University
[2] Research Reactor Institute, Kyoto University
[3] *Professor Emeritus,* Kyoto University
[4] School of Engineering, The University of Tokyo

Abstract
We measured chemical speciation of ^{137}Cs and ^{129}I in the surface soil of Kanto loam after Fukushima nuclear disaster. We observed the behavior of ^{137}Cs and ^{129}I in soil samples of the Kanto loam layer: more than 90% of ^{137}Cs was fixed by organically bound and residual fractions, while ^{129}I was mainly fixed by Fe-Mn oxidation and organically bound.

Keywords –Cs-137, I-129, Fukushima nuclear disaster, Kanto loam, Solid-phase extraction, leaching

Introduction

Sequential extraction has been proven to be a useful and practical technique for the speciation analysis of radionuclides in the soil and sediment samples (Desideri, et al., 2001; Desideri et al., 2002 ; Oughton et al., 1992; Riise et al.,1990; Tessier et al., 1979). We extracted ^{137}Cs and ^{129}I from surface soil samples from the Kanto-loam layer in eastern Tokyo metropolitan area.

Methods

The two soil samples of depths of 0−2.5cm were reduced by cone and quartering to approximately 10 g. Approximately 10 g of the samples were used in the sequential-extraction experiment. A solution/sample ratio of 5 (v/w) was used for extraction in each step (Fraction 1, 2, 3, 4, 5 and residue).
Fraction 1: Ultrapure water was added to the soil sample, and the sample was shaken for 24 h at room temperature. The sample was stored overnight. This fraction represents water-soluble species. The remaining solid on the filter paper was combined with the residue for the leaching in the next step.
Fraction 2: 1 M of NaAc was added to the residue from Fraction 1. The sample was shaken for 12 h at room temperature and stored overnight. This fraction represents exchangeable species.
Fraction 3: 1-M NaAc−HAc (pH 5) was added to the residue from Fraction 2, and the sample was shaken for 12 h at room temperature. This fraction represents carbonate-bound species.
Fraction 4: 0.04-M NH_2OH・HCl in 25% (v/v) HAc (pH 2) was added to the residue from the fraction and stirred in a hot-water bath at 80 °C for 4 h. This fraction represents species associated with solids via chemical-sorption mechanisms which can be released into the extraction solution with a weak reducing agent, and they mainly include species bound to Fe/Mn oxides.
Fraction 5: 30% H_2O_2 was added to the residue, in which HNO_3 had already been added to adjust the final pH to 2, and the sample was agitated for 2 h at 85 °C. After the sample solution was cooled to room temperature, 1.8-M NH_4Ac in 11% HNO_3 (v/v) was added, and the extraction continued for 30 mins at room temperature. This fraction is associated with organic matter.
After extraction, each solution was separated from the soil residue by centrifugation at 2000 rpm for 5 mins. The solution was filtered through a filter paper with a pore size of 0.45 μm. After each fraction was stored into the U-8 vessel, ^{137}Cs was measured by gamma-ray spectrometry (Hokkaido University). I-129 was measured by AMS (Tokyo University).

Result

The amount of ^{137}Cs leached into water (F1) from the Kanto-loam soil was below the detection limit. The rate of ^{137}Cs exchange from the two soil samples was less than 1%, with 50–60% of ^{137}Cs remaining in the residue. Approximately more than 90 % of ^{137}Cs was adsorbed on organic matter and the residue, while ^{129}I was mainly fixed by Fe-Mn oxidation and organically bound.

References

[1] Desideri, D., et al., 2001. Speciation of natural and anthropogenic radionuclides in different sea sediment samples. J. Radioanal. Nucl. Chem. 248, 727–33.
[2] Desideri, D., et al., 2002. Geochemical partitioning of actinides, ^{137}Cs and ^{40}K in a Tyrrhenian sea sediment sample: comparison to stable elements. J. Radioanal. Nucl. Chem. 251, 37–41.
[3] Oughton, D.H., et al., 1992. Radionuclide mobility and bioavailability in Norwegian and Soviet soils. Analyst. 117, 481–6.
[4] Riise, G., et al., 1990. A Study on Radionuclide Association with Soil Components using a Sequential Extraction Procedure. J. Radioanal. Nucl. Chem. 142, 531–8.
[5] Tessier, A., et al., 1979. Sequential extraction procedure for the speciation of particulate trace metals. Anal. Chem. 51, 844–50.

FKO-04

Transfer of radiocesium and radioiodine in the environment following the Fukushima nuclear accident

Yasuyuki Muramatsu[1], Takeshi Ohno[1], Naoya Inagawa[1], Kazumasa Oda[1], Mamoru Sato[2], Hiroyuki Matsuzaki[3]
[1]Gakushuin University, [2]Fukushima Agricultural Technology Centre, [3]The University of Tokyo

Abstract- Following the Fukushima accident, intensive studies have been carried out regarding the distribution and transfer of radionuclides that have been released into the environment. In this paper, the following two topics related to this theme are presented: (1) The importance of translocation pathways to understand the transfer of radiocesium into some crops such as tealeaves and citrus fruit. (2) The reconstruction of I-131 deposition in different places in Fukushima Prefecture through the analysis of long-lived I-129.

Keywords – Radiocesium transfer to plant, translocation pathway, I-129 analysis for the reconstruction of I-131 deposition

I. INTRODUCTION

Among radionuclides released from the accident of Fukushima Daiichi Nuclear Power Plant, radioiodine and radiocesium are very important from the viewpoint of environmental safety. Shortly after the accident, high I-131 concentrations were observed in leafy vegetables in Fukushima and in the surrounding Prefectures. The levels of I-131 in vegetables decreased markedly with time due to its short half-life (8 days), as a consequence more attention has been paid to the longer-lived radiocaesium (Cs-134 and Cs-137) deposited in soil. Results of the monitoring for agricultural crops harvested during spring to autumn in 2011 showed that most of crops had not exceeded the provisional guideline for radiocaesium of 500 Bq/kg for 2011. (After 2012 the guideline was changed to 100 Bq/kg.) However, values higher than the guideline were found in some crops such as bamboo shoots, some fruits (e.g. Japanese citron 'Yuzu') and new tealeaves. These high values could not be explained solely by root-uptake, which was previously assumed to be the primary pathway.

In this study we analyzed radiocesium concentrations in a variety of crops and studied the mechanisms of radiocesium transfer. Apart from radiocesium, we have studied the distribution of I-131 (half-life: 8 days) deposited in Fukushima Prefecture. Due to the short half-life of I-131, most of it decayed away after some months and there were not enough data to construct a deposition map for I-131. Since a long-lived I-129 (half-life: 15.7 million years) was also released from the accident, we have analyzed it for reconstructing I-131 deposition.

II. EXPERIMENTALS

Concentrations of radiocesium were determined with a Ge-detector in crop samples collected in Fukushima following the accident. For I-129 analysis, iodine fractions were separated from soil samples to make a AgI target for the determination of this nuclide by AMS.

III. RESULTS AND DISCUSSION

The distribution of radiocesium in an entire tea tree (old leaves, new leaves, bark, roots and soil) was studied and it was found that the new tealeaves that had not appeared until March 2011 also showed high values for this nuclide. It was found that translocation pathway from the contaminated old leaves and bark should be important to understand the high values observed in new leaves. Higher concentrations found in 'Yuzu' were also explained by the translocation pathway. The levels in tealeaves and 'Yuzu' harvested in the second year decreased significantly. High radiocesium concentrations found in bamboo shoots should be the effect of both translocation and root-uptake pathways.

Soil samples that had been determined for I-131 were analyzed for I-129 to estimate I-131/I-129 ratio. Amounts of I-131 deposition in different areas were reconstructed through the analysis of I-129 together with the obtained I-131/I-129 ratio.

APSORC'13 - 5th Asia-Pacific Symposium on Radiochemistry
Kanazawa, Japan, 22-27 September 2013

States of existence of the Cesium and Silver radionuclides at the sandy beach in Iwaki city, Fukushima

Yukihiko SATOU[1], Keisuke SUEKI[1], Kimikazu SASA[1] , Jun-ichi KITAGAWA[1,2], Satoshi IKARASHI[1]
[1]Graduate school of Pure and Applied Sciences, University of Tsukuba
[2]Radiation Science Center, High Energy Accelerator Research Organization and J-PARC Center

Abstract
We have made an investigation that shows the states of existence of radionuclides from the Fukushima Dai-ichi nuclear power plant (FDNPP) accident on the sandy beach in Iwaki city, Fukushima Prefecture, Japan. The ^{137}Cs and ^{110m}Ag were observed different behavior along the depth distribution of sand layer. As a result of the checking of the imaging plate photograph, ^{137}Cs from the FDNPP were attached to the granular spots. In addition, it is suggested that ^{110m}Ag and ^{137}Cs were independent for the same layer.

Keywords
^{110m}Ag, ^{137}Cs, Sandy beach, Depth distribution, Particle

I. INTRODUCTION

The Fukushima Daiichi nuclear power plant (FDNPP) disaster occurred in March 2011, various radionuclides were emitted from the FDNPP and deposited to a wide area of the northeastern Japan associated with precipitation. We already reported the fall out radionuclides were easily penetrated deeper layer in the sandy beach at the Iwaki city [1]. However, the cause of such a phenomenon is not yet understood clearly. For this reason, we have made a research that shows behavior and dynamics of months or longer half-life radionuclides such as ^{134}Cs, ^{137}Cs, and ^{110m}Ag in the sandy beach.

II. MATERIALS AND METHODS

Core soil sample (depth 30cm, D 5.0 cm) was collected at Yotsukura district, Iwaki city (E140.993, N37.1074) on 2 June 2011. Radionuclides in the sample were measured by a HPGe. More than one year has elapsed from the initial sample measurement, we have took the imaging plate photographs of the layer of more had accumulated ^{137}Cs in core sample. In addition, include soil sample of ^{110m}Ag was divided into 7 samples. Further were these samples measured radionuclides by using a HPGe detector.

III. RESULTS AND DISCUSSION

Figure 1(a) shows the depth distribution of radionuclides from the FDNPP. ^{137}Cs, ^{129m}Te, and ^{131}I were distributed broadly. On the other hand, ^{110m}Ag are predominantly confined in the 5-6 cm layer from top. Figure 1(b) shows imaging plate (IP) photograph of the sample containing a relatively large amount of ^{137}Cs. The granular radioactive nuclides were observed, and it seems that granular spots were consist on ^{137}Cs from the FDNPP resulting gamma ray spectrometry. In Figure 1(c), shows the fraction activity of ^{110m}Ag and ^{137}Cs in each sample. From the above observational results can be shown that ^{137}Cs and ^{110m}Ag were independent. In order to make clear for relationship between ^{137}Cs and ^{110m}Ag, additional chemical experiments required.

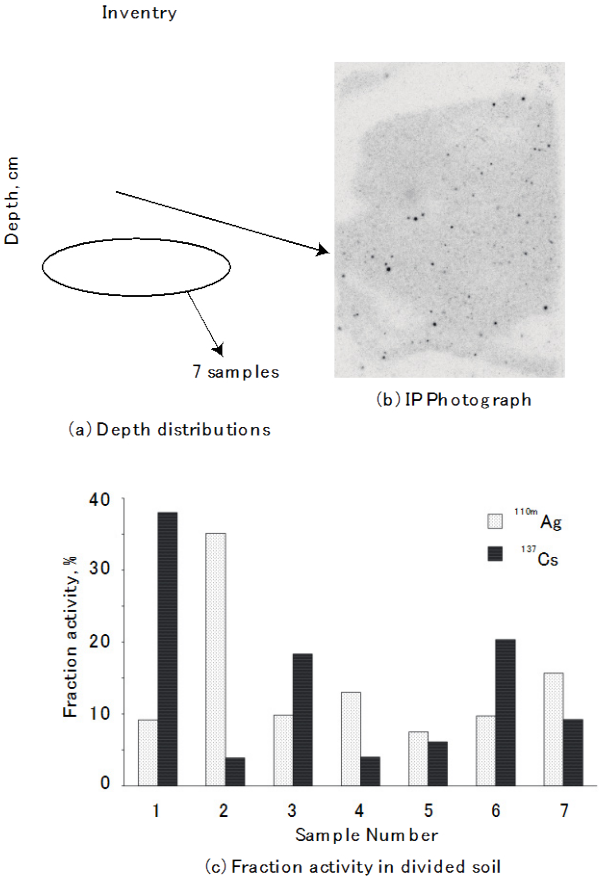

Figure 1 (a) Depth distribution of radioactivity inventories in the sandy beach core sample, (b) Imaging plate photograph in layer 4 from top level, (c) Fraction activity of 7 samples. Fraction activities are expressed as a percentage of the total activity (%)

REFERENCES

[1] Satou, Y., et al., J. Rad. Nucl. Sci. **12** Suppl. 116, 2011(Japanese)

Vertical transport of FNPP1-derived radiocesium by settling particles in the Western North Pacific

Makio C. Honda[1], Hajime Kawakami[1], Shuichi Watanabe[1], Toshiro Saino[1], Seiya Nagao[2], Ken Buesseler[3], Chris German[3], Steven Manganini[3]

[1]Japan Agency for Marine-Earth Science and Technology [2]Kanazawa University [3]Woods Hole Oceanographic Institution

Keywords – FNPP1, radiocesium, Western North Pacific, settling particle, sediment trap

Introduction

On March 2011, the 2011 Tohoku-Oki Earthquake occurred. This earthquake and the tsunami seriously damaged the Fukushima Daiichi Nuclear Power Plant (FNPP1). As a result, large quantities of radionuclides were emitted. About one month after the FNPP1 accident, FNPP1-derived radiocesium was dispersed to broad area in the Western North Pacific (WNP). Based on mathematical simulation, it was suspected that radiocesium detected in the WNP originated from not only contaminated water directly discharged, but also eolian input (Honda et al., 2012). It is well known that biogenic and lithogenic materials in the surface ocean are quickly transported to the ocean interior by settling particles. At the time of the FNPP1 accident, settling particles' collectors (sediment traps) had already been deployed at time-series stations in the WNP. We measured radiocesium (^{134}Cs, ^{137}Cs) in settling particles collected by sediment traps and verified how FNPP1-derived radiocesium was transported to the ocean interior.

Methods

Sediment traps were deployed at 500 m and 4810 m of time-series stations K2 (47°N/160°E, ca. 2000 km from FNPP1) and S1 (30°N/145°N, ca. 1000 km from FNPP1) in July 2010 and successfully collected settling particles before and after the FNPP1 accident. In July 2011, 4 months after the accident, sediment traps were also deployed at 500 m and 1000 m of F1 (36-30°N/141-30°E, ca. 100 km from FNPP1) and started collection of settling particles. After recovery, collected samples < 1 mm were dried and pulverized. Specific activities (activities) of ^{134}Cs and ^{137}Cs were measured by gamma spectrometry with a Ge detector.

Results and discussion

At stations K2 and S1, radiocesium was detected at 4810 m by middle April 2011 (Fig. 1 a, b). The sinking velocity was estimated to be 8 – 36 m day^{-1} between surface and 500 m, and > 180 m day^{-1} between 500 m and 4810 m. At 4810 m of K2, maximum ^{134}Cs flux and activity were observed in June 2011 and, thereafter, ^{134}Cs flux and activity decreased gradually. At 4810 m of S1, the highest ^{134}Cs flux was observed in early May 2011. It was notable that the maximum ^{134}Cs activity and relatively higher flux was observed in late November and early December 2011. Total ^{137}Cs flux (^{137}Cs inventory) at 4810 m was about 3 Bq m^{-2} at K2 and 2 Bq m^{-2} at S1. These corresponded to about 0.7% and 0.3% of ^{137}Cs eolian input to respective stations by one month after FNPP1 accident. The ^{134}Cs was detected, at the earliest, by April 2012 at K2 and by February 2012 at S1. At 500 m of F1, the highest ^{134}Cs activity was observed in late August 2011 and ^{134}Cs activity decreased thereafter (Fig. 1 c). However ^{134}Cs activity temporary increased in March 2012 and ^{134}Cs flux was the maximum at that time during observation. ^{137}Cs inventory at 500 m of F1 during observation was about 60 Bq m^{-2} and 20 – 30 times higher than that at 4810 m of K2 and S1. It might be attributed to much higher ^{137}Cs inventory to surface around F1 (30000 – 40000 Bq m^{-2} by June 2011. Buesseler et al., 2011). In addition, lithogenic materials were pre-dominant in settling particle collected at F1 while biogenic materials such as biogenic opal and $CaCO_3$ were pre-dominant at K2 and S1. Station F1 was located on the continental shelf slope and the "nepheloid layer" was observed around 600 m depth and near seafloor. Lateral transport of radiologically contaminated clay minerals from/near the land might also contribute the higher ^{137}Cs inventory at sediment trap depth at F1.

References

Buesseler et al. (2011) Proc. Natl. Acad. Sci. 109, 5984-5988.

Honda et al. (2012) Geochem. J. 46, e1-e9.

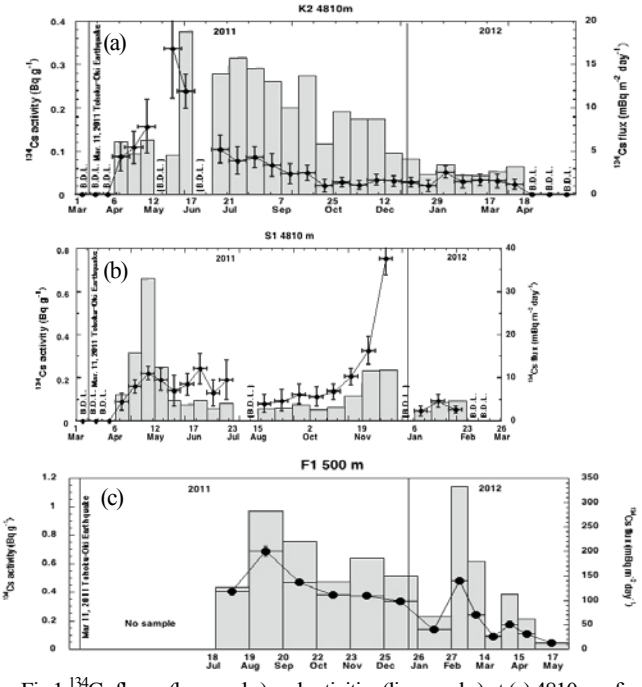

Fig.1 ^{134}Cs fluxes (bar graphs) and activities (line graphs) at (a) 4810 m of K2, (b) 4810 m of S1 and (c) 500 m of F1 (after Honda et al. submitted to Biogeosciences). Note that vertical scale is different between figures.

Strontium-90 determination in air dust filter using solid phase extraction after the accident of FD-NPS

ZiJian Zhang[1], Shunsuke Kakitani[1], Kazuhiko Ninomiya[1], Naruto Takahashi[1], Yoshiaki Yamaguchi[2], Takashi Yoshimura[2], Takashi Saito[3], Kazuyuki Kita[4], Haruo Tsruta[5], Shogo Higaki[6], Atsushi Shinohara[1]

[1] Graduate School of Science, Osaka University, [2] Radioisotope Research Center, Osaka University,
[3]Faculty of Comprehensive Human Sciences, Shokei Gakuin University, [4] College of Science, Ibaraki University,
[5]Atmosphere and Ocean Research Institute, the University of Tokyo, [6]Radio Isotope Center, the University of Tokyo

Abstract - Radioactivities of Sr-90 in air-dust filters collected in Hitachi, Kawasaki and Toyonaka were determined using solid state extraction method and low background beta-ray counting system. In Hitachi, though the Sr-90 activity concentration was decreased with time, the activity rates of Sr-90/Cs-137 kept about 10^{-3} order. This fact suggests that Sr-90 transportation behavior in the atmosphere is similar to that of Cs-137 during the time of sample collection.

Key word – Sr-90, solid-phase extraction, air dust

I. INTRODUCTION

On 12th March, 2011, a large amount of radioactive nuclides have been released into the environment by the nuclear accident at the Fukushima Daiichi Nuclear Power Station. Measurement about radioactive nuclides will give us much information about the accident circumstance. There are many measurement results of I-131, Cs-134, Cs-137 in natural samples. However, for other nuclides, such as the pure beta emitter nuclide Sr-90 has not been measurement sufficiently. Strontium-90 is considered one of the harmful radioactive nuclides. Therefore, measurement of Sr-90 in air dust is important for calculating exposure. We developed a new simple and quick strontium isolation technique using solid phase extraction and determined Sr-90 activities in air dust.

II. EXPERIMENTAL

In this study, we used the 3M Empore™ Strontium Rad Disk to extract strontium ion. This filter can collect mg order of Sr^{2+} ion efficiently. However, it is known that this filer also catches Pb^{2+}[1]. Natural radioactive nuclide Pb-210 seriously will be interferences for Sr identification in beta ray counting. In this study, cation exchange with EDTA solution was adopted for Sr purification after solid phase extraction. We made test experiments with radioactive Sr tracer and obtained high chemical yield as 90 %. The time for chemical operation of this method was 3-4 hours. The activity of Sr-90 was determined by the growth curve in sequential measurements of Cherenkov light from Y-90 by the low background liquid scintillation counter. Using Sr-90 standard solution, we determined that Cherenkov light detection efficiency for Y-90 68.7% and detection limit of Sr-90 is 0.004 Bq in this system.

III. RESULTS

We measured Sr-90 in air dust samples of Hitachi, Kawasaki and Toyonaka City. We analyzed some air dust samples for Sr-90 detection that had high Cs-137 activity, and strontium isolation with solid phase extraction was performed. The measurement result of Hitachi is shown in Table.1 and Fig.1. Without Pb separation, we can easily observe the Cherenkov light form Bi-210, that is daughter nuclide of Pb-210. However, there is a ND(not detectable) result and it indicates that the measurement sample was sufficiently Pb-210. In Hitachi, the Sr-90 activity concentration in air was decreased with time. All of the ratios of Sr-90/Cs-137 were about 10^{-3}. It is possible that after April, Sr-90 has been the same behavior of Cs-137. Strontium-90 was also determined in samples of Kawasaki and Osaka. In the presentation, we will discuss about the results of Sr-90 in air dust and compare with the results by other group about Sr-90 in soil and fallout.

Table.1 Sr-90 detection results of Hitachi

	Sampling Date	^{90}Sr Bq/m^3 error%	^{90}Sr /^{137}Cs error%
1	4/9	1.5×10^{-3} 3%	1.6×10^{-3} 10%
2	4/16	2.6×10^{-4} 3%	3.1×10^{-3} 11%
3	4/18	3.7×10^{-4} 3%	1.1×10^{-3} 10%
4	4/19	ND	
5	5/4	3.1×10^{-5} 15%	1.5×10^{-3} 18%
6	5/21	6.3×10^{-5} 12%	3.7×10^{-3} 16%

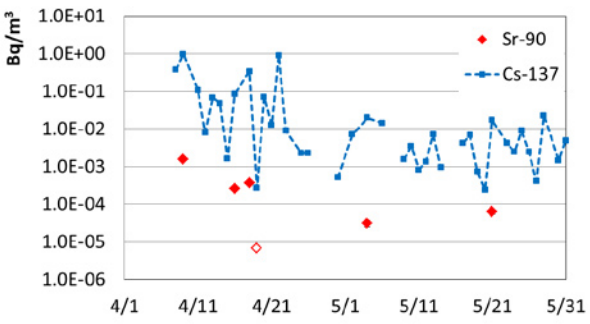

Fig.1 The time dependence change of Sr-90 and Cs-137 in Hitachi

[1]L.L.Smith and K.A.Orlandini. Radiochimica Acta 73,165-170(1996)

Dosimetric Implications of the Fukushima Release for Pacific albacore in the Northern California Current

Delvan R. Neville[1], A. Jason Phillips[1], Kathryn A. Higley[1]
[1]Oregon State University, Corvallis, OR; nevilled@onid.orst.edu

Abstract – Using activity concentrations in Pacific albacore at both pre-Fukushima and post-Fukushima levels, the average annual whole body internal dose for these nekton is estimated. MCNP & voxelized phantoms applied for determination of absorbed fraction. Analyzed tissues include both edible tissue, viscera and other non-edible tissues.

Keywords – Cs-137, Cs-134, Pacific albacore, radioecology, Fukushima

I. INTRODUCTION

An unfortunate result of the already devastating earthquake and tsunami on March 11, 2011 was a release of radionuclides from the Fukushima Daichi power generating station. It will be several years before this release into the North Pacific Gyre will be carried, at diluted and decayed activity concentrations, to the West Coast of North America[1]. During the interim, migratory species may be passing through the extent of this liquid plume, and feeding throughout that range. This work intends to address the dosimetric implications for migratory Pacific albacore, *Thunnus alalunga.*

A. State of existing body of knowledge

Historically, reported activity concentrations in the United States have almost exclusively sampled the edible tissues. In the case of albacore, this excludes not just skin, bone and viscera, but the fatty red muscle tissue along the belly. These were conducted at national labs, with the primary goal of ensuring Cold War-era radionuclides releases were not affecting food quality.

However, muscle tissue is one of the most radio-resistant tissues in the body. One goal of this work is to address the dosimetric impact to biota by determining concentrations for the whole body, rather than simply in edible tissue.

There is a large body of work reporting concentration ratios for nekton in the Pacific, which is the ratio of the activity concentration in the tissue over the activity concentration in the water, by mass. These concentration ratios vary wildly, as they depend on the assumption that the animal sampled is in equilibrium with activity in the surrounding environment, including the complicated food web transfer through other species. Nonetheless, they are still widely used for determinations of the expected concentrations after a release until a more thorough determination may be made. Another goal of this work is to relate edible muscle concentrations to concentrations elsewhere in the animal, to allow utilizing this existing body of work for animal dosimetric estimations

B. Whole Body Dosimetry

Absorbed fractions were calculated for activity in different body compartments using MCNP and a voxelized model developed from CT & MRI of a pelagic fish. Activity concentrations for Cs-134 and Cs-137 measured in Pacific albacore were then used to calculate annual internal dose to the animal for both those that exhibited trace concentrations of Fukushima effluents and those that remained at pre-Fukushima concentrations. The internal and external dose from naturally occurring K-40 is also provided for comparison. Additionally, dose estimates using the prior "edible-only" paradigm are presented.

[1] Behrens, E., Schwarzkopf, F.U., Lubbecke, J.F. & Boning, C.W. 2012. Model simulations on the long-term dispersal of 137Cs released into the Pacific Ocean off Fukushima. Environmental Research Letters 7:1-10.

ANNRI at J-PARC

Hideo Harada[1]
(on behalf of ANNRI project)
[1]Nuclear Science and Engineering Directorate, Japan Atomic Energy Agency

The Accurate Neutron-Nucleus Reaction measurement Instrument (ANNRI) has been installed at the beam line no. 4 of the Material and Life science experimental Facility (MLF) in the Japan Proton Accelerator Research Complex (J-PARC). It was constructed in order to supply accurate neutron capture cross sections of minor actinides and fission products required for developing innovative nuclear systems [1].

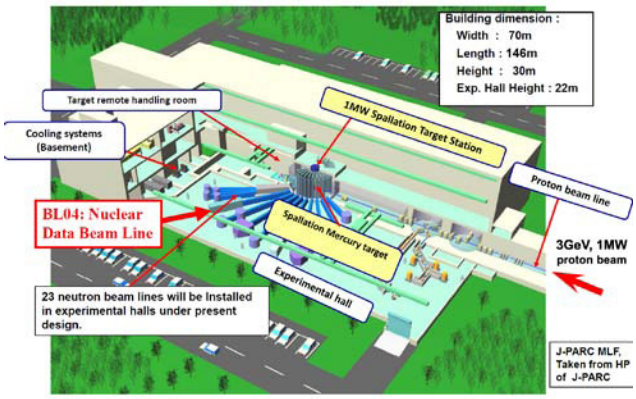

Fig. 1 A bird's-eye view of the layout of J-PARC/MLF

Fig. 2 Photo of ANNRI (outside) and Ge spectrometer

The ANNRI project team has developed the neutron beam line optimized for neutron time-of-flight experiments [2, 3], the advanced Ge [4] and NaI [5] spectrometers for detecting prompt γ rays, and the measurement method of neutron capture cross sections. The team has started the measurements of neutron capture cross sections of minor actinides and fission products since 2009, and successfully obtained the neutron capture cross sections of $^{244, 246}$Cm and ^{237}Np [6-8].

At the time of the Great East Japan Earthquake on March 11, 2011, the ANNRI suffered serious damages. However, the team members of BL04 immediately recovered from the situation. The recovered ANNRI has been used again for the user program since Feb. 2012. The project research using the ANNRI entitled as "Research on nuclear astrophysics, nuclear data, and trace-element analysis using pulsed neutrons" has also been started since April 2012.

The ANNRI is a unique instrument for high-resolution neutron-capture γ-ray spectroscopy by utilizing the world's strongest pulsed-neutron beam as shown in Fig. 3 and the high-efficiency Ge and NaI spectrometers. The ANNRI is expected to be usefully utilized not only for nuclear data measurements for the study of innovative nuclear systems, but also for the study of nuclear astrophysics [9-10] and for the analyses of trace elements [11-12].

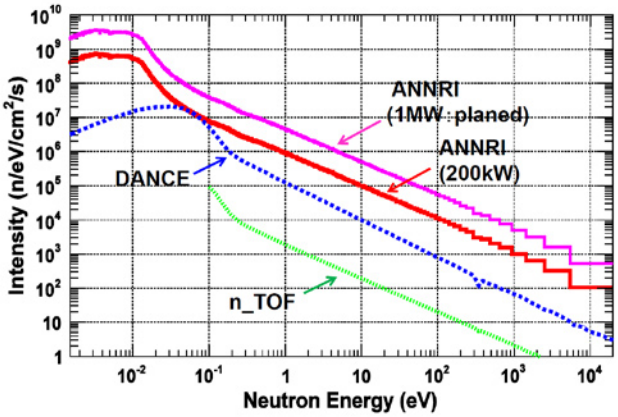

Fig. 3 Comparison of neutron flux of J-PARC /MLF/ANNRI with CERN/n_TOF and LANL/LANCE/DANCE

Current status and recent topics of the ANNRI will be reviewed in this symposium.

References

[1] OECD/NEA WPEC Subgroup 26 Report, "Uncertainty and Target Accuracy Assessment for Innovative Systems Using Recent Covariance Data Evaluations", 2008.
[2] K. Kino, *et al.*, Nucl. Instru. Method. **A 626-627**, 58 (2011).
[3] Y. Kiyanagi, J. Korean Phys. Soc. **59**, 779 (2011).
[4] H. Harada, *et al.*, J. Korean Phys. Soc. **59**, 1547 (2011).
[5] T. Ohsaki et al., Nucl. Instru. Method. **A 425**, 302 (1999).
[6] S. Goko, *et al.*, J. Nucl. Sci. Technol. **47**, 1097 (2010).
[7] A. Kimura, *et al.*, J. Nucl. Sci. Technol. **49**, [7], 708 (2012).
[8] K. Hirose et al., J. Nucl. Sci. Technol. **50**, [2], 188-200 (2013).
[9] T. Hayakawa et al., *Astrophysical Journal,* **707**, 859 (2009).
[10] F. Kappeler et al., Reviews of Modern Physics, 83, 157 (2011).
[11] M. Islam, et al., Analytical Chemistry, **83**, 7486 (2011).
[12] Y. Toh et al., Applied Radiation and Isotopes **70**, 984 (2012).

Nanomaterial and nanotechnology in nuclear energy chemistry

Yu-Liang Zhao[1,2], Wei-Qun Shi[1], Li-YongYuan[1], Zhi-Fang Chai[1]

[1]Nuclear Energy Chemistry Group, CAS Key Laboratory of Nuclear Analytical Techniques, and CAS Key Laboratory for Biomedical Effects of Nanomaterials and Nanosafety, Institute of High Energy Physics, Chinese Academy of Sciences (CAS), Beijing 100049, China
[2] National Center for Nanosciences and Technology, Beijing 100190, China

Keywords: Nanomaterial, Nanotechnology, Nuclear energy chemistry

With the increasing human demands for energy, applications of newly emerging technology for safer and cheaper energy become new challenges and new front in energy sciences. Major nuclear countries in the world have initiated forward-looking researches toward future advanced nuclear energy systems, in which nanomaterials and nanotechnologies play important roles. Nanomaterials and nanotechnology show some exciting application potentials in future nuclear energy systems. In the talk, we will discuss the recent research progress in nanomaterials and nanotechnologies associated with advanced nuclear fuel fabrication, spent nuclear fuel reprocessing, nuclear waste disposal and nuclear environmental remediation, etc. We will focus mostly on chemical aspects of above processes. The talk will highlight research activities in our Laboratory and China, and future challenges and opportunities of nanomaterials and nanotechnologies in nuclear energy chemistry.

For example, graphene nanomaterials has been demonstrated to effectively loaded ions, molecules, and atomic clusters onto their basal plane through weak interactions such as van der Waal's forces, electrostatic interactions, and π-π stacking. Due to relatively strong noncovalent interactions, decorated graphene can be highly stable in both acidic and basic media. Carbon nanomaterials have great potentials in areas whose issues are difficultly solved by conventional methods or bulk materials. We may use nanoparticles-loading graphene layered materials (like a 3D network material) as fillers of separation columns for nuclear fuel cycling and radioactive wastes treatments. The enhanced performances make the graphene material be able to selectively adsorb heavy metals (e.g., lanthanides or actinide) with a super loadage and an in-situ rebirth capacity, which may bring revolutionary progress into the nuclear fuel cycling industries.

To integrate the advance of nanomaterials and the need of nuclear energy production is a challenge in nuclear energy chemistry. For example, a variety of tetradentate ligands, 6,6`-bis(5,6-dialkyl-1,2,4-triazin-3-yl)-2,2`-bipyridines (BTBPs), have been experimentally proved as effective ligands for selective extraction of Am(III) over Eu(III). Recently, in exploring the origin of their selectivity, we found that in 1:1 (metal:ligand) type complexes substitution of electron-donating groups to the BTBP molecule can enhance its coordination ability and thus the energetic stability of the formed Am(III) and Eu(III) complexes in the gas phase. Eu(III) can coordinate to the BTBPs with higher stability in energy than Am(III), no matter whether there are nitrate ions in the inner-sphere complexes. The presence of nitrate ions leads to formation of the probable Am(III) and Eu(III) complexes, $M(NO_3)_3(H_2O)_n$ (M = Am, Eu), in nitric acid solutions. It has been found that the changes of Gibbs free energy play an important role for Am(III)/Eu(III) separation. In fact, the weaker complexing ability of Am(III) with nitrate ions and water molecules makes the decomposition of $Am(NO_3)_3(H_2O)_4$ more favorable in energy, which may thus increase the possibility of formation of $Am(BTBPs)(NO_3)_3$. These findings may shed light on the design of novel extractants for Am(III)/Eu(III) separation. However, the single atom lay of the graphene nanomaterials can first use as novel substrate and then as novel designs of a complex-based the extractant-platform for Am(III)/Eu(III) separation, and for selective separations of other Ln and Ac ions, or selective separations of ions among Ac elements.

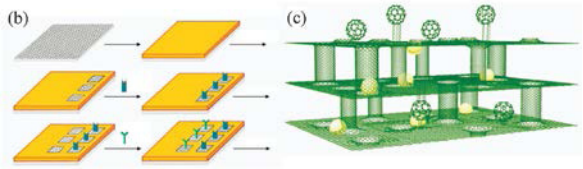

Figure 1, The superior performance of graphene-based materials. Basal plane functionalization could lead to graphene-based integrated function nanomaterials. Regiofunctionalization of graphene towards multifunctional and all-purpose devices. In the example, different functional groups for Am(III)/Eu(III) separation, or for separations of other Ln and Ac ions, or selective separations of ions among Ac elements, can be bonded in turn to the graphene substrate (Copyright @ RSC)[3].

References

1. W. Q Shi, L. Y Yuan, Z. J Li, J. H Lan, Y. L Zhao, Z. F Chai. ***Radiochim Acta***. 2012, 100: 727.
2. L. Y Yuan, Y. L Liu, W. Q Shi, Z. Li, J. H Lan, Y. X Feng, Y. L Zhao, Z. F Chai, ***J. Mater. Chem***. 2012, 22: 17019.
3. L. Yan, Y. B Zheng, F. Zhao, S. J Li, X. F Gao, B. Q Xu, P. Weiss, Y. L. Zhao, ***Chem. Soc. Rev.***, 2012, 41: 97-114.
4. J.H Lan, W.Q Shi, L.Y Yuan, Y.L Zhao, J Li, Z.F Chai, ***Inorg. Chem***., 2012, DOI: org/10.1021/ic200078j.
5. Y. L Zhao, C. L Bai, et al, Progress of Nanosciences in China, ***Front. Phys***. DOI 10.1007/s11467-013-0324-x, 1-32, 2013.

APSORC'13 - 5th Asia-Pacific Symposium on Radiochemistry
Kanazawa, Japan, 22-27 September 2013

Development of Real-Time Radioisotope Imaging System to Study Plant Nutrition

Tomoko M. Nakanishi[1], Natsuko I. Kobayashi[1], Atsushi Hirose[1], Takayuki Saito[1], Ryohei Sugita[1], Hisashi Suzuki[2], Ren Iwata[3], Keitaro Tanoi[1]

[1]Graduate School of Agricultural and Life Sciences, The University of Tokyo
[2] National Institute of Radiological Sciences
[3]Cyclotron and Radioisotope Center, Tohoku University

Abstract – We have been developing two types of real-time radioisotope imaging systems, one for macroscopic imaging targeting the whole plant itself and the other for microscopic imaging under modified fulorescent microscope to get both fluorescent and radioisotope images (Hirose et al. 2012; Kanno et al. 2012; Kobayashi et al. 2012). Now we can visualize the real-time movement of C-14, Na-22, Mg-28, P-32, S-35, K-42, Ca-45, Rb-86 or Cs-137, from root kept in dark to up-ground part where light was irradiated. There are a wide range of application of this imaging , such as to measure the uptake manner in root, speed or distribution or translocation manner, as well as distribution, translocation or deposition of the nutrient element in upground part. Here we present some representative real-time images in plants.

Keywords – real-time radioisotope imaging system, plant nutrition, C-14, Na-22, Mg-28, P-32, S-35, K-42, Ca-45, Rb-86 or Cs-137

Plants Prepared for Imaging

Rice (*Oryza sativa*. L. cv. *Nipponbare*) seedlings and *Arabidopsis thaliana* seedlings were grown for about 12 days and 40days, respectively, in culture solution. Then the plant was placed in front of the fiber optic plate where CsI scintilator was deposited. Then the radioisotope (RI) was supplied to the water culture solution and the RI image from roots ro up-ground part was monitored by highly sensitive CCD camera (Fig.1).

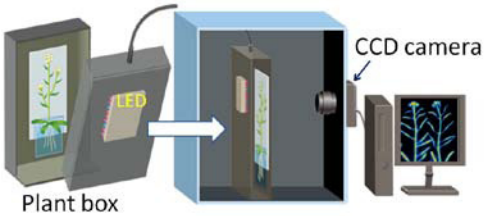

Fig.1a macoscopic real-time RI imaging system

The real-time images

The real-time images of absorption manner using varuious radioisotopes allows to calculate uptake amount and transfer rate both in macroscopic and microscopic images. As an example, Mg-28, P-32 and K-42 uptake manners were shown as successive images.

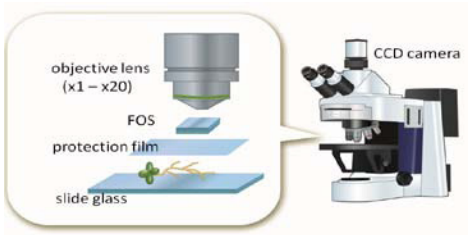

Fig.1b micoscopic real-time RI imaging system

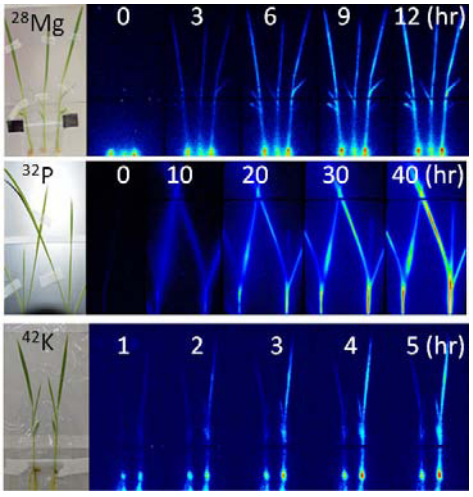

Conclusion

The real-time imaging system we developed showed the uptake manner of the wide range of the nutrient elements. There are two great advantages of RI imaging, allows imaging under light and enables numerical treatment of the image, since the image is based on radiation count. The imaging system for C-14 labeled carbon dioxide gas is now developing to study real-time photosynthesis.

References

Kanno, S.et al. Philosophical Transactions of The Royal Society B 367: 1501 (2012)
Kobayashi, I.N. et al. Radioisotopes 61:121 (2012)
Hirose, A. et al. J. Radioanal. Nucl. Chem.,in press.

MCNP study on the development of industrial SPECT in terms of a radiation measurement design and void influence in multiphase media

Sung-Hee Jung[1], Jang-Guen Park[1], Jong-Bum Kim[1], Jin-Ho Moon[1], Chan-Hyeong Kim[2]
[1]Korea Atomic Energy Research Institute, Daedeok-daero 989-111, Yuseong-gu, Daejeon, 305-353, Korea
[2]Dept. of Nuclear Engineering, Hanyang Univ., 17 Haengdang-dong, Seongdong-gu, Seoul, 133-791, Korea

Abstract – There have been extensive studies on the development of SPECT (Single Photon Emission Computer Tomography) for industrial applications. Owing to its intrinsic limitation originated from the dimensions and density of objects in industrial process units, it has been a challenging issue to get a spatial resolution good enough to draw informative data from it. This study demonstrates the feasibility of a radiation measurement array proposed for a greater region of interest resulting in better spatial image resolution. Considering that the industrial process units are designed to mix up different materials in different phases, the influence of a void ratio into the image quality of the industrial SPECT was investigated with the Monte Carlo code for a Liquid/Vapor phase system.

Keywords –Industrial SPECT, Radioisotope tracer, Multiphase flow investigation, Gamma radiation collimation, MCNPX

I. INTRODUCTION

Industrial image diagnosis technology based on the medical SPECT principle has been studied at the Korea Atomic Energy Research Institute [1]. The technology visualizes the distribution of process media as a function of time at a certain cross-section of the object under investigation [2]. The system was redesigned in a diverging collimator configuration substituting the conventional parallel configuration.

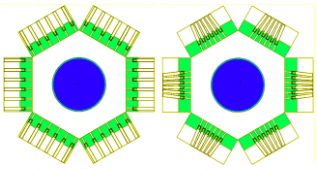

Fig. 1. Radiation detection geometry for MCNP simulation with conventional (left) and proposed (right) collimator arrays of industrial SPECT.

II. METHODS AND RESULTS

A. Redesign of radiation collimator configuration

The configurations in Fig. 1 show the conventional and newly proposed radiation measurement arrays for an MCNPX simulation. Besides the diverging orientation of collimation, the proposed array is identical to the conventional one. The cylindrical vessel is 40 cm in diameter and contains water. Radiation probes are NaI(Tl) with 1.3 cm in diameter and 2.5 cm in length. The radioisotope is ^{68}Ga with 511 keV of gamma radiation and the energy window for measurement was set to ±10% of it, 460-562 keV. The radioisotope was positioned at five different points, 0, 4, 8, 12, and 16 cm from the center to evaluate the precision of the reconstructed images at various locations.

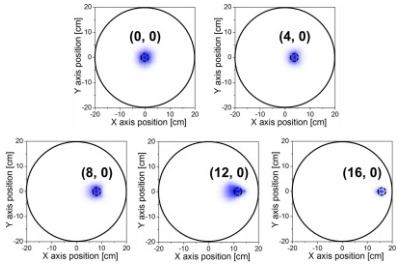

Fig. 2. Reconstructed images of the radioisotope with the geometry of diverging configuration.

B. Influence of void fraction to image quality

Homogeneous void formation at the same layer with the 6 detectors of industrial SPECT was modeled with MCNP code.

Table 1. NRMSE for quantitative comparison of image quality

Source	Counting Method	Void volume fraction		
		5%	10%	20%
^{68}Ga (511 keV)	Gross	1.93	2.33	3.67
	Peak	1.69	2.02	2.60
^{137}Cs (662 keV)	Gross	1.88	2.19	3.59
	Peak	1.42	1.99	2.52

III. CONCLUSION

The study showed that the diverging collimator demonstrates a better image quality because the collimators cover a wider angle being able to reconstruct the location of radioisotope more precisely compared to a parallel geometry.

Void formation in the vessel hardly affects the image quality in industrial SPECT. There are two reasons for these results: (1) the homogeneous void distribution in the vessel uniformly influences the signals of every detector, and (2) there are few gamma interactions in the void because the density of the void is as low as 0.001205 g/cm^3.

ACKNOWLEDGEMENT

This work was carried out under the Nuclear R&D Program of the Korean Government.

REFERENCES

[1] J. G. Park, et. al., Development of an Industrial SPECT to Study Dynamic Behavior of Plant Process Flow, Trans. Korean Nucl. Soc., Autumn Meeting, Pyeongchang, Korea, Oct. 30, 2008
[2] S. Legoupil, G. Pascal, D. Chambellan, and D. Bloyet, Tomograph for Industrial Flow Visualization Using Radioactive Tracers, IEEE Transactions on Nuclear Science, Vo.43, No.2, pp.751, 1996.

Tracking the Deportment of Uranium Chain Daughters during Alkaline Leaching of an Australian Monazite

Mellodee Anvia[1,2] and Susan A. Brown[1]
[1]ANSTO Minerals, Locked Bag 2001, Kirrawee DC, NSW 2232, Australia
[2]School of Chemistry, The University of Sydney, NSW 2006, Australia

Monazite contains between 50–68% rare earths and is the second most abundant source of the rare earth elements after bastnasite [1, 2]. Monazite may contain up to 20% thorium and 0.3% uranium and so is an example of a naturally occurring radioactive material (NORM). The deportment of radionuclides from NORM is of particular concern during rare earth extraction [3]. Standard methods for measuring activity concentrations in order to track radionuclide deportment using techniques such as gamma, alpha and beta spectrometry have in general proved to be unsuccessful. In this work, we have developed an analytical method to track the deportment of ^{238}U and ^{235}U daughters during the alkaline leaching of an Australian monazite concentrate. During the alkaline leaching stage it was found that uranium isotopes (^{238}U and ^{235}U) and ^{210}Pb reported to both the trisodium phosphate liquor (leach liquor) and the rare earth hydroxide residue; while ^{230}Th, ^{226}Ra, ^{210}Po (^{238}U) and ^{231}Pa and ^{227}Ac (^{235}U) reported to the rare earth hydroxide. Following hydrochloric acid leaching of the rare earth hydroxide, the major contaminants found in the leach liquor included ^{210}Pb, ^{226}Ra and ^{210}Po. These contaminant radionuclides were later removed from the hydrochloric acid leach liquor by a 'deactivation' and 'lead elimination' step, which is commonly used in industry. The results indicated that removal for most radionuclides was greater than 90%.

[1] Gupta, C. K.; Krishnamurthy, N. *Extractive Metallurgy of Rare Earths*; CRC Press Florida, 2005.
[2] Bashir, V. S. *Mater. Sci. Forum*. **1988**, *30*, 33.
[3] International Atomic Energy Agency. *Radiation Protection and NORM Residue Management in the Production of Rare Earths from Thorium Containing Minerals*, Safety Reports Series No.68, IAEA Vienna, 2011.

Nuclear chemistry and radiochemistry studies at IMP

Z. Qin[1*], F.-L. Fan[1], Y. Wang[1], F.-Y. Fan[1], X.-L. Wu[1], J. Bai[1], X.-J. Yin[1], L.-L. Tian[1],

W. Tian[1] , Z. Li[1], C.-M. Tan[1],

[1] Institute of Modern Physics, Chinese Academy of Sciences, Lanzhou 730000, China

This paper will review the relative research of nuclear chemistry of IMP.

(1) Synthesis and chemical properties of the superheavy elements

The study of the chemistry of transactinide elements ($Z \geq 104$) is a topic of great interest in current nuclear chemistry research. In IMP, two new transactinide isotopes of ^{259}Db and ^{265}Bh have been produced successfully via the reactions of ^{241}Am (^{22}Ne, 4n)^{259}Db and ^{243}Am (^{26}Mg, 4n)^{265}Bh, respectively[1,2]. In order to study the gas phase chemical behaviour of transactinide elements, an on-line isothermal chromatography apparatus has been established at IMP [3]. The isothermal gas chromatographic behaviour of the group 5 elements Nb, Ta and Db was investigated in a brominating atmosphere using the OLGA technique [4]. The nuclide ^{258}Db was synthesized successfully by the nuclear reaction ^{243}Am (^{20}Ne, 5n)^{258}Db registering ^{258}Db – ^{254}Lr α-decay chains. It was found that Db forms a very volatile compound, most likely the pentabromide, being more volatile than similar compounds formed under identical conditions with Nb and Ta, respectively. This observation is in disagreement with previous experimental investigations of the same compound [5] but in agreement with theoretical prediction [6].

At the same time, metal carbonyl complexes were used for studying the gas-phase chemical behavior of Mo and W isotopes with an on-line low temperature isothermal gas chromatography apparatus. The result showed that short-lived isotopes of Mo and W can form carbonyl complexes which are very volatile and interact most likely in physisorption processes. The first Sg(CO)6 experiment have been completed at RIKEN under a large scale international collaboration between GSI/Maunz, RIKEN, JAEA, LBNL and IMP.

The liquid-liquid extraction behavior of short-lived molybdenum and tungsten isotopes from HCl and HNO_3 as well as HF/HNO_3 acid media was also studied using the α-benzoinoxime/chloroform system [7].

(2) Synthesis of radiopharmaceutical

Positron emission tomography (PET) has become a powerful and widely used imaging technology. The most commonly used PET radiopharmaceutical is 2-[^{18}F] fluoro-2-deoxy-D-glucose ([^{18}F]-FDG). 10 MeV proton mini-medical cyclotron are under construction at IMP, [^{18}F]-FDG system will be developed by ourselves. The water target system was ready to test with proton beam.

(3) Extraction of uranium from the salt-lake

Many materials were developed and as the absorbent to remove uranium from salt lake. Adsorption of uranium from aqueous solution onto the yeast cells (*Rhodotorula glutinis*), magnetically modified yeast cells, magnetic $Fe_3O_4@SiO_2$ composite particles and magnesium silicate hollow spheres was investigated in a batch system [8,9]. The result showed that these absorbents exhibit much higher sorption capability for uranium.

At the present, the fabric containing amidoxime group as the absorbent for uranium has been synthesized by graft acryloonitrile (AN) onto polypropylene (PP) and amidoximation after electro-beam (EB) irradiation. The detail experiment is still underway.

(4) Transmutation chemistry

In order to transmutation of long-lived fission products and minor-actinides in ADS, the production of minor-actinide containing sphere-pac fuel is under development in collaboration with the international and domestic scientists.

[1] Gan, Z. G. Qin, Z. Fan, H. M. et al., European Physical Journal A10, 21, **2001.**
[2] Gan, Z. G. Guo, J. S. Wu, X. L. et al., Euro. Phys. J. A20,385, **2004**
[3] Lin, M. S., Qin, Z., Lei, F. A., et al. Radiochimica Acta 98, 321-326 **2010**.
[4] Qin, Z., Lin, M. S., Fan, F.L., et al., *Radiochimica Acta.* 100:285-289, **2012**.
[5] Gäggeler, H. W., Jost, D. T., Kovacs, J., et al. Radiochim. Acta 57, 93, **1992.**
[6] Pershina, V., Sepp, W.-D., Fricke, B., et al. J. Chem.Phys**.** 97, (2): 1116, **1992.**
[7] Fan, F. L. Lei, F. A. Zhang, L. N. et al. *Radiochimica Acta*. *97*:297-302. **2009**.
[8] Bai, J., Wu X. L., Fan, F. L. et al., Enzyme and Microbial Technology, 51:382, **2012**
[9] Fan, F. L., Qin Z., Bai J., et al. *Journal of Environmental Radioactivity*, 106: 40-46, **2012**

APSORC'13 - 5th Asia-Pacific Symposium on Radiochemistry
Kanazawa, Japan, 22-27 September 2013

Preparation of Low Valent Technetium Metal-metal Bonded Species via Solvothermal Reduction of Pertechnetate Salts

W.M. Kerlin[1], F. Poineau[1], P.M. Forster[1], A.P. Sattelberger[2], K.R. Czerwinski[1]
[1]Department of Chemistry, Radiochemistry Program, University of Nevada Las Vegas, Las Vegas, NV 89154, USA
[2]Energy Engineering and Systems Analysis Directorate, Argonne National Laboratory, Argonne, IL 60439, USA

Abstract – A new one-step solvothermal synthesis route for reduction of pertechnetate salts to low valent technetium metal-metal bonded dimers will be presented. The reaction of potassium pertechnetate with glacial acetic acid plus either halo acids or halo salts under in-situ hydrogen production by sodium borohydride at various temperatures yields multiple products consisting of tetraacetate Tc-Tc (II,III) and Tc-Tc (III,III) paddle wheel dimers. Solid products isolated and analyzed via Single Crystal X-ray Diffraction (SC-XRD) in these reactions consist of polymeric chains Tc_2^{+5} core: $Tc_2(\mu\text{-}O_2CCH_3)_4(O_2CCH_3)$, $Tc_2(\mu\text{-}O_2CCH_3)_4Cl$, $Tc_2(\mu\text{-}O_2CCH_3)_4Br$, $Tc_2(\mu\text{-}O_2CCH_3)_4I$, molecular Tc_2^{+5} core: $Tc_2(\mu\text{-}O_2CCH_3)_3Cl_2(H_2O)_2{\cdot}H_2O$, $K[Tc_2(\mu\text{-}O_2CCH_3)_4Br_2]$, and molecular Tc_2^{+6} core: $Tc_2(\mu\text{-}O_2CCH_3)_4Cl_2$, $Tc_2(\mu\text{-}O_2CCH_3)_4Br_2$. Of the compounds listed, four are newly discovered using the one-step technique and two more additions to crystal database. Additional spectroscopic (X-ray Absorbance Fine Structure, UV-Vis, and FT-IR) characterization of the new compounds will be shown and used to propose a mechanism. Analysis of the mother liquor of each reaction by UV-Vis and formation of crystals over time due to oxidation of solutions affords a possible insight into mechanism of the Tc_2^{+5} to Tc_2^{+6} core formation. The oxidation states of Tc-Tc dimers formed is also dependent on temperature and pH of the starting solutions and will be explained in extensive detail. These one step reactions of reducing Tc(VII) to low valent technetium provides high yield intermediates for potential waste forms, use in nuclear fuel cycle separations, and radiopharmaceuticals.

Keywords – technetium carboxylates; metal-metal bonds; metal-halogen bond; hydro/solvo-thermal reactions; polymers

I. INTRODUCTION

Transition metals of groups six through nine exhibit unique direct multiple metal-metal bonding cores. The isotope ^{99}Tc (β^- = 293 keV) is a group seven radioactive element that is of concern in radioactive waste due to the long-lived half-life (2.13 x10^5 years). Exploring and understanding the role of metal-metal bonding in Tc can provide routes for the development of novel and stable waste forms. The fundamental chemistry of low valent Tc is not well explored compared to the surrounding elements Mo, Re, and Ru. Currently over 200 compounds containing the Re_2^{+n} (n = 4, 5, 6) cores are known, whereas less than 30 compounds with Tc_2^{+n} (n = 4, 5, 6) core exist.[1] One example of a Tc_2^{+6} core is $Tc_2(O_2CCH_3)_4Cl_2$ and has been shown to be a stable starting compound for synthesis of technetium binary halides.[2,3] The reduction of pertechnate, a waste product of spent nuclear reprocessing, to lower valent intermediates provides potential waste forms and insight into radiopharmaceuticals cores.

II. EXPERIMENTAL

A. Synthesis of Tc_2^{+5} and Tc_2^{+6} cores

Addition of 6.0 mL of glacial acetic acid into a small glass vial containing 0.25 mmol potassium pertechnetate, and 4 molar equivalent of desired halogen salt (such as sodium iodide) or haloacid (such as hydrobromic acid) is placed into a 23 mL Teflon lined Parr 4749 autoclave vessel containing 320 mg of sodium borohydride and 200 uL of DI water. The autoclave system is sealed and placed in a oven at 210 °C for 72 hrs, Equations 1-3. Figure 1, shows single-crystals of the polymeric chain $Tc_2(\mu\text{-}O_2CCH_3)_4I$ and molecular view of $Tc_2(\mu\text{-}O_2CCH_3)_4Br_2$.

$$2\ KTcO_4 + 4\ CH_3COOH + NaI + \text{ex. } NaBH_4 \rightarrow Tc_2(\mu\text{-}O_2CCH_3)_4I \quad (1)$$

$$2\ KTcO_4 + 4\ CH_3COOH + 2\ HBr + \text{ex. } NaBH_4 \rightarrow Tc_2(\mu\text{-}O_2CCH_3)_4Br_2 \quad (2)$$

$$2\ KTcO_4 + 5\ CH_3COOH + \text{ex. } NaBH_4 \rightarrow Tc_2(\mu\text{-}O_2CCH_3)_4(O_2CCH_3) \quad (3)$$

Bond lengths of Tc_2^{+5} cores are shorter than the Tc_2^{+6} cores and the effects of the bonding halogens will be discussed. These compounds are being considered potential waste forms sue to insolubility in all organic solvents and acidic solutions.

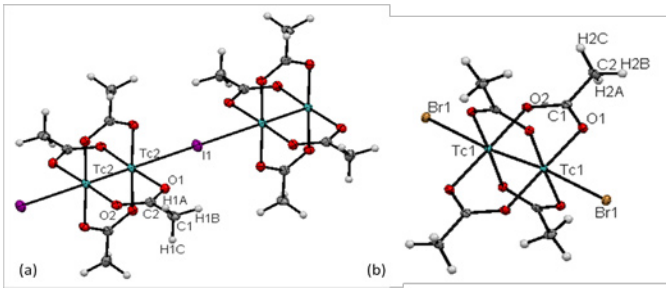

Figure 1. Ortep views of the (a) $Tc_2(\mu\text{-}O_2CCH_3)_4I$, (b) $Tc_2(\mu\text{-}O_2CCH_3)_4Br_2$

Acknowledgement: Funding for this research was provided by a SISGR Grant from the U.S. Department of Energy, Office of Science, Office of Basic Energy Sciences, under Contract No. 47824B.

REFERENCES

[1] Cotton, A., C. Murillo, R. Walton.; *Multiple Bonds Between Metal Atoms,* Springer, Inc.: New York, 2005, Chapter 7, p. 251-269.
[2] Zaitseva, L. I., et *al*., *Russ. J. Inorg. Chem.* 1980, 25, 1449
[3] Poineau, F.; *et al*., *J. Am.Chem. Soc.,* 2010, 132, 15864

The Statues of Chemical Characterization of a Spent Nuclear Fuel

Yeong-Keong Ha, Soon-Dal Park, Yang-Soon Park, Jung-Suk Kim, Kyuseok Song
Korea Atomic Energy Research Institute, 989-111 Daedeokdaero, Yuseong, Daejeon, 305-353, Korea

Abstract –The high burnup nuclear fuel requires an experimental data to support the fuel integrity, a safety analysis, and a shielding design. At high burnups, the composition of a nuclear fuel changes in a non-homogeneous manner throughout the radius. We present the R&D activities being performed in KAERI for spent fuels discharged from PWR in Korea; focused on the local chemical properties such as 'local burnup', 'structural changes' and 'the distribution of retained fission gas'.

Keywords – spent fuel, burnup, actinide, isotopic distribution, lattice parameter, fission gas

I. INTRODUCTION

To provide basic data about the local chemical properties of a spent fuel, 'radial distribution of isotopes', 'lattice changes along the radius' and 'the quantitative analysis of retained fission gas' were performed.

For the analysis of isotopic distribution and lattice changes, a shielded LA-ICP-MS and a micro-XRD were used, respectively. The generation yield, release fraction and retained fraction of fission gas of a fuel are important factors for determination of maximum burnup of commercial nuclear fuel. Thus, the gas analysis was performed along the axis and radius of a fuel rod.

II. EXPERIMENTAL

For the determination of average burnup of a PWR nuclear fuel, IDMS using ^{148}Nd-isotope as a burnup monitor was used. A shielded LA-ICP-MS system was used for the analysis of isotopic distribution of the spent fuel. A shielded micro-XRD system was used for the analysis of structural changes of a fuel pellet. The inert gas fusion method was used for the analysis of retained fission gas. A hydrogen analyzer equipped with electrode furnace was employed for complete fusion of a fuel to extract the retained gas, and a QMS was used as a gas analyzer.

III. RESULTS AND DISCUSSION

A. Isotopic Distribution and Structural Changes

By LA-ICP-MS system, radial distribution of actinides with respect to ^{235}U was measured successfully. The ^{236}U to ^{235}U ratio was almost constant, while the isotopic ratio of Pu and minor actinides were increased significantly at the pellet periphery. For a comparison, ORIGEN2 code was used to calculate the isotope ratios. The measured values agreed comparatively well with that of the calculated one.

The lattice parameters of the irradiated fuel revealed the larger values than that of non-irradiated UO_2 due to the radiation damage during the reactor operation and cooling after discharge.

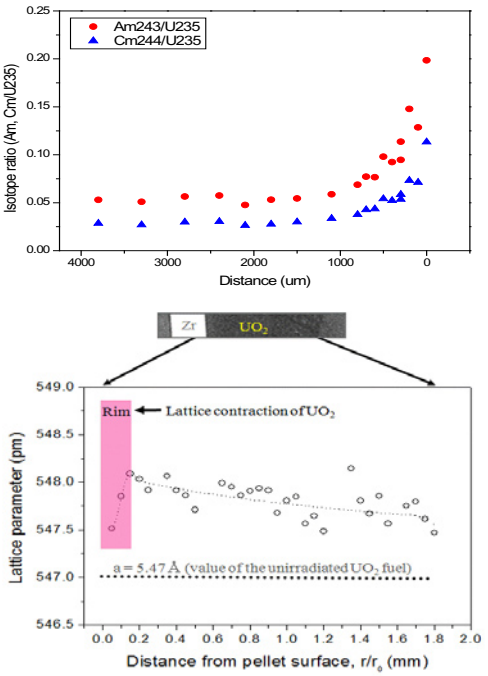

Fig. 1. The local chemical properties of a spent nuclear fuel; (top) actinides distribution, (bottom) changes in lattice parameters

B. Quantitative Analysis of Retained Fission Gas

A small fragment of spent fuel was fused with tin and nickel at a fussion current of 850A for 120 sec. The recovery of Kr and Xe was ca. 96~108 % during 2 min collection for reference materials in Al foil. The axial and radial distribution of RFG was investigated. The amount of retained Xe and Kr increased along the radius, and it decreased along the axis. The measured values were in the range of 75-84% of fission gas generation expected by code calculation. When combined with the released gas, the measured value was approached 95% of calculated one.

IV. CONCLUSION

The measured data can contribute to provide data needed for understanding an irradiation behavior of a high burnup fuel, and can contribute to study the advanced fuel such as ultra high burn-up fuel under developing.

ACKNOWLEDGEMENTS

This work was supported by the National Research Foundation of Korea (NRF) grant funded by the Korea government (MSIP).

NCO-04

Determination of ^{93}Zr from intermediate level radioactive effluent

I. Laszak[1], J.P. Degros[2], C. Gautier[2], P. Fichet[2], F. Goutelard[2], J.N. Saas[3], A. Vian[3], J.F. Valéry[4]
[1]*CEA Saclay, DEN/DANS/DPC/SEARS/LANIE, Nuclear, Isotopic Elementary Analytical Development Laboratory, Building 391, PC33, 91191 GIF SUR YVETTE CEDEX, FRANCE*
[2]*CEA Saclay, DEN/DANS/DPC/SEARS/LASE, Operator Support Analyses Laboratory, Building 459, PC171, 91191 GIF SUR YVETTE CEDEX, FRANCE*
[3]*AREVA NC La Hague, Central Control Laboratory, 50444 BEAUMONT-HAGUE CEDEX, FRANCE*
[4]*AREVA NC, Recycling Business Unit, AREVA tower, 92084 PARIS La Défense CEDEX*

The French Atomic Energy Commission (CEA) was asked by AREVA to develop a methodology in order to perform ^{93}Zr measurements on an intermediate level radioactive effluent. The difficulty encountered related to the solution containing high contents of fission products which is incompatible with the sample acceptance criteria of the CEA laboratory in charge of this development (Operator Support Analyses Laboratory - LASE). Indeed, the total radioactivity was about 400 GBq/L for the beta emitters and 4 GBq/L for the alpha emitters when the expected concentration of ^{93}Zr was roughly 2 MBq/L, thus implying a drastic decontamination step before acceptance and measurement. This study is a joint work between the LASE and the LCC (Central Control Laboratory, AREVA NC La Hague) and required to establish a proper scientific and experimental coordination between these two laboratories.

The first experimental steps were performed at the LCC. Because zirconium was essentially contained in the solid phase within the sample solution, it was decided to separate the precipitate using centrifugation prior to mineralization. Once the Zr was perfectly and entirely solubilized, a simple 500 fold dilution was needed for the samples to be accepted at the LASE for further analysis. The main goal was then to perform additional decontamination on the samples and to eliminate the various interfering species, mostly ^{93m}Nb and ^{93}Mo, as the ^{93}Zr would be measured by ICP-MS because of the very low detection limit offered (0.05ng/g) and because it also allowed us to follow the ^{93}Zr decontamination completion. The main separating steps involve a co-precipitation of zirconium with $Ba_3[AlF_6]_{2(s)}$ followed by several solvent extraction steps. These are alternating stages of zirconium and of niobium / molybdenum extraction in the organic phase, using either N-benzoyl-N-phenylhydroxylamine or cupferron in $CHCl_3$ while tuning accordingly the aqueous phase in order to retrieve a maximum amount of zirconium (forming highly stable complexes). Ultimately, the aqueous phase contained all of the zirconium as an oxalate complex and ICP-MS measurement was performed to determine the ^{93}Zr concentration. The separation yield was then determined by measuring the total concentration of zirconium using ICP-AES. Care was taken throughout the whole procedure to circumvent any zirconium cross-contamination. The ^{93}Zr concentration was found to be of 15Bq/µg (Zr, total) with a separation yield above 90%. A 2g/L total concentration of zirconium was determined, leading to a 30 MBq/L ^{93}Zr concentration in the effluent, a result one order higher than the one expected.

Keywords – ^{93}Zr; zirconium; radiochemistry; ICP-MS; intermediate level radioactive effluent; AREVA; CEA.

Selective Separation of Cesium from Simulated High Level Liquid Waste using a Silica-based (Calix[4] + Dodecanol)/SiO_2-P Adsorbent

Yuanlai Xu[1], Seong-Yun Kim[1]*, Tatsuya Ito[2], Haruki Tokuda[1], Tsutomu Tada[1], Keitaro Hitomi[1], Keizo Ishii[2]

[1]Cyclotron and Radioisotope Center, Tohoku University, Aramaki-Aza-Aoba 6-3, Sendai, 980-8578 Japan

[2]Graduate School of Engineering, Graduate School of Engineering, Tohoku University, Aramaki-Aza-Aoba 6-6-01-2, Sendai, 980-8579 Japan

*Corresponding author: Tel.: +81-175-72-4227; fax: +81-175-72-4611.
E-mail address: kim@cyric.tohoku.ac.jp (S.-Y. Kim)

Keywords – Cesium; Separation; (Calix[4] + Dodecanol)/SiO_2-P Adsorbent; High level liquid waste (HLLW); Macroporous silica-based supramolecular absorbent.

In order to separate Cs(I) from high level liquid waste (HLLW), a macroporous silica-based supramolecular recognition absorbent, (Calix[4] + Dodecanol)/SiO_2-P, was prepared by impregnating and fixing the 1,3-[(2,4-Diethylheptylethoxy)oxy]-2,4-crown-6-calix[4]arene (Calix[4]arene-R14) extractant and its molecule modifier 1-dodecanol into a macroporous SiO_2 silica based polymer support (SiO_2-P). Adsorption and separation behavior of Cs(I) or other typical fission produces (FPs) onto adsorbent were investigated by batch and column methods, respectively. It was found that (Calix[4] + Dodecanol)/SiO_2-P adsorbent showed strong adsorption affinity to Cs(I). A relatively large K_d value of Cs(I) above 90 cm^3/g was obtained in the presence of 4 M HNO_3 solution and reach equilibrium state within 1hr at 298 K. From calculated thermodynamic parameters, this adsorption process for Cs(I) could occur spontaneously at the given temperature and was confirmed to be an exothermic reaction. Meanwhile, low value of TOC (total organic carbon) in separated liquid phase from batch experiment reflected that (Calix[4] + Dodecanol)/SiO_2-P adsorbent had excellent chemistry stability against concentrated HNO_3 solution. In addition, tested Cs(I) were eluted out with distilled water chromatographically and separated from simulated HLLW successfully using (Calix[4] + Dodecanol)/SiO_2-P packed column. All results showed that (Calix[4] + Dodecanol)/SiO_2-P adsorbent had excellent adsorption affinity and high selectivity for Cs(I) from HLLW.

APSORC'13 - 5th Asia-Pacific Symposium on Radiochemistry
Kanazawa, Japan, 22-27 September 2013

Age Determination of a single Pu and Pu/U mixed oxide particle

Yutaka MIYAMOTO, Fumitaka ESAKA, Daisuke SUZUKI, Masaaki MAGARA
Research Group for Analytical Chemistry, Nuclear Science and Engineering Directorate
Japan Atomic Energy Agency (JAEA), Tokai, Ibaraki 319-1195, JAPAN

Abstract – *Age-dating of a single Pu oxide particle and a Pu/U mixed oxide (MOX) particle ~1 μm in diameter was demonstrated. The particles were prepared from the U and Pu standard reference materials for this demonstration. They were separately dissolved, and Am, U, and Pu were chemically separated from the solution via anion-exchange chromatography. The isotope ratios of Am and Pu in the eluted fractions were measured using a high-resolution inductively coupled plasma mass spectrometer (HR-ICP-MS). The precision and accuracy of the Pu age were improved through the addition of ^{243}Am or ^{243}Am-^{242}Pu mixed spikes to the sample solutions and by the trace chemical separation of Pu and Am. The determined age in this work was in good agreement with the expected age with high accuracy and precision. These results indicate that a combination of measurement using a mass spectrometer and chemical separation of the spiked samples provides an effective tool for the analysis of environmental samples collected during nuclear safeguard inspections.*

Keywords – Age dating, MOX, Plutonium, Trace analysis, Ion-exchange separation, Safeguards

I. INTRODUCTION

Isotopic and quantitative analyses of U and Pu in environmental swipe samples collected during routine International Atomic Energy Agency (IAEA) safeguard inspections are important for detecting undeclared nuclear activities. Age determination of nuclear materials collected as environmental samples from nuclear facilities is also useful for detecting undeclared activities, as the age provides information regarding the origins and history of the nuclear material. Plutonium of less than nanograms (ng) purified within a few years may be contained in the environmental samples collected during IAEA safeguard inspections. We present a method for determining the purification age of a single Pu oxide and a Pu/U mixed oxide (MOX) particle. These oxide particles ~1 μm in diameter were prepared from U and Pu standard reference materials for this work, and accuracy and precision of the analytical results were evaluated.

II. EXPERIMENTAL

Some Pu oxide particles and five types of MOX particles which consist of different Pu/U atomic ratio were prepared from the standard reference materials, NBS-SRM 947 purified 3.9 years ago and NBL-CRM U010. Small portion of the mixture of these solutions was calcined, and the obtained oxides were ground[1]. The particles 0.5–2 μm in diameter were selected under SEM observation. Each particle was dissolved in a mixture of HF and HNO_3. Finally, an 8 M HNO_3 solution was prepared. The sample solution was spiked with an ^{243}Am or ^{243}Am-^{242}Pu mixed solution purified by anion-exchange chromatography. One-third of the sample solution was used for measurement of the Am/Pu atomic ratio via ICP-MS. The remaining portion was passed through a single anion-exchange column to chemically separate Pu, U, and Am. The isotope ratios in the collected each fraction were measured with a HR-ICP-MS (Element-1) equipped with an Apex-Q desolvating inlet system. All treatments, except for the particle preparation from the standard solution, were carried out in clean rooms (ISO Class 5 and 6) at the "CLEAR" clean laboratory at JAEA.

III. RESULT AND DISCUSSIONS

The Pu purification age was determined using the ^{241}Am/^{241}Pu ratio and the general age-dating equation. The addition of ^{243}Am and ^{242}Pu spikes to the samples gave a precise and accurate Pu age. The determined ages of both the Pu oxide and MOX particles were in good agreement with the expected age (3.9 years). The accuracy in the determined age in the Pu oxide particle was 7.1–105 days and the uncertainty was 0.16–0.5 years. Addition of purified spikes, including ^{243}Am and ^{242}Pu, to the samples led to more precise and accurate age determination, even for a young Pu particle purified only a few years ago[2].

ACKNOWLEGEMENT

The authors would like to acknowledge Mr. N. Kohno for the particle production. The authors are also thankful to Mr. H. Fukuyama, Mr. T. Onodera, and Ms. R. Usui for the sample preparation and Mr. Y. Takahashi for the ICP-MS measurements. This work was supported by the Nuclear Regulation Authority, Japan.

REFERENCES

[1] F. Esaka *et al.*, Talanta, **83**, 569 (2010).
[2] Y. Miyamoto *et al.*, Radiochim. Acta, in press (2013).

APSORC'13 - 5th Asia-Pacific Symposium on Radiochemistry
Kanazawa, Japan, 22-27 September 2013

Radiochemical measurement of 10-15 MeV proton induced fission yields for U-238

Narek Gharibyan[1], Kenton J. Moody[1], Thomas A. Brown[2], John D. Despotopulos[1], Julie M. Gostic[3], Roger A. Henderson[1], Evgeny Tereshatov[1], Scott J. Tumey[2] and Dawn A. Shaughnessy[1]
[1]Chemical Sciences Division, Lawrence Livermore National Laboratory
[2]Atmospheric, Earth, and Energy Division, Lawrence Livermore National Laboratory
[3]Air Force Technical Applications Center, Patrick Air Force Base, Florida

Abstract – The production of realistic nuclear forensics debris requires an accurate knowledge of cross sections and fission yields for large number of systems. Proton induced fission of U-238 was examined for incident energies in the range of 10-15 MeV. Fission yields were first measured directly from the irradiated materials. The valley and wing fission products were then isolated in various chemical fractions in order to increase the counting statistics leading to improvements in the fission yields. In addition to the total fission cross section and the fission mass yields for U-238, proton based reaction cross sections on U-238 and U-235 were also measured.

Keywords – Fission yields, protons, fission product separation, U-238

I. INTRODUCTION

The improvements in fidelity of nuclear forensic exercise samples require the development of analytical reference materials with the end goal of establishing a realistic exercise sample. This is designed to test the national laboratory analysis and data evaluation communities through a truly coupled, end-to-end "unknown sample" exercise. The fabrication of such a sample requires an accurate knowledge of cross sections and fission yields for numerous reactions that can be explored to obtain fission products and/or short-lived actinide isotopes. Due to the limited amount of nuclear data and the large uncertainties associated with the reported values of proton-induced fission for U-238, experiments were performed to measure the fission mass yields and the cross section. Radiochemical separations were established for fission products of interest in order to improve the fission yields in comparison to those obtained from the initially irradiated samples.

II. EXPERIMENTAL

A stacking foil technique was employed in the irradiation of nat. U foil with 10-15 MeV protons with Y as the beam intensity monitor. A series of irradiations were performed using the tandem Van De Graff accelerator located at the Center for Accelerated Mass Spectrometry at Lawrence Livermore National Laboratory (LLNL). Irradiated samples were transferred to the Nuclear Counting Facility on site at LLNL for the initial counting. After sufficient data were obtained, the uranium foils were dissolved and separated into three fractions: one as a standard and one each for the separation of wing and valley fission products. Various chemical separation methods were developed based on the sorption behavior of the fission products on ion exchange resins. Chemical fractions containing the fission products of interest were counted individually and the total fission yields were back calculated for each sample.

III. RESULTS

The measured fission yields are based on the results generated by the GAMANAL program [1] evaluation of the raw gamma spectra. Fission yields for short lived fission products, as low as $t_{1/2}$=14 minutes, were acquired. An example of a fission mass yield obtained from these experiments is provided in Figure 1. The measured values of the cross sections and fission yields are relatively close to those reported in literature [2-4].

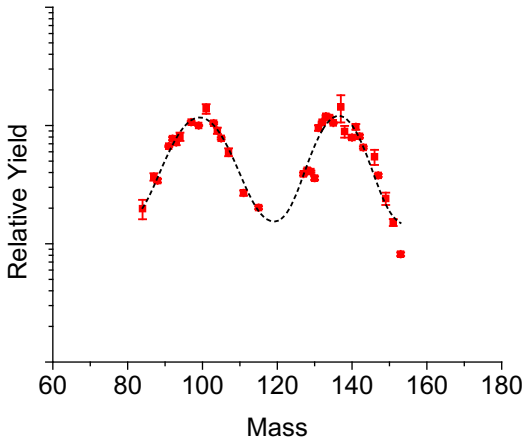

Figure 1. Fission mass yield from 11.9 MeV protons on U-238.

Acknowledgements – This work was performed under the auspices of the U.S. Department of Energy by Lawrence Livermore National Laboratory under contract DE-AC52-07NA27344.

[1] Gunnink, R., Niday, J.B., UCRL-51061, Vol. I (1972)
[2] Yokoyama, A., *et al.*, Z. Phys. A **356**, 55-60 (1996)
[3] Baba, H., *et al.*, Z. Phys. A **356**, 61-70 (1996)
[4] Karttunen, E., *et al.*, Nucl. Sci. Eng. **109**, 350-359 (1991)

APSORC'13 - 5th Asia-Pacific Symposium on Radiochemistry
Kanazawa, Japan, 22-27 September 2013

Effect of Interferences on Actinide and Strontium Separations in Unusual Matrices

Ralf Sudowe[1], Evelyn M. Bond[2], Ashlee R. Dailey[1], Derek R. Mclain[1], Audrey R. Roman[1]
[1]University of Nevada Las Vegas, Las Vegas, Nevada 89154, USA
[2]Los Alamos National Laboratory, Los Alamos, New Mexico 87545, USA

Abstract – Insufficient information is currently available about the effects that the interferences present in complex matrices can have on radiochemical separations utilizing extraction chromatography. This poses a particular challenge for sample analysis in the aftermath of a nuclear incident involving an Improvised Nuclear Device or a Radiological Dispersion Device. This research aims at obtaining this information by examining the composition of common urban materials and by investigating the influence that their constituents have on radioanalytical separations. To address this issue the compositions of several different sample matrices of interest has been investigated. Subsequently the uptake of Sr, Pu, Am and Cm on different commercially available resins was studied in the presence of varying concentrations of potentially interfering elements such as Al, K, Ca, K, Cr, Fe, Ni, Zr and Nd.

Keywords – Extraction chromatography, Actinide, Strontium, Separations

I. INTRODUCTION

Most current radioanalytical methods have been developed for the analysis of air, water, soil and bioassay samples. While these protocols build the foundation of operational environmental monitoring, they are not necessarily suitable for the analysis of samples that will be encountered in the aftermath of a nuclear incident involving an improvised nuclear device or a dirty bomb. Of particular interest for emergency response and nuclear forensics are therefore methods that can be applied to the analysis of steel, concrete, melt glass, asphalt and bone samples. Extraction chromatographic resins have been used for radiochemical separations for many years now, and a large body of data has been published on the retention capabilities of many of these resins for a large variety of elements that can be found in environmental samples. Little can be found, however, on the effect that the matrix constituents found in debris samples can have on analyte uptake. Even though it is known that the elements of interested are retained on the respective resins to a high degree, the samples analyzed will have a much more complex composition than previously encountered. Their behavior might therefore potentially deviate from normal sorption characteristics. In particular the competition between the potential interference and the analyte of interest has to be studied in a systematic manner. The goal of this study is to obtain information about the major and minor constituents that are present in several sample matrices of interest for emergency response and to investigate the influence that they can have on the radiochemical determination of several actinide elements and radiostrontium.

II. EXPERIMENTAL

The composition of several different matrices of interest was determined by either obtaining information from reference materials or by performing elemental analysis on suitable samples. Batch studies were then used to determine the uptake of the analyte of interest on a particular resin in the presence of varying concentrations of different alkali, earth alkali and transition metals, as well as lanthanides. The uptake of Sr on SR resin [1] was investigated in addition to the uptake of Pu, Am and Cm on DGA and UTEVA resin [2, 3]. Single analyte solutions were contacted with small amounts of resin in the presence of varying concentrations of the potential interference. Aliquots were taken and the amount of analyte remaining in solution was determined using either LSC measurement or gamma spectroscopy. Simultaneously the concentration of the interfering element after contact with the resin was measured by ICP-AES.

III. RESULTS

The compositions of several different sample matrices of interest, such as bone ash, steel, concrete, asphalt and melt glass has been investigated. The uptake of Sr on Sr resin was studied in the presence of varying concentrations of Mg, Al, P, K, Ca, Cr, Fe, Ni, Cu and Zr. The adsorption of Pu, Am and Cm on DGA and UTEVA resin was studied in the presence of varying concentrations of Fe, Zr, Mo, Sr, Tc, Cs and Nd. The presence of several of the interferences studied led to a significant decrease in uptake of the element of interest on the resin. Others appeared to have no influence. In some cases the presence of the interference lead to an increased adsorption of the analyte on the resin, hinting at a synergistic effect that needs to be studied in greater detail.

REFERENCES

[1] E.P. Horwitz et al, *A novel strontium-selective extraction chromatographic resin*, Solvent Extraction Ion Exchange **10**, 313 (1992)
[2] E.P. Horwitz et al, *Novel extraction of chromatographic resins based on tetraalkyldiglycolamides: Characterization and potential applications*, Solvent Extraction Ion Exchange **23**, 319 (2005)
[3] E.P. Horwitz et al, *Separation and preconcentration of uranium from acidic media by extraction chromatography,* Analytica Chimica Acta, **266**, 25 (1992)

Oral Presentations

Tuesday, 24 September 2013

Hall & Meeting Room, Kanazawa Bunka Hall

	Tuesday, 24 September				
Time		Hall		Meeting Room	
09:00-09:10	9:00	PL-03	**Plenary**		
09:10-09:20					
09:20-09:30			A. Tuerler		
09:30-09:40	9:30	PL-04	**Plenary**		
09:40-09:50					
09:50-10:00			S. Nagao		
10:00-10:10	10:00	**Coffee Break**			
10:10-10:20					
10:20-10:30	10:20	ENI-01	**Invited**	NCI-01	**Invited**
10:30-10:40					
10:40-10:50			H. Foerstendorf		S. Dmitriev
10:50-11:00	10:50	ENO-01	General	NCI-02	**Invited**
11:00-11:10			Z.J. Guo		
11:10-11:20	11:10	ENO-02	General		Ch.E. Duellmann
11:20-11:30			H. Tuovinen	NCI-03	**Invited**
11:30-11:40	11:30	ENO-03	General		
11:40-11:50			M.- C. Wu		H. Haba
11:50-12:00	11:50	ENO-04	General	NCO-06	General
12:00-12:10			T. Ohnuki		V. Pershina
12:10-13:20	12:10	**Lunch Time**			
13:20-13:30	13:20	ENO-05	General	NCO-07	General
13:30-13:40			S. Sachs		D. Rudolph
13:40-13:50	13:40	ENO-06	General	NCO-08	General
13:50-14:00			Y. Iwahana		A. Yakushev
14:00-14:10	14:00	ENO-07	General	NCO-09	General
14:10-14:20			J. Krmela		J. Even
14:20-14:30	14:20	ENO-08	General	NCO-10	General
14:30-14:40			K. Masumoto		H. Nitsche
14:40-14:50	14:40	ENO-09	General	NCO-11	General
14:50-15:00			H.W. Gaeggeler		R. Eichler
15:00-15:10	15:00	ENO-10	General	NCO-12	General
15:10-15:20			A. Sakaguchi		T.K. Sato
15:20-15:30	15:20	**Coffee Break**			
15:30-15:40					
15:40-15:50	15:40	ENI-02	**Invited**	NEI-01	**Invited**
15:50-16:00					
16:00-16:10			J.V. Krtaz		Z.F. Chai
16:10-16:20	16:10	ENO-11	General	NEI-02	**Invited**
16:20-16:30			J.H. Park		
16:30-16:40	16:30	ENO-12	General		A. Goswami
16:40-16:50			J. Zheng	NEO-01	General
16:50-17:00	16:50	ENO-13	General		E. Loefstroem-Engdahl
17:00-17:10			I. Milanovic	NEO-02	General
17:10-17:20	17:10	FKI-05	**Invited**		Y. Tomobuchi
17:20-17:30				NEO-03	General
17:30-17:40			K. Minato		F. Poineau
17:40-17:50	17:40	FKO-09	General	NEO-04	General
17:50-18:00			Y. Oura		A. Braatz
18:00-18:10	18:00	FKO-10	General	NEO-05	General
18:10-18:20			K. Hirose		R. Chen
18:20-18:30					
18:30-18:40					
18:40-18:50					
18:50-19:00	18:50	**Poster Session**			
19:00-19:20					
19:20-19:40					
19:40-20:00					
20:00-	20:00				

Advances in the Production and Chemistry of the Heaviest Elements

Andreas Türler[1,2]

[1] Laboratory of Radiochemistry and Environmental Chemistry, Paul Scherrer Institute, Villigen-PSI, Switzerland
[2] Laboratory of Radiochemistry and Environmental Chemistry, University of Bern, Bern, Switzerland

Abstract – Now that the discovery of all elements in the 7th period has been announced, has the far end of the Periodic Table of the Elements been reached? What is the heaviest element in the Periodic System? Are there still undiscovered ones which might even be found in nature? Is there an 8th period and how many elements will it contain? Will we need to introduce the g-orbitals and will the current principles governing the groups and periods of the Periodic Table still be valid for the heaviest elements? These intricate questions are the topic of current research in fundamental nuclear chemistry.

Keywords – APSORC'13 Keywords

I. INTRODUCTION

For increasingly heavy nuclei the electrostatic repulsions of protons cannot be sufficiently compensated by the attractive nuclear force through an increasing number of mediating neutrons. Therefore, the heaviest stable known nucleus is already reached with ^{208}Pb. All isotopes of heavier elements, including some elements such as Bi, Th, and U that still can be found in nature as remnants of the last nucleosynthesis process, are radioactive and decay preferentially by successive α-particle and β^--particle emissions back to the last stable element Pb.

A. Synthesis of Heavy Elements

All elements heavier than Pu (Z=94) are man-made. Transactinide elements ($Z \geq 104$) are synthesized currently only in complete heavy ion fusion reactions at high power accelerators on a "one atom at a time" level. Spectacular progress was obtained by using the very tightly bound, doubly magic nucleus ^{48}Ca and actinide target nuclei. Oganessian et al. were able to synthesize single atoms of elements 113 through 118 (with ^{294}118 currently being the heaviest observed nucleus) and observe their radioactive decay [1]. So far, only elements 114 and 116 have been authenticated by IUPAC and the element names flerovium, Fl, and livermorium, Lv, suggested by the team of discoverers, have recently been made official by IUPAC.

The addition of 6 new elements in the past decade was remarkable in several ways. First, the maximum production cross sections of elements Rf through Cn (Z=104-112) could be described rather well by an exponential decay law, where the cross sections dropped by roughly a factor of 10 when increasing the atomic number by 2 units. In the synthesis of ^{277}Cn production cross sections of less than 1 pb (10^{-36} cm^2) were determined. However, by using ^{48}Ca projectiles, this trend was broken and rather constant maximum production cross sections of several picobarns were measured for synthesis of elements Cn through Lv (Z=112-116) and even for elements 117 and 118 values near or slightly below 1 pb were observed. Nevertheless, even under optimum conditions a production cross section of 1 pb translates into the synthesis of only 1 atom of a superheavy nuclide every 36 h on average. Second, of the more than 50 new nuclides produced in these experiments a number of them have $t_{1/2} > 1$ s and, thus, live long enough for chemical investigations. This result is in strong contrast to the previously known, more neutron deficient isotopes of Mt, Ds, Rg, and Cn in the range of few milliseconds.

B. Chemical Investigations of Heavy Elements

The place an element occupies in the Periodic Table is not only defined by its atomic number, i.e. the number of protons in the nucleus, but also by its electronic configuration, which defines its chemical properties. Strictly speaking, a new element is assigned its proper place only after its chemical properties have been sufficiently investigated. In some cases it has been possible to experimentally investigate chemical properties of transactinide elements and even synthesize simple compounds. Due to the predicted strong influence of relativistic effects, the experimental investigation of superheavy elements is especially fascinating.

The difficulties involved in the production and rapid chemical isolation of few single atoms of a transactinide element from numerous other reaction products and the subsequent detection of the nuclear decay require the development of unique separation methods. Chemical studies of transactinide elements and simple transactinide compounds have been accomplished in the liquid as well as in the gaseous phase. For the heavy transactinides, which very likely are volatile in their elemental state, gas phase chemistry is the method of choice [2]. Lately, the required decontamination factors from interfering nuclear reaction products grew so large that chemical experiments were coupled to kinematic preseparators that already remove a substantial fraction of the primary beam and of transfer reaction products.

In this contribution the advances made in the synthesis and chemical investigations of transactinide elements are reviewed [3]. Latest results on attempts to synthesize elements beyond Z=118 and experiments to chemically investigate Fl will be highlighted as well as the first synthesis of volatile transactinide carbonyl complexes.

[1] Yu. Ts. Oganessian, Radiochim. Acta 99, 429 (2011).
[2] R. Eichler et al., Angew. Chem. Int. Ed. 47, 3262 (2008).
[3] A. Türler, V.G. Pershina, Chem. Rev. 113, 1237 (2013).

Study on transport of particulate organic matter in river and coastal marine systems using radiocarbon

Seiya Nagao
Low Level Radioactivity Laboratory, Institute of Nature and Environmental Technology, Kanazawa University

This study applies a combined use of carbon isotope composition ($\Delta^{14}C$ and $\delta^{13}C$) to suspended solids in river waters and surface sediments from the river mouth, continental shelf off the coast of Japan. This study is intended to investigate the fate of terrestrial particulate organic matter that is released from the river to the coastal marine environment at three river-coastal systems. Our results indicate that the combined $\Delta^{14}C$ and $\delta^{13}C$ measurements of the particulate organic matter can provide unique information on the sources and age of sediments and their transport behavior.

Keywords –$\delta^{13}C$, $\Delta^{14}C$, suspended solids, transport

Global riverine discharge of organic matter to the ocean represents a substantial source of dissolved terrestrial matter and organic carbon particulates. Continental margins are recognized as the dominant reservoir for organic carbon burial in the marine environment. An accurate inventory for terrestrial and marine organic carbon in continental margin sediments is important for quantitative understanding of biogeochemical cycles.

A variety of geochemical approaches have been employed to define the mixing ratio of marine and terrestrial organic matter, including $\delta^{13}C$ and lignin biomarker analyses. Radiocarbon abundances have become an additional indicator of terrestrial versus marine sources because nuclear weapons testing in the 1950s and 1960s injected large quantities of ^{14}C into the atmosphere. The $\Delta^{14}C$ values of organic matter in river suspended particles range from −980 to +75‰, but plankton and particulate organic carbon in marine environments have enriched ^{14}C values ranging from −45 to +110‰. Therefore, the simultaneous use of $\Delta^{14}C$ and $\delta^{13}C$ values adds a second dimension to isotopic studies of carbon cycling in surface aquatic environments.

This study investigates the fate of terrestrial particulate organic matter that is released from the river to the coastal marine environment at three research fields in Japan.

We selected a river in wetland, Bekanbeushi River, and rivers in forest and paddy field such as the Ishikari, Kuzuryu and Hino Rivers. The river-coastal systems were set up at the Bekanbeuchi River-Lake Akkeshi, the Tokachi River and the Kumaki River-off the coast of the rivers in Japan.

^{14}C measurements were performed by accelerator mass spectrometry at the Japan Atomic Energy Agency and the Institute for Environmental Studies in Japan. The $\Delta^{14}C$ is defined as the deviation in parts per thousand from the modern standard. $\delta^{13}C$ values were determined for sub-samples of the CO_2 gas generated during graphite production, using an isotope ratio mass spectrometer.

Figure 1 shows the $\Delta^{14}C$ values of organic matter in the riverine suspended solids plotted as a function of $\delta^{13}C$ values. The paired $\Delta^{14}C$ vs. $\delta^{13}C$ distributions vary with sampling site and divided into two groups. Riverine POC in wetland has lower in $\delta^{13}C$ and higher in $\Delta^{14}C$ rather than those of rivers in forest and fluvial plain. This indicates higher contribution of younger organic matter at the wetland river systems.

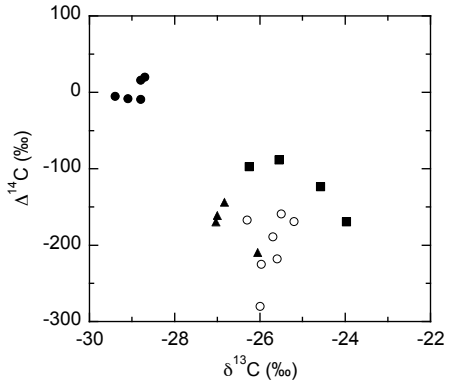

Figure 1 Relationship between $\Delta^{14}C$ and $\delta^{13}C$ of organic matter in the suspended solids for the Bekanbeushi (●), Ishikari (○), Kuzuryu (■) and Hino Rivers (▲).

Figure 2 shows $\Delta^{14}C$ and $\delta^{13}C$ values of organic matter in riverine suspended solids and surface marine sediments at the Kumaki-Nanao Bay system. The $\Delta^{14}C$ decreased from the headwater to the middle sites at the Kumaki River, but increased to the coastal sediments. These results indicate that the middle and lower watershed area has main sources of particulate organic matter exported to the costal marine environments.

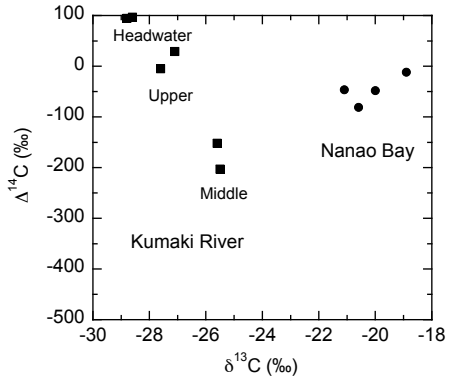

Figure 2 $\Delta^{14}C$ and $\delta^{13}C$ of organic matter in the Kumaki River suspended solids (■) and the Nanao Bay sediments (●).

APSORC'13 - 5th Asia-Pacific Symposium on Radiochemistry
Kanazawa, Japan, 22-27 September 2013

Surface speciation of dissolved radionuclides on mineral phases – A vibrational and X-ray absorption spectroscopic study

H. Foerstendorf[1], K. Gückel[1], N. Jordan[1], A. Rossberg[1,2], V. Brendler[1]
[1]Helmholtz-Zentrum Dresden-Rossendorf, Institute of Resource Ecology, Dresden, Germany
[2]Rossendorf Beamline at the European Synchrotron Radiation Facility (ESRF), Grenoble, France

Abstract – Binary and ternary surface complexes of U(VI) and Np(V) on gibbsite were spectroscopically identified. Se(VI) forms two different types of outer-sphere complexes depending on the solid metal oxide.

Keywords – Surface complexes, minerals, spectroscopy

INTRODUCTION

A detailed description of the molecular interactions of radionuclides with minerals is required for the prediction of their dissemination in the environment. In the past decade, vibrational spectroscopy has been developed to a powerful tool for the study of surface complexes of heavy metal ions on solid phases. In particular, a combined approach of vibrational and X-ray absorption spectroscopy potentially provides comprehensive molecular information. In this study, a survey of very recent results obtained from sorption reactions of radionuclides, namely U(VI), Np(V) and Se(VI) on metal oxides is given.

RESULTS

A. Surface processes of U(VI) and Np(V) on gibbsite

Gibbsite is widely used as a model system for alumosilicate minerals and clays. In addition, it is a ubiquitous weathering product of these minerals and the most common crystalline aluminum hydroxide.

The results of the U(VI) sorption experiments indicate the formation of a monomeric binary inner-sphere surface complex irrespective of the prevailing atmospheric condition and surface loading (Fig. 1A). In addition, it was found that U(VI) surface precipitation occurs at a micromolar concentration level in an inert gas atmosphere. This is circumvented by lowering the initial U(VI) concentration or in the presence of atmospheric CO_2 due to the formation of ternary uranyl carbonato surface complexes. The ternary complex was identified as a dimeric inner-sphere uranyl surface species containing a bidentately coordinated carbonate ligand by EXAFS spectroscopy (Fig. 1B)[1].

Inner-sphere complexation was also derived from spectroscopic results of the Np(V)/gibbsite sorption system. Whilst the neptunyl(V) ion forms a mononuclear surface species under inert gas condition (Fig. 1C), a ternary surface complex in the presence of atmospherically derived CO_2. This ternary species is most likely a mononuclear Al–O–NpO_2–O_2CO-surface species with a bidendately coordinated carbonate ligand (Fig. 1D).

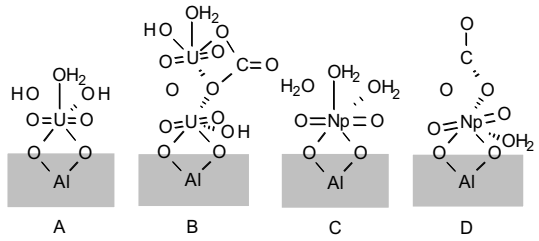

Fig. 1: Proposed surface complexes of U(VI) and Np(V) on gibbsite.

B. Surface speciation of Se(VI)

The sorption of selenate ions on different metal oxide phases exhibits a new type of outer-sphere complexes. As it was already postulated for transition metal cations to form classical and extended outer-sphere complexes [2], this is obviously also true for oxoanions, such as SeO_4^{2-}. With respect to the high sensitivity of vibrational spectroscopy to symmetry properties of molecules, the spectra of the sorption complexes of selenate ions on anatase [3] and maghemite (γ-Fe_2O_3) [4] clearly indicate the formation of different types of outer-sphere complexes (Fig. 2). These findings are corroborated by macroscopic analytical techniques.

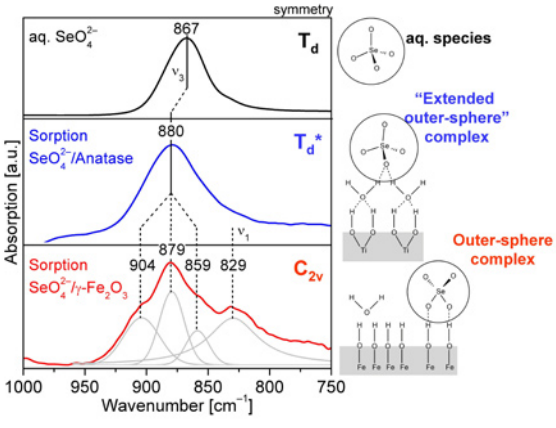

Fig. 2: IR spectra of SeO_4^{2-} species and the derived surface species.

REFERENCES

[1] Gückel, K. et al. (2012) *Chem. Geol.* **326-327**, 27-35.
[2] Lee, S. S. et al. (2010) *Langmuir* **26**, 16647-16651.
[3] Jordan, N. et al. (2011) *Geochim. Cosmochim. Acta* **75**, 1519-1530.
[4] Jordan, N. et al. (2013) *Geochim. Cosmochim. Acta* **103**, 63-75.

APSORC'13 - 5th Asia-Pacific Symposium on Radiochemistry
Kanazawa, Japan, 22-27 September 2013

Adsorption of Eu(III) and Am(III) on granite: Effects of temperature, fulvic acid and background electrolyte

Z.J. GUO, Z.Y. CHEN, Q. JIN, W.S. WU
School of Nuclear Science and Technology, Lanzhou University, Lanzhou, 730000, China
E-mail: guozhj@lzu.edu.cn

Abstract –The adsorption of Eu(III) and Am(III) on crushed Beishan granite (BS03, 600m) was investigated as a function of temperature, background electrolyte and the presence of fulvic acid at different concentrations. It was found that temperature did not affect apparently the distribution coefficient (K_d) of Eu(III) in the range of 25-80 ^oC. At pH < 5.0, the K_d value decreased in $CaCl_2$ solution as compared to that in NaCl solution at the same ionic strength, suggesting cation exchange reactions occurred in low pH range. Whereas in high pH range, the K_d values in $CaCl_2$ and NaCl solutions at the same ionic strength are identical, which indicate inner-sphere surface complexes formed. FA significantly decreased K_d of Eu(III) especially at pH > 4 and the extent of the decrease depended on FA concentration and varied with aqueous pH as well. Aging of freshly crushed granite in synthetic underground water at 150 ^oC for two weeks did not affect apparently Eu(III) K_d values. A surface complexation model (SCM) using Generalized Composite (GC) approach was constructed based on experimental data of Eu(III) in NaCl solutions and verified by experimental data of Eu(III) in $CaCl_2$ solutions as well as in synthetic underground water. The SCM was used to predict Am(III) adsorption on the granite and the calculated results were in accordance with the experimental data of Am(III)

Keywords –Eu(III), Am(III), adsorption, granite, temperature effect, fulvic acid, surface complexation model

I. INTRODUCTION

Beishan granite (Beishan, Gansu province) has been considered as a preliminary selection of host rock for geological disposal of high-level radioactive waste in China, [1]. Considering temperature variation, potential change in electrolytes of underground water, and the presence of humic substances in the near field of a repository, it is necessary to evaluate adsorption of radionuclides on the granite at variable conditions.

II. MATERIAL AND METHODS

$^{152+154}$Eu(III) and ^{241}Am(III) radiotracers were obtained from Chinese Atomic Energy Institute. All other chemicals used were of analytical grade. Beishan granite was sampled from the borehole BS03 at a depth of 600 m. To simplify the adsorption system, carbonates in Beishan granite was removed and the exchangeable cations were transformed into Na-form or Ca-form. Batch sorption was carried out with polyethylene tubes in nitrogen atmosphere glove box.

III. RESULTS AND DISCUSSION

In Generalized Composite (GC) approach [2], a rock is integrally considered and surface reactions on which are assumed to occur on a type of "general sites", although the chemical environmental of surface sites on different minerals and even those on different crystal planes of the same mineral are actually different. In addition, the GC approach ignores electrostatic effect. As a result, a GC model for a radionuclide sorption on a rock is actually the simplest model with the least adjustable parameters.

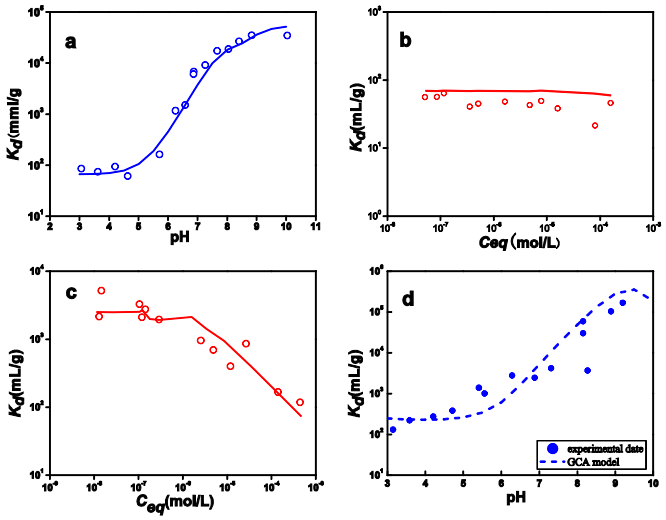

Figure. Eu(III) sorption in $CaCl_2$ and "real" systems, (a) Sorption edge of Eu(III) on Ca-granite, $C_o = 6.74\times10^{-8}$ M, m/V = 1 g/L and C_{CaCl2} = 0.033 M; (b) Sorption isotherm of Eu(III) on Ca-granite, C_{CaCl2} = 0.033M, m/V = 1g/L and pH = 4.00±0.10; (c) Sorption isotherm of Eu(III) on Ca-granite, C_{CaCl2} = 0.033 M, m/V = 1g/L and pH = 6.50±0.10; (d) Sorption edge of Eu(III) on Na-granite with simulated underground water $C_o = 6.74\times10^{-8}$ M, m/V = 1 g/L and C_{NaCl} = 0.1 M.

[1] Guidelines for the R&D for geological disposal of high-level radioactive waste. Beijing: China Atomic Energy Authority (CAEA), Ministry of Environmental Protection, Ministry of Science and Technology, 2006 (in Chinese)
[2] Davis J A, Meece D E, Kohler M, Curtis G P. Approaches to surface complexation modeling of Uranium(VI) adsorption on aquifer sediments. Geochimica et Cosmochimica Acta, 2004, 68: 3621-3641.
[3] Guo Z, Chen Z, Wu W, Liu C, Chen T, Tian W, Li C, The adsorption of Eu(III) on Beishan granite, SCIENTIA SINICA Chimica, 2011, 41: 907-913.

Behaviour of radionuclides and secondary mineral formation in the Talvivaara mining process

Hanna Tuovinen[(1)], Esa Pohjolainen[(2)], Daniela Vesterbacka[(1)], Caroline Kirk[(3)], David Read[(3)], Dina Solatie[(4)], Jukka Lehto[(1)]

[(1)] Laboratory of Radiochemistry, Department of Chemistry, University of Helsinki, P.O. Box 55, FI-00014 University of Helsinki, Finland
[(2)] Geological Survey of Finland, Betonimiehenkuja 4, FI-02151 Espoo, Finland
[(3)] Department of Chemistry, Loughborough University, Loughborough, Leicestershire, LE11 3TU, UK
[(4)] Regional Laboratory of Northern Finland, Finnish Radiation and Nuclear Safety Authority, Lähteentie 2, FI-96400 Rovaniemi, Finland

The Talvivaara nickel deposits are located in Sotkamo, Eastern Finland. The deposits comprise one of the largest known nickel sulphide resources in Europe. Talvivaara is an operational, open cast mine where Talvivaara Mining Company uses bioheap leaching to extract the metals (Ni, Zn, Cu, Co) from the black schist ore. In 2010 the company announced the commencement of uranium production as an addition to its normal mining operations. In heap leaching, uranium dissolves in the pregnant leach solution (PLS) along with main base metals and will be extracted using the solvent extraction (SX) process. The uranium produced will be in the form of yellowcake with an estimated annual production of approximately 350 tons. Currently, the uranium is diverted into a gypsum pond and part of it also ends up in the nickel concentrate as an impurity.

Bioheap leaching is a naturally occurring exothermic process catalysed by indigenous bacteria. The key parameters are particle size (< 8 mm), pH of the pregnant leach solution (2 – 2.5), temperature (20-90 ^{o}C) and the oxidation and aeration rates. The ore is first extracted using conventional large scale open pit drill and blast methods, then crushed and screened in four stages. It is agglomerated in a rotating drum, where recirculated PLS is added to the ore in order to consolidate the finer particles. It is then stacked eight meters high on the primary heap pad for primary leaching. The heap is irrigated from above and the leachate collected from the base of the heaps. The pregnant leach solution is collected in the PLS ponds where a 10% side flow is taken for metals recovery; the remaining 90% per cent is recycled back to irrigation to increase the metal grade. The metals are precipitated from the PLS using hydrogen sulphide and the resulting intermediate products transported for further processing in refineries. After approximately 2 years bioleaching on the primary pad, the leached ore is reclaimed, conveyed and restacked onto secondary heap pads. At this stage, the main part of copper and cobalt is recovered. After secondary leaching, the barren ore will remain permanently in the secondary heaps.

The leaching process oxidizes U(IV) to U(VI) in the form of the uranyl ion (UO_2^{2+}) at low pH. Radioactive progeny from the ^{238}U series are also mobilized and fractionate depending on chemical properties and the ambient conditions. The aim of this study is to generate new data leading to a better understanding of the behaviour of radionuclides, especially ^{226}Ra, ^{210}Pb and ^{210}Po, at each stage of the Talvivaara mining process. In addition the formation of secondary minerals during the leaching process is poorly understood.

Samples were collected from the primary heaps, secondary heaps, the PLS-ponds and gypsum pond in 2011, 2012 and 2013. After pre-treatment, gamma spectrometry was used for direct determination of uranium and thorium progeny. Samples were then analysed by X-ray diffraction (XRD) to determine the main minerals present. The uranium-bearing minerals were determined by electron probe micro-analysis (EPMA). Uranium, thorium and heavy metals were determined by ICP-MS. For alpha spectrometry, uranium and thorium were separated using anion exchange chromatography, ^{210}Po with silver plate precipitation and ^{210}Pb was precipitated from the remaining solution. Leaching experiments were performed in order to determine ^{226}Ra, ^{210}Pb and ^{210}Po – bearing mineral phases.

Preliminary results provide information on the formation of secondary phases and the relative abundance of the initial ore minerals. Uranium in the gypsum pond is found at least in association with goethite (FeO(OH)). The high content of sulphate restricts solubility of radium; ^{226}Ra concentrating in precipitated sulphate minerals. For lead, the formation of anglesite ($PbSO_4$) is probable and polonium is also likely to be bound to secondary minerals in the heaps. The results of this work will play an important role in estimating radiation doses and potential health implications to the local population resulting from past and anticipated disposal. A summary of the main results obtained to date is given in the presentation.

Evaluation of HTO and selenium diffusion behavior in compacted bentonite with different lengths

Chuan-Pin Lee [1], Ming-Chee Wu [1,*],Ching-Yuan Liu [2], Chun-Hua Pan [1], Tsuey-Lin Tsai [3], Hwa-Jou Wei [3], Lee-Chung Men [3]

[1]* Department of Earth Sciences, National Cheng Kung University, Tainan, Taiwan, 70101
[2]Department of Chemical and Materials Engineering, National Central University, Taoyuan, Taiwan, 32001,
[3] Chemistry Divisions, Institute of Nuclear Energy Research, Taoyuan, Taiwan, 32546

Abstract – *n this study, diffusion behavior of selenium(Se) with a concentration of 0.1mM in bentonite (MX80) was investigated using through-diffusion methods with various lengths (0.25, 0.5, 0.75, 1.0, 2.0, 2.5 cm), respectively. Before performing the through-diffusion experiments of Se, a non-reactive tracer (HTO) was applied and achieved to characterize the physical process in compacted MX80 columns with different lengths. It shows that the diffusion process of Se in synthetic seawater (SW) and groundwater (GW) reached equilibrium after 250 and 300 days, respectively. Moreover, both retardation factor (Rf^{cal}) and distribution coefficients (K_d^{cal}) of Se obtained from accumulative concentration's method in through-diffusion test showed an obvious discrepancy in an increasing length/diameter (L/D) ratio. In fact, it presented an agreement of $Rf^{H/Se}$ and $K_d^{H/Se}$ in an increasing L/D ratio in comparison between HTO and Se. It appears that the $Rf^{H/Se}$ and $K_d^{H/Se}$ obtained from the through-diffusion experiments are higher than those derived from the batch experiments. Therefore, it demonstrates that reliable Rf and K_d of Se by through-diffusion experiments could be achieved at a non-reactive radiotracer(HTO) prior to tests and would be more confident for long-term performance assessment.*

Keywords – *Diffusion, Selenium, distribution coefficients, apparent diffusion coefficient*

Sorption Behavior of Dy(III) and Np(V) on microbial consortia

Toshihiko Ohnuki[1], Naofumi Kozai[1], Fuminori Sakamoto
[1]Japan Atomic Energy Agency, Tokai, Ibaraki, 319-1195 Japan

Abstract – To elucidate sorption of trivalent and pentavalent actinides by the consortia of microorganisms sampled at Horonobe, Hokkaido, Japan. In the sorption experiments of Nd(III), Dy(III) (analogue of trivalent actinides), and Np(V) were contacted with the consortia in the solution at pH between 3 and 7 in resting condition. The coordination environment of the sorbed Dy by the consortia was analyzed by EXAFS. For the sorption of Nd and Dy on the consortia, the K_d increased with increasing pH, and was nearly the same as that by single species of *S. putrefaciens*. For the sorption of Np on the consortia, the K_d was higher than that for a single species of *S. putrefaciens*, indicating that the sorption behavior of Np on the consortia is different from that by a single species of *S. putrefaciens*. These results indicate that the consortia poses higher affinity to Np than a single species of S. putrefaciens.

Keywords – Neptunium, trivalent actinides, sorption, consortia of microorganisms

I. INTRODUCTION

The presence of actinides (ANs) in radioactive wastes is a major environmental concern due to their long radioactive half-lives, and its chemical toxicity. The high capacity of microbial surfaces to bind ANs may affect the migration of ANs in the environment. Unfortunately, we have only limited knowledge of the role of microorganisms in the migration of ANs in the environment.

Many researches have been carried out to study adsorption of ANs on the cell surface o microorganisms. Usually in the adsorption experiment single species of microorganism was used, even though microorganisms habit in consortia in environment. The adsorption of divalent cations of Cd, Cu, Ca, Pb, Sr, and Zn by the consortia was nearly the same as that by a single species. However, sorption behavior of ANs by consortia has not been elucidated.

In the present study, sorption behavior of trivalent lanthanides of Nd(III) and Dy(III) (alternative use for Am(III) and Cm(III), and of Np(V), by consortia of microorganisms using batch type sorption experiments..

II. EXPERIMENTAL

Sample locations were at 140 m in depth in the site of JAEA Horonobe Deep Geological Research Center, Horonobe, Hokkaido, Japan. Samples were collected 3 different points on February, 2011. The samples were inoculated in the Fe-reducing bacteria growth medium containing $NaHCO_3$ 1g: NH_4Cl 0.6g: KH_2PO_4 0.24g: KCl 0.04 g: Na-acetate 1 g: Na-citrate 0.4 g: $Fe(OH)_3$ 0.4g in 1 L distilled water under anaerobic condition. The pre-grown consortia were cultured in the medium containing beef extract or shewanella medium under aerobic condition. Culture in the consortia were analyzed by 16S rRNA analysis.

For the sorption experiments of Nd(III), Dy(III), and Np(V) by the consortia were conducted in resting condition. The solution sampled at 4 and 24 hrs after the exposure were centrifuged for 10 min at 4000 rpm. The supernatant was filtered through a membrane filter of 0.2 μm to measure concentrations of the dissolved elements. The concentration of Nd and Dy was 0.1 mM, and Np was 0.01 mM. The sorption experiments were performed in aerobic condition.

The concentrations of Nd and Dy were measured by ICP-AES, and that of Np by liquid scintillation analyzer. The coordination environments of the sorbed Dy(III) by consortia were determined by XAFS analysis using KEK PF.

III. RESULTS AND DISCUSSION

The consortia contained many kind sof bacteria involving Pseudomona and *Shewanella* family by random clone analysis.

For the sorption of Nd and Dy on the consortia, distribution coefficients (K_d) were between 10^4-10^5 ml/g at pH between 3-7. The K_d for Nd and Dy increased with increasing pH. Higher Kd in Dy than Nd was determined. The K_d of Nd and Dy for the single species of *Shewanella putrefaciens*, was approximately 10^4 ml/g at pH around 4, and increased with increasing pH. XAFS analysis showed that the FT spectrum of Dy sorbed on the consortia resembled to that of Dy sorbed on a single species of *Shewanella putrefaciens*, but not to $DyPO_4$, indicatng that the coordination environment of Dy was nearly the same as that on *P. putrefaciens*. These results indicate that the sorption behavior of Nd and Dy on the consortia is nearly the same as that by a single species of *S. putrefaciens*.

For the sorption of Np on the consortia, the K_d was approximately 10^4 ml/g at pH 4. The K_d remained constant with increasing pH of the solution. The K_d for a single species of *S. putrefaciens* was about 10^2 ml/g at pH between 4 and 6.5. The Kd increased with increasing pH. These results indicate that the sorption behavior of Np on the consortia is different from that by a single species of *S. putrefaciens*. Since higher K_d is measured in the consortia than a single species of *S. putrefaciens*, the consortia poses higher affinity to Np than a single species of S. putrefaciens.

This research project has been conducted as the regulatory supporting research funded by the Nuclear Regulation Authority (NRA), Japan.

APSORC'13 - 5th Asia-Pacific Symposium on Radiochemistry
Kanazawa, Japan, 22-27 September 2013

Interaction of Eu(III) with Mammalian Cells as a Function of Eu(III) Concentration and Nutrient Composition

Susanne Sachs, Anne Heller, Gert Bernhard
Helmholtz-Zentrum Dresden-Rossendorf e.V., Institute of Resource Ecology, P.O. Box 510 119, 01314 Dresden, Germany

The Eu(III) toxicity onto FaDu cells is influenced by its chemical speciation that is determined by the composition of the culture medium. However, independent from its speciation, Eu(III) seems to be bound to the cell surface and does not significantly enter the cells.

Eu(III), interaction, mammalian cells, toxicity, speciation

I. INTRODUCTION

In case of the release of long-lived radionuclides, e.g., actinides, into the environment, knowledge about their behavior in biosystems is necessary to assess and prevent health risks for humans. This includes knowledge about bioavailability and toxicity of actinides for/onto cells, which are governed to a large extent by their speciation [1]. In order to enable a better understanding of these processes, we study interaction processes of trivalent actinides/lanthanides with mammalian cells on a cellular level combining biochemical and spectroscopic methods. In the present work we studied the cellular tolerance of FaDu cells (human squamous cell carcinoma cell line) toward Eu(III), as an analog for trivalent actinides, and its uptake into the cells as a function of the metal concentration and the nutrient composition. In parallel, the Eu(III) speciation in the culture media was studied by time-resolved laser-induced fluorescence spectroscopy (TRLFS) to correlate Eu(III) toxicity and uptake with its chemical speciation.

II. EXPERIMENTAL

FaDu cells were grown in Dulbecco's modified eagle medium supplemented with fetal bovine serum (FBS), non-essential amino acids, HEPES buffer, penicillin/streptomycin, sodium pyruvate (37°C, 5% CO_2, 95% humidity) and subcultivated as described in [2]. The Eu(III) toxicity onto FaDu cells ([Eu]: 5-2000 µM) and its uptake into the cells ([Eu]: 10, 1000 µM) was studied in the presence and absence of FBS as described in [2,3]. In addition, the impact of citrate was studied. To differentiate between chemotoxic and radiotoxic effects of Eu(III), first experiments were performed in the presence of FBS ([Eu]: 10, 1000 µM) applying ^{152}Eu as radioactive tracer. The Eu(III) speciation was studied by TRLFS as described in [4].

III. RESULTS

As an example, the viability of FaDu cells after 24 h of incubation with 5-2000 µM Eu(III) in the presence and absence of FBS (no citrate present) is shown in Fig. 1. The Eu(III) toxicity is higher in the absence of FBS than in its presence. This discrepancy is attributed to the different Eu(III) species in the media and points to an unequal bioavailability of Eu(III). In the presence of FBS, Eu(III) is stabilized in solution by complexation with FBS constituents, most probably serum proteins, which was verified by ultrafiltration. In contrast, in the absence of FBS, the Eu(III) solubility is very low. ICP-MS analysis of Eu(III) precipitates as well as TRLFS point to the occurrence of ternary or higher Eu(III) complexes with phosphate as the dominant ligand. The additional presence of citrate does not significantly affect the Eu(III) toxicity onto the cells in the presence of FBS. However, in its absence, an excess of citrate decreases the Eu(III) toxicity most probably due to a change of the chemical speciation.

Independent from the initial Eu(III) speciation, the Eu(III) uptake by the cells is low. It is predominantly located on the cell surface.

Under the studied experimental conditions, the tolerance of FaDu cells versus Eu(III) appears to be not significantly influenced by the presence of ^{152}Eu, i.e., there seems to be no additional radiotoxic effect.

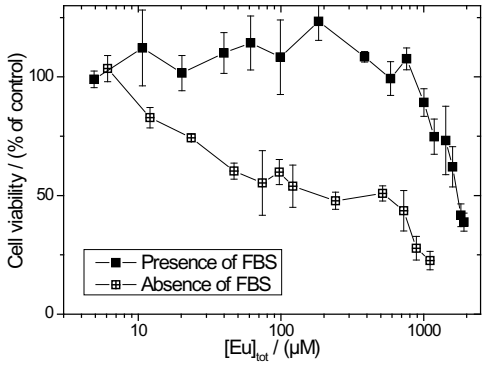

Fig. 1: Cell viability after 24 h of incubation with Eu(III).

ACKNOWLEDGMENTS

We thank J. Seibt, S. Heller, A. Ritter, C. Eckardt, and S. Weiß for experimental and technical support as well as J. Pawelke and E. Leßmann for the first batch of FaDu cells, FBS and training in cell cultivation techniques.

[1] Ansoborlo, E. et al., Biochimie 88 (2006), 1605.
[2] Sachs, S., Bernhard, G., *Annual Report 2011, HZDR-013.* Helmholtz-Zentrum Dresden-Rossendorf, Dresden (2012), p. 12.
[3] Sachs, S., Heller, A., *Annual Report 2012, HZDR-030.* Helmholtz-Zentrum Dresden-Rossendorf, Dresden (2013), p. 26.
[4] Heller, A. et al., *Annual Report 2011, HZDR-013.* Helmholtz-Zentrum Dresden-Rossendorf, Dresden (2012), p. 13.

ENO-06

Monitoring and Elution Characteristics of Radioactive Cs in Incinerator Fly ashes of Municipal Solid Waste

Yuki Iwahana, Yuya Koike, Masaru Kitano, Toshihiro Nakamura
Meiji University

Abstract – Radioactive Cs in incinerator fly ash was monitored and Notification No. 13 test was applied to the ashes in order to estimate the Cs elution. In monitoring, ^{40}K, ^{134}Cs, ^{137}Cs, ^{226}Ra, ^{228}Ra, and ^{228}Th were detected in fly ashes. These concentrations were ^{40}K, 445 – 2,556 Bq kg^{-1}; ^{134}Cs,0 – 10.0 Bq kg^{-1}; ^{137}Cs, 4.2 – 18.4 Bq kg^{-1}; ^{226}Ra,15.0 – 20.1 Bq kg^{-1}; ^{228}Ra, 24.2 – 33.9 Bq kg^{-1}; and ^{228}Th, 23.4 – 33.3 Bq kg^{-1}; respectively. ^{134}Cs was only detected in sample of January, while ^{137}Cs existed in all measured samples, but activity concentrations tended to decrease. As results of pure water and Notification No. 13 elution test, 50–60% of radioactive Cs moved to liquid phase in each case. Since no γ-ray peaks of radioactive Cs were detected on the spectra of elution residues, it was indicated that radioactive Cs in incinerator fly ashes had high water solubility.

Keywords – Radioactive Cs, Notification No. 13 Test, Incinerator Fly Ashes Monitoring

I. INTRODUCTION

Incinerator ashes of municipal solid wastes contain a large amount of hazardous heavy metals and dioxins. They are known as 'specially controlled industrial wastes', and the concentration of hazardous materials in the ashes and leachate from disposal sites are strictly controlled. In Japan, a certification of elution procedure is provided by the Environment Agency of Japan as Notification No. 13 test. In the certification, pH 6.0 of HCl and/or pH8.0 of NaOH solutions were applied to elution. In addition, Fukushima nuclear power plant accident was caused by the Great East Japan Earthquake on March 11, 2011; subsequently radioactive contamination with released radioactive Cs was reported. Following the accident, the Japanese Government established 100, 000 Bq kg^{-1} as the activity concentration limit for radioactive Cs in the incinerator ashes of the MSW that were destined for the landfill. In this report, radioactive Cs in incinerator fly ash was monitored and Notification No. 13 test was applied to the ashes in order to estimate Cs elution.

II. EXPERIMENTAL

The γ-ray measurement were performed with γ-ray spectrometer (γ-PGT) equipped high purity Ge semi-conductor detector. The incinerator fly ashes were obtained in an incinerator plant, located in northern Kyushu, from January to August, 2012.

The elution procedure was followed by the Notification No. 13 test. Eluted materials were added to 2 mL of conc. HNO_3 to rip eluted materials from glass beaker. These solutions were evaporated on evaporation dish to make dried salt. Elution residues and salt were dried at 110°C for a period of 24 h in the drying oven.

About 4 g of solid samples were placed in tin containers (3.8 cmϕ, 1.1 cmh). The containers were made gas tight by sealing with an epoxy resin adhesive and stored for three weeks at least in order to achieve radioactive equilibrium among ^{226}Ra and its daughters. These measurement samples were set away from the Ge-detector to prevent considering the coincidence sum effect. The γ-rays were measured for 48 h.

III. RESULTS AND DISCUSSION

A. *Cs monitoring*

In the fly ahses, ^{40}K, ^{134}Cs, ^{137}Cs, ^{226}Ra, ^{228}Ra, and ^{228}Th were identifed. These concentrations of nuclides were ^{40}K, 445 – 2,556 Bq kg^{-1}; ^{134}Cs,0 – 10.0 Bq kg^{-1}; ^{137}Cs, 4.2 – 18.4 Bq kg^{-1}; ^{226}Ra,15.0 – 20.1 Bq kg^{-1}; ^{228}Ra, 24.2 – 33.9 Bq kg^{-1}; and ^{228}Th, 23.4 – 33.3 Bq kg^{-1}; respectively. ^{134}Cs was only detected in sample of January, while ^{137}Cs existed in all measured samples, but activity concentrations tended to decrease. Therefore, it was considered that the influence of ^{134}Cs, which had been released from Fukushima nuclear power plant, faded away. By contrast, concentrations of natural radioactive nuclides were constant.

B. *Results of Notification No. 13 Test*

To estimate Cs elution, Notification No. 13 test was applied to fly ashes collected on January and August. Pure water elution was also performed under the same condition of official certification. About 50% of ^{134}Cs and 60% of ^{137}Cs eluted when pure water had been used. Comparable results were obtained as the pH 6.0 of HCl and pH 8.0 of NaOH solutions were used for elution. While no γ-ray peaks of radioactive Cs were detected on spectra of each elution residues. Hence, it was indicated that radioactive Cs in incinerator fly ashes had high water solubility.

IV. CONCRUSIONS

Radioactive Cs in incinerator fly ashes tends to decrease from January to August, 2012. From Result of pure water and Notification No. 13 elution test, radioactive Cs in incinerator fly ashes had high water solubility for deposit site of incinerator fly ashes.

APSORC'13 - 5th Asia-Pacific Symposium on Radiochemistry
Kanazawa, Japan, 22-27 September 2013

The Issue of Separation of Uranium from Drinking Water in the Czech Republic

Jan Krmela[1]
[1]UJV Řež a.s., Hlavní 130, Řež, 250 68 Husinec, The Czech Republic, jan.krmela@ujv.cz

Abstract

Natural ground water used for the preparation of drinking water contains a number of cations, anions, elements and other substances depending on the bedrock composition (Ca, Mg, Fe, Mn, heavy metals, radioactive elements, arsenic, chromium, carbonates, sulfates, phosphates, silicates, fulvic and humic acids etc.). Information about composition of drinking water is important to comply with all the requirements on sanitary of drinking water.

The elements that affect the quality of drinking water mainly from groundwater, also includes radioactive elements contained in bedrock sections where water is extracted. These are the elements with long half-lives, mainly alpha emitters (U, Ra, Rn, Th, and elements of the decay series).

Uranium and its decay products are found in all environmental compartments. Radionuclides come to the environment both naturally - weathering and leaching of the rocks, and as a consequence of human activities in connection with the use of raw materials.

Uranium occurs naturally in four oxidation states. The most mobility has hexa-valent state (uranyl ion). Uranyl is highly soluble form of uranium in water. Mobility of uranium in soil and water is affected by many factors.

Complex processes in soil and rock lead to redox reactions forming both insoluble compounds (lower valence forms of uranium) and soluble form of U (VI) (forming by reoxidation), which is again leachable into groundwater. The content of uranium in groundwater depends on the geological composition of the ground, and can reach up to hundreds of μg/L.

At present the issue associated with removing uranium from drinking water is solved in the Czech Republic. New limit for the concentration of natural uranium (^{234}U, ^{235}U and ^{238}U) was recommended at a level of 15 μg/L as the highest limit based on the World Health Organization (WHO). Advice of the Chief Health Officer of the Czech Republic came into force on 1st January 2010, which decreased the limit for uranium in drinking water from original 30 μg/L to new 15 μg/L recommended by WHO. However, the WHO reported a new limit value of 30 μg/L in 2011 based on a new studies, which proved that 30 μg/L uranium in drinking water has not negative effect on the human organism (chemical toxicity) [1]. Limit in the Czech Republic remained at the same level 15 μg/L.

Change the limit leaded to solving the issue on the waterworks in the Czech Republic, which had not any experiences with radioactivity. Some waterworks installed a new device from Germany (ion exchanges), but did not solve what they do with saturated ion exchanges. Ion exchanges as the most suitable material for removing of uranium from drinking water is not reused (without regeneration), but it is used in the uranium industry, where is putted to start of processing of uranium ore. Ion exchanges are replaced with a new one in the waterworks and saturated ion exchanges are discarded in the uranium industry.

Regeneration of ion exchanges could be cheaper, because ion exchanges could be reused and processing of ion exchangers could be cheaper, because it is possible to put the regenerant before the process of precipitation of "yellow cake" in the processing of uranium ore.

This project TA02010044 was supported by TA CR.

Key words - Uranium, Drinking water, Ion exchanger

[1] WHO: Uranium in Drinking-water, Background document for development of WHO guidelines for Drinking-water Duality, WHO/SDE/WSH/03.04/118/Rev/1, 2011.

Air-born contamination caused in a high-energy proton accelerator room

K. Mausmoto[1], A. Toyoda[1], H. Matsumura[1], T. Kunifuda[2]
[1]High Energy Accelerator Research Organization, Tsukuba, 305-0801, Japan
[2]Tokyo Nuclear Service, Tsukuba, 300-2646, Japan

Abstract – Surface contamination caused during the operation of 12-GeV proton synchrotron, KEK have been studied by gamma-ray spectrometry and imaging plate technique. The surface of accelerator component was wiped with the filter paper. PSL value of imaging plate contacted on the filter paper decreased according to the half-life of 2 weeks. Therefore, it was assumed that ^{32}P might be produced from Ar by the high-energy protons and neutrons and deposited on the accelerator components.

Keywords – Air-born activity, High-energy accelerator, ^{32}P, Imaging plate

I. INTRODUCTION

It is well known that various radioisotopes are induced in the stratosphere by cosmic rays. During the operation of a high-energy proton accelerator, air components are also activated by primary protons and secondary neutrons and similar radioisotopes are produced. It is interesting to know the behavior of radioisotopes in an accelerator room. The radioisotopes are deposited on the surface of accelerator components and cause surface contamination problem. In this work, these radioisotopes were wiped with a filter paper. The radioactivity was measured by the gamma-ray spectrometry and the imaging plate technique.

II. EXPERIMENTAL

This work was performed at the 12-GeV proton synchrotron, KEK. After stopping, smeared samples were obtained from on beam pipes, magnets, wall and floor in the accelerator room. In order to measure the activity of beta and gamma nuclides, a GM-counter, a liquid scintillation counter, a Ge-detector and an imaging plate were used.

III. RSULTS AND DISCUSSIONS

(1) A liquid scintillation counter

Tritium was only observed. Carbon-14 could not detected by the background effect.

(2) GM-counter and Imaging plate

Figure 1 shows the decay curves of seven filter papers sampled from the beam line. It was found that the half-life of major activity was 2 weeks. Therefore, it was assumed that ^{32}P was produced and deposited. As the similar result was obtained by a GM-counter, Imaging plate was also detected beta activity. A polyethylene film pasted on the wall and surface was wiped with a filter after beam stopping. In this case, ^{32}P was also observed as a major activity.

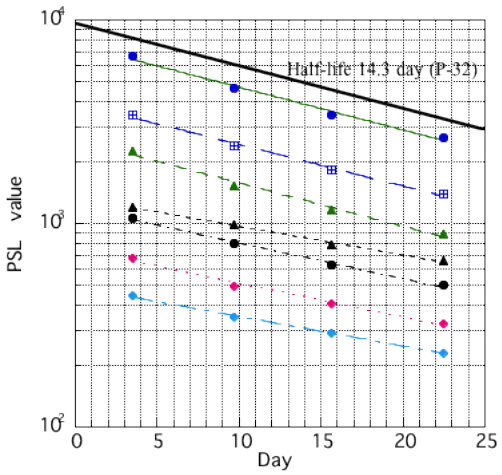

Fig. 1 Decay curves of radioactivity collected on filter

(3) Ge-detector

Many radioisotopes such as ^{7}Be, ^{54}Mn, were observed. ^{7}Be was produced by the spallation reactions of oxygen and nitrogen in air and deposited on the surface of beam line. The gamma activity obtained by the Ge-detector was not correlated with the result of imaging plate technique. Therefore, beta activity is important for surface contamination.

IV. CONCLUSION

An imaging plate technique is very useful to measure the radioactive decay of many samples simultaneously on the same condition.

Induced radioisotopes in air were deposited on the beam line. Because, the radioisotopes attached to aerosol and deposited on the surface of beam line. A major acitivity was ^{32}P, which might be produced by the spallation reaction of Ar in air.

In case of high-energy and high-intensity accelerators, radioactive aerosol formation will become important problem of radiation control. And this phenomenon was interesting subject to achieve the cosmic ray reaction in the stratosphere on the ground level.

APSORC'13 - 5th Asia-Pacific Symposium on Radiochemistry
Kanazawa, Japan, 22-27 September 2013

Application of ^{210}Pb in Glaciology

H.W. Gäggeler, L. Tobler, M. Schwikowski
Paul Scherrer Institut, Labor für Radio- und Umweltchemie, 5232 Villigen, Switzerland

Keywords – ^{210}Pb dating, climate research, environmental pollution, non-dating application of ^{210}Pb

I. *ABSTRACT*

Glaciers are increasingly used as proxies for climate change. Advances and retreats of these ice bodies are prime information on climate variability. Moreover, glaciers have found widespread application as archive of current and past atmospheric information. To fully benefit from such information, the glaciers have first to be dated. ^{210}Pb is one of the most frequently used radionuclide that enables dating for one to two centuries BP (before present). ^{210}Pb is ubiquitous in atmosphere, since it is a decay product of natural radon (^{222}Rn). Attached to aerosol particles ^{210}Pb is then scavenged by precipitation and deposited on the Earth surface. ^{210}Pb has proven to be much more versatile as information species besides dating. This contribution summarizes some examples that includes (besides dating, see e.g. figure 1);

Determination of annual snow accumulation rates at remote sites using the ^{210}Po/^{210}Pb disequilibria.

Thinning of glaciers as a function of depth caused by the increasing mass of overlying fresh snow and ice.

Folding of low lying ice layers due to topographic conditions that lead to non regular age-depth relationships.

Variability of seasonal deposition at high altitudes due to convective processes in summer.

Study of heavy metal percolation in temperate glaciers

Determination of sublimation rates at glacier sites in arid areas such as the Andes.

^{210}Pb activity concentrations as indicator of air masses, with low values for precipitation from marine air and high values for continental air, respectively.

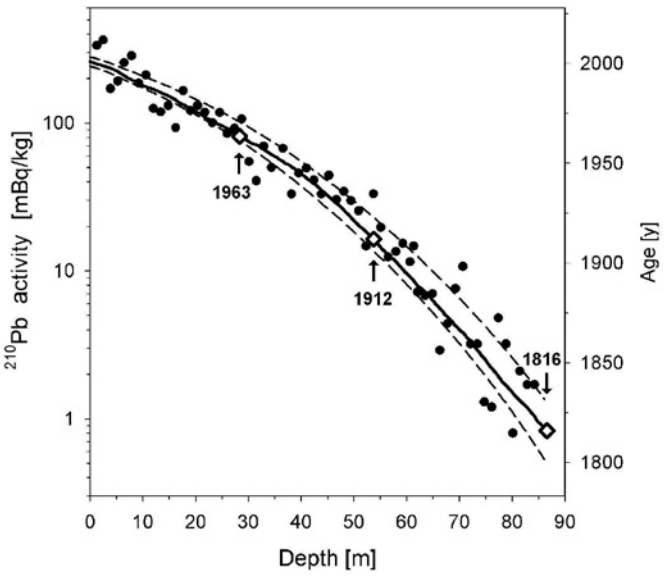

Fig. 1: ^{210}Pb activity concentrations along an ice core from the Belukha saddle in the Altai mountains (Siberia, Russia) together with three additional time horizons from the nuclear weapons testing (1963: measured via tritium), and the well known volcanic eruptions from Katmai (1912) and Tambora (1816) identified via increased excess sulphate concentrations. The right axis depicts the age deduced from the ^{210}Pb measurement (deduced from [1])

Presented examples originate from glaciers studied at our institute. Ice core drillings were performed in the European Alps, the South American Andes, the Russian and Mongolian Altai, the Mt. Cook area in New Zealand and in Svalbard (Norway).

References

[1] Olivier, S.., C. Blaser, S. Brütsch, N. Frolova, H.W. Gäggeler, K.A. Henderson, A.S. Palmer, T. Papina, M. Schwikowski, Temporal variations of mineral dust, biogenic tracers and anthropogenic species during the past two centuries from Belukha ice core, Siberian Altai, J. Geophys. Res. Atmospheres, 111, DO5309, doi:10.1029/2005/Doo5830 (2006)

APSORC'13 - 5th Asia-Pacific Symposium on Radiochemistry
Kanazawa, Japan, 22-27 September 2013

Depth distributions of uranium-236 and cesium-137 in the Japan Sea; toward the potential use as a new oceanic circulation tracer

Aya Sakaguchi[1], Akinobu Kadokura[1], Peter Steier[2], Yoshio Takahashi[1], Kiyoshi Shizuma[3], Tomoeki Nakakuki[1], Masayoshi Yamamoto[4]
[1] Graduate School of Science, Hiroshima Univ.
[2] VERA-Laboratory, Univ. of Vienna
[3]Graduate School of Engineering, Hiroshima Univ.
[4]Low Level Radioactivity Laboratory, Kanazawa Univ.

We present a feasibility study for using ^{236}U as an oceanic circulation tracer based on depth profiles of ^{236}U and ^{137}Cs in the Japan/East Sea. The concentration of the predominantly anthropogenic ^{236}U, measured with Accelerator Mass Spectrometry (AMS), decreased from the order of 10^7 atom/kg in surface water to 10^6 atom/kg close to the sea floor (3000 m). The profile has a smooth trend with depth and concentration values are generally proportional to that of ^{137}Cs for the same water sample. The cumulative inventory of dissolved ^{236}U in the water column was estimated to be 10^{12}-10^{13} atom/m^2, which is similar to the global-fallout level ($17.8x10^{12}$ atom/m^2) in Japan. Additional analyses of suspended solids (SS) and bottom sediments yielded negligible amounts of ^{236}U. Our results suggest that ^{236}U behaves as a conservative nuclide in seawater, with potential advantages over other tracers of oceanic circulation.

Keywords – *the Japan Sea, GEOTRACES, U-236, Cs-137, globalfallout*

I. INTRODUCTION

^{137}Cs ($T_{1/2}$=30.2 y) has been spread all over the world as a fission product of atmospheric nuclear weapons tests in the 1960s. This nuclide has been used as a powerful tool for oceanography due to the well-defined origin and conservative behaviour in water. However, the number of atoms has decayed already to one thirds compared with its initial levels, and it will become more difficult to measure. In this situation, we focus on ^{236}U ($T_{1/2}$=2.342×10^7 y) as a candidate for a new isotopic tracer for oceanography. The detection of ^{236}U in the environment has become possible only recently, by the development of measuring techniques with high sensitivity based on AMS. Our group showed that global fallout from bomb tests contains ^{236}U, which might be produced as nuclear reactions of $^{235}U(n,\gamma)$ and/or $^{238}U(n,3n)$[1]. So ^{236}U has been therefore globally distributed in the surface environment. Thus, ^{236}U has a similar potential as a tracer for environmental dynamics as ^{137}Cs, especially for oceanography.

In this study, a comprehensive attempt was made to measure the concentration of ^{236}U in marine samples such as water, suspended solid and bottom sediments to clarify the environmental behaviour of this isotope. Furthermore, the discussion of the circulation of deep and bottom water in "Miniature Ocean", the Japan Sea, has been attempted.

II. MATERIAL AND METHOD

Bottom sediments (4 sites) and seawater samples (7 sites) were collected from the Japan Sea in the research cruise with R/V Hakuhomaru, 2010 . The sediment core was cut into 1 cm segments from the surface to 5 cm in depth within a few hours after the sampling. About 20 L of seawater samples were collected from some depths in each site, and immediately after the sampling, the water was filtered with 0.45 μm pore-size membrane-filters. After the appropriate pre-treatment for each sample, uranium isotope and ^{137}Cs were measured with AMS and Ge-detector, respectively. The detail of these methods were published in Sakaguchi et al., (2012)[2].

III. RESULTS AND DISCUSSION

^{236}U was successfully detected for all seawater samples, and $^{236}U/^{238}U$ atom ratios in seawater were in the range of (0.19-1.75)×10^{-9}. The dissolved ^{236}U concentration showed a subsurface maximum and decreased steeply with depth. The minimum value was found at a depth of 2500 m and bottom (about 3000 m in depth) in the northern and the southern areas, respectively. These profiles are markedly different from that of natural ^{238}U which is nearly constant over the depth, suggesting that ^{236}U has not yet reached steady state. For the SS sample, ^{236}U could not be detected in significant levels. The total ^{236}U inventory of the water column was estimated at 10^{12}-10^{13} atom/m^2. This value is nearly the same as the global fallout level (17.8×10^{12} atom/m^2)[1][2]. ^{236}U was also found in the bottom sediments, and the inventory was about 1/40 compared with that in water column. All above characters are comparable with ^{137}Cs which is anthropogenic conservative nuclide in ocean. Actually, the diffusion coefficients for both nuclides show the nearly same value. The detail discussion of this study has been shown in Sakaguchi et al., (2012)

[1] A. Sakaguchi, K. Kawai, P. Steier et al. Science of the Total Environment. 407, 4238-4242, 2009.
[2] A. Sakaguchi, K. Kawai, P. Steier, et al., Science of the Total Environment, 408, 5392-5398, 2010.
[3] A. Sakaguchi, A. Kadokura, P. Steier,et al, Earth and Planetary Science Letters, 333-334, 165-170, 2012.

Ultratrace Analysis of Long-lived Radionuclides by Resonance Ionization Mass Spectrometry (RIMS)

J.V. Kratz
Institute for Nuclear Chemistry, Johannes Gutenberg-University, Mainz, Germany

Keywords – Ultratrace analytical method, resonant laser ionization, isotopic composition, plutonium analyses, actinide ionization potentials, optical spectroscopy with ^{255}Fm, IONTOF-SIMS coupled with RIMS

Abstract For long-lived radionuclides such as actinides, conventional radioanalyses by α spectroscopy suffer from unsatisfactory limits of detection (LOD). Resonance ionization mass spectrometry, on the contrary, achieves limits of detection of 10^6 atoms and is free from isobaric interferences [1,2]. The multiple step resonant excitation of evaporated atoms with laser light and the mass selective detection is presented for isotopes of plutonium as an example. We use a frequency-doubled Nd:YAG laser with a repetition rate of 10 kHz to pump three titanium-sapphire lasers delivering wave lengths of 420.76 nm, 847.28 nm, and 767.53 nm to resonantly excite plutonium into a Rydberg state from where ionization is achieved by applying an electric field [3]. For isotopic composition measurements, the wavelengths of lasers 1 and 2 must be readjusted for each isotope while laser 3 can be maintained at the same wavelength. The accuracy of isotopic ratios determined this way is demonstrated with a certified NIST standard. Applications are presented for fallout plutonium, reactor plutonium, samples from the Chernobyl area, wapons plutonium from the Mururoa island, seawater plutonium from the Northern Sea, and from the Irish Sea. Migration of plutonium through a granite fracture in the Grimsel underground laboratory has also been investigated [4].

By detecting ionization thresholds as a function of the applied electric field, accurate ionization potentials IP of Ac, Th, U, Np, Pu, Am, Cm, Bk, Cf, and Es have been determined by extrapolation to zero field strength [5, 6, 7]. In a first attempt to determine also the IP of Fm, a sample of 20.1-h ^{255}Fm produced at the HFIR at Oak Ridge has been investigated. By resonance excitation with a dye laser and ionization with an excimer laser in a buffer gas cell, two excited states of Fm ($5f^{12}$ 7s 7p) have been identified and mass spectra of $^{255}Fm^+$ and the daughter $^{251}Cf^+$ have been measured by a quadrupole mass spectrometer coupled to a channeltron detector [8]. By measuring the drift times of these ions and of $^{238}UO^+$, ion mobilities in the electric field could be determined. These are potentially useful to determine ionic radii of the heavy actinides and superheavy elements.

By using a commercial IONTOF-SIMS apparatus, analyses of hot micro particles with high lateral resolution in the sub-micron range have been exploited [9]. For the determination of the location of these hot particles (x,y coordinate on the target holder) their content of fissile material via fission track analysis [10] has been used. In order to avoid isobaric interferences, the sputtered ions (SIMS) were suppressed by a pulsed counter voltage applied to the target holder, and the abundantly sputtered neutral particles were resonantly excited and ionized by RIMS. The resulting ions were directed by an alternating acceleration voltage into the TOF mass spectrometer.

[1] N. Erdmann, G. Herrmann, G. Huber, S. Köhler, J.V. Kratz, A. Mansel, M. Nunnemann, G. Passler, N. Trautmann, A. Turchin, A. Waldek
Fresenius J. Anal. Chem. 359, 378 (1997)
[2] M. Nunnemann, N. Erdmann, H.-U. Hasse, G. Huber, J.V. Kratz, P. Kunz, A. Mansel, G. Passler, O. Stetzer, N. Trautmann, A. Waldek
J. Alloys and Compounds 271-273, 45 (1998)
[3] C. Grüning, G. Huber, P. Klopp, J.V. Kratz, P. Kunz, G. Passler, N. Trautmann, A. Waldek, K. Wendt
Int. J. Mass Spectrometry 235, 171 (2004)
[4] S. Bürger, R.A. Buda, H. Geckeis, G. Huber, J.V. Kratz, P. Kunz, Ch. Lierse von Gostomski, G. Passler, A. Remmert, N. Trautmann
in: Radioactivity in the environment – Volume 8, series editor: M.S. Baxter, Elsevier 2006, 581
[5] S. Köhler, R. Deißenberger, K. Eberhardt, N. Erdmann, G. Herrmann, G. Huber, J.V. Kratz, M. Nunnemann, G. Passler, P.M. Rao, J. Riegel, N. Trautmann, K. Wendt
Spectrochimica Acta, Part B 52, 717 (1997)
[6] J.R. Peterson, N. Erdmann, M. Nunnemann, K. Eberhardt, G. Huber, J.V. Kratz, G. Passler, O. Stetzer, P. Thörle, N. Trautmann, A. Waldek
J. Alloys and Compounds 271-273, 876 (1998)
[7] N. Erdmann, M. Nunnemann, K. Eberhardt, G. Herrmann, G. Huber, S. Köhler, J.V. Kratz, G. Passler, J.R. Peterson, N. Trautmann, A. Waldek
J. Alloys and Compounds 271-273, 837 (1998)
8] H. Backe, A. Dretzke, K. Eberhardt, S. Fritzsche, C. Grüning, G. Gwinner, R. G. Haire, G. Huber, J.V. Kratz, G. Kube, P. Kunz, J. Lassen, W. Lauth, G. Passler, R. Repnow, D. Schwalm, P. Schwamb, M. Sewtz, P. Thörle, N. Trautmann, A. Waldek
J. Nucl. Sci. Tech., Suppl. 3, 86 (2002)
[9] N. Erdmann, J. V. Kratz, N. Trautmann, G. Passler
Anal. Bioanal., Chem. 395, 1911 (2009)
[10] O. Stetzer, M. Betti, J. van Geel, N. Erdmann, J.V. Kratz, R. Schenkel, N. Trautmann
Nucl. Instr. and Meth. in Physics Research A525, 582 (2004)

APSORC'13 - 5th Asia-Pacific Symposium on Radiochemistry
Kanazawa, Japan, 22-27 September 2013

The Bulk Analysis with TIMS Measurements Performed in KAERI for Nuclear Safeguards

Jong-Ho Park, Sunyoung Lee, Young-Geun Ha, Seon A Lee, Kahee Jeong, Kyuseok Song
Nuclear Chemistry Research Division, Korea Atomic Energy Research Institute, Daejeon 305-353, Korea.

Abstract

KAERI has been developing the techniques for bulk analysis of environmental samples to support the international society for nuclear safeguards purpose. The analytical procedure, which consists of screening, ashing, acid digestion, chemical separation, and isotopic measurements by TIMS, was established. The analytical results of simulated environmental samples prepared from certified reference materials fell into the criteria that the IAEA requires for the NWAL qualification.

Environmental Sample, Safeguards, Isotopic Analysis, TIMS

I. INTRODUCTION

Highly accurate and precise analysis of nuclear materials in environmental samples plays essential roles in monitoring undeclared nuclear activities.[1] The IAEA has been maintaining a Network of Analytical Laboratories (NWAL) for nuclear safeguards. Since 2009, Korea Atomic Energy Research Institute (KAERI) has been developing the techniques for bulk analysis of environmental samples to support the international society as one of the members of NWAL. The analytical techniques that KAERI is utilizing with TIMS measurements for bulk analysis are briefly introduced in this paper.

A. Sample Analysis Procedure

Decomposition and acid digestion of environmental samples were carried out to prepare sample solutions in nitric acid, called as the mother solution. The solutions were weighed precisely, and then divided into three for determination of U isotope ratios and Pu quantity, for determination of U quantity and Pu isotope ratio, and for archive, respectively. Appropriate spike isotopic reference materials were added to the corresponding mother solution portion. IRMM 040a (^{233}U) and IRMM 085 (^{242}Pu) were used for quantification of uranium and plutonium, respectively.

The Pu isotopes were eluted into the conical PFA vial through the UTEVA columns with 2M HNO_3/0.02M ascorbic Acid/0.02M $NH_2OH \cdot HCl$ after loading the sample solution adjusted with 8M HNO_3/0.3% H_2O_2 on the UTEVA columns. The uranium isotopes were eluted through the columns with 0.007M ammonium oxalate solution. The purified Pu and U solutions were evaporated to dryness with concentrated nitric acid, HF and $HClO_4$ until any residue was not found in the PFA vial. Each sample was loaded on a pre-degassed rhenium filament with minimized residue. A thermal ionization mass spectrometer (TRITON, Thermo Fisher Scientific) was utilized for isotopic measurement.

A simulated samples were prepared with cotton swipe containing known amounts of uranium (CRM 112-A) and plutonium (REIMEP 16D) reference materials. The routine procedure was applied for the bulk analysis of the simulated samples.

B. Result

The analytical results of simulated environmental samples prepared from certified reference materials are shown in Table 1. The accuracy and the precision of the result fell into the criteria that the IAEA requires for the NWAL qualification. The measured n(^{235}U)/n(^{238}U) of the samples agreed with the certified value within less than 1% of accuracy.

Table 1. The result of bulk analysis of simulated environmental samples

	n(^{234}U)/n(^{238}U)	n(^{235}U)/n(^{238}U)	n(^{240}Pu)/n(^{239}Pu)
Cert.	5.2841e-5	7.2543e-3	1.110e-1
#1	5.32[±0.52]e-5	7.27[±0.18]e-3	1.150[±0.005]e-1
#2	6.71[±0.97]e-5	7.28[±0.11]e-3	1.140[±0.002]e-1

Numbers in parentheses indicate expanded uncertainties $U = k \cdot u_c$

[1] D. L. Donohue, *J. Alloy Compd.* **1998**, 271-273, 11.

APSORC'13 - 5th Asia-Pacific Symposium on Radiochemistry
Kanazawa, Japan, 22-27 September 2013

Determination of plutonium isotopes at ultratrace level in seawater samples by sector-field ICP-MS combined with chromatographic separation

Wenting Bu[1,2], Jian Zheng*[2], Qiuju Guo*[1], Tatsuo Aono[2], Keiko Tagami[2], Shigeo Uchida[2]
[1]School of Physics, Peking University, China
[2]National Institute of Radiological Sciences, Japan

Plutonium isotopes are released into the environment as a consequence of human nuclear activities including nuclear weapon testing, nuclear fuel reprocessing and nuclear accident. As the world's ocean covers ca. 70 % of the earth surface, it received majority of Pu isotopes released into the environment by atmospheric nuclear weapons tests. For example, it has been estimated that the total global fallout $^{239+240}$Pu released into the environment was about 10.87 PBq, and 6.6 PBq entered the world's ocean[1]. Besides, a significant amount of Pu isotopes were injected directly to the world's ocean by close-in fallout from the nuclear explosions conducted at the Pacific Proving Ground by US and the French Polynesia by France.

Due to their radiotoxicity and long half-lives, Pu isotopes are regarded as highly hazardous pollutants in the marine environment and are of great research interest. Accurate and precise determination of plutonium isotopes in marine samples is important for radioecological assessment. In addition, Pu isotopes have also been used for tracing of oceanographic processes, such as water mass circulation, transport and scavenging of particulate matter, etc.

The concentration of Pu in seawater is extremely low ($^{239+240}$Pu, 1.2-7.4 mBq/m^3 in the surface seawater of the NW Pacific Ocean).[2] By the traditional alpha spectrometry method, usually large volume (~ 200 L) of seawater sample is needed for the analysis of Pu, and the ^{240}Pu/^{239}Pu atom ratio, which is an important fingerprint for Pu source identification and for tracing of oceanographic processes, cannot be obtained.[3] Due to the low detection limit and the relatively simple sample preparing procedures, ICP-MS has been treated as a promising method for the analysis of Pu in environmental samples in recent years. However, when using ICP-MS, the detection of ^{239}Pu and ^{240}Pu can be affected by spectral interferences caused by $^{238}UH^+$ and $^{238}UH_2^+$ formations, especially for the environmental samples with high U concentrations. The concentration of U in seawater in the Pacific Ocean is about several μg/L and the atom ratio of ^{238}U/^{239}Pu can be up to 10^{11}.[4] Thus, complex procedures for the preconcentration of Pu and separation of Pu from U were employed for the determination of Pu in seawater prior to the analysis by ICP-MS, which somehow may lead to a low Pu recovery.

In this work, we presented a simple method for the analysis of Pu concentration and its isotopic composition in seawater samples by sector field ICP-MS combined with chromatographic separation technique. High precision and accuracy were achieved by using this method. The detailed analytical procedures and the merits of this method will be discussed at the conference.

Acknowledgments
This work was supported by the Ministry of Education, Culture, Sports, Sciences and Technology (MEXT) (24110004), Japan, and partly supported by the Agency for Natural Resources and Energy, the Ministry of Economy, Trade and Industry (METI), Japan.

References
[1] Aarkrog, A., Deep-Sea Res. II, 50, 2597-2606, 2003.
[2] Povinec, P. P., Livingston, H. D., Shima, S. et al., Deep-Sea Res. II, 50, 2607-2637, 2003.
[3] Yamada, M. and Zheng, J., Appl. Radiat. Isot., 66, 103-107, 2008.
[4] Chen, J. H., Edwards, R. L., Wasserburg G. J., Earth Planet. Sci. Lett., 80, 241-251, 1986.

APSORC'13 - 5th Asia-Pacific Symposium on Radiochemistry
Kanazawa, Japan, 22-27 September 2013

Semi-automated Procedure for the Determination of ^{89,90}Sr in Environmental Samples by Cherenkov Counting

Ivana Milanović, Željko Grahek
Division for marine and environmental research, Ruđer Bošković Institute, Zagreb, Croatia

Abstract - Development of new chromatographic resins in the last two decades Sr resin, AnaLig-01 and SuperLig 620 has significantly simplified separation of strontium from various types of samples. These resins, that have principles based on molecular recognition, are highly selective for strontium binding. In combination with appropriate detection methods they enable automatic determination of radioactive strontium. Sequential injection analysis and equilibration based sensor column analysis were developed for the determination of long lived ^{90}Sr (28.8 y) in liquid radioactive waste and water samples.[1-3] However, ^{89}Sr that has short half-life (50.5 d), can also be present in samples, especially in those exposed to fresh fallout from nuclear reactor. Classical analysis of ^{89}Sr requires isolation of ^{90}Y, usually after attaining of secular equilibrium of ^{90}Sr-^{90}Y and the whole procedure takes at least 16 days. However, by using Cherenkov counting technique, determination time may be significantly reduced. Unlike ^{90}Sr that emits low energy electrons, its daughter ^{90}Y as well as ^{89}Sr, generates Cherenkov photons in aqueous media. Consequently, by successive counting within 64 hours, ^{89}Sr and ^{90}Sr via ^{90}Y can be determined. Therefore, the main aim of this research is development of semi-automated procedure for the determination of ^{89,90}Sr. It includes solid phase extraction (SPE) of strontium from liquid samples and Cherenkov counting of its isotopes. The procedure is based on sample - column equilibration and off-line detection of bound ^{89,90}Sr on the column. Sample is pumped through column at constant flow rate until the breakthrough or saturation point is achieved. The ^{89,90}Sr is determined by counting on column in PE vial. It will be shown how strontium can be selectively bound on the Sr resin, AnaLig-01 and SuperLig 620 resins and separated from interfering radionuclides. Also, influence of column geometry, amount of resin and media in PE vial around the column on quantity determination, detection efficiency and achievable lower detection limits will be discussed. The method is tested in proficiency testing samples and natural water samples.

Keywords – semi-automated procedure, solid phase extraction, Cherenkov counting, ^{89,90}Sr determination

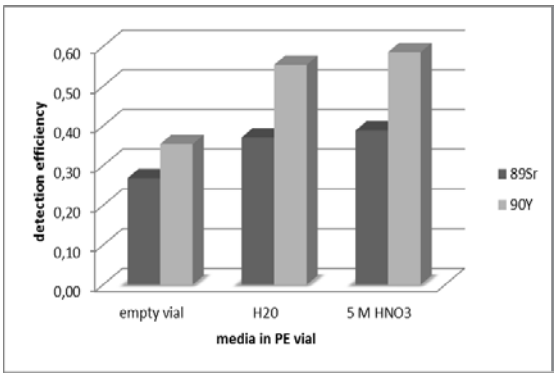

Figure 1. Detection efficiency of ^{89}Sr and ^{90}Y bound on AnaLig-01 resin depending on surrounding media (TriCarb 3180)

REFERENCES

[1] O. B. Egorov, M. J. O'Hara, J. W. Grate, Equilibration-Based Preconcentrating Minicolumn Sensors for Trace Level Monitoring of Radionuclides and Metal Ions in Water without Consumable Reagents. *Anal. Chem.* **2006** 78(15) 5480-5490.

[2] J. W Grate, O. B. Egorov, M. J. O'Hara, T. A. Devol, Radionuclide Sensors for Environmental Monitoring: From Flow Injection Solid-Phase Absorptiometry to Equilibration-Based Preconcentrating Minicolumn Sensors with Radiometric Detection. *Chem. Rev*. **2008** 108(2) 543-562.

[3] M. J. O'Hara, S.R. Burge, J. W. Grate, Automated radioanalytical system for the determination of Sr-90 in environmental water samples by Y-90 Cherenkov radiation counting. *Anal. Chem.* **2009** 81(3) 1228-1237.

Research and Development towards Decommissioning of Fukushima Daiichi Nuclear Power Plants

Kazuo Minato
Nuclear Science Research Institute, Tokai Research and Development Center,
Japan Atomic Energy Agency
Tokai-mura, Ibaraki-ken 319-1195, Japan

Abstract – Towards the decommissioning of Fukushima Daiichi Nuclear Power Plants, science-based research and development is important and useful, as well as technology and engineering development. Research and development activities based on radiation chemistry, radiochemistry, thermodynamics, etc., have contributed to safe and efficient decommissioning of the plants.

Keywords – Fukushima Daiichi, Decommissioning, Radiation Chemistry, Radiochemistry, Thermodynamics

I. INTRODUCTION

Two and a half years have passed since the accident at Fukushima Daiichi Nuclear Power Station Units 1-4, Tokyo Electric Power Company, Inc. (TEPCO). The research and development towards decommissioning of the plants, concerning the removal of fuels from spent fuel pools, removal of fuel debris, processing and disposal of radioactive waste, and remote control equipment and devices, have been being made as national projects, which are based on the Mid-and-Long-Term Roadmap towards the Decommissioning of TEPCO's Fukushima Daiichi Nuclear Power Station Units 1-4 [1]. Besides TEPCO, plant makers, research institutes, etc., jointly participate in the projects. Among them the Japan Atomic Energy Agency is playing an important part in science-based research and development to support the decommissioning of the plants.

II. RADIOLYSIS OF SEAWATER

One of the distinguishing features of the accident is that seawater was injected to the damaged reactor cores and spent fuel pools in the early stage of actions. The accumulated radioactive water, including seawater, in the reactor and turbine buildings has been being processed for decontamination and desalination. This process generates spent zeolites highly contaminated with radioactive cesium. For safe storage of the spent zeolites, hydrogen generation should be clarified.

Gamma-ray irradiation experiments revealed that the yield of hydrogen from seawater was larger than that from pure water and comparable to the primary yield, indicating that oxidation of hydrogen by radical products of water radiolysis is not effective in seawater due to the presence of Cl^- and Br^- ions. Furthermore, hydrogen generation was increased by addition of the zeolite to seawater. This means that the radiation energy deposited on zeolite is involved in hydrogen formation [2].

Based on the experimental data, hydrogen generation in the vessels was evaluated, and the procedures to repress hydrogen generation in the spent zeolite were suggested.

III. RADIOCHEMICAL ANALYSIS OF WASTE

The radioactive materials were released into the environment by the accident. A huge amount of the waste contaminated with the radioactive materials was generated. To classify the waste and to establish ways of processing and disposal of the waste, inventory of radioactive materials in the waste should be clarified.

The analysis of rubbles, trees, and accumulated water sampled in the site of the nuclear power station revealed that the main radionuclide was ^{137}Cs (and ^{134}Cs) with very small amounts of fission products, actinides, and activation products, which is quite different from those of the radioactive waste generated from ordinary nuclear power stations and reprocessing plants. The development of separation method of a target nuclide before radiochemical analysis was inevitable, and the analytical scheme and methods have been developed for the nuclides, such as ^{3}H, ^{14}C, ^{36}Cl, ^{79}Se, ^{90}Sr, ^{99}Tc, ^{129}I, ^{60}Co, ^{94}Nb, ^{137}Cs, ^{152}Eu, ^{154}Eu, ^{238}Pu, ^{239}Pu, ^{240}Pu, ^{241}Am, and ^{244}Cm.

IV. THERMODYNAMIC ANALYSIS OF FUELS

A large amount of seawater was injected into the reactor pressure vessels in the accident. Several elements contained in seawater possibly reacted with degraded fuel debris and molten corium. These reactions may have affected volatilization of fission products, property of fuel debris, and formation of corrosive gases.

Thermodynamic evaluation indicated that volatility of Cs, Sr, and Te was potentially increased due to the change in stable chemical species, and that corrosive gases, such as HCl and H_2S, were possibly generated, depending on temperature and oxygen potential [3].

Experiments on the high temperature reaction between sea salt deposit and $(U,Zr)O_2$ simulated fuel debris (sim-debris) were also made. A dense layer of calcium and sodium uranate formed on the surface of a sim-debris under airflow. When the oxygen partial pressure was low, calcium was dissolved into the cubic sim-debris phase to form solid solution $(Ca,U,Zr)O_{2+x}$ [4].

REFERENCES

[1] http://www.meti.go.jp/english/earthquake/nuclear/decommissioning/index.html
[2] Y. Kumagai, R. Nagaishi, et al., At. Energy Soc. Jpn., 10, 235-239 (2011).
[3] M. Kurata, N. Shirasu and T. Ogawa, Trans. At. Energy Soc. Jpn., in press.
[4] M. Takano and T. Nish, J. Nucl. Mater., 443, 32-39 (2013).

APSORC'13 - 5th Asia-Pacific Symposium on Radiochemistry
Kanazawa, Japan, 22-27 September 2013

Determination of atmospheric radiocesium on filter tapes used at automated SPM monitoring stations for estimation of transport pathways of radionuclides from Fukushima Daiichi Nuclear Power Plant

Yasuji Oura[1], Mitsuru Ebihara[1], Haruo Tsuruta[2], Teruyuki Nakajima[2], Toshimasa Ohara[3]
Mitsunori Ishimoto[4], Yosuke Katsumura[4]
[1]Department of Chemistry, Tokyo Metropolitan University
[2]Atmosphere and Ocean Research Institute, The University of Tokyo
[3]Center for Regional Environmental Research, National Institute for Environmental Studies
[4]Nuclear Professional School, The University of Tokyo

I. INTRODUCTION

Enormous amount of artificial radionuclides were emitted into the atmosphere by a nuclear accident at Fukushima Daiichi nuclear power plant (FDNPP) in March 2011. The radionuclide in the atmosphere was transported with atmospheric stream into eastern Japan area widely. Since some institutes in Kanto region monitored atmospheric radioactivity periodically, it was partially evident that when radioactive plumes passed through Kanto region. However, data on atmospheric radioactivity during an initial period in Tohoku region in where FDNPP presents is nothing, thus passing routes of radioactive plumes in Tohoku region and how radioactivity went though is not clear.

A lot of automated air pollution monitoring stations are placed by local governments around in Japan. Suspended particulate matters (SPM) are also monitored hourly in the station. SPM collected during the accicdent at the stations in Tohoku and Kanto region must play an important role to solve when and how much atmospheric radionuclides passed through in Tohoku and Kanto regions. So we determined ^{134}Cs and ^{137}Cs contents in SPM collected on filer tapes at SPM monitoring stations. The determined contents are also expected to help a development of air pollution transport model calculation.

II. EXPERIMENTAL

Filter tapes used at 3 stations in Miyagi, 19 stations in Fukushima, 8 stations in Ibaraki, 4 stations in Saitama, and 6 stations in Chiba prefectures were subjected to gamma spectroscopy. SPM was collected on roll paper tape continuously and SPM on a paper tape was visible as a black circle (we call it spot in this article). Spots of SPM collected from 15 to 16 March and from 20 to 23 March in 2011 were cut one-by-one. Each spot was sandwiched between medical papers, and it was fixed on a thin plastic sheet by an adhesive tape. Gamma rays from samples were measured for 1 to 3 hours with a Ge detector.

III. RESULTS AND DISCUSSION

We observed the different arrival time of radioactive plume on 15 and 20-21 March among stations. For example, ^{137}Cs concentrations at 3 stations in Fukushima city and 4 stations in Ibaraki prefecture are shown in Figs. 1 and 2, respectively. It was found that high ^{137}Cs concentration (> 10 Bq/m^3) continued for about 12 hours in Fukushima city. This peak was not observed by radiation dose monitoring around that time. In Ibaraki prefecture, a high ^{137}Cs concentration (> 200 Bq/m^3) appeared at 8 am, 21 March at 2 stations in Tsuchiura but not observed in both Shimozuma and Tsukuba. This difference is expected to be helpful for solving passways of radioactive plume in Ibaraki. Analysis of radioactive Cs on filter tapes collected by automated SPM monitoring stations even at 1 - 2 years after FDNPP accident is concluded to give very valuable information.

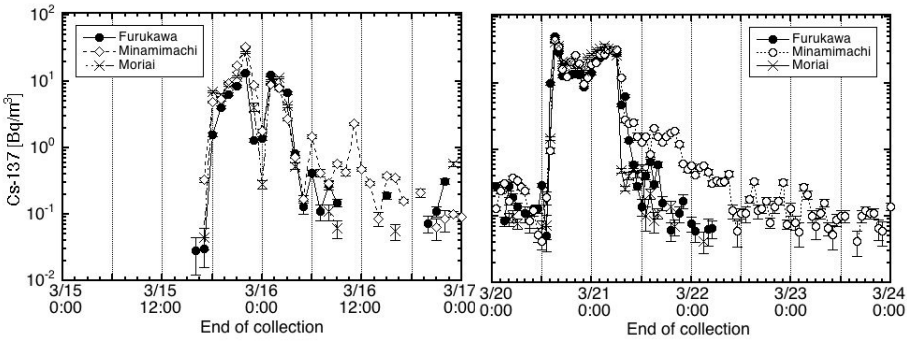

Fig.1 Atmospheric ^{137}Cs concentration at 3 stations in Fukushima city.

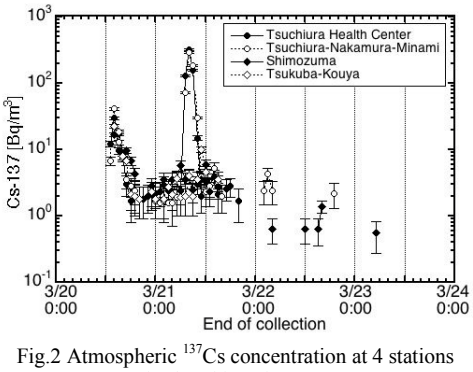

Fig.2 Atmospheric ^{137}Cs concentration at 4 stations in Ibaraki prefecture.

Two-Years Trend of Monthly ^{137}Cs Deposition Observed within 300 km of the Fukushima Dai-ichi Nuclear Plant

Katsumi Hirose [1,2]

[1] *Department of Materials and Life Sciences, Faculty of Science and Technology, Sophia University, 7-1 Kioicho, Chiyodaku, Tokyo 102-8554, Japan*

[2] *Geosphere Research Institute, Saitama University, 255 Shimo-okubo, Sakura-ku, Saitama, 338-8570, Japan*

Abstract – Monthly depositions, which directly reflect atmospheric processes including emission from the Fukushima Daiichi nuclear power plant (FDNPP), are an important tool to re-construct accident sequence. In order to elucidate deposition behavior of the FDNPP-derived radionuclides after the major emission in March 2011, two-years trends of the monthly ^{137}Cs deposition at monitoring stations within 300 km of the FDNPP were examined. The monthly ^{137}Cs deposition showed marked peaks in winter 2012 and winter 2013 at the Futaba site about 5 km of the FDNPP, whereas 2013 winter the peak at the sites in south Kanto and Tohoku regions was not pronounced. We discuss two-years trend of the monthly ^{137}Cs deposition taking into account its spatial variation and effect of precipitation amount.

Keywords – Fukushima Dai-ichi nuclear power plant, monthly deposition, ^{137}Cs, temporal variation, emission history

I. INTRODUCTION

The 2011 Great East Japan Earthquake and resulting tsunami caused severe accident in the Fukushima Dai-ichi nuclear power plant (FDNPP). As a result, large amounts of radionuclides have been released in the environment. In order to trace long-term trend of FDNPP-derived radionuclides emitted into atmosphere, it is important to do continuous monitoring of radionuclides in surface air and deposition. Especially monthly deposition of the FDNPP-derived radionuclides is one of the powerful tools to elucidate long-term environmental effects of the FDNPP accident. The results of monthly ^{137}Cs deposition [1,2] revealed that the effects of the FDNPP accident at least continued until the early 2012. In this paper, we describe two-years trend of the monthly ^{137}Cs deposition observed in the Kanto and Tohoku regions and discuss processes controlling temporal variation of the monthly ^{137}Cs deposition.

II. SAMPLING AND METHOD

Monthly deposition samples (rainwater and falling dust) were collected by rainwater samplers with surface areas of 0.5 m^2, respectively, which are usually installed on the roof of main monitoring building in each monitoring site. Monthly deposition sampling in 45 monitoring sites covering Japanese Island has been stationary performed to monitor basic levels of radioactivity deposition. Monthly rainwater and falling dust samples was collected in appropriate bottles on the first day morning of every month. Water sample was transferred into an evaporation dish and dried on a hot plate. The resultant residues were weighted after drying in an oven at 110°C and then transferred to a plastic container. Dried residue sample in a plastic container was subjected by gamma spectrometry. Gamma spectrometry was performed in each measurement laboratory of local government. Major radionuclides in monthly deposition samples were radiocesium (^{134}Cs and ^{137}Cs). In this analysis, we focused ^{137}Cs deposition because at initial stage, the ^{134}Cs/^{137}Cs activity ratio was constant (Hirose, 2012). All of monthly deposition data has been recorded in NRA homepage.

III. RESULT AND DISCUSSION

Two-years trend of the monthly ^{137}Cs deposition at the monitoring stations within 300 km of the FDNPP was examined. The FDNPP-derived ^{137}Cs has been still measured in January 2013 at most of the monitoring stations within 300 km of the FDNPP. A typical time sequence of the monthly ^{137}Cs deposition is as follows: 1. Pronounced high ^{137}Cs deposition (3.34 MBq m^{-2}) occurred in March 2011 at the Futaba monitoring station, where is located about 5 km of the FDNPP. 2. The monthly ^{137}Cs deposition at Futaba rapidly decreased in April 2011 as a result of cease of major radioactivity emission from the FDNPP. 3. A minimum monthly ^{137}Cs deposition (1.55 kBq m^{-2}) appeared in October 2011 and then gradually increased to a maximum (19.5 kBq m^{-2}) in February 2012. 4. A cause of higher ^{137}Cs deposition in winter, 2012 was presumed to be resuspension of ^{137}Cs-enriched particles [2]. 5. After a peak in February 2012, the monthly ^{137}Cs deposition deceased and reached a minimum in August 2012. However, the monthly ^{137}Cs deposition increased in winter, 2013 (January 2013: 18.9 kBq m^{-2}).

The temporal variations of the monthly ^{137}Cs deposition at the monitoring stations within 300 km of the FDNPP spatially differed from each other. In order to have better understanding of temporal variations of the monthly ^{137}Cs deposition and its spatial difference, we calculate ^{137}Cs concentrations in rainwater from the ^{137}Cs deposition and precipitation amount to eliminate effect of precipitation amount. The temporal variation of the ^{137}Cs concentration in rainwater at Hitachinaka is similar to that at Futaba. This finding suggests that the temporal change of the ^{137}Cs concentration in rainwater at Hitachinaka was predominantly affected by that at Futaba, in other words, source intensity at the FDNPP.

REFERENCES

[1] Hirose, K., *J. Environ. Radioact*., **111**, 13-17, 2012.
[2] Hirose, K., Appl. Radiat. Isot. doi.org/10.1016/j.apradiso.2013.03.076

Synthesis and study of properties of superheavy elements status, problems, and prospects

S. Dmitriev
The Flerov Laboratory of Nuclear Reactions, JINR, Dubna,
dmitriev@jinr.ru

The study of nuclear physical and chemical properties of recently discovered superheavy elements (SHE, Z = 112–118) as well as synthesis of new elements (Z>118) remain one of the most crucial tasks in modern science. Over the past decade, the unique results [1] have been obtained that are of utmost importance both in nuclear physics and astrophysics (experimental evidence of existence of islands of increased stability of SHE) as well as in chemistry (influence of relativistic effects on the chemical properties of the elements 112–114). As per the IUPAC decision, the two new elements are now officially called Fl - Flerovium (element 114) and Lv - Livermorium (element 116). The discovery of elements 117 [2] and 118 closed the 7th period of Mendeleev's Periodic Table of the Elements. Possibilities to study synthesis of heavier elements in reactions with the double-magic ^{48}Ca nucleus are exhausted because production of actinides with Z>98 (Es, Fm, etc.) in necessary quantity (several mg) is impossible in neutron-capture reactions within the framework of existing today reactor technologies. One needs to use ions heavier than ^{48}Ca, for example, ^{50}Ti, ^{58}Fe, and ^{64}Ni; however, production cross sections with these ions are expected to be at least one order of magnitude less. Implementation of the large-scale program on the study of earlier synthesized SHE requires, in turn, significant experiment efficiency improvement.

Further development implies the construction of a first-ever SHE factory at JINR FLNR, which shall include the following:

- a new accelerator complex with the average-mass ion beam intensity 10-20 times higher than that of today;
- physical and chemical new-generation experimental set-ups (highly effective gas-filled recoil separator, gas catcher, selective laser ionization, etc.).

The work was carried out with the financial support from the Russian Foundation of Basic Research (project code # 13-03-12058-ofi-m-2013).

[1] Yu. Ts. Oganessian, S. N. Dmitriev, Russian Chem.Review, 78, 1077, 2009.
[2] Yu. Ts. Oganessian et al., Phys. Rev. Lett., 104, 142502, 2010.

APSORC'13 - 5th Asia-Pacific Symposium on Radiochemistry
Kanazawa, Japan, 22-27 September 2013

The Search for New Chemical Elements and the Possibilities to Synthesize Transactinide "Chemistry" Isotopes

Christoph E. Düllmann[1,2,3]
[1]Johannes Gutenberg-Universität Mainz, 55128 Mainz, Germany
[2]GSI Helmholtzzentrum für Schwerionenforschung, 64291 Darmstadt, Germany
[3]Helmholtz Institute Mainz, 55099 Mainz, Germany

On overview on nuclear reactions leading to isotopes of the transactinide (Z≥104) elements with sufficiently long half-lives for chemical study will be presented.

Transactinides, Superheavy elements, Nuclear fusion reactions

Elements up to Z=112 as well as 114 and 116 are officially recognized as discovered and have been named [1]. The current literature contains reports about the synthesis of all elements up to Z=118 [2], meaning that more than 10% of all elements are members of the transactinide series with Z=104-118. Search experiments for the new elements with Z=119 and Z=120 have been performed, e.g., at the GSI Darmstadt. Elements up to Hs (Z=108) as well as Cn (Z=112) and Fl (Z=114) have been chemically investigated [3], using isotopes with half-lives of at least about one second, which is the current limit for chemical studies. The figure shows the cutout of the current chart of nuclei of the more than 100 transactinide isotopes, synthesized in nuclear fusion reactions. Selecting the optimum nuclear reaction to synthesize a certain isotope is a sensible topic, which requires proper attention in any experiment with the heaviest elements, regardless of the specific aspect under study. The figure shows that isotopes suitable for chemistry studies with current technology exist for all elements up to Fl (Z=114).

I will first present the search for new elements using the recoil separator TASCA [4] at GSI and then discuss the optimum reactions leading to the relatively long-lived isotopes of the transactinides as they are frequently used in chemical studies of these elements, including elements which were not studied chemically to date.

[1] R. D. Loss and J. Corish, Pure Appl. Chem. **84**, 1669 (2012).
[2] Y. Oganessian, Radiochim. Acta **99**, 429 (2011).
[3] A. Türler and V. Pershina, Chem. Rev. **113**, 1237 (2013).
[4] A. Semchenkov et al., Nucl. Instrum. Meth. B **266**, 4153 (2008)

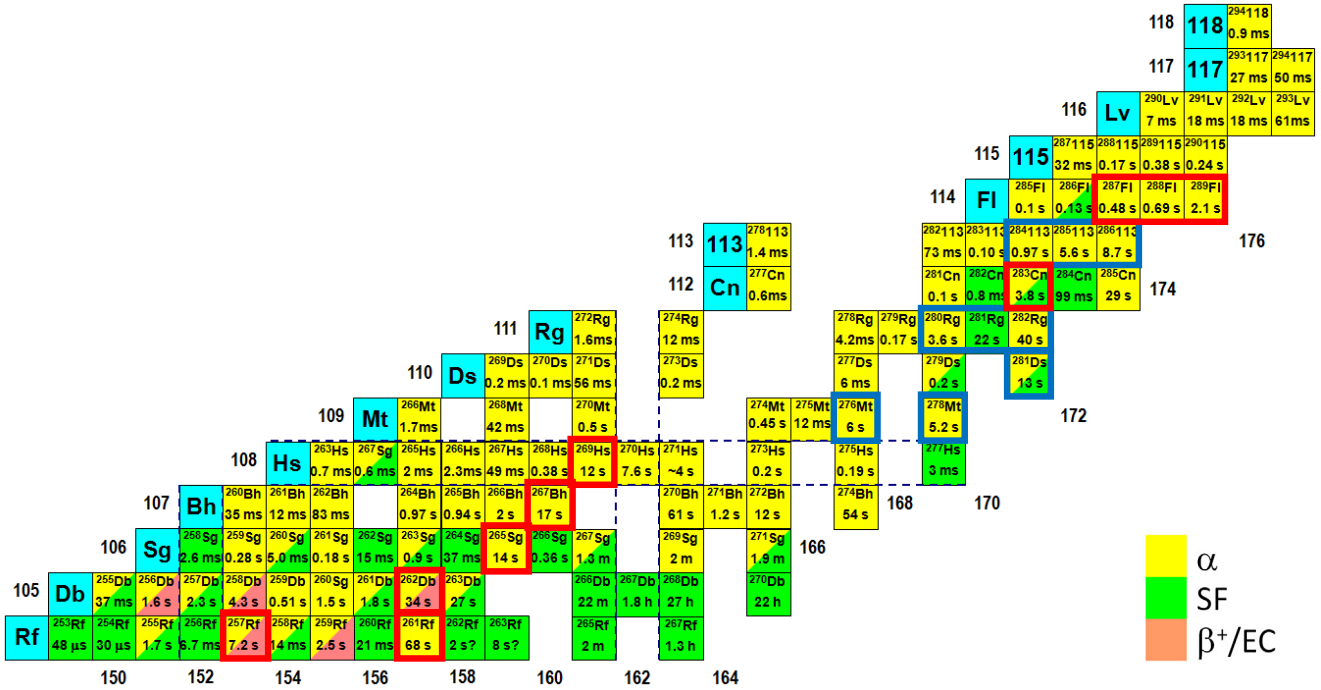

Chart of nuclei of transactinide elements. Half-lives are given, and decay modes color coded. Isotopes often used in chemical studies are shown in a red border. Long-lived isotopes of elements that were not studied chemically so far are shown in a blue border. Dashed lines show nuclear shell closures.

Production and Decay Studies of Transactinide Nuclides with GARIS at RIKEN

Hiromitsu Haba
Nishina Center for Accelerator-Based Science, RIKEN, Wako, Saitama 351-0198, Japan

Abstract – The isotopes of ^{261}Rf, ^{262}Db, and ^{265}Sg were produced in the ^{248}Cm(^{18}O,5n)^{261}Rf, ^{248}Cm(^{19}F,5n)^{262}Db, and ^{248}Cm(^{22}Ne,5n)^{265}Sg reactions, respectively, using a gas-jet transport system coupled to the gas-filled recoil ion separator, GARIS at RIKEN. Production and decay properties of those nuclides were investigated in detail with a rotating wheel apparatus for α and spontaneous fission spectrometry under low background conditions.

Keywords – Superheavy elements; RIKEN gas-filled recoil ion separator, GARIS; ^{261}Rf; ^{262}Db; ^{265}Sg

Chemical characterization of superheavy elements (SHEs, atomic numbers $Z \geq 104$) is an extremely interesting and challenging research subject in modern nuclear and radiochemistry [1,2]. We have been developing a gas-jet transport system coupled to the RIKEN gas-filled recoil ion separator GARIS as a novel technique for the next-generation SHE chemistry [3–5]. With this method, breakthroughs in SHE chemistry are expected: (i) the background radioactivities originating from unwanted by-products are strongly suppressed, (ii) the intense primary heavy-ion beam is absent in a gas-jet chamber and hence high gas-jet yield is achieved, and (iii) the beam-free conditions also make it possible to investigate new chemical reactions. In this work, we investigated production and decay properties of isotopes of ^{261}Rf (Z = 104), ^{262}Db (Z = 105), and ^{265}Sg (Z = 106) available for chemical studies using the GARIS gas-jet system.

A schematic of the experimental setup is shown in Fig. 1. Oxygen-18, ^{19}F, and ^{22}Ne beams were extracted from the RIKEN Linear Accelerator, RILAC. The isotopes of ^{261}Rf^{a,b}, ^{262}Db, and ^{265}Sg^{a,b} were produced in the reactions of ^{248}Cm(^{18}O,5n)^{261}Rf, ^{248}Cm(^{19}F,5n)^{262}Db, and ^{248}Cm(^{22}Ne,5n)^{265}Sg, respectively. The evaporation residues of interest were separated in flight from the beam and the majority of the nuclear transfer products by GARIS and were guided to a gas-jet chamber at the focal plane of GARIS. The evaporation residues were thermalized in He gas, attached to KCl aerosol particles, and were transported through a Teflon capillary to a chemistry laboratory. Alpha and spontaneous fission (SF) decays of ^{261}Rf^{a,b}, ^{262}Db, and ^{265}Sg^{a,b} were then investigated with the rotating wheel apparatus MANON (Measurement system for Alpha-particle and spontaneous fissioN events ON line) under low background conditions.

The 1.9-s isomeric state (^{261}Rf^{b}) in ^{261}Rf was directly populated in the ^{248}Cm(^{18}O,5n)^{261}Rf^{b} reaction for the first time [6]. The identification of ^{261}Rf^{b} was based on six α-α correlations linking α decays of ^{261}Rf^{b} and its daughter ^{257}No. The α-particle energy of ^{261}Rf^{b} was measured to be E_α = 8.52 ± 0.05 MeV. The half-life was determined to be $T_{1/2}$ = 1.9 ± 0.4 s based on both 8.52-MeV α and SF decays. The SF branch is b_{SF} = 0.73 ± 0.06. The cross section for the ^{248}Cm(^{18}O,5n)^{261}Rf^{b} reaction is σ(^{261}Rf^{b}) = 11 ± 2 nb at 95.1 MeV, which gives a cross section ratio of σ(^{261}Rf^{a})/σ(^{261}Rf^{b}) = 1.1 ± 0.2. In the ^{265}Sg experiment [7], eighteen and twenty four events were assigned to ^{265}Sg^{a} and ^{265}Sg^{b}, respectively, based on α-α(-α) and α-SF correlations. The half-life and α-particle energy of ^{265}Sg^{a} were measured to be $T_{1/2} = 8.5^{+2.6}_{-1.6}$ s and E_α = 8.84 ± 0.05 MeV, respectively, and those of ^{265}Sg^{b} were $T_{1/2} = 14.4^{+3.7}_{-2.5}$ s and E_α = 8.69 ± 0.05 MeV. As a daughter product of ^{265}Sg^{a,b}, the decay properties of ^{261}Rf^{b} were derived: $T_{1/2} = 2.6^{+0.7}_{-0.5}$ s, E_α = 8.51 ± 0.06 MeV, and b_{SF} = 0.82 ± 0.09. These results confirm and refine the complicated decay pattern suggested for the decay chain ^{265}Sg^{a,b} → ^{261}Rf^{a,b} → ^{257}No → in [8]. The production cross sections for ^{265}Sg^{a} and ^{265}Sg^{b} were determined to be σ(^{265}Sg^{a}) = 180^{+80}_{-60} pb and σ(^{265}Sg^{b}) = 200^{+60}_{-50} pb at 117.8 MeV. Recently, decay properties of ^{262}Db and its α-decay daughter ^{258}Lr were investigated [9]: E_α = 8.46 ± 0.04 MeV (α intensity I_α = 70 ± 6%) and 8.68 ± 0.04 MeV (I_α = 30 ± 6%), $T_{1/2} = 34^{+4}_{-3}$ s, and b_{SF} = 55 ± 4% for ^{262}Db; $T_{1/2} = 3.5^{+0.5}_{-0.4}$ s and b_{SF} (and/or b_{EC}) = 2.6 ± 1.8% for ^{258}Lr. Based on those decay properties, the cross section for the ^{248}Cm(^{19}F,5n)^{262}Db reaction in [10,11] was revised to σ(^{262}Db) = 2.2 ± 0.7 nb at 103 MeV. In the conference, perspectives of SHE nuclear chemistry opened by GARIS will be also presented.

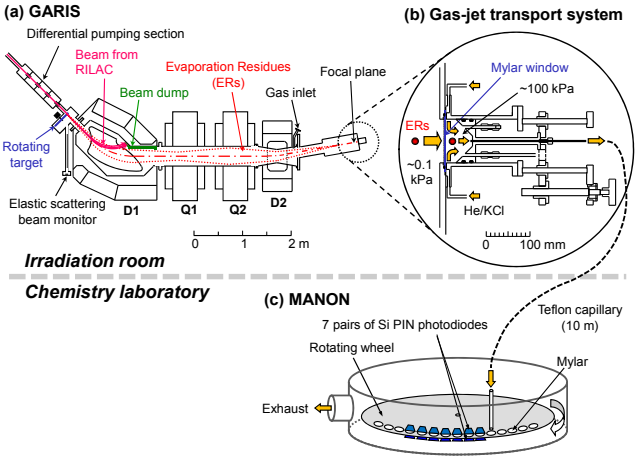

Fig.1. (a) RIKEN gas-filled recoil ion separator, GARIS. (b) Gas-jet transport system coupled to the focal plane of GARIS. (c) The rotating wheel apparatus MANON for α/SF-spectrometry.

[1] M. Schädel, Angew. Chem. Int. Ed. **45**, 368 (2006).
[2] A. Türler and V. Pershina, Chem. Rev. **113**, 1237 (2013).
[3] H. Haba *et al.*, J. Nucl. Radiochem. Sci. **8**, 55 (2007).
[4] H. Haba *et al.*, J. Nucl. Radiochem. Sci. **9**, 27 (2008).
[5] H. Haba *et al.*, Chem. Lett. **38**, 426 (2009).
[6] H. Haba *et al.*, Phys. Rev. C **83**, 034602 (2011).
[7] H. Haba *et al.*, Phys. Rev. C **85**, 024611 (2012).
[8] Ch. E. Düllmann and A. Türler, Phys. Rev. C **77**, 064320 (2008).
[9] H. Haba *et al.*, EuCheMS International Conference on Nuclear and Radiochemistry (NRC8), Sept. 18, 2012, Como, Iraly.
[10] Y. Nagame *et al.*, J. Nucl. Radiochem. Sci. **3**, 85 (2002).
[11] K. Tsukada *et al.*, Radiochim. Acta **97**, 83 (2009).

APSORC'13 - 5th Asia-Pacific Symposium on Radiochemistry
Kanazawa, Japan, 22-27 September 2013

Theoretical Predictions of the Electronic Structure and Properties of the Heaviest Elements

Valeria Pershina[1]
[1]Helmholtzzentrum für Schwerionenforschung, Planckstr. 1, D-64291 Darmstadt, Germany

Abstract - Recent theoretical works on predictions of chemical properties and experimental behaviour of the heaviest elements are presented and critically compared

Keywords – Superheavy elements/Electronic structure/Relativistic calculations

I. INTRODUCTION

One of the main aims of studies in the area of the chemistry of the heaviest elements is to place a newly produced element in the proper position of the Periodic Table [1]. It is achieved by comparing behaviour of the new element with that of its lighter homologs in the chemical group. Having this in mind, a large number of interesting and important chemical experiments on the heaviest elements were performed in the recent years [2]. Theoretical investigations in this area have also been very fruitful and resulted in some remarkable achievements [2, 3]. In the presentation, recent advances in the relativistic electronic structure calculations for the heaviest elements and predictions of their experimental behaviour are overviewed. An emphasis is put on the reliability of the theoretical approaches and models with respect to the experimental outcome.

II. THEORETICAL METHODS AND RESULTS

For the heaviest elements, electronic structure calculations should be made with the use of methods that treat relativistic and electron correlation effects at the highest possible level of theory. In the recent years, the relativistic quantum theory and computational algorithms received tremendous developments [4]. As a result, very accurate calculations of the electronic structure and properties of superheavy atoms and molecules became possible. On their basis, reliable predictions of experimental behaviour of these elements in the sophisticated and expensive experiments with single species have been made [5].

For atoms, Dirac-Coulomb-Breit (DCB) calculations with electron correlation at the highest level of theory, i.e., a coupled-cluster (CC) method, were performed for elements till Z=122 [6]. Accurate predictions of such properties like electronic configurations, ionization potentials, polarizabilities, that are important for the placement of the elements and for the chemical experiments, have been made.

In the molecular theory, fully relativistic (4-component) and 2-component wave-function (*ab initio* Dirac-Fock) [7] and Density-Functional-Theory (DFT) [8] methods have been developed to such an extent that very accurate predictions of binding molecular energies, optimized geometry, electronic density distributions, etc. are now available. On their basis, predictions of experimental behaviour for gas-phase and aqueous chemistry chromatography experiments have been made [2, 3, 5]. For the gas-phase experiments, direct calculations of adsorption energy of atoms and molecules on metal or other surfaces using relativistic DFT methods are now possible via a cluster approach [9].

In the presentation, we will overview results of atomic calculations till Z=122 that are important for placing these elements in the Periodic Table. They are also used for predictions of adsorption of atoms of these elements on neutral surfaces to guarantee their transportation from an accelerator to the chemistry set up.

For the gas-phase chemistry experiments, predictions of volatility of group-4 through 8 compounds are presented and compared. General trends and a common character of the chemical behaviour are outlined. Predictions of volatility of elements in the atomic state, like of element 112, Cn, element 113, and element 114, Fl, as adsorption on neutral and metal surfaces are also described and compared [9]. Interesting cases of volatility of even heavier elements, like 115, or 119 and 120 are considered.

Influence of relativistic effects on properties and experimental behaviour of the heaviest elements is elucidated.

Future perspectives for the chemical studies on the heaviest elements from the theoretical point of view are outlined.

Acknowledgment: The author is thankful to her free-will collaborators J. Anton, T. Jacob, A. Borschevsky, E. Eliav and U. Kaldor. She also thanks her colleagues, experimentalists, for valuable discussions of experimental results.

REFERENCES

[1] *The Chemistry of Superheavy Elements*, M: Schädel ed., Kluwer, Dorderecht, 2003.
[2] A. Türler and V. Pershina, Chem. Rev. **113**, 1237 (2013).
[3] V. Pershina, Radiochim. Acta **99**, 459 (2011).
[4] *Relativistic Electronic Structure Theory*, P. Schwerdtfeger ed., Parts I and 2, Elsevier, Dordrecht, 2002 and 2004.
[5] V. Pershina, In: *Relativistic Methods for Chemists*, Y. Ishikawa, M. Barysz, eds., Springer, Dordrecht (2010), pp. 452-520.
[6] U. Kador, E. Eliav, In: Ref. [4], Part 2, pp. 279-350.
[7] K. G. Dyall and K. Faegri, *Relativistic Quantum Chemistry*, Oxford University Press, 2007.
[8] J. Anton, B. Fricke, E. Engel, Phys. Rev. A **69**, 012505 (2004).
[9] V. Pershina, J. Anton and T. Jacob, J. Chem. Phys. **131**, 084713 (2009).

APSORC'13 - 5th Asia-Pacific Symposium on Radiochemistry
Kanazawa, Japan, 22-27 September 2013

Spectroscopy of Element 115 Decay Chains

D. Rudolph[1], U. Forsberg[1], P. Golubev[1], L.G. Sarmiento[1], A. Yakushev[2], L.-L. Andersson[3], Ch.E. Düllmann[2,3,4], J.M. Gates[5], K.E. Gregorich[5], F.P. Heßberger[2,3], R.-D. Herzberg[6], J. Khuyagbaatar[2,3], J.V. Kratz[4], K. Rykaczewski[7], M. Schädel[2,8], S. Åberg[1], D. Ackermann[2], M. Block[2], H. Brand[2], B.G. Carlsson[1], D. Cox[6], X. Derkx[3,4], A. Di Nitto[4], K. Eberhardt[4], J. Even[3], C. Fahlander[1], J. Gerl[2], C.J. Gross[7], E. Jäger[2], B. Kindler[2], J. Krier[2], I. Kojouharov[2], N. Kurz[2], B. Lommel[2], A. Mistry[6], C. Mokry[4], H. Nitsche[5], J.P. Omtvedt[9], P. Papadakis[6], I. Ragnarsson[1], J. Runke[2], H. Schaffner[2], B. Schausten[2], P. Thörle-Pospiech[4], T. Torres[2], A. Türler[10], A. Ward[6], D. Ward[1], N. Wiehl[3,4]

[1]Lund University, S-22100 Lund, Sweden
[2]GSI Helmholtzzentrum für Schwerionenforschung GmbH, D-64291 Darmstadt, Germany
[3]Helmholtz Institute Mainz, D-55099 Mainz, Germany
[4]Johannes Gutenberg-Universität Mainz, D-55099 Mainz, Germany
[5]Lawrence Berkeley National Laboratory, Berkeley, CA 94720, USA
[6]University of Liverpool, Liverpool L69 7ZE, United Kingdom
[7]Oak Ridge National Laboratory, Oak Ridge, TN 37831, USA
[8]Advanced Research Center, Japan Atomic Energy Agency, Tokai, Japan
[9]University of Oslo, NO-0315 Oslo, Norway
[10]Paul Scherrer Institute and University of Bern, CH-5232 Villingen, Switzerland

During the past decade, a number of correlated α-decay chains, which all terminate by spontaneous fission, have been observed in several independent experiments using ^{48}Ca-induced fusion-evaporation reactions on actinide targets [1]. These are interpreted to originate from the production of neutron-rich isotopes with proton numbers Z = 113 to 118. However, neither their mass, A, nor their atomic number, Z, have been measured directly.

In November 2012, a three-week experiment was conducted at the GSI Helmholtzzentrum für Schwerionenforschung GmbH in Darmstadt, Germany, using high-resolution α-, electron, X-ray and γ-ray coincidence spectroscopy to observe α-X-ray events to identify uniquely atomic numbers of isotopes in Z = 115 decay chains. The reaction ^{48}Ca+^{243}Am was used, with fusion-evaporation products being focused into the TASISpec set-up [2-4], which was coupled to the gas-filled separator TASCA [5,6].

A beam integral of roughly $7 \cdot 10^{18}$ ^{48}Ca particles led to the observation of about 25 correlated α-decay chains with characteristics similar to those previously published [7,8].

Results from the ongoing data analysis will be presented.

[1] Yuri Oganessian, J. Phys. G **34**, R165 (2007).
[2] L.-L. Andersson *et al.,* Nucl. Instrum. Meth. A **622,** 164 (2010).
[3] L.G. Sarmiento, L.-L. Andersson and D. Rudolph, Nucl. Instrum. Meth. A **667**, 26 (2012).
[4] U. Forsberg *et al.*, Acta Phys. Pol. B **43**, 305 (2012).
[5] A. Semchenkov *et al*., Nucl. Instrum. Meth. B **266**, 4153 (2008).
[6] J.M. Gates *et al.*, Phys. Rev. C **83**, 054618 (2011).
[7] Yu. Ts. Oganessian *et al*., Phys. Rev. C. **69**, 021601 (2004).
[8] Yu. Ts. Oganessian *et al*., Phys. Rev. Lett**. 108**, 022502 (2012).

APSORC'13 - 5th Asia-Pacific Symposium on Radiochemistry
Kanazawa, Japan, 22-27 September 2013

Chemistry at a one-atom-per-week level

A. Yakushev
GSI Helmholtzzentrum für Schwerionenforschung GmbH, 64291 Darmstadt, Germany

Keywords – superheavy elements, element 114, flerovium, gas chromatography, adsorption

INTRODUCTION

Long-lived isotopes of superheavy elements (SHE) with atomic number $Z \geq 108$ can be produced via fusion reactions between heavy actinide targets and neutron-rich projectiles at a rate of single atoms per day or per week only. Investigating the neutron-rich SHE nuclei using rapid chemical separation and subsequent on-line detection provides an independent chemical characterization and an alternative separation technique to electromagnetic recoil separators. The highly efficient separation of Hs in the form of HsO_4 is an impressive example for such studies of the nuclear reaction mechanism and nuclear structure [1,2]. Approaching the heaviest elements, copernicium (Cn), element 113 and flerovium (Fl), which are accessible for chemistry experiments, the coupling of chemistry setups to a recoil separator promises extremely high sensitivity due to strong suppression of background from unwanted species.

FL: NOBLE GAS OR VOLATILE METAL?

Electron shells of SHE are influenced by strong relativistic effects caused by the high value of *Z*. Early atomic calculations for Fl predicted this to have quasi-closed electron shell configuration $6d^{10}7s^27p_{1/2}^2$, and to be noble gas-like due to very strong relativistic effects [3]. Recent fully relativistic calculations studying Fl in different environments suggest this to be less reactive compared to its lighter homologues in the group, but still exhibiting metallic character [4]. The dilemma, is Fl a noble gas or a noble metal, calls for experiments. Comparative studies of the interaction of Fl, Cn, Pb, Hg and Rn in the elemental state with metal surfaces are a powerful tool for distinguishing between metallic and noble-gas-like chemical behaviour. This was shown in experiments with Cn [5]. For Fl, the formation of a weak physisorption bond upon adsorption on gold was inferred from first experiments [6].

GAS-SOLID CHROMATOGRAPHY OF FL AT TASCA

The present gas chromatography study on Fl upon the adsorption on gold was performed at a gas-filled separator TASCA [7]. Flerovium isotopes were produced in the nuclear reaction ^{244}Pu(^{48}Ca;3,4n)^{288,289}Fl. Thez were separated in TASCA and stopped in a gas-filled chamber and flushed by a He/Ar gas mixture within 0.8 s to a detection setup COMPACT [1,2]. Two detector arrays connected in series were used, both covered with a thin gold layer. The first detector array was connected directly to the exit of TASCA and kept at room temperature. A negative temperature gradient from +20 to −162 °C was applied along the second detector array placed downstream of the first one. The use of two detectors in series allowed the detection of species in a wide volatility range – from the non-volatile Pb to the noble gas Rn.

RESULTS

Two decay chains, one from ^{288}Fl and one ^{289}Fl were detected. Both decays from Fl isotopes occurred in the first detector array at room temperature. The positions of decay chain members are shown in Fig. 1 together with distributions of Pb, Hg, and Rn and the Monte–Carlo simulated deposition peak for ^{285}Cn (dashed line). The observed behavior of Fl in the chromatography column is indicative of Fl being less reactive than the nearest homolog Pb. The evaluated lower limit of the adsorption enthalpy $-\Delta H_{ads}$(Fl) > 48 kJ/mol reveals the formation of a metal-metal bond with Au, which is at least as strong as that of Cn, and thus demonstrates the metallic character of Fl.

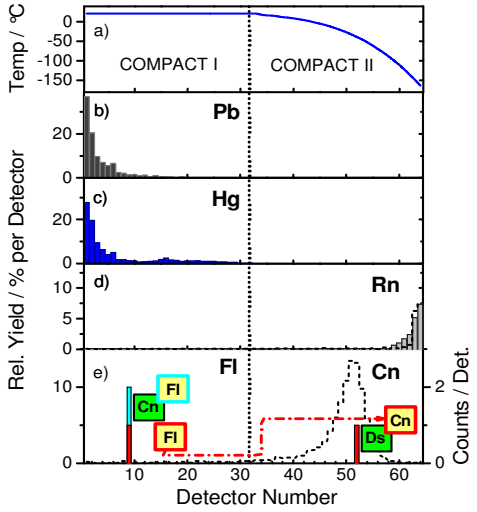

Fig.1: The observed gas-chromatography behavior of Fl and Cn in COMPACT compared to those of Pb, Hg and Rn.

[1] J. Dvorak *et al. Phys. Rev. Letters* **97**, 242501 (2006).
[2] J. Dvorak *et al. Phys. Rev. Letters* **100**, 132503 (2008).
[3] K.S. Pitzer. *J. Chem. Phys*. **63**, 1032 (1975).
[4] V. Pershina *et al. J. Chem. Phys*. **131**, 084713 (2009).
[5] R. Eichler *et al. Angew. Chem, Int. Ed.* **47**, 3262-3266 (2008).
[6] R. Eichler *et al. Radiochim. Acta* **98**, 133-139 (2010).
[7] A. Semchenkov et al. *NIM B* **266**, 4153-4161 (2008).

APSORC'13 - 5th Asia-Pacific Symposium on Radiochemistry
Kanazawa, Japan, 22-27 September 2013

$Sg(CO)_6$ – The First Organometallic Transactinde Complex opening a Window to a New Compound Class

J. Even [1], A. Yakushev[2], Ch.E. Düllmann[1,2,3], H. Haba[4], M. Asai[5], T.Sato[5], H. Brand[2], A. Di Nitto[3], R. Eichler[6,7], F. Fangli[8], W. Hartmann[2], M. Huang[4], E. Jäger[2], D. Kaji[4], J. Kanaya[4], Y. Kaneya[5], J. Khuyagbaatar[1], B. Kindler[2], J.V. Kratz[3]; J.Krier[2],Y. Kudou[4], N. Kurz[2], B. Lommel[2], S. Miyashita[5], K. Morimoto[4], K. Morita[4], Y. Nagame[5], H. Nitsche[9,10], K. Ooe[11], M. Schädel[5], J. Steiner[2], T. Sumita[4], K. Tanaka[4], A. Toyoshima[5], K. Tsukada[5], A. Türler [6,7], I. Usoltsev [6,7], Y. Wakabayashi[4], Y. Wang[8], N. Wiehl[1,3], S. Yamaki[4,12], Q. Zhi[8]

[1]Helmholtz-Institut Mainz, Johannes Gutenberg-Universität, 55099 Mainz, Germany;
[2] GSI – Helmholtzzentrum für Schwerionenforschung, Planckstr. 1, 64291 Darmstadt, Germany;
[3]Johannes Gutenberg-Universität Mainz, 55099 Mainz, Germany;
[4]Nishina Center for Accelerator-Based Science, RIKEN, Wako, Saitama 351-0198, Japan;
[5]Advanced Science Research Center, Japan Atomic Energy Agency, Tokai, Ibaraki 319-1195, Japan;
[6]University of Berne, Freiestrasse 3, CH-3012 Berne, Switzerland;
[7]Paul Scherrer Institute, CH-5232 Villigen, Switzerland;
[8]Institute of Modern Physics Lanzhou; Chinese Academy of Sciences, 509 Nanchang Road, CN-730000 Lanzhou, China;
[9]University of California, Berkeley, CA 94720-1460; U.S.A.;
[10] Lawrence Berkeley National Laboratory, Berkeley, CA 94720-8169 U.S.A.,
[11]Niigata University, Niigata, Niigata 950-2181, Japan,
[12]Saitama University, Saitama 338-8570, Japan.

Abstract – We report on the synthesis and chemical investigation of the first organometallic compound of a transactinide element, namely seaborgium hexacarbonyl.

Keywords – Seaborgium, Carbonyl Complex, Adsorption, Hot chemistry

In the last decades, simple inorganic compounds of the transactinde elements (TAN) were studied in gas phase chemical reactions [1]. Accessing, e.g., metal complexes with organic ligands or organometallic compounds was impossible due to technical restrictions, like the destructive plasma present behind the target created by the intense heavy ion beam. Thanks to the novel approach of physical preseparation in a recoil separator to reject the beam [2], these limitations could be overcome [3]. In previous experiments, we demonstrated the formation of volatile d-element carbonyl complexes with recoiling ions thermalized in a carbon monoxide containing atmosphere [4]. Short-lived isotopes of the lighter homologs of seaborgium – molybdenum and tungsten showed this to be an appropriate method to study group 6 elements under conditions relevant for a transactinide chemistry experiment.

Seaborgium hexacarbonyl has been predicted to be stable [5]. The π-back bonding, characteristic for the metal-carbon bond in carbonyl complexes, is expected to be stronger than in the complexes of the lighter homologues due to the relativistic expansion of the d-orbitals. Furthermore, $Sg(CO)_6$ is predicted to be as volatile as tungsten hexacarbonyl and therefore suitable for, e.g., thermochromatography studies [6]. Based on previous studies with molybdenum and tungsten, an experiment aiming at the study of seaborgium hexacarbonyl was conducted at the gas-filled recoil ion separator GARIS at RIKEN. In our experiment, $^{265a,b}Sg$ ($t_{1/2}$=8.5 s, 14.4 s) [7] was synthesized in the reaction $^{248}Cm(^{22}Ne,5n)$. Seaborgium was separated within GARIS from the primary beam and was guided to the recoil transfer chamber (RTC) mounted in the focal plane of GARIS [8]. The ^{265}Sg was thermalized within the RTC in a helium carbon-monoxide mixture under ambient conditions. This way it formed volatile carbonyl complexes and was transported in the gas stream to the radiochemistry laboratory. There, its adsorption on silicon dioxide was studied with the thermochromatography detector COMPACT. The combination of preseparation with GARIS and detection in COMPACT allowed the study of seaborgium under background-free conditions.

Our results indicate the observation of $Sg(CO)_6$ and allow to compare its behavior to that of $W(CO)_6$ and to theoretical predictions. At the moment, the data analysis is ongoing. Experimental details and results will be presented at the conference.

[1] A. Türler and V. Pershina, *Chem. Rev*. **2013**, *113*, 1237−1312.
[2] Ch E. Düllmann et al., *Nucl. Instr. Meth. A* **2005**, *551*, 528–539.
[3] Ch.E. Düllmann et al., *Radiochim. Acta* **2009**, *97*, 403-418.
[4] J. Even, et al., *Inorg.Chem.* **2012**, *51*, 6431-6422.
[5] C.S. Nash, B. E. Bursten, *J. Am. Chem. Soc.* **1999**,*121*, 10830-10831.
[6] V. Pershina and J. Anton, *submitted to J. Chem Phys.* **2013**.
[7] H. Haba et al., *Phys. Rev. C* **2012**, *85*, 024611.
[8] H. Haba et al, *Chem. Lett.* **2009**, *38*, 426-427.

This experiment was performed at RI Beam Factory operated by RIKEN Nishina Center and CNS, University of Tokyo. We thank the ion source and RILAC operators Financial support from the German BMBF under contract 06MZ7164 and from JAEA Tokai, Advanced Science Research Center's Reimei research program is gratefully acknowledged..

APSORC'13 - 5th Asia-Pacific Symposium on Radiochemistry
Kanazawa, Japan, 22-27 September 2013

Superheavy Element Z and A Measurements at the Berkeley Gas-Filled Separator

H. Nitsche [1, 2], G. K. Pang [2], J. M. Gates [2], K. E. Gregorich [2] N. E. Esker [1], O. R, Gothe [1]
[1] University of California, Berkeley, Department of Chemistry, Berkeley, CA 94720-1460, USA
[2] Lawrence Berkeley National Laboratory, Nuclear Science Division, Berkeley, CA 94720-8169, USA

Since the dawn of the new Millenium, six new superheavy elements (SHE) (113, 114, 115, 116, 117, and 118) have been produced in reactions of ^{48}Ca beams with actinide targets. So far, these experiments have led to the discovery of 52 new isotopes [1,2]. Several independent confirmation experiments led to the recent naming of flerovium, Fl, and livermorium, Lv, for elements 114 and 116, respectively [3-6]. The α-decay chains of these SHE terminate by spontaneous fission, before reaching the part of the Chart of the Nuclides where Z and A are well-established. The SHE Z and A assignments have been made by comparing experimental α-particle decay energies with model calculations [7], supplemented with cross-bombardment information. Thus, neither Z nor A have been directly measured. Before using measured α-decay energies to adjust mass models, these Z and A assignments must be proven to be correct. Otherwise a situation could arise where data from incorrect assignments are used to modify mass models which, in turn, reinforce the incorrect assignments. Identifying Z by detecting α - K x-ray coincidences [9], known as x-ray fingerprinting, is an already established process. The first results of x-ray finger printing experiments conducted for element 115 produced in the ^{243}Am(^{48}Ca,3n)^{288}115 reaction using the Berkeley Gas-Filled Separator (BGS) at the 88-inch cyclotron at Lawrence Berkeley National Laboratory will also be presented.

However, to simultaneously identify both Z and A with the BGS, we are making several upgrades to its detection setup, design and construct a new mass analyzer, as well a gas catcher and a radiofrequency quadrupole ion trap (RFQ) to match the output of the BGS to the acceptance of the mass analyzer. The first SHE to be studied using these new upgrades at the BGS will be ^{289}Fl [9] produced in the fusion evaporation reaction of ^{244}Pu(^{48}Ca,3n). Z-identification is conducted in the same manner as described above and coupling of the x-ray fingerprinting setup with a mass analyzer, then provides a simultaneous determination of A and Z.

[1] Y.T. Oganessian, J. Phys. G 34, R165 (2007).
[2] Y.T. Oganessian, Radiochim. Acta 99, 429 (2011)
[3] L. Stavsetra, K. E. Gregorich, J. Dvorak, P. A. Ellison, I. Dragojevic´, M. A. Garcia, and H. Nitsche, Phys. Ref. Let. 103, 132502 (2009).
[4] Ch. E. Düllmann et al., Phys. Ref. Let. 104, 252701 (2010).
[5] P. A. Ellison, K. E. Gregorich, J. S. Berryman, D. L. Bleuel, R. M. Clark I. Dragojevic´, J. Dvorak, P. FallonC. Fineman-Sotomayor, J. M. Gates, O. R. Gothe, I.Y. Lee, W. D. Loveland, J. P. McLaughlin, S. Paschalis, M. Petri, J. Qian, L. Stavsetra, M. Wiedeking, and H. Nitsche, Phys. Ref. Let. 105, 182701 (2010).
[6] J. M. Gates et al., Phys. Rev. C 83, 054618 (2011).
[7] A. Sobiczewski et al., Prog. Part. Nucl. Phys. 58, 292 (2007).
[8] C.E. Bemis et al., Phys. Rev. Lett. 31, 647 (1973).
[9] Y.T. Oganessian et al., Phys. Rev. C 69, 054607 (2004).

Acknowledgement:
This work is supported by U.S. Department of Energy, Office of Science, Nuclear Physics, Low Energy Physics Program, and was performed at Lawrence Berkeley National Laboratory under Contract No. DE-AC02-05CH11231.

Intermetallic Actinide compounds for SHE Production Targets

R. Eichler[a,b], I. Usoltsev[a,b], J.P. Omtvedt[d], O. V. Petrushkin[c], D. Piguet[a], A. V. Sabel'nikov[c], A. Türler[a,b], G. K. Vostokin[c] , A. V. Yeremin[c]

[a] Laboratory for Radiochemistry and Environmental Chemistry, Paul Scherrer Institute, CH-5232 Villigen, Switzerland
[b]Department of Chemistry & Biochemistry, University of Berne, Freiestrasse 3, CH-3012 Berne, Switzerland
[c]Flerov Laboratory of Nuclear Reactions, Joint Institute for Nuclear Research, 141980 Dubna, Russia
[d]University of Oslo, 0316 Oslo, Norway

*R*ecent experiments with superheavy elements require high intensive heavy ion beams and highly sophisticated target technologies able to stand the harsh irradiation conditions. Especially, stationary target technologies based on painting and molecular plating of actinide oxides onto thin Ti foils reveal severe target degradation by the intensive beams. These effects lead to a considerable drop in the production rates and transport yields of SHE to chemical setups. Seeking for better target material possibilities we focused our research onto metallic targets. These metallic targets are expected to be superior to the widely used nowadays solely electroplated targets due to higher thermal conductivity, electrical conductivity, chemical stability, and mechanical stability. We proposed a simple method which allows producing Pd-based intermetallic targets for high intensity irradiations [1]. Based on the molecular plating technique [2] followed by coupled reduction [3] this method was successfully applied to different lanthanide and actinide isotopes [1]. First irradiation experiments with intermetallic targets were carried out at the Oslo Cyclotron Laboratory, University of Oslo, Norway. Here, a 3.5 µm ^{238}U/Pd target was irradiated at the MC-35 Scanditronix cyclotron using a 0.5 □A proton beam with cyclotron energy of 30 MeV. This experiment showed the possibility of safe handling of such targets in accelerator environments. Two ^{243}Am/Pd intermetallic targets have been prepared and irradiated at the U-400 cyclotron at the Flerov Laboratory for Nuclear Reactions for several days. Both ^{243}Am targets were characterized by alpha-particle spectroscopy and light microscopy before and after irradiation with high intensity beams of ^{48}Ca. For direct comparison, the performance of a 'classical' electroplated $^{243}AmO_2$/Ti target was investigated. Figure 1 shows optical micrographs revealing the clear superiority of intermetallic targets. Challenges and possibilities connected to the use of intermetallic compounds as high power irradiation targets will be presented.

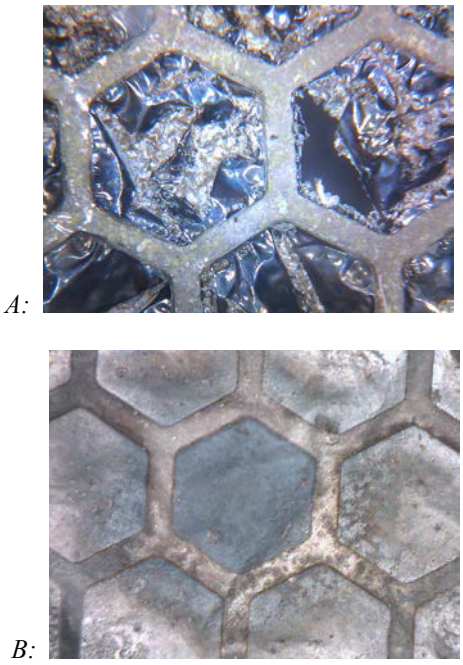

A:

B:

Figure 1: Micrographs of irradiated targets. A) titanium based target after irradiation with ^{48}Ca particles at intensities of up to $7\cdot10^{12}$ ^{48}Ca per second for about 120 hours; B) palladium based target after irradiation with ^{48}Ca particles at almost two times higher intensities compared to the titanium based target of up to $1.2\cdot10^{13}$ ^{48}Ca per second for about 60 hours. The Pd foil and the actinide distribution remain nearly unchanged.

Acknowledgments: We thank the crews form the ion source and U-400 cyclotron of FLNR Dubna for providing intense beams of ^{48}Ca. This research was supported by Swiss National Science Foundation grant 200020_126639.

References

[1]I. Usoltsev, et al., Preparation of Pd-based intermetallic targets for high intensity irradiations, Nucl. Instr. and Meth. Phys. Res.A691, 5–9 2012.
[2]W. Parker, et al., Nucl. Instr. and Meth. 26, 61 (1964).
[3]S. Möbius, L. Hellwig, C. Keller, J. Less-Common Met. 121, 43 (1986).

The First Successful Observation of Mass-separated Lawrencium (Lr, Z = 103) Ions with ISOL Technique

T. K. Sato[1], M. Asai[1], N. Sato[2], Y. Kaneya[1,3], K. Tsukada[1], A. Toyoshima[1], S. Miyashita[1], Y. Nagame[1], M. Schädel[1], A. Osa[3], S. Ichikawa[1,4], K. Ooe[5], T. Stora[6], J. V. Kratz[7]

[1]Advanced Science Research Center, Japan Atomic Energy Agency, Tokai, Ibaraki 319-1195, Japan
[2] Nuclear Science and Engineering Directorate, Japan Atomic Energy Agency, Tokai, Ibaraki 319-1195, Japan
[3]Graduate School of Science and Engineering, Ibaraki University, 2-1-1, Bunkyo, Mito, Ibaraki 310-8512, Japan
[3]Department of Research Reactor and Tandem Accelerator, Japan Atomic Energy Agency, Tokai, Ibaraki 319-1195, Japan
[4]Nishina Center for Accelerator-Based Science, RIKEN, 2-1 Hirosawa, Wako, Saitama 351-0198, Japan
[5]Institute of Science and Technology, Niigata University, Niigata 950-2181, Japan
[6]ISOLDE, CERN, CH-1211 Geneva 23, Switzerland
[7]Institut für Kernchemie, Universität Mainz, D-55099 Mainz, Germany

*Abstract – In order to determine the first ionization potential of the heaviest actinide lawrencium (Lr, Z=103), we have developed a surface ionization ion-source as part of the JAEA-ISOL (**I**sotope **S**eparator **O**n-**L**ine) setup, which is coupled to a He/CdI_2 gas-jet transport system. We will report on the first successful ionization and mass separation of 27-s ^{256}Lr produced in the ^{249}Cf+^{11}B reaction.*

Keywords – Lawrencium (Lr), Heavy actinide, Ionization potential, ISOL, Surface ionization, Ion source

I. INTRODUCTION

The ground-state electronic configuration of lawrencium (Lr, Z = 103) that is the heaviest actinide element is predicted to be [Rn]5f^{14}7$s^2$7$p_{1/2}$, which is different from that of the lanthanide homolog lutetium (Lu) [Xe]4f^{14}6$s^2$5d. The reason for this change in the ground state configuration is that the 7p orbital of Lr is stabilized below the 6d orbital by strong relativistic effects [1]. The weakly-bound outermost electron results in a significantly lower first ionization potential of Lr as compared to its neighboring heavy actinides [2]. The ionization potential of Lr, however, has not been determined experimentally owing to its low production rate and short half-life. In order to determine the ionization potential of Lr, we have developed a surface ionization type ion-source for the JAEA-ISOL coupled to a gas-jet transport system [3]. As a step to determination of the ionization potential of Lr, we conducted to ionize a short-lived Lr isotope by using the ion-source in several ionization conditions.

II. EXPERIMENTAL

The isotope ^{256}Lr ($T_{1/2}$ = 27 s) was produced in the reaction of ^{249,250,251}Cf(^{11}B, xn)^{256}Lr [4]. A ^{249,250,251}Cf target (^{249}Cf: 63%, ^{250}Cf: 12%, and ^{251}Cf : 25%) with 185 ± 25 μg/cm^2 on a 1.85 mg/cm^2 thick Be backing foil was irradiated with a 67.9-MeV (63 MeV in the middle of the target) $^{11}B^{4+}$ beam from the JAEA tandem accelerator. For comparison the lutetium isotopes ^{168m}Lu and ^{168g}Lu, with half-lives of 6.7 min and 5.5 min, respectively, were synthesized in the ^{162}Dy(^{11}B, 5n) reaction. The nuclear reaction products recoiling from the targets were transported to the ion-source by a He/CdI_2 gas-jet transport system. The products were ionized in the ion-source, accelerated with 30 kV, and then mass-separated with a mass-separator in ISOL. The amount of ions collected at the end of the ISOL after mass-separation was determined by α- or γ-ray measurements. To calculate ionization efficiencies, nuclear reaction products transported from a target recoil chamber were collected directly and measured prior to the ionization experiments. To compare the ionization efficiencies on different surface material of the ion-source, a rhenium (Re) surface and a tantalum (Ta) surface were employed in this study.

III. RESULTS AND DISCUSSION

We successfully ionized and mass-separated ^{256}Lr for the first time by using the developed ion-source and applying the ISOL technique. The Ionization efficiencies of Lr and Lu on the Re surface were obtained to be 42^{+20}_{-19} % and 19.9 ± 7.0 %, respectively. In the case of the Ta surface, the efficiency of Lr was 19^{+9}_{-8} % while that of Lu was 4.0 ± 1.4 %. The ionization efficiency of each element on the Re surface was larger than that on the Ta surface because the work function of Re is higher than that of Ta.

Under both conditions, the ionization efficiencies of Lr are larger than those of Lu. The results indicate that the ionization potential of Lr must be lower than that of Lu. This is consistent with the theoretical prediction from a coupled cluster (CC) calculation that takes into account relativistic effects [3].

In the presentation, we will report on the first experimental determination of the first ionization potential of Lr based on our latest results.

[1] Zou, Y. and Fischer, C. F. Phys. Rev. Lett. **88** (2002) 183001.
[2] Borschevsky, A. et al. Eur. Phys. J. D**45** (2007) 115.
[3] Sato, T. K. et al. Rev. Sci. Instrum. **84** (2013) 023304.
[4] Sato, N. et al. JAEA Rev. **2010-056** (2010) 52.

NEI-01

Nuclear Energy Chemistry in China: Present Status and Future Perspectives

Zhi-Fang Chai
Nuclear Energy Chemistry Group, Key Laboratory of Nuclear Analytical Techniques
Institute of High Energy Physics, Chinese Academy of Sciences, Beijing 100049, China
E-mail: chaizf@ihep.ac.cn

Nuclear energy chemistry is one of the most challenging subjects in modern science, and its development is tightly related to the advanced nuclear fuel cycle and persistent development of nuclear energy. Nuclear energy chemistry in China is now experiencing a renaissance, which is being strongly motivated by China's huge energy demand. In this talk, the recent progresses in nuclear energy chemistry of China are selectively highlighted, with emphasis on the front-end chemistry, actinide solid-state chemistry associated with nuclear fuel fabrication, actinide solution chemistry and nuclear fuel reprocessing as well as chemistry in nuclear waste disposal and management. Some positive measures about how to promote the nuclear energy chemistry in China are discussed, and future perspectives are briefly outlined as well.

Acknowledgement – This work was supported by Natural Science Foundation of China (Grants 91026007, 91226201 and 11275219) and the "Strategic Priority Research Program" of the Chinese Academy of Sciences (Grants.XDA030104).

[1] WQ Shi, YL Zhao, ZF Chai. *Radiochim Acta*. 2012, 100: 529.

Evaluation of new extractants relevant to the back-end of nuclear fuel cycle

A. Goswami

Radiochemistry Division, Bhabha Atomic Research Centre, Trombay, Mumbai – 400 085, INDIA

E-mail: agoswami@barc.gov.in

Abstract:. *Conventionally, PUREX and THOREX processes have been proposed for the reprocessing of U and Th based spent fuels employing tri-n-butyl phosphate (TBP) as extractant. However, some major limitations of TBP have been identified and need to be addressed. Evaluation of alternative extractants is, therefore, desirable which can overcome at least some of these problems. Extensive studies have been carried out on the evaluation of N,N-dialkyl amides as extractants in the back-end of the nuclear fuel cycle for addressing the issues related to the reprocessing of U and Th based spent fuels. Similarly, efforts have been made on the evaluation of new solvents for the partitioning of minor actinides (MA) from high-level waste (HLW) solutions. This talk presents an overview of studies carried out at Radiochemistry Division on (a) spent fuel reprocessing of U/Th based spent fuels employing N,N-dialkyl amides as extractants, and (b) partitioning of minor actinides using novel solvents .*

Keywords – Reprocessing; Actinide partitioning; Tributyl phosphate; Dialkyl amides; Diglycolamides

The challenging task of recovery and purification of ^{239}Pu from irradiated U and of ^{233}U from irradiated Th are accomplished presently by the well known PUREX and THOREX processes, respectively [**1**]. These processes employ tri-n-butyl-phosphate (TBP) in n-dodecane as solvent. However, a few drawbacks associated with the use of TBP have been identified: (i) deleterious nature of its degradation products (ii) relatively lower distribution coefficient of Pu(IV) as compared to that of U(VI) (iii) significant solubility of TBP towards aqueous phase, and (iv) non-incinerable nature of the spent solvent yielding large volumes of secondary radioactive waste. These shortcomings may pose a serious challenge particularly during the reprocessing of short-cooled (MOX) thermal reactor, Advanced Heavy Water Reactor (AHWR, being developed in India based on Th) as well as fast reactor spent fuels with larger Pu content and significantly higher burn up [**2**]. In this context, large number of eco-friendly *N,N*-dialkyl amides were evaluated as alternative extractants at Radiochemistry Division, BARC, Mumbai, India. Amongst these amides, N,N-dihexyloctanamide (DHOA) and *N,N*-di(2-ethylhexyl)isobutyramide (D2EHIBA) received considerable attention as potential alternatives extractants for the reprocessing of U and Th based spent nuclear fuels, respectively [**3**]. Batch extraction, mixer settler/ centrifugal contactor runs were carried out with these reagents under Pu rich feed (relevant to fast reactor) and AHWR feed conditions, respectively. These data were compared with those obtained with TBP as extractant under identical experimental conditions and a flow sheet for AHWR spent fuel reprocessing has been proposed [**4**].

Actinide partitioning is the proposed strategy for effective mitigation of the long term hazards associated with high-level waste (HLW). Octyl-(phenyl)–*N,N*-diisobutyl carbamoyl methyl phosphine oxide (CMPO) has been studied extensively during eighties for actinide partitioning from wastes of different origin. However, the last two decades, substituted malonamide extractants such as *N,N'*-dimethyl-*N,N'*-dibutyl tetradecyl malonamide (DMDBTDMA) and *N,N'*-dimethyl-*N,N'*-dioctyl hexylethoxy malonamide (DMDOHEMA) have emerged as viable green alternatives to phosphine oxides. Recently, diglycolamide based extractants such as *N,N,N′,N′*-tetraoctyl diglycolamide (TODGA) and *N,N,N′,N′*-tetra-2-ethylhexyl diglycolamide (TEHDGA) have received considerable attention due to overwhelmingly favorable extraction and stripping efficiencies of minor actinides from different types of transuranium (TRU) wastes (**Fig.1**) [**5,6**]. We have carried out comparative evaluation of the key physical and chemical properties (including extraction/stripping) of these extractants for hydrometallurgical applications. A flow sheet has been proposed using DHOA as extractant. Merits of flow-sheets proposed for the separation and recovery of minor actinides from HLW have also been discussed. Detailed batch as well as mixer settler studies have shown that tridentate diglycolamide based ligands such as TODGA and TEHDGA have excellent properties for the partitioning of actinides from HLW solution.

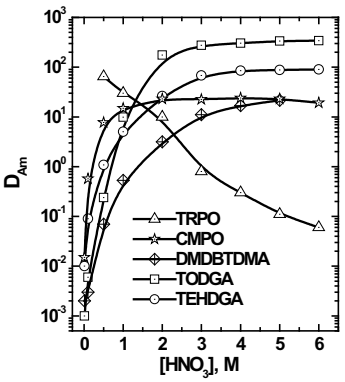

Fig.1: Variation of D_{Am} with HNO_3 concentration; Extractants: 30% TRPO, 0.2M CMPO+1.2M TBP, 1M DMDBTDMA, 0.1M TODGA + 0.5M DHOA and 0.2M TEHDGA + 30% *iso*-decanol; Diluent: *n*-dodecane; Temperature: 25°C

Acknowledgement: Author thanks Dr. P.K. Mohapatra and Dr. P.N. Pathak for their help in preparing this paper.

References

1. "Reactor Hand Book", S.M. Stoller and R.B. Richards (Eds.), v. 2, "*Fuel reprocessing*", Interscience Publishers & Inc., New York, 1961.
2. R.K. Sinha, A. Kakodkar, A. *Nucl. Engg. Design*, 2006, 236, 683.
3. V.K. Manchanda, P.N. Pathak, *Sep. & Purif. Technol.*, 35 (2004) 85.
4. N. Kumari, D.R. Prabhu, A.S. Kanekar, P.N. Pathak. *Ind. Engg. Chem. Res.,* 51 (44) (2012) 14535.
5. S.A. Ansari, P.N. Pathak, Prasanta K. Mohapatra, Vijay K. Manchanda. *Chemical Reviews*, 112(3) (2012) **1751**.
6. Seraj A. Ansari, Priyanath Pathak, Prashant K. Mohapatra and Vijay K. Manchanda. *Sep.& Purif. Reviews*, 40 (2011) 43.

Hexanoic acid as alternative diluent in a GANEX process based on TBP and CyMe4-BTBP

Elin Löfström-Engdahl[1], Emma Aneheim[1], Christian Ekberg[1], Hanna Elfversson[1] and Gunnar Skarnemark[1]

Nuclear chemistry[1], Industrial Materials Recycling[2], Department of chemical and Biological Engineering, Chalmers University of Technology, SE 412 96 Gothenburg, Sweden

Abstract – Used nuclear fuel is radiotoxic for mankind and its environment for a long time. However, if it can be transmuted the radiotoxicity can be reduced. Simultaneously the long term heat load is decreased, making a final storage more volume efficient. Before the transmutation the actinides within the used fuel need to be separated from the fission, corrosion and activation products. This separation can be achieved by using the technique liquid-liquid extraction.

One extraction process that can be used for such a separation is the GroupActiNideEXtraction (GANEX) process. In a GANEX process all the actinides are to be separated from the rest of the fuel as one group. This extraction leaves all the fission, corrosion and activation products in the aqueous stream. One GANEX process that can successfully accomplish the An(III)/Ln(III) separation utilizes the diluent cyclohexanone in combination with the extractant tributylphosphate (TBP) (30 % vol) and a second ligand, CyMe4-BTBP (10 mM). However, there are some issues when using cyclohexanone as diluent, for example; it has a low flash point and it degrades in contact with the acidic aqueous phase. In this work an alternative diluent has therefore been tried in order to rule out if it can replace cyclohexanone. The diluent used was hexanoic acid. In the system containing 12 mM CyMe4-BTBP and 30 % vol TBP in hexanoic acid and the aqueous phase being 4 M HNO_3 the distribution ratio for plutonium is high (D_{Pu} = 76 ± 17), while the one for uranium is lower (D_U = 2.2 ± 0.25). The distribution ratios for americium and curium are unfortunately much lower than that of plutonium (D_{Am}= 1.1 ± 0.27, D_{Cm}=1.6 ± 1.81). The concentration CyMe4-BTBP ligand, the extractant of curium and americium, could unfortunately not be increased, because of limited solubility in hexanoic acid. The distribution ratios for fission, corrosion and activation products were low for mostly metals; however, silver, cadmium, palladium and molybdenum all have distributions ratios above 1 is therefore troublesome. Europium is used as a representative lanthanide, which are similar to the trivalent actinides and therefore hard to separate. The distribution ratio for europium is low in this system (D Eu = 0.12 ± 0.016). However, to conclude, the low americium and curium extractions indicate that hexanoic acid cannot replace cyclohexanone in a GANEX process.

APSORC'13 - 5th Asia-Pacific Symposium on Radiochemistry
Kanazawa, Japan, 22-27 September 2013

Effect of alcohols on separation behavior of rare earth elements using benzimidazole-type anion-exchange resin in nitric acid solutions

Tomobuchi Yusuke[1], Yu Tachibana[1], Masao Nomura[2] and Tatsuya Suzuki[1]
[1]Department of Nuclear System Safety Engineering, Graduate School of Engineering, Nagaoka University of Technology,
[2]Laboratory for Nuclear Reactors, Tokyo Institute of Technology

Abstract - Chromatographic separation experiments of trivalent rare earth elements were performed using benzimidazole type anion-exchange resin in nitric/alcohol mixed solvent systems at room temperature. As a result, it was found those trivalent rare earth elements are able to be separated mutually in a 20 % HNO_3 and 80 % MeOH mixed solvent. Based on these results, we systematically examined using various alcohols to make clear the role of alcohols in anion-exchange reactions at various temperatures.

Keywords - rare earth elements, alcohols, benzimidazole-type anion-exchange resin, mutual separation

I. INTRODUCTION

As a final disposal method for the high level liquid waste(abbreviated as HLLW) generated by spent-nuclear-fuel reprocessing plants, the geologic disposal concept of the vitrified HLLW has been proposed and investigated globally. Especially, from the viewpoint of minimizing the long-term radiological risk and facilitating the management of HLLW, a separation of the long-lived minor actinides(MA = Am and Cm) from HLLW is strongly desired.[1)] Moreover, a mutual separation of Am and Cm is also required after the separation of MA from HLLW because the relatively high decay heat of Cm makes it difficult to fabricate nuclear fuels reproduced from spent nuclear fuels.[2)] On the other hand, it has been well known that the difficulty of a mutual separation between trivalent Am and Cm is due to similar chemical properties.[2)] In fact, although a few reports by Hale et al. using diethylenetriaminepentaacetic acid and Suzuki et al. with tertiary pyridine have been reported, little systematic information is available on the mutual separation mechanisms between Am and Cm.[2,3)] Therefore, as a part of the fundamental researches to innovate conventional separation technologies, we have studied on the chromatographic separation of trivalent rare earth elements(abbreviated as REE (REE = La, Ce, Pr, Nd, Sm, Eu, and Gd)) which have the same valence level in solutions and the similar ion radii as compared with those of MA, using benzimidazole type anion-exchange resin (abbreviated as AR-01) embedded in high-porous silica beads in nitric acid/alcohol mixed solvent systems.

II. EXPERIMENTAL

All REE were used without further purification. The purity of all REE was more than 98.0%. All chemicals for sample preparations were of special pure grade. AR-01 resin consisted of styrene-divinylbenzene copolymers with 4-(1-methylbenzoimidazole-2-yl)phenyl and 4-(1,3-dimethyl-benzoimidazole-2-yl)phenyl, was supplied from Asahi Kasei Corporation. Each concentration of REE species in the solutions were determined by ICP-MS(7700x, Agilent).

III. RESULTS

Chromatographic separation experiments of trivalent REE were performed using AR-01 resin in a nitric acid solvent system and a nitric/alcohol mixed solvent system at room temperature. As a result, it was found that mutual separations of REE cannot be achieved completely in HNO_3 solutions(data no shown), but REE are able to be separated mutually in a 20 % HNO_3 and 80 % MeOH mixed solvent(see Figure 1). In addition, retention times obtained from these chromatograms of the REE increase with increasing the ion radii in order of Gd, Eu, Sm, Nd, Pr, Ce, and La, *i.e.*, it could be estimated that the separation mechanisms proceed through anion-exchange reactions between 4-(1,3-dimethyl-benzoimidazole-2-yl)phenyl groups of AR-01 and $[Ln(NO_3)_n]^{3-n}$ ($n \geq 4$). Based on these results, we concluded that the examined separation technique is applied to mutual separation of Am and Cm.

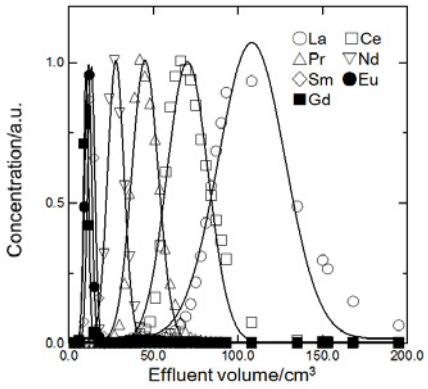

Figure 1. Chromatograms of La, Ce, Pr, Nd, Sm, Eu, and Gd species with AR-01 in 20 % HNO_3 and 80 % MeOH mixed solvent.

ACKNOWLEGEMENT

This work was partially supported by the Grant-in-Aid for Scientific Research (B) (KAKENHI No. 23360423).

REFERENCES

[1] Kolarik, Z., Journal of Nuclear Fuel Cycle and Environment, 5, 21-35 (1998)
[2] Suzuki, T., Otake, K., Sato, M., Ikeda, A., Aida, M., Fujii, Y., Hara, M., Mitsugashira, T.,Ozawa, M., Journal of Radioanalytical and Nuclear Chemistry, 272, 257-262 (2007)
[3] Hale, W.H., Lowe, J.T., Inorganic and Nuclear Chemistry Letters, 5, 363-368 (1969)

APSORC'13 - 5th Asia-Pacific Symposium on Radiochemistry
Kanazawa, Japan, 22-27 September 2013

Speciation and Reactivity of Heptavalent Technetium in Concentrated Acids.

Frederic Poineau[1], Philippe Weck[2], Benjamin P. Burton-Pye[3], Alesya Maruk[4], Gayane Kirakosyan[4], Ibthihel Denden[5], Daniel. B Rego[1], Erik V. Johnstone[1], William Kerlin[1], Eunja Kim[1], Mairlynn Ferrier[1], Alfred P. Sattelberger[7], Wayne Lukens[6], Massoud Fattahi[5], Lynn C. Francesconi[3], Konstantin E. German[4], and Kenneth R. Czerwinski[1].

[1] Department of Chemistry, University of Nevada Las Vegas, Las Vegas, NV, USA.
[2] Sandia National Laboratories, Albuquerque, NM 87185, USA.
[3] Department of Chemistry, Hunter college of the City University of New York, NY, USA
[4] A. N. Frumkin Institute of Physical Chemistry and Electrochemistry, Russian Academy of Sciences, Moscow, Russian Federation
5 Laboratory Subatech, Ecoles des Mines de Nantes, Nantes, France
[6] Energy Engineering and Systems Analysis Directorate, Argonne National Laboratory, Lemont, IL, USA.
[7] Chemical Sciences Division, Lawrence Berkeley National Laboratory, Berkeley, 94720, USA

Keywords – Technetium, Speciation, EXAFS spectroscopy.

Discovered 75 years ago, technetium is the lightest radioelement. Thirty four isotopes are known; the most common isotopes being ^{99}Tc ($t_{1/2}$ = 2.1 x 10^5 y) and ^{99m}Tc ($t_{1/2}$ = 6 h). The isotope ^{99}Tc is a fission product of the nuclear industry, while the isotope ^{99m}Tc is used in nuclear medicine as an imaging agent. Current researches focus on the development of ^{99m}Tc radiopharmaceuticals, and on the development of separation process and waste form storage for ^{99}Tc. Technetium exhibits nine oxidation states (-1 to +7). Under oxidizing conditions, the aqueous chemistry of Tc(+7) is dominated by the pertechnetate anion, TcO_4^-. In high acid concentration, TcO_4^- can be protonated and pertechnetic acid, $HTcO_4$, is formed. The structure and reactivity of $HTcO_4$ is poorly studied. Studying the chemistry of Tc(+7) in concentrated acids is relevant to the fundamental and applied chemistry of technetium; it will allow to better understand the behavior of Tc(+7) in separation processes where concentrated acids are used. In this work, the speciation and reactivity of Tc(+7) in concentrated HNO_3, H_2SO_4 and $HClO_4$ is investigated. The resulting complexes are characterized by NMR, UV-visible and EXAFS spectroscopy and DFT calculations. Results show the formation of $TcO_3(H_2O)_2(OH)$ in concentrated H_2SO_4 and $HClO_4$ while TcO_4^- in concentrated HNO_3. The complex $TcO_3(H_2O)_2(OH)$ reacts in 13 M H_2SO_4 with MeOH to produce $TcO(HSO_4)_3(OH)^-$. In HNO_3 > 7 M , the pertechnetate anion reacts with hydrogen peroxide to produce $TcO(O_2)_2(H_2O)OH$. The results demonstrate the complex and little explored chemistry of Tc in concentrated acids.

NEO-04

Fluorescence Studies of Complex Stoichiometry of Metal ions in Extraction Systems Combining Dibutyl Phosphoric Acid and Tri-n-butyl Phosphate

Alexander Braatz and Mikael Nilsson
University of California, Irvine
Department of Chemical Engineering & Materials Science
916 Engineering Tower
Irvine, CA 92697-2575
abraatz@uci.edu

Advanced nuclear fuel cycles are dependent on successful chemical separation of the various elements present in the used fuel. Numerous extraction systems have been developed for the recovery and separation of the various metal ions present in the used fuel. Extraction of lanthanides and actinides by tri-n-butyl phosphate (TBP) and dibutyl phosphoric acid (HDBP) is of importance for one of these processes, the PUREX process. The combination of these two extraction reagents have been shown to synergistically enhance metal ion extraction and display characteristics of microemulsion aggregates of reverse micelle type. To improve our understanding of the complexes formed in this system we further studied the extraction of lanthanides and actinides, in our case dysprosium, Dy, and uranium, U, with TBP and HDBP in conjunction with 2D fluorescence spectrometry. Aqueous samples containing Dy^{3+} and UO_2^{2+} in nitric acid were contacted with organic phases containing varying ratios of TBP and HDBP in n-dodecane and the distribution was followed by neutron activation analysis. 2D Fluorescence spectra were examined for all lanthanides and uranium. Typically, europium is used as a benchmark for lanthanides in fluorescence studies but we show here that several other lanthanides exhibit excellent spectroscopic characteristics using this technique. The effects of acid on the fluorescence spectra will be investigated. Possible explanations of phenomena and comparison to existing Eu studies found in literature will also be presented.

Column study on electrochemical separation of cesium ions from wastewater using copper hexacyanoferrate film

Rongzhi Chen [1)], Hisashi Tanaka [1)], Miyuki Asai [1)], Chikako Fukushima [1)], Tohru Kawamoto [1)], Manabu Ishizaki [2)], Masato Kurihara [1,2)], Makoto Arisaka [3)], Takuya Nankawa [3)] and Masayuki Watanabe [3)]

[1)] Nanosystem Research Institute, AIST, Tsukuba central 5, 1-1-1 Higashi, Tsukuba, Ibaraki 305-8565, Japan

[2)] Department of Material and Biological Chemistry, Faculty of Science, Yamagata University, 1-4-12 Kojirakawa-machi, Yamagata 990-8560, Japan

[3)] Japan Atomic Energy Agency, 2-4 Shirane Shirakata, Tokai-mura, Naka-gun, Ibaraki 319-1195, Japan

Abstract – We coated the copper hexacyanoferrate (CuHCF) on the gold electrodes, and then performed the Cs removal by electrochemical separation (ES). The prepared CuHCF nanoparticles can be simply and uniformly coated on electrodes by wet process like conventional printing methods, so any sizes or patterns are feasible at low cost, which indicated the potential as a promising sorption electrode of large size in the columns for sequential removal and recycle of Cs from wastewater.

Keywords: Metal hexacyanoferrate complex, Electrochemical separation, Cesium, Radioactive waste, Nanoparticle ink, Prussian blue complex.

Introduction

Transition metal hexacyanoferrates (HCFs) are preferred to be competitive ion exchangers over other materials due to their selectivity and high capacity. Among them, copper (II) hexacyanoferrate (III) (CuHCF) is often selected as the agent in practical analysis. This compound has been much used as precipitants for alkali metal cations, especially cesium, to remove them from aqueous radioactive wastes [1].

However, small sized CuHCF particles can easily contaminate water, which restricts its direct use for column operations. Herein, we developed and coated the water-dispersible CuHCF nanoparticles on the electrode substance, and then performed Cs removal. This study evaluates the electrochemical Cs sorbability of CuHCF NPs film and estimates the potential as a promising sorption electrode of large size in the columns for sequential removal and recycle of Cs from wastewater.

Experimental & Results

The Cs adsorption was performed in a three-electrode cell in which an $Hg/Hg_2Cl_2/KCl$ (saturated solution) as reference electrode, a platinum electrode (as counter electrode), and the CuHCF film coated adsorbent electrode were used as the working electrodes. The redox reaction for Cs separation process is proposed as follows [1]:

$$Cu_3[Fe^{III}(CN)_6]_2) + 2e^- + 2Cs^+ \leftrightarrow Cs_2Cu_3[Fe^{II}(CN)_6]_2$$

To examine the effect of temperature, electrochemical characterization of CuHCF film and its Cs adsorptions were conducted at 298, 313, and 323 K, respectively. Cs removal decreased with the increase in temperature for CuHCF film (Fig. 3b). Namely, the Cs adsorption process was exothermic in nature.

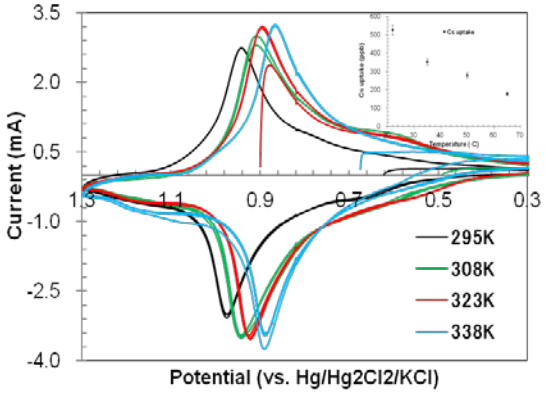

Fig. CV of a Cu-HCF film under different temperatures (from 298 to 338 K), and effect of temperature on Cs sorption using CuHCF film

In order to using our film for practical analysis in the field-scale applications, column study is needed. We synthesized water-dispersed nanoparticle CuHCF ink and then coated its nanoparticles on SUS316L sheet electrodes. The Cs adsorption and desorption were alternately repeated for 5 cycles (30 min/cycle), initial Cs conc. is 9.858 ppm.

The well balance of Cs desorption and adsorption, indicated the CuHCF film has a long life in the columns for sequential removal and recycle of Cs from wastewater.

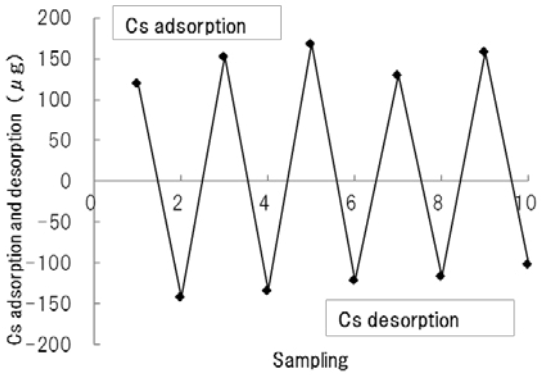

Fig. Cs alternate adsorption and desorption performance using CuHCF film

Effective regeneration and large surface coating will allow it to be used in the column for sequential removal processes.

[1] RZ. Chen, et al., *Electrochimica Acta,* **2013**, *87* 119

Oral Presentations

Wednesday, 25 September 2013

Hall & Meeting Room, Kanazawa Bunka Hall

	Wednesday, 25 September				
Time		Hall		Meeting Room	
09:00-09:10	9:00	PL-05	**Plenary**		
09:10-09:20					
09:20-09:30			M. A. Denecke		
09:30-09:40	9:30	PL-06	**Plenary**		
09:40-09:50					
09:50-10:00			J. Hatazawa		
10:00-10:10	10:00	**Coffee Break**			
10:10-10:20					
10:20-10:30	10:20	RPI-01	**Invited**	ACI-01	**Invited**
10:30-10:40					
10:40-10:50			D. S. Wilbur		J. Li
10:50-11:00	10:50	RPI-02	**Invited**	ACI-02	**Invited**
11:00-11:10					
11:10-11:20			S. Lahiri		Y. Kitatsuji
11:20-11:30	11:20	RPO-01	General	ACO-01	General
11:30-11:40			E. Aneheim		A. Kirishima
11:40-11:50	11:40	RPO-02	General	ACO-02	General
11:50-12:00			Y. Hatsukawa		H. Hayashi
12:00-12:10	12:00	**Group Photo (Hall)**			
12:10-13:20		**Lunch Time**			
13:20-13:30	13:20				
13:30-13:40					
13:40-13:50	13:40	**JNRS General Assembly (For Member of JNRS))**			
13:50-14:00					
14:00-14:10	14:00				
14:10-14:20					
14:20-14:30	14:20				
14:30-14:40					
14:40-14:50	14:40	**JNRS Meeting**			
14:50-15:00					
15:00-15:10	15:00				
15:10-15:20					
15:20-15:30	15:20	**Coffee Break**			
15:30-15:40					
15:40-15:50	15:40	RPO-03	General	ACO-03	General
15:50-16:00			L. Safavi-Tehrani		T.H. Park
16:00-16:10	16:00	FKO-11	General	ACO-04	General
16:10-16:20			E. Rasmussen		N. Aoyagi
16:20-16:30	16:20	FKO-12	General	NCO-13	General
16:30-16:40			K. Minami		A. Toyoshima
16:40-16:50	16:40	FKO-13	General	NCO-14	General
16:50-17:00			T. Kawamoto		P. Steinegger
17:00-17:10	17:00	FKO-14	General	NCO-15	General
17:10-17:20			D. Parajuli		R. Tripathi
17:20-17:30	17:20	**Coffee Break**			
17:30-17:40					
17:40-17:50					
17:50-18:00	17:50	**JNRS Award Presentation (Open Session) T. Kimura**			
18:00-18:10					
18:10-18:20					
18:20-18:30					
18:30-18:40	18:30				
18:40-18:50					
18:50-19:00	18:50	**Poster Session**			
19:00-19:20					
19:20-19:40					
19:40-20:00					
20:00-	20:00				

Actinide speciation using synchrotron-based methods

M. A. Denecke[1]
[1]Dalton Nuclear Institute, University of Manchester, Manchester, M13 9PL, UK

Abstract – *Synchrotron-based techniques are increasingly used to characterize materials and elucidate determinant processes relevant to the nuclear fuel cycle. Most recent advances are driven by the need to characterize materials with high spatial resolution, for example localized components of heterogeneous systems or interstitial/interfacial junctions. In this presentation, examples of synchrotron-based investigations covering a wide range of wavelengths (infra-red to hard X-ray) and spatial resolution (nanometer range to bulk) will be introduced. The examples are chosen to illustrate various themes of research and development over the entire range of the nuclear fuel cycle, from power plant lifetime extension scenarios to nuclear waste disposal and future fuel/target development.*

Keywords –Actinide speciation, X-ray techniques, synchrotron radiation

PL-06

Radionuclides in Diagnostic Nuclear Medicine

Jun Hatazawa
Department of Nuclear Medicine and Tracer Kinetics, Osaka University Graduate School of Medicine
WPI-Immunology Frontier Research Center, Osaka University

Abstract – Diagnostic Nuclear Medicine (NM) is an essential procedure in modern medical practice. Recent survey reported that more than 2 million NM examinations are conducted every year in Japan. Around 75% of diagnostic NM employs single photon emission tomography (SPECT) with ^{99m}Tc, ^{123}I, ^{133}Xe, or ^{201}Tl-labeled compound, and 25% positron emission tomography (PET) with ^{18}F-fluorodeoxy glucose, ^{15}O-labeled H_2O, CO, O_2, or ^{11}C-labeled compounds. Modern medicine is based on the intervention of molecular pathology of the diseases. Therefore, NM is expanding in number and in quality in daily medical practice including early diagnosis of Alzheimer's diseases, cancer, and cardiovascular diseases, strategy decision of treatment, evaluation of regeneration medicine. Furthermore, the NM is being utilized to facilitate new drug development. Combining molecular diagnosis with radionuclide therapy (Theranostics) is another future direction of clinical NM.

Keywords – Nuclear Medicine, Molecular Imaging, Theranostics

Nuclear Medicine is now employed as a major tool of sensitively detecting molecular changes of the diseases before symptom onset. In Alzheimer's disease, amyloid deposition in brain tissue can be detected more than 10 years earlier than the onset. Abnormality in cerebral perfusion predicts a probability of ischemic stroke onset. PET examination can detect small cancer in volume before invasion and remote metastasis. Therapy response can be detected most sensitively among imaging modalities. The number of NM examination is therefore increasing dramatically recent years.

The application of NM is extending to facilitate new drug development (PET micro-dosing test). Because of high specific activity of radionuclide-labeled compound, pharmaco-kinetics of candidate compounds can be examined in humans. Combining molecular diagnosis of NM with radio-nuclide therapy (Theranostics) is another direction of NM. Nano particles with designed chemistry, size, surface charge, and target-specific binding ligands can extend "Nuclear Medicine Theranostics" by specifically carrying therapeutic radioisotopes and drugs to diseased tissues.

There are several problems to expand clinical NM. The shortage of ^{99}Mo supply is most critical. ^{99}Mo is now being produced by old nuclear reactors of specific countries. ^{99}Mo-99mTc generator completely depends on the import of ^{99}Mo. We are now trying to produce ^{99}Mo with accelerator by ^{100}Mo(n,2n)^{99}Mo reaction. After improving irradiation of solid target, separation and purification of ^{99}Mo in solid target, we obtained ^{99m}Tc for bone scintigraphy of rats. Following steps of this project are mass production, clinical trial, approval by regulatory authority, and commercial delivery.

For the NM theranostics, we need radio-nuclides with specific characteristics. It should emit gamma ray with appropriate energy (100~200keV) for imaging and beta particles for therapy. Nowadays, ^{89}Sr and ^{90}Yo are utilized to treat bone metastasis of cancers and malignant lymphoma, respectively. Since these tracers are pure beta particle emitting radionuclides, an evaluation of radio-nuclides accumulation is not possible by NM imaging. ^{131}I (gamma ray of 364keV, beta particle of 606keV) is utilized for the treatment of hyperthyroidism, pheochromo-cytoma, and thyroid cancer. Imaging is possible by adapting heavy collimation of high energy gamma ray.

Functional nano particles are now applied to NM. Non-radioactive nano particles have been safely used in clinical trials of anti-cancer drugs (Nature 496:S58-60, 2012). The difficulty of radionuclides labeled nano particles is that the labeling process should be rapid because of physical decay of radionuclides. Long enough physical decay (13 hour of ^{64}Cu, 13 hour of ^{123}I, and 100 hour of ^{124}I) is required for this purpose.

Finally, the process from experimental study to clinical trial (translational medical center) has been installed in Osaka University Hospital under the support of Ministry of Health, Labor, and Welfare, Japan, which will be introduced in this presentation.

Addressing Challenges in Preparation of ^{211}At-Labeled Biomolecules for Use in Targeted Alpha Therapy

D. Scott Wilbur[1], Donald K. Hamlin[1], Ming-Kuan Chyan[1], Ethan R. Balkin[1], John M. Pagel[2,3], Oliver W. Press[2,3], and Brenda M. Sandmaier[2,3]
[1]Radiation Oncology and [2]Medicine, University of Washington, Seattle, WA, USA
[3]Fred Hutchinson Cancer Research Center, Seattle, WA, USA

Abstract – There are significant challenges in the development of ^{211}At-labeled biomolecules for application to targeted alpha therapy. Challenges that we have addressed include development of: (1) labeling methods to obtain high in vivo ^{211}At-label stability, (2) approaches to consistently obtain high recovery yields of Na[^{211}At]At from irradiated bismuth targets, (3) methods to optimize biomolecule labeling yields, (4) reagents for use of ^{211}At in pretargeting approach to cancer therapy, and (5) ^{211}At-labeled antibodies in conditioning for hematopoietic cell transplantation.

Keywords – Astatine-211, antibodies, pretargeting, biotin

I. INTRODUCTION

There are only ten α-emitting radionuclides identified as having properties suitable for targeted alpha therapy [1]. Of that small group of radionuclides, astatine-211 (^{211}At) is particularly attractive due to its reasonable half-life ($t_{1/2}$ = 7.21 h), lack of α-emitting daughter radionuclides, and relative ease of preparation from an inexpensive target material (bismuth metal). However, application of ^{211}At to the development of targeted alpha therapy has been difficult due to the low number of cyclotrons with (operating) alpha beams used in its production [2], and a host of problems involving the labeling chemistry and in vivo stability of ^{211}At-labeled biomolecules [3]. We have investigated ^{211}At-labeled biomolecules for over two decades and have had to address many challenging problems associated with ^{211}At during that time.

II. RESULTS AND DISCUSSION

One of the most impactful challenges to development of ^{211}At-labeled biomolecules has been their low in vivo stability. Early studies demonstrated that the ^{211}At label was stabilized on non-activated aryl compounds. However, the in vivo stability is only retained in slowly metabolized biomolecules, such as intact monoclonal antibodies (MAbs). Thus, in vivo stability has been a problem with MAb fragments, peptides or smaller biomolecules, where the aryl-At bond can be rapidly cleaved in vivo. We have investigated chelation of ^{211}At, oxidation of ^{211}At on aryl groups, and changing the bonding atom to boron for stabilization of the ^{211}At bonding. In the latter approach, a number of boron cage molecules have been evaluated as pendant groups for attachment of ^{211}At to biomolecules.

Of the different types of boron cage molecules studied, the *closo*-decaborate(2-) cage [B10 cage] has proven to provide high in vivo stability. In addition to high stability, that pendant group has made labeling of proteins much more efficient and easy to conduct. This is due to the fact that the high electrophilic reactivity of the *closo*-decaborate(2-) moiety permits conjugation with proteins prior to astatination. This is in contrast to using a 2-step labeling procedure required with aryl-astatine reagents.

Another significant challenge became apparent when the size of the bismuth target was increased in preparation for translating ^{211}At-labeled MAbs into clinical studies. Our standard method for isolation of ^{211}At was "dry distillation". However, the larger bismuth target and requisite larger quartz glassware resulted in low and inconsistent distillation yields of ^{211}At. Therefore, we switched to a "wet chemistry" isolation approach. That approach has provided very consistent and high recovery yields. Another advantage of the wet chemistry approach is that it may permit automation of the isolation process.

Developing ^{211}At-labeled reagents for use in pretargeting approaches to cancer therapy has been another challenge. For example, it initially appeared that preparation of an ^{211}At-labeled biotin reagent might be relatively straight-forward. However, many of the biotin derivatives prepared localized to kidneys or liver, or did not work in the pretargeting protocol. In some studies, biotin derivatives that did not localize in tumor bound with MAb-streptavidin conjugates. We knew the lack of binding with tumor could be due to formation of biotin-sulfone. We investigated formation of biotin-sulfone with chloramine-T (ChT) oxidant, but believed that our labeling conditions did not form the sulfone as the labeled product bound to an avidin column. Presently, we are investigating labeling biotin derivatives with other oxidants or no oxidant.

The oxidant ChT has also been found to cause problems with ^{211}At-labeled MAb-B10 conjugates. Studies to decrease the amount of ChT in the radiolabeling reactions with MAb-B10 conjugates have shown that no oxidant is required in the ^{211}At reactions. We now know that under acidic or neutral conditions, At is electropositive enough to undergo electrophilic reactions with *closo*-decaborate(2-) cages. In reactions without oxidant we obtain labeling yields equivalent to those with oxidant.

A further challenge is developing methods to keep ^{211}At-labeled small biomolecules from localizing in kidneys. We have conducted a number of studies in that area as well. An overview of some of our research to circumvent challenges encountered when using ^{211}At in development of Targeted Alpha Therapy agents will be presented.

REFERENCES

[1] D. S. Wilbur, *Current Radiopharm.* **4**, 214 (2011).
[2] M. R. Zalutsky, M. Pruszynski, *Current Radiopharm.* **4**, 177 (2011)
[3] D. S. Wilbur, *Current Radiopharm.* **1**, 144 (2008).

Generation of nuclear data for the production of ^{97}Ru from ^{12}C+^{89}Y reaction

Moumita Maiti[1], Susanta Lahiri[2]
[1]Department of Physics, Indian Institute of Technology Roorkee, Roorkee-247667, India
[2]Saha Institute of Nuclear Physics, 1/AF Bidhannagar, Kolkata-700064, India

Abstract – This article reports the measurement of cross section and yield of ^{97}Ru in ^{12}C induced reaction on natural yttrium target in the 40-75 MeV incident energy range. Cumulative cross section/yield of ^{97}Ru was measured by stacked foil technique followed by off line γ-ray spectrometry. Measured data follows the trend of theoretical estimation.

Keywords – ^{97}Ru, cross section measurement, yield, stacked foil technique, ^{89}Y target, ^{12}C projectile

I. INTRODUCTION

Due to the suitable nuclear properties, ^{97}Ru has been proposed for a number of applications. Besides high chemical reactivity of ruthenium helps to produce various ^{97}Ru-labelled complexes concerned to the application. Investigation on the production cross section of ^{97}Ru is important as it helps to optimize the production and to maintain the purity of the product.

Several attempts to produce ^{97}Ru through p, ^{3}He and α-particle induced reactions on suitable targets have been reported. In a recent attempt we produced no-carrier-added (NCA) ^{97}Ru through ^{93}Nb(^{7}Li,3n)^{97}Ru reaction and developed radiochemical separations[1]. This article reports the experimental measurement of production cross section and yield of ^{97}Ru from ^{12}C+^{89}Y reaction.

II. EXPERIMENTAL

Production cross sections and yield of ^{97}Ru produced in ^{12}C+^{89}Y reactions were measured by the stacked foil technique followed by off-line γ-ray spectroscopy. Thin self supporting Y foils (99.9% purity) of thickness 1.9-2 mg/cm^2 were prepared by proper rolling. A target stack was assembled with 3 such Y foils; each Y foil was backed by an aluminum catcher foil of thickness 1.5 mg/cm^2, and was irradiated with ^{12}C^{6+} ions. A total of four such target stacks were irradiated independently varying the incident energy with an overlap between them. The experiment was carried out at the BARC-TIFR pelletron accelerator facility, Mumbai, India. The integrated charge was recorded in each irradiation by an electron-suppressed Faraday cup stationed at the back of the target assembly. The cross sections of ^{97}Ru produced at various incident energies were calculated using the standard activation equation whose detail description is available elsewhere [2].

III. RESULTS AND DISCUSSION

Production ^{97}Ru was contributed by the direct reaction (i) ^{nat}Y(^{12}C,p3n)^{97}Ru and (ii) indirect reaction, through the decay of short-lived ^{97}Rh(30.7min),^{97m}Rh(46.2min) produced through ^{nat}Y(^{12}C,4n)^{97}Rh(EC)^{97}Ru & ^{nat}Y(^{12}C,4n)^{97m}Rh(EC: 94.4%, IT: 5.6%) ^{97}Ru reactions. Measured cross sections of ^{97}Ru at different projectile energies are therefore cumulative of all reaction channels. All possible errors are considered in the error analysis and the data presented up to the 95% confidence level. Figure 1 shows the maximum cross section of ^{97}Ru is ~780 mb at ~67 MeV bombarding energy and the trend of the measured data nicely follows the theoretical estimation of PACE4, which essentially calculates the fusion-evaporation cross section following the Hauser-Feshbach model. Moreover, measured cross sections of ^{97}Ru are comparable to the sum of cross sections of ^{97}Ru+^{97}Rh. Figure 2 shows the measured yield of ^{97}Ru at various bombarding energies. The maximum yield of 110 kBq/μA.h was obtained at ~67 MeV energy. However, a thick target yield of >0.5 MBq/μA.h can easily be achieved if the thickness of the Y foil and proper projectile window is chosen.

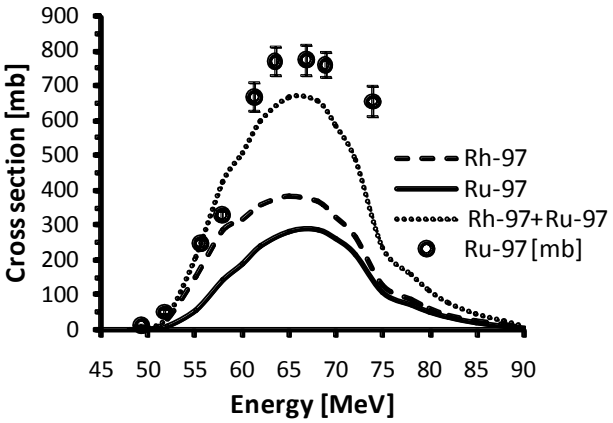

Figure 1. Comparison of cross sections of ^{97}Ru (symbol) with the theoretical excitation functions (lines) of ^{97}Ru, ^{97}Rh and sum of (^{97}Rh+^{97}Ru) as obtained from PACE4

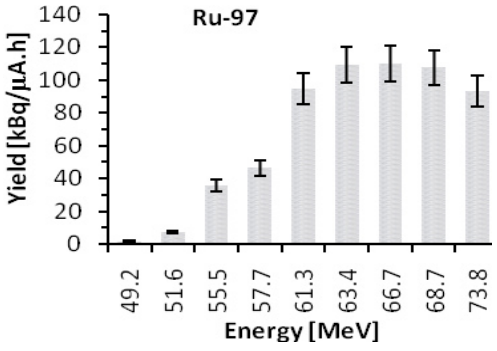

Figure 2. Measured yield of ^{97}Ru at different projectile energies

[1] M. Maiti, S. Lahiri, Radiochim. Acta 99, 359 (2011)
[2] M. Maiti, S. Lahiri, Phys. Rev. C 81, 024603 (2010)

APSORC'13 - 5th Asia-Pacific Symposium on Radiochemistry
Kanazawa, Japan, 22-27 September 2013

Towards an automatic procedure for the production of astatinated antibodies

Emma Aneheim[1], Sture Lindegren[1], Holger Jensen[2]
[1]Targeted Alpha Therapy group, Department of Radiation Physics, Sahlgrenska Academy at Gothenburg University, SE41345 Gothenburg, Sweden
[2]Cyclotron and PET Unit, KF-3982, Rigshospitalet, Copenhagen, Denmark

In recent time targeted radiotherapy of cancer tumors have been given a larger interest. For microscopic tumors, alpha therapy is especially interesting due to the high LET of the alpha particles. One promising nuclide for targeted alpha therapy is ^{211}At. ^{211}At decays with 100% alpha-emission along two different branches and does not emit any major quantities of gamma, allowing for safe handling of large activities. At Sahlgrenska Academy in Sweden, research regarding alpha therapy using astatine and monoclonal antibodies has been ongoing for over fifteen years. The research has been taken from bench to bedside including a number of preclinical studies and a phase I clinical trial on nine patients with recurrent ovarian cancer. However, to be able to move forward towards phase II/III studies the current synthesis of radiolabeled antibodies would benefit from being automated. The automation will be performed using a custom made radiopharmaceutical module from Scintomics Gmbh. This procedure, however, requires both modifications of the synthesis, as well as an adaptation of the astatine distillation process. The work presented here concerns such an automation of the production of astatinated antibodies.

Keywords – Astatine-211, antibodies, radiopharmaceutical module

Production of ^{95m}Tc for Compton Camera Imaging

Yuichi Hatsukawa[1], Kazuyuki Hashimoto[1], Kazuaki Tsukada[1], Tetsuya Sato[1], Masato Asai[1], Atsushi Toyoshima[1], Yasuki Nagai[1], Toru Tanimori[2], Shinya Sonoda[2], Shigeto Kabuki[3], Hideo Saji[4], Hiroyuki Kimura[4]

[1]Japan Atomic Energy Agency
[2]Department of Physics, Kyoto University
[3]School of Medicine, Tokai University
[4]Faculty of Pharmaceutical Sciences, Kyoto University

Abstract – With the development of the Compton camera which can realize high position resolution, technetium isotopes emitting high energy gamma-rays are required. In this study, technetium-95m which emits some gamma rays with higher than 500 keV was produced by the ^{95}Mo(p,n)^{95m}Tc reaction. Image of gamma-rays from Tc-95m was taken by a Compton gamma-ray camera

Keywords –Technetium-95m, Compton gamma-ray camera, MDP labeling, ^{95}Mo(p,n)^{95m}Tc reaction,

I. INTRODUCTION

Technetium-99m is used in radioactive medical diagonostic tests, for example as a radioactive tracer that medical equipment can detect in the human body. It is well suited to the role because it emits readily detectable 141 keV gamma rays, and its half-life is 6.01 hours (meaning that about 94% of it decays to technetium-99 in 24 hours). There are at least 31 commonly used radiopharmaceuticals based on technetium-99m for imaging and functional studies of the brain, myocardium, thyroid, lungs, liver, gallbladder, kidneys, skeleton, blood, and tumors. Recent years, with the develop-ment of the Compton camera which can realize high position resolution, technetium isotopes emitting high energy gamma-rays are required. In this study, technetium-95m which emits some gamma rays around 800 keV was produced by the ^{95}Mo(p,n)^{95m}Tc reaction.

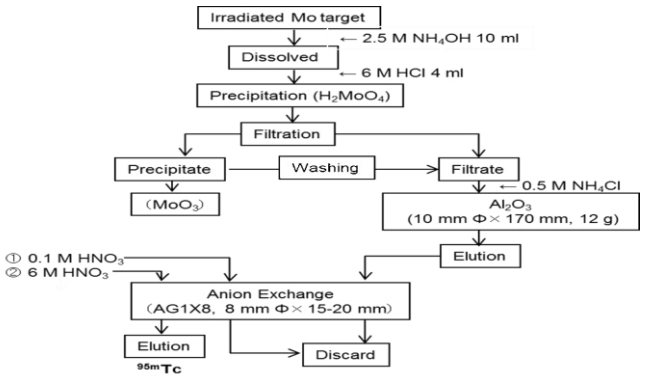

Fig.1 Chemical purification procedure of Tc-95m from MoO_3 target.

II. EXPERIMENTAL and RESULTS

A 300-700 miligrams of $^{nat}MoO_3$ targets were irradiated with 15 MeV proton beam for 7 hours at the JAEA Tandem accelerator. Averaged beam currents were 1.2 μA. After a few weeks cooling time, about 300-500 kBq of ^{95m}Tc were extracted from the irradiated MoO_3 target after a chemical separation shown in Fig.1

Using purified ^{95m}Tc, a labeled compound, ^{95m}Tc-MDP (methylene diphosphate) was synthesized. In order to examine quality of the labeled compounds obtained in this study, thin-layer chromatography (TLC) method was carried out. A spot of solution of the labeled compound was placed at the edge of the TLC plate, and the plate stood up-right in a solvent. Two kind of solvents, Methyl ethyl ketone (MEK) and physiological saline were used. After about 10 -30 min dipping time, TLC plates were dried and taken autoradiography images using imaging plates for 12 hours. The result of labeling experiment was shown in Fig. 2. According to this result, labeled compound, ^{95m}Tc-MDP was synthesized well.

Then, Compton camera imaging was taken by the Electron-tracking Compton gamma-ray camera which was developed by prof. T. Tanimori's group of Kyoto university for medical usage.[2-3] The results obtained from these experiments will be discussed in the APSORC meeting.

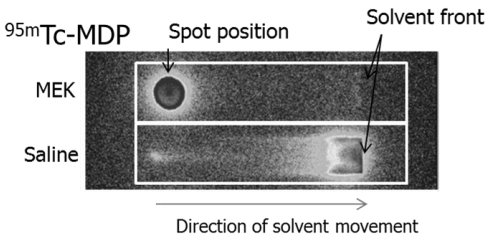

Fig.2 Autoradiography images form ^{95m}Tc-MDP. MEK and physiological saline was used as solvents.

Reference

[1] M.Izumo, et al., Appl. Radiat. Isot. 42 297-310 (1991)
[2] T. Tanimori et al., New Astron. Rev. 48 (2004) 236.
[3] S.Kabuki et al., NIM,A623(2010) 606

Relativistic Quantum Chemical Studies on Electronic Structures and Photoelectron Spectra of Actinide Complexes

Jing Su and Jun Li*
Department of Chemistry, Tsinghua University, Beijing 100084, China
*E-Mail: junli@tsinghua.edu.cn

Abstract – Investigations of the actinide spectroscopy and chemistry have been an active field of research recently. Actinide complexes are challenging for theoretical studies because of their significant relativistic effects and strong electron correlation effects. Photoelectron spectroscopy (PES) is a powerful experimental technique in providing detailed information about the electronic structures of ground states and excited states of actinide species. In this talk we will present our recent results from a series of joint relativistic quantum mechanical and photoelectron spectroscopy studies on actinyl complexes and uranium halides. Computational details on how to accurately describe excited states with spin-orbit coupling (SOC) will be given. We will focus on the electronic structures of $UO_2X_3^-$ and $UO_2X_4^{2-}$ (X = F, Cl, Br, I) complexes. Theoretical simulation of their experimental photoelectron spectra will also be discussed.

Keywords – Actinyl, Relativistic Effects, Spin-Orbit Coupling, Photoelectron Spectrum, Ab initio Wavefunction Theory

I. INTRODUCTION

Uranyl halides play important roles in the extraction of uranium into the aqueous phase and in serving as useful starting materials for the syntheses of a wide variety of uranium compounds. In this work, we report a joint photoelectron spectroscopy (PES) and relativistic quantum chemistry study on the bonding and stability of a series of gaseous tricoordinate uranyl halide complexes: $UO_2X_3^-$ (X = F, Cl, Br, I). Low temperature PES spectra were obtained at 20 K for the first time by Wang and coworkers at Brown University and these uranyl trihalides were observed to be highly stable electronically with extremely high electron binding energies. Theoretical results from *ab initio* wavefucntion theory (WFT) calculations agree well with experiments (Table 1). Extensive bonding analyses for $UO_2X_3^-$ and the doubly-charged tetracoordinate complexes ($UO_2X_4^{2-}$) show that the U–X bonds are dominated by ionic interactions with weak covalency. Further theoretical calculations show that the gaseous $UO_2X_4^{2-}$ complexes are thermodynamically unstable against dissociation to $UO_2X_3^-$ + X^- with decreasing dynamic stability from X = F to I. The competition between the U–X bonding and the Coulomb repulsions determines the kinetic stability of $UO_2X_4^{2-}$ (Figure 1).[1-4]

Table 1. Observed and calculated adiabatic (ADE) and vertical (VDE) detachment energies for $UO_2X_3^-$ (X = F, Cl, Br, I).[a]

		Exp [b]	DFT/PBE		CCSD(T)	
			SR	SO	SR	SO [c]
$UO_2F_3^-$	ADE	6.25 (5)	5.44	5.31	6.48	6.35
	VDE	6.53 (5)	5.62	5.52	6.81	6.71
$UO_2Cl_3^-$	ADE	6.64 (5)	5.47	5.41	6.82	6.76
	VDE	6.72 (5)	5.52	5.47	6.88	6.83
$UO_2Br_3^-$	ADE	6.27 (5)	5.24	5.18	6.45	6.39
	VDE	6.37 (5)	5.24	5.18	6.45	6.39
$UO_2I_3^-$	ADE	5.60 (5)	4.84	4.71	5.86	5.73
	VDE	5.72 (5)	4.85	4.72	5.86	5.73

[a] All the energies are in eV. [b] The numbers in parentheses represent the experimental uncertainties in the last digit. [c] These SO results are estimated using the SR CCSD(T) energies with the *ad hoc* SO-corrections from the DFT/PBE calculations.

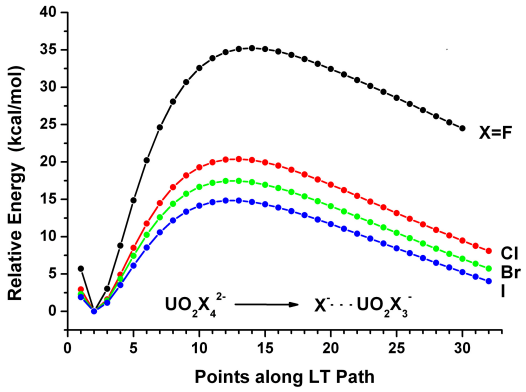

Figure 1. Linear transit (LT) energy curves illustrating the dissociation of $UO_2X_4^{2-} \rightarrow UO_2X_3^- + X^-$ (X = F, Cl, Br, I). The energies are obtained from the DFT/PBE calculations.

REFERENCES

[1] J. Su, P. D. Dau, Y.-H. Qiu, H.-T. Liu, C.-F. Xu, D.-L. Huang, L.-S. Wang, J. Li, "Probing the Electronic Structure and Chemical Bonding in Tricoordinate Uranyl Complexes $UO_2X_3^-$ (X = F, Cl, Br, I)." ***Inorg. Chem.*** *52*, 6617-6626 (**2013**).

[2] P. D. Dau, J. Su, H.-T. Liu, J.-B. Liu, D.-L. Huang, J. Li , L.-S. Wang, "Observation and investigation of $UO_2F_4^{2-}$ and its solvation complexes with water and acetone nitrile", ***Chem. Sci***. *3*, 1137−1146 (**2012**).

[3] F. Wei, G. Wu, W. H. E. Schwarz, J. Li, "Excited States and Absorption Spectra of UF_6: A RASPT2 Theoretical Study with Spin-Orbit Coupling", ***J. Chem. Theory Comp.*** *7*, 3223-3231 (**2011**).

[4] J. Su, Y.-L. Wang, F. Wei, W. H. E. Schwarz, J. Li, "Theoretical Study of the Luminescent States and Electronic Spectra of UO_2Cl_2 in an Argon Matrix", ***J. Chem. Theory Comp.*** *7*, 3293-3303 (**2011**).

[5] J. Su, K. Zhang, W. H. E. Schwarz, J. Li, "Uranyl-glycine-water complexes in solution: comprehensive computational modeling of coordination geometries, stabilization energies, and luminescence properties." ***Inorg. Chem.*** *50*, 2082-2093 (**2011**).

Flow electrolysis of actinide ions utilizing electrocatalysis

Yoshihiro Kitatsuji
Nuclear Science and Engineering Directorate, Japan Atomic Energy Agency

Abstract – Flow electrolysis enables the exhaustive redox reaction rapidly even the electrochemically irreversible reaction such as reduction of actinide (V) ions. The flow electrolysis cell with platinized glassy carbon fiber working electrode which acts as electrocatalyst is effective to decrease overpotentials of reduction of NpO_2^+ and PuO_2^+. A rapid and precise method for the preparation of U, Np and Pu ions of a desired oxidation state was proposed by taking advantage of the electrocatalytic reaction.

Keywords – platinized electrode, actinide ion, flow electrolysis, selective redox reaction

I. INTRODUCTION

Actinide ions (An) such as U, Np and Pu exist stably as trivalent to hexavalent ions in acidic and neutral solutions. Control of the oxidation state of these ions to a desired one and determine them are inevitable for the efficient chemical separation or the precise analyses of them, because chemical reactions such as liquid-liquid distribution and complex formation with ligands depend strongly on the oxidation state of the ions.

Electrode reactions of An^{4+}/An^{3+} and AnO_2^{2+}/AnO_2^+ couples are electrochemically reversible, and they have been well studied. On the other hand, those of An^{4+} and AnO_2^+ ions couples, which accompanying formation or cleavage of An-O bond, are generally electrochemically irreversible and required a large overpotential. For this reason, selective control of oxidation state of actinide ions by electrolysis is difficult.

Flow electrolysis can attain the exhaustive redox reduction even irreversible one, because electrolytes are electrolyzed repeatedly during the stay of the sample solution in the flow cell. It was reported that reduction of AnO_2^+ and oxidation of U^{4+} can be carried out rapidly when flow electrolysis was applied[1].

Catalytic reaction can decrease the overpotential as a result of facilitation of the charge transfer between the ion and the electrode. The author has studied redox mechanisms of actinide ions, and clarified that electrocatalytic reaction at Pt electrode can decrease overpotential of reduction of NpO_2^+ ion[2]. Based on these studies, platinized carbon fiber electrode as a working electrode of the flow electrolysis is expected to be a rapid and precise electrolytic method for controlling oxidation state of actinide ions.

II. EXPERIMENTAL

Flow electrolysis was performed by using the column electrode system with glassy carbon (GC) fiber working electrode. The GC fiber was packed tightly in a porous glass cylinder of 8 mm inner diameter and 50 mm long. The platinization of GC working electrode (abbreviated as Pt/GC-WE, hereafter) was carried out by electrodeposition of platinum black onto GC fiber from an aqueous H_2PtCl_6 solution.

Flow electrolysis was performed by passing a solution containing an actinide ion through narrow paths among GC fibers in the column electrode at a constant flow rate.

III. RESULTS AND DISCUSSION

Relations between current and potential for reductions of UO_2^{2+}, NpO_2^+ and PuO_2^{2+} in 1 M $HClO_4$ were investigated. Two-electron reduction of NpO_2^+ to Np^{3+} is occurred at -0.14 V when the ordinary GC-WE were employed. This reduction is explained by the catalytic reaction where Np^{4+}/Np^{3+} couple acts as an electron transfer mediator for NpO_2^+ reduction. So the potential observed for the NpO_2^+ reduction is close to that of Np^{4+} reduction. On the other hand, overpotential of NpO_2^+ reduction is mitigated by Pt/GC-WE electrode, and two-step reduction, i. e. the one-electron reduction of NpO_2^+ to Np^{4+} followed by that of Np^{4+} to Np^{3+}, proceeded at the Pt/GC-WE. The overpotential of reduction of PuO_2^+ is also decreased at Pt/GC-WE, but reduction of UO_2^{2+} to U^{4+} in 1 M $HClO_4$ was less affected by the electrode materials.

Based on the results of the flow electrolysis with Pt/GC-WE, the selective adjustment of the oxidation states of actinide ions can utilize. For example, when a solution containing Np ions of various oxidation states is electrolyzed at the potential in the ranges more positive than +1.1 V, from +0.2 to 0 V, and more negative than −0.26 V, the oxidation state of Np is adjusted to NpO_2^{2+}, Np^{4+} and Np^{3+}, respectively; when a solution containing U, Np and Pu ions is electrolyzed at the potential in the range between +0.20 and +0.15 V, U, Np and Pu ions of different oxidation states (i.e., UO_2^{2+}, Np^{4+} and Pu^{3+}) can be prepared[3].

REFERENCES

[1] H. Aoyagi, Y. Kitatsuji, Z. Yoshida, S. Kihara, Anal. Chim. Acta, 538(2005)283.
[2] Y. Kitatsuji, T. Kimura, S. Kihara, J. Electroanal. Chem., 641(2010)83.
[3] Y. Kitatsuji, T. Kimura, S. Kihara, Electrochim. Acta, 74(2012)215.

APSORC'13 - 5th Asia-Pacific Symposium on Radiochemistry
Kanazawa, Japan, 22-27 September 2013

Determination of the thermodynamic quantities of U(VI) complexation with "aliphatic" and "aromatic" di-carboxylic acids by calorimetry

Akira Kirishima and Nobuaki Sato
Institute of Multidisciplinary Research for Advanced Materials, Tohoku University,
2-1-1, Katahira, Aoba-ku, Sendai,980-8577, Japan

The thermodynamic quantities (ΔG, ΔH, ΔS) of complex formation of U(VI) with four "aliphatic" di-carboxylic acids, *i.e.*, glutalic acid (GA)[1], oxydiacetic acid (ODA), thiodiacetic acid (TDA), iminodiacetic acid (IDA), and four "aromatic" di-carboxylic acids, *i.e.*, isopthalic acid (IPA), 2,5-frandicarboxylic acid (FDA), 2,5-thiophenedicarboxylic acid (TDCA) and dipicolinic acid (DPA) were determined by the potentiometric titration and micro-calorimetric titration. So far, extensive data on stability constant have been obtained and summarized in databases for a variety of combinations of actinide ions and ligands, which plays important role as the basic parameters for the prediction of migration behavior of these elements in the geosphere, and for the development of new separation process. However, enthalpy and entropy data of actinide elements are scarce in comparison with stability constants. These data are demanded not only for the understanding of the reaction mechanism but also for the estimation of stability constants at elevated temperatures outside the range of 20 – 30 ^{o}C by the extrapolation from those at a room temperature with using thermodynamic models. Following our previous study reporting thermodynamic data (ΔG, ΔH, ΔS) of complexation of 8 di-carboxylates with U(VI) [1], this paper presents the thermodynamic quantities of U(VI) complexation with four "aliphatic" di-acetic acids and four "aromatic" di-acetic acids. Those ligands have a different center atom between two carboxylic groups, i.e., carbon for GA and IPA, oxygen for ODA and FDA, sulfur for TDA and TDCA, and nitrogen for IDA and DPA, which may coordinate with a metal cation. The obtained thermodynamic quantities are compared with each other for the discussion of the effect of structural difference *i.e.*, aliphatic- and aromatic structure and types of central atom in the ligands on the complex formation thermodynamics.

From the obtained thermodynamic quantities, it is indicated that these reactions are mainly driven by the entropy change while the enthalpy change is not promoting the progress of the reaction. The ΔG, ΔH and ΔS of 1:1 IDA complex show remarkable difference from those of GA complex, while those of ODA and TDA complex are almost equal to those of GA complex. The $-\Delta G$ of 1:1 IDA complex with U(VI) was 30 kJ/mol larger than that of GA complex, which is attributed to the chelate effect of the ligand. Our calorimetric measurement has revealed that this "chelate effect" should be ascribed to the "entropy effect" since $T\Delta S$ of IDA complex was 50 kJ/mol larger than that of GA complex.

[1] A. Kirishima, Y. Onishi, N. Sato and O. Tochiyama, *Radiochim. Acta* **96** (2008) 581–589.

Electrochemical Behavior of Americium in NaCl-2CsCl Melt

Hirokazu Hayashi[1], Mitsuo Akabori[1], Kazuo Minato[1,2]
[1]Nuclear Science and Engineering Directorate, Japan Atomic Energy Agency,
2-4 Shirakata-shirane, Tokai-mura, Naka-gun, Ibaraki-ken 319-1195, Japan
[2]Present address: Tokai Research and Development Center, Japan Atomic Energy Agency,
2-4 Shirakata-shirane, Tokai-mura, Naka-gun, Ibaraki-ken 319-1195, Japan

Abstract –The behavior of Am in NaCl-2CsCl melt was investigated by voltammetry, and potentiometry with an yttria-stabilized zirconia membrance electrode. Redox reactions of Am(III)/Am(II) and Am(II)/Am(0) were observed. Chemical reaction of Am^{3+} ions with O^{2-} ions in NaCl-2CsCl melt at 823K has been considered to make Am_2O_3 precipitates.

Keywords – Am, molten salt, electrochemistry

I. INTRODUCTION

For a basis of the future nuclear fuel cycle, it is very important to understand and control the behavior of TRU (Np, Pu, Am, Cm) in the nuclear fuel cycle. Experimental study of pyrochemical process of fuels containing TRU is one of the important topics. But, few data are available in literature on the behavior of TRU such as americium in NaCl-2CsCl melt which is considered to be used as one of the solvents for pyrochemical reprocessing. In the present study, the behavior of Am in NaCl-2CsCl melt was investigated by electrochemical methods.

II. EXPERIMENTAL

Anhydrous NaCl-2CsCl mixed salts (99.99%, Anderson Physical Laboratory Engineered Materials (APL)), cadmium chloride (99.9%, APL), and silver chloride (99.9%, APL) were used as purchased in this study. $AmCl_3$ was prepared by the solid-solid reaction of americium nitride and cadmium chloride [1]; $^{241}AmO_2$ sample prepared 35 years ago was used as a starting material. All the materials were handled in a glove box or a hot cell maintained with a purified argon gas atmosphere [2]. Typical impurities in the argon gas were H_2O < 1 ppm and O_2 < 1 ppm.

The sample in an alumina crucible was heated under an Ar gas flow after setting a cover of the furnace having the electrodes, and a stirrer made of Mo metal. Electrochemical measurements with 3 electrodes were carried out for $AmCl_3$-(NaCl-2CsCl) system with $X(AmCl_3)=4.0\times10^{-4}$ mainly at 823K using a PAR263A potensiostat/galvanostat with a CorrWare electrochemical software (Scribner Associates Inc.). The working electrode was a 1mmϕ tungsten wire. Assembled two tungsten wires (1mmϕ) were used as the counter electrode. The reference electrode was a silver wire (1mmϕ) dipped in the AgCl (X(AgCl)= 0.0487) - (NaCl-2CsCl) placed in a mulite tube. Potentiometric titration of Am^{3+} ion with O^{2-} ion using BaO (mixture of BaO and NaCl-2CsCl) was carried out at 823K. The values for pO^{2-} were monitored with a pO^{2-} indicator electrode made with yttria-stabilized zirconia filled with molten NaCl-2CsCl containing oxide ion and silver ion ($[O^{2-}]$=0.01mol/kg, $[Ag^{+}]$=0.37mol/kg) in which a silver wire was dipped. The electromotive forth (EMF) of the cell $Ag|NaCl\text{-}2CsCl\text{-}AgCl\text{-}O^{2-}|ZrO_2\text{-}Y_2O_3|NaCl\text{-}CsCl\text{-}AmCl_3\text{-}O^{2-}|Mulite|NaCl\text{-}2CsCl\text{-}AgCl|Ag$ was measured with an electrometer (Keithley Model6514). Temperatures of the molten salt sample were measured with R type thermocouple set in an alumina tube.

III. RESULTS AND DISCUSSION

A typical cyclic voltammogram shows 2 groups of signals close to the lower limit of the electrochemical window. The lower limit signals around –2.3V correspond to electrodeposition of alkaline metal. The higher limit signal around +1.0V corresponding to evolution of chlorine gas was also observed. The signals can be assigned to redox reactions of Am(III)/Am(II) and Am(II)/Am(0) comparing with those in LiCl-KCl eutectic melt [3].

The EMF values were measured during the additions of BaO from $\alpha = [O^{2-}]/[Am^{3+}]=0$ to 2.22. α is defined as the ratio of added oxide ion over the initial Am(III) ion. The titration curve shows only one equivalent point at $\alpha = 1.5$. This value corresponds to the formation of Am_2O_3 according to the reaction, $2Am^{3+}+3O^{2-}=Am_2O_3(s)$. The chemical form of the precipitation of plutonium in the molten salts has been reported as Pu_2O_3 [4, 5]. Our results indicate the similarity of the precipitation behavior of Am with that of Pu in molten salts.

ACKNOWLEDGMENTS

Part of the present study was carried out within the collaborative research program of TRU behavior in pyrochemical processes with Tohoku Electric Power Company, Tokyo Electric Power Company and The Japan Atomic Power Company.

REFERENCES

[1] H. Hayashi, M. Takano, M. Akabori, K. Minato, J. Alloys Compd. 456, 243-246 (2008).
[2] K. Minato, M. Akabori, T. Tsuboi, S. Kurobane, H. Hayashi, M. Takano, H. Otobe, M. Misumi, T. Sakamoto, I. Kato, T. Hida, JAERI-Tech 2005-059 (2005) (in Japanese).
[3] H. Hayashi, M. Akabori, K. Minato, Nucl. Technol., 162, 129-134 (2008).
[4] D. Lambertin, S. Ched'homme, G. Bourges, S. Sanchez, G. Picard, J. Nucl. Mater., 341, 124-130 (2005).
[5] C. Caravaca, A. Laplace, J. Vermeulen, J. Lacquement, J. Nucl. Mater., 377, 340-347 (2008).

RPO-03

Production of High Specific Activity Radiolanthanides for Medical Purposes using the UC Irvine TRIGA Reactor

Leila Safavi-Tehrani[1], George E. Miller[2] and Mikael Nilsson[1]
University of California, Irvine
[1]Department of Chemical Engineering & Materials Science
[2]Department of Chemistry
916 Engineering Tower, Irvine, CA 92697-2575
Lsafavit@uci.edu

Radioactive lanthanides have become an important imaging, diagnostic and therapeutic tool in the medical field. For example, the neutron rich samarium isotope of ^{153}Sm has been proven to have desirable characteristics for treatment of bone cancer. However, for medical purposes, the radioactive lanthanide isotope must be produced at high specific activity, i.e. low concentration of inactive carrier, so they are both beneficial for therapy and the concentration of the metal ions does not exceed the maximum sustainable by the human body. The objective of our research is to produce radioactive lanthanides with high specific activity in a small-scale research reactor using the Szilard-Chalmers method. The Szilard-Chalmers process is a method that separates radioactive ions away from a bulk of nonradioactive ions by neutron capture. We propose an innovative experiment setup to instantaneously separate the radioactive recoil product formed during irradiation from the bulk of non-radioactive ions. The instant separation prevents the recoiled radioactive nucleus from reforming its original bonds with the target matrix and chemically separates it from the non-radioactive target matrix, resulting in a carrier free radiolanthanide with increased specific activity. We will present methods for preparation and synthesis of the material used for irradiations and the results of enrichment factors and extraction yields in radioactive lanthanide solutions. We will also investigate degradation by ionizing radiation that occurs during neutron activation to determine the stability of the target material during irradiations. The obtained results will be compared to previously published methods and their corresponding results.

Mycoremediation: Fungus-based Soil Remediation of Radioisotope Contamination

Steven LaZar [1], Eric Rasmussen, MD, MDM, FACP [2], and Paul Stamets, D.Sc.[3]
[1]Managing Director and Department of Energy (DOE) Program Manager, MGI, Seattle, Washington
[2]Research Professor, Environmental Security and Global Medicine, San Diego State University, San Diego, California
[3]Chief Scientist, Fungi Perfecti Research Laboratories, Kamilche Point, Washington, USA

Abstract – Fungal mycelia in soil can hyperaccumulate radioisotopes at up to 25,000 Bq per kg of mushrooms [1]. Mycelium Group International (MGI) here introduces mycelial radioactive decontamination techniques (mycoremediation) that can potentially restore safe soil levels on Fukushima farmland in less than ten years with high efficiency, without loss of topsoil, and less expensively than current destructive methods.

Keywords – cesium, farmland, Fukushima, fungi, mycelium, remediation, topsoil

1. Introduction

Mycoremediation uses selected fungi to reduce contaminants in a step-function based on species and soil characteristics, weather and season parameters, harvest frequency, and contamination concentration.

The 2011 Fukushima nuclear disaster released more than 538,000 teraBecquerels (TBq) of radioactive Iodine-131, Cesium-134, and Cesium-137. As a result of that cesium deposition, the Japanese government has declared more than 1,300 square kilometers of northern Japan to be unsafe for human habitation and unsafe for food production. Conventional remediation is currently removing valuable farm topsoil at a rapid rate.

MGI has developed new capabilities for reducing radioactive Cesium-137 contamination in soil to achieve safety goals set by the IAEA, while retaining valuable topsoil and restoring safe farming decades earlier than anticipated. MGI's mycological research and industrial process designs are currently undergoing independent testing at two US Department of Energy Laboratories.

Our mycoremediation technique uses our unique strains of cultivated fungi to remove Cesium-137 by either biosorption or metabolism-dependent intracellular uptake. Our fungi start as microscopic spores that form spreading mycelial strands similar to a spider's web in topsoil, with measurements in some species of 300 square meters per meter of plant root [2]. The mycelia in the soil then concentrate the Cesium-137 in their strands as they form into mushrooms which are then harvested as radioactive waste. Since, in some fungal biochemistry, cesium mimics potassium - a necessary element in cellular metabolism - local cesium uptake can be rapid. Also, since mycelium are only a single cell thick and yet can comprise up to 45% of soil biomass in temperate zones [3], the calculated mycelial surface area available for cesium absorption is enormous.

Some hyper-accumulating fungal species can form mushrooms from mycelial mats every 60 days. Harvesting radioactive mushrooms therefore results in the removal of significant fractions of cesium contamination from topsoil multiple times each year. Our current research is showing that we can very likely use our mycoremediation techniques on radioactive farmland around Fukushima to meet IAEA safety standards in less than ten years while preserving topsoil critical to the restarting of a productive farm economy.

2. Mycoremediation Processes

MGI's mycoremediation processes include in-situ remediation, post-sort hot-pile remediation, and acid-leach resin column adsorption. The processes are safe, nearly silent, rapidly implemented, have low infrastructure requirements and can, in many cases, improve the soil to better than pre-contamination condition. The result is land again available for crop production earlier than anticipated, with far less volume for radioactive waste disposal, and at a cost that is substantially less than any other remediation process.

[1]Epik and Yprack, 2003
[2]Jones, 1991
[3]Stamets, 2005

APSORC'13 - 5th Asia-Pacific Symposium on Radiochemistry
Kanazawa, Japan, 22-27 September 2013

Automatic Cs-Uptake Device for Radioactive-Cs Evaluation in Environmental Water

Kimitaka Minami[1], Takayuki Funabashi[2], Ryuichi Kamimura[2], Tetsuo Yasutaka[1], Hisashi Tanaka[1], Akiko Kitajima[1], Hiroshi Ogawa[1], and Tohru Kawamoto[1]
[1]National Institute of Advanced Industrial Science and Technology (AIST)
[2]Tokyo Power Technology Ltd.

Abstract –We developed an automatic Cs-uptake device for concentrating the dilute radioactive cesium (r-Cs) in environmental water, especially paddy fields water. The device was set onto paddy fields and the r-Cs in more than 400 L of water in 24 hours was automatically concentrated in the small columns without external power supply. With this device, 0.01 Bq/L of r-Cs concentration can be evaluated by the r-Cs measurement of the columns.

Keywords – Prussian blue, radioactive cesium, environmental water, monitoring

I. INTRODUCTION

By the Fukushima Daiichi Nuclear Power Plant accident by the March 2011 Great East Japan Earthquake and subsequent tsunami, radioactive materials were released into the atmosphere and deposited over widespread agricultural, forest, and urban areas.

Now, radioactive materials, especially radioactive cesium (r-Cs), gradually migrate into environmental water and affect farm products even if these are low-level concentration. We have developed a monitoring method to investigate the low-level r-Cs concentration in environmental water by each existence form. Yasutaka et al. (2013) developed a method to adsorb 90% of dissolved r-Cs in 20 L water within 10 minutes using Prussian Blue (PB) impregnated nonwoven fabric. Tsuji et al. (2013) developed a cartridge filter which can concentrate up to 30 g of suspended solid in environmental water and more than 98% of suspended solid r-Cs in 20 L water was concentrated within 10 minutes. In this way, we can easily evaluate level of r-Cs in a short time by using germanium detector.

In this study, we developed another device for concentrating dilute r-Cs in environmental water, especially paddy fields water, as the average for a long time more than 1 day automatically without external power supply.

II. SETUP AND RESULTS

The developed device was shown in Fig 1. It includes pump, battery, cartridge filter, cesium adsorbed column with PB nanoparticles, and flow meter. The pump and the battery were chosen so that flow rate continually became 0.3 L/min for 24 hours. Suspended solid in environmental water was filtrated and concentrated by cartridge filter with large filtration area and 1 μm of pore-size. Dissolved Cs in the filtrate was adsorbed and concentrated onto PB. This PB column was developed for the structure that was measured by simple operation when it was measured by germanium detector. The device was designed so that less than 5 cm sank in order to use in the paddy with the very shallow water depth.

The r-Cs concentrations in a pond and paddy in Fukushima evaluated with the device were shown in Table 1. By passing more than 400 L of water through the device, around 0.01 Bq/L of dissolved r-Cs in paddy water can be evaluated in the 1,800 seconds measurement by the germanium semiconductor detector.

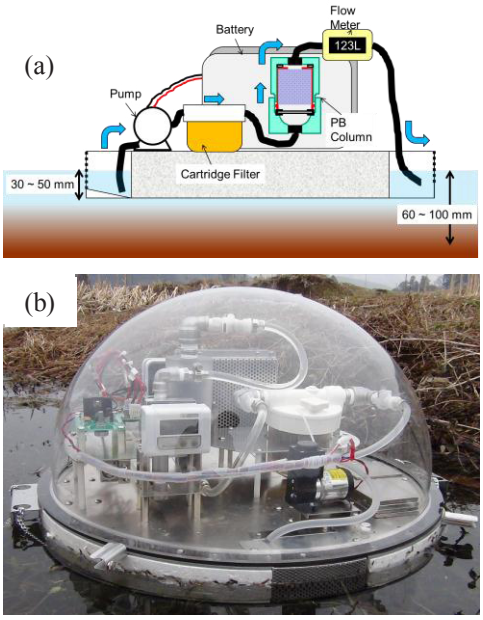

Fig 1. The automatic r-Cs uptake device (a) schematic view (b) appearance

Table 1. r-Cs Concentration in environmental water

Measuring Time of Ge 1,800 sec

Environmental Water	Flow Rate (L/min)	Pass Water (L)	Sample	r-Cs※ Concentration (Bq/L)	Counting Error (±Bq/L)	Detection Limit (Bq/L)
Paddy	0.3	419	SS Cartridge	0.068	0.0034	0.0036
			PB Column	0.014	0.0020	0.0031
Pond	0.3	348	SS Cartridge	0.042	0.0031	0.0047
			PB Column	0.049	0.0038	0.0037

※Cs^{134}+Cs^{137}

[1] Yasutaka et al.(2013), Appl. Chem. (in Japanese), in press
[2] Tuji et al. (2013), APSORC13

APSORC'13 - 5th Asia-Pacific Symposium on Radiochemistry
Kanazawa, Japan, 22-27 September 2013

Pilot plant for volume reduction of Cs-contaminated combustible materials

Kimitaka Minami[1], Hiroshi Ogawa[1], Hisashi Tanaka[1], Akira Takahashi[1], Tatsuya Uchida[1], Akiko Kitajima[1], Durga Parajuli[1], Tohru Kawamoto[1], Masaki Yamaguchi[2], Mitsuo Osada[2], Nobuaki Otake[2], Syuichi Sato[2], Ryuichi Kamimura[2], and Yukiya Hakuta [1]
[1]Nanosystem Research Institute, AIST, Japan
[2] Tokyo Power Technology Ltd., Japan

Abstract –We report the pilot plant test for volume reduction of radioactive-Cs (r-Cs)-contaminated combustible materials for the volume reduction of the contaminated waste, and to reduce the r-Cs leaching from the waste. the combustible wood is incinerated by the biomass boiler. The radioactive-Cs stored in ash is extracted into the water, and finally is captured into the Prussian blue-nanoparticle adsorbents.
Keywords – radioactive-Cs, Prussian blue, incineration, adsorbents

I. INTRODUCTION

Around Fukushima area, there are so much combustible materials contaminated by the radioactive Cs (r-Cs), e.g. the wood in forests, municipal waste, and waste from agriculture. Japan government showed the policy that the municipal waste with r-Cs contamination should be incinerated. In addition, the biomass power system with the incineration of the contaminated wood materials is also planned around Fukushima area.

There are problems in the management of the incineration of the combustible material. One is the large amount of the volume of ash and the other is the r-Cs leaching from the ash. In order to solve the problems, the extraction of leachable r-Cs from the ash as the pre-treatment before disposal is gathering attention. In order to confirm the method for the safety management based on the incineration and the r-Cs extraction from the ash, we carried out the plant-scale test.

II. METHOD AND RESUTS

The firewood was incinerated in a biomass boiler shown in Fig. 1(a). To avoid the emission of the r-Cs in the exhaust, the bag filter and HEPA filter is prepared. The r-Cs is trapped in ash mainly stored in the boiler and the bottom of the bag filter. In the next step, the r-Cs is extracted from the ash into the water in the ash-decontamination unit shown in Fig.1(b)[1]. Finally the r-Cs is captured by the adsorbents with Prussian blue nanoparticles shown in Fig.2.

When 465 kg of firewood was incinerated (r-Cs concentration ~ 0.3 kBq/kg), 1.35 kg of ash was obtained. The highest r-Cs concentration of was ~ 210 kBq/kg at the bag filter. The r-Cs in the exhaust in the incineration was undetectable. The r-Cs extraction ratio from the ash into water was 50-90%. The r-Cs in the water after the decontamination of the adsorbent was also undetectable.

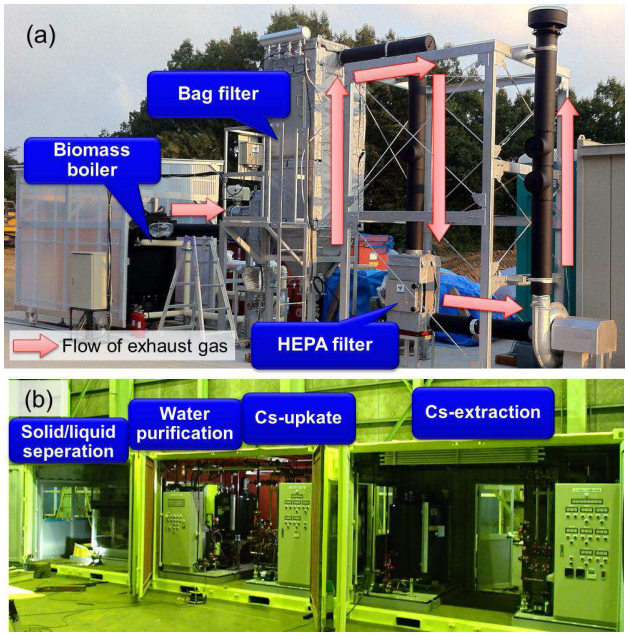

Fig. 1. for volume reduction of Cs-contaminated combustible materials. (a) biomass boiler with gas-filters for Cs-reduction from exhaust, (b) Ash-decontamination unit.

Fig. 2. Various Cs-adsorbents with Prussian blue nanoparticles

[1] D Parajuli et al., Env. Sci. Tech., *in press*.

APSORC'13 - 5th Asia-Pacific Symposium on Radiochemistry
Kanazawa, Japan, 22-27 September 2013

Decontamination of Radioactive Cesium from Ash and Soil

Durga Parajuli[1], Hisashi Tanaka[1], Shigeharu Fukuda[2], Ryuichi Kamimura[2], Tohru Kawamoto[1]
[1]Nanosystem Research Institute, AIST, [2]Tokyo Power Ltd., Japan

Abstract – Methods for the removal of Cesium from contaminated tsunami-debris, top-soil, and forest litter was studied. Incineration of tree bark resulted over 95% volume reduction. Fly ashes from wood, municipal garbage, and sewage sludge with enriched Cesium were washed with water at varying temperatures. Cesium along with other alkali metals was easily washed from the garbage ash and wood ash. But, only acid treatment at higher temperature could release Cesium from sewage sludge ash. Also, Cesium removal from soils with acid solutions was studied from 25 to 200 ºC. Though the release was higher at higher temperatures, results varied with the soil type.

Keywords – Radioactive Cesium, Extraction, Ash, Soil, Soil type

I. INTRODUCTION

Now two years after the Fukushima Daiichi Nuclear Power Plant disaster, the main problem is exposure to the radioactivity due to the long living radioisotopes of Cesium, ^{134}Cs (approx. 1.8 x 10^{16} Bq) and ^{137}Cs (approx. 1.5 x 10^{16} Bq).[1-3] So, we are conducting elaborated study to address the issues of Cs contaminated tsunami-debris, paddy field soil, forest litter and stream water so as to control the long term entry of the radioactive Cs to the ecosystem.

II. EXPERIMENTAL

Wood incineration ash, municipal garbage incineration ash, and sewage sludge ash were studied for Cs extraction. Also, soil samples collected from different areas in Fukushima prefecture were also tested for Cs removal. Ash samples were washed with water in flow or batch by varying ash-water ratio, temperature, etc. For comparison, dilute acid solutions were also studied. Acid solutions were tested for the extraction of Cs from clay containing substrates: sludge ash and soil.

III. RESULTS AND DISCUSSION

Incineration of contaminated waste and extraction of Cs

Incineration is the most suitable option for volume reduction and compaction of burnable wastes like tsunami debris, forest litter, plants, and household garbage. For this, incineration experiment taking the radioactive cesium contaminated tree bark was performed. When the volume was reduced to 5% of the initial mass, its fly ash showed 137 kBq/kg Cs-activity. Because the current Japanese Government's guideline allows landfill of wastes showing less than 8 kBq/kg, the disposal of enriched ash is problematic. Therefore, Cs-extraction study was performed taking ashes of tree-bark, household garbage, and municipal sewage sludge. Over 70% Cs-133 along with other alkali metals was easily washed with water from the garbage ash and wood ash. Figure 1 shows the change in the residual mass of the wood fly ash, Cs, and K in after washing with water in 1:10 ratio at different temperatures. The residual mass was 18-25% less, with higher drop at higher temperature. This result shows 70-80% dissolution of Cs and more than 90% K. These outcomes suggest the feasibility of compaction of the burnable waste by incineration followed by decontamination by washing with water.

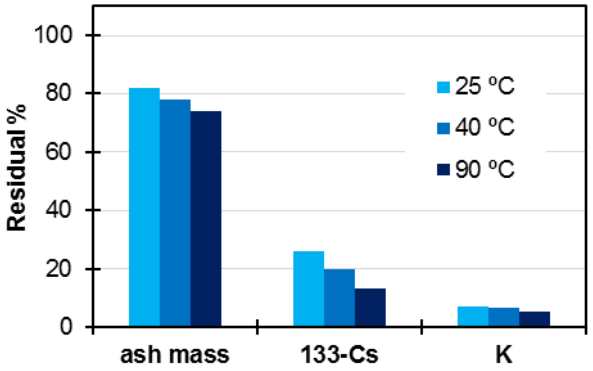

Figure 1. Change in residual mass of ash, Cs, and K with respect to the initial mass in the wood ash before and after washing with water.

Extraction of Cs from Soil and Sludge ash

Unlike the significant Cs removal observed with wood ash or garbage ash, the method was ineffective for the removal of Cs from soil and sewage sludge. So, a number of reagents were tested, and mineral acid solutions at higher temperature were found to be effective. However, the results varied widely depending upon the soil type. At 95 ºC with 0.5 M nitric acid solution, Cs removal from the brown forest soil was around 50%, however only 20% release was observed for Kuroboku-soil. Results to the date showed that Cs extraction from soils other than Kuroboku type is effective with acid at higher temperature.

References

[1] IAEA Radiological Assessment Report Series (2006)
[2] Y. Masumoto, et al. *Elements*, *8*, 207 (2012)
[3] R. Stone, *Science*, 331, 1507 (2011).

APSORC'13 - 5th Asia-Pacific Symposium on Radiochemistry
Kanazawa, Japan, 22-27 September 2013

Rapid radioanalytical determination of U, Pu, and Am in radioactive wastes via extraction chromatography, alpha spectrometry, and thermal ionization mass spectrometry

Tae-Hong Park, Yong Sul Choi, Jong-Ho Park, Jong-Yun Kim, Sang-Eun Bae, Young-Hwan Cho, Jei-Won Yeon, Kyuseok Song

Nuclear Chemistry Research Division, Korea Atomic Energy Research Institute,989-111 Daedeok-daero, Yuseong-gu, Daejeon, 305-353, Korea

Abstract

We optimize extraction chromatographic separation procedures to assay alpha particle emitting nuclides for disposal purpose of radioactive wastes generated from power plants and pyroprocessing laboratories. In particular, U isotopes are isolated on UTEVA resin, whereas Pu and Am/Cm isotopes are subsequently separated on TRU resin.

Keywords

Actinides, Extraction chromatography, Radioactive wastes

I. INTRODUCTION

Management of radioactive wastes requires sensitive and accurate radioanalytical determination procedures that include rapid and reliable chemical separation methods for a broad range of sample types, and radiometric evaluation tools [1]. Extraction chromatography has been successfully applied to separate the radionuclides of interest for a wide variety of environmental samples and thus many reliable procedures have been also developed with commercially available resin [2]. Here, we optimize rapid and reliable radiochemical determination of U, Pu, and Am/Cm isotopes via extraction chromatography, coprecipitation, alpha spectrometry, and isotope dilution-thermal ionization mass spectrometry (IDMS-TIMS) by which we estimate the alpha-emitting nuclide activities of low-level wastes generated from power plants and pyroprocessing laboratories.

II. EXPERIMENTAL

A radiochemical determination procedure of Pu, and Am/Cm nuclides is illustrated in Scheme 1.

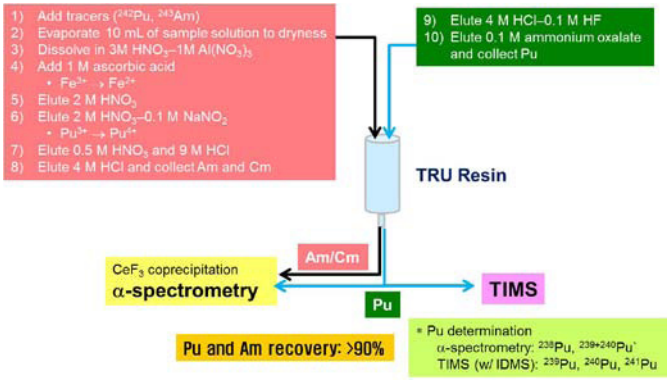

Scheme 1. Radiochemical determination of Pu and Am/Cm

III. RESULTS

The method in scheme 1 typically presented recovery yields of nuclides > 90% when a cocktail of ~0.1 Bq of ^{242}Pu, and ^{243}Am was separated on TRU resins. We also separated out Pu, Am, and Cm isotopes from low-level waste samples, and determined the nuclide activities via alpha spectrometric measurements of CeF_3 coprecipitating alpha-emitters and ID-TIMS especially for ^{239}Pu, ^{240}Pu, and ^{241}Pu.

IV. CONCULUSION

The methods developed in this report have shown good separation of U, Pu, and Am/Cm nuclides from radioactive wastes with high recovery yields. Because the isolated nuclides are determined by alpha spectrometry and ID-TIMS that can effectively quantify the nano- and picogram amounts of alpha emitters, the rapid and efficient chromatographic separation procedures in this report need marginal amounts of radioactive samples leading to reduction of chemical waste and radiation exposure.

[1] M. H. Lee, E. C. Jung, W. H. Kim, K. Y. Jee, J. Alloys Compd. 444-445 (2007) 544-549
[2] S. L. Maxwell III, B. K. Culligan, G. W. Noyes, J. Radioanal. Nucl. Chem. 286, (2010), 273-282

Luminescence Spectroscopy of Uranium Complexes in Non-Aqueous Media

Noboru Aoyagi[1*], Masayuki Watanabe[1], Akira Kirishima[2], Nobuaki Sato[2], Takaumi Kimura[1]
[1]Nuclear Scicence and Engineering Directorate, Japan Atomic Energy Agency,
Shirakatashirane 2-4, Tokai-mura Naka-gun, Ibaraki, 319-1195, Japan
[2]Institute of Multidisciplinary Research for Advanced Materials, Tohoku University,
1-1 Katahira, 2-chome, Aoba-ku, Sendai, 980-8577, Japan

Abstract – Syntheses and optical properties of tetravalent or hexavalent uranium compounds were studied to understand photo-physics under the unexplored condition such as in non-aqueous media or the cryogenic temperature. Uranium dioxide, halides or uranium metal were used as starting materials to yield the luminescent compounds in a series of organic solvents; the luminescence-solvent structure relationship was investigated using UV-Vis absorption and time-resolved laser-induced luminescence spectroscopies.

Keywords – Uranium(IV), (VI) complexes, Luminescence, Time-Resolved Laser-induced Fluorescence Spectroscopy (TRLFS)

Luminescence studies on uranium compounds have been mainly related to $U^{VI}O_2$ for the stability under ambient conditions and its high quantum yield of luminescence. In contrast, only a few studies on the luminescence properties of U^{4+} are known[1-3] due to the lack of information on the structure-spectrum relationship and its much less quantum yield. A fundamental study to further understand the optical property is indispensable and considered in two approaches; a molecular design to enhance the luminescence intensity using asymmetric complexes or ligand-to-metal energy transfer, or a spectroscopic method performed at cryogenic temperatures. Wang et al.[4] and our previous studies[5,6] report on the advantages in measuring luminescence of $U^{VI}O_2^{2+}$ at 77 K or below 77 K, however, such studies are uncommon. And thus we demonstrate a photophysical study on a series of uranium compounds designed to make luminescence intensity enhanced in order to elaborately obtain well-defined spectra in the present work.

A series of uranium sulfides, oxides, or halides such as US_2, UOS, UF_4, UCl_4, UBr_4, UI_4 were synthesized as starting materials via the reaction of uranium metal with halogen gasses at elevated temperature, and the resulting powder was characterized by XRD. In an Ar-operated glove box the powder were added into 1,4-dioxane, ethanol, tetrahydrofuran (THF), 1-methyl-THF, etc. The solution was put into non-luminescent cell. Under the irradiation of excitation UV-lamp at 302 nm, luminescence spectra are observed (Fig. 1) in time-gated ICCD camera.

Emission spectra of $[Li(THF)_4][UCl_5(THF)]$, **1** which forms a crystalline solid is first characterized and investigated by Baker[3], reporting three featureless bands observed in the UV and visible region centered at 365 nm, 421 nm, and 518 nm for the solution of **1** in THF with λ_{ex}= 260 to 390 nm as an excitation wavelength. While the present spectrum of UCl_4 in THF, **2** also exhibits the structureless bands with two peaks around 368 nm and 416 nm at room temperature, the third peak seen for **1** in THF was not observed. However, UCl_4 in dioxane, **3** provides more intense and featured spectrum having peaks at 349 nm, 378 nm, and 459 nm. Compared to **1** in THF, the remarkable blue shifts for all peaks appeared in **3**. This still seems a structureless band of U^{4+} ion, so that the spectral shape might be almost identical to that of $UCl_4(THF)_3$ in THF, except different peak values: 362 nm, 410 nm, and 500 nm. There was no peak of UCl_4 found in ethanol in which quenching of luminescence is taken place or the higher symmetrical structure could presumably provide the less probability in the f-f transitions. Further spectroscopic data such as TRLFS and low temperature measurements are to be discussed with regard to possible structures in solutions by digging into unexplored photoluminescence.

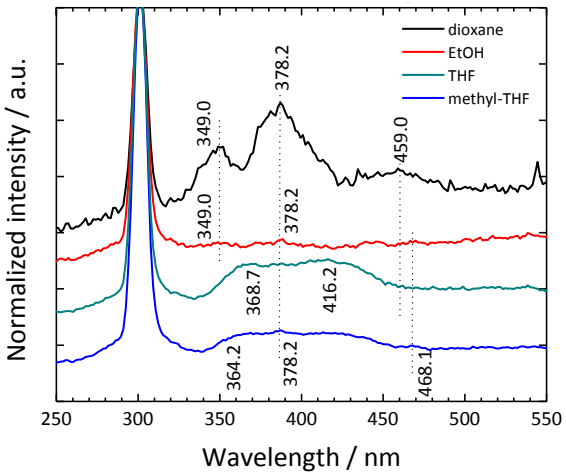

Fig. 1. Luminescence spectra of UCl_4 in organic solvents: λ_{ex} = 302 nm.

References

[1] A. Kirishima, T. Kimura, O. Tochiyama, Z. Yoshida, *Chem. Commun.* **2003**, 910.
[2] L. S. Natrajan, *Coord. Chem. Rev.* **2012**, 256, 1583-1603.
[3] E. Hashem, A. N. Swinburne, C. Schulzke, R. C. Evans, J. A. Platts, A. Kerridge, L. S. Natrajan, R. J. Baker, *RSC Advances*, **2013**, 3, 4350-4361.
[4] Z. Wang, J. M. Zachara, W. Yantasee, P. L. Gassman, C. Liu and A. G. Joly, *Environ. Sci. Technol.*, **2004**, 38, 5591-5597.
[5] R. N. Collins, T. Saito, N. Aoyagi, T.E. Payne, T. Kimura and T.D. Waite, *J. Environ. Qual.* **2011**, 40, 731-741.
[6] N. Aoyagi, K. Shimojo, N. R. Brooks, R. Nagaishi, H. Naganawa, K.V. Hecke, L.V. Meervelt, K. Binnemans and T. Kimura, *Chem. Commun.* **2011**, 47, 4490-4492.
[7] L. S. Natrajan, *Dalton Trans.*, **2012**, 41, 13167.

Chemical studies of Mo and W in preparation of a seabogrium (Sg) reduction experiment using MDG, FEC, and SISAK

A. Toyoshima[1], S. Miyashita[1], M. Asai[1], T. K. Sato[1], Y. Kaneya[1], K. Tsukada[1], Y. Kitatsuji[1], Y. Nagame[1], M. Schädel[1], H. V. Lerum[2], J. P. Omtvedt[2], Y. Oshimi,[3] K. Ooe[3], Y. Kitayama[4], A. Yokoyama[4], A. Wada[5], Y. Oura[5], H. Haba[6], J. Kanaya[6], M. Huang[6], Y. Komori[7], T. Yokokita[7], Y. Kasamatsu[7], A. Shinohara[7], V. Pershina[8], J. V. Kratz[9]

[1]Advanced Science Research Center, Japan Atomic Energy Agency, Tokai, Ibaraki 319-1195, Japan
[2]Department of Chemistry, University of Oslo, Oslo 0371, Norway
[3]Institute of Science and Technology, Niigata University, Niigata 950-2181, Japan
[4]College and Institute of Science and Engineering, Kanazawa University, Kanazawa 920-1192, Japan
[5]Graduate School of Science and Engineering, Tokyo Metropolitan University, Hachioji, Tokyo 192-0397, Japan
[6]Nishina Center for Accelerator-Based Science, RIKEN, Wako, Saitama 351-0198, Japan
[7]Graduate School of Science, Osaka University, Toyonaka, Osaka 560-0043, Japan
[8]GSI Helmholtzzentrum für Schwerionenforschung GmbH, D-64291 Darmstadt, Germany
[9]Institut für Kernchemie, Universität Mainz, 55128 Mainz, Germany

Abstract –We are developing a new chemistry assembly to perform continuous reduction experiments of seaborgium (element 106, Sg). In preparation for the Sg experiment, we have begun studies on the dissolution, reduction, and extraction of Mo and W isotopes. Our present status of the preparation with Mo and W will be presented.

Keywords – Superheavy elements, Seaborgium (Sg), Electrochemistry, Solvent extraction, Flow electrolytic column, SISAK, Membrane degasser

Seaborgium (Sg) is expected to be redox-active similarly to its lighter group-6 homologs, Mo and W. Theoretical calculation show that Sg can be reduced from the most stable hexavalent state Sg(VI) to, e.g., the tetravalent one [1]. They also predict that the Sg(VI)/Sg(IV) couple will have a more negative redox potential than those of the corresponding W ions in acidic solution [1]. In such reduction reactions, electrons occupy the vacant valence 6d orbital of the Sg(VI) ion. The redox potential of the Sg(IV)/Sg(VI) couple, therefore, provides information on the stability of the 6d orbital which is anticipated to be influenced by increasingly strong relativistic effects.

Because of low production rates of ^{265a,b}Sg (a and b stand for two different states) in the ^{248}Cm(^{22}Ne, 5*n*) reaction and their short half-lives of 8.5 and 1.4 s [2], only single atoms of Sg are present. This means that standard electrochemical techniques are not applicable to its reduction study. In our previous works, we have developed a novel electrochemical method of electrolytic column chromatography available for single ions [3]. Carbon fibers modified with Nafion perfluorinated cation-exchange resin were employed as a working electrode as well as a cation-exchanger. This technique was successfully applied to the oxidation of nobelium (No) [4] and the reduction of mendelevium (Md) [5]. It is, however, technically difficult to apply this batch-wise chromatographic method to the reduction study of Sg because of its very short half-lives. We are, therefore, developing a new chemistry assembly consisting of a membrane degasser (MDG), a flow electrolytic column (FEC), the continuous liquid-liquid extraction apparatus, and the liquid scintillation counting system (SISAK) [6] to continuously perform the dissolution, reduction, separation, and detection of Sg, respectively.

In preparation for our future experiment with Sg, we have begun studies on the dissolution, reduction, and extraction of Mo and W isotopes. On-line experiments using the newly developed MDG were carried out to examine the dissolution efficiency of nuclear reaction products transported by a gas-jet. The aqueous solution dissolving the reaction products was successfully separated from the carrier gas using the MDG after continuous mixing of the carrier gas with the aqueous solution. Electrolytic reduction of Mo and W was examined using a FEC. Redox couples of Mo(VI)/Mo(V) and W(VI)/W(V) in HCl have been so far characterized for macro amounts of Mo and W with cyclic voltammetry and UV/Vis. absorption spectrometry. Batch extractions of hexavalent ^{93m}Mo and ^{181}W were performed to search for suitable conditions in the separation between Sg(IV) and Sg(VI). Variations of extraction ratios of Mo(VI) and W(VI) between toluene containing hinokitiol (HT) and HCl were successfully observed as a function of HT and HCl concentrations. On-line extractions of short-lived ^{91m}Mo and ^{176}W were also carried out using SISAK and MDG. Extraction ratios of these elements were increased with increasing HT concentration, reflecting results of the batch experiments. In the symposium, our present status of the preparation with Mo and W will be presented.

[1] V. Pershina *et al*., J. Phys. Chem. A**103**, 8463 (1999).
[2] H. Haba et al., Phys. Rev. C**85**, 024611 (2012).
[3] A. Toyoshima et al., Radiochim. Acta **96**, 323 (2008).
[4] A. Toyoshima et al., J. Am. Chem. Soc. **126**, 9180 (2009).
[5] A. Toyoshima et al., to be submitted.
[6] For example, J. P. Omtvedt et al., Eur. Phys. J. D**45**, 91 (2007).

APSORC'13 - 5th Asia-Pacific Symposium on Radiochemistry
Kanazawa, Japan, 22-27 September 2013

Diamond Detectors for Isothermal Vacuum Chromatography

P. Steinegger[1,2], R. Dressler[1], R. Eichler[1,2], A. Türler[1,2]

[1] Paul Scherrer Institut, CH-5232 Villigen PSI, Switzerland
[2] University of Bern, CH-3012 Bern, Switzerland

Keywords: Superheavy elements, isothermal vacuum chromatography, diamond detectors.

I. INTRODUCTION

On-line thermochromatography is a well established gas phase experiment for the chemical characterization of the superheavy elements. However, recent experiments with state of the art detectors such as COLD [1] and COMPACT [2] are limited in terms of the upper bound of the applied temperature gradient. Therefore, the experimental characterization of less volatile elements with stronger adsorption interaction is not feasible. Already the rather volatile mercury with $-\Delta H_{ads}^{Au}$ (Hg) = 98 kJ/mol [3] - corresponding to a deposition temperature of about 430 K using the experimental conditions of the COLD system - reveals the constrained range of the currently used setups. Pushing the starting temperature of the gradient above the current limit, would open up a new range of elements accessible by on-line thermochromatography, including candidates like element 113.

A. Diamond Detectors

The upper limit of the temperature gradient however, evolves due to the maximum operation temperature of the currently applied Si PIN-diodes or Si PIPS-detectors respectively at around 315 K. Above this threshold, thermal excitation of the low band gap material (1.1 eV) prevents any spectroscopic measurement.

In recent years the development of chemical vapor deposition (CVD) single crystal diamonds made a considerable progress concerning the available size, quantity, and most importantly the quality. Diamond, as a large band gap material (5.5 eV), can be operated under IR and UV-Vis irradiation as well as at elevated temperatures even higher than 500 K without any spectroscopic degradation [4]. In addition, diamond has the largest known thermal conductivity, which is important for a reliable reconstruction of the surface temperature at vacuum conditions.

B. Experimental Section

In the course of the development of an isothermal vacuum chromatography setup for application in SHE chemistry experiments, we tested the new detector material with respect to the change of the spectroscopic behavior under heating and in first experiments with carrier-free ^{211}Pb, where the detector was successfully tested in the immediate vicinity of the isothermal oven held at temperatures up to T_{max} = 1193 K (see Fig. 1).

Acknowledgment: This project is supported by the Swiss National Foundation project number 200020_144511 / 1.

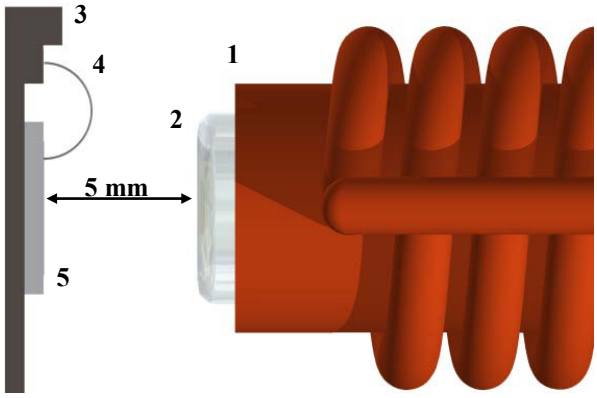

Fig. 1: Isothermal vacuum chromatography with carrier-free ^{211}Pb; **1** isothermal oven, **2** quartz column exit, **3** ceramic carrier, **4** wire bonds, **5** CVD diamond detector.

[1] R. Eichler et al., *Radiochim. Acta* **98(3)** (2010) 133
[2] J. Dvořák, *Ph.D. TU Munich* (2007)
[3] B. Eichler et al., *Radiochim. Acta* **33** (1983), 121
[4] J. H. Kaneko et al., *Nucl. Instr. and Meth. A* **422** (1999), 211

Angular distribution of projectile like fragments in $^{16}O+^{89}Y$ reaction

R. Tripathi[1], S. Sodaye[1], K. Mahata[2], P. K. Pujari[1]
[1]Radiochemistry Division, Bhabha Atomic Research Centre, Mumbai, India
[2]Nuclear Physics Division, Bhabha Atomic Research Centre, Mumbai, India

Abstract – Angular distribution of projectile like fragments have been measured in $^{16}O+^{89}Y$ reaction at E_{lab}=62 and 84 MeV. A systematic change in the angular distribution of PLFs was observed with increasing mass transfer indicating the evolution of reaction mechanism from quasi-elastic transfer to massive transfer or incomplete fusion. Elastic scattering measurements have been carried out to obtain grazing angle and total reaction cross section.

Keywords – Incomplete fusion, angular distribution

I. INTRODUCTION

Reactions involving incomplete mass transfer, namely direct and quasi-elastic transfer (QET), incomplete fusion (ICF) or massive transfer and deep inelastic collisions (DIC), have been an active area of investigation. Study of these reactions at beam energies below ~<10 MeV/nucleon has been actively investigated in the recent past [1-5] as existing theories and models [6-9] explain the observations of such reactions at higher beam energies. Measurement of angular distribution and cross sections data of PLFs (Z=3-7) in $^{19}F+^{66}Zn$ [3], ^{89}Y [4], ^{159}Tb [5] showed a systematic decrease of PLF cross sections with their decreasing Z. A comparison of PLF cross sections with those of respective evaporation residues gave information about the relative magnitude of cross section for total projectile break-up and break-up followed by the capture of one of the fragments [5]. As projectile structure plays an important role in these reactions [10,11], angular distributions of projectile like fragments (Z=3-7) have been measured in $^{16}O+^{89}Y$ reaction at E_{lab}=62 and 84 MeV corresponding to $E_{c.m.}/V_b$ value of 1.18 and 1.58 respectively. Elastic scattering measurements have been carried out at to determine the grazing angle and total reaction cross section.

II. EXPERIMENTAL DETAILS

Experiments were carried out at BARC-TIFR pelletron accelerator facility, Mumbai. Self-supporting metallic target of ^{89}Y was bombarded with ^{16}O beam and projectile like fragments were measured in the forward hemi-sphere using Si detector based E-ΔE telescopes. Telescope data were normalized for the target thickness and beam current using the data from a monitor detector kept at 20^0 with respect to the beam direction to obtain absolute cross sections.

III. RESULTS AND DISCUSSION

Lab Angular distribution of PLFs at E_{lab}=62 and 84 MeV, obtained from a preliminary data analysis is shown in Fig. 1 (a) and (b) respectively. It can be seen from Fig. 1(a), that the angular distribution of PLFs become more and more forward peaked with increasing mass transfer. This indicates the increasing overlap of the projectile and target nuclei with increasing mass transfer. This observation is consistent with our earlier measurements in ^{19}F induced reactions [3-5]. However, the comparable cross sections of C and N PLFs indicate the role of alpha cluster structure, leading to a large cross section for even Z C PLF. Also, ^{12}C yield was significantly larger than the other isotopes indicating the preferential break-up of the ^{16}O projectile into $^{12}C+^{4}He$. At higher beam energy, angular distributions of all the PLFs become forward peaked, suggesting the formation of even lighter PLFs in collision trajectories with deeper interpenetration. A qualitative comparison of angular distributions of PLFs at the two beam energies shows a larger decrease in the yields of lighter PLFs with decreasing beam energy. This is consistent with the picture that the formation of these PLFs involves substantial overlap of the projectile and the target nuclei, which was indicated by the sharp fall in the cross sections of lighter PLFs with decreasing beam energy [3,4].

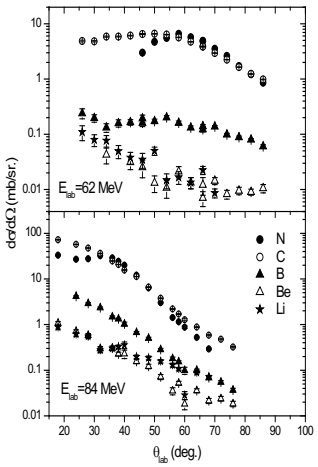

Fig. 1. Angular distribution of PLFs in $^{16}O+^{89}Y$ reaction

In the further analysis, angular distributions and kinetic energy spectra of PLFs would be analyzed in more detail. Integrated cross section data for PLFs would be compared with the incomplete fusion cross section data obtained from evaporation residue measurements [12] as well as those obtained in ^{19}F induced reactions.

REFERENCES

[1] Abhishek Yadav et al., Phys. Rev. C **85**, 064617 (2012).
[2] Rahbar Ali et al., J. Phys. G **37**, 115101 (2010).
[3] R. Tripathi et al., Phys. Rev. C **79**, 064604 (2009).
[4] R. Tripathiet al., J. of Physics. G. **35**, 025101 (2008).
[5] Amit Kumar et al., Eur. Phys. J A **49**, (2013).
[6] K. Siwek-Wilczynska et al.,Phys. Rev. Lett. **42**, 1599 (1979).
[7] T. Udagawa and T. Tamura, Phys. Rev. Lett. **45**, 1311 (1980).
[8] V. Zagrebaev and Yu. Penionzhkevich, Prog. Part. Nucl. Phys. **35**, 575 (1995).
[9] B.G. Harvey, Nucl. Phys. A **444**, 498 (1985).
[10] R. Tripathi et al., Eur. Phys. J. A **42**, 25 (2009).
[11] Chr. V. Christov, Z. Phys. A **325**, 221 (1986).
[12] B. S. Tomar et al., Z. Phys. A **343**, 223 (1992).

JNRS Award

Studies on Solution Chemistry of Actinides and Lanthanides by Time-resolved Laser-induced Fluorescence Spectroscopy

Takaumi Kimura
Nuclear Science and Engineering Directorate, Japan Atomic Energy Agency
Shirakata-shirane 2-4, Tokai-mura Naka-gun, Ibaraki, 319-1195, Japan

Abstract – Several topics on solution chemistry of actinides(An) and lanthanides(Ln) studied by time-resolved laser-induced fluorescence spectroscopy(TRLFS) will be mentioned in this presentation. Those are hydration studies of An(III) and Ln(III) and its applications, speciation study of U(VI), and luminescence of U(IV) in aqueous solution.

Keywords – Hydration, Speciation, Actinides, Lanthanides, Time-resolved Laser-induced Fluorescence Spectroscopy(TRLFS)

As a highly sensitive and selective speciation method, time-resolved laser-induced fluorescence spectroscopy (TRLFS) is a powerful tool to study luminescent actinides(An) and lanthanides(Ln) in solution, in solid and at their interface. We have started hydration study of Cm(III)[1] and speciation study of U(VI)[2] by TRLFS in the beginning of the nineteen-nineties.

A luminescence study of Cm(III) has shown a linear correlation between the reciprocal of the excited-state lifetime τ_{obs} and the number of water molecules N_{H2O} in the first coordination sphere of complexes. From measurements of τ_{obs} of Cm^{3+} in D_2O-H_2O solutions and of Cm(III) doped lanthanum compounds, the following correlation for τ_{obs}(ms) *vs.* N_{H2O} was established: $N_{H2O} = 0.65(1/\tau_{obs}) - 0.88$[1]. This relationship was applied to study the residual hydration of Cm(III) complexes of polyaminopolycarboxylate ligands and to determine the N_{H2O} of Cm(III) in various aqueous solutions. All of the N_{H2O} values calculated from the lifetime were chemically reasonable[3]. For Am(III) and several Ln(III)(Ln=Nd, Sm, Eu, Tb and Dy), the similar calibration relations were also proposed and the validity was confirmed through the study of a series of polyaminopolycarboxylate complexes[4-6]. The N_{H2O} of Ln(III) in concentrated aqueous salt solutions at room and liquid nitrogen temperatures was estimated on the basis of the correlation obtained at each temperature[7]. To understand the solvation of An(III) and Ln(III) in non-aqueous solutions, their τ_{obs} in perprotonated and perdeuterated solvents, i.e., DMSO, DMF, MeOH and water, were measured systematically and the quenching behavior of the ions in the solvents and the preferential solvation of them in water/non-aqueous solvent mixtures were evaluated[8,9].

The determination of the N_{H2O} by the measurement of τ_{obs} is a simple and effective method for the speciation study of An(III) and Ln(III). This method makes it possible to study chemical species at solid-water interface. TRLFS accelerated the speciation study on sorption behavior of Eu(III) and Cm(III) at mineral-water interface in the presence or absence of humic substances[10] and on the cell surfaces of microorganisms[11]. This also makes it possible to compare directly the coordination environment between An(III) and Ln(III) using same experimental technique. TRLFS improved the understanding of separation mechanisms of An(III) and Ln(III) using ion exchange resin[12] and solvent extraction[13].

Chemical species of U(VI) in 0.1 M $NaClO_4$ in equilibrium with 0.03 % CO_2 partial pressure were investigated by TRLFS[2]. The emission spectra of U(VI) solutions (pH = 3.8 to 7.0) in solid-liquid equilibrium with schoepite $UO_3 \cdot 2H_2O$ were interpreted by the summation of the emission spectra of the individual components, UO_2^{2+}(aq), $(UO_2)_2(OH)_2^{2+}$(aq), $(UO_2)_3(OH)_5^{+}$(aq) and UO_2CO_3(aq). Numerical evaluation of the species gave a satisfactory agreement with the distribution of the species calculated from the formation constants of U(VI). Furthermore, the speciation study of U(VI) by TRLFS with an optical cell system was extended to the hydrothermal conditions[14]. The results shows that TRLFS is an effective *in-situ* speciation method not only U(VI) hydrolysis but also for complexation at elevated temperatures(25-200 ^{o}C) and pressures(0.1-40 MPa).

U(IV) in aqueous solution has been considered to have no luminescence except for phosphate complex. From an analysis of transition energy level structure of U(IV), we found there was a possibility of U^{4+} exhibiting luminescence in aqueous solution and discovered the emission spectrum consisting of 12 bands in the range 280 to 560 nm[15]. Temperature dependence and isotope effect between H and D on the τ_{obs} suggest that water molecules in a bulk solution participates considerably in quenching process of the luminescence, which is quite different from the luminescence properties of An(III) and Ln(III).

REFERENCES

[1] T. Kimura, G.R. Choppin, J. Alloy Compd., **213/214**, 313-317 (1994).
[2] Y. Kato, G. Meinrath, et al., Radiochim. Acta, **64**, 107-111 (1994).
[3] T. Kimura, G.R. Choppin, et al., Radiochim. Acta, **72**, 61-64 (1996).
[4] T. Kimura, Y. Kato, J. Alloy Compd., **225**, 284-287 (1995).
[5] T. Kimura, Y. Kato, J. Alloy Compd., **271-273**, 867-871 (1998).
[6] T. Kimura, Y. Kato, J. Alloy Compd., **275-277**, 806-810 (1998).
[7] T. Kimura, Y. Kato, J. Alloy Compd., **278**, 92-97 (1998).
[8] T. Kimura, R. Nagaishi, et al., Radiochim. Acta, **89**, 125-130 (2001).
[9] T. Kimura, R. Nagaishi, et al., J. Alloy Compd., **323-324**, 164-168 (2001).
[10] Y. Takahashi, T. Kimura, et al., Geochim. Cosmochim. Acta, **66**, 1-12 (2002).
[11] T. Ozaki, T. Kimura, et al., Radiochim. Acta, **94**, 715-721 (2006).
[12] T. Kimura, Y. Kato, et al., J. Alloy Compd., **271-273**, 719-722 (1998).
[13] G. Tian, T. Kimura, et al., Radiochim. Acta, **92**, 495-499 (2004).
[14] T. Kimura, R. Nagaishi, et al., J. Nucl. Sci. Technol., **Suppl. 3**, 233-239 (2002).
[15] A. Kirishima, T. Kimura, et al., Radiochim. Acta, **92**, 705-710 (2004).

Oral Presentations

Thursday, 26 September 2013

Hall & Meeting Room, Kanazawa Bunka Hall

	Thursday, 26 September				
Time		Hall		Meeting Room	
09:00-09:10	9:00	PL-07	**Plenary**		
09:10-09:20					
09:20-09:30			S. B. Clark		
09:30-09:40	9:30	PL-08	**Plenary**		
09:40-09:50					
09:50-10:00			H. Ueno		
10:00-10:10	10:00	**Coffee Break**			
10:10-10:20					
10:20-10:30	10:20	NPI-01	**Invited**	EDI-01	**Invited**
10:30-10:40					
10:40-10:50			W. Sato		J. John
10:50-11:00	10:50	NPO-01	General	EDI-02	**Invited**
11:00-11:10			K. Nomura		
11:10-11:20	11:10	NPO-02	General		W.S. Wu
11:20-11:30			J. Wang	EDI-03	**Invited**
11:30-11:40	11:30	NPO-03	General		
11:40-11:50			M. Kaneko		A. Yokoyama
11:50-12:00	11:50	NPO-04	General	EDO-01	General
12:00-12:10			G. Yoshida		S. B. Sarmani
12:10-13:20	12:10	**Lunch Time**			
13:20-13:30	13:00	**Excursion (Shirakawa-go)**			
13:30-13:40					
13:40-13:50					
13:50-14:00					
14:00-14:10					
14:10-14:20					
14:20-14:30					
14:30-14:40					
14:40-14:50					
14:50-15:00					
15:00-15:10					
15:10-15:20					
15:20-15:30					
15:30-15:40					
15:40-15:50					
15:50-16:00					
16:00-16:10					
16:10-16:20					
16:20-16:30					
16:30-16:40					
16:40-16:50					
16:50-17:00					
17:00-17:10	17:00				
17:10-17:20					
17:20-17:30					
17:30-17:40					
17:40-17:50					
17:50-18:00					
18:00-18:10					
18:10-18:20					
18:20-18:30					
18:30-18:40					
18:40-18:50					
18:50-19:00					
19:00-19:20	19:00	**Banquet**			
19:20-19:40					
19:40-20:00					
20:00-					

Preparing the Next Generation of Radiochemists for Global Challenges

Sue B. Clark
Washington State University, Department of Chemistry, Pullman, WA 99164

Abstract – Nuclear and radiochemists are needed to support the expansion of nuclear energy, nuclear medicine, and environmental management. In this presentation, the changing needs for educating future generations of radiochemists are described. Consideration of the global nature of these market sectors is given, along with observations and recommendations for changes in academic curricula and training opportunities.

Keywords– nuclear chemistry, education, curriculum development

I. INTRODUCTION

Nuclear and radiochemistry is a sub-discipline within chemistry, and is referred to simply as radiochemistry in this presentation. These chemists study nuclear properties, nuclear reactions, and the chemical manipulation of radioactive substances for applications in physics, chemistry, biology, medicine, earth and space sciences [1]. The global radiochemistry workforce includes individuals employed in basic research and the allied fields of nuclear energy, nuclear medicine, defense, and the interface of these sectors with the environment. As nuclear energy and nuclear medicine grow world-wide, the need for a well-educated global workforce of critical thinkers is a challenge for many countries. In this presentation, the preparation of radiochemists for these future opportunities and challenges is discussed.

II. RADIOCHEMISTS IN ENERGY

Nuclear power plants provided more than 12% of the world's electricity production in 2011, generated by over 400 reactors in 30 countries worldwide, with a 70 new nuclear plants under construction in 14 countries [2]. The global nuclear power industry requires radiochemistry expertise to support (1) the operation of existing nuclear power plants and supporting facilities within a country's nuclear energy cycle, (2) the licensing and regulation of these facilities, and (3) research into future generations of nuclear energy facilities and approaches.

Chemists who work in these areas require expertise in areas such as nuclear reactions, radiation detection, radiation effects, separations, and chemical engineering, to name a few. As some countries move towards closing their fuel cycles and implementation of fusion energy technologies to transmute nuclear wastes while generating energy, developing unique expertise in the chemistry of materials and their corrosion in extreme, high radiation environments, and challenging chemical separations will be required. Anticipating these needs and altering university curricula to provide the necessary skills for those working in fusion energy will be important for advancing such new nuclear energy systems.

III. RADIOCHEMISTS IN MEDICINE

Nuclear medicine involves the use of radiopharmaceuticals for imaging to assess physiological processes, and to diagnose and treat diseases [3]. Future generations of radiochemists are needed for careers in academia, government laboratories, industry, and pharmacy. Academic radiopharmaceutical chemists typically provide the initial education and training, and the basic research that drives innovation in this technical area. Radiochemists working in government laboratories build upon the basic research foundation from academia to further develop radiopharmaceutical compounds. Industrial radiochemists synthesize radiopharmaceuticals, and conduct clinical trials of potential new pharmaceuticals. Nuclear pharmacists are the practitioners who prepare and sometimes administer the drugs, in collaboration with physicians. As the use of isotopes in the diagnosis and treatment of disease continues to expand, a global workforce of radiochemists who are also knowledgeable in biochemistry, molecular biology, synthetic chemistry and medicine are needed worldwide.

IV. RADIOCHEMISTS IN ENVIRONMENTAL MANAGEMENT

As with any industrial sector, nuclear energy and nuclear medicine both generate waste streams that require management for eventual disposal. Nuclear accidents and past radioactive waste management practices in countries that have used nuclear technologies for national defense and/or energy production have resulted in environmental legacies that require remediation. A new generation of radiochemists who are prepared to resolve such environmental legacies is needed. For example, as a result of the Fukushima accident in Japan, a new professional society of scientists was formed [4]. Developing strategies that meet international regulatory requirements relies on development of a pipeline of radiochemists who are also knowledgeable in disciplines such as environmental science and engineering, communications, sociology, and political science.

V. REFERENCES

[1] National Research Council, "Assuring a future US-based nuclear and radiochemistry expertise", 2012
[2] www.nei.org, accessed on30 May 2013
[3] www.snm.org, accessed on30 May 2013
[4] Society for Remediation of Radioactive Contamination in the Environment; http://www.uili.org/Cms/CmsArticlesReadOnly.aspx ?__item__=4077

Researches with stopped radioisotopes at the RIKEN RIBF facility

H. Ueno
RIKEN Nishina Center for Accelerator-Based Science, 2-1 Hirosawa, Wako, Saitama 351-0198, Japan

RIKEN has started the operation of the new facility for the Radioactive-Isotope Beam Factory (RIBF) project [1] since 2006. In this project, intense primary beams are delivered at the energy E/A = 350–440 MeV over the whole range of the atomic number utilizing newly constructed three cyclotrons, K = 700 fixed-frequency Ring Cyclotron (fRC), K = 980 Intermediate-Stage Ring Cyclotron (IRC), and K = 2500 Superconducting Ring Cyclotron (SRC) together with the existing K = 540 RIKEN Ring Cyclotron (RRC). Beams are delivered in the cyclotron cascade-acceleration scheme, in which AVF, RILAC, or RILAC2 is also included as an injector depending on the energy and the mass of a beam. The beam extracted from SRC is then transported to superconducting in-flight RI separator BigRIPS [2] in order produce radioactive-isotope beams (RIBs). BigRIPS is characterized by its large acceptance and two-stage scheme. The former is realized by the large aperture superconducting triplet Q-lens system, which enables BigRIPS efficiently to collect in-flight ^{238}U fission products. The latter is effective in the isotope separation and particle identification event-by-event basis. After the first beam was delivered on December 2006, the beam time for 1701 days, including 298 days for BigRIPS-based experiments, will be conducted until the end of September 2013. The beam current and the stability in beam delivery have been improved significantly by the improved performance of the 28-GHz ECR ion source and fRC, and the installation of a He-gas charge-stripping system [3], where the maximum beam currents 415, 100, 38, and 15 pnA, have been recorded for typical primary beams of BigRIPS-based experiments, ^{48}Ca, ^{70}Zn, ^{124}Xe, and ^{238}U, respectively [4].

In order to fully capitalize the RIBF facility, several experimental key devices have been installed downstream of the BigRIPS separator. Many nuclear-physics experiments are performed by means of the in-flight secondary nuclear reaction of radioactive-isotope beams (RIBs). For this purpose, a multi-function spectrometer for particle identifications (ZeroDegree [2]), a superconducting large acceptance and multi-particle detection spectrograph (SAMURAI [5]), and a high-resolution spectrograph under the scheme of the dispersion matching (SHARAQ [6]) were constructed following BigRIPS. In addition, the construction of the Rare-RI Ring [7], which is an isochronous storage ring to measure the mass of rare radioactive isotopes, is underway. Aiming at the first e-RI scattering experiments, the SCRIT [8] system is also under development.

Apart from the reaction-based approaches, nuclear-structure studies have also been conducted using stopped RIBs, where measurements are performed on the techniques of nuclear spectroscopy that take advantage of intrinsic nuclear properties. In particular, at the BigRIPS site, the EURICA (Euroball RIKEN Cluster Array) project [9] had been unfolded taking a high priority over the period of year and half since April 2012. In this program, structure of far unstable nuclei, which can be currently accessible only with the RIBF, have been investigated through the β-γ spectroscopy with the γ-ray detector array consisting of twelve high purity germanium cluster detectors from the Euroball IV array [10]. Combining the recently developed new method to produce spin-oriented RIBs [11], spin-related observables of RIs such as nuclear moments and spin parities will be measured in the stopped-RI type experiments. As for slowed-down and stopped RIBs, it should be noted that the construction of the SLOWRI system [12], which is a system to stop and extract the fast fragmentation RI by means of He and Ar gas catchers combined with the RF ion guide technique, has just started. The system is expected to provide a unique opportunity to investigate nuclear structure of RIs through atomic-physics techniques such as the laser spectroscopy.

Besides these BigRIPS-based experiments, which is categorized as the high-energy mode in RIBF, beams are also available in the low-energy mode whose acceleration scheme is AVF or RILAC (→RRC), where the accelerators in parentheses can be skipped in the cascade acceleration, depending on the beam used. RIBs are also available at E/A ~ 70 MeV in this mode with the former projectile-fragment separator RIPS [13]. Researches with stopped RIBs are actively conducted in the low-energy mode, in which an advanced usage of RIPS by changing the configuration of the beam-transport line has been proposed [14].

In the talk, after the overview of the RIBF facility, researches with stopped RIBs at BigRIPS and RIPS sites will be presented.

Reference

[1] Y. Yano, Nucl. Instrum. Methods Phys. Res. Sect. **B261**, 1009 (2007).
[2] T. Kubo, Nucl. Instrum. Methods Phys. Res. Sect. **B204**, 97 (2003).
[3] H. Okuno, N. Fukunishi, O. Kamigaito, Prog. Theor. Exp. Phys. (2012) 03C002.
[4] Technical information on the available beams are found at http://www.nishina.riken.jp/RIBF/
[5] K. Yoneda et al., RIKEN Accel. Prog. Rep. **43**, 178 (2010).
[6] T. Uesaka et al., Nucl. Instrum. Methods Phys. Res., Sect. B266, 4218 (2008).
[7] Y. Yamaguchi *et al*., Nucl. Instrum. Methods Phys. Res. Sect. **B266**, 4575 (2008).
[8] M. Wakasugi *et al*., Nucl. Instrum. Methods Phys. Res. Sect. **A532**, 216 (2004).
[9] S. Nishimura *et al*., RIKEN Accel. Prog. Rep. **45**, x (2012).
[10] M. Wilhelm *et al*., Nucl. Instrum. Meth. **A381**, 462 (1996).
[11] T. Ichikawa *et al*., Nature Phys. **8**, 918 (2012).
[12] M.Wada *et al*., Nucl. Instrum. Methods Phys. Res. Sect. **A532**, 40 (2004).
[13] T. Kubo et al., Nucl. Instrum. Methods Phys. Res. Sect. **B70**, 309 (1992).
[14] H. Ueno, Eur. Phys. J-Spec. Top. **162**, 221 (2008).

Local Structure at the In Impurity Site in ZnO Probed by the TDPAC Technique

W. Sato[1,2], S. Komatsuda[2], Y. Yamada[3], and Y. Ohkubo[4]
[1]Institute of Science and Engineering, Kanazawa University, Kanazawa, Ishikawa 920-1192, Japan
[2]Graduate School of Natural Science and Technology, Kanazawa University, Kanazawa, Ishikawa 920-1192, Japan
[3]Department of Chemistry, Tokyo University of Science, Shinjuku-ku, Tokyo 162-8602, Japan
[4]Research Reactor Institute, Kyoto University, Kumatori, Osaka 590-0494, Japan

Abstract – Local structures produced in 0.5 at.% In-doped ZnO were investigated by means of the time-differential perturbed angular correlation method using the ^{111}Cd probes generated in the disintegration of different parents, ^{111}In and ^{111m}Cd. From distinct perturbation patterns, it was ascertained that the doped In atoms locally form a unique structure dispersed in ZnO matrix without forming macroscopic agglomerates of their own. The microscopically associated structure of In atoms is discussed based on the hyperfine parameters at the probes in comparison with those for other metal oxide compounds.

Keywords – Zinc Oxide, Perturbed Angular Correlations, Indium, Impurity, Local Structure

I. INTRODUCTION

Zinc oxide (ZnO) is an intrinsic *n*-type semiconductor having optoelectronic properties, and its wider industrial application as functional devices has been highly expected. For the control of the *n*-type conductivity, it is of importance to understand the state of being of impurities on an atomic scale.

From this point of view, we have studied the local fields at the impurity sites in ZnO doped with group 13 elements (Al[1], Ga[2], In[3]) by means of the time-differential perturbed angular correlation (TDPAC) method using the ^{111}Cd(← ^{111}In) probe. Among these impurity doped samples, the TDPAC spectrum for 0.5 at.% In-doped ZnO exhibits a single high-frequency component reflecting a characteristic local structure surrounding the probe, which is distinct from the one appearing in the spectrum for undoped ZnO[3]. In addition to the structural uniqueness, we found that this component is thermally stable in ZnO matrix. In the present paper, the characteristic local structure formed in the In-doped ZnO is discussed.

II. EXPERIMENTS

For the production of 0.5 at.% In-doped ZnO, a conventional solid state reaction was applied to a mixture of stoichiometric amounts of ZnO and $In(NO_3)_3 \cdot 3H_2O$[3]. Two different parents of the ^{111}Cd probe were then introduced to the synthesized samples as impurities: droplets of ^{111}In HCl solution were added onto a disk of the In-doped ZnO, and it was heated in air at 1373 K for 2 h for diffusion of the probe[3]; ^{111m}Cd prepared by thermal neutron irradiation of enriched ^{110}CdO was doped into the In-doped ZnO by heat treatment[4]. TDPAC measurements were performed for both of the heat-treated samples using the same probe descended from different parents: ^{111}Cd(←^{111}In) and ^{111}Cd(←^{111m}Cd).

III. RESULTS

The TDPAC spectrum of ^{111}Cd(←^{111}In) in 0.5 at.% In-doped ZnO is shown in Fig. 1(a). One can see a characteristic pattern in the spectrum. This signifies that the doped In ion(s) produces a greater electric field gradient at the ^{111}Cd(←^{111}In) probe compared with the case for undoped ZnO[3]; that is, nonradioactive In ion(s) is adjacent to the probe, forming a certain association in the host.

Figures 1(b) and 1(c) show the TDPAC spectra of ^{111}Cd(←^{111m}Cd) in undoped and 0.5 at.% In-doped ZnO, respectively. (Note that 5 at.% Cd is inevitably introduced in the system when the probe as in ^{110}CdO is doped.) As is evident from the quadrupole frequency in Fig. 1(b), the ^{111}Cd(←^{111m}Cd) probe resides at the substitutional Zn site. For 0.5 at.% In-doped ZnO in Fig. 1(c), a spectral damping is observed; this trend becomes more pronounced with increasing concentration of In dopants[4]. These observations reveal the fact that a large number of microscopic local associations of a specific In compound are widely dispersed in ZnO matrix. In order to identify the compound formed in ZnO, we are now working on comparative studies about metal oxides comprised of Cd and In in expectation of their synthesis in ZnO matrix.

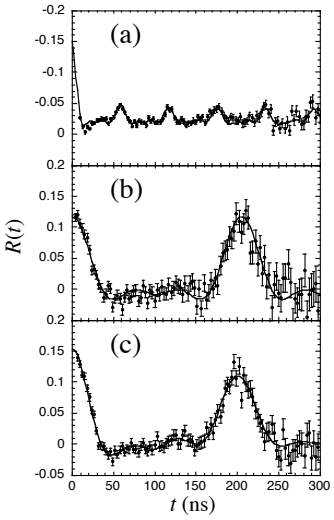

Fig. 1. TDPAC spectra of ^{111}Cd measured at room temperature: (a) ^{111}Cd(←^{111}In) in 0.5 at.% In-doped ZnO, (b) ^{111}Cd(←^{111m}Cd) in undoped ZnO, and (c) ^{111}Cd(←^{111m}Cd) in 0.5 at.% In-doped ZnO.

[1] S. Komatsuda et al. J. Phys. Soc. Jpn. 80, 095001 (2011).
[2] W. Sato et al. Proc. Radiochim. Acta 1, 435 (2011).
[3] W. Sato et al. Phys. Rev. B 78, 045319 (2008).
[4] W. Sato et al. Phys. Rev. B 86, 235209 (2012).

Mössbauer Analysis of Iron Ore and Rapidly Reduced Iron Ore by Micro-Discharge

Kiyoshi Nomura[1], Paulo de Souza[2], and Shoji Hirai[3], Norimichi Kojima[1]

1) Graduate School of Art and Science, The University of Tokyo, Komaba 3-8-1, Meguro-ku, 153-8902, Japan

2) University of Tasmania, Australia, 3) Tokyo Toshi University, Japan

Abstract

Several samples of iron ore were analyzed by Mössbauer spectrometry. Almost all iron ores are composed of hematite, goethite, and fine grains of oxides, of which the ratios are different among production area. The amount of hematite, magnetite and geothite are consistent with those obtained by conventional chemical analysis. MD method is proven to be efficient in rapidly reducing iron ores.

I. INTRODUCTION

Iron ore contains several kinds of iron oxides such as Hematite (α-Fe_2O_3), and Magnetite (Fe_3O_4), and iron oxy-hydroxides such as Goethite (α-FeOOH), and Lepidocrocite (γ-FeOOH). A chemical analysis is generally used for determining chemical composition of iron ore [1]. On a number of different ores, we compared qualitative and quantitative results obtained by Mossbauer spectrometry with those by chemical analysis. Further, we tried to perform the rapid reduction of iron ore by using micro discharge (MD) using carbon felt (CF) for shirt time [2].

II. EXPERIMENT

Using five ore samples (A and B from Brazil, C, E and M from Australia) and a reference Japanese standard sample (JSS805), the content ratios of Fe_2O_3, FeOOH, and Fe_3O_4 were determined by Japanese Industrial Standard (JIS) method. The content ratios of Fe_2O_3, FeOOH, and Fe_3O_4 obtained are as follows: sample A (91.7%, 2.8% 0.4%), sample B (85.4%, 10.2%, 0.2%), sample C (78.6%, 23.7%, 63.3%), sample E (23.7%, 63.7%, 0.2%), sample M (63.3%, 29.3%, 1.1%)[1)].

Mössbauer spectra of the same samples were measured at room temperature by using ^{57}Co(Cr) source.

III. RESULT AND DISCUSSION

Results by Mössbauer spectra

Mössbauer spectra of Australian iron ores (C, E, and M) are shown in Fig. 1. A outer sextet with a large magnetic field (B_{hf} =51.5T, IS= 0.37mm/s, QS(2ε)= -0.20 mm/s) is assigned to α–Fe_2O_3, and the inner sextet with a small magnetic field (B_{hf} = 37T, IS = 0.37mm/s, QS(2ε) = 0.30mm/s) is to α–FeOOH. The Mössbauer spectrum of sample E show the broaden sextet due to α–Fe_2O_3 and paramagnetic peaks in addition to the more broaden sextet peaks of α–FeOOH due to fine grains of iron ore or isomorphic substitution of Fe^{3+} by Al^{3+}. The amounts of α–Fe_2O_3 and α–FeOOH were consistent with the results by chemical analysis.

Reduction treatment of iron ore by micro-discharge (MD) using carbon felt (CF)[2)]

A sample can be heated up to 1000°C by MD/CF for about 100 seconds. Mössbauer spectrum of sample M, treated in alumina crucible by MD/CF with 500 W for 2 min, is shown in Fig. 2. Two sextets and two doublets were additionally observed in the Mössbauer spectrum. The Mössbauer parameters indicate that the two sextets come from the Fe^{2+} and Fe^{3+} species occupied in octahedral (site B) and Fe^{3+} in tetrahedral (site A) sites of inverse-spinel, magnetite. Two doublets with small and large QS values were observed. The former is due to Fe^{2+} species as wüstite (FeO). The latter doublet with large QS is considered due to formation of siderite ($FeCO_3$) although the QS value is larger than expected for this mineral. The large QS may be a result of the dispersion in oxide matrix. Unquestionably the micro-discharge method produces a noticeable fast reduction of all treated ores.

1) M. Yasutaka, S. Hirai, Japanese J. Iron and Steel, 97 (2011) 70,

2) H. Kurihara, T. Yajima, K. Nomura, J. of Powder Metallurgy Association, 56 (2009) 116.

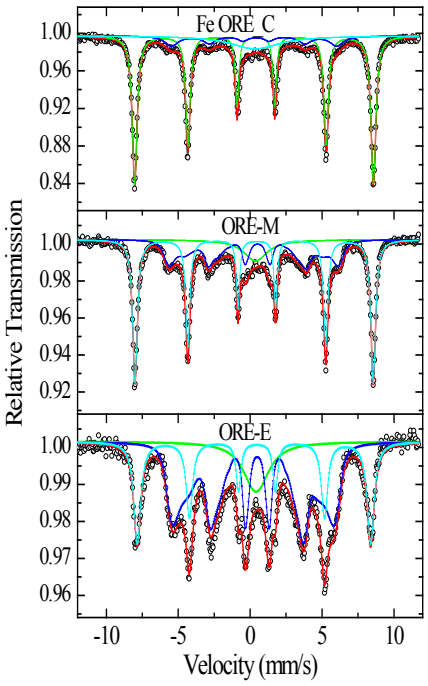

Fig.1 MS spectra of Austrian iron ore.

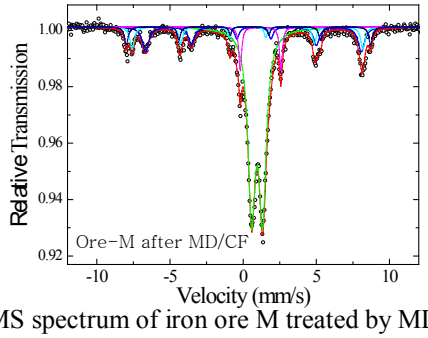

Fig.2 MS spectrum of iron ore M treated by MD/CF.

APSORC'13 - 5th Asia-Pacific Symposium on Radiochemistry
Kanazawa, Japan, 22-27 September 2013

Three Ways to Fix Cs in Prussian Blues

Junhu WANG[1], Alexandre I. RYKOV[1],
and Kiyoshi NOMURA[2]
[1]Mössbauer Effect Data Center, Dalian Institute of Chemical Physics, CAS, Dalian 116023, China
[2]School of Engineering, The University of Tokyo, Hongo 7-3-1, Bunkyo-ku 113-8656, Japan

Prussian Blue (PB) and its analogues have a very high capacity for incorporation, or sorption, of various alkali ions. Among all the alkali elements in PB Cs is absorbed most firmly. The mobility of alkali ions in channels of the hexacyanometalate structure drops dramatically with increasing the alkali ionic radius. We have explored three routes towards fixation of Cs in the solid phases of the PB analogues. Our sorption experiments showed that the insoluble hexacyanocobaltates are rather slow sorbents, however, our newly synthesized soluble PB analogues are having much larger sorption capacity accessible at short times.

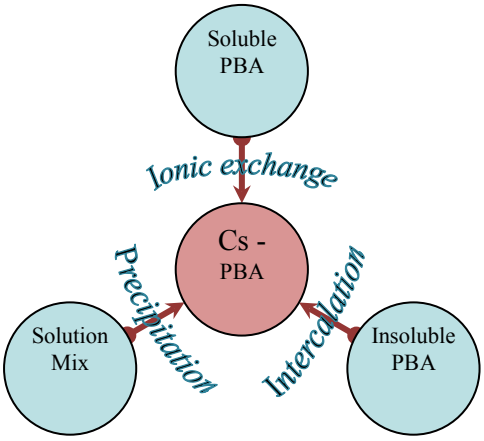

Fig 1. Explored routes of Cs fixation in PB.

The sorption rate is the crucial functionality parameter of a sorbent for sorption of the radioactive isotopes. This is because in a realistic radioactive contaminated environment the PB sorbent attains too much activity well before the saturation in Cs. Therefore, it is vital to compare the rates for known ways of the synthesis of a target cyanometallate $CsFe[Co(CN)_6]$ in Fig.1.

Measuring the Mössbauer spectra of the sorbents allows to understand the changes in local surrounding of the Fe^{2+} ions [1]. In Fig. 2, we show that the ionic charge of Fe^{2+} becomes distributed more isotropically with increasing Cs content. The latter is controlled by the Rietveld analysis of x-ray diffraction patterns.

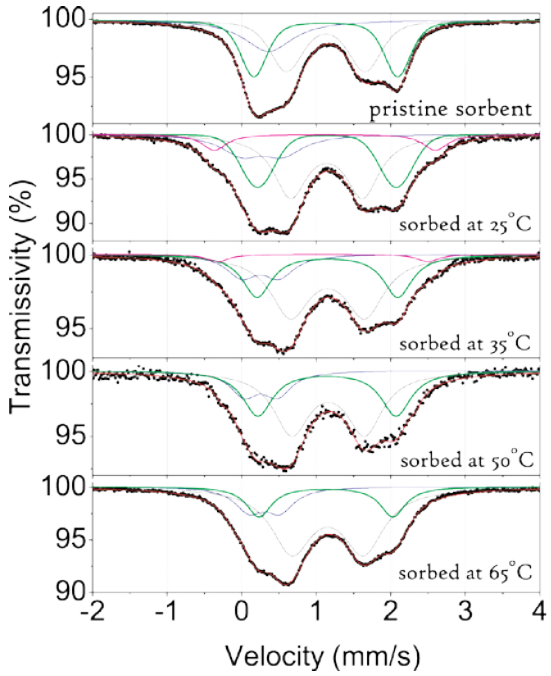

Fig.2. Mössbauer spectra of the insoluble pristine sorbent

$Fe_3[Co(CN)_6]_2 \cdot xH_2O$ and the products of its reaction after soaking in solutions containing the Cs ion. The aliquotes of 35 mg of the sorbent were stirred in a beaker with 25 mL of 0.1 M solution of CsCl for 40 h at the temperatures of 20 °C, 35 °C, 50 °C and 65 °C. Inner doblet (lower EFG owing to smaller charge anisotropy) is increasing with Cs content from top to bottom.

This work was supported by the Chinese Academy of Sciences Visiting Professorships for Senior International Scientists. Grant No. 2011T1G15. Financial support obtained from the Chinese Academy of Sciences for "100 Talents" Project, the National Natural Science Foundation of China (No. 11079036) and the Natural Science Foundation of Liaoning Province (No. 20092173) is also greatly acknowledged.

[1] A.I. Rykov, J. Wang, T. Zhang and K. Nomura, Hyperfine Interact. DOI 10.1007/s10751-012-0705-5.

Theoretical study on Mössbauer parameters of iron assembled complexes

KANEKO Masashi[1], DOTE Haruka[1], NAKASHIMA Satoru[2]
[1]Graduate School of Science, Hiroshima University
[2]Natural Science Center for Basic Research and Development (N-BARD), Hiroshima University

Abstract – The calculation of ^{57}Fe Mössbauer parameters (δ_{Fe}, ΔE_Q) using density functional theory to 20 benchmark complexes was performed and showed a good correlation with experiment values. And the calculation to the mononuclear model of iron assembled complexes was also performed. The result of isomer shift was in good agreement with experiment, while that of quadrupole splitting did not show a good correlation with experiment.

Keywords – ^{57}Fe Mössbauer spectroscopy, density functional theory, iron assembled complex

I. INTRODUCTION

Assembled complexes with transition metal ion as a center metal can show various structures and properties. And assembled iron(II) complexes bridged by bipyridine-type ligands (L) $[Fe(NCX)_2(L)_2]_n$ (X = S, Se, BH_3; L = 1,2-bis(4-pyridyl)ethane (bpa), 1,3-bis(4-pyridyl)propane (bpp)) showed a stereospecific structure depending on the conformer of L[1][2]. Furthermore, in these system, the quadrupole splitting values obtained by ^{57}Fe Mössbauer spectroscopy experiment showed a drastic change depending on anions, which were NCX^-, in spite of isomorphous structures[1][2].

Then we can easily perform the molecular orbital calculation including transition metals using density functional theory (DFT) thanks to the progress of arithmetic capacity. And benchmark studies of Mössbauer parameters (δ_{Fe}, ΔE_Q) on mononuclear complexes which possess noncubic electric field gradient show a good correlation between experiment and calculation value[3].

In the present study, we report the electronic states of assembled systems using DFT to reveal the quadrupole interaction by changing anions.

II. COMPUTATION DETAILS

All DFT calculations were performed using the ORCA software package. The spin-unrestricted Kohn-Sham method has been used for iron(II) high-spin octahedral system. In the present study, we have used the simple cluster model $[Fe(NCX)_2(pyridine)_4]$ referenced by single crystal X-ray analyses to 1D chain structures of bpa and bpp complexes. Single-point energies were calculated by using a B3LYP functional. CP(PPP) for Fe and TZVP for other atoms were assigned to basis functions. Isomer shift was calculated by fitting experiment δ_{Fe} with calculated ρ_0, which is the electron density at Fe nucleus, using benchmark study. ^{57}Fe quadrupole splittings were calculated using electric field gradient tensor (V_{ii}) and asymmetry parameter (η) obtained by DFT calculation.

III. RESULTS AND DISCUSSION

As shown in Figs.1 and 2, calculated δ_{Fe} and ΔE_Q were strongly correlated with experiment values. The correlation coefficients of δ_{Fe} and ΔE_Q were 0.99 and 0.98 respectively.

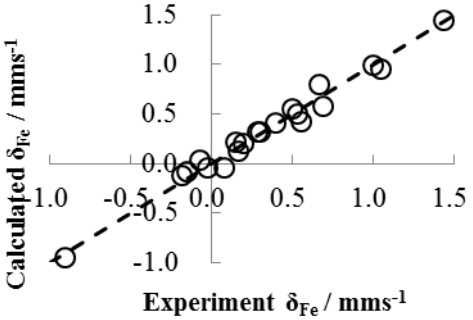

Fig.1 The correlation of δ_{Fe} between calculation and experiment.

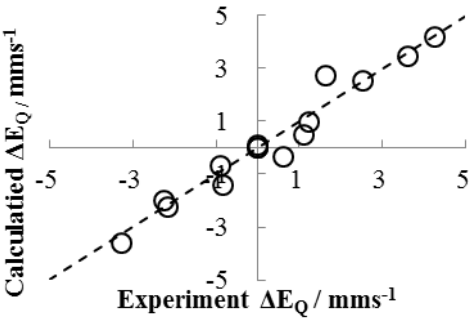

Fig.2 The correlation of ΔE_Q between calculation and experiment.

And the result of mononuclear models referenced by iron assembled complexes was shown in Tbl.1. Calculated δ_{Fe} values were in good agreement with experiment while calculated ΔE_Q values did not correlate with experiment. These results suggest the effect of assembly and these reasons are under study.

Tbl.1 Mössbauer parameters of pyridine model referenced by $[Fe(NCX)_2(L)_2]$ (unit in mm s^{-1}).

L	X	δ_{Fe}^{exp}	δ_{Fe}^{calc}	$\lvert\Delta E_Q^{exp}\rvert$	ΔE_Q^{calc}
bpa	S	1.18	1.03	2.17	3.12
bpa	Se	1.18	1.03	0.74	3.32
bpa	BH_3	1.19	1.03	1.51	3.94
bpp	S	1.20	1.03	2.19	2.96
bpp	Se	1.19	1.02	1.24	3.07
bpp	BH_3	1.19	1.00	1.71	3.27

[1] T. Morita, *et al.*, *Bull. Chem. Soc. Jpn.*, 79, 738 (**2006**).
[2] M. Atsuchi, *et al.*, *Inorg. Chim. Acta*, 370, 82 (**2011**).
[3] F. Neese, *et al.*, *Inorg. Chem.*, 44, 2245 (**2005**).

Study on muon capture process for gaseous molecules containing C and O atoms

G. Yoshida[1], K. Ninomiya[1], M. Inagaki[1], T.U. Ito[2], W. Higemoto[2], T. Nagatomo[3], P. Strasser[3], N. Kawamura[3], K. Shimomura[3], Y. Miyake[3], T. Miura[4], M.K. Kubo[5], and A. Shinohara[1]

[1]Graduate School of Science, Osaka University
[2]Advansed Science Research Center, Japan Atomic Energy Agency
[3]Institute of Materials Structure Science, High Energy Accelerator Research Organization (KEK)
[4]Radiation Science Center, High Energy Accelerator Research Organization (KEK)
[5]Colleage of Liberal Arts, International Christianity University

Abstract –Muonic atom is an atomic system which has a negative muon substituted an electron. When a muon is stopped in a substance, a muonic atom is formed. It is known that muonic atom formation processes are influenced by the chemical environment of muon capturing atom such as molecular structure (chemical effect). However chemical effects still have not been well investigated. In this study, we performed muon irradiation for CO, CO_2 and COS molecules, and measured muonic X-rays precisely to investigate the chemical effect on muon capture processes.
Keywords – muon, muonic atom, exotic atom, muon capture

I. INTRODUCTION

A negative muon is one of the elementary particles (lepton) that has charge and approximately two hundred times heavier mass than that of an electron. When a muon is stopped in a substance, a muonic atom is formed. It is know that muon capture processes are strongly influenced by the structure of the muon capturing molecule; the muon capture probability of each atom (muon capture ratios) and the initial quantum state (*n*; principal quantum number and *l*; angular momentum quantum number) of the captured muon are changed drastically. For example muon capture probability ratio of boron atom to nitrogen atom for cubic structure boron nitride is 20% smaller than that of hexagonal structure [1]. This is called chemical effect.

To reveal the chemical effect on muonic atom formation processes, we previously performed muon irradiations for simple gaseous molecules containing nitrogen and oxygen atoms (NO, N_2O and NO_2). In high density condition, such as solid, liquid and high pressure gas samples, sample density affects muonic cascade processes after muon capture, hence we conducted all experiments at low pressure condition below 1 atm. In this study, we focused on gaseous simple molecules containing carbon and oxygen atoms (CO, CO_2 and COS).

II. EXPERIMENTAL

All muon irradiation experiments were performed at muon science facility (MUSE) in J-PARC. Low pressure sample gases (0.2 to 0.4 atm CO, CO_2 and COS) were put into a gas chamber and irradiated with low momentum muon beam (18.8MeV/c). Muonic X-rays were measured by germanium semi-conductor detectors.

III. RESULTS AND DISCUSSION

Muonic X-ray spectrum for CO_2 sample obtained by this experiment is shown in Fig.1. In this study, we discussed the experimental results about following two topics; muon capture probabilities of C and O atoms, and muonic X-ray structures (K_β/K_α and K_γ/K_α X-ray ratio etc.).

The muon capture probabilities of C and O atoms were determined from total intensity of muonic Lyman X-ray series of each atom. The muon capture ratios compared with the previous reports in high pressure sample conditions were in agreement [2,3].

The muonic X-ray structure reflects initial quantum state of the captured muon. The initial quantum state of muon was estimated using a simulation of muonic cascade processes [4]. The experimental structure of muonic C X-rays for CO_2 resembles that for COS, but that for CO resembles neither. This implies that the initial quantum state of muons captured by C atom differs between CO and other molecules. In fact, we found that muons captured by C atoms in CO molecule tend to have large angular momentum quantum number compared with that of CO_2 and COS from the cascade calculation. In the presentation, we will also discuss the initial quantum state of muons captured by O atoms for CO, CO_2 and COS samples.

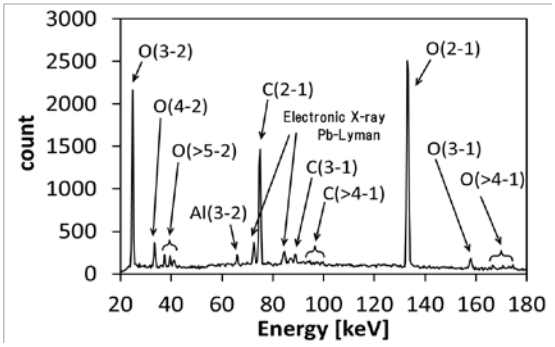

Fig.1 Muonic X-ray spectra of CO_2 sample. C(2-1) means the muonic X-ray series at muon transition from principal quantum number two to one on muonic carbon atom (K_αX-ray).

[1] H.Schneuwly et al., Physical Review A **27**, 950 (1983)
[2] J.D.Knight et al., Physics Letters **79**A 377 (1980)
[3] M K.Kubo et al.,Radiochimica Acta **47** 77 (1989)
[4] V.R. Akylas et.al., Computer Physics Communications **15**, 291 (1978)

EDI-01

CINCH–II Project – Next Step in the Coordination of Education in Nuclear- and Radiochemistry in Europe

Jan John[1], Václav Čuba[1], Mojmír Němec[1], Teodora Retegan[2], Christian Ekberg[2], Gunnar Skarnemark[2], Jukka Lehto[3], Teija Koivula[3], Paul J. Scully[4], Clemens Walther[5], Jan-Willem Vahlbruch[5], Nick Evans[6], David Read[6], Eric Ansoborlo[7], Bruce Hanson[8], Lindis Skipperud[9], Brit Salbu[9], Jon Petter Omtvedt[10]

[1] Czech Technical University in Prague, Czech Republic
[2] Chalmers University of Technology, Gothenburg, Sweden
[3] University of Helsinki, Finland
[4] National Nuclear Laboratory Ltd., Warrington, United Kingdom
[5] University of Hanover, Germany
[6] Loughborough University, Great Britain
[7] Commissariat à l'énergie atomique et aux énergies alternatives, France
[8] Leeds University, United Kingdom
[9] Norwegian University of Life Sciences, Aas, Norway
[10] University of Oslo, Norway

Abstract

Any of the potential options for the nuclear power – both the renaissance, if any, or the phase out – will require significant numbers of the respective specialists, amongst others the nuclear and/or radiochemists. In parallel, a significant demand exists for these specialists in non-energy fields, such as environmental protection, radiopharmacy, nuclear medicine, biology, authorities, etc. Since the numbers of staff in teaching and the number of univerzities with facilities licensed for the work with open sources of ionizing radiation has decreased on or sometimes even below the critical level, coordination and collaboration are required to maintain the necessary teaching and training capabilities.

The CINCH-II project, aiming at the Coordination of education and training In Nuclear CHemistry in Europe, will be a direct continuation of the CINCH-I project which, among others, identified the EuroMaster in Nuclear Chemistry quality label recognized and guaranteed by the European Chemistry Thematic Network Association as an optimum common mutual recognition system in the field of education in Nuclear Chemistry in Europe, surveyed the status of Nuclear Chemistry in industry / the needs of the end-users, developed an efficient system of education/training compact modular courses, or developed and tested two electronic tools as a basis of a future efficient distance learning system.

In the first part of this paper, the achievements of the CINCH-I project will be described. This description will cover both the status review and the development activities of this Collaboration. In the status review field, the results of a detailed survey of the universities and curricula in nuclear- and radiochemistry in Europe and Russia will be presented. Another survey mapped the nuclear- and radiochemistry in industry – specifically the training and education needs of the end users. In the development activities field, the main achievements of the CINCH project will be presented. They are particularly the NukWik – an open platform for collaboration and sharing teaching materials in nuclear- and radiochemistry based on a wiki engine. Further outputs are a set of compact joint modular courses in different branches of modern nuclear- and radiochemistry, or an e learning platform (CINCH Moodle) available for both education and training (applicable at the Ph.D., life-long learning, and MSc. levels).

The expected outcomes of the follow-on CINCH-II project will be described in detail. The CINCH-II project is built around three pillars - Education, Vocational Education and Training (VET), and Distance Learning - supported by two cross-cutting activities – Vision, Sustainability and Nuclear Awareness that includes also dissemination, and Management. Its main objectives, expected to have the broadest impact to the target groups, are further development and implementation of the EuroMaster in Nuclear Chemistry, completion of a pan-European offer of modular training courses for the customers from the end users, development of a Training Passport in Nuclear Chemistry and preparing the grounds for the European Credit system for Vocational Education and Training (ECVET) application in nuclear chemistry, implementation of modern e-learning tools developed in CINCH-I and further development of new tools for the distance learning, laying the foundations of a Nuclear Chemistry Education and Training Platform as a future sustainable Euratom Fission Training Scheme (EFTS) in Nuclear Chemistry, development of a Sustainable Systems for Mobility within the Nuclear Chemistry Network, or development of methods of raising awareness of the possible options for nuclear chemistry in potential students, academia and industry. The CINCH-II project will mobilize the identified existing fragmented capabilities to form the critical mass required to implement the courses and meet the nuclear chemistry postgraduate education and training needs, including the high-level training of research workers, of the European Union. Networking on the national level and with existing European as well as international platforms will be an important feature of the project.

Fostering of Personnel for Nuclear and Radiochemistry according to China's NPP Prospects after Fukushima Daiich Accident

Wangsuo WU[1] Zhifang CHAI[1,2]

[1]Radiochemistry Laboratory, School of nuclear Science and Technology, Lanzhou University, Lanzhou 730000, China
[2]Institute of High Energy Physics, Chinese Academy of Science, P.O. Box 918, Beijing 100049, China

PartI China's NPPs Prospects after Fukushima Daiichi Accident

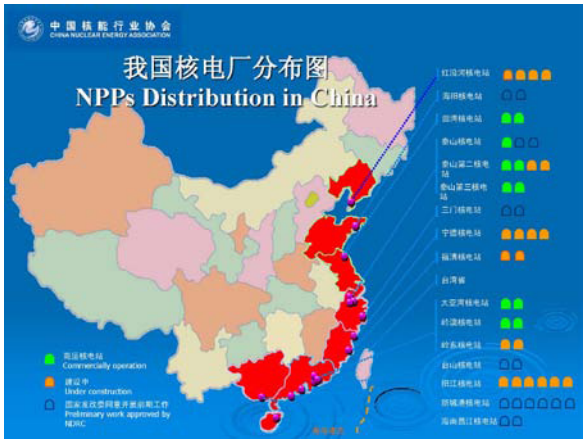

Fig.1 NPPs Distribution in China

PartII Fostering of Personnel for Nuclear and Radiochemistry

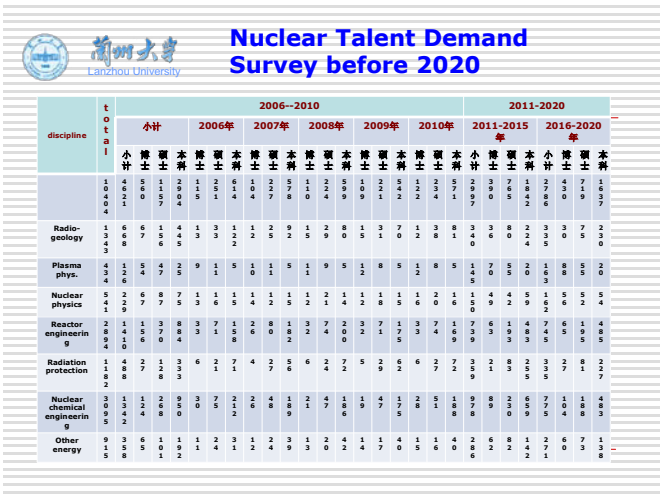

discipline	total	2006--2010														2011-2020					
		小计			2006年			2007年			2008年			2009年			2010年			2011-2015年			2016-2020年		
		小计	博士	硕士	本科	博士	硕士	本科	博士	硕士	本科	博士	硕士	本科	博士	硕士	本科	博士	硕士	本科	小计	博士	硕士	本科	博士	硕士	本科
	10404	4621	520	1157	2904	1151	2511	6144	1047	2278	5781	1102	2244	5991	1091	2121	5422	1224	2344	5713	2997	3905	7655	1842	2786	4300	719	1637
Radio-geology	1343	668	67	156	445	133	33	122	125	92	152	99	80	155	31	70	12	38	81	340	36	80	224	335	30	75	230			
Plasma phys.	434	126	54	47	25	9	11	5	10	11	5	11	9	5	12	8	5	12	8	5	145	70	55	20	163	88	55	20		
Nuclear physics	541	229	67	87	75	13	16	15	14	12	15	12	21	14	12	18	15	16	20	16	150	49	42	59	162	56	52	54		
Reactor engineering	2894	1410	156	370	884	33	71	158	26	80	182	32	74	200	32	71	175	33	74	169	739	63	193	483	45	65	195	485		
Radiation protection	1182	488	27	128	333	6	21	71	4	27	56	6	24	72	5	29	62	6	27	72	359	21	83	255	335	27	81	227		
Nuclear chemical engineering	3095	1342	124	268	950	30	75	212	26	48	189	21	47	186	19	47	175	28	51	188	978	89	230	659	754	104	183	483		
Other energy	915	358	65	101	192	11	24	31	12	24	39	13	20	42	14	17	40	15	16	40	286	62	82	142	271	60	73	138		

A strong impetus for radiochemistry is attributed to the rapid development of nuclear energy in China. In average, two nuclear power facilities per year will be installed even after Fukushima Daiich Accient. Nowadays there are 27 schools (or colleges) of nuclear science and technology (or engineering) in Chinese universities, of which 13 have nuclear and radiochemistry education and training with about 300 undergraduate students per year. The number of master and doctorate students in radiochemical field is about 50-60 annually. Several universities and institutes have research reactors, accelerators, neutron generators and other nuclear facilities used for radiochemical education and training. An exciting fact is that some big scientific platforms have been, are being or will be constructed, e.g. the Chinese Advanced Research Reactor, Shanghai Advanced Light Source, Chinese Spallation Neutron Source, Thorium Melted Salt Reactor (TMSR), Accelerator Driven Sub-critical System (ADS) and other big nuclear facilities, which are providing or will provide radio-chemists with advanced nuclear arsenal.

However, a quite number of problems in Chinese nuclear and radiochemical educations still exist, among which the biggest one is shortage of bright young radio-chemists in China. In the meantime, experienced radiochemical teachers are urgently needed. Some radiochemical laboratories in Chinese universities are outdated and ill-equipped.

Some measures and strategies for pushing nuclear and radiochemistry research and education in China will be proposed in this text as well.

APSORC'13 - 5th Asia-Pacific Symposium on Radiochemistry
Kanazawa, Japan, 22-27 September 2013

Post-Fukushima Situation on Radiation Awareness Activities and Nuclear and Radiochemistry Education in Japan

Akihiko Yokoyama,

Faculty of Chemistry, Institute of Science and Engineering, Kanazawa University,
Kakuma, Kanazawa, Ishikawa 920-1192, Japan

Abstract – The accident at Fukushima Daiichi Nuclear Power Plant in 2011 altered the working environment for radiochemists in Japan, who are supposed to be in charge of several problems such as radioactive contamination and nuclear wastes from reactors. Under the circumstances, we are compelled to reexamine the education relating to such matters. I discuss the effect of the accident on some aspects of education of the field.

Keywords – Fukushima accident/ radioactive contamination/ radiation awareness/ education

Research work in any field is affected by the educational prospects of the respective fields in both positive and negative ways. I would like to describe the present situation and future prospects for nuclear and radiochemistry education in Japan from my point of view, as a radiochemist, radiochemistry being one small part of the total discussion.

After the accident at Fukushima Daiichi Nuclear Power Plant in 2011, radiation-related topics such as radioactive contamination and nuclear wastes from reactors came to be the center of attention of people in this country. Furthermore, people's orientation concerning the nation's energy policy seems to be changing here. Under these circumstances I am compelled to reexamine the radiation awareness activities conducted for ordinary people (including children) as a university contribution to local communities. All these new situations cannot help affecting the educational content in many fields to some extent. I will discuss here the effect of the accident on the education for my field.

Nuclear science is still important in many industries and research fields in relation to nuclear medicine, material science, and the nuclear power industry to name a few.[1] Momentum towards the development of human resources is increasing in the nuclear power industry because of international pressure for carbon-oxide reduction and the need for development of nuclear waste treatment in Japan.[2] As a result, engineers, researchers and leaders of research groups have had to gain a broad perspective regarding energy crisis and environmental problems.

On the other hand, the number of students in the nuclear field, including radiochemistry, has decreased in recent years in Japan. Tight budgets at universities interfere with the maintenance of nuclear facilities, which in turn has largely discouraged students.[1,2]

Besides those aspects, the Fukushima accident has added several more complicated factors. We face several problems such as decontamination of everything in the area around the nuclear power plant, not to mention the decommissioning of the plant itself, all of which require radiochemical knowledge.

Primary education and secondary education had not paid attention to radiation awareness for many years. Nowadays, the situation is changing due to an education guideline change made by the government. It requires more opportunities to lecture to young people and their teachers and to discuss about radiation matters. The accidents have created more opportunities to talk to the general population on these issues, too. I am, however, not sure of the future contents to teach in relation to the Fukushima issues

On the university and graduate school level, a new methodology for human resources development for nuclear science and technology had been proposed by several universities in Japan and the Japan Atomic Energy Agency (JAEA). The network system has established a program by utilizing unique courses at universities and a real-time multi-directional network system as well as effective curriculums with practical exercises by utilizing JAEA's training and experimental facilities.[3] The network aims to implement the system with an eye to improving it with expanded experiences and increased the number of participant universities as well as to update the curriculums learning from the Fukushima issues.

Despite many difficulties, we have to overcome the current crisis to move towards a brighter dawn of the nuclear sciences and I think we still have a good chance of realizing the dream.

REFERENCES

[1] The Japan Society of Nuclear and Radiochemical Sciences, Fifty Years' History of Radiochemistry in Japan (CD), *in Japanese* (2007).

[2] References on Human Resources for Nuclear Science and Technology in Japan: http://www.jaif.or.jp/ja/news/2007/jinzai-kenkyukai.html, *in Japanese* (2007), http://www.jaif.or.jp/ja/seisaku/jinzai-kyogikai _report0807.pdf, *in Japanese* (2008), http://www.aec.go.jp/jicst/NC/iinkai/teirei/siryo2009/siryo15/siryo1.pdf, *in Japanese* (2009).

[3] Y. Fujii, T. Nakanishi, T. Fukui, H. Kato, and H. Ojima, Japan Nuclear Education Network (JNEN), A Multi-Directional Education System among JAEA and Several Universities, Presentation by J. Sugimoto in Conference on Nuclear Training and Education (2009)

EDO-01

Radiochemistry course in the undergraduate Nuclear Science Program at Universiti Kebangsaan Malaysia

S. B. Sarmani, R. B. Yahaya, M. S. Yasir, A. Ab. Majid, K. S. Khoo,
I. A. Rahman, F. Mohamed
Nuclear Science Programme, Universiti Kebangsaan Malaysia, 43600 Bangi, Malaysia

Universiti Kebangsaan Malaysia (UKM), is the only university in Asia offering an undergraduate degree program in Nuclear Science since 1978. The program has undergone several modifications due to changes in national policy and priority. The last adjustment was made in 2011 to ensure that the program is aligned with the aims and strategies of the National Nuclear Policy that guided the realization of Malaysia's first Nuclear Power Plant by 2021. The program covers nuclear sub-disciplines such as nuclear physic, radiobiology, radiochemistry and radiation safety. To graduate with a Bachelor of Science in Nuclear Science students are required to pass a total of 122 credits comprising of 20 credits of university courses and 102 credits of compulsory courses or core courses. Radiochemistry course involves both lectures and laboratory practicals. During the first year students are taught about basic physical and chemical properties of radioactive materials, radiation interaction and detection, radiation safety. In the second year lecture topics cover basic theory in radioanalytical chemistry, neutron activation, XRF, XPS and PIXE, tracer techniques, isotope dilution analysis, radioimmunoassay, nuclear dating and analysis of radionuclides in the environment. In the third year lectures are given on the chemistry of uranium, thorium and other actinides, isotope production and chemical aspects of nuclear fuel cycle. In the final year students may do a short project on applications of radioanalytical techniques, measurements of radioactivity in the environment or radiochemical separation. Recently, more students are enrolled into the program because of the National Nuclear Policy implementation and the program is in tandem with the thrusts and strategies of the policy. However, it is very difficult in getting new text books on radiochemistry particularly and nuclear science and technology generally. In the absence of good text book students are using on-line references published by reputable universities and organisations world wide.

Oral Presentations

Friday, 27 September 2013

Hall & Meeting Room, Kanazawa Bunka Hall

	Friday, 27 September		
Time		Meeting Room	
09:00-09:10	9:00	AAI-01	**Invited**
09:10-09:20			
09:20-09:30			A. Chatt
09:30-09:40	9:30	AAI-02	**Invited**
09:40-09:50			
09:50-10:00			T. Miura
10:00-10:10	10:00	**Coffee Break**	
10:10-10:20			
10:20-10:30	10:20	AAO-01	General
10:30-10:40			J.H. Moon
10:40-10:50	10:40	AAO-02	General
10:50-11:00			Y. Toh
11:00-11:10	11:00	AAO-03	General
11:10-11:20			K. Ninomiya
11:20-11:30	11:20	AAO-04	General
11:30-11:40			M. Fukushima
11:40-11:50	11:40	AAO-05	General
11:50-12:00			N. Shirai
12:00-12:10	12:00	**Lunch Time**	
12:10-13:20			
13:20-13:30	13:20	API-03	**Invited**
13:30-13:40			
13:40-13:50			Y. Hamajima
13:50-14:00	13:50	APO-04	General
14:00-14:10			C. Gautier
14:10-14:20	14:10	APO-05	General
14:20-14:30			T.Yoshimura
14:30-14:40	14:30	APO-06	General
14:40-14:50			J.D. Despotopulos
14:50-15:00	14:50	**Coffee Break**	
15:00-15:10			
15:10-15:20	15:10	**Closing Ceremony**	
15:20-15:30			
15:30-15:40			
15:40-15:50			
15:50-16:00			
16:00-16:10			
16:10-16:20			
16:20-16:30			
16:30-16:40			
16:40-16:50			
16:50-17:00			
17:00-17:10			
17:10-17:20			
17:20-17:30			
17:30-17:40			
17:40-17:50			
17:50-18:00			
18:00-18:10			
18:10-18:20			
18:20-18:30			
18:30-18:40			
18:40-18:50			
18:50-19:00			
19:00-19:20			
19:20-19:40			
19:40-20:00			
20:00-			

APSORC'13 - 5th Asia-Pacific Symposium on Radiochemistry
Kanazawa, Japan, 22-27 September 2013

Simultaneous Analysis for As, Sb, and Se Species in Water by Chemical Separation and Neutron Activation

W. Menendez Sanchez, Y. Shi, and A. Chatt

Trace Analysis Research Centre, Department of Chemistry, Dalhousie University, Halifax, NS, B3H 4J3, Canada

Abstract – APSORC'13 Abstract

Keywords – solid-phase extraction, solvent extraction, HPLC, INAA, speciation analysis, arsenic, antimony, selenium

I. INTRODUCTION

Arsenic speciation analysis has become an increasing health concern since the toxicity of the element depends upon the chemical species. Inorganic arsenic species are more toxic than their organic counterparts. Among the inorganic forms, As(III), the major arsenic species present in fresh water systems, is considered to be more toxic than As(V). It is well known that As(III) and As(V) undergo interconversion in aqueous solutions depending on pH, temperature, oxygen content, microorganisms, *etc*. Co-contaminants such as species of antimony and selenium in water can also affect arsenic speciation. There exists a need for simultaneous analysis of all these species.

Simultaneous speciation neutron activation analysis (SSNAA) technique has been developed in our laboratory over the last 20 years or so. This technique can now be used for the simultaneous determination of not only various species of a single element but also species of other elements present in the same sample. Almost all speciation techniques consist of two steps. The first step involves the separation of species from a sample followed by the second step of element-specific detection. Neutron activation analysis (NAA) methods in combination with high-performance liquid chromatography (HPLC) were developed first for the determination of low levels of five arsenic species, namely As(III), As(V), monomethylarsonic acid (MMA), dimethylarsinic acid (DMA), and arsenobetaine (AsB) in water samples. Organically bound arsenic (OBAs) and total arsenic levels were measured. These methods were then extended to include the determination of arsenic, antimony and selenium species, namely As(III), As(V), AsB, OBAs, MMA, DMA, Sb(III), Sb(V), and Se(IV), in natural water samples by solvent extraction and solid-phase extraction (SPE).

II. EXPERIMENTAL

In the HPLC method [1], OBAs was first separated by solid phase extraction using a C_{18} silica column. Next DMA and AsB were separated in a cation exchange column followed by injection into HPLC with 10 mM $NH_4H_2PO_4$/ $(NH_4)_2HPO_4$ buffer as the mobile phase. The effluent containing MMA, As(III), and As(V) species was then injected into HPLC with 75 mM $NH_4H_2P0_4$/$(NH_4)_2HP0_4$ buffer at pH 5.5.

An independent solvent extraction method was developed to separate soluble As(III) and As(V) compounds in water using APDC/MIBK [2].

In the SPE method [3], As(V), MMA, and DMA were separated and preconcentrated by an Alltech strongly anion exchange (SAX), namely Extract-Clean SPE SAX, column and strongly cation exchange (SCX), namely Extract-Clean SPE SCX, column in tandem while As(III) remained in the effluent. Once the columns were physically separated, acetate buffer at pH 3.4 was used to elute MMA from the SAX column. Then 5 mL of 1 M nitric acid was used to elute As(V). The SCX column was also eluted with 5 mL of 1 M nitric acid for DMA determination. This SPE method was further extended to separate As(III), As(V), AsB, OBAs, MMA, DMA, Sb(III), Sb(V), and Se(IV) in natural water samples [4].

All samples were irradiated in the Dalhousie University SLOWPOKE-2 Reactor facility at a neutron flux of either 5 or 2.5×10^{11} cm^{-2} s^{-1}. Samples were counted using either a conventional or a Compton suppression gamma-ray spectrometer. The 559.1-keV γ-ray of ^{76}As ($t_{1/2}$ = 26.3 h) was used for arsenic determination.

III. RESULTS AND DISCUSSION

The detection limits (ng mL^{-1}) of the HPLC-NAA method were found to be 0.005 for OBAs, 0.02 for AsB, DMA, MMA, As(III), and As(V) and 0.12 for total arsenic. The detection limits of As(III) and As(V) in the solvent extraction methods were 0.007 for fish/shellfish, 0.005 for As(III) and 0.006 mg kg^{-1} for As(V) in plants. The detection limits (ng mL^{-1}) were 0.9, 1.7, 1.6, 3.8 and 16 for As(III), As(V), MMA, DMA and total arsenic, respectively.

References

[1] Y. Shi, R. Acharya, A. Chatt, J Radioanal Nucl Chem, 262(2004) 277-286.
[2] R. Zwicker, B.M. Zwicker, S. Laoharojanaphand, A. Chatt, J Radioanal Nucl Chem, 287(2011)211-216.
[3] W. Menendez Sanchez, B. Zwicker, A. Chatt, J Radioanal Nucl Chem, 282(2009)133-138
[4] W. Menendez Sanchez, Ph.D. Thesis, Dalhousie University, Halifax, NS, Canada, 2009.

Precise Determination of Bromine in PP Resin Pellet by Instrumental Neutron Activation Analysis using Internal Standardization

Tsutomu Miura[1], Ryo Okumura[2], Yuto Iinuma[2], Shun Sekimoto[2], Koichi Takamiya[2], Masaki Ohata[1], Akiharu Hioki[1]

[1]National Metrology Institute of Japan, AIST
[2]Kyoto University Research Reactor Institute

Abstract – Instrumental neutron activation analysis with the internal standardization was applied the precise determination of bromine in PP resin. Gold was used as an internal standard. The analytical results of Br were in excellent agreement with the values obtained by ID-ICPMS. The relative expanded uncertainty (k=2) was 1.9 %, and it was comparable to that of ID-ICP-MS.

Keywords – Neutron activation analysis, Bromine, certified reference material, Uncertainty

I. INTRODUCTION

National Metrology Institute of Japan is responsible for developing certified reference materials (CRMs) and for establishing the traceability of SI (The International System of Units) on chemical metrology in Japan. To establish SI traceability, the primary method of measurements should be applied to the characterization of the CRMs. Recently, neutron activation analysis (NAA) using comparator standard is recognized as a potential primary ratio method [1]. Despite the potential of NAA as primary ratio method, the evaluation of the measurement uncertainty is required in any analysis. In general, there are three main components of uncertainty in NAA, that is, sample preparation uncertainty, neutron flux homogeneity, and gamma ray measurement uncertainty. Usually, flux monitor is used to correct the neutron flux in-homogeneity. However, although the flux monitor can correct the neutron flux variation using the count rate of the known amount of the monitor nuclide, it does not reflect the neutron flux of the actual sample. The most practical method to eliminate neutron flux in-homogeneity and to improve gamma ray measurement uncertainty is an internal standard method [2]. In this paper, we presented that notable capability of internal standardization in NAA for determination of Br in polypropylene (PP) resin pellet as a candidate CRM.

A. Instruments and methods

The PP resin pellet candidate CRM was produced by a mixing machine. The calibration solution was prepared from NMIJ primary Bromide standard solution. The Au solution for the internal standard was prepared from a high purity metal. The calibration solutions contained Br and Au. One hundred mg of the PP resin pellet samples was used for Br analysis. The Au solution was added to the samples before neutron irradiation. The neutron irradiations were performed by KUR (Kyoto University Research Reactor) PN-3(thermal neutron flux: 4.6×10^{12} $cm^{-2}s^{-1}$) for 10 min and TCPn (thermal neutron flux: 8.0×10^{10} $cm^{-2}s^{-1}$) for 30 min. The γ ray measurement system consisted of a Canberra GC4070-7500 Ge detector and a Laboratory Equipment Corporation MCA600.

B. Results and discussions

It was found that the neutron flux varied according to the sample position in the irradiation capsule. The relative standard uncertainty of the in-homogeneity was estimated to be about 5.1 % by ^{198}Au sensitivity (cps/μg) at 411 keV of the internal standard (n=19). The uncertainty related to the neutron flux homogeneity significantly contributes to the overall uncertainty, if an internal standard is not applied. The calibration curve linearity was also improved by internal standardization. The calibration curves of ^{82}Br showed good and sufficient linearity. The relative uncertainty related to the calibration curve linearity was improved to 0.97 % from 2.0 % for ^{82}Br by using an internal standardization. The analytical results of Br by proposed method were in excellent agreement with the values obtained by Isotope dilution-Inductively Coupled Plasma Mass Spectrometry (ID-ICPMS). The relative expanded uncertainty (k=2) was 1.9 %, and it was comparable to that of ID-ICP-MS.

APSORC'13 HEADING (WITHOUT NUMBER)

[1] Greenberg, R., Bode, P., De Nardi Fernandes, E., *Spectrochim. Acta B*, 66 (2011) 193-241.
[2] Miura, T, Chiba, K, Kuroiwa, T, Narukawa, T, Hioki, A, Matsue H., *Talanta*, 82 (2010) 1143-1148.

Analysis of most popular and/or consumed fish species by neutron activation analysis in six Asian countries

J. H. Moon[1], B. F. Ni[2], R. M. Theresia[3], N. A. Abd. Salim[4], B. Arporn[5], C. D. Vu[6]
[1]Korea Atomic Energy Research Institute, Daejeon, Korea
[2]China Institute of Atomic Energy, Beijing, P.R. China
[3]National Nuclear Energy Agency, Serpong, Indonesia
[4]Malaysian Nuclear Agency, Bangi,Kajang, 43000 Selangor, Malaysia
[5]Thailand Institute of Nuclear Technology, Bangkok, Thailand
[6]Vietnam Atomic Energy Agency, Dalat, Vietnam

Abstract – Since 2000, collaborative studies for applying NAA have been performed through the Forum for Nuclear Cooperation in Asia (FNCA) sponsored by the Japanese Government. Fish were selected as a common target sample for a collaborative study in 2011. Six Asian countries, China, Indonesia, Korea, Malaysia, Thailand, and Vietnam, are greatly concerned about the composition of arsenic, heavy metals, and essential trace elements and took part in this work. Fish samples were purchased from commercial markets and prepared by following a protocol that had been proposed for this study. Samples were analyzed by their own NAA systems. Each country has determined toxic and/or essential elements. These data will be very helpful in the monitoring of the levels of food contamination and to evaluate the nutritional status for people living in Asia.

Keywords–Neutron Activation Analysis, FNCA, Fish Species, Toxic Metals

I. INTRODUCTION

Since 2000, collaborative studies applying a neutron activation analysis (NAA) have been carried out as one of FNCA (Forum for Nuclear Cooperation in Asia) projects for the application of nuclear technology for socio-economic development. Six Asian countries, China, Indonesia, Korea, Malaysia, Thailand, and Vietnam agreed to participate in the analysis of the most popular and/or consumed fish species as a sub-theme of the NAA project in 2011. The aims of this study were to determine the inorganic elemental contents in fish species of six Asian countries by NAA and to evaluate the dietary intake levels of nutritional and toxic elements for population of the participating countries.

II. EXPERIMENTAL

Each participating country selected six to ten fish species and purchased them from the commercial market for this study. Analytical samples were prepared by cutting the edible parts of the fish, cleaning, grounding, freeze-drying, and homogenizing fish samples. The samples prepared by each country were analyzed using their own NAA facilities. Samples were activated by short and long irradiation to detect short-, median- and long-lived nuclides. To detect the gamma-rays emitted from the irradiated samples, HPGe detectors coupled to multichannel analyzers were used. The elemental content was determined by relative method and/or k_0-method.

III. RESULTS

China determined 14 elements from 10 fish species and most element concentration from the sea fish is higher than freshwater fish. Indonesia determined 17 elements from 6 types of fish samples, and As concentrations in sea fish is higher than in freshwater fish and Hg is contained in all types of fish. In Korea, 17 elements including As, Cr, and Hg were analyzed from 7 fish species. Malaysia determined Cr, Hg, Se, and Zn on eight species of marine fish, and the level of mercury in several fish showed a high value in dietary intakes levels compared to the EPA guideline value. Thailand analyzed As, Cd, Co, Cr, Fe, Hg, Rb, Sb, Sc, Se and Zn in 10 fish species As in all fresh water fish species does not exceed the standard recommended (2ug/g) but exceeds it in all marine fish species, while Hg in two fresh water fish species and three marine fish species exceed the standard recommended (0.5ug/g). Vietnam analyzed 18 elements in 10 samples of 6 sea fish species and As from Scad fish in the Vinh Hai district is higher than the WHO tolerable value.

ACKNOWLEDGEMENT

This research has been carried out by the support of the Ministry of Education, Culture, Science and Technology of Japan.

REFERENCES

[1] Ebihara M, Chung YS, Chueinta W, Ni BF, Otoshi T, Oura Y, Santos FL, Sasajima F, Sutisna, Wood AKBH (2006) J. Radioanal. Nucl. Chem. 269(2): 259-266
[2] World Health Organization (2006) Trace elements in human nutrition and health. Geneva, WHO, Belgium

APSORC'13 - 5th Asia-Pacific Symposium on Radiochemistry
Kanazawa, Japan, 22-27 September 2013

Current status and future perspective on time-of-flight prompt gamma-ray analysis combined with gamma-ray coincidence technique

Y. Toh[1], M. Ebihara[2], K. Hara[1], A. Kimura[1], H. Harada[1], S. Nakamura[1], M. Koizumi[1], K. Furutaka, F. Kitatani[1]

[1] Research Group for Applied Nuclear Physics, Japan Atomic Energy Agency, Tokai, Ibaraki 319-1195, Japan
[2] Graduate School of Science and Engineering, Tokyo Metropolitan University, 1-1 Minami-osawa, Hachioji, Tokyo 192-0397, Japan

Keywords – Prompt gamma-ray analysis (PGA); Time-of-flight (TOF); Coincidence method; Pulsed neutron; High-purity Ge detectors

Prompt gamma-ray analysis (PGA) is a rapid, non-destructive and a nuclear analytical technique which can perform both qualitative and quantitative multi-element analysis of elemental and isotopic compositions. The multiple gamma-ray detection method, also known as the coincidence method, is widely used in nuclear spectroscopy. By applying the multiple gamma-ray detection method to PGA, called MPGA (multiple prompt gamma-ray analysis), the signal-to-noise ratio (S/N) can be improved. The kinetic energy of a neutron can be measured with the time-of-flight (TOF) technique at a pulsed neutron source by measuring the time it takes a neutron to reach a sample. The neutron capture cross sections of most nuclides exhibit strong variations with the energy of neutron. Therefore, the energy of the neutron obtained by TOF method can be used for identification of nuclides (elements). For further improvements of the S/N and sensitivity, we have developed a time-of-flight prompt gamma-ray analysis combined with multiple gamma-ray detection method (TOF-MPGA).

The Accurate Neutron-Nucleus Reaction Measurement Instrument (ANNRI) has been designed and developed for PGA, nuclear cross-section data and nuclear astrophysics (See Fig.1). ANNRI is located at the beamline No. 04 at the Material and Life Science Experimental Facility (MLF) of the Japan Proton Accelerator Research Complex (J-PARC). MLF is high intensive pulsed neutron facility, which operates at approximately 300 kW proton beam power, and will be increased up to 1 MW in the near future. The germanium detector-array, which consists of two cluster-Ge detectors, eight coaxial-Ge detectors and BGO Compton suppression detectors surrounding cluster-Ge and coaxial-Ge detectors, was installed at the flight length of 21.5m in ANNRI. It is designed to provide high gamma-ray energy resolution and high detection efficiency. The typical time resolution of Ge detector is rather poor but this is not a disadvantage because of the proton beam pulse width of approximately 100ns (100ns double pulse, bunches separated by 600 ns). Frame overlap occurs when fast neutrons from a given pulse can catch-up with slower neutrons from a succeeding pulse. Whenever there is frame overlap there is a problem because the neutron energy cannot be unambiguously determined. Disk choppers consisting of a neutron absorbing disk are placed upstream of the Ge detectors. The disc choppers are used to prevent frame-overlap problems by limiting the neutrons which arrive at a sample. The rotation frequency of the choppers is the same as the source repetition rate (25Hz) under normal operation.

We present some remarks regarding the current status of experiments in TOF-MPGA development and its future perspective. The results of some standard sample measurements are discussed. These are compared with the results of the experiments of MPGA at Japan Research Reactor-3, and the similarity and difference are also discussed.

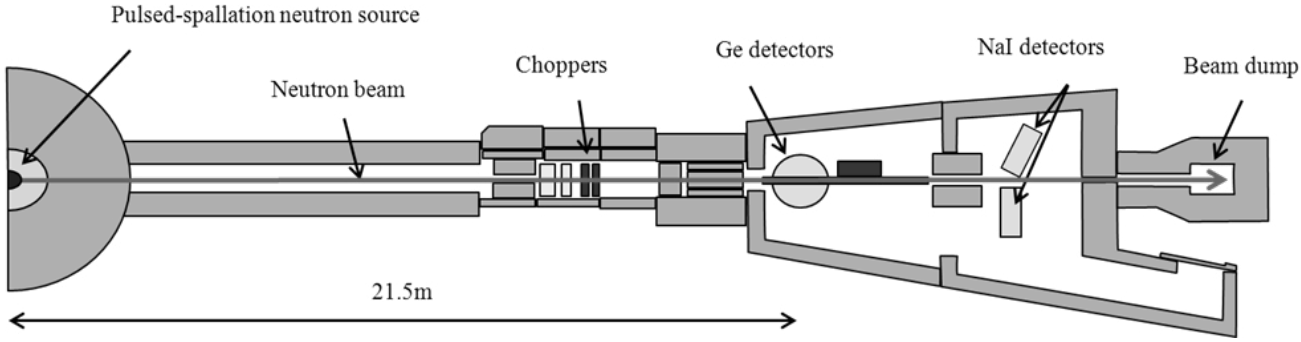

Figure 1 The Accurate Neutron-Nucleus Reaction Measurement Instrument (ANNRI)

Simultaneous and Multielemental Analysis by Muonic X-rays for Inside Japanese Bronze and Gold Coins

K. Ninomiya[1], M. K. Kubo[2], T. Nagatomo[3], G. Yoshida[1], M. Inagaki[1], A. Shinohara[1], T. Suzuki[2], N. Kawamura[3], P. Strasser[3], K. Shimomura[3], Y. Miyake[3], Y. Kobayashi[4], W. Higemoto[5], S. Sakamoto[5],
T. Saito[6]

[1]Graduate School of Science, Osaka University
[2]Colleage of Liberal Arts, International Christianity University
[3]Institute of Materials Structure Science, High Energy Accelerator Research Organization (KEK)
[4]Nishina Center for Accelerator-Based Science, RIKEN
[5]J-PARC Center, Japan Atomic Energy Agency (JAEA)
[6] National Museum of Japanese History

Abstract – A nondestructive, quantitative and multielemental analysis method for bulk samples was developed, which was based on the measurement of high-energy muonic X-rays emitted from muonic atoms inside material after muon irradiation. We demonstrated quantitative determination of the elemental composition inside archaeological artifacts without sample destruction.

Keywords – Elemental Analysis, Muonic Atom, Muonic X-ray

I. INTRODUCTION

Quantitative elemental analysis is one of the most important themes in the field of natural science. In particular, non-destructive elemental analysis for inside material is very useful in the field of archeology. The archeological sample surface is usually oxidized and coated. The destructive analysis methods are never applied to the very valuable sample. The elemental analysis methods inside bulk material are strongly desired.

In this paper, we report the development of a non-destructive, position-sensitive, quantitative and simultaneous multielemental analysis method for bulk samples by muonic X-ray measurements [1]. Muonic atom is the exotic atoms that has one negatively charged muon in its atomic orbital. When a muon is stopped in material, a muonic atom is formed, and characteristic X-rays (muonic X-rays) were emitted from the muonic atom. Because the mass of a muon is 207 times larger than that of an electron, the energies of muonic X-rays are very high. Therefore muonic X-ray can penetrate a bulk sample layer and the muonic X-rays from inside sample are detectable. In addition, this elemental analysis method has position sensitivity; the depth of muonic atom formation in the sample is controllable by adjusting the incident muon energy.

II. EXPERIMENTAL

We performed muon irradiation experiments at Muon Science Establishment (MUSE) in J-PARC (Japan). We measured muonic X-rays emitted from an old Japanese bronze coin (tempo-tsuho) and an old Japanese gold coin (tempo-koban) using high purity germanium detectors. For quantitative analysis, we also carried out muon irradiation for some standard alloys to obtain the relation between their elemental compositions and the muonic X-ray intensities.

III. RESULTS AND DISCUSSION

Muonic X-ray spectrum of the tempo-koban is shown in Figure 1. Muonic X-rays originated muon capture in Au and Ag atoms were identified. We easily determined that tempo-koban was alloy made from Au and Ag, and the compositions of the other elements were low. We also found incident muon momentum dependence of muonic Au X-ray intensity for the tempo-koban. This result showed that elemental composition of tempo-koban changed as its depth. The elemental composition inside the tempo-koban (> 5 μm in depth) was quantitatively determined (Au: 56%, Ag: 44%). Our result well reproduced the previous analysis result with destructive method [2]. The details will be reported in our presentation.

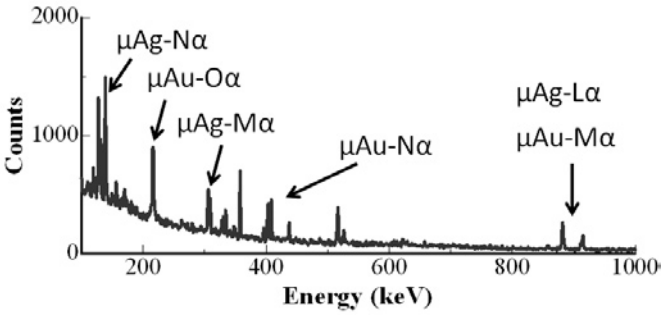

Figure 1: Muonic X-ray spectrum for old Japanese gold coin (tempo-koban). Muonic Au and Ag X-rays were clearly detected and no X-ray peaks originated from the other elements were identified.

[1] K. Ninomiya et. al., *Bull. Chem. Soc. Jpn*., **85**, 228 (2012)
[2] M. Ueda et. al., *IMES Discussion paper series*, 96-E-26 (1996)

Rapid Analysis for Selenium in Urine Samples using the 17.4-s Neutron Activation Product ^{77m}Se

Michiko Fukushima[1], Amares Chatt[2], Yoshitaka Nakamura[3], Megumi Haga[4], Seiko Hoshi[5], Takashi Sakata[1]

[1] Ishinomaki Senshu University, Ishinomaki, Miyagi, Japan;
[2] Dalhousie University, Halifax, NS, Canada;
[3] Meiji Co., Ltd., Odawara, Kanagawa, Japan;
[4] formerly at Shokei Gakuin University, Natori, Miyagi, Japan;
[5] Shokei Gakuin University, Natori, Miyagi, Japan

Abstract – APSORC'13 Abstract

Keywords – Selenium, urine samples, NAA, short half- life nuclide

I. INTRODUCTION

Selenium is an essential trace element for humans. Selenium deficiency causes dysfunction of various organs, including skeletal and cardiac muscles. The recommended dietary allowance (RDA) levels for Se in Japan [1] are 10 and 15 μg d^{-1} for 1-2 and 3-5 years old children, respectively. Although Se intake levels can be estimated by directly analyzing foods and diets [2], some researchers prefer to use bodily fluids or excretions as a better reflection of body burden of Se. For example, Dael *et al.* [3] used stable isotopes, namely ^{76}Se as selenate and ^{74}Se as selenite as supplements given to infants, analyzed their urine samples, and reported total Se intake of 60.8 ± 4.6 μg per 72 h, apparent Se absorption of 45.6 ± 5.2 μg per 72 h, and total urinary Se excretion 21.0 ± 4.2 μg per 72 h.

The techniques commonly used for the determination of Se in biological fluids are atomic absorption spectrometry (AAS), inductively-coupled plasma (ICP) atomic emission spectrometry (AES), and ICP mass spectrometry (ICP-MS). All of these techniques are suitable but time-consuming. The objective of the present project was to investigate a rapid method for the quantitative determination of Se in urine samples of children. We have developed an instrumental neutron activation analysis (INAA) method for this purpose using the short-lived nuclide ^{77m}Se (half-life = 17.4 s).

II. EXPERIMENTAL

24-h urine samples were collected from 75 healthy 3-5-year-old children by their families in their own houses living in two different cities of Miyagi Prefecture, Japan. The average total volume of urine was 503 mL d^{-1}. The urine samples were kept in cold and dark place for two days. After bringing the samples to the laboratory, they were frozen until the analysis.

Prior to analysis the urine samples were defrosted and 1 mL of each sample was transferred to a precleaned polyethylene irradiation vial using a calibrated Eppendorf pipette. These vials were precleaned using the following steps: soaking overnight in 2 mL of 4 M HNO_3, washing them with tap water followed by distilled water, and drying them in an oven. About 0.7 g of pure sucrose was added to each vial containing 1 mL urine and dried under IR lamp overnight in a fumehood. The vials were then heat-sealed. Comparator standards, for calculating Se concentrations in urine samples using the relative NAA method, were prepared by adding 1 mL of the Se standard solution containing 0.2, 0.5, or 1.0 μg of Se to 0.7g of sucrose using the same procedure as the urine samples. Samples, comparator standards and various reference materials were irradiated for 10 s in a neutron flux of 5×10^{11} $cm^{-2}s^{-1}$ at the Ghana Research Reactor-1 (GHARR-1). After a 10-s decay time the samples were counted for 30 s using a conventional gamma-ray spectrometer. The Se levels were assayed using the 161.9-keV gamma-ray of ^{77m}Se. It is evident that the INAA part of the analysis can be accomplished within 60 s which is quite rapid.

III. RESULTS AND DISCUSSION

To evaluate the accuracy of the INAA method developed here the following standard reference material (SRM) and certified reference material (CRM) were used: NIST SRM 2670a Toxic Elements in urine (Freeze Dried), NIST SRM 1549 Non-Fat Milk Powder, NIST SRM 1577b Bovine Liver, and NRC DOLT-3 Dogfish Liver. Our values agreed within ± 10% of the certified values. Out of the 75 urine samples analyzed by the INAA method described above, only 4 samples were below the detection limit of 10 ng mL^{-1}. The average level of 71 samples was 79.2 ± 46.8 ng mL^{-1} with the highest value of 242 ng mL^{-1}.

References

[1] Ministry of Health, Labour and Welfare of Japan. Dietary Reference Intakes for Japanese, 2010.
[2] Reiko Yamamoto, Rie Okita, Akane Hiruta, Tosiko Konno, Research Reports of Shohkei Gakuin College 52 (2006) 205-218.
[3] Peter Van Dael, Lena Davidsson, Rafael Munoz-Box, Laurent B. Fay, Denis Barclay, British J. Nutrition 85 (2001) 157-163.

Neutron activation analysis of iron meteorite

Naoki Shirai[1], Yoshihiro Hidaka[1], Shun Sekimoto[2], Mitsuru Ebihara[1], Hideyasu Kojima[3,4]
[1]Tokyo Metropolitan University
[2]Kyoto University Research Reactor Institute
[3]National Institute of Polar Research
[4]Graduate University for Advanced Sciences

I. INTRODUCTION

Iron meteorites are made of Fe-Ni metal phases with such minor minerals as schreibersite, troilite, cohenite and other Fe-Ni carbides [e.g., 1]. As most iron meteorites are believed to be samples of the metallic core of asteroidal parent bodies, petrological, mineralogical and chemical studies of iron meteorites are fundamental for unraveling the process of planetary differentiation.

Based on structure, iron meteorites were classified into hexahedrites, octahedrites and ataxites. Hexahedrites and ataxites are nearly made of kamacite and taenite, respectively. Octahedrites consist of kamacite and taenite and they are further divided into six subgroups on the basis of the width of the kamacite from finest (<0.2 mm) to coarsest (>3.3 mm). Almost all iron meteorites are classified into octahedrites. Therefore, it is difficult to determine representative elemental abundances of iron meteorites due to their heterogeneity. Bulk elemental abundances for iron meteorites have been obtained by using neutron activation analysis (NAA) [e.g., 2]. Other analytical methods such as inductively coupled plasma mass spectrometry (ICP-MS) have not been very often applied to iron meteorites [3, 4]. As subgroup IVB iron meteorites are made of ataxites and these chemical compositions are highly homogeneous, Campbell and Humayun [3] applied laser ablation with ICP-MS (LA-ICP-MS) to this subgroup. However, other subgroups have not been analyzed by using LA-ICP-MS for determination of their bulk chemical compositions. D'Orazio and Folco [4] analyzed iron meteorites by using solution nebulization ICP-MS. However, elements having smaller mass number than 80 significantly suffered spectral interferences caused by molecular ions such as FeO^+. There is a possibility of vaporization of Ge as $GeCl_4$ during the digestion of iron meteorites. Kong et al. [5] developed the INAA procedure for iron meteorites by using a TRIGA Mark II reactor at the Institute for Atomic Energy, St. Paul's University. In this study, Kyoto University Research Reactor was used for determination of elemental abundances of iron meteorites and the analytical capability was evaluated in comparison with the procedure of Kong et al. [5].

II. EXPERIMENTAL

As the Canyon Diablo iron meteorite was used for control sample in considering that it has been vigorously analyzed and its elemental abundances were well established. A piece of Canyon Diablo was cut into square plates weighing 33 and 41 mg by using a ISOMET Low Speed Saw. In INAA, samples were firstly irradiated for 10 sec at a neutron flux of 4.6 x 10^{12} $cm^{-2}s^{-1}$ at KURRI for determination of Cu, Ge and Rh. The samples were reirradiated for 4 hrs at a neutron flux of 5.6 x 10^{12} $cm^{-2}s^{-1}$ at KURRI and were measured for gamma rays several times with different cooling intervals. JB-1 and the Allende meteorite were also analyzed for reference samples. In addition, chemical standard samples were prepared for the determination of Cu, Ga, Ge, Mo, Ru, Rh, Pd, Sb, W, Re, Os, Ir, Pt and Au. The analytical procedure used in this study is basically similar to that described by Kong et al. [5].

III. RESULTS AND DISCUSSIONS

In short irradiation of Canyon Diablo, ^{60m}Co, ^{65}Ni, ^{66}Cu, ^{75}Ge and ^{104}Rh could be detected. Among these elements, Cu, Ge and Rh contents were calculated and shown in Table 1, where literature values were also indicated for comparison. Our values are in good agreement with literature values [2,6].

The plots of Ni vs. Ga, Ge and Ir can separate iron meteorites into about 12 subgroups. Usually, Ge has been determined by using radiochemical NAA [2] and Ni data have been obtained by INAA with long irradiation. Considering that short-irradiation INAA is able to determine both Ni and Ge. Therefore, our INAA procedure is simple and effective in classification of iron meteorites.

Reference: [1] Goldstein J. I. et al. (2009) Chemie der Erde, 69, 293-325. [2] Wasson J.T. and Kallemeyn G. W. (2002) GCA, 66, 2445-2473. [3] Campbell A. J. and Humayun M. (2005) GCA, 69, 4733-4744. [4] D'Orazio M. and Folco L. (2003) Geostand. Newsl., 27 (3), 215-225. [5] Kong P. et al. (1996) Anal. Chem., 68, 4130-4134. [6] Nichiporuk W. and Brown H. (1965) J. Geophys. Res., 70 (2), 459-470.

Table 1. Cu, Ge and Rh abundances (in ppm) of Canyon Diablo in comparison with literature.

	This work				Literature
Cu	136	± 11	154	± 10	148, 150[2]
Ge	329	± 22	314	± 21	323, 330[2]
Rh	1.33	± 0.11	1.08	± 0.10	1.5[6]

APSORC'13 - 5th Asia-Pacific Symposium on Radiochemistry
Kanazawa, Japan, 22-27 September 2013

What has been revealed in the Low-Level Radioactivity Measurement?

- Low Level Gamma-Ray Counting in Ogoya Underground Laboratory -

Yasunori Hamajima
Kanazawa Univ. LLRL.

Abstract – *In Ogoya Underground Laboratory, low-level radioactivity measurement is performed. We have 18 low background Ge detectors and all detectors provide excellent counting efficiency. We report recent results.*

Keywords – low-level counting, underground laboratory, well-type Ge detecto

I. INTRODUCTION

In gamma ray measurements, it is important to reduce the background noise of detectors and activation of shielding materials derived from secondary cosmic ray components (muons and neutrons). It is difficult to reduce these components by conventional shield at aboveground. The intensity of secondary components decreases with the depth of overburden at the underground facility. Ogoya Underground Laboratory (OUL) is in a 546 m tunnel of the former Ogoya Copper Mine. It is located 270 m from the tunnel entrance, where the overburden is 270 mwe. The background count rates of OUL detectors are about 1/100 of the aboveground ones.

II. DETECTORS AND SHIELDING IN OUL

OUL has 11 well, 6 planar, and 1 coaxial Ge detectors, as shown in Table 1. In order to measure a wide energy range from 20 keV to about 3 MeV, the planar type detectors have large diameters and thicknesses and the well type detectors have also large diameters. For most of detectors, ultra low-background aluminum was used for the end-cap. The cryostat is the J-type and/or U-type and the preamplifier is located outside of the lead shield. The lead shield is 15 to 25 cm thick, and its upper part is covered by 10 to 15 cm of iron. The inner 3 to 5 cm of the lead shield is made of lead refined 200 years ago. The space near the detector head is filled with Hg shield encapsulated in a polyethylene bag and nitrogen gas from the Dewar is blown to the top of the end cap.

III. RECENT RESULTS IN OUL

Some significant measurements have been made at OUL such as the detection of low level cosmogenic nuclides, natural radio nuclides, fission products and activated nuclides induced by environmental neutrons and fission neutrons.

In the recent results of extraterrestrial science, "Neutron Activation Analysis of a Particle Returned from Asteroid Itokawa" was in Science, 333, 1119-1121, (2011), and "Radar-Enabled Recovery of the Sutter's Mill Meteorite, a Carbonaceous Chondrite Regolith Breccia" was reported in Science 338, 1583-1587, (2012).

In those of Oceanography, "Surface pathway of radioactive plume of TEPCO Fukushima NPP1 released 134Cs and 137Cs" was reported in Biogeosciences, 10, 3067-3078, (2013), and "Cross equator transport of 137Cs from North Pacific Ocean to South Pacific Ocean (BEAGLE2003 cruises)" was in Progress in Oceanography, 89, 7-16, (2011).

Table 1. Specifications of Ge crystals and background counting rates.

Ge	Type (Al end cap)	Relative Eff, (size)	BG (min^{-1})
I	planar	18%(28cm² x 2cm)	0.48
J	planar	34%(38cm² x 3cm)	0.57
K	planar	34%(38cm² x 3cm)	0.52
L	planar	18%28cm² x 2cm)	0.57
M	planar	22%(28cm² x 2.8cm)	
N	planar	22%(28cm² x 3cm)	
C	well(10ϕx40mm)	37%(61ϕx56mm,)	0.9
D	well(21ϕx62mm)	56% (72.0ϕx74.8mm)	2.51
A	well(21ϕx62.5mm)	56% (72.0ϕx75.0mm)	2
B	well(21ϕx62.5mm)	56% (72.0ϕx74.7mm,)	1.93
G	well(21ϕx66.5mm)	71.5%(74.0ϕx79mm)	2.83
H	well(21ϕx66.5m	71.7%(74.0ϕx80mm)	2.09
W	well(21ϕx60mm)	65% (75.1ϕx81mm)	1.72
X	well(21ϕx68mm)	73.4%(74.3ϕx80mm)	1.69
Y	well(21ϕx68mm)	70.5%(74.3ϕx80mm)	1.4
E	well(21ϕx60mm)	68%(74.06ϕx80mm)	1.7
F	well(21ϕx55mm)	56%(75ϕx55mm)	2.1
U	coaxial	94% (78.9ϕx81mm)	1.12

BG: integrated count rate (50 – 2000 keV)

APSORC'13 - 5th Asia-Pacific Symposium on Radiochemistry
Kanazawa, Japan, 22-27 September 2013

Zr and U determination at trace level in simulated deep groundwater by Q ICP-MS using TRU-based and TODGA-based extraction chromatography

C. Gautier[1], M. Coppo[1], C. Caussignac[2], I. Laszak[2], P. Fichet[1], F. Goutelard[1]
[1]*Operator Support Analyses Laboratory, Atomic Energy Commission, CEA Saclay, DEN/DANS/DPC/SEARS/LASE, Building 459, PC171, 91191 GIF SUR YVETTE CEDEX, FRANCE*
[2]*Nuclear, Isotopic Elementary Analytical Development Laboratory, Atomic Energy Commission, CEA Saclay, DEN/DANS/DPC/SEARS/LANIE, Building 391, PC33, 91191 GIF SUR YVETTE CEDEX, FRANCE*

Abstract – APSORC'13 Abstract

In the past decades, metallic fuels, such as UZr metallic alloys, were used as nuclear fuels. Direct disposal in deep geological repository can be an option for the long-term management of spent nuclear fuels. In the framework of such an issue, it is necessary to develop a source-term model for the release of radionuclides from the spent nuclear fuels. The validation of the dedicated model requires the implementation of leaching experiments in the conditions of a deep geological repository. For the spent UZr fuels studied in France, the leaching and the release of two major radionuclides, ^{235}U and ^{93}Zr, have to be investigated in the reference groundwater which is planned to be a deep clayey Callovo-Oxfordian groundwater containing high concentrations of salts (alkali and alkaline earth metals). Given the expected concentrations of ^{235}U and ^{93}Zr isotopes ($< 10^{-6}$ mol L^{-1} or < 0.2 mg L^{-1}) in leaching solutions, Q ICP-MS can be considered as the most promising technique for their simultaneous measurements. However, due to the groundwater composition, sample dilution has to be applied before ICP-MS analysis to avoid matrix effects. This option is incompatible with our requirements in terms of detection limits. Consequently, a full analytical procedure was implemented to determine Zr and U at trace level in a simulated deep Callovo-Oxfordian groundwater by Q ICP-MS.

Separation procedures based on extraction chromatography were developed to eliminate the high salt contents and to concentrate Zr and U simultaneously. Since U and Zr display different chemical behaviors in solution, their speciation was first discussed. Theoretical and experimental speciation studies showed the importance of adjusting the medium to HNO_3/HF (0.5M/0.005M) to guarantee the stability over time of the analytes before removal of the matrix. Two preconcentration methods based on TRU® and TODGA® resins were optimized for the simultaneous isolation of Zr and U prior to Q ICP-MS measurements. Using TRU resin, alkali and alkali earth metals contained in the deep groundwater were removed with 2M HNO_3 whereas Zr and U were recovered with a $HNO_3/NH_4HC_2O_4$ (0.02M/0.05M) medium. For the separation protocol based on TODGA resin, alkali and alkali earth metals were eliminated with 3M and 11M HNO_3 while Zr and U were simultaneously stripped with a HNO_3/HF (0.5M/0.2M) medium. The procedure optimized on TODGA resin was the only one validated with the French AFNOR NF T90-210 standard by studying linearity, limits of quantification (LOQ) and separation yields. The LOQ was determined to be 0.008 µg L^{-1} for Zr and U after the separation. Both analytes were recovered quantitatively. Compared to a direct Q ICP-MS analysis after sample dilution, the developed preconcentration method allowed improving the sensitivity up to a 20 fold factor for Zr and U measurements at trace level by Q ICP-MS.

The leaching experiments are requested to be performed in hot cells of the LECI laboratory (Laboratory for Studies on Irradiated Fuel) at CEA (French Alternative Energies and Atomic Energy Commission) Saclay. Blank samples (containing 0.5M HNO_3 + 0.005M HF) were introduced during one week in the selected hot cell where spent fuels are usually handled. The solutions were analyzed by Q ICP-MS to check whether the atmosphere of the hot cell induces problems of blank contamination for Zr and U measurements at trace level. The measured concentrations were lower than the limits of quantification validated at 0.008 µg L^{-1} after separation, which proved the feasibility of the scheduled experiments.

The developed procedure was demonstrated to be very efficient for this application but it could be also used for many other issues concerning analysis of trace amount of radionuclides contained in high salt matrix.

APSORC'13 - 5th Asia-Pacific Symposium on Radiochemistry
Kanazawa, Japan, 22-27 September 2013

Photoluminescence of Five- and Six-coordinate Tetracyanidonitridotechnetium(V) and –rhenium(V) Complexes

Takashi Yoshimura[1], Hayato Ikeda[2], Akitaka Ito[3], Eri Sakuda[3], Noboru Kitamura[3], Tsutomu Takayama[4] Tsutomu Sekine[5], Atsushi Shinohara[2]

[1]Radioisotope Research Center, Osaka University
[2]Department of Chemistry, Graduate School of Science, Osaka University
[3]Department of Chemical Sciences and Engineering, Graduate School of Chemical Sciences and Engineering, Hokkaido University
[4]Department of Chemistry, Daido University
[5]Center for Advancement of Higher Education, Tohoku University

Abstract – Six-coordinate tetracyanidonitrido Re(V) and Tc(V) complexes with a volatile organic compound (VOC) and five-coordinate complexes were synthesized and characterized. Reversible luminescence switching between six- and five-coordinate Re(V) complexes and between the relevant six-coordinate Re(V) complexes was achieved by exposing them to VOC vapor in the solid state at room temperature. Luminescence changes were observed from the five-coordinate Tc(V) complexes in a MeOH vapor atmosphere in the solid state. In contrast, no vapochromic luminescence was observed from the five-coordinate and six-coordinate complexes in an acetone vapor atmosphere.

Keywords – Technetium, Rhenium, Photoluminescence

I. INTRODUCTION

Among the Group 7 metal ions, a very small number of technetium complexes have been reported to show photoluminescence. In coordination compounds, molecular sensing can be done based on the color change of a complex through changes in the coordination environments and/or direct interaction of the metal ion with a molecule to be sensed. In contrast, molecular sensing based on the vapochromic luminescence through a ligand substitution reaction and the coordination number of a metal ion in the solid state has been rarely reported. We report novel six-coordinate nitrido Re(V) and Tc(V) complexes and their five-coordinate square pyramidal complexes without an axial ligand. The present study demonstrated for the first time that the nitrido Tc(V) complex showed luminescence in the solid phase at room temperature. We demonstrate for the first time interconversion between the six-coordinate Re(V) complexes through a solid state substitution reaction upon exposure to VOC vapor, and between the five-/six-coordinate complexes by a solid state ligand coordination/elimination reaction.[1]

II. RESULTS AND DISCUSSION

Six-coordinate Re(V) and Tc(V) complexes with a VOC, $(PPh_4)_2[MN(CN)_4L]$ (M = Re, L = MeOH, EtOH, acetone, or MeCN; M = Tc, L = MeOH), and five-coordinate $(PPh_4)_2[MN(CN)_4]$ (M = Re or Tc), were synthesized and their spectroscopic and photophysical properties were investigated. Results demonstrate that the tetracyanidonitrido Re(V) and Tc(V) complexes were bistable between the five-coordinate square pyramidal and six-coordinate octahedral coordination environments. All of the five-coordinate square pyramidal and six-coordinate octahedral complexes showed photoluminescence in the solid state at room temperature. The emission spectra and photophysical data of the five-coordinate $[ReN(CN)_4]^{2-}$ were significantly different from those of the relevant six-coordinate complexes.

Vapochromic luminescence between the bistable five- and six-coordinate Re complexes with the VOCs (MeOH, EtOH, acetone, or MeCN) and between the six-coordinate complexes was investigated. We found unique reversible coordination and elimination of a VOC at the axial site of the Re complex in the solid state that gave rise to changes in the emission maximum wavelength, demonstrating photoluminescence switching and sensing of VOC by the present Re(V) complexes at room temperature. Upon exposure of MeOH vapor to the five-coordinate Tc complex, the emission spectrum changed to that of the MeOH coordinate complex. The coordinating MeOH molecule can be removed by evacuation of the complex in vacuo. In contrast, the emission band shapes of the five-coordinate Tc complex remained unchanged even upon exposure of acetone vapor. The emission spectrum of MeOH coordinate Tc complex changed to that of the five-coordinate complex by exposure to acetone vapor. This suggests that the coordinating MeOH molecule in the Tc complex was eliminated under acetone vapor atmosphere, but acetone was not incorporated and did not coordinate at the axial site in the Tc complex.

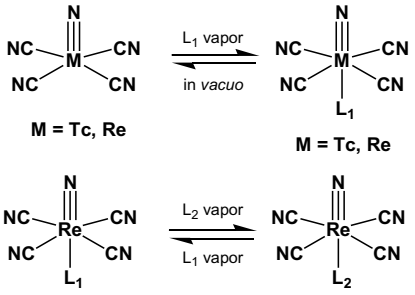

Scheme 1.

[1] H. Ikeda, T. Yoshimura, A. Ito, E. Sakuda, N. Kitamura, T. Takayama, T. Sekine, A. Shinohara, *Inorg. Chem.*, **51**, 12065-12074 (2012).

APSORC'13 - 5th Asia-Pacific Symposium on Radiochemistry
Kanazawa, Japan, 22-27 September 2013

Studies of Flerovium and Element 115 Homologs with Macrocyclic Extractants

John D. Despotopulos[1,2], Narek Gharibyan[1], Roger A. Henderson[1], William Kerlin[2], Kenton J. Moody[1], Dawn A. Shaughnessy[1], Evgeny Tereshatov[1], Ralf Sudowe[2]
[1]Lawrence Livermore National Laboratory,Chemical Sciences Division, Livermore, California 94551, USA
[2]University of Nevada Las Vegas, Las Vegas, Nevada 89154, USA

Abstract – Recent studies of the chemical behavior of Copernicium (Cn, element 112) and Flerovium (Fl, element 114) together with the discovery of isotopes of these elements with half-lives suitable for chemical studies have spurred a renewed interest in the development of rapid systems designed to study the chemical properties of elements with Z ≥ 114 [1,2]. Due to the short half-lives of the transactinide elements, fast and efficient separations are necessary to evaluate their properties, such as ionic radii and chemical speciation, by comparing to their lighter homologs. Separations based on extraction chromatography resins using macrocyclic extractants show promise for achieving the short separation times, large extraction yields, and high separation factors required for transactinide studies. In this study the potential of different macrocyclic extractants for their future application to a Fl and element 115 chemical system has been investigated.

Keywords – Transactinide, homolog, element 114/115, separations

I. INTRODUCTION

Studies of the chemical properties of superheavy elements (SHE) pose interesting challenges due to their short half-lives and low production rates. Chemical systems must have extremely fast kinetics to be able to probe the chemical properties of interest, such as chemical speciation, before the SHE decays to another element. To achieve chemistry on such time scales (~ seconds), the chemical system must also have the potential to be easily automated. The transactinides (elements with Z > 103) are predicted to exhibit changes in their chemical behavior compared to that of their lighter homologs (elements in the same chemical group) or pseudo-homologs (elements with the same oxidation state and similar ionic radii) due to relativistic effects [3].

II. EXPERIMENTAL

A. Extractants and Resins

Crown ethers and their derivatives show high selectivity for metal ions based on their size compared to the cavity of the ether. Di-t-butylcyclohexano-18-crown-6 (fig. 1) is known to show high affinity for the Pb^{2+} ion.

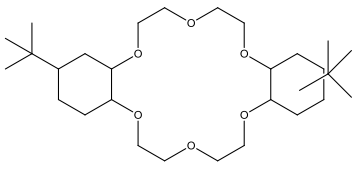

Fig. 1: Di-t-butylcyclohexano-18-crown-6.

Eichrom's commercially available Pb resin is based on the di-t-butylcyclohexano-18-crown-6 extractant sorbed to the resin backbone in isodecanol. Consequently, this resin exhibits high selectivity for Pb^{2+} [4]. Thiacrown ethers, which replace the oxygen atoms with sulfur, act as softer Lewis bases compared to traditional crown ethers [5]. This unique property of thiacrowns should make them even better extractants for softer metals such as Pb. Hexathia-18-crown-6 (fig. 2) was synthesized and investigated.

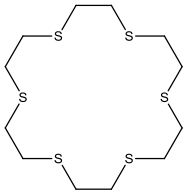

Fig. 2: Hexathia-18-crown-6.

B. Extraction Studies

Batch experiments were performed for the direct homologs of Fl (Pb and Sn) and element 115 (Bi and Sb) using the Eichrom Pb resin. Promising results were obtained from HCl/KI matrices as well as from simple mineral acid matrices. Column studies were performed to asses these extractions under dynamic conditions. Liquid-liquid extractions were also performed using hexathia-18-crown-6 to determine its suitability and compare it to that of the standard crown ether.

Acknowledgment: This work was performed under the auspices of the U.S. Department of Energy by Lawrence Livermore National Laboratory under Contract DE-AC52-07NA27344. This work was funded by the Laboratory Directed Research and Development Program at LLNL under project tracking code 11-ERD-011.

REFERENCES

[1] R. Eichler *et al.*, Chemical characterization of element 112, *Nature*, **2007**, 447, 72-75.
[2] R. Eichler *et al.*, Indication for a volatile element 114, *Radiochim. Acta*, **2010**, 98, 133-139.
[3] P. Pyykko, Relativistic effects in structural chemistry, *Chemical Reviews*, **1988**, 88, 563-594.
[4] E. P. Horwitz, *et al.*, A lead-selective extraction chromatographic resin and its application to the isolation of lead from geological samples, *Analytical Chemica Acta,* **1994**, 292, 263-273.
[5] E. Sekido, *et al.,* Liquid-liquid extraction of some class b metal ions with thiacrown ether 1,4,8,11-tetrathiacyclotetradecane, *Analytical Sciences*, **1985**, Vol. 1, 363-368.

LLNL-ABS-631618

Poster Session 1

Monday, 23 September 2013

18:50 ~ 20:00

Scientific Topics (Abbrev.)

1. Fukushima issues (FK)
2. Education in nuclear and radiochemistry (ED)
3. Nuclear forensics (NF)
4. Nuclear energy chemistry (NE)
5. Nuclear chemistry (NC)
6. Actinide chemistry (AC)
7. Environmental radiochemistry (EN)
8. Radiopharmaceutical chemistry and Nuclear medicine (RP)
9. Nuclear probes for materials science (NP)
10. Activation analysis (AA)
11. Application of nuclear and radiochemical techniques (AP)

APSORC'13 - 5th Asia-Pacific Symposium on Radiochemistry
Kanazawa, Japan, 22-27 September 2013

^{137}Cs Accumulation Enhanced by Potassium Starvation in *Lotus japonicus*

Jun Furukawa[1], Hiroki Noda[2], Ryohei Sugita[3], Keitaro Tanoi[3], Tomoko M. Nakanishi[3], Shinobu Satoh[1]
[1]Faculty of Life and Environmental Sciences, University of Tsukuba
[2]Graduate School of Life and Environmental Sciences, University of Tsukuba
[3]Graduate School of Agricultural and Life Sciences, The University of Tokyo

Abstract – Radionuclides released from Fukushima Dai-ich Nuclear Power Plant spread to the environment. The transfer of ^{137}Cs from soil to land plants is one of the most important steps for considering the influx of ^{137}Cs into ecosystem. To identify the responsible genes for ^{137}Cs uptake and translocation in plants, we focused on the K+ transport system in the model legume, Lotus japonicus. The dynamics of ^{137}Cs uptake and translocation was differed between two accessions, B-129 and MG-20, and K starvation drastically enhanced ^{137}Cs uptake in B-129. The expression levels of known K+ transporters were also investigated under several K conditions.

Keywords – cesium-137, potassium, accumulation, Lotus japonicus

I. INTRODUCTION

After the Fukushima Dai-Ichi Nuclear Power Plant accident, large amount of radioactive materials were released into the environment and the major radionuclides leaking was ^{137}Cs. Cesium is known as an analog of potassium in the plant nutrition and, therefore, one of the main route of ^{137}Cs into the ecosystem is an uptake process in land plant. Uptake and translocation of ^{137}Cs is thought to be carried out by the K^+ transport systems in plants [1]. However, because of the complexity of K^+ transport system, the responsible transporters, which transport ^{137}Cs, were not well identified. In this research, the identification of the K^+ transport system, which involved in the ^{137}Cs uptake and transport, in *Lotus japonicus* was attempted. *L.japonicus* has been proposed as a model legume for molecular biology, and the results obtained from *L.japonicus* are applicable to one of the major crops, soybean.

II. MATERIAL AND METHODS

Plant Materials and Growth Conditions

Two *L.japonicus* accessions, Gifu B-129 (B-129) and Miyakojima MG-20 (MG-20), were obtained from the Biological Resource Center in *Lotus* and *Glycine*, University of Miyazaki, Japan. Seedlings were grown with continuously aerated 1/10 strength Hoagland's solution in a 2 L plastic container under light- and temperature-controlled condition; light 16 h, darkness 8 h, 24°C. The solution was renewed every 3 days. At the last 3 days before ^{137}Cs uptake experiment, the solutions with and without K were prepared.

^{137}Cs Uptake

Plants grown for one month were transferred to 50 mL of 1/10 strength Hoagland's solution (without K) containing ^{137}CsCl and non-radioactive Cs (10 μM) for 12 h. After harvesting shoots and roots, distribution and radioactivity of ^{137}Cs was detected with an image analyzer (BAS) and gamma counter, respectively.

Real-time Radioisotope Imaging

RRIS (Real-time Radioisotope Imaging System) was used for obtaining the images of ^{137}Cs uptake and translocation in *L.japonicus*. RRIS is a non-destructive digital autoradiography system specialized for the use in living plant research [2]. The plants prepared as previous BAS experiment were placed in RRIS and the ^{137}Cs distribution images were obtained for 24 h.

III. RESULTS AND DISCSSION

As for the plants grown under normal K condition, ^{137}Cs in B-129 root was about twice the concentration of that in MG-20. However, ^{137}Cs concentration in shoot was not differed between two accessions. In the plants treated with -K solution for 3 days, drastic enhancement of ^{137}Cs uptake was observed in B-129 root. The increase of ^{137}Cs translocation from root to shoot was observed both in B-129 and MG-20. Because of the constant ^{137}Cs concentration in MG-20 root, the increase of ^{137}Cs concentration in MG-20 shoot suggested the high ^{137}Cs translocation activity in MG-20 under K starvation. Real-time ^{137}Cs images clearly indicated the ^{137}Cs uptake site in root and the rapid uptake and translocation of ^{137}Cs in B-129 (Figure 1).

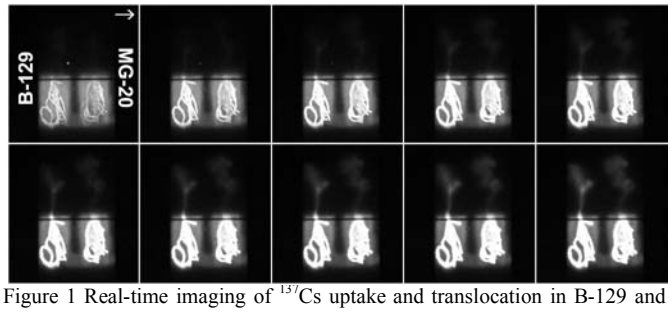

Figure 1 Real-time imaging of ^{137}Cs uptake and translocation in B-129 and MG-20 treated with -K solution for 3 days. Each panel indicates the radioactivity image obtained for every 2.4 h.

Potassium starvation promotes K uptake system, especially high affinity K^+ transporter, in root [3]. Therefore, the expression levels of known K^+ transporters in *L.japonicus* will be discussed.

IV. REFERENCES

[1] White PJ and Broadley MR (2000) *New Phytol.*, **147**, 241-256.
[2] Kanno S *et al.* (2012) *Philos. Trans. R. Soc. B*, **367**, 1501-1508.
[3] Wang TB *et al.* (1998) *Plant Physiol.*, **118**, 651-659.

APSORC'13 - 5th Asia-Pacific Symposium on Radiochemistry
Kanazawa, Japan, 22-27 September 2013

Decontamination of the Contaminated Water on Severe Nuclear Accidents by Titanium Oxide Adsorption

Youko Takahatake[1], Masahiro Nakamura[1], Atsuhiro Shibata[1], Kazunori Nomura[1], Yoshikazu Koma[1], Yasuo Nakajima[1]
[1]Japan Atomic Energy Agency

Abstract – In order to establish a decontamination process for contaminated water that generated in a severe nuclear power plant accident such as the Fukushima accident, we proposed a new decontamination process. A new decontamination process is composed of co-decontamination of radioactive transition metals and Cs with hexacyanoferrate(II) ion, and decontamination of radioactive metals including Sr with titanium oxide adsorption. This study discussed the adsorptivity of a new titanium oxide and its applicability to the radioactive water after co-decontamination of transition metals and Cs.
Keywords – Sr decontamination, titanium oxide adsorption, contaminated water of Fukushima accident

The massive amount of radioactive contaminated water was generated in Fukushima Dai-ichi NPP. This water is unique compared to contaminated water generated in previous treated radioactive contaminated waters, concerning the amount of minerals due to the utilization of seawater during the emergency cooling of reactor cores. According to the analysis of the water, it contains fission products (^{90}Sr, ^{125}Sb and ^{134,137}Cs), corrosion products and large amount of non-radioactive metals. The special treatment system was applied to decontaminate it. If NPP accidents may be occur in the future, the experience on this accident is utilized effectively.

In order to minimize the amount of secondary waste from the water treatment system, we proposed a new decontamination process (figure 1) for radioactive contaminated water generated at NPP accidents. At first, this process decontaminates transition metals and Cs simultaneously by adding hexacyanoferrate(II) ion. This step was already discussed [1]. The next step is decontamination of Sr, Sb and remaining Co and Mn by titanium oxide adsorption. This study discusses the adsorptivity of a new titanium oxide and its applicability to the radioactive water after co-decontamination of transition metals and Cs.

Titanium oxide adsorption is commonly used to decontaminate Sr and Co. One of adsorbents is "READ-Sr", which will be used for the treatment of low level liquid waste at the Tokai Reprocessing Plant in Japan. An investigation of its applicability to the decontamination of Sr from the contaminated water containing seawater suggested that titanium oxide adsorb other alkaline earth elements those are abundant in seawater[2]. Therefore, selectivity of Sr from other alkaline earth elements is necessary.

We synthesized a new titanium oxide with titanium sulfate and ammonium solution, and obtained distribution coefficient (K_d) of Sr, and separation factor (SF) between Sr and alkaline earth elements by batch method. And then the titanium oxide was added to the radioactive water after co-decontamination of transition metals and Cs. This mixture was stirred for 45 minutes and filtrated with 0.1 μm membrane, and then decontamination factor (*DF*) was calculated from concentration of each radioactive and non-radioactive elements.

On experiment of radioactive water, Sr, Mn, Co and Sb was successfully decontaminated, and their *DF*s were >16, 460, 260, 230, respectively. But Mg and Ca were adsorbed to titanium oxide; particularly Ca was adsorbed as much as Sr. Selectivity of Sr to alkaline earth elements is important to reduce secondary waste, so further improvement is necessary.

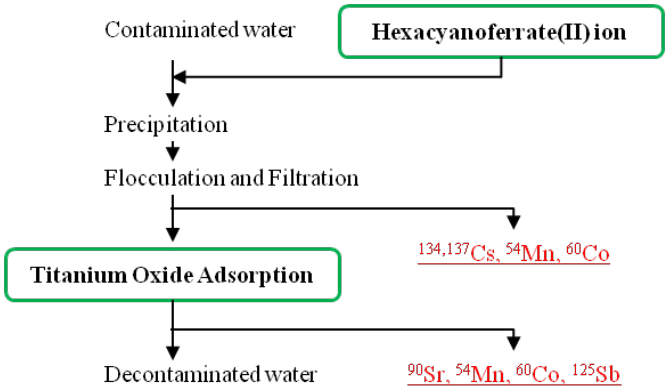

Figure 1. Schematic flow of a new decontamination process

[1] Decontamination of radioactive liquid waste with hexacyanoferrate(II), Takahatake et. al., Procedia Chemistry , 7: 610-615 (2012)
[2] Strontium decontamination from the contaminated water by titanium oxide adsorption, Takahatake et. al., Proceedings of International Conference on Toward and Over the Fukushima Daiichi Accident (GLOBAL 2011), CD-ROM. (2011)

ACKNOWLEDGEMENTS

The authors would like to thank Masashi Kaneko, Kaname Kubo and Jun Hashimoto of Fuji Sangyo KK for synthesizing titanium oxide.

APSORC'13 - 5th Asia-Pacific Symposium on Radiochemistry
Kanazawa, Japan, 22-27 September 2013

Iodine-129 in the aquatic environment adjacent to a spent nuclear fuel reprocessing plant, Rokkasho, Japan

Shinji Ueda[1], Hideki Kakiuchi[1], Hidenao Hasegawa[1]
Naofumi Akata[1], Hidehisa Kawamura[2], Shun'ichi Hisamatsu[1]
[1] Department of Radioecology, Institute for Environmental Sciences, 1-7 Rokkasho, Aomori 039-3212, Japan
[2] Kyushu Environmental Evaluation Association, 1-10-1, Higashi, Fukuoka 813-0004, Japan

Abstract – The spent nuclear fuel reprocessing plant in Rokkasho, Aomori Prefecture, Japan, has been undergoing final testing since March 2006. Iodine-129 is one of radionuclides released into the atmosphere and the coastal water by the operation of the plant. We measured the concentrations of ^{129}I in various environmental samples such as water, sediment, and aquatic biota collected in the aquatic environment adjacent to the reprocessing plant from 2005 to 2012. The concentration of ^{129}I in the environmental samples increased during testing of the chemical separation of dissolved fuel. Since the end of that stage, the ^{129}I concentration in lake water and aquatic biota samples has been rapidly decreasing, whereas the concentration in sediment samples has remained steady.

Keywords – iodine-129, spent nuclear fuel reprocessing plant, water, sediment, aquatic biota

I. INTRODUCTION

Japan's first commercial spent nuclear fuel reprocessing plant, which is in Rokkasho, Aomori Prefecture (Fig. 1), is undergoing final testing. Since the cutting and chemical separation using actual spent nuclear fuel started in March 2006, small amounts of radionuclides (^{85}Kr, ^{3}H, ^{129}I, and ^{14}C) have been released into the atmosphere and the Pacific Ocean. Iodine-129 released from the plant into the atmosphere and the ocean enters Lake Obuchi, which is adjacent to the plant (Fig. 1), through various routes: from the ocean by tides, from river water, and from the atmosphere by deposition.
The aim of this study was to investigate the fluctuations of ^{129}I concentrations in water, sediment, and aquatic biota samples collected in the aquatic environment, mainly in Lake Obuchi, from 2005 to 2012.

II. MATERIALS AND METHODS

Water was sampled from five locations (Sts. 1–5), and sediment from two locations (Sts. 2, 3); samples from aquatic biota (fish, seagrass, shellfish, shrimp, and plankton) were collected from the lake in an area near the north shore (Fig. 1). The samples were analyzed for ^{129}I with an accelerator mass spectrometer (PRIME Lab, Purdue University, USA).

III. RESULTS AND DISCUSSION

The concentrations of ^{129}I in the water samples collected from Lake Obuchi during 2006 to 2008 were approximately an order of magnitude higher than the background level in 2005, whereas the concentrations in the seawater samples collected off the Rokkasho coast (St. 5) showed no increase over the background level during the study period. The ^{129}I concentrations in aquatic biota samples during 2006 to 2008 were also approximately one order of magnitude higher than the background level. Most of the chemical separation of fuel material was finished by 2008, and the rate of ^{129}I release from the plant markedly decreased thereafter. Corresponding with the decrease in the release rate, the ^{129}I concentrations in the lake water and aquatic biota samples rapidly decreased after 2008. In contrast, the ^{129}I concentrations in the sediment samples were stable even after the chemical separation was finished.
The committed effective dose due to annual ingestion of foods with the maximum ^{129}I concentration in the biota sample in Lake Obuchi was calculated as 6.7 nSv y^{-1}.

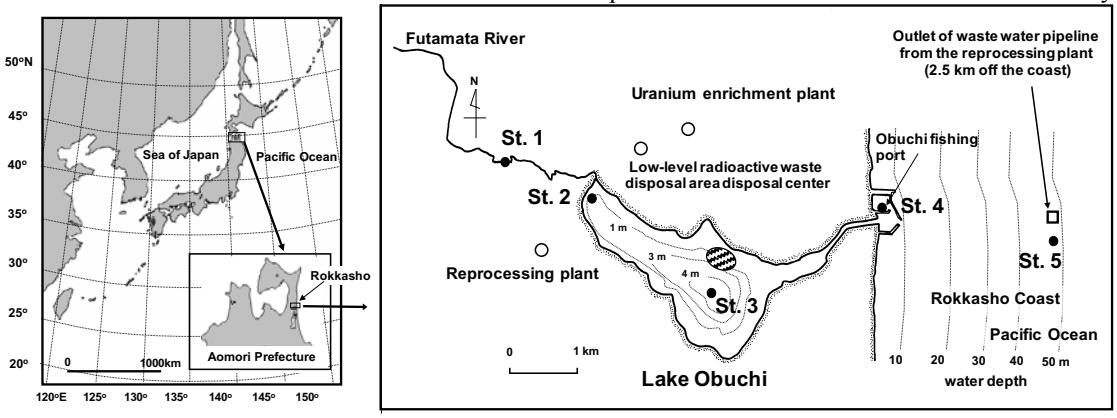

Fig. 1. Map of the sampling stations. Aquatic biota samples were collected in the hatched area.

This study was performed under a contract with the government of Aomori Prefecture, Japan.

APSORC'13 - 5th Asia-Pacific Symposium on Radiochemistry
Kanazawa, Japan, 22-27 September 2013

Specific activity and time dependence of radionuclides in soils affected by the accident of the Fukushima Dai-ichi nuclear power plant (Part 2).

Tatsuya Shimasaki[1], Yoshioki Shiraishi[1], Osamu Kawahara[1], Kumiko Goto[1], Masako Shimamoto[1],Akihiro Kojima[1] and Seiji Okada[2]
[1]Institute of Source Development and Analysis, Kumamoto University
[2]Center for AIDS Research, Kumamoto University

Abstract – The purpose of this study is to clear the specific activity and the time dependence of the radionuclides in soils at Fukushima prefecture and neighborhood area. We performed soil sampling for six times at several points within 60km from FDNPP and at Tokyo to October 30, 2012 from March 23, 2011. The concentration of ^{131}I, ^{134}Cs, ^{136}Cs, ^{137}Cs and ^{129m}Te were obtained, but only trace amounts of ^{95}Nb, ^{110m}Ag and ^{140}La were detected whitch were too low to provide accurate concentrations. The concentration of radioactivity on March 15, 2011 is 8234 kBq/m^2 for ^{131}I and 882 kBq/m^2 for ^{137}Cs at Fukaya, Iitate village. Some radionuclides, such as ^{103}Ru, and ^{106}Ru and ^{140}Ba, observed in the Chernobyl accident, were not measured in the soil samples. This is estimated that mainly noble gasses and volantile radionuclides were released from FDNPP. For the time dependence of ^{137}Cs concentration in soil, it was decreased approximately 30% in 19 months at Fukaya, Iitate village. However, at some sampling points, there was not a change at all.

Keywords – Fukushima Dai-ichi N, ^{137}Cs, specific activity, time dependence, ^{134}Cs

I. INTRODUCTION

The Fukushima Dai-ichi Nuclear Power Plant (FDNPP) lost all electricity due to a huge tsunami after the Richter-scale magnitude 9 earthquake of March 11, 2011. The water circulation system was severely damaged, and the radionuclides were released to the environment, specially for days in the middle of March. The purpose of this study is to clear the specific activity and the time dependence of the radionuclides in soils at Fukushima prefecture and neighborhood area.

II. MATERIALS AND METHODS

We performed soil sampling for eight times at several points within 60km from FDNPP and at Tokyo from March 23, 2011 to October 30, 2012. Soil samples, at 0-2, 0-3, 3-6 and 6-10 cm depths, were taken using a scraper with a sampling area of 100cm^2 (10cm×10cm). The second and the subsequent sampling were carried out at 3 m intervals from the previous sampling points. The specific activity of samples were measured by Ge detectors (SEIKO EG&G) and decay corrected to March 15, 2011.

III. RESULTS AND DISCUSSION

Specific activity in soils

We were taken soil samples in Iitate village, Fukaya , on March 23, 2011. The concentration of ^{131}I, ^{134}Cs, ^{136}Cs, ^{137}Cs and ^{129m}Te were obtained, but only trace amounts of ^{95}Nb, ^{110m}Ag and ^{140}La were detected whitch were too low to provide accurate concentrations. Some radionuclides, such as ^{103}Ru, and ^{106}Ru and ^{140}Ba, observed in the Chernobyl accident, were not measured in the soil samples. This is estimated that mainly noble gasses and volantile radionuclides were released from FDNPP. The concentration of radioactivity on March 15, 2011 is 8234±1654 kBq/m^2 for ^{131}I and 882±182 kBq/m^2 for ^{137}Cs at Fukaya, Iitate village. The highest difference was more than 100 times in Fukusima. Only ^{137}Cs from global fallout was observed in the soil collected at kumamoto city. The ratio of the total amounts of ^{137}Cs in each section depth was shown in Fig.5. Approximatery 95% of deposited ^{137}Cs were found in the upper 3 cm of the soil. The ratio of the depth profiles did not change at all sampling points during the measurement period.

Time dependence of radionuclides in soils

Fig.1 shows the temporal changes of ^{137}Cs concentration in soil at several sampling points during from March 23, 2011 to October 30, 2012. For the time dependence of ^{137}Cs concentration in soil, it was decreased approximately 30% in 19 months at Iitate village, Fukaya district. It was decreased approximately 20% in 15 months at Minamisouma city. However, at some sampling points, there was not a change of the time dependence of ^{137}Cs concentration at all. For the environment half life of the cesium-137 in the comparatively land with a little vegetation, it was with the range for four years from two years except a physical half life.

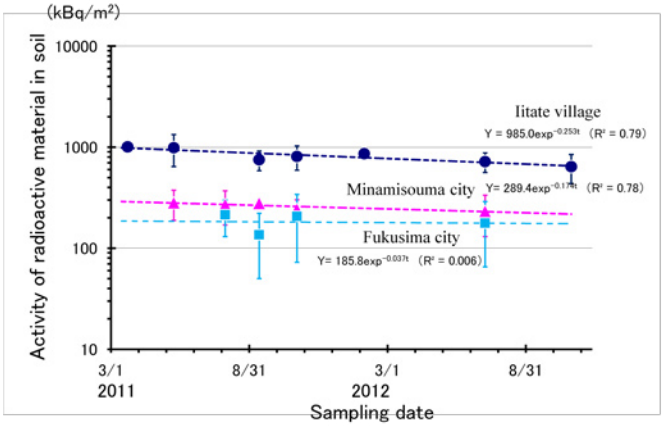

Fig. 1 The temporal changes of ^{137}Cs concentration in soil at several sampling points during from March 23, 2011 to October 30, 2012.

APSORC'13 - 5th Asia-Pacific Symposium on Radiochemistry
Kanazawa, Japan, 22-27 September 2013

Differences between year 2011 and 2012 in Cs-137 concentration in brown rice grown in Fukushima Prefecture

Shigeto Fujimura[1,2], Yuuki Sakuma[1], Toshimi Yamauchi[1], Kazutoshi Niitsuma[1], Norio Sato[3], Mutsuto Sato[1], Takashi Saito[1], Kunio Yoshioka[1]
[1]Fukushima Agricultural Technology Centre, [2] NARO Tohoku Agricultural Research Center
[3]Inawashiro Town

Abstract – Brown rice was collected from ten paddy fields located in four sites in Fukushima Prefecture in year 2011 and 2012 to clear the year difference in radiocesium concentration in brown rice. Paddy fields with the same management including fertilization in both years were selected. Cs-137 concentration in brown rice was in the range of 2.8-290 Bq kg^{-1} in 2011 and 1.3-160 Bq kg^{-1} in 2012. The concentration of Cs-137 was decreased by 40 % in the average from year 2011 to year 2012.

Keywords – brown rice, Cs-137, paddy field, aging

I. INTRODUCTION

Radionuclides was released into the environment as a consequence of the accident at Fukushima Daiichi Nuclear Power Plant (FNPP) that was triggered by the earthquake and subsequent tsunami that occurred on 11 March 2011. Brown rice (unpolished rice) produced during the 2011 growing season was contaminated by radiocesium released from FNPP. Concentration of radiocesium in agricultural products is annually declined because radiocesium is fixed to sorption site for cesium of soil. In addition, potassium and/or zeolite was applied to farmland in Fukushima Prefecture to avoid the contamination of radiocesium to brown rice in the year 2012. In the results, concentrations of radiocesium in brown rice were much lower in the year 2012 than in the year 2011. The aim of this study is to clear the annually declined effect on the concentration of brown rice to evaluate the effects of potassium and zeolite application on uptake of radiocesium by crops.

II. MATERIALS AND METHODS

A. Brown rice sampled

Rice was grown in ten paddy fields in four sites (Aizu Bange, Inawashiro Koriyma and Nihonmatsu) located in Fukushima Prefecture during the year 2011 and 2012. Management including fertilizer followed the conventional practices in each site in both year except in Aizubange and Inawashiro. In these two sites, potassium had not been applied more than ten years in one paddy field and practical fertilizer had been applied in another one. Brown rice was sampled from the paddy fields in the year 2011 and 2012.

B. Measurement of Cs-137 concentration

The concentration of Cs-137 was determined using a germanium detector with a multichannel analyzer system. The actual decay date was determined as October 1, 2011, using the half-life (i.e., decay constant) of the Cs-137. Brown rice was dried for 48 h at 105 °C and dry weight was determined.

III. RESULTS AND DISCUSSION

Concentration of Cs-137 in brown rice investigated in this study was in the range of 2.8-290 Bq kg^{-1} in 2011 and 1.3-160 Bq kg^{-1} in 2012 (Table 1). There were differences in the concentration of Cs-137 between paddy fields in the same site in both years. The differences between paddy fields in the same sit would be due to the differences in exchangeable potassium content and/or the sorption sites for cesium in soil. The details will be published else where.

The concentration of Cs-137 in brown rice was 30-114 % in 2012 compared to those in 2011. It was increased in one of ten paddy fields. The concentration of Cs-137 in brown rice was decreased by 40 % in the average from year 2011 to year 2012. It was suggested that uptake of radiocesium by rice plant in the second year from the radiocesium contamination is a half of that in the first year without decontamination nor the application of potassium, zeolite and so on.

Table 1. Concentration of Cs-137 in brown rice.

Site	No.	Concentration of Cs-137 (Bq kg^{-1} dw)		2012 / 2011 (%)
		2011	2012	
Aizu Bange	1	22	10	48
	2	3.3	2.0	61
Inawashiro	1	17	19	114
	2	3.8	3.1	82
Koriyama	1	2.8	1.3	48
Nihonmatsu	1	200	160	80
	2	290	160	56
	3	130	50	41
	4	61	26	42
	5	74	22	30
Maximum		290	160	114
Minimum		2.8	1.3	30
Average		29	16	60

Geometric average is shown for the concentration of Cs-137.

APSORC'13 - 5th Asia-Pacific Symposium on Radiochemistry
Kanazawa, Japan, 22-27 September 2013

Size-distribution of airborne radioactive particles from the Fukushima Accident

H. Muramatsu[1], K. Kawasumi[1], T. Kondo[1], and K. Matsuo[2]
[1] Department of Chemistry, Faculty of Education, Shinshu University, Nishinagano, Nagano-shi, Nagano 380-8544, Japan
[2] Graduate School of Education, Shinshu University, Nishinagano, Nagano-shi, Nagano 380-8544, Japan

Abstract –The particle size distribution of radioactive aerosols has been observed using the Andersen-type classifier combined with a high volume air sampler. Estimated AMADs of ^{131}I-, ^{134}Cs- and ^{137}Cs-aerosols were ranging from 0.56 to 0.60 μm, which were larger than that of ^{7}Be-aerosols, about 0.2 μm.

Keywords – particle size distribution, radioactive aerosols, airborne radionuclide, nuclear power plant accident

INTRODUCTION

The release of radioactive materials from the Fukushima I nuclear power plant accident brought about seroius and wide contaminations in the area of northeastern Japan. Released radioacive materials from the reactors would migrate as radioactive aerosols, attaching to non-radioactive aerosols suspended in the surface air and being affected by a transport of air masses which is somewhat complex and strongly depends on the distribution of high and low atmospheric pressure regions around the Japanese Islands. In this report, we describe the results of radioactivity measurements in the region far from the site where the present nuclear accident had occurred. Especially, are shown the results obtained in the experiment done by using a high-volume cascade impactor to estimate the size distribution of aerosols attached by fission products.

EXPERIMENTAL

Air samplings were carried out at the sampling station on the roof of the building (height above ground level 12 m) located in our university campus (36º39′N, 138º12′E). Suspended particles attached by fission products were collected by using the Andersen-type classifier combined with the high volume air sampler (Model AH-600). The sampler is a jet cascade impactor consisting of five multi-jet stages (including a backup stage) and a filter, vertically stacked, designed for use at a flow rate of 566 L/min, and it can collect the particles classified into five sizes from 1.1 μm to 7.0 μm.

RESULTS AND DISCUSSION

The sampling was carried out at the sampling station from April 7 to April 24, during 17 days, with the flow rate of 566 L/min and the total volume of 138400 m^3. Aerosol particles were classified and collected on four glass fiber filters, and on a back-up filter for aerosols smaller than 1.1 μm in diameter. About 60% of collected activities were found on the back-up filter, which means that the majority of radioactivity would attached to aerosols with the diameters less than 1.1 μm. This tendency is much more remarkable for the case of ^{7}Be-aerosols, which is formed through attaching by the cosmogenic radionuclide of ^{7}Be and whose size distributions have been measured by using the same manner mentioned below during a couple of years.

In order to estimate a size distribution and a mean particle diameter, we used only three data, which the particle-size range is neatly known, that is, corresponding to particle-size ranges of 3.3-7.0, 2.0-3.3 and 1.1-2.0 μm. Under the assumption that the particle size distribution of radioactive aerosols in surface air is in a *lognormal* and *unimodal* distribution, the cumulative probability was plotted against the particle diameter, as is shown in Fig.1. Activity Median Aerodynamic Diameter (AMAD) was estimated by the value when the cumulative probability is 50%. Estimated AMADs of ^{131}I-, ^{134}Cs- and ^{137}Cs-aerosols were ranging from 0.56 to 0.60 μm, which were larger than that of ^{7}Be-aerosols, around 0.2 μm.

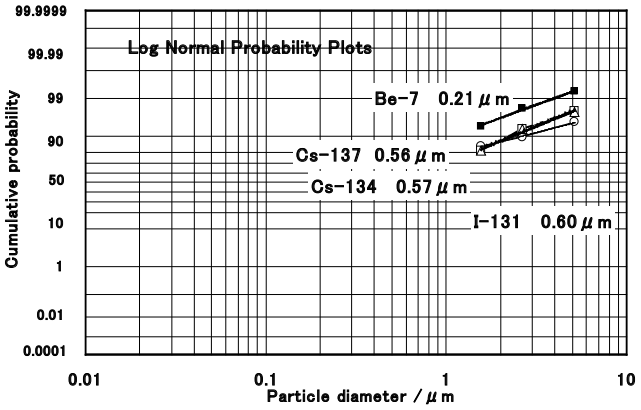

Fig.1 Probability plot for the cumulative percent as a function of aerosol particle diameter.

According to the physical characteristics reported by Whitby for sulfur aerosols [1], the geometric mean radii of 0.57, 0.60, and 0.56 μm for ^{131}I-, ^{134}Cs- and ^{137}Cs-aerosols, respectively, seem to belong to the *accumulation mode* whose mean value is (0.48 ± 0.1) μm. Beyond the difference in origin and chemistry between cosmogenic ^{7}Be and fission products of ^{131}I, ^{134}Cs and ^{137}Cs, what controls mean radius of radioactive aerosols is not clarified yet. It is surely considered that the difference in the formation and growth of both radioactive aerosols would be important.

[1] Whitby, K. T., Atmos. Envir. **12**, 135-159 (1978).

APSORC'13 - 5th Asia-Pacific Symposium on Radiochemistry
Kanazawa, Japan, 22-27 September 2013

Long-term effects of radionuclides originating from the Fukushima nuclear power plant accident in airborne particulate matters in Kawasaki

Ko Nakamachi[1], Hirotaka Matsuno[1], Teruyuki Honda[1], Yoshikazu Kikawada[2]
[1] Graduate School of Engineering, Tokyo City University
[2] Faculty of Science and Technology, Sophia University

Abstract – This study is intended to elucidate the long-term effects of atmospheric radioactive cesium in Kawasaki City, Kanagawa. As a result, it became clear that the radioactive cesium activity concentration in December 2012 had decreased to about 1/10^5 of that observed immediately after the Fukushima Daiichi nuclear power plant (FDNP) accident in March 2011 and sulfate aerosols may act as a carrier and transport radioactive cesium.

Keywords – Fukushima Daiichi nuclear power plant accident, radioactive cesium, carrier, airborne particulate matters, Kawasaki

I. INTRODUCTION

The FDNP accident was caused by the Great East Japan Earthquake, which occurred on March 11, 2011. The artificial radionuclides ^{131}I, ^{134}Cs, and ^{137}Cs were detected in the Kanto region.

In this study, we focused on ^{131}I, ^{134}Cs, ^{137}Cs, and other radionuclides contained in airborne particulate matters (APM) sampled from filters in the Atomic Energy Research Laboratory of Tokyo City University located in the west of Kawasaki City, Kanagawa, which is about 250 km south-southwest from the FDNP.

The aim of this study was to determine the time series of the radioactive decay and the atmospheric dispersion of the artificial radionuclides by γ-ray spectrometry. Moreover, because we have been sampling the APM continuously from before the FDNP accident, we can compare the results before and after the FDNP accident.

II. METHODS

After sampling the APM from the filters, we compressed the filter into an acrylic case to measure the γ-rays. A high purity germanium semiconductor detector was used for the analysis. The measurements were carried out for 80,000 s. The Seiko EG&G spectrum navigator environmental analysis program was used for nuclide analysis.

III. RESULTS AND DISCUSSION

Immediately after the accident at the FDNP in March 2011, ^{95}Nb, ^{97}Nb, ^{110m}Ag, ^{129}Te, ^{129m}Te, ^{131}I, ^{134}Cs, and ^{137}Cs were detected. The activity concentrations of ^{131}I, ^{134}Cs, and ^{137}Cs immediately after the accident were 1.66, 0.61, and 0.60 Bq/m^3 respectively, and the ^{131}I/^{137}Cs activity concentration ratio was 2.78. The time series of the radioactive cesium activity concentration after the FDNP accident is shown in Fig. 1. The ^{134}Cs and ^{137}Cs activity concentration in December 2012 had decreased to about 1/10^5 of the activity concentration observed immediately after the FDNP accident. Sulfate aerosols can act as carriers of radioactive cesium. Because sulfates are formed from sulfur dioxide in the atmosphere, we indirectly examined the relationship between radioactive cesium and sulfate by comparing the activity concentration of radioactive cesium and the sulfur dioxide levels recorded by the Kawasaki pollution monitoring center. The fluctuations in the radioactive cesium concentration were similar to the fluctuation in the sulfur dioxide concentration. This finding suggests that sulfate acts as a carrier and transports radioactive cesium.

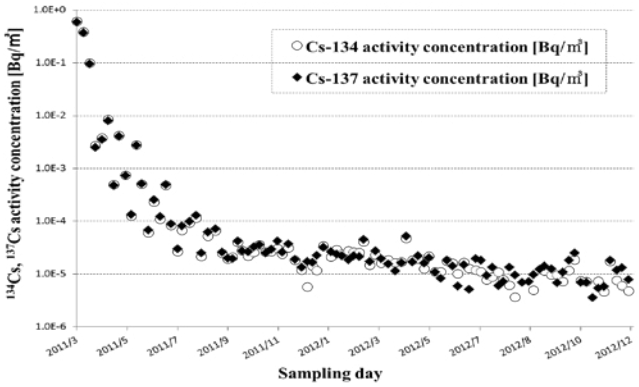

Fig.1 Time series of ^{134}Cs and ^{137}Cs activity concentration in Kawasaki

IV. CONCLUSION

(1) Immediately after the accident at the FDNP in March 2011, ^{95}Nb, ^{97}Nb, ^{110m}Ag, ^{129}Te, ^{129m}Te, ^{131}I, ^{134}Cs, and ^{137}Cs were detected.

(2) The activity concentrations of ^{131}I, ^{134}Cs, and ^{137}Cs immediately after the FDNP accident were 1.66, 0.61, and 0.60 Bq/m^3, respectively, and the ^{131}I/^{137}Cs activity concentration ratio was 2.78.

(3) The ^{134}Cs and ^{137}Cs activity concentration in December 2012 had decreased to about 1/10^5 of the activity concentration observed immediately after the FDNP accident (March 2011).

(4) The fluctuation in the radioactive cesium activity concentration was similar to the fluctuations in the sulfur dioxide concentration; therefore, sulfate aerosols may act as a carrier and transport radioactive cesium.

APSORC'13 - 5th Asia-Pacific Symposium on Radiochemistry
Kanazawa, Japan, 22-27 September 2013

Measurement of Iodine-129 concentration in water samples in relation with Fukushima Daiichi Nuclear Power Plant accident

Hiroyuki Matsuzaki[1], Hironori Tokuyama[1], Yasuto Miyake[1], Maki Honda[2], Takeyasu Yamagata[3], Yasuyuki Muramatsu[4]

[1]Department of Nuclear Engineering and Management, School of Engineering, The University of Tokyo, Japan
[2] Graduate School of Integrated Basic Sciences, Nihon University, Japan
[3] College of Humanities and Sciences, Nihon University, Japan
[4] Department of Chemistry, Gakushuin University, Japan

Abstract – Iodine-129 (^{129}I) concentration in several water samples were measured by means of Accelerator Mass Spectrometry and discussed in relation with Fukushima Daiichi Nuclear Power Plant (FDNPP) accident. ^{129}I concentration of river waters collected Iitate village and Minami-Soma city (North to North-west of FDNPP) showed as high as $1.0 \cdot 10^9$ atoms/L and had not vary significantly during period from March to October, 2012. The combination of $^{129}I/^{127}I$ ratio and ^{127}I concentration of these water samples can be explained as mixture of fossil rain water (ground water) and the rain radioactively contaminated by FDNPP accident.

Keywords – FDNPP accident, Iodine-129, Accelerator Mass Spectrometry, tap water, environmental water

I. INTRODUCTION

According to Fukushima Dai-ichi Nuclear Power Plant (FDNPP) accident, vast amount of radioactive nuclides including radioactive iodine were spilled out into the environment. A rare isotope Iodine-129 (^{129}I) was also widely distributed in a very short time by the FDNPP accident. ^{129}I directly landing on the soil surface had been trapped in the upper layer of the soil and the depth profile should indicate the migration and the interaction with the soil. If ^{129}I was trapped in the woods, it seems to take rather longer time for landing on the ground. Either way, a certain portion of the ^{129}I should be moving downward and finally washed out by the groundwater or river with a certain rate and transported into the sea. The concentration of ^{129}I in environmental water samples taken from rivers and ponds are considered to reflect the iodine transportation process by the fluvial system.

II. EXPERIMENTAL

River water samples and lake water samples were collected from the South-west region (Abukuma area) and North to North-west region (Minami-Soma city and Iitate village) during the period from April, 2011 to March, 2013. 500mL or 1 L of each water sample was served for analysis. 2mg of iodine carrier was added to water and mixed well in a little reduced condition. Iodine was extracted by the solvent extraction and the back extraction process and precipitated as a Silver Iodide (AgI). Collected AgI was mixed with Niobium powder and pressed into a cathode of Accelerator Mass Spectrometry (AMS). $^{129}I/^{127}I$ ratio was measured at MALT (Micro Analysis Laboratory, Tandem accelerator), The University of Tokyo. An aliquot taken from the water sample before adding carrier was analyzed for iodine concentration by ICP-MS.

III. RESULTS AND DISCUSSION

^{129}I concentration of river waters collected Iitate village and Minami-Soma city (North to North-west of FDNPP) showed as high as $1.0 \cdot 10^9$ atoms/L and had not vary significantly during period from March to October, 2012. This concentration is quite high compared to the pre-accident level ($1\text{-}2 \cdot 10^6$ atoms/L), which was determined from the result of measurement for tap water collected in 2006. The combination of $^{129}I/^{127}I$ ratio and ^{127}I concentration of these water samples can be explained as mixture of fossil rain water (ground water) and the rain radioactively contaminated by FDNPP accident (Fig. 1).

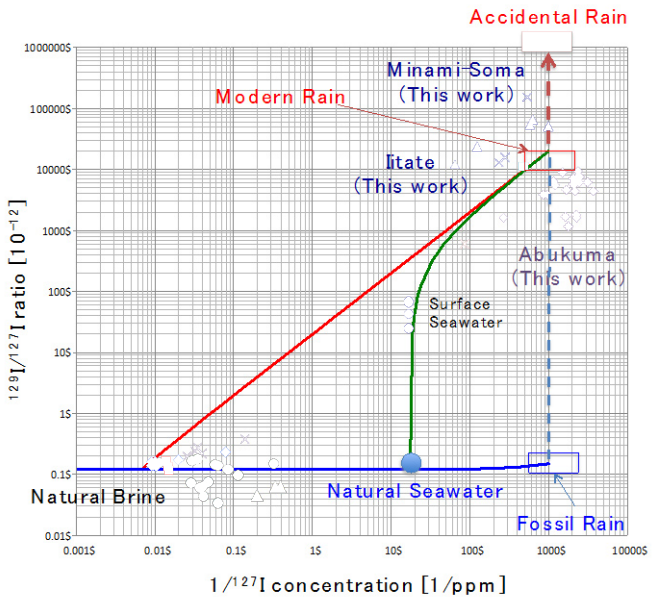

Fig. 1. $^{129}I/^{127}I$ – $1/^{127}I$ plots of several water samples. Lines are the mixing lines between the end members.

Considering the accidental ^{129}I deposition in Northwest of FDNPP ($\sim 1.4 \cdot 10^{14}$ atoms/m^2) and annual precipitation rate (~1300 mm), it is figured out that no more than 1% of total inventory is transported by the river system annually.

APSORC'13 - 5th Asia-Pacific Symposium on Radiochemistry
Kanazawa, Japan, 22-27 September 2013

Observed radioactivities and activity ratios in aerosols from April 2011 at the Geological Survey of Japan, Tsukuba, Japan

Yutaka KANAI[1]
[1]Geological Survey of Japan, National Institute of Advanced Industrial Science and Technology

Abstract – The aerosol monitoring was started at the GSJ, Tsukuba, from the end of March 2011 for the assessment of environmental impact and residents' dose rate. This paper reviewed the obtained data and the geochemical behaviors of natural and artificial radionuclides were studied. Many artificial nuclides derived from the FDNPP accident as well as natural ^{7}Be and ^{210}Pb were observed in this study and the most of them with short half-lives became below the detection limit in June, 2011. Several high concentration peaks of ^{134}Cs and ^{137}Cs were observed after June, and around 10^{-4} Bq/m^3 concentration was estimated as temporal background level. After middle April 2012, it became in half level. The observed $^{134}Cs/^{137}Cs$, $^{136}Cs/^{137}Cs$ and $^{132}Te/^{137}Cs$ activity ratios showed relatively good attenuation corresponding to their half-lives. For ^{131}I and ^{129m}Te, the activity ratios showed a decreasing trend with fluctuations. ^{110m}Ag showed a bigger attenuation rate than its half-life and ^{95}Nb showed increasing trend. The variation of activity ratio with time observed at the GSJ was supposed to depend on particle size, their chemical species, the source, discharge amount, mixing and the transportation processes of nuclides.

Keywords – Radioactivity, Aerosol, the Geological Survey of Japan, Tsukuba, Activity ratio, Natural and artificial nuclides

I. INTRODUCTION

A big earthquake (M. 9.0) and the subsequent tsunami on 11 March 2011 resulted in severe damages to the Fukushima Daiichi Nuclear Power Plant (FDNPP). All the power supply was lost and the luck of cooling system caused the release of a large amount of radioactive nuclides such as ^{131}I and ^{137}Cs into the environment.

We started the monitoring of radionuclides in aerosols at the Geological Survey of Japan (GSJ) in Tsukuba from the end of March, about 20 days after the FDNPP accident, for the purpose of assessing their environmental impacts and the radiation dose for safety of the habitant. In this paper we summarize and focus on the geochemical behavior of artificial radionuclides as well as natural radionuclides using their activity ratios.

II. OBSERVED RADIOACTIVITIES IN AEROSOLS

Tsukuba is located about 170 km south-southwestward from the FDNPP. The radionuclide concentrations observed at the GSJ would be greatly dependent on those emitted from the FDNPP and the climate conditions, because the released radioactive nuclides would move as a plume. ^{95}Nb, $^{99}Mo/^{99m}Tc$, ^{110m}Ag, $^{129m}Te/^{129}Te$, ^{131}I, $^{132}Te/^{132}I$, ^{134}Cs, ^{136}Cs, ^{137}Cs, $^{140}Ba/^{140}La$, ^{141}Ce and ^{144}Ce were main artificial nuclides observed in this study and the most of them with short half-lives became below the detection limit in June, 2011. Several high concentration peaks of ^{134}Cs and ^{137}Cs were observed after June, and around 10^{-4} Bq/m^3 concentration was estimated as temporal background level, which is about 2 orders of magnitude higher level than that before the accident. After middle April 2012, it became in a half level.

III. ACTIVITY RATIOS BETWEEN NUCLIDES

Supposing the nuclear reactions almost stopped at the time of accident, activity ratio of nuclide versus ^{137}Cs should decrease nearly with the half-life of nuclide because that of ^{137}Cs is by far larger. Variations of the activity ratio of ^{134}Cs, ^{136}Cs, ^{131}I, ^{129m}Te, ^{132}Te, ^{110m}Ag and ^{95}Nb versus ^{137}Cs were examined.

The observed macroscopic $^{134}Cs/^{137}Cs$, $^{136}Cs/^{137}Cs$ and $^{132}Te/^{137}Cs$ activity ratios showed relatively good attenuation corresponding to their half-lives, although these nuclides might be released from the different three reactors that might have different activity ratios owing to the different burn-up. As ^{134}Cs, ^{136}Cs and ^{137}Cs are isotopes of the same element, the change and large fluctuation of activity ratio during transport would not occur. The small fluctuation after several months from the accident might suggest complex release and mixing of the source reactors at different situations. The $^{131}I/^{137}Cs$ activity ratio in aerosol showed a decreasing trend with a little fluctuation, and also the tendency of a little higher concentration after 60 d. The change of composition (gas/particle), the release rate and temperature at the reactors, transport processes and their mixing would contribute to the activity ratios. Although ^{129m}Te and ^{132}Te show the decreasing trend, the former showed rather large fluctuation with a high value. There may be complicated processes concerning the older and younger air masses whose $^{132}Te/^{129m}Te$ activity ratios differ from each other because of half-lives. On the other hand, ^{110m}Ag showed a bigger attenuation than that supposed from its half-life, probably owing to its chemistry and the discharge rate. Although ^{95}Nb was emitted in the atmosphere together with other radioactive nuclides in the accident, $^{95}Nb/^{137}Cs$ activity ratio showed increasing trend with time.

It was shown that the activity ratios of artificial nuclides observed at the GSJ might depend on their chemical species, particle size, diversity of the source, change of discharge and the transportation processes of nuclide. These facts would help the better understanding of the reactor conditions in and after the accident in addition to other information.

APSORC'13 - 5th Asia-Pacific Symposium on Radiochemistry
Kanazawa, Japan, 22-27 September 2013

Chemical forms of radioactive Cs in soils originated from Fukushima Dai-ichi nuclear power plant accident, as studied by extraction experiments

Masaaki Hirose[1], Yoshikazu Kikawada[1], Atsushi Tsukamoto[2], Takao Oi[1], Teruyuki Honda[2], Katsumi Hirose[1], Hiroaki Takahashi[3]

[1]Faculty of Science and Technology, Sophia University
[2] Graduate School of Engineering, Tokyo City University
[3]Graduate School of Engineering, Tohoku University

We conducted extraction experiments on soil samples contaminated with radioactive cesium originated from the Fukushima Dai-ichi nuclear power plant (FDNPP) accident in Japan in March 2011. The experimental results suggested that the majority of the radioactive cesium deposited on land surface was first adsorbed on exchangeable sites of clay minerals, and eventually it was strongly fixed in interlayer spaces of some 2:1 clay minerals. The experiment revealed that a very small amount of Cs-137 extractable with acetic acid solution existed in the surface soil layer.

Keywords: radioactive cesium, Fukushima Dai-ichi nuclear power plant accident, sequential extraction, soil contamination.

I. INTRODUCTION

The FDNPP accident in March 2011 resulted in radiological contamination mainly by radioactive Cs widely in Japan. It is highly probable that the behavior of radioactive Cs newly deposited on soils due to the accident is different from that of stable Cs that has existed in soils before the accident, because of the difference in chemical forms between them [1]. In this study, we discuss chemical forms of radioactive Cs in soils originated from the FNPP accident based on the results of extraction experiments conducted for Cs on soil samples.

II. EXPERIMENTAL

We first performed preliminary extraction experiments on some soil samples with various extracting solutions. The contents of Cs-133, the stable isotope of cesium, in the centrifuged/filtered extract solutions were determined.

Based on the results of preliminary experiments, we then performed two-step sequential extraction on a soil sample collected at Toride City, Ibaraki, Japan, which is located about 200 km southwest of the FDNPP and is one of the small radioactive hotspots near Tokyo found after the accident.

The soil core sample, collected with a core sampler (10 cm in diameter and 10 cm in length) in August 2011, was cut with 1 cm width layers. The contents of Cs in the surface layer of the sample were Cs-133, Cs-134, and Cs-137 in the 3.8 μg/g, 1.1 Bq/g, and 1.3 Bq/g , respectively. Five grams of the dried soil (upper three layers) samples were subjected to sequential extraction with 200 mL of 1 M ammonium acetate solution and then 0.11 M acetic acid for 24 hours each. The contents of Cs-133 and radioactive Cs (Cs-134 and Cs-137) in each extract solution were determined with spectrometry respectively.

III. RESULTS AND DISCUSSION

The preliminary experiments revealed that stable Cs in soil was hardly extracted with Milli-Q water and 0.11 M acetic acid, and that only the extractants prepared from ammonium salts could partially extract Cs from the soil samples. This indicates that stable Cs is predominantly extractable from clay minerals with the extractants including ammonium ion by ion exchange process.

Fig. 1 shows the results of the extraction experiments on the Toride soil layer sample. About 10 to 20% of radioactive Cs in the layer samples was extracted with 1 M ammonium acetate solution, while only about 3% of the stable Cs, Cs-133, was extracted. It is likely that the extracted radioactive Cs was incorporated in ion-exchangeable sites of clay minerals. Thus, radioactive Cs has apparently higher mobility than Cs commonly existing in soil. The portion of the radioactive Cs extracted with ammonium acetate solution is higher in deeper layers, which suggests that radioactive Cs has migrated into the deeper layer of the soil *via* ion-exchangeable sites of clay minerals. On the other hand, in the case of acetic acid as extractant, a small amount of Cs-137 was extracted from only the surface layer (0-1cm).

As a whole, more than 70% of radioactive Cs was not extracted by either ammonium acetate solution or acetic acid. A dominant part of radioactive Cs, which was not extracted from present extractants, is probably strongly fixed to interlayer spaces of 2:1 clay minerals.

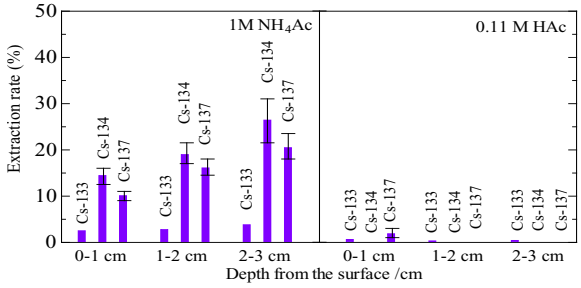

Fig.1 Extraction rates of Cs in the Toride soil sample with NH_4Ac-aq (left) and acetic acid (right).

REFERENCE

[1] Kaneyasu. H. et al, *Environ. Sci. Technol.* **46**, 5720-5726, 2012.

APSORC'13 - 5th Asia-Pacific Symposium on Radiochemistry
Kanazawa, Japan, 22-27 September 2013

Thermal Oxidation of Cesium Loaded Prussian Blue as a Precaution for Exothermic Phase Change in Extreme Conditions

Durga Parajuli, Hisashi Tanaka, Akira Takahashi, and Tohru Kawamoto
Nanosystem Research Institute, AIST, Japan

Abstract – Cesium adsorbed Prussian blue is studied for the thermal oxidation. The TG-DTA shows exothermic phase change of micro aggregates of nano-PB at above 270 ºC. For this reason, Cs loaded PB was heated between 180 to 260 ºC. Heating at 180 removed only the water. Neither the oxidation of Iron nor the removal of cyanide is observed at this temperature. Oxidation of cyanide is observed upon heating above 200 ºC while loaded Cs is released after heating at >250 ºC followed by washing with water. Thermal oxidation between 200 to 220 ºC for more than 2 h showed control on exothermic phase change and loaded Cs is also not solubilized.

Keywords – Prussian blue, Cesium, Exothermic Phase Change

I. INTRODUCTION

Prussian blue (PB), ferric hexacyanoferrate (Fe-HCF), is an inorganic complex, mostly known in the history for its peculiar Cesium (Cs) selectivity.[1] In reference to the PB parent molecule, a number of transition metal hexacyanoferrate are synthesized and named as PB-analogues. The PB forms an open cage structure that possesses a typical zeolytic characteristic, an adjective typically given to any molecule capable of trapping other ions within its lattice cavities.[2] Interestingly, PB, different from the common zeolytic materials, possesses unique selectivity for the Cs-ion. Due to this structural coincidence, PB has become the ultimate Cs-trapper. From Ni-HCF for Cs in alkaline solutions to Cu-HCF for electrochemical removal of Cs or Fe-HCF for neutral to acidic solutions, no materials show high Cs selectivity, faster kinetics, and high capacity like PB-analogues. However, based on the Sax's Dangerous Properties of Industrial Materials some concerns were raised regarding the stability of used HCF analogues during long term storage.[3] Cash et. al. performed extensive study on ferrocyanide storage tanks in Hanford site (USA) for resolving such issues.[4] Their report ruled out all these postulations. Therefore, any speculations on the long-term storage of PB are unlikely. Even so, to ensure the post-use safety of the PB adsorbent for assured long-term storage, we propose the thermal oxidation of the Cs loaded adsorbent prior to the storage.

II. EXPERIMENTAL

As a parent molecule of number of analogues, PB itself is used for the thermal oxidation experiment. For this, PB is loaded with given amount of Cs from pure water or fly-ash extracted solution containing Cs along with high concentration other alkali metals, and other ions. Then it is heated at different temperature. The oxidized sample was washed with water and analyzed for the release of loaded Cs. ICP-MS, TG-DTA, IR, Mossbauer, etc. were used for different analyses.

III. RESULTS AND DISCUSSION

The phase change behavior of PB was studied by taking micro aggregates of PB nanoparticles. The TG-DTA taken with air, Figure 1, Shows the exothermic oxidation at about 272 ºC. Therefore, Cs loaded PB was heated at 180 ºC to 250 ºC. No oxidation of iron or cyanide but only water removal was observed at 180 ºC, while the loaded Cs is released upon washing the PB oxidized at 250 ºC. Heating above 200 ºC is necessary to induce the oxidation. But, the process may get vigorous when heated above 250 ºC. So, optimum oxidation temperature is above 200 ºC and below 250 ºC. Exothermic phase change was disappeared for a sample loaded with 0.2 wt% Cs when heated at 210 ºC for 3 h. Washing this sample after oxidation, Cs release was not observed.

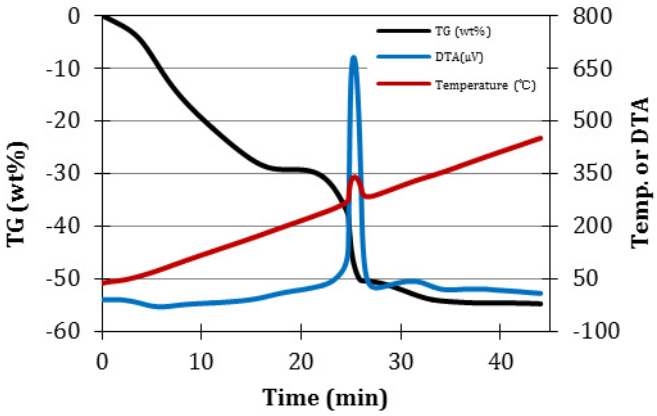

Figure 1. TG-DTA of Cs adsorbed PB taken in air. 10 mg, 10 ºC/min.

References

[1] M.T. Ganzerli Valentini, S. Meloni, V. Maxia, J Inorg. Nucl. Chem., 34, 1427, 1972.
[2] M. Ware, Prussian Blue: Artists' Pigment and Chemist's Sponge. J Chem. Edu., 8,612, 2008
[3] R. J. Lewis, Sr., "Sax's Dangerous Properties of Industrial Materials," Van Nostrand Reinhold (1992).
[4] R.J. Cash, J.E. Meacham, M.A. Lilga, H. Babad, Resolution of the Hanford Site Ferrocyanide Safety Issue. Proceeding of the Waste Management Symposium 1997.

Analysis of ^{134}Cs and ^{137}Cs distribution in soil of Fukushima prefecture and their specific adsorption on clay minerals

A. Maekawa[1], N. Momoshima[2], S. Sugihara[2], R. Ohzawa[1], A. Nakama[1]

[1] Graduate School of Sciences, Kyushu University, 6-10-1, Hakozaki, Higashi-ku, Fukuoka 812-8581, Japan
[2] Radioisotope Center, Kyushu University, 6-10-1, Hakozaki, Higashi-ku, Fukuoka 812-8581, Japan

Keywords – Radiocesium Interception Potential, Fukushima Daiichi Nuclear Power Plant accident

Various kinds of radionuclides were released from the Fukushima Daiichi Nuclear Power Plant (FDNPP) due to the accident that occurred in March of 2011. Of the radionuclides released from the FDNPP, ^{134}Cs and ^{137}Cs are the major radionuclides of concern in radiation dose because of large amounts in deposition on surface soil and their long half-lives. Cs is known to be adsorbed specifically on clay minerals in soil. The strong affinity of clay minerals for Cs is considered to be due to the presence of the frayed edge sites (FES). Cremers et al. (1988) proposed that the strength of the affinity can be explained by the radiocesium interception potential (RIP), which was defined by the product of the FES capacity and Cs-K selectivity coefficient on the FES [1]. The RIP would be usable as an index of the mobility of radiocesium in soil and expected to be used to predict the downward migration of radiocesium.

We collected surface soil samples within 60 km from the FDNPP and analyzed spatial and temporal radiocesium distributions with a Ge semiconductor detector. No large change in vertical distribution pattern of radiocesium has observed on the samples collected in April 2011 and April 2012 at the same location, suggesting strong adsorption of ^{134}Cs and ^{137}Cs on soil (Fig. 1). To confirm the specific adsorption of Cs on clay minerals, we divided the soil into different particle sizes by sieving and sedimentation method and measured the activity in each size fraction. The activity was highest in the clay fraction (< 2 μm) and it tended to decrease as the particle size increased. The RIP measurement was carried out based on the procedure adopted from Wauters et al. (1996) [2]. One g of soil was equilibrated with carrier free ^{137}Cs in a 100 cm^3 of 0.1 mol dm^{-3} $CaCl_2$ and 0.5 mmol dm^{-3} KCl solution. Under the above condition the amount of Cs adsorbed on the FES is negligibly small compared to that of K. A known amount of carrier-free ^{137}Cs was used for the equilibration experiment and the activity of ^{137}Cs in the solution was measured with a NaI scintillation detector for the determination of the solid-liquid distribution coefficient for Cs (K_d^{Cs}). The RIP can be calculated from the K_d^{Cs} and the K concentration in solution. The obtained RIP value ranged 200-1500 mmol kg^{-1} that seemed to be high enough to adsorb ^{134}Cs and ^{137}Cs derived from the accident. The relationship between the RIP and Cs soil depth profile will be discussed.

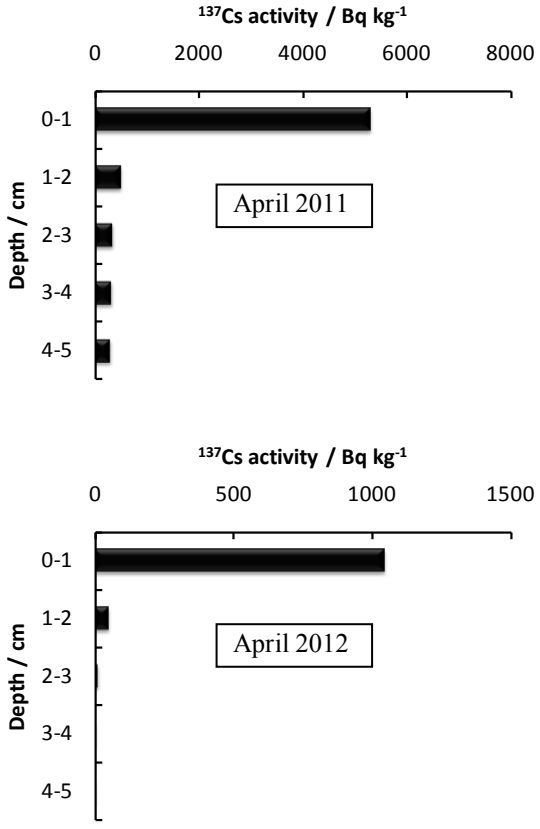

Fig. 1. Vertical distribution of ^{137}Cs in soil collected at the same location (30 km west of the FDNPP) in 2011 and 2012. The concentrations differ but the vertical distribution pattern was similar.

[1] A. Cremers, A. Elsen, P. De Preter, A. Maes, Nature 335, 247-249 (1988)
[2] J. Wauters, A. Elsen, A. Cremers, A. V. Konoplev, A. A. Bulgakov, R. N. J. Comans, Applied Geochemistry 11, 589-594 (1996)

Distribution of radionuclides in seabed sediments off Ibaraki coast after the Fukushima Daiichi Nuclear Power Plant accident

M. Nagaoka[1], H. Yokoyama[1], H. Fujita[1], M. Nakano[1], H. Watanabe[1], S. Sumiya[1]
[1]Nuclear Fuel Cycle Engineering Laboratories, Japan Atomic Energy Agency, 4-33 Tokai-mura, Naka-gun, Ibaraki 319-1194, Japan

Abstract – Various kinds of radionuclides were released into the atmosphere and the sea from the Fukushima Daiichi Nuclear Power Plant of Tokyo Electric Power Co. (TEPCO) by the accident and then reached to the neighboring prefectures. Therefore the accident influence in Ibaraki prefecture was investigated by measuring the concentrations of cesium-134, cesium-137, strontium-90 and plutonium isotopes in seabed sediments. The values for ^{137}Cs ranged from 6.1 to 300 Bq/kg (dry wt) and the ratio of ^{134}Cs/^{137}Cs ranged from 0.48 to 0.77. The highest point of ^{137}Cs concentration was observed at the northernmost station and the concentration was similar to that reported by MEXT[1].

Keywords – seabed sediments, Ibaraki coast, Fukushima Daiichi Nuclear Power Plant accident, cesium-134, cesium-137

I. INTRODUCTION

Various kinds of radionuclides were released into the atmosphere and the sea by the Fukushima accident, and then reached around the Tokai Reprocessing Plant (TRP) located about 120 km south of the Fukushima Daiichi Nuclear Power Plant. The influence of the radioactivity on the environment should be investigated because we have performed the routine environmental radiation monitoring around TRP. In this research, strontium-90, cesium-134 and cesium-137 concentrations in the additional special seabed sediments were measured with plutonium isotopes (^{238}Pu, $^{239+240}$Pu), to find out the accident influence on sea area. Moreover, strontium-90/cesium-137 radioactivity ratio was compared with the ratio before the accident. Finally, each radioactivity distribution in sea area was arranged to acquire the influence of the accident.

II. METHODS

From May to July in 2012, fifty-one Seabed sediments were collected by the Smith–McIntyre sampler set on a monitoring ship. The samples were dried at 105 °C for 3 days and then packed in measurement vessels. Cesium-134 and ^{137}Cs radioactivity concentrations were measured by high-purity germanium semiconductor detectors for 10,000 sec. On the other hand, Strontium-90 and plutonium isotopes were purified by chemical separation and were then measured by a beta gas-flow counter and a silicon semiconductor detector, respectively.

III. RESULTS AND DISCUSSION

Distributions of ^{137}Cs concentration in seabed sediments at each place are shown in Fig. 1(a), (b). Radioactivities of ^{137}Cs ranged from 6.1 to 300 Bq/kg (dry wt) and the ratio of ^{134}Cs/^{137}Cs ranged from 0.48 to 0.77. The concentration of ^{134}Cs and ^{137}Cs before the accident at the sea area in the past 10 years were < DL* and < DL* to 1.0 Bq/kg, respectively. The highest ^{137}Cs concentration was observed at the northernmost station near Kitaibaraki City and was similar to that reported by MEXT [1]. The higher ^{137}Cs concentrations were also observed along the coastal area of Tokai-mura including the mouth of the Kuji River. Therefore, the influence of the Kuji River on sea area should be investigated in detail. Radioactivity concentrations of ^{90}Sr and plutonium isotopes are under measurements.

* DL: detection limit (^{134}Cs:1 Bq/kg, ^{137}Cs:0.8Bq/kg)

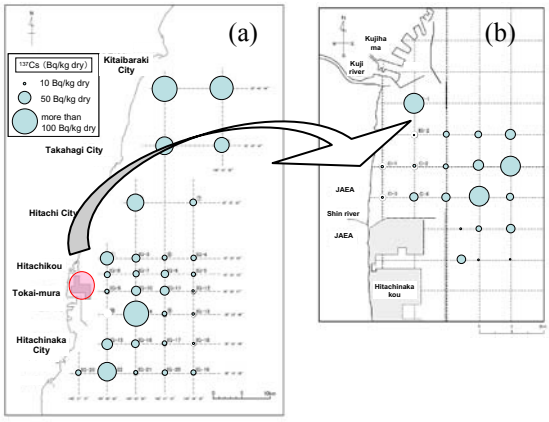

Fig.1 Distribution of ^{137}Cs concentration in seabed sediments of (a) Ibaraki coast and (b) Tokai coast

IV. CONCLUSION

In order to identify the accident influence, distribution of radionuclides in seabed sediments off Ibaraki coast was investigated. Cesium-137 concentrations had more than hundreds times higher than that before the Fukushima accident. Furthermore, the Fukushima accident influence was observed from the ratio of ^{134}Cs/^{137}Cs. The highest point of ^{137}Cs radioactivity was located at the northernmost station.

[1] MEXT, http://radioactivity.mext.go.jp/ja/contents/6000/5704/24/229_so_0710.pdf, Accessed on March 28, 2013.

Radiocesium Concentration Change in Tree Leaves Before and After Defoliation

Shigeo Uchida[1], Keiko Tagami
[1]Office of Biospheric Assessments for Waste Disposal, National Institute of Radiological Sciences

Abstract – Understanding the fate of radiocesium in a tree is of great important to estimate the removal rates of radiocesium. Defoliation is one of the important removal pathways, however, radiocesium might retranslocate from senesced leaves to other tree parts like potassium. In this study, several tree species were measured the cesium-137 concentrations in leaves before and after defoliation. It was found that a portion of radiocesium retranslocate from senesced leaves to other tree tissues; this mechanism will extend radiocesium retention time in trees.

Keywords – Cesium-137, Potassium-40, retranslocation, defoliation

I. INTRODUCTION

Two years after the TEPCO's Fukushima Daiichi Nuclear Power Plant (FDNPP) accident, radiocesium ($^{134+137}$Cs) is recognized as the only major contaminant in the terrestrial environment. Decontamination of houses, public places as well as some agricultural fields have been proceeded, however, forests are difficult to clean up because they occupies large areas in contaminated areas and countermeasures have not been established yet. Thus, radiocesium will be recycled in natural forest ecosystems.

Under these circumstances, it is important to know the reduction rate of radiocesium from a tree to understand the fate in forests after contamination. The most important removal pathway is defoliation; the old leaves fell off with some radiocesium in them so that radiocesium concentrations could decrease with time [1]. However, as it was found for potassium [2] retranslocate to developing tissues or internal stores before defoliation would occur for radiocesium because both elements are in the same group. The mechanism extends the radiocesium residence time in trees. However, there was no data on Cs retranslocation from senesced leaves to green leaves. In this study, therefore, we measured concentrations of radiocesium before and after defoliation to see whether the mechanism was found or not.

II. MATERIALS AND METHODS

Eight species of deciduous trees and evergreen trees were studied in October to November 2011, within the grounds of our institute (NIRS), Chiba Prefecture, Japan. Tree leaves both just after defoliated (senesced leaves) and the green leaves still remained on the tree branches were collected on the same sampling day. They were dried at 80˚C for 3 days at least to obtain constant weight. Each sample mass was 8-22 g on dry weight basis. After drying, each sample was mixed well and transferred into a plastic bottle to measure ^{137}Cs and ^{40}K concentrations with a Ge detecting system (Seiko EG&G). In order to check the stable Cs and K concentration change, a 0.1-g amount of selected leave sample was decomposed with mineral acids and the concentrations were measured by ICP-MS (Agilent 7500a) for Cs and ICP-OES for K (Seiko Vista-Pro).

III. RESULTS AND DISCUSSION

The retranslocate percentage (T_r) is defined as follows

$$T_r=(A_{green}-A_{senesced})/A_{green}x100$$

Where A_{green} is activity concentration of green leaves of a tree (Bq kg^{-1}-dry) and $A_{senesced}$ is activity concentration of fallen leaves of the tree (Bq kg^{-1}-dry). The T_r values of *Somei-yoshino* cherry trees (3 samples from different tree stands) showed 19-49% for ^{137}Cs while 16-40% for ^{40}K. Deciduous tree stands tended to show radiocesium translocation (Tr=0-81%) however, no clear result was found for evergreen tree stands because direct deposition effect on senesced leaves remained. The stable isotope determination results for K agreed well with ^{40}K data, however, the data for radiocesium and stable cesium did not agree due to the above mentioned reason. The T_r values of stable Cs for deciduous tree ranged 0-63%, while less Cs translocation was found for evergreen tree stands (0-17%).

The second year results will be added and discussed at the presentation.

Acknowledgement: This study was partially supported by the Agency for Natural Resources and Energy, Ministry of Economy, Trade and Industry (METI), Japan.

REFERENCES

[1] Tagami, K., Uchida, S., Ishii, N., Kagiya, S.: Translocation of radiocesium from stems and leaves of plants and the effect on radiocesium concentrations in newly emerged plant tissues. J. Environ. Radioactiv. 111, 65-69 (2011).

[2] Ares, A., Gleason, S. M.: Foliar nutrient resorption in trees species. In: New Research on Forest Ecology, Eds. Archibald K.S., pp. 1-32. Nova Science Pub. New York (2007).

APSORC'13 - 5th Asia-Pacific Symposium on Radiochemistry
Kanazawa, Japan, 22-27 September 2013

Distributions and Concentrations of Radionuclides in Giant Butterbur after the Fukushima Nuclear Power Plant Accident

Keiko Tagami[1], Shigeo Uchida[1]
[1]Office of Biospheric Assessment for Waste Disposal, National Institute of Radiological Sciences, Japan

Abstract – Distributions of radiocesium (^{137}Cs) and radioiodine (^{131}I) in giant butterbur (Petasites japonicus) was studied to investigate translocation of these radionuclides. The concentration ratios (on dry weight basis) between petiole and leaf for the first samples (28 March 2011) showed about 0.2 for both isotopes, however, the ratio increased to ca 0.7 for ^{131}I while that for ^{137}Cs was ca. 0.4 by 5 May 2011. The newly emerged shoots showed the concentrations in between.

Keywords – translocation, radioiodine, radiocesium, herbaceous plants

I. INTRODUCTION

Radioiodine and radiocesium released due to the Fukushima Daiichi Nuclear Power Plant (FDNPP) accident were deposited around Kanto Plain, mainly on 20-22 March 2011 with rain [1]. Radionuclide behavior in herbaceous plants after deposition will provide information of radionuclide mobility and uptake from roots and through plant surfaces after emergency situation. Previously, newly emerged part concentrations were reported [2], however, the distribution patterns between old plant parts, which directly affected by deposition, and newly emerged plant part has not been reported yet.

In this study, we focused on giant butterbur (*Petasites japonicus*), which is a herbaceous plant and had already been grown at the time of FDNPP accident occurred. Distributions of radioiodine and radiocesium in this plant will provide us the fate differences between radioiodine and radiocesium after deposition.

II. MATERIALS AND METHOD

Plant samples were collected from 28 March 2011 at NIRS, about 210 km SSW from FDNPP. Newly emerged parts were collected from 13 April to 5 May 2011. The sampled plant parts are shown in figure 1. Immediately after the collection, each parts were cut and mixed well. The radioactivity concentrations were measured with a Ge detecting system (Seiko EG&G). Concentrations of iodine-131 (^{131}I) and cesium-137 (^{137}Cs) in the ground were 4500 and 8300 Bq m^{-2} at 25 April 2011. About 200 days after the first sampling, the concentrations of radiocesium in leaves and petiole samples were collected again, however, due to the low concentrations, the samples were dried to reduce volume.

The samples collected between 28 March to 5 May 2011 were measured in wet weight mass, thus, the concentration was estimated to dry weight mass using the following data.

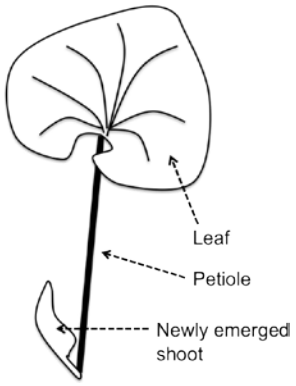

Figure 1. Schematic of giant butterbur sampling parts

III. RESULTS AND DISCUSSION

The average concentration ratios (on dry weight basis) between petiole/leaf for ^{137}Cs and ^{131}I showed 0.42 (0.34-0.51) and 0.59 (0.40-0.76), respectively, for the samples collected between 12 April to 5 May. The ratio for the first sampling date were the same (ca. 0.2), thus these radionuclide translocation showed different increments in the petiole part. The concentrations of ^{137}Cs and ^{131}I in newly emerged shoots were between those of leaves and petioles. Compared to other herbaceous plants, ^{137}Cs concentration in giant butterbur shoots was almost the same after 22 April, thus it was assumed that the root uptake pathway became major by that time. However, the concentration in shoots collected on 13 April was about 2.5 times higher than 22 April sample; probably, translocation from leaf surface to newly emerged shoots would partially affect.

Acknowledgement: This study was partially supported by the Agency for Natural Resources and Energy, Ministry of Economy, Trade and Industry (METI), Japan.

REFERENCES

[1] Ishii, N., Tagami, K., Takata, H. Fujita, K., Kawaguchi, I., Watanabe, Y., Uchida, S.: Deposition in Chiba Prefecture, Japan, of Fukushima Daiichi Nuclear Power Plant Fallout. Health Phys. 104, 189-194 (2013).

[2] Tagami, K., Uchida, S., Ishii, N., Kagiya, S.: Translocation of radiocesium from stems and leaves of plants and the effect on radiocesium concentrations in newly emerged plant tissues. J. Environ. Radioactiv. 111, 65-69 (2011).

The Behavior of Cs Adsorption of Microcapsule Beads Nano-Prussian Blue

Akiko Kitajima[1], Hiroshi Ogawa[1], Kazunori Yoshino[2], Mikihiro Takasaki[2], Hisashi Tanaka[1] and Tohru kawamoto[1]

[1]Nanosystem Research Institute, AIST, 1-1-1 Higashi, Tsukuba, Ibaraki 305-8565, Japan
[2]Kanto Chemical Company Inc., Inari, Soka, Saitama 340-003, Japan

Abstract – A granular cesium adsorbent for column-type decontamination has been developed using Prussian blue nanoparticles with micro-capsule technique (MC-nPB). The MC-nPB shows the extraordinary Cs-adsorption capacity, over 120g(Cs)/Kg(Adsorbent). The lattice constant of MC-nPB was expanded after Cs adsorbed, indicating that Cs cations are adsorbed in the nano-PB crystalline frameworks.

Keywords – Cesium, Cesium adsorbent, Nano-Prussian blue, Microcapsule beads

I. INTRODUCTION

Prussian blue is known as an excellent cesium-ion adsorbent[1-3]. For the decontamination of the radioactive-Cs from the aqueous solution, a column of the adsorbent is quite effective. For the purpose, we have developed the granular adsorbent with Prussian blue nanoparticles by microcapsule technique (MC-nPB). Here we show its quite high adsorption capacity.

II. METHOD

The Cs adsorption properties of MC-nPB were evaluated in a batch adsorption experiment. 12.5 mg of the MC-nPBs were immersed in 10 mL of Cs solution and shaken at 25 °C for 24 h. (solid /liquid ratio = 800 mL/g). The Cs^+ concentration was determined using an inductively coupled plasma mass spectrometer (ICP-MS).

The crystal structure of MC-nPB before and after the Cs-adsorbed is examined by an X-ray diffract meter (XRD). The lattice constant a, b and c were estimated using XRD spectra or miller indices (200) (220) (400) (420) (422) and (440) assuming a cubic structure. The lattice constant a, b and c were refined with WPPF (Whole Powder Pattern Fitting); Pawley Method.

III. RESULTS

Figure 1 shows the Cs-adsorption isotherm of MC-nPB with the 1 mg/L Cs-solution. Over 6 hours, the Cs-adsorption is almost complete. The adsorption rates at 6, 12, and 24 hours are 96.0, 99.0 and 99.9 %, respectively. The adsorption speed is roughly proportional to the solid/liquid ratio.

With the solution with the high Cs-concentration until 500 mg/L, adsorption capacity is determined as the 120 g (Cs) /kg (adsorbent).

Figure 2 shows the XRD patterns of MC-nPB (a), that after 7% Cs-adsorbed (b) and that after 15% Cs-adsorbed (c). Accordingly to these results, a cubic structure shown in a stoichiometric PB was retained even after the Cs-adsorption. In addition, it was observed that the peaks for the Cs 15% adsorbed PB were sifted to be lower degrees compared to that of the MC-nPB. The lattice constants for the MC-nPB, 7% Cs adsorbed and 15% Cs adsorbed were determined as 10.167(4), 10.171(7) and 10.193(4) Å, respectively.

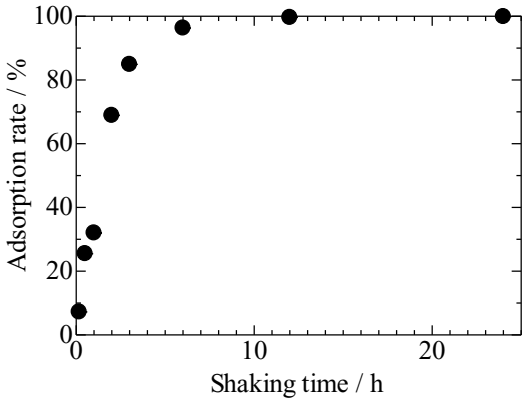

Figure 1 Relationship between Shaking time and Adsorption rate

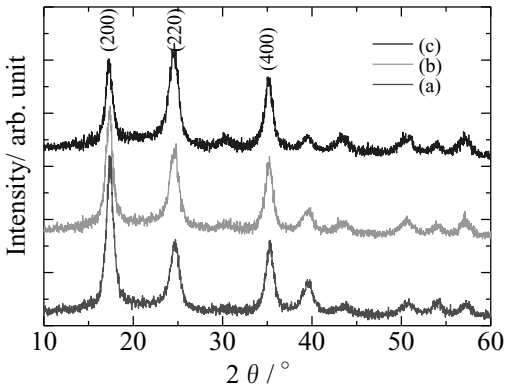

Figure 2 XRD pattern of microcapsule beads nano-PB (a), 7% Cs adsorbed PB (b), and 15% Cs adsorbed PB (c).

REFERENCES

[1] H. Vandenhove, M. Van Hees, S. De. Brouwer, C. M. Vandecasteele, *The Science of Total Environment*, **1996,** 187, 237.
[2] S. Taj, D. Muhammad, M. A. Chaudhry, M. Mazha, *Radional Nucl Chem*, **2011**, 288, 79.
[3] A. Kitajima, H. Tanaka, N. Minami, K. Yoshino and T. Kawamoto, *Chem. Lett.* **2012**, 41,1473

Transfer of Radiocesium from Soil to Cut Flowers

Yasukazu Suzuki[1,2], Hiroyuki Munakata[1], Yutaka Yajima[1], Yosihiro Tooyama[3], Hirokazu Suzuki[1], Hirofumi Tsukada[4], Kazuyuki Inubushi[2]

[1]Fukushima Agricultural Technology Centre, [2] Graduate School of Horticulture, Chiba University
[3]Ken-poku District Agriculture and Forestry Office, Fukushima, Japan , [4]Fukushima University

Abstract – Concentration and transfer factor of radiocesium, which was derived from the Fukushima Daiichi Nuclear Power Plant Accident, from soil to cut flowers was determined. Field experiment was performed in Gray Lowland soil located in Fukushima Prefecture from May to October of 2011 and seven species of plants, gypsophila paniculata, sunflower, chrysanthemum, gentian, lily, dahlia and eustoma, were cultivated. Concentration of radiocesium ($^{134+137}$Cs) in the soil was 1800-4400 Bq kg^{-1} and the range of the transfer factor in the plants was 0.008-0.066, which was within one order of magnitude.

Keywords – cut flower, Fukushima Daiichi Nuclear Power Plant, radiocesium, transfer factor

I. INTRODUCTION

A huge amount of radionuclide was released into the environment at the Fukushima Dai-ichi Nuclear Power Plant accident. Radiocesium, which is major radionuclide, was deposited on the soil and agricultural products were contaminated. Radiocesium is an important radionuclide for the assessment of radiation exposure to the public and also need to know the contamination level of agricultural products for the public relief. Few data available on behavior in soil-cut flower interactions. This study was conducted to clarify the concentration and transfer factor of radiocesium in cut flowers.

II. MATERIALS AND METHODS

Field experiment was performed in Gray Lowland soil located in Fukushima Prefecture from May to October of 2011. The soils was sampling of 0–15 cm depth in five points and mixing. Seven species of cut flowers such as gypsophila paniculata (*Gypsophila paniculata*), sunflower (*Helianthus annuus*), chrysanthemum (*Dendranthema grandiflorum*), gentian (*Gentian triflora*.), lily (*Lilium* × *formolongo*), dahlia (*Dahlia pinnata.*) and eustoma (*Eustoma grandiflorum*) were cultivated in the field experiment. Cut flowers were harvested as when flowering.

After the plants maturing, they were collected from the fields. The samples were rinsed with water, and dried at 80°C for 3 d. The dried samples were pulverized with cutter blender and compressed into plastic vials (U-8). The soil samples were collected after harvesting the cutting flowers, air-dried at 25°C for 10 d, and passed through a 2-mm mesh sieve. The soil samples were also compressed into the plastic vials. The radioactivity of the samples was measured with a germanium semiconductor detector with a multichannel analyzer, over a period of 2,000-48,000 seconds for the plant and 1,200 seconds for the soil samples.

III. RESULTS AND DISCUSSION

The concentration of radiocesium in the soil was 1800-4400 Bq kg^{-1}. The concentration of radiocesium in cut flowers was from 33 to 120 Bq kg^{-1} dry wt, which was 4.0 times differences between the eustoma and gypsophila paniculata. The transfer factor of radiocesium in the seven plant was 0.008-0.066 which was 8.3 times differences between the eustoma and gypsophila paniculata. The transfer factor in cut flowers was a relatively similar order to the reported values in leafy vegetables.[1][2]

[1]http://www.maff.go.jp/j/press/syouan/nouan/pdf/110527-01.pdf (in Japanese)
[2]http://www-pub.iaea.org/MTCD/publications/PDF/trs472_web.pdf

Table 1 Concentration and transfer factor of radiocesium in cut flowers

Cut flower	Sampling day	Radiocesium concentration				Transfer factor
		soils $^{134+137}$Cs	Plants ^{134}Cs	Plants ^{137}Cs	Plants $^{134+137}$Cs	
		(Bq kg^{-1} dry wt)		(Bq kg^{-1} dry wt)		
Gypsophila paniculata	2011/8/18	1800 ± 260	60 ± 32	64 ± 34	120 ± 66	0.066 ± 0.028
Sunflower	2011/7/25	3500 ± 1100	39 ± 21	44 ± 30	84 ± 50	0.024 ± 0.013
Chrysanthemum	2011/8/17	2900 ± 310	20 ± 4.8	24 ± 5.9	44 ± 11	0.016 ± 0.005
Gentian	2011/10/5	3100 ± 170	19 ± 4.6	23 ± 3.9	42 ± 8.0	0.014 ± 0.003
Lily	2011/9/5	3000 ± 350	32 ± 3.3	33 ± 7.2	65 ± 11	0.022 ± 0.003
Dahlia	2011/8/5	4400 ± 880	42 ± 3.3	48 ± 6.4	90 ± 8.9	0.021 ± 0.006
Eustoma	2011/8/16	4400 ± 450	13 ± 4.0	19 ± 3.7	33 ± 7.7	0.008 ± 0.002

Decay correction was done from sampling day. Average ± SD (n = 3).

APSORC'13 - 5th Asia-Pacific Symposium on Radiochemistry
Kanazawa, Japan, 22-27 September 2013

CLEVASOL, a novel radiation hard cation exchanger suitable for treatment of liquid radioactive waste with high salinity

A. Yakushev[1], A. Türler[2], Z. Dvorakova[3], K. von Bremen[2]
[1]GSI Helmholtzzentrum für Schwerionenforschung GmbH, 64291 Darmstadt, Germany
[2]University of Bern, CH-3012 Bern, Switzerland
[3]Neplachova 17, 37004 Ceske Budejovice, Czech Republic

Keywords – cation exchanger, ion selective, radiation resistant, radioactive waste treatment, water purification

I. INTRODUCTION

CLEVASOL is a novel strongly acidic inorganic cation exchanger designed for the purification of aqueous solutions from metal cations, and especially from caesium. This macroporous cation exchange resin has an ultra-high capacity, as well as a very high chemical stability and radiation hardness. The resin is absolutely not soluble in aqueous solutions at pH = 0÷14, and in common organic solvents. In general, the selectivity increases in the order $M^+ < M^{2+} < M^{3+} < M^{4+}$, but CLEVASOL has extremely high selectivity for heavy monovalent cations (caesium(I), silver(I), thallium(I) etc.) and for transition metal cations (e.g., Ni^{2+}, Co^{2+}, Mn^{2+}). High K_D values for cations of *d*-transition metals increase significantly by adding chelating ligands to solution. CLEVASOL has excellent kinetics resulting in high loading capacity and minimal ionic leakage. This product is ideal for use in radioactive waste treatment, water purification and nuclear medicine.

II. STRUCTURE OF CLEVASOL

CLEVASOL has an ionic structure – cations as counter ions are distributed inside of a resin grain. Solid crystal grains of a salt containing the dodecahydro-closo-dodecaborate anion $[B_{12}H_{12}]^{2-}$ are polymerized by cross linking monomeric anions $[B_{12}H_{12}]^{2-}$ to a polymeric anion $[B_{12}H_{(12-x)}L_x]_n^{2n-}$. Each polymeric anion is as big as a single crystal grain. The monomer unit is a regular boron icosahedron with a highly delocalized electron density. The icosahedron itself is a resonance hybrid involving both two-centre two-electron B-B and three-centre two-electron B-B-B bonds. Each boron atom contributes with two valence electrons to the B_{12} cage. The position and distances between monomers are given by the crystal structure of the initial salt.

III. PROPERTIES OF CLEVASOL

CLEVASOL is used usually as a solid cation exchanger loaded with H_3O^+ ions. The determined total ion-exchange capacity of the resin is 5.4±0.2 meq/g. We found that CLEVASOL has a high stability against ionizing radiation. Irradiating the resin with gamma-rays from ^{60}Co, an integral dose of ~$6 \cdot 10^6$ Gray did not cause any changes in the ion-exchange capacity. CLEVASOL is chemically stable and not soluble in concentrated acids, bases, and in common organic solvents. A change of CLEVASOL colour from dark grey to yellow occurs by loading the resin in H^+-form with metal cations (Fig. 1).

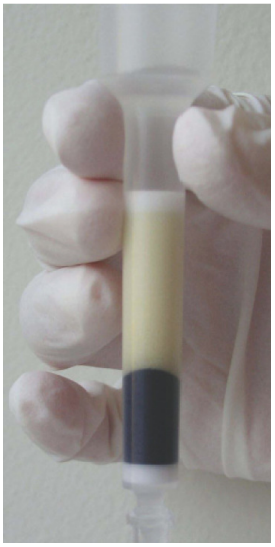

Fig. 1. Colour change from dark grey (H^+-form) to yellow (Na^+-form).

The distribution coefficients (K_D) for the following cations in nitric and/or hydrochloric acid media were determined in batch and column experiments: Na^+, Cs^+, Ag^+, Tl^+, Mg^{2+}, Ca^{2+}, Sr^{2+}, Ba^{2+}, Ra^{2+}, Mn^{2+}, Fe^{2+}, Co^{2+}, Ni^{2+}, UO_2^{2+}, Y^{3+}, Ac^{3+}, Eu^{3+}, Yb^{3+}, Lu^{3+}, Th^{4+} (see Fig. 2). The K_D values usually decrease with increasing the acid or salt concentration. For many cations K_D values obtained with CLEVASOL are significantly higher then values of the common used cation exchanger AG 50W-X8. By adding chelating ligands to solutions containing cations of transition metals, K_D value remains very high (~10^4) even at very high acid concentrations.

CLEVASOL can find application also in nuclear medicine, where ion exchangers are used to separate or purify medical radionuclides. It is especially suited for the separation of heavy monovalent cations (Cs, Tl, Ag) from various cation mixtures. CLEVASOL can be also employed for group separations of mono-, di-, and trivalent cations. Column experiments showed that the chromatographic separation of divalent and trivalent cations is feasible on CLEVASOL, even when one element is present in macro amounts.

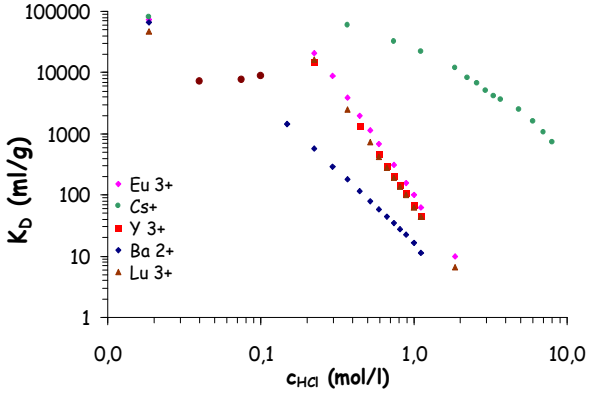

Fig. 2. Distribution coefficients of bi-, trivalent cations and Cs^+ in acid solutions.

APSORC'13 - 5th Asia-Pacific Symposium on Radiochemistry
Kanazawa, Japan, 22-27 September 2013

Estimation of I-131/I-129 ratios and vertical distribution of radioiodine in soil collected from Fukushima Prefecture

N. INAGAWA[1], Y. MURAMATSU[1], T. OHNO[1], T. TOYAMA[1], C. SATOU[2], M. OUTSUKI[3], T. MATSUZAKI[4]
[1]Gakushuin University
[2]Fukushima Agricultural Technology Centre
[3] Tohoku University
[4] University of Tokyo

I-131 was released by the accident of Fukushima Daiichi Nuclear Power Plant. However, due to its short half-life and there are not enough data for this nuclide to understand its dispersal. In this study we determined I-129 (half-life: 1.57×10^7 years) in soil samples by AMS for estimating I-131/I-129 ratios. We also studied vertical distribution of radioiodine in soil and compared it with the profile of radiocesium in soil.

Keywords – I-131, I-129, I-131/I-129 raitos, vertical distribution of radioiodine

I. INTRODUCTION

A severe nuclear accident occurred at Fukushima Daiichi nuclear power plant in March 2011, resulting in the release of enormous amounts of I-131 and Cs-137. Subsequently, soils in Fukushima Prefecture were contaminated. Because radioiodine accumulates in thyroid glands in human body, it is important to obtain data of I-131 in the environment at the time of the accident. However, I-131 was below the detection limit after a few months because its short half-life of 8.02 days. On the other hand, I-129 released simultaneously with I-131 still remained in soil in Fukushima Prefecture, due to its long half-life of 1.57×10^7 years. Therefore, we determined I-129 in Fukushima soil samples in which I-131 concentrations were known, and calculated I-131/I-129 ratios for radioiodine derived from the Fukushima accident.

II. EXPERIMENTALS

The soil sample collected in Fukushima Prefecture after the accident was measured for I-131 and Cs-137 by Ge-detector. Soil samples were dried and pulverized with ball mill. The powdered sample was placed in in a quartz tube and heated at 1000℃ to collect the evaporated iodine in alkaline trap solution (TMAH). Stable iodine (I-127) concentrations in the trap solution were measured by ICP-MS. Solvent extraction was performed using remaining solution, and iodine was separated and purified. Silver nitrate was added to precipitate AgI as a target for AMS and the I-129/I-127 ratios were measured for about 150 samples. For the estimation of I-129 concentrations the I-129/I-127 ratios and I-127 concentrations were used.

III. RESULTS AND DISCUSSION

The observed concentration of I-129 in soil samples showed a wide range, (4.1×10^{-5} to 6.3×10^{-2} Bq/kg). It is interested to note that a good correlation was found between the concentrations of I-131 and I-129. This finding suggests the possibility to estimate previous I-131 levels in soil samples through the analysis of I-129. We obtained an average I-131/I-129 ratio as $(2.1 \pm 0.7) \times 10^7$. However, due to the variations in the data, it is possible that the ratios are different according to the area.

We examined the depth distribution of I-129 and Cs-137 for investigating their behavior in soil. Most of the nuclides were found to be retained in surface soil. If we compare the distribution pattern for these two nuclides, we found that I-129 moved deeper than Cs-137. We also examined different soils such as wheat field, rice field and forest soils. It was found that I-129 did not migrate deeper in rice field (uncultivated) because of its dense nature, while in wheat field (uncultivated) I-129 penetrated deeper due to its high porosity. In case of forest soils, about 90% retained in the layer of leaf litters.

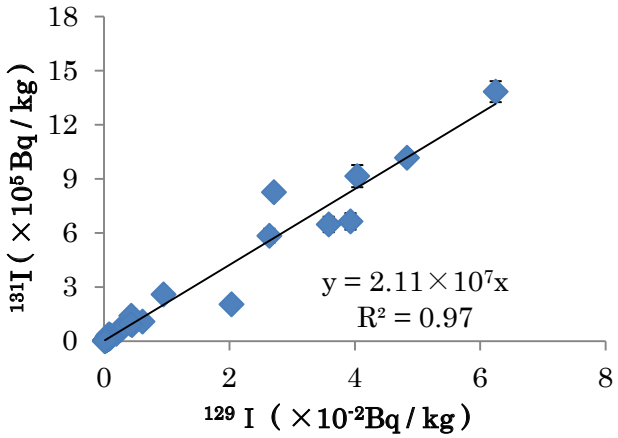

Fig.1 Relationship between the concentration of I-129 and that of I-131

APSORC'13 - 5th Asia-Pacific Symposium on Radiochemistry
Kanazawa, Japan, 22-27 September 2013

Effects of soil types on the transfer of radiocesium to plant

K. ODA[1], Y. MURAMATSU[1], T. OHNO[1], T. KOBAYASHI[2], S. FUJIMURA[2]
[1]Gakushuin University
[2]Fukushima Agricultural Technology Centre

Following the accident of Fukushima Daiichi Nuclear Power Plant, radiocesium was detected in agricultural crops cultivated in Fukushima Prefecture. Although the activity levels in crops significantly decreased in second year, some crops still exceeded the guideline (100 Bq/kg). In this study we cultivate agricultural crops using different types of soils contaminated by the accident and discuss the mechanisms of transfer.

Keywords – radiocesium, soil-plant transfer, agricultural crops

I. INTRODUCTION

Agricultural fields in Fukushima Prefecture were contaminated with radiocesium released from the accident of Fukushima Daiichi Nuclear Power Plant. From a perspective of agricultural safety, Cs-137 (half-life 30.1 y) and Cs-134 (half-life 2.06 y) are very important. Following the accident, radiocesium was detected in many agricultural crops. More than 2 years after the accident, however, some crops still show high concentrations. The mechanisms responsible for the transfer of radiocesium from soil to plants are poorly understood. Therefore, we investigated radiocesium and stable element concentrations in agricultural crops grown in different types of soils. For the purpose of our investigation, soils were collected from the contaminated fields in Fukushima Prefecture. We discuss mechanisms of radiocesium transfer with special reference to the soil characteristics in this study.

II. EXPERIMENTALS

Cultivation experiments using soil that was contaminated with radiocesium were carried out in Fukushima Agricultural Technology Centre and the radiocesium concentrations of both soil and plant samples were determined by a Ge-detector at Gakushuin University. Four different types of soil collected in Fukushima Prefecture were used in our experiments. The plant samples used in these experiments are: komatsuna (a leafy vegetable) and rice plants. The plants were cultivated in Wagner pots (3 L) in a greenhouse at Fukushima Agricultural Technology Centre. Some soils were mixed with contaminated fallen leaves or humus in order to examine whether there is a relationship between the transfer of radiocesium and the organic content of the soils. The soil and plant samples were decomposed with acid to determine concentrations of stable elements by ICP-MS. In addition, we operated extraction experiments with ammonium acetate to verify whether there is any correlation between the extractible radiocesium and the transfer factor to plants.

III. RESULTS AND DISCUSSION

Radiocesium concentrations in both the paddy rice and the komatsuna harvested in this study were found to be influenced by the soil types. The highest values for transfer coefficient were observed in agricultural crops grown in brown forest soils, while the plants cultivated in gray lowland soil showed the lowest values.

In order to compare soils with different radiocesium levels, we collected them from the top layer with high radiocesium concentrations (upper 5 cm) and from the underlying soil with lower concentrations (5–15 cm). We cultivated komatsuna and found that the transfer coefficients of plants grown in the underlying soils are greater than the transfer coefficients of komatsuna planted in the surface soils. This might be related to the speciation of radiocesium in the soils. Deeper layers may have more labile, plant-available radiocesium, while less labile particulate-bound radiocesium from the accident may be more common in the surface soils.

Additionally, we also noted that the transfer coefficients of komatsuna cultivated with the underlying soils mixed with contaminated fallen leaves or humus are higher than the transfer coefficients of komatsuna grown with underlying soils alone. Therefore, we speculate that the radiocesium that exists in organic materials is more mobile, and is subsequently more readily taken up by plants.

As a result of the analysis of stable cesium, we found that komatsuna absorbed more radiocesium than stable cesium. It would seem that stable cesium exists in a less labile form and is adsorbed tightly within the soils, particularly clay minerals.

The extraction experiments show that there is no clear relationship between transfer coefficients and the proportion of radiocesium that is extractable along with potassium using ammonium acetate. Further research should be done another methodologies for extracting plant-available radiocesium from soil.

Temporal distribution of plutonium isotopes in marine sediments off Fukushima and Ibaraki after the Fukushima Dai-ichi Nuclear Power Plant accident

Wenting Bu[1,2], Jian Zheng*[2], Tatsuo Aono[2], Shigeyoshi Otosaka[3], Keiko Tagami[2], Qiuju Guo[1], Shigeo Uchida[2]
[1]School of Physics, Peking University, China
[2]National Institute of Radiological Sciences, Japan
[3]Japan Atomic Energy Agency, Japan

Large amounts of radionuclides were released into the atmosphere as well as discharged into the sea as a consequence of the Fukushima Dai-ichi Nuclear Power Plant (FDNPP) accident caused by the earthquake and subsequent tsunami on March 11, 2011. The radionuclide contamination in the marine environment due to the FDNPP accident is of great public and scientific concern. Radiocesium (^{137}Cs and ^{134}Cs) were detected in the sediment traps in the deep sea in Pacific Ocean one month after the FDNPP accident, indicating the quick incorporating of radiocesium in seawater with the sediments.[1] In the coastal area of Fukushima and Ibaraki, spatial and temporal distributions of radiocesium in the marine sediments from June 2011 to February 2012 were determined.[2,3] Nevertheless, information about the temporal distribution of Pu in the sediments off Fukushima and Ibaraki after the FDNPP accident is limited.

Plutonium isotopes derived from the FDNPP accident have been detected in the soil and liter samples in the 20-30 km zone around the FDNPP, revealing the release of Pu from the accident.[4] In our previous works, we determined the distribution of Pu isotopes in the marine sediments off Fukushima and Ibaraki collected from April 2011 to July 2012, and observed no detectable Pu contamination from the FDNPP accident.[5,6] However, as no information about the Pu isotopes in the discharged liquids from the FDNPP accident is available to date and the release of radionuclides from the FDNPP site continued one year after the accident, Pu contamination in the marine sediments off Fukushima needs continuous investigation.[7]

In this work, we determined vertical distribution of Pu activities and Pu atom ratios (^{240}Pu/^{239}Pu and ^{241}Pu/^{239}Pu) in a sediment core collected from the coastal areas off Fukushima in January 2013. For the analysis of Pu isotopes, ca. 2.0 g dried sediment sample was weighted out and spiked with 1 pg ^{242}Pu as yield monitor. The extraction of Pu was performed in a Teflon tube with 20 mL concentrated HNO_3 on a hot plate at 180-200ºC for at least 4 h. A two-stage anion-exchange chromatographic method was employed for the separation of Pu and for the further purification of Pu prior to the ICP-MS analysis. Combined with our previous results, the temporal distribution of Pu isotopes in marine sediments off Fukushima and Ibaraki will be discussed to understand the source and transport of Pu in the sediments after the FDNPP accident.

Acknowledgments This work was supported by the Agency for Natural Resources and Energy, the Ministry of Economy, Trade and Industry (METI), Japan, and partly supported by the Ministry of Education, Culture, Sports, Sciences and Technology (MEXT) (24110004), Japan.

References

[1] Honda, M. C., Kawakami, H., Watanabe, S. et al., Biogeosciences Discuss., 10, 2455-2477, 2013.
[2] Otosaka, S. and Kobayashi, T., Environ. Monit. Assess, doi:10.1007/ s 10661-012-2956-7, 2012.
[3] Kusakabe, M., Oikawa, S., Takata, H. et al., Biogeosciences Discuss., 10, 4819-4850, 2013.
[4] Zheng, J., Tagami, K., Watanabe, Y. et al., Sci. Rep., 2: 304, doi:10.1 038/srep00304, 2012.
[5] Zheng, J., Aono, T., Uchida, S. et al., Geochem. J., 46, 361-369, 2012.
[6] Bu, W. T., Zheng, J., Aono, T. et al., Biogeosciences Discuss., 10, 643-680, 2013.
[7] Kanda, J., Biogeosciences Discuss., 10, 3577-3595, 2013.

APSORC'13 - 5th Asia-Pacific Symposium on Radiochemistry
Kanazawa, Japan, 22-27 September 2013

Evaluation of Iodine-129 mobility and deposition amount in the soil contaminated by the Fukushima Daiichi nuclear power plant accident

Maki Honda[1], Hiroyuki Matsuzaki[2], Takeyasu Yamagata [3], Yoko (Sunohara)Tuchiya[2], Chuichiro Nakano[2], Yuki Matsushi[4], Yuji Maejima[5], Hisao Nagai[3]
[1]Graduate School of Integrated Basic Sciences, Nihon university, Japan
[2]Department of Nuclear Engineering and Management, School of Engineering, The University of Tokyo, Japan
[3]College Humanities and Sciences, Nihon University, Japan
[4]Disaster Prevention Research Institute, Kyoto University, Japan
[5]National Institute for Agro-Environmental Sciences, Japan

Abstract – Iodine-129 depth profiles of 13 soil cores were analyzed to evaluate the ^{129}I distribution and mobility in soil. The cores were sampled from various fields around the Fukushima Daiichi Nuclear Power Plant (FDNPP). Four cores out of the 13 were collected from almost the same position in Kawauchi village crop field 20 km apart from FDNPP at different times between May 2011 and June 2012 to observe the temporal variation of depth profile of ^{129}I in soil. Clear enhancement of the accidental origin ^{129}I was observed but no positive evidence of ^{129}I migration was found. Other 9 cores were collected from various fields including crop fields and man-made soils within 30 km from FDNPP on June 2012. These cores showed large variation of depth profile of FDNPP origin ^{129}I. The fraction of top 5 cm to the total inventory was varied from 56% to 100%.

Keywords – FDNPP accident, Iodine-129 concentration depth profile, crop field

I. INTRODUCTION

FDNPP accident (on 11 March, 2011) released a large amount of radionuclide into atmosphere such as ^{129}I ($T_{1/2}$= 1.57x10^7 y), ^{131}I ($T_{1/2}$= 8.01d). Subsequently it caused extensive radioactive contamination. Among them, ^{131}I is absolutely essential radionuclide for the estimation of primary dose. However the data on deposition amount and distribution pattern of ^{131}I most contaminated area, is totally lacking because of its short half-life. Through the ^{129}I data, the ^{131}I levels at the time of accident can be estimated [2]. The accidental origin ^{129}I has also a great potential as a geographic and oceanographic tracer [3]. Predominant source of ^{129}I in global environment, including Japan, before FDNPP accident have been two large nuclear reprocessing facilities at Sellafield and La Hauge. They have released ^{129}I totally over 1.03 TBq (7.35x10^{26} atoms) [4] to atmosphere. To evaluate the distribution and the mobility of ^{129}I, it is essential to identify ^{129}I of FDNPP origin from that of previously existed. From this point, crop field is ideal because soil should have been tilled and well mixed by farmers to the depth of around 30cm until just before the FDNPP accident. Therefore it is speculated that the crop field soil had been made homogeneous, so that the direct accumulation from the accident should be clearly observed. This was confirmed by the observations that depth profiles of ^{127}I concentration, as well as carbon content, of these soil cores were roughly constant.

II. EXPERIMANTAL PROCEDURE

Collected column soil was cut into 1.5 or 3 cm layers. The soil sample were first dried by oven (80℃, 48h). Then homogenized well. An amount of about 0.2 or 0.5 g was mixed with V_2O_5 in a ceramic boat and placed in a quartz tube. The sample is then heated at 990℃ under a flow of oxygen gas and water vapor. The evaporated iodine is collected with a trap solution (2% TMAH solution). (Here, an aliquot was separated for ICP-MS for the determination of the stable iodine concentration.) Iodine in the aliquot of trap solution (2-9 mL) with 2-4 mg iodine carrier is purified by a sequential solvent extraction and back extraction and a finally extracted as AgI precipitation. Extracted AgI was dried well and pressed into a cathode of AMS system. ^{129}I was measured at MALT-AMS system, The University of Tokyo.

III. RESULTS AND DISCUSSION

The ^{129}I depth profiles of four cores from Kawauchi village commonly showed particularly high concentration at the top most layer, steep exponential decrease as a depth and constant blow 10 cm depth (Fig. 1). This enhancement in the top 10 cm layer can be considered as the direct accumulation from the FDNPP after the accident. However no positive evidence of ^{129}I migration was found because there was only a small difference among these profiles which can easily explained by the spatial variation of ^{129}I deposition amount suggested by other observation [1]. In any of the four cores, more than 89% of FDNPP origin ^{129}I was existed within top 5 cm and 98% within top 10 cm. Other 9 cores showed larger variation of depth profile of FDNPP origin ^{129}I. Especially the fraction of total inventory existed within top 5 cm were varied from 56% to 100%. This large profile variation for crop field and Man-made soil should be controlled by the soil properties such as porosity. Sampling site and/or should be carefully chosen not to underestimate the total deposition amount of ^{129}I originated from FDNPP.

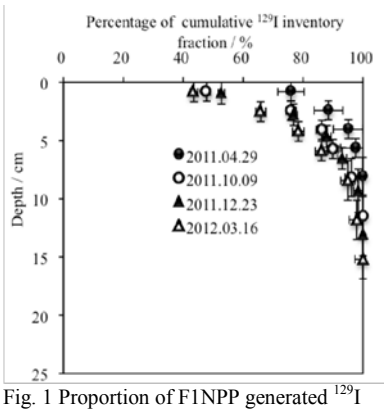

Fig. 1 Proportion of F1NPP generated ^{129}I per depth in Kawauchi village crop field

[1] T. Ohno et al., J. Radiat. Res. **50**, 325-332, 2009
[2] S. K. Sahoo et al., Geochem. Cosmochim. Acta **63**, 1927-1938, 2009
[3] U. Rao et al., Geochem. Cosmochim. Acta **63**, 1927-1938, 1999
[4] UNSCEAR 2008, Annex C

APSORC'13 - 5th Asia-Pacific Symposium on Radiochemistry
Kanazawa, Japan, 22-27 September 2013

Vertical distribution of the Fukushima-derived radiocesium in the western North Pacific in January and February 2011

Yuichiro Kumamoto[1], Akihiko Murata[1], Takeshi Kawano[1], Michio Aoyama[2]
[1] Japan Agency for Marine-Earth Science and Technology, Japan
[2] Meteorological Research Institute, Japan

Abstract – The radiocesium in seawaters from surface to 800-m depth at stations more than hundreds km away from the Fukushima Dai-ichi nuclear power plants in the western North Pacific Ocean were measured in January and February 2012. Activity of the Fukushima-derived Cs-134 in the surface mixed layer (0 ~ 200-m depth approx.) was highest (~ 20 Bq m^{-3}) in the transition area between the subarctic (north of 40°N approx.) and subtropical regions (south of 35°N approx.), which was due to the direct discharge of radiocesium from the plants. In the subtropical region, we observed Cs-134 maxima just below the mixing layer (200 ~ 300-m depth approx.). The Cs-134 activities in the maxima corresponded to those in the surface mixed layers in the transition area, which implies that the Cs-134-rich waters in the transition area have been transported southwardly to the subtropical region across the Kuroshio Extension Current along isopycnal layers.

Keywords – Fukushima Dai-ichi nuclear power plants, radiocesium, North Pacific Ocean

I. INTRODUCTION

The massive Tohoku earthquake and consequent giant tsunami of March 11, 2011 resulted in global releases of radiocesium (Cs-134 and Cs-137) from the Fukushima Dai-ichi nuclear power plants (FDNPPs). In the North Pacific Ocean, a large portion of Fukushima-derived radiocesium has been settled in both through atmospheric deposition and direct discharge of contaminated waters. The total amount of the radiocesium derived from the direct discharge was estimated to be about 4 PBq for Cs-137 (Kawamura et al, 2011 [1]; Tsumune et al., 2012 [2]; Estournel et al., 2012[3]). On the other hand, evaluation of the radiocesium derived from the atmospheric deposition contains large uncertainty mostly due to the restriction of available data in the vast North Pacific Ocean. In particular, vertical distribution of the Fukushima-derived radiocesium in the open ocean is hardly known. We measured the radiocesium in seawaters from surface to 800-m depth at stations more than hundreds km away from FDNPPs in the western North Pacific Ocean in January and February 2012.

II. METHODS

We conducted water sampling during a cruise of R/V Mirai, Japan Agency of Marine-Earth Science and Technology (MR11-08) along the 149°E meridional line approximately. The seawater samples were collected into 20-L cubitainers using a bucket and a conductivity-temperature-depth rosette with Niskin water samplers. The sample were filtrated and acidified by nitric acid on board. Radiocesium in the seawater was concentrated onto ammonium molybdophosphate (AMP). The radiocesium in the AMP/Cs compound was measured using a gamma-spectrometry with well-type Ge detector. Detection limit of the radiocesium measurement was 0.2 ~ 0.3 Bq m^{-3}. Uncertainties for the measurement was about 8 %. The radiocesium decay were corrected to the sampling date.

III. RESULTS AND DISCUSSION

Before the FDNPPs accident, Cs-134 derived from the nuclear weapon tests and the Chernobyl accident was not detected in the environment because of its short half-life (about 2 years). Therefore Cs-134 observed in the North Pacific was derived from FDNPPs after the accident. Cs-134 was found in surface waters at all the stations from 20°N to 42°N about ten months after the disaster. Activity of Cs-134 in the surface mixed layer (0 ~ 200-m depth approx.) was highest (~ 20 Bq m^{-3}) in the transition area between the subarctic (north of 40°N approx.) and subtropical regions (south of 35°N approx.). Those in the subarctic and subtropical regions were less than 5 and 1 Bq m^{-3}, respectively. This meridional distribution was due to the direct discharge of radiocesium into the transition area from FDNPPs located at 37.4°N/ 141.0°E.

Below the surface mixed layer Cs-134 activity decreased sharply and was not detected in deeper layers than 400-m depth at stations in the subarctic region and transition area, which is explained by vertical one-dimensional penetration of radiocesium from the surface mixed layer to the deeper layers. However, at stations in the subtropical region, south of the Kuroshio Extension Current, we observed Cs-134 maxima just below the mixing layer (200 ~ 300-m depth approx.). The Cs-134 activities in the maxima corresponded to those in the surface mixed layers in the transition area, which implies that the Cs-134-rich waters in the transition area have been transported southwardly to the subtropical region across the Kuroshio Extension Current along isopycnal layers.

[1] Kawamura, H., Kobayashi, T., Furuno, A., In, T., Ishikawa, Y., Nakayama, T., Shima, S., and Awaji, T., J. Nucl. Sci. Technol., 48, 1349–1356, 2011.
[2] Tsumune, D., Tsubono, T., Aoyama, M., and Hirose, K., J. Environ. Radioactiv., 111, 100–108, doi:10.1016/j.jenvrad.2011.10.007, 2012.
[3] Estournel, C., Bosc, E., Bocquet, M., Ulses, C., Marsaleix, P., Winiarek, V., Osvath, I., Nguyen, C., Duhaut, T., Lyard, F., Michaud, H., and Auclair, F.,J. Geophys. Res., 117, C11014, doi:10.1029/2012JC007933, 2012.

Effect of Application Timing of Potassium Fertilizer on Root Uptake of ^{137}Cs in Brown Rice

Takashi Saito[1], Kazuhira Takahashi[1], Tomoyuki Makino[2], Hirofumi Tsukada[3, 4], Mutsuto Sato[1], Kunio Yoshioka[1]

[1]Fukushima Agricultural Technology Centre,
[2] National Institute for Agro-Environmental Sciences
[3] Institute for Environmental Sciences
[4] Fukushima University

Abstract – We have already reported that potassium fertilizer is effective to reduce radiocesium in brown rice. In this study, we tried to find the most appropriate timing for potassium fertilizer application during the rice cultivation period in terms of ^{137}Cs concentrations in brown rice. The concentration of ^{137}Cs in brown rice cultivated without application of potassium fertilizer was 32 Bq kg^{-1}, while that with application of basal fertilizer including potassium was 5 Bq kg^{-1}. The concentration of ^{137}Cs in brown rice was increased with the late application timing. Therefore, application of potassium fertilizer in the early growing period reduced the uptake of ^{137}Cs by rice plant from contaminated soils effectively.

Keywords –^{137}Cs, Brown rice, Potassium fertilizer, Soil-to- brown rice transfer factor

I. INTRODUCTION

After the accident of Fukushima Daiichi Nuclear Power Plant, in 2011, the concentration of radiocesium in brown rice collected in some areas of Fukushima prefecture exceeded the provisional regulation value for brown rice (500Bq kg $^{-1}$). It is reported that the concentration of radiocesium in brown rice decreases with increasing exchangeable potassium concentrations in soil (Saito et al, 2012). In terms of more positive application method of potassium fertilizer for reducing radioactive concentration in rice, concentrations of ^{137}Cs in brown rice according to application timing of potassium fertilizer were investigated in the present study.

II. MATERIALS AND METHODS

A field test was carried out in the northern part of Fukushima Prefecture. Plowing, puddling and transplanting were performed on April 20, May 4 and May 10, 2012, respectively. The planting density was 17.1 hill m^{-2} (30× 19.5 cm). The nitrogen and phosphorus fertilizer (g m^{-2}) were applied to each plot of paddy field in the proportion 6.0:10 (N-P_2O_5) on April 17, 2012. The potassium fertilizer was applied to each plot of the field at a rate of 8.0 g m^{-2} before plowing, 50, 70 and 80 day after transplanting, respectively.

Rice straw had been applied to the test field every year. The soil in the rice paddy field was classified as Gray lowland soil. Soil samples (at the depth of 0-15cm) were collected from each plot of experimental rice paddy field after the cultivation of the rice plant on September 19, 2012. In order to determine the soil-to brown rice transfer factor, we collected soil from the vicinity of the rice plant. After the soil samples were air-dried for 21 days, the soil in each sample was properly mixed and sieved through a 2 mm sieve. Rice seeds were collected from the soil where the soil was sampled. After threshing rice samples were passed through a 1.80-mm sieve and grains remained on the sieve were used for the analysis. The dried soil was compressed into cylindrical polystyrene containers. The brown rice samples were compressed into 0.7 L Marinelli beakers. The concentration of ^{137}Cs in the soil and brown rice were measured using a Ge gamma- ray detector connected to a multichannnel analyzer system by counting for 3600-7200 s.

III. RESULTS AND DISCUSSIONS

The concentration range of ^{137}Cs in the soils of the experimental plot was 3262-3983 Bq kg^{-1}. The ^{137}Cs concentration in brown rice cultivated without potassium fertilizer was 32 Bq kg^{-1}, while that decreased to 5 Bq kg^{-1} with application of basal potassium fertilizer. On the other hand, the ^{137}Cs concentrations of brown rice to which potassium fertilizer was applied at 50, 70 and 80 d after transplanting were 15, 23 and 36 Bq kg^{-1}, respectively. As a result, the concentrations of radiocesium in brown rice increased with late application timing. These results show that application of potassium fertilizer in the early growing period decreases the uptake of ^{137}Cs by rice plants from contaminated soils effectively.

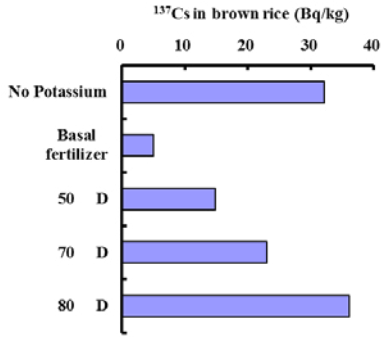

Fig.1 Concentrations of ^{137}Cs in brown rice by difference of application timing using potassium fertilizer

[1] Saito T et al : Effect of potassium application on root uptake of radiocesium in rice, KUR Research Program for Scientific Basis of Nuclear Safety, 165-170, 2012

Low levels of ^{134}Cs and ^{137}Cs in bottom sediments along the Japanese Archipelago side of the Sea of Japan after the Fukushima Dai-ichi NPP accident

M. Inoue[1,*], S. Ochiai[1], T. Murakami[1], S. Oikawa[2],
M. Yamamoto[1], S. Nagao[1], Y. Hamajima[1], H. Kofuji[1], J. Misonoo[2]
[1]Low Level Radioactivity Laboratory, Kanazawa University
[2]Marine Ecology Research Institute

Abstract

We examined radiocesium concentrations in bottom sediment samples collected along the Japanese Archipelago side of the Sea of Japan before/after the Fukushima Dai-ichi Nuclear Power Plant (FDNPP) accident. Low levels of ^{134}Cs were detected in an area located near estuaries. This was considered to be due to the riverine discharge rather than direct radioactive depositions to sea surface.

Key words- radiocesium; bottom sediment; riverine discharge; Fukushima Dai-ichi Nuclear Power Plant accident

I. INTRODUCTION

The FDNPP accident on March 11, 2011 resulted in the widespread release of large amounts of ^{134}Cs (half-life: 2.06 y) and ^{137}Cs (30.2 y) to the atmosphere and to land and sea surfaces over a wide region of eastern Japan. We analyzed the ^{134}Cs and ^{137}Cs concentrations in sediment samples collected in the Japanese Archipelago side of the Sea of Japan in May 2011, which indicated the slight contamination of the FDNPP-derived radiocesium in a sediment sample from site *D1* (Fig. 1) [1]. In the present study, we examined radiocesium concentrations of sediments in area *D* and clarify delivery process of radiocesium from the FDNPP.

II. SAMPLES and EXPERIMENTAL

We collected a total of 11 bottom sediment samples (0–3 cm depths) at four sites in Niigata offshore (*D*) area (230–530 m depths) during 2010–2012 (Fig. 1). Sediment samples were freeze-dried and crushed into a powder with an agate mortar after washing with distilled water (5–25 g-dry). γ-Spectrometry was performed on all samples using Ge-detectors designed for low-background counting and located at the Ogoya Underground Laboratory [2].

III. RESULTS and DISCUSSION

In area *D*, ^{134}Cs was detected in bottom sediments collected in 2011 and 2012 (*e.g.*, 7.7 mBq/g-dry at site *D2*

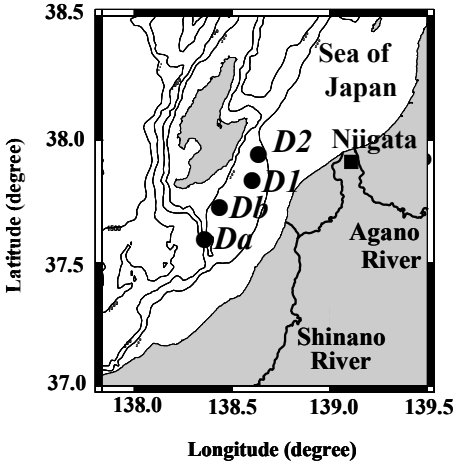

Fig. 1 sampling sites for sediment samples

in 2011) in contrary to the sediments at other coastal areas along the Japanese Archipelago side which were below the detectable limit [1]. In estuary areas, particle materials play important roles in the transportation of radiocesium. Due to the existence of the thermocline, the contamination of ^{134}Cs in sediment samples in area *D* could not be ascribed to the contribution of the soluble fraction accompanying downward water circulation, but to the transportation of the reactive fraction together with particle materials. Agano River and Shinano River meet around area *D*. Detection of ^{134}Cs in samples collected in May 2011 suggests that introduction of contaminated riverine particles from the estuary may lead to radiocesium contamination in the sediment samples, showing immediate transportation (within 1–2 months) of radioactive particle materials to the bottom of this area. Further clarification of the contamination levels and delivery patterns for ^{134}Cs and ^{137}Cs in this area can be achieved by obtaining additional sediment samples, including riverine sediments. This is an operation that we are currently engaged in.

References

[1] Inoue, M. *et al.* (2013) *Appl. Radiat. Isot*. (in press)

[2] Hamajima, Y. and Komura, K. (2004) *Appl. Radiat. Isot.* **61**, 179-183

The heavy-ion reactions ^{238}U + ^{238}U and ^{238}U + ^{248}Cm and actinide production close to the barrier revisited

J.V. Kratz[1a], M. Schädel[1b], H.W. Gäggeler[1c]
[1]Gesellschaft für Schwerionenforschung mbH, 64291 Darmstadt, Germany
[a]currently at Institut für Kernchemie, Johannes Gutenberg-Universität, 55099 Mainz, Germany
[b]currently at Advanced Science Research Center, Japan Atomic Energy Agency, Tokai-mura, Ibaraki 319-1195, Japan
[c] currently at Paul Scherrer Institut, 5232 Villigen, Switzerland

Keywords – Quasi-elastic and damped collisions/Sequential fission/Total kinetic energy loss/Production of surviving heavy actinides/Excitation functions/Survival probabilities

Recent theoretical work [1,2] has renewed interest in radiochemically determined isotope distributions in reactions of ^{238}U projectiles with heavy targets that had previously been published only in parts [3,4]. These data are being revisited. The cross sections $\sigma(Z)$ below the uranium target have been determined as a function of incident energy in thick-target bombardments. These are compared to predictions by a diffusion model [5] whereby consistency with the experimental data is found in the energy intervals 7.65 – 8.30 MeV/u and 6.06 – 7.50 MeV/u. In the energy interval 6.06 – 6.49 MeV/u, the experimental data are lower by a factor of 5 compared to the diffusion model prediction indicating a threshold behaviour for massive charge and mass transfer close to the barrier. For the intermediate energy interval, the missing mass between the primary fragment masses deduced from the generalised Q_{gg} systematics including neutron pair-breaking corrections and the centroid of the experimental isotope distributions as a function of Z have been used to determine the average excitation energy as a function of Z. From this, the Z dependence of the average total kinetic-energy loss $\overline{TKEL}$ has been determined. This is compared to that measured in a thin-target counter experiment at 7.42 MeV/u [6,7]. For small charge transfers, the values of $\overline{TKEL}$ of this work are typically about 30 MeV lower than in the thin-target experiment with the difference decreasing with increasing charge transfer developing into even slightly larger values in the thick-target experiment for the largest charge transfers. This is the expected behaviour which is also found in a comparison of the partial cross sections for quasi-elastic and deep-inelastic reactions in both experiments. The cross sections for surviving heavy actinides, e.g., $_{98}$Cf, $_{99}$Es, and $_{100}$Fm indicate that these are produced in the low-energy tails of the dissipated energy distributions, however, with a low-energy cutoff on the order of 35 MeV. Excitation functions show that identical isotope distributions are populated independent of the bombarding energy indicating that the same bins of excitation energy are responsible for the production of these fissile isotopes. A comparison of the survival probabilities of the residues of equal charge and neutron transfers in the reactions of ^{238}U projectiles with either ^{238}U or ^{248}Cm targets [4] is consistent with this cutoff as evaporation calculations assign the surviving heavy actinides to the 3n and/or 4n evaporation channels.

[1] V. Zagrebaev et al., Nucl. Phys. A787, 363c (2007)
[2] V. Zagrebaev et al., Phys. Rev. C78, 034610 (2008)
[3] M. Schädel et al., Phys. Rev. Lett. 41, 469 (1978)
[4] M. Schädel et al., Phys. Rev. Lett. 48, 852 (1982)
[5] C. Riedel et al., Z Physik A290, 385 (1979)
[6] K.D. Hildenbrand et al., Phys. Rev. Lett. *39*, 1065 (1977)
[7] H. Freiesleben et al., Z. Physik A292, 171 (1979)

Mechanism of Mo-99 Adsorption and Tc-99m Elution from Zirconium-Based Material in Mo-99/Tc-99m Generator Column Using Neutron-Irradiated Natural Molybdenum

Rohadi Awaludin[1], Adang Hardi Gunawan[1], Hotman Lubis[1], Sriyono[1], Herlina[1], Abdul Mutalib[1], Akihiro Kimura[2], Kunihiko Tsuchiya[2], Masakazu Tanase[3], Masahiro Ishihara[2]
[1]Center for Radioisotope and Radiopharmaceutical, National Nuclear Energy Agency of Indonesia.
rohadi_a@batan.go.id
[2]Neutron Irradiation and Testing Reactor Center, Oarai Research and Development Center, Japan Atomic Energy Agency
[3] Chiyoda Technol Corporation, Japan

Keywords – adsorption mechanism/Mo-99/Tc-99m radionuclide generator/neutron-irradiated natural molybdenum

It is expected that the use of fission product Mo-99 for Tc-99m production can be replaced by neutron-irradiated natural molybdenum. The challenge in using neutron-irradiated molybdenum is that the Mo-99 has low specific radioactivity. Zirconium-based material has a great opportunity as an adsorbent in Mo-99/Tc-99m radionuclide generator using neutron-irradiated natural molybdenum since the material can adsorb molybdenum with high capacity. However, until now, there is still no data to explain the mechanism of Mo adsorption and Tc-99m elution process from the material. It is very important to investigate the mechanism for increasing the adsorption capacity, increasing the Tc-99m elution yield as well as reducing the Mo-99 breakthrough in Mo-99/Tc-99m generator using irradiated natural molybdenum. In this study, the Mo-99 adsorption and Tc-99m elution mechanism were investigated using Scanning Electron Microscope-Energy Dispersive X-ray Spectroscopy (SEM-EDS) to analyze the elemental composition of the material surfaces before Mo adsorption, after Mo adsorption and after Tc-99m elution using saline solution. The results were compared with the value of adsorption capacity of the material to irradiated natural Mo and elution yield of Tc-99m. From the changes of elemental composition in the surface, it was found that molybdate ions were adsorbed into the adsorbent by ion exchange with Cl^- ions in the material. It was also revealed that Tc-99m can be eluted from the material column in high oxidation state ($^{99m}TcO_4^-$) since oxidizing agent was needed in the elution process. It was considered that in lower oxidation state the Tc-99m easily made coordination bonds with other elements in the adsorbent.

APSORC'13 - 5th Asia-Pacific Symposium on Radiochemistry
Kanazawa, Japan, 22-27 September 2013

Startup of a new gas-filled recoil separator GARIS-II

D. Kaji[1], K. Morimoto[1], H. Haba[1], Y. Wakabayashi[1], Y. Kudou[1], M. Huang[1], S. Goto[2], M. Murakami[2], N. Goto[2], T. Koyama[2], N. Tamura[2], S. Tsuto[2], T. Sumita[3], K. Tanaka[3], M. Takeyama[4], S. Yamaki[5], and K. Morita[1]

[1] Nishina Center for Accelerator Based Science, RIKEN, Saitama 350-0198, Japan
[2] Niigata University, Niigata 950-2181, Japan
[3] Tokyo University of Science, Chiba 278-8510, Japan
[4] Yamagata University, Yamagata 990-8560, Japan
[5] Saitama University, Saitama 338-8570, Japan

Abstract – We developed a new gas-filled recoil separator GARIS-II, which consists of 5 magnets in a Q-D-Q-Q-D configuration, to study on actinide-based fusion reaction. The solid angle of the separator was determined to be 18.2 msr measured by a standard α-source of ^{241}Am. Basic characteristics of the separator, such as a background suppression and transmission, was studied by using fusion products via well-known nuclear reactions of ^{169}Tm(^{40}Ar,4n)^{205}Fr and ^{208}Pb(^{40}Ar,3n)^{245}Fm, respectively.

Keywords – gas-filled recoil ion separator, GARIS, new element, superheavy element, SHE chemistry

We designed and constructed a new gas-filled recoil ion separator GARIS-II [1, 2] and installed it in an experimental hall at the RIKEN heavy-ion linear accelerator (RILAC) facility in March 2009. This separator has been developed for studying on actinide-based fusion reactions. The most interesting subjects studied by GARIS-II are a new element search with $Z \geqq 119$, chemical investigations of superheavy element, studies on nuclear reaction and nuclear structure of SHE nuclides, and understanding the operating principles of gas-filled typed recoil separators such as the equilibrium charge state with various filling gases.

This device consists of five magnets in a Q_v-D-Q_h-Q_v-D configuration as shown in **Fig. 1**, where Q and D denote quadrupole and dipole magnets, respectively. The Q1 magnet acts as a strong vertical focusing. This enables better matching to D1 acceptance. The D1 magnet has a large deflecting angle of 30 degree. This enables separation of evaporation residue ER from primary beam immediately. The Q2 and Q3 magnets have a large bore radius of 300 mm. These magnets act as a horizontal and vertical focusing to the focal point. The D2 magnet has a deflecting angle of 7 degree. This enables separation of ER from transfer products and light charged particles. The total path length is 5.06 m from the target position to the focal point. The solid angle of the separator was determined to be 18.2 msr measured by a standard α-source of ^{241}Am. This value well agrees with 18.5 msr estimated from ion optical characteristics.

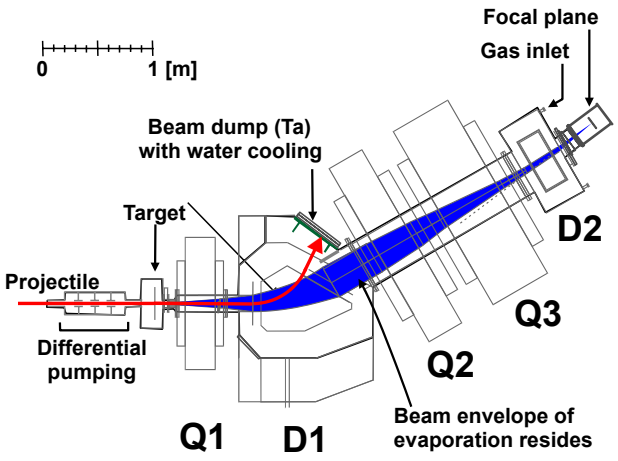

Fig. 1. Schematic of a new gas-filled recoil ion separator GARIS-II [2].

A gas-cooled rotating target system with differential pumping system was installed at an upstream of GARIS-II. Projectiles from accelerator is stopped at water-cooled Ta-beam dump. Filled gas is inlet from downstream of the separator. A pressure/ flow controller regulates continuous filling gas flow into the target chamber. The reaction products were separated in flight from projectiles and other by-products by GARIS-II, and guided into a focal plane detection system. The GARIS can be transported the ER with a magnetic rigidity $B\rho < 2.43$ T·m to focal plane. For the identification of ER and their successive radioactive decays, a system of a time-of-flight (TOF) detector, a double side silicon detector (DSSD) array, and a VETO silicon detector array were installed at the focal plane of GARIS-II.

In this symposium, we will talk about status of GARIS-II R&D and some operating tests by using 0 degree target recoils and reaction products, which were used as low energy ion-source, via the fusion reactions of ^{169}Tm(^{40}Ar,4n)^{205}Fr and ^{208}Pb(^{40}Ar, 3n)^{245}Fm.

[1] D. Kaji et al., RIKEN Accel. Prog. Rep. **42**, 179 (2008).
[2] D. Kaji et al., Submitted to Nucl. Instrum. Methods B.

APSORC'13 - 5th Asia-Pacific Symposium on Radiochemistry
Kanazawa, Japan, 22-27 September 2013

Purification of Scintillation Cocktails containing the alpha emitters americium and plutonium

E. Löfström-Engdahl*, G. Skarnemark, K. El Tayara, J. Eriksson, N. Halldin, J. Halleröd, M. Malmberg, J. Mattiasson Bjugren
Nuclear chemistry, Department of Chemical and Biological Engineering,
Chalmers University of Technology, SE 412 96 Gothenburg, Sweden
*Corresponding author, elinlo@chalmers.se

ABSTRACT

One efficient way of measuring alpha emitters is by the usage of liquid scintillation counting (LSC). A liquid sample is placed in a vial containing a scintillation cocktail. The alpha particles excite electrons in the surrounding liquid, and when they are de-excited photons are emitted. The photons are detected and the activity can be quantified. LSC has a high efficiency for alpha radiation and is therefore a fast and easy way for measuring alpha emitting samples. One drawback is that it does not differentiate very well between alpha energies; measurements of for example curium and plutonium simultaneously are impossible and demand other techniques. Another drawback is the production of a liquid alpha active waste.

In Sweden alpha radioactive waste liquids with an activity over some kBq per waste container cannot be sent for final storage. If, however, the activity of the liquids could be reduced by precipitation of the actinides, it would be possible to send away the liquid samples to municipal incineration. In this work a method for a purification of alpha active scintillation cocktails was developed. The method was first tried on a lab scale, and then scaled up. Until today (March, 2013) more than 20 liters of scintillation liquids have successfully been purified from americium and plutonium at Chalmers University of Technology in Sweden.

The four scintillation cocktails used were Emulsifier Safe®, Hionic-Fluor®, Ultima Gold AB® and Ultima Gold XR®. The scintillation cocktails could all be purified from americium with higher yield than 95 %. The yield was kept when the liquids were mixed. Also plutonium could be precipitated with a yield over 95 % in all cocktails except in Hionic-Fluor® (>55 %). However, that liquid in particular could be purified (>95 %) by mixing it with the three other cocktails. Up-scaling was performed to a batch size of 6-8 L of scintillation cocktail. In neither the americium nor the plutonium system, adverse effects of increasing the volume were detected. The products of the process are a solid fraction that can be sent to final storage and a practically non-radioactive liquid fraction that can be sent to municipal incineration.

Liquid scintillation counting, Alpha emitting waste, Co-precipitation

APSORC'13 - 5th Asia-Pacific Symposium on Radiochemistry
Kanazawa, Japan, 22-27 September 2013

Formation and stability of sulfides of the superheavy elements Cn and Fl

N.M. Chiera[1,2], R. Eichler[1,2*], A. Türler [1,2]
[1]Department of Chemistry & Biochemistry, University of Berne, Freiestrasse 3, CH-3012 Berne, Switzerland
[2]Laboratory for Radiochemistry and Environmental Chemistry, Paul Scherrer Institute, CH-5232 Villigen, Switzerland

First chemistry experiments with Cn and Fl revealed a relativistic stabilization of their elemental state leading to a much weaker metallic interaction with gold compared to their lighter homologues in the groups 12 and 14 of the periodic table [1,2]. Extrapolative predictions, in which thermochemical state functions were correlated mutually, showed that Cn and Fl may form stable sulfides. However, the stability trends in group 12 and 14 are predicted to be opposite. Hence, FlS is expected to be more stable compared to CnS. An experimentally exceptionally favourable case for comparative studies of Cn and Fl is the possibility of a simultaneous production of both elements in Ca-48 induced nuclear fusion reactions with Pu-242/Pu-244 [3]. The affinity of mercury towards sulfur is well known, and the formation of HgS is thermodynamically favored [4]. Hence, this chemical system is an ideal model system to investigate the kinetics and thermodynamics of the adsorption and reaction of a volatile noble metal with sulfur surfaces. For this purpose the method of isothermal reaction chromatography is used. Here, first results from these investigations will be presented. Some conclusions will be drawn, which are important for the preparation of further chemical investigations of Cn and Fl.

[1] R. Eichler et al., Nature 447, 72 (2007)
[2] R. Eichler et al., Radiochim. Acta 98, 133 (2010)
[3] Y. Oganessian, J. Phys. G: Nucl. Part. Phys, 34 (2007)
[4] M. Svensson, Sci. Tot. Env. 368, 418 (2006)

APSORC'13 - 5th Asia-Pacific Symposium on Radiochemistry
Kanazawa, Japan, 22-27 September 2013

Development of a Batch-Type Solid-Liquid Extraction Apparatus for Repetitive Extraction Experiment of Element 104, Rf

Y. Kasamatsu[1], T. Yokokita[1], A. Kino[1], K. Nakamura[1], K. Toyomura[1], Y. Komori[1], N. Takahashi[1], H. Haba[2], J. Kanaya[2], M. Huang[2], Y. Kudou[2], T. Yoshimura[3], A. Shinohara[1]
[1]Graduate School of Science, Osaka University
[2]Nishina Center for Accelerator-Based Science, RIKEN
[3]Radioisotope Research Center, Osaka University

Abstract – For the extraction of element 104, Rf, an automatic and rapid solid-liquid extraction apparatus by batch method was newly developed. On-line solid-liquid extraction experiments using an accelerator were performed in the TIOA/HCl system with ^{89m,g}Zr and ^{175}Hf produced in the nuclear reactions. As a result, the distribution coefficients in equilibrium were obtained within 10 s in 7–11 M HCl. This indicates the applicability of the present apparatus to Rf experiment.

Keywords – Solid-liquid extraction, Triisooctylamine (TIOA), Zr, Hf, Superheavy element

Chemical properties of transactinide elements ($Z \geq 104$) are expected to be characteristic due to strong relativistic effects on their electronic shells. Therefore, transactinide chemistry is very fascinating. It is, however, very difficult to perform chemical experiments of these elements because of their short half-lives and low production rates in the nuclear reactions. On-line chemical experiments on a "one-atom-at-a-time" basis are required. In recent years, the fluoride complex formation of Rf was successfully investigated under the condition that chemical equilibrium is attained for its homologues. To systematically study the complex formation of Rf, we are interested in the chloride complexation of Rf.

Purpose of the present study is to clarify the chloride complex formation of Rf based on the extraction data in equilibrium and further to investigate time dependence of the chemical behavior of Rf for the first time. In our previous work [1], solid-liquid extraction of Zr and Hf, the homologues of Rf, using triisooctylamine (TIOA) from HCl was performed by batch method. In this work, we newly developed the automatic apparatus to perform batch-wise solid-liquid extraction of transactinide elements rapidly and repeatedly. On-line experiments using this apparatus were conducted with ^{89m,g}Zr and ^{175}Hf tracers produced at the AVF cyclotron in RIKEN. We investigated the equilibrium time in extraction in several HCl concentrations by determining time dependences of the K_d values.

Schematic view of the solid-liquid extraction apparatus is shown in Fig. 1. Nuclear reaction products transported by the gas-jet system are deposited on the collection site of the dissolution section and then dissolved with an aqueous solution. The solution sample passes through two valves and a slider which moves horizontally to three positions, and then enters a Teflon reactor containing TIOA resin, reactor 1 in Fig. 1. After shaking the reactor using a vortex mixer, only the liquid phase is pneumatically pushed out of the reactor, and is subjected to the radiation measurement. To measure the radioactivity on the resin, the control experiment without the resin is performed using reactor 2. The present apparatus is controlled by a computer through a LabVIEW system.

In the on-line experiment, ^{89g,m}Zr ($T_{1/2}$ = 3.27 d, 4.18 min) and ^{175}Hf ($T_{1/2}$ = 70 d) were produced in the ^{89}Y(p,n)^{89g,m}Zr and ^{175}Lu(p,n)^{175}Hf reactions, respectively. Extraction experiments were performed by the above operations with the 25–57 wt. % TIOA resin (2.6–3.8 mg) and 6–11 M HCl (160–230 μL). Shaken time was varied to be from 10 s to 120 s. Remained Zr and Hf on the resin were eluted by washing the resin with ca. 220 μL of the mixture of 5.1 M HNO_3 and 0.01 M HF three times. The TIOA resin was reused 3–6 times. Each solution sample was assayed by γ-ray spectrometry using a Ge detector to obtain the K_d values by the equation K_d (mL/g) = $[M]_{resin}/[M]_{soln}$ (M = Zr or Hf).

It was found that the K_d values are basically constant in the studied time range, and are consistent with those obtained in our previous batch experiment [1] in 7–11 M of HCl. This result suggests that chemical reactions in the extraction reach the equilibrium within 10 s for ^{89m}Zr and ^{175}Hf under the present experimental conditions. It took about 35 s until the end of elution of the HCl solutions. These results suggest the applicability of the present apparatus to Rf experiment.

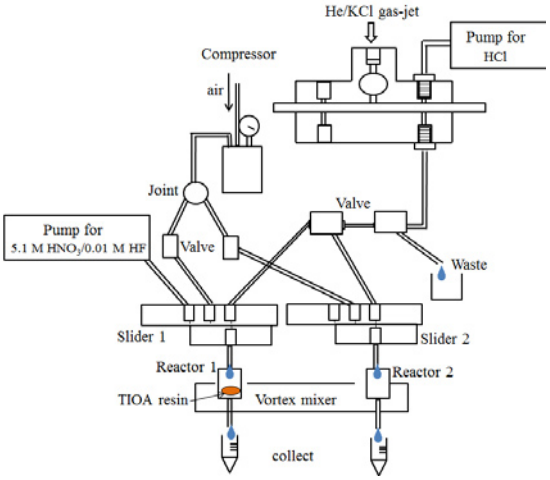

Fig. 1 Schematic view of the solid-liquid extraction apparatus

[1] A. Kino et al., 4th International Conference on the Chemistry and Physics of the Transactinide Elements, Sochi, Russia, 5-11 Sep. (2011).

Coprecipitation of Zr, Hf, and Th with Sm Hydroxide for Chemical Study of Rf

K. Toyomura[1], Y. Kasamatsu[1], N. Shiohara[1], T. Yokokita[1], Y. Komori[1], K. Nakamura[1], N. Takahashi[1], T. Yoshimura[2], H. Haba[3], Y. Kudou[3], H. Kikunaga[4], T. Ohtsuki[4], K. Takamiya[5], T. Mitsugashira[6], and A. Shinohara[1]

[1]Graduate School of Science, Osaka University

[2]Radioisotope Research Center, Osaka University

[3]Nishina Center for Accelerator-Based Science

[4]Research Center for Electron Photon Science, Tohoku University

[5]Research Reactor Institute, Kyoto University

[6]International Research Center for Nuclear Materials Science, Institute for Material Research, Tohoku University

Abstract – The purpose of our study is to perform hydroxide coprecipitation experiments of element 104, rutherfordium (Rf), to investigate its complex formation with hydroxide ions. In this work, we investigated the hydroxide coprecipitation behaviors of the group-4 homologues Zr and Hf, and the pseudo homologue Th in aqueous NH_3 and NaOH solutions by coprecipitation method with Samarium (Sm) hydroxide. In addition, we developed the semiautomatic and rapid suction filtration apparatus for repetitive experiment of Rf, and tested its performance by on-line experiments of Zr and Hf using an accelerator.

Keywords – Superheavy elements, Rutherfordium, Coprecipitation

I. INTRODUCTION

Elements with the atomic numbers $Z \geq 104$ are called superheavy elements (SHEs). They have short half-lives and are produced only by nuclear reaction with an accelerator. Therefore, much repetition of rapid experiments targeting one atom is required. This is why it is difficult to perform experiments of SHEs, and their chemical properties are hardly elucidated. So far, chemical properties of SHEs have been studied mainly by chromatographic methods. Experiments of SHEs in more various chemical systems should be performed to study their chemical properties in more detail. We have been developing a new method to investigate chemical properties of SHEs.

The purpose of our study is to perform coprecipitation experiments of element 104, rutherfordium (Rf), to investigate its complex formation with hydroxide ions by the coprecipitation method with samarium (Sm) hydroxide. By this method [1], we can prepare a precipitate sample which has good energy resolution in α spectroscopy in a few min. Therefore, this method is expected to be applicable to SHE chemistry that requires rapid operations. In this work, we investigated the hydroxide coprecipitation behaviors of the group-4 homologues Zr and Hf, and the pseudo homologue Th with Sm in aqueous NH_3 and NaOH solutions with various concentrations. In addition, we developed a semiautomatic and rapid suction filtration apparatus for repetitive experiments of Rf and tested its performance by on-line experiments of Zr and Hf using an accelerator.

II. EXPERIMENTS AND RESULTS

The Sm standard solution (1 M HNO_3) with the volume of 20 μL containing 20 μg of Sm was added into the HCl solution containing ^{88}Zr, ^{175}Hf, and ^{228}Th radiotracers. The solution was stirred and then the basic solution (dilute and concentrated aqueous NH_3, and 0.1–12 M NaOH solutions) was added. The solution was stirred for 10 s or 10 min. The solution containing the precipitate was filtrated by suction with a polypropylene membrane filter. The filtrate was collected in a vial. Both the precipitate and filtrate were dried on the heater at 100°C. The precipitate, filtrate, and beaker used were subjected to α and γ spectrometry. The precipitation yields of Zr, Hf, and Th were determined from each radioactivity. Above experiments were performed changing conditions such as solution volume and filter stick size to determine suitable conditions for Rf experiment. The precipitation behaviors of Zr, Hf, and Th without Sm were investigated using macro amounts of Zr, Hf, and Th samples in the same conditions to coprecipitation experiments with radioactive tracers.

As a result, the coprecipitation yields of Zr and Hf were lower as concentration of the hydroxide ions increases. On the other hand, the precipitation yields of Th were approximately 100% under all conditions. We observed clear differences in precipitation yields among these elements, suggesting that it is possible to investigate the stability of complex formation with hydroxide ions by this method. Because precipitation yields of the samples stirred for 10 s and 10 min were almost the same, it was found that precipitate is rapidly formed within 10 s. We were able to prepare a precipitate sample of Th with good energy resolution in α spectrometry. These results are preferred in Rf experiment. In the presentation, we will also report the development of the semiautomatic apparatus and results of the on-line experiments using an accelerator, and propose suitable conditions for Rf experiment.

[1] H. Kikunaga et al.: Appl. Radiat. Isot. **67**, 539 (2008).

Development of modified epoxy paint films to reduce the volatile iodine source term in the containments of LWRs during severe nuclear accidents

Sabrina Tietze[a]

[a] PhD student, Severe Nuclear Accident Chemistry, Nuclear Chemistry Department, Department of Chemical and Biological Engineering, Chalmers University of Technology, Göteborg, Sweden, sabrina.tietze@chalmers.se

During a severe nuclear accident in a light water reactor (LWR) significant amounts of iodine will be released from damaged UO_2 fuel into the containment. Primarily released cesium iodide aerosols and elemental iodine will partly dissolve in steam or the containment water pools. The remaining gaseous species can undergo complex reactions with released radiolysis- (e.g. ozone) and pyrolysis products such as volatile short chained organics released from e.g. cable plastics to form under the conditions of a severe nuclear accident (high temperatures, high radiation field) a series of different volatile iodine species. While inorganic iodine oxide aerosols (IOx) are rather water soluble and are likely to deposit on metal surfaces, organic iodides such as methyl- and ethyl iodide are less reactive with metal surfaces and more hydrophobic and thus are more likely to remain in gaseous phase. While gaseous elemental iodine can be sufficiently trapped with the currently used charcoal-, spray- and wet-scrubber filter systems, the used filter materials are less selective for organic iodides. Thus, both in case of a venting of the containment and in case of a failure of the containment these highly volatile species are more likely to be released into the environment and cause harm to the public. In case of a Fukushima like containment pressure increase in a nuclear power plant which is not equipped with an external wet-scrubber filter system through which the vented air can be filtered, significant amounts of both volatile inorganic and organic iodine species will be released into the environment.

In modern nuclear power plants bisphenol-A based epoxy paints are commonly used as coatings within the containment. These aromatic rich paints withstand higher radiation doses and thus they are expected to contribute less to the formation of highly volatile organic iodides such as methyl iodide than formerly used (partly) oil based paint films.

Experimental studies at Chalmers University of Technology on Teknopox Aqua VA epoxy paint, which is recently used in Swedish and Finish nuclear power plants, have shown that the paint can chemisorb significant amounts of both inorganic- and organic iodine species. The chemisorbed iodine will be partly washed out in steam or can be revapourised under the increased temperature and gamma irradiation field during a severe nuclear accident.

Attempts are made at Chalmers University of Technology to develop a modified epoxy paint to increase the retention of gaseous iodine species already inside the containment. For this purpose different organic and inorganic, irradiation stable, water insoluble and for different iodine species reactive additives are tested using e.g. a Co-60 gamma irradiator with a dose rate of 14 kGy/h.

23-NCP-09

New insights into the formation and stability of Molybdenum carbonyl compounds

I. Usoltsev[1,2], Wang Yang[3], R. Eichler[1,2], A. Türler[1,2], Qin Zhi[3]
[1]Department of Chemistry & Biochemistry, University of Berne, Freiestrasse 3, CH-3012 Berne, Switzerland;
[2]Laboratory for Radiochemistry and Environmental Chemistry, Paul Scherrer Institute, CH-5232 Villigen, Switzerland;
[3]Institute of Modern Physics Lanzhou; Chinese Academy of Sciences, 509 Nanchang Road, CN-730000 Lanzhou, China

The "Ms. Piggy" ^{252}Cf spontaneous fission (SF) source installed at the University of Bern allows for production of different transition metal fission products with a wide variety of half-lives. Volatile metal carbonyl compounds were formed in situ and transported by flushing pure CO or CO mixed with inert gas (N_2, Ar, He) through the recoil chamber of this source at a flow rate of 1 l/min [1]. Thus, these compounds are available outside of the source for radiochemical experiments. Our work focuses on the decomposition or thermal stability of the formed complexes. Therefore, the carbonyl complexes are transported trough a decomposition column held at variable temperatures between 25°C and 800°C. The surviving complexes are trapped in a charcoal filter, which was monitored by a HPGe gamma-ray detector. The fused silica decomposition column (1 m, 4 mm i.d.) covered by selected stationary surface materials was heated up within a steel cladding tube by means of a resistance furnace. By performing a gamma spectrometric measurement of the charcoal trap decomposition curves for carbonyl complexes were obtained. We will discuss here the results obtained for ^{104}Mo. Several different surface materials were examined: quartz, silver, gold, palladium, and PFA-Teflon®. Formation and decomposition of the complexes has been studied also in dependence on the CO concentration and on the inert gas used to dilute the CO. Thus, decomposition curves were obtained for different isotopes and different carrier gas mixtures, which allowed for determination of a pseudo-reaction order on carbon monoxide in the metal carbonyl formation. For the first time formation of nitrogen containing carbonyl complexes with the neutral transition metal atom Mo was observed. It was also shown that the beta decay of the Mo central atom in the carbonyl complex does not lead to the formation of volatile compounds of the daughter nuclide Tc. Obtained results are discussed in the light of upcoming decomposition studies of transactinide carbonyl complexes.

[1] Even J. et al: *Inorg. Chem.* 51, 6431 (2012).

Adsorption behavior of super-heavy elements (Z ≥ 112) on metal and inert surfaces

J. Anton[1], T. Jacob[1], V. Pershina[2]
[1]Institut für Elektrochemie, Universität Ulm, Albert-Einstein-Allee 47, D-89069 Ulm, Germany
[2]Gesellschaft für Schwerionenforschung, Planckstr 1, D-64291 Darmstadt, Germany

Investigation of chemical and physical properties of the heaviest elements (those beyond Lr) is a hot topic since several decades. In this time period, many new elements were discovered and after a proper characterization were added to the Periodic Table of the elements. The main problem of such investigations, however, is the rather short half-life of these elements, which requires the development of innovative experimental techniques. Nowadays the research focusses on the chemical properties of the element 114. So far, two gas chromatography experiments to study the interaction strength of element 114 with a gold surface have been performed with conflicting results. One experiment [1] reported a weak interaction of element 114 with a gold surface, leading to adsorption only at very low temperatures of approximately -90°C, while in the second experiment [2] adsorption on gold has been observed at the room temperature, indicating a much stronger bond between element 114 and gold. To resolve this conflict, further experiments on chemical properties of the element 114 will be performed at GSI and PSI/JINR in the next two years. For theoretical studies, standard quantum-mechanical packages that treat a system mostly non- or only scalar-relativistically are not satisfactory: Due to rather significant relativistic effects on the electron shells of the heaviest elements a fully-relativistic four-component description is required.

Recently, we have studied the adsorption behavior of elements 112, Cn, and 114 and their lighter homologues Hg and Pb, respectively, on gold surfaces [3] by using a cluster-approach [4]. We found that Hg/Cn and Pb/114 prefer different adsorption sites. Also, the adsorption energies of elements 112 and 114 are related to those of their lighter homologues in a different way. Thus, E_b(Cn) is only slightly (0.1-0.2 eV) lower than E_b(Hg), while E_b(114) is much lower (1.4 eV) than E_b(Pb). This is due to the fact, that in element 112 both the relativistically stabilized 7s and destabilized 6d AOs take part in the binding, while for element 114 binding is mostly determined by the relativistically stabilized $7p_{1/2}$ orbital. In contrast to Pb, where $6p_{3/2}$ strongly contributes to the surface bond, the $7p_{3/2}$ participate much less due to its large relativistic destabilization (the spin-orbit splitting between $7p_{1/2}$ and $7p_{372}$ is about 3.5 eV). Furthermore, binding of element 114 to gold is similar to that of Cn, however, about 0.2 eV stronger. Our predicted sequence in the E_b values is Cn < Hg < E114 << Pb. Thus, we predicted that in the thermochromatography experiments, element 114 will adsorb right at the beginning of the chromatography column with the hot end of 35°C, at the position of Hg. This prediction was recently confirmed experimentally [2].

In this talk we will present theoretical results on adsorption energies and distances of the elements from 112 to 114 and their homologues on metal (gold) and inert (SiO_2) surfaces.

Acknowledgment – J.A. gratefully acknowledges the support by the Deutsche Forschungsgemeinschaft (DFG) and BMBF

[1] R. Eichler et al. *Radiochim. Acta*, **98**, 133 (2010).
[2] A. Yakushev, NUSTAR-SHE-11, *GSI Scientic Report* 2009.
[3] V. Pershina, J. Anton, and T. Jacob, *J.Chem. Phys*., **131**, 084713 (2009).
[4] J. Anton, B. Fricke, E. Engel, Phys. Rev. A**69**, 012505 (2004).

Structural studies of the Eu(III) and U(VI) interactions with pentapeptides

A. Jeanson[1], J. Roques[1], S. Safi[1], E. Simoni[1], D. Aitken[2]
[1]IPN - Université Paris Sud, 91406 Orsay Cedex, France
[2]ICMMO - Université Paris Sud, 91406 Orsay Cedex, France

It is of great importance to assess the mechanisms governing radionuclide impact on the environment (particularly the biosphere) and to unravel the molecular processes underlying actinide transport and deposition in tissues. But most data available on the interaction of actinides with biological systems are based on physiological or biokinetic measurements, with scarce information on the microscopic factors such as structure of the actinide coordination site within biological molecules (proteins, peptides...). These structural data are essential to understand structure, function and affinity interdependence, which governs the organ deposition of such elements. In this paper, we will present first results on the complexation of trivalent and hexavalent metals (in a first step, Eu^{3+} was used as a surrogate to Am^{3+} and UO_2^{2+} represented the VI oxydation state) with peptides containing various, biologically relevant, geometrical constraints. The pentapeptide sequences contain sequential differences that induce conformational change, but relatively close enough so one parameter was varied at a time. We used the three DGDGD, ADPDA and DPDPD peptides, since they are differentiated by the number of proline (P) residues, that induce different angular strains. Both experimental (EXAFS, micro-calorimetry, laser fluorescence, ATR-FTIR) and theoretical (DFT methodology) approaches have been performed in order to determine the structure of the obtained complexes and the consequences on their stability.

APSORC'13 - 5th Asia-Pacific Symposium on Radiochemistry
Kanazawa, Japan, 22-27 September 2013

Solubility of Amorphous UO_2 and NpO_2 in Nitrate Media Containing Platinum Catalyst

Akira Kitamura[1], Satoko Shimoda[2]
[1]Japan Atomic Energy Agency, Tokai, Ibaraki 319-1194, Japan
[2]Mitsubishi Materials Corporation, Naka, Ibaraki 311-0102, Japan

Significant amount of nitrate salts are contained in a group of TRU wastes which may be disposed under deep underground together with high-level radioactive waste. Nitrate may oxidize redox-sensitive elements, e.g., uranium and neptunium. Although it was found that no effects of nitrate on solubility of amorphous neptunium(IV) dioxide (NpO_2(am)) was observed under anoxic conditions [1], it is still concerned that some catalysts may promote redox reactions between nitrate and elements reduced. Therefore, solubility of NpO_2(am) was investigated under nitrate media containing platinum catalyst. Similar experimental study was applied to amorphous uranium(IV) dioxide (UO_2(am)) to compare results with those for NpO_2(am).

An oversaturation method was applied to prepare the UO_2(am) and NpO_2(am) using stock solutions of uranium(VI) and neptunium(V), respectively, with addition of the reducing agent sodium dithionite ($Na_2S_2O_4$). After removing the solution containing $Na_2S_2O_4$ and washing several times, various concentration of sodium nitrate ($NaNO_3$) solution was added to UO_2(am) and NpO_2(am). A porous platinum black powder was added to some samples as a catalyst. The pH of solution was adjusted around 9, and no adjustment of redox potential was carried out. After contacting from 2 weeks to 5 months, an aliquot of sample solution was picked up, centrifuged (CF), filtered with 0.45 μm membrane, and filtered with molecular weight cut-off of 10^4. All the experimental procedures were performed in an argon-filled glove box to avoid contamination of oxygen gas.

The obtained solubility values of UO_2(am) and NpO_2(am) as a function of $NaNO_3$ concentration are shown in Figs. 1 and 2, respectively. Due to no dependences of nitrate concentrations on solubility of UO_2(am) and NpO_2(am) containing platinum black powder, no redox effects of $NaNO_3$ on their solubility were found. On the other hand, it was found that the obtained solubility values of UO_2(am) and NpO_2(am) containing porous platinum black powder were larger than those without porous platinum black powder. Considering with large difference of solubility by filtration types, aqueous uranium and neptunium species may form colloidal species in lower $NaNO_3$ concentrations and be physically absorbed into porous platinum black powder in higher $NaNO_3$ concentrations.

It was found that the oxidation state of uranium solid was 4 even after the solubility experiment using X-ray diffractometry. According to thermodynamic calculations, the oxidation state of neptunium solid can also be 4.

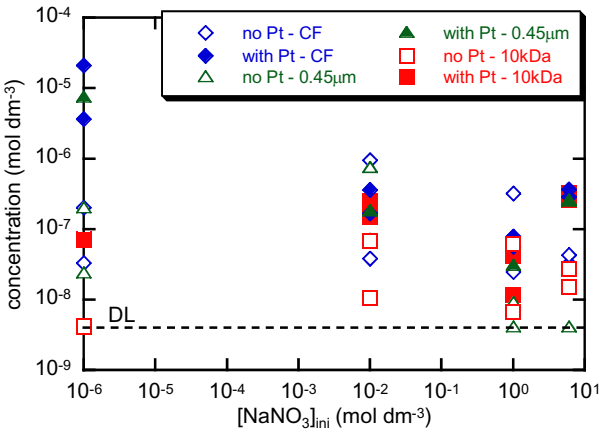

Fig. 1 – Solubility of UO_2(am) as a function of $NaNO_3$ concentration with/without platinum black

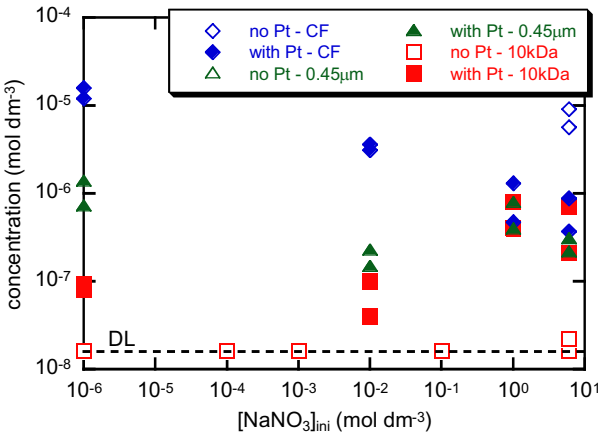

Fig. 2 – Solubility of NpO_2(am) as a function of $NaNO_3$ concentration with/without platinum black

[1] M. Mihara et al., Proc. ASME 13th Intl. Conf. on Environmental Remediation and Radioactive Waste Management (ICEM2010), October 2010, Tsukuba, Japan, Paper No. ICEM2010-40040 (2010).

This work was performed in the project "TRU waste disposal technology – Combined development of nitrate salt removal technology and an assessment system for the impact of nitrate on the co-locational disposal of TRU waste and HLW" in FY 2012 funded by the Ministry of Economy, Trade and Industry of Japan.

APSORC'13 - 5th Asia-Pacific Symposium on Radiochemistry
Kanazawa, Japan, 22-27 September 2013

Apparent formation constants of actinide complexes with humic substances determined by solvent extraction

Takayuki Sasaki[1], Yury M. Kulyako[2], Katharina Müller[3], Taishi Kobayashi[1], Maxim Samsonov[2], Boris F. Myasoedov[2]

[1] Department of Nuclear Engineering, Kyoto University, Kyoto daigaku-Katsura, Nishikyo, Kyoto 615-8540, Japan
[2] V.I. Vernadsky Institute of Geochemistry and Analytical Chemistry RAS, Kosygin str. 19, Moscow, Russia
[3] Helmholtz-Zentrum Dresden-Rossendorf e.V., Institute of Resource Ecology, 510119, D-01314 Dresden, Germany

Abstract – Apparent formation constants of Pu(IV) with two kinds of humic substances (HSs) were determined in 0.1M $NaClO_4$ at 25 °C using a back-solvent extraction method. The effect of solution conditions, such as the pH, the initial metal and HS concentrations, and the ionic strength, on the formation constants was investigated. The obtained data were compared with the other actinide series.

Keywords – Humic substances / Actinides / Apparent formation constant / Solvent extraction

Organic substances may greatly affect the speciation and solubility of tetravalent actinides in groundwater, depending on the complex formation constants, pH, the ionic strength, the organic ligand-to-metal concentration ratio, and so on. In order to estimate how these parameters influence the apparent solubility, reliable thermodynamic data on the interaction of tetravalent actinide ions with counter anions in aqueous solutions are required in the safety assessment of geological disposal. In the present study, we investigate the formation constants of Pu(IV) with typical HSs in groundwater.

The formation constants were determined using the solvent extraction method which was conducted in a similar manner as described in a previous study [1,2]. The organic phase of xylene containing thenoyltrifluoroacetone (HTTA) without further purification and the aqueous phase containing Pu at a pH_c ~3 were placed in a polypropylene tube and shaken by hand for several minutes. The concentration of $Pu^{IV}(TTA)_4$ complexes extracted into the organic phase was ca. $10^{-6\sim-9}$ M, while the hydrophilic polymer/colloidal species and species with other oxidation states such as $Pu^{III,V}(TTA)_x$ could not be co-extracted under the present condition. Soon after, the organic phase was isolated and brought into contact with fresh aqueous phases containing HS of pH_c 4 to 8, and ionic strength I = 0.1 M ($NaClO_4$). In this back-extraction, two kinds of humic acids were used. One is the purified Aldrich humic acid (ALHA). The other is the Elliott soil humic acid (1S102H, the International Humic Substance Society) abbreviated to SHA. Back-extraction was performed using a mechanical shaker at 25 ± 1 °C, and the pH_c and E_h values were measured.

The E_h values were stable at around +0.5–+0.6V (*vs*.SHE) throughout the measurement period at the examined pH values. The predominant species of plutonium was tetravalent state as discussed in ref. [1]. The concentration in both phases was determined by alpha spectrometry (5.16MeV). Though the recovery ratio for Pu was approximately 50% due to strong adsorption of Pu on the polypropylene vessel wall, the ratio was not dependent on the shaking time. Hence, the presence of the adsorbed Pu was ignored in the analysis.

The apparent formation constant is expressed by the binary or ternary complex, depending on the definition of the species.

$$\beta_{\mathrm{app},q} = \frac{[\mathrm{M(OH)}_q\mathrm{L}]}{[\mathrm{M}^{4+}][\mathrm{OH}]^q[\mathrm{R}^-]},$$

where q=0 or 1 is assumed in the present study. From the difference of the distribution ratio between the presence (D) and absence (D_0) of HSs,

$$\log\left(D_0/D\right) = \log\left(\frac{1+\sum\beta_{\mathrm{OH},p}[\mathrm{OH}^-]^p + \beta_{\mathrm{app},q}[\mathrm{OH}^-]^q[\mathrm{R}^-]}{1+\sum\beta_{\mathrm{OH},p}[\mathrm{OH}^-]^p}\right)$$

For $A = 1 + \sum\beta_{\mathrm{OH},p}[\mathrm{OH}]^p$,

$$\log D = \log D_0 - \log(A + \beta_{\mathrm{app},q}[\mathrm{OH}^-]^q[\mathrm{R}^-]) + \log A$$

where the $\beta_{\mathrm{OH},p}$ values at a given ionic strength calculated from specific ion interaction theory (SIT). In Figure, the $\log\beta_{\mathrm{app}}$ values for tetravalent Pu are higher than those for Th due to an effect of actinide contraction.

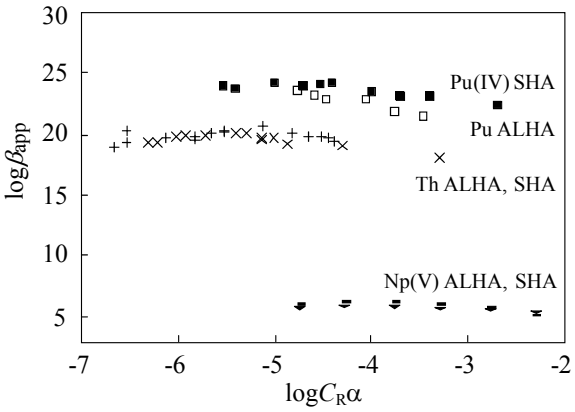

Fig. Comparison of the $\log\beta_{\mathrm{app}}$ (I=0.1 ($NaClO_4$) and 25ºC) values for Pu– and Th–OH–HS (as q=1) ternary complexes at pH 4 [1] and Np-HS binary complexes at pH 6 [2] as a function of C_R.

[1] T. Sasaki, S. Aoyama, H. Yoshida, Y.M. Kulyako, M. Samsonov, T. Kobayashi, I. Takagi, B.F. Myasoedov, H. Moriyama, *Radiochim. Acta*, 100, 737-745 (2012).
[2] K. Müller, T. Sasaki, *Radiochim. Acta*, 101, 1-6 (2013).

APSORC'13 - 5th Asia-Pacific Symposium on Radiochemistry
Kanazawa, Japan, 22-27 September 2013

The solubility of Np(IV) under alkaline and anoxic conditions

Göran Källvenius[1], Stefan Allard[2], Christian Ekberg[2]
[1]AB SVAFO, SE-611 23 Nyköping, Sweden
[2]Chalmers University of Technology, Nuclear Chemistry, SE-41296 Göteborg, Sweden

The solubility of Np(IV) has been studied under alkaline (10 < pH < 14) and reducing conditions. Previously the solubility of Np(IV) has been studied under acidic and near neutral conditions, with just a few studies in the range of 11 < pH < 13. In these studies the analysis technique used was liquid scintillation counting on ^{237}Np, resulting in a detection limit of about 10^{-8} M. The results from these studies have indicated solubility around or below this limit resulting in a high degree of uncertainty. Another problem with the previous studies is that they have been made on the amorphous hydrous hydroxide which may not be a uniquely defined phase. This study was initiated to test if the alkaline solubility of $NpO_2(c)$ would be within the detection limit using ICP-MS technique.

Experiments on Np(IV) in the form of $NpO_2(c)$ were performed in (Na^+, OH^-, ClO_4^-) media at 8 different pH values in the range of 10 to 14 and an ionic strength of 2 M. In trying to achieve reducing conditions hydrogen atmosphere was used, and Pt(s) catalyst added to the solutions. The neptunium concentration was determined using ICP-MS technique thereby lowering the detection limit to between 10^{-12} and 10^{-11} M. In most of the studied pH region the solubility of Np(IV) was found to be below the detection limit. However, at two pH values, 10.4 and 13.5 the Np(IV) concentration was found to be at least $3 \cdot 10^{-10}$ and $3 \cdot 10^{-11}$ M respectively.

Np(IV), solubility, LSC, ICP-MS, detection limit

APSORC'13 - 5th Asia-Pacific Symposium on Radiochemistry
Kanazawa, Japan, 22-27 September 2013

Separation of Am and Cm by Using TODGA and DOODA(C8) Adsorbents with Hydrophilic Ligand-Nitric Acid Solution

Shigekazu Usuda[1], Kei Yamanishi[1], Hitoshi Mimura[1], Yuji Sasaki[2], Akira Kirishima[3], Nobuaki Sato[3], Yuichi Niibori[1]

[1] Department of Quantum Science and Energy Engineering, Graduate School of Engineering, Tohoku University
[2] Research Group for Aqueous Separation Chemistry, Japan Atomic Energy Agency
[3] Institute of Multidisciplinary Research for Advanced Materials, Tohoku University

Abstract – Extraction chromatographic separation of Am and Cm was studied by using TODGA and DOODA(8) adsorbents and nitric acid eluents containing hydrophilic ligands, DOODA(C2) and TEDGA, respectively, in order to produce a synergistic effect in mutual separation properties.

Keywords – Chromatographic Separation of Am and Cm, TODGA and DOODA(C8) Adsorbents, Hydrophilic Ligands

For an improved partitioning of high level radioactive waste containing trivalent minor actinides (MA: Am, Cm) [1,2], extraction chromatographic separation of Am and Cm was studied by using porous silica/polymer support (SiO_2-P particles), into which two lipophilic diamide-type extractants, tridentate ligands TODGA (*N,N,N',N'*-tetraoctyl-1,3-oxapentane-1,5-diamide) and tetradentate ligands DOODA(8) (*N,N,N',N'*-tetraoctyl-3,6-dioxaoctane-1,8-diamide) were impregnated (TODGA and DOODA(C8) adsorbents, respectively). For the TODGA and DOODA(C8) adsorbents, nitric acid eluents containing hydrophilic ligands, DOODA(C2) (*N,N,N',N'*-tetraethyl-3,6-dioxaoctanediamide) and TEDGA (*N,N,N',N'*-tetraethyl-diglycolamide), respectively, were selected as masking agents in order to produce a synergistic effect in mutual separation of trivalent lanthanides (Ln) and/or MA.

Mutual separation properties of Ln were preliminarily investigated in both separation systems by batch and column methods, especially paying attention of separation between Nd and Sm. In nitric acid solution, the uptake of Ln onto the TODGA and DOODA(C8) adsorbents increased with nitric acid concentration. While the distribution coefficient (K_d) values of Ln for the TODGA adsorbent increased with atomic number of Ln, those for the DOODA(C8) adsorbent decreased with atomic number of Ln [3]. In nitric acid solution containing hydrophilic ligands, the K_d (Ln) values onto the TODGA and DOODA(C8) adsorbents decreased with concentration of DOODA(C2) and TEDGA ligands [4]. Relative separation factors (*SF*) of Ln (Nd~Tb) for the TODGA/DOODA(C2) system were almost the same degree irrespective of DOODA(C2) concentration, but those for the DOODA(C8)/TEDGA system were enlarged in lower TEDGA concentration. Consequently satisfactory eluent concentration of hydrophilic extractant and nitric acid concentration for each adsorbent was determined to be 0.05 M DOODA(C2)-0.1 M nitric acid eluent for TODGA adsorbent and 0.005 M TEDGA-3 M nitric acid eluent for DOODA(C8) adsorbent. Chromatographic separations of Ln (Nd~Tb) by both systems were effectively performed (*SF* (Nd/Sm): 4.2 for the TODGA system and 2.7 for the DOODA(C8) system and peak resolution (*R*) of Nd/Sm: 2.5 for the TODGA system and 2 for the DOODA(C8) system).

In this presentation, separation of MA(III) in both systems was demonstrated using not only Am-241 and Cm-243 but also Eu-152 for comparison between MA and Ln adsorbabilities. In the TODGA system, *SF* (Am/Cm) was considerably large (4.2), but chromatographic development was not sufficient and *R* (Am/Cm) was *ca.* 0.9 since the K_d (Am) value was unexpectedly small (0.7~0.8). In the DOODA(C8) system, *SF* (Am/Cm) was not so large (2.3) and *R* (Am/Cm) was *ca.* 1.2 because of adequate developed elution. It seems that the DOODA(C8) system is better than the TODGA system for practical use from a viewpoint of 3 M nitric acid eluent. On the other hand, the latter was superior to the former from an angle of mutual separation of Ln (Nd~Gd). In near future, the optimum elution condition will be searched for more effective separation of MA in pursuit of higher peak resolution between Am and Cm ($R \geq 1.5$).

A part of this study is the result of "Development of mutual separation technology of minor actinides by the novel hydrophilic and lipophilic diamide compounds" entrusted to "Japan Atomic Energy Agency" by the Ministry of Education, Culture, Sports, Science and Technology of Japan.

[1] Y. Sasaki, Y. Kitatsuji, Y. Tsubata, Y. Sugo, Y. Morita, "Separatiion of Am, Cm and lanthanides by solvent extraction with hydrophilic and lipophilic organic ligands," *Solvent Extraction Research and Development, Japan,* 18, p.93-101 (2011).

[2] Y. Sasaki, Y. Kitatsuji, Y. Sugo, Y. Tsubata, T. Kimura and Y. Morita, "Actinides extractability trends for multidentate diamides and phosphine oxides", *Solvent Extraction Research and Development, Japan,* 19, p.51-61 (2012).

[3] K. Yamanishi, H. Mimura, S. Usuda, Y. Sasaki, Y. Morita, "Adsorption properties of lanthanoids for SiO_2-polymer adsorbents impregnated with extractants", Extended Abstracts of IEX 2012 (The International Ion Exchange Conference, 19-21 September 2012, Queens' College, University of Cambridge, UK).

[4] K. Yamanishi, H. Mimura, S. Usuda, Y. Sasaki, Y. Morita, "Separation of lanthanoids by SiO_2-P adsorbent impregnated with extractants", Proceedings of WM2013 Conference (The annual Waste Management Symposia, 24-28 February, 2013, Phoenix, Arizona USA).

APSORC'13 - 5th Asia-Pacific Symposium on Radiochemistry
Kanazawa, Japan, 22-27 September 2013

Growth of uranyl hydroxide nanowires and nanotubes with electrodeposition method

Lin Wang, Li-Yong Yuan, Zhi-Fang Chai, and Wei-Qun Shi*
Key Laboratory of Nuclear Analysis Techniques, Institute of High Energy Physics, Chinese Academy of Sciences
Email: shiwq@ihep.ac.cn

Abstract –Actinides nanomaterials have great potential applications in fabrication of novel nuclear fuel and spent fuel reprocessing in advanced nuclear energy system. [1-2] *However, the relative research so far still lacks systematic investigation on the synthetic methods for actinides nanomaterials. In this work, we use track-etched membranes as hard templates to synthesize uranium based nanomaterials with novel structures by electrodeposition method. Through electrochemical behavior investigations and subsequent product characterizations such as energy dispersive spectrometer (EDS), fourier transform infrared spectroscopy (FTIR), the chemical composition of deposition products have been confirmed as the uranyl hydroxide. More importantly, accurate control of morphology and structures (nanowires and nanotubes) could be achieved by carefully adjusting the growth parameters such as deposition time and deposition current density. It was found that the preferred morphology of electrodeposition products is nanowire when a low current density was applied, whereas nanotubes could be formed only under conditions of high current density and the short deposition time. The mechanism for the formation of nanowires in track-etched membranes is based on the precipitation of uranyl hydroxide from uranyl nitrate solution, according to the previous researches about obtaining nanostructures of hydroxides from nitrate salt solutions.* [3-4] *And we have concluded that the formation of nanotubes is attributed to the hydrogen bubbles generated by water electrolysis under the condition of over-potential electro-reduction. The conveying of hydrogen bubbles plays the role of dynamic template which can prevent the complete filling of uranyl hydroxide in the channels. Additionally, we transform the chemical composition of deposition products from uranyl hydroxide to triuranium octoxide by calcining them at 500 and 800 degree centigrade, respectively, and SEM results show the morphologies of nanowires and nanotubes are maintained very well. Our work provides new idea for synthesizing one-dimension uranium based nanomaterials. Further investigations are needed to unveil the size and shape effect on the physical and chemical properties of these nanowires and nanotubes, and to demonstrate their potential applications.*

Keywords – uranium based nanomaterials, uranyl hydroxide, electrodeposition, track-etched membranes, template method, nanowires, nanotubes.

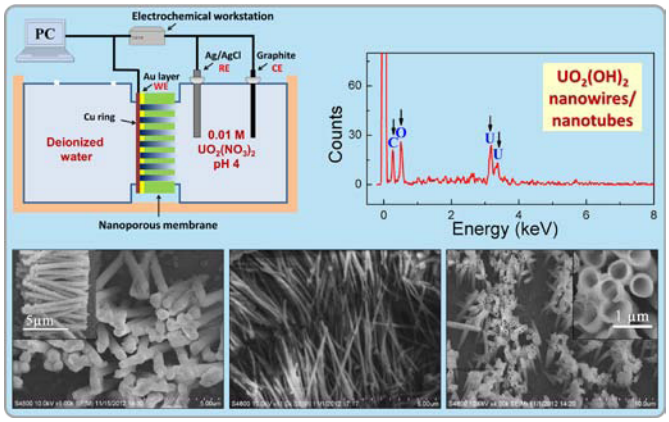

Figure 1. Growth of uranyl hydroxide nanowires/nanotubes with electrodeposition method. Top left, scheme of electrodeposition system; top right, result of elemental analysis for nano-structured products; down left, SEM images of uranyl hydroxide nanowires with diameters of 400 nm; down middle, SEM image of uranyl hydroxide nanowires with diameters of 50 nm; down right, SEM images of uranyl hydroxide nanotubes.

REFERENCES

[1] T. E. Albrecht-Schmitt, *Angewandte Chemie-International Edition*, 2005, *44*, 4836-4838.
[2] P. C. Burns, K. A. Kubatko, G. Sigmon, et al., *Angewandte Chemie-International Edition*, 2005, *44*, 2135-2139.
[3] L. Gonzalez-Rovira, J. M. Sanchez-Amaya, M. Lopez-Haro, et al., Nanotechnology, 2008, *19*, 495305.
[4] D. Z. Zheng, J. Y. Shi, X. H. Lu, et al., *CrystEngComm*, 2010, *12*, 4066-4070.

APSORC'13 - 5th Asia-Pacific Symposium on Radiochemistry
Kanazawa, Japan, 22-27 September 2013

Adsorption Behavior of Neptunium Ions on Pyridine Resin in Hydrochloric Acid Solutions

Yu Tachibana[1], Yusuke Tomobuchi[1], Masafumi Inaki[1], Yuki Yamazaki[1], Tatsuya Suzuki[1], Tomoo Yamamura[2]
[1]Department of Nuclear System Engineering, Nagaoka University of Technology,
[2]Institute of Material Research, Tohoku Univeristy

Abstract - The adsorption behavior of neptunium ions on pyridine resin in hydrochloric acid solutions has been studied at room temperature. Neptunium has many kinds of valence states of ions; mainly tetravalent, pentavalent, and heptavalent ions. We controlled the neptunium valence states and confirmed the valence states in hydrochloric acid solution by a UV-vis. spectrometry. The adsorption study on the neptunium ions which has the confirmed valence states, using pyridine resin was studied by batch-wise experiments. The distribution coefficients of neptunium on pyridine resin in hydrochloric acid solution were obtained.

Keywords – neptunium, pyridine resin, nuclear fuel reprocessing

I. INTRODUCTION

The noble nuclear reprocessing process based on chromatography in hydrochloric acid solutions has been developed [1]. This pyridine resin is used as the adsorption medium. In our previous works, the adsorption behavior of many elements was investigated, and the reprocessing process with nuclide separation system has been proposed from these results [2]. However we have not obtained the adsorption behavior of neptunium ions on pyridine resin in hydrochloric acid solution. It is well known that the neptunium has many valance states in solution. Thus, we controlled the valence states of neptunium, and obtained the adsorption behavior of each valence state of neptunium.

II. EXPERIMENTAL

1. Confirmation of valance states of neptunium

An ultraviolet-visible absorption photospectrometry (Lambda750, Perkin Elmer) was used for confirmation of valence states of neptunium. The wavelength of absorption peaks used for confirmation of Np(IV), Np(V), and Np(VI) species are about 750 and 960 nm, 980 nm, and 1230 nm, respectively.

Neptunium we used was confirmed to consist of pentavalent and heptavalent ions in original solution. In addition, we also confirmed that the neptunium can be controlled to be heptavalent by twice treatments of evaporation to dryness with the concentrated nitric acid solution and the perchloric acid solution. Tetravalent condition was confirmed to be able to be obtained by adding 0.5 M of hydroxylamine hydrochloride to the original solution. It was confirmed that Np(V) species are able to be obtained by adding peroxide to Np(VI) solution.

2. Adsorption experiments

Adsorption behavior was investigated by batch-wise experiments at room temperature. The neptunium with the controlled valences in a hydrochloric solution was added to the hydrochloric acid solution of adjusted concentrations. 0.1 g of pyridine resin was added to 1.0 mL of a neptunium solution. Adsorptions of neptunium ions on pyridine resin were evaluated by comparison of activity of neptunium before and after adding the pyridine resin.

III. RESULTS

We confirmed the methods of neptunium valence control. Distribution coefficients of neptunium with each controlled valence in hydrochloric acid solutions were obtained. Distribution coefficients of heptavalent neptunium are shown in Fig. 1. In this experiment, the neptunium-239 obtained by milking of americium-244 decay was used. The gamma-ray spectrometry was used for measurement of neptunium activity. We found that the heptavalent neptunium is strongly adsorbed on pyridine resin in higher concentrated hydrochloric acid solution, and this behavior is similar to heptavalent uranium.

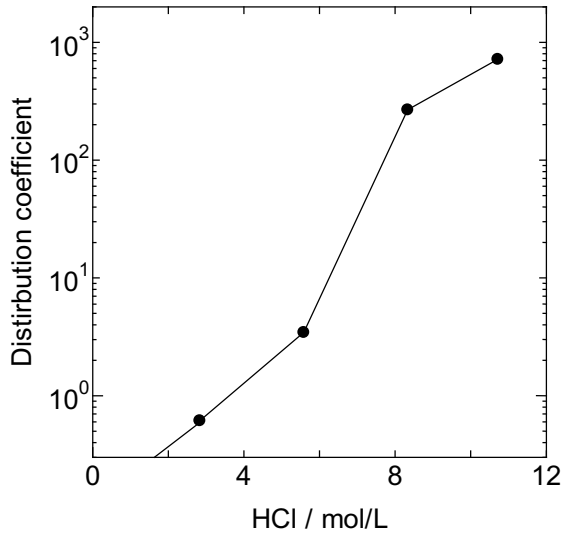

Fig. 1 Distribution coefficients of heptavalent neptunium on pyridine resin in hydrochloric acid solution.

REFERENCES

[1] S. Koyama, et al ., J. Nucl. Sci & Technol. 43 (2006) 681.
[2] T. Suzuki, et al., Prog. Nucl. Energy. 50 (2008) 476.
T. Suzuki, et al., Energy Procedia 7 (2011) 421., etc.

A method for ^{237}Np determination with liquid scintillation counting in the experiment of neptunium sorption onto bentonite

LI Ping, LIU Zhi, GUO Zhijun, WU Wangsuo*
Radiochemistry Laboratory, School of Nuclear Science and Technology, Lanzhou University, Lanzhou 730000, China

Among various analytical methods developed and used for the determination of neptunium (alpha spectroscopy, Neutron Activation Analysis (NAA), High Resolution γ-Spectroscopy (HRGS), Inductively Coupled Plasma Mass Spectrometry (ICP–MS), luminescence method and Liquid Scintillation Counting (LSC) etc.), The Liquid Scintillation Counting (LSC) method does not require extensive sample preparation and is very sensitive for alpha-decaying radionuclides such as ^{237}Np[1]. However, direct determination of ^{237}Np from its β-active daughter ^{233}Pa is difficult.

In this study, a new method was developed for the determination of ^{237}Np with liquid scintillation counting (LSC), the α/β discrimination is carried out with the function of pulse shape analysis (PSA) without a pure α emitter or a pure β emitter. Before we use the PSA technique to discriminate α/β, an approach was developed to set the optimum PSA by measuring a mixed α/β emitters sample and a background sample. The mathematic treatment of neptunium peak indicated that at the selected PSA-level (38), we detected ~86% of the total α emission[2]. It is suitable for the sample determination in the sorption experiments at this PSA-level with LSC. Moreover, we confirmed that, at m/V(bentonite) = 0~10g/L the suspension in sample did not influence LSC determination obviously. Thus, we could detect ^{237}Np samples containing bentonite suspension directly with LSC by setting PSA-level=38.

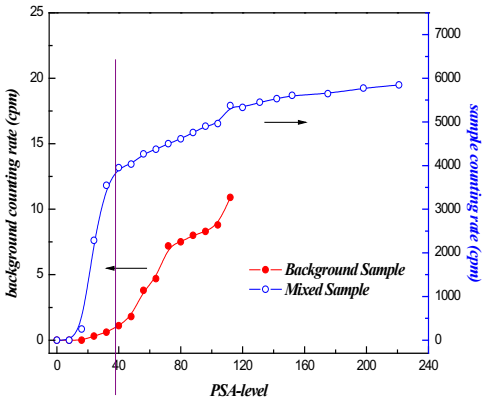

Fig.1 Count rate of a mixed sample and a background sample as a function of the PSA-level used.

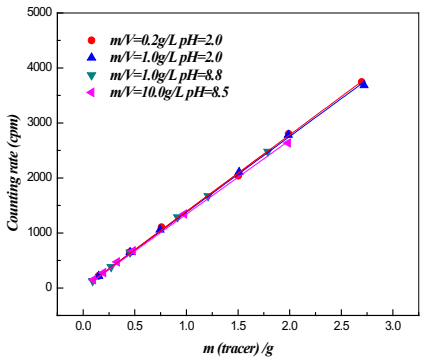

Fig. 2 Influence of bentonite on LSC measurement at a PSA-level=38.

[1] Thakur P, Mulholland G P. Determination of ^{237}Np in environmental and nuclear samples: A review of the analytical method [J]. Appl Radiat Isotopes, 2012, 70: 1747-1778.
[2] Aupiais J, Dacheux N, Thomas A C, Matton S. Study of neptunium measurement by alpha liquid scintillation with rejection of β-γ emitters [J]. Anal Chim Acta. 1999, 398: 205-218.

Determination of Stability Constants for the Thorium Iminodiacetic acid Complexes

D. Rama Mohana Rao, R. M. Sawant, B. S. Tomar.
Radioanalytical Chemistry Division, Bhabha Atomic Research Centre, Trombay, Mumbai 400085

Abstract: *Potentiometric method of determining the stability constants was employed to study the complexation of thorium with iminodiacetic acid. All the stability constant values have been determined at temperature of 298 K and in 1 M $NaClO_4$ medium. The formation and determination of log β was not reported in the literature for ML_2 complex. Under our experimental conditions 1:1 and 1:2 complexes are found to be formed and no partially protonated ligand metal complexes such as MLH, ML_2H were observed. The determined log β values for ML and ML_2 complexes are 10.78 ± 0.03 and 19.81 ± 0.07 respectively.*

Keywords:*Thorium, Iminaodiacetic acid, stability constants*

INTRODUCTION

The complexation of actinides with various naturally present and anthropogenic organic ligands plays a vital role in understanding their speciation and migration in the environment. Thermodynamics of complexation of actinides with various organic and inorganic ligands have been reported in the literature. To know the binding nature and the effect of hetero atom present in the ligand on complexation with actinides, we initiated the study to determine the thermodynamic parameters for complexation of actinide ions with carboxylates containing hetero atom like nitrogen, sulphur, etc. As a part of this study, in the present paper the stability constants for the complexation of thorium with iminodiacetic acid have been reported. The complexation of thorium with iminodiacetic acid have also been reported in the literature [1] which show the formation of MLH and ML complexes whereas in our study we determined for the completely deprotonated ligand metal complexes ML and ML_2.

EXPERIMENTAL

The details on the preparation and standardization of Th(IV) solution was given elsewhere [2]. The iminodiacetic acid (IDA) was procured from sigma Aldrich and was used as such. Carbonate free NaOH was used for the electrode calibration. Potassium hydrogen phthalate as a primary standard has been used to standardize the NaOH. The ligand solution was prepared by adding known amount of standardized NaOH to iminodiacetic acid solution. The acidic metal ion solution was titrated with the ligand solution to determine the stability constants of the Th(IV) – Iminodiacetate complexes. The data collection was stopped before the appearance of turbidity and the collected data was analyzed by Hyperquad software.

RESULTS AND DISCUSSION

There is always a competition from H^+ during the complexation of metal with a ligand containing dissociable proton. Therefore, in order to determine the stability constants of the metal ligand complexes, knowledge of the protonation constants is essential. The protonation constants of iminodiacetate ion were taken from our previous experiment results [3]. During the titration of acidic metal ion solution with the buffered ligand solution, following reaction can occur in the reaction vessel.

$$H^+ + L^{2-} \rightarrow HL^-$$
$$H^+ + HL^- \rightarrow H_2L$$
$$Th^{4+} + nL^{2-} \rightarrow ThL_n^{(4-2n)+}$$

The overall stability constant for the complex formed by thorium can be given by

$$\beta_{ML_n} = \frac{[ThL^{(4-n)+}]}{[Th^{4+}][L^{2-}]^n}$$

Figure:1 shows the speciation diagram for the complexation of thorium with iminodiacetic acid along with the fitted data of pH. Under the experimental conditions, ML and ML_2 complexes are observed predominantly and the log β values for these complexes are shown in the table 1. The log β for the complex ML was comparable with literature value (log β =9.69) [1]. The higher values of log β indicate the role of chelation in these complexes. Studies on the coordination structure in these complexes are in progress.

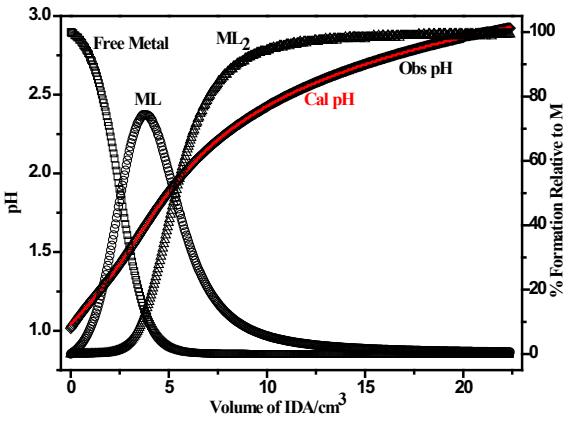

Figure:1 Speciation diagram of complexation of thorium with iminodiacetic acid along with the fitted data of both calculated and observed pH. ([Th] = $3*10^{-3}$ M, [H] = 0.0890 M and [IDA] = 0.2997 M, [H] = 0.2987 M, initial volume = 25 cm^3, I = 1 M $NaClO_4$, T = 298 K).

Table: 1 stability constants of thorium complexes with IDA ([Th] = $3*10^{-3}$ M, [H] = 0.0890 M and [IDA] = 0.2997 M, [H] = 0.2987 M, initial volume = 25 cm^3, I = 1 M $NaClO_4$, T = 298 K)

S.No.	Reaction				log β		
2	Th	+ IDA	→	[Th(IDA)]	10.78	±	0.03
3	Th	+ 2 IDA	→	$[Th(IDA)_2]$	19.81	±	0.07

Reference

1. P di Bernardo, A. Cassol, G. Tomat et al, J. Chem. Soc., Dalton trans., 733 (1983)
2. "Thermodynamics of Complexation of Actinides and Lanthanides with Ligands", Ph. D. Thesis by Neetika Rawat submitted to Homi Bhabha National Institute, Mumbai, March 2011.
3. D. Rama Mohana Rao, R. M. Sawant, B. S. Tomar, "Study of Complexation of Uranyl with iminodiacetic acid by Potentiometry", NUCAR 2013, Govt. Model Science College (A), R. D. University, Jabalpur, M. P. February 19-2013.

Time-resolved laser fluorescence spectroscopy combined with parallel factor analysis: a robust speciation technique for UO_2^{2+}

Takumi Saito[1], Noboru Aoyagi[2], Takaumi Kimura[2]
[1]Nuclear Professional School, School of Engineering, The University of Tokyo
[2]Nuclear Science and Engineering Directorate, Japan Atomic Energy Agency

Speciation is a key issue for the fate of actinides and fission products in natural environments. Time-resolved laser fluorescence spectroscopy (TRLFS) is a popular speciation technique for fluorescent metal ions and can be further extended by combining multivariate data reduction methods such as parallel factor analysis (PARAFAC). This study demonstrates the applicability of TRLFS combined with PARAFAC for the speciation of UO_2^{2+} in solution as well as on mineral surface.

Uranium, time-resolved laser spectroscopy, PARAFAC, speciation, adsorption, complexation

I. INTRODUCTION

Chemical speciation governs the reactivity and migration of radionuclides released from nuclear waste disposal or an accident of a nuclear power plant in environments. Various analytical techniques are used for this purpose. Preferably, such speciation techniques shall possess all of the following capabilities: (i) discrimination of species by their different chemical and/or physical properties, (ii) quantification, and (iiii) structural determination of the species. Time-resolved laser fluorescence spectroscopy (TRLFS) is a particular speciation technique for fluorescent actinide ions such as UO_2^{2+} and Cm^{3+}. The above three characteristics are well-balanced in TRLFS; the discrimination and quantification of species can be achieved, based on their excitation/emission spectra and decay lifetimes; the concentrations of the species are proportional to their fluorescence intensities. The favorable characteristics of TRLFS as a speciation technique largely rely on the inherent multi-dimensional nature of its data, which makes the combination of multivariate statistics method suitable for the data reduction. Parallel factor analysis (PARAFAC) is a multi-model factor analytic method, which can only be applied for data having more than three dimensions. It has been shown that combining TLRFS with PARAFAC provides robust speciation capability for the speciation of Eu^{3+}, a chemical homologues of the trivalent actinide ions [1-3]. In this study, the applicability of TRLFS-PARAFAC for the speciation of UO_2^{2+} is firstly demonstrated.

II. EXPERIMENTAL

A set of the time-resolved fluorescence spectra of UO_2^{2+} complexed with orthosilicate (H_2SiO_4) or adsorbed on gibbsite (α-$Al(OH)_3$) surface were obtained with a TRLFS system equipped with the forth harmonics of Nd:YAG laser. The complexation of UO_2^{2+} with H_2SiO_4 was studied as a function of the H_2SiO_4 concentration at different pH; the adsorption of UO_2^{2+} on gibbsite as a function of pH at the different concentrations of UO_2^{2+}. The entire data set in each series was processed by PARAFAC, using the N-way toolbox for MATLAB®[4].

III. RESULTS AND DISCUSSION

Three species were found for the complexation of UO_2^{2+} with H_2SiO_4 at pH 4, exhibiting the characteristic fluorescence spectra (Figure 1) and decay curves. The fluorescence intensity profiles, which approximated the concentration profiles of the species as a function of the H_2SiO_4 concentration, were used to determine the stability constants of the complexation.

Three surface species of UO_2^{2+} on gibbsite were obtained from the TRLFS data set by applying PARAFAC. Based on the fluorescence spectra, decay lifetimes, and the dependence of the intensity profiles on pH and the UO_2^{2+} concentration, these species likely corresponded to mono-nuclear surface complexes with and without hydrolysis and a multi-nuclear surface complex.

IV. CONCLUSION

It was shown that the combination of TRLFS with PARAFAC was capable of discriminating the contribution of multiple species of UO_2^{2+}. The obtained spectra, decay curves, and intensity profiles were invaluable to understand and model the underlying speciation both in solution and on mineral surface.

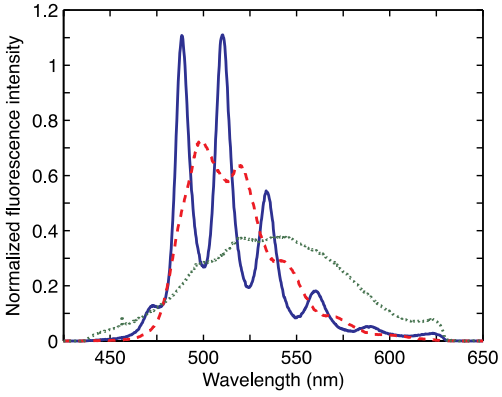

Figure 1. Fluorescence spectra of the three UO_2^{2+} species with H_4SiO_4 obtained from a series of TRLFS spectra by PARARAC.

REFERENCES

[1] Saito, T., et al., *Environ. Sci. Technol.* **2010**, *44*, 5055–5060.
[2] Ishida, K. et al., *J. Colloid Interface Sci.* **2012**, *374*, 258–266.
[3] Lukman, S., et al., *Geochim. Cosmochim. Acta* **2012**, *88*, 199–215.
[4] Andersson, C. and Bro, R., *Chemometr. Intell. Lab.* **2000**, *52*, 1–4.

APSORC'13 - 5th Asia-Pacific Symposium on Radiochemistry
Kanazawa, Japan, 22-27 September 2013

Determination of ^{55}Fe and ^{89,90}Sr in liquid samples using Sr and/or Pb resins for the mutual separation of Fe and Sr

Marijana Nodilo, Ivana Milanović, Željko Grahek
Division for marine and environmental research, Rudjer Bošković Institute, 10000 Zagreb, Croatia

Abstract. The determination of ^{55}Fe and strontium isotopes is complicated and time-consuming, especially the determination of ^{89,90}Sr. In the last decade, a number of methods have been developed for radioactive strontium isolation and determination in various types of samples. On the other hand, only few methods for ^{55}Fe determination are developed, mainly in liquid radioactive waste samples. Since strontium isotopes are highly radiotoxic fission products (especially ^{90}Sr with long half-life), they are an interesting subject for various investigations, from their distribution and behavior in natural systems to the influences on the human health. In distinction from strontium isotopes, ^{55}Fe is an activation product, low energetic emitter with approximately 2.74 year half-life. As such, it is not as interesting as strontium, but environmental concerns prompted the responsible institutions in the radiological monitoring program to include ^{55}Fe determinations in their procedures. In almost all published methods, isolation and determination of ^{89,90}Sr and ^{55}Fe are separated. Therefore, the aim of the paper is to present a method for the isolation of ^{55}Fe and ^{89,90}Sr from liquid sample in one step by using Sr and/or Pb resin and mixture of nitric and hydrochloric acid, because Fe and Sr can be bound on Sr resin from mixture of HNO_3+HCl as shown earlier.[1] Namely, Sr and Pb resins were primarily developed as Sr, Pb specific resins which enable very efficient separation of Sr and Pb from other elements as well as for their mutual separation. The main focus in the literature was directed on their application in the determination of ^{89,90}Sr and ^{210}Pb in different kinds of samples,[2,3] while determination of ^{55}Fe was not in focus from above mentioned reason. Therefore, it will be shown how Fe and Sr can be bound and mutually separated (and from many other elements) on Sr and Pb resin column. It will be shown that binding strength and selectivity on both resins depend on concentration of HCl and HNO_3. By changing the eluent composition, separation of Fe from Sr, as well as Pb from Fe and Sr ions, can be achieved on both resins. Based on these results, methodology for rapid determination which involves, binding of Fe and Sr on the column from the mixture of HNO_3+HCl, elution of Sr with HCl, Fe with H_2O and detection on LSC is created. It will be shown that ^{55}Fe and ^{89,90}Sr can be easily separated on both resins from different types of samples with almost same efficiency. Methodology is tested by determination of ^{55}Fe and ^{89,90}Sr in proficiency testing samples and radioactive waste samples and obtained results will be presented and discussed in detail.

Keywords: Sr and Pb resin, Iron-55, Strontium-89, 90, separation

Table 1. Distribution coefficients of elements on Pb resin

K_d [mLg^{-1}]	Pb resin				
	Sr	Mn	Fe	Ni	Pb
0,5 M HCl	-	-	-	-	322
2 M HCl	-	-	-	-	218
4 M HCl	-	-	220	-	68,7
6 M HCl	-	-	442	-	8,94
6 M HCl + 1 M HNO_3	58,91	-	796	-	3,54
6 M HCl + 3 M HNO_3	101,12	-	210	-	-
6 M HCl + 5 M HNO_3	105,66	-	102,5	-	-
5 M HNO_3	108,42	-	-	-	>399

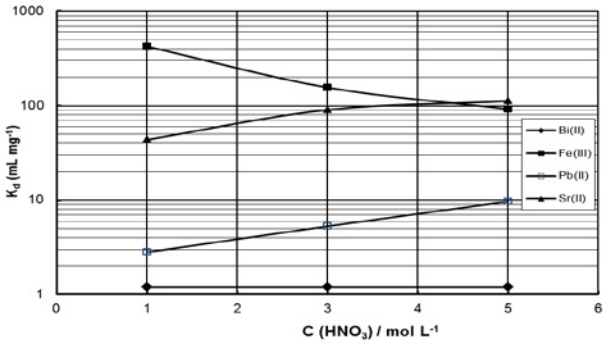

Figure 1. Distribution coefficients of elements in mixture of 6M HCl and HNO_3 on Sr resin

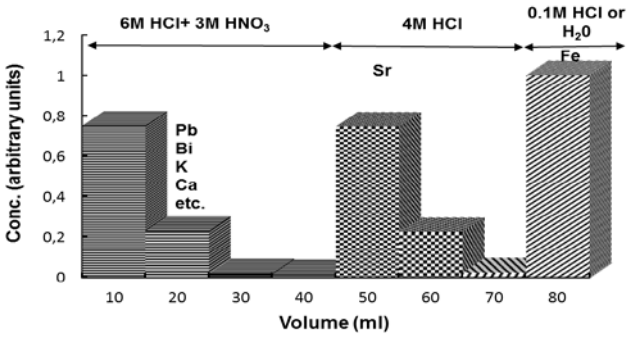

Figure 2. Separation of Sr and Fe from other elements on Pb resin column

[1] Ž. Grahek, I. Milanović, M. Nodilo, M. Rožmarić, Sequential separation of Fe and Sr from liquid samples by using Sr resin and rapid determination of ^{55}Fe and ^{89,90}Sr. Appl. Radiat. Isot. *In press*
[2] Horwitz E.P., Dietz M, Chiarzia R, Novel Strontium-Selective Extraction Chromatographic Resin. Solvent Extraction & Ion Exchange, 10 (1992) 313-336.

APSORC'13 - 5th Asia-Pacific Symposium on Radiochemistry
Kanazawa, Japan, 22-27 September 2013

Implementation of Dry Cow Dung Powder for Biosorption of ^{90}Sr(II) from Simulated Radioactive Waste

Roshan P. Khilnani, Hemlata K. Bagla
Department of Nuclear and Radiochemistry, K. C. College, Mumbai – 20, India.

Abstract – ^{90}Sr is one of the major fission product found in the radioactive waste. The anthropogenic activities such as nuclear weapon testing, reprocessing of liquid spent fuel etc. are major sources of ^{90}Sr in our environment. Some of the well-established processes such as chemical precipitation, membrane process, liquid extraction and ion exchange have been applied as a tool for the removal of this metal ion. All the above methods are not considered to be greener due to some of their shortcomings such as incomplete metal ion removal, high requirement of energy and reagents, generation of toxic sludge or other waste materials which in turn require further treatments for their cautious disposal. The present investigation entails the biosorption studies of ^{90}Sr(II) from simulated radioactive waste employing dry cow dung powder (DCP) as an indigenous, inexpensive and, eco-friendly material without any pre or post treatments. As DCP is easily available, it is superior to other processed natural adsorbent considering their cost, time and energy efficiency. The Batch experiments were conducted employing ^{90}Sr as a radiotracer and the effect of process parameters such as pH, temperature, amount of resin, time of equilibration, agitation speed and distribution co-efficient have been studied for simulated reactor and reprocessing waste with and without carrier. The efficiency of adsorption was found to be more than 70%. The prime amenity of using DCP over other biosorbents is that it doesnot require any degree of physical and chemical enhacement for optimization of the method and inturn adds to the economy of entire adsorption process. Thus use of DCP manifests the principles of Green Chemistry and proves to be an eco-friendly alternative for the remediation of radiotoxic ^{90}Sr(II).

Keywords – Biosorption, Strontium, Dry cow dung powder, Simulated radioactive waste

APSORC'13 - 5th Asia-Pacific Symposium on Radiochemistry
Kanazawa, Japan, 22-27 September 2013

Application of Simplified Desorption Method to Sorption Study: (1) Sorption of Americium (III) on Bentonite and Its Major Components

Naofumi Kozai[1], Toshihiko Ohnuki[1]
[1]Japan Atomic Energy Agency, Tokai, Ibaraki, 319-1195 Japan

Abstract – To elucidate the sorption behavior of americium on bentonite, which is a mixture of montmorillonite clay, quartz and so on, simplified desorption experiments were applied to the solid phases collected after the sorption experiments. Almost 100% of Am was sorbed on bentonite and montmorillonite at pH from 2 to 8. A fraction of the Am sorbed on the solid phases was desorbed by twice treatment with a 1M KCl aqueous solution, and the residual Am was completely desorbed by twice treatment with a 1M HCl aqueous solution. The desorption behaviors of Am from bentonite and montmorillonite were very similar to each other and symmetrical at pH 7. Most of the Am sorbed below pH 7 was desorbed with 1M KCl solutions and that above pH 7 was not desorbed with 1M KCl but with 1M HCl solutions. The trend in the KCl-desorbable fraction vs. pH is very similar to the abundance ratio of cationic Am species (Am^{3+}) and so is the trend in the KCl-nondesorbable fraction to that of the hydrolyzed species of Am.

Keywords – Americium, sorption, desorption, pH, montmorillonite, bentonite, quartz

I. INTRODUCTION

Sorption is one of the key mechanisms to control the subsurface environmental behavior of the radionuclides. It is known that sorption behavior of elements on solid phases may vary depending on the concentration of the element [1]. Thus, for the environmental study, it is desirable to examine sorption behaviors at tracer concentrations (nanomolar or less). To date it is however impossible to apply any instrument analysis except radiation measurements to the analysis of the tracer level radionuclides on solid phases.

To analyze the tracer level neptunium sorbed on clays, a simplified desorption method sequentially using two kinds of desorption agent solutions was effective [2]. This paper applies the desorption method to the sorption study of Am on bentonite and discuss the sorption and Am species. Bentonite is a clay found ubiquitously in soil environment. Its main component is montmorillonite, and minor components are calcite, dolomite, quartz, pyrite, cristobalite, zeolite, etc. Owing to high cation exchange capacity of montmorillonite, bentonite clay plays a very important role for migration of radionuclides in the subsurface environment.

II. EXPERIMENTAL

Tsukinuno montmorillonite (Kunipia F®, Kunimine Industries Co. Ltd.) was used after the montmorillonite was converted to homoionic Na^+ forms (Na-montmorillonite). Tsukinuno bentonite (Kunigel V1®, Kunimine Industries Co. Ltd.) was used with no pretreatment. Kunipia F is a purified product from this bentonite. An Am (III) nitrate stock solution was diluted with 0.01 M $NaClO_4$ to yield a working solution having an Am concentration of about $5x10^{-10}$ M.

For the sorption experiments, the initial pH of the Am solution was adjusted over a range of 1.8 to 10. A weighed amount (0.06 g) of sold phases was soaked in 6 cm^3 aliquots of the Am solution and stored at 20°C. This solid-solution mixture was agitated once a day. After 10 days, a supernatant was collected by centrifugation.

Desorption experiments were conducted in two steps. First, 6 cm^3 of 1 M KCl solution was added to the solid phases collected after the sorption experiments. After 2 days, the KCl solution was separated by centrifugation. Second, desorption with a 1 M HCl solution was undertaken in the same way as the desorption with a 1 M KCl solution. The desorption with each solution was carried out twice to confirm complete desorption of Am.

III. RESULTS AND DISCUSSION

In the examined final pH range (2 – 8), almost 100% of Am was sorbed on bentonite and montmorillonite. All of the Am sorbed on bentonite and montmorillonite were desorbed by the two step desorption procedures. The desorption behaviors of Am from bentonite and montmorillonite were very similar to each other. Most of the Am sorbed below pH 5 was desorbed by the twice treatment with 1M KCl solutions. The KCl-desorbable fraction of Am sharply decreased with increasing pH above pH 5 and most of the Am sorbed above pH 7 was not desorbed with 1M KCl solution but with 1M HCl solution. The trend in the KCl-desorbable fraction vs. pH is very similar to the abundance ratio of cationic Am species (Am^{3+}) and so is the trend in the KCl-undesorbable fraction to that of the hydrolyzed species of Am. It is intuitively understand that the Am desorbable from the bentonite with KCl solution is the Am sorbed on the montmorillonite fraction in the bentonite.

This paper further discuss the sorption behavior of Am on bentonite with the result of blank experiments to examine the sorption on the reaction vessels and with that of sorption and desorption experiments on quartz, which is the second major mineral in the bentonite.

[1] Ohnuki T et al., J. Nucl. Sci. Technol., in press.
[2] Kozai N et al., Radiochimica Acta, 75, 149-158 (1996).

APSORC'13 - 5th Asia-Pacific Symposium on Radiochemistry
Kanazawa, Japan, 22-27 September 2013

Effect of aging on availability of iodine in grassland soil collected in Rokkasho, Japan

Akira Takeda, Hirofumi Tsukada, Yuichi Takaku, Shun'ichi Hisamatsu
Department of Radioecology, Institute for Environmental Sciences

Abstract – In the laboratory, we investigated the time-dependent changes in the availability of I in soil over the course of 23 months. Stable I was added as iodide or iodate to a soil sample collected from a grassland area in Rokkasho, Japan. Whether I was added as iodide or iodate, its water solubility, and soil-to-grass transfer factor decreased drastically over the course of 4 months after addition and then slightly decreased thereafter.

Keywords – iodate, iodide, radioiodine, soil-to-plant transfer

I. INTRODUCTION

The first commercial nuclear fuel reprocessing facility in Japan, located in Rokkasho, Aomori Prefecture, is undergoing its final testing using actual spent nuclear fuel. Iodine-129 (half-life, 1.6×10^7 y) is discharged from the facility, and the radiation dose to the public resulting from discharge of this radionuclide must be assessed. Some of the ^{129}I discharged to the atmosphere is deposited on the land surface and retained in surface soil. The mobility of I in soil is expected to decrease with time after its deposition, and investigation of the time-dependent changes in I mobility in soil is necessary for the better prediction of long-term I behavior in the surface soil environment. We conducted a laboratory study of the changes in the water solubility and phytoavailability of trace I added to soil collected from Rokkasho.

II. MATERIALS AND METHODS

A soil sample was collected from the surface of a pasture field in Rokkasho, Japan. Aliquots (200 g) of the dried soil sample were placed in plastic pots, and a solution of NaI or $NaIO_3$ was added to the soil in each pot at a concentration of 20 mg-I kg^{-1}-soil. The pots were stored in an artificial climate chamber for about 23 months. The water content of the soil was adjusted to 60% of its maximum water-holding capacity every 2 weeks. The soil in the pots was stirred every 4 weeks. As controls, pots of soil without added I were treated the same way.

Soil samples were collected from the pots at 0, 2, 9, 29, 64, 113, 204, 372, and 687 d after addition of the I solution. The soil samples were extracted with deionized water, at a 1:10 w/v ratio of soil to water, for 1 h at 20°C. The supernatants were separated from the soil by means of high-speed centrifugation and then filtered through a 0.22-μm-pore membrane filter.

Orchardgrass (*Dactylis glomerata*) was cultivated in the pots 2–29 d, 37–64 d, 86–113 d, 117–204 d, 345–372 d, and 660–687 d after the addition of I. The cultivation experiments were carried out in triplicate for each time period. Twenty germinated seeds were sown in each pot. The water content of the soil was adjusted with deionized water to 60% of maximum water-holding capacity of the soil three times a week during the cultivation period. The aboveground parts of the plants were sampled at 28 d after sowing. The plant samples were freeze-dried and finely ground. Iodine in the plant samples was extracted with tetramethyl ammonium hydroxide at 60ºC overnight. The concentrations of I in the soil and plant extracts were determined by inductively coupled plasma mass spectrometry. Concentrations of added I in the soil extract and plant were calculated by subtracting the I concentrations in the control samples, to which I had not been added.

III. RESULTS AND DISCUSSION

The water-solubility of I in the soil decreased with time after its addition. Soon after addition, 98% of the I added as iodide and 54% of the I added as iodate were extracted with water. In contrast, the extraction yield of the added I at 113 d after addition was 2%, and no difference was observed between the chemical forms of the added I. The extraction yield of the added I was nearly constant thereafter, and was 1.5% at 687 d after the addition.

The concentration of added I in the orchardgrass plants was relatively lower in the later stage compared to soon after addition of I to the soil. The soil-to-plant transfer factor, which is defined as (concentration of added I in the aboveground part of the plant)/(concentration of added I in the soil) (mg kg^{-1} dry plant)/(mg kg^{-1} dry soil), decreased with time after the addition: from 0.80 to 0.042 for the soil with added iodide, and 1.3 to 0.041 for the soil with added iodate over the course of the experiment (Fig. 1). The decreasing trend was similar to that for the water extractability from the soil.

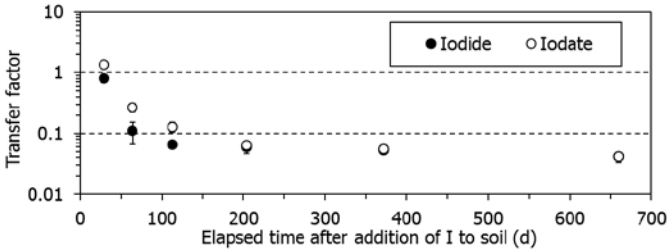

Fig. 1 Time-dependence of soil-to-plant transfer factor of I after its addition to the soil. Error bars indicate standard deviations (n = 3). Orchardgrass was cultivated for 28 d in each pot experiment. The plotted transfer factors are values for the end of each cultivation period.

This study was performed under a contract with the government of Aomori Prefecture, Japan.

Study on ^{14}C spatial distribution around Qinshan nuclear power plant in China

Zhongtang Wang[1], Dan Hu[2], Qiuju Guo[1]
[1] State Key Laboratory of Nuclear Physics and Technology, Peking University Beijing 100871,China.
[2]Radiation Monitoring Technical Center of Ministry of Environmental Protection, Hangzhou 310012, China

Abstract –To understand the spatial distribution of ^{14}C discharged by Qinshan nuclear power plant (NPP), where two heavy water reactors (Plant III) are on commercial operation, both experimental investigation and model prediction (Gaussian plume model) were carried out by this work. Twenty one moss samples were collected in five different wind directions near Qinshan NPP, and analyzed by accelerator mass spectrometry (AMS). The ^{14}C specific activities in moss samples ranged from 265.6 to 233.0 Bq/kg C (the background is 233.8 ±1.1 Bq/kg C), decreasing with increased distance from the stacks of Plant III. Simulation of ^{14}C spatial distribution in air was calculated by using a Gaussian plume model, which was based on monthly meteorological data, ^{14}C discharge record, local dispersion parameter and other parameters. A good fit was found between the predicted and measured values, indicating that the spatial distribution of ^{14}C follows a Gaussian model. It can be concluded furthermore, that the influence of the Hill Qinshan (located at W of Plant III, 170 meters high) on ^{14}C's distribution is quite limited at this site - compared to meteorological influences.

Key words: Qinshan NPP; ^{14}C; Gaussian plume model

APSORC'13 - 5th Asia-Pacific Symposium on Radiochemistry
Kanazawa, Japan, 22-27 September 2013

Atmospheric deposition of radionuclides (^{7}Be, ^{210}Pb, ^{134}Cs, ^{137}Cs, and ^{40}K) during 2000–2012 at Rokkasho, Japan, and impact of the Fukushima Dai-ichi Nuclear Power Plant accident

Naofumi Akata[1], Hidenao Hasegawa[1], Hitoshi Kawabata[1], Hideki Kakiuchi[1], Yuki Chikuchi[2]
Nagayoshi Shima[3], Toshitaka Suzuki[4], Shun'ichi Hisamatsu[1]
[1]Institute for Environmental Sciences
[2]Aomori JGC PLANTECH
[3]Fukushima University
[4]Yamagata University

Abstract – Radionuclides, including radiocesium (^{134}Cs and ^{137}Cs), were measured in atmospheric deposition samples collected in Rokkasho, Aomori, Japan, from 2000 to 2012. After the accident at the Fukushima Dai-ichi Nuclear Power Plant, radiocesium deposition rapidly increased and reached a maximum in April 2011. Since then, monthly radiocesium deposition has gradually decreased. Monthly ^{137}Cs deposition has almost reached pre-accident levels, although ^{134}Cs is still being detected.

Keywords – atmospheric deposition, Rokkasho Village, Fukushima Dai-ichi Nuclear Power Plant accident

I. INTRODUCTION

Natural and anthropogenic radionuclides are useful tracers for studying processes in the atmospheric environment. Atmospheric deposition of radionuclides has been measured at many sites for geochemical studies and radiation protection. We have been measuring atmospheric deposition of radionuclides in the village of Rokkasho, Aomori Prefecture, Japan, since 2000 [1, 2]. In this study, we report the impact of the accident at the Fukushima Dai-ichi Nuclear Power Plant (FDNPP) on the atmospheric deposition of radiocesium (^{134}Cs and ^{137}Cs) in Rokkasho.

II. EXPERIMENTAL

Atmospheric deposition samples were collected on the roof of a building at the Institute for Environmental Sciences in Rokkasho (40° 57′ N, 141° 21′ E), approximately 13 m above ground level. Bulk atmospheric deposition samples were collected biweekly in a polyethylene basin from March 2000 until March 2006, and samples were collected monthly after April 2006. Each sample was passed through a Powdex resin (Ecodyne Co., USA) column to separate ionic radioactive species and particulates from the sample. The homogenized resin was dried and packed into a plastic case for γ-ray spectrometry. The concentrations of γ-ray-emitting radionuclides, including ^{7}Be, ^{210}Pb, ^{137}Cs, and ^{40}K, in the sample were measured with a low-energy photon spectrometer with a Ge detector. After the accident at the FDNPP, ^{134}Cs concentrations were also measured.

III. RESULTS AND DISCUSSION

Annual deposition of ^{137}Cs from 2001 to 2010 ranged from 0.04 to 0.69 Bq m^{-2} with a mean value of 0.21 Bq m^{-2}. We have already reported that recent background ^{137}Cs deposition was affected by Asian dust [1]. On 11 March 2011, large amounts of radiocesium were released into the atmosphere from the accident at the FDNPP. After the accident, monthly radiocesium deposition increased, reaching a maximum in April 2011. Thereafter, monthly ^{137}Cs deposition decreased rapidly until September 2011 (apparent half-time ~0.8 month) and more gradually (half-time ~0.7 y) from September 2011 until December 2012. Annual deposition of ^{137}Cs was 86.9 Bq m^{-2} in 2011 and 1.89 Bq m^{-2} in 2012. Monthly ^{137}Cs deposition has dropped almost to the pre-accident level, although ^{134}Cs is still detectable.

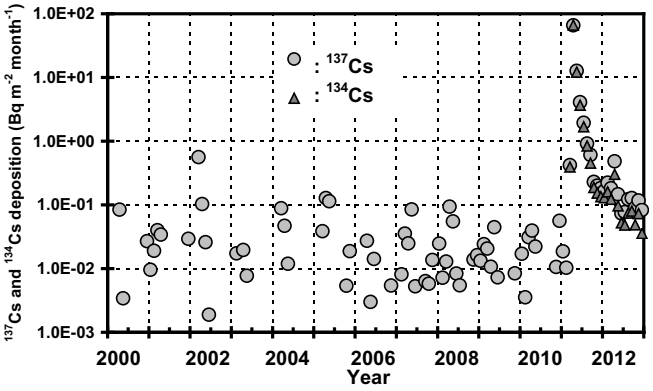

Fig. 1 Monthly atmospheric deposition of ^{137}Cs and ^{134}Cs in Rokkasho

REFERENCES

[1] Akata, N., Hasegawa, H., Kawabata, H., Chikuchi, Y., Sato, T., Ohtsuka, Y., Kondo, K. and Hisamatsu, S. (2007) Deposition of ^{137}Cs in Rokkasho, Japan and its relation to Asian dust, Journal of Environmental Radioactivity, 95, 1-9.

[2] Akata, N., Kawabata, H., Hasegawa, H., Sato, T., Chikuchi, Y., Kondo, K., Hisamatsu, S. and Inaba, J. (2008) Total deposition velocities and scavenging ratios of ^{7}Be and ^{210}Pb at Rokkasho, Japan, Journal of Radioanalytical and Nuclear Chemistry, 277, 347-355.

This study was performed under a contract with the government of Aomori Prefecture, Japan.

APSORC'13 - 5th Asia-Pacific Symposium on Radiochemistry
Kanazawa, Japan, 22-27 September 2013

Effect of Aging on Water Extractability of Radioactive Iodine and Cesium from Soil

Hirofumi Tsukada, Akira Takeda, Shunichi Hisamatsu
Department of Radioecology, Institute for Environmental Sciences

Abstract – Water extractabilities of radioactive ^{125}I and ^{137}Cs from soil were determined by tracer experiments. Career free ^{125}I (iodide or iodate) or ^{137}Cs was spiked to soil samples, which were then stored in an artificial climate chamber where a wetting-and-drying treatment was repeated. Extraction yield of ^{125}I at 4 h after spiking with iodide was higher than that with iodate, and then both yields decreased with aging independent of the chemical forms. Chemical form of ^{125}I in the water extracts at 29 d was predominantly iodide, regardless of whether the spiked form was iodide or iodate. Water extraction yield of ^{137}Cs immediately decreased after spiking in the soil, which was 0.015 at 4 h, and then less than 0.001 at 320 d after spiking.

Keywords – radioactive ^{125}I, iodide, iodate, ^{137}Cs, water extractability, aging

I. INTRODUCTION

Aging of radionuclides in soils after deposition can play an important role in the change of the physicochemical form, which is an important factor in determining the fate of radionuclides in the environment. Radioactive iodine and cesium were the major radionuclides released from the Fukushima Daiichi Nuclear Power Plants after the accident in March 2011. Water extractable forms in soil make up the most mobile fraction, which can migrate and be taken up by plants. In the present study, water extractabilities of radioactive ^{125}I (iodide and iodate) and ^{137}Cs were determined at different elapsed time intervals.

II. MATERIALS AND METHODS

Volcanic ash soil (Andosol), which is a typical upland soil in Japan, was collected from the surface of a grassland in Aomori Prefecture (40°52'23"N, 141°16'57"E). The soil was dried at 50°C and passed through a 2 mm sieve. Career free ^{125}I (iodide or iodate) or ^{137}Cs of 10 kBq was spiked to 1 g of soil sample. Iodate solution was prepared by the oxidation of iodide solution by adding bromine water. The samples were stored in an artificial climate chamber (17°C, 60% relative humidity, 30 klx, 12 h of daylight), and wetting-and-drying treatments were repeated by adding 1 ml of deionized water every 2 weeks. The soil samples were extracted with deionized water for 1 h at room temperature with a 1:10 ratio of soil weight to extract. The samples were extracted from 4 h to 320 d after spiking for ^{125}I, and 4 h to 1110 d for ^{137}Cs. The extracts were filtered through a 0.22 μm pore membrane filter (Millipore, Steriflip®) after centrifugation at 10,000 rpm for 5 min. Chemical forms of ^{125}I in the water extracts were also determined at 2 and 29 d after spiking by using an anion exchange disk (3M, Empore Anion-SR®). Radioactivity of the extract and disk samples were measured with NaI(Tl) detectors.

III. RESULTS AND DISCUSSION

Water extraction yield of ^{125}I at 4 h after spiking with iodide was 0.87, which was higher than that with iodate (0.33), and both yields after spiking decreased to 0.033-0.034 at 320 d independent of the spiking chemical forms (Fig. 1). Content of $^{125}IO_3^-$ in the water extract at 2 d after spiking with iodate was 28%, and that it decreased to 1% at 29 d. Iodine-125 in the water extract at 2 and 29 d after spiking with iodide existed as $^{125}I^-$. This suggests that the chemical form of ^{125}I in the water extracts was predominantly iodide excluding the time just after spiking, regardless of whether the spiking form was iodide or iodate.

Water extraction yield of ^{137}Cs in the soil immediately decreased after spiking, from 0.015 at 4 h to 0.0075 at 30 d. After that, the yield was gradually decreased from 0.0012 at 120 d to less than 0.001 at 320 d, and was 0.00050 at 1110 d after spiking. It is well known that radioactive Cs is strongly fixed in clays, and that its mobility is limited.

The results show that transferability of radioactive iodine and cesium in soil immediately decreases in early stage after deposition.

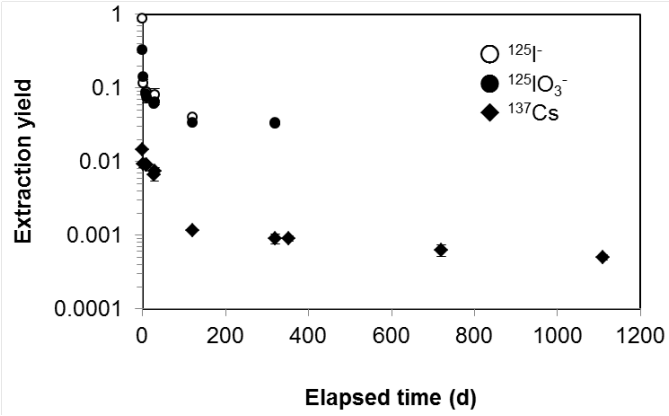

Fig. 1 Time dependecy of water extractabilities of ^{125}I (iodide and iodate) and ^{137}Cs from soil. Error bars indicate one standard deviation (n=3).

This study was performed under a contract with the government of Aomori Prefecture, Japan.

Background internal dose rates of earthworm and arthropod species in the forests of Aomori, Japan

Yoshihito Ohtsuka, Yuichi Takaku, Shun'ichi Hisamatsu
Department of Radioecology, Institute for Environmental Sciences

Abstract – We measured naturally occurring radionuclides in samples from an earthworm species and 11 arthropod species collected in coniferous forests in Rokkasho, Aomori, Japan, to assess background internal radiation dose rates. The rates were calculated from the measured concentrations of the radionuclides and dose coefficients from the literature. The mean internal dose rate of composite earthworm samples was 0.35 μGy h^{-1}, whereas the mean dose rates of the arthropod samples ranged from 36 nGy h^{-1} to 0.79 μGy h^{-1}. Polonium-210 was the radionuclide with the highest contribution to the internal dose rate for all the species, except the longhorn beetle.

Keywords – non-human species, background radiation, naturally occurring radionuclides, forest ecosystem

I. INTRODUCTION

Protection of the environment from radiation and assessing effects of radiation on nonhuman species have been discussed by international organizations such as the International Commission on Radiological Protection [1]. Many researchers have reported concentrations of artificial radionuclides in animals living in terrestrial environments contaminated by the nuclear accidents at Chernobyl and Fukushima [e.g., 2, 3]. However, few studies have compared background radiation doses with artificial radionuclide doses.

In this study, samples of an earthworm species and 11 arthropod species were collected in coniferous forests around the nuclear fuel reprocessing plant currently under construction in Rokkasho, Aomori, Japan, and the internal background dose rates of natural radionuclides were determined.

II. MATERIALS AND METHODS

One species of earthworm and 11 species of arthropods were collected monthly in coniferous forests in Rokkasho from June to October 2008; the animals were collected with falling traps buried in the ground in four areas (Fig. 1). After being washed with pure water, the animals were freeze-dried. For each animal species, a composite sample was prepared from the dried animals for each sampling site and each collection month. The composite samples were analyzed for ^{210}Po, ^{210}Pb, ^{238}U, ^{232}Th, ^{40}K, and ^{87}Rb by γ-ray and α-ray spectrometry, and ICP-AES and ICP-MS.

III. RESULTS AND DISCUSSION

Polonium-210 was the natural radionuclide with the highest concentration in the earthworm samples, whereas ^{40}K was the radionuclide present at the highest concentration in the samples of all the arthropods, except for a millipede and a Japanese ground beetle. The mean ^{210}Po concentration in the earthworm samples was 0.10 Bq g^{-1}-wet, and the mean ^{210}Po concentrations in the arthropods varied widely, from 0.0042 Bq g^{-1}-wet in a longhorn beetle to 0.24 Bq g^{-1}-wet in a millipede.

The internal dose rates were calculated by using the measured concentrations of ^{210}Pb, ^{210}Po, ^{232}Th, ^{238}U, and ^{40}K, and the dose coefficients for the earthworm and the woodlouse reported by the Framework for Assessment of Environmental Impact [4]; the dose coefficients for the woodlouse were applied to all the arthropods. The mean internal dose rate for the earthworm was calculated to be 0.35 μGy h^{-1}, approximately 90% of which was due to ^{210}Po. The dose rates for the arthropods ranged from 36 nGy h^{-1} to 0.79 μGy h^{-1}, with the actual value depending mainly on the ^{210}Po concentration. The contribution of ^{210}Po to the dose rate of the arthropods varied from 36% to 95%.

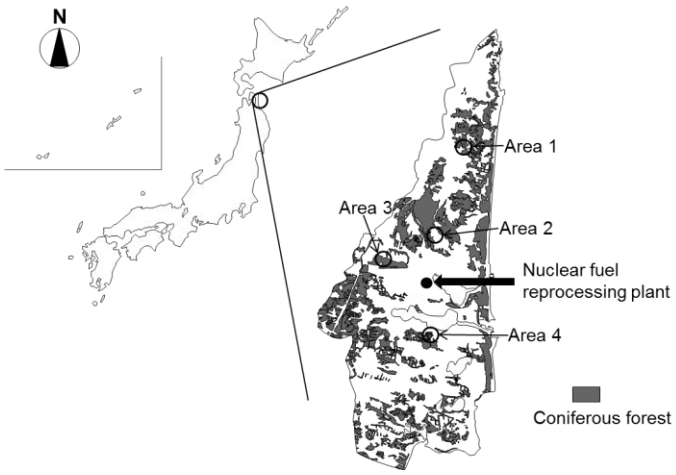

Fig. 1 Sampling areas for earthworms and arthropods, along with the distribution of coniferous forests in Rokkasho, Aomori, Japan.

This study was performed under a contact with the government of Aomori Prefecture, Japan.

REFERENCES

[1] International Commission on Radiological Protection (2007) The 2007 recommendation of the Internal Commission on Radiological Protection, Publication 103.
[2] J. W. Mietelski et al. J. Radioanal. Nucl. Chem., 262, (2005) 645.
[3] T. Fukuda et al., PLOS ONE, 8, (2013) e54312.
[4] Framework for Assessment of Environmental Impact (2003) The EC 5th Framework programme, Contact FIGE-CT-2000-00102.

APSORC'13 - 5th Asia-Pacific Symposium on Radiochemistry
Kanazawa, Japan, 22-27 September 2013

An EXAFS Study on the Effect of Natural Organic Matter and Mineralogy Composition on Cesium Mobility in Environment

Qiaohui FAN, Masato TANAKA and Yoshio TAKAHASHI

Department of Earth and Planetary Systems Science, Graduate School of Science, Hiroshima University, 1-3-1 Kagamiyama, Higashi-Hiroshima, Hiroshima 739-8526, Japan
(Corresponding mail: fanqiaohui@gmail.com)

Abstract: The sorption of Cs was clearly inhibited in the ternary clay+HA+Cs system (the addition sequence of reagent) with respect to the blocking to the access of frayed edge sites (FESs) and interlayer sites by HA for both illite and vermiculite. Both inner-sphere complexes (ISCs) and outer-sphere complexes (OSCs) of Cs^+ have attribution to its adsorption on illite (non-expansion). However, on vermiculite (intermediate expansion), the partially dehydrated Cs^+ was liable to be present as ISCs associated with the siloxane group of the ditrigonal cavity in the SiO_4 sheet. However, nearly complete OSCs were observed at the planar sites of montmorillonite (high expansion).

Keywords: Cesium, EXAFS, Clay mineral, Mobility, Natural organic matter

Introduction

There is a consensus that radiocesium (RCs) strongly and selectively interacts with the phyllosilicate fraction of soil, sediment, and suspended particles such as illite, vermiculite, and montmorillonite. Natural organic matters (NOMs) normally play various important roles in the environment because of its correlations with soil properties and Cs bioavailability. Herein, the speciation of Cs on clay minerals in presence of humic acid (HA) were investigated by batch experiment, modified sequential extraction [1] and Cs L_{III}-edge EXAFS approaches.

Experimental

IMt-1 illite (Cambrian shale, Silver Hill, Montana) and SWy-2 montmorillonite (Mont) from the University of Missouri were purchased from The Clay Minerals Society. Vermiculite (Verm) from Kent, Connecticut was supplied by Ward's Natural Science Establishment, Rochester, NY, USA.

Cs L_{III}-edge extended X-ray absorption fine structure (EXAFS) spectra were collected at BL-12C and BL-9A stations at KEK Photon Factory (Tsukuba, Japan). EXAFS analysis was performed using REX 2000 (Rigaku Co. Ltd) and FEFF 7.0 [2].

Results and Discussion

Cesium sorption on vermiculite increased significantly over the pH range of 3.0 to 7.0, whereas weak pH dependence was observed for Cs sorption on illite. The pH dependence can be ascribed to the competitive sorption with proton, wherein the available exchange site for Cs increases with pH increasing. In Verm+HA+Cs system, Cs sorption is clearly depressed, but this inhibition becomes weaker with increasing pH. A similar phenomenon could also be found in the illite+HA+Cs system.

EXAFS analysis demonstrated that Cs speciation strongly depends on mineralogy and NOMs. The increase in pH from 3.0 to 7.0 increases ISCs from 42% to 80% for illite. However, in vermiculite system, ISCs mostly dominate Cs fixation and weakly depend on pH. Vermiculite with a 1.4 nm layer distance is enough to the entrance of Cs^+ and to form the ISCs associated with the siloxane groups of ditrigonal cavities even at low pH. XRD patterns showed that the characteristic peak of vermiculite (6.1°) shifted to a large angle after Cs adsorption at low Cs concentration even in the presence of HA and disappears at high Cs concentration. The dehydrated Cs^+ replacement of Mg^{2+} or K^+ causes the partial collapse of vermiculite layers at low Cs coverage and complete collapse at high Cs coverage, which is a more stable state to Cs [2]. However, no such change was observed in the illite systems. The negative charge of montmorillonite with a 2.0 nm layer distance (high expansibility) is mainly derived from the isomorphic substitution of Mg^{2+} for Al^{3+} in the octahedral AlO_6 sheet, which drives hydrated Cs^+ to form OSCs in the interlayer sites.

EXAFS analysis indicates that HA molecules could efficiently block the accesses to FESs and interlayer even at relative large layer distance such as vermiculite (1.4 nm) to reduce Cs sorption to a large extent. Obviously, the OSCs proportion increase in the illite+HA+Cs system, because the coated HA molecules make Cs form OSCs through electrostatic attractive force, which was also consistent with the sequential extraction results.

Conclusion

The strong retard Cs in soil or sediment could attribute to the ISCs related to the FESs and interlayer of illitic clay minerals. However, the presence of NOMs could provoke Cs mobility largely by the indirect effect, i.e., the blocking effect.

Reference

[1] Rigol A., Roig M., Vidal M. and Rauret G. Environ. Sci. Technol. 33 (**1999**) 887-895.
[2] Zabinsky S. I., Rehr J. J. and Ankudinov A. *Phys. Rev. B* 52 (**1995**) 2995-3009.
[3] Kogure T., Morimoto K., Tamura K., Sato H. and Yamagishi A. *Chem. Lett.* 41 (**2012**) 380-382.

APSORC'13 - 5th Asia-Pacific Symposium on Radiochemistry
Kanazawa, Japan, 22-27 September 2013

Using Factorial Design to the Robustness Analysis of the Classic Sample Preparation Method for ^{90}Sr Determination in Tea Leaf

Chi-Chang Liu[1*], Wen-Hsien Tsai[1], Ming-Chi Horng[1], Ching-Chung Huang[1], Yuh-Wern Wu[2]
[1]Radiation Monitoring Center, AEC, Taiwan, ROC
[2] Department of Chemical Engineering, I-Shou University, Taiwan, ROC

Abstract

The classic sample pretreatment method for ^{90}Sr determination based on a series of precipitations including the separation of Sr from Ca by fuming nitric acid is the standard and popular method around world. To select a best set of operational conditions for such an analytical method with numerous of experimental steps is a difficult task. Even when the optimum values of these factors are found, practically it is difficult in accurately controlling them and sometimes leads to wide variations of results. Procedures for optimization of factors by multivariate techniques have been encouraged, as they are faster, more economical and effective, and allow more than one variable to be optimized simultaneously for sample preparation. However, the application of these techniques for the robustness analysis in the method for radiochemical analysis has been limited. In this study, a robustness test was performed to provide a better insight into which critical process affect ^{90}Sr determination in the sample preparation method. To assess method robustness, the empirical optimum procedures set for this method have been test by slightly modified and were evaluated using the factorial design approach at two levels. The evaluated sensitivity of parameters includes pHs in precipitation procedures, concentration of fuming nitric acid, and times for reactions. The result allows us to analyze the influence of significant factors upon the ^{90}Sr radioactivity and the recovery of carrier and to establish intervals that ensure the robustness of our method.

Keywords ^{90}Sr, robustness, factorial design, fuming nitric acid method

[1] Y. Vander Heyden, A. Nijhuis, J. Smeyers-Verbeke, B. G. M. Vandeginste, and D. L. Massart, "Guidance for robustness/ruggedness tests in method validation," Journal of Pharmaceutical and Biomedical Analysis, vol. 24, no. 5-6, pp. 723–753, 2001.
[2] D.G. Montgomery, Design and Analysis of Experiments, 7th Edition, John Wiley and Sons, New York, 2009.

A simple method for dehydrogenase assay of soil microorganisms to evaluate the biospheric behavior of C-14 originated in transuranic waste

Kayoko Iwata, Nobuyoshi Ishii, Keiko Tagami, Shigeo Uchida
Office of Biospheric Assessment for Waste Disposal, National Institute of Radiological Sciences

Abstract – When carbon-14 (^{14}C) that originated in transuranic (TRU) waste reaches the ground surface in low molecular weight organic forms, it is reported that soil microbial activity has influence on $^{14}CO_2$ gas production. This study aims to develop a simple method to determine soil microbial respiratory activity, which results can be applied to evaluate their correlations with ^{14}C gasification ratios. Respiratory activity was measured using 2-(p-iodophenyl)-3-(p-nitrophenyl)-5-phenyltetraxolium chloride (INT). Agricultural soil samples were incubated at a solid: liquid ratio of 1 to 10, often used in the gasification ratio experiments. Primarily, INT incubation time, INT-formazan extraction method, and storage time for the extracted INT-formazan were examined.

Keywords – C-14, Soil microbial activity, CO_2 production

I. INTRODUCTION

Carbon-14 (^{14}C) is one of the important radionuclides in transuranic (TRU) waste, which are concerns to human dose assessment due to its relatively long half-life (5730 y) and potential for migration to the biosphere. It was reported that ^{14}C released from TRU waste is partially released as low molecular weight organic forms, such as acetic acid, formic acid, and methanol. These forms have low adsorption properties and are expected to pass through barrier materials. However, there is little information available on the fate of organic ^{14}C after reaching the ground surface. Although it has been showed that soil microbial activity influences CO_2 gas production [1], few studies have been conducted to estimate the gasification ratio using soil microbial activity as an indicator. Understanding the relationship between soil microbial activity and CO_2 gas production may enable to estimate gasification ratio of ^{14}C in different soil in the future.

Since CO_2 gas production is influenced by microbial decomposition of organic ^{14}C, microbial respiratory activity is involved. However, the microbial respiratory activity determination method corresponding to the $^{14}CO_2$ gas production study has not been developed yet. Therefore, this study was conducted to develop a suitable and easily replicable method to determine soil microbial respiratory activities, which results can be applied to evaluate the correlation with ^{14}C gasification ratio. For the microbial activity determination, electron transport system (ETS) was measured by dehydrogenase assay using the redox dye 2-(p-iodophenyl)-3-(p-nitrophenyl)-5-phenyltetraxolium chloride (INT) as the substrate, which is reduced to INT-formazan by the dehydrogenase enzyme. In the method development, primarily three points were examined—INT incubation time, extraction method, and storage time for the extracted INT-formazan.

II. MATERIALS AND METHODS

Agricultural soil samples that were air-dried and sieved through a 2-mm mesh were incubated beforehand at a solid: liquid ratio of 1 to 10 (0.5 g to 5 mL), which is commonly used in the experiments to determine $^{14}CO_2$ gasification ratio, so as to share the method [2]. After the incubation, 4mL of supernatant was discarded, and INT aqueous solution (0.05%) was added to the sample. INT incubation time was evaluated up to four hours by comparing the amount of extracted INT-formazan detected with a spectrophotometer at 480 nm. INT-formazan extraction methods using methanol as the extractant were also evaluated, regarding the volume of methanol and extracting time. Storage time of extracted INT-formazan before absorbance reading was assessed by keeping samples in the dark at 4℃ or room temperature (approx. 20℃).

III. RESULTS AND DISCUSSION

Based on the experiments, three hours was chosen for INT incubation time because resultant INT-formazan increased over time for the first three hours and then started to be stabilized. As regards INT-formazan extracting method, our experiment showed that mixing samples with 8mL of methanol vigorously for one minute was sufficient. Extracted INT-formazan was stable in both conditions at least for 24 hours. Because our method considered the method of gasification ratio experiments, it enables the evaluation of correlation between soil microbial activity and gasification ratio.

This work was partially supported by the Agency for Natural Resources and Energy, the Ministry of Economy, Trade and Industry (METI), Japan.

REFERENCES

[1] Koga, K. The roles of soil microbes in the global environment. *Netsu Sokutei* 34 (2): 77-86, 2007

[2] Ishii, N., Koiso, H., Takeda, H., Uchida, S. Partitioning of ^{14}C into solid, liquid, and gas phases in various paddy soils in Japan. *J. Nuc. Sci. Technol.* 47: 238-243, 2010

Effect of humic acid on the sorption of selenium (VI) on ferric oxide hydrate

N. Guo, Z. L. Niu, Y. L. Ye, R. Zhang, Z. J. Guo
School of nuclear science and technology, Lanzhou University, Lanzhou, China, 730000

Abstract – Selenium-79 ($T_{1/2}$= 6.5×10^5 a) is one of the long-lived fission products, which is chemically and radiologically toxic, and one of the main radionuclides of special concerned in the disposal of high level nuclear waste. In this paper we studied the effect of humic acid (HA) on the sorption of selenium (VI) on ferric oxide hydrate (HFO) via *batch-type experiments. We researched the effects of contact time, pH, ion strength, concentration of Se (VI) and HA on the sorption of Se (VI) and found that the equilibrium time of the Se (VI) sorption on HFO was around 3 h, the sorption decreased with the increasing pH and increased with the decreasing ion strength. The sorbed amount decreased with equilibrium concentration in aqueous phase, and the sorption isotherms were fitted to Langmuir equation to figure out the max sorbed amount which was 3.82×10^{-4} mol/g. HA significantly suppressed the sorption of Se (VI).*

Keywords – selenium, sorption, ferric oxide hydrate, humic acid

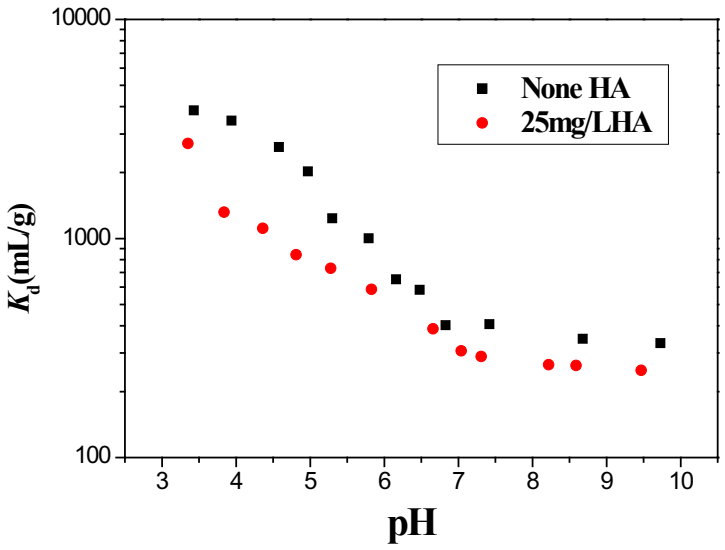

Fig 1. Effect of HA on the sorption of Se (VI) on HFO: C_{Se} = 1.5×10^{-4} mol/L, I = 0.1 mol/L (NaCl), T = 25±1 ℃

APSORC'13 - 5th Asia-Pacific Symposium on Radiochemistry
Kanazawa, Japan, 22-27 September 2013

Uranyl ions Adsorption to Na-GMZ and Interactions with FA Adsorption: experiments and modeling

Ye Yuanlv, Guo Zhijun*, Wu Wangsuo
Radiochemistry Laboratory, School of Nuclear Science and Technology, LanzhouUniversity, Lanzhou, 730000, China

Abstract –In this work, data for the interactions betwee fulvic acid (FA) with uranyl ions at the surface of Na-GMZ are presented. U adsorption to Na-GMZ in the presence of FA can be well predicted with the SCD model (surface and complex distribution). According to the model calculations, the nature of the interactions between FA and U at Na-GMZ surface is mainly surface complex.
Keywords –Uranyl ions, Na-GMZ, FA, Surface Complex Model

I. INTRODUCTION

In the enviromnent, an important factor of radionuclide mobility is their interaction with mineral–water interfaces. To predict radionuclide mobility, it is necessary to understand fundamental processes such as surface precipitation and surface complexation. Studies of uranium sorption onto mineral surfaces have great practical importance for risk assessment.what's more, in recent years it has been revealed that many groundwaters in granitoidic environments contain excessive amounts of dissolved U[1].In addition to the effects for sorption, NOM may influence U(VI) distribution via some other mechanisms. In addition, some studies also postulated that U(VI) can form organic complexes with NOM possibly via metal ion bridging The formation of organic U(VI) complexes at the mineral surface or in the solution may decrease or increase U(VI) solubility in groundwater[1-2].

A. Uranyl ions Adsorption to Na-GMZ and Interactions with FA Adsorption

Figures 1 and 2 show the two relatively gentle sorption edges from pH 2 to 8. It is also seen that FA causes a relative enhancement in the U(VI) sorption at pH<6. U adsorption to Na-GMZ in the presence of adsorbed FA can be well predicted with the SCD model (surface and complex distribution) U adsorption to Na-GMZ in the presence of adsorbed FA can be well predicted with the SCD model (surface and complex distribution).

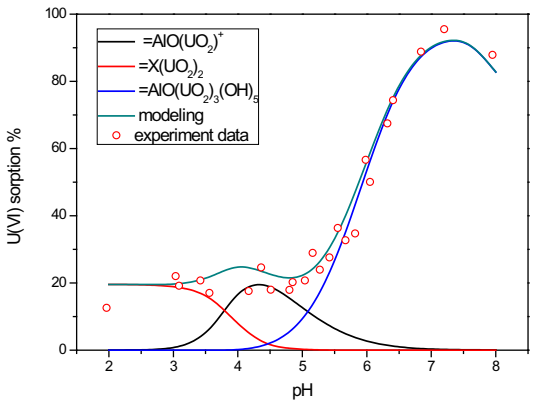

Figure 1 Adsorption curves of U(VI) vs. pH on Na-GMZ , C[U(VI)] =1.003E-4 mol/ L, m/ V = 20 g/ L , T = 22±1 ℃, I =0.1 mol/ L (NaCl).

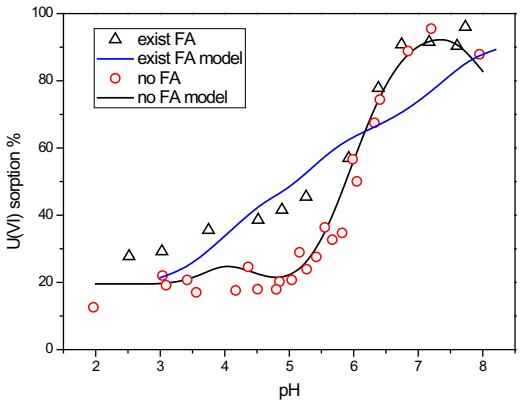

Figure. 2 Adsorption curves of U(VI) vs. pH on Na-GMZ in the absence and presence of FA, C[U(VI)] =1.012E-4 mol/ L, C[FA] =10 mg/L, m/ V = 20 g/ L , T = 22±1 ℃, I =0.1 mol/ L (NaCl).

[1] Gustafsson, J.P., Dassman, E. and Backstrom, M. (2009) Towards a consistent geochemical model for prediction of uranium(VI) removal from groundwater by ferrihydrite. Applied Geochemistry 24(3), 454-462
[2] Weng, L.P., Van Riemsdijk, W.H. and Hiemstra, T. (2008) Humic Nanoparticles at the Oxide-Water Interface: Interactions with Phosphate Ion Adsorption. Environmental Science & Technology 42(23), 8747-8752.

* coresponding author:Guo Zhijun email:Guohij@lzu.edu.cn

APSORC'13 - 5th Asia-Pacific Symposium on Radiochemistry
Kanazawa, Japan, 22-27 September 2013

Foliar uptake and translocation of stable cesium and iodine by radish

Hidenao Hasegawa[1], Hirofumi Tsukada[1], Hitoshi Kawabata[1], Yuichi Takaku[1], Shun'ichi Hisamatsu[1]
[1]Institute for Environmental Sciences

Abstract – We studied foliar uptake of Cs and I by radish (Raphanus sativus L. cv. Redchim) by applying droplets of a solution of Cs (as CsCl or $CsNO_3$) or I (as NaI or $NaIO_3$) on an upper leaf surface. The uptake of Cs decreased with increasing $CsNO_3$ concentration in the applied solution. Approximately 80% of applied Cs was absorbed no matter what the initial concentration of the applied solution. The uptake of I in either form was independent of the concentration of the applied solution. Approximately 80% of applied I was absorbed, whereas 90% of IO_3^- remained on the surface.

Keywords – foliar uptake, translocation, cesium, iodide, iodate

I. INTRODUCTION

Direct deposition of radioactive materials onto crops is an important pathway for radiation dose assessment of radionuclides released from nuclear facilities. Cesium and iodine radioisotopes are transferred into agricultural products both by direct deposition from the atmosphere onto the plants and by absorption from the soil via the roots. We have already reported that foliar uptake of stable Cs is higher from droplets of a CsCl solution than from droplets of a $CsNO_3$ solution. In this study, we investigated the concentration dependence of the foliar uptake of Cs from a CsCl or $CsNO_3$ solution applied as droplets onto the leaf surface of radish plants (*Raphanus sativus L.* cv. Redchim). A similar experiment was carried out with NaI and $NaIO_3$ solutions.

II. MATERIALS AND METHODS

Details of radish plant cultivation and the method for applying the solutions to leaf surfaces are described elsewhere [1]. A solution of CsCl or $CsNO_3$ at a concentration of 0.001, 0.01, 0.1, or 1 g Cs L^{-1} was applied to the upper surface of radish leaves (*Raphanus sativus L.* cv. Redchim) 28 d after germination. A solution of NaI or $NaIO_3$ at a concentration of 0.2, 0.5, or 1 g I L^{-1} was also applied in a similar manner. The plants were harvested 4 d after the application of test solutions and were divided into leaves, root tubers, and lateral roots. The leaves were washed with a solution containing detergent. The washing solution, leaves, and root tubers were analyzed for Cs and I by means of inductively coupled plasma mass spectrometry.

III. RESULTS AND DISCUSSION

We determined the absorption ratios of Cs and I, calculated as (amount of Cs or I detected in the inner leaf or root tuber)/(applied amount of Cs or I), and we plotted the ratios against the Cs or I concentration of the applied solution (Fig. 1). When Cs was applied as a $CsNO_3$ solution, the Cs absorption ratio decreased with increasing Cs concentration in the applied solution. In contrast, when Cs was applied as a CsCl solution, the absorption ratio was nearly constant. There was a clear difference in I absorption ratio between NaI and $NaIO_3$. This result suggests that the chemical form of I strongly affected the absorption ratio of I.

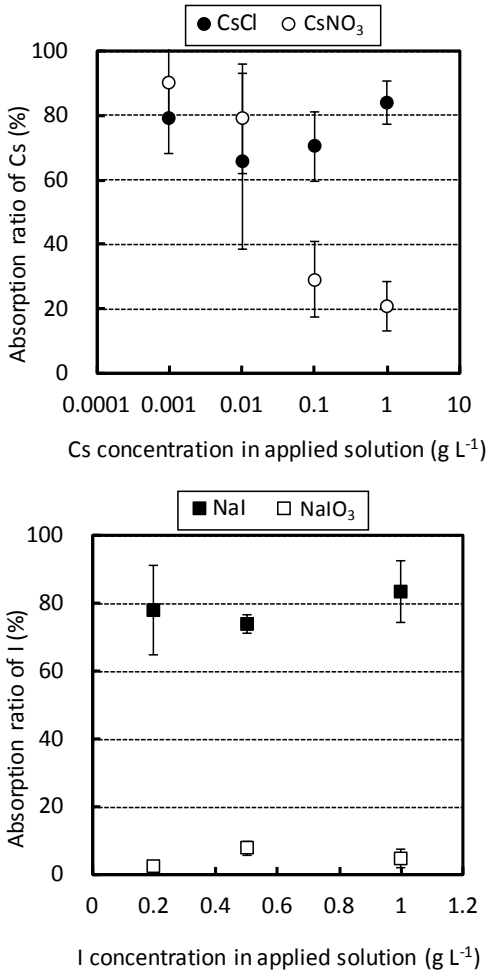

Fig. 1 Absorption ratios of Cs and I into radish plants from upper leaf surfaces

REFERENCES

[1] H. Hasegawa, H. Tsukada, H. Kawabata, Y. Chikuchi, Y. Takaku, S. Hisamatsu, J. Environ. Radioact., 100 (2009) 54.

This study was performed under a contract with the government of Aomori Prefecture, Japan.

APSORC'13 - 5th Asia-Pacific Symposium on Radiochemistry
Kanazawa, Japan, 22-27 September 2013

The rapid determination of radiostrontium from a large amount of seawater (within 72hrs) for an emergency situation

Hyuncheol Kim*, Kun-Ho Chung, Hyo-Kook Park, Jong-Myoung Lim, Mun-Ja Kang
Environmental Radioactivity Assessment Team, Korea Atomic Energy Research Institute
989-111 Deadeok-daero, Yuseong-gu, Daejeon, 305-353, Korea

Abstract – This paper describes the results of the development of an automated radionuclide separator from a large seawater sample. It consists of two parts, which are a concentration part with a cation exchange resin (Dowex50Wx8, Sigma-Aldrich) and a purification part with Sr resin (Eichrom Technology). The volume of raw seawater sample was reduced by about 25% at the concentration part, and radiostrontium was purified at the Sr-resin part. The chemical yield ranged from 92% to 96%. This automated system can simultaneously execute four samples. Using liquid scintillation counting (LSC) and Cherenkov counting, the analysis of Sr-89/90 from seawater could be completed within 3 days.

Keywords – radiostrontium, seawater, automated system, rapid determination

Radiostrontium is one of the main fission products and can be released into the environment through nuclear test or NPP accidents. During emergency situations such as FDNPP, a radionuclide analysis should be completed in a short time to support rapid decision making and maintain public safety. The determination of radiostrontium following traditional methods involves a significant number of separation steps such as precipitation which are time-consuming and labor intensive. This paper describes Modular Automated Radionuclides Separator Sr-seawater (MARS Sr-sw) which allows the purification of radiostrontium from four seawater samples at the same time within 3 days. MARS Sr-sw can reduce the analytical time and labor intensity.

MARS Sr-sw was based on column chromatography. It consists of a concentration part and purification part, which contain a control module, a pump module, a valve module, and four column modules. We developed the control software using LabVIEW (National Instrument). The operational procedure is shown in figure 1.

In the concentration part, Dowex50Wx8(100~150um) was used to concentrate a large seawater sample, the volume of which was reduced from 20% to 30%. Seawater consists of many cations, such as Ca^{2+}, Mg^{2+} and Sr^{2+}. However, the selectivity of Sr for Dowex50Wx8 is relatively higher than that of Ca or Mg, which are dominant ions in seawater. It enables Sr concentration from seawater without significant loss of Sr. In a Sr breakthrough test, 500g of Dowex50Wx8 can isolate 99% of Sr from 10L seawater (0.16mg Sr/g of Dowex50Wx8). The low level of Ca was found in the elution sample, which did not affect the Sr recovery by Sr resin. The Sr recovery was quantitative for Ca levels of up to 320mg, which was higher than that of Ca in the elution sample. About 99% of Sr in seawater from 1L to 10L was collected by the concentration part. A pre-concentration of Sr from 10L seawater was completed within 5hrs.

We prepared a Sr resin column using a benchmark glass column (Omnifit Ltd.) in the purification part. The amount of Sr resin depends on the sample size because the level of Sr in seawater is around 8ppm. All procedures were automatically completed by MARS Sr-sw. It took 4hrs to complete the purification of Sr from 10L of seawater The Sr recovery was about 93%.

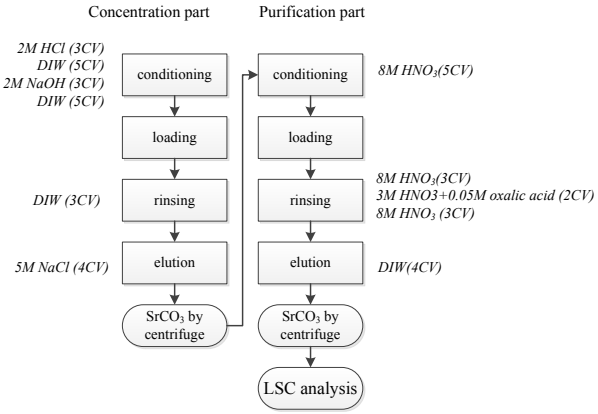

Figure 1 Procedure of MARS Sr-sw (CV: column volume)

This study suggests that MARS Sr-sw can complete the determination of radiostrontium from a large amount of seawater within 3 days using LSC and Cherenkov counting which provide spectral information. It allows the identification of Sr-89/90. The remarkable aspects of MARS Sr-sw are the automation and capability to handle multiple samples at the same time.

[1] Chung, G.H., Choi, S.D., Choi, G.S., Kang, M.J. Design and performance of an automated radionuclide separator: its application on the determination of 99Tc in groundwater. *Applied Radiation and isotopes* (in press)
[2] Vajda, N. and Kim, C.H. Determination of radiostrontium isotopes: A review of analytical mehtodoly. *Applied Radiation and isotopes*, 2010. 2306-2326.

*Corresponding author. E-mail: hckim3@kaeri.re.kr

APSORC'13 - 5th Asia-Pacific Symposium on Radiochemistry
Kanazawa, Japan, 22-27 September 2013

Peak Tailing Correction in Measurement of $^{222}Rn/^{220}Rn$ Activity Concentration with α Spectrum Method

Lei Zhang[1], Qiuju Guo[2], Ruoyun Ma[2], Lu Guo[2]
[1]Solid Dosimetric Detector and Method Laboratory, Beijing, 102205, China
[2]State Key Laboratory of Nuclear Physics and Technology, School of Physics, Peking University, Beijing 100871, China

Abstract – α spectrum method is one of the most important methods for $^{222}Rn/^{220}Rn$ concentration measurement. The peak tailing from high energy α particle to low energy region influences the measurement accurateness. To improve α spectrum method, the theory of peak tailing was analyzed and a series of calibrating experiments was carried out. For a commercial radon monitor ERS-2, the experiment values of peak tailing correction factors C_5 and K_4 is 15.25%±0.24% and 36.23%±0.68%, the calibration factors of ^{222}Rn and ^{220}Rn(KF_{Rn} and KF_{Tn}) is 2.08±0.02 Bq•m^{-3}/cph and 5.23±0.28 Bq•m^{-3}/cph. After peak tailing correction, the measurement results agree with reference value very well.

Keywords – $^{222}Rn/^{220}Rn$; α spectrum method; peak tailing correction factor; calibration factors

Underwater Analysis of Sediment Chemistry using an Autonomous Platform

Jeremy Breen[1], Paulo de Souza[1,2,3], Greg Timms[3], Robert Ollington[1]

[1]School of Computing and Information Systems, University of Tasmania, Hobart TAS 7001 Australia

[2] Vale Institute of Technology, Belem, PA, Brazil

[3] Intelligent Sensing and Systems Laboratory, ICT Centre, CSIRO, Hobart TAS 7000 Australia

Abstract – The increasing number and size of marine reserves comes with additional challenges and responsibilities concerning environmental monitoring, including sediment chemistry. The characterisation of sediments can shed light on past events like anthropogenic contamination and natural events as well as provide information to guide mineral exploration. However, the costs associated with the monitoring of sediment chemistry are high and traditional methods can disturb the sediment and influence the results. Here we present original results of X-ray fluorescence measurements performed underwater, in-situ, using an autonomous underwater vehicle in the Derwent Estuary, which is located in South East Tasmania Australia and has a long history of contamination from heavy metals. To demonstrate the capability of performing in situ, underwater analysis of sediments we analysed three distinctive sites on the Derwent estuary floor. XRF spectra with good signal-to-noise ratios have been recorded. The results show spatial variation of zinc, lead and iron concentration. The contamination of heavy metals we found reflects proximity to potential sources and patterns of the hydrodynamics of the estuary. We suggest that XRF in submersible autonomous platforms could be used to perform an initial, cost effective, assessment of heavy metals contamination of sediments to guide comprehensive surveys.

Keywords – XRF, Sediments, AUV

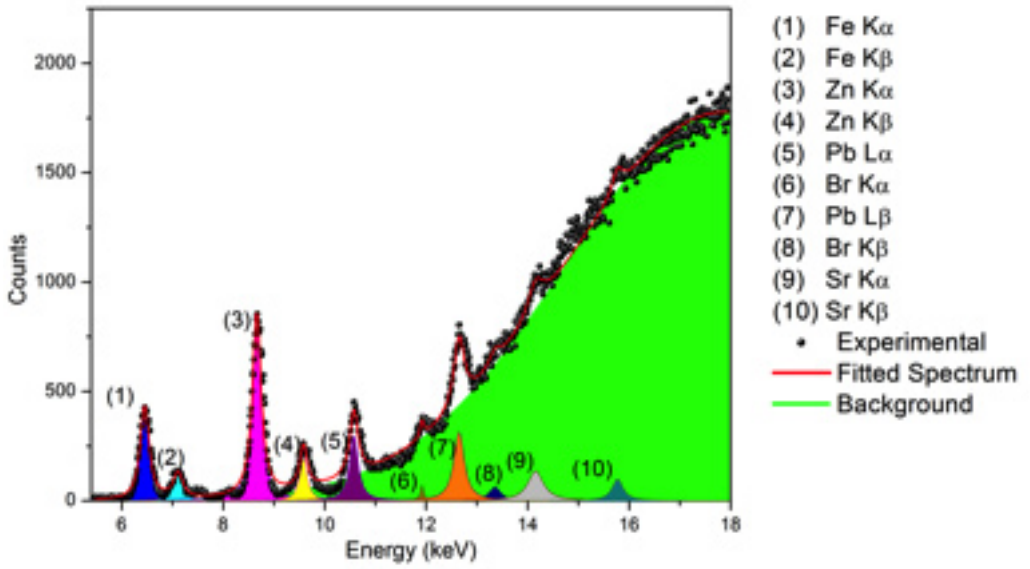

XRF spectra recorded underwater. Typical least-squares fitted XRF spectrum record at site D (Ralphs Bay) at 10m-depth. The broader line between 10 keV and 30 keV overlaps Lead, Bromine and Strontium signals and are caused by bremsstrahlung from the XRF housing (high density polypropylene).

Development of the in-line, multiple elution cartridge-based radioisotope concentrator device for increasing ^{99m}Tc and ^{188}Re concentration of commercial radionuclide generator eluates

Le, Van So[1,2*]; Morcos, Nabil[1]; McBrayer, James[1]; Bogulski, Zac[1]; Buttigieg, Charles[1]; Phillips, Graham[1]

[1]CYCLOPHARM Ltd, NSW, Australia
[2]MEDISOTEC, NSW, Australia

I. INTRODUCTION

^{99m}Tc is used in approximately 85% of diagnostic imaging procedures in nuclear medicine world-wide. ^{188}Re is important radio-therapeutic radionuclide. The expansion of ^{99m}Tc and ^{188}Re application depends on the generator availability. However, the cost-effective utilisation of ^{99m}Tc and ^{188}Re generators and the quality of SPECT imaging diagnosis and radiotherapy are controlled by the ^{99m}Tc and ^{188}Re generator operation/elution management, which is determined by the ^{99m}Tc and ^{188}Re concentration in the generator eluate. Generally ^{99m}Tc and ^{188}Re eluates are produced from the generators in fixed volume and the ^{99m}Tc and ^{188}Re concentration of the eluates decreases with the life time of the generators due to radioactive decay of parent nuclides ^{99}Mo and ^{188}W, respectively. Consequently, the useful life time of the generator is also a function of available ^{99m}Tc and ^{188}Re concentration of the eluate. The injection dose activity of ^{99m}Tc- and ^{188}Re-based radiopharmaceuticals delivered in 1 mL solution (^{99m}Tc- or ^{188}Re- concentration, mCi/mL) is an important factor in determining the useful life time of the ^{99m}Tc and ^{188}Re generators and the quality of ^{99m}Tc based SPECT imaging diagnosis or ^{188}Re –based radiotherapy, respectively. So, the radioisotope concentrator device should be developed to increase the concentration and quality of injectable ^{99m}Tc and ^{188}Re eluates and the life time of the generators.

II. METHODS

A multi-elution, radioisotope concentrator device [1], in-line eluted via evacuated-vial and through disposable sterile filters was developed to increase the concentration of ^{99m}Tc or ^{188}Re in the elution of aged commercial ^{99m}Tc or ^{188}Re generators. The increase in ^{99m}Tc concentration in the eluate enhances the utilisation of technetium in Technegas generator-based lung perfusion (100-250 mCi/mL) and other SPECT (20-30 mCi/mL) imaging studies. A self-shielded radioisotope concentrator device (Fig. 1a) was created based on a newly developed sorbent/concentrator column which selectively retains $^{99m}TcO_4^-$ ions from downstream of 10 mL ^{99m}Tc solution eluted from the generator. The eluate is freed from Cl^- and MoO_4^- ions by passing through a competitive ion-selective column. ^{99m}Tc is then eluted from the concentrator column with 1.0 mL saline into an evacuated vial through a millipore filter and ready for injection. The design of the device in form of a disposable cartridge was optimised to make elution process effective, simple, sterile and radiation safe. Gentech ^{99m}Tc generator of 110 GBq activity eluted with 10 mL saline was chosen to test our radioisotope concentrator device.

III. RESULTS

As a result obtained from our project, the ^{99m}Tc eluate was concentrated more than 10-fold with a ^{99m}Tc recovery yield of > 85% using this radioisotope concentrator device. 5 or 10 repeated elutions were successfully performed with each cartridge coupled to the 10 mL or 5 mL saline solution eluted generators, respectively. So, each cartridge can be effectively used for one week in the hospital environment for radiopharmaceutical formulation. The useful lifetime of the ^{99m}Tc generator was significantly extended from 10-20 days for the generators of 300-3000 mCi activity, respectively. The ^{99}Mo impurity in the ^{99m}Tc solution eluted from the Gentech generator was totally eliminated by this radioisotope concentrator device (Fig. 1c).

IV. CONCLUSION

We conclude that the radioisotope concentrator device functioned well and is robust in operation. This device will, to some extent, mitigate the global ^{99m}Tc crisis. This concentrator device is under patent-pending.

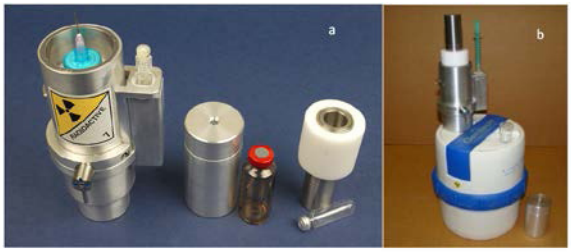

Fig. 1. Radioisotope concentrator device with standard accessories (a) and the radioisotope concentrator device coupled with ^{99m}Tc generator for in-line elution/concentration of ^{99m}Tc eluate (b).

REFERENCE

[1] Le V.S, McBrayer J., Morcos N. (2012) Australian Patent AU2012904683APSORC'13 Body Text

APSORC'13 - 5th Asia-Pacific Symposium on Radiochemistry
Kanazawa, Japan, 22-27 September 2013

Production and Preclinical Evaluation of Diagnostic and Therapeutic Radionuclides in Tumor-Bearing Mice: Recent Developments at Paul Scherrer Institute

A. Türler[1,2], M. Behe[3], M. Bunka[1,2], H. Dorrer[1,2], A. Hohn[3], K. Johnston[4], U. Köster[5], C. Müller[3], J. Reber[3], R. Schibli[3], N.T. van der Walt[6], K. Zhernosekov[1,2]

[1]Laboratory of Radiochemistry and Environmental Chemistry, Paul Scherrer Institute, Villigen-PSI, Switzerland
[2]Laboratory of Radiochemistry and Environmental Chemistry, University of Bern, Bern, Switzerland
[3]Center for Radiopharmaceutical Sciences ETH-PSI-USZ, Paul Scherrer Institute, Villigen-PSI, Switzerland
[4]Physics Department, ISOLDE/CERN, Geneva, Switzerland
[5]Institut Laue-Langevin, Grenoble, France
[6]Faculty of Applied Sciences, Cape Peninsula University of Technology, Bellville, South Africa

Abstract – At PSI we have initiated a close collaboration of the Laboratory of Radiochemistry and Environmental Chemistry and the Center for Radiopharmaceutical Sciences to bring novel diagnostic and therapeutic radiopharmaceuticals to the point of clinical trials. Pre-clinical studies using tumor-bearing mice were conducted at PSI and ETH Zürich. At the university hospital in Bern the required infrastructure for clinical trials was established.

Keywords – theranostics, diagnostic radionuclides, ^{44}Sc, ^{152}Tb, ^{155}Tc, therapeutic radionuclides, ^{149}Tb, ^{161}Tb, DOTA-folate conjugate, targeted radionuclide therapy,

I. INTRODUCTION

Radiopharmaceuticals which comprise metallic radionuclides are valuable diagnostic and therapeutic tools in nuclear oncology. Several clinics worldwide have started targeted radionuclide therapies based on ^{177}Lu- or ^{90}Y-DOTA-TOC, a somatostatin receptor targeting peptide to treat metastatic gastro-entero-pancreatic neuroendocrine tumors. For diagnostic purposes ^{177}Lu can be replaced with the short-lived positron emitter ^{68}Ga available from a ^{68}Ge/^{68}Ga generator system.

Further development and implementation of such innovative radiometallated drugs depend, however, directly on the availability of radiometals. Compared to other lanthanides, the element Tb comprises a quadruplet of clinically attractive radionuclides, such as ^{152}Tb and ^{155}Tb, with suitable decay properties for PET and SPECT imaging, and, ^{149}Tb and ^{161}Tb, suitable for targeted alpha- and beta-radionuclide therapy. To assess the diagnostic and therapeutic features of these four radioisotopes we employed the folic acid/folate receptor (FR)-targeting strategy.

In addition, we investigated the use of ^{44}Sc ($t_{1/2}$ = 3.97 h, E+av = 632 keV) as a valuable alternative to short-lived ^{68}Ga ($t_{1/2}$ = 68 min, $E\beta^+_{av}$ = 830 keV) for imaging of cancer prior to ^{177}Lu-based radionuclide therapy. The aim of the study was the preclinical evaluation of a folate conjugate labeled with cyclotron-produced ^{44}Sc and to compare these data with those of the ^{177}Lu-labeled match.

A. Production of Radionuclides

The neutron deficient ^{149}Tb, ^{152}Tb, and ^{155}Tb were obtained in several beam times at CERN-ISOLDE by spallation of a Ta target with 1 GeV protons followed by mass separation. The low energy isobaric ion beams were implanted in Zn covered Au foils.

A production facility for up to 20 GBq of n.c.a. ^{161}Tb was established at PSI. Samples of enriched ^{160}Gd were irradiated at PSI-SINQ, FRM-II Munich, or ILL Grenoble. It was possible to routinely produce ^{161}Tb of excellent radionuclidic purity and highest specific activity (i.e. >3700 GBq/mg), so that labeling of i.e. DOTATATE was possible with a molar ^{161}Tb:DOTATATE – ratio of 1:3.5 with 99.41 % yield.

^{44}Sc was produced via the ^{44}Ca(p,n)^{44}Sc-nuclear reaction at the PSI Injector 2 cyclotron using highly enriched ^{44}Ca-targets. Separation from the target material was carried out by a semi-automated process using extraction- and cation exchange chromatography.

B. Preclinical Evaluation

A summary of results obtained in *in-vivo* experiments with all four Tb-isotopes is shown in Figure 1.

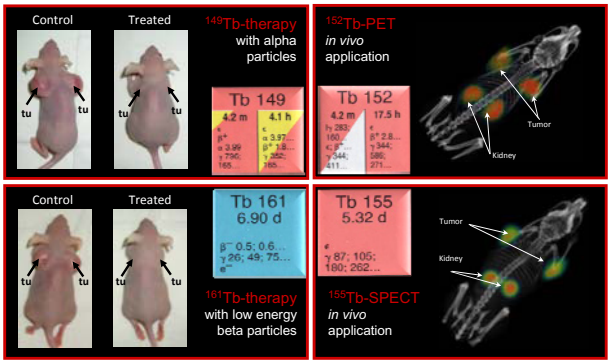

Figure 1: Left-hand side: treatment of tumor bearing mice with ^{149}Tb (α-particle therapy) and ^{161}Tb (β-particle therapy) DOTA-FOLATE. Right-hand side: PET and SPECT images of tumor bearing mice with ^{152}Tb and ^{155}Tb DOTA-FOLATE, respectively.

[1] C. Müller et al., J. Nucl. Med. **53**, 1951-1959 (2012).

APSORC'13 - 5th Asia-Pacific Symposium on Radiochemistry
Kanazawa, Japan, 22-27 September 2013

^{99}Mo production by ^{100}Mo(n,2n)^{99}Mo using accelerator neutrons

Nozomi SATO[1], Masako KAWABATA[1], Yasuki NAGAI[1], Kazuyuki HASHIMOTO[1], Yuichi HATSUKAWA[1], Hideya SAEKI[1], Shoji MOTOISHI[1], Tadahiro KIN[2], Chikara KONNO[3], Kentaro OCHIAI[3], Kosuke TAKAKURA[3], Futoshi MINATO[4], Osamu IWAMOTO[4], Nobuyuki IWAMOTO[4], and Shintaro HASHIMOTO[4]

[1]Nuclear Engineering Research Collaboration Center, Japan Atomic Energy Agency
[2] Faculty of Engineering Sciences, Kyushu University
[3] Fusion Research and Development Directorate, Japan Atomic Energy Agency
4 Nuclear Science and Engineering Directorate, Japan Atomic Energy Agency

Abstract – We proposed a new route to produce a medical radioisotope ^{99}Mo by the ^{100}Mo(n,2n)^{99}Mo reaction using accelerator neutrons. A high-quality ^{99}Mo with a minimum level of radioactive waste can be obtained by the proposed reaction. The decay product of ^{99}Mo, ^{99m}Tc, is separated from ^{99}Mo by the sublimation method. The proposed route could bring a major breakthrough in the solution of ensuring a constant and reliable supply of ^{99}Mo.

Keywords – ^{99}Mo radioisotopes, diagnosis, accelerator neutrons, neutron induced reaction, SPECT

I. INTRODUCTION

^{99m}Tc (half-life, $T_{1/2}$ = 6.0 h), the daughter nuclide of ^{99}Mo ($T_{1/2}$ = 66 h), is the most common radioisotope used in diagnosis, and its use accounts for 80% of all nuclear medicine procedures worldwide.[1)] ^{99m}Tc has a versatile chemistry that allows it to be incorporated into all sorts of molecules, and because of the short half-life of ^{99m}Tc, ^{99m}Tc is routinely produced in ^{99}Mo/^{99m}Tc generators. ^{99}Mo has been mostly produced by the fission reaction of highly enriched ^{235}U in research reactors. However, an unscheduled shutdown of some of these reactors has recently caused a crisis shortage of ^{99}Mo worldwide, which triggered widespread discussions on the ^{99}Mo supply.[2)] The ^{99}Mo production using a charged-particle induced nuclear reaction, such as the ^{100}Mo(p,pn)^{99}Mo, ^{100}Mo(d,$p2n$)^{99}Mo, and ^{100}Mo(p,$2n$)^{99m}Tc reactions, has been investigated.[3)] We proposed a new route to produce ^{99}Mo using fast neutrons from an accelerator,[4)] and we have been carrying out important steps necessary to obtain high-quality ^{99m}Tc.

II. ^{99}MO PRODUCTION BY ACCERELATOR NEUTRONS

Intense neutrons with an average energy of 14 MeV are necessary to produce a large amount of ^{99}Mo by the ^{100}Mo(n,$2n$)^{99}Mo reaction. Neutrons can be produced from the ^{nat}C(d,n) or ^{9}Be(d,n) reactions at deuteron energy of 40 MeV. The production yield of ^{99}Mo was estimated using the evaluated cross section of ^{100}Mo(n,$2n$)^{99}Mo,[5)] and the neutron intensity. Typically, we assumed a metallic ^{100}Mo sample (251 g, 100% enriched) with a radius of 2 cm and a thickness of 2 cm was irradiated by neutrons. The sample was placed 2 cm downward from the ^{nat}C or ^{9}Be target.

The ^{99}Mo harvest frequency, determined by the ratio, R = N(^{99}Tc)/N(^{99m}Tc), is also important. Here, N(^{99}Tc) and N(^{99m}Tc) are the numbers of ^{99}Tc ($T_{1/2}$ = 2.1 × 10^5 y, useless in diagnostic use), and ^{99m}Tc. The calculated R values were 1.2, 3.0, and 11 for one, two and six-days of irradiation. The harvest frequency will be every two or three days by considering the available amounts of ^{100}Mo and the ^{99}Mo decay during the ^{100}Mo sample irradiation.

III. EXPERIMENT AND RESULT

^{99}Mo was produced by irradiating an enriched ^{100}MoO$_3$ sample with ~14 MeV neutrons from the ^{3}H(d,n)^{4}He reaction at the Fusion Neutronics Source (FNS) facility of Japan Atomic Energy Agency (JAEA). Gamma-rays from the decay of ^{99m}Tc and ^{99}Mo were clearly observed. Yields of impurity isotopes, such as ^{97}Zr and ^{97}Nb, were much smaller than that of ^{99}Mo.

To separate high-quality ^{99m}Tc from the produced ^{99}Mo, we used the sublimation method, which is based on a different volatility of Tc_2O_7 and MoO_3.[6)] The irradiated ^{100}MoO$_3$ sample was placed in a furnace, and heated so as to form gaseous materials containing vaporized ^{99m}Tc$_2$O$_7$ in a stream of oxygen carrier gas. ^{99m}Tc was condensed at the exit of the furnace, and was eluted with a saline solution. As a result of the γ-ray measurement of the separated ^{99m}Tc, the upper limits of γ-rays from any impurity isotopes were found to be very small. A sublimation method allows us to recycle any irradiated enriched ^{100}Mo. Labeling efficiency, an important factor in the compounding and dispensing of radiopharmaceuticals, was shown to be higher than 90% by formulating a radiopharmaceutical.

REFERENCES

[1] F. F. Knapp, Jr. and S. Mirzadeh: Eur. J. Nucl. Med. 21 (1994) 1151.
[2] J. R. Ballinger: J. Labelled Compd. Radiopharm. 53 (2010) 167.
[3] K. Bertsche: Proceedings of IPAC'10, Kyoto, Japan. (2010) 121.
[4] Y. Nagai and Y. Hatsukawa: J. Phys. Soc. Jpn. 78 (2009) 033201.
[5] K. Shibata, et al.: J. Nucl. Sci. Technol. 48 (2011) 1.
[6] C. Perrier and E. Segre: J. Chem. Phys. 5 (1937) 712.

APSORC'13 - 5th Asia-Pacific Symposium on Radiochemistry
Kanazawa, Japan, 22-27 September 2013

Production and Separation of ^{64}Cu and ^{67}Cu using 14 MeV Neutrons

Masako Kawabata[1], Kazuyuki Hashimoto[1], Hideya Saeki[1], Nozomi Sato[1], Shoji Motoishi[1], Kosuke Takakura[2], Chikara Konno[2] and Yasuki Nagai[1]
[1]Nuclear Engineering Research Collaboration Centre, [2]Fusion Research and Development Directorate
[1,2]Japan Atomic Energy Agency (JAEA), 2-4 Shirane, Shirakata, Tokai, Naka-gun, Ibaraki, 319 1195, Japan

Abstract –^{64}Cu and ^{67}Cu were produced from 14 MeV neutron irradiated natural ZnO and enriched ^{64}ZnO targets via ^{64}Zn(n, p)^{64}Cu and ^{67}Zn(n,p)^{67}Cu reactions. The ZnO disc targets were irradiated for 6 hours by 14 MeV neutrons, which are generated by bombarding a tritiated titanium target with deuteron beam at the Fusion Neutronics Source (FNS) at Japan Atomic Energy Agency (JAEA). After irradiation, ion chromatographic separations were carried out to obtain purified no-carrier-added Cu radionuclides. Elution pattern clearly showed separation of ^{64}Cu and ^{67}Cu giving a yield of > 90%, and a very low radionuclide impurity ratio of ^{65}Zn within the purified ^{64}Cu.

Keywords – ^{64}Cu, ^{67}Cu, radioisotope production, 14 MeV neutrons, nuclear medicine,

I. INTRODUCTION

^{64}Cu ($T_{1/2}$ 12 h, E.C.= 43%, β^+ = 18%, β^- = 40%) and ^{67}Cu ($T_{1/2}$ 62 h, β^- = 100%) [1] have attracted attention in radiopharmaceutical applications for their unique decay properties and chemical characteristics [2]. Being a positron and a beta emitter, ^{64}Cu is a strong candidate for the agents of both positron emission tomography imaging and targeted radiotherapy. ^{67}Cu, a longer-lived beta emitter can be used for radiotherapy to treat small tumors with a diameter of 2-3 mm [3]. Cu radionuclides can be produced either with cyclotrons by bombarding Ni or Zn targets with proton beams, *e.g.* ^{64}Ni(p,n)^{64}Cu, ^{68}Zn(p,αn)^{64}Cu, ^{68}Zn(p,2p)^{67}Cu, or in a nuclear reactor by bombarding a target with thermal neutrons [4,5]. The studied methods using cyclotron generated proton beams, however, include relatively expensive targets, unwanted radionuclides or complex chemical separation [5-8]. The current study investigates a production route of ^{64}Cu and ^{67}Cu from ^{64}Zn(n,p)^{64}Cu and ^{67}Zn(n,p)^{67}Cu reactions, by irradiating ^{nat}ZnO or ^{64}ZnO with 14 MeV neutrons [9], and a subsequent chemical separation.

II. EXPERIMENTAL

^{nat}ZnO and ^{64}ZnO (99.935% enriched ^{64}Zn) disc targets (20ϕ × 5 mm, 5 g) were individually irradiated by 14 MeV neutrons at FNS in JAEA for 6 hours. The average neutron flux was *ca.* 1.0×10^{11} n/s generated via ^{3}H(d,n)^{4}He reaction. The irradiated target was dissolved in 20 ml of 36 wt% HCl after which the pH was adjusted to 3.5-4.0 with 10 M NaOH. The sample was passed through a Chelex-100 exchange column (1.1ϕ × 11.5 cm) followed by washing with 100 ml of 0.001 M HCl to remove Zn [10]. The ^{64,67}Cu was then eluted with 20 ml of 2 M HCl and passed through an AG1-X8 column (0.8ϕ × 12.0 cm) to remove traces of Zn followed by a washing with 10 ml 2 M HCl [10]. The drop rate was regulated to be 1 ml/min throughout the separation. The purified ^{64,67}Cu solution was evaporated and dissolved in 1 ml 0.4 M ammonium acetate (pH5.5), filtered, and then reacted with TETA (1,4,8,11-tetraazacyclotetradecane-1,4,8,11-tetraacetic acid) solution for 2 hours [11]. The labeling yield was determined by silica gel TLC / 1:1 methanol-10 % ammonium acetate.

III. RESULTS & DISCUSSION

The production of $^{64, 67}$Cu by irradiating $^{nat, 64}$ZnO with 14 MeV neutrons reduced the consequent chemical separation process because of fewer side products (*e.g.* only ^{65}Zn if enriched ^{64}ZnO is used), which saves considerable time in comparison with $^{64, 67}$Cu production by proton-irradiation [8, 10]. The time required for the column separation process was 3 hours and could be shortened further if the system was fully automated. Over 95% of the $^{65, 69}$Zn side products were separated by the ion exchange Chelex-100 column, which can be recovered as $Zn(OH)_2$ by alkaline precipitation and decomposed to ZnO upon heating [8]. Radioactivity of 0.79 MBq/g ^{64}Cu, 6.3 kBq/g ^{67}Cu from ^{nat}ZnO and 2.5 MBq/g ^{64}Cu were obtained from ^{64}ZnO at the end of bombardment. A high separation efficiency was observed from the Chelex-100 (98%) and the AG1-X8 (95%) based on the ^{64}Cu yield of two experiments, with the final product having a ^{65}Zn radionuclide impurity below the detection limit of gamma-ray spectrometry. The labeling efficiency of Cu-TETA for clinical radiotherapy applications was found to be good at 94.4%.

REFERENCES

[1] Monographie BIPM-5, Table of radionuclides, Vol. 2, 2004
[2] Blower P.J, Lewis J.S. et al., Nucl med biol, 23, 957, 1996
[3] Ting G.,Chang,C.-H. et al., J Biomed Biotechnol, 2010, ID953537, 2010
[4] Qaim S.M., Radiochim Acta, 100, 635, 2012
[5] Novak-Hofer I. and Schubiger P.A., Eur J Nucl Med, 29(6), 821, 2002
[6] McCarthy D.W., Shefer R.E. et al., Nucl med biol, 24, 35, 1997
[7] Le,V.S., Pellegrini P. et al, J Radioanal Nucl Ch, 277(2), 451, 2008
[8] Katabuchi T., Watanabe S. et al., J Radioanal Nucl Ch, 277(2), 467, 2008
[9] Kin T., Nagai, Y. et al., J Phys Soc Jpn, 82,034201-1, 2013
[10] Schwarzbach R., Zimmermann K. et al., Appl Radiat isot, 46(5), 329, 1995
[11] Sun X., Wuest M. et al., J Biol Inorg Chem, 8, 217, 2003

APSORC'13 - 5th Asia-Pacific Symposium on Radiochemistry
Kanazawa, Japan, 22-27 September 2013

Novel radiochemical separation of arsenic from selenium for $^{72}Se/^{72}As$ generator.

Ewelina Chajduk[1], Halina Polkowska-Motrenko[1], Aleksander Bilewicz[1]
[1]Institute of Nuclear Chemistry and Technology, Dorodna 16, 03-195 Warsaw, Poland

Keywords – selenium-arsenic separation, extraction chromatography, PET, $^{72}Se/^{72}As$ generator

The potential usage of arsenic isotopes for nuclear medicine has been reported recently. One of the way for obtaining appropriate radioarsenic species is using radionuclide generator, where As is formed by the radioactive decay, eg.$^{72}Se \rightarrow {}^{72}As$. A new radiochemical separation scheme based on extraction chromatography for isolation As from Se is presented. The distribution coefficients of As and Se on prepared sorbents were determined in order to find the best condition for separation of both elements. Batch experiments were verified by column studies. Elaborated radiochemical separation scheme insures high selectivity and radionuclide purity of separated arsenic fraction, whereas examined sorbents have been found to have a very high selectivity with reference to selenium (IV). Arsenic is easily eluted by diluted HCl and NaCl solutions. Proposed approach insures high selectivity and radionuclide purity of separated arsenic fraction; it is also characterized by high elution efficiency (>95 %) using small volume (2 mL) of 0.9 % NaCl with very low breakthrough (<0.01 %) of selenium.

Acknowledgments: This work was partly supported by the grant of Polish Ministry of Science and Higher Education, Poland, (Nr 2713/B/H03/2011/40)

APSORC'13 - 5th Asia-Pacific Symposium on Radiochemistry
Kanazawa, Japan, 22-27 September 2013

Training Program of Synthesizing a Radiopharmaceutical in KAERI

S. Yang[1], Y. H. Chung[2]
[1]Advanced Radiation Technology Institute, Korea Atomic Research Institute, Jeongeup, 580-185, Korea
[2]Department of Chemistry, Hallym University, 1 Hallymdaehak-gil, Chuncheon 200-702, Korea; yhchung@hallym.ac.kr

Radiopharmaceuticals have widely been used in diagnoses of various medical conditions. Medical facilities using radiopharmaceuticals such as 2-deoxy-2-[^{18}F]fluoroglucose (^{18}F-FDG) have increased in number in Korea. ^{18}F-FDG is absorbed into cells such as brain and kidney along with cancer cells. Without the hydroxyl group replaced to ^{18}F it fails to undergo glycolysis in the cell and cannot leave it before its radioactive decay, which provides a quantitative distribution of glucose uptake and phosphorylation in cells. As ^{18}F-FDG is used in many medical facilities, a reliable quality control system is needed in its synthesis in addition to technical staff who can handle the process. KAERI recently started to operate its own 30-MeV cyclotron at Jeongeup, where ^{18}F-FDG is to be produced. A month-long training program is planned for college undergraduates and graduates to learn synthesis of ^{18}F-FDG and its handling, which would fill national future demand of skilled technical personnel.

Synthesis of ^{64}Cu-Labeled MARSGL Peptide as an Imaging Probe for HER2/neu Overexpressing Tumors

Yumi Sugo, Ichiro Sasaki, Shigeki Watanabe, Yasuhiro Ohshima, Noriko S. Ishioka
Quantum Beam Science Directorate, Japan Atomic Energy Agency

Abstract – ^{64}Cu was produced by the cyclotron using ^{64}Ni(p,n)^{64}Cu nuclear reaction. MARSGL peptide has high affinity to HER2/neu overexpressing in various cancer cells. In this study, ^{64}Cu-DOTA-MARSGL was designed and synthesized as a novel PET imaging probe for HER2/neu overexpressing tumors.

Keywords – ^{64}Cu, Positron, DOTA, Peptide, HER2/neu

Copper-64 is an attractive radionuclide for positron emission tomography (PET) imaging as well as radiotherapy due to its half-life ($T_{1/2}$=12.7 h) and decay characteristics (β^+ 17.4%, β^- 39%). MARSGL (H-Met-Ala-Arg-Ser-Gly-Leu-OH) is a linear peptide having high affinity to HER2/neu overexpressing in various cancer cells [1]. 1,4,7,10-Tetraazacyclododecane-1,4,7,10-tetraacetic acid (DOTA) is a macrocyclic ligand for various metal ions.

In this study, we designed ^{64}Cu-labeled MARSGL peptide conjugated with DOTA as an imaging probe for HER2/neu overexpressing tumors.

^{64}Cu was produced by the AVF cyclotron of Takasaki Ion Accelerators for Advanced Radiation Application facility at Japan Atomic Energy Agency using the nuclear reaction of ^{64}Ni(p,n)^{64}Cu. Radiochemical separation of ^{64}Cu was carried out by chelating ion-exchange method [2].

Protected MAR(Pbf)S(^{t}Bu)GL-Trt(2-Cl) resin was prepared by solid-phase peptide synthesis using automatic peptide synthesizer (Aapptec, Titan 357). As shown in Fig.1, tri-*tert*-butyl 1,4,7,10-tetraazacyclododecane-1,4,7,10-tetraacetate was allowed to react with the peptide resin by 1-ethyl-3-(3-dimethylaminopropyl)carbodiimide hydrochloride (EDCI·HCl) and 1-hydroxy-1H-benzotriazole (HOBt) in dimethylformamide. And then the cleavage and the deprotection were performed at the same time using trifluoroacetic acid (TFA), 1,2-ethanedithiol (EDT), and triisopropylsilane (TIS).

^{64}Cu-labeling of DOTA-MARSGL was carried out in acetate buffer. The formation of ^{64}Cu-DOTA-MARSGL was determined by reversed-phase TLC and HPLC.

In order to evaluate the usefulness of ^{64}Cu-DOTA-MARSGL peptide as a PET imaging probe, *in vitro* stability and affinity to HER2 are under investigation.

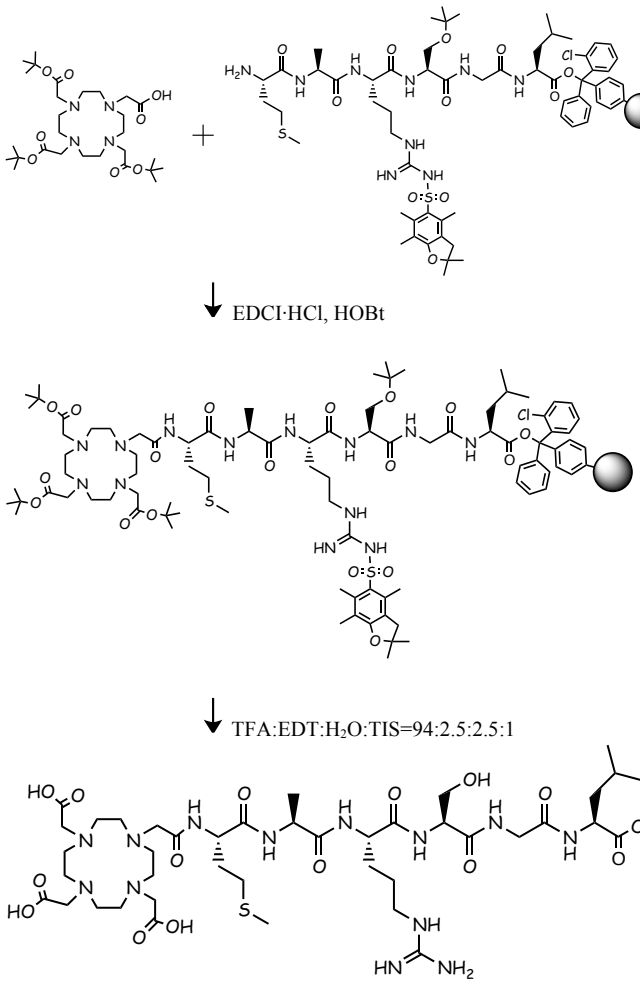

Fig. 1 Synthesis of DOTA-MARSGL by solid-phase conjugation.

REFERENCES

[1] M. Houimel et al., *Int. J. Cancer*, **92**, 748 (2001).
[2] Sh. Watanabe et al., *Nucl. Med. Biol*, **36**, 587 (2009).

Molybdenum Isotope Fractionation in Ion Exchange Reaction by using Anion Exchange Chromatography

Masafumi Inaki[1], Yu Tachibana[1], Masao Nomura[2] and Tatsuya Suzuki[1]
[1]Department of Nuclear System Safety Engineering, Nagaoka University of Technology
[2]Reserch Laboratory for Nuclear Reactors, Tokyo Institute of Technology

Abstract – The molybdenum isotope fraction in ion exchange reaction in hydrochloric acid solution was investigated by using the anion exchange chromatography. We confirmed that the heavier isotopes are enriched in solution phase.

Keywords – technetium-99m, molybdenum-99, molybdenum isotope, isotope enrichment

I. INTRODUCTION

Technetium-99m (^{99m}Tc) is one of the most important radioisotopes in nuclear medicine. ^{99m}Tc is generated from molybdenum-99 (^{99}Mo). Now, ^{99}Mo is mainly produced by fission of highly enriched uranium-235 (HEU). However, the supply of 99Mo becomes unsteady, since the reactors for the generation of ^{99}Mo become older. In addition, the use of HEU causes the problem of nuclear proliferation. Thus, new production technologies for ^{99}Mo and ^{99}mTc by non-use of HEU are required and investigated [1,2]. The typical technologies use the molybdenum targets, such as ^{100}Mo(n, 2n)^{99}Mo [3], ^{100}Mo(p,x)^{99}Mo or ^{99m}Tc [4], ^{98}Mo(n,γ)^{99}Mo [5]. These methods are required the enriched molybdenum isotopes. We are investigating the molybdenum isotope separation by chemical exchange. In the present work, the molybdenum isotope fractionation by ion exchange is studied. The geochemists have also much interest in the molybdenum isotope fraction in chemical reaction, recently [6,7]. Our study may help the understanding of molybdenum fraction in nature.

II. EXPERIMENTAL

1. Materials

$Na_2MoO_4 \cdot 2H_2O$ supplied by Junsei Chemical Co., Ltd. was used. The purity of Mo(VI) was more than 99.0 %. The acidic concentrations of the solutions dissolved Mo species of 0.1 M(M = mol/L) were adjusted to 0.1, 0.5, 1.0, 2.0, 4.0, 6.0, 9.0, and 11.2 M using HCl. The high-porous benzimidazole-type anion-exchange resin embedded in high-porous silica beads which has two functional groups consisted of 4-(1-methylbenzoimidazole-2-yl)phenyl and 4-(1,3-dimethyl-benzoimidazole-2-yl)phenyl was used for Mo isotope fractionation.

2. Chromatography Experiments

Five columns connected in series were used for the isotope fractionation chromatography. Each column has the diameter of 0.8 cm and the length of 100 cm. Total volume of the resin packed into these columns was 84.8 mL. The temperature of columns was kept at 308 K. The breakthrough experiments using 0.1 M of Mo species dissolved in 0.10 - 11.2 M HCl were performed. The flow rate was controlled at 0.35 mL/min by using the high pressure pump made of Nihon Seimitsu Kagaku Co., Ltd. The Mo isotope ratios were measured using ICP-MS(7700x, Agilent). Mo concentrations in samples for isotope ratio measurements were adjusted at *ca.* 1.0 ppb (ppb = ng/g), and all sample solutions was used as 2.0 % HNO_3.

III. RESULTS AND DISCUSSION

The breakthrough experiments for Mo isotope fractionation were carried out under conditions, $[Mo]_T$ = 0.1 M(subscript T means total concentration), $[HCl]_T$ = 0.1 - 11.2 M, and Temp. = 308 K. The typical result of Mo isotope fractionation was shown in Figure 1. As shown in the figure, it was found that heavier isotopes are disproportionately distributed into a solution phase. The hexavalent molybdenum in solution is known to have many type of chemical species, such as oxoacid ions, complexes, and their combines. Mo isotope fractionations are attributed to the chemical exchange among their species.

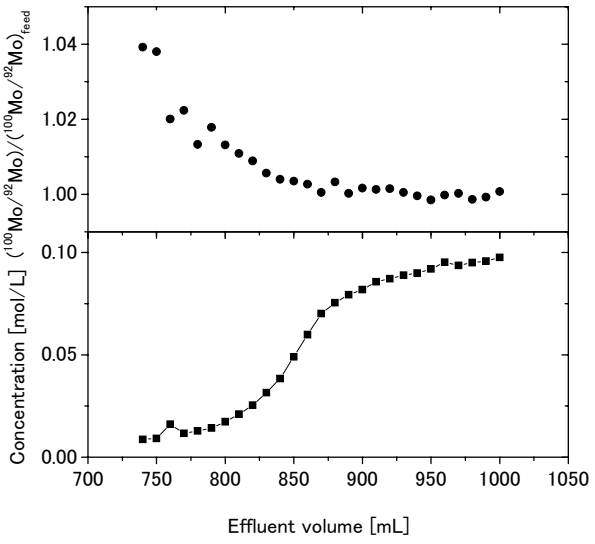

Figure 1. Molybdenum breakthrough curve and molybdenum isotope fractionation by anion exchange chromatography using 2 M HCl solution.

ACKNOWLEDGEMENT

This work was partially supported by the Grant-in-Aid for Challenging Exploratory Research (KAKENHI No. 24656567).

[1] IAEA Nuclear Energy Series No. NF-T-5.4 (2013)
[2] IAEA TecDoc 1065 (1999)
[3] Y.Nagai, Y. Hatsukawa, J. Phys Soc. Jpn. 78(2009)33201
[4] K. Gagnon, et al. Nucl. Medicine & Biology 38(2011)907.
[5] A. Kimura, et al, IOP conf. Series : Mat. Sci & Eng. 18(2011)42001
[6] T. Kashiwabara, et al. Geochem. J. 43(2009e31.
[7] J. Barling, A.D.Anbar Earth & Planetary Sci. Lett. 217(2004)315.

APSORC'13 - 5th Asia-Pacific Symposium on Radiochemistry
Kanazawa, Japan, 22-27 September 2013

The Mechanism of Oxidized Multi-walled Carbon Nanotubes across Placental Barrier and Its Effects on Pregnany

QI Wei[1], BI Juanjuan[1], WANG Jing[1], LI Zhan[2], LIU Peng[1], WU Wangsuo[1*]
[1] Radiochemical Laboratory, Lanzhou University, Lanzhou, Gansu, China, 730000
[2] Institute of Modern Physics, Chinese Academy of Sciences, Lanzhou, Gansu, China, 730000

Abstract
The mechanism of nanoparticles across placental barrier was studied post injected intravenously with solution of oxidized multi-walled carbon nanotubes (oMWCNTs) labeled by technetium-99m into pregnant mice, the rate and mechanisms of abortion were also investigated via measuring content of progesterone and estradiol in maternal serum. The results indicated that oMWCNTs could across placental barrier and enter into fetus body, and caused high distribution of fetal lung, and then eliminated gradually; oMWCNTs could decrease level of progesterone and increase level of estradiol in serum, that depended on exposure dosage and time, but weakened with the extension of gestational ages; the abortion rate of primiparous, second-parous and fourth-parous pregnant mice caused by oMWCNTs was 70%, 40% and 50%, respectively, and also the maternal body weight growth were inhibited until gestational age of 13, 10 and 11 days, respectively. Therefore, oMWCNTs can damaged normal pregnancy, and that was more serious for primiparous.

Keywords: oMWCNTs; placenta; biodistribution; abortion rate; progestational hormone.

Table 1.The statistics of abortion rates after exposure oMWCNTs (n=10).

Group	Ectroma (colpo-bleeding)	Normal parturition	Average weight change before and after production /g	Total abortion rate
First-oMWCNTs	7	3	8.57±8.95*	70%
First-control	1	9	20.73±9.00	10%
Second-oMWCNTs	4	6	13.99±9.44	40%
Second-control	0	10	15.83±4.24	0
Fourth-oMWCNTs	5	5	11.18±5.82	50%
Fourth-control	3	7	12.72±5.78	30%

*p<0.05, group *vs.* normal.

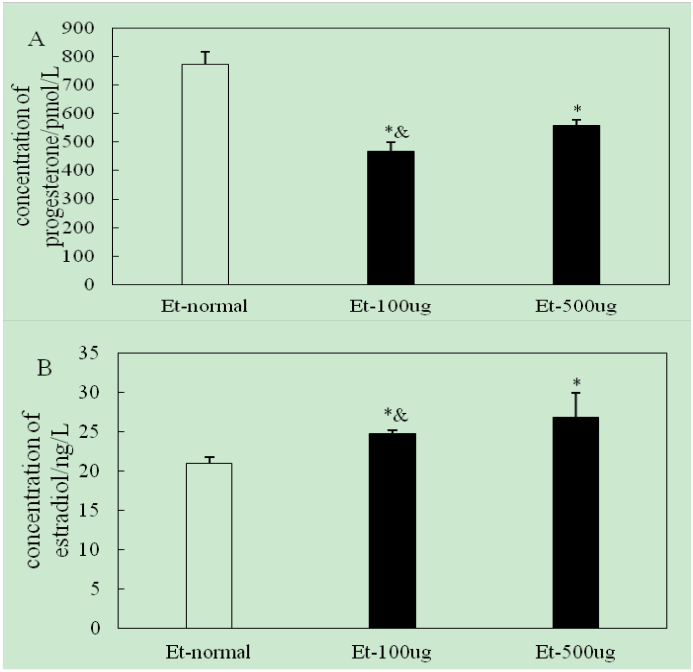

Figure. The exposure time of oMWCNTs effects on the progesterone in the mice at gestational age of 18 days (n=4-5, *p<0.05, group.*vs* normal, &p<0.05,group *vs.* Et-500ug).

*Corresponding author: WU Wangsuo, Tel & Fax:(+86)09318913594, Email address: wuws@lzu.edu.cn,

Prompt Gamma Test of a Large Volume Lanthanum Bromide Detector

Naqvi, A. A[*1] , M. A. Gondal[1]; M. Raashid[1]; Khateeb-ur-Rehman[1], M. Dastegeer[1]

[1]Department of Physics,
King Fahd University of Petroleum and Minerals, Dhahran, Saudi Arabia

Abstract – Response of a large $LaBr_3$:Ce detector has been tested over broad range of gamma rays using prompt gamma ray neutron activation analysis technique,. Due to its larger size, the detector has poorer energy resolution a 76 mm x 76 mm (diameter x height) cylindrical $LaBr_3$:Ce detector

Keywords – Large $LaBr_3$:Ce detector, performance tests using prompt gamma rays, portable neutron generator, chlorine, mercury and cadmium contaminated bulk water samples

I. INTRODUCTION

The application of Prompt Gamma-ray Neutron Activation Analysis (PGNAA) technique is growing further due to the fabrication of radiation hardened lanthanum-halide ($LaBr_3$:Ce and $LaCl_3$:Ce) gamma ray detectors. Although $LaCl_3$:Ce detectors and $LaBr_3$:Ce detectors have a fast rise time, excellent light output and energy resolution but they have intrinsic activity, which increases with detector volume. This may limit their utilization in PGNAA application. King Fahd University of Petroleum and Minerals , Dhahran, Saudi Arabia has acquired a cylindrical 100 mm x 100 (diameter x height) $LaBr_3$:Ce detector for its prompt gamma ray program. Performance test of the large volume detector were carried **out** over broad range of gamma ray energies emitted in thermal neutron capture in bulk samples.

A prompt gamma ray neutron activation analysis setup has been developed using a MP320 D-D reaction-based portable neutron generator to analyze elemental concentration of bulk samples. Response of the cylindrical 100 mm x 100 mm (diameter x height) $LaBr_3$:Ce detector has been measured for detection of chlorine, mercury and cadmium contaminated bulk water samples, Compared with performance of a smaller 76 mm x 76 mm $LaBr_3$:Ce detector reported earlier [1], the larger volume $LaBr_3$:Ce detector has higher intrinsic activity and poorer energy resolution. Results of the study will be presented.

[1] Naqvi A. A., M.S. Al-Anezi, Zameer Kalakada, Faris A. Al Matouq, M. Maslehuddin , M. A. Gondal , A. A. Isab, Khateeb-ur-Rehman and M. Dastageer Response Tests of a $LaCl_3$:Ce Scintillation Detector With Low Energy Prompt Gamma Rays From Boron and Cadmium. Applied Radiation and Isotopes, Vol.70 (2012) pp. 882-887.

APSORC'13 - 5th Asia-Pacific Symposium on Radiochemistry
Kanazawa, Japan, 22-27 September 2013

Radiation-Induced Reactions in D, L-α-Alanine Adsorbed in Solid Surfaces

E Aguilar, A. Negrón-Mendoza, and C. Camargo
Instituto de Ciencias Nucleares, Universidad Nacional Autonoma de Mexico, Mexico DF 04510, Mexico

Abstract
The aim of this work is to study the behavior under irradiation of D, L and D-L α-alanine adsorbed in solid surfaces, as possible phase in the chemical evolution that may have occurred on the primitive Earth or in extraterrestrial environments and to evaluate the contribution of solids (a clay mineral) as shields for the adsorbed amino acids against a external energy source. The results show that α-alanine is adsorbed in the surfaces as function of pH and its yield of decomposition in mineral suspension is lower than the system without the solid surface. These results show the importance of nuclear techniques in these types of studies.

Keywords – α-Alanine, chemical evolution, gamma radiation, clay mineral

I. INTRODUCTION

The emergence of life on Earth needed a physical and chemical preamble. There is a large variety of experimental data to support the hypothesis for the abiotic formation of organic compounds [1, 2]. Although much knowledge has been obtained, many questions remain. One important factor in chemical evolution is related to the importance of random chemical synthesis/decomposition *versus* more selective pathways forming compounds of biological relevance. It is important then to explore chemical mechanisms able to narrow the variety of prebiotic chemical compounds liable to be used in the construction of primitive living systems. We study a simple chemical system: an amino acid adsorbed in a clay mineral and exposed to ionizing radiation.

Our interest is twofold: (1) to evaluate the role that a solid surface plays to protect the compound adsorbed in the solid. (2) To show experimentally that biased reactions might have occurred in geologically relevant conditions on the primitive Earth, for example to study if there is a preferential destruction by ionizing radiation of one of the optical isomers of α-alanine.

II. EXPERIMENTAL PROCEDURES

The solid surface was sodium montmorillonite of Wyoming bentonite. Aqueous solutions of α-alanine were tested (racemic and pure enantiomeric forms) at concentrations of 0, 01 M and different pH values (2, 4, and 6). The oxygen was removed by passing argon through the solutions. The irradiations were carried out in a ^{60}Co- gamma source. The radiation doses were from 0 to 91 kGy. The analyses were made by high pressure liquid chromatography with a Chiral column (ChirobioticT®), coupled to light scattered detector (ELSD). The solid phase was analyzed by X-ray, IR and electron spin resonance. The experiment was carried out 15 times to check the repeatability of the results.

III. RESULTS

The adsorption data shows that the α-alanine (D and L or D; L) is absorbed readily in the clay. The adsorption occurs to a maximum degree at low pH. At basic pH the adsorption was very low. The gamma irradiation of samples show low yield of recovery of the amino acid without clay. The summary of the recovery percent is in Table I.

Table I Survival Percent of α-Alanine after irradiation

SAMPLE	TREATMENT	SURVIVAL % DOSES 91 kGy	
		L-Alanine	D-Alanine
D, L Alanine	without clay	3.49	2,47
	with clay	73.76	62.85
L-Alanine	without clay	2.56	
	with clay	54.45	
D-Alanine	without clay		3.32
	with clay		45.84

IV. REMARKS

It was observed that the presence of mineral drastically decreases the damage to that amino acid by action of the gamma radiation. The observed general tendency shows the L-α-alanine as the most resistant to ionizing radiation, especially when is radiated in enantiomerically pure solutions, the difference is very slight, but this small difference may be amplified with time and by other mechanism. This result shows the important role of minerals in chemical evolution processes.

ACKNOLEDGEMENTS

This work was supported by PAPIIT Grant No. IN110712-3 and the CONACyT Grant No. 168579/11. The technical support from C. Camargo, B. Leal, and F. García-Flores is acknowledged.

REFERENCES

[1] A. Negrón Mendoza, S. Ramos-Bernal and G. Mosqueira, Int. J. Astrobiol. 3, 295-300, 2005
[2] . S. L. Miller and L. Orgel, The Origins of Life on Earth, Prentice-Hall, Inc. New Jersey, 1974.

APSORC'13 - 5th Asia-Pacific Symposium on Radiochemistry
Kanazawa, Japan, 22-27 September 2013

^{36}Cl determination in steel radioactive waste

F. Goutelard[1], P. Perret[1], C. Hamon[1], R. Brennetot[1], C. Andrieu[2]

[1]*Operator Support Analyses Laboratory, Atomic Energy Commission, CEA Saclay, DEN/DANS/DPC/SEARS/LASE, Building 459, PC171, 91191 GIF SUR YVETTE CEDEX, FRANCE*

[2]*Electricité de France, EDF – CIDEN / Département Etudes - Division Déconstruction/Groupe Inventaire et Agréments, 154 Avenue Thiers, CS 60018, 69458 LYON CEDEX 06*

Abstract – APSORC'13 Abstract

Within the framework of the nuclear power plants dismantling, approximately 3600 tons of metallic radioactive wastes will be generated. Located near the reactor core, some of them are highly activated and ^{36}Cl produced from the natural stable isotope ^{35}Cl, due to high mobility and long half life, becomes one of the radionuclides that significantly control the ultimate disposal. In steel materials, concentrations between 0.15 and 12.9ppm have been reported [1, 2]. Depending on neutron flux intensity, ^{36}Cl activity calculated for a stable chlorine concentration of 1ppm varies from 0.03 to 91 Bq/g, while the upper acceptance limit for medium activity waste is 5 Bq/g. 200 steel samples have already been collected in nuclear plants under dismantling. Without further available data on stable chlorine content, ^{36}Cl has to be measured.

French standard methods [3] dedicated to ^{36}Cl measurement in wastes does not describe this first step in details and the radiochemical method includes no more than 3mmole of stable chlorine used as carrier and chemical yield tracer. ^{36}Cl is measured by liquid scintillation. A radiochemical process dedicated to ^{36}Cl measurement in steel radioactive waste, has been developed in order to

- *ensure a detection limit far below 5Bq/g,*
- *treat a great flow of samples.*

Furthermore, it must be adapted to as well as carbon than stainless steel samples. And, as ^{36}Cl is an activated product, a total dissolution must be guaranteed.

A dissolution mixture of nitric and chlorhydric acid needed to assure a complete dissolution specially for stainless steel samples has been optimized in order to minimize the quantity of chlorine added. Nevertheless, 25mmole of chlorine are required to dissolve 0.2g of stainless steel, while 15mmole are necessary for 1g of carbon steel. As a result, the following separation steps have to be adapted. The experimental set-up for the dissolution step is a three-neck flask, containing the sample and KCl as chloride source. After gently added nitric acid, nitrogen is bubbled in the solution in order to carry on the gas Cl_2, in a trapped bottle. With this process, only volatile radionuclides such as ^{14}C, ^{129}I… are trapped.

In order to sort the samples, an aliquot of the bubbler solution is directly analyzed. For sample with an activity higher than 3Bq/g, the radiochemistry is carried on to isolate ^{36}Cl in a pure fraction in only two days. The recovery yield is determined at the different stages of the radiochemical procedure, measuring stable chlorine by ionic chromatography.

The method has been evaluated in terms of recovery yield and limit of detection according to the French AFNOR NFT90-210 standard [4]. Thus, a limit of quantification of 0,15Bq has been experimentally verified. Considering the mass analyzed and the limit of quantification the limit of detection is 3 times lower than this limit of quantification, leading to a limit of detection at 0,3Bq/g and 0,15 Bq/g for stainless steel and carbon steel samples respectively.

Results on activated steel will be presented.

[1] C.S. Sastri, G. Blondiaux, P. Mijller, H. Petri Determination of chlorine in metals and ceramics materials by low energy deuteron activation analysis, Nuclear instruments and methods in physics research B, vol.119,1996 p425-428.

[2] NIREX report 772, T/REP/20021/P/08 (date d'émission : 31/03/1997).

[3] Norme NF M 60-332, Détermination du chlore-36 dans les effluents et déchets par scintillation liquide, mai 2009.

[4] Norme NF T 90-210, Protocole d'évaluation initiale des performances d'une méthode dans un laboratoire, mai 2009.

APSORC'13 - 5th Asia-Pacific Symposium on Radiochemistry
Kanazawa, Japan, 22-27 September 2013

Naturally Occurring Radioactive Materials(NORM) in Malaysian Oil Sludge Samples

[1]Mohamed B.A. Teiara and [2]Sukiman B. Sarmani
[1]Department of Physics, University of Al-Zaituna, Tarhruna, Libya
[2]School of Chemical Sciences and Food Technology, Faculty of Science and Technology, Universiti Kebangsaan, Malaysia, Bangi, 43600, Malaysia

It was in the early 70's, when concern was started regarding the presence of NORM associated with the oil & gas production. During 1980's a lot of work has been devoted to the hazards arising from the measured elevated concentration of NORM in this field. Recently, most publications concern about the effect of NORM on personnel and environment. It was the scope of this paper to analyze the sludge waste resulted from the Malaysian oil fields for the presence of Naturally Occurring Radioactive Materials (NORM) and investigated the hazardous risk associated. This can be also used in future as a reference data to monitor any level changes. About 30 dried sludge samples were characterized using gamma-ray spectroscopy based on a well shielded HPGe detector for the determination of the activity concentrations of ^{238}U, ^{232}Th, their important progenies and ^{40}K. The range of activity concentrations were (10.1 – 51.0) Bq/Kg for ^{226}Ra (186 keV), (6.2 – 34.8) Bq/Kg for ^{214}Pb (352keV), (4.7 – 17.7) Bq/Kg for ^{208}Tl (583 keV), (5.8 – 40) Bq/Kg for ^{214}Bi (609keV), (5.45 – 15.7) Bq/Kg for ^{228}Ac (911keV) and (9.2 – 46) Bq/Kg for ^{40}K (1460keV). The radiation doses resulted from the sample total activities were measured and compared with standard dose limits which would be investigated in the full manuscript.

APSORC'13 - 5th Asia-Pacific Symposium on Radiochemistry
Kanazawa, Japan, 22-27 September 2013

On the Use of ^{233}U and ^{237}Np as Radiotracers for Redox Potential Measurements

Stellan Holgersson
Chalmers University of Technology, Department of Chemical and Biological Engineering, Nuclear Chemistry, Kemivägen 4, SE41296 Göteborg , Sweden

Abstract

Reduction/oxidation (redox) potential measurements in environmental samples are usually made with electrodes. However, these have certain weaknesses in terms of stability and memory effects. Alternative methods for determination of redox are therefore of interest and the use of radioactive tracer elements may be one such method, which is the subject of this investigation. It is suggested that the actinides are particularly appropriate for use as indicators of redox, provided that their different redox states can be separated in a fast and reliable way. A literature survey show that solvent extraction is an established method for separation of tracer amounts of actinides into their redox states and three of the most commonly used extraction reagents of the beta-diketone type were investigated: thenoyltrifluoroacetone (TTA), dibenzoylmethane (DBM) and 4-benzoyl -3-methyl-1-phenyl pyrazol-5-one (PMBP). U and Np were reduced to tetravalent state, which was confirmed with spectropscopic measurements. Extraction curves in the pH range 0.6-7 were then measured for An(IV),(V) and (VI) . It was found that 0.5M DBM in chloroform and 0.05M PMBP in xylene gave the best separation factor (SF=1700 resp. 1100) for actinide (IV)/(VI) and (IV)/(V) oxidation state separation, respectively, when pH of aqueous phase was in the region 1-2. Actinide tracer was used for redox determinations of prepared samples with an artificial groundwater, with or without addition of grains of rock and pyrite and also a Fe(II)/Fe(III) redox-buffer. Comparison with electrode (Pt/Ag/AgCl) measurements gave values that were considerable lower: for example 30mV for a non-redox-buffered synthetic groundwater measured with actinide speciation, compared with about 300mV with electrode. The actinide speciation reflects a slower response to redox changes and a preservation of an earlier redox state of the groundwater, while the electrode responds seems to respond fasterto changes but is thereby also more sensitive to undesirable Eh drift. It was also found that U and Np redox speciation method also have a limited working range of about -100>Eh<100 mV so an absolute correspondence between the methods may therefore be impossible to attain if Eh is outside this range.

Keywords – Redox potential measurements, Groundwater, Uranium, Neptunium, Solvent extraction

Analysis of $^{129}I/^{127}I$ ratios from underground fluids collected in Japan

N. Okabe[1], Y. Muramatsu[1], M. Arai[1], H. Matsuzaki[2], M. Takahashi[3], K. Kazahaya[3]
[1]Gakushuin University, Japan
[2]University of Tokyo, Japan
[3]AIST, Japan

Keywords – I-129, dating, underground fluids

1. INTRODUCTION

There are many isotopes of iodine. Specialty, the long-lived iodine isotope, ^{129}I is produced by the spallation of atmospheric and by spontaneous fission ^{238}U. ^{129}I and the stable isotope ^{127}I are in steady state before being released and mixed with anthropogenic ^{129}I. So this ratio was measured in order to provide an estimation of the age of iodine.

The purpose of this study is to understand the origin of high salinity groundwaters related to the geological settings of the area. In this study we analyzed ^{129}I (half-life 15.7 m.y.) in the fluids in older to estimate the age of the dissolved iodine in hot spring waters collected from various places in Hokkaido. It is known that several hot springs in Hokkaido, the northern Japanese island, contain high concentrations of halogens including iodine. However, the origin of the salts in these springs is not well known. We analyzed I, Br and Cl concentrations.

2. Samples and Analytical method

Hot springs and groundwaters were collected in Hokkaido. In the sampling interpretation of sample types we considered the classification based on Matsunami et al (1999).

Concentrations of Cl in the hot spring samples were determined by an ion chromatography. Concentrations of I and Br were determined by ICP-MS.

The $^{129}I/^{127}I$ ratios were determined by accelerator mass spectrometry (AMS). Samples were precipitated as AgI (target cell) after separated iodine, and analyzed by AMS at MALT (Micro Analysis Laboratory, Tandem accelerator, University of Tokyo).

3. Results and discussion

In the Hokkaido hot spring samples, the relationship between iodine concentration and $^{129}I/^{127}I$ ratios is classified in 2 types. In general, if iodine concentrations increase, $^{129}I/^{127}I$ ratios are higher. But, a part of sample didn't show this trend.

$^{129}I/^{127}I$ ratios ranged between 0.05×10^{-12} and 0.38×10^{-12} in Hokkaido hot springs samples. Samples collected from north-western area showed very low $^{129}I/^{127}I$ ratios of 0.05×10^{-12} to 0.1×10^{-12}. Low values are also observed along the longitude 141-142. These values are markedly lower than the $^{129}I/^{127}I$ ratios observed in iodine-rich fluids in other areas in Japan, such as Chiba (0.18×10^{-12}), Niigata ($0.3\text{-}0.4\times10^{-12}$, Tomaru et al. 2009) and Satsuma-Iwojima (0.78×10^{-12}, Snyder et al. 2002). Considering the ^{129}I systematics (Fehn et al. 2004), iodine age in Hokkaido samples of the lowest $^{129}I/^{127}I$ ratios is estimated to be 60-70 Ma. This indicates that the iodine-rich fluids are likely be derived from old marine sediment, which was later uplifted to form older rock formations in the present day coastal region of Hokkaido.

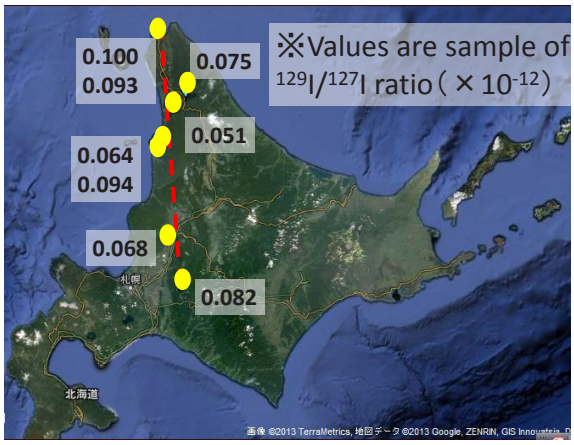

Fig. 1 Mapping of location of low $^{129}I/^{127}I$ ratio samples in Hokkaido

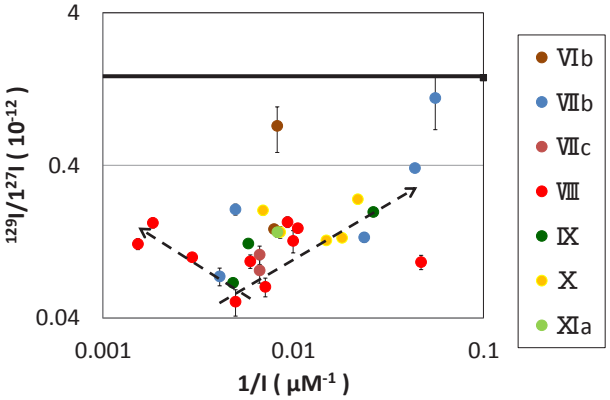

Fig. 2 Iodine concentrations vs. $^{129}I/^{127}I$ ratios

APSORC'13 - 5th Asia-Pacific Symposium on Radiochemistry
Kanazawa, Japan, 22-27 September 2013

Radiocarbon Dating of Ancient Japanese Calligraphy Sheets: Checks with Ancient Documents of Known Age and Its Application to Kohitsugire Calligraphies

Hirotaka Oda[1], Kazuomi Ikeda[2], Hiroaki Yasu[3], Shoji Sakamoto[4]
[1]Center for Chronological Research, Nagoya University
[2]Faculty of Letters, Chuo University
[3]Taga High School
[4]Degital Archives Research Center, Ryukoku University

Abstract – Radiocarbon ages of ancient documents, sutras and books of known age were measured by AMS. The calibrated radiocarbon ages corresponded to the years in which they were written. The result shows that Japanese paper is suitable for radiocarbon dating. Radiocarbon dating on ancient calligraphies of unknown age clarified their historical ages and academic value.

Keywords – AMS, Radiocarbon dating, Ancient calligraphy.

I. INTRODUCTION

Kohitsugire are ancient paper sheets or fragments containing elegant calligraphy. They were originally pages of ancient manuscripts. The old manuscripts written before the 14th century hardly remain as complete books; therefore, kohitsugire potentially has high academic value. However, among kohitsugire attributed to famous calligraphists, many copies and counterfeits written several centuries later are in circulation. Therefore, in this study, we measured radiocarbon ages of kohitsugire by accelerator mass spectrometry (AMS). In the first, we measured ancient documents, sutras and books of known age for check of the method. Then, we applied to kohitsugire calligraphies of unknown age to determine their historical ages and academic value.

II. EXPERIMENTAL

Paper samples were cut from the margins of kohitsugire. A kohitsugire is commonly mounted on other paper sheets that form a lining. The samples were soaked in distilled water to peel the surface sheet of the calligraphy from the mounts. The surface sheets were first washed in distilled water with an ultrasonic cleaner and then treated with 1.2N HCl and 1.2N NaOH solutions (60-70°C). After re-treating with 1.2N HCl and rinsing with distilled water, they were combusted using CuO (850°C, 3h) to form CO_2. The CO_2 was reduced to graphite by H_2 (650°C, cat-Fe, 6h). The radiocarbon ages were measured by AMS.

III. RESULTS AND DISCUSSION: THE KNOWN-AGE DOCUMENTS

The results of the known-age documents, sutras and books were plotted on the calibration curve (Fig. 1). The obtained radiocarbon ages of the documents correspond to the paleographical ages. Although ancient Japanese paper can be considered as a wooden sample, it was made from short-lived branches of trees. In addition, old paper is not used for calligraphy because it repels India ink and is unsuitable for elegant handwriting. The result indicates that ancient Japanese paper is suitable for radiocarbon dating.

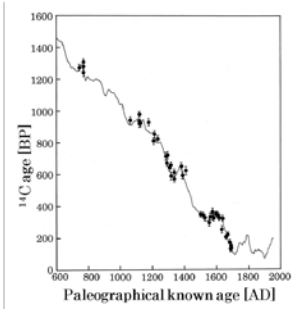

Fig. 1. Result on the known-age documents

IV. RESULTS AND DISCUSSION: KOHITSUGIRE CALLIGRAPHIES

We applied to kohitsugire of unknown age to clarify their historical ages and academic value. For example, Fig. 2 is kohitsugire attributed to Nakatomi no Kamatari (614-669). However, radiocarbon dating indicated that it was written in the 14th century and is not his genuine handwriting. According to legend, calligraphy of Fig. 3 is Shibunritsu sutra brought from China by the priest Ganjin (688-763). Although radiocarbon dating cannot show that the legend is true or not, it indicated that it is old sutra written in the 7-8th centuries as the legend.

Fig. 2. Kohitsugire attributed to Nakatomi no Kamatari

Fig.3 Shibunritsu sutra

APSORC'13 - 5th Asia-Pacific Symposium on Radiochemistry
Kanazawa, Japan, 22-27 September 2013

μ-XRF study on Wiangkalong pottery

K. Won-in[1], S. Tancharakorn[2], W. Tanthanuch[2], P. Dararutana[3]
[1]Department of Earth Sciences, Faculty of Science, Kasetsart University, Bangkok 10900 Thailand
[2]Synchrotron Light Research Institute, Nakhon Ratchasima 30000 Thailand
[3]The Royal Thai Army Chemical School of the Royal Thai Army Chemical Department, Bangkok 10900 Thailand

Abstract- It was proved that non-destructive and non-sampling methods were used to analyze the composition of the archaeological objects. It was well-known that differences of them found in Thailand such as glasses, potteries and metal wares. Due to the complex nature of materials and objects, extremely sensitive, spatially resolved, multi-elemental and versatile analytical instruments are needed. In this work, micro-beam X-ray fluorescence spectroscopy (μ-XRF) based on synchrotron radiation was firstly used to characterize the elemental composition of ancient Wiangkalong pottery. Wiangkalong was one of major ceramic production cities in northern of Thailand, once colonized by the ancient Lanna Kingdom (1290 A.D.). Potteries were produced with shapes and designs as similar as those of the Chinese Yuan and Ming Dynasties. The results showed the variations in elemental composition of the body matrix, the glaze and the painting. μ-XRF was successfully to characterize the elemental composition of this ancient pottery.

Keywords – Wiangkalong pottery, μ-XRF

[1] Praichanjit, S. (2011). Archaeology of Ceramics in Lanna Northern Siam, Samaphun Publishing Co.Ltd., Bangkok.
[2] Won-in, K., Pongkrapan, S, Dararutana, P., Thawwornmongkolkij, M. and Wathanakul, P. (2010). Raman spectroscopic study of ancient potteries in Thailand: Wiangkalong pottery, 5th Mid-European Clay Conference; August 25-29, 2010: Budapest, Hungary.

Poster Session 2

Tuesday, 24 September 2013

18:50 ~ 20:00

Scientific Topics (Abbrev.)

1. Fukushima issues (FK)
2. Education in nuclear and radiochemistry (ED)
3. Nuclear forensics (NF)
4. Nuclear energy chemistry (NE)
5. Nuclear chemistry (NC)
6. Actinide chemistry (AC)
7. Environmental radiochemistry (EN)
8. Radiopharmaceutical chemistry and Nuclear medicine (RP)
9. Nuclear probes for materials science (NP)
10. Activation analysis (AA)
11. Application of nuclear and radiochemical techniques (AP)

APSORC'13 - 5th Asia-Pacific Symposium on Radiochemistry
Kanazawa, Japan, 22-27 September 2013

Determination of short-lived ^{241}Pu in environmental samples by inductively coupled plasma mass spectrometry

Jian Zheng*, Keiko Tagami, Shigeo Uchida
Office of Biospheric Assessment for Waste Disposal, National Institute of Radiological Sciences

Plutonium isotopes have been released into the environment mainly from the atmospheric nuclear weapons tests in last century, the discharges from nuclear fuel reprocessing facilities, and the nuclear accidents, such as the Chernobyl and the Fukushima Daiichi Nuclear Power Plant (FDNPP) accidents [1-3]. Accurate determination of Pu isotopic composition is important for the source identification of radioactive contamination in the environment since Pu isotopic composition is characteristic for various Pu sources. Among Pu isotopes (^{238}Pu, ^{239}Pu, ^{240}Pu, and ^{241}Pu) observed in the environment, the short-lived ^{241}Pu ($t_{1/2}$ = 14.4 y), a beta emitter, is a sensitive indicator for the identification of any new contamination of Pu isotopes resulted from nuclear power plant accident. For ^{241}Pu originated from the global fallout, the activity of ^{241}Pu in the environment is quite low due to the dacay with time. The activity ratio of ^{241}Pu/$^{239+240}$Pu is ca. 1.2 in 2011 for the global fallout-sourced Pu isotopes. Therefore, higher activity ratio of ^{241}Pu/$^{239+240}$Pu in the environment will provide evidence of additional Pu input.

Due to its short half-life and beta emission, determination of ^{241}Pu in environmental samples has been a great analytical challege. Conventional technique is the low level liquid scintillation counting, which requires tedious sample preparation and long measurement time (typically 13-24 h). In the past years, we have developed sensitive analytical method using inductively coupled plasma mass spectrometry for the determination of ^{241}Pu in various environmental samples, such as atmospheric fallou material, marine sediments, and seawater reference material [4-6]. In this work, we report the determination of ^{241}Pu in environmental samples, such as litter, soil and marine sediments collected in Fukushima Prefecture after the FDNPP accident in 2011. Fig. 1 shows the results of ^{241}Pu activity in litter and surface soils collected in 20-30 km zone of the FDNPP, and in Cities of Mito, Kamagaya and Chiba. High activities of ^{241}Pu ranging from 4.5 to 34.8 mBq/g were detected in the J-Village surface soil (0-2 cm) and two litter samples. This finding of high ^{241}Pu activities in environmental samples after the FDNPP accidnet provided evidence of the release of Pu isotopes from the accident.

Acknowledgement: This study was partially supported by the Agency for Natural Resources and Energy, Ministry of Economy, Trade and Industry (METI), Japan.

References

[1] J. M. Kelley, L. A. Bond, T. M. Beasley. Sci. Total Environ. 237/238 (1999) 483-500.
[2] M. E. Ketterer, K. M. Hafer, J. W. Mietelski. J. Environ. Radioact. 73 (2004) 183-201.
[3] J. Zheng, K. Tagami, Y. Watanabe et al. Sci. Rep. 2:304; DOI:10.1038/srep00304. 2012
[4] J. Zheng, M. Yamada. J. Oceanogr. 64 (2008) 541-550.
[5] J. Zheng, M. Yamada, Appl. Radio. Isot. 70 (2012) 1944-1948.
[6] Y. S. Zhang, J. Zheng, M. Yamada et al. Sci. Total Environ. 408 (2010) 1139-1144.

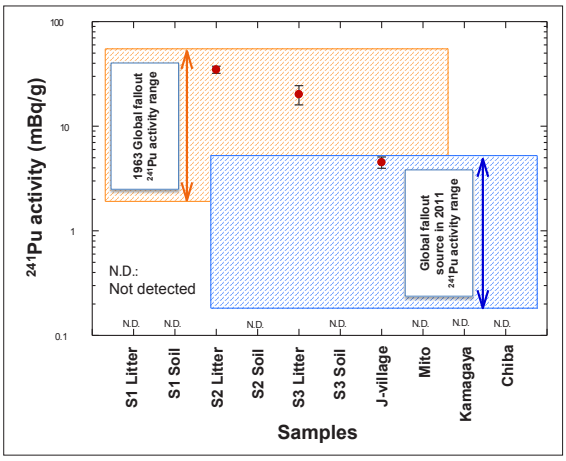

Figure 1. Results of activities of ^{241}Pu detected in the environmental samples collected after the FDNPP accident.

Numerical evaluation of Cs adsorption in PB column by extended Langmuir formula and one-dimensional adsorption model

Hiroshi Ogawa, Akiko Kitajima, Hisashi Tanaka, and Tohru Kawamoto
Nanosystem Research Institute, Advanced Industrial Science and Technology (AIST), Tsukuba, 305-8568, Japan.

Abstract – Amount of Cs adsorption in PB column was numerically evaluated based on extended Langmuir formula and one-dimensional adsorption model. The extended Langmuir formula successfully reproduced the experimental K_d distribution coefficient of Cs adsorption that cannot be explained by traditional Langmuir model. The time-variation of the Cs adsorption in column experiment was also explained by one-dimensional adsorption model.

Keywords – Cs decontamination, Cs adsorption, extended Langmuir formula, column experiment, simulation

I. INTRODUCTION

The accident of the Fukushima-daiichi nuclear plant in March, 2011 has caused heavy radioactive pollution in surrounding regions. Decontamination of radioactive elements, especially Cs-134 and Cs-137, is an urgent issue. One of the most effective procedures for the Cs-decontamination from contaminated water is to use Prussian-Blue (PB) as a Cs adsorbent [1,2]. In this paper, the authors propose a numerical method for expecting the amount of Cs reduction by PB adsorbent based on extended Langmuir formula and one-dimensional adsorption model.

II. METHOD

The Langmuir formula is extended as,

$$w = \Sigma_{i \le Ni}\, w_i\,, \qquad (1)$$

$$w_i = K_i\, c\, (w_i^{\max} - w_i), \qquad (2)$$

where w is the total amount of the adsorbed Cs in the adsorbent, N_i the number of adsorption site, w_i the amount of the adsorbed Cs at i-th adsorption site, K_i the equilibrium constant between liquid and adsorbent at the i-th site, $w_i^{\max}$ the saturation value of the Cs adsorption at the i-th site, and c the Cs concentration in the liquid.

Time-variation of Cs reduction in a column experiment was calculated by one-dimensional adsorption model as,

$$\mathrm{d}c\,(x, t) / \mathrm{d}t' = -\,c\,(1 - \zeta\,(x, t)) / \zeta^{\max}\,\tau, \qquad (3)$$

where x, t, t', $\zeta^{(\max)}$, and τ are the one-dimensional position in the column, wall-clock time, contact time of the water with the adsorbent, (maximum capacity of) Cs-concentration in the adsorbent, and time constant of Cs-concentration reduction, respectively.

The column and shaking experiments were carried out by using granular adsorbent with PB nanoparticle supplied by Kanto Chemical Co. Inc. [2]

III. RESULTS

In Fig. 1 the experimental K_d values are shown as a function of initial Cs concentration in comparison with the results of Langmuir fittings of N_i = 1 and 2. Large discrepancy is found in the case of N_i = 1 (dashed line) especially at high Cs concentration. The fitting is, however, drastically improved if the second adsorption site is included (solid line).

Figure 2 gives the comparison between experimental and calculated time-variation of Cs concentration in column experiment. Our one-dimensional model gives time-variation of the Cs concentration after column adsorption accurately. It is expected that precise simulation of the Cs adsorption in actual plant will be possible by combining extended Langmuir formula and one-dimensional adsorption model.

[1] Kitajima et al., Chem. Lett., 41, 1403 (2012).
[2] Kitajima et al., in APSORC 13 abstract.

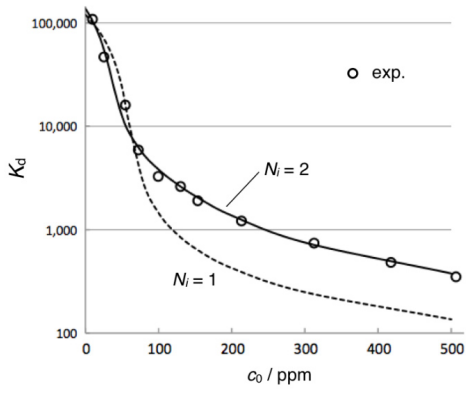

Fig. 1 Experimental and calculated K_d values of the adsorbent used in this study.

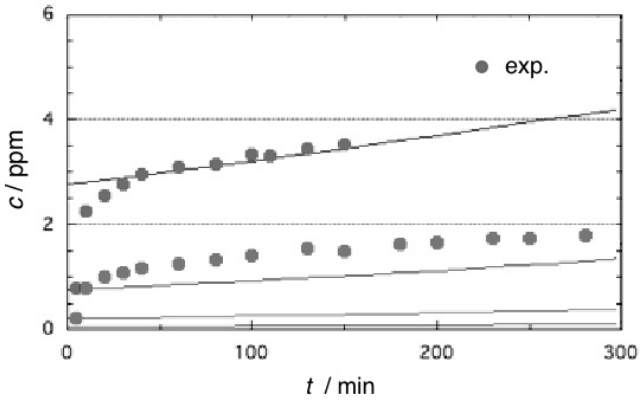

Fig. 2 Experimental and calculated (solid lines) time-variation of Cs concentration in liquid after column adsorption.

Secular distribution of radioactive concentration in the atmosphere at Fukushima, Hitachi and Marumori

ZiJian Zhang[1], Shunsuke Kakitani[1], Kazuhiko Ninomiya[1], Naruto Takahashi[1], Yoshiaki Yamaguchi[2], Takashi Yoshimura[2], Kazuyuki Kita[3], Akira Watanabe[4], Atsushi Shinohara[1]
[1] Graduate School of Science, Osaka University, [2] Radioisotope Research Center, Osaka University,
[3]Faculty of Symbiotic Systems Science, Fukushima University,
[4]College of Science, Ibaraki University

Abstract - Our group started gamma ray measurement of air dust sample after the Fukushima Dai-ichi nuclear power station accident. Air dust filters was collected at Hitachi, Fukushima and Marumori. The activity of Cs-134 and Cs-137 was determined by germanium semiconductor detector. The radiocesium activity concentration in air dust(Bq/m^3) after October 2011 were stable and 6.2×10^{-6} at Hitachi, 3.0×10^{-4} at Fukushima and 1.3×10^{-4} at Marumori.

Key word –radioactive cesium, air dust

I. INTRODUCTION

On 11th March 2011, the earthquake occurred and a large tsunami destroyed coasts of Eastern Japan. As a result, the nuclear accident of Fukushima Dai-ichi nuclear power station (in the following FD-NPS) was arisen. The accident caused massive release of radioactivity into the atmosphere. Many material transportation models were used for simulating the behavior of radioactive nuclides in environment. From these simulations, we can estimate the amount of radioactive deposition to land and sea, and calculate the internal exposure. However, there are some unclear points about nuclides transportation in the environment, and the accuracy of precision simulation was limited by these problems. We need accurate measurement data of radioactive nuclides in the atmosphere. Our group started collection of air dust after the accident of FD-NPS at three locations. In this study, we discuss about the seculer distribution of radioactive concentration in the atmosphere.

II. MEASUREMENT

Our group has been collecting air dust in Fukushima City, in 68 km east of FD-NPS, Hitachi, in 87 km south and Marumori, in 50 km north. Sampling duration was 3-4 days. All gamma ray measurements were carried out at Osaka University in low background condition with 1-2 days. Radioactivities in air (Bq/m^3) of I-131, Cs-134 and Cs-137 were determined. We also measured Be-7 that is one of index of cosmogenic radionuclides, to discuss transportation process of Cs-137.

III. RESULT AND DISCUSSION

The time variation of activity concentration in Hitachi and Fukushima is shown in Fig.1. In Hitachi, activity concentrations for Cs-134 and Cs-137 were very high at April 2011(～Bq/m^3).They were rapidly decrease with time passing, and in October, they were about one-thousandth of the concentration in April. The average of radiocesium activity concentration after October 2011 were 6.2×10^{-6} Bq/m^3 at Hitachi, 3.0×10^{-4} Bq/m^3 at Fukushima and 1.3×10^{-4} Bq/m^3 at Marumori. Ratios of Cs-134/Cs137 were about 1 in three locations. There are many studies that observe the same results in environmental samples.

The activity concentration of beryllium-7 was always about 10^{-3} Bq/m^3. The seasonal variation was likely some previous report [1]. Beryllium-7 is known for attaching to aerosol and being transported to all over the world. We could not find out some correlation between Be-7 and Cs-137. Therefore, main sources of Cs-137 in environment behave differently with cosmic ray radionuclides. We suggest that most of radiocesium in the atmosphere come from some local sources, likely releasing from soil and forest.

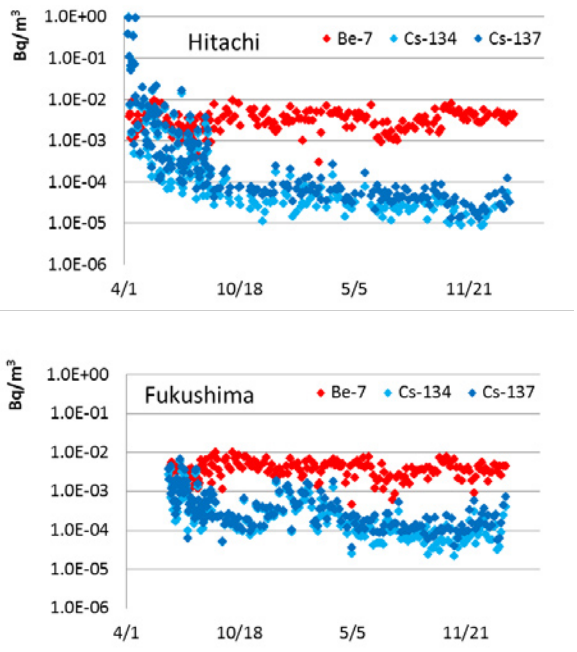

Fig.1. Cs-134, Cs-137 and Be-7 activity concentration. Upper one is data of Hitachi and Under one is data of Fukushima

[1]R.Winkler and F.DIETL, Atmospheric Environment 32, No6, 983-991(1998)

APSORC'13 - 5th Asia-Pacific Symposium on Radiochemistry
Kanazawa, Japan, 22-27 September 2013

Concentration of ^{137}Cs in atmospheric coarse and fine particles collected in Fukushima

Kyo Kitayama[1], Hirofumi Tsukada[1], Kenji Ohse[1], Chika Suzuki[1], Akira Kanno[1], Kencho Kawatsu[1],
[1]Fukushima University Future Center for Regional Revitalization

Abstract – Concentration of ^{137}Cs in atmospheric coarse and fine particles was determined in Fukushima city and Date city collected every 2 weeks from August 2012 to January 2013. Total average concentration of ^{137}Cs in Fukushima and Date were 182 and 173 μBq m^{-3}, respectively and the range was within a factor of 2. The concentration of ^{137}Cs in the coarse fraction was higher than that in the fine fraction except for one sample collected in Fukushima city. The variation of ^{137}Cs concentration in the fine fraction was smaller than that in the coarse fraction and the concentration ratio of ^{137}Cs in the fine fraction to that in the total was approximately 1/3.

Keywords – ^{137}Cs, fine particle, coarse particle, Fukushima city, Date city

I. INTRODUCTION

On 11 March, 2011, the Fukushima Dai-ichi Nuclear Power Plant accident was caused by the tsunami following the earthquake to release radioactive nuclides into the atmosphere. Cesium-137 is a major radionuclide released into the environment and is important to estimate radiation dose for the public. In order to estimate radiation dose from inhalation, the particle size distribution of ^{137}Cs in the atmosphere is required. In this study, concentration of ^{137}Cs in atmospheric coarse and fine particles was determined in Fukushima city and Date city.

II. METHOD

Coarse and fine particles were collected from two sites such as 62 km (Fukushima) and 55 km (Date) distant from Fukushima Dai-ichi Nuclear Power Plant from August 2012 to January 2013. Fukushima is in the urban site and Date is in the rural site. Coarse and fine particles were divided at 50 % cutoff diameter of 1.1 μm with an Andersen sampler (AH-600, Tokyo Dylec), and were collected on polytetrafluoroethylen filters at flow rate of 566 L min^{-1}. The filters were exchanged every two weeks.

The sampled filters were cut into small pieces and compress into a plasitic bottle. Radioactivety of ^{137}Cs in the samples was measured for 0.5-2 days by Ge detector.

III. RESULTS AND DISCUSSION

Total concentration of ^{137}Cs in coarse and fine particles in Fukushima was ranged from 84 to 347 μBq m^{-3} with an average of 182 μBq m^{-3} (Fig. 1-a). The total ^{137}Cs concentration of Date was in the range of 103 to 311 μBq m^{-3} where the average was 173 μBq m^{-3} (Fig. 1-b). The range of

a) Fukushima city

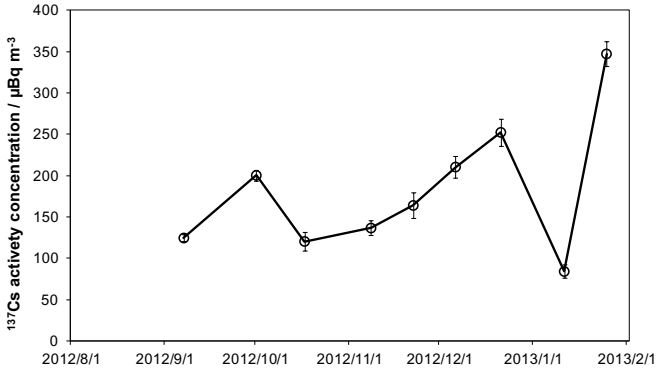

b) Date city

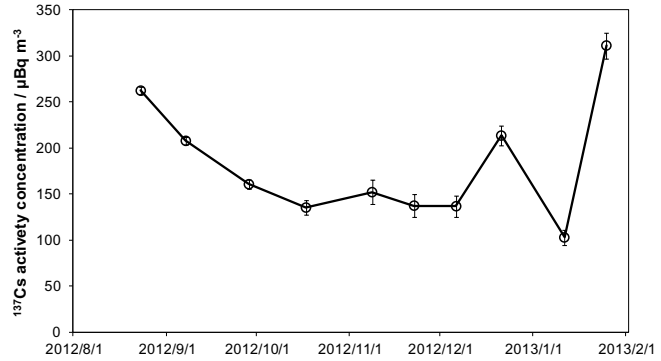

Fig. 1 Concentration of ^{137}Cs in atmospheric coarse and fine particles. Error bars indicate one sigma of deviation.

the concentration of ^{137}Cs in the total particles was within a factor of 2. Tsukada et al. (2012) reported that ^{137}Cs concentration in Fukushima city was 164 mBq m^{-3} in early April 2011 and the value decreased to one thousandth in September 2011. The observed values in the study also maintained a similar order of magnitude to the value in September 2011.

The concentration of ^{137}Cs in the coarse fraction was higher than that in the fine fraction except for one sample collected in Fukushima. The variation of ^{137}Cs concentration in the fine fraction was smaller than that in the coarse fraction and the concentration ratio of ^{137}Cs in the fine fraction to that in the total was approximately 1/3. However, mass concentration ratio in the fine fraction to the total was approximately 1/2. It may attribute that the sources of coarse and fine particles were different.

[1] Tsukada H. et al. (2012) Atomic Energy Society of Japan, Hiroshima.

APSORC'13 - 5th Asia-Pacific Symposium on Radiochemistry
Kanazawa, Japan, 22-27 September 2013

Electrochemical cesium sorption under coexisting other ions using nanoparticle film of copper hexacyanoferrate

Hisashi Tanaka [1)], Rongzhi Chen [1)], Miyuki Asai [1)], Chikako Fukushima [1)], Tohru Kawamoto [1)], Manabu Ishizaki [2)], Masato Kurihara [1,2)], Makoto Arisaka [3)], Takuya Nankawa [3)] and Masayuki Watanabe [3)]

[1)] Nanosystem Research Institute, AIST, Tsukuba central 5, 1-1-1 Higashi, Tsukuba, Ibaraki 305-8565, Japan

[2)] Department of Material and Biological Chemistry, Faculty of Science, Yamagata University, 1-4-12 Kojirakawa-machi, Yamagata 990-8560, Japan

[3)] Japan Atomic Energy Agency, 2-4 Shirane Shirakata, Tokai-mura, Naka-gun, Ibaraki 319-1195, Japan

Abstract – Copper hexacyanoferrate (CuHCF) is known as a good adsorbent for Cs. We developed water-dispersible CuHCF ink by nanoparticulation and surface treatment, and fabricated the thin film of CuHCF on metal electrodes. Cs adsorption/desorption can be controlled electrochemically using this thin film CuHCF electrode, repetitively. Cs sorption capability under coexisting other ions were examined for alkali metals, alkali earth metals, transition metals, etc, and determined to be few affected.

Keywords – Copper hexacyanoferrate, Prusian blue analogues, Nanoparticle ink, Electrochemical adsorption/desorption, Cs adsorption, Nuclear waste water, Fukushima daiichi nuclear disaster

I. INTRODUCTION

The radioactive cesium such as ^{137}Cs ($T_{1/2}$ ~ 30.1 years) is one of heat sources in radioactive wastes. To remove the radioactive nuclide, extensive studies have been done using metal hexacyanoferrates (MHCFs), which have a selective affinity for Cs^+ over a wide pH range and good resistance to radiation. Especially, copper hexacyanoferrate (CuHCF, $Cu_3[Fe(CN)_6]_2$) is stable for electrical use. We fabricated the thin films of CuHCF on metal electrodes by conventional spin coating and succeeded in developing electrochemical Cs^+ recovery system. Here we report the electrochemical Cs^+ adsorption/desorption control and Cs sorption capability under coexisting other ions.

II. EXPERIMENTAL & RESULTS

The nanoparticle CuHCF ink was synthesized according to our previous paper [1]. Uniform film about 100-150 nm thickness was fabricated by spin coating on Au substrate. After insolubilizing process, the CuHCF electrode was able to treat in aqueous electrolyte solution. The Cs^+ concentration in solution was measured with inductivity coupled plasma mass spectrometry (ICP-MS, NexION 300D, Perkin Elmer).

The electrochemical Cs^+ adsorption/desorption was executed by three-electrode system, nanoparticle CuHCF film electrode (20x25 mm^2) as working electrode, saturated calomel electrode (SCE) as reference electrode, and Pt wire as counter electrode. The aqueous electrolyte solution for adsorption contained 10 ppm Cs^+ and 1 ppm Na^+, and for desorption contained 1 ppm Na^+. In the case of coexisting Sr, the adsorption solution contained 10 ppm Cs^+, 10 ppm Sr^{2+} and 1 ppm Na^+. After executing 5 cycle adsorption and desorption, the Cs^+ concentration decreased about 2.5 ppm in adsorption and increased 2.5 ppm in desorption solutions, in the only Cs case and Cs+Sr coexisting case (Fig. 1). In contrast, the Sr concentration kept about 10 ppm in adsorption and 0 ppm in desorption solution. That means the coexisting of Sr ion does not affect the electrochemical Cs sorption capability of CuHCF thin film, and it suggests the possibility of selective recovery of Cs. We also checked it for other alkali metals, alkali earth metals, transition metals, etc.

[1] A. Gotoh, et al., Nanotechnology **2007**, *18*, 345609

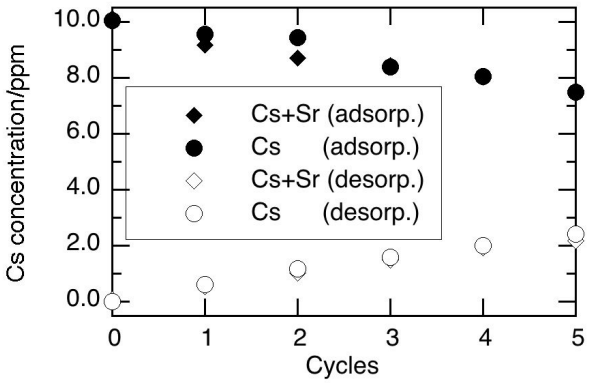

Figure 1. Cs concentration in adsorption solution and desorption solution.

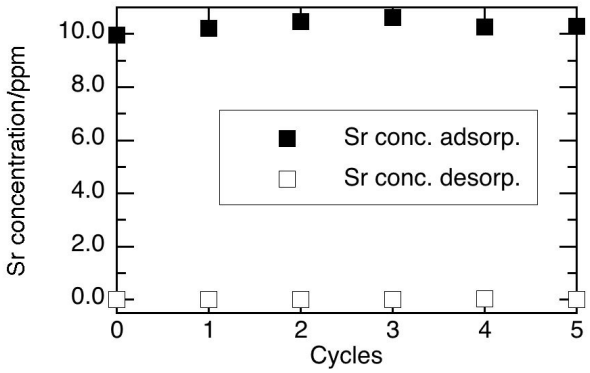

Figure 2. Sr concentration in adsorption solution and desorption solution.

APSORC'13 - 5th Asia-Pacific Symposium on Radiochemistry
Kanazawa, Japan, 22-27 September 2013

Determination of ^{129}I in Fukushima Soil Samples by ICP-MS

Takeshi Ohno[1], Yasuyuki Muramatsu[1], Hiroyuki Matsuzaki[2]
[1]Faculty of Science, Gakushuin University
[2]School of Engineering, The University of Tokyo

Abstract – A method was developed for the determination of ^{129}I in soil samples, which uses a ICP-MS with an octopole reaction system, permitting the investigation of radioiodine released by the Fukushima Daiichi nuclear power plant (FDNPP) accident. The determination of ^{129}I by ICP-MS is capable of providing a high sample throughput compared to other methods.

Keywords – Radioiodine, Fukushima Daiichi nuclear power plant accident, ^{129}I, ICP-MS, Octopole reaction system

I. INTRODUCTION

The accident at the Fukushima Daiichi nuclear power plant (FDNPP) resulted in a substantial release of radionuclides into the environment, including atmospheric of radioiodine and radioceium.[1, 2] The distribution of radio-cesium has been studied, and a map of the radiocesium contamination was made. On the other hand, ^{131}I could only be determined within a couple of months, due to its short half life (8 days), resulting in a lack of data on the deposition of this nuclide. Because iodine is an essential element, and plays an important role in thyroid development, radioiodine that is ingested readily and becomes enriched in the human thyroid. In the event of a nuclear plant accident, an effective dose estimation of released ^{131}I is important.

Another iodine isotope, ^{129}I (half-life: 1.57×10^7 y), was released simultaneously with ^{131}I, although the amount was very small. To reconstruct the early distribution of ^{131}I in the environment, ^{129}I has been used as a follow-up tracer due to its much longer half-life. The determination of ^{129}I in soils in Fukushima is of importance to investigate the distribution of radioiodine released from the FDNPP. Recent advances in inductively coupled plasma mass spectrometry (ICP-MS) using a octopole reaction cell have enabled us to determine the long-lived radionuclide ^{129}I in soil samples.[3]

II. EXPERIMENTAL

The analytical method used in this study is based on the method for AMS measurements.[4] Soil samples (about 2 g) were mixed with V_2O_5 in a ceramic boat before being placed in a quartz tube. The sample was heated at 1000°C in a tube oven for 30 min under a flow of oxygen with water vapor. The iodine released by heating was collected with a trap containing 10 ml of a solution of 1% TMAH. The iodine fraction was then purified by a combination of solvent-extraction and back extraction using carbon tetrachloride as the solvent. The back-extracted solution was concentrated to about 1 mL on a hotplate at 100°C. The purified samples were subjected to measurements of ^{129}I/^{127}I by the ICP-MS. Any mass-discrimination effect in the mass spectrometer was monitored using NIST SRM 3231 Level 1.

III. RESULTS AND DISCUSSION

In order to improve the precision and accuracy of the ^{129}I/^{127}I isotopic ratio measurements, interfering signals, such as $^{129}Xe^+$, must be reduced. In this study, $^{129}Xe^+$ was suppressed by O_2 as a reaction gas using the following reaction: $Xe^+ + O_2 \rightarrow Xe + O_2^+$. The oxygen flow rate was optimized while aspirating an iodine solution (10 ppb, ^{129}I/^{127}I=10^{-13}) so as to maximize the ^{127}I intensity/background (m/z = 129) ratio. When increasing the oxygen flow rate from 0 L/min to the optimum value at 0.8 mL/min, a twenty-fold improvement of ^{129}I background-equivalent concentration was observed.

We investigated the production ratio of $^{127}IH_2^+/^{127}I^+$ while aspirating iodine solution (100 ppm, ^{129}I/^{127}I=10^{-13}). The results demonstrated that the production ratio of $^{127}IH_2^+/^{127}I^+$ in the ICP-MS was about 3×10^{-8}. The contribution from this interference could be corrected by subtracting of $^{127}IH_2^+$ according to the production ratio. The production ratio was monitored before and after measuring the samples, and the contribution of $^{127}IH_2^+$ was subtracted from the signal intensity of ^{129}I when calculating the ^{129}I/^{127}I isotopic ratios.

In order to confirm the applicability to measurements of the ^{129}I/^{127}I ratios of soils we measured ^{129}I in six samples which were collected from an orchard in Ohkuma-machi (about 5 km from the FDNPP), a rice paddy in Iitate-mura and Namie-machi (about 30 km from the FDNPP) and an orchard in Koriyama-shi (about 60 km from the FDNPP). The measured ^{129}I/^{127}I ratios in the samples by ICP-MS are consistent with the value determined by AMS within the analytical error, suggesting the applicability of this method to measurements of ^{129}I/^{127}I in Fukushima soil samples. Our results indicate that ^{129}I can also be determined outside of the 30 km districted area, i.e. 60 km or more from the FDNPP. This method could provide a powerful tool for the investigation of the radioiodine contamination.

[1] M. Chino, H. Nakayama, H. Nagai, H. Terada, G. Katata, and H. Yamazawa, J. Nucl. Sci. and Tech., 2011, 48, 1129.
[2] N. Kinoshita, K. Sueki, K. Sasa, J. Kitagawa, S. Ikarashi, T. Nishimura, Y.-S. Wong, Y. Satou, K. Handa, T. Takahashi, M. Sato, and T. Yamagata, PNAS, 2011, 108, 19526.
[3] T. Ohno, Y. Muramatsu, C. Toyama, K. Nakano, S. Kakuta, and H. Matsuzaki, Anal. Sci., 2013, 29, 271.
[4] Y. Muramatsu, Y. Takada, H. Matsuzaki, and S. Yoshida, Quarter. Geochronol., 2008, 3, 291.

APSORC'13 - 5th Asia-Pacific Symposium on Radiochemistry
Kanazawa, Japan, 22-27 September 2013

Measurement of soil-to-crop transfer factor of tellurium for estimation of potential radiotellurium ingestion from crops

Guosheng Yang, Keiko Tagami*, Jian Zheng, Shigeo Uchida
Office of Biospheric Assessment for Waste Disposal, National Institute of Radiological Sciences

The Fukushima Daiichi Nuclear Power Plant (FDNPP) accident discharged large amounts of radionuclides into the environment, including ^{127m}Te ($T_{1/2}$=109 d), ^{129m}Te ($T_{1/2}$=33.6 d), ^{131m}Te ($T_{1/2}$=30 h) and ^{132}Te ($T_{1/2}$=3.204 d) [1]. Since relatively long-lived ^{127m}Te could transfer from soil to crops through roots, people would ingest ^{127m}Te; however, the isotope is a beta-emitter and the concentration data in food crops were unavailable. Now, ^{127m}Te has been decayed out and it is difficult to measure ^{127m}Te in crops samples. However, it is still important to estimate how much amount of ^{127m}Te might have been ingested from food for public safety purpose. The soil-to-crop transfer factor (TF) is a useful tool to estimate Te concentrations in crops. Unfortunately, the TF data of Te are scarce in the world [2] and there are no data for crops native to Japan.

In order to obtain the TF data of Te for crops, we focused on stable Te as an analogue of radioactive Te. We measured 79 soil and associated crop samples collected nationwide to calculate TFs of Te. Te concentrations in soil and crop samples were measured by using sector field inductively coupled plasma mass spectrometry (SF-ICP-MS) after *aqua regia* digestion and appropriate dilution to reduce the matrix effect [3]. The Te contents in Japanese soil and crops ranged from 12.6 to 479 ng g^{-1} (mean: 55.3 ng g^{-1}) and from 0.06 to 3.8 ng g^{-1} (mean: 0.7 ng g^{-1}), respectively. The Te concentrations in soil were higher than previous report in Japan (10–109 ng g^{-1}), while Te contents in plant samples were much lower than those (18–33 ng g^{-1}) in Japanese plants [4]. Then, TF values from 8.7×10^{-4} to 1.1×10^{-1} (mean: 1.8×10^{-2}) were obtained for the first time in Japan (Figure 1), which were relatively low compared to those reported by IAEA-TRS-472 (0.1–1) [2]. These data could be used to estimate the internal radiation dose from ^{127m}Te after the FDNPP accident.

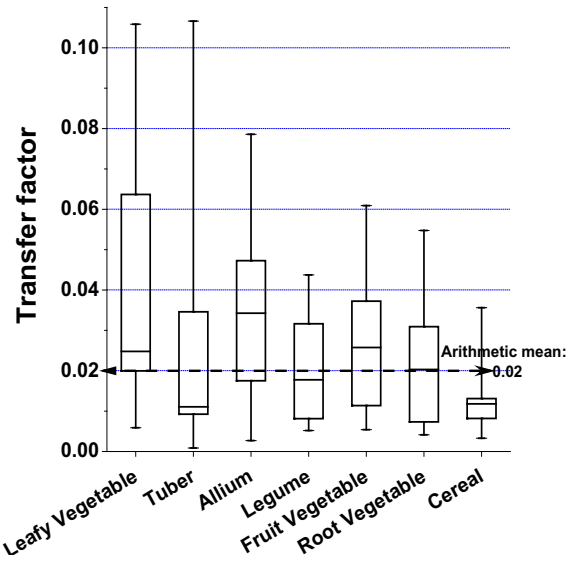

Figure 1. The variations of soil-to-crop transfer factors of Te from different crop groups in Japan. Bars show maximum and minimum values. Boxes show the 75% and 25% values.

Acknowledgement: This work was partially supported by the Agency for Natural Resources and Energy, the Ministry of Economy, Trade and Industry (METI), Japan.

[1] METI (Ministry of Economy, Trade and Industry), Data on the amount of released radioactive materials, http://www.meti.go.jp/press/2011/08/20110826010/20110826010-2.pdf. 2011.
[2] IAEA. *Handbook of Parameter Values for the Prediction of Radionuclide Transfer in Terrestrial and Freshwater Environments*. Technical Reports Series No. 472, IAEA, 2010.
[3] G. Yang, J. Zheng, K. Tagami, S. Uchida, Direct determination of tellurium in Japanese soil and plant samples by sector-field inductively coupled plasma mass spectrometry (submitted).
[4] T. Asami, Metal pollution in Japanese soils (in Japanese), Heiwa Kogyo Co., Ltd., Tokyo, Japan, 2010, p. 447.

* Corresponding author. Tel: +81 43 206 3268; fax: +81 43 206 3267. E-mail address: k_tagami@nirs.go.jp (K. Tagami).

APSORC'13 - 5th Asia-Pacific Symposium on Radiochemistry
Kanazawa, Japan, 22-27 September 2013

Retention of radiocesium incorporated in tree leaves contaminated by fallout of the radionuclides emitted from the Fukushima Daiichi Nuclear Power Plant

Kazuya Tanaka[1], Hokuto Iwatani[2], Aya Sakaguchi[2], Yoshio Takahashi[2], Yuichi Onda[3]
[1] Institute for Sustainable Sciences and Development, Hiroshima University, 1-3-1 Kagamiyama, Higashi-Hiroshima, Hiroshima 739-8530 Japan
[2] Department of Earth and Planetary Systems Science, Graduate School of Science, Hiroshima University, 1-3-1 Kagamiyama, Higashi-Hiroshima, Hiroshima 739-8526 Japan
3 Graduate School of Life and Environmental Sciences, University of Tsukuba, 1-1-1 Tennodai, Tsukuba, Ibaraki, 305-8572, Japan

Abstract – We analyzed fresh and dead leaves collected in forests in Fukushima after the Fukushima Daiichi Nuclear Power Plant (FDNPP) accident using autoradiography. We examined how strongly radiocesium was incorporated in contaminated leaves of Cryptomeria japonica, Quercus serrata and Pinus densiflora. More than half of radiocesium in the contaminated leaves remained in leaf tissues after leaching treatment using pure water, surfactant and acetone.

Keywords – Fukushima, radioactivity, radiocesium, tree leaves, autoradiography

I. INTRODUCTION

A large amount of radionuclides was emitted by the Fukushima Daiichi Nuclear Power Plant (FDNPP) accident. Tree canopies and underlying litters above the soil layers are critical parts when forests are directly contaminated by fallout of radionuclides. Considering cycles of radiocesium in ecosystems, it is very important to know the distribution of radionuclides that were deposited directly on litters or intercepted by tree canopies [1-3]. In this study, we investigated the distribution of radioactivity in various samples of fresh and dead leaves contaminated by the fallout of radionuclides after the FDNPP accident, and examined how strongly radiocesium was incorporated in the leaves [4].

II. SAMPLES AND METHODS

We collected fresh and dead leaf samples (*Cryptomeria japonica*, *Quercus serrate* and *Pinus densiflora*) from Kawamata Town in Yamakiya District, in the northern part of Fukushima Prefecture on December 15, 2011. Leaching experiments were carried out to examine how strongly radiocesium was incorporated in leaf tissues. Leaching experiments consisted of three steps using leachates in the order of pure water, 0.14% of fatty acid potassium salt (surfactant) solution and 100% acetone. Leaf samples were immersed in each leachate and sonicated in an ultrasonic water bath at room temperature for 30 min. Leaf samples before and after each treatment were analyzed using autoradiography. All the samples were treated in the same way to obtain comparable autoradiographs. Reduction of radioactivity by each leaching treatment was evaluated using the differences in signal intensity of autoradiographs before and after leaching treatments.

III. RESULTS AND DISCUSSION

It was clearly observed in autoradiographs that both fresh and dead leaves of *C. japonica* were contaminated by radionuclides (^{134}Cs and ^{137}Cs). Contamination of the fresh leaves was possibly attributed to interception of radionuclides by tree canopies, whereas the dead leaves indicated the direct deposition of radionuclides by fallout and/or washout of radionuclides intercepted by tree canopies. Fallen leaves of *Q. serrata*, which started growing after the FDNPP accident, did not show radioactivity. This means that significant amounts of translocation from other parts to new leaves did not occur. Fallen leaves of *Q. serrata* collected from a litter showed hot spots originating from direct fallout. Needles of *P. densiflora* were also contaminated by fallout. Leaching with pure water removed soluble fractions of radiocesium and radiocesium-bearing particles from the surface of the contaminated leaves, but significant amounts of radioactivity remained. This suggests that foliar absorption occurred in both fresh and dead leaves. The surfactant was used to remove the wax coating from leaf surfaces. This treatment showed that 10 to 20% of radiocesium was removed as a wax fraction of leaf surface. However, the further treatment using acetone did not effectively removed radiocesium. After the three step leaching experiments using pure water, surfactant and acetone, more than half of radiocesium remained in the contaminated leaves. In conclusion, our results indicate that radiocesium in the contaminated leaves is strongly fixed in leaf tissues and is not readily released unless leaf tissues are decomposed.

REFERENCES

[1] Desmet G, Myttenaere C (1988) J Environ Radioact 6:197-202
[2] Bunzl K, Schimmack W, Kreutzer K, Schierl R (1989) Sci Total Environ 78:77-87
[3] Ronneau C, Sombre L, Myttenaere C, Andre P, Vanhouche M, Cara J (1991) J Environ Radioact 14:259-268
[4] Tanaka K, Iwatani H, Sakaguchi A, Takahashi, Y, Onda Y (2013) J Radioanal Nucl Chem 295:2007–2014

Decontamination of Radioactive Cesium in the Soil

Makoto YANAGA, Ayumi OISHI
Department of Chemistry, Graduate School of Science, Shizuoka University

Abstract – Decontamination of radioactive cesium from the agricultural soil was attempted by extraction method using potassium solution. The result of experiments using the soil artificially contaminated with ^{137}Cs showed that radioactive cesium was extracted by potassium solution. However, the extraction rate decreased when time after contamination passed.

Keywords – Decontamination, Radioactive cesium, Nuclear power plant accident, soil

I. INTRODUCTION

A huge amount of radioisotopes was released by the Fukushima Daiichi Nuclear Power Plant accident in March 2011. The radioactive materials released in the atmosphere contaminated not only air but also the earth surface. Decontamination of the radioactive cesium from the soil is one of the current serious problems. In the present work, the decontamination of radioactive cesium from soil, especially agricultural soil, was attempted using the contaminated soil which was made artificially.

II. EXPERIMENTAL

Many commercial plastic containers usually for storing and preserving food were prepared. About 400 grams of commercially obtained mixture of many kinds of soil, used for gardening, was put into each plastic container. Then, 5 ml of ^{137}Cs solution (1 kBq/ml) was dropped in each container. After selected time (from several hours to dozens of weeks) was passed, one container was opened and homogenized in another container.

The homogenized soil was separated to by 60 grams, and each radioactivity was measured. Then, 200 ml of pure water, 1M KNO_3, 1M KI, or 2M KI solution was poured into the beaker which soil was in and the mixture was stirred. After two days standstill, radioactivity of each extract was measured.

III. RESULTS AND DISCUSSION

Relation between the removal rate and time after contamination is shown in Fig. 1. As shown in Fig. 1, it was hardly extracted in pure water. The extraction rate for 1M KI solution and the 1M KNO_3 solution was about the same, and the extraction rate for the 2M KI water solution was higher than them. This indicates that radioactive cesium in the soil was extracted by ion exchange with potassium.

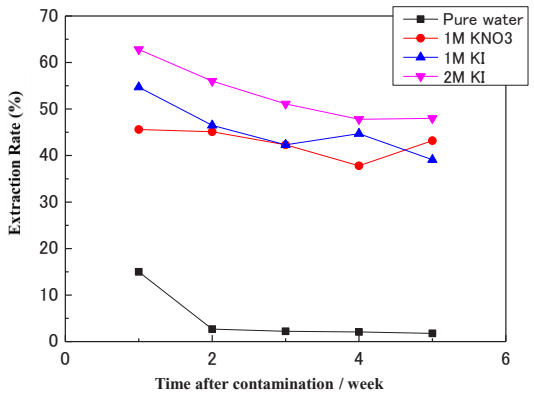

Fig. 1 Time variation of removal rate of ^{137}Cs from the gardening soil.

On the other hand, when time after soil was contaminated by radioactive cesium passed, in the case of any solution used in the present work, the removal rate decreased. It is thought that cesium ion moved to the site that is strongly combined with cesium ion in minerals.

APSORC'13 - 5th Asia-Pacific Symposium on Radiochemistry
Kanazawa, Japan, 22-27 September 2013

Altitude distribution of radioactive cesium at Mt. Fuji due to Fukushima No.1 nuclear power plant accident.

T. Saito[1], Y. Kurihara[2], Y. Koike[2], I. Tanihata[3], M. Fujiwara[3], H. Sakaguchi[3], A. Shinohara[4], H. Yamamoto[5]
[1]Faculty of Comprehensive Human Sciences, Shokei Gakuin University
[2] School of Science and Technology, Meiji University
[3] Research Center for Nuclear Physics, Osaka University
[4]Graduate School of Science, Osaka University
[5]Department for the Administration of Safety and Hygiene, Osaka University

Abstract – Altitude distributions of radioactive cesium (^{134}Cs and ^{137}Cs) fallout at Mt. Fuji due to Fukushima No.1 nuclear power plant accident have been investigated. Radioactive cesium from Fukushima No.1 nuclear plant is found to reach at the height of 2700 m. It is inferred that some amounts of radioactive cesium are attributable to the global fallout due to the nuclear weapons tests in the atmosphere.

Keywords – radioactive cesium, altitude distribution, Mt. Fuji

I. INTRODUCTION

Radioactive materials, released by the Fukushima No.1 nuclear power plant accident have been spread through the atmosphere, and have deposited on the soil surface all over Japan. Over the past two years, a considerable number of studies have been conducted on deposition of radioactive materials on the soils, but very few attempts have been made for measuring the altitude distribution of radioactive materials. In this study, the altitude distribution of radioactive cesium (^{134}Cs and ^{137}Cs) at Mt. Fuji, and floated height of radioactive plume from the power plant have been investigated.

II. EXPERIMENTALS

The soil samples at Mt. Fuji were collected in Sep. 2011 and Sep. 2012, and its details are given in Table. Each sample was packed in the U-8 container, and activities were determined by means of γ-ray spectrometry with a HPGe semiconductor detector. The 605 keV and 662 keV γ-rays from ^{134}Cs and ^{137}Cs, respectively, were used for the determination of radioactivity fallout, and the decay correction of measured activities were made for the date of Mar. 11, 2011.

Table Sampling point information of Mt. Fuji.

Sampling date	Climbing route	Altitude (m)	Remarks
Sep.23. 2011	Fujinomiya	3720 - 2502	scoriaceous lava
Sep.10. 2012	Gotenba	2800 - 1491	scoriaceous lava

III. RESULT AND DISCUSSIONS

The altitude distribution of radioactive cesium inventory (Bq/m^2) and the activity ratios of ^{134}Cs/^{137}Cs are given in Fig.1. Figure 1 shows that the ^{134}Cs and ^{137}Cs inventories are in the range of triple-digit, being higher in the lower altitude.

The significant amount of radioactive cesium at the place lower than the altitude of 2500 m was detected, while radioactivity levels at the altitude higher than 2700 m was extremely low, especially for the ^{134}Cs activity. Therefore, it is suggested that the radioactive plume, which was caused due to Fukushima No.1 nuclear power plant accident, was floated at the upper limit of about 2500 m around of Mt. Fuji.

The activity ratio of ^{134}Cs/^{137}Cs is known as about 1, but in this study, most of the ratio is less than 1. It is inferred from these data that some amounts of radioactive cesium is attributable to the global fallout due to the nuclear weapons tests in the atmosphere.

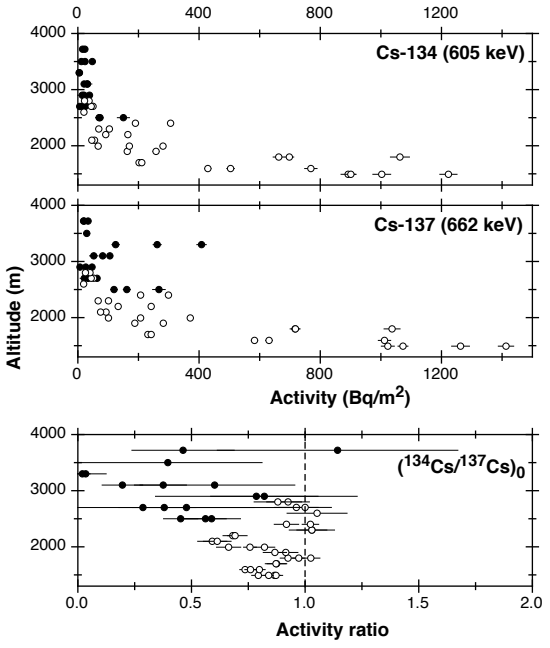

Fig.1: Radioactivities of ^{134}Cs and ^{137}Cs and the activity ratios of ^{134}Cs/^{137}Cs in scoriaceous lava at Mt. Fuji.
(filled cycle: Fujinomiya route, open cycle: Gotenba route)

APSORC'13 - 5th Asia-Pacific Symposium on Radiochemistry
Kanazawa, Japan, 22-27 September 2013

Isotope Compositions of Strontium in Environmental Samples in Fukushima Prefecture

Y. Shibahara[1], S. Fukutani[1], T. Fujii[1], T. Kubota[1], M. Yoshikawa[2], T. Shibata[2], T. Ohta[3], K. Takamiya[1], N. Sato[1], M. Tanigaki[1], Y. Kobayashi[1], R. Okumura[1], H. Yoshinaga[1], H. Yoshino[1], A. Uehara[1], S. Mizuno[4], T. Takahashi[1], and H. Yamana[1]

[1]Research Reactor Institute, Kyoto University
[2]Institute for Geothermal Sciences, Kyoto University
[3]Faculty of Engineering, Hokkaido University
[4]Nuclear Power Safety Division, Fukushima Prefectural Government

Abstract – Strontium was recovered from environmental samples in Fukushima prefecture. The isotopic composition of ^{84}Sr, ^{86}Sr, ^{87}Sr, ^{88}Sr, and ^{90}Sr was evaluated by mass spectrometry and β spectrometry. The source of radioactive strontium released during the Fukushima Daiichi nuclear power plant accident was discussed.

Keywords– strontium-90, strontium isotope ratio, mass spectrometry

On the accident of Fukushima Daiichi nuclear power plant, huge amount of fission product containing radioactive strontium were widely released. The most important radioactive strontium are ^{89}Sr and ^{90}Sr, whose half-lives are 50.5 days and 28.90 years, respectively. The cumulative yields of thermal neutron induced fission of ^{235}U are 4.73% (^{89}Sr) and 5.77% (^{90}Sr) [1]. As shown in Fig. 1, the isotopic composition of Sr via fission of uranium and plutonium [1] are totally different from the natural abundance. The information on the origin of radioactive strontium release would also be obtained from the analytical data.

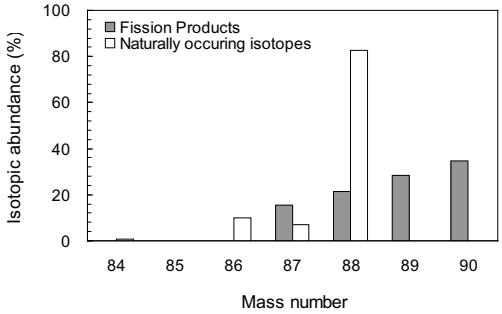

Fig. 1 Isotopic abundances of Sr. The sum of cumulative fission yields of Sr isotopes from ^{235}U by thermal neutron irradiation [1] was set to 100% for comparing them with the natural abundance. The natural abundance of ^{84}Sr is 0.56%. The fission yields of ^{84}Sr and ^{86}Sr are less than 10^{-4}%.

The purpose of the present study is to enhance the analysis of Sr isotopes in environmental samples in Fukushima prefecture for safety assessment about ^{90}Sr dose. Generally, concentration of ^{90}Sr is determined by β spectrometry. Since this method gives no data of stable isotopes, the thermal ionization mass spectrometry (TIMS) was applied for high precision isotopic analysis in parallel. The isotopic composition of ^{84}Sr, ^{86}Sr, ^{87}Sr, ^{88}Sr, and ^{90}Sr was evaluated

Environmental samples (soils, plants, and so on) were immersed in concentrated HNO_3 and heated at 413 K. After evaporation of HNO_3, diluted HNO_3 was added and this was used as the source material. Strontium was recovered from the samples by extraction chromatography with UTEVA-resin and Sr-resin following ion-exchange chromatography with ion-exchange resin. Concentration of recovered strontium was analyzed with a quadrupole inductively coupled plasma mass spectrometer, and that of ^{90}Sr was analyzed by β spectrometry. Correlation between ^{90}Sr and ^{137}Cs was also checked. These samples were supplied for TIMS.

Isotopic ratios of Sr were measured with a TIMS (Triton-T1, Thermo Fisher Scientific). About 100 ng of strontium was loaded on a rhenium single filament with TaO activator. The isotopic reference material SRM987 was used as the standard. Our analytical result of SRM987 agreed with the certified value within 2σ analytical error. As a possible source of ^{89}Sr and ^{90}Sr, on the other hand, 10 mg of UO_2 of natural uranium was irradiated at the Kyoto University Research Reactor. Similar to the environmental samples, strontium was recovered from UO_2 irradiated and analyzed. Since the amounts of ^{89}Sr and ^{90}Sr were much smaller than those of stable Sr isotopes, their mass spectra were obtained with a secondary electron multiplier detector. The isotopic data obtained are discussed by conjunction with the results of β spectrometry.

[1] K. Shibata *et al.*, *J. Nucl. Sci. Technol.*. **48**, 1 (2011).

Distribution of radioactive caesium in the North Pacific one year and a half after the Fukushima Dai-ichi Nuclear Power Plant accident

K. Tsujita[1], A. Hasegawa[1], N. Harada[2], T. Yamagata[2], H. Nagai[2], M. Aoyama[3]
[1]Graduate School of integrated Basic Sciences, Nihon University
[2]College of Humanities and Sciences, Nihon University
[3]Geochemical Research Department, Meteorological Research Institute

Abstract – In stations off Fukushima, ^{137}Cs concentration in surface seawater were 3.9±0.2 and 2.7±0.2 mBq/kg. Between stations off Fukushima and open ocean station (K2; 47°N, 160°E), average ^{137}Cs concentration was 2.9±0.2 mBq/kg. From 160°E to 170°W along 47°N in the North Pacific, average ^{137}Cs concentration was 4.9±0.2 mBq/kg. It was higher than that off Fukushima, and ^{134}Cs was also detected. Thus, the effects of the Fukushima Dai-ichi Nuclear Power Plant accident were observed. But it was not observed in Bering Sea and east of 170°W.

Keywords – Fukushima Dai-ichi Nuclear Power Plant; ^{137}Cs; ^{134}Cs; North Pacific

I. INTRODUCTION

On 11 March 2011, the accident occurred at the Fukushima Dai-ichi Nuclear Power Plant (F1NPP) due to the Tohoku earthquake and tsunami. A large amount of ^{134}Cs ($T_{1/2}$=2.06 y) and ^{137}Cs ($T_{1/2}$=30.07 y) were released to the environment. The estimated total amounts of ^{137}Cs released from the F1NPP reactors to the atmosphere and ocean were 15 [1] and 3.5±0.7 PBq [2], respectively. In this study, we measured the distributions of ^{134}Cs and ^{137}Cs in seawater off Fukushima and in the North Pacific to investigate the spread of the radionuclides about a year and a half after the accident.

II. EXPERIMENTAL

Seawater samples (20 L) were collected with an underway pump and a large-volume water sampler during the KH-12-4 cruise (23 Aug. to 3 Oct. 2012). The sample was acidified to pH1.8 by adding concentrated nitric acid, stirred for 1 hour after adding 200 mg of stable cesium, then stirred again for 1 hour after adding 4 g of ammonium phosphomolybdate (AMP). The sample was settled for 12 hours and filtrated to collect AMP-Cs compound onto a membrane filter (0.45 μm). The AMP-Cs compound was dried for 12 hours at 100 °C, transferred to a counting tube, then measured ^{134}Cs (Eγ=604 keV, 795 keV) and ^{137}Cs (Eγ=661 keV) gamma rays using a well-type HPGe detector.

III. RESULTS AND DISCUSSION

In regions off Fukushima, ^{137}Cs concentration in surface water from BD-02 and 03 located 30 km east of F1NPP were 3.9±0.2 and 2.7±0.2 mBq/kg, respectively. The ^{137}Cs concentrations reduced by two orders of magnitude from those observed in MR-11-03 cruise (Apr. 2011) [3] and KOK cruise (Jun. 2011) [4]. For distant stations about 190 km south (BD-01) and 250 km east (BD-04) of F1NPP were 1.4±0.1 and 1.3±0.1 mBq/kg, respectively. It was almost same as those before the accident (1.5 mBq/kg) [5]. Between off Fukushima and open ocean (47°N, 160°E, BD-05~07), average ^{137}Cs concentration in surface water was 2.9±0.2 mBq/kg, still high compared to that before the accident (1.8 mBq/kg) [6]. From 160°E to 170°W along 47°N (BD-08~14), average ^{137}Cs concentration was 4.9±0.2 mBq/kg. It is higher than those off Fukushima. For all stations of high ^{137}Cs concentration, ^{134}Cs were also detected. In those regions the effects of the F1NPP accident were observed. In Bering Sea and east of 170°W (BD-15~17), ^{137}Cs concentration in surface water were equal to or lower than those before the accident and ^{134}Cs were not detected. In those regions the effects of the F1NPP accident were not observed.

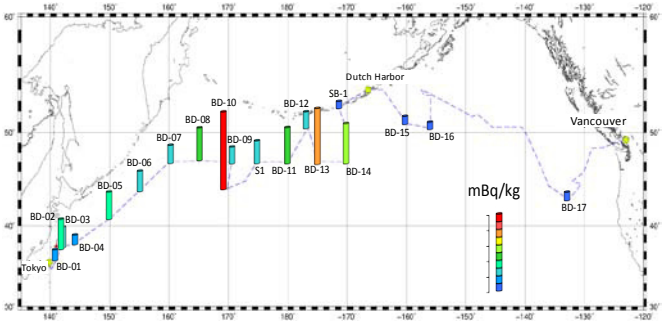

Fig.1 The surface ^{137}Cs concentration in the North Pacific and the KH-12-4 cruise track

REFERENCES

[1] NERH (Nuclear Emergency Response Headquarters, Government of Japan) (2011) Report of Japanese Government to the IAEA Ministerial Conference on Nuclear Safety—The Accident at TEPCO's Fukushima Nuclear Power Stations.
[2] D. Tsumune et al., J. of Environ. Radioact., **111** (2012) 100e108.
[3] M. C. Honda et al., Geochemical J., 46 (2012) e1- e9.
[4] N. Harada, Bachelor thesis (2011).
[5] K. Buesseler et al., Environ. Sci. Technol., 45(2011) 9931-9935.
[6] K. Hirose et al., Deep-Sea Res. II, 50 (2003) 2675-2700.

APSORC'13 - 5th Asia-Pacific Symposium on Radiochemistry
Kanazawa, Japan, 22-27 September 2013

Image analysis for the study of radiocesium distribution in coniferous trees: two years after the Fukushima Daiichi Nuclear Power Plant accident

Haruka Minowa
Radioisotope Research Facility, The Tokyo Jikei University School of Medicine

Abstract – The accident at the Fukushima Daiichi Nuclear Power Plant in March 2011 resulted in the deposition of radioactive fallout over wide area in eastern Japan. Environmental samples were examined with an imaging plate to investigate the characteristics and the behavior of fallout deposits. In the autoradiographs, so-called "hot particles" were evident in many samples. There were no particulate contamination on new leaves which grown after the accident. The state and adsorption amount of fallout was different depending on the locality and the timing of sampling. The results of this study confirm that deposition on the leaves and the barks would remain several years and radiocesium concentration would be decrease with the growing of new leaves.

Keywords – radiocesium, autoradiography, coniferous tree

I. INTRODUCTION

Radioactive fallout from the March 2011 disaster at the Fukushima Daiichi Nuclear Power Plant (NPP) spread across much of eastern Japan. Deposition of fallout on land was affected by rain, wind, and geographical features [1]. The purpose of this research is to investigate the characteristics and behavior of the fallout. Because it was early spring in eastern Japan at the time of the accident, many trees were bare of leaves except for evergreen trees include coniferous trees. Radioactivity on the perennial leaves of coniferous trees would be an appropriate indicator for the monitoring of the radionuclides in the environmental system.

II. SAMPLES AND METHODS

Samples were collected at Naraha-machi, Hirono-machi and Iwaki city in Fukushima prefecture, which are located approximately 20 to 50km in south or southwest side from Fukushima Dai-ichi NPP. It was considered that the dried deposition were more principal than the wet deposition in these area [2]. As a typical coniferous tree, Pine trees (*Pinus thunbergii, Pinus densiflora*), Japanese cypress (*Chamaecyparis obtusa*), Japanese cedar (*Cryptomeria japonica*), and Chinese juniper (*Juniperus chinensis*) were selected.

Samples were flattened and covered with a wrapping film and exposed to an imaging plate BASIII 2040 (Fujifilm Co., Tokyo, Japan) for time periods ranging from overnight to one week. Autoradiographs were scanned using an image analyzer Typhoon FLA7000 (GE Healthcare Japan Co., Tokyo, Japan).

III. RESULTS AND DISCCUSION

Autoradiographs are shown in Figure 1 and 2. Samples were collected from Naraha-machi at Nov. 2012. It was observed that the fallout seemed to be granular, so-called "hot particles". These radioactive particles had not moved from the initial site of adhesion on the leaf despite repeated exposure to rain. Particulate contaminations were distributed only the bottom leaves spread before the accident and did not seen in the top leaves grown after the accident. This confirms that particulate deposition on the leaves and the barks would remained several years and radiocesium concentration would be decrease with the growing of new leaves.

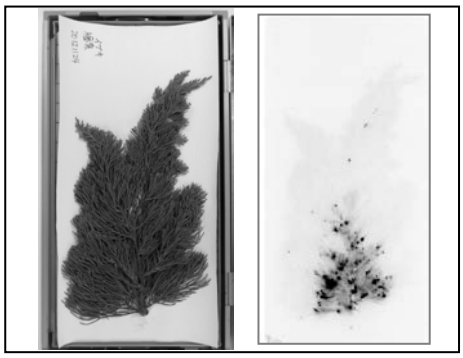

Fig. 1. Leaves of *Juniperus chinensis* from Naraha-machi at Nov. 2012. Particulate contaminations were seem only on the bottom leaves and not seem on the top leaves.

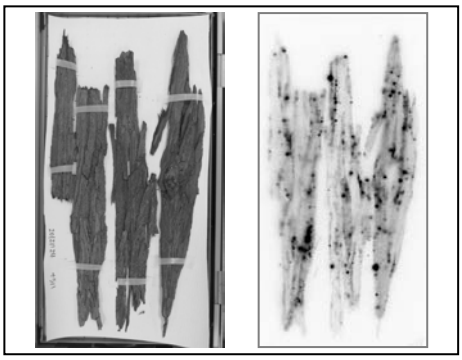

Fig. 2. Tree barks of *Chamaecypars obtusa* from Naraha-machi at Nov 2012. Heterogeneously contaminations were visible throughout on the bark.

[1] Kinoshita et al. (2011) PNAS 108, 19526-19529
[2] Katata et al. (2012) J. Environ. Radioact. 109, 103-113

Distribution of Iodine-129 in off Fukushima and the North Pacific one year and a half after the Fukushima Dai-ichi Nuclear Power Plant accident

A. Hasegawa[1], T. Yamagata[2], H. Nagai[2], M. Aoyama[3], H. Matsuzaki[4]
[1]Graduate School of integrated Basic Sciences, Nihon University
[2]College of Humanities and Sciences, Nihon University
[3]Geochemical Research Department, Meteorological Research Institute
[4]School of Engineering, the University of Tokyo

Abstract – High ^{129}I concentrations were observed in samples from stations off Fukushima (BD02, 03) located 30 km away from Fukushima Dai-ichi Nuclear Power Plant (F1NPP). In these stations, ^{129}I inventory down to 100 m water depth was not decrease since three month after the F1NPP accident. In adjacent stations off Fukushima (BD01, 04), ^{129}I concentrations were almost identical to those observed in seawater collected in the Kuroshio region before the F1NPP accident. In the North Pacific (BD05~17), ^{129}I concentrations in surface seawater were 2 times higher than those in the Kuroshio region.

Keywords – Iodine-129, seawater, Fukushima Daiiti Nuclear Power Plant, North Pacific

I. INTRODUCTION

The Fukushima Dai-ichi Nuclear Power Plant (F1NPP) was damaged by the great earthquake of magnitude 9.0 and the associated tsunami on 11 March 2011. As a result, Many radionuclides such as, ^{134}Cs (2.06 yr), ^{137}Cs (30.2 yr), ^{131}I (8.01 d), ^{129}I (1.57 x 10^7 yr) were discharged from F1NPP into the ocean. These nuclides were transported by the Oyashio current and the Kuroshio current, and supposed to spread along the Kuroshio extension. Many data for ^{137}Cs discharged into ocean from F1NPP in seawater has already reported[1][2] but few data for ^{129}I have reported[3][4].

A large amount of ^{129}I discharged from nuclear activities such as, weapons testing until the 1970's, nuclear power plant accidents, nuclear fuel reprocessing plants, into the environment. As a result, most of ^{129}I present in the environment is anthropogenic, and ^{129}I concentrations in seawater are higher than pre-nuclear activities. Due to the F1NPP accident, ^{129}I concentration in seawater may enhanced. In this study, we measure of ^{129}I concentration in seawater, to investigate the influence of the F1NPP accident in the North Pacific.

II. EXPERIMENTAL PROCEDURE

Seawater samples (1L) were collected with an underway pump and a large-volume water sampler during the cruise of the R/V Hakuho-maru in 23 Aug. to 3 October 2012 (KH-12-4). The cruise track and positions of the station are shown in Fig. 1. First, seawater samples were filtered through a membrane filter (0.45 μm), them iodine carrier (I^- : 1 mg) were added to filtered seawater samples. Secondly, separation of iodine from seawater samples has carried out solvent extraction and back-extraction. The molecular iodine extracted into carbon tetrachloride (CCl_4), then back-extracted into aqueous layer. Finally, silver nitride solution was added to make silver iodide precipitation. The $^{129}I/^{127}I$ ratios of samples were measured by Accelerator Mass Spectrometry (AMS) at MALT, the University of Tokyo. All measured ratios were normalized to the standard reference material having $^{129}I/^{127}I=63.6 \times 10^{-12}$(S-Puredue2).

III. RESULTS AND DISCUSSION

^{129}I concentrations in surface seawater in the Western North Pacific (BD05~09) and Eastern North Pacific (BD11~17) were almost constant (12.7~17.1 x 10^6 atoms/kg). On the other hand, ^{129}I concentrations in stations off Fukushima were higher than those in the North Pacific. Maximum ^{129}I concentration 71.4 x 10^6 atoms/kg was observed at BD03 (about 30 km away from F1NPP). ^{129}I inventory down to 100 m water depth at BD03 was 35.3 x 10^{11} atoms/m^2, which is comparable to those observed three month after the F1NPP accident (KOK cruise). Therefore, the effects of the F1NPP accident still remain in this region. In other stations off Fukushima (BD01 and BD04), ^{129}I concentrations were almost identical to those observed in seawater collected in the Kuroshio region before the F1NPP accident (KT-09-13). In the North Pacific (BD05~17), ^{129}I concentrations were 2 times higher than those in the Kurosio region. It considered with high ^{129}I concentration seawater inflow from the Bering Sea.

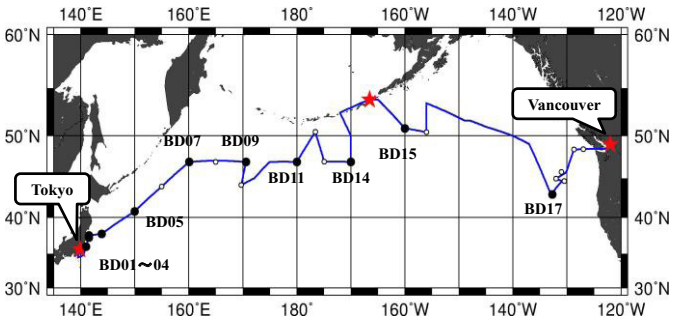

Fig. 1 The KH-12-4 cruise track and sampling stations

[1] http://www.mri-jma.go.jp/Topics/hotyouhi/houtyouhi_sea.html
[2] P. P. Povinec et al., Biogeosciences Discuss, 10, 6377-6416, 2013
[3] T. Suzuki et al., Biogeosciences Discuss, 10, 1401-1419, 2013
[4] X. Hou et al., Environ. Sci. Technol. 47, 3091-3098, 2013

APSORC'13 - 5th Asia-Pacific Symposium on Radiochemistry
Kanazawa, Japan, 22-27 September 2013

Agricultural Implications for Fukushima Nuclear Accident

Tomoko M. Nakanishi

Graduate School of Agricultural and Life Sciences, The University of Tokyo

Abstract – The overview of our research projects for Fukushima is presented including how they were derived. Then, where the fallout was found, right after the accident, is briefly summarized for soil, plants, trees, etc. The time of the accident was late winter, there were hardly any plants growing except for the wheat in the farming field. Most of the fallout was found at the surface of soil, tree barks, etc., which were exposed to the air at the time of the accident. The fallout found was firmly adsorbed to anything and did not move for months from the site when they first touched. Therefore, the newly emerged tissue after the accident showed very low radioactivity. The fallout contamination was not uniform, therefore, when radiograph of contaminated soil or leaves were taken, fallout was shown as spots. Generally, plants could not absorb radiocesium adsorbed to soil. Some of the results we obtained will be presented.

Keywords – *Fukushima nuclear accident, research in agiriculture, research project, research site, fallout, the way of contamination*

Introduction

After the accident of Fukushima Daiichi nuclear power plant, thousands of measuring data have been piling up, especially in the web sites of government agencies. However, most of them are two kinds of the data. One is the radio activities of the places, including soil, air dust or sea water and the other is the measurement of the foods. These are just the monitoring data and it is difficult to find out the research data related to agriculture, such as, how much amount of radioactivity was found or estimated when the plants were grown in the contaminated field or how much radioactivity was accumulated in mountains and what about the contamination of river water coming from the mountain, etc.

Research groups

Right after the accident, about 40 academic staffs in our Graduate School had started the research project for Fukushima in plants, soil, animals, fish, etc. Our activities were classified into several groups as follows but most of them were developed based on voluntary activities. research project for Fukushima for plants, soil, animals, fish, etc. Our activities were classified into several groups as follows but most of them were developed based on voluntary activities.

Research projects

Influence of fallout (distribution & movement)

1. crop plants and soils
2. stock raising & dairy products
3. fishery
4. environment, including wild life
5. radiation measurement & radiochemistry
6. science communication

Research sites

Results & discussion

The Cs movement in soil showed that Cs is so firmly adsorbed on soil and there was no further washout of Cs by rain, therefore, Therefore, it was suggested that this thin contaminated surface soil can thus be collected and buried on site, leaving the land safe to work again, as the radionuclides are unlikely to be leached from the soil. The downward movement of the radiocesium in soil was further monitored. The study of fruit tree showed that Cs was transferred from bark surface to fruits and there was not any radiocesium taken up from roots. Animals are now investigated how radiocesium is distributed among the tissues. We have now expanded our investigations into a long-term study that will also cover trees and fisheries.

Reference

Agricultural Implications for Fukushima Nuclear Accidents. Nakanishi, T.M. and Tanoi, K. ed. Springer (2013)

APSORC'13 - 5th Asia-Pacific Symposium on Radiochemistry
Kanazawa, Japan, 22-27 September 2013

Concentration of Radiocesium in Rice, Vegetables, and Fruits Cultivated in Evacuation Area at Okuma Town, Fukushima

Kenji Ohse[1], Kyo Kitayama[1], Seiich Suenaga[2], Kiyoyuki Matsumoto[2], Akira Kanno[1], Chika Suzuki[1], Kencho Kawatsu[1], Hirofumi Tsukada[1]
[1]Fukushima Future Center for Regional Revitalization, Fukushima University
[2] Okuma Government Office

Abstract – Rice, vegetables, and fruits were cultivated in the evacuation area at Okuma town, and the radiocesium concentration of the crop samples cultivated in contaminated and decontaminated soil was compared. Decrease of the concentration in every crop by decontamination was observed. The TF of brown rice was higher than previous reports.

Keywords – evacuation area, test cultivation, radiocesium

I. INTRODUCTION

Okuma Town which Fukushima Daiichi nuclear power plant locates, the whole region contaminated severely by radioactive nuclides including ^{134}Cs and ^{137}Cs and was designated the evacuation area. The prospect for reactivate of agriculture was not found in the regions. However, in order to obtain the scientific data for recultivation in the future, test cultivations of several crops in the contaminated and decontaminated soils and collected fruits grown in the town were carried out. In this study, the concentration and translate factor of radiocesium in rice, vegetables, and fruits cultivated in the contaminated and decontaminated sites are reported.

II. MATERIALS AND METHODS

Test cultivation site, which had paddy and upland field, was located about 6 km far from Fukushima Daiichi Nuclear Power Plant. Each paddy and upland field was divided into two parts, which was contaminated and decontaminated by removing surface soil. Several crops including rice plant, eggplant, green soybean, sweet potato, pumpkin, and cabbage were cultivated in both sites. After harvest, the crops were washed and separated in several parts. They were dried and pulverized to powder. An ancient black rice plant was also harvested from other paddy field. Soil samples were corrected for the depth of 30 cm, cut into sections 0-2, 2-5, 5-10, 10-15, 15-20, 20-25, 25-30 in depth, oven dried and sieved 2 mm mesh. ^{134}Cs and ^{137}Cs in the samples were determined by germanium semiconductor detector.

III. RESULTS AND DISSCUSSION

The abundance of radiocesium in the soils at contaminated upland, decontaminated upland, contaminated paddy, decontaminated paddy and ancient black rice paddy field was 3680, 877, 1820, 1640, and 1070 kBq m^{-2}, respectively and the weighted average of the concentration for the depth of 15 cm was 31.6, 7.46, 15.4, 13.7, and 14.8 kBq kg^{-1},. The concentration of radiocesium in the decontaminated upland soil decreased 1/4 by removing the soil of 0-15 cm depth. However, the radiocesium concentration in decontaminated paddy soil was slightly decrease compared to the contaminated paddy soil because the paddy field was disturbed by animals and radiocesium mixed in deeper before cultivation.

The radiocesium concentration in crops and their transfer factor (TF) were shown in Table 1. The concentration of radiocesium in every crop cultivated in the decontaminated field was lower than that cultivated in the contaminated field. The concentration of radiocesium in eggplant and pumpkin of edible part cultivated in the decontaminated field was lower than standard limit (100 Bq kg^{-1}). However, the TF values of the crops cultivated in the contaminated fields were within a factor of 3 to those cultivated in the decontaminated fields. More techniques are required to decrease the radiocesium concentration in crops.

Table 1 Concentration and translate factor of radiocesium in crops.

Crop	Sampling date	contaminated field			decontaminated field		
		Cs-134	Cs-137	TF	Cs-134	Cs-137	TF
		(Bq kg^{-1} fresh weight)			(Bq kg^{-1} fresh weight)		
rice plant							
brown rice	3-Oct-12	117	195	0.0203	82.7	139	0.0162
rice hull	3-Oct-12	264	438	0.0456	197	322	0.0379
reaf and straw	8-Aug-12	89.0	132	0.0144	39.2	57.5	0.0071
reaf and straw	3-Oct-12	185	300	0.0315	113	187	0.0219
ancient black rice							
brown rice	3-Oct-12	258	424	0.0461			
rice hull	3-Oct-12	474	762	0.0835			
reaf and straw	22-Aug-12	178	271	0.0303			
reaf and straw	3-Oct-12	285	464	0.0506			
eggplant							
edible part	8-Aug-12	58.5	90.0	0.0047	7.01	11.0	0.0024
edible part	3-Oct-12	32.4	52.9	0.0027	7.39	11.5	0.0025
stalk	3-Oct-12	69.1	116	0.0059	12.2	20.4	0.0044
reaf	3-Oct-12	161	262	0.0134	46.4	77.1	0.0166
green soybean							
bean	3-Oct-12	161	257	0.0132	69.4	116	0.0249
pod	3-Oct-12	240	395	0.0201	97.0	158	0.0342
stalk	3-Oct-12	302	492	0.0251	91.8	153	0.0329
reaf	3-Oct-12	627	992	0.0512	136	226	0.0486
sweet potato							
edible part	3-Oct-12	151	261	0.0130	84.4	139	0.0300
coat	3-Oct-12	223	356	0.0183	68.6	115	0.0246
vine	3-Oct-12	171	284	0.0144	101	163	0.0354
reaf	3-Oct-12	215	361	0.0182	137	226	0.0487
pumpkin							
edible part	3-Oct-12	113	184	0.0094	13.4	21.7	0.0047
coat	3-Oct-12	145	234	0.0120	16.0	24.5	0.0054
gut	3-Oct-12	191	319	0.0161	14.6	22.6	0.0050
vine and reaf	3-Oct-12	143	234	0.0119	41.7	62.8	0.0140
cabbage							
head	3-Oct-12	250	402	0.0206	148	241	0.0522
un-head reaf	3-Oct-12	375	634	0.0319	321	520	0.1129

APSORC'13 - 5th Asia-Pacific Symposium on Radiochemistry
Kanazawa, Japan, 22-27 September 2013

Isotopic U, Pu, Am and Cm signatures in environmental samples from the Fukusima Dai-ichi Nuclear Power Plant accident

Masayoshi Yamamoto[1], Aya Sakaguchi[2], Shinya Ochiai[1],Takahiro Takada[1], Seiya Nagao[1], Peter Steier[3]
[1] Low Level Radioactivity Laboratory, KINET, Kanazawa University, Nomi, Ishikawa 923-1224, Japan
[2] Graduate School of Science, Hiroshima University, Higashi-Hiroshima, 739-8526, Japan
[3] VERA-Laboratory, Faculty of Physics, University of Vienna, Währinger Str. 17, A-1090 Vienna, Austria

Abstract – Alpha-ray spectrometry and AMS measurements of U, Pu Am and Cm isotopes isolated from black materials of roadsides collected at areas within the 20-km exclusion zones (Minami-Souma, Namie, Futaba and Okuma Towns) and Iitate Village are reported. For most of the samples, low levels of ^{236}U, ^{238}Pu, $^{239,240}Pu$, ^{241}Am, ^{242}Cm and $^{243,244}Cm$ were successfully determined. The results provide a coherent isotopic data set, indicating that traces of U and transuranic nuclides were released into the environment without their large fractionations, probably with forms of fine particles. These data are also very important in order to check the validity of estimation of fuel compositions in the FDNPP.

Keywords – FDNPP accident, ^{236}U, transuranic elements, black materials of roadside, alpha-ray spectrometry, AMS

I. INTRODUCTION

In the Fukushima Dai-ichi Nuclear Power Plant (FDNPP) accident which occurred in connection with the *M9* Great East Japan Earthquake and subsequent tsunami on 11 March 2011, large amounts of radionuclides, especially volatile ones such as ^{131}I, ^{134}Cs and ^{137}Cs, have been accidently released into the environment from the FDNPP. By broadly survey of these nuclides and researches, whole picture about levels and spreading areas of contaminants has been becoming clear, together with the situation of plant accident. However, information on releases of U and transuranic nuclides as refractory elements in fuel core was extremely limited due to the difficulties of analyzing these nuclides. In this paper, we intended to clarify a full picture about these elements released into the environment. For this purpose, ^{236}U, Pu isotopes (^{238}Pu, ^{239}Pu and ^{240}Pu), ^{241}Am and Cm isotopes (^{242}Cm and $^{243,244}Cm$) were measured for roadside dust collected at the Fukushima areas heavily contaminated. Their released levels and isotopic compositions will be discussed, compared with the fuel compositions in FDNPP estimated by Nishihara et al. (2012).

II. MATERIAL AND METHODS

The road dusts, called "Black Materials", whose color is apparently black, are browned in a corner and/or dip of residential streets and roadside by wind and rain. These materials are composed with fine aerosol particles, fine car-cut asphalt materials, residue of lichens, soil and so on, and contaminated with extremely high levels of radionuclides released. They seemed to be suitable for getting information on isotopic composition of trace amount of U and transuranic elements. The samples were mainly collected from areas within the 20-km exclusion zones (Minami-Souma, Namie, Futaba and Okuma Towns) in Sep.- Nov., 2012. Also were samples taken from Iitate Village heavily contaminated. The collected samples were air-dried, and sieved through a 2-mm mesh to remove pebbles and big plant remains, and pulverized in an agate mortar to obtain homogeneous samples. After chemical separation of each element, Pu (^{238}Pu and $^{239,240}Pu$), ^{241}Am and Cm (^{242}Cm and $^{243,244}Cm$) were determined by alpha-ray spectrometry, respectively. Uranium-236 was determined by AMS installed at VERA-Laboratory, University of Vienna (Vienna, Austria).

III. RESULTS AND DISCUSSION

The collected black materials samples were found to be contaminated with extremely high levels of ^{134}Cs and ^{137}Cs over 1000 kBq/kg by the FDNPP accident. More than 100 samples from areas within the 20 km-exclusion zones were determined for ^{238}Pu, $^{239,240}Pu$, ^{241}Am. ^{242}Cm and $^{243,244}Cm$ by α–ray spectrometry. Furthermore, in some samples, ^{236}U was successfully determined by AMS.

The results provided a coherent isotopic data set as follows: 1) traces of $^{239,240}Pu$ (range: 0.0n-1.8 Bq/kg) and high levels of $^{238}Pu/^{239,240}Pu$ activity ratios (range; ca.1-2.7, but mostly around 2.1-2.4) were detected; for samples showing $^{238}Pu/^{239,240}Pu$ ratios of more than 2 (most (or all) of Pu detected is due to the accident); 2) $^{241}Am/^{239,240}Pu$ activity ratios were in the range from 0.32-0.75 with the mean value of 0.53 ± 0.12 (n=35); 3) $^{242}Cm/^{243,244}Cm$ activity ratios (decay-corrected to 11 March, 2011) were 25.1 ± 8.9 (n=61) on average; 4) $^{242}Cm/^{239,240}Pu$ activity ratios (decay-corrected to 11 March, 2011) were 33.6 ± 10.6 (n=52) on average; and 5) $^{236}U/^{239,240}Pu$ activity ratios were in the range of (1.96-18.4) $x10^{-4}$ with the weighted mean value of $7.87x10^{-4}$ (n=12).

When these activity ratios are compared with those of fuel compositions in the FDNPP estimated by Nishihara et al (2012) of the JAEA group, fairly good agreement was found, indicating that traces of U and transuranic nuclides, probably with forms of fine particles, were released into the environment without their large fractionations.

K. Nishihawa et al. (2012), JAEA-Data/Code, 2012-018.

Influence of the Fukushima Daiichi nuclear disaster on the tritium concentration in the precipitation of Kanazawa city

Yoshimune Yamada[1], Kaeko Yasuike[1], Toshiyuki Kawabata[2], Akihiro Fujii[2], Hitoshi Kakimoto[2]
[1]Faculty of Pharmaceutical Sciences, Hokuriku University, Kanagawa-machi, Kanazawa, 920-1181, Japan
[2]Ishikawa Prefectural Institute of Public Health and Environmental Science, Taiyogaoka, Kanazawa, 920-1154, Japan

Abstract – The variation in tritium concentration in the precipitation of Kanazawa city was measured the day after the Fukushima Daiichi nuclear disaster, which occurred on 11 March, 2011. The most interesting result in the period from March to August 2011 is that a secondary peak of 4.6 Bq/L was observed on 22 March after the maximum peak of 15.0 Bq/L on 16 March. This fact suggests that a sudden release of a large amount of tritium from the Fukushima Daiichi nuclear power plant occurred between 21 March and 22 March, followed by the release from 11 March to 15 March. Another interesting result is that dramatic increases in the tritium concentration of 131.6 Bq/L and 99.9 Bq/L were observed on 30 May and 13 June in the variation patterns of the tritium concentration in the precipitation of Kanazawa city. These increases may have been caused by wind blowing down from the upper atmosphere during a storm. A large amount of tritium which had been released by hydrogen explosions from the Fukushima Daiichi nuclear reactors was considered to exist in the bulk air in the upper atmosphere.

Keywords – Tritium, Fukushima Daiichi nuclear disaster, precipitation of Kanazawa city

I. INTRODUCTION

Tritium distribution in nature is mainly the result of continuous production by cosmic rays in the upper atmosphere and prolonged exposure from thermonuclear bomb tests carried out during the 1950's and early 1960's.

The tritium concentration of the precipitation in Ishikawa Prefecture, Japan, showed the highest annually averaged value of 74.1 Bq/L[1] in 1963, which corresponded to the year of the maximum fallout of tritium in the northern hemisphere. After the maximum, it decreased year by year for the past four or five decades, and returned to levels lower than 1 Bq/L in 2007.

Tritium is generated by various nuclear reactions and presents as tritiated water (HTO), tritiated hydrogen gas (HT) and other chemical forms in nuclear reactors. A large amount of tritium was released from the Fukushima Daiichi nuclear power plant caused by the damage of the nuclear reactors in consequence of the Great East Japan Earthquake on 11 March 2011. In this paper, the variations in tritium concentration in the precipitation of Kanazawa city are reported for the period from March to August 2011. This was done to determine the influence of the tritium released into the environment by the Fukushima Daiichi nuclear disaster on the tritium concentration in the precipitation of Kanazawa city.

II. MATERIAL AND METHODS

The precipitation of Kanazawa city (36.52°N, 136.71°E) Ishikawa Prefecture, Japan, was collected during every rainfall in a stainless tray of 560 mm x 405 mm, and then distilled after the addition of $KMnO_4$ and Na_2O_2 to remove any acidic contaminants. The counting source for a liquid scintillation spectrometer was prepared by mixing 40 mL of distilled water with 60 mL of cooled sol-gel emulsifier-type scintillating cocktail, ULTIMA GOLD LLT （PerkinElmer Inc.） in a 100 mL Teflon vial. It was allowed to stand under cool, dark conditions for three days before counting to suppress chemical luminescence. The tritium activity was measured under temperature-stabilized conditions at 12°C using a low background liquid scintillation counter, Aloka LB-5. The counting was carried out for at least four cycles of 1,150 min (50 min x 23) run. The background count rate was 2.22-2.48 cpm at an efficiency of 30.0-30.8 %, which was determined by the external standard channels ratio method.

III. RESULTS AND DISCUSSION

The first rainfall in Kanazawa city after the occurrence of the Fukushima Daiichi nuclear disaster was observed on 15 March 2011 (from 15:50) and it changed to intermittent snow the next day. The tritium concentration in the precipitation of Kanazawa city (36.52°N, 136.71°E) Ishikawa Prefecture, Japan was at levels of 0.35-0.54 Bq/L during the period from February to early March in 2011. It began to increase following the snow of 4:10-9:00 on 16 March, and through to a maximum peak of 15.0 Bq/L after the snow of 9:00-19:00 on 16 March. It decreased to the normal level of 0.5 Bq/L in the rainfall of 9:00-13:30 on 21 March, and thereafter increased again rapidly to 4.6 Bq/L in the sleet from 19:10 on 22 March to 9:00 on 23 March. These facts suggests that a sudden release of a large amount of tritium from the Fukushima Daiichi nuclear power plant occurred between 21 March and 22 March, followed by the accidental or uncontrolled release of tritium from 11 March to 15 March.

A dramatic increase in tritium concentrations of 131.6 Bq/L and 99.9 Bq/L was observed in the rainfalls of 9:30-13:40 on 30 May and those from 21:30 on 13 June to 9:00 on 14 June in the variation patterns of tritium concentration in the precipitation of Kanazawa city, although no marked change was observed in the period from April up to the end of May. This may have been caused by the wind violently blowing down from the upper atmosphere during a storm. A large amount of tritium which had been released by hydrogen explosions from the Fukushima Daiichi nuclear reactors is considered to exist in the bulk air in the upper atmosphere.

[1] Y. Yamada, K. Yasuike, K. Komura, J. Nucl. Radiochem. Sci., 6, 17-20 (2005)

Sediment transport processes in reservoir-catchment system inferred from sediment trap observation and fallout radionuclides

Shinya Ochiai[1], Seiya Nagao[1], Masayoshi Yamamoto[1], Taeko Itono[2], Kenji Kashiwaya[3]
[1]Low Level Radioactivity Laboratory, Institute of Nature and Environmental Technology, Kanazawa University, Japan
[2]Graduate School of Natural Science & Technology, Kanazawa University, Japan
[3]Institute of Nature and Environmental Technology, Kanazawa University, Japan

Abstract – Sediment trap observation of ^{210}Pb, ^{137}Cs, and ^{134}Cs in an artificial reservoir located in central Japan indicates that the discharge rate of these radionuclides from the catchment is largely influenced by the precipitation, with high precipitation in typhoon and snow season. The annual discharge rate of ^{134}Cs from the catchment is larger than that of ^{137}Cs, suggesting that FDNPP-derived ^{134}Cs is concentrated at the erodible surface soil and it is a major sediment source for the annual timescale. The $^{137}Cs/^{210}Pb_{ex}$ activity ratio was high during rainy season and typhoon season, corresponding to the change in 10 mm/h excess rainfall. The soil erosion during the heavy rainfall may extend to the high ^{137}Cs accumulated part in the catchment where is not erodible in the normal condition. This result suggests that heavy rainfall affects the source of eroded sediment and the erosion process in the catchment.

Keywords – sediment transport, sediment trap, ^{210}Pb, $^{134,137}Cs$, Fukushima Dai-ichi NPP

I. INTRODUCTION

The sediment transport processes in the catchment are important to understand the landform development and material transport to downstream rivers, lakes and ocean. The fallout radionuclides ^{137}Cs and ^{210}Pb have been widely used to investigate soil erosion and sediment transport processes. ^{210}Pb is continuously supplied on the soil through atmospheric deposition, while the supply of ^{137}Cs is negligible at the present and its distribution has been changed by downward migration and erosion during the past several decades. Additionally, ^{134}Cs was newly accumulated on the surface soil by the Fukushima Dai-ichi Nuclear Power Plant (FDNPP) accident in 2011. The difference in horizontal and vertical distribution of these radionuclides in the catchment may provide the information on the eroded sediment sources and its response to erosional forces (e.g., hydrological and geomorphological conditions).

This study aims to investigate the sediment transport processes in the reservoir-catchment system based on the continuous sediment trap observation and these fallout radionuclides.

II. SAMPLES AND METHOD

Study site is an artificial reservoir Takidani-ike for agricultural irrigation located in Ishikawa Prefecture in central Japan. Sediment trap observations have been performed since 2000 in Takidani-ike. Deposited sediments collected monthly using a sediment trap on the bottom were oven dried at 110°C to obtain their dry weights and sedimentation rates. Samples collected during the period from February 2010 to December 2011 were used for the radioactivity measurements. Soil samples were also obtained in the catchment using a steel tube (30 cm length) to estimate inventory of the radionuclides. The activity concentration of ^{210}Pb (peak energy: 46 keV), ^{214}Pb (352 keV), ^{137}Cs (661.6 keV), and ^{134}Cs (604.7 keV) were determined by gamma-ray spectrometry using low background Ge detectors. The activity of excess $^{210}Pb_{ex}$ was estimated by subtracting the activity of ^{214}Pb from that of ^{210}Pb.

III. RESULTS AND DISCUSSION

Sedimentation fluxes of $^{210}Pb_{ex}$ and ^{137}Cs in Takidani-ike range 3.5–80 and 0.1–2.6 Bq/m^2/day, respectively, and were high during autumn and winter than in spring and summer. ^{134}Cs was first observed just after the FDNPP accident and showed the similar seasonal fluctuation ranging n.d.–0.15 Bq/m^2/day. These fluctuations correspond to the changes in precipitation, with high precipitation in typhoon and snow season, indicating that the discharge of these radionuclides from the catchment is largely influenced by the precipitation.

Based on the average sedimentation flux, the annual $^{210}Pb_{ex}$, ^{137}Cs, and ^{134}Cs discharge rates from the catchment were estimated as 222, 7.1, and 0.62 Bq/m^2/year, respectively. These values correspond to 0.72, 0.25, and 4.2 %/year of the inventory of $^{210}Pb_{ex}$ (31 kBq/m^2), ^{137}Cs (2.8 kBq/m^2), and ^{134}Cs (14.7 Bq/m^2). The annual discharge rate of ^{134}Cs is much larger than that of ^{137}Cs, suggesting that FDNPP-derived ^{134}Cs was accumulated at the erodible surface soil and it is a major sediment source for the annual timescale.

The $^{137}Cs/^{210}Pb_{ex}$ activity ratio of the trap samples temporally changes from 0.02 to 0.045, and was high during rainy season and typhoon season. This fluctuation well corresponds to the change in 10 mm/h excess rainfall (total rainfall exceed 10 mm/h for each sampling interval) reflecting the heavy rainfall events. This fluctuation may result from the soil erosion at the high ^{137}Cs accumulated part in the catchment during the heavy rainfall where is not erodible in the normal condition. This result suggests that heavy rainfall affects the source of eroded sediment and the erosion process in the catchment.

Transfer of Radiocesium to Crops Cultivated in Fukushima

Shinji Sugihara[1], Toshio Hara[2], Akihiro Maekawa[3], Noriyuki Momoshima[1]
[1]Radioisotope Center, Kyushu University, 6-10-1 Hakozaki, Higashi-ku, Fukuoka 812-8581, Japan
[2]Molecular Engineering Institute, Kinki University, 11-6 Kayanomori, Iizuka, Fukuoka 820-8555, Japan
[3]Graduate School of Sciences, Kyushu University, 6-10-1 Hakozaki, Higashi-ku, Fukuoka 812-8581, Japan

Abstract – Several kinds of crops were cultivated by using the contaminated soil in the field of Fukushima Prefecture and the radioactivity of soil and crops was measured. The soil-to-crops transfer factor of a radiocesium was calculated, and a different value was calculated by corps and the part of crops. But the level of the calculated value is almost equal to already reported.

Keywords – Transfer factor, Radiocesium, Crop, Fukushima Dai-ichi Nuclear Power Plant

I. INTRODUCTION

A large amount of radioactive materials were discharged into the atmosphere during the Fukushima Dai-ichi Nuclear Power Plant accident. As a consequence, a wide region of Japan has been contaminated by mainly radiocesium.

As part of the proof examination of the revival model after the Fukushima nuclear disaster, several kinds of crops were cultivated and the effect of decontamination and desalinization of the contaminated farmland were inspected. The soil-to-plant transfer factor (TF) of radiocesium is extremely variable among soils.

Radionuclides can reach the human body through several food chains in the environment. A lot of data in the targeted environment such as TF is necessary to evaluate the influence on the human body.

II. METHOD

The cultivation examination ground was set by two places (A area: Harashita, B area: Kekaya) in Tomioka, Fukushima Prefecture. B area had received the flood damage of the tsunami. After the disaster, the area was left because these areas were specified for the no-go zone though both areas were originally rice fields. The radiation measurement, the ploughing and the sowing were done in May, 2013. Crops were sorghum (*Sorghum bicolor*), corn (*Zea mays*), rapeseed (*Brassica napus*) and Sugar beet (*Beta vulgaris ssp*). Sorghum and corn were harvested in the middle of November, 2013 at A area. Because the cultivation period was different, the flowering of the rapeseed was difficult. Only the sugar beet grew and it harvested in December, 2013 though sorghum and corn were fruitless on B area due to the salt damage. The radioactivity of the soil before and after the ploughing and the harvested crops sample was measured. The soil sample was cut at intervals of 1cm. The samples of Crops were made separately for the leaf, the stalk and the seed. A dry sample was put in the U8 container, and the Cs concentration was measured with the Ge solid state detector. The radioactivity of the sunflower (Helianthus annuus) grown at the field in A area was measured similarly.

III. RESULTS AND DISCUSSION

Figure 1 shows the depth distribution of the Cs in the soil before the ploughing of A area. Cs that deposited to surface on the field by the Fukushima nuclear disaster remained in the surface layer after two years passed, and most was detected within 5cm in depth. The radiation dose rate at A area was 1.14 μSv/h by 1m on the ground. The Cs concentration was about 1/3 of that of A area, and the dose rate was 0.71 μSv/h on B area.

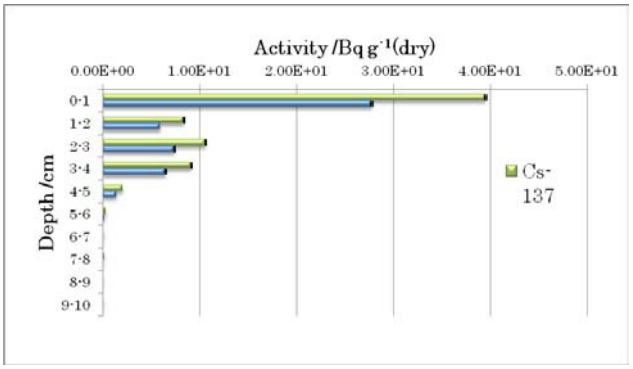

Fig.1 Depth distribution of Cs in A area before the ploughing

Soil-to-crop transfer factor (TF) was calculated as the ratio of the radionuclide concentration in crops (Bq/kg dry weight) to its concentration in soil (Bq/kg dry weight). Both the dry weight and the fresh weight were used as for the numerator, and the dry weight was used here. TF differed according to the part of the crop, and existed in the range of 0.01 to 0.1. Because TF of the seed was small, the seed might be able to use as fodder.

It will be necessary to obtain the basic data for the revival by changing the kind of the soil and crops in addition and accumulating the vast scope of data in the future.

Dynamics of radiocesium in bamboo forests after the accident of Fukushima Daiichi nuclear power plant

Tsutomu KANASASHI, Mitsutoshi UMEMURA, Yuki Sugiura , Chisato TAKENAKA

Graduate School of Bioagricultural Sciences, Nagoya University

Abstract – To understand the dynamics of radiocesium in bamboo forests, we compared the ^{137}Cs concentrations in one-year old bamboo with older ones. The leaves from one-year bamboo contained ^{137}Cs at similar concentration to those of older bamboos. Since bamboo shoot of 2012 also contained ^{137}Cs, cesium should be actively transported in bamboo body.
Keywords – bamboo, radiocesium, leaves, branch, shoot

I. INTRODUCTION

The accident of Fukushima daiichi nuclear power plant on 2011 caused serious problems through the deposition of radionuclide in a large area of Fukushima prefecture. Bamboo forests, which have been familiar to peoples as producing area of various livelihoods like bamboo shoots, were also contaminated with radionuclide, especially ^{137}Cs. The decontamination of ^{137}Cs from bamboo forests has been expected but supposed to be difficult because of the existence of a large amount of subterranean stems. In order to design an effective decontamination procedure of ^{137}Cs and resume the usage of bamboo forests in Fukushima, it is essential to understand the dynamics of ^{137}Cs in bamboo forests. We aimed to clarify the absorption and transport of ^{137}Cs in bamboo by comparing the ^{137}Cs concentration in one-year old bamboo with older one.

II. MATERIAL & METHODS

Bamboo samples were collected from three moso bamboo (*Phyllostachys pubescens*) forests in Fukushima prefecture during spring season of 2012. At one site (site A), since the age of each bamboo could be defined, not only an one-year old bamboo, which sprouted after the accident of FNPP, but also 2,4,5,10,11-years old bamboos were collected. At the other two sites (sites B and C), three one-year old bamboos and three bamboos older than one year were sampled. A bamboo shoot was also collected at site C. Litters and soils were collected from three sites.

Each bamboo was divided into stem, branch and leaves. For the samples from site C, branch and leave samples were prepared from top and middle parts of a stem.

Every plant samples were pulverized after drying. The activity of ^{137}Cs was counted by a Ge- semiconductor detector (Seiko EG & G). Each counting was continued until the count error becomes below 10%.

III. RESULTS & DISCUSSION

Table 1 shows the concentration of ^{137}Cs per area in litter and soil layers at three moso bamboo forest sites. From these data, the radioactivity at site A was almost a third of those at sites B and C. In addition, at the sites A and B, the concentrations of ^{137}Cs in soil layer were higher than those in litter layer, whereas the activity of litter was almost twice of that of soil layer at site C. These observations suggested that the degree of ^{137}Cs infiltration into root system were different among three sites.

The concentrations of ^{137}Cs in leaves and branches collected at site A were shown in Fig.1. The ^{137}Cs concentration in leaves from one-year bamboo, which sprouted on 2011 after the accident, was not so different from the values of leaves in the other samples (2 to 11-years old bamboos), whereas the data in branch of one-year bamboo was quite low comparing with those of the other bamboos. Since the bamboos older than one year adsorbed ^{137}Cs on their surface at the accident of FNPP, the difference of concentrations among branches with various aged bamboo should reflect the direct deposition. On the contrary, the similar concentrations of ^{137}Cs in leaves of one-year bamboo with the others might indicate the uptake of ^{137}Cs through root system. The same results were obtained from the data of site B and C. The bamboo shoot sprouted on 2012 also contained ^{137}Cs at the same level as leaves.

Table 1. Acticity of Cs-137 in litter and soil at three moso forests (kBq/m2)

	A	B	C
Litter	44	161	254
Soils	66	186	132

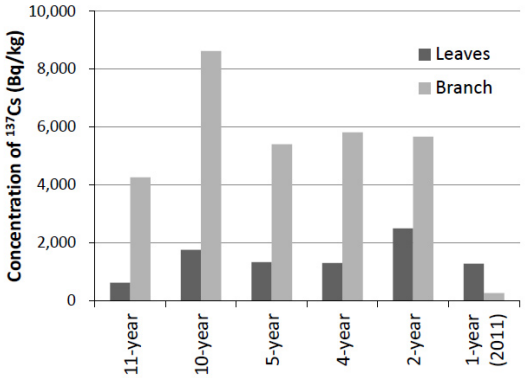

Figure 1. Concentration of ^{137}Cs of leaves and branches in various aged bamboos

Reaction Behavior of Uranium and Zirconium Oxides in Oxidative and Reductive Conditions

Nobuaki Sato, Kohei Fukuda and Akira Kirishima
Institute of Multidisciplinary Research for Advanced Materials, Tohoku University,
2-1-1, Katahira, Aoba-ku, Sendai,980-8577, Japan

To investigate the treatment of fuel debris formed in the damaged reactors at Fukushima Daiichi NPP, study on the reaction behavior of main constituents in the reactor is essential. The main component in the damaged reactor is the mixture of uranium and zirconium since there are the fuel and cladding. As for the reaction between fuel oxide and fission products in oxidative condition, the phase relation of the oxides in the U_3O_8 and Nd_2O_3 system was reported [1]. Then the reaction behavior of the uranium and zirconium oxides at elevated temperatures in oxidative and reductive atmospheres was studied by XRD method. After the heat treatment of the mixture of UO_2 and ZrO_2 with a Zr amount of 50 mol % under vacuum at elevated temperature, the UO_2 solid solution phase such as $Zr_yU_{1-y}O_{2+x}$ seemed to be formed at temperatures lower than 1273 K. However, phases similar to U_3O_8 structure appeared in the temperature range from 1073 K to 1473 K. Over this temperature, a new phase similar to the UO_2 phase seemed to be formed showing the decomposition of U_3O_8 phase at high temperature. When the mixture of zirconium to uranium oxides was treated by mechanochemical method under reducing condition , the X-ray pattern of the products showed that they were the same fluorite structure and the lattice parameter of linearly decreased with increasing zirconium ratio. This suggests that the UO_2 and ZrO_2 form the solid solution from low Zr/U ratio to high one. These results were also discussed with the phase diagram.

Keywords: Fuel debris, Uranium oxides, Zirconium, UO_2 solid solution, Phase relation

[1] N. Sato, G. Shinohara, A. Kirishima and O. Tochiyama, *High Temp. Mat. Proc.,* **29** (2010) 461–468.

Radiocesium in zooplankton in seawaters off Miyagi, Fukushima, and Ibaraki Prefectures

H. Takata[1], M. Kusakabe[2], S. Oikawa[1]
[1]Central Laboratory, Marine Ecology Research Institute
[2]Head Office, Marine Ecology Research Institute

Abstract – Zooplankton samples in seawaters were collected off Miyagi, Fukushima, and Ibaraki prefectures from May 2012 to January 2013. Activity concentrations of ^{134}Cs and ^{137}Cs in zooplankton varied from 0.1to 9.1 Bq/kg-wet weight, and from 0.1 to 12.8 Bq/kg-wet weight, and were higher in May 2012 than in the other sampling months. We also estimated the zooplankton-to-water activity ratio of ^{137}Cs to be 20-754 L/kg.

Keywords – zooplankton, radiocesium, concentration ratio, Fukushima Dai-ichi nuclear power plant

I. INTRODUCTION

The East Japan earthquake and tsunami of March 11, 2011, resulted in unprecedented radioactivity releases from the Fukushima Dai-ichi nuclear power plant (FDNPP) to the Northwest Pacific Ocean. Radionuclides (e.g., ^{134}Cs ($t^{1/2}$ =2 y), and ^{137}Cs ($t^{1/2}$=30 y)) originated from the FDNPP migrated horizontally (e.g., Aoyama et al., [1]); however, the vertical transport mechanisms for radiocesium in the coastal areas off Japan are not fully understood. Zooplankton activity such as excretion and vertical migration can be one of candidates to play an important role in vertical transport of man-made radionuclides (e.g. Fowler et al. [2]).

We report here the results from a radiochemical analysis of zooplankton for raiocesium (^{134}Cs and ^{137}Cs) collected in the waters off Miyagi, Fukushima, and Ibaraki prefectures in 2012 and 2013.

II. MATERIALS AND METHODS

Zooplankton were collected at seven stations during four cruises (May 2012, Aug. 2012, Oct. 2012, and Jan. 2013) at the depths of around 20-80 m with a large ring net (160 cm mouth diameter, 0.5 mm mesh) during daytime by a 30-min horizontal towing. To ensure sufficient amounts of sample for radionuclide analyses, 2–3 hauls per station were combined into one sample. After the collection, samples on the mesh were transferred to plastic buckets. A small amount of samples were preserved immediately in 5% (v/v) formalin–seawater buffered with borax for microscopic observation, and the rest of the sample was stored in a freezer at -20°C.

Zooplankton samples were weighed (wet weight), ovendried (105°C), and weighed again to obtain dry weight. The activity of radiocesium in dried samples was measured with coaxial type Ge detectors for a few hours. The radioactivities of ^{134}Cs and ^{137}Cs in the samples were decay-corrected to the sampling date.

III. RESULTS AND DISCUSSION

Activity concentrations of radiocesium in zooplankton ranged from 0.1 to 9.1 Bq/kg-wet weight, and from 0.1 to 12.8 Bq/kg-wet weight for ^{134}Cs and ^{137}Cs, respectively during May 2012 to January 2013 (Fig. 1). In addition, relatively high activity concentrations of radiocesium were observed near off Ibaraki prefecture during May 2012 cruise, and near off Fukushima prefecture during January 2013 cruise (Fig. 1). The variation in activity concentrations would be due to changes in activity concentrations of radiocesium in their ambient waters. However, there was no significant correlation between radiocesium activity concentration in the ambient water and in the zooplankton.

Another possible reason is probably due to the difference in the composition of zooplankton at each station; however, so far it is unclear as to the relationship between planktonic species and their ^{137}Cs contents.

We also estimated the zooplankton-to-water activity ratio of ^{137}Cs to be 20-754 L/kg; most of them are higher than the one (40 L/kg) published by the IAEA[3].

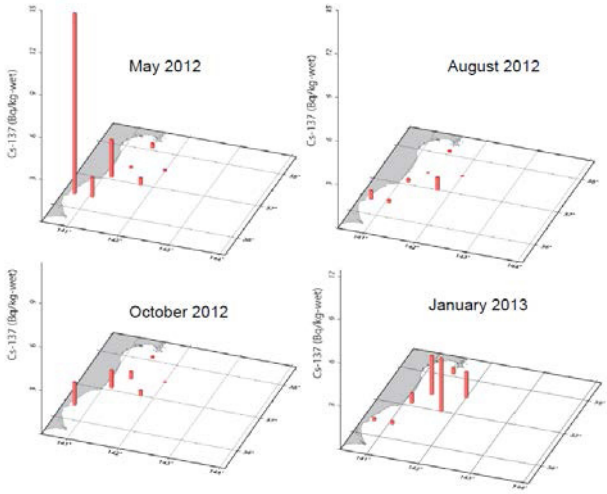

Fig. 1 Activity concentrations of ^{137}Cs in zooplankton at 7stations during each sampling cruise.

REFFERENCES

[1] Aoyama, M., Uematsu, M., Tsumune, D., and Hamajima, Y.: Surface pathway of radioactiveplume of TEPCO Fukushima NPP1 released 134Cs and 137Cs, *Biogeosciences Discuss.,* 10, 265–283, doi:10.5194/bgd-10-265-2013, 2013.

[2] Fowler, S.,W., Buat-Menard, P., Yokoyama, Y., Ballestra, S., Holm, E., and Nguyen, H.,V.: Rapid removal of Chernobyl fallout from Mediterranean surface waters by biological activity, *Nature* 329, 56–58, 1987.

[3] IAEA: Sediment distribution coefficients and concentration factors for biota in the marine environment, Technical Report Series no. 422, IAEA, Vienna, 1–95, 2004.

This work was part of a research project contracted from the Ministry of Education, Culture, Sports, Science and Technology, Tokyo, Japan.

Plutonium isotopes and ^{241}Am in surface sediments off the coast of the Japanese islands after the Fukushima accident

S. Oikawa[1], T. Watabe[2], H. Takata[1], J. Misonoo[2], M. Kusakabe[2]
[1] Central Laboratory, Marine Ecology Research Institute
[2] Head Office, Marine Ecology Research Institute

Abstract – We determined concentrations of Pu isotopes and ^{241}Am in surface (upper 3cm) bottom sediments collected in a sea area along the coast of the Japanese islands after the Fukushima Dai-ichi Nuclear Power Plant (FDNPP) accident. The concentration in the sediments collected immediately after the accident was at almost the same levels as those obtained before the accident.

Keywords – plutonium; ^{241}Am; bottom sediment; Fukushima Dai-ichi Nuclear Power Plant accident

I. INTRODUCTION

As a result of the FDNPP accident on March 11, 2011, a large amount of ^{131}I (half-life: 8 d), ^{134}Cs (2 y), ^{137}Cs (30 y) and other radionuclides were released into the atmosphere. In addition, a remarkable amount of radionuclides was also released directly from the plant as the leakage of coolant seawater poured into the reactor. Comprehensive survey projects were immediately initiated after the accident for clarifying the distribution of radionuclides especially with high volatility such as ^{131}I, ^{134}Cs and ^{137}Cs in the environment. However, a survey of actinides derived from the accident in the marine environment has been yet to be sufficient to evaluate their impact. This paper represents the results of a nationwide survey project to figure out the extent of the accident impact in the levels of Pu isotopes and ^{241}Am in the bottom sediments collected from the 15 sampling areas. And a comparison was made of the pre-accident data to the post-accident ones.

II. MATERIALS AND METHODS

The radioactivity survey project was implemented in nationwide 15 sampling areas (Fig. 1). Bottom sediment samples were collected by a box-type sampler, which retrieves a 1600 cm^2 of sediment from the ocean floor without disturbing their surface. The upper 3 cm of the sediments were taken for analysis. Plutonium and ^{241}Am analysis was performed using 50 g aliquot of dried sample, and alpha spectrometry and beta counting method was used to measure $^{239+240}$Pu (alpha), ^{241}Pu (beta) and ^{241}Am (alpha). We also used SF-ICP-MS to measure ^{240}Pu/^{239}Pu atom ratio.

III. RESULTS AND DISCUSSION

The activity concentrations of $^{239+240}$Pu found in these surface sediment samples collected in May-July 2011, immediately after the accident ranged from 0.42 to 3.7 Bq/kg-dry, which was comparable to those reported by Zheng et al. [1] and Oikawa et al. [2]. The highest $^{239+240}$Pu activity concentration of 3.7 Bq/kg-dry was found in the clayey sediment collected in the Aomori area and the lowest of 0.42 Bq/kg-dry in the sandy sediment in the Ehime area. Although the ^{241}Pu was detected from some samples having relatively high $^{239+240}$Pu concentration (*ca.* >0.7 Bq/kg-dry), the ^{241}Am was detected from all of the sediments. The ^{241}Pu/$^{239+240}$Pu activity ratio found in the sediments varied among the sites even if the sediments collected in the same period of time and ranged from 0.75 to 1.2. The ^{241}Am/$^{239+240}$Pu activity ratio in the sediments were nearly constant (*ca.* 0.6), and the ^{240}Pu/^{239}Pu atom ratios were also nearly constant (*ca.* 0.24) throughout the nationwide sites. The concentrations of Pu isotopes and ^{241}Am, and their ratios found even in the sediments taken in the vicinity of the FDNPP accident have no significant differences between prior to and after the accident. Thus, our nationwide survey results showed that the accident at the FDNPP did not contribute so greatly to the inventory of Pu isotopes and ^{241}Am even in the coastal area off Fukushima Prefecture.

Fig. 1 Locations of sampling areas.

REFERENCES

[1] Zheng, J. et al., Distribution of Pu isotopes in marine sediments in the Pacific 30km off Fukushima after the Fukushima Daiichi nuclear power plant accident. *Geochem. J.* 46, 361-369 (2012).
[2] Oikawa, S. et al., Plutonium isotopes concentration in seawater and bottom sediment off the Pacific coast of Aomori sea area during 1991-2005. *J. Environ. Radioact.* 102, 302-310 (2011).

This work was a part of a research project contracted from the Ministry of Education, Culture, Sports, Science and Technology, Tokyo, Japan.

APSORC'13 - 5th Asia-Pacific Symposium on Radiochemistry
Kanazawa, Japan, 22-27 September 2013

A theoretical study of actinide and lanthanide extraction with carbamoylmethylphosphine oxide ligands

Cong-Zhi Wang, Jian-Hui Lan, Yu-Liang Zhao, Zhi-Fang Chai, Wei-Qun Shi*
Nuclear Energy Nano-Chemistry Group, Key Laboratory of Nuclear Analytical Techniques and Key Laboratory For Biomedical Effects of Nanomaterials and Nanosafety, Institute of High Energy Physics, Chinese Academy of Sciences, Beijing 100049, China
E-mail: shiwq@ihep.ac.cn

Abstract – With the development of nuclear energy, safe disposal of the spent nuclear fuel especially high level liquid waste (HLLW) generated during the PUREX (Plutonium Uranium Extraction) process has become the key factors affecting the sustainable development of nuclear energy. The n-octyl(phenyl)-N,N-diisobutyl-methylcarbamoyl phosphine oxide (CMPO) used in the so-called TRUEX (Transuranium Extraction) process was found to possess excellent extracting ability for actinide and lanthanide cations in acidic media.[1,2] In this work, The UO_2^{2+}, NpO_2^{+}, Pu^{4+}, Am^{3+} and Eu^{3+} extraction complexes with CMPO and diphenyl-N,N-diisobutyl carbamoyl phosphine oxide (Ph_2CMPO) have been investigated by density functional theory (DFT) in conjunction with relativistic small-core pseudopotentials. For most extraction complexes, the CMPO and Ph_2CMPO molecules are coordinated as bidentate chelating ligands through the carbonyl oxygen and phosphoric oxygen atoms. The metal-ligand bonding is mainly ionic for all of these complexes. The neutral $UO_2L_2(NO_3)_2$, $NpO_2L_2(NO_3)$, $PuL_2(NO_3)_4$, $AmL_3(NO_3)_3$ and $EuL_3(NO_3)_3$ complexes are predicted to be the most thermodynamically stable molecules according to the metal-ligand complexation reactions. As reported in the literature,[3-5] the extractability of these actinides decrease in the order of $Pu^{4+} > UO_2^{2+} > Eu^{3+} \approx Am^{3+} > NpO_2^{+}$. In addition, hydration energies may play an important role in the extractability of CMPO and Ph_2CMPO for these actinide ions. In most cases, the complexes with CMPO and Ph_2CMPO ligands have comparable metal-ligand binding energies, i.e., the substitution of a phenyl ring for the n-octyl at the phosphoryl group of CMPO has little influence on the extraction of these actinides and lanthanides.

Keywords – actinide, lanthanide, extractant, relativistic quantum chemistry

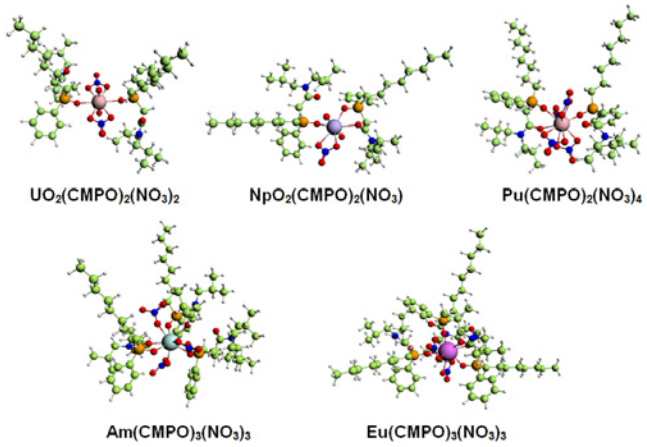

Fig. 1 Extraction complexes of UO_2^{2+}, NpO_2^{+}, Pu^{4+}, Am^{3+} and Eu^{3+} from nitric acid solutions with CMPO

[1] Horwitz, E. P.; Kalina, D. G.; Diamond, H.; Vandegrift, G. F.; Schulz, W. W. *Solvent Extr. Ion Exch.* 1985, 3, 75.
[2] Horwitz, E. P.; Kalina, D. G.; Diamond, H.; Kaplan, L.; Vandegrift, G. F.; Leonard, R. A.; Steindler, M. J.; Schulz, W. W. DE85 010251, 1985.
[3] Visser, A. E.; Jensen, M. P.; Laszak, I.; Nash, K. L.; Choppin G. R.; Rogers, R. D. *Inorg. Chem.* 2003, 42, 2197.
[4] Wisnubroto, D. S.; Nagasaki S.; Enokida Y.; Suzuki A. *J. Nucl. Sci. Technol.* 1992, 29, 263.
[5] Mathur, J. N.; Murali, M. S.; Natarajan P. R. *Taianta* 1992, 39, 493.

APSORC'13 - 5th Asia-Pacific Symposium on Radiochemistry
Kanazawa, Japan, 22-27 September 2013

The role of microorganisms during the wet nuclear fuel storage in Slovak Republic

Martin Pipíška[1], Lenka Tišáková[2], Miroslav Horník[1], Jozef Augustín[1]
[1]Department of Ecochemistry and Radioecology, University of SS Cyril and Methodius, J. Herdu 2, Trnava, SK-917 01, Slovak Republic (pipiska@ucm.sk)
[2]Institute of Molecular Biology, Slovak Academy of Sciences, SK-845 51, Bratislava, Slovak Republic

Abstract

The role of short-term and long-term effects of microbial activity on the wet disposal of spent nuclear fuel in storage facilities is relatively discussed question. Deionized water in storage pools serves as a coolant and, at the same time, as a protection against radiation. However, microorganisms have been shown to survive and grow in high levels of radiation and in highly pure water and they can tolerate both high and low osmolarity and extreme pH and temperature values [1, 2]. This work is focused on a characterization of bacterial contamination in pool water of the Interim spent nuclear fuel storage (ISFS, JAVYS Inc.) in Slovakia. The ISFS consists of 4 interconnecting pools: 3 fuel storage pools and 1 reserve pool built from austenitic steel and permanently filled with deionized water (Fig 1). The mean specific radioactivity of pool water for β emitters was 3.910 ^{5} Bq/L, for γ emitters 3.7 $\times 10^5$ Bq/m^3. Tritium participated by the activity 1.3 $\times 10^5$ Bq/m^3 and contribution of radionuclides increased in the order: ^{60}Co < ^{134}Cs < ^{3}H < ^{137}Cs. From the microbiological point of view, the pool water represents oligotrophic environment which enables the growth of mesophilic bacteria, where chronic radiation exerts selective pressure, altering both the diversity and abundance of bacteria.

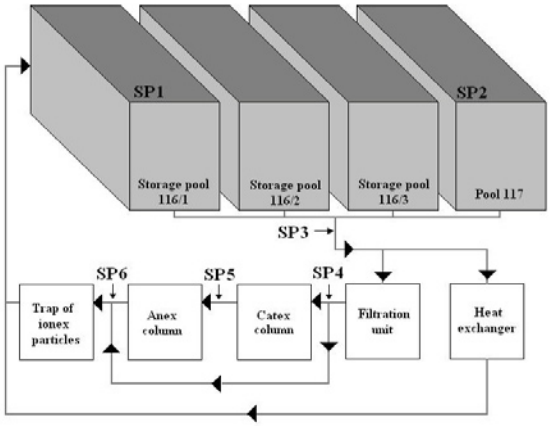

Fig. 1 Circulation system of pool water in spent nuclear fuel storage facility at ISFS. Samples of water were collected from fixed 6 sampling points: SP1 and SP2 – near the water surfaces, SP3 – from the bottom, SP4, SP5 and SP6 – after filtration unit, after catex and anex columns, respectively.

Bacterial content in pool waters is kept on very low level by extremely low concentration of solutes in deionized water and by both the efficient water and air filtration systems. During the monitoring from 2009 to 2012, bacterial densities in the water samples from the surface of pools (SP1, 2) were within the range from 50 to 4 525 CFU/L. Viable counts in the water from the bottom of the pool SP 3 and SP4 to SP6 fluctuated between 100 and 5 500 CFU/L, although noticeable higher values were observed in August and October 2011 and from April to June 2012. Observed higher values up to 250 000 CFU/L can be caused by manipulation procedures such as filling the new fuel assemblies or manipulation in filtration units and by the facility reconstruction. In our primary screening 7 different bacterial isolates from spent nuclear fuel pools were obtained. Only 4 isolates showed stable growth on DEV nutrient agar. Subsequently, these isolates were identified by 16S rDNA as *Kocuria palustris, Micrococcus luteus, Ochrobactrum* spp. and *Pseudomonas aeruginosa.*

In laboratory experiments, the bioaccumulation of ^{137}Cs and ^{60}Co by isolated bacteria were also studied [3]. The maximum specific uptake of Cs^+ after 48 h cultivation in mineral medium (MM) reached 7.54 ± 0.48 µmol/g dw. (*Ochrobactrum* spp.), 19.6 ± 0.1 µmol/g dw. (*M. luteus*) and 20.1 ± 2.2 µmol/g dw. (*K. palustris*). The maximum specific uptake of Co^{2+} after 24 h cultivation in MM reached 31.1 ± 3.5 µmol/g dw. (*Ochrobactrum* spp.), 86.6 ± 12.2 µmol/g dw. (*M. luteus*) and 16.9 ± 1.2 µmol/g dw. (*K. palustris*).

Analyzing of bacterial communities inhabiting an environment exposed to radiation gives opportunities to find bacterial strains with interesting properties such as radioresistance and radionuclide sequestering, able to survive in extremely nutrient deficient environment. We found that bacteria *K. palustris*, *Ochrobactrum* spp. and *M. luteus* isolated from ISFS pool water effectively accumulate both ^{137}Cs and ^{60}Co under growth conditions indicating that these bacteria affect the fate of radionuclides in pool water. Presented results should serve also as the basis for further studies relating to the microbial safety of wet nuclear waste storage in Slovak Republic.

Keywords spent nuclear fuel, storage pools, bacteria, bioaccumulation, ^{60}Co, ^{137}Cs

References

[1] Wolfram JH, Dirk, WJ (1997) Biofilm development and the survival of microorganisms in water systems of nuclear reactors and spent fuel pools. In: Wolfram JH, Rogers RD, Gaszó LG (Eds) Microbial degradation process in radioactive waste repository and in nuclear fuel storage areas. Dordrecht, Kluwer Academic Publishers, pp. 139-147
[2] Diósi G, Telegdi J, Farkas G, Gazso LG, Bokori E (2003) Corrosion influenced by biofilms during wet nuclear waste storage. Int Biodeterior Biodegrad 51: 151-156
[3] Tišáková L, Pipíška M, Godány A, Horník M, Vidová B, Augustín J (2013) Bioaccumulation of ^{137}Cs and ^{60}Co by bacteria isolated from spent nuclear fuel pools. J Radioanal Nucl Chem 295: 737-748

APSORC'13 - 5th Asia-Pacific Symposium on Radiochemistry
Kanazawa, Japan, 22-27 September 2013

Single centrifugal contactor test of a proposed group actinide extraction process for partitioning and transmutation purposes

Emma Aneheim[1,2], Christian Ekberg[1], Giuseppe Modolo[3], Andreas Wilden[3]
[1]Nuclear Chemistry, Department of Chemical- and Biological Engineering, Chalmers University of Technology, SE41296 Gothenburg, Sweden
[2]Targeted Alpha Therapy group, Department of Radiation Physics, Sahlgrenska Academy at Gothenburg University, SE41345 Gothenburg Sweden
[3]Forschungszentrum Jülich GmbH (FZJ), Institut für Energie- und Klimaforschung, Nukleare Entsorgung und Reaktorsicherheit (IEK-6), 52428 Jülich, Germany

Partitioning and Transmutation (P&T) is one of the future strategies for handling of used nuclear fuel. Within P&T, compared to conventional reprocessing, not only uranium and plutonium are to be recycled, but also the rest of the actinides present in the used fuel. By doing this, the idea is to decrease the storage time needed for the residual waste as well as to lower the strain on the final repository. Group Actinide Extraction (GANEX) is a process scheme for P&T where the actinides are extracted as a group directly from the dissolution liquor, after removal of bulk uranium. A solvent intended for GANEX purposes, utilizing two well-known extractants (tri-butyl phosphate and bis-triazine,bi-pyridine) in cyclohexanone has previously been intensely investigated. The extraction system has in batch tests been found to extract the actinides as a group and, with some modifications, separate them from most of the fission products. The solvent was also found to be resistant both towards strong nitric acid and irradiation up to ca 200 kGy. Due to these positive findings, the extraction system has in this work been used in a single centrifugal contactor test on a simulated high active raffinate solution, spiked with radiotracers. The kinetics of the system was found to be relatively slow in the equipment of choice, especially regarding the stripping. However, it was still possible to recover more than 87% of all actinides in one extraction step with a flowrate of 30ml/h.

Keywords – GANEX, TBP, BTBP, Centrifugal contactor

Application of Flow Analytical Methods for Determination of Radionuclides in Cooling Water and Wastes from Nuclear Plants

Anna Bojanowska-Czajka[1], Kamila Kołacińska[1], Marek Trojanowicz[1]
[1]Institut of Nuclear Chemistry and Technology, Dorodna 16, 03-195 Warsaw, Poland

I. INTRODUCTION

Flow analytical systems can be described as measuring devices, in which all operations of sample pretreatment and detection of analyte are carried out in flowing streams. This concept of analytical measurements is widely employed in process analysis, and for laboratory measurements was primarily developed for clinical analysis. In last decades these methods have gained a lot of interest especially for environmental applications [1]. This is proved by vast number of research papers and developed methods, increasing number of commercially available instruments and increasing number of methods, which are recognized by national and international authorities as standard methods.

The methodology of flow-injection analysis (FIA), being developed since 1970-ties, has gained numerous technical modifications such as *e.g.* systems with sequential injection of sample and reagents into a single line system (named as *sequential injection analysis* - SIA), flow measurements with direct injection to the detector sensing surface (named as *batch injection analysis* – BIA), or application in flow-injection systems with a moveable solid particles, also named as *bead-injection analysis*. [2]. Commonly, as major advantages of flow methods of analysis are considered possibility of efficient on-line methods of sample processing prior to the detection step, and improvement of precision and efficiency compared to batch procedures. From the point of view of application of flow analysis in determination of trace level of selected radionuclides especially valuable is possibility of effective on-line preconcentration of trace analytes [3], and carrying out elemental speciation analysis.

Flow methods are mainly developed for non-gamma or low-energy gamma emitters with application for detection of individual radioisotopes mainly α– and β-spectrometry (gas proportional counters, liquid-scintillation counters) [4]. Some developments reported so far include determinations of such radioisotopes as ^{90}Sr, ^{99}Tc, ^{226}Ra or ^{231,240}Pu and ^{241}Am. For design of flow-injection setups different configurations of instrumentation can be employed, including FIA, SIA, and also multi-syringe and multi-pumping devices. Most commonly both in environmental samples or cooling waters from nuclear plants those isotopes are determined in trace or ultra-trace levels, hence, in flow systems especially efficient preconcentration steps are developed. As the most efficient is considered extraction chromatography, but among other methods possible for this purpose are sorption on solid sorbents including recently also nanostructured materials, and precipitation or co-precipitation processes. Those operations can be especially efficient in flow conditions, hence construction of such monitoring systems is very advantageous for monitoring of selected radionuclides in nuclear power reactors.

APSORC'13 HEADING (WITHOUT NUMBER)

[1] M. Trojanowicz (Ed.), *Advances in Flow Analysis*, Wiley-VCH, Weinheim, 2008.
[2] M. Trojanowicz, *Flow Injection Analysis. Instrumentation and Applications*. World Scientific Publishing, Singapore, 2000APSORC'13 Reference
[3] Z. Fang, Flow Injection Separation and Preconcentration, VCH, Weinheim, 1993
[4] Y. Fajardo, J. Avivar, L. Ferrer, E. Gomez, M. Casas, V. Cerda, *Trends Anal. Chem*., 29 (2010) 1399.

Acknowledgments:
Research task No. 8 „Study of processes occurring under regular operation of water circulation systems in nuclear power plants with suggested actions aimed at upgrade of nuclear safety" financed by the National Research and Development Centre in the framework of the strategic research project entitled „Technologies Supporting Development of Safe Nuclear Power Engineering".

APSORC'13 - 5th Asia-Pacific Symposium on Radiochemistry
Kanazawa, Japan, 22-27 September 2013

Determination of low level ^{99}Tc in the primary coolant water by ICP-MS. Analysis of potential interferences.

Ewelina Chajduk[1], Sylwia Witman-Zając[1], Halina Polkowska-Motrenko[1]
[1]Institute of Nuclear Chemistry and Technology, Dorodna 16, 03-195 Warsaw, Poland

Keywords – technetium-99, primary coolant water, inductively coupled plasma mass spectrometry (ICP-MS)

Tc-99 is produced by the fission of U-235 and Pu-239. Information on technetium and other fission and activation product content in the primary coolant and at various locations in the purification system can be of considerable value in assessing fuel integrity and performance of purification system component. Nowadays, mass spectrometry methods are complementary to radiometric techniques for radionuclide determination. Using inductively coupled plasma mass spectrometry (ICP-MS) for long-lived radionuclides improves detection limit and accuracy. However, in accurate measurements by ICP-MS method, the contribution of isobaric interferences from atomic- and molecular ions created by plasma gas and/or solvent used should be defined and appropriate ways of their elimination should be introduced. During the determination of Tc-99, the following interferences can be taken into account: $^{99}Ru^{+}$, $^{64}Zn^{35}Cl^{+}$, $^{98}Mo^{1}H^{+}$, $^{198}Hg^{2+}$, $^{198}Pt^{2+}$, $^{157}Gd^{40}Ar^{2+}$, $^{40}Ar_{2}{}^{18}O^{1}H^{+}$ etc. In this work, possibility of presence isobaric inferences has been investigated. From obtained results, it could be concluded, that some of interference examined can be recognized as insignificant. However, a careful chemical separation of Tc species before the measurements, for the removal of interfering elements, such as Ru traces, as well as for the high recovery of Tc is necessary.

Acknowledgments:

Research task No. 8 „Study of processes occurring under regular operation of water circulation systems in nuclear power plants with suggested actions aimed at upgrade of nuclear safety" financed by the National Research and Development Centre in the framework of the strategic research project entitled „Technologies Supporting Development of Safe Nuclear Power Engineering".

APSORC'13 - 5th Asia-Pacific Symposium on Radiochemistry
Kanazawa, Japan, 22-27 September 2013

Extraction of Homologous Elements of Dubnium and Seaborgium from HCl Solution

T. Yokokita[1], K. Nakamura[1], A. Kino[1], Y. Komori[1], K. Toyomura[1], Y. Kasamatsu[1], N. Takahashi[1], T. Yoshimura[2], K. Ooe[3], Y. Kudou[4], K. Takamiya[5], A. Shinohara[1]
[1]Graduate School of Science, Osaka University
[2]Radioisotope Research Center, Osaka University
[3]Faculty of Science, Niigata University
[4]Nishina Center for Accelerator Based Science, RIKEN
[5]Research Reactor Institute, Kyoto University

Abstract – We aim at studying aqueous chemistry of element 105, dubnium (Db), and element 106, seaborgium (Sg). In this work, we carried out extraction experiments of Nb, Mo, Ta, W, and Pa which are homologous elements of Db and Sg by batch method. These data are significant to investigate the chemical properties of Db and Sg and to determine the experimental conditions of these experiments.

Keywords – Hydrochloric acid, Niobium, Molybdenum, Tantalum, Tungsten, Protactinium

I. INTRODUCTION

It is predicted that the chemical properties of transactinide elements, atomic numbers $Z \geq 104$, show some difference from periodicity in the Periodic Table due to increasingly strong relativistic effect. These elements are produced only by nuclear reactions with very low production rates as one atom at a time, and their half-lives are short, μs to ca. 1 min. Therefore, we must repeat rapid chemistry by such as partition method and alpha-particle measurement. In these studies, the complex formation and chemical species of the transactinides were investigated based on the comparison of their chemical behaviors with those of lighter homologues and pseud homologues. To the chemistry of element 104 (Rf), 105 (Db), and 106 (Sg), we have studied extraction experiments of homologous of Rf, Db, and Sg. Moreover, we have developed rapid extraction apparatuses. In this presentation, we report on solid-liquid and liquid-liquid extraction of Nb, Mo, Ta, W, and Pa as homologous elements of Db and Sg in HCl solution. For Db only one result obtained in HCl solution, so far, and Sg is expected to show different behavior with oxidation states.

II. EXPERIMENTAL

We carried out extraction experiments using carrier-free radiotracers of ^{95}Nb, ^{99}Mo, ^{179}Ta, ^{181}W, and ^{233}Pa. Two kinds of macro amounts of Mo(V) samples were used; one is $[MoCl_5]$ and the other is prepared by electrochemical reduction of $Na_2[MoO_4]$ solution. Macro amounts of W(V) was prepared by reducing $Na_2[WO_4]$ containing ^{181}W tracer by $SnCl_2$. Liquid-liquid extraction was performed by mixing 1–2 mL of the 0.1–11 M HCl solutions containing RI tracers or Mo(V) or W(V) with the same volumes of Aliquat 336 in chloroform or carbon tetrachloride solutions. The mixture was mechanically shaken at 25 °C. After centrifuging the solution, both the phases were pipetted in separate tubes and then subjected to γ- or X-ray spectrometry. The quantity of Mo(V) was determined by thiocyanate method. In solid-liquid extraction, cation-exchange resin (DOWEX^{TM} 50W×8) or MCI GEL CHP20/P30 powder sorbed by Aliquat 336 and 0.5–1 mL of 0.1–11 M HCl solution containing ^{95}Nb, ^{179}Ta, and ^{233}Pa tracers was mixed. The aqueous solution was pipetted into another tube and the sample was subjected to γ- or X-ray spectrometry. In all solid-liquid extraction, control experiments without the resin were performed to determine the radioactivities on the resin indirectly. We also carried out solvent extraction with a flow-type extraction apparatus. Distribution ratio (D) and distribution coefficient (K_d) were determined from radioactivity of RI tracer or concentration of Mo(V).

III. RESULTS AND DISCUSSION

In the results of the cation-exchange of Nb, Ta, and Pa, the K_d value was in the sequence of Ta > Pa > Nb. In the liquid-liquid extraction and solid-liquid extraction of the anionic complexes of Nb, Ta, and Pa using Aliquat 336, the D value and K_d value were in the sequence of Pa > Nb > Ta. From HCl concentration dependences of the K_d and D values, Nb forms neutral and anionic complexes in 0.1–4 M and 5–11 M HCl, respectively. The Ta forms cationic and neutral complexes in 0.1–5 M and 6–11 M HCl, respectively. The Pa forms cationic, neutral, and anionic complexes in 0.1–1 M, 1–3 M, and 4–11 M HCl, respectively. Based on the comparison with these elements, we are planning to investigate the chloride complex formation of Db. In the liquid-liquid extraction of group-6 elements using Aliquat 336, the D values of Mo(VI) were higher than those of W(VI). The D values of Mo(V) were higher than those of Mo(VI). The D values of Mo(V) obtained by the reduction of Mo(VI) were in good agreement with those obtained with $[MoCl_5]$. These results suggest that reduction behavior of Sg can be observed by solvent extraction in Aliquat 336/HCl system. In contrast, the D values of W(VI) and W(V) were similar to each other. This suggests that the behavior of W(V) is similar of that of W(VI). The alternative interpretation is that W(VI) could not be reduced or W(V) was rapidly oxidized to recover W(VI) species.

Evaluation of Stopping Powers of Superheavy Ions in Al and U

Y. H. Chung
Department of Chemistry, Hallym University, 1 Hallymdaehak-gil, Chuncheon 200-702, Korea
yhchung@hallym.ac.kr

Electronic and nuclear stopping powers of superheavy ions with Z>120 in Al and U were estimated in the energy range of 0.01-0.20 MeV/u. In the previous study [1], the corresponding stopping powers of a superheavy ion with Z=120 and A=300 in several media were estimated using stopping powers of ions with 6≤Z≤92 obtained from SRIM [2]. Results were compared with those deduced from Northcliffe and Schilling's stopping-power tables [3]. In the lower energy regime the contribution of nuclear stopping powers is substantially significant in both media while it is not negligible even in the higher energy regime.

[1] Y. H. Chung, Int. J. Mod. Phys. E **19**, 1117 (2010).
[2] http://www.srim.org.
[3] L. C. Northcliffe and R. F. Schilling, Nuclear Data Tables A **7**, 233 (1970).

Separation of tungsten from LEU fission-produced ^{99}Mo solution to improve technological performance in both the processes of ^{99}Mo and ^{99m}Tc generator production

Van So Le[1] , Cong Duc Nguyen[2]
[1]Medisotec, NSW, Australia
[2]ChoRay Hospital , HCM, Vietnam

I. INTRODUCTION

^{99}Mo is a parent nuclide of the ^{99m}Tc radioisotope generator which is used in diagnostic imaging procedures in nuclear medicine world-wide. The ^{99}Mo production is mainly based on the ^{235}U fission using HEU and/or LEU targets and on the ^{98}Mo (n, γ) ^{99}Mo reaction. The conversion of present HEU-based technology to those using LEU requires a 5-6 fold increase in total uranium target weight. Consequently, LEU target possibly contains approximately five times more W contaminant than HEU target, assuming the same purity of the both types of the targets. The large amount of W is seriously challenging the performance of both the processing of ^{99}Mo stock solution and the ^{99m}Tc generator production. So the development of the method of W separation from LEU-produced ^{99}Mo solution should be addressed.

II. METHODS

A ^{99}Mo/^{188}W-spiked simulator of the fission ^{99}Mo solution containing (0.05 mg Mo + 0.06 mg W) per mL and the contaminant ions was used for W/Mo separation method development. The element composition of the simulator solution is mimicked based on an elemental analysis result of a real ^{99}Mo solution sample which is obtained from the chemical processing steps in which a base-dissolution-processed ^{99}Mo solution of LEU (20% ^{235}U) target is passed through anion exchange (AG-1 X8 and AGMP) and Chelex resin columns to remove the majority of fission products.

K_d values of molybdate and tungstate ions adsorption on the acidic alumina in the above mentioned simulator solution of variable acidity were first studied as described in the literature [1]. The separation process was then performed using a chromatographic column of 1.0 g acidic alumina sorbent, on which a given amount of the simulator solution was loaded. The elution of ^{99}Mo-molybdate ions was performed by sulphuric and/or nitric acid solutions with an acidity optimised based on the K_d measurement results. Tungstate ions were then striped out of the column with 5 mL 1.0 M NH_4OH solution. The elution fractions of 5 mL were collected and their ^{99}Mo/^{188}W radioactivity was measured using an Ortec gamma-ray spectrometer coupled with HpGe detector.

III. RESULTS

The K_d values versus acidity of H_2SO_4 solutions and the elution profile of ^{99}Mo/W separation are shown in Fig.1 and Fig. 2, respectively. Based on the obtained results it is stated that the separation of ^{99}Mo from W contaminant can be effectively performed using a small acidic alumina column and H_2SO_4 eluant. This process can be conveniently integrated with the base-dissolution technology process of LEU target-based ^{99}Mo production. This additional alumina column separation step, following the step of AG-1 X8/AGMP anion exchange and Chelex resin column separation, is proposed to eliminate or reduce W contaminant content from ^{99}Mo solution. A typical design of a chromatographic column loaded with 5-10 g acidic alumina and the elution of ^{99}Mo with 50-70 mL 4 M H_2SO_4 solution can be effectively used to remove more than 80% W contaminant content (~ 100 mg W) from a 3665 Ci activity (E.O.B) ^{99}Mo solution (~ 70 mg Mo) produced using 18.4 g ^{235}U LEU target neutron-activated for 120 hours in the OPAL reactor. The ^{99}Mo recovery yield is >96 %.

REFERENCE

[1] Le, VS, Morcos N. (2008) New SPE column packing material: Retention assessment method and its application for the radionuclide chromatographic separation, J Radioanal nucl Chem, 277: 651-661

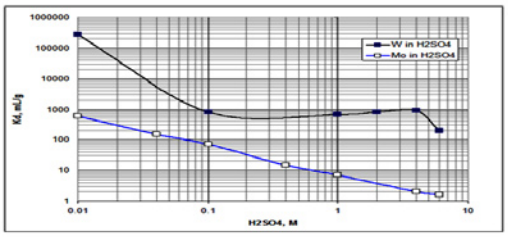

Fig. 1. Weight distribution coefficient of WO_4^{2-} and MoO_4^{2-} ions vs. H_2SO_4 solution acidity for alumina sorbent

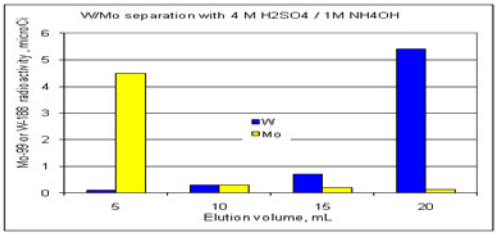

Fig. 2. Elution profile of WO_4^{2-} and MoO_4^{2-} ions (Column: 1 g alumina; Eluent: 4 M H_2SO_4 for MoO_4^{2-} and 1 M NH_4OH for WO_4^{2-}; Loading solution: Simulator solution containing 8 mg Mo + 10 mg W.

APSORC'13 - 5th Asia-Pacific Symposium on Radiochemistry
Kanazawa, Japan, 22-27 September 2013

Effecting Separation of Fission Products from the Actinides By Direct Reaction with Diketones

Daniel B. Rego, Paul M. Forster, Kenneth R. Czerwinski
University of Nevada, Las Vegas

Abstract – The use of diketone ligands, such as hexafluoroacetylacetone (Hhfac) and tetramethylheptandione (Htmhd), can react in solvent -free and solvent-minimal routes to effect separation fission products from uranium matrices without any pre-preparation of the isotopes in question, and provides a path to drastically simplify the separations process and limits the potential for contamination and waste formation due to extensive handling, while increasing the rapidity of separation and isolation of target elements. In particular, the reactivity cesium, barium, strontium, silver, and lead [1] with Hhfac can allow for rapid separations from uranium matrices such as oxide mixtures, in some cases in a matter of minutes.

Keywords – Fission Products, Uranium, Cesium, Strontium, Volatility, Separations.

I. INTRODUCTION

Current radioelement separations necessitate the dissolution of solids in either an acidic aqueous solution or a molten salt. The resulting solutions must be manipulated through a variety of means to achieve the desired separation. These manipulations can involve a complex set of conditions (e.g., the UREX+ suite of separations). Volatile dikeotones, such as hexafluoroacetylacetone (Hhfac) and tetramethylheptandione (Htmhd), have been used to react with, and isolate with crystalline purity, fission products [2,3] and actinides [4,5] such as uranium (figure 1) and neptunium.

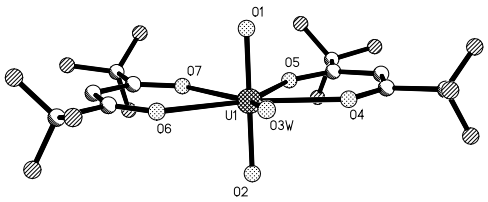

Ball and stick diagram of $UO_2(hfac)_2(H_2O)$.

Initial studies have focused on characterizing the coordination with the diketone ligands. The use of coordinating ethers to help break up matrices in order to maximize volatility has been examined and can increase the volatility and separatability of species from uranium matrices: For example, cesium hexafluroacetylacetonate forms an extended polymeric structure with extensive Cs-O and Cs-F coordination; in contrast, the use of diglyme or 18-crown-6 reduces this extensive cross-coordination significantly.

Direct separation of reactive species from uranium containing oxide mixtures has been demonstrated. The additional ability of exploiting differences in volatility of these diketone complexes themselves serves as a secondary method of separating the isotopes in question with limited handling and processing. [6] The flexibility of this system can allow for customization to fit specific scenarios and situations. Single solvent extraction from solid material, or volatilization of treated solid samples, are utilizable routes. An additional route is that these metal complexes are often used as metal vapor deposition precursors. [7] Thus, a pure metal could be obtained directly from vapor phase volatile complexes formed directly in the reaction mixture from the oxides and vaporous ligands *in situ*, which would allow for the potential combination of separations with metal formation in a single step.

[1] (a) Evans, W. J.; Rego, D. B.; Ziller, J. W. *Polyhedron* **2006**, *25*, 2691-2697. (b) Malandrino, G.; Nigro, R. L.; Rossi, P.; Dapporto, P.; Fragalá, I. L. *Inorg. Chim. Acta* **2004**, *357*, 3927. (c) Rego, D. B. Lanthanide Reduction Chemistry of the LnZ_3/M and LnZ_2Z'/M Systems and Related Coordination Chemistry Dissertation, University of California, Irvine, **2007**.
[2] (a) Evans, W. J.; Giarikos, D. G.; Johnston, M. A.; Greci, M. A.; Ziller, J. W. *J. Chem. Soc., Dalton Trans.* **2002**, 520-526. (b) Fragalà, L.; Maladrino, G.; Benelli, C.; Castelli *Chem. Mater.* **1998**, *10*, 3434. (c) Fragalà, L. Maladrino, G.; Incontro, O.; Castelli, F. *Chem. Mater*, **1996**, *8*, 1292.
[3] (a) Krisyuk, V.V.; Sysoev, S. V.; Fedotova, N. E.; Igumenov, I. K.; Grigorieva, N. V. *Thermochim. Acta* **1997**, *307*, 107-115. (b) Drake, S. R.; Hursthouse, M. B.; Abdul Malik, K. M.; Miller, S. A. S. *Inorg. Chem.* **1993**, *32*, 4653-4657. (c) Darr, J. A.; Poliakoff, M.; Blake, A. J.; Li, W.-S. *Inorg. Chem.* **1998**, *37*, 5491-5496. (d) Strasser, A.; Vogler, A. *Inorg. Chem. Comm.* **2004**, *7*, 528-530. (e) Azad Malik, M.; O'Biren, P.; Motevalli, M.; Jomes, A. C.; Leedham, T. *Polyhedron* **1999**, *18*, 1641-1646. (f) Fenton, D. E.; Newman, R. *J. Chem. Soc., Dalton Trans.* **1974**, 655-657. (g) Cotton, F. A.; Holm, R. H. *J. Am. Chem. Soc.* **1960**, *82*, 2979-2983.
[4] (a) Nikitenko, S. I.; Moisy, Ph.; Tcharushnikova, I. A.; Blanc, P.; Madic, C. *Ultrasonics Sonochemistry*, **2000**, *7*, 177-182. (b) Danford, M. D.; Burns, J. H.; Higgins, C. E.; Stokely, J. R., Jr.; Baldwin, W. H. *Inorg. Chem.* **1970**, *9*, 1953-1955. (c) Morris, M. L.; Moshier, R. W.; Sievers, R. E. *Inorg. Chem.* **1962**, *1*, 411-412.
[5] (a) Giarikos, D.G. Dissertation. University of California, Irvine, **2003**. (b) Yamamura, T.; Shiokawa, Y.; Yamana, H.; Moriyama, H. *Electochim. Acta* **2002**, *48*, 43-50. (c) Kramer, G. M.; Dines, M. B.; Kaldor, A.; Hall, R.; McClure, D. *Inorg. Chem.* **1981**, *20*, 1421-1426. (d) Kramer, G. M.; Dines, M. B.; Hall, R. B.; Kaldor, A.; Jacobson, A. J.; Scanlon, J. C. *Inorg. Chem.* **1980**, *19*, 1340-1347.
[6] Sedai, B.; Heeg, M. J.; Winter, C. H. *Organometallics*, **2009**, *28*, 1032-1038.
[7] Lin, W., Warren, T.H., Nuzzo, R.G., and Girolami, G.S.: J. Am. Chem. Soc., **115 (24),** 11644–11645 (1993).

APSORC'13 - 5th Asia-Pacific Symposium on Radiochemistry
Kanazawa, Japan, 22-27 September 2013

Muonic Atom Formation by Muon Transfer Process in C_6H_6 / C_6H_{12} + CCl_4 Mixtures

M. Inagaki[1], K. Fujihara[1], G. Yoshida[1], K. Ninomiya[1], Y. Kasamatsu[1], A. Shinohara[1], M. K. Kubo[2], W. Higemoto[3], Y. Miyake[4], T. Miura[5]
[1]Graduate School of Science, Osaka University
[2]Colleage of Liberal Arts, International Christian University
[3]Advanced Science Research Center, Japan Atomic Energy Agency
[4]Institute of Materials Structure Science, High Energy Accelerator Research Organization (KEK)
[5]Radiation Science Center, High Energy Accelerator Research Organization (KEK)

Abstract – Negative muon transfer process in the mixtures of C_6H_6 / C_6H_{12} + CCl_4 was studied. The muonic Cl X-ray structure of C_6H_6 + CCl_4 mixture sample was similar to that of pure CCl_4 sample. However, the muonic Cl X-ray structure of C_6H_{12} + CCl_4 mixture sample was different from that of pure CCl_4 sample. This result can be explained by assuming that the number of muons transferred to chlorine atoms in C_6H_6 + CCl_4 mixture sample is smaller than that in C_6H_{12} + CCl_4 mixture sample. This fact suggests that the muon transfer rate for carbon atoms of C_6H_6 is higher than that for carbon atoms of C_6H_{12}.

Keywords – Muonic Atom, Exotic Atom, Muon Transfer, Muonic X-ray

I. INTRODUCTION

A muonic hydrogen is one of the simplest exotic atom that consists of a muon and a proton. The charge of a proton is strongly shielded by a muon in the muonic hydrogen because the mass of a muon is 206 times larger than that of an electron. The muonic hydrogen can diffuse in the substance like a neutron and transfer the muon to the other heavier atoms. This process is known as muon transfer process. The transfer process occurs also in the case of a pionic hydrogen, which consists of a pion and a proton.

It is reported that the structure of molecule affects the formation or transfer process of the exotic atom. This effect is called as chemical effect. In the previous study on pion transfer process, we investigated the chemical effect in mixtures of C_6H_6 / C_6H_{12} + CCl_4. The pion transfer rate for carbon atoms of C_6H_6 is twice higher than that for C_6H_{12} [1]. In this study, we examined the chemical effect on the muon transfer in the same sample system.

II. EXPERIMENTAL

The muon irradiation experiments were performed at the MUSE D2 beam line of Materials and Life Science Experimental Facility in Japan Proton Accelerator Research Complex (J-PARC). We selected the following samples for measurement; C_6H_6 + CCl_4 (33%) mixture, C_6H_6 + CCl_4 (3%) mixture, C_6H_{12} + CCl_4 (33%) mixture, C_6H_{12} + CCl_4 (3%) mixture, pure C_6H_6, pure C_6H_{12}, and pure CCl_4. Muonic X-rays, which are emitted after formation of muonic atoms, were measured by Ge detectors.

III. RESULTS AND DISCUSSION

The experimental muonic Cl X-ray structure (muonic X-ray intensity ratios) in pure CCl_4, C_6H_{12} + CCl_4 (33%) mixture and C_6H_6 + CCl_4 (33%) mixture samples are shown in Fig. 1.

The relative intensity of Cl (5–3) / Cl (4–3) and Cl (4–2) / Cl (3–2) in C_6H_{12} + CCl_4 mixture sample was smaller than that in pure CCl_4 sample. The difference indicates that initial state (principal and angular momentum quantum number) of the muon captured by chlorine atoms in C_6H_{12} + CCl_4 mixture sample is different from that in pure CCl_4 sample. Because the muon transfer occurs in C_6H_{12} + CCl_4 mixture sample while no muon transfer in pure CCl_4 sample, it seems that the muon transfer process changes the initial state of the muon captured by chlorine atoms in C_6H_{12} + CCl_4 sample. On the other hand, although the muon transfer also occurs in C_6H_6 + CCl_4 sample, the muonic X-ray structure of that was similar to pure CCl_4 sample. This can be explained by assuming that the number of muons transferred to chlorine atoms in C_6H_6 + CCl_4 sample is smaller than that in C_6H_{12} + CCl_4 sample. This fact suggests that the muon transfer rate for carbon atoms of C_6H_6 is higher than that for carbon atoms of C_6H_{12}. Despite using different particle, this result is consistent with the previous study for pion transfer in the same sample system [1].

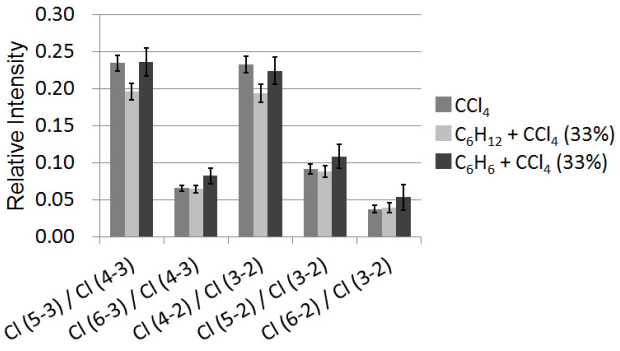

Fig. 1. Muonic chlorine X-ray structure. Cl (n–n′) means muonic Cl X-ray emitted with muon deexcitation from principal quantum number n to n′.

[1] A. Shinohara *et al.*, Hyperfine Interact. **106**, 301 (1997).

Research for Fusion Reaction Mechanisms with Deformed Nuclei

S. Ueno[1], K. Toda[1], A. Asano[1], N. Takahashi[2], Y. Kasamatsu[2], T. Yokokita[2], A. Yokoyama[3],
[1]Graduate School of Natural Science and Technology, Kanazawa Univ.
[2]Graduate School of Science, Osaka Univ.
[3]Institute of Science and Engineering, Kanazawa Univ.

Abstract – In order to better understand the reaction on the fusion reaction, we have focused on the deformation of the nuclei. We have researched for the fusion reactions of $^{169}Tm+^{16}O$ [1], $^{169}Tm+^{20}Ne$, and $^{165}Ho+^{20}Ne$ [2]. The cross sections for fusion were compared between systems of different entrance channels. The results are consistent with the idea that the degree of deformation makes an effect on the rising edge of excitation functions near the Coulomb barrier.

Keywords – Fusion reaction/ Excitation function/ Deformed nucleus

I. INTRODUCTION

Heavy ion fusion reaction is often used in the synthesis of heavy elements recently. For the synthesis of trans-actinides, evaporation residues cross section is very small compared to fission. Briefly, it is important to understand the reaction mechanism and to know the conditions for efficient synthesis.

We have focused on the deformation of nuclei. In this study, in order to study the effect of the degree of nuclear deformation on the fusion reaction, we have researched for the fusion reactions of $^{169}Tm+^{16}O$ [1], $^{169}Tm+^{20}Ne$, and $^{165}Ho+^{20}Ne$ [2]. Figure 1 shows deformed nuclei in a spheroid model and Table 1 shows the degree of nuclear deformation of ^{20}Ne, ^{16}O, ^{169}Tm and ^{165}Ho based on the model. In $^{169}Tm+^{20}Ne$ and $^{165}Ho+^{20}Ne$ systems, the target nucleus ^{165}Ho is more deformed than ^{169}Tm. In $^{169}Tm+^{16}O$ and $^{169}Tm+^{20}Ne$ systems, the projectile nucleus ^{16}O is spherical, while ^{20}Ne is deformed. Both systems of $^{169}Tm+^{16}O$ and $^{159}Ho+^{20}Ne$ form the same compound nucleus, $^{185}Ir^{*}$.

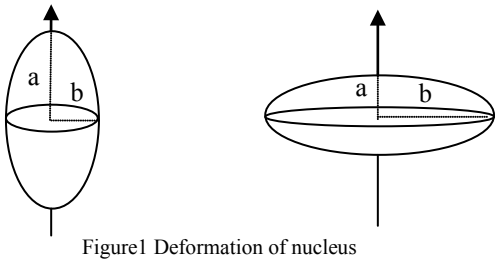

Figure1 Deformation of nucleus

Table1 Degree of deformation of relevant nuclei

	^{20}Ne	^{16}O	^{169}Tm	^{165}Ho
a/b	0.75	1.00	0.95	1.16

II. EXPERIMENTAL

The bombardment for synthesis was carried out using ^{16}O and ^{20}Ne beam supplied from the AVF cyclotron facility at Research Center for Nuclear Physics (RCNP), Osaka University. The targets were prepared by electrodeposition with standard solution on an Al foil of 2.7 mg/cm^2 thickness. For instance, the ^{169}Tm content was 4.5-5.1 mg/cm^2 in thickness. In order to achieve experiments of wide energy range in a single irradiation, energy degradation technique was used. In the present experiment using two stacks with four targets each, each target was irradiated at a different energy below 155 MeV in $^{169}Tm+^{20}Ne$ system. Typical beam intensity was 1 particle-μA. The activities produced in each target were assayed using a high resolution HPGe detector. Excitation function was made from the measured activities.

III. RESULTS AND DISCUSSION

The evaporation residues detected, for instance, in $^{169}Tm+^{20}Ne$ system were ^{185}Pt, $^{183-185}Ir$, $^{181,182}Os$ and ^{181}Re. Figure 2 shows the excitation function for fusion reaction of $^{169}Tm+^{20}Ne$, $^{169}Tm+^{16}O$ [1] and $^{165}Ho+^{20}Ne$ [2] compared with the theoretical calculations using code HIVAP taking into consideration degree of deformation of nucleus. In order to compare the systems between different entrance channels, let the value obtained by subtracting the Coulomb barrier [3] from the incident energy, ($E_{cm}-B_c$), be the horizontal axis in the figure. Comparing $^{169}Tm+^{16}O$, $^{169}Tm+^{20}Ne$ and $^{159}Ho+^{20}N$ systems, more deformed system of $^{159}Ho+^{20}Ne$ induced fusion reaction from lower incident energy. Comparing $^{169}Tm+^{20}Ne$ and $^{165}Ho+^{20}Ne$ systems, starting points for fusion reaction were nearly the same. The trends were reproduced by HIVAP calculation.

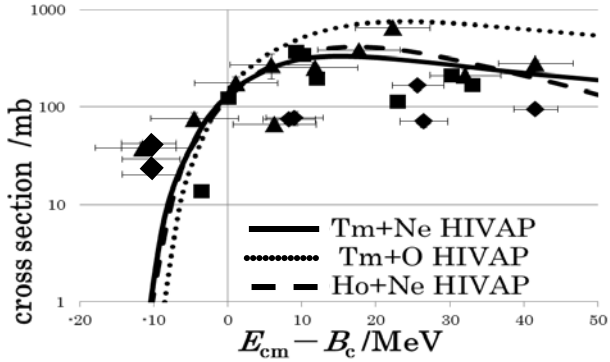

Figure2 Excitation function of $^{169}Tm+^{20}Ne$ (◆), $^{169}Tm+^{16}O$ (■) [1] and $^{165}Ho+^{20}Ne$ (▲) [2] compared to theoretical values of each system

[1] A. Asano, master thesis of Kanazawa Univ. (2010)
[2] K. Toda, master thesis of Kanazawa Univ. (2013)
[3] R. Bass, *Nuclear Reactions with Heavy Ions*, Springer-Verlag, New York (1980)

Extraction behavior of Nb and Ta in HF solutions with tributyl phosphate

M. Murakami[1,2], S. Tsuto[1], K. Ooe[1], H. Haba[2], J. Kanaya[2], S. Goto[1], and H. Kudo[1]
[1]Department of Chemistry, Faculty of Science, Niigata University, Niigata 950-2181, Japan
[2]Nishina Center for Accelerator-Based Science, RIKEN, Saitama 351-0198, Japan

Abstract – Extrtaction behavior of carrier-free Nb and Ta with tributyl phosphate (TBP) from HF solutions was studied by a batch method. Tantalum is extracted well to an organic phase, while Nb is left in an aqueous phase at 0.053–1.0 M HF concentrations. The similar extraction trends of Nb and Ta are shown in the solid phase extraction using a TBP resin. The extraction equilibria in the solid phase extraction are attained within ~10 s.

Keywords – niobium, tantalum, extraction, tributyl phosphate

I. INTRODUCTION

In the synthesis experiment of an element 115, chemically separated 27-h spontaneously fissioning nuclide was assigned to ^{268}Db which is the descendant of ^{288}115 [1,2]. To clarify this 27-h nuclide is actually Db, further chemical investigations are needed for both of known nuclides of dubnium, ^{262}Db ($T_{1/2}$ = 34 s), and 27-h spontaneously fissioning nuclide.

Tributyl phosphate (TBP) is one of the most effective extractants used for industrial separation of Nb and Ta [3]. In this work, solvent extraction behavior of Nb and Ta with TBP was first studied by a batch method. Solid phase extraction with a TBP resin was also performed to examine the feasibility of this resin to an automated rapid reversed-phase chromatography apparatus for ^{262}Db.

II. EXPERIMENTAL

The radiotracers ^{95g}Nb ($T_{1/2}$ = 34.991 d) and ^{179}Ta ($T_{1/2}$ = 1.82 y) were produced in the bombardments of 14-MeV proton beam supplied by the RIKEN AVF cyclotron on ^{nat}Zr and ^{nat}Hf target foils, respectively.

In the experiment of the solvent extraction, 1 mL of HF solution containing ^{95g}Nb and ^{179}Ta tracers were shaken with 1 mL of TBP−1,2-dichloroethane solution for 180 min at 25°C. After centrifugation, 700 μL of each phase was transferred to an polypropylene tube separately, and then subjected to γ- and X-ray measurements with a Ge detector. The distribution ratios (D) of Nb and Ta were deduced from the observed radioactivities.

The solid phase extraction was performed with following procedures. TBP resin was prepared by adsorbing TBP on a support material (MCI GEL CHP20/P30, Mitsubishi Chemical Co.) [4]. A portion of 20 to 30 mg of the TBP resin was shaken with 400 μL of HF solution containing ^{95g}Nb and ^{179}Ta tracers for 6 s to 60 min. After filtration, 200 μL aliquot was transferred to a polypropylene tube. The distribution coefficients of Nb and Ta were calculated with the observed radioactivities and the weight of the used resin.

III. RESULTS AND DISCUSSION

Figure 1 shows the dependence of the D values of Nb and Ta on the initial HF concentration ($[HF]_{ini}$) with 1.8 M TBP − 1,2-dichloroethane solution as an organic phase. Tantalum was extracted well at the $[HF]_{ini}$ of 0.053 to 1.0 M, while Nb was left in an aqueous phase.

The number of TBP molecules combined with the Nb and Ta compounds was examined by varying the TBP concentration at the constant $[HF]_{ini}$. The number of combined TBP molecules was found to be 3 for Ta at $[HF]_{ini} \leq 2.7$ M. This agrees with the results in Refs. [3,4]. Although the number of TBP molecules combined with the Nb compound is reported as 3 [3], our results show that the number is 2 independently of $[HF]_{ini}$. This results show that Nb and Ta are extracted with different chemical forms.

Using the 48 wt-% TBP resin, the dependence of the distribution coefficients of Ta on $[HF]_{ini}$ was similar to that of the D values in the liquid-liquid solvent extraction. Niobium was not extracted at ≤ 10 M. The time required for the extraction equilibrium was less than 12 s for both of Nb and Ta. This indicates that the present extraction system could be applicable to an on-line experiment with the short-lived ^{262}Db.

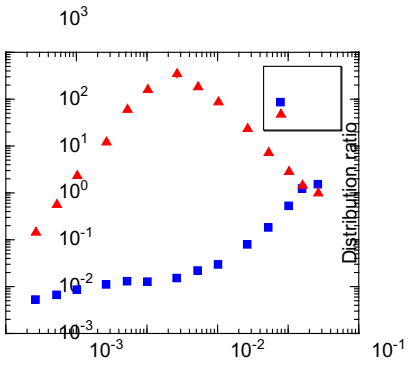

Fig. 1. Distribution ratios of Nb and Ta.

[1] S. N. Dmitriev et al., Mendeleev Commun. **15**, 1 (2005).
[2] N. J. Stoyer et al., Nucl. Phys. A **787**, 388c (2007).
[3] Z. Zhu and C. Y. Cheng, Hydrometallurgy **107**, 1 (2011).
[4] H.Haba *et al.*, Radiochim. Acta **95**, 1 (2007).
[5] S. Nishimura et al., Trans. JIM **5**, 79 (1964).

A MODIFIED METHOD FOR SYNTHESIS OF [γ-^{32}P] LABELLED ADENOSIN TRIPHOSPHATE

Wira Y Rahman[1]*, Endang Sarmini[1], Herlina[1], Triyanto[1], Rien Ritawidya[1], Abdul Mutalib[1] and Santi Nurbaiti[2]

[1] Center for Radioisotope and Radiopharmaceuticals (PRR) - BATAN)
[2]Biochemistry Research Division, faculty of Mathematics and Natural Sciences, Institut Teknologi Bandung, Jl. Ganesha 10 Bandung, Indonesia, 40132
*Tel/fax : (6221)7563141, email: wira@batan.go.id

ABSTRACT

Adenosine triphosphate-labelled with γ-^{32}P (γ-^{32}P]-ATP) has been widely used in the biotechnology research, usually as a tracer to study aspects of physiological and pathological processes. In order to support biotechnology research in Indonesia, a process for production of [γ-32P]-ATP in accordance with a more simple glycolysis enzymatic reaction utilizing glyceraldehid 3-phosphate dehydrogenase, 3-phosphoglyceryc phosphokinase and lactate dehydrogenase has been conducted. DL-glyceraldehydde 3-phosphate, *Adenosine Diphosphate (ADP) and $H_3{}^{32}PO_4$ was used as precursors for this reaction. Purification of [γ-^{32}P]-ATP was performed by using DEAE-Sephadex column chromatography. The results showed that radiochemical purity of [γ-^{32}P]-ATP was 99,49% with radioactivity was 1,175 mCi for 20 minutes enzymatic reaction. The result suggested that this modification method can be used for producing [γ-^{32}P]-ATP to support the provision of radiolabeled nucleotide for biotechnology research in Indonesia.*

Key words *: labeled nucleotide [γ-^{32}P]-ATP, synthesis, enzymatic reaction, DEAE-Sephadex column chromatography*

Production of ^{88}Nb and ^{170}Ta for chemical studies of element 105 Db using the GARIS gas-jet system

M. Huang,[1] M. Asai,[2] H. Haba,[1] D. Kaji,[1] J. Kanaya,[1] Y. Kasamatsu,[3] H. Kikunaga,[4] Y. Kikutani,[3] Y. Komori,[3] H. Kudo,[5] Y. Kudou,[1] K. Morimoto,[1] K. Morita,[1] M. Murakami,[5] K. Nakamura,[3] K. Ozeki,[1] R. Sakai,[1] A. Shinohara,[3] T. Sumita,[1] K. Tanaka,[1] A. Toyoshima,[2] K. Tsukada,[2] Y. Wakabayashi[1] and A. Yoneda[2]

[1]Nishina Center for Accelerator-Based Science, RIKEN
[2]Advanced Science Research Center, JAEA
[3]Graduate School of Science, Osaka University
[4]Research Center for Electron Photon Science, Tohoku University
[5]Department of Chemistry, Niigata University

Abstract – We developed a production technology for radioisotopes of Ta and Nb for chemical studies of element 105, Db, using the RIKEN gas-filled recoil ion separator, GARIS. Isotopes of ^{170}Ta and ^{88}Nb produced via the ^{nat}Gd(^{19}F, xn)^{170}Ta and ^{nat}Ge(^{19}F, xn)^{88}Nb reactions, respectively, were successfully extracted by the gas-jet method to a chemistry laboratory after physical separation by GARIS.

Keywords – superheavy element chemistry, Nb, Ta, Db, GARIS, gas-jet method, recoil transfer chamber

We plan to study chemical properties of element 105, Db, produced in the ^{248}Cm(^{19}F,5*n*)^{262}Db reaction using the gas-jet transport system coupled to the RIKEN gas-filled recoil ion separator, GARIS[1]. It is important to perform Db chemistry together with Ta and Nb under identical conditions to find different chemical behavior among the homologues. In this work, we tried to produce isotopes of ^{170}Ta ($T_{1/2}$ = 6.76 min) and ^{88}Nb ($T_{1/2}$ = 14.55 min) in the ^{nat}Gd(^{19}F, *xn*)^{170}Ta and ^{nat}Ge(^{19}F, *xn*)^{88}Nb reactions, respectively, using the GARIS gas-jet system.

A 106.4-MeV ^{19}F^{9+} beam was extracted from the RIKEN linear accelerator. A ^{nat}Ge target of 0.29 mg/cm^2 thickness was prepared by vacuum evaporation onto a 0.89 mg/cm^2 Ti backing foil, while a ^{nat}Gd_2O_3 target of 0.34 mg/cm^2 was prepared by electro-deposition on a 0.87 mg/cm^2 Ti foil. The two arc-shaped Ge targets and two Gd_2O_3 were mounted together with four 0.95 mg/cm^2 Ti blank foils on a rotating wheel of 100-mm diameter, which was rotated at 1000 rpm. The beam energy was 103 MeV in the middle of the target and the typical intensity was approximately 3 particle μA (pμA). The working He pressure of GARIS was 33 Pa. At the focal plane of GARIS, a recoil transfer chamber (RTC) of 100-mm inner diameter and 0~100-mm adjustable depth was installed. Evaporation residues separated with GARIS were passed through a 0.5-μm Mylar window, thermalized in RTC, and were transported by the He/KCl-aerosol-gas-jet system to a chemistry laboratory. The He flow rate was 2.0 L/min, and the inner pressure of RTC was 47 kPa. After collection of the aerosols on a glass filter (ADVANTEC GB-100R) for 1 and 3 min for ^{170}Ta and ^{88}Nb, respectively, the filters were subjected to γ-ray spectrometry using a Ge detector. The magnetic setting of GARIS was varied in the magnetic rigidity ($B\rho$) range of 1.51–1.80 Tm for ^{170}Ta and 0.850–0.979 Tm for ^{88}Nb. In the GARIS separation of ^{88}Nb at low $B\rho$ values, the beam particles with lower charge states broke the thin Mylar foil of RTC. Thus, we installed a retractable Al shutter of 2-mm thickness and 30×100-mm^2 size at the focal plane to protect the Mylar foil from the undesired beam particles. The gas-jet efficiencies are very sensitive to the depth of RTC and recoil ranges of the evaporation residues in RTC. To effectively collect ^{88}Nb atoms in RTC, a 3-μm Al degrader foil was used to reduce their recoil ranges before entering the RTC.

The 221.2-keV and 671.2-keV γ-rays are useful for chemical studies of ^{170}Ta and ^{88}Nb, respectively. Yield distributions of ^{170}Ta and ^{88}Nb related to $B\rho$ are displayed in Fig. 1. The optimal $B\rho$ of 1.64±0.01 and 0.936±0.001 Tm were determined for ^{170}Ta and ^{88}Nb, respectively. Under the optimal $B\rho$ and with the 100-mm depth RTC, the production yields of ^{170}Ta and ^{88}Nb in the chemistry laboratory were evaluated to be 8.65±0.56 and 0.61±0.02 kBq/pμA after 1-min and 3-min aerosol collection, respectively. The gas-jet efficiency of ^{88}Nb was 41±2%, while that of ^{170}Ta was 77±3%.

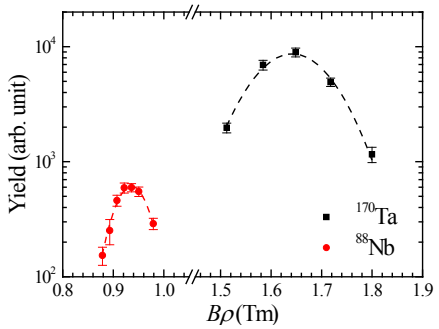

Fig.1. Yields of ^{170}Ta and ^{88}Nb as a function of $B\rho$.

[1] H. Haba et al.: Chem. Lett. **38**, 426 (2009).

Half-life measurement of ^{7}Be in several materials

T. Ohtsuki
Research Center for Electron Photon Science, Tohoku University
1-2-1, Mikamine, Taihaku, Sendai, 982-0826, Japan

Abstract – The formation of atom-doped C60 and C70 etc. has been investigated by using several types of radionuclides produced by nuclear reactions. From the trace of the radioactivities after high performance liquid chromatography (HPLC), it was found that formation of endohedral fullerenes of Be atom is possible by a recoil process following the nuclear reaction. The decay rate of ^{7}Be electron capture (EC) was measured in C 7 0 and Be metal with a reference method. The half-lives of ^{7}Be endohedral C70 and ^{7}Be in Be metal (Be metal(^{7}Be)) were found to be 52.45±0.04 and 53.25±0.04 days, respectively. This amounts to a 1.5% difference in the EC-decay half-life between ^{7}Be@C70 and Be metal(^{7}Be). The results are a reflection of the different electron wave-functions in nuclear site for ^{7}Be inside C70 compared to when ^{7}Be is in a Be metal. The further theoretical interpretation is needed for these experimental results.

Keywords – Electron Capture Decay, Beryllium-7, Half-life

I. INTRODUCTION

A long-standing challenge has been to establish the degree to which manipulation of the environmental factors can in practice change nuclear decay rates in experiments to determine the decay rate of ^{7}Be compounds. In addition, there have been several observations of variations in the half-life with host metals, chemical forms, and pressure. From the early data, the half-life of ^{7}Be as a function of different chemical forms and/or host materials have been limited almost to within 0.2%. In recent studies, however, large variations have been observed as a function of different chemical forms and pressures. Therefore, a precise measurement is still needed to obtain the absolute decay rate in different circumstances.

After the discovery of C_{60} and the subsequent successful production of several kinds of fullerenes, endohedral fullerenes which have one or more atoms inside the C_{60}, C_{70}, cages etc. currently have attracted great interest. If their mass production becomes possible, they would have many interesting applications such as stable molecular devices in nano-meter scales and/or as functionalized materials in many fields. We have examined the formation of endohedral fullerenes by a nuclear recoil implantation of several foreign atoms following nuclear reactions[1,2]. We found that the ^{7}Be atom can be endohedrally doped to create the ^{7}Be endohedral fullerenes.

Because of the unique chemical form of fullerenes and/or several factors contributing to give rise to this environment; many π-electrons of $C_{60}(C_{70})$, and special dynamic motions inside $C_{60}(C_{70})$ etc., the electron contact density on the ^{7}Be nuclei can be affected significantly by the electron environment of $C_{60}(C_{70})$. Therefore, it is intriguing to measure the half-life of the ^{7}Be inside $C_{60}(C_{70})$; "how does the EC decay rate in ^{7}Be change inside the $C_{60}(C_{70})$ cage relative to other situations?"

So far, we compared the half-life of ^{7}Be when it is encapsulated in a C_{60} cage to that of ^{7}Be in Be metal as a reference. We found a surprisingly shorter half-life of ^{7}Be inside C_{60}[3,4]. This fact implied that the ^{7}Be atoms are located in a unique environment inside C_{60} cage. Furthermore, in order to see the size effect of fullerenes, we demonstrate the change of decay rete of ^{7}Be in ^{7}Be@C_{70} and in Be metal [Be metal(^{7}Be)]. The decay rate of ^{7}Be electron capture (EC) was measured in C 7 0 and Be metal with a reference method. The half-lives of ^{7}Be endohedral C70 and ^{7}Be in Be metal (Be metal(^{7}Be)) were found to be 52.45±0.04 and 53.25±0.04 days, respectively.

[1] T. Ohtsuki *et al*., Physical Review Letters 77 (1996) 3522.

[2] T. Ohtsuki *et al*., Physical Review Letters, 81 (1998) 967-970.

[3] T. Ohtsuki *et al*., Physical Review Letters 93 (2004) 112501.

[4] T. Ohtsuki *et al*., Physical Review Letters 98 (2007) 252501

APSORC'13 - 5th Asia-Pacific Symposium on Radiochemistry
Kanazawa, Japan, 22-27 September 2013

Verification of anticlockwise gyre in the semi-closed water area of Lake Nakaumi, southwest Japan, by using $^{224}Ra/^{228}Ra$ activity ratios

Ritsuo Nomura[1],* Mutsuo Inoue[2], Hisaki Kofuji[3] and Shota Ikeda[1]
[1] Foraminiferal Laboratory, Faculty of Education, Shimane University, Matsue 690-8504 Japan
[2] Institute of Nature and Environmental Technology, Kanazawa University, Wake, Nomi, Ishikawa 923-1224 Japan
[3] Mutsu Marine Laboratory, Japan Marine Science Foundation, Minato, Mutsu, Aomori, 035-0064 Japan

Abstract –
The Honjyo area in Lake Nakaumi is a semi-closed brackish water area where some mixing of up-flowing marine water and down-flowing lake water take place. A large-scale gyre that caused by the residual circulation was once indicated by a temporal algal blooming that spread over the semi-closed Honjyo area in brackish Lake Nakaumi. In order to verify this type of water circulation, we examined ^{224}Ra ($t_{1/2}$=3.66 d)/^{228}Ra ($t_{1/2}$=5.75 y) activity ratios of both upper and lower waters that differentiated by a well-developed halocline. The $^{224}Ra/^{228}Ra$ ratios in the upper water were lowest in the central area, suggesting the formation of anticlockwise gyre. The ratios in the lower water were rather uniform, but a basin-wide anticlockwise flow of water is also indicated. The $^{224}Ra/^{228}Ra$ ratio is clearly effective to trace the water flow for both the deep and surface waters.

Keywords – $^{224}Ra/^{228}Ra$ ratio, Water flow, Lake Nakaumi

I. INTRODUCTION

Estuarine biota has been critically influenced by an increased eutrophication in Japan. The environmental and biological interaction is complicate, but the water characters and the dynamic water movement are major factor to understand the total environment of estuarine water.

The Honjyo area, occupying ~20 % of Lake Nakaumi, was closed for 28 years. This closed area is now partly opened and permitted the exchange of marine water and lake water through the opened slit [1]. After the closed area opened, the original massive low salinity water changed to form a density stratification of bottom and surface waters. In order to clarify the deep and surface water dynamics, we analyzed $^{224}Ra/^{228}Ra$ ratio of both deep and surface waters to understand the water residence time and the circulation of water.

A. Methods of study

Ten sampling locations were set in and out of the Honjyo area (Fig. 1). We used Mn-fiber to collect Ra from lake water (40-60 L) prefiltered with a polypropylene filter cartridge (~1 L/min; 0.5 μm median pore size). Mn-fiber was dried and then ashed within 24 hours. Ash powder was completely sealed in the styrene bottle.

γ-Spectrometry was performed using a coaxial-type Ge-detector. The ^{224}Ra and ^{228}Ra activities were evaluated from the γ-ray peaks of ^{212}Pb (235 keV) and ^{228}Ac (338 and 911 keV), respectively. The first γ-ray counting time for ^{224}Ra and ^{228}Ra was 18,000 seconds and the second counting time was 85,000 seconds. Owing to the short half-life of ^{224}Ra, first γ-ray counting for ^{224}Ra was conducted between 3-5 days after the sampling.

II. RESULTS AND DISCUSSION

Both the upper and lower waters in the Honjyo area show lower $^{224}Ra/^{228}Ra$ ratio, compared to that in the Sakai Channel. The ratios of the upper water show the range between 0.02-0.15, and those of the lower water are 0.08-0.20. These ratios are similar to the ratio of the Nakaumi water. It is noted that the $^{224}Ra/^{228}Ra$ ratio of the upper water shows regional difference, which is higher in western and northern sides, while the central and eastern sides are lower. The $^{224}Ra/^{228}Ra$ ratios of lower water are characterized by similar ratios, excepting the place near the Ohmisaki slit.

In 2010, algae blooming spread over the surface of the Honjyo area, showed a large-scaled anticlockwise gyre in the area. Our reconstructed surface water flow, using $^{224}Ra/^{228}Ra$ ratios, is similar to the large-scale anticlockwise gyre shown by the algae powder. The $^{224}Ra/^{228}Ra$ ratios in the lower water are rather uniformly distributed, but the lower water may form a large-scale anticlockwise flow over the basin.

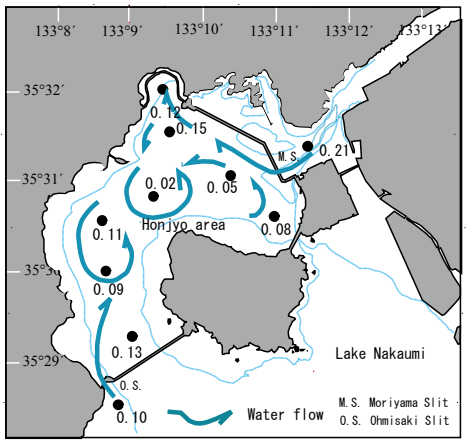

Figure 1. Distribution of $^{224}Ra/^{228}Ra$ ratios in the Honjyo area and the supposed flow of upper water.

[1] Nomura, R. et al., 2013. Opening of the closed water area and consequent changes of $^{228}Ra/^{226}Ra$ activity ratios in coastal lagoon Lake Nakaumi, Southwest Japan. Applied Radiation and Isotopes. DOI: 10.1016/j.apradiso.2013.03.069

APSORC'13 - 5th Asia-Pacific Symposium on Radiochemistry
Kanazawa, Japan, 22-27 September 2013

Effect of hydroxylated fullerene on U(VI) Adsorption onto oxidized multi-walled carbon nanotubes

Jing WANG[1], Zhan LI[2], Peng LIU[1], Wei QI[1], Juanjuan BI[1], Wangsuo WU[1]*
1 Radiochemistry Laboratory, School of Nuclear Science and Technology, Lanzhou University, Lanzhou 73000, China
2 Institute of Modern Physics, Chinese Academy of Sciences, Lanzhou 73000, China

Abstract –Herein, hydroxylated fullerene ($C_{60}(OH)_n$) was chosen as the third phase to investigate its impact on U(VI) adsorption onto carbon nanotubes. The results showed that the drastic effect of $C_{60}(OH)_n$ on U(VI) adsorption of oMWCNTs was not significant at low concentration of $C_{60}(OH)_n$, whereas a negative effect was observed at higher concentration. The adsorption of U(VI) onto oMWCNTs was enhanced with increasing pH values at pH < 6, but decreased after pH reached 6. The main mechanism may be the adsorbed Cu(II) on oMWCNTs is "squeezed" down to the solution by the adsorption of $C_{60}(OH)_n$ onto oMWCNTs. The double sorption site model was applied to simulate the adsorption isotherms of U(VI) in the presence of $C_{60}(OH)_n$ and fitted the experimental data well. This provides reference for studying the interactions between carbon nanomaterials and radionuclide in various conditions of natural environment. Meanwhile, it also brings theoretical basis for studying the biological safety problems caused by multi-component environment pollution.

Keywords –Effect, Hydroxylated fullerene, U(VI) adsorption, Oxidized multi-walled carbon nanotubes

I. INTRODUCTION

Carbon nanotubes has potential application in the disposal of nuclear fuel reprocessing, due to the large specific surface area, the surface is easy to be modified, resistant to heat and radiation. As far as we known, the study concerning the mechanism for radionuclide selective adsorption on a variety of carbon nanomaterials in the ternary system was sparse. However, it is difficult to achieve the adsorption contribution of each carbon nanomaterial when they are all chosen as adsorbent in the experiment. Two different water-soluble carbon nanomaterial must be selected as the adsorbent to resolve this problem.

$$A\% = \frac{C_2}{C_0} + \frac{e^{C_1}}{C_0} \times e^{(k \cdot b \cdot C_f)} \qquad (1)$$

Where Co (mg/L) is the initial concentration of U(VI) before adsorption; Cs (mg/g) for the equilibrium concentration of U(VI) in the solid phase after adsorption; Ce (mg/L) is the equilibrium concentration of U(VI) in the liquid phase; Cf (mg/L) is definited as the initial concentration of C60(OH)n; b is the parameter for characterization the adsorption of C60(OH)n, it depends on the species and surface character of C60(OH)n and the nature of oMWCNTs; C_1 and C_2 are the performance parameters for the sorption characterization of oMWCNTs, these parameters depend on the surface character of oMWCNTs and the nature and species of U(VI); k represents the rate constant.

Table 1 Parameters of double adsorption site model*

m/V(g·L^{-1})	DSSM model			
	C_2/C_0	e^{C_1}/C_0	k · b	R^2
1	267.26	-165.72	-773.41	0.9485
0.5	-4148.21	4246.26	12867.49	0.9739
0.25	-10.97	104.89	127.13	0.9757
0.1	-7.72	185.38	55.43	0.9457

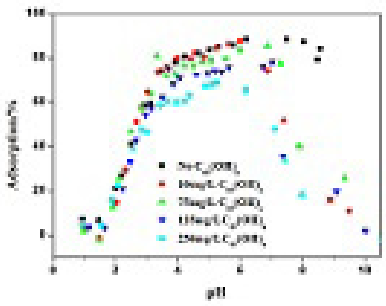

Fig. 1 Effect of $C_{60}(OH)_n$ on U(VI) adsorption onto oMWCNTs as a function of pH, *m/V* =0.5 g/L, *T* = 25±1 ºC, *I*=0.01 mol/L $NaNO_3$, C[UO_2^{2+}]initial =1.12×10^{-4} mol/L.

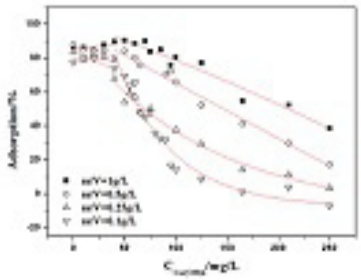

Fig. 2 Effect of oMWCNTs dosage on U(VI) adsorption onto oMWCNTs as a function of $C_{60}(OH)_n$ initial concentrations, pH=7.00±0.10, *I*=0.01 mol/L $NaNO_3$, *T* = 25±1 ºC, C[UO_2^{2+}]initial =1.12×10^{-4} mol/L.

*Corresponding author: Wangsuo Wu,
Tel & Fax:+8609318913594,
E-mail:wuws@lzu.edu.cn(W.Wu).

APSORC'13 - 5th Asia-Pacific Symposium on Radiochemistry
Kanazawa, Japan, 22-27 September 2013

Corrosion of Copper in Water and Colloid Formation under Intense Radiation Field

Kotaro Bessho[1], Yuichi Oki[2], Naoya Akimune[3], Hiroshi Matsumura[1], Kazuyoshi Masumoto[1], Shun Sekimoto[2], Naoyuki Osada[4], Norikazu Kinoshita[5], Hideaki Monjushiro[1], Seiichi Shibata[2]
[1] Radiation Science Center, High Energy Accelerator Research Organization (KEK),
[2] Research Reactor Institute, Kyoto University (KURRI), [3] Graduate School of Engineering, Kyoto University,
[4] Graduate School of Engineering, Tohoku University, [5] Institute of Technology, Shimizu Corporation

Abstract – Radiation effects on corrosion of copper in water and colloid formation were investigated. Irradiation experiments using ^{60}Co γ-ray irradiation facility and electron LINAC demonstrated that high-energy photons promote corrosion and elution of copper into water and formation of copper-related colloids / particles in water phase.

Keywords – Radiation effect, Corrosion, Colloid

I. INTRODUCTION

At high-energy accelerator facilities, colloid formation in cooling water is an important subject for radiation management at high-energy accelerator facilities, because the presence of colloidal species complicates the behavior of radionuclides in the cooling water systems [1]. It's possible that intense radiation field inside accelerator facilities affects the corrosion of metal components and formation of metal-related colloid in the cooling water. Effects of radiation on corrosion of copper and formation of copper-related colloid in water were studied.

II. EXPERIMENTS

Irradiation experiments were carried out at the ^{60}Co γ-ray irradiation facility or the electron linear accelerator (e-LINAC) at the Research Reactor Institute, Kyoto University (KURRI). Cu vessels (Inside:19ϕ x 75 mm) filled with pure water (26 ml) were irradiated by γ-rays from ^{60}Co source, or bremsstrahlung and neutrons generated by a 30 MeV electron beam striking a Ta target assembly. At the ^{60}Co γ-ray irradiation facility, samples were irradiated by γ-ray with the dose rates of 2.9 kGy/h or 21 kGy/h for 2 to 240 h. At the e-LINAC facility, irradiation experiments were carried out with several beam-current conditions, and the irradiation times were varied between 2 to 24 h.

After the irradiations, water samples in the Cu containers were collected and filtrated with four kinds of ultrafiltration (UF) units for particle size separation. Estimated pore sizes of the UF units were 200 nm, 16 nm, 7 nm, and 3 nm. Elemental concentrations of Cu in each UF filtrate and original samples before UF were determined by ICP-AES analyses.

III. RESULTS AND DISCUSSION

Figure 1 shows soluble and size-separated colloidal concentrations of Cu in water without irradiation or after the irradiation at the γ-ray irradiation facility or the e-LINAC facility. The results for the LINAC experiments were obtained at the downstream (0-deg) sample position, where flux of neutrons can be neglected compared to flux of bremsstrahlung. The results demonstrate that irradiation of high-energy photons (γ-ray or bremsstrahlung) clearly affects the elution of Cu into water and formation of Cu-related colloid / particle in water phase.

Concentration of soluble Cu species increased with photon intensity. Formation of colloidal species was also noticeable at intense photon environment. Furthermore, qualitative evaluations using water-quality test kits clarified that H_2O_2 and O_3 were generated in water by irradiating γ-ray or bremsstrahlung. These results imply that high-energy photons produce active species, such as H_2O_2, O_3 and OH radicals, in water. These active species may affect various processes, such as corrosion of Cu materials, transfer of Cu species into water as a soluble species or colloidal species, and growth of colloidal species in water phase.

Time dependence of size-profiles for Cu species formed at constant dose rates imply that dissolution of Cu materials in water and formation of Cu-related colloid occurring in intense radiation environments progress in the time scale of several hours to hundreds hours.

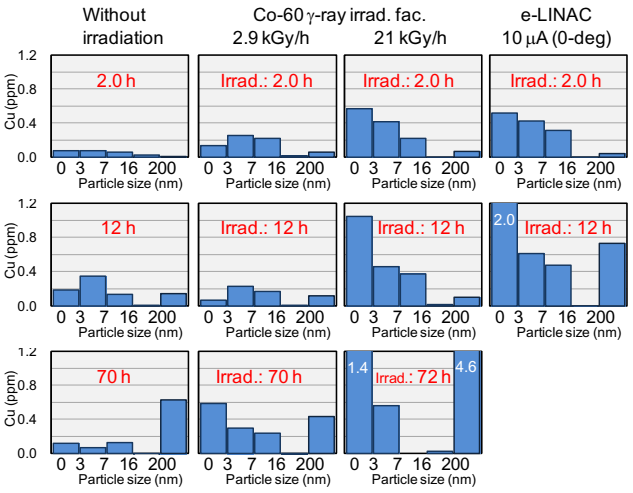

Figure 1 Soluble (0-3 nm) and colloidal concentrations (3-7, 7-16, 16-200 nm) of Cu in water without irradiation, after the irradiation at Co-60 γ-ray irradiation facility, and after the irradiation at electron LINAC. Irradiation time : 2.0 h, 12 h

[1] K. Bessho *et al.*, Eleventh Meeting of the Task-Force on Shielding Aspects of Accelerators, Targets and Irradiation Facilities (2012)

Study on Unattached Fraction of Radon Progeny and its Environmental Influence Factors

Lu GUO[1], Lei ZHANG[2], Qiuju GUO[1]
[1]State Key Laboratory of Nuclear Physics and Technology, Peking University, Beijing 100871,China
[2]Solid Dosimetric Detector and Method Laboratory, Beijing 102205, China

Abstract – *The exposure of radon and its progeny contributes more than half of the natural radiation exposure received by the public. The unattached fraction of radon progeny is an important parameter in radiation dose estimation through dosimetric process; however, not so much data has been reported. For a better understanding on temporal variation and its environmental influence factors of the unattached fraction of radon progeny, a series of field measurements were performed periodically by adopting a new developed integrating monitor for measuring unattached fraction of radon progeny, and an instrument for measuring aerosol concentration in both indoor and outdoor environments.*

It was shown by the measurement results that the ranges of unattached fraction of radon progeny in indoor and outdoor environments all over the year were 8.4%~16.5% and 9.4%~28.2%, respectively. Seasonal and diurnal variations of the unattached fraction of radon progeny were also analyzed. It comes to the conclusion that during the winter season the unattached fraction of radon progeny is stable in indoor environment because of the little change on aerosol concentration、temperature and humidity indoor in Beijing area, while on the other hand, it changes a lot in outdoor environment due to the great undulation of atmospheric factors, and the average of the unattached fraction of radon progeny is higher in outdoor environments than that of indoors. While in summer, the unattached fraction of radon progeny in indoor environment was close to the values of outdoor environment, and both of them had lower average than that in winter.

Keywords – radon; unattached fraction; aerosol; dose conversation factor

APSORC'13 - 5th Asia-Pacific Symposium on Radiochemistry
Kanazawa, Japan, 22-27 September 2013

Preliminary Study on Measuring Radon Progeny Concentration Using Alpha/Beta Spectroscopic Method

Abdumomin Kadir[1], Lei Zhang[2], Qiuju Guo[1], and Juncheng Liang[3]
[1] State Key Laboratory of Nuclear Physics and Technology, School of Physics, Peking University, Beijing, 100871, China
[2]Solid Dosimetric Detector and Method Laboratory, Beijing, 102205, China
[3]Ionizing Radiation and Medical Science, National Institute of Metrology, Beijing, 100013, China

Abstract – The accurate measurement of radon progeny concentration is essential for dose evaluation of radon exposure. Alpha/beta spectroscopic methods have great advantage comparing with traditional total counting methods as well as alpha-spectrum methods. This work introduces a radon progeny measurement method using alpha/beta spectroscopy. Sample 10 min with unit flow rate (1 L/min), 1 min delay and then record the alpha/beta spectroscopy at 3 min internals for 30 min, the uncertainty of this method is 9.3% in a typical indoor environment (C_{Rn}=40 Bq/m^3, F=0.4). Experiment comparison results confirm that this method could greatly improve the measurement precision of radon progeny concentration.

Keywords – radon progeny; spectroscopic method; least-square calculation; accurate measurement;

The Measurement Comparability of ^{134}Cs and ^{137}Cs in Foodstuff Samples in Japan - Result of Inter-Laboratory Experiment for Certification of Certified Reference Material

Tsutomu Miura[1], Yoshitaka Minai[2], Shoji Hirai[3], Hiroshi Iwamoto[4], Chushiro Yonezawa[5], Yoshinobu Uematsu[6], Akira Okada[7], Masami Shibukawa[8], Koichi Chiba[1], Kiyoshi Kitamura[9], Takahiro Yamada[10], Kazutoshi Kakita[11], Isao Kojima[11]

[1]National Metrology Institute of Japan, AIST, [2] Musashi University, [3]Tokyo City University, [4]Environmental Technology Service Co, Ltd., [5]Japan Institute of International Affairs, [6]Japan Accreditation Board, [7]TERM, [8]Saitama University, [9]Japan Chemical Analysis Center, [10]Japan Radioisotope Association, [11]The Japan Society for Analytical Chemistry

Abstract – The measurement comparability of ^{134}Cs and ^{137}Cs in foodstuff samples in Japan was evaluated based on the inter-laboratory experiment for certification of certified reference material (CRM) for environmental radioactivity analysis.

Keywords – measurement comparability, certified reference material, Environmental radioactivity, ^{134}Cs, ^{137}Cs, inter-laboratory experiment method, Uncertainty

I. INTRODUCTION

Following the mega earthquake, tsunami, and the accident at the Fukushima No.1 nuclear power plant on March 11, 2011, a massive amount of radioisotopes were released in the environment. This situation required urgent measurements of radioactive isotopes in foodstuff samples for human health. The CRM is essential to accurate and precise measurement of radioisotopes in the samples. The Japan Society of Analytical Chemistry was developed the certified reference material of brown rice (JSAC0731 and JSAC0732) and bovine muscle flakes (JSAC0751 and JSAC0752) for measuring radioactive isotopes of ^{134}Cs and ^{137}Cs support by Grant-in-aid Japan Science and Technology Agency. The certification of the ^{134}Cs, ^{137}Cs and ^{40}K in candidate CRM of brown rice and bovine muscle for environmental radioactivity analysis was performed by the inter-laboratory experiment method. Twelve laboratories, including the research institutes, JCSS (Japan Calibration Service System) accredited calibration labs, universities, and industrial testing labs in Japan participated in the inter-laboratory experiment for certification. The certified values and associated expanded uncertainties (k=2) of ^{134}Cs, ^{137}Cs, and ^{40}K in brown rice CRM were 141 Bq kg^{-1} ± 9 Bq kg^{-1}, 210 Bq kg^{-1} ± 13 Bq kg^{-1}, and 75 Bq kg^{-1} ± 7 Bq kg^{-1}, respectively [1]. And also, the certified values and associated expanded uncertainties (k=2) of ^{134}Cs, ^{137}Cs, and ^{40}K in bovine muscle CRM were 174 Bq kg^{-1} ± 12 Bq kg^{-1}, 297 Bq kg^{-1} ±20 Bq kg^{-1}, and 276 Bq kg^{-1} ± 46 Bq kg^{-1}, respectively [2].

In this paper, we present a measurement comparability of ^{134}Cs and ^{137}Cs in foodstuff samples in Japan resulting from that of the inter-laboratory experiments.

Instruments and methods

All participants of the inter-laboratory experiments measured ^{134}Cs, ^{137}Cs, and ^{40}K in the candidate CRM using the Ge semiconductor detector.

Results and discussions

The example of the results of inter-laboratory experiments is shown in Fig.1. In that case, the z-score of the all reported values ranged from -3 to 3, the all data were used for calculation of the certified value.

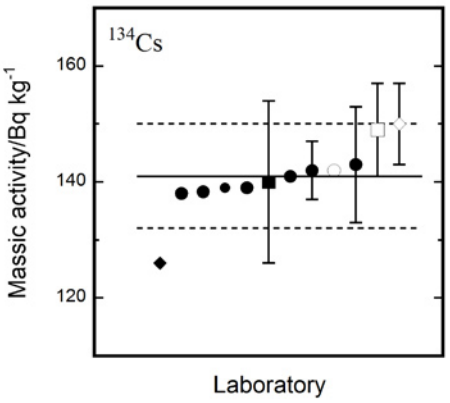

Fig.1 The result of inter-laboratory experiment of ^{134}Cs in JSAC 0731 brown rice CRM.

Acknowledgement

Our deepest appreciation goes to participants the inter-laboratory experiment for certification of CRMs.

APSORC'13 HEADING (WITHOUT NUMBER)

[1] Certificate of JSAC 0731, 0732 Brown rice certified reference material for environmental radioactivity, www.jsac.or.jp/srm/CRMJSAC0731.
[2] Certificate of JSAC 0751, 0752 Bovine muscle flakes certified reference material for environmental radioactivity www.jsac.or.jp/srm/CRMJSAC0751.

APSORC'13 - 5th Asia-Pacific Symposium on Radiochemistry
Kanazawa, Japan, 22-27 September 2013

Synthesis and Characterization of Volatile Technetium Compound

Bradley C. Childs[1], Frederic Poineau[2], Ken R. Czerwinski[2]
[1]University of Nevada Las Vegas, Las Vegas, Nevada 89154, USA

Abstract – Technetium-99 is an important fission ($T_{1/2}$= 2.13.105 y) product of the nuclear industry. Technetium in its highest oxidation state (VII) is highly mobile and can represent a threat to the environment [1]. There are over 55 million gallons of high level mixed waste located at the Hanford site. Waste tanks at the Hanford site contain Tc that could potentially leak, and in the context of management of technetium, a glass waste form was proposed to counteract the issue [2]. In the process of synthesizing melt glass between the temperatures of 600 °C and 1100 °C, volatile technetium compounds were observed in the reaction tube. These compounds displayed characteristic colors based upon the reaction environments of either breathing air or nitrogen gas. A breathing air atmosphere produces a red compound that adheres to the walls of the reaction tube. An atmosphere of nitrogen gas produces a white compound that was observed on the walls of the reaction tube.

Keywords – Technetium, Red, Volatile,

I. INTRODUCTION

A study of how technetium behaves as a waste-form and the speciation that correlates with the waste-form has garnered much attention. One of the proposed methods to create a waste-form was vitrification. The main issue with vitrication is dealing with volatile products that form in the process of manufacturing the glass from vitrification. The temperatures that are reached allow for radioactive compounds to become airborne and can present a problem when trying to retain all of the radioactive material. As it pertains to technetium, Tc_2O_7 boils at 311 °C and TcO_2 boils at temperatures above 900 °C which is problematic because melting temperatures exceed the boiling points of those compounds very easily [3]. Most speciation studies go into how the glass is formed, but the focus of the study at hand is to look at the volatilized species.

A. Vitrification Process

The process that was used to produce volatile species involves making glass material. Melt glass formers based on the LAWE4H batch composition were used while loading 1% technetium by mass to this mixture by way of sodium pertechnetate ($NaTcO_4$) [4]. A temperature range between 600 °C and 1100 °C will be used to produce the material. Two different environments will be created while producing volatile species. The first of which will be breathing air. Under these conditions we expect to see a red volatile species (Fig.1). The second environment will be nitrogen gas. It is expected that a white volatile species will be observed from this synthesis (Fig.2).

B. Additional Synthetic Routes

One way to determine the exact species being volatilized is to observe the technetium compound being used in the batch synthesis material. $NaTcO_4$ will also be observed without adding it to the batch material to see if volatile species are still produced in the same manner. Other pertechnetate salts will be observed as well with and without the batch material.

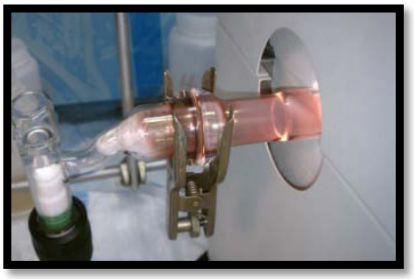

Fig.1: Volatile Red Compound

Fig.2: Volatile White Compound

REFERENCES

[1] Y. Liu, J. Terry and S. Jurisson, *Radiochim. Acta*, 2007, **95**, 717–725
[2] W.W. Lukens et al., Dissimilar behavior of technetium and rhenium in borosilicate waste glass as determined by X-ray absorption spectroscopy. Chem. Mater. 19, (2007) 55-56.
[3] J.G. Darab and P.A. Smith *Chem. Mater.* 1996, *8,* 1004-1021.
[4] DM-100 Melter Testing to Support LAW Glass Formulation Correlation Development," K. Abel and J. Westsik, WTP Test Specification, 24590-WTP-TSP RT-04-0004, Rev. 0, 1/12/05.

APSORC'13 - 5th Asia-Pacific Symposium on Radiochemistry
Kanazawa, Japan, 22-27 September 2013

Time Variation of Concentrations of Radioactive Cesium-134, 137 and Iodine-129 in the Ohori River, Chiba Prefecture, Japan

Nao Shibayama[1], Keisuke Sueki[2], Kimikazu Sasa [2,3], Yukihiko Satou[1], Tsutomu Takahashi[3], Masumi Matsumura[3], Hiroyuki Matsuzaki[4], Michio Murakami[5], Rey Yamashita[6], Mahua Saha[6], Hideshige Takada[6], Yukio Koibuchi[7], Soulichan Lamxay[7], Taikan Oki[8]

[1]Graduate School of Pure and Applied Sciences, Univ. of Tsukuba
[2]Faculty of Pure and Applied Sciences, Univ. of Tsukuba
[3]Research Facility Center for Science and Technology, Univ. of Tsukuba
[4]MALT, The Univ. of Tokyo
[5] "Wisdom of Water" (Suntory), The Univ. of Tokyo
[6]Tokyo Univ. of Agri. & Tech.
[7]Graduate School of Frontier Sciences, The Univ. of Tokyo
[8]Insitute of Industrial Science, The Univ. of Tokyo

Abstract

Radioactive nuclides emitted from the Fukushima Dai-ichi nuclear power plant were observed for the long term in Ohori River, Chiba Prefecture, Japan. In this presentation, we report time variation of concentrations of ^{134}Cs, ^{137}Cs and ^{129}I in the suspended soils (SS) and dissolved matter (DM) from the flow of the river were measured. The concentrations of radioactive cesium 134 and 137 in SS were gradually decreasing in long term observation and rising on the rainy day. The DM/SS ratios of ^{137}Cs were almost constant over time. In the DM, the ^{129}I data showed strong correlation with cesium data.

Keywords

Cesium-134, 137 ; Iodine-129 ; time variation ; river water

I. INTRODUCTION

Radioactive cesium and iodine emitted from the Fukushima Dai-ichi nuclear power plant were detected from environmental water, reflecting an aspect of dynamics of these radioactive nuclides in the environment. In the metropolitan area, comparatively high concentration of radioactive cesium isotopes were detected from sediment of Ohori River in Chiba Prefecture[1]. In this work, the long-term variations of the concentrations of the radioactive cesium and iodine in the suspended soils (SS) and dissolved matter (DM) were measured for Ohori River, and the trend of nuclides was discussed.

II. METHODS

The SS samples of two or three weeks are collected by the SS Auto-Sampler[2] which installed at the middle of river near the Showa-bridge, and the river water samples are collected every two or three weeks in the same place from May, 2012 at Ohori River. The river water was filtrated. The SS was defined as residue of 0.7 μm filter and the DM was defined as the component passing through the 0.2 μm filter. The concentrations of ^{134}Cs and ^{137}Cs were determined from the γ-ray spectrum obtained by HPGe detectors. ^{129}I in the river was investigated about the same samples by AMS at MALT, The Univ. of Tokyo[3].

III. RESULTS AND DISCUSSION

Time variations of concentration of radioactive cesium in the SS of Ohori River are shown in Fig.1. The average concentrations of radioactive cesium were gradually decreasing in long term observation. The concentration of radioactive nuclides in the SS sampled by Auto-Sampler was treated as average for a certain period. The momentary concentrations of radionuclides in the SS were obtained from the river water sampled every two or three weeks. In most points, the momentary concentration was lower than the average concentration, but a few points which corrected in rainy differed from the tendency due to rain fall. The DM/SS ratios of ^{137}Cs were almost constant, which may considered as the equilibrium constant of cesium between SS and DM. In the DM, the ^{129}I data showed strong correlation with cesium data. The iodine data, however, is insufficient.

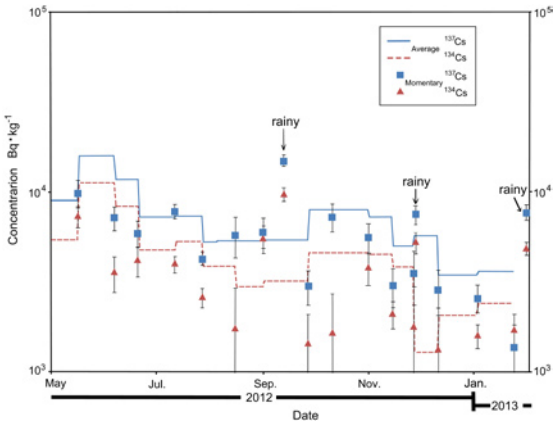

Fig.1. Time variation of concentration of radioactive cesium in SS of Ohori River. Solid line and dashed line show the average concentration of ^{137}Cs and ^{134}Cs, respectively. Square points and triangular points show momentary concentrations of ^{137}Cs and ^{134}Cs, respectively.

REFERENCES

[1] Ministry of Environment, 2011, http://www.env.go.jp/jishin/monitoring/result_pw111222-1.pdf
[2] Phillips et al. (2000) Hydrol. Process. 14, 2589-2602.
[3] H. Matsuzaki et al., Nucl. Instr. and Meth. B, 259, 2007, 721–726.

Ra isotopes in Na-Cl type groundwater in Japan

Junpei Tomita[1, a], Takahiro Takada[1], Seiya Nagao[1], Masayoshi Yamamoto[1]
[1] Low Level Radioactivity Laboratory, Institute of Nature and Environmental Technology, Kanazawa University, Wake, Nomi, Ishikawa 923-1224, Japan
[a] Department of Radiation Protection, Nuclear Science Research Institute, Japan Atomic Energy Agency, Tokai-mura, Ibaraki 319-1195, Japan.

Abstract – Radium isotopes (^{226}Ra and ^{228}Ra) were measured for Na-Cl type groundwater samples collected from Hokkaido, Aomori, Akita and Yamagata Prefectures in Japan. The ^{226}Ra contents varied in the wide range from 9 - 5000 mBq kg^{-1} and their values were roughly correlated to the total dissolved solid (TDS). Activity ratios of ^{228}Ra/^{226}Ra in groundwater ranged from 0.3 – 4.2 and most of them clustered around those of ^{232}Th/^{238}U of common rocks in Japan. These observations agreed well with the previous results from Ishikawa, Toyama and Niigata Prefectures, and overall indicated that Ra was mainly transported into the groundwater by α-recoil process and its concentration in groundwater was constrained by adsorption-desorption reaction depending on salinity.

Keywords – Ra isotopes, Na-Cl type groundwater, α-recoil, adsorption-desorption reaction

I. INTRODUCTION

Radium isotopes (^{226}Ra ($T_{1/2}$=1600 y) and ^{228}Ra ($T_{1/2}$= 5.75 y)) in groundwater have been investigated worldwide from the various viewpoints such as geochemical interest and radiation protection. Activities of Ra isotopes in groundwater vary widely, and anomalously high ^{226}Ra contents over several tens of Bq kg^{-1} have been found in saline waters and brines.

In Japan, Ra isotopes in groundwater have been investigated mainly in relation to the radioactive hot spring, and groundwaters with high ^{226}Ra concentration over 1 Bq kg^{-1} have been found at hot springs such as Arima and Masutomi. Since these hot springs are commonly originated from granite areas where have relatively high U contents, it was considered that such higher ^{226}Ra in water was attributed to the U in granite. Recently, Na-Cl type groundwaters with intermediate salinity (ca.1-36‰) have been obtained from the deep wells with the development of more sophisticated drilling techniques. We have studied the distribution of Ra isotope concentrations in these Na-Cl type groundwaters from coastal area and sedimentary basin in Ishikawa, Toyama and Niigata Prefectures facing to the Japan Sea of Central Japan, and found that some of them contained relatively high ^{226}Ra over 1 Bq kg^{-1} even in coastal areas and sedimentary basin.

Authors are interested in clarifying the geochemical mechanism of such high ^{226}Ra occurrence, and expanded research to groundwater at Hokkaido and Tohoku Districts (Aomori, Akita and Yamagata Prefectures). In this study, we report the Ra contents in Na-Cl type groundwaters from these areas. Constraining factors which Ra content becomes higher in groundwater will be mainly discussed, including the results obtained previously from other areas such as Ishikawa, Toyama and Niigata Prefectures.

II. MATERIAL AND METHODS

Na-Cl type groundwater samples were collected from the coastal area and sedimentary basin in Hokkaido, Aomori, Akita and Yamagata Prefectures in Japan. Radium isotopes were co-precipitated with $BaSO_4$, and their activities were determined by γ-ray spectrometry.

III. RESULTS AND DISCUSSION

Activities of ^{226}Ra in groundwater from Hokkaido, Aomori, Akita and Yamagata Prefectures were observed in the wide range from 9 - 5000 mBq kg^{-1}. These ^{226}Ra activities in groundwater samples showed an increasing tendency with increasing total dissolved solid (TDS) (Fig. 1). Activity ratios of ^{228}Ra/^{226}Ra of them varied from 0.3 – 4.2, and most of them clustered around 0.5 - 2. These ratios were nearly similar to those of ^{232}Th/^{238}U of common rocks in Japan. These observations agreed well with the previous results from Ishikawa, Toyama and Niigata Prefectures.

Ra isotopes are supplied into groundwater by some processes: 1) decay of dissolved parent nuclides (Th is considered as insoluble element); 2) weathering and/or dissolution of aquifer rock; 3) α-recoil at water-rock interface; and 4) desorption reaction at water-rock interface.

Results both relationships between ^{226}Ra and TDS and activity ratios of ^{228}Ra/^{226}Ra in groundwater samples obtained here indicated that Ra was mainly ejected into the groundwater by α-recoil process and its Ra was constrained by adsorption-desorption reaction depending on salinity.

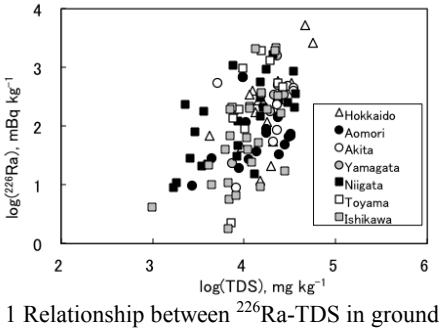

Fig. 1 Relationship between ^{226}Ra-TDS in groundwater

A new method to estimate $^{210}Po/^{210}Pb$ activity ratio in atmospheric aerosol by alpha spectrometry

N. Momoshima[1], S. Nishio[2], K. Hibino[2], S. Sugihara[1]
[1] Radioisotope Center, Kyushu University, Hakozaki, Higashi-ku, Fukuoka 812-8581, Japan
[2] Graduate School of Science and Technology, Kumamoto University, Kurokami, Kumamoto 860-8555, Japan

Keywords – aerosol, ^{210}Po ^{210}Pb activity ratio, alpha spectrometry

Various kinds of radionuclides are observed in the atmosphere, among them radon and its daughter nuclides attached to aerosol are most abandon and the daughter nuclides finally decay to ^{210}Pb within a few hours. The formed ^{210}Pb (22.3 y) decays to ^{210}Bi (5 d) followed by ^{210}Po (138 d). The half life of ^{210}Po is rather long compared to the removal process functioning to atmospheric aerosols; therefore $^{210}Po/^{210}Pb$ activity ratio as well as $^{210}Bi/^{210}Pb$ activity ratio is usable to estimate residence time of aerosol in the atmosphere.

The growth curves of ^{210}Po from ^{210}Pb in aerosol are shown in Fig.1 as a function of initial $^{210}Po/^{210}Pb$ activity ratios. The growth pattern differs depending upon the initial $^{210}Po/^{210}Pb$ activity ratio. The initial activity ratio varies in the environment due to additional input of ^{210}Po to atmosphere from such as volcanic release, fire burning of vegetation etc. Atmospheric migration of soil dusts increases the initial activity ratio because of secular radioactive equilibrium in soil. Under the general environmental circumstances major radionuclide in aerosol would be ^{210}Pb and then, ^{210}Po is considered to be the main alpha particle emitted from aerosol. If we measure a growth of ^{210}Po activity with time and compared with growth pattern shown in Fig. 1, we can estimate the $^{210}Po/^{210}Pb$ activity ratio of the aerosol samples.

The theoretical calculation of ^{210}Pb-^{210}Bi-^{210}Po equilibrium suggests that $^{210}Po/^{210}Pb$ slightly depends on initial $^{210}Bi/^{210}Pb$ activity ratio. The measurement time of a few days would be necessary for alpha spectrometry to obtain statistically acceptable counts. Then, the ^{210}Po growth pattern dependent on the initial $^{210}Bi/^{210}Pb$ activity ratio would be obscure. However, the proposed method is simple and no chemical separation is necessary.

The growth of ^{210}Po activity in the aerosol collected on a membrane filter and measured several times with a silicon surface barrier detector of an alpha spectrometer is shown in Fig. 2 as an example. The growth pattern is analyzed under the assumption that the initial $^{210}Bi/^{210}Pb$ activity ratio is 0.6, which would be the representative value in the general environment [1]. The least square fitting was carried out to obtain the initial ^{210}Pb and ^{210}Po counts. The measurements were done at the identical geometrical configuration between the detector and the sample, and in a series of measurements the same detector of the same alpha spectrometer system was used.

[1] Rangarajan, C., J. Environ. Radioactivity, 15, 193-206(1992)

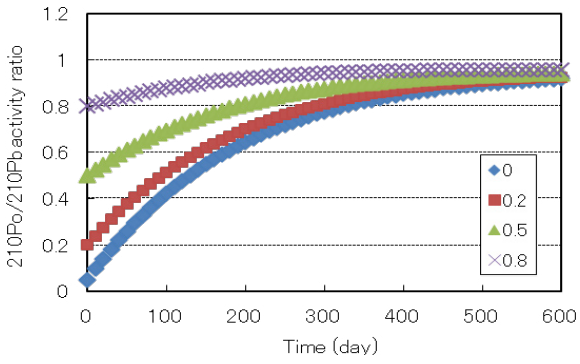

Fig. 1 Theoretical change in $^{210}Po/^{210}Pb$ activity ratio with time at different initial $^{210}Po/^{210}Pb$ activity ratio.

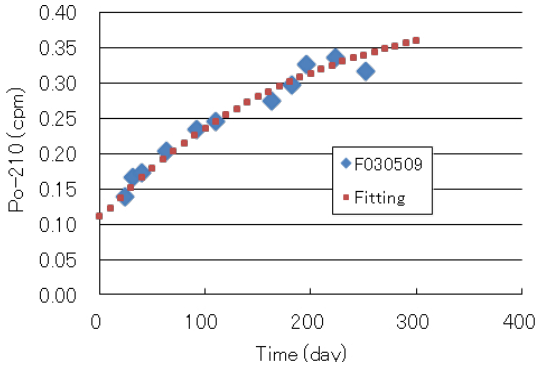

Fig. 2 Counts of ^{210}Po measured with the alpha spectrometer for the aerosol collected on a membrane filter and the theoretical counts obtained by least square fitting.

APSORC'13 - 5th Asia-Pacific Symposium on Radiochemistry
Kanazawa, Japan, 22-27 September 2013

Sedimentary environment inferred from sedimentation rates by ^{210}Pb and ^{137}Cs and their inventories in Mutsu Bay, Japan

Kazuhito Hamataka[1], Seiya Nagao[1], Michio Kato[2], Isao Kudo[3], Masayoshi Yamamoto[1]
[1] Low Level Radioactivity Laboratory, KINET, Kanazawa University, Ishikawa 923-1224, Japan
[2] Graduate School of Science, Kanazawa University, Kanazawa, Ishikawa 920-1192, Japan
[3] Graduate School of Fisheries Sciences, Hokkaido University, Sapporo 060-0808, Japan

Abstract –Fourteen sediment cores were collected from Mutsu Bay, Aomori in Japan, and excess ^{210}Pb and ^{137}Cs were measured γ-spectrometrically. The spatial distributions of sedimentation rates by ^{210}Pb$_{ex}$ and ^{137}Cs and their inventories were studied in order to clarify whole pictures about the sedimentary environment of Mutsu Bay. Excessively post-depositional mixing (up to a depth of 10-15 cm) of surface sediments by bioturbation was observed on the ^{210}Pb$_{ex}$ depth profiles in cores from the offshore areas. The sedimentation rates calculated varied in the wide range from 0.04 to 0.2 g/cm^2/y. The sedimentation rates using ^{137}Cs method could not be applied. Apart from the ^{210}Pb$_{ex}$ inventories from the nearshore area, the responding inventories (17-30 kBq/m^2) from the offshore area were higher than the reported value of ca.15 kBq/m^2 in the surrounding soils, indicating that the sediment focusing due to the inner current etc., to the deeper area from the surrounding nearshore area, affects the sediment accumulation in the offshore area.

Keywords –Mutsu Bay, Aomori, sedimentation rate, inventory, ^{210}Pb, ^{137}Cs, sedimentary environment

I. INTRODUCTION

Semi-enclosed bay is sensitive to human activity and change of natural environment, and these directly and strongly impact in its sedimentary environment.

Mutsu Bay (surface area of 1580 km^2, average depth of 34 m, and maximum depth of 75 m), which is located in the north of Honshu in Japan, is indirectly connected with the open sea by a narrow channel through which seawater flows in and out the bay. The east floor of Mutsu Bay is relatively flat and shallow (40 m deep on average). The coastal areas are excessively populated and extensive scallop farming has been popularly practiced since 1970s. The present–day, death of scallop due to overcrowded cultivation and generation of red tides by declining water quality are going on, and muds are markedly accumulating in the offshore areas (Minoura *et al*. (1992)).

We have been interested in clarifying whole pictures about such sedimentary environment of Mutsu Bay, investigating the sediment rates by using radioactive ^{210}Pb and ^{137}Cs and their inventories in sediments.

II. MATERIAL AND METHODS

Core sampling: The core sediment samples were collected during cruises in May and August 2011, and June and September 2012. A small gravity corer (3.5 or 8.0 cm in diameter) was used to collect surface sediments (20-40 cm long) at 14 locations (Fig. 1). The obtained cores were immediately cut every 1 cm from top along the core, and after taking them to laboratory the samples were freeze-dried.

Measurements of ^{210}Pb and ^{137}Cs: The samples were then sieved through a 2-mm mesh to remove pebbles and fragments of shell, and pulverized in an agate mortar to obtain homogeneous samples. An aliquot of 5-10 g of sample was packed into a plastic vessel and stored for more than 3 weeks. The ^{210}Pb, ^{226}Ra (from daughter nuclide ^{214}Pb) and ^{137}Cs were measured by a low–background γ-ray spectrometer with a high pure Ge detector (planar or well type). The spectrometer was calibrated with standards prepared by the New Brunswick Laboratory (NBL) reference materials No. 42-1 (4.04% uranium), and analytical grade KCl. Unsupported ^{210}Pb activity (^{210}Pb$_{ex}$) was calculated from the difference between the total ^{210}Pb and the ^{226}Ra (from ^{214}Bi) contents.

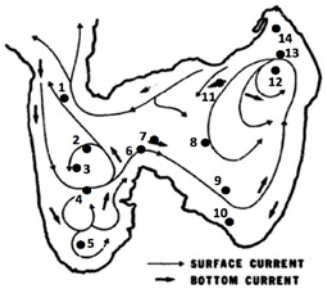

Fig. 1 Sampling sites in Mutsu Bay

III. RESULTS AND DISCUSSION

To date, activity measurements of ^{210}Pb and ^{137}Cs were finished for cores from St.1 to St.10. Overall, the sediments (Sts. Sts. 2-4 and 6-8) from the offshore area were mostly mud, while sand and coarser sediments, with their low mud contents, are restricted to the nearshore area. Surface mixed layers (up to a depth of 10-15 cm) were observed on the ^{210}Pb$_{ex}$ depth profiles from the offshore area, evidencing the excessively post-depositional mixing of surface sediments by bioturbation and so on. For other sites, ^{210}Pb$_{ex}$ concentrations declined more or less exponentially with depth. Sedimentation rates calculated for these cores varied in the wide range from 0.04 to 0.2 g/cm^2/y. Sedimentation rates using ^{137}Cs method could not be applied. A generally increasing trend in sedimentation rate after the late 1970s, when correspond to the rapid increase of scallop-production activity, was clearly observed at St.10.

Excess ^{210}Pb and ^{137}Cs inventories were calculated as the sum of ^{210}Pb$_{ex}$ and ^{137}Cs through a sediment core, respectively. The ^{210}Pb$_{ex}$ inventories ranged from 7-30 kBq/m^2. Apart from the values (7-9 kBq/m^2) from the nearshore areas, the responding inventories (17-30 kBq/m^2) for cores (Sts. 2-4 and 6-8) from the offshore areas were somewhat higher than the reported value of ca.15 kBq/m^2 estimated for the surrounding soils, indicating that the sediment focusing due to the inner current etc., to the deeper area from the surrounding nearshore area, affects the sediment accumulation in the offshore area. The ^{137}Cs inventories (0.08-0.14 kBq/m^2) were clearly lower than its inventories (around 3 kBq/m^2) in the surrounding soils. Further works are going on organic contents and grain-size of sediments.

K. Minoura et al. (1992), *Marine Geology,* 103, 487-502.

Distribution of radiocarbon in Japanese agricultural soils

Nobuyoshi Ishii, Keiko Tagami, Shigeo Uchida
Office of Biospheric Assessment for Waste Disposal, National Institute of Radiological Sciences

Abstract – Distributions of C-14 in solid, liquid, and gas phases were determined by batch sorption tests using 142 Japanese agricultural soil samples. The agricultural soils used were classified into "paddy" and "upland" soils. Each of the soil samples was suspended in deionized water containing [1, 2-C-14] sodium acetate and shake-incubated for 7 days. After the incubation, the distributions of C-14 in solid, liquid and gas phases were approximately 35%, 5% and 60% of the spiked C-14, respectively. These results suggested that if the C-14 of acetate migrated from a TRU repository site to agricultural soils, most of the C-14 would be released into the air and the rest would be distributed in the soil solid phase. The distribution of C-14 in gas phase was lower for upland soils than for paddy soils..

Keywords – TRU waste, Radiocarbon, Distribution, Agricultural soils

I. INTRODUCTION

Transuranic (TRU) waste is generated during the operation and dismantling of reprocessing facilities and mixed oxide (MOX) fuel fabrication facilities, and the waste contains radionuclides that have long half-lives. The dominant nuclides contributing to the dose from TRU waste are C-14 and I-129 [1]. These radionuclides, therefore, are very important in safety assessments for geological repositories of TRU waste.

C-14 could be released from a geological repository over a timescale of several thousand years. Because there is little information regarding reliable migration and realistic transport models, the possible migration of C-14 from a TRU repository site to the biosphere through groundwater presents some concern. It is, therefore, required to clarify the behavior of C-14 in the environment due to the reduction of exposure to C-14.

In general the environmental behavior of chemicals is influenced by various factors such as land use, soil type, temperature, pH, oxidative conditions and so on. The behavior of C-14 may differ between paddy and upland soils. In this study, distribution of C-14 for both Japanese paddy and uplands was determined and compared. The relationships among the distribution of C-14 and selected soil properties were discussed.

II. MATERIALS AND METHODS

A total of 142 agricultural soils (63 paddy soils and 79 upland soils) were collected throughout Japan. The soil samples were dried at room temperature, and then passed through a 2 mm mesh sieve to obtain fine particles.

[1,2-C-14] sodium acetate was used as the chemical form of C-14. This solution was diluted with deionized water to a specific activity of 1.8 kBq mL^{-1} and was filter-sterilized to remove microorganisms [2]. The specific activity corresponded to 4.2 x 10^{-1} nmol mL^{-1}.

For batch culture experiments, 0.5-g of air-dried soil sample was soaked with a 5-mL of the radioactive solution. The culture was shake-incubated at 25℃ for 7 days in the dark. After the incubation, the C-14 activities of the culture were determined to estimate the distribution of C-14 in solid, liquid and gas phases by measuring C-14 in solid, liquid phase with a liquid scintillation counter.

III. RESULTS AND DISCUSSION

Distribution of C-14 in solid, liquid and gas phases were determined on day 7 of incubation. The mean values of those distributions were 59.1 ± 8.6% in as phase, 35.4 ± 7.7% in solid phase, and 5.5 ± 5.4% in liquid phase. For each phase, a positive excess kurtosis was found (2.7 for solid, 7.1 for liquid and 4.2 for gas), and the interquartile range, which is the difference between the third and first quartiles, was less than 10%. Results of these statistical analyses mean that the distribution of C-14 in each phase had small variation ranges for Japanese agricultural soils. It should, however, note that there were big differences between the two extreme values for each phase. These values were far from the average and thus must be paid attention in safety assessments for geological repositories of TRU waste.

Distribution in liquid phase was correlated positively with pH of the culture solution. Similar results were found in our previous study [3].

Significant differences in the distribution of C-14 between paddy and upland soils were found for all phases. Distributions in solid and liquid phases were higher for the upland soils than for paddy soils, but, on the other hand, distribution in gas phase was lower for upland soils than for paddy soils. The difference in distribution in liquid phase may be explained by pH of the solution because pH of the upland samples was significantly higher than that of the paddy samples.

This work was supported by the Agency for Natural Resources and Energy, the Ministry of Economy, Trade and Industry (METI), Japan.

REFERENCES

[1] JAEA, FEPC, Second progress report on research and development for TRU waste disposal in Japan –Repository design, safety assessment and means of implementation in the generic phase-, JAEA-Review 2007-010, FEPC TRU-TR2-2007-01(2007).

[2] N. Ishii, S. Uchida, "Bacteria contributing to behaviour of radiocarbon in sodium acetate," Radiat. Prot. Dosimetry. 146, 151-154 (2011).

[3] N. Ishii, H. Koiso, H. Takeda, S. Uchida, "Partitioning of ^{14}C into solid, liquid and gas phases for various paddy soils in Japan," J. Nucl. Sci. Technol., 47, 238-243 (2010).

APSORC'13 - 5th Asia-Pacific Symposium on Radiochemistry
Kanazawa, Japan, 22-27 September 2013

Lateral distributions of $^{228}Th/^{228}Ra$ and $^{228}Ra/^{226}Ra$ ratios in surface waters of the Sea of Japan and their physical implications

Y. Furusawa[1], M. Inoue[1], S. Nagao[1], M. Yamamoto[1], Y. Hamajima[1], H. Kofuji[1], K. Yoshida[1]
Y. Nakano[1], K. Fujimoto[2], A. Morimoto[3], T. Takikawa[4], Y. Isoda[5]
[1]Low Level Radioactivity Laboratory, Kanazawa University
[2] Fisheries Research Agency, National Research Institute of Fisheries Science
[3]Hydrospheric Atmospheric Research Center, Nagoya University
[4]National Fisheries University
[5]Graduate School of Fisheries Sciences, Hokkaido University

Abstract –
We examined $^{228}Th/^{228}Ra$ and $^{228}Ra/^{226}Ra$ ratios in surface waters from the Sea of Japan by low background γ-spectrometry. These lateral distributions clarified the aspects of physical movement of geochemical species on surface.

Keywords –
$^{228}Th/^{228}Ra$ ratio, $^{228}Ra/^{226}Ra$ ratio, Sea of Japan

I. INTRODUCTION

Many researchers have studied the flow pattern of the Tsushima Warm Current (TWC), a major feature of the flow patterns in the Sea of Japan, using various techniques [1]. However, the origin and characteristics of the circulation pattern of the TWC have not yet been well clarified because of the markedly complicated seasonal variation in the circulation. The seasonal variation in the $^{228}Ra/^{226}Ra$ ratio recorded for the surface waters of the Sea of Japan is considered to be mainly controlled by the remarkable changes in the mixing ratio of the ^{228}Ra-poor Kuroshio ($^{228}Ra/^{226}Ra$ = 0.2) and the ^{228}Ra-rich continental shelf waters ($^{228}Ra/^{226}Ra$ = 3.5) within the East China Sea (ECS) [2]. Activity of particle-reactive ^{228}Th (half-life, 1.91 y) in seawater is governed by biogenic particle behavior, and therefore the combination of ^{228}Th and ^{228}Ra activities ($^{228}Th/^{228}Ra$ ratio) in seawater samples is useful for the study of scavenging processes in the Sea of Japan.

II. METHOD AND SAMPLING SITE

We collected 165 surface water samples (20 L) during the research expeditions of T/V *Oshoro Maru*, R/Vs *Mizuho Maru*, *Tansei Maru*, *Soyo Maru*, and *Tenyo Maru* (Fig. 1). Low-background γ-spectrometry was performed on the samples using Ge-detectors at the Ogoya Underground Laboratory in Japan [3, 4].

III. RESULTS AND DISCUSSION

Along the Tsushima Strait, the $^{228}Ra/^{226}Ra$ ratio of samples on the transect A gradually increased from south to north (from 0.8 to 2.3). On the transect B, the $^{228}Ra/^{226}Ra$ ratio of coastal-side waters (0.6-0.8) was lower than that of offshore-side waters (1.2). This reflects a higher mixing ratio of the Kuroshio water in the Honshu Island side. On the other hand, $^{228}Th/^{228}Ra$ ratio of waters on the transect A exhibited gradual decrease (<0.01 to 0.12) from south to north, dominantly reflecting a higher flux of biogenic particles in shelf water [5]. In this study, we examined the lateral distributions of $^{228}Th/^{228}Ra$ ratio as well as $^{228}Ra/^{226}Ra$ ratio on surface of the Sea of Japan and clarify the circulation patterns of particles and water masses. This is an operation that we are currently engaged in, by obtaining additional surface water samples.

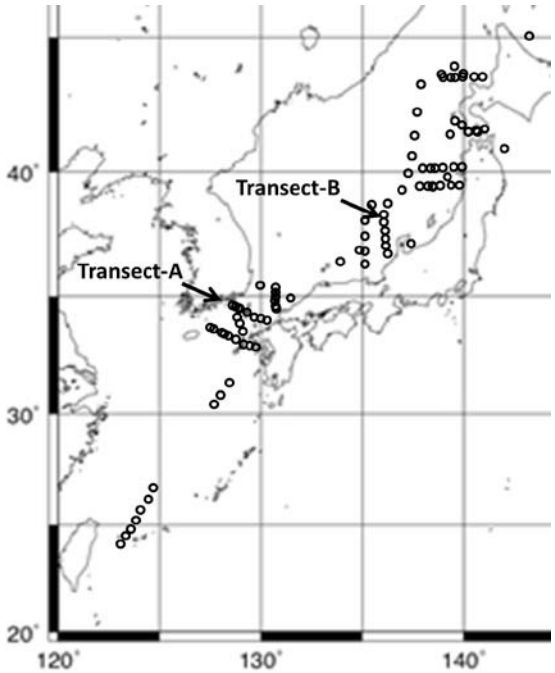

Fig. 1. Sample locations for seawater

References
[1] Hase *et al.* (1999) *J. Oceanogr.* **55**, 217-234
[2] Nozaki *et al.* (1989) *Geophys. Res. Lett.* **16**, 1297-1300
[3] Y. Nakano *et al.* (2008) *J. Oceanogr.* **64**, 713-717
[4] Y. Hamajima & K. Komura (2004) *Appl. Radiat. Isot.* **61**, 179-183
[5] M. Inoue *et al.* (2012) *Geochem. J.* **46**, 311-320

Vertical profiles of ^{228}Ra and ^{226}Ra activities in the Sea of Japan and their implications for water circulation

M. Inoue[1], M. Minakawa[2,*], K. Yoshida[1], Y. Nakano[1], H. Kofuji[1], S. Nagao[1], M. Yamamoto[1], Y. Hamajima[1]

[1]Low Level Radioactivity Laboratory, Kanazawa University
[2]Fisheries Research Agency, National Research Institute of Fisheries Science
*present address; National Research Institute of Aquaculture

Abstract-

By employing low-background γ-spectrometry combined with minimal radiochemical processing, we examined vertical profiles of ^{226}Ra ($t_{1/2}$ = 1600 y) and ^{228}Ra (5.75 y) activities in water columns in the Sea of Japan. The results indicate continuous delivery of ^{228}Ra to the Deep Proper Water (DPW), and clarify aspects of the transport of ^{226}Ra and ^{228}Ra by water circulation.

Keywords- ^{226}Ra, ^{228}Ra, Deep Proper Water, residence time, low-background γ-spectrometry

I. INTRODUCTION

The Sea of Japan is surrounded by the Eurasian continent and the Japanese Archipelago, and is connected to the Pacific and other marginal seas by the very shallow Tsushima, Tsugaru, and Soya Straits (≤~150 m of depth). Therefore, the deep water, so-called the Proper Water of the Sea of Japan, has no influx from a surrounding sea, indicating unique vertical water circulation [1]. ^{226}Ra and ^{228}Ra of seawater have been used as powerful tracer for studying the migration of water masses. However, standard γ-spectrometry for measuring ^{228}Ra of deep seawater usually required very large volumes (hundreds to thousands of liters) because of its low activity and previously reported data are not sufficient to allow investigating the details of the vertical distribution of ^{228}Ra in oceans. In the present study, we analyzed seawater samples from the Japan Basin, Yamato Basin, and Tsushima Basin within the Sea of Japan, for ^{226}Ra and ^{228}Ra.

II. SAMPLES and EXPERIMENTAL

We analyzed a total of seawater samples collected in water columns in the Sea of Japan for ^{226}Ra and ^{228}Ra. Low-background γ-spectrometry was performed using well-type Ge-detectors, which are located at the Ogoya Underground Laboratory, Japan [2]. Detailed explanations of these experimental procedures were presented elsewhere [3]. γ-Peaks for ^{228}Ra measurement (^{228}Ac; 338 and 911 keV) on a blank sample, which was performed our experimental procedures on 50 L of distilled water, were "not detected" level. Therefore, we corrected only least Ra-contaminated Ba-reagent blank, which accounted for <1% ^{228}Ra for our water samples.

III. RESULTS and DISCUSSION

In the Japan Basin, the ^{226}Ra activity of the water samples gradually increased from surface to the DPW (1.5-2.3 mBq/L). The ^{228}Ra activity of the water exhibited steep gradients with depth from the surface to the Upper Proper Water (1.8-0.2 mBq/L), and short-lived ^{228}Ra is continuously delivered to the DPW by the active water circulation before it radioactively decays. The results indicate continuous delivery of ^{228}Ra to the DPW, and clarify aspects of the transport of ^{226}Ra and ^{228}Ra by water circulation. The residence time of the DPW is calculated to be about 100 y.

Acknowledgements

We thank the researchers, captain, and crew of R/V *Soyo Maru* for their assistance during sampling.

References
[1] Gamo, T. and Horibe, Y. (1983) *J. Oceanogr. Soc. Jpn* **39**, 220-230:
[2] Hamajima, Y. and Komura, K. (2004) *Appl. Radiat. Isot.* **61**, 179-183:
[3] Nakano, Y. *et al*. (2008) *J. Oceanogr*. **64**, 713-717.

Induced radioactivity in air and water at medical accelerators

K. Masumoto[1], K. Takahashi[1], H. Nakamura[1], A. Toyoda[1], K. Iijima[1], K. Kosako[2], K. Oishi[2], F. Nobuhara[3]

[1]High Energy Accelerator Research Organization (KEK)
[2]Shimizu Co.
[3]Tokyo Nuclear Service Co

Abstract – Activation of air and water has been evaluated at the 10 and 15 MeV linear electron accelerator facilities. At 15 MeV irradiation, the activity of 10-min-half-life ^{13}N was observed in the case of the air in the glove box. Air and water samples were also bombarded by 250 MeV protons and 400 MeV/u carbon, and the irradiation dose was 10 Gy at the isocenter. Upon the ion-chamber monitoring of the air sampled from the glove box, ^{15}O, ^{13}N, and ^{11}C activities were mainly observed. At the end of proton and carbon irradiation, the activity of the water was found to be about 10 kBq•cm^{-3} and several kBq•cm^{-3}, respectively. From the decay analysis of the induced activity in water, ^{15}O, ^{13}N, and ^{11}C were detected.

Keywords – Activation, Air, Water, Medical accelerator

I. INTRODUCTION

Accelerators have been widely used in medical applications, especially in cancer treatment. Electron linear accelerators have been used in hospitals for the X-ray irradiation of diseased organs. Particle accelerators have also been used in recent times as a powerful tool for cancer therapy. In this work, we investigated the activation of air and water in treatment rooms in hospitals for radiation safety management. In the case of photonuclear reaction, several positron emitting radioisotopes such as ^{15}O and ^{13}N can be produced by the bremsstrahlung at higher than 15 MeV in air. In case of hadron irradiation, many radioisotopes might be produced by high-energy particles. In this work, we measured the induced activity in air and water caused by the electron and hadron accelerators employed for medical use, in order to determine whether the concentration of radioactivity was below regulated levels.

II. EXPERIMENTAL

A. Activation of air and water

(1) Electron accelerator:10 and 15MeV irradiations for 10 min were performed by Varian Clinac 2100C and Clinac iX, respectively. Doses were 40 and 60 Gy at the isocenter, respectively.
(2) Proton accelerator: 200 MeV proton beam was irradiated for 3.25 min on an area of 0.15 m × 0.15 m, and 10 Gy at the isocenter.
(3) Heavy ion accelerator: Carbon beams of 400 MeV/nucleon was irradiated for 2 min on an area of 0.15 m × 0.15 m, and 10 Gy at the isocenter.

B. Activity measurement

(1) Air: The air in a glove box of 250L was irradiated and sampled with a vacuum ionization chamber for measurement. An aerosol was also collected on a HEPA filter by an air sampler.
(2) Water: After irradiation, dose rate of water surface was monitored using a NaI(Tl) survey meter and the gamma-ray spectrum was measured using a $LaBr_3$(Ce) scintillation spectrometer.

III. RESULTS AND DISCUSSION

At the 15 MeV irradiation of bremsstrahlung, the activity of ^{13}N was 0.87 Bq•cm^{-3} at the end of the irradiation. As the activity of ^{13}N was also detected on the filter paper, NO_x fomation was presumed. Activity of water could not be detected.

In case of 250 MeV proton irradiation, activities of ^{15}O, ^{13}N, and ^{11}C were found to be 1.9, 0.6, and 0.6 Bq•cm^{-3} at the end of irradiation in air sampled from the glove box. The activity of ^{13}N was also detected on the filter paper. By the decay curve analysis of water activity obtained from the surface dose rate of the polyethylene tank, activities of ^{14}O, ^{15}O, ^{13}N, and ^{11}C were found to be 91000, 12000, 1100, and 190 Bq•cm^{-3} at the end of irradiation, respectively.

In case of carbon irradiation, we performed irradiation of air for two times and fitted the decay curve for ^{14}O, ^{15}O, ^{13}N, ^{11}C, and ^{41}Ar. Average activities of ^{14}O, ^{15}O, ^{13}N, ^{11}C, and ^{41}Ar were 0.8, 1.1, 0.08, 0.09, and 0.006 Bq•cm^{-3} at the end of irradiation. By the decay curve analysis of water activity obtained from the surface dose rate of the polyethylene tank, activities of ^{14}O, ^{15}O, ^{13}N, and ^{11}C were found to be 2100, 2000, 100 and 180 Bq•cm^{-3} at the end of irradiation, respectively.

IV. CONCLUSION

In case of 10 MeV irradiation, we could not detect the residual activity in air and water. In the case of 15 MeV irradiation, we observed ^{13}N in the air sampled from the glove box irradiated in front of the beam exit window and on the filter collected by the air samplers in the irradiation room and the maze. In the case of 250 MeV proton activation and 400 MeV/u carbon irradiation, activation of air was not excessively high and the induced activity was comparable to that induced by 15 MeV irradiation for the electron accelerator. But induced activity of water was extremely high. The main radionuclides detected were ^{13}N and ^{11}C, 10 min after irradiation with protons and ^{11}C, 20 min after irradiation with carbon

Radioactivity determination of ^{14}C and ^{3}H in solid waste samples by liquid scintillation counter

Jong-Myoung Lim[1*], Mun-Ja Kang[1], Kun-Ho Chung[1], Chang-Jong Kim[1], Geun-Sik Choi[1]
[1]Environmental Radioactivity Assessment Team, Korea Atomic Energy Research Institute
989-111 Deadeok-daero, Yuseong-gu, Daejeon, 305-353, Korea

Abstract –This study reports the comprehensive efforts made to evaluate the analytical procedure for ^{3}H and ^{14}C in solid sample. The sludge samples from National Physical Laboratory (NPL) proficiency program (Environmental Radioactivity Proficiency Test Exercise 2012) were combusted by high temperature furnace and analyzed in LSC. The various performance tests of analytical method were conducted with standard solutions. The detection limit and uncertainty of the method were also evaluated in detail. Major factors of standard uncertainty were grouped into counting error, sample homogeneity, and efficiency calibration. Finally, sensitivity tests of these major factors were performed.

Keywords – tritium, ^{14}C, radioactivity, combusting, sludge,

As an attempt to reduce social costs and apprehension arising from the radioactivity in environments, an accurate and rapid assessment of radioactivity is highly desirable. Nuclear wastes (e.g., sludge, activated carbon, oils, resins, etc.) have been consistently generated by actions to prevent the emission of radioactive pollutants from nuclear sites. To decide a proper disposal option of these nuclear wastes, we need an analytical method that can determine the radioactivity of ^{3}H and ^{14}C which exists in very low levels.

The ^{3}H in the water (tritiated water; HTO) is major chemical form in the environment. Through the natural or industrial process with organic compounds, tritium is easily converted into organic bound tritium (OBT). The HTO form is easily lost at a temperature around 120°C, whereas the strongly-bounded tritium with the form of non-HTO requires high temperature of a few hundred degrees in centigrade for complete extraction. The ^{14}C decays into ^{14}N through beta decay(E_{max}=156 kev). The main anthropogenic origin of ^{14}C is thermal neutron activation of ^{14}N in the nuclear reactor by a neutron capture reaction $^{14}N(n,p)^{14}C$. For extraction of ^{14}C which exist in lattice structure, it requires also high temperature to oxidize $^{14}CO_2$ gas.

Radioactivity of ^{3}H and ^{14}C in waste water sludge has been determined by the following combustion method. The sludge samples were combusted in a purpose-designed tubular high temperature furnace (Raddec Pyrolyser Trio^{TM}) which consist of six quartz tubes with the length of 1.5 m and the diameter of 1.5 cm. The combusting temperature was controlled stepwise up to 800°C. The ^{3}H and ^{14}C were trapped in 0.1 M HNO_3 and carbon absorber solution (Carbo-Sorb® E, Perkin Elmer), respectively. The measuring of the radioactivity was carried out in LSC (Walac 1220 Quantulus, Perkin Elmer).

This study reports the comprehensive efforts made to evaluate the analytical procedure for ^{3}H and ^{14}C in solid sample. The sludge samples from National Physical Laboratory (NPL) proficiency program (Environmental Radioactivity Proficiency Test Exercise 2012) were combusted by high temperature furnace and analyzed in LSC. The various performance tests of analytical method were conducted with standard solutions. In order to evaluate dynamic range of the method, real samples with spiking ^{3}H and ^{14}C standard solution were analyzed. Duplicated samples (n=6) were analyzed to see the repeatability of this method. The results showed that relative standard deviations for ^{3}H and ^{14}C are about 11% and 2.9%, respectively. The activity concentrations were compared statistically with the assigned values. The deviation between the two values for ^{3}H and ^{14}C are about 14.5% and 5.7%, respectively. The detection limit and uncertainty of the method were also evaluated in detail. Major factors of standard uncertainty were grouped into counting error, sample homogeneity, and efficiency calibration. Finally, sensitivity tests of these major factors were performed.

Table 1. Uncertainty budget of the analytical procedure for solid sample

	Uncertainty factor	^{3}H	^{14}H	Unit
Standard uncertainty	Counting error	0.53	2.15	%
	Sample homogeneity	5.3	1.1	
	Lab control standard	2.0	2.0	
	Efficiency calibration	5.0	5.0	
	Overall process	3.0	3.0	
Combined uncertainty		8.1	6.6	
Measured values		66.7	2.0	Bq/g
Uncertainty(k=1)		5.3	0.1	

[1] Kim, H.R., Kang, M.J., Choi, G.S. An experiment on the radioactivity characteristics of the tritium contaminated metal sample, *Annals of Nuclear Energy*, 2011. 1074- 1077.
[2] Hou, X., Roos, P. Critical comparison of radiometric and mass spectrometric methods for the determination of radionuclides in environmental, biological and nuclear waste samples. *Analytica chimica Acta* , 2008. 105-139.

*Corresponding author. E-mail: jmlim@kaeri.re.kr

Preparation of pure TiO_2 sorption material

Irena Špendlíková, Jakub Raindl, Mojmír Němec
Czech Technical University in Prague, Department of Nuclear Chemistry, Brehova 7, 115 19 Prague, Czech Republic

Abstract

Among the natural or anthropogenic radionuclides of very low concentrations nowadays measured in environmental samples, the radionuclide of ^{236}U has been recently included. In these ultra-trace analyses, the purity of sorption materials is very important and the traditional preparation procedures have to be optimized to minimize possible contamination. In the case of the determination of natural concentration of ^{236}U ($^{236}U/^{238}U \sim 10^{-10} - 10^{-14}$), the sample treatment procedure has to be modified in order to eliminate possible contamination from anthropogenic ^{236}U that may result even in more than ten thousand times higher $^{236}U/^{238}U$ ratios.

Many inorganic and organic materials have been proposed for the extraction of uranium. However, only several of them are suitable for the uranium sorption from the solutions of low uranium concentration, but relatively high salt content, such as fresh water, sea water etc. At the same time they have to meet other limiting parameters such as fast kinetics, chemical stability, and low costs. Among the inorganic sorption materials, titanium dioxide has been studied for years with promising results.

Titanium dioxides can be prepared via the hydrolysis of titanium compounds, either inorganic salts or organic derivatives, but their properties strongly depend on the preparation conditions. In classical procedures, titanium dioxides are prepared from commercial inorganic salts, such as sulphates or chlorides, or even from industrial intermediates of the titanium white production. Typically, the resulting titanium dioxides are contaminated with uranium already from the origin. Assuming that most organic compounds do not contain uranium and that it is possible to find "uranium free" water, titanium dioxide free of uranium contamination could be prepared by the hydrolysis of organic titanium derivatives.

The aim of this study was to find a suitable way of pure titanium dioxide preparation and to optimize the preparation procedure with respect to the sorption properties of the resulting material towards uranium. Therefore, an organic compound, tetrabutylorthotitanate, was used for the preparation of a series of titanium dioxide samples. The conditions of the preparation procedure slightly varied (e.g. different washing solutions – ethanol, acetone or both) but the important steps like sample drying remain unchanged.

One of the aspects which should be considered in the preparation of TiO_2-based absorbers is the fact that the sorption properties of titanium dioxide strongly depend on the crystal structure and their capacities increase in order: rutile < anatase < amorphous. Therefore, the first characterization of the new prepared materials was carried out using the X-Ray Powder Diffraction method. The presence of the organic compound residue in the materials after the hydrolysis was monitored using the thermogravimetry and IR methods and the size and shape of the particles were measured using the SEM/TEM.

Other important characteristic of new sorption material are specific surface area, sorption capacity and possible correlation among them. Specific surface area of the prepared oxides was determined by selective sorption of nitrogen gas from catalytically deoxygenated mixture of 5 H_2 : 1 N_2 at the temperature of 77 K. Sorption capacities for uranium were deduced from their sorption isotherms determined with fixed uranium concentration (20 $mmol.L^{-1}$) and variable values of V/m (10 - 1400 $mL.g^{-1}$).

Based on this characterization, the most promising material has been chosen. In the future study, this material will be prepared in larger quantity using "uranium free" water and used for the uranium concentration from environmental samples and for the consecutive determination of $^{236}U/^{238}U$ ratios using Accelerator Mass Spectrometry which will outline the contamination with anthropogenic ^{236}U and/or its natural abundance.

Keywords

Titanium dioxide, uranium sorption, ^{236}U

APSORC'13 - 5th Asia-Pacific Symposium on Radiochemistry
Kanazawa, Japan, 22-27 September 2013

Mössbauer Study of Iron Carbide Nanoparticles Produced by Sonochemical Synthesis

R. Miyatani[1], Y. Yamada[1], Y. Kobayashi[2,3]
[1]Department of Chemistry, Tokyo University of Science
[2]Department of Engineering Science, The University of Electro-Communications, [3]RIKEN

Abstract – Iron carbide nanoparticles were synthesized by ultrasonic irradiation of iron pentacarbonyl or ferrocene in diphenylmethane. Mössbauer spectra of the as-prepared particles measured at room-temperature and 6 K indicated only one doublet. The particles were annealed at 600 °C under argon for 2 h, and the Mössbauer spectrum measured at room-temperature consisted of Fe_3C, α-Fe, and a paramagnetic component.

Keywords – Sonochemistry, Iron carbide, Iron pentacarbonyl, Ferrocene, Nanoparticles

I. INTRODUCTION

Iron carbide nanoparticles of various compositions have been studied extensively due to their magnetic properties. Recently, Fe/Fe_3C nanoparticles were synthesized by sonicating iron pentacarbonyl $Fe(CO)_5$ in diphenylmethane and subsequent annealing [1]. But the mechanism of the sonochemical reaction and the effect of annealing are yet to be investigated. In this study, we performed sonolysis of $Fe(CO)_5$ in diphenylmethane and both the as-prepared nanoparticles and the particles after annealing were measured. The similar experiments were performed using ferrocene $FeCp_2$ in order to investigate the difference of the products depended on precursors.

II. EXPERIMENT

0.1mol of $Fe(CO)_5$ in diphenylmethane was irradiated using a high intensity ultrasonic horn (Ti-horn, 20 kHz) under argon flow for 1 h. 15 mmol of $FeCp_2$ in diphenylmethane was also sonicated under argon flow for 6 h. After the sonication, the products were centrifuged, washed with hexane and dried in vacuum. The product was annealed under argon flow for 2 h. The product was investigated by Mössbauer spectroscopy, X-ray diffraction (XRD), and transmission electron microscope (TEM).

III. RESULTS AND DISCUSSION

Nanoparticles were produced by sonolysis of $Fe(CO)_5$ in diphenylmethane. Mössbauer spectra were measured at 293 K and 7 K, and there observed only one doublet; $\delta = 0.35$ mm/s, $\Delta E_q = 0.94$ mm/s at 293 K and $\delta = 0.48$ mm/s, $\Delta E_q = 0.94$ mm/s at 7 K. Thus, the product was a paramagnetic compound. The XRD patterns with broad peaks and the TEM images showed that the nanoparticles were amorphous. Then, the sample were annealed at 300 °C, also the Mössbauer spectrum exhibited a doublet ($\delta = 0.35$ mm/s, $\Delta E_q = 0.88$ mm/s) at 293 K. However, Mössbauer spectrum measured at 6 K of the sample consisted of two sextets ($\delta = 0.45$ mm/s, $H = 491$ kOe and $\delta = 0.42$ mm/s, $H = 428$ kOe) and a doublet ($\delta = 0.41$ mm/s, $\Delta E_q = 1.12$ mm/s). The some of the XRD patterns of the sample corresponded to those of Fe_3O_4. It was presumed that the particles after annealing consisted of Fe/O/C. Room-temperature Mössbauer spectrum of the sample annealed at 700 °C showed only one sextet ($\delta = 0.35$ mm/s, $H = 511$ kOe) which was assigned to α-Fe_2O_3.

Next, nanoparticles were produced by sonolysis of $FeCp_2$ in diphenylmethane in order to eliminate the effects of oxygen in the sample. Mössbauer spectra measured at room temperature showed a doublet ($\delta = 0.36$ mm/s, $\Delta E_q = 0.94$ mm/s) (Fig.1a) while the spectrum measured at 6 K also showed one doublet ($\delta = 0.44$ mm/s, $\Delta E_q = 0.98$ mm/s). However, Mössbauer spectrum of the sample after annealing at 600 °C showed two sextets and a doublet (Fig.1b). The sextets were assigned to cementite Fe_3C ($\delta = 0.20$ mm/s, $H = 211$ kOe) and α-Fe ($\delta = 0.02$ mm/s, $H = 333$ kOe). Iron oxides were not found in the sample produced from $FeCp_2$.

IV. CONCLUSION

Nanoparticles produced by ultrasonic irradiation of $Fe(CO)_5$ in diphenylmethane consisted of Fe/O/C, whereas the nanoparticles produced by sonolysis of $FeCp_2$ in diphenylmethane did not contain oxygen. As-prepared particles were paramagnetic amorphous, and the particles with magnetic nature were produced after annealing. $FeCp_2$ is an adequate starting material to produce iron carbide particles.

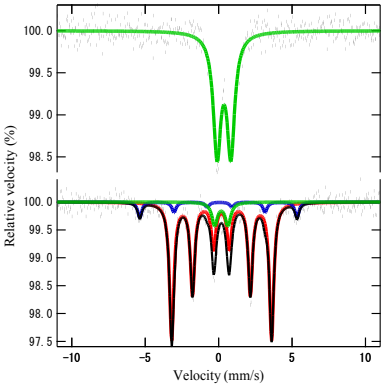

Fig.1 Room-temperature mössbauer spectra of (a) as-prepared nanoparticles produced by sonolysis of $FeCp_2$ in diphenylmethane and (b) the sample after annealing at 600 °C under argon flow for 2 h.

[1] S. I. Nikitenko, Yu. Koltypin, I. Felner, I. Yeshurun, A. I. Shames, J. Z. Jiang, V. Markovich, G. Gorodetsky, and A. Gedanken, *J.Phys. Chem. B*. 108, 7620-7626 (2004)

MÖSSBAUER STUDY OF IRON FLUORIDE FILMS PRODUCED BY PULSED LASER DEPOSITION

K. Shiga[1], Y. Yamada[1], Y. Kobayashi[2,3]
[1]Department of Chemistry, Tokyo University of Science
[2]Department of Engineering Science, The University of Electro-Communications, [3]RIKEN

Abstract – Iron fluoride thin films were produced by a reaction of laser-evaporated iron atoms with sulfur hexafluoride gas. The composition of thin films changed varying a pressure of ambient SF_6 gas: FeF_3 was obtained at a high pressure while FeF_2 was obtained at a low pressure. It was also demonstrated that the crystalline size of FeF_3 in the film was controlled by the substrate temperature while PLD.

Keywords – Iron fluoride, Film, Pulsed laser deposition, Mössbauer spectroscopy

I. INTRODUCTION

Pulsed laser deposition PLD in an ambient gas is a very useful method to produce compound films controlling the compositions [1-4]. In this study, we performed PLD of Fe metal in SF_6 atmosphere to produce iron fluoride films deposited onto Al substrates, and their structures and compositions were investigated. While SF_6 is known as an inert gas, it decomposes to produce F atoms in a plasma plume produced by the laser ablation followed by a production of iron fluorides.

II. EXPERIMENTAL

A block of Fe metal in a vessel filled with pure SF_6 gas was irradiated using Nd: YAG laser (523 nm, 85 mJ/pulse, 10 Hz) for 110000 pulses, and the laser-evaporated Fe atoms were deposited onto an Al substrate. The SF_6 atmosphere was maintained at a desired pressure between 1 and 5 Pa, and the Al substrate was kept at desired temperature between 298 and 873 K using a heater. The synthesized iron fluoride films were investigated by Mössbauer spectroscopy, powder X-ray diffraction (XRD), and scanning electron microscopy (SEM).

III. RESULTS AND DISCUSSION

PLD of Fe onto Al substrate at 298 K was performed in a SF_6 ambient gas of 5 Pa to produce an iron fluoride film. The Mössbauer spectrum of the film was measured at 298 K (Fig. 1a) and only one doublet (δ = 0.49 mm/s, ΔE_q = 0.58 mm/s) was observed. When the same sample was measured at 6 K (Fig. 1b), Mössbauer spectrum changed to show a sextet (δ = 0.59 mm/s, $H\iota$ = 561 kOe) which was assigned to FeF_3. It was considered that the crystalline size of FeF_3 in the film was very small showing the superparamagnetic nature at a high temperature. The XRD pattern of the sample showed broad lines, and it was also confirmed that the film consisted of small crystalline. Next, PLD of Fe in SF_6 of 5 Pa onto the Al substrate at 873 K was performed. The Mössbauer spectrum of the film measured at 298 K (Fig. 2a) showed a sextet (δ = 0.49 mm/s, $H\iota$ = 395 kOe) of FeF_3 as well as an unassigned doublet (δ = 0.46 mm/s, ΔE_q = 1.71 mm/s). The crystal growth on the substrate surface was enhanced by increasing the substrate temperature while deposition to show the sextet at 298 K. SEM images of the films revealed that the film produced at 873 K had rugged surface because of the crystal growth, whereas the film produced at 293 K had a smooth surface. Similar experiment was performed at a low pressure 1 Pa of SF_6, and the Mössbauer spectra measured at room temperature (Fig. 2b) showed a doublet (δ = 1.39 mm/s, ΔE_q = 2.76 mm/s) of FeF_2. The assignments of the films were also confirmed by the XRD patterns. The composition of the films clearly depended on the ambient SF_6 pressures.

IV. CONCLUSION

PLD of Fe in SF_6 gas produced FeF_3 or FeF_2 films. The crystalline size in the film was controlled by the substrate temperature while deposition. Composition of films was controlled by the pressure of ambient gas.

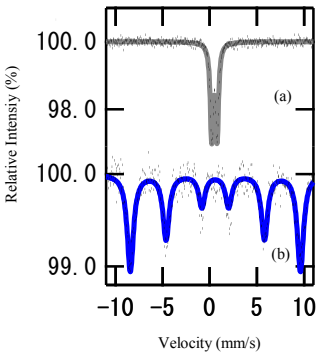

Fig.1 Mössbauer spectra of an iron fluoride film produced by PLD onto an Al substrate at 298 K in 5 Pa of SF_6 ambient gas. The film was measured at (a) 298 K and (b) 6 K.

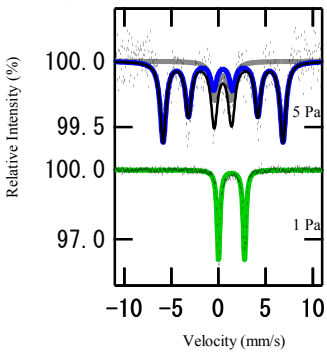

Fig.2 Room-temperature Mössbauer spectra of iron fluoride thin films produced by PLD onto an Al substrate at 873 K.
The pressures of SF_6 are indicated in the figure.

[1] D. Yokoyama, K. Namiki, H. Fukasawa, J. Miyazaki, K. Nomura, Y. Yamada, J. Radioanal. Nucl. Chem., 272, (2007) 631
[2] Y. Yamada, H. Yoshida, K. Kouno, J. Phys.: Conf. Ser. 217, 012096 (2010)
[3] Y. Yamada, H. Yoshida, Y. Kobayashi, Hyper. Int. 198, (2010) 55
[4] R. Usui, Y. Yamada, Y. Kobayashi, Hyper. Int. **205** (2012) 13

APSORC'13 - 5th Asia-Pacific Symposium on Radiochemistry
Kanazawa, Japan, 22-27 September 2013

Iron sulfide particles synthesized in liquid phase

R. Shimizu[1], Y. Yamada[1], Y. Kobayashi[2,3]
[1]Department of Chemistry, Tokyo University of Science
[2]Department of Engineering Science, The University of Electro-Communications, [3]RIKEN

Abstract – Iron sulfide particles were prepared by a polyol method using ferrocene as a precursor. The composition of the particles changed varying a mixture ratio of 1,2-hexadecanediol and 1-octadecanethiol. Iron (III) sulfide (Fe_2S_3) which has not been available in normal conditions was obtained.

Keywords – Iron (III) sulfide, Particles, Mössbauer spectroscopy, polyol method

I. INTRODUCTION

Generally, iron sulfide is stable having divalent iron Fe(II), and few Fe(III) sulfides have been reported. As the iron (III) sulfide have been appeared in an amorphous form, and thus, the existence has been the subject of discussion. Mössbauer spectra of Fe(III) sulfide (Fe_2S_3) was reported in a literature [1], but the crystal structure was not clear. An unstable phase could be stabilized in a form of small particles. In this study, we synthesized iron sulfide particles using a polyol method, and their Mössbauer spectra were measured.

II. EXPERIMENTAL

A mixture of ferrocene (2 mmol), oleylamine (30 mL), 1,2-hexadecanediol (HD), and 1-octadecanethiol (OT) (varying the mixture ratio of HD / OT = 0 mmol / 8 mmol, 8 mmol / 2 mmol, 8 mmol / 4 mmol, 8 mmol / 8 mmol) was heated to reflux for 2 h at 320 °C under a flow of argon. Particles were washed three times with ethanol and hexane after air cooling. The synthesized iron sulfide particles were investigated by Mössbauer spectroscopy, powder X-ray diffraction (XRD), and scanning electron microscopy (SEM).

III. RESULTS AND DISCUSSION

Fig. 1 shows SEM images of iron sulfide particles. Particle size changed dramatically by a presence of polyol: the particles produced without HD were ~ 1 μm (Fig. 1a), whereas the particle produced with HD were 100 ~ 200 nm (Fig. 1b).

Fig. 2 shows the Mössbauer spectra measured at room temperature of iron sulfide particles obtained in various mixture ratio of HD / OT. The particles produced without HD were assigned to $Fe_{1-x}S$ (pyrrotite) (Fig. 2a). When the small amount of OT (2 mmol) was added, two sets of sextet were observed, which were assigned to FeS (troilite) and α-Fe (Fig. 2d). Two sets of doublet (δ = 0.38 mm/s, ΔE_q = 0.73 mm/s and δ = 0.44 mm/s, ΔE_q = 0.47 mm/s) were observed in all the samples produced under the conditions with HD (Fig. 2b-d). Mössbauer parameters of the doublets had the similar values of iron (III) sulfide (Fe_2S_3) reported in the literature [1].

XRD patterns of the samples were shown in Fig. 3, and the yields of FeS, $Fe_{1-x}S$ and α-Fe were in good agreement with the results obtained by the Mössbauer spectra. Besides these well assigned XRD patterns, unassigned XRD patterns were observed. The peaks marked 'X' in Fig. 3 may correspond to Fe_2S_3 with a long-range periodic structure which were observed for the first time.

IV. CONCLUSION

Iron sulfide particles were prepared by the polyol method. Iron(III) sulfide (Fe_2S_3) particles having a long-range periodic structure were found. The Mössbauer spectra of Fe_2S_3 showed that it was paramagnetic.

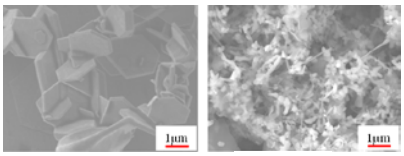

Fig. 1. SEM images of the iron sulfide particles synthesized with the molar ratio of HD / OT (a) 0/ 8 and (b) 8 / 4.

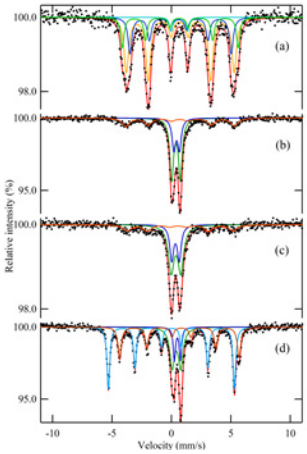

Fig. 2. Room-temperature Mössbauer spectra of the iron sulfide particles synthesized in a mixture of HD / OT = (a) 0 / 8, (b) 8 / 8, (c) 8 / 4, and (d) 8 / 2.

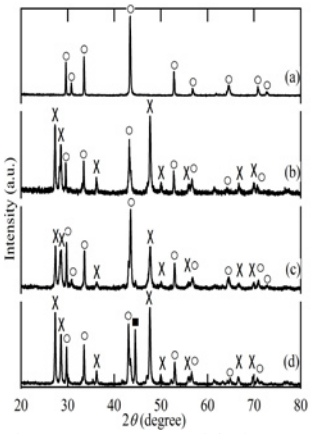

Fig. 3. XRD patterns of the iron sulfide particles synthesized in a mixture of HD / OT (a) 0 / 8, (b) 8 / 8, (c) 8 / 4, and (d) 8 / 2. (○) FeS or $Fe_{1-x}S$, (■) α-Fe, (×) unidentified peaks

[1] A. H. Stiller, B. Jack MaCormick, P. Russell, P. A. Montano, J. Am. Chem. Soc. 100, 2553-2554 (1978)

APSORC'13 - 5th Asia-Pacific Symposium on Radiochemistry
Kanazawa, Japan, 22-27 September 2013

Mössbauer and XRD studies of NiCuZn ferrites By Sol-Gel auto-combustion

Chenglong Lei[1], Qing Lin[1,2]*, Haifu Huang[3], Hui Zhang[1], Yun He[1]
[1]*College of Physics and Technology, Guangxi Normal University, Guilin 541004, China*
[2]*Department of Information Technology, Hainan Medical College, Haikou 571101, China*
[3]*Nanjing National Laboratory of Microstructures and Jiangsu Provincial Laboratory for NanoTechnology,,Department of Physics, Nanjing University, Nanjing 210093, China*
e-mail:hy@gxnu.edu.cn

Abstract:
The $Ni_{0.6}Cu_{0.2}Zn_{0.2}Ce_xFe_{2-x}O_4$ ferrites（0≤x≤0.85） have been prepared by Sol-Gel auto-combustion method and we have investigated the effect of impurity CeO_2 phase to the microstructure and hyperfine magnetic field in spinel ferrite. The results of XRD patterns confirm the average crystallite size of samples decreases with Ce^{3+} substitution increasing and the lattice parameters vary as a function of x content. ^{57}Fe Mössbauer spectra at room temperature for all samples confirm the [Fe^{3+}- O^{2-}-Fe^{3+}] super exchange interaction decrease due to cerium substitution. For low temperature auto-combustion samples it reveals one normal sextet line and one doublet line x≤0.25, which shows well-resolved ferromagnetic order. Lattice defects are determined and Mössbauer spectrums vary from magnetic sextet to relaxation doublet at x≥0.45 due to a mass of CeO_2 phase. In contrast, the Mössbauer spectra for the samples sintered at 800℃/3h detect the secondary phaseα -Fe_2O_3 where the cation distribution occurs and it collapses to paramagnetic doublet(x≥0.85). Ce^{3+} substitution has its maximum limit values of super exchange interaction and high sintering temperature will affect this interaction.

Keywords: NiCuZn ferrite, Rare earth, Cerium substitution, Mössbauer, XRD

I. RESULTS AND DISCUSSION

We have successfully prepared ferrite system Ce^{3+} doped $Ni_{0.6}Cu_{0.2}Zn_{0.2}Fe_2O_4$ by Sol-Gel auto-combustion method. The XRD patterns of ferrite as-brunt and sintered at 800℃/3h powders are shown in Fig.1-3, respectively.

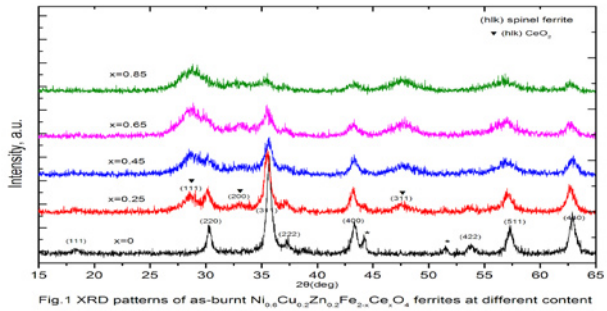

Fig.1 XRD patterns of as-burnt $Ni_{0.6}Cu_{0.2}Zn_{0.2}Fe_{2-x}Ce_xO_4$ ferrites at different content

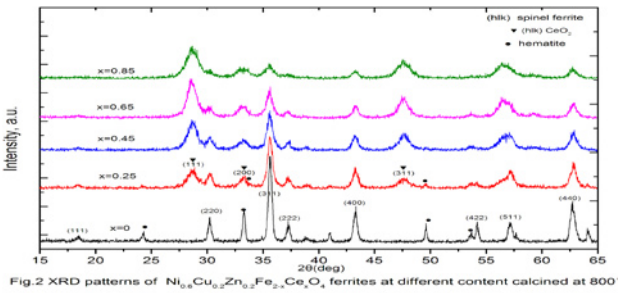

Fig.2 XRD patterns of $Ni_{0.6}Cu_{0.2}Zn_{0.2}Fe_{2-x}Ce_xO_4$ ferrites at different content calcined at 800℃

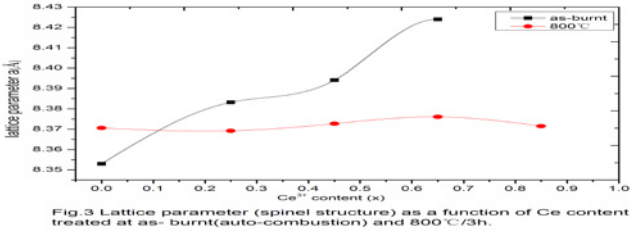

Fig.3 Lattice parameter (spinel structure) as a function of Ce content treated at as- burnt(auto-combustion) and 800℃/3h.

Fig.4 and Fig.5 show the Mössbauer spectra (RT) of $Ni_{0.6}Cu_{0.2}Zn_{0.2}Ce_xFe_{2-x}O_4$ nanocrystalline ferrites measured at room temperatures , respectively.

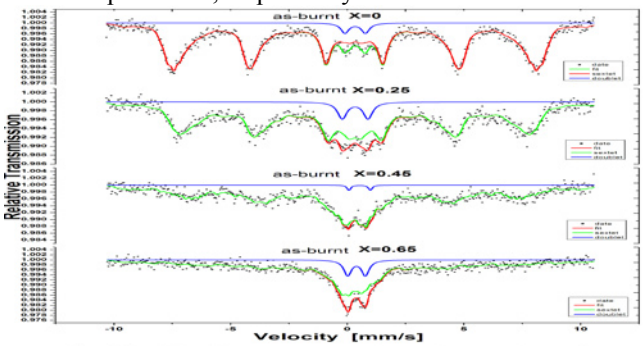

Fig.4 The Mossbauer spectra at room temperature of as-burnt $Ni_{0.6}Cu_{0.2}Zn_{0.2}Ce_xFe_{2-x}O_4$ at different content

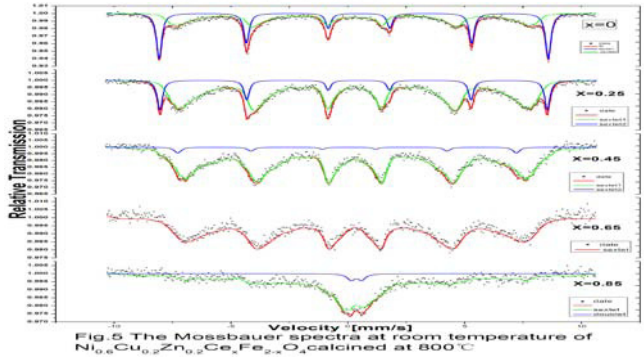

Fig.5 The Mossbauer spectra at room temperature of $Ni_{0.6}Cu_{0.2}Zn_{0.2}Ce_xFe_{2-x}O_4$calcined at 800℃

The lattice parameter changes as a function of the cerium substitution. The Mössbauer spectra (RT) results illustrate that only after low temperature auto-combustion the samples exhibit ferromagnetism and a super para-magnetism.

[1] Aphesteguy, J.C., et al., *Characterization of nanosized spinel ferrite powders synthesized by coprecipitation and autocombustion method.* Journal of Alloys and Compounds, 2010. 495(2): p. 509-512.
[2] Nedkov, I., R.E. Vandenberghe, and A. Zaleski, *Surface magnetic disorder in nanostructured $Ni_{0.5}Zn_{0.5}Fe_2O_4$ particles.* Journal of Magnetism and Magnetic Materials, 2010. 322(18): p. 2732-2736.
[3] S.I.Moussa, R.R.Sheha, E.A.Saad, N.A.Tadros, Synthesis and characterization of magnetic nano-material for removal of Eu^{3+} ions from aqueous solutions, *Journal of Radioanalytical and Nuclear Chemistry*, 2013. 295: 929–935.

Thermal Stability of Locally-Associated Al and In Impurities in Zinc Oxide

S. Komatsuda[1], W. Sato[1,2], and Y. Ohkubo[3]
[1]Graduate School of Natural Science and Technology, Kanazawa University
[2]Institute of Science and Engineering, Kanazawa University
[3]Research Reactor Institute, Kyoto University

Abstract – Local structures in 100 ppm Al-doped ZnO were investigated by means of the time-differential perturbed angular correlation method. From distinct perturbation patterns obtained for the samples annealed in different conditions, we found that the ^{111}In, which is strongly associated with Al ions in ZnO, gradually breaks the interaction and occupies the defect-free substitutional Zn site in high-temperature vacuum.

Keywords – Al-doped ZnO, electric field gradient, In-111, perturbed angular correlation

I. INTRODUCTION

Zinc Oxide (ZnO) doped with group 13 elements (Al, Ga, In) as impurity donors is expected to be applied to functional devices as *n*-type semiconductors. For a practical use of ZnO as a conduction-controlling device, it is of great importance to study the physical and chemical states of the dilute impurity ions in ZnO. The time-differential perturbed angular correlation method (TDPAC) is very suited for that purpose because it can directly provide atomic-level information of impurity atoms. In our previous TDPAC studies, we found that Al ions and ^{111}In probe doped in ZnO can form local associations even at extremely dilute concentrations[1]. In this work, we have investigated the stability of the interaction between Al and In impurities in various conditions.

II. EXPERIMENTS

For the synthesis of 100 ppm Al-doped ZnO, stoichiometric amounts of $Al(NO_3)_3 \cdot 9H_2O$ and ZnO powder were mixed in ethanol. The suspension was heated to evaporate the ethanol until dryness. The powders were pressed into disks and sintered in air at 1273 K for 3 h. For TDPAC measurements, commercially available ^{111}In solution was added in droplets onto each of the sintered disks at the concentration of 100 ppt. The disks again underwent heat treatment in air at 1373 K for 2 h. Then the disk samples were ground into powder, and sealed in a quartz tube in vacuum respectively. The samples underwent further heat treatment in vacuum at 1023 K and 1173 K for 24 h. The TDPAC measurements were carried out for the 171-245 keV cascade γ rays of ^{111}Cd($\leftarrow^{111}$In) probe with the intermediate state of I = 5/2 having a half-life of 85.0 ns.

III. RESULTS

Figure 1(a) shows a TDPAC spectrum obtained for the sample heat-treated in air. The directional anisotropy, $R(t)$, is plotted as a function of the time interval between the cascade γ-ray emissions, t, during which the probe is perturbed by the outer surrounding field. This spectrum shows that 100 ppm Al and 100 ppt ^{111}In are locally-associated in ZnO matrix, suggesting that there is a strong attractive force between Al and In in ZnO[1]. Figure 1(b) and 1(c) show TDPAC spectra obtained for the samples annealed in vacuum at 1023 K and 1173 K respectively, for 24 h after the probe was doped. For the spectrum in Fig. 1(b), two different components appearing in the spectra for the Fig. 1(a) and undoped ZnO[2] were observed. The component appearing in the spectrum for undoped ZnO has become more visible in Fig.1 (c). These observations imply that in high-temperature vacuum, the probe resides solely at the substitutional Zn site being independent of the field produced by Al ions. Showing TDPAC spectra of the samples annealed in various conditions, we discuss the stability of locally-associated Al and In impurities doped in ZnO.

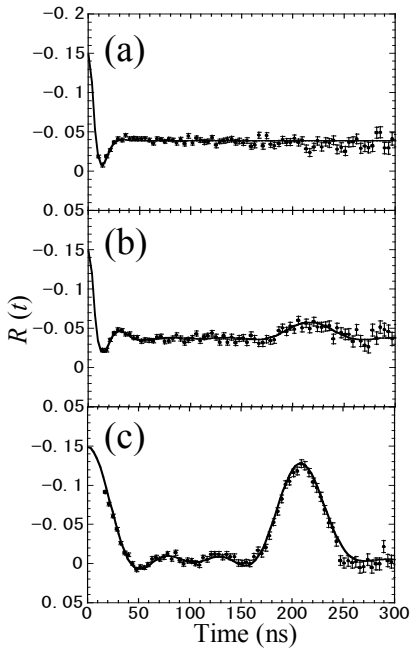

Fig.1 Room temperature TDPAC spectra of ^{111}Cd($\leftarrow^{111}$In) embedded in 100 ppm Al-doped ZnO annealed (a) in air at 1373K, (b) in vacuum at 1023 K, and (c) in vacuum at 1173K.

[1] S. Komatsuda, W. Sato, S. Kawata, and Y. Ohkubo, J. Phys. Soc. Jpn. **80**, (2011) 095001.
[2] W. Sato, Y. Itsuki, S. Morimoto, H. Susuki, S. Nasu, A. Shinohara, and Y. Ohkubo, Phys. Rev. B **78** (2008) 045319.

Structure and Antimony-121 Mössbauer Spectra of Hypervalent Antimony Compounds with an Antimony–Gold Bond in Equatorial Position

Masashi Takahashi, Asumi Sato, Shiro Matsukawa
Department of Chemistry, Toho University
Funabashi, Chiba 274-8510 Japan

Abstract – Hypervalent antimony compounds having Sb–Au bond in equatorial position are studied. [$Rf_2SbAu(PPh_3)_2$] (Rf = $C_6H_4C(CF_3)_2O^-$) has a short Sb–Au bond (2.6813 Å). ^{121}Sb Mössbauer spectrum of [$Rf_2SbAu(SMe_2)$] indicates a large electron density along the Sb–Au bond. These results suggests a dative interaction of the gold fragments to hypervalent antimony atom.

Keywords –Mössbauer Spectroscopy, Hypervalent Compound, Dative Bond, Antimony, Gold

I. INTRODUCTION

Since the first report on the ruthenaboratrane, in which the boron atom at the pivot position of a tripodal ligand acts as the Lewis acid [1] , unconventional metal to ligand donation (M→□) attracts keen interests. Although the investigations are mostly carried out using the electron deficient borane ligands such as $R_nB(C_6H_4PR'_2)_{3-n}$, the heavier main group elements such as phosphorus, antimony, silicon and tin can be used as the Lewis acidic point because these elements accept the electron pair to form hypervalent compounds. Indeed quite recently Wade and Gabbai have demonstrated such M→□ interactions using [$(C_6H_4PPh_2)_3$ SbAuI] (**1**) [2]. On the other hand we have already suggested that the existence of electron flow from organometallic fragment to antimony atom in the hypervalent antimony compounds $Rf_2SbMCpL_n$ [M = Fe, Ru, Cr, Mo, W; L = CO, PPh_3 etc; Rf = $C_6H_4C(CF_3)_2O^-$] (**2**) using ^{121}Sb Mössbauer spectroscopy. [3] These results inspired us to extend our investigation to the Au fragments.

II. EXPERIMENTAL

material: Rf_2SbAuL (L = SMe_2, PPh_3) were prepared by the reaction of $[Rf_2Sb]^-$ with AuLCl using a modified method for [$Rf_2SbFeCpL_n$]. The compounds were characterized using ^{1}H, ^{19}F and ^{31}P NMR.
Structural determination: X-ray diffraction data were collected on a SMART APEX (Bruker) at 150 K. Data were processed as routine.
^{121}Sb Mössbauer spectrum: Mössbauer spectrum was measured at 20 K using a $Ca^{121}SnO_3$ source on a Mössbauer measurement system from Wissel (MDU-1200, DFG-1200, MVC-450, CMCA-550). The spectrum was analyzed using a MossWin software. The value of the isomer shift was given relative to InSb.

III. RESULTS AND DISCUSSION

The reaction product with $AuCl(PPh_3)_2$ was confirmed to be [$Rf_2SbAu(PPh_3)_2$] (Fig. 1), which has unexpectedly a three coordinated gold atom. The antimony atom adopts trigonal bipyramidal geometry as expected. The Sb–Au length (2.6813 Å) is shorter than that of (**1**) (2.7086 Å). The Sb–O and Sb–C lengths are slightly longer than those of **2**. The O–Sb–O and C–Sb–C angle is almost the same to those of **2**. These results suggest the high electron density along the equatorial Sb–Au bond due to the strong electron donation from gold atom. Two phosphine ligands at gold atom should afford the electron density to Sb atom effectively and might stabilize the Sb–Au bond.

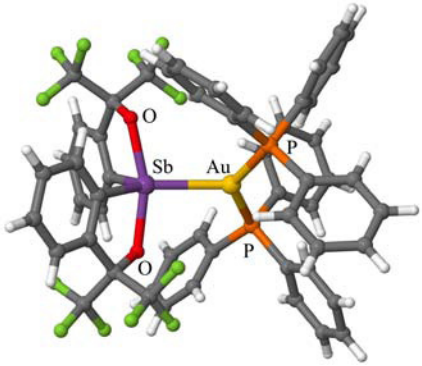

Figure 1 Crystal Structure of [Rf_2Sb–$Au(PPh_3)_2$] Sb–O = 2.1095, 2.1237; Sb–C = 2.123, 2.123 Å; O–Sb–O = 161.75; C–Sb–O = 107.10°.

Fig. 2 shows the Mössbauer spectra of [$Rf_2SbAu(SMe_2)$] (**3**). As expected 3 has a large negative quadrupole coupling constant (–23.91 mm s^{-1}) and a large asymmetry parameter (0.67). The isomer shift value (2.63 mm s^{-1}) is an intermediate value between typical Sb(V) and Sb(III) complexes. The Mössbauer parameters indicate considerable electron density is present along the Sb–Au bond, suggesting a strong electron donation of gold atom.

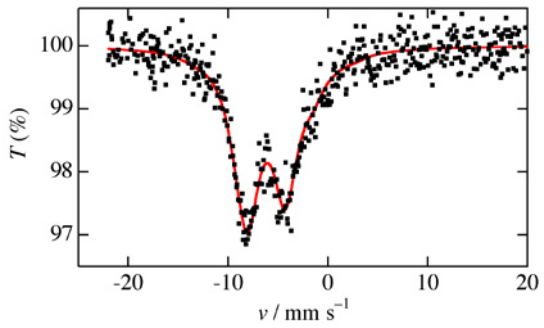

Figure 2 ^{121}Sb Mössbauer spectrum of [$Rf_2SbAu(SMe_2)$] at 20 K.

[1] Hill, A. F. et al. *Angew. Chem. Int. Ed.* **1999**, *38*, 2759.
[2] Wade, C. R.; Gabbai, F. P. *Angew. Chem. Int. Ed.* **2011**, *50*, 7369.
[3] Takahashi, M. et al. *Z. Naturforsch.* **2001**, *57a*, 631.

APSORC'13 - 5th Asia-Pacific Symposium on Radiochemistry
Kanazawa, Japan, 22-27 September 2013

Local Structure of ^{57}Mn/^{57}Fe Implanted into Lithium Hydride

Jun Miyazaki[1], Takashi Nagatomo[2], Yoshio Kobayashi[3, 4], Michael K. Kubo[5], Yasuhiro Yamada[6], Mototsugu Mihara[7], Wataru Sato[8], Kazuya Mae[5], Shinji Sato[9], Atsushi Kitagawa[9]
[1]College of Industrial Technology, Nihon University
[2]J-PARC Center, High Energy Accelerator Research Organization
[3]Department of Engineering Science, The University of Electro-Communications
[4]RIKEN Nishina Center for Accelerator-Based Science, RIKEN
[5]The Division of Arts and Sciences, International Christian University
[6]Department of Chemistry, Tokyo University of Science
[7]Department of Physics, Osaka University
[8]Institute of Science and Engineering, Kanazawa University
[9]Department of Accelerator and Medical Physics, National Institute of Radiological Sciences

Abstract – We report the in-beam Mössbauer Spectra of ^{57}Mn implanted into polycrystalline LiH at under room temperature. As compared with the result of DFT calculations, ^{57}Fe atoms were implanted into Li or H substitutional site in LiH crystal. With an increase the sample temperature, we could observe the decrease of lattice defects.

Keywords – In-beam Mössbauer Spectroscopy, β-decay of ^{57}Mn, Lithium hydride, DFT Calculations

I. INTRODUCTION

In-beam Mössbauer spectroscopy is a powerful technique to obtain the direct information on exotic chemical or physical state of the nuclear probe that was implanted into the sample such as metal or inorganic solid. Lithium hydride (LiH) is an ionic solid having the rock salt type crystal structure in which one Li^+ cation is surrounded by six H^- anions. In our previous study[1], we reported the in-beam Mössbauer spectra of ^{57}Mn implanted into LiH from room temperature to over 800 K. In this study, we report the spectra under room temperature and discus the local structure of ^{57}Mn/^{57}Fe implanted into LiH.

II. EXPERIMENTAL

The measurements were performed using Heavy Ion Medical Accelerator in Chiba (HIMAC) at National Institute of Radiological Science (NIRS) in Chiba, Japan. ^{57}Mn beam (E =~ 260*A* MeV) was produced from the projectile fragment process of nuclear collisions between ^{58}Fe ions (500*A* MeV, ~ 1×10^6 particles per beam) and ^{9}Be nuclei in a 27 mm thick production target. The beam pulse was generated every 3.3 s with a ~300 ms duration and with 1×10^6 particles/pulse. The energy of the ^{57}Mn nuclei was adjusted using energy degraders to stop the ions at an appropriated depth in the sample. The polycrystalline LiH (Wako Pure Chemical) was mounted on a cold finger or BN heater in a vacuum chamber in order to control the sample temperature from 11 K to over 800 K. A parallel-plate avalanche counter (PPAC) was employed as a detector. The anti-coincidence method that uses a plastic scintillation detector to detect and reject extraneous β-rays was employed to obtain high-quality in-beam Mössbauer spectra with improved S/N ratios.

III. RESULTS AND DISCUSSION

In-beam Mössbauer spectra of ^{57}Mn/^{57}Fe implanted into LiH at 11, 274, 294 K were shown in Fig. 1. Obtained spectra were fitted with some single lines and doublet lines. In the spectra at 3 temperatures, the single line peaks of S (IS = -0.54 mm/s) and S' (IS = 0.07 mm/s) were observed. As compared with the result from DFT calculations, S is assigned to be in ^{57}Fe at the substitutional Li site and S' is assigned to be in ^{57}Fe at the stubstitutional H site in LiH crystal. Symmetrical doublet peaks of D1 (IS = -0.59 mm/s, ΔE_Q = 0.57 mm/s) and D' (IS = -0.03 mm/s, ΔE_Q = 0.58 mm/s) were also observed, and new doublet peak of D2 (IS = -0.60 mm/s, ΔE_Q = 2.34 mm/s) was observed at 11K (Fig.1c). In the result from DFT calculations, doublet peaks are assigned to be in ^{57}Fe at the substitutional Li or H site with a neighboring atom deficiency. The temperature dependence of the relative intensities in this study suggests that the lattice defects recover with an increase temperature.

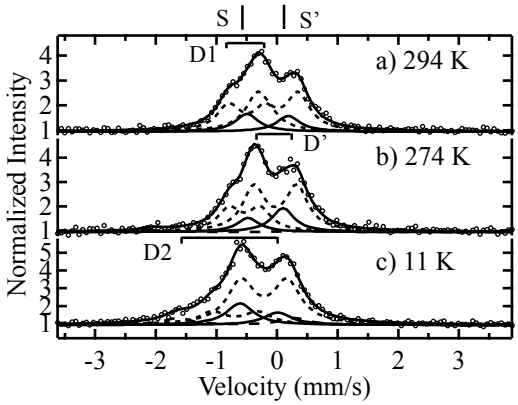

Fig.1 In-beam Mössbauer spectra of ^{57}Mn implanted into LiH

[1] T. Nagatomo *et al.*, *Hyperfine Interact*, **204**, 125-128 (2012)

Evaluation of Vacancy-Type Defects in ZnO by the Positron Annihilation Lifetime Spectroscopy

R. Ono[1], T. Togimitsu[1], and W. Sato[1,2]
[1]Graduate School of Natural Science and Technology, Kanazawa University
[2]Institute of Science and Engineering, Kanazawa University

Abstract – Annealing-temperature dependence of the formation of vacancy-type defects in ZnO has been studied by means of the positron annihilation lifetime spectroscopy. It was found that the lifetime does not drastically change for ZnO samples annealed at the temperature range below 600 ℃, whereas annealing-temperature dependence of the lifetime was observed above 600 ℃, showing the minimum value at 1000 ℃.

Keywords – positron annihilation lifetime spectroscopy, ZnO, annealing effect, vacancy, grain boundary

I. INTRODUCTION

Zinc oxide (ZnO) is an intrinsic n-type semiconductor having optoelectronic properties. Because vacancy-type defects brought about in the formation process of ZnO is known to affect the intrinsic properties, for future applications, it is important to understand various behaviors of defects in ZnO such as generation, recovery, agglomeration and diffusion. For the evaluation of their vacancy-type defects, positron annihilation lifetime spectroscopy (PALS) is one of the most powerful methods and we have applied this spectroscopy to part of our studies on local structures of ZnO. In the present study, we examined annealing-temperature dependence of positron lifetime to evaluate the concentration and size of vacancy-type defects formed in ZnO.

II. EXPERIMENTS

Polycrystalline ZnO powders (purity 99.99%) were pressed into pellets at 75 MPa. They were annealed in air at different temperatures ranging from 200 to 1200℃ for 2h. A ^{22}Na (as in NaCl) positron source covered with Kapton film was sandwiched with the sample disks. Positron annihilation lifetime was measured with a conventional circuit at room temperature. BaF_2 scintillators were used for the detection of 1275- and 511-keV γ rays.

III. RESULTS

It was found from the PALS measurements that the lifetime does not drastically change for ZnO samples annealed at the temperature range between 200 to 600℃. However, obvious temperature dependence was seen for those annealed at higher temperatures. In Fig.1 is shown the PALS spectra obtained for the ZnO samples annealed (a) at 600℃ and (b) at 1000℃. The spectra reproduced by the lines named A are made up of three different decay components as numbered 1-3. Components 1 and 2 originate from self absorption in the source materials, and Component 3 corresponds to positron annihilations in the ZnO samples. The lifetime of Component 3 is the average of those in the bulk and defects in ZnO samples. It is obvious from the slopes of the decay curves of Component 3 that the lifetime of positrons in ZnO annealed at 1000℃ is shorter than that for 600℃. The short lifetime can be explained as a result of the recovery of vacancy-type defects. Particle growth arising from the heat treatment may be another cause of the lifetime shortening because the amount of vacancy-like defects present in grain boundaries is considered to become less by the phenomenon. The positron lifetime, to the contrary, increases in ZnO samples annealed at temperatures above 1000℃. The reason for the increase has not been understood yet. For the total understanding of the defect formation process, further data acquisition at other sample-preparation conditions is now underway.

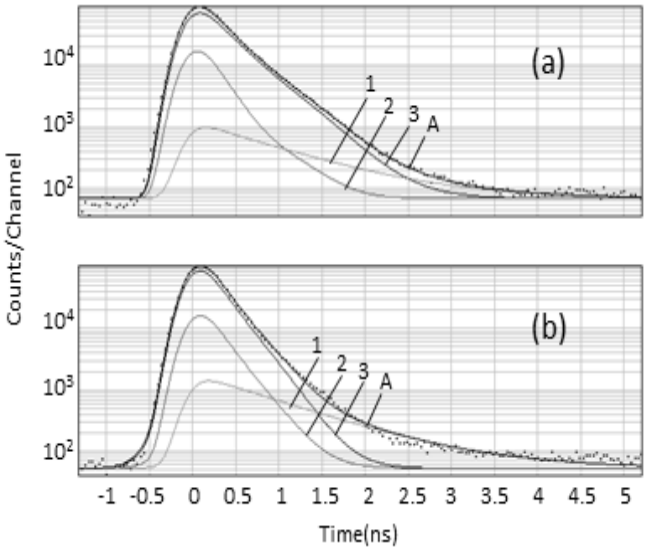

Fig.1 PALS spectra for ZnO pellets annealed (a) at 600℃ and (b) at 1000℃.

APSORC'13 - 5th Asia-Pacific Symposium on Radiochemistry
Kanazawa, Japan, 22-27 September 2013

Determination of ultratrace-levels of ^{99}Tc using ICP-QMS in the low level radioactive waste samples

Te-Yen Su, Tsuey-Lin Tsai, Hsin-Chieh Wu, Lee-Chung Men
Chemistry Division, Institute of Nuclear Energy Research, Longtan, Taoyuan 32546, Taiwan, R.O.C.

Abstract –A rapid, accurate and less labor intensive approach was developed to determine ^{99}Tc in the low level radioactive wastes (LLW). Only 0.1 g of solid radwastes was firstly dissolved using microwave digestion and then the specific TEVA resin was used for chemical separation to remove most of the matrices piror to inductively coupled plasma- quadrupole mass spectrometry (ICP-QMS) measurement. The minimum detectable activity (MDA) of ICP-QMS for the determination of ^{99}Tc in LLW samples was 8.5 mBq g^{-1} (13.6 pg g^{-1}), which was comparable to that of double-focusing magnetic sector field inductively coupled plasma mass spectrometry (ICP-SFMS), 5.3 mBq g^{-1}. The sensitivity of the ICP-QMS method for the determination of ^{99}Tc was much superior to that of the alternative radiochemical methods (e.g., liquid scintillation analyzer; LSA) when accounting for the data acquisition time for identical, low-concentration samples. Approximately 88 % of the chemical recovery was achieved and this developed technique was successfully applied to LLW samples for ^{99}Tc measurement within 5 minutes.

Keywords –^{99}Tc; inductively coupled plasma-quadrupole mass spectrometry (ICP-QMS); low level radioactive wastes (LLW)

APSORC'13 - 5th Asia-Pacific Symposium on Radiochemistry
Kanazawa, Japan, 22-27 September 2013

Development of an Automatic Prompt Gamma-ray Activation Analysis System

Takahito OSAWA[1]
[1]Neutron Imaging and Quantum Beam Analysis Group, Quantum Beam Science Directorate,
Japan Atomic Energy Agency (JAEA),

Abstract – An automatic prompt gamma-ray activation analysis system was developed and installed at the Japan Research Reactor No. 3 Modified (JRR-3M). The main control software, referred to as AutoPGA, was developed using LabVIEW 2011 and the hand-made program can control all functions of the analytical system. The core of the new system is an automatic sample exchanger and measurement system with several additional automatic control functions integrated into the system. Up to fourteen samples can be automatically measured by the system.

Keywords – Prompt gamma-ray analysis; Automatic analysis; Revolute robot; LabVIEW

Prompt gamma-ray analysis (PGA) using a neutron beam generated by a nuclear reactor is a convenient and nondestructive elemental analytical technique. PGA can be widely used in various science and technology fields [e.g. 1], because the analytical methods have high sensitivity for certain specific light elements.

The PGA system at the JRR-3M at the Japan Atomic Energy Agency (JAEA) was constructed in 1992 [2]. Although the system using cold and thermal neutron beams achieved a very low gamma-ray background level, it was outdated because no improvements had been made since its construction. In this study, an automatic system for PGA was developed in order to update the old analytical system and improve its measurement efficiency.

The new automatic PGA system is mainly composed of two computers (PC1 and PC2), four programs, a six-axis vertical revolute joint robot (Mitsubishi RV-3SD, Fig.1), and data acquisition devices. Although the inside of the shielding body is not changed most of the devices and systems on the outside of the shielding body are completely improved in this work. The core of the new system is an automatic sample exchanging and measurement system, and several automatic control functions: such as helium flow control, neutron flux recording, internet functions, and machine vision, have been integrated into the system.

In the system, fourteen samples hung on the center of Teflon frames with Teflon strings that can be placed onto a sample stand. Each sample frame is selected and introduced into a Teflon sample box using a revolute joint robot. Opening and closing of the loading hatch is enabled with compressed air and air bulbs that are controlled using a digital output module. A physical interlock on the loading hatch that synchronizes with the neutron beam shutter is operated by a single-pole single-throw relay, and the relay can also control the opening and closing of the neutron beam shutter.

Fig.1 A revolute joint robot of the automatic PGA system

A robot sequence program written in MELFA BASIC V was designed by the author. The AutoPGA program is installed in PC1 and controls the entire series of automatic analytical operations. When the user clicks the start button AutoPGA starts the servomechanism of the robot and initiates the sequence program. It then closes the neutron beam shutter, releases the interlock, and opens the loading hatch. When the machine vision system judges that the lid is not placed in the correct position, the sequence program stops working. The robot begins operating, and the Teflon lid on the Teflon sample box is removed and placed on a lid stand. The robot selects the sample frame and introduces it into the sample box and then places the lid on the sample box. The loading hatch is closed, the neutron shutter is opened, and the measurement is begun. An existing measurement program (SEIKO EG&G Spectrum Navigator) is installed in PC2 and is used for the measurements. In the automatic analysis, a batch processing mode is utilized that calls a communication program (PGA-Talk created by the author) after each measurement. PGA-Talk sends a signal to PC1 via TCP, and AutoPGA recognizes the completion of the gamma-ray recording and begins to exchange the sample. When the sample exchange is complete, AutoPGA sends a signal to PC2 and PGA-Talk is automatically shut down. Spectrum Navigator then begins the measurement of the next sample.

[1] T. Osawa, Y. Hatsukawa, P. W. U. Appel, H. Matsue, Nucl. Instrum. Meth. Phys. Res. B 269 (2011), pp. 717-720.
[2] C. Yonezawa, A.K.H. Wood, M. Hoshi, Y. Ito and E. Tachikawa, Nucl. Instr. and Meth. A 329 (1993), pp. 207-216.

APSORC'13 - 5th Asia-Pacific Symposium on Radiochemistry
Kanazawa, Japan, 22-27 September 2013

Concentration of Heavy Metal Elements in Chinese Medicine by INAA

S. Ishihara[1], E. Furuta[2], N. Iwasaki[1], Y. Yoshihara[3], R.Okumura[4], Y.Iinuma[4]
[1] Ochanomizu University, Facility of Sciences
[2]Ochanomizu University, Graduate School of Humanities and Sciences
[3]Ochanomizu University, Facility of Human Life and Environmental Sciences
[4]Kyoto University, Research Reactor Institute

Abstract – *An instrumental neutron activation analysis of Chinese medicines and medicinal herbs was performed, in which they have possibilities to contain toxic elements. By the preliminary experiments, there were some medicines that arsenic and mercury were included by observing gamma-ray spectroscopy with neutron irradiation. The Chinese medicine can be purchased through the Internet easily; however, it is considered that some regulations may be necessary.*

Keywords – Chinese medicine, Arsenic, Mercury, INAA

I. INTRODUCTION

Chinese medicine is used all over the world because of its safer image than Western pharmaceutical products. It is possible to purchase everywhere through the Internet. However, a few reports mentioned some of them included some kinds of toxic elements like arsenic (As), lead (Pb), mercury (Hg) and cadmium (Cd) [1]. Chinese medicines and medicinal herbs may be taken in continuously for a long term. So, if they include some toxic elements, it develops a health problem. Therefore, many kinds of Chinese medicines and medicinal herbs which can be purchased in an Asian area were analyzed by neutron activation at the KUR for the purpose of clarifying the actual situation. The preliminary experimental results were shown in the presentation.

II. EXPERIMANTAL

Many kinds of Chinese medicine and medicinal herbs were purchased from 5 routes to analyze the heavy metal elements; 1. 12 kinds of Chinese medicines were sold with a prescription by a hospital doctor in China; they were not sold to public in a market, 2. 8 kinds of Chinese medicines were bought through the Internet from China, 3. 11 kinds of Chinese medicines were bought at a market of Korea, 4. 47 kinds of medicinal herbs were bought at a market of Vietnam, and 5. 25 kinds of Chinese medicines were bought at a medical corner of a super market in Japan; they were produced in Japan. Each of them was enclosed almost 100 mg in a double polyethylene bag. The standard samples used were JA-2 and JR-2 of rock standard. The samples were put in capsules with standards and irradiated 5MW × 10 min or 1MW × 30 min at KUR. After cooling among 5 days, the capsules were opened to take out samples, each sample was enclosed in a new polyethylene bag, and then started measurement of medium and long half-life radionuclides.

III. RESULTS

Table shows the results of 4 elements in the samples from route-1. Among 12 kinds of Chinese medicines, 6 kinds of them included As, and 5 kinds of them included Hg. On the other hand, these 4 elements were not included in 2 of them. Other elements detected were sodium, potassium, calcium, scandium, iron, manganese, lanthanum, and selenium and these elements were included a few ten ppm except for calcium of a few thousand ppm.

Table Four elements concentrations in 10 Chinese medicines (ppm)

Sample	^{51}Cr	^{60}Co	^{76}As	^{203}Hg
牛黄解毒片 Niuhuang Jiedu Pian			7.1%	
青果丸 Fluit, Lonicera	8.0	1.1		
十全大と丸 Shiquan Dabu Wan	3.3	1.6		1.7
天麻首烏片 Tenma Shouwu Pian		1.8	1.9	
麻仁丸 Cannabis sativa				47
六神丸 (Musk) Liu Shen Wan			6.7%	6.7%
胃气痛片 Weiqitong Pian	76	1.8	14	3.8
黄进上清片 Hou –Hashi			2.8	
木香順气丸 Muxiang Shunqi Wan		1.4		4.9
六味地黄丸 Rehmannia glutinosa			1.6	

IV. CONCLUSION

Some of Chinese medicines included high concentration of toxic elements such as As and Hg. It is considered that a regulation how to sell or a limitation of the purchase method is necessary.

[1] Agilent Technologies; www.agilent.com/chem/jp

Application of instrumental neutron activation analysis to assess dietary intake of selenium in Korean adults from meat and eggs

Jong-Hwa Moon[1], Sun-Ha Kim[1], Yong-Sam Chung[1], Ok-Hee Lee[2]
[1]Korea Atomic Energy Research Institute, Daedeok-daero 989-111, Yuseong-gu, Daejeon, 305-353, Korea
[2]Dept of Food Science and Nutrition, Yongin University, 470, Samga-dong, Cheoin-Gu, Yongin, 449-714, Korea

Abstract – Selenium is a key constituent of enzyme in glutathione peroxidase, which is effective in decreasing various types of oxidative stress, Thus, the adequacy of selenium intake is very important in decreasing the risks of various degenerating diseases such as cardiovascular disease, or certain cancers. Lately, the intake of animal foods is increasing among Koreans owing to a dietary transition toward a western style. This study was conducted to measure the selenium content in meat and eggs, and then assessed the selenium intake from these foods. Forty frequently eaten items among meat and eggs were analyzed using an Instrumental Neutron Activation Analysis. The selenium content in 100g of raw meat and eggs ranged from 8.1ug to 50.9ug. In particular, 100g of beef contained 12.4ug to 50.9ug of selenium; pork, 11.2ug to 22.6ug chicken, 10.2ug to 13.7ug and eggs, 28.6ug to 43.0ug. Thus, beef viscera and chicken eggs contain the highest amounts of selenium among these groups. 100g of Pork belly, the most frequently eaten meat type among Koreans, contains 14.6ug of selenium. An evaluation of dietary selenium intake shows that the total selenium supply from meats and eggs was 28.4ug/day and 27.5 ug/day in adult men and women, respectively. These are over one-half of the Korean RNI(Recommended Daily Intake) of 55ug/day.

Keywords–Instrumental Neutron Activation Analysis, Selenium, Meat and Eggs, Dietary Intake

I. INTRODUCTION

As the biological activity of food selenium in humans is dependent, sometimes to a very large degree, on the source and chemical form of the selenium consumed, an increased intake of animal food can facilitate meats and eggs as important sources for selenium intake in Koreans. Considering these points, an evaluation of selenium intake in Koreans from animal foods is very important. This study was conducted to analyze the selenium contents in meats and eggs, and to assess the consumption pattern of selenium in Koreans from these animal foods.

II. EXPERIMENTAL

The number of meat items used in the selenium analysis was 13 items for raw beef, 8 items for raw pork, 3 items for raw chicken, 4 items for raw eggs, and 12 items for the processed meat products, respectively. Most of the foods were bought between September 2009 and February 2010. All domestically produced and imported meats and eggs in a raw or processed state were purchased from markets with a nationwide network around Seoul and Keunggido. The meat sample was ground using a blender with a titanium blade, and freeze-dried in a lyophilizer at various times of 24 - 96 hours. The analysis of selenium was performed by instrumental neutron activation analysis using the HANARO research reactor.

III. RESULTS

The selenium contents in the different parts of beef were ranged from 12.4ug to 50.9ug in 100g of the edible portions, where the highest value was shown with beef liver. The selenium contents in raw Korean pork ranged from 11.2ug to 22.6ug in 100g of food, showing a difference according to the pork region. Pork belly, the most frequently eaten meat among Koreans, contained selenium at an amount of 14.6ug at 100g. The raw chicken contained selenium with a range of 10.2ug to 13.7ug in 100g, showing only a small difference by the chicken part. The selenium contents in the frequently eaten eggs were in the range of 28.6ug 43.0ug for 100g. Eggs were distinct in that they contained the highest amount of selenium among the meats with a range of 38.9ug to 43.0ug for chicken eggs, and of 28.6ug for the quail egg per 100g of eggs. The processed pork products contained selenium in a range of 8.8 - 14.9 ug for 100g, which is lower than the raw unprepared pork meat. Among the pork products, Pyeonuk and pork hocks, cooked pork products, showed selenium contents of 19.4 and 21.1ug for 100g, respectively. The prepared chicken, mostly from fast food eateries, contained selenium in a range of 7.4 to 11.5ug for 100g. An evaluation of dietary selenium intake shows that the total selenium supply from meat and eggs was 28.4ug/day and 27.5ug/day in adult men and women, respectively. These are over one-half of the Korean RNI (Recommended Daily Intake) of 55ug/day.

ACKNOWLEDGEMENT

This work was carried out under the Nuclear Research and Development Program of the Korean Ministry of Education, Science, and Technology.

REFERENCES

[1] J Rotruck JT, Pope AL, Ganther HE, Swanson AB, Hafeman DG, Hoekstra WG. Selenium: biochemical role as a component of glutathione peroxidase. Science 1973, 179:588-90.
[2] The Korean Nutrition Society, Dietary Reference Intake for Koreans, Seoul, 2010, p 481-97.

APSORC'13 - 5th Asia-Pacific Symposium on Radiochemistry
Kanazawa, Japan, 22-27 September 2013

Evaluation of Hypoxia at Dredged Trenches in Tokyo Bay by Determination of Redox Sensitive Elements in the Sediments

T. Yamagata[1], K. Shozugawa[1], R. Okumura[2], K. Takamiya[2], M. Matsuo[1]
[1]Graduate School of Arts and Sciences, The Univ. of Tokyo
[2]Research Reactor Institute, Kyoto Univ.

Abstract – Sediment samples were collected from Tokyo Bay, and the concentrations of some elements were determined by instrumental neutron activation analysis (INAA).Though hypoxia has been observed in dredged trenches, it is suggested that upper layers of the sediments are more oxidative than lower layers.

Keywords – Hypoxia, Sediment in Tokyo Bay, Instrumental neutron activation analysis (INAA)

I. INTRODUCTION

Hypoxia is water mass contained little dissolved oxygen (DO) (< 2 ml of O_2 / liter) [1], which is known as dead zone in coastal sea. At the seabed in Tokyo Bay, large-scale dredging operations had been done in 1970s. In particular, the dredged trenches off Makuhari have the maximum area and depth. In dredged trenches severe hypoxia has been observed in annual summer seasons, and the hypoxia has disappeared in winter. But the influence of dredged trenches on hypoxia is not revealed yet. Therefore, it is important to estimate the interannual variations of hypoxia by analyzing sediments.

To evaluate the sedimentary environment such as redox conditions, the method using the Th/U-Ce/U plot based on the data obtained by INAA was reported by Honda et al [2]. It is very useful because the correlation coefficient between the Th/U and Ce/U ratios is high, but it hasn't been used for evaluating the sedimentary environment at dredged trenches, where the conditions are unique. In this study, sediment cores were collected from the Makuhari dredged trenches in Tokyo Bay. Concentrations of U, Th, and Ce in the sediments were analyzed by INAA. And then the sedimentary environment is discussed in connection with the depth profiles of the elements and the Th/U-Ce/U plot.

II. EXPERIMENTAL

The sediment samples were collected at dredged trenches (water depth 25.5 m and 18.9 m) and reference site (non-dredged seabed, water depth 10.7 m) off Makuhari in Tokyo Bay on August 2012. Sediments were collected by a core sampler at each point. Water quality data were also obtained by a multichannel water quality meter and an oxidation-reduction potentiometer. All cores were cut in the vertical direction at 0.6 – 3.0 cm intervals after freezing.

Approximately 30 mg of freeze-dried sediments were packed in double polyethylene film bags. All samples were irradiated at the pneumatic tube, Kyoto University Reactor (KUR). Two types of gamma-ray measurement were carried out depending on half-lives of elements. For analysis of U, samples were irradiated for 20 min at 1 MW or 4 min at 5 MW, and then gamma-ray was measured for 1200 seconds (live time) by Ge detector after 3 days cooling. Regarding Th and Ce, samples were irradiated for 20 min at 1 MW or 4 min at 5 MW, and the measurement time of gamma-ray was for 9000 seconds (live time) after 3 weeks cooling.

III. RESULTS AND DISCUSSION

The DO in the seawater at dredged trenches and reference site (non-dredged area) indicated the similar vertical distribution at each station. From the depth of 8 m, the DO decreased suddenly. And below the depth of 10 m, the water became anoxic in dredged trenches. It turned out that strong hypoxia has developed at the dredged trenches.

From the depth profiles in dredged trenches, the Th/U and Ce/U ratios are higher in the upper layers than in the lower layers. It is said that the concentrations of Th and Ce in sediments increase when condition of seawater is oxidative. On the other hand, the concentration of U increases when condition is reductive. It is considered that the sedimentary environment of the upper layers is more oxidative than the lower layers.

Figure shows the Th/U-Ce/U plots of the sediments. The correlation coefficient between the Th/U and Ce/U ratios is high enough. Therefore, this method is also useful for evaluating the hypoxia at dredged trenches, in which the environment changes drastically on each summer and winter season.

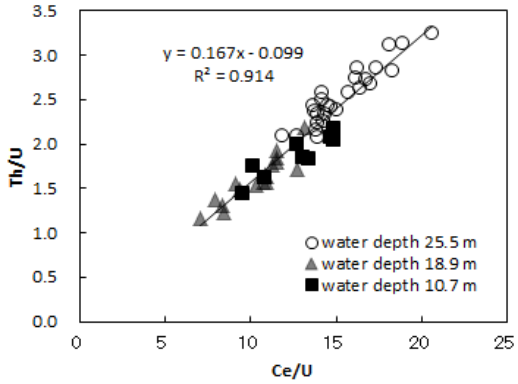

Fig. Th/U-Ce/U plots of the sediments collected from Tokyo Bay

[1] R. J. Diaz and R. Rosenberg, Science, 321, 926-929 (2008).
[2] T. Honda and K. Kimura, Bull. Soc. Sea Water Sci., Japan, 57, 166-180 (2003) (in Japanese).

APSORC'13 - 5th Asia-Pacific Symposium on Radiochemistry
Kanazawa, Japan, 22-27 September 2013

Determination of ultra trace amounts of Mn in iron meteorites by preconcentration neutron activation analysis

Y. Tanaka[1], Y. Arai[1], T. Imamura[1], Y. Oura[1]
[1]Department of Chemistry, Tokyo Metropolitan University

I. INTRODUCTION

Meteorites contain cosmogenic nuclides produced by a nuclear reaction with cosmic rays. Cosmogenic nuclides are useful for determination of exposure and terrestrial ages. In general, only radionuclides and noble gas stable-isotopes can be detected as cosmogenic nuclides. Although it is difficult to detect cosmogenic stable nuclides in stony meteorites, some cosmogenic stable nuclides could be detected in iron meteorites, which consist of mainly an iron–nickel alloy, since iron meteorites have little geochemical lithophile elements. Among such stable nuclides we focus on Mn.

Natural Mn is a monoisotopic (^{55}Mn) element. But iron meteorites have also a cosmogenic radioisotope, ^{53}Mn, which has longest half life among detectable cosmogenic radionuclides. One of practical methods for determination of ^{53}Mn is a preconcentration neutron activation analysis (preNAA) using ^{53}Mn(n, γ)^{54}Mn reaction. We suggested that ^{55}Mn content should be required for determination of ultra trace ^{53}Mn in iron meteorites by preNAA because of correction of ^{55}Mn(n, 2n)^{54}Mn. But accurate concentration in iron meteorites is rarely reported. Almost ^{53}Mn in iron meteorites is extrapolated to be comsogenic by ^{45}Sc contents [1]. If accurate ^{55}Mn concentration can be determined, ^{55}Mn-^{53}Mn system for exposure age will be also established. And estimation of original ^{55}Mn concentration is interesting for considering a differentiation of planets. Determination of ^{55}Mn in iron meteorites by NAA is well known to be interfered by ^{56}Fe(n, p)^{56}Mn reaction. Therefore, the removal of iron prior to irradiation or irradiation at a channel with high Cd ratio is required. Thus we tried to determine ^{55}Mn concentration in iron meteorites by preNAA using well thermalized neutrons.

II. EXPERIMENTAL

Using radiotracers, a chemical procedure using an ion-exchange method was developed for separation of Mn from iron meteorites based on one by Fujimoto and Shimura [2]. After dissolution of a sample in 2 M HF, the HF solution was loaded on a cation exchange resin. Adsorbed Mn was eluted by 8M HCl, and then Mn in HCl - 2-propanol solution was purified by an anion exchange method. This procedure was applied to Japan steel standard samples and Gibeon iron meteorites followed by irradiation of separated Mn fraction for 4 hours at the thermal column pneumatic transport system (Tc-Pn) and for 1 hour at Pn-2 in Kyoto University Research Reactor (KUR). In addition, sensitivity of ^{55}Mn(n, γ)^{56}Mn and contribution of ^{56}Fe(n, p)^{56}Mn at Tc-Pn in KUR and at PN-3 in the Japan Research Reactor-3 (JRR-3), Japan Atomic Energy Agency were evaluated by using Mn standard and Ti plate, respectively.

III. RESULT AND DISCUSSION

In Mn fraction irradiated for 1 h at Pn-2, no ^{59}Fe and ^{60}Co was observed. Our chemical procedure removed > 99.99% of Fe and Co and > 99.5% of Ni, Ir and Cr, and overall procedure blank of Mn was about 30 ng. Determined Mn concentration in steel standards (JSS003-5 and JSS001-5) and Gibeon meteorites are shown in Table 1. Low determination values in Run-1 were guessed to be caused by low chemical yield. In Run-2 a chemical yield was estimated to be 91% and determined concentrations on Mn in steel standards were consistent with certified values. It is concluded that down to 30 ppb of Mn can be determined by our method.

Sensitivities of Mn were 930 cps/μg and 2400 cps/μg for 4 h irradiation at Tc-Pn and 20 min irradiation at Pn-3, respectively. And contributions of (n, p) reaction were corresponding 16 ngMn/gFe and 97 ngMn/gFe for Tc-Pn and PN-3, respectively. Since Fe was sufficiently removed, contribution of ^{56}Fe(n, p) reaction was more than 150 times smaller than the present procedure blank. A detection limit of Mn by preNAA was 30 ppb, assuming that a half of induced ^{56}Mn is resulted by a blank. Even INAA using Tc-Pn can determine such concentration of Mn. Reducing a procedure blank is highly required for lower detection limit.

TABLE 1: Result of Mn content

Sample	Unit	INAA*	preNAA run1	preNAA run2	Certified Value
JSS003-5	ppm	24.9 ± 0.2	19.8 ± 0.4	26.0 ± 0.3	27 ± 1
JSS001-5	ppb	36.1 ± 2.2		27.5 ± 2.2	30 ± 10
Gibeon	ppb		273 ± 9	415 ± 7	

*Corrected for (n, p) reaction.

[1] Oura et al., Proc. Radiochim. Acta 1.383 (2011).
[2] K. Fujimoto and M. Shimura, Bunseki Kagaku 50, 175 (2001).

Instrumental photon activation analysis of geological and cosmochemical samples

Naoki Shirai[1], Shun Sekimoto[2], Mitsuru Ebihara[1]
[1]Tokyo Metropolitan University
[2]Kyoto University Research Reactor Institute

I. INTRODUCTION

Bulk chemical compositions for terrestrial and cosmochemical materials are significantly important to elucidate the formation, evolution processes and magmatism of planetary bodies. Compared to geological samples, cosmochemical samples pose several severe requirements to their analytical methods for chemical compositions. High sensitivity and accuracy for as many as elements as possible are required for analytical methods applied to such samples because of the limitation of sample amounts usable for analysis. Non-destructive analysis for many elements is equally favorable. Nuclear analytical methods represented by prompt gamma-ray analysis (PGA), instrumental neutron activation analysis (INAA) and instrumental photon activation analysis (IPAA) meet almost all these requirements. Among these nuclear analytical methods, INAA has been commonly used as an analytical tool in comomochemistry for a long time, while PGA and IPAA have not been very often applied to cosmochemical samples.

In PAA, (γ,n) reaction is used for determination of elemental abundances which is an opposite reaction ((n, γ) reaction) used in INAA. Thus, IPAA could determine elemental abundances which cannot or hardly be determined by INAA. Ebihara et al. [1] examined the suitability of PAA by analyzing cosmochemical samples (chondrites) and concluded that PAA is as effective as NAA for analyzing chondritic meteorites. Usually samples are irradiated by using 30 MeV electrons in IPAA. However, corrections of interferences caused by secondary nuclear reactions such as (γ,p) and (γ,pn) are necessary. Although the sensitivity obtained by activation with 20 MeV electrons are suppressed compared to the activation with 30 MeV electrons, activation with 20 MeV electrons reduces the degree of such interferences. In this study, we performed IPAA by using a linear electron accelerator at Kyoto University Research Reactor Institute (KURRI) and compared the results obtained the activation with 20 MeV with those for activation with 30 MeV.

II. EXPERIMENTAL

In this study, four Geological Survey Japan standards materials (JA-2, JB-3, JR-1 and JG-1) were analyzed. In addition to these terrestrial geological samples, the Allende meteorite was analyzed as a cosmochemical samples. Each samples was taken into a sample container (9 mmϕ) made of highly Al foil (Al: 99.5 %, Niraco Co., Ltd). In addition to rock samples, chemical reagents were irradiated to correct the spectral interferences. Five to ten samples were stacked, among which thin foil disks (9 mmϕ) of Au were placed for as monitoring the intensity of photon. Samples in a block were put in a quartz tube. Irradiations were performed by using a linear electron accelerator at KURRI. Electrons were accelerated by the linear accelerator to about 20 and 30 MeV. After irradiation (about 30 hrs), samples were taken into new Al foil and measured for gamma rays several times with different cooling intervals at KURRI and the Laboratory of Radioisotopes, Tokyo Metropolitan University. Elemental abundances were determined by comparison method by using JB-1.

III. RESULTS AND DISCUSSION

Table 1 shows the interfering reactions and their contributions to nuclides produced by corresponding reactions for activation with 20 MeV and 30 MeV electrons. As shown in Table 1, significant contributions from interfering reactions were found in activation with 30 MeV electrons. Thus, determinations of Cr, Co and Mn abundances need the correction of corresponding interferences. As expected, contributions from interfering reactions with 20 MeV electrons were lower than those in activation with 30 MeV electrons.

A total of 17 elements (Ca, Sc, Ti, Cr, Mn, Fe, Co, Ni, Zn, As, Rb, Y, Zr, Nb, Cs, Ba and Ce) were determined in geological reference standard materials and the Allende meteorite. Our Cr and Mn values obtained from activation with 30 MeV electrons were different from literature values. Improper corrections of the interfering reactions were responsible for these differences. In contrast, our Cr and Mn values obtained from activation with 20 MeV electrons were in good agreement with literature values. For other elements, there were no differences between the two sets of our values obtained from the activations with 20 and 30 MeV electrons, which were consistent with literature values.

Table 1. Interfering reaction and correction rate for interference.

Element interfered	Reaction used for determination	Interfering reaction	Correction rate 30 MeV	Correction rate 20 MeV
Cr	$^{52}Cr(\gamma,n)^{51}Cr$	$^{56}Fe(\gamma,\alpha n)^{51}Cr$	0.036 mgCr/gFe	-
Co	$^{59}Co(\gamma,n)^{58}Co$	$^{60}Ni(\gamma,pn)^{58}Co$	3.7 mgCo/gNi	0.88 mgCo/gNi
Mn	$^{55}Mn(\gamma,n)^{54}Mn$	$^{56}Fe(\gamma,pn)^{54}Mn$	6.2 mgMn/gFe	0.1 mgMn/gFe

Reference: [1] Ebihara M. et al. (2000) J. Radioanal. Nucl. Chem., 244 (3), 491-496.

Monte Carlo Calculation of Chloride Diffusion in Concrete

A. A. Naqvi[1], Khateeb-ur-Rehman[1], M. Maslehuddin[2], O.S.B. Al-Amoudi[3] and M. Raashid[1]
[1]Department of Physics, [2]Center for Engineering Research, and [3]Department of Civil and Environmental Engineering
King Fahd University of Petroleum and Minerals, Dhahran, Saudi Arabia

Abstract – Coefficient of chloride diffusion is calculated by applying the Fick's second law of diffusion to a chloride concentration profile. Then from the signal strength for various chlorine gamma-ray energies was then calculated at the detector. of the portable D-D neutron generator based PGNAA setup. An excellent agreement was noted between the reported results of the calculations for the ^{252}Cf neutron source-based portable PGNAA setup and the D-D portable *neutron generator based PGNAA setup developed by the authors.*

Keywords –Coefficient of chloride diffusion ; Fick's second law of diffusion; DD based Portable neutron generator based PGNAA setup; detector chloride signal strength calculation

I. INTRODUCTION

Corrosion of reinforcing steel is mainly caused due to the chloride ions. These ions either diffuse to the steel surface from the service environment or they are contributed by the mixture ingredients. The penetration of chloride ions from the service environment is a diffusion controlled process [1]. Consequently, the coefficient of chloride diffusion is calculated by applying the Fick's second law of diffusion to a chloride concentration profile. A prompt gamma-ray neutron activation (PGNAA) setup has been designed utilizing a portable neutron generator by the authors [2]. The setup, which mainly consists of a D-D portable neutron source along with its moderator placed side by side with a shielded gamma-ray detector, allows the determination of chloride concentration in a concrete structure from one side. The D-D portable PGNAA setup has been modeled for the determination of chlorine concentration at various depths using a MCNP simulation code following the procedure described elsewhere [1] for a ^{252}Cf neutron source based PGNAA setup.

.

In the reported study, the chloride diffusion profile was modeled for several values of diffusion coefficients as a function of time. These chloride concentrations are then utilized as an input to the MCNP based model [1]. The signal strength for various chlorine gamma-ray energies was then calculated at the detector. An excellent agreement was noted between the reported results of the calculations for the ^{252}Cf neutron source-based portable PGNAA setup [1] and the D-D portable neutron generator based PGNAA setup developed by the authors

[1] Livingston, R.A., Al-Sheikhly, M., Mohamed, A.B. "Numerical simulation of the PGNA signal from chlorine diffusion gradients in concrete," *Applied Radiation and Isotopes*, Vol. 68 (2010), pp. 679–682.

[2] Naqvi, A. A., Kalakada, Z., Al-Matouq, F.A., Maslehuddin, M. and Al-Amoudi, O.S.B., "Chlorine detection in fly ash concrete using a Portable Neutron Generator," *Applied Radiation and Isotopes,* Vol. 70(2012), pp.1671-4.

APSORC'13 - 5th Asia-Pacific Symposium on Radiochemistry
Kanazawa, Japan, 22-27 September 2013

Catalysis Induced by Radiation in Fatty Acids Adsorbed on Clay Minerals

A. Negron-Mendoza[1]*, S. Ramos-Bernal[1], M. Colin-Garcia[2] and F.G. Mosqueira[3]
[1]Instituto de Ciencias Nucleares, Universidad Nacional Autonoma de Mexico, UNAM. A.P. 70-543, México, D.F. 04510, México.
Instituto de Geología, Universidad Nacional Autonoma de Mexico, México, D.F. 04510, México
[3]Dirección General de Divulgación de la Ciencia, Universidad Nacional Autonoma de Mexico, D.F. 04510, México

Abstract – We have studied the behavior of small fatty and dicarboxylic acids adsorbed in sodium-montmorillonite and exposed to gamma radiation. It is observed that the radiation-induced decomposition of the clay-acid system goes along a definitive path (oxidation) rather than following several modes of simultaneous decomposition, as in the case of the radiolysis without the clay. This preferential synthesis promotes the formation of a hydrocarbon compound with one carbon atom less than the parent compound

Keywords –Decarboxylation reaction, carboxylic acids, gamma radiation, montmorillonite, $^{14}CO_2$

I. INTRODUCTION

The adsorption of certain organic compounds by clays gives rise to the transformation of the adsorbate by the action of clays. These kinds of reactions play an important role in many natural and industrial processes. In the context of oil and gas exploration, for example, the source and trap of petroleum hydrocarbons frequently are clay-rich rocks. Clay-water based muds are also seen as environmental friendly alternatives to toxic oil-based fluids [1].

In this perspective, several investigators [2, 3] have studied the thermal decomposition of fatty acids in the presence of clay minerals. The differences found by several workers for the distribution patterns of hydrocarbons may be caused largely by thermal alteration. In addition, radioactive bombardment alters these sediments. It is an important subject that has not been extensively studied.

The modification by ionizing radiation of the activity of heterogeneous catalysis is a relatively new problem in radiation chemistry. The sensitization of radiation-chemical reactions by solid surfaces may increase the catalytic activity of the clay. The aim of this paper is to study the radiation-induced decomposition of carboxylic acids adsorbed in a clay mineral as an example of heterogeneous radiation catalysis that can be correlated to natural and industrial processes.

II. MATERIALS AND METHODS

The experimental part is divided in two stages: (1) Radiolysis of aqueous solutions of the carboxylic acids, (2) Study of heterogeneous radiolysis of the water-carboxylic acid-clay system

(1) Aqueous solutions of carboxylic acids (0.1 mol L^{-1}), oxygen free, prepared in a glass syringe (acetic, succinic, aconitic); (2) Aqueous solutions of acids containing 0.3 g of the clay were prepared. The addition of the clay into the solution was in an oxygen-free bag, with continues agitation. (3) For gas analysis, 0.1 g of the clay was evacuated for one hour and 1 mL of the solution was added, in an oxygen-free bag. The samples were in special glass tubes with a stopcock that was connected to a Toepler pump. We used blanks to correct the yield of gas samples. Some runs were made with 14-carbon label acetic acid ($CH_3{}^{14}COOH$) to show that the CO_2 obtained was from the target acid. $^{14}CO_2$ was measured by a scintillation technique. The irradiations were carried out in a high intensity gamma source of ^{60}Co (Gammabeam 651 PT). The radiation doses were from 46. kGy to 300 kGy

III. RESULTS AND REMARKS

The irradiation of aqueous carboxylic acid produced many compounds, for example for acetic acid, the total yield of polycarboxylic acids was 22% and for succinic acid was about 35%. The principal feature of these series of radiolysis experiments was the production of the dimer of the acid, as the principal way of decomposition of the target compound, but many other acids were formed. For example, in the radiolysis of acetic acid (CH_3CO_2H), the main product was succinic acid $(CH_2CO_2H)_2$, the dimeric product. The formation of CO_2 from the decarboxylation reaction was only 7%. The decomposition of the target compound increased as a function of the dose.

The radiolysis performed in presence of clay decreased considerably the number of formed products. For example, in acetic acid, the production of polycarboxylic acids was 4.8 % and the formation of carbon dioxide increased to 81 %.

The main result obtained shows that the radiolysis of the system clay-acid goes along a defined path rather than showing various pathways of decomposition. The main pathway was the decarboxylation of the target compound rather than condensation/dimerization reactions.

ACKNOLEDGEMENTS

This work was supported by PAPIIT Grant No. IN110513 and the CONACyT Grant No. 168579/11.

REFERENCES

[1] Skipper, N. Hannon, A., and Buchanan, P. ISIS Experimental Report, Rutherford Appleton Laboratory, RB 1205 (2001).
[2] Eisma, E. and Jurg, W.J. in G. Eglinton and M.J. Murphy (Editors) Organic Geochemistry, Springer Verlag, New York, (1969).
[3] Simoyama, A. and Johns, W.D., Nature, 232, 14 (1971).

APSORC'13 - 5th Asia-Pacific Symposium on Radiochemistry
Kanazawa, Japan, 22-27 September 2013

Preliminary Study for Highly Sensitive Airborne Radioiodine Monitor

Yoshimune Ogata[1], Tadashi Yamasaki[2], Ryuji Hanafusa[3]
[1]Nagoya University
[2]CEPCO
[3]Fuji Electric

Abstract – Airborne radioiodine monitoring has a problem in that conventional radioiodine gas monitors have inadequate sensitivity. To solve the problem, we designed a highly sensitive gas monitor. The higher counting efficiency and lower background brought sufficient sensitivity. The properties of the monitor were investigated using air including gaseous ^{125}I. The minimum detectable activity concentration for ^{125}I was 1×10^{-4} Bq cm^{-3} for one minute counting, which corresponded to one tenth of the legal limit of ^{125}I for the radiation controlled areas in Japan.

Keywords – Radioiodine, Gas monitor, Highly sensitivity

I. INTRODUCTION

There are several issues regard with airborne radioiodines. It caused significant social fear that large amount of ^{131}I was released from the nuclear disaster of Fukushima Daiichi NPP, TEPCO. On the other hand, small amounts of ^{129}I are gradually released from nuclear reprocessing plants and decommissioning sites of NPPs. Another issue is the contamination of patient rooms by exhalation of ^{131}I from patients undergoing thyroid gland therapy. Furthermore, ^{125}I is frequently used for radioimmunoassay and research programs in medical examination facilities and/or research laboratories. To guarantee radiation safety, radioiodine concentration should be measured.

However, the legal limits of airborne radioiodine are quite low, and conventional gas monitors have inadequate sensitivity to measure such low-level airborne radioiodine[1]. One method for detecting low-level airborne radioiodine is to adsorb the radioiodine with activated charcoal by air suctioning, and measure it with laboratory detectors. But, since it is carried out in a batch process, it needs a relatively long time to obtain results.

Highly sensitive, real-time airborne radioiodine monitor are required for safety work in radiation areas and for environmental safety. In this study, a novel monitor to measure the airborne radioiodine was designed, which has sufficient sensitivity to detect the airborne radioiodines toward the legal limits.

II. MATERIALS AND METHODS

The detector consists of an adsorption column containing activated charcoal, a well-type NaI(Tl) scintillation detector, an air suction pump, and a flow regulator. The column was put in the well of the NaI(Tl) detector. The detector was surrounded by a shield with lead and copper. The air was introduced into the bottom of the column and suctioned by an air pump.

The electric signal from the detector was collected with a multichannel analyzer (MCA) through an amplifier. The MCA had two modes: a pulse height analysis (PHA) mode, and a multichannel scaling (MCS) mode. The PHA mode was used for the initial settings, and the MCS mode was used for the time-series measurements as continuous monitoring.

The characteristics of the system were investigated using ^{125}I. Before application of the airborne iodine monitoring, the counting efficiency of the detector was estimated using a set of ^{125}I solutions with several volumes. The activities of the solutions were estimated according to coincidence method[2]. Then, sample air including gaseous ^{125}I in a balloon was drawn into the detector. The concentration of ^{125}I in the air and the adsorption factor of the column were estimated using a set of tandem adsorption column. The minimum detectable concentration (MDC) of the system was evaluated by the experimental results.

III. RESULTS AND DISCUSSION

The counting efficiencies of the detector for ^{125}I were 50% – 85%, which depended on the sample height. The adsorption factor for iodine was higher than 99%. The ^{125}I concentration prepared in the balloon was 3.5×10^{-4} Bq cm$^{-3}_{\text{-air}}$.

When the flow rate was 3 L min^{-1}, the MDC is estimated as 1×10^{-4} Bq cm^{-3} for one minute counting, which was one tenth of the legal limits of the air in radiation controlled areas, 1×10^{-3} Bq cm^{-3}. In the case of 15 minute counting, the MDC is estimated as 2×10^{-6} Bq cm^{-3}, which was one fourth the legal limits of the exhausted air, 8×10^{-6} Bq cm^{-3}. Lower MDCs will be expected by improving of the detection arrangement.

This detection system can be used for ^{129}I monitoring as it is, and it needs a minor modification for ^{131}I monitoring. The MDCs of this system were almost two orders of magnitude lower than conventional radioiodine gas monitors. The system will be effective in radioactive gas monitoring applications in decommissioning sites, nuclear plants, medical and laboratorial facilities, and environment in general.

[1] Matsuda. N., Effluent monitor – Technical guideline for safe management of radioiodine. Japanese J Radiation Safety Management, 8 (2), 162 (2009) (in Japanese).
[2] Horrocks, D,. et al., Theoretical considerations for standardization of ^{125}I by the coincidence method. Nucl. Instrum. Methods, 124 (2), 585-589 (1975).

Radiation synthesis and cesium removal of cellulose microsphere based hybrid adsorbent

Long Zhao[1*], Yanliang Chen[1], Yuezhou wei[1]
[1] *School of Nuclear Science and Engineering, Shanghai Jiao Tong University, Shanghai 200240, China*
Corresponding author: Fax: (+86) 213420-7654; E-mail address:* ***ryuuchou@sjtu.edu.cn*

Abstract –A novel cellulose-based hybrid adsorbent was successfully prepared by radiation-induced grafting of glycidyl methacrylate (GMA) onto the surface of cellulose microspheres, followed by epoxy ring-opening reaction to introduce ammonium 12-molybdo phosphate (AMP). The characterization of the obtained adsorbent was investigated in detail. To evaluate the adsorption performance of the novel adsorbent, batch and column mode adsorption experiment against cesium (Cs) was conducted.
Keywords –radiation grafting; ammonium12-molybdophosphate; cellulose microsphere; cesium; adsorption

I. INTRODUCTION

It is well known that the leakage and spread of ^{137}Cs generated from the accident of atomic power plant such as Fukushima nuclear disaster can affect human health, and lead to severe environmental problem [1-2]. Several techniques have been employed for treating Cs containing aqueous solutions, which include adsorption, reverse osmosis, extraction and precipitation. Among these methods, adsorption has the advantages on high efficiency, easy handling, availability of different adsorbents and cost effectiveness.

Ammonium 12-molybdophosphate (AMP), which shows high selectivity toward Cs ion, can act as one of the most promising adsorbent materials for this purpose. [3]. However, AMP is still not employed on a large scale because of its fine powder form which hinders simple column operation. To overcome this disadvantage, in this study, we proposed a novel hybrid adsorbent which could be easily prepared by radiation grafting. In current work, AMP can be introduced onto glycidyl methacrylate (GMA) grafted cellulose microsphere surface through epoxy ring-opening reaction. The whole preparation procedures are rather simple.

To evaluate the adsorption performance of the novel adsorbent, batch and column mode adsorption experiments by using a nonradioactive Cs solution will be conducted.

In this report, the synthesis conditions and adsorption properties of the novel adsorbent prepared by radiation grafting are introduced in detail.

II. EXPERIMENTAL AND RESULTS

Adsorbent was prepared by pre-irradiation grafting polymerization. Initially, trunk polymer was sealed in polyethylene bags purged with nitrogen gas. The sample bags were irradiated by EB generated from an accelerator, at a voltage of 750 keV and a dose rate of 10 kGy per pass under the cooling of dry-ice. After getting rid of oxygen by nitrogen flow, monomer solution was injected into the sample bags. The grafting reaction was then performed in a water bath at desired temperature and reaction time. The homopolymer and unreacted monomer were removed by eligible solvent and then grafted polymers were dried in vacuum. Thereafter, the grafted cellulose microsphere with GMA having epoxy groups was reacted with AMP in a turbid liquid state at 80°C for 18h. The resulting adsorbent was washed with water and dried in vacuum and kept for further use. The structure of the resulting adsorbent was confirmed by micro-FTIR spectra, TG and XPS analysis.

The batch adsorption of Cs has been investigated as a function of contact time, pH, Cs and NaCl concentration. A column-mode adsorption test was carried out using 15ml volume column at a flow rate of space velocity $10h^{-1}$ for initial Cs of 5 mg L^{-1} at pH5.4. The concentration of Cs was measured by atomic absorption spectrophotometer (AAS) and Inductively Coupled Plasma Mass Spectrometer (ICP-MS).

It was found that adsorption equilibrium could be achieved within 30 min for initial Cs of 5 mg L^{-1}. It is believed that the functional groups concentrated in surface result in such quick adsorption. Cs uptake of adsorbent depends on solution pH, with a maximum Cs uptake at pH 5.4. The adsorption kinetics was well described by the pseudo-second order model equation, and the adsorption isotherm was better fitted by the Langmuir mode. Fig.1. showed the breakthrough curves of column adsorption experiment. The breakthrough curve indicated that the Cs adsorption amount at the breakthrough point was 0.75g-Cs/L-adsorbent, and the Cs can be completely removed till the flux reached roughly 150 bed volumes.

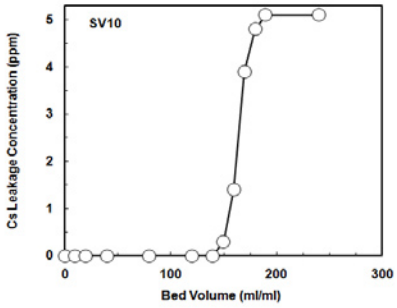

Fig.1. Breakthrough curves of adsorbent.

Lastly, it was found that 80% adsorption capacity can be kept even though the adsorbent was exposed to 1000kGy γ-irradiation. These results suggested that obtained adsorbent could be used to removal Cs from wastewater.

REFERENCES

[1] *IAEA Technical Report Series*, *No. 356* (1993).
[2] K. Takeshita and T. Ogata, *J. Ion Exchange.23,*1 (2012).
[3] W. Faubel and S. A. Ali, *Radiochim. Acta*, *40*, 49 (1986).

Study about separation mechanism of endohedral metallofullerenes with Lewis acid

K. Chiba[1], T. Hamano[1], E. Takeuchi[1], K. Akiyama[1], S. Kubuki[1], and H. Shinohara[2]

[1]Department of Chemistry, Tokyo Metropolitan University, Hachioji, 192-0397, Japan

[2]Graduate School of Science, Nagoya University, Nagoya 464-8602, Japan

Keywords – Metallofullerene, Lewis acid, Separation

I. INTRODUCTION

Recently, a method for the separation and purification of endohedral metallofullerenes (EMFs) with Lewis acid was reported[1]. It is found that EMFs in fullerene crude extract are selectively oxidized with Lewis acid and separated with especially high yield (>99 %) by the liquid Lewis acid such as $TiCl_4$ and $SnCl_4$. On the other hand, the method using solid Lewis acids like $AlCl_3$ needs long time for the separation compared to liquid Lewis acid and the separation efficiency is decreased to around 40 % for the same reaction time. Based on the previous study, it is presumed that homogeneous diffusion of Lewis acid in crude extract solution lead to the efficient interaction between EMFs and Lewis acid.

In this session, we will report the effect of diffusion of $AlCl_3$ to the separation and the detail of separation mechanism of EMFs.

II. EXPERIMENTAL

Soot containing La EMFs were produced by arc discharge method with La/C composite rods (La:C=1:130). The produced soot were dissolved to 1,2,4,-trichlorobenzene (TCB), and then refluxed for 12 hours. The TCB solution including crude extracts of fullerenes was filtered and evaporated to dryness. After that, the crude extracts were re-dissolved to *o*-dichlorobenzene (DCB). EMFs of ^{141}Ce, which are known to behave as with La EMFs, were added to these solutions as a radioactive tracer. Chlorobenzene solution of $AlCl_3$ ($AlCl_3$/CB) was added to the crude extract. These mixed solutions were stirred and then separated by PTFE membrane filter (pore diameter is 0.2 μm, Millex, Merck Millipore). The EMFs remaining on the filter were washed by water and acetone. After that, DCB was passed through the filter to recover the EMFs. The gamma-ray emitted from ^{141}Ce in the samples was measured for the determination of separation efficiency by germanium semiconductor detector (GMX25, SEIKO EG&G).

$AlCl_3$/CB was also added to purified La@C_{82} DCB solutions and their vis-NIR absorption spectra were measured (UV-3600, SHIMADZU) in order to investigate the electronic states of the EMF.

III. RESULTS AND DISCUSSION

In comparison of the radioactivity of ^{141}Ce at before / after separation, the efficiency with $AlCl_3$/CB was determined as about 40 %. This is corresponding to that with solid $AlCl_3$. It suggests that the separation efficiency is not much affected by homogeneous diffusion of Lewis acid.

In the vis-NIR spectra of the mixed solution of La@C_{82} and $AlCl_3$/CB, two characteristic absorption bands at 1000, 1400 nm of La@C_{82} were disappeared but new band was raised at 1300 nm after 5 min of adding $AlCl_3$/CB. This result indicate that neutral La@C_{82} is immediately oxidized by the addition of Lewis acid and cationic species of La@C_{82} is produced within 5 minute.

Detail of the mechanism of separation will be discussed in the session.

[1] K. Akiyama *et al., J. Am. Chem. Soc.,* **134,** 9762-9767, (2012).

CRYSTAL STRUCTURE AND SPIN STATE OF MIXED-CRYSTALS OF $Fe(NCS)_x(NCBH_3)_{2-x}(bpp)_2$ (bpp = 1,3-BIS(4-PYRIDYL)PROPANE)

Haruka Dote[1], Hiroki Yasuhara[1], Satoru Nakashima[2]
[1]Graduate School of Science, Hiroshima University
[2]Natural Science Center for Basic Research and Development (N-BARD), Hiroshima University

Abstract
New mixed crystals, $Fe(NCS)_x(NCBH_3)_{(2-x)}(bpp)_2$ were synthesized. ^{57}Fe Mössbauer spectroscopy showed that the ratio of low-spin state in the $Fe(NCBH_3)_2$ unit changed with the change of x. The results revealed that the high spin site of $Fe(NCS)_2$ unit affects the spin state of $Fe(NCBH_3)_2$ unit.

Keywords
Mössbauer spectroscopy, mixed crystals, spin-crossover, assembled complexes

I. INTRODUCTION

Self-assembled coordination polymers containing transition metal ions and organic bridging ligands have attracted intensive interests because of their potential abilities for selective inclusion and transformation of ions and molecules.[1)] It is possible to construct various structures for porous assembled iron complexes bridged by bis(4–pyridyl) type ligand. We have studied iron complexes bridged by 1,3–bis(4–pyridyl)propane (bpp), which has three methylenes, by using single crystal X–ray diffraction analysis, Mössbauer spectroscopy, and SQUID measurements. $Fe(NCX)_2(bpp)_2$ (X = S, Se, and BH_3) had a 2D interpenetrated structure and the $NCBH_3$ complex showed a spin–crossover phenomenon.[2)] We also synthesized $Fe(NCX)_2(bpp)_2 \cdot 2(benzene)$ (X = S, Se, and BH_3). They had a 1D structure and were in temperature-independent Fe^{II} high-spin state. Both 2D interpenetrated and 1D structures were converted to each other by desorption and adsorption of benzene molecules.[3)] Recently, we discussed the spin state of the mixed crystals with zinc or cobalt ion both in the 2D interpenetrated and 1D structures for the assembled complexes bridged by bpp.[4)] In the present study, we discussed the structure of the mixed crystals of iron with NCS and $NCBH_3$ for the assembled complexes bridged by bpp, and then we discussed the spin state of the mixed crystals.

Ⅱ. Results and Discussions

Elemental analysis of $Fe(NCS)_X(NCBH_3)_{2-X}(bpp)_2$ showed that x is 0.25, 0.65, 0.95, 1.15, 1.1, 1.25, 1.4, 1.7, 1.8, and 1.9, when the preparation ratio of x is 0.2, 0.4, 0.6, 0.8, 1, 1.1, 1.2, 1.4, 1.6,and 1.8, respectively. This reveals that the obtained crystals show a trend that the ratio of NCS increases compared with the preparation ratio. All the mixed crystals showed the similar powder X-ray diffraction patterns, and the (002) diffractions of the mixed crystals are not the superposition of those from $Fe(NCS)_2(bpp)_2$ and $Fe(NCBH_3)_2(bpp)_2$. The (002) diffractions are shifted to higher degree by increasing ratio of NCS.

We carried out single crystal X-ray diffraction analysis of $Fe(NCS)_{1.8}(NCBH_3)_{0.2}(bpp)_2$. By comparing $Fe(NCS)_{1.8}(NCBH_3)_{0.2}(bpp)_2$ with $Fe(NCS)_2(bpp)_2$, and $Fe(NCBH_3)_2bpp_2$, we found that the structure is similar to $Fe(NCS)_2(bpp)_2$ but has shorter b-axis and longer c-axis. The result is consistent with the result of powder X-ray diffraction.

We measured Mössbauer spectra of the present mixed crystals. All the spectra consist of $Fe(NCS)_2$ unit and $Fe(NCBH_3)_2$ unit. Fig. 1 shows that ratio of $NCBH_3$ and fraction of low spin in mixed anion crystal. The result reveals that the ratio of low-spin state in the $Fe(NCBH_3)_2$ unit changed with the change of x and revealed the high-spin site of $Fe(NCS)_2$ unit affects the spin state of $Fe(NCBH_3)_2$ unit. The results suggest the chemical pressure effect, in which $Fe(NCS)_2$ unit next to $Fe(NCBH_3)_2$ unit makes $Fe(NCBH_3)_2$ unit to become high spin from low spin at low temperature.

Ⅲ. Conclusion

We synthesized new mixed anion crystals, $Fe(NCS)_x(NCBH_3)_{(2-x)}(bpp)_2$. ^{57}Fe Mössbauer spectroscopy showed that the high-spin site of $Fe(NCS)_2$ unit affects the spin state of $Fe(NCBH_3)_2$ unit.

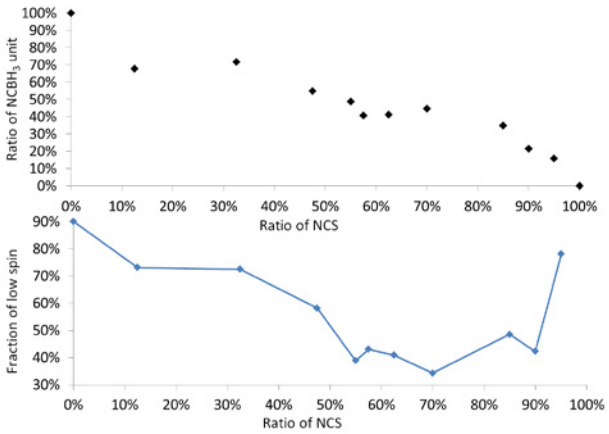

Fig 1. Ratio of $NCBH_3$ and fraction of low spin in mixed anion crystal

[1] B. Moulton, M. J. Zaworotko, Chem Rev., 101 (2001) 1629
[2] M. Atsuchi, H. Higashikawa, Y. Yoshida, S. Nakashima, and K. Inoue, Chem. Lett., 36 (2007) 1064.
[3] M. Atsuchi, K. Inoue, and S. Nakashima, Inorg. Chim. Acta, 370 (2011) 82
[4] S. Nakashima, T. Dote, M. Atsuchi, and K. Inoue, J. Phys., C217, 01035 (2010).

Analysis of Fragments of a Roman Mask using Mössbauer spectroscopy

Paulo de Souza[1,2], G. Klingelhöfer[3], P Gütlich[3], M. Egg[4]
[1]University of Tasmania, Hobart TAS 7001 Australia
[2]Commonwealth Scientific and Industrial Research Organisation, Hobart TAS 7001 Australia
[3]Johannes Gutenberg-Universität Mainz D-55128 Germany
[4]Römisch-Germanisches Zentralmuseum, Mainz D-55116 Germany

Abstract – *A fragmented roman mask was found in excavations at "Villa von Allmend", Saarland, Germany. The mask is made of iron, covered externally by bronze. Such objects were used in war games during the height Roman times. During the excavations around the mask other metallic objects were also found. Some clearly belong to the mask, such as the left ear (Figure 1, top left), among other fragments that cannot be associated with the mask without further investigation. Some of these fragments were investigated using backscattering Mössbauer spectroscopy. The objective was to determine whether the fragment was a piece of the roman mask or was part of another object laying in the excavated area, and shed additional light on the manufacturing process of the mask itself.*

The current communication discusses the results of the analysis of fragments from this roman mask using the miniaturised Mössbauer spectrometer (MIMOS II). This instrument was developed by Dr. Klingelhöfer's research group in Mainz for space exploration [1] and was successfully used onboard NASA's Mars Exploration Rovers [2]. Thanks to MIMOS II portability, robustness, low-power consumption and relative good radiation shielding, in situ characterization became possible. These advantages of MIMOS II were explored in a number of outdoor applications [3, and references therein]. In archaeology the instrument has been applied in the analysis of rock paintings [3] and on a greek Vase [4].

On this roman mask, the results yield the understanding of the provenance of fragments and were used to guide the process of its restoration. The Mössbauer spectra on pieces that clearly belong to the mas show the presence of many iron oxides including wüstite (FeO_{1-x}). Wüstite has been interpreted as the indication of production of 'brand patina' on the surface of the object. This oxide phase could be produced by fast cooling under reducing atmosphere (e.g., putting the hot metal in a bath of animal fat). Patina was a surface treatment used by romans to improve resistance to corrosion and for aesthetics purposes. Therefore, the absence of wüstite would imply in a possible mismatch with the original mask.

Keywords – Mössbauer spectroscopy, archaeology.

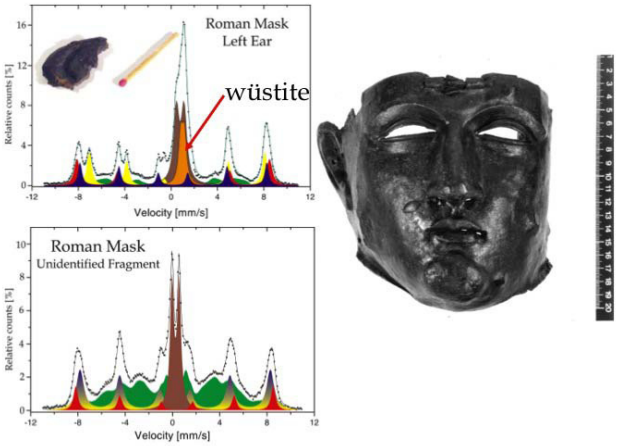

Fig. 1. Room temperature Mössbauer spectra of some of the studied metallic fragments. On the top, the left ear of the mask; on the bottom, an unidentified fragment (probably from the metallic box where it was placed), and on the left, the final appearance of the reconstructed mask.

REFERENCES

[1] G. Klingelhöfer, R. V. Morris, B. Bernhardt, D. Rodionov, P. A. de Souza, S. W. Squyres, J. Foh, E. Kankeleit, R. Gellert, C. Schröder, S. Linkin, E. Evlanov, B. Zubkov, O. Prilutski (2003) The Athena MIMOS II Mössbauer Spectrometer Investigation. ***Journal of Geophysical Research***, v. 108, No. E12, 8067. doi: 10.1029/2003JE002138.

[2] G. Klingelhöfer, R. V. Morris, B. Bernhardt, C. Schröder, D. Rodionov, P. A. de Souza, A. Yen, R. Gellert, E. N. Evlanov, B. Zubkov, J. Foh, U. Bonnes, E. Kankeleit, P. Gutlich, D. W. Ming, F. Renz, T. Wdowiak, S. W. Squyres, R. E. Arvidson (2004) Jarosite and Hematite at Meridiani Planum from Opportunity's Mössbauer Spectrometer. ***Science***, 306,1740-1745. doi: 10.1126/science.1104653.

[3] C. Schröder, G. Klingelhöfer, R. V. Morris, B. Bernhardt, M. Blumers, I. Fleischer, D. S. Rodionov, J. Gironés López, P. A. de Souza (2010) Field-portable Mössbauer Spectroscopy on Earth, the Moon, Mars, and Beyond, ***Geochemistry: Exploration, Environment, Analysis***, 11 (2011) 2, 129-143. doi: 10.1144/1467-7873/09-IAGS-018.

[4] P. A. de Souza, B. Bernhardt, G. Klingelhöfer, P. Gütlich (2003) Surface Analysis in Archaeology Using the Miniaturized Mössbauer Spectrometer MIMOS II. ***Hyperfine Interactions***, v. 151, 125-130. doi: 10.1023/A:1025444209059.

Synthesis of ^{14}C labeled C_{60} with higher specific activity

T. Tadai[1], K. Akiyama[1], H. Aoshima[2], R. Ibuki[2], S. Kubuki[1]
[1]Department of Chemistry, Tokyo Metropolitan University, Hachioji, 192-0397, Japan
[2]Vitamin C60 BioResearch Corporation, Chuo-ku, Tokyo 103-0028, Japan

Keywords Keywords – ^{14}C-labeled C_{60}

I. INTRODUCTION

Recently, Fullerenes and their derivatives have been attracted to the medical and cosmetics fields. However, there are some problems for the application of fullerenes, such as nano toxicity. To overcome these problems, further study about drug disposition is required. As one of the most useful technique, the radioactive tracer method using ^{14}C-labeled C_{60} is applicable for this purpose. Synthesis of ^{14}C-labeled C_{60} has been reported so far [1, 2]. However, synthesis of ^{14}C-labeled C_{60} with higher specific radioactivity is desired for the detail study. In this session, we will report the development of synthesis and the properties of produced ^{14}C-labeled C_{60} such as specific radioactivity.

II. EXPERIMENTAL

$Ba^{14}CO_3$ (0.2 mmol, 57 mCi/mmol) was mixed with $PbCl_2$ and AgCl and then put into the electric furnace for heating at 450 ^oC to produce labeled CO_2 under He gas flow. The produced CO_2 gas was stored in the plastic bag, and then introduced to the Et_2O solution of 2-lithiofuran to produce the furoic acid. The produced furoic acid was reduced with $LiAlH_4$ in THF solution to obtain the labeled furfuryl alcohol. This alcohol was condensed by the evaporator, and then dissolved into *o*-dichlorobenzene (*o*-DCB). For the polymerization of this alcohol, *p*-toluenesulfonic acid was added into this *o*-DCB solution. The polymer solution was adsorbed on a porous carbon rod (PC5060G, Tokai Carbon Inc.) and dried at 200 ^oC under He gas stream for 1 hour. After that, carbon rod was set into fullerene generator and sintered by the electric resistance heating method. The resulting ^{14}C-impregnated graphite electrode was then employed as an anode for the arc discharge for the fullerene production. The soot containing ^{14}C-labeled C_{60} were recovered from the generator as a CS_2 solution and then filtered to remove the insoluble substances. The ^{14}C-labeled C_{60} was purified from these filtered crude fullerenes by HPLC (Buckyprep, Nakarai tesque Inc.). Their total weight and specific radioactivity were determined by UV/vis absorption and liquid scintillation counter (LSC).

III. RESULTS AND DISCUSSION

The yield of ^{14}C was estimated from the radioactivity in $Ba^{14}CO_3$ and in obtained C_{60}, and found to be 0.73 %. This is about 3 times larger than that of previously reported value [1]. As the results of UV/vis absorption measurement, the total weight of purified C_{60} is found to be about 3 mg. The specific radioactivity of these C_{60} estimated from the radioactivity determined by the results of LSC measurement and total weight of $C_{60,}$ were found to be 18.4 mCi/mmol. Enrichment of ^{14}C for this sample was about ^{14}C: ^{12}C = 1: 200. This value is the highest among that of previous reports and indicate that the most enriched ^{14}C-labeled C_{60} is produced by our method.

[1] W. A. Scrivens, *et al., J.Am.Chem.Soc.,*116, 4517-4518, 1994.
[2] S. R. Wilson, *et al., Fullerene Sci. & Technol.,* 4, 43-48, 1996.

Adsorption Behavior of Zr and Hf to TTA-resin in Microcolumn for Determining the Forming Ability of Rf Monofluoride Complex

Y. Kitayama[1], Y. Shigeyoshi[1], A. Yokoyama[2], A. Toyoshima[3], K. Tsukada[3], K. Ooe[4], E. Maeda[1], H. Kimura[1], H. Kikunaga[5], Y. Kudou[6], J. Kanaya[6], M. Huang[6], and H. Haba[6]

*1 Graduate School of Natural Science and Technology, Kanazawa University
*2 Institute of Science and Engineering, Kanazawa University
*3 Japan Atomic Energy Research Institute
*4 Institute of Science and Technology, Niigata University
*5 Research Center for Electron Photon Science, Tohoku University
*6 Nishina Center for Accelerator-Based Sience, RIKEN

Abstract — *We study aqueous chemistry of Rf to determine the forming ability of monofluolide complex of Rf. Reversed-phase chromato-graphic behaviors of non-carrier tracers of Zr and Hf with TTA-resin were observed for simulation of the Rf experiment. Although we obtained good adsorption behavior and short equilibrium time for the batch experiment, the chemical system in microcolumn does not appear to come to equilibrium and needs further improvement.*

Keywords — *Reversed-phase chromatography, Zirconium(Zr), Hafnium(Hf), Rutherfordium(Rf)*

I. INTRODUCTION

Rutherfordium (Rf) has attracted a lot of attention in research on the chemical properties of a super heavy element. For the purpose of its speciation in aqueous solution, we aim to observe the chemical behavior of Rf by means of reversed-phase chromatography with a chelate extractant of 2-thenoyl-trifluoroacetone (TTA) as the stationary phase. It extracts quadrivalent metal ions preferentially, and, that is, it will make possible determination of a specific complex formation constant of Rf. [1]

In this work, we observed chemical equilibrium times and distribution coefficients of non-carrier tracers of Zr and Hf with TTA-resin in the acid solutions of HF/HNO_3 for simulation of the Rf experiment. Then, on-line reversed-phase chromatography of Zr was performed with Automated Rapid Chemistry Apparatus (ARCA), which was also used for an on-line chemical system for the Rf experiment.

II. EXPERIMENTAL

In the batch experiments with ^{88}Zr and ^{175}Hf tracers, we observed equilibrium times and distribution coefficients on TTA-resin in the solution of 9.5×10^{-5} – 10^{-1} M HF / 10^{-1} M HNO_3 , 1×10^{-4} M HF / 10^{-2} –10^{-1} M HNO_3. and 1.0×10^{-4} M HF / 10^{-2} –10^{-1} M HNO_3 by assaying in γ-ray spectrometry with a Ge detector.

In the on-line experiment, an reversed-phase chromato-graphy was performed with the ^{89m}Zr atoms produced in the ^{89}Y (p, n) reaction at the RIKEN K70 AVF cyclotron. They were transported with KCl/He gas jet and collected in ARCA. They were dissolved in acid solutions of HF/HNO_3, and the solutions were introduced in the microcolumns (1.6mm ϕ × 7mm) filled up with TTA-resin at flow rate of 0.1-1 mL/min. The solutions eluted through TTA-resin were collected and subjected to γ-ray spectrometry by using a Ge detector.

III. RESULTS AND DISCUSSION

The batch experiment demonstrated that the best perfor-mance in adsorption was obtained for TTA (octanol) resin on Kel-F resin and TTA (octanol) on CHP20/P20 resin. The equilibration was attained in less than 1 min for the cases. Besides, it was found that the results of experimental with TTA resin agree with those of solvent extraction behavior for Zr and Hf at the lower acid concentrations.

In the on-line experiment, an example of the obtained elution curves is shown in Fig. 1 for TTA on CHP20/P20 resin with a ^{89m}Zr tracer. It shows the tracer atoms are adsorbed on the resin. However, the equilibration times in the on-line experiment appears to be not as short as we had expected from the batch experiment; K_d value from the on-line experiment was observed lower than that for the batch experiment. Therefore, we should find better conditions for shorter equilibration time for the experimental with Rf.

In conclusion, reversed-phase chromatography with TTA resin has the potential for speciation of a Rf chemical species although the resin preparation needs further improvement to optimize the experimental condition for Rf. Thus far we have succeeded in introducing ^{261}Rf into ARCA system and its measurement by α -ray spectrometry.

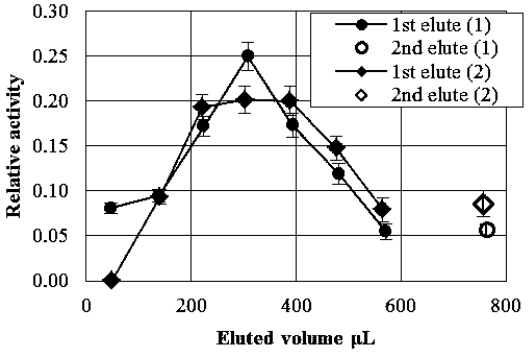

Fig. 1. An example of elution curve of Zr on the TTA resin.
The conditions were 1.0×10^{-4}M in [HF], 0.01M in [HNO_3] for the 1st elute and 1.0×10^{-4}M in [HF], 0.01M in [HNO_3] for the 2nd elute at 0.1 mL/min in flow rate

Reference:
[1] M. Araki, T. Nanri., Y. Takeda, M. Nishio, M. Nishikawa, Y. Kasamatsu, Y. Ezaki, Y. Kudou, H. Haba, and A. Yokoyama: RIKEN Accel. Prog. Rep. **43**, 271 (2010).

Poster Session 3

Wednesday, 25 September 2013

18:50 ~ 20:00

Scientific Topics (Abbrev.)

1. Fukushima issues (FK)
2. Education in nuclear and radiochemistry (ED)
3. Nuclear forensics (NF)
4. Nuclear energy chemistry (NE)
5. Nuclear chemistry (NC)
6. Actinide chemistry (AC)
7. Environmental radiochemistry (EN)
8. Radiopharmaceutical chemistry and Nuclear medicine (RP)
9. Nuclear probes for materials science (NP)
10. Activation analysis (AA)
11. Application of nuclear and radiochemical techniques (AP)

APSORC'13 - 5th Asia-Pacific Symposium on Radiochemistry
Kanazawa, Japan, 22-27 September 2013

$^{235}U/^{238}U$ Isotopic Ratio in Environmental Samples at the Fukushima Area

Y. Shibahara[1], T. Fujii[1], S. Fukutani[1], T. Kubota[1], R. Okumura[1], T. Ohta[2], K. Takamiya[1], N. Sato[1], M. Tanigaki[1], Y. Kobayashi[1], H. Yoshinaga[1], H. Yoshino[1], A. Uehara[1], S. Mizuno[3], T. Takahashi[1], and H. Yamana[1]

[1]Research Reactor Institute, Kyoto University
[2]Faculty of Engineering, Hokkaido University
[3]Nuclear Power Safety Division, Fukushima Prefectural Government

Abstract – $^{235}U/^{238}U$ isotopic ratio of environmental samples in Fukushima prefecture was analyzed by thermal ionization mass spectrometry and inductively coupled plasma mass spectrometry. A possibility of atmospheric release of uranium during the accident of Fukushima Daiichi nuclear power plant was discussed.

Keywords– uranium isotope ratio, thermal ionization mass spectrometry, inductivity coupled plasma mass spectrometry

Uranium has three major isotopes (^{234}U, ^{235}U, and ^{238}U) and is widely distributed in the environment. The relative isotopic abundances are 0.0054% (^{234}U), 0.7200% (^{235}U), and 99.2745% (^{238}U), respectively [1]. The range of natural variations of uranium isotopes [1] are shown in Table 1. Fukushima Daiichi nuclear power plant used UO_2 and mixed oxide (MOX) fuels, in which the averaged ^{235}U concentrations are 3.4-3.7 wt% and 1.2 wt%, respectively.

Table 1. Isotopic composition of uranium[1]

Isotope	Range of natural variations [%]
^{234}U	0.0050-0.0059
^{235}U	0.7918-0.7207
^{238}U	99.2739-99.2752

On the accident of Fukushima Daiichi nuclear power plant, huge amount of fission products were widely released. Since uranium is a heavy element, if it was released, the fallout may have been distributed at the near site of nuclear power plant.

The purpose of the present study is, from the viewpoint of safety assessment, to check that the $^{235}U/^{238}U$ ratio in environmental samples at the Fukushima area falls within the range of natural variations. The spent nuclear fuel includes ^{236}U generated via the neutron capture of ^{235}U. The $^{236}U/^{238}U$ ratio in the river and ocean close to the Fukushima area has been investigated with accelerator mass spectrometer [2]. In the present study, we analyzed $^{235}U/^{238}U$ in environmental samples (soils, plants, and so on) at the Fukushima area with thermal ionization mass spectrometer (TIMS) and inductively coupled plasma mass spectrometer (ICP-MS).

Samples were immersed in concentrated HNO_3 and heated at 413 K. After evaporation of HNO_3, diluted HNO_3 was added, and then, uranium was recovered from the samples by ion-exchange chromatography with ion-exchange resin and extraction chromatography with UTEVA-resin. The concentration of uranium recovered was analyzed with quadrupole ICP mass spectrometer (ICP-QMS) or ICP atomic emission spectrometer (ICP-AES).

Uranium isotopic ratios were analyzed with a TIMS (Triton-T1, Thermo Fisher Scientific) with a rhenium double filament system and/or an ICP-MS (Element 2, Thermo Fishier Scientific). As the reference material of mass spectrometry, standard material CRMU010, in which the atomic percent of ^{235}U is certified to be 1.0037±0.0010% [3], was used.

The sample solution of 1 ppm uranium in 1 M HNO_3 was prepared for TIMS. Each solution of 1 μL (1 ng of U) was loaded onto a rhenium evaporation filament. The mass spectrum was obtained with a secondary electron multiplier detector. The sample solution of 10 ppb uranium in 0.1% HNO_3 was also prepared for ICP-MS. Our analytical result of CRMU010 agreed with the certified value within 2σ analytical error. Based on the validity of isotopic analysis, the $^{235}U/^{238}U$ ratio in the environmental samples inside the 3 km range from the Fukushima Daiichi nuclear power plant was analyzed. A possibility of atmospheric release of nuclear fuel matrix during the accident of Fukushima Daiichi nuclear power plant is discussed.

[1] J. K. Böhlke *et al*., *J. Phys. Chem. Ref. Data*, **34**, 57 (2005).
[2] A. Sakaguchi *et al*., *Geochemical. J*., **46**, 355 (2012).
[3] E. L. Garner *et al*., Nat. Bur. Stand. (U.S.), Spec. Publ. 267-27 (1971).

Particulates of Ag and Pu radioisotopes released from Fukushima Daiichi nuclear power plants

H. Kimura[1], M. Uesugi[2], A. Muneda[2], R. Watanabe[1], A. Yokoyama[3], T. Nakanishi[4]

[1]Grad. School Nat. Sci. Tech., Kanazawa Univ., [2]Col. Sci. Eng., Kanazawa Univ., [3]Inst. Sci. Eng., Kanazawa Univ., [4]Adv. Sci. Res. Cent., Kanazawa Univ.

Abstract –Due to Fukushima Daiichi nuclear power plants accident, a large amount of radionuclides were released into environment. The radioactivities of ^{134}Cs, ^{137}Cs, ^{110m}Ag, ^{238}Pu, and $^{239+240}Pu$ in a soil sample collected in Futaba, Fukushima were determined by α spectrometry or γ spectrometry. We searched for the dispersion of these radioactivities in a soil sample, which suggests the existence of hot particles for Pu contamination.

Keywords –^{238}Pu,, ^{110m}Ag ,^{137}Cs, hot particle,

I. INTRODUCTION

Massive radionuclides were released into environment due to the Fukushima Daiichi nuclear power plant (FDNPP) accident. The volatile fission products, such as ^{137}Cs, ^{134}Cs were considered to be deposited as several chemical forms through dry deposition and wet deposition. On the other hand, the deposition procedures of non-volatile nuclides such as Pu isotopes and ^{110m}Ag were not clear, and it is predicted that these radionuclides were deposited as hot particles. The existence of hot particles may cause their radioactivity concentrations to vary over a wide range even if soil samples are collected in a place. In this work, we researched for the dispersion of radioactivities in a homogenized soil sample collected in Futaba, Fukushima.

II. EXPELIMENTS

Sample collection

A soil sample was collected in Futaba located at 4km north-west of Fukushima DNPP.

Preparation

Firstly, the sample was agitated by hand hundred times, and it was dried at 105℃ overnight. Secondly, it was crushed in a mortar, and sieved through at 2mm sieve. Finally, it was heated at 450℃ for 4 hours to decompose organics.

1 Measurement of Pu

After addition of a tracer of ^{242}Pu, six aliquots of 10g soil were leached with 10 M HNO_3-0.01M HF. And then, after isolation of Pu atoms through an ion exchange procedure the atoms were electrodeposited on a steel plate and subjected to α spectrometry.

2 Measurement of ^{110m}Ag

Some aliquots of 1.0g soil sample were prepared, and they were subjected to γ spectrometry.

III. RESULTS

Figure 1 shows correlation between ^{238}Pu and ^{137}Cs for six aliquots. The radioactivity of ^{238}Pu in one aliquot is clearly higher than the others, and the ratio of $^{238}Pu/^{239,240}Pu$ of the former is also higher. This result suggests the existence of hot particle of Pu in that aliquot. Figure 2 shows the good correlation between ^{137}Cs and ^{110m}Ag. Therefore it was suggested that hot particles of ^{110m}Ag did not exist in the soil sample. These results suggest the difference of the release processes of ^{110m}Ag and ^{238}Pu although both of them are non-volatile nuclides.

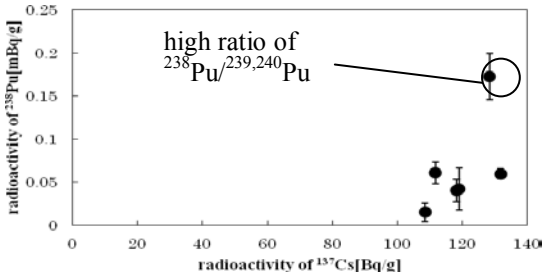

Fig.1 Correlation between ^{238}Pu and ^{137}Cs

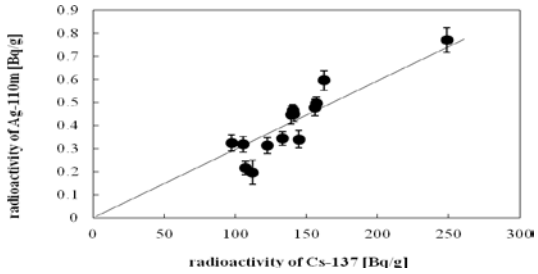

Fig.2 Correlation between ^{110m}Ag and ^{137}Cs

The measurement of $^{14}C/^{12}C$ ratios in Japanese plant samples affected by anthropogenic sources

Risa Hashimoto [1], Aki Inoue [1], Yasuyuki Muramatsu [1], Hiroyuki Matsuzaki [2]
[1]Depertment of Chemistry, Gakushuin University
[2]School of Engineering, the University of Tokyo

In relation to anthropogenic influences of ^{14}C in the atmosphere, we have carried out the following two different studies;

(1) secular variation of $^{14}C/^{12}C$ ratio in rice harvested in Japan,

(2) influence of the Fukushima nuclear accident on $^{14}C/^{12}C$ ratio in plant leaves in the region.

Analytical results by AMS for rice collected from 1951 to 2012 showed that $^{14}C/^{12}C$ ratios decreased exponentially after the Partial Test Ban Treaty in 1963. The residence time of ^{14}C in the atmosphere is estimated to be about 10 years.

Plant leaves collected about 9km from the reactor showed a weak increase of $^{14}C/^{12}C$ ratios. This suggests that ^{14}C was released by the accident and influenced the $^{14}C/^{12}C$ ratios in plant leaves collected near the reactor.

Keywords – ^{14}C; anthropogenic sources; plant samples; secular variation; Fukushima; AMS

I. INTRODUCTION

^{14}C is produced in nature by cosmic ray reactions in the upper atmosphere, and its production changes by the flux of cosmic rays. The produced ^{14}C immediately reacts with an oxygen molecule, resulted in the production of $^{14}CO_2$ and it is absorbed by plants through photosynthesis. Therefore plants are reflected atmospheric $^{14}C/^{12}C$ ratios at that time.

^{14}C is also released into the atmosphere by anthropogenic sources such as nuclear weapons tests and nuclear accidents. In this study, we focus on ^{14}C released from anthropogenic sources and carried out the following two studies using AMS. We determined $^{14}C/^{12}C$ ratios in rice harvested in Japan to study recent influence of the past nuclear weapons tests. We also studied whether there were influences on $^{12}C/^{14}C$ ratios in the plants due to the accident at the Fukushima Daiichi Nuclear Power Plant (FDNPP) occurred in March, 2011. Although there are many papers reporting the release of several nuclides, there are almost no data for ^{14}C. In the last year, we have determined $^{14}C/^{12}C$ ratios in Japanese cedars and pine needles collected in Fukushima prefecture. Some enhancements of ^{14}C levels were observed. However, we still have lack of ^{14}C data. Therefore, we analyzed additional samples collected near the FDNPP and studied whether the $^{14}C/^{12}C$ ratios in the plants were affected by the accident.

II. EXPERIMENT

Rice samples harvested from 1951 to 2012 were used for the analysis. They were homogenized in a blender and oxidized to produce CO_2. Then, the CO_2 was purified in a vacuum line and reduced to prepare graphite target for AMS. $^{14}C/^{12}C$ ratio in the graphite was measured by AMS at the University of Tokyo and Japan Atomic Energy Agency.

In order to examine the possible influences of ^{14}C for plants, we have collected leaves of Japanese cedar in Okuma, 9km far from FDNPP, in September, 2011. Since cedars are evergreen, leaves were contaminated at the time of the accident. We analyzed old leaves, which were grown before the accident, and new leaves, which were grown after the accident. Cedar leaves were washed with pure water in order to remove particulate matters deposited on the plant surface. For comparison with background samples collected far from FDNPP, we analyzed pine needles in Chiba prefecture and rice samples collected in Niigata prefecture. The samples were also homogenized in a blender, and prepared graphite targets for AMS.

III. RESULTS

Results obtained for rice showed that $^{14}C/^{12}C$ ratios decreased exponentially with time after the Partial Test Ban Treaty in 1963. The residence time of ^{14}C in the atmosphere is estimated to be about 10 years.

For the cedar samples collected in Okuma, $^{14}C/^{12}C$ ratios in the old leaves (grown before the FDNPP accident) were found to be higher than the new leaves (see Fig.1). Since $^{14}C/^{12}C$ ratios in new leaves were almost the same as the ratios in the other samples collected from outside of Fukushima. From the above-mentioned results, ^{14}C in the old leaves was increased because of the influence of ^{14}C released by the FDNPP accident. $^{14}C/^{12}C$ ratios did not change so much, even the samples were washed. Therefore, we assume that most of ^{14}C were taken as gaseous forms and associated with plant tissues in the leaves. Contribution of ^{14}C associated with particulate matters deposited on the leaves seems to be small.

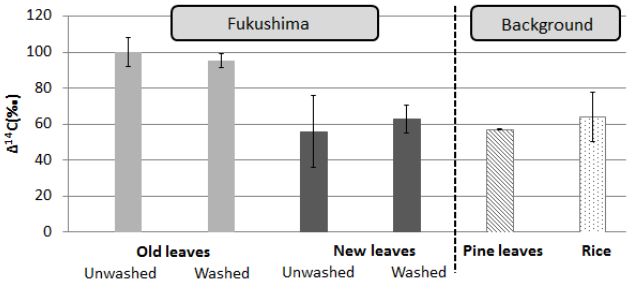

Fig 1. $^{14}C/^{12}C$ ratios in Japanese cedar leaves collected from Fukushima and those in other samples from background areas

Radiocesium and stable cesium in edible wild plants (Sansai) collected from forests in Fukushima Prefecture

SUGIYAMA, M.[1], MURAMATSU, Y.[1], OHNO, T.[1], SATO, M.[2]
[1]Gakushuin University
[2]Fukushima Agricultural Technology Center

Abstract –
High concentrations of radiocesium were observed in edible wild plants and bamboo shoots collected from forests in Fukushima Prefecture following the nuclear accident. We have analyzed radiocesium and stable cesium in a variety of plant samples. The highest concentrations of radiocesium and stable cesium were found in leaves of Acanthopanax sciadophylloides. The Cs/Rb ratios and the Cs/K ratios were also high in this species. These results suggest that leaves of Acanthopanax sciadophylloides absorb Cs selectively from surface forest soil.

Keywords – radiocesium, stable cesium, edible wild plants, transfer to plants

I. INTRODUCTION

An accident occurred at the Fukushima Dai-ichi Nuclear Power Plant in March 2011, consequently large quantities of radioactive materials were released into the environment. Farmlands and forests in Fukushima Prefecture were widely contaminated and their products were affected by the released radionuclides. The most important radionuclides related to vegetation are Cs-134 (half-life: 2y) and Cs-137 (half-life: 30y), which have relatively long half-lives. Concentrations of radiocesium in vegetables and rice decreased with time. However, radiocesium concentrations in edible wild plants and mushrooms often exceeded the guideline (100 Bq/kg) for foods stuffs. Therefore, it is important to identify plants which accumulate cesium and to clarify the transfer mechanism of radiocesium. In this study, we analyzed both radiocesium and stable cesium and considered the mechanism of high radiocesium transfer into the plants. We also compared the transfer of stable cesium with other stable elements to examine the availability of cesium to plants.

II. MATERIALS AND METHODS

Four different edible wild plants, *Acanthopanax sciadophylloides* (Koshiabura), *Kalopanax septemlobus* (Harigiri), *Aralia elata* (Taranoki), bamboo shoots (Takenoko), were collected from forests in Iitate-mura, Fukushima, and they were measured with a Ge-detector. Then the samples were freeze-dried and milled with a mixer. Powdered samples (0.1 g) were digested in teflon vessels with an acid mixture (HNO_3, HF and $HClO_4$) on a hot plate. After digestion, the samples were evaporated to dryness. Then, the residues were dissolved in 2% HNO_3. Concentrations of stable elements (Li, Na, Mg, K, Ca, Mn, Co, Cu, Zn, Rb, Sr, Cs and Ba) were determined by ICP-MS. To have a better precision in the analysis, triplicate samples were prepared and determined for these elements.

III. RESULTS AND DISCUSSION

Radiocesium concentrations differed by the plant species. We first expected that the concentrations of radiocesium should be similar within a same group (*Araliaceae*) collected from the same area. However, leaves of *Acanthopanax sciadophylloides* showed very high concentrations up to about 20,000 Bq/kg. Therefore, transfer mechanism of cesium for *Acanthopanax sciadophylloides* seems to be different from the other two species of *Araliaceae*. For stable cesium, we also found the highest concentration in this species. This suggests that the transfer through roots should be a dominant pathway to explain high radiocesium concentrations in *Acanthopanax sciadophylloides*. The high uptake of stable cesium in this species suggests that the contribution of translocation pathways from barks and leaves might be low, because stable cesium exists mainly in soils and not in barks of the trees. In addition, we also compared stable Cs with K and Rb which are also one of the alkali elements. The Cs/Rb ratios and the Cs/K ratios in leaves of *Acanthopanax sciadophylloides* were higher than those in the other species of *Araliaceae* and bamboo shoots. These findings indicate that *Acanthopanax sciadophylloides* absorbs cesium selectively than the other alkaline elements. In forests, radiocesium is accumulated in surface soil layers (including litter layer) in which contents of organic matters are high. Since radiocesium is more mobile in organic layers compared to mineral soil, it was more readily taken up by the plant.

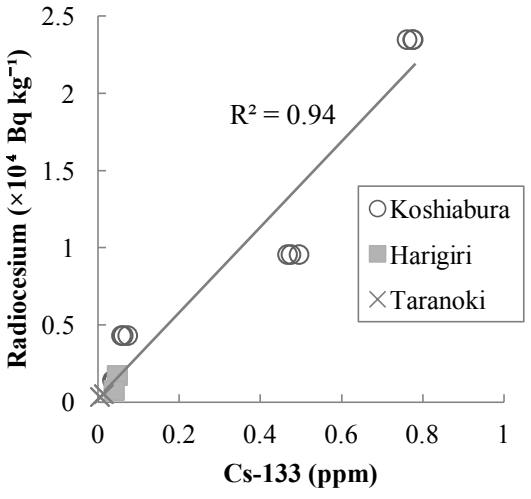

Fig. 1. Relationship between radiocesium and stable cesium in plant leaves of *Araliaceae* collected from Iitate-mura, Fukushima.

Annual Variation of Radioactivity in Marine Biota in the Pacific off Fukushima after TEPCO's Fukushima Daiichi Nuclear Power Station Accident

TatsuoAono [1], Satoshi Yoshida[1], Tadahiro Saotome [2],Takuji Mizuno [2],
Yukari Ito[3], Jota Kanda[3], Takashi Ishimaru [3]
[1] National Institute of Radiological Sciences
[2] Fukushima prefecture fisheries experimental station
[3] Tokyo University of Marine Science and Technology

Abstract – Many kinds of marine biota could be observed in the coastal area around off Fukushima after this accident, and it is suggested that the changes of activity are caused by the feeding and sediment effects in biota.

Keywords – Marine organisms, ^{134}Cs, ^{137}Cs, ^{110m}Ag

I. Introduction

The pollution in marine environment spread by radioactive substances widely after the accident of TEPCO's Fukushima Daiichi Nuclear Power Station (F1NPP) with the 2011 Great East Japan Earthquake and Tsunami. It's been 2.5 years since this accident. The activities of Cs-134 and Cs-137 decreased exponentially in seawater. When the activities of radionuclides had decreased in seawater, it was thought that these gradually decreased in marine biota and sediment before this accident. However, the high activities of radio casesium have been monitored in fish in the coast area around off Fukushima. Little notice of the benthos was taken, because there are not edible as foodstuff. Marine biota were collected around off Fukushima due to investigate the activities of radionuclides. The aims of the present study were to examine the temporal changes in radioactivity and to clarify the variation factor in marine biota.

II. Method

Marine biota samples were collected with plankton net, dredge sampler, and trawl during the cruise of T/S Umitaka, T/S Shinyo, and some research and fishing vessels. After being classified into species (Polychaete, Sea Urchin, Starfish, Sea Slug and Crab etc.) and packed into a plastic container. The radioactivity was determined by gamma ray spectrometry using a HPGe detector (Canberra, GX-2019). The activities of radionuclides of biota in the sampling date were calculated with the correction of the decay and the coincidence - summing of ^{134}Cs. Detection limits of ^{134}Cs, ^{137}Cs, and ^{110m}Ag were estimated within 1 and 0.5 Bq/kg (wet wt), respectively.

III. Results and Discussion

The radioactivities of ^{137}Cs and ^{110m}Ag in marine biota were from 1 to 400 Bq/kg (wet wt) and from less than 1 to 55 Bq/kg (wet wt), respectively. The high correlation between the activities in biota and densities in dry samples were observed in the benthos. It is suggested that it is caused by the feeding and sediments effects in biota.

Migration behavior of ^{134}Cs and ^{137}Cs in the Niida River water in Fukushima Prefecture, Japan during 2011-2012

Seiya Nagao[1], Masaki Kanamori[2], Shinya Ochiai[1], Masayoshi Yamamoto[1]
[1]Low Level Radioactivity Laboratory, Kanazawa University
[2]Graduate School of Natural Science and Technology, Kanazawa University

Abstract – The radioactivity of ^{134}Cs and ^{137}Cs in the water samples from the Niida River, which flows through high contaminated area, was measured with gamma-spectrometry using ammonium molybdophosphate (AMP)/Cs compound method. Total radioactivity of ^{134}Cs and ^{137}Cs ranged from 0.254 to 4.18 Bq/L during May 2011-August 2012 and decreases with increasing time except for the rain events. The radioactivity was 1.20 Bq/L for ^{134}Cs and 1.83 Bq/L for ^{137}Cs after the rain event due to the typhoon No.4 in June 2012. The particulate phase of ^{134}Cs and ^{137}Cs was 47-93% in normal flow condition and 86-91% in high flow condition by rain events. These results indicate that suspended solids are major carrier of ^{134}Cs and ^{137}Cs in the Niida River.

Keywords – radiocesium, radioactivity, heavy rain, suspended solids

I. INTRODUCTION

A nuclear accident at the Fukushima Daiichi Nuclear Power Plant (NPP) occurred after the 2011 Tohoku earthquake and tsunami. About 15 PBq of both ^{134}Cs and ^{137}Cs was released from the NPP as a result of venting operations and hydrogen explosions. Surface deposition of ^{134}Cs and ^{137}Cs reveals considerable external radioactivity above 3000k Bq/m^2 in a zone extending northwest from the NPP. Therefore, it is important to elucidate the short-term to long-term impacts of the Fukushima Daiichi NPP accident on ecosystems of river watershed environments. This study investigated the transport of ^{134}Cs and ^{137}Cs in a small river, Niida River running through IIdate, in Fukushima Prefecture, Japan at normal and high flow conditions during 2011-2012.

II. MATERIALS AND METHODS

Niida River is located in Fukushima Prefecture, Japan and flows through IIdate with higher contaminated area of radiocesium and Minami-Souma with medium to low accumulation area. It has a watershed area of 585 km^2 and 78 km in length.

Field experiments were conducted at a fixed station in the lower Niida River during the period of May 2011-November 2012. The 20 L of surface river water samples were collected at the station using buckets. In normal flow condition, dissolved and particulate phase of radiocesium was separated using cartridge filters with pore sizes of 10 µm, 1 µm, and 0.45 µm. The radioactivity of ^{134}Cs and ^{137}Cs in the river waters before and after the filtration was measured with gamma-ray spectrometry using ammonium molybdophosphate (AMP)/Cs compound method. In heavy rain events with typhoon, particles were separated using centrifugation and filtration with No. 5A (approximate pore size of 7 µm) filters and a pore size of 0.45 µm membrane filters. Filtration was conducted using No. 5A filters and then filtered with membrane filters.

The ^{134}Cs and ^{137}Cs were measured using gamma-ray spectrometry with a low background Ge detector at the Low Level Radioactivity Laboratory and the Ogoya Underground Laboratory of Kanazawa University.

III. RESULTS AND DISCUSSION

Radioactivity of ^{134}Cs and ^{137}Cs in the river waters ranged from 0.15 Bq/l to 3.83 Bq/l, and from 0.19 Bq/l to 4.18 Bq/L, respectively during May 2011-August 2012 (Fig. 1). Highest value was found in May 2011. The radiocesium concentration indicates decreasing trend with increasing time after the Fukushima Daiichi NPP accident. However, the higher radioactivity was observed in March and June 2012 after rain events.

Percentage of ^{134}Cs and ^{137}Cs associated with riverine suspended solids was 47-48% at normal flow condition in July and September 2011, but after December 2011 ranged from 75 to 93% at normal flow condition and 86-91% at high flow condition due to rain events. It appears to be differences in the radioactivity and existence forms between early period of July-September and after December 2011.

These results indicate that the transport processes of ^{134}Cs and ^{137}Cs from watershed to river vary with river watershed condition and water discharge condition.

Figure 1. Radioactivity and percentage of particulate phase of ^{137}Cs in waters from the Niida River.

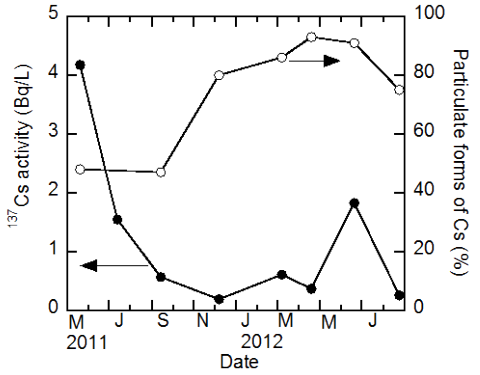

Migration Behavior of Radiocesium Released from Fukushima Daiichi Nuclear Power Plant Accident

Toshihiko Ohnuki[1], Naofumi Kozai[1], Fuminori Sakamoto
[1]Japan Atomic Energy Agency, Tokai, Ibaraki, 319-1195 Japan

Abstract – The migration behavior of radiocesium in plants and soil collected in Fukushima, Japan have been studied by the analyses of contaminated plants and soil using autoradiography, sequential desorption, size fractionation, XRD, and SEM analysis. Autoradiography analysis of tree samples collected after 2 and 8 months after the accident showed that radiocesium was mainly distributed as like spots on the branches and leaves of the trees emerged before the accident, and was little detected in new branch and leaves emerged after the accident. On the contrary, radiocesium was detected at the outermost tip of branches in the trees collected after 20 months of the accident. More than 65% of radiocesium were remained in the residual fraction of the soil samples after the sequential desorption. Approximately 70% of radiocesium in the residual fraction were associated with the size fractions larger than the elutriated one, even though mica like minerals were contained in the elutriated one. Therefore, plants and soil act as retardation barrier in the migration of radiocesium.

Keywords – Radiocesium, migration, autoradiography, desorpion

I. INTRODUCTION

The nuclear accident at the Fukushima Daiichi Nuclear Power Plant (FDNPP) occurred as a consequence of the massive earthquake and associated tsunami that struck the Tohoku and north Kanto regions of Japan on 11 March 2011. A series of hydrogen explosion was occurred from 13 March to 15 March at the units 1, 2, and 3. The release rate of ^{137}Cs on 15 March is estimated between 10^{12} and 10^{15} Bq/h. This fallout radioactive Cs were dispersed from FDNPP to ocean and land. Some of the released radioactive Cs was deposited on the ground of the area located north-west direction from FDNPP. Many scientists have studied migration of radiocesium to estimate dose rate and to estimate the fate in the terrestrial environment. However, the migration behavior of radiocesium is not fully understood.

In the present study, migration behavior of radiocesium has studied by the analyses of contaminated plants and soil using autoradiography, sequential desorption, size fractionation, XRD, and SEM analysis.

II. EXPERIMENTAL

The samples of plants were collected on the places located between 4 and 55 km from FDNPP at approximately 2, 8, 20, and 22 months after the accident. The spatial distribution of radiocesium on the plants was analyzed by autoradiography analyses.

Soil was sampled in Iitate, Fukushima on 1 month after the accident. For the analyses of soil spatial distribution was measured by autoradiography, and mobility was examined by sequential desorption using appropriate desorption reagent solutions. Size distribution of residual radiocesium after the sequential desorption was analyzed by size fractionation using sieve and the elutriation. The mineralogical components of soil were analyzed by XRD and SEM-EDS analyses.

III. RESULTS AND DISCUSSION

The autoradiography analyses of *Cryptomeria japonica*, *Torreya nucifera*, and *Thujopsis dolabrata* var. *hondae* collected on approximately 2 and 8 months after the accident showed that radiocesium was mainly distributed as like spots on the branches and leaves of the trees emerged before the accident, and was little detected in new branch and leaves emerged after the accident. On the contrary, radiocesium was detected at the outermost tip of branches in the trees collected after 20 months of the accident. *Morus alba* collected after 22 months contained radiocesium in and outside of the stem, even though no radiocesium was detected in the root, strongly suggesting that some radioacesium was translocated from the outside stem to inside. These results indicate that distribution of radiocesium deposited on/in the trees has been gradually changed with time in the scale of the year.

Autoradiography analysis of the thin section of soil showed that radiocesium in soil was distributed as like spots on the soil particles. More than 65% of radiocesium were remained in the residual fraction of the soil samples after treatment of a 1 mole L^{-1} NH_4Cl solution and a 1 mole L^{-1} CH_3COOH solution. Approximately 70% and 10% of radiocesium in the residual fraction were associated with the size fractions larger than the elutriated one and with elutriated one, respectively. XRD and SEM-EDS analyses showed that a variety of minerals were present in the soil involving mica like minerals. XRD spectrum of elutriated soil fraction showed the presence of mica like minerals. These results strongly suggest that radiocesium was irreversibly associated with soil components other than mica like minerals in the contaminated soil.

Therefore, plants and soil function as barrier to retard the migration of radiocesium deposited by the accident of FDNPP.

Research on Atmospheric Radionuclides from the Fukushima Nuclear Accident at the MRI, Japan

Yasuhito Igarashi[1], Koji Adachi [1], Taichu Tanaka[1], Mizuo Kajino[1], Tsuyoshi Sekiyama[1], Takashi Maki[1], Yuji Zaizen[1], Masao Mikami[1]
[1]Meteorological Research Institute, Japan

Abstract – By the Fukushima nuclear accident, atmospheric environments over Japan, especially the eastern part, were seriously polluted by a massive amount of the anthropogenic radionuclides. The Meteorological Research Institute, Japan (MRI) has devoted into the clarification of these earlier environmental impact not only by the observations but also by model simulation endeavors. Major research activities at the MRI are briefly introduced in this presentation.

Keywords – Fukushima nuclear accident, radio-Sr, radio-Cs, Radioactive aerosol, Numerical transport and deposition modeling

I. INTRODUCTION

The Meteorological Research Institute, Tsukuba, Japan (MRI) has carried out observations on the atmospheric radionuclides for more than 50 years. In order to clarify the impacts of the Fukushima nuclear accident in the atmospheric environment and its control factors, the observations have continued after the disaster in March 2011. Also, the model simulations were conducted to reconstruct radioactive plume transport and depositions of the radioactive contaminants over the regional as well as the global environment.

II. OBSERVATION ENDEVOURS

The MRI locates ca.170 km southwest of the accidental site. The monthly total deposition of ^{137}Cs at the MRI was 23±0.9 kBq/m^2 in March, 2011. This amount is 6-7 digits higher than the level prior to the disaster. The total ^{137}Cs deposition was 25.5 kBq/m^2 for the year 2011. Simple sum of the monthly ^{137}Cs deposition flux due to the global weapon tests since 1954 gives about 7 kBq/m^2. Considering the physical decay for the global fallout ^{137}Cs, the Fukushima ^{137}Cs contamination could be about 20 times larger than the global fallout. Almost the same extent of ^{134}Cs deposited, thus the surface radio-Cs contamination extended about 50 kBq/m^2. This value almost corresponds to that around Tsukuba obtained by the air-borne survey conducted by the Ministry of Education, Culture, Sports, Science and Technology, Japan (MEXT).

On the contrary, the monthly ^{90}Sr deposition at the MRI was 4.4±0.1 Bq/m^2 in March, 2011, which was about 1/5000 of that of ^{137}Cs during the same month. Referring to the level before the disaster, this deposition exhibits 2-3 digits of enhancement; the environmental and health impacts were not as enormous as radio-Cs. The total ^{90}Sr deposition was about 11 Bq/m^2 for the year 2011 and it was about 1/2500 of ^{137}Cs. Until the middle of 2012, the ^{90}Sr/^{137}Cs activity ratio varied about 400~5000 and after all the degree of the pollution by the radio-Sr can confirm trivial compared with Cs over the metropolitan region.

As further trials an imaging plate (IP) analysis, which visualizes the radioactivity distributions in air filter samples, and particle analysis using a scanning electron microscope (SEM) with energy-dispersive X-ray spectrometer (EDS), have been carried out. The purpose of these analyses is to identify the host particles which carry the radionuclides.

III. SIMULATION ENDEVOURS

In order to improve our understanding of the temporal and spatial distributions of transport and depositions of the radionuclides due to the Fukushima accident, both global and regional atmospheric transport models have been employed. For the global transport MASINGAR (Model of Aerosol Species IN the Global AtmospheRe), with horizontal model grid of about 0.56^o and 40 vertical layers (from surface to 0.4hPa), was used. The horizontal wind components were nudged by global analysis of Japan Meteorological Agency (GANAL) dataset. The model deals with ^{137}Cs, ^{133}Xe, and ^{131}I. Emission flux estimates by Chino et al. (2011) and Stohl et al. (2011) were used for ^{137}Cs and ^{131}I, and ^{133}Xe, respectively. The model simulated advective transport, eddy diffusion, convective transport, dry and wet depositions, and radioactive decay.

More detailed distribution and processes for the Fukushima radioactivity, a regional transport model MRI-PM/r (Passive-tracers Model for Radioactivity) has been developed. This model classifies the aerosol particles into 6 categories, and considers condensation, evaporation, cohesion, activation of cloud condensation nuclei and ice nuclei, dissolution, collision (washout), cloud microphysical processes (conversion processes among rainout, cloud water, ice clouds, raindrops, snow, hail) and dry deposition. The model also incorporated physical and chemical processes of radionuclides and the interaction with the environment aerosol.

In addition to these, emission analysis from the accident by inverse modeling approach, and advanced approach of ensemble simulation of atmospheric dispersion of radionuclides during the accident have been performed.

The overview of the current status and challenges of these observations as well as simulation studies are given.

[1] Igarashi et al., 2013EGU
[2] Adachi et al., 2013EGU
[3] Maki et al., 2013EGU
[4] Sekiyama et al., 2013EGU
[5] Tanaka et al., 2013AMS
[6] Kajino et al., 2011JMSJ Fall Meeting

Presuming techniques of radioactive cesium concentration in muscle for beef cattle

T. Ohtsuki[1], F. Koga[2], M. Uchida[2], Y. Ishikawa[2], T. Takase[3], K. Kawatsu[3], M. Mogi[4] S. Murayama[4], Y. Izumi[4], H. Kikunaga[1], T. Tachiya[5], Y. Shiraishi[2], K. Endo[2]

[1]Research Center for Electron Photon Science, Tohoku University
[2]Fukushima Agricultural Technology Center Livestock Industry Research Center, Fukushima Prefecture
[3]Faculty of Symbiotic System Science, Fukushima University
[4]Japan Environment Research Co., LTD,
[5]Comtec Eng. Co., LTD, Fukushima

Abstract – The contamination of livestock products by the radioactive cesium (Cs134 and Cs137) is a serious problem in Tohoku area after the accident of the Fukushima No.1 nuclear power plant. The presuming techniques of the radioactive cesium concentration in muscle and blood for these beef cattle were developed in this study. We found that the measurements of the radioactive cesium from outside of body are really possible by using several inches(") NaI scintillation detectors.

Keywords – radioactive cesium, beef cattle, measurement from outside of body, NaI scintillation detector

I. INTRODUCTION

The contamination to the livestock products, by radioactive cesium is becoming a serious problem in Tohoku area after the accident of the No.1 nuclear power plant of Fukushima. Especially, beef cattle which fed excessively contaminated stock food should be still continuously monitored. Since Ge-detectors are restricted and if we use them, so much time is needed for presuming of the cesium contamination by taking blood sample[1], then, another technique for the concentration check inside body(muscle) for the living cattle should be considered. Here we demonstrate the monitoring system by using NaI scintillation detectors from outside of cattle body.

II. MONITORING SYSTEM AND MEASURENENTS

The monitoring system is consist of 2", 2.5" and 5" NaI scintillation detectors for measuring the Cs134 and Cs137 concentrations in the cattle body, collimators (Pb material), phantoms (plastic tank: the specific liquid like inside materials are contaminated by several concentrations of Cs134 and Cs137), special frame for keeping the cattle body on the inside and its radiation shielding materials consist of several sheets of Pb curtains. We use a portable MCA system for data acquisition. The 5" NaI detector and its collimator are shown in Fig. 1(a) and the special frame for keeping the cattle body and the portable MCA system are also shown in Fig. 1(b). Firstly, we took calibration curves between the Ge and NaI detectors by using phantoms by which the cesium concentration is known. The practical measurements were performed by comparison of contamination-free cattle and contaminated them. The measurement time and position were set to 600 sec at the thigh and haunches (further shorter time like 300 sec. is needed for the measurements). The data are analyzed by the code Fukushima by provided Niki Grass Co. Ltd. for doing better deconvolution.

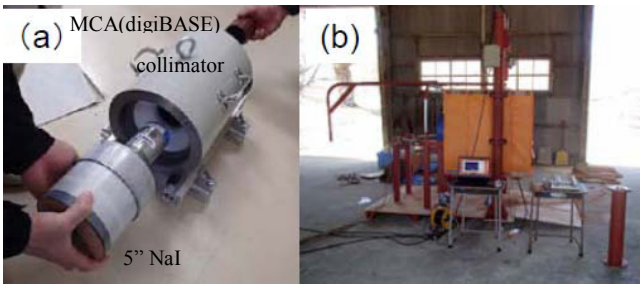

Fig. 1(a) 5" NaI detector and its collimator: setting inside the collimator, (b)Measurement system of cattle from outside of the body (special frame for keeping the cattle body).

III. RESULTS

Results of the measurements are shown in Fig. 2. From the figure it is clearly seen the cesium peaks, namely, the cesium contaminated cattle has much higher count rates of Cs134 and Cs137 than those of the contamination-free cattle even though the similar count rates of K40 between them. Small peaks of Cs134 and Cs137 for contamination-free cattle are due to the back ground from atmosphere. Detail of the results will be shown and discussed in the conference.

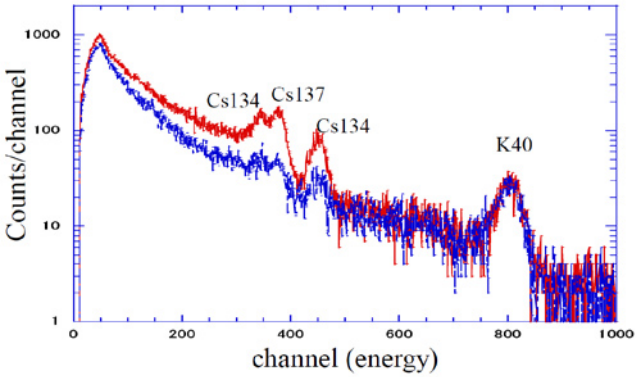

Fig. 2 Two spectra with 5" NaI scintillation detector are shown, the results of contaminated cattle fed by the contaminated stock food (higher count rate) and the contamination-free cattle (lower count rate).

[1] T. Takase et. al., Radioisotopes 62 (2013), in press.

Spatio-temporal distribution of atmospheric radiocesium at monitoring stations for Suspended Particulate Matter in Fukushima area released from the TEPCO Fukushima Daiichi Nuclear Power Plant accident

Haruo Tsuruta[1], Yasuji Oura[2], Mitsuru Ebihara[2], Mitsunori Ishimoto[3], Yosuke Katsumura[3], Toshimasa Ohara[4], Teruyuki Nakajima[1]

[1] Atmosphere and Ocean Research Institute, The University of Tokyo, Japan
[2] Department of Chemistry, Tokyo Metropolitan University, Japan
[3]Center for Regional Environmental Research, National Institute for Environmental Studies
[4]Nuclear Professional School, The University of Tokyo, Japan

Keywords Spatio-temporal distribution, atmospheric ^{137}Cs, Fukushima, filter tapes of SPM monitor

I. INTRODUCTION

No data has been found of continuous monitoring of radioactive materials in the atmosphere in Fukushima area after the Fukushima Daiichi Nuclear Power Plant (FD1NPP) accident on March 11, 2011, although it greatly contributes to accurate evaluation of the internal exposure dose, to reconstruction of emission time series of released radionuclides, and to validation of numerical simulations by atmospheric transport models. Then, we have challenged to retrieve the radioactivity in atmospheric aerosols collected every hour on a filter tape which was installed in Suspended Particulate Matter (SPM) monitor with beta-ray attenuation method used at air pollution monitoring networks in Japan. In the previous paper [1], the concentration of ^{134}Cs and ^{137}Cs collected on the filter tapes has been successfully measured by a Ge detector, and time series of hourly atmospheric concentrations of ^{134}Cs and ^{137}Cs was also made at many monitoring stations for SPM in Fukushima prefecture and the adjasent areas. The purpose of this paper is that, by using these data, spatio-temporal distribution of ^{137}Cs will be shown in Fukushima area, and the transport of radioactive materials from the FD1NPP will be discussed by analyzing meteorological data and radiation dose rate.

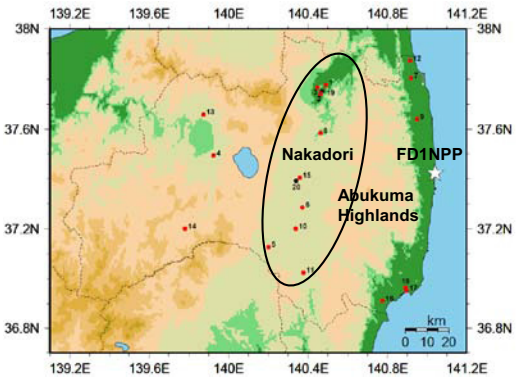

Fig. 1 SPM monitoring stations in Fukushima prefecture

II. DATA FOR ANALYSIS

Hourly atmospheric concentrations of ^{134}Cs and ^{137}Cs in several monitoring stations in Nakadori of Fukushima prefecture (Fig. 1) during March 15-16 and 20-23, 2011, was used for a detailed analysis. Meteorological data of AMeDAS stations, GPV (Grid Point Value) and Radar-AMeDAS precipitation by Japan Meteorological Agency was also used. Regional deposition rate for ^{137}Cs on the earth's surface with airborne measurements by MEXT was used in comparison with spatial distribution of the polluted air masses.

III. RESULTS AND DISCUSSION

High concentrations of ^{137}Cs (>10 Bq m^{-3}) were measured in Nakadori twice, the first period from 9:00 (JST) Mar. 15 to 3:00 Mar. 16, and the second period from 13:00 Mar. 20 to 06:00 Mar. 21. In the first period, the polluted air masses transported from the FD1NPP over Abukuma Highlands, were found in the afternoon of Mar. 15. The time of the maximum concentration changed from the early afternoon in the south to the night in the north, and the maximum concentration was much higher in the south than in the north. According to the deposition rate of ^{137}Cs on the soil surface in regional scale measured by MEXT [2], higher deposition rate was measured in the northern part than in the southern part, possibly due to more precipitation in the northern part. In the second period, however, higher ^{137}Cs concentrations began to be measured in the northern part in the early afternoon of Mar. 20. In the night, the time of the maximum ^{137}Cs was found early in the north and late in the south. During the second period, radiation dose rate in Nakadori did not show any increase due to no precipitation. Thus, the radiocesium dataset by measuring filter tapes installed in the SPM monitor is very useful to retrieve the spatio-temporal distribution of ^{137}Cs in an area which has no continual data of radionuclides in the atmosphere.

[1] Oura, Y. et al.: a paper in this Symposium, 2013
[2] MEXT: Intensive field study on the measurements of radionuclides deposited on the soil surface in east Fukushima, HP of MEXT, 2011.

Education of Nuclear and Radiochemistry in Hallym University, Korea

Y. H. Chung
Department of Chemistry, Hallym University, 1 Hallymdaehak-gil, Chuncheon 200-702, Korea
yhchung@hallym.ac.kr

Nuclear and radiochemistry course has been provided by Department of Chemistry in Hallym University (HU) for more than ten years. It is designed mainly for undergraduates who want to pursue their career in the pertinent fields such as chemistry of spent fuel of nuclear reactors, radiopharmaceutical chemistry, radiation chemistry and nuclear chemistry. There are twenty-two reactors currently operating in Korea and a few research facilities are treating cancer patients using an accelerator. A heavy-ion accelerator, RAON, will be commissioned in 2017 and provide various rare isotopes produced by IF (in-flight fragment) and ISOL (Isotope Separation On-Line) methods [1]. RAON's superconducting linear accelerator will accelerate uranium beam up to 200 MeV/u with 400 kW beam power. In addition to RAON, a KHIMA (Korea Heavy Ion Medical Accelerator) project for cancer therapy was initiated in 2010 by KIRAMS (the Korea Institute of Radiological & Medical Sciences) and will include a superconducting cyclotron to be completed at the end of 2016 [2]. The cyclotron will provide heavy ions whose maximum energy and beam intensity are 430 MeV/u and 1.7×10^{10} pps, respectively. Nuclear and radiochemistry program in Hallym University is going to embrace the ongoing progress in Korea.

[1] S. K. Kim, *RAON: Heavy Ion Accelerator for Rare Isotope Science in Korea*, The 16th Inter. Conf. on Accelerators and Beam Utilizations, November 8-9, 2012, Gyeongju, Korea.
[2] G. B. Kim, *Current Status of KHIMA Project*, The 16th Inter. Conf. on Accelerators and Beam Utilizations, November 8-9, 2012, Gyeongju, Korea.

APSORC'13 - 5th Asia-Pacific Symposium on Radiochemistry
Kanazawa, Japan, 22-27 September 2013

Use of Small $^{68}Ge/^{68}Ga$ Generators in Experiments for the Education of Radioisotope-related Fields as well as of Natural and Social Sciences in General

Tadashi Nozaki,[1] Koji Ogawa[2]

[1]School of Sciences, Kitasato University
[2]School of Allied Health Sciences, Kitasato University

Experiments undertaken in schools usually give more vivid and unforgettable impression to the students than lectures. Several characteristics of radioisotopes can be used efficiently in the education of radioisotope-related fields as well as of natural and social sciences in general. Many radioisotopes useful for education are given from isotope generators, of which $^{68}Ge/^{68}Ga$ generator has proved to be of the widest use, as understood from the decay properties of both nuclides shown here and from chemical properties of the daughter, ^{68}Ga.

^{68}Ge: 271 d, EC, no γ ---- Black matter for many detections
^{68}Ga: 67.7 m; β^+, 90 % 1.9 MeV; EC, 10 %
γ, 1.07 MeV 1.0 %, etc.

Although large scale $^{68}Ge/^{68}Ga$ generators for PET use are commercially available, we were unable to find any stable supply of small types. For full use of this generator, thus we should become able to make it by ourselves. First we examined the method of preparing the adsorbent for parent-daughter separation, and have proved the following procedure to be highly useful: (1) prepare gelatinous precipitate of hydrated SnO_2 from $SnCl_4$ and NaOH solutions and wash it by repeated centrifugation and re-suspension in water; (2) collect and warm gently the centrifuged mass with occasional turn-over with a non-metallic spatula to give moist particles; (3) push gently the particles on a sieve of 200 μm mesh size to crash them into smaller sizes, and leave them over potassium acetate (CH_3CO_2K) at room temperature for drying; (4) after 1 week, treat the particles just as in Step 3 but with a sieve of about 100 μm mesh size; (5) collect by sieving particles of about 50 to 100 μm size, and keep them over CH_3CO_2K; (6) after more than 2 weeks, dip the particles in refluxing 0.1 M HNO_3 for 3 hours, and (7) after being left to cool, replace the HNO_3 with 1 M HCl. After 2 days, the particles, hydrated SnO_2, is ready for use.

Usually 1 mL disposable plastic syringe is used for the generator column, to which the adsorbent (apparent volume of 0.3 - 0.4 mL) suspended in HCl is added. Then 1 M HCl solution of ^{68}Ge (1 to 100 kBq) with daughter ^{68}Ga is added to the column. The column is further washed with 100 mL of 1 M HCl flowing slowly through it for wash away some fine suspensions . In Japan, the generator with ^{68}Ge activity under 100 kBq can be used free from law regulation.

The ^{68}Ga is eluted into 1/3 mL of 1 M HCl in about 30 sec with 65-70 % yield. Since quantitative separation is possible for ^{68}Ge and ^{68}Ga in 1 M HCl, some hot-atom effect is thought to make ^{68}Ga formed in the column partly non-elutable. Under frequent milking, the breakthrough of ^{68}Ge is a few tens ppm. No change was observed in these characteristics in 9 months, the half-life of ^{68}Ge.

Self-making of the generator is thought to be a common experimental theme, and can be guessed to give joy and satisfaction to the participants in handling samples prepared by their self-made devices, even when ready-made adsorbent was supplied them in the generator making. Comparison of the growth curve of ^{68}Ga observed after milking with the curve obtained by calculation from the differential equation is expected to be highly effective in the study of how to treat some observed phenomena by mathematical means. The eluted ^{68}Ga is highly suitable for the following chemical experiments: adsorption on cellulose under various pH; solvent extraction and ion exchange separation; and isotopic exchange between Ga^{3+} and Ga-EDTA complex.

We have almost completed a guide book for the experiments given above, and now are working further for the following themes: (1) utilizing the generator as the source of annihilation radiation, γ-ray absorption by various substances, and coincidence measurement for localization and for low background counting; and (2) utilizing ^{68}Ga as tracer, studies on contamination and decontamination, leak hunting, synthesis of radiopharmaceuticals, and measurement of uptake by plants.

Since a vast variety exists in the principal aim, experiences and scientific levels of possible candidates to the experimental study, at least three courses should be prepared. Also, the guide book should be so made as the teachers and instructors are able to select adequately the themes for each course. As for usual high school curriculums, only a few to several days are allotted to the education related with nuclear phenomena. Hence, it is of prime importance, we believe, to set up a rental system, in which generators, radiation detectors, etc., are sent to individual high schools from regional centers according to predetermined schedules, preferably together with instructor(s).

Application of alpha spectrometry to the measurement of a single plutonium particle for nuclear safeguards

Kenichiro Yasuda, Daisuke Suzuki, Fumitaka Esaka and Masaaki Magara
Research group for analytical chemistry, Japan Atomic Energy Agancy

Abstract – For rough estimation of isotopic composition in a single plutonium particle before precise measurement by thermal ionization mass spectrometry (TIMS), alpha spectrometry was demonstrated using 10 particles in a standard reference material NBS947. The particles with diameters of around one micrometer were picked up and put onto TIMS filaments by a micromanipulator attached to a scanning electron microscope (SEM). The particle on the filament was transferred to an alpha spectrometer chamber. And then, the activity ratio of (^{238}Pu+^{241}Am)/(^{239}Pu+^{240}Pu) was measured for each particle. Finally, precise Pu isotope ratios of ^{240}Pu/^{239}Pu and ^{241}Pu/^{239}Pu were determined with TIMS. The measured activity ratios and isotope ratios were in good agreement with the reference data within the measurement uncertainty.

Keywords – alpha spectrometry, plutonium particle, nuclear safeguards

I. INTRODUCTION

The International atomic energy agency (IAEA) has adopted environmental sampling as a new method for the strengthened safeguards system [1-2]. The objectives of this method are to detect undeclared nuclear materials and activities. One of the analytical methods for environmental sampling is particle analysis, which is a powerful tool for nuclear safeguards to detect undeclared nuclear activities. In this method, isotope ratios of nuclear materials in individual particles were measured by secondary ion mass spectrometry (SIMS) [3-5] or thermal ionization mass spectrometry (TIMS) [6-8]. Prior to the analysis with TIMS, the particle containing nuclear materials should be put onto a filament. However, there is no conclusive proof that nuclear materials exist in the particle on the filament. The purpose of this study is to check if the particle on the filament contains nuclear materials before measuring the isotope ratios by TIMS, and to compare the activity ratios and the isotope ratios of the particle.

[1] D.L. Donohue, J. Alloys Compd., 11, 271-273 (1998).
[2] D.L. Donohue, Anal. Chem., 74, 28A-35A (2002).
[3] G. Tamborini, M. Betti, V. Forcina, T. Hiernaut, B. Giovannone, L. Koch, Spectrochim. Acta B53, 1289-1302 (1998).
[4] M. Betti, G. Tamborini, L. Koch, Anal. Chem., 71, 2616-2622 (1999).
[5] F. Esaka, K.T. Esaka, C.G. Lee, M. Magara, S. Sakurai, S. Usuda, K. Watanabe, Talanta, 71, 1011-1015 (2007).
[6] C.G. Lee, L. Iguchi, F. Esaka, M. Magara, S. Sakurai, K. Watanabe, S. Usuda, Jpn. J. Appl. Phys., 45, L294-L296 (2006).
[7] C.G. Lee, D. Suzuki, F. Esaka, M. Magara, N. Shinohara, S. Usuda, J. Nucl. Sci. Technol., 46, 809-813 (2009).
[8] O. Stetzer, M. Betti, J. van Geel, N. Erdmann, J.V. Kratz, R. Schenkei, N. Trautmann, Nucl. Instrum. Meth. Phys. Res. A525, 582-292 (2004).

High LET Radiolytic Degradation Studies of Separation Processes for Spent Nuclear Fuel

Jeremy Pearson and Mikael Nilsson
University of California – Irvine, USA
Department of Chemical Engineering and Materials Science,916 Engineering Tower, Irvine, CA, 92697
E-mail: nilssonm@uci.edu

Treatment of used nuclear fuel through solvent extraction separation processes is hindered by radiolytic damage from radioactive isotopes present in used fuel. The nature of the damage caused by the radiation may depend on the radiation type, whether it be low linear energy transfer (LET) such as gamma radiation or high LET such as alpha radiation. Used nuclear fuel contains beta/gamma emitting isotopes but also a significant amount of transuranics which are generally alpha emitters. The effects of gamma radiation on solvent extraction ligands have been more extensively studied than the effects of alpha radiation. This is due to the inherent difficulty in producing a sufficient and confluent dose of alpha particles within a sample without leaving the sample contaminated with long lived radioactive isotopes. Helium ion beam and radioactive isotope sources have been studied in the literature. We have developed a method for studying the effects of high LET radiation *in situ* via ^{10}B activation and the high LET particles that result from the $^{10}B(n,\alpha)^{7}Li$ reaction which follows. This method has been applied to organic solutions of TBP and CMPO, two ligands common in TRU solvent extraction treatment processes. Rates of degradation of TBP and CMPO and their respective degradation products in the presence of high LET radiation are presented and discussed. These results are also compared to gamma studies performed in our lab and other gamma and alpha studies found in the literature. The possible application of this method to a variety of other solvent extraction ligands to study the effects of high LET radiation is also considered.

Effects of helium retention and lithium depletion on tritium behaviors in Li_2TiO_3

Makoto Kobayashi[1], Hiromichi Uchimura[1], Kensuke Toda[1], Misaki Sato[1],
Katsuyoshi Tatunuma[2], Yasuhisa Oya[1] and Kenji Okuno[1]
[1]*Radioscience Research Laboratory, Faculty of Science, Shizuoka University, Shizuoka, Japan*
[2]*Kaken Co. Ltd., 1044, Hori, Mito-city, Ibaraki, 310-0903, Japan*

Abstract – The effects of helium retention on tritium behaviors in lithium-titanate (Li_2TiO_3) were investigated. The synergetic effect of helium retention and lithium-depletion was also examined with using lithium-depleted $Li_{1.8}TiO_{2.9}$. Deuterium introduced into Li_2TiO_3 by ion implantation was desorbed as three peaks at 400, 490 and 620 K. Deuterium retention at 400 K for $Li_{1.8}TiO_{2.9}$ was larger than that for Li_2TiO_3 due to the existence of larger amount of lithium vacancies. Deuterium retention by lithium vacancies was decreased by He implantation because of the occupation of vacancies by He.

Keywords – Tritium, Li_2TiO_3, Helium, TDS

I. INTRODUCTION

For the establishment of D-T fusion reactors, a comprehensive model of tritium migration processes in solid tritium breeder materials must be developed. Tritium migration behavior in lithium-titanate (Li_2TiO_3), which is one of candidates for tritium breeder materials, has been studied by out-of-pile annealing experiments. However, the effects of helium generated by Li(n,α)T reaction on tritium migration in Li_2TiO_3 have not been focused in detail. It is generally known that helium can retain in the materials by forming bubbles, which will exist in Li_2TiO_3 after long-term operation, and affect on tritium migration process by acting as diffusion passes and/or trapping sites. These predictions motivated us to investigate the contributions of helium retention on trapping and release of hydrogen isotopes in Li_2TiO_3. The pre-irradiation of He^+ was performed into sintered Li_2TiO_3 pellet. Thereafter, D_2^+ irradiation was carried out. Thermal desorption spectroscopy (TDS) measurements were adopted for the elucidation of deuterium retention and release behaviors. The same experimental procedure was also done for lithium-depleted Li_2TiO_3 ($Li_{1.8}TiO_{2.9}$) to understand the effects of helium retention with lithium burn-up, which are simultaneously occurred in actual environment.

II. EXPERIMENTAL

The powders of Li_2TiO_3 and $Li_{1.8}TiO_{2.9}$ were pressed into a disc shape with the size of 10 mm^{ϕ} × 0.5 mm^{t}, and sintered at 1173 K for 3 h. These samples were installed into a vacuum system and heated at 1173 K for 3 h to remove impurities. The He^+ implantations were done with the implantation energy of 3 keV He^+, ion flux of 1.0×10^{18} He^+ m^{-2} s^{-1} and ion fluence of 1.0×10^{22} He^+ m^{-2}. Thereafter, 3.0 keV D_2^+ implantations were carried out with the ion flux and ion fluence of 2.0×10^{18} D^+ m^{-2} s^{-1} and 2.0×10^{22} D^+ m^{-2}, respectively. The deuterium desorption behaviors were examined by TDS using a high resolution mass spectrometer to separate He^+ and D_2^+ from room temperature to 1173 K with the heating rate of 5 K min^{-1}..

III. RESULTS AND DISCUSSION

D-TDS spectra for Li_2TiO_3 and $Li_{1.8}TiO_{2.9}$ are shown in the figure. D-TDS spectrum for only D_2^+ irradiated Li_2TiO_3 showed that D release was distributed in the temperature of 350- 750 K. The D release spectrum was consisted of three release peaks at around 400, 490 and 620 K. The TDS spectrum for the D_2^+-irradiated $Li_{1.8}TiO_{2.9}$ also showed the same D release peaks. However, the deuterium retention in the peak at 400 K was increased compared to that for Li_2TiO_3. This fact indicates that deuterium released at 400 K was weakly trapped by lithium vacancies. He^+ pre-irradiated Li_2TiO_3 showed the decrease of deuterium retention in the release peaks at 400 and 490 K. The deuterium trapping sites for the release peaks at 490 K and 620 K would be the irradiation defects such as oxygen vacancies and the dangling oxygen atoms, respectively. Therefore, helium retention would only reduce the deuterium retention in irradiation defects. These results suggest that helium would disturb deuterium to retain at irradiation defects by substituting them, however, hardly affects for chemical binding due to the little chemical affinity of helium.

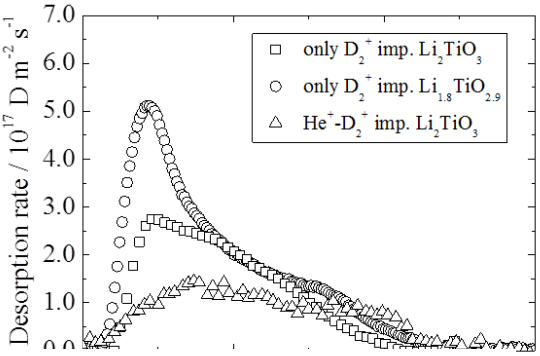

Fig. D-TDS spectra for Li_2TiO_3 and $Li_{1.8}TiO_{2.9}$ with D_2^+ and He^+ implantations

APSORC'13 - 5th Asia-Pacific Symposium on Radiochemistry
Kanazawa, Japan, 22-27 September 2013

Adsorptivity of Various Metal Ions onto Benzo-18-crown-6 and Dibenzo-18-crown-6 Resins

Masanobu Nogami[1], Tomohiro Haratani[1], Yu Tachibana[2], Toshitaka Kaneshiki[3], Masao Nomura[3], Tatsuya Suzuki[2]
[1]Department of Electric and Electronic Engineering, Kinki University
[2]Department of Nuclear System Safety Engineering, Nagaoka University of Technology
[3]Research Laboratories for Nuclear Reactors, Tokyo Institute of Technology

Abstract – Adsorptivity of various metal ions onto silica-supported resins consisting of benzo-18-crown-6 (B18C6) and dibenzo-18-crown-6 (DB18C6), repectively, was investigated in hydrochloric acid and nitric acid media. Pd(II) and Ag(I) for HNO_3 and Fe(III) and Ba(II) for HCl were found to be adsorbed by both resins, respectively. It was also found that Sr(II) for HCl and Ca(II) for HNO_3 were adsorbed by B18C6 and DB18C6 resins, respectively. These facts indicate that the two resins which have almost the same ring size adsorbed metal ions with smaller cationic diameters except Ba(II) with different selectivity.

Keywords – benzo-18-crown-6, dibenzo-18-crown-6, resin, nuclide separation

I. INTRODUCTION

It is well known that macrocyclic compounds such as crown ethers selectively form complexes with metal ions, and their applications to the treatment of radioactive liquid wastes by liquid-liquid extraction have widely been investigated. Recently we have synthesized silica-supported resins where crown ethers are chemically bonded to the polymer network[1,2]. The chemical structure of dibenzo-18-crown-6 (DB18C6) resin, for example, is shown Figure 1. So far the resins have mainly been studied for the purpose of isotope separation, e.g. zinc and calcium, and little information on adsorptivity of various metal ions by these resins is available. In the present study, adsorptivity of various metal ions onto benzo-18-crown-6 (B18C6) and DB18C6 resins was investigated in hydrochloric acid and nitric acid media.

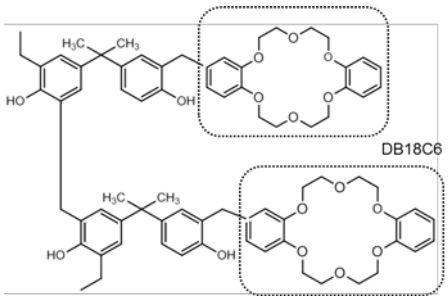

Figure 1 Chemical structure of DB18C6 resin

II. EXPERIMENTAL

B18C6 and DB18C6 resins were synthesized by following the earlier paper[2]. Adsorptivity of metal ions by the resins to at equilibrium was examined by a batch method at 25°C using solutions of HNO_3 or HCl up to 9 mol/dm^{-3} (= M) containing each metal ion (1mM).

III. RESULTS AND DISCUSSION

Pd(II) and Ag(I) for HNO_3 and Fe(III) and Ba(II) for HCl were found to be adsorbed by both resins, respectively. It was also found that Sr(II) for HCl and Ca(II) for HNO_3 were adsorbed by B18C6 and DB18C6 resins, respectively. In general, the distribution ratios increased with increasing concentrations of HCl. On the other hand, dependence of HNO_3 concentrations on the distribution ratios was found much smaller for HNO_3 system. No or very little adsorptions were observed for the other examined metal ions. These facts indicate that the two resins which have almost the same ring size adsorbed metal ions with smaller cationic diameters except Ba(II) with different selectivity. Extraction experiments using DB18C6 and dichloromethane as the diluent showed different selectivity, *i.e.*, Zn(II) and Zr(IV) were extracted from HNO_3 of higher concentrations and Fe(III) was extracted from HCl of higher concentrations, respectively. No or very little extractions were observed for the other examined metal ions. Such a difference may result from the structure except the part of DB18C6, e.g. oxygen atoms of the hydroxyl group. Investigation of detailed adsorption mechanisms is the task in the future.

ACKNOWLEDGMENT

This work was partially supported by the Grant-in-Aid for Scientific Research (B) (KAKENHI No. 23360423).

[1] Ding X, Suzuki T, Nomura M, Kim HJ, Sugiyama Y, Fujii Y (2007) J Radioanal Nucl Chem 273:79-84
[2] Hayasaka K, Kaneshiki T, Nomura M, Suzuki T, Fujii Y (2008) Prog Nucl Energy 50:510-513

Cesium adsorption ability and stability of metal hexacyanoferrate irradiated with gamma-rays

Makoto Arisaka[1], Masayuki Watanabe[1], Manabu Ishizaki[2], Masato Kurihara[2], Rongzhi Chen[3], Hisashi Tanaka[3]

[1]Research Group for Radiochemistry, Nuclear Science and Engineering Directorate, Japan Atomic Energy Agency
[2]Department of Material and Biological Chemistry, Faculty of Science, Yamagata University
[3]Nanosystem Research Institute, National Institute of Advanced Industrial Science and Technology

Abstract – The influence of irradiation with gamma-rays to metal hexacyanoferrate (MHCF: M = Fe, Cu or Ni), which is known as an adsorbent for selective adsorption of cesium (Cs) ion in solution, on Cs adsorption ability and stability was investigated in HNO_3 solutions. Under the adsorbed dose conditions (50 - 300 kGy), it was found that the MHCF is fully stable although the radiolytic decomposition of MHCF was slightly observed with an increase of the total adsorbed dose, which was confirmed by an increment of Fe, Cu or Ni concentration in HNO_3 solution after the irradiation. The weight percent of the metal in the solution to initial weight of MHCF was less than unity. Moreover, no change in composition of carbon, hydrogen and nitrogen in MHCF was observed. On the other hand, the distribution coefficients of Cs to the irradiated MHCF were independent of the total adsorbed dose. This indicates that the Cs adsorption ability was maintained under gamma-ray irradiation.

Keywords – cesium, metal hexacyanoferrate, gamma-irradiation, adsorption ability, stability

I. INTRODUCTION

Metal hexacyanoferrate, MHCF, is known as an adsorbent for selective adsorption of cesium (Cs) ion in solutions. In nuclear industry, an application of MHCF (M = Fe, Cu or Ni) to recovery of Cs from high level radioactive waste has been studied. Recently, we reported an electrochemical application of MHCF for Cs recovery [1, 2].

It has been commonly accepted that the selectivity of MHCF to Cs ions are caused by regular lattice spaces surrounded by cyanide-bridged metals. However, the intrinsic mechanism of Cs ion adsorption still has not been made clear. So far, we have revealed that synthesized FeHCF, obtained as a charge-compensated salt ($Fe^{III}_4[Fe^{II}(CN)_6]_3$), has much higher Cs adsorption ability than that of commercially purchased FeHCF, i.e., prussian blue having ideal perfect lattice. The higher ability is attributed to the presence of lattice defect sites [3].

In this study, the influence of irradiation with gamma-rays to MHCF having lattice defect sites on Cs adsorption ability and stability in HNO_3 solutions was investigated for application of MHCF to practical Cs separation process.

II. EXPERIMENTAL

Irradiated sample is a mixture of MHCF and HNO_3 solution. MHCF used in this study is as follows; $Fe^{III}_4[Fe^{II}(CN)_6]_3$ (FeHCF), $Cu^{II}_3[Fe^{III}(CN)_6]_2$ (CuHCF), $Ni^{II}_3[Fe^{III}(CN)_6]_2$ (NiHCF).

Irradiation with gamma-rays was done at the Co-60 gamma ray irradiation facilities in Takasaki Advanced Radiation Research Institute of Japan Atomic Energy Agency. Samples in glass tubes were intermittently irradiated with gamma-rays from 1.0×10^{16} Bq ^{60}Co source at an absorbed dose rate of 10 kGy h^{-1} in air at room temperature for a maximum of 27 hours. A dose absorbed by each sample was corrected for an electron density. Absorbed doses were calibrated by a cellulose triacetate film dosimeter.

III. RESULTS AND DISCUSSION

After gamma-ray irradiation, the HNO_3 solutions were separated from the sample by filtration. To evaluate the radiolytic degradation of MHCF, the amount of M (= Fe, Cu or Ni) in HNO_3 solution was determined by ICP-AES. The result for CuHCF was shown in Fig.1 as an example. It was found that the amounts of Fe and Cu increased slightly with an increase of the total adsorbed dose. The increase was attributed to radiolytic decomposition of CuHCF. Under the adsorbed dose conditions (50 - 300 kGy), the weight percent of Fe and Cu in the solutions to initial weight of CuHCF was less than 0.05%. From the viewpoint of usage for a long period, it suggests that the CuHCF is fully stable. Moreover, the composition of carbon, nitrogen and hydrogen in CuHCF is independent of the total adsorbed dose.

The Cs adsorption experiment was performed using the irradiated MHCF as adsorbent. The distribution coefficients of Cs into MHCF were independent of the total adsorbed dose. This indicates that the Cs adsorption ability was maintained under gamma-ray irradiation.

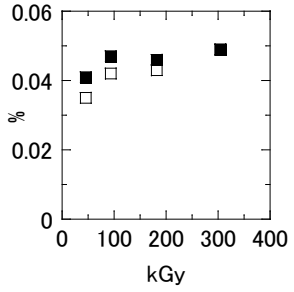

Fig.1 Weight percent of Fe (■) and Cu (□) to initial weight of CuHCF in HNO_3 solutions after the irradiation.

[1] R. Chen et al., Electrochem. Commun., **25**, 23-25 (2012).
[2] R. Chen et al., Electrochim. Acta, **87**, 119-125 (2013).
[3] M. Ishizaki et al., Phys. Chem. Chem. Phys., submitted.

Residual Actinides Separation from the DIAMEX/SANEX Secondary Waste and Decontamination of the Spent DIAMEX Solvent from the "Difficult-to-Strip" Elements

Jan John, Ferdinand Šebesta, Kamil V. Mareš, František Klimek, Martin Vlk
Czech Technical University in Prague, Department of Nuclear Chemistry, Brehova 7, 115 19 Prague, Czech Republic

Abstract

One of the contemporary issues connected with the spent nuclear fuel is its reprocessing. The presence of long-lived radionuclides in the spent nuclear fuel is responsible for its long-term radiotoxicity. A decrease of the long-term radiotoxicity may be achieved by partitioning of minor actinoids with their subsequent transmutation. The main goals of the Partitioning and Transmutation are decreasing the time and the volume needed to store high radioactive waste, and a reduction of the hazard associated with the spent fuel and radioactive waste.

Among the processes under development for the Partitioning, the families of DIAMEX and SANEX processes studied by the broad international collaborations in Europe should be mentioned. This paper summarizes the results of the studies of two process-relevant issues of these processes – development of materials and processes for the residual actinides separation from the secondary waste, and decontamination of the spent organic solvent from the "difficult-to-strip" elements.

During the study of *materials and processes for residual actinides separation*, the behaviour of TODGA–PAN solid extractant in applications involving processing of large volumes of solutions was tested. In an experiment with 5.10^{-5}M $Eu(NO_3)_3$ sorption from 3M HNO_3, it was confirmed that no significant washing of TODGA from the solid extractant occurs even during the processing of more than 300 BV of the simulated waste. In another experiment, it was shown that the repeated sorption / elution cycles do not significantly influence the practical sorption capacity of the solid extractant.

For the mutual separation of An and Ln, pre-concentrated from the secondary waste streams, two novel solid extractants (SEXs) – the E5-C_5BTBP[nitrobenzene] and E5-$CyMe_4$BTBP(cyclohexanone) – were proposed and developed. With the E5-C_5BTBP[nitrobenzene] SEX, very good separation of americium and europium was achieved. From a loaded column, 98.6 % of europium was washed in 8.7 BV of the eluant; the europium fraction contained only 0.3 % of the total amount of americium sorbed on the column. Then, americium was efficiently eluted with 0.5M glycolic acid with pH ~ 4. In the total volume of the eluant used (3.1 BV), 99.7 % of americium was recovered; the americium fraction contained 1.4 % of the amount of europium originally sorbed on the column.

The E5-$CyMe_4$BTBP(cyclohexanone) SEX was tested for the selective separation of An from Ln and other components of the simulant of a model secondary waste stream – PUREX raffinate without both the major and minor actinides. In batch experiments, the Am D_g was found to display a pronounced maximum at 1M HNO_3. As expected on the basis of the liquid-liquid extraction experiments, the kinetic studies revealed that the uptake of Am by the new SEX is much faster than for the similar materials with 1-octanol or nitrobenzene diluents.

Two dynamic experiments were performed with a column loaded by the new E5-$CyMe_4$BTBP(cyclohexanone) SEX. The experiments revealed that the maximum achievable flow-rate for a negligible Am break-through is ~ 5 BV/hr for the given experimental set-up. An almost quantitative uptake of Am from a mixed carrier free Am – Eu solution in 1M HNO_3 was achieved during the treatment of all the ~ 60 BV of the feed; Am could be easily eluted from the column by 0.5M HGlyc at pH = 4. The cumulative data for the experiment were: americium: recovery > 98 %, < 1 % of Eu in Am fraction; europium fraction: recovery > 99 %, contaminated by < 2 % of Am.

A serious obstacle in industrialization of the DIAMEX process is accumulation of *"difficult-to-strip" elements* (e.g. Ru, Y, Mo, Pd, Zr, Sr etc.) *in the spent solvents*. The aim of the study performed was to verify the possibility to decontaminate such spent solvents by solid sorbents. A problem in the pre-selection of potentially suitable sorbents turned out to be the fact that for the case of spent solvents and the metals like Ru or Pd, their speciation in organic phase is hardly predictable and may well be of non-ionic nature (colloids or pseudo-colloids containing reduced species etc.).

For the experimental part of this work, the DIAMEX solvent based on TODGA in kerosene / 1-octanol (5 vol.%) mixture was used as a reference system. An attempt to characterize speciation of the elements of interest in the simulant of the spent solvent was done by FTIR, ESI-MS, APCI-MS, and thin layer chromatography.

More than 50 solid sorbents of various nature, identified as potentially prospective, were obtained and their efficiency for the removal of Ru and Y from the simulated spent solvent was screened in batch contact experiments. The results obtained revealed that relatively high weight distribution ratios D_g, sufficient for the design of a process for quantitative separation of the contaminants from the solvent, can be achieved for some of the solid sorbents, e.g. Amberlyst A26 or Fe-EDA-SAMMS. For the prospective materials, sorption kinetics and sorption isotherms were determined. The materials with the highest sorption capacity were tested in dynamic column experiments. The results obtained in these tests will be presented in detail.

Thorium based Molten Salt Fuel Cycle

Qing-nuan Li*, Lan Zhang, Wen-xin Li, Guo-zhong Wu
Shanghai Institute of applied physics, Chinese Academy of Sciences, Shanghai*, China*
*Corresponding author. Tel: +86 21 39194059. Email: liqingnuan@sinap.ac.cn

Abstract –In 2011, Chinese Academy of Sciences (CAS), after discontinuing the research and development activity in nuclear energy for decades, started to implement Strategic Priority Research Program "Future Advanced Fission Nuclear Energy (FANE)". To perform this program, two sub-bases, the north and the south, were deployed in CAS. Shanghai Institute of applied physics (SINAP), as the south sub-base, is taking in charge of research and development of "Thorium-based Molten Salt Reactor Nuclear Energy System (TMSR)". According to this research plan, two kinds of molten salt nuclear reactors, i.e. 2MW uranium-thorium fluoride molten salt reactor (TMSR-LF1)and 2MW pebble bed fluoride salt-cooled high temperature reactor (TMSR-SF1), will be designed and developed. Three fuel cycle models will also be implemented orderly, one-through fuel cycle on TMSR-SF, modified open fuel cycle on TMSR-SF and TMSR-LF, and closed fuel cycle on TMSR-LF.

Pyrochemical processing methods are judged to be the only technologies for the fuel of MSRs with integrated reprocessing technologies. Because the liquid fuel for MSR is a mixture of molten fluorides, the fuel processing and reprocessing technologies planned are pyrochemical or pyrometallurgical techniques, which are based on separation of ^{233}U and fission products in molten fluoride salt. Considering the special advantages of fluoride volatility and electrometallurgical techniques, a preliminary protocol based on closed fuel cycle has been proposed for the treatment of fuel from TMSR. The recycling techniques of fuels proposed in this protocol include fluoride volatilization, distillation of molten salt carriers, electrochemical deposition. The simple experimental devices for above techniques have been established, and the feasibility studies are ongoing in SINAP.

Keywords –TMSR; fuel cycle; reprocessing; pyrochemical techniques

Study on electrochemical behaviors of rare earth elements in FLINAK eutectic salt

Li-fang Tian, Wei Huang, Feng Jiang, Chang-feng She, Hai-yang Zheng, De-wu Long*, Qing-nuan Li
Shanghai Institute of applied physics, Chinese Academy of Sciences, Shanghai, *China*
*Corresponding author. Tel: +86 21 39194677. Email: longdewu@sinap.ac.cn

Abstract –The reliable data on the electrochemical behaviors of key elements, such as lanthanides and actinides, is the foundation to assess the feasibility of application of the electrometallurgical method in recovery of the valuable actinides from fission products. For this purpose, the electrochemical behaviors of some rare earth elements (REs) in FLINAK eutectic salt (46.5 LiF - 11.5 NaF - 42.0 KF, mol %) at 550℃ were studied, including samarium (Sm^{3+}), europium (Eu^{3+}), yttrium (Y^{3+}), neodymium (Nd^{3+}), and gadolinium (Gd^{3+}) ions. The redox potentials, the number of exchanged electrons and the diffusion coefficients were determined by electrochemical transient techniques, such as cyclic voltammetry, square wave voltammetry and chronopotentiometry. For Y^{3+}, Gd^{3+} and Nd^{3+}, the results showed a three-electron reduction from the trivalent ions to metals near the potential of -1.95 V (or more negative) vs Ni/NiF_2 reference electrode. However, no metallic Sm and Eu could be formed because only the reduction of their trivalent ions to divalent ions occurred in the electrochemical window of FLINAK eutectic salt. Further work on the electrochemical extraction of REs from FLINAK is ongoing.

Keywords –FLINAK eutectic salt; Electrochemical behavior; Rare earth elements; Sm^{3+}, Eu^{3+}, Y^{3+}, Nd^{3+} and Gd^{3+}

APSORC'13 - 5th Asia-Pacific Symposium on Radiochemistry
Kanazawa, Japan, 22-27 September 2013

Measurement of cosmogenic nuclides in meteorites by well-type Ge detector in Ogoya Underground Laboratory

- Correction of coincidence sum effect for Al-26, Co-56, Na-22, and Co-60 -

Yasunori Hamajima
Kanazawa Univ. LLRL.

Abstract – *Two carbonaceous chondrite samples of about 3 ~ 5g, which have fallen in California on April 22, 2012, were measured by well-type Ge detector in Ogoya Underground Laboratory from May 21, 2012 for 30 days. Cosmogenic Co57, Cr51, Be7, Co58, Mn54, Co56, Co60, Na22, and Al26 were detected within the error of 20% or less, (That of Al26 is about 33%). The correction of coincidence sum effect would require for Al26, Co56, Na22 and Co60. The correction factors of these nuclides have been estimated from total efficiency as a function of gamma-ray energy.*

Keywords – chondrite cosmogenic nuclides, well-type Ge detector, sum coincidence effect, total efficiency

I. INTRODUCTION

Measurement of cosmogenic nuclides in meteorite, usually several tens of g, has been carried out by using a coaxial Ge detector. In case of small samples, a well-type Ge detector will be advantageously, because of high counting efficiency. And also, the efficiency does not depend much on the sample shape and its height up to about 40 mm in the well. On the other hand, coincidence sum effect is not negligible small, for annihilation and cascade gamma-ray.

In this experiment, two carbonaceous chondrites were measured by a well-type Ge detector in Ogoya Underground Laboratory. The correction of coincidence sum effect would require for Al26, Co56, Na22 and Co60. The correction factors of these nuclides have not been estimated from peak to total ratio, but from total efficiency as a function of gamma-ray energy. In this paper, I will discuss the method of the correction that will be required for all Ge detectors.

II. EXPERIMENTAL

Two carbonaceous chondrite samples of about 3.15 g and 5.16 g, which have fallen in Sutter's Mill, California on April 22, 2012, were measured by well-type Ge detector in Ogoya Underground Laboratory from May 21, 2012 for 30 days. Counting efficiency was determined by JRIA mixing standard volume source (Cd109, Co57, Ce139, Cr51, Sr85, Cs137, Mn54, Y88, and Co60), Na22 source and natural Lu176.

III. RESULTS AND DISCUSSION

Cosmogenic Co57, Cr51, Be7, Co58, Mn54, Co56, Co60, Na22, and Al26 were detected within the error of 20% or less, (That of Al26 is about 33%). The corrections of coincidence sum effect with annihilation gamma-ray for Na22 and Al26, and with cascade gamma-ray for Co56 and Co60 have been required. Those of Na22 and Co60 are corrected by standard.

Total efficiency as a function of energy was estimated as following equation;

$$\varepsilon_1^* = \varepsilon_1(1-T_2), \quad (1)$$

here, ε_1^*, ε_1 and T_2 are apparent peak and single peak, and total efficiency, respectively. Figure 1 shows the results of efficiency. The lower cross marks are apparent efficiencies, triangles and diamonds are single peak efficiencies, and upper line shows the total efficiency. The total efficiency curve as a function of energy leads to correction of coincidence sum effect of all of nuclides including those with extremely complicate decay scheme, such as Co56.

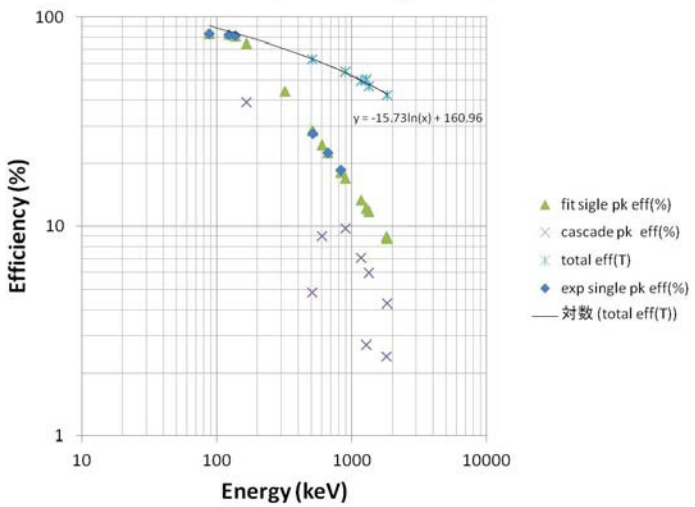

Figure 1. Efficiency of well Ge detector

I have estimated the apparent efficiency of 1809 keV of Al26 from the total efficiency of 511 keV of Na22. This estimated apparent efficiency (2.62%) was consistent with the result of Al26 standard AMS source (2.69%).

Correction of coincidence sum effect by total efficiency is practical.

Development of Multipurpose Neutron Irradiation Apparatus at KUR

K. Takamiya[1], Y. Yoshida[2], H. Tanaka[1], T. Fujii[1], S. Fukutani[1], T. Sano[1], H. Yoshino[1], Y. Iinuma[1], R. Okumura[1], S. Shibata[1]

[1]Research Reactor Institute, Kyoto University
[2]Graduate School of Engineering, Kyoto University

Abstract – A new apparatus for various neutron irradiation experiments has been developed at Kyoto University Reactor. The apparatus can transport a larger space gently to a neutron irradiation field adjacent to the reactor core. Therefore, various samples, for examples, large and liquid samples can be irradiated with neutrons. And also samples can be joined to experimental instruments with tubes that realize online measurements and cyclic irradiation experiments. Since setting samples at different range from the reactor core can change irradiated neutron flux, various experiments by wide range neutron flux can be performed. Neutron activation analysis for large samples and liquid samples becomes enabled by these characteristics. In order to apply the apparatus effectively, the neutron flux and gamma-ray dose rate has been measured at various irradiation position. And changing spectrum of irradiating neutrons has been tried using polyethylene blocks as a moderator. The characteristics of the apparatus and the future plan are reported in this paper.

Keywords – Neutron Irradiation, Neutron Activation Analysis, Online Measurement

I. INTRODUCTION

Neutron irradiation experiments, such as neutron activation analysis and isotope production, have been performed using various apparatuses at research reactors. One of the most general apparatus is a pneumatic system, which transport small capsules enclosing samples from a laboratory to a neutron irradiation field near a reactor core. However, sizes and weights of samples are limited by the transporting capacity of capsules, and irradiating liquid samples is difficult for reactor safety in the pneumatic system. A new neutron irradiation apparatus has been developed at Kyoto University Reactor (KUR, 5 MW thermal power) to overcome such limitations.

II. APPARATUS

The developed neutron irradiation apparatus transport samples loaded on a carrier from an experimental room adjacent to the reactor to nearby the reactor core through a horizontal beam hole (B-2) of KUR. The sample carrier has a capacity of about 6 cm × 6 cm × 30 cm and materials of up to 10 kg can be loaded. The carrier can be connected with plastic tubes to monitors and instruments placed at the experimental room at a distance of about 4 m from the reactor wall. Circulating liquid samples can be irradiated using pumps and the tube.

III. MEASUREMENT OF NEUTRON FLUX AND GAMMA-RAY DOSE RATE

The neutron flux and gamma-ray dose rate at various position of irradiation field of the apparatus have been measured. The neutron flux was measured by activation method using gold wires. The gamma-ray dose rate was measured by thermo luminescence dosimeters. Both measurements were performed at the positions of 100 to 300 cm at intervals of 50 cm, and only neutron flux measurements were carried out additionally at 0 and 50 cm from the reactor-side edge. The results of the measurements are shown in Fig. 1. The wide range of neutron flux that is from 10^8 to 10^{12} n/cm^2/s was observed, which realizes various kinds of neutron irradiation experiments. The neutron flux and gamma-ray dose rate decrease as the range from the edge increases. The decreasing trend of neutron flux changes around the range at 100 cm because the sectional shape of the beam hole changes here. The uniformity of neutron flux was also measured by activation method using PET films[1)] at every 100 cm from the reactor-side edge, and it was found the neutron flux at a section is uniform.

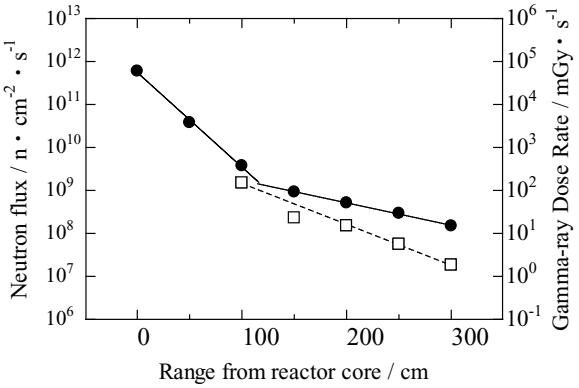

Fig. 1 Variation of neutron flux and gamma-ray dose rate at various positions in the B-2 beam hole.

[1] K. Takamiya, et al, Proc. Radiochim. Act 1 (2011) 63-66.

Development of a new continuous dissolution apparatus with a hydrophobic membrane for superheavy element chemistry

K. Ooe[1,2], K. Tsukada[2],M. Asai[2], T. K. Sato[2], A. Toyoshima[2], S. Miyashita[2], Y. Nagame[2], M. Schädel[2], Y. Kaneya[3], H. V. Lerum[4], J. P. Omtvedt[4], J. V. Kratz[5], H. Haba[6], A. Wada[7], Y. Kitayama[8]
[1]Institute of Science and Technology, Niigata University
[2]Japan Atomic Energy Agency
[3]Graduate School of Science and Engineering, Ibaraki University
[4]Department of Chemistry, University of Oslo
[5]Institut für Kernchemie, Universität Mainz
[6]Nishina Center for Accelerator-Based Science, RIKEN
[7]Department of Chemistry, Tokyo Metropolitan University
[8]Graduate School of Natural Science and Technology, Kanazawa University

Abstract –A new continuous dissolution apparatus of gas-jet transported products was developed for superheavy element chemistry. The new apparatus has a hydrophobic membrane for separation of aqueous solution from the gas. We investigated the dissolution efficiencies with the apparatus for short-lived nuclides. In the conference, the dependence of the efficiencies on the aqueous- and gas-flow rates will be reported.

Keywords – Molybdenum, Tungsten, Continuous dissolution, Hydrophobic membrane

I. INTRODUCTION

For investigation of the redox potentials of element 106, seaborgium (Sg), we plan to combine a flow electrolytic column (FEC) [1] with the rapid liquid-liquid extraction apparatus SISAK [2]. There is a technical problem in connection with these two apparatuses; a typical liquid flow rate for SISAK of ~24 mL/min is quite higher than that for FEC of ~1 mL/min. To successfully work with these two apparatuses, it is required to reduce the liquid flow rate of the SISAK system. However, the dissolution efficiency with the SISAK centrifuging degasser, which continuously dissolves gas-jet transported nuclear reaction products into an aqueous solution, drops with decreasing liquid flow rate. In the present study, therefore, we fabricated a completely new continuous dissolution apparatus which successfully works with a lower liquid flow rate.

II. NEW CONTINUOUS DISSOLUTION APPARATUS WITH A HYDROPHOBIC MEMBRANE

Our new degasser utilizes a hydrophobic Teflon membrane to separate aqueous solution from gas (hereafter called membrane degasser, MDG). It continuously dissolves transported products by a gas-jet as follows. The mixture of gas and aqueous solution enters the MDG. Then, only the gas is sucked through the membrane with a vacuum pump. On the other hand, the aqueous solution does not pass through the hydrophobic membrane and elutes from an outlet.

III. PERFORMANCE TEST

Dissolution efficiencies of gas-jet transported products were measured using the MDG. Short-lived isotopes, ^{91m}Mo ($T_{1/2}$ = 65 s), ^{93m}Mo ($T_{1/2}$ = 6.9 h), and ^{176}W ($T_{1/2}$ = 2.5 h), which are lighter homologues of Sg, were produced simultaneously in the ^{89}Y(^{7}Li, 5n)^{91m}Mo, ^{89}Y(^{7}Li, 3n)^{93m}Mo, and ^{175}Lu(^{7}Li, 6n)^{176}W reactions, respectively, at the JAEA tandem accelerator. Reaction products recoiling out of the targets were transported to the chemistry laboratory by a He/KCl gas-jet. The pressure in the target chamber was 130–140 kPa. The transported products were mixed with 1 M HCl/10^{-4} M HF solution before entering the MDG. The carrier gas was then sucked through the membrane in the MDG, while the aqueous solution was eluted from the MDG. The aqueous sample was collected in a plastic bottle and was then measured with a Ge detector.

IV. RESULTS AND DISCUSSION

The dissolution efficiencies for Mo and W at a He gas flow rate of 1.5 L/min were investigated as a function of aqueous flow rate. In the result, a dependence of the dissolution efficiencies on the half-life was observed; the efficiency for ^{93m}Mo ($T_{1/2}$ = 6.9 h) was higher than that for ^{91m}Mo ($T_{1/2}$ = 65 s) at aqueous flow rate of 0.6–6 mL/min. The dissolution efficiency for ^{176}W ($T_{1/2}$ = 2.5 h) was almost the same as that for ^{93m}Mo. Nevertheless, a dissolution efficiency of more than 80% was obtained for short-lived ^{91m}Mo at aqueous flow rates of 6–24 mL/min. A high yield of around 70% was also observed at flow rates of 1.8–3 mL/min. These results show that the MDG works with a lower aqueous flow rate than the previous SISAK degasser.

In the conference, the dependence of dissolution efficiency on the He gas flow rate will be also reported.

[1] A. Toyoshima et al., *Radiochim. Acta* **96**, 323-326 (2008).
[2] J. P. Omtvedt et al., *Eur. Phys. J. D* **45**, 91-97 (2007).

Cross-section Measurements of High Energy Neutron-induced Reactions for Cu and Nb

K. Ninomiya[1], T. Omoto[1], R. Nakagaki[1], N. Takahashi[1], Y. Kasamatsu[1], A. Shinohara[1], S. Sekimoto[2], H. Yashima[2], S. Shibata[2], T. Shima[3], H. Matsumura[4], M. Hagiwara[4], Y. Iwamoto[5], D. Satoh[5], M. W. Caffee[6] and K. Nishiizumi[7]

[1] Graduate School of Science, Osaka University
[2] Research Reactor Institute, Kyoto University
[3] Research Center of Nuclear Physics, Osaka University
[4] Radiation Research Center, High Energy Accelerator Organization
[5] Nuclear Science and Engineering Directorate, Japan Atomic Energy Agency
[6] Department of Physics, Purdue University
[7] Space Sciences Laboratory, University of California

Abstract – High-energy monoenergetic neutron-induced reactions above 100 MeV have been studied for Cu and Nb targets. Excitation functions of short-lived radionuclides were determined by gamma-ray spectrometry. We also measured cross-sections by proton-induced reactions with the same energy range and compared with each other. The cross-sections of neutron-rich nuclides by neutron-induced reaction were systematically larger than these by proton-induced reactions.

Keywords – cross-section, neutron-induced reaction, monoenergetic neutron

The determination of cross-sections by neutron-induced nuclear reaction is very important in the view point of space and planetary sciences to investigate the history of cosmic ray exposure. These data are also required for estimation of residual radioactivities in accelerator facilities. However, cross section measurements in the energy region > 100 MeV have scarcely been undertaken because of the difficulty in obtaining high energy monoenergetic neutrons. So neutron-induced cross-sections are estimated by a proton-induced cross-section with the same energy or calculated using theoretical models.

Our group has developed a method for determination of high energy monoenergetic neutron cross-sections at the Research Center for Nuclear Physics (RCNP), Osaka University [1]. This method is based on two neutron irradiation experiments produced by ^{7}Li (p, n) ^{7}Be reaction with two different angles for the axis of the primary proton beam to correct the contribution of the low energy neutron reaction [2]. In this study, we performed cross-section measurements with 197, 287 and 386 MeV neutrons for Cu and Nb.

All neutron irradiation experiments were performed at N0 beam line in RCNP. We obtained quasi monoenergetic neutron fluence with 197, 287 and 386 MeV from 200, 300 and 392 MeV incident proton beam, respectively. The details of the experimental methods were written in elsewhere [1]. Produced short-lived radionuclides were identified by high-purity germanium detectors, and neutron cross-sections were determined. We also performed proton irradiation experiments at the same beam line to obtain proton cross sections with the same incident energies.

The excitation function of ^{60}Co for Cu target by proton- and neutron-induced reactions are shown in Figure 1 with the related literature values [2-5]. We found the cross-sections of neutron-rich nuclides such as ^{60}Co by neutron bombardment reactions have a tendency larger than these by proton reactions, and proton-rich nuclides such as ^{58}Co have an opposite trend. In the presentation, we will report the detail experimental cross-section data and discuss such cross-section difference by projectile using empirical models for nuclear spallation reactions.

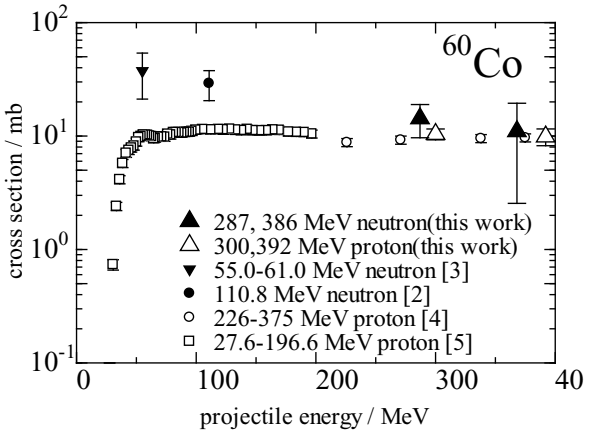

Figure 1. Excitation function for ^{nat}Cu (n, x) ^{60}Co and ^{nat}Cu (p, x) ^{60}Co reactions.

[1] K. Ninomiya et. al., *Proc. Radiochim. Acta*., **1**, 123 (2011)
[2] J. M. Sisterson et. al., *Nucl. Instrum. Meth*., **B240**, 617 (2005)
[3] E. J. Kim et. al., *Nucl. Sci. Technol*., **36**, 29 (1999)
[4] Th. Shiekel et. al., *Nucl. Instrum. Meth*., **B114**, 91 (1996)
[5] S. J. Mills et. al., *Appl. Radiat. Isot.*, **43**, 1019 (1992)

APSORC'13 - 5th Asia-Pacific Symposium on Radiochemistry
Kanazawa, Japan, 22-27 September 2013

Development of a rapid solvent extraction technique with flow injection analysis for superheavy element chemistry

T. Koyama[1], N. Goto[1], M. Murakami[1,2], K. Ooe[1], H. Haba[2], J. Kaneya[2], S. Goto[1], and H. Kudo[1],
[1]Department of Chemistry, Faculty of Science, Niigata University, Niigata 950-2181, Japan
[2]Nishina Center for Accelerator-Based Science, RIKEN, Saitama 351-0198, Japan

Abstract –A rapid solvent extraction system with flow injection analysis based on microchip chemistry was developed to study chemical properties of superheavy elements. Using this system, solvent extraction experiments of ^{95g}Nb were performed as model experiments of element 105, dubnium. The extraction equilibrium of Nb was reached in approximately 2 s. For on-line liquid-liquid phase separation, a phase separator was also developed by use of a membrane filter.

Keywords – microchip, flow injection analysis, liquid-liquid extraction, niobium, phase separation

I. INTRODUCTION

For the chemical investigation of superheavy elements with atomic numbers ≥ 104, a rapid chemical separation apparatus is needed because of their extremely short half-lives. As a rapid chemistry apparatus, we developed a solvent extraction system with flow injection analysis (FIA) based on microchip chemistry. This FIA system consists of solvent extraction and phase separation parts. In the solvent extraction part, aqueous and organic phases are mixed in a tube with a very small inner diameter of 100-200 μm. Because of a large specific interfacial area and a short diffusion length in the tube, chemical equilibrium is rapidly reached. In the phase separation part, on-line liquid-liquid phase separation is achieved with a hydrophobic Teflon membrane. In this work, solvent extraction of 35-d ^{95g}Nb with this system was investigated as a model experiment of element 105, dubnium. The performance of the membrane phase separator was also investigated separately.

II. EXPERIMENTAL

The ^{95g}Nb tracer was produced in the bombardment of a ^{nat}Zr target foil with a 14-MeV proton beam supplied by the RIKEN AVF cyclotron. The carrier-free ^{95g}Nb tracer was prepared by the chemical separation from the target using anion-exchange technique[1].

A schematic view of the FIA system is shown in Figure 1. Aqueous and organic solutions introduced in each reservoir coils were pumped with double-plunger pumps, and mixed in T-connector. As aqueous and organic solutions, 5 M HCl solution containing ^{95g}Nb tracer and 0.1 M Aliquat 336 in 1,2-dichloroethane solution were used, respectively. The mixture was fed into the extraction coil of poly(tetrafluoroethylene) (PTFE) tube of 0.17 mm i.d..

In order to examine the time needed for the extraction equilibrium, a flow rate and an extraction coil length were independently varied. After extraction, both solutions were collected in a polypropylene tube and two phases were separated by centrifugation. The separated two phases were then subjected to γ-ray spectrometry using a Ge detector. A batch extraction experiment of ^{95g}Nb using the same solutions was also performed to compare with these using FIA system.

Two phase separation experiment with the membrane phase separator was performed without radiotracers. The flow rate was 0.5 mL/min, and the length of extraction coil was 1 m. The phase separation was checked by weighing the separated solutions varying backpressure coil length in the aqueous outlet (0.17 mm i.d.). The length of outlet tube for organic phase was 10 cm.

III. RESULTS AND DISCUSSION

In the batch experiment, shaking time of 40 min was needed to attain the extraction equilibrium. On the other hand, the equilibrium was reached within the contact time of 2 s using the FIA system.

In the two phase separation experiment, a clear phase separation was observed with back pressure coil length of about 5-15 cm. And the separator withstood 6 h continuous operation without replaining a membrane.

Therefore, this FIA system can be used for the solvent extraction experiments of superheavy elements with half-lives of several tens of seconds.

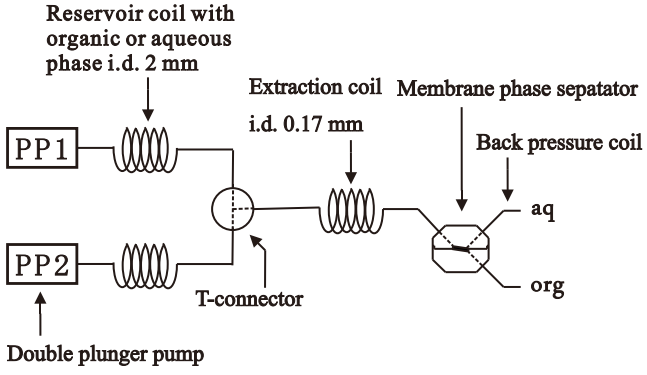

Figure 1. Schematic view of the FIA system

[1] Y.Kasamatsu et al, J. Nucl. Radiochem. Sci. **8**, 69 (2007).

Solid-liquid extraction of Mo and W by Aliquat 336 from HF and HCl solutions towards extraction chromatography experiments of Sg

Y. Komori[1], T. Yokokita[1], K. Toyomura[1], K. Nakamura[1], Y. Kasamatsu[1], H. Haba[2], J. Kanaya[2], M. Huang[2], Y. Kudou[2], A. Toyoshima[3], N. Takahashi[1], A. Shinohara[1]
[1]Graduate School of Science, Osaka University
[2]Nishina Center for Accelerator-Based Science, RIKEN
[3]Advanced Science Research Center, Japan Atomic Energy Agency

Abstract –We are aiming to investigate complex formation properties of Sg with fluoride and chloride ions by extraction chromatography from HF and HCl solutions. We have selected Aliquat 336 as an extractant for anionic species in aqueous solution. In this study, solid-liquid extraction behaviors of carrier-free radiotracers Mo and W on Aliquat 336-loaded resin from 1–10 M HF and 0.1–10 M HCl solutions were investigated.

Keywords – Superheavy elements, Seaborgium (Sg), Molybdenum, Tungsten, Solid-liquid extraction

Element 106, seaborgium (Sg) is a group-6 element and the most stable oxidation state of Sg in aqueous solution is expected to be 6+ as with its lighter homologues, molybdenum (Mo) and tungsten (W). The pioneering aqueous chemical studies on complex formation and hydrolysis of Sg were carried out by Schädel et al. with cation-exchange chromatography in 5×10^{-4} M HF/0.1 M HNO_3 [1] and in HNO_3 [2] using a liquid chromatography apparatus, ARCA [3]. However, there are no reports on aqueous chemical studies of Sg following these works. It is extremely difficult to perform chemical experiments of Sg due to its low production rates and short half-lives of the isotope $^{265}Sg^{a,b}$ ($T_{1/2}$ = 8.5 s/14.4 s [4]). To progress chemical studies of Sg, it is important to search for experimental systems and conditions applicable to the Sg experiment.

We are aiming to investigate complex formation properties of Sg with fluoride and chloride ions by extraction chromatography from HF and HCl solutions using ARCA. We have selected Aliquat 336 as an extractant for anionic species in aqueous solution. In this study, we have investigated solid-liquid extraction behaviors of carrier-free radiotracers Mo and W on Aliquat 336-loaded resin (Aliquat 336/CHP20Y resin) from 1–10 M HF and 0.1–10 M HCl solutions by a batch method. Extraction reaction kinetics was investigated and distribution coefficients (K_d) of Mo and W were obtained as functions of HF and HCl concentrations. Extraction chromatography with ARCA was also performed in 2–8 M HCl solutions.

The short-lived isotopes ^{90}Mo ($T_{1/2}$ = 5.7 h) and ^{173}W ($T_{1/2}$ = 7.6 min) were produced using the RIKEN K70 AVF cyclotron. The K_d values of ^{90}Mo and ^{173}W were obtained as functions of HF and HCl concentrations by a batch method. Reaction products transported by the He/KCl gas-jet system were deposited on a Naflon sheet for 1 or 5 min. The collected reaction products were dissolved in 240 μL of 0.1–10 M HCl (or 1–10 M HF) solutions. A 10–20 mg of 51.9-wt.% Aliquat 336/CHP20Y resin, 100 μL of the HCl (or HF) solution containing ^{90}Mo and ^{173}W, 400 μL of a certain concentration of HCl (or HF) solution were mixed in a PP tube. These samples were shaken for 5 min at 25 ºC. Standard samples of ^{90}Mo and ^{173}W which contained no resin were also prepared and were shaken together with the resin-containing samples. After centrifugation, the aqueous phase was pipetted into another PP tube which was subjected to γ-ray spectrometry using a Ge detector to determine radioactivities of ^{90}Mo and ^{173}W. Reaction kinetics was also investigated at 25 ºC by varying the shaking time to be 10 s, 5 min, and 10 min in each 4 M HF and 2, 6, and 10 M HCl solution. These batch solid-liquid extractions were also performed using the isotopes ^{93m}Mo ($T_{1/2}$ = 6.9 h) and ^{181}W ($T_{1/2}$ = 121 d).

The on-line extraction chromatography of Mo and W was performed with ARCA. The 51.9-wt.% Aliquat 336/CHP20Y resin was filled into the 1.0 mm i.d. × 3.5 mm microcolumn of ARCA. The reaction products transported by the gas-jet system were deposited on the collection site of ARCA for 5 min. After the collection, the reaction products attached to the KCl aerosols were dissolved with 2, 4, 6, and 8 M HCl solutions and were subsequently fed onto the column at a flow rate of 1 mL/min for 30 s. The effluents were collected in PP tubes for every 50 or 80 μL. Then, the remaining ^{90}Mo and ^{173}W in the column were eluted with 400–500 μL of 6 M HNO_3/0.01 M HF solution and were collected in another PP tube. These fractions of the effluents were assayed by γ-ray spectrometry with a Ge detector.

It was found that extraction reaction kinetics in 4 M HF and 6 and 10 M HCl solutions is fast enough to reach the equilibrium state within approximately 10 s. In the extraction chromatography of Mo and W in 2–8 M HCl solutions with ARCA, the order of extractability was Mo > W, which is consistent with the of order of the K_d values obtained in the batch experiment.

[1] M. Schädel et al., Radiochim. Acta **77**, 149 (1997).
[2] M. Schädel et al., Radiochim. Acta **83**, 163 (1998).
[3] M. Schädel et al., Radiochim. Acta **48**, 171 (1989).
[4] H. Haba et al., Phys. Rev. C **85**, 024611 (2012).

APSORC'13 - 5th Asia-Pacific Symposium on Radiochemistry
Kanazawa, Japan, 22-27 September 2013

Off-line isothermal gas chromatography of Zr and Hf compounds

Y.Oshimi, S.Goto, T.Taguchi, T.Tomitsuka, K.Ooe, H.Kudo
Department of Chemistry, Faculty of Science, Niigata University, Niigata 950-2181, Japan

Abstract –We obtained isothermal chromatographic data of Zr and Hf chlorides in a macro-scale (about 10^{18} molecules). The adsorption enthalpies(ΔH_a) of the Zr and Hf chlorides on a quartz surface were determined to be about –78 kJ/mol and –73 kJ/mol, respectively, with analyzing these retention curves. The present ΔH_a values are very different from the earlier work[1] in micro-scale, but agree with the volatility deduced from the vapor pressure in macro-scale.

Keywords – isothermal gas chromatography, zirconium and hafnium, adsorption enthalpy

I. INTRODUCTION

Gas-phase chemical separation is one of the most utilized method to study chemical properties of superheavy elements. Using this method, adsorption enthalpies (ΔH_a) of volatile compounds of these elements can be determined based on their adsorption-desorption processes on a column surface. To clarify chemical property of element 104, Rf, gas chromatographic behavior of chlorides of Rf and its homologs, Zr and Hf, has been studied in the single-atom scale[1]. The reported sequence of volatility was Zr ≳ Rf > Hf. But this volatile relation between Zr and Hf chlorides differ from volatile sequence requested from the macro-scale these vapor pressure curves[2]. Appropriate explanation about this difference has not been given until now.

In this study, we investigated gas chromatographic behavior of volatile compounds which were formed with thermal decomposition of oxychlorides of Zr and Hf.

II. EXPERIMENTAL

In this work, stable isotopes of Zr and Hf were used to confirm whether the experimental technique is suitable before the experiments under tracer scale. Schematic view of the experimental equipment is shown Fig. 1. Quartz wool was impregnated with 80 μL of $ZrOCl_2$ or $HfOCl_2$ water solution containing about 2240 μg of Zr or Hf, and dried at 200 °C. After drying, the wool was mounted in the reaction part which is composed of a quartz tube. Because the deposited oxychloride may be hydrate, the reaction part was heated at 210 °C to remove hydration water completely. Then, heating the reaction part at above 400 °C, the oxychlorides decomposed into nonvolatile dioxide and volatile tetrachloride, for example,

$$2HfOCl_2 \rightarrow HfO_2 + HfCl_4.$$

The produced tetrachloride was fed into an isothermal chromatographic quartz column with He gas (1.0 L/min, purity ≳ 99.999 %). The tetrachloride compounds of Zr and Hf through the column were collected in quartz wool plugged in a quartz tube connected just behind the column. An absorption photometry using arsenazo III was applied to determine the quantity of collected Zr and Hf.

III. RESULT AND DISCUSSION

The passed-through yields for Zr and Hf were obtained as a function of the temperature of the isothermal column. Adsorption enthalpies were calculated using a simulation which is generally used in gas phase chemistry[3] and taken into account the fact that thermal decomposition reaction of the oxychlorides takes time. Adsorption enthalpies(ΔH_a) on a quartz surface for the Zr and Hf chlorides were obtained about –78 kJ/mol and –73 kJ/mol, respectively. The present ΔH_a values for Hf are very different from the previously reported values. This result is consistent with the fact that $HfCl_4$ is more volatile than $ZrCl_4$. Our results agree with the volatility deduced from the vapor pressure. Hence, there is some possibility that the Hf compound observed in the previous work was not pure tetrachloride.

In the symposium, the experiments and the results will be presented in more detail.

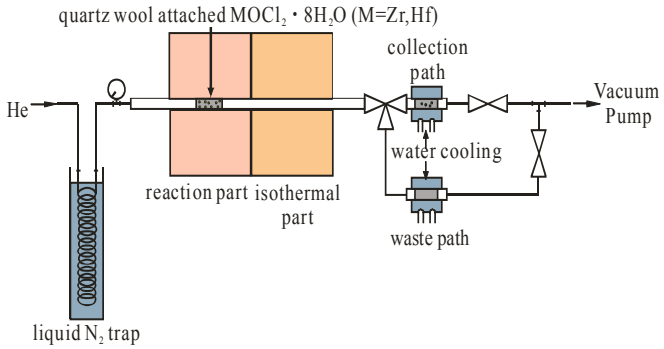

Fig.1. schematic views of the experimental equipment

[1] B. Kadkhodayan *et al.*, *Radiochim. Acta* **72**, 169 (1996)
[2] A. Türler *et al.*, *J. Alloys Comp* **271**, 287 (1998)
[3] I. Zvara, *Radiochim. Acta* **38**, 95 (1985).

Chemical studies of Rf and Db in liquid-phases using automated rapid chemical separation apparatuses at JAEA

K. Tsukada[1], A. Toyoshima[1], M. Asai[1], Y. Kasamatsu[2], Z. J. Li[3], Y. Ishii[1], H. Haba[4], T. K. Sato[1], Y. Nagame[1], M. Schädel[1]

[1] Japan Atomic Energy Agency, Tokai, Ibaraki 319-1195, Japan
[2] Graduate School of Science, Osaka University, Toyonaka, Osaka 560-0043, Japan
[3] Institute of High Energy Physics, Chinese Academy of Science, China
[4] Nishina Center for Accelerator Based Science, RIKEN, Wako, Saitama 351-0198, Japan

Abstract – We present chemical studies of element 104, rutherfordium (Rf), and element 105, dubnium (Db), in liquid-phases at JAEA. The experiments based on an atom-at-a-time scale have been performed using an automated rapid ion-exchange separation apparatuses, AIDA and AIDA-II. We have found interesting information for the complex formations of Rf with chloride, nitrate, sulfate, and fluoride ions and Db with fluoride ions in aqueous solutions.

Keywords – Superheavy elements, Ratherfordium, Dubnium, Ion-exchange separation, Complex formation with chloride, nitrate, sulfate and fluoride, Automated apparatus

I. INTRODUCTION

Chemical studies of the superheavy elements are extremely challenging subjects in the fields of nuclear and radiochemistry [1]. An interesting aspect is to clarify basic chemical properties of these elements, such as ionic radii, complex formation and so on, and to elucidate the influence of relativistic effects on valence electrons of the superheavy elements [2]. The superheavy elements produced in heavy-ion-induced nuclear reactions at accelerators with low production rates. As the available isotopes are short-lived, they are usually available in quantities of only a few atoms at a time. Chemical characterization of the superheavy elements in liquid-phase experiments is performed by a partition method with single atoms. In order to have statistically significant results, it needs to repeat same experimental procedures over several hundred times within a cyclic time of a life-time of objective nuclides. In JAEA we have developed automated rapid chemical separation apparatuses to study chemical properties of Rf and Db in liquid-phases.

II. EXPERIMENTAL

The nuclides ^{261}Rf ($T_{1/2}$ = 78 s) and ^{262}Db ($T_{1/2}$ = 34 s) were produced in the reactions ^{248}Cm(^{18}O, 5*n*) and ^{248}Cm(^{19}F, 5*n*), respectively, at the JAEA tandem accelerator. For characterization of Rf, we conducted cyclic discontinuous column chromatographic separations of short-lived nuclides in aqueous solutions and automated detection of α-particles within a typical cycle of 1 min using the automated rapid ion-exchange separation apparatus AIDA (Automated Ion-exchange separation apparatus coupled with the Detection system for Alpha spectroscopy) [3] that consists of a modified computer-controlled liquid chromatography system ARCA (Automated Rapid Chemistry Apparatus) [4] and an automated on-line α-particle detection system. The experimental approach involves comparative studies on the chemical properties of the superheavy elements with those of respective lighter homologues and a pseudo-homologue. Thus, the experiments should be conducted together with the lighter homologues under identical conditions. To shorten the time for the sample preparation, the newly developed rapid ion-exchange apparatus AIDA-II was introduced. The apparatus is based on continuous sample collection and evaporation of effluents, and successive α-particle measurement. The ion-exchange part is the same as that of AIDA. The AIDA-II was successfully applied for the chemical experiments with Db.

III. RESULTS

We have investigated the ion-exchange chromatographic behaviors of Rf in HCl, HNO_3, H_2SO_4/HNO_3, HF/HNO_3 and HF solutions [3,5-10]. It has been found that the chemical properties of Rf are quite similar to those of the group-4 homologues, Zr and Hf, in the formation of chloride, nitrate, and sulfate complexes, although there are some differences in complexation strength between Rf and the lighter homologues [3,5,6]. In contrast, fluoride complex formation of Rf was found to be remarkably weaker than those of Zr and Hf studied over a wide range of fluoride ion concentrations [7,8]. The formation constant of $[RfF_6]^{2-}$ was observed to be at least one order of magnitude smaller than those of $[ZrF_6]^{2-}$ and $[HfF_6]^{2-}$ [5]. This result on the fluoride complexation is in agreement with theoretical calculations including relativistic effects.

Anionic fluoride complexation of Db has also been studied [9,10]. The result demonstrates that the fluoride complex formation of Db is considerably different from that of the group-5 homologue Ta, while the behavior of Db is similar to that of the lighter homologue Nb [10].

[1] M. Schädel (ed), The Chemistry of Superheavy Elements, Kluwer Academic Publishers, Dordrecht (2003).
[2] Pyykkö P, Chem. Rev .88, 563 (1988).
[3] Y. Nagame *et al*., J. Nucl. Radiochem. Sci. 3, 85 (2002).
[4] M. Schädel *et al*., Radiochim. Acta 48, 171(1989).
[5] Y. Ishii *et al*., Chem. Lett. 37, 288-289 (2008).
[6] Z. J. Li *et al*., Radiochim. Acta 100, 157 (2012).
[7] H. Haba *et al*., J. Am. Chem. Soc. 126, 5219 (2004).
[8] A. Toyoshima *et al*., Radiochim. Acta 96, 125-134 (2008).
[9] K. Tsukada *et al*., Radiochim. Acta 97, 83 (2009).
[10] Y. Kasamatsu *et al*., Chem. Lett. 38, 1084 (2009)

APSORC'13 - 5th Asia-Pacific Symposium on Radiochemistry
Kanazawa, Japan, 22-27 September 2013

Solvent extraction of hexavalent Mo and W using 4-isopropyltropolone (Hinokitiol) for Seaborgium (Sg) reduction experiment

S. Miyashita[1], A. Toyoshima[1], K. Ooe[2], M. Asai[1], T. K. Sato[1], K. Tsukada[1], Y. Nagame[1], M. Schädel[1], Y. Kaneya[3], H. Haba[4], J. Kanaya[4], M. Huang[4], Y. Kitayama[5], A. Yokoyama[5], A. Wada[6], Y. Oura[6] J. V. Kratz[7], H. V. Lerum[8] and J. P. Omtvedt[8]

[1] Advanced Science Research Center, Japan Atomic Energy Agency, Tokai, Ibaraki 319-1195, Japan
[2] Institute of Science and Technology, Niigata University, Niigata 950-2181, Japan
[3] Graduate School of Science and Engineering, Ibaraki University, Mito, Ibaraki 310-8512, Japan
[4] Nishina Center for Accelerator-Based Science, RIKEN, Wako, Saitama 351-0198, Japan
[5] College and Institute of Science and Engineering, Kanazawa University, Kanazawa 920-1192, Japan
[6] Graduate School of Science and Engineering, Tokyo Metropolitan University, Hachioji, Tokyo 192-0397, Japan
[7] Institut für Kernchemie, Universität Mainz, 55128 Mainz, Germany
[8] Department of Chemistry, University of Oslo, P.O. Box 1033 - Blindern, NO-0315, Oslo, Norway

Abstract – Solvent extraction of ^{93m}Mo and ^{176}W using 4-isopropyltropolone (Hinokitiol, HT) was investigated. Extraction mechanism of Mo and W with HT was examined by slope analysis. The slopse of the distribution ratio of Mo and W vs. [HT] in logarithmic scale are 1.88 and 1.54, respectively.
Keywords – Superheavy elements, Solvent extraction, Hinokitiol, Molybdenum, Tungsten, Seaborgium

I. INTRODUCTION

For the determination of the reduction potentials of Seaborgium (Sg), we plan to carry out reduction experiments using a rapid and continuous system consisting of a flow electrolytic column (FEC) [1] combined with the liquid-liquid extraction apparatus SISAK [2]. The oxidation states of Sg will be chemically characterized its extraction behavior, and thus, rapid extraction enabling separation of Sg with different oxidation states is required. From our results of extraction-kinetics studies of ^{181}W as lighter homologue of Sg into toluene containing several extractants from 0.1 M HCl, we found that 4-isopropyltropolone (Hinokitiol, HT) has fast kinetics enough to be used together with SISAK. In the work presented here, we examined the extraction with HT of ^{93m}Mo ($T_{1/2}$ = 6.9 h) and ^{176}W ($T_{1/2}$ = 2.5 h) from a mixed solution 1.0 M HCl and 1.0 M LiCl solution.

II. EXPERIMENTAL

^{93m}Mo and ^{176}W were produced in the ^{89}Y(^{7}Li, 3n)^{93m}Mo and ^{175}Lu(^{7}Li, 6n)^{176}W reactions, respectively. ^{89}Y metallic foil and $^{nat}Lu_2O_3$ on Be foil were irradiated by a 62 MeV ^{7}Li beam from a tandem accelerator in JAEA. Reaction products recoiling out of the target foils were transported with a He/KCl gas-jet to the chemistry laboratory. Transported products were collected on a PTFE sheet, and dissolved by a mixed solution of 1.0 M HCl and 1.0 M LiCl. Then, a hydrogen ion concentration of solution was adjusted to desired ones. An organic phase was toluene containing a certain concentration of HT. 700 μL of each aqueous and organic phase was mixed in a vial and shaken for 600 s using a mechanical shaker. After shaking, two phases were separated by centrifugation for 30 s. 500 μL of each aqueous and organic phase was taken into the vials. Radioactivity of both phases, 263 keV γ-rays of ^{93m}Mo and 102 keV γ-rays of ^{176}W, was detected by a Ge-detector. The distribution ratio (D) was calculated by the ratio of radioactivity of ^{93m}Mo and ^{176}W in the two phases.

III. RESULT AND DISCUSSION

Figure 1 show that the variation of the D value of Mo and W with respect to the concentration of HT in the organic phase ([HT]) when the concentration of hydrogen ion in the aqueous phase was 0.1 M. The D value of Mo and W increased by increasing of [HT]. The slopes of the D value of Mo and W vs. [HT] in logarithmic scale are 1.88 and 1.54, respectively. Those results indicated that Mo is formed an extractable complex with two HT molecules and W is one and/or two molecules.

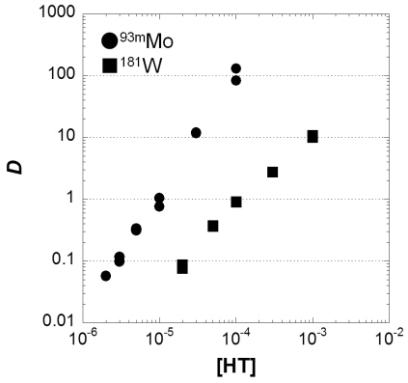

Figure 1. Variation of the distribution ratio of Mo and W vs. the concentration of HT in the organic phase when aqueous phase was 0.1 M HCl / 0.9 M LiCl. Closed cycles and squares represent Mo and W, respectively.

[1] A. Toyoshima et al., *Radiochim. Acta,* **2008**, *96*, 323
[2] J. P. Omtvedt et al., *Eur. Phys. J. D,* **2007**, *45*, 91

Development of Surface Ionization Ion-source for Determination of the First Ionization Potentials of Heavy Actinides

Y. Kaneya[1,2], T. K. Sato[2], M. Asai[2], K. Tsukada[2], A. Toyoshima[2], S. Miyashita[2], Y. Nagame[1,2], M. Schädel[2], N. Sato[3], K. Ooe[4], A. Osa[5], S. Ichikawa[2,6], T. Stora[7], J. V. Kratz[8]
[1]Graduate School of Science and Engineering, Ibaraki University, Mito, Ibaraki 310-8512, Japan
[2]Advanced Science Research Center, Japan Atomic Energy Agency, Tokai, Ibaraki 319-1195, Japan
[3]Nuclear Science and Engineering Directorate, Japan Atomic Energy Agency, Tokai, Ibaraki 319-1195, Japan
[4]Institute of Science and Technology, Niigata University, Niigata 950-2181, Japan
[5]Department of Research Reactor and Tandem Accelerator, Japan Atomic Energy Agency, Tokai, Ibaraki 319-1195, Japan
[6]Nishina Center for Accelerator Based Science, RIKEN, Wako, Saitama 351-0198, Japan
[7]ISOLDE, CERN, CH-1211 Geneva 23, Switzerland
[8]Institut für Kernchemie, Universität Mainz, 55128 Mainz, Germany

Abstract – We have developed a surface ionization ion-source as part of the JAEA-ISOL that is coupled to a He/CdI_2 gas-jet transport system to determine the first ionization potential (IP) of heavy actinides. Separation efficiencies of various short-lived lanthanide isotopes as homologs of actinides that were produced in nuclear reactions were measured with the present system. Obtained results demonstrate that the developed ion-source would be applicable to a measurement of the IP of heavy actinides.

Keywords – ionization potential ; lanthanide ; surface ionization ; ISOL

I. INTRODUCTION

The first ionization potential (IP) directly reflects an atomic valence state influenced by relativistic effects which are significantly noticeable for heavy elements. Therefore information on the IP of heavy elements give us a better understanding of relativistic effects. IPs of the heavy actinides, however, have not been measured because of their short half-lives and low reaction cross-sections. In order to measure the IP of the heavy actinides, we need an apparatus which has higher separation efficiency.

In our previous work, we utilized a surface ionization ion-source coupled to a gas-jet transport system to study nuclear decay properties and spectroscopy of short-lived lanthanides and actinides [1]. Then, have improved the ion-source to measure the IP of lawrencium (Lr, Z = 103) and other heavy actinides [2]. In this work, to evaluate a performance of the developed ion-source, we measured separation efficiencies of various short-lived lanthanide isotopes as homologs of actinides.

II. EXPERIMENTAL

Short-lived lanthanide isotopes, ^{140m}Pm, ^{142m}Eu, ^{143}Eu, ^{143m}Sm, ^{148m}Tb, ^{154}Ho, ^{157}Er, and ^{165}Yb, were produced in the irradiation of a 67.9 MeV $^{11}B^{4+}$ beam from the JAEA tandem accelerator on ^{136}Ce / ^{141}Pr / ^{159}Tb and ^{142}Nd / ^{147}Sm / ^{nat}Eu targets. Short-lived ^{168}Lu was also produced in the reaction of ^{162}Dy with a $^{11}B^{4+}$ beam. Nuclear reaction products recoiling from the targets were transported to the ion-source by a He/CdI_2 gas-jet transport system. The products were ionized in the ion-source, accelerated with 30 kV, mass-separated at mass-separator in ISOL, and collected on the aluminized Mylar tape. The amounts of ions were determined by γ–ray measurement with a HP-Ge detector. To calculate separation efficiencies, nuclear reaction products transported from a target recoil chamber were directly collected on a separate catcher system.

III. RESULTS AND DISCUSSION

Separation efficiencies of various short-lived lanthanide isotopes were measured. We compared the efficiencies obtained by the developed ion-source with those the previous ion-source. It is clearly found that the yields of all the isotopes with the developed ion-source are larger than those with the previous one. The separation efficiency of Sm, for example, was 12% with the developed ion-source while that with the previous ion-source was 3%. Furthermore, separation efficiency of Lu whose volatility would be similar to that of Lr was about 4.2%.

From this result, the present system has sufficient separation efficiencies to apply to measurement of the IP of the heavy actinides.

[1] S. Ichikawa, et al. Nucl. Instr. and Meth. A **374** (1996) 330.
[2] T. K. Sato, et al. Rev. Sci. Instrum. **84** (2013) 023304

Comparison of the decay constants of ^{51}Cr with various valence states

H. Kikunaga[1], K. Takamiya[2], K. Hirose[1*], and T. Otsuki[1]
[1]Research Center for Electron Photon Science, Tohoku University
[2]Research Reactor Institute, Kyoto University
[*]Present address: Advanced Science Research Center, Japan Atomic Energy Agency

Abstract – We have precisely measured the decay constants of ^{51}Cr with 0, +3, and +6 valence states to investigate the effects of chemical states on the decay constants of ^{51}Cr. The value of $\{\lambda(Cr^{6+})-\lambda(Cr^0)\}/\lambda(Cr^0)$ was determined to be $(5.3\pm2.2)\times10^{-4}$, whereas the difference less than 1.4×10^{-4} was observed for $\{\lambda(Cr^{3+})-\lambda(Cr^0)\}/\lambda(Cr^0)$. The results are compared with theoretical estimated values calculated with a simple model.

Keywords – half-life, decay constant, chemical effect

I. INTRODUCTION

The decay constants of more than ten nuclides from ^{7}Be to ^{235}U^{m} were changed with changing environmental factors such as its chemical state [1]. Kakiuchi and Mukoyama reported the change in the decay constant of an electron capture decay nuclide ^{51}Cr was observed between two chemical forms of $CrCl_3$ and Na_2CrO_4 [2]. They also estimated the value for the relative change in the decay constant among 0, +3, and +6 valence states with a simple theoretical model. The estimation shows that the relative change in the decay constant between 0 and +3 state is in the same degree as that between +3 and +6 state. In this study, the decay constants of ^{51}Cr have been precisely measured with 0, +3, and +6 valence states to investigate the effects of chemical states on the decay constants of ^{51}Cr.

II. EXPERIMENTAL

The decay constants of ^{51}Cr were measured for three chemical forms: chromium metal (Cr^0), chromium (III) oxide Cr_2O_3 (Cr^{3+}), and potassium chromate K_2CrO_4 (Cr^{6+}). The isotopes ^{51}Cr was produced in the ^{nat}Cr(γ, xn)^{51}Cr reactions. Target materials were about 100 mg of Cr metal, Cr_2O_3, and potassium dichromate $K_2Cr_2O_7$. Each target material was sealed in a quartz tube and irradiated with bremsstrahlung photons. The irradiation was carried out with the electron linear accelerator at Tohoku University. The accelerator was operated at an electron energy of 30 MeV with a mean current of around 0.12 mA during the 8 h irradiation.

After the irradiation, the metal target and the Cr_2O_3 target was maintained at 800°C for 5 h in argon and atmosphere, respectively, with an electric furnace. The $K_2Cr_2O_7$ target irradiated was mixed into 250 mg of a non-radioactive $K_2Cr_2O_7$ reagent and then dissolved in 3 mL of distillated water. The solution was heated on a hot-plate and alkalified with potassium carbonate to produce CrO_4^{2-}. The solution was filtered and the filtrate was evaporated to less than 1 mL on a hot-plate. Finally, a K_2CrO_4 sample was prepared by recrystallization from the solution. The metal, Cr_2O_3, and K_2CrO_4 samples were placed in aluminum cups separately and sealed with an epoxy resin adhesive.

These samples were measured in pairs of Cr_2O_3-metal and K_2CrO_4-metal to reduce the influence caused by the difference of detectors. The sample pairs were set in an automated sample changer [3] and alternately placed in front of a high-purity Ge detector at intervals of 7200 s. The procedures were repeated over at least 95 d. A ^{137}Cs source was attached to near the Ge detector as a reference source to correct for influential factors for determination of half-life such as pile-up effect.

III. RESULTS AND DISCUSSION

The decay constant of ^{51}Cr was determined based on a reference source method [4]. The ratio $R(t)$ is given by the following equation:

$$R(t) = C^0_{sample}(t) \Big/ C^0_{ref}(t) \ , \qquad (1)$$

where $C^0_{sample}(t)$ and $C^0_{ref}(t)$ are count rates of a sample and a reference source at the beginning of each data acquisition, respectively. The decay constant of the radionuclide in the sample λ_{sample} is described in the following equation:

$$\lambda_{sample} = \lambda_{ref} - a_{slope} \ , \qquad (2)$$

where a_{slope} is the slope of the graph of ln $R(t)$ against time. λ_{ref} is the decay constant of the reference source, here that of ^{137}Cs.

In the present work, the relative difference in the decay constant of ^{51}Cr, $\{\lambda(Cr^{6+})-\lambda(Cr^0)\}/\lambda(Cr^0)$ was determined to be $(5.3\pm2.2)\times10^{-4}$. On the other hand, the difference less than 1.4×10^{-4} at a 68% confidence level was observed for $\{\lambda(Cr^{3+})-\lambda(Cr^0)\}/\lambda(Cr^0)$. Kakiuchi and Mukoyama reported the value of $(5.3\pm2.1)\times10^{-4}$ for $\{\lambda(Cr^{6+})-\lambda(Cr^{3+})\}/\lambda(Cr^{3+})$ [2], which is in good agreement with the our value of $\{\lambda(Cr^{6+})-\lambda(Cr^0)\}/\lambda(Cr^0)$. In the presentation, we will discuss the comparison between the results obtained and the theoretical estimation with a simple model calculation [2].

[1] G. T. Emery: Ann. Rev. Nucl. Sci. **22**, 165 (1972)
[2] S. Kakiuchi and T. Mukoyama: Bull. Inst. Chem. Res., Kyoto Univ. **59**, 27 (1981)
[3] T. Ohtsuki et al.: Phys. Rev. Lett. **93**, 112501 (2004)
[4] H. Kikunaga et al.: Proc. Radiochim. Acta **1**, 113 (2011)

25-NCP-12

Selective Separation of Strontium (II) from Nitric Acid Solution by a Macroporous Silica-based DtBuCH18C6 Adsorbent Modified with Surfactants

WU Yan, CHEN Zi, WEI Yuezhou*
School of Nuclear Science and Engineering, Shanghai Jiao Tong University, China
* *Corresponding author*. Tel.: +86-21-34207654. *E-mail address:yzwei@sjtu.edu.cn*.

Keywords – Sr(II); silica-based support; crown ether; dodecyl benzenesulfonic acid; adsorption

4',4'(5")-di(*tert*-butylcyclohexano)-18-crown-6 (DtBuCH18C6), a microcyclic crown ether, has the ability to extract Sr(II) due to the effective complexation of Sr(II) with hydrophilic crown ether, and a good match between the cavity of crown ether and ionic radius of Sr(II) ion. The SiO_2-P support is a kind of inorganic material, which is prepared by synthesizing the SDB-copolymer inside the macroporous SiO_2 substrate. In this study, DtBuCH18C6 modified with dodecanol and dodecyl benzenesulfonic acid (DBS) was impregnated onto SiO_2-P ((DtBuCH18C6+ dodecanol + DBS)/SiO_2-P). The equilibrium and kinetics of (DtBuCH18C6 + dodecanol + DBS)/SiO_2-P for adsorption of Sr(II) were investigated under the conditions: varying the shaking times, HNO_3 concentration, and initial concentration of metal ions. The chemical stability of absorbent in HNO_3 medium was examined by measuring the leakage of total organic carbon(TOC) in liquid phase. In order to confirm the effect of surfactant(DBS) on adsorption of Sr(II), the (DtBuCH18C6+ dodecanol)/SiO_2-P are synthesized for comparison. Compared to (DtBuCH18C6 + dodecanol)/SiO_2-P, much higher distribution coefficient (K_d) for (DtBuCH18C6+ dodecanol + DBS)/SiO_2-P was obtained in the range of 0.5 to 4 M nitric acid. The uptake rate of Sr(II) on (DtBuCH18C6+ dodecanol + DBS)/SiO_2-P in the presence of 0.5 M HNO_3 was attained equilibrium within 1 h, and the relatively large K_d value around 4×10^2 cm^3/g was obtained, which was improved 428 times compared with (DtBuCH18C6+ dodecanol)/SiO_2-P. The adsorbent had almost no uptake for other tested metals such as Cs(I), Na(I), K(I), Pd(II), Ru(III), Y(III), La(III), Nd(III) and Gd(III). The uptake of Sr(II) for (DtBuCH18C6+ dodecanol + DBS)/SiO_2-P was explained by Langmuir adsorption equation and the saturated amount of adsorption was estimated to be 0.24 mmol/g in 0.5 M HNO_3. The leakage of TOC from the (DtBuCH18C6+ dodecanol + DBS)/SiO_2-P into aqueous phase were below 95 ppm even in 4 M HNO_3. These findings suggest that the (DtBuCH18C6+ dodecanol + DBS)/SiO_2-P are stable in HNO_3 solution and would be effective for the selective separation of Sr(II) from radioactive liquid waste.

Exploring the Synthesis and Characterization of Binary Technetium Chlorides and Bromides

Erik Johnstone[1], Frederic Poineau[1], Paul M. Forster[1], Phillippe Weck,[2] Christos D. Malliakas[3], Eunja Kim[4], Mercouri G. Kanatzidis[3], Brian L. Scott[5], Alfred P. Sattelberger[6], and Kenneth R. Czerwinski[1]

[1] Department of Chemistry, University of Nevada Las Vegas, Las Vegas, NV, USA.
[2] Sandia National Laboratories, Albuquerque, NM, USA.
[3] Department of Chemistry, Northwestern University, Evanston, IL, USA
[4] Department of Physics and Astronomy, University of Nevada Las Vegas, Las Vegas, NV,USA
[5] Materials Physics and Applications Division, Los Alamos National Laboratory, Los Alamos, NM, USA
[6] Energy Engineering and Systems Analysis Directorate, Argonne National Laboratory, Lemont, IL, USA.

Keywords –Technetium, solid-state synthesis, binary transition metal halides

Technetium (Z = 43) is the lightest element on the periodic table with no stable isotopes. The most common isotope, ^{99}Tc ($t_{1/2}$ = 2.1 x 10^5 a), is produced in nuclear fuels as a primary fission product in ~6% yield. In comparison to the surrounding stable transition metals, the fundamental chemistry of technetium has been poorly studied. An example of this is the binary halide system, which prior to 2008 consisted of 3 known compounds for technetium (TcF_6, TcF_5, and $TcCl_4$), whereas for rhenium there have been 12 identified.[1] In this work low-valent binary technetium chlorides and bromides were synthesized in the solid state and analyzed using various physicochemical characterization methods including single-crystal and powder X-ray diffraction (XRD), IR spectroscopy, X-ray absorption fine structure (XAFS), and elemental analysis.

A. Binary Technetium Chlorides

Technetium dichloride was synthesized from the stoichiometric reaction of the elements as a novel compound with a new structure-type containing a Tc-Tc triple bond. The α-phase of technetium trichloride was prepared from the reaction of $Tc_2(O_2CCH_3)_4Cl_2$ with passing HCl(g) at elevated temperatures.[3] It is isostructural to $ReCl_3$ with a triangular Tc_3^{9+} core structure containing Tc=Tc bonds. The β-phase of the trichloride was synthesized from the stoichiometric reaction of Tc metal with Cl_2(g) and it exhibits structural characteristics comparable to the trichlorides of ruthenium and molybdenum.[4] Technetium tetrachloride was synthesized from the metal and excess chlorine gas in sealed Pyrex tubes and used as a starting material for decomposition to $TcCl_2$ and $TcCl_3$.[5]

[1] Schwochau, K. Technetium: Chemistry and Radiopharmaceutical Applications; Wiley-VCH: Weinheim, Germany, 2000.
[2] Poineau, F., et. al., *J. Am. Chem. Soc.*, **2010**, *132*, 15864-15865.
[3] Poineau, F., et. al. *J. Am. Chem. Soc.*, **2011**, *133*, 8814-8817.
[4] Poineau, F., et. al. *Inorg. Chem.*, **2012**, *51*, 4915-4917.

B. Binary Technetium Bromides

$TcBr_3$ has been prepared via two different methods: the stoichiometric reaction of the elements in sealed Pyrex tubes or by passing HBr(g) over $Tc_2(O_2CCH_3)_4Cl_2$ at elevated temperatures. Both synthetic methods yield the infinite-chain structure of distorted $TcBr_6$ face-sharing octahedra. Technetium tetrabromide was synthesized from the reaction of Tc metal with excess Br_2(l).[6] It is isostructural to technetium tetrachloride, and similarly decomposes to lower-valent technetium bromides. When performed in Pyrex tubes the decomposition of the tetrabromide yields a novel trigonal prismatic Tc(II) bromide cluster, $Na\{[Tc_6Br_{12}]_2Br\}$.[7]

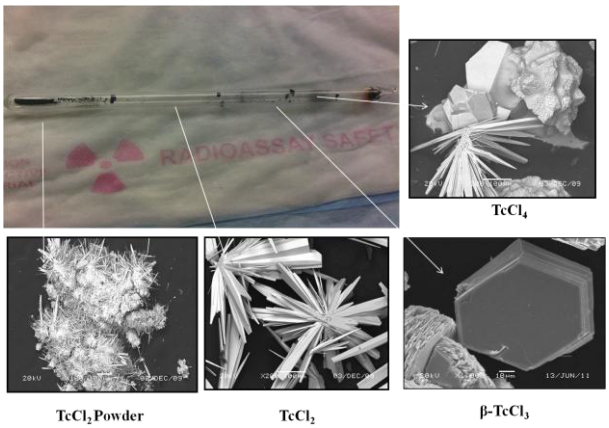

Figure 1. Binary Tc chlorides synthesized from the stoichiometric reaction of Tc metal and elemental chlorine in sealed tubes at elevated temperatures.

The low-valent technetium chlorides and bromides synthesized exhibit interesting chemical and physical properties, and may serve as potential synthetic inorganic and radiopharmaceutical precursors, as well as potential waste form-type material in the nuclear fuel cycle.

[5] Johnstone, E. V., et. al. *Inorg. Chem*. **2012**, *51*, 8462-8467.
[6] Poineau, F., et. al. *J. Am. Chem. Soc.* **2009**, *131*, 910-911.
[7] Johnstone, E. V., et. al., *Inorg. Chem.*, **2013**, *52(10),* 5660-5662.

APSORC'13 - 5th Asia-Pacific Symposium on Radiochemistry
Kanazawa, Japan, 22-27 September 2013

Solvent Extraction of Americium(III) and Europium(III) Using Hydroxyoctanoic Acid and N-heteroaromatic Compound

Moe Seike[1], Mai Eguchi[1], Atsushi Shinohara[1], Takashi Yoshimura[2]
[1]Graduate School of Science, Osaka University
[2]Radioisotope Research Center, Osaka University

*Abstract – Solvent extraction of Am(III) and Eu(III) was investigated using two hydroxyoctanoic acids including a new 2-hydroxy-2-trifluoromethyl-octanoic acid (**L1-CF$_3$**) and two bidentate N-heteroaromatic compounds as extractants. The new lanthanide(III) complexes with bidentate N-heteroaromatic ligands were synthesized and the structures were characterized to eight- or nine-coordinate. Solvent extraction of Am(III) and Eu(III) in 1-octanol/acetic acid buffer solution was performed. The separation factor using **L1-CF$_3$** was about 2.*

Keywords – lanthanides, actinides, extraction, complex

I. INTRODUCTION

It is recognized that separation of trivalent lanthanides and actinides is difficult because of their similar chemical properties. To date, various methods such as chromatography, extraction, and electrophoresis have been investigated. In the present study, we report on solvent extraction using hydroxyoctanoic acids and bidentate N-heterocyclic compounds that have π electron-accepting ability. We synthesized four extractants: two hydroxyoctanoic acids and two bidentate N-heteroaromatic ligands. The crystal structures of lanthanides(III) with bidentate N-heteroaromatic ligands were determined. The solvent extraction of ^{152}Eu and ^{241}Am was performed using hydroxyoctanoic acids and N-heteroaromatic compounds in 1-octanol/acetic acid.

II. EXPERIMENTAL

Figure 1 shows the new 2-hydroxy-2-trifluoromethyl-octanoic acid (**L1-CF$_3$**) and three known compounds, 2-hydroxy-2-methyl-octanoic acid (**L1-CH$_3$**), 3-(2-pyrazinyl)-pyrazole (**L2-pz**), and 2-(1*H*-pyrazole-3-yl)-pyridine (**L2-py**)[1][2]. **L1-CF$_3$** was synthesized by referring to the literature to prepare a hydroxycarboxylic acid with a long alkyl chain[3].

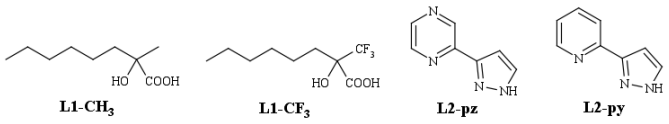

Figure 1. Extractants in this study.

Nineteen new lanthanide(III) complexes with **L2-pz** or **L2-py** were synthesized by the reactions of $[Ln(H_2O)_9](CF_3SO_3)_3$ (Ln = La, Nd, Sm, Eu, Gd, Tb, Dy, Ho, Er, Tm, Yb) with bidentate N-heteroaromatic ligands.

The solvent extraction experiment was performed in the acetic acid buffer solution or nitric acid solution as the aqueous phase and 1-octanol containing the extractant as the organic phase. The tube containing the same volume of two phases were shaken for 24 h in a thermostatic bath at 20 ℃. The distribution ratios (D) of ^{152}Eu and ^{241}Am were determined by gamma-ray measurement of each phase by means of a germanium semi-conductor detector.

III. RESULTS AND DISCUSSION

In the case of **L2-pz**, the three types of structures with eight- or nine-coordinate were obtained by changing the central lanthanide ions. The change of coordination number from nine to eight occurred between Gd and Ho. The eight-coordinate complexes exhibited intramolecular hydrogen bonds between triflate and **L2-pz**. In the case of **L2-py**, the eight-coordinated dinuclear complexes (Ln = Tb – Yb) were afforded.

The D value of 0.60 for Eu and that of 0.50 for Am were obtained at pH 4.8, when **L1-CH$_3$** was used as the extractant. The D values were about 200 times larger than the values without extractant: $D = 3.0\times10^{-3}$ for Eu and $D = 2.2\times10^{-3}$ for Am. When **L1-CH$_3$** and **L2-pz**/**L2-py** were added to the organic phase, the D values were not changed from the values using **L1-CH$_3$** in the pH region of 4 - 5.5. This indicates that synergetic extraction of **L2-pz** and **L2-py** is not shown to be effective in this condition. This may cause that 1-octanol coordinates to Eu and Am to inhibit coordination of bidentate N-heteroaromatic ligands. In the case using only **L1-CF$_3$**, the D value of 2.83 for Eu and that of 1.29 for Am were obtained at pH 5.0. The values are several times larger compared with those using **L1-CH$_3$** under the similar condition. This would be due to decrease of pK_a of extractant by substituting from CH_3 to CF_3 group. Namely, carboxylate proton in **L1-CF$_3$** easily dissociates by the existence of electron-withdrawing CF_3 group. The value of separation factor of Eu and Am was about 2. In the case using **L1-CH$_3$** or **L1-CF$_3$** as the extractant, the log$D$ values were increased with increasing pH. The slope values suggest that two **L1-CH$_3$**/**L1-CF$_3$** coordinate to the metal ions.

[1] T. Yabuuchi, *et al.*, *Chem. Pharm. Bull*., **1999**, *47*, 684-686.
[2] K. L. V. Mann, *et al*., *Polyhedron*, **1999**, *18*, 721-727.
[3] Blay, *et al*., *Tetrahedron*, **2002**, *58*, 8565-8571.

Stability of uranyl peroxo-carbonato complex ions in the presence of metal oxide in carbonate media

Dong-Yong Chung[1], Min-Sung Park[1], Keun-Young Lee[1], Han-Beom Yang[1], Eil-Hee Lee[1], Kwang-Wook Kim[1], Jei-Kwon Moon[1]

[1]Korea Atomic Energy Research Institute, Daedeok-daero 989-111, Yuseong-gu, Daejeon, 305-353, Republic of Korea

Abstract – This work studied the stability of uranyl peroxo carbonato complex ions in a carbonate solution with hydrogen peroxide in the presence of various metal oxides using absorption spectroscopy. The uranyl peroxo carbonato complex ions self-decomposed into uranyl triscarbonato complex ion in the presence of various metal oxides.

Keywords – Uranyl peroxo-carbonato complex, Hydrogen peroxide, Metal oxides, Absorption spectra

I. INTRODUCTION

Uranium is selectively dissolved to form uranyl peroxo-carbonato complex ions, $UO_2(O_2)_x(CO_3)_y^{2-2x-2y}$, with a high solubility in carbonate solutions that contain hydrogen peroxide, H_2O_2. Recently, several carbonate-based processes have been studied and suggested to treat uranium-bearing waste and scraps generated during uranium fuel fabrication, uranium sludge and spent nuclear fuel [1–2]. Hydrogen peroxide is easily decomposed into water and oxygen in aqueous solutions. Additionally, uranyl peroxo-carbonato complex solution can self-decompose into uranyl tris-carbonato complex ions, $UO_2(CO_3)_3^{4-}$, which are stable in a carbonate solution. When a carbonate-based uranium leaching process using hydrogen peroxide is applied to treat uranium-bearing compounds, the stability of the uranium peroxo-carbonato complex ions must be known to ensure that the concentration does not change during prolonged storage [3]. In this study, the decomposition of hydrogen peroxide and the stability characteristics of a uranium peroxo-carbonato complex in a carbonate solution were investigated in the presence of various metal oxides using absorption spectroscopy.

II. RESULTS AND DISCUSSION

A. Decomposition of hydrogen peroxide in the presence of the metal oxides in a carbonate solution

The decomposition of H_2O_2 in the presence of metal oxide follows first-order kinetics. The rate constants for RuO_2, PdO and MoO_2 are 115.1, 15.97 and 0.561 hr^{-1}, respectively. Rate constants of other metal oxides are similar to the value, 0.292 hr-1 of rate constant in a 0.5 M carbonate solution (Fig. 1). The decomposition rate of hydrogen peroxide in the presence of metal oxide powders was almost not affected with metal oxides except RuO_2, PdO and MoO_2.

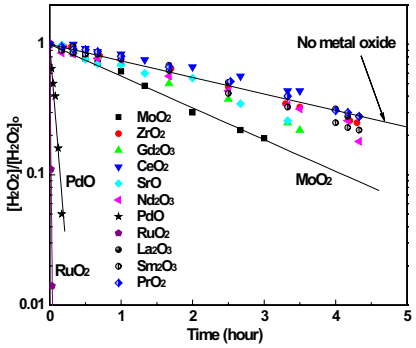

Fig. 1. Change of hydrogen peroxide concentration with time in the presence of each metal oxide at $[Na_2CO_3]$=0.5M, $[H_2O_2]$=1.0M, amount of metal oxide = 0.5 g/L.

B. Stability of uranyl peroxo-carbonato complex ions in the presence of the metal oxides

When the absorbance of the uranyl peroxo-carbonato complex ion solutions were measured in the presence of Ru oxide powder. The features of the absorption spectrum of the uranyl peroxo-carbonato complex solution gradually disappeared with time. The peaks of uranyl tris-carbonato complex appeared at 435, 448, and 462 nm (Fig. 2).

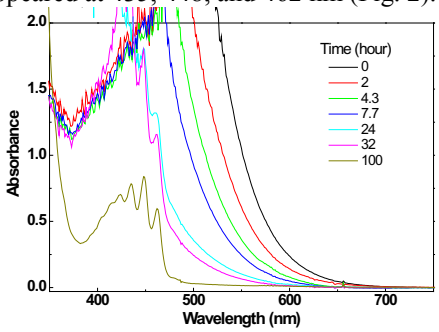

Fig. 2. Variation of asorption spectra of uranium dissolved solution ([U]=3.25x10^{-2} M) in the presence of Ru oxide powder in 0.5M Na_2CO_3 solution (0.02g powder/30ml Na_2CO_3 solution).

ACKNOWLEDGMENT

This work was supported by the National Research Foundation of Korea grant funded by the Korea government (MSIP).

[1] Kim, K.W.; Chung, D.Y; Yang, H.B.; Lim, J.K; Lee, E.H.; Song, K.C.; Song, K-S. *Nucl. Technol.,* **2009**, 166, 170−179.
[2] Chung, D.Y.; Seo, H.S.; Lee, J.W.; Yang, H.B.; Lee, E.H.; Kim, K.W. *J. Radioanal. Nucl. Chem.*, **2010**, 284,123-129.
[3] Kim, K.W.; Lee, K.Y.; Chung, D.Y.; Lee, E.H.; Moon, J.K.; Shin, D.W. *J. Hazardous materials*, **2012**, 233-234, 213-218.

Raman Spectroscopic Study on Uranyl and Neptunyl Complexes in Highly Concentrated Calcium Chloride

Toshiyuki Fujii[1], Akihiro Uehara[1], Yoshihiro Kitatsuji[2], and Hajimu Yamana[1]
[1]Division of Nuclear Engineering Science, Research Reactor Institute, Kyoto University
[2]Nuclear Science and Engineering Directorate, Japan Atomic Energy Agency

Abstract – In order to understand the coordination circumstance of actinyl ions in concentrated inorganic electrolytes, U and Np species in concentrated $CaCl_2$ were analyzed by Raman spectrometry. The ν_1 symmetric vibrational frequency of actinyl ions was found to decrease with the increase of [$CaCl_2$]. This may be attributable that hydration water molecules at the equatorial plane of actynyl were substituted by Cl^- ions.

Keywords – Raman spectrometry, uranyl, neptunyl, calcium chloride, hydrate melt

Calcium chloride hexahydrate, $CaCl_2 \cdot 6H_2O$, possesses a low melting point, 303 K. The melt is identical with 6.9 mol dm^{-3} (M) $CaCl_2$ aqueous solution. The chemical properties of the hydrate melt are considered to be intermediate between aqueous solutions and anhydrous molten salts. A structural study on UO_2^{2+} in 6.9 M $CaCl_2$ by X-ray absorption fine structure (EXAFS) analysis showed that the possible structure is $UO_2Cl_2(H_2O)_2$ [1]. This is distinctly different from the hydrated UO_2^{2+} in diluted acidic solutions, that is, $UO_2(H_2O)_5^{2+}$. The coordination and redox behavior of UO_2^{2+} in 6.9 M $CaCl_2$ has been studied by Raman spectrometry and by using electrochemical methods [2]. A change in the vibrational frequency of symmetrical stretching (ν_1) of UO_2^{2+} suggested that the complexation between U(VI) and Cl^- at the equatorial plane of UO_2^{2+} depresses the bonding strength of U=O.

In the present study, we investigated the ν_1 frequencies of uranyl and neptunyl in highly concentrated calcium chlorides by Raman spectrometry. The ν_1 frequency was also estimated by using *ab initio* methods. The ligand exchange reaction between hydrated water and Cl^- at the equatorial plane is discussed.

Calcium chloride dihydrate, $CaCl_2 \cdot 2H_2O$, of analytical grade (Wako Pure Chemical Industries, Ltd.) was used without purification. Weighed amounts of $CaCl_2 \cdot 2H_2O$ and water were mixed for preparing various concentrations of $CaCl_2$. As a starting material, U_3O_8 was dissolved in 6 M HCl. A nitric acid solution containing Np was also used. A portion of these solutions was once dried by heating and then the $CaCl_2$ solution prepared was added. The concentration of U or Np was 0.01 M. The sample was taken in a quartz cell and the cell was sealed. Electronic absorption spectra of the samples were measured in the wavelength range from 340 to 1350 nm at 0.5 nm intervals by using an UV/Vis/NIR spectrophotometer (Shimadzu, UV-3100PC).

Raman spectra were measured by using a Raman spectrophotometer (NRS-3100, JASCO). A green laser with the wavelength of 531.9 nm was used at the output power of 57.6 mW. The measurement interval of a charge-coupled device (CCD) detector was set to be every 0.3 cm^{-1}. The operations of each 3-seconds measurement were accumulated by 25 times. The experimental temperature was 298 K.

The ν_1 frequency of UO_2^{2+} in 6.8 M $CaCl_2$ was found at ~855 cm^{-1}. This agreed with the literature value [2]. With the decrease of water content in the $CaCl_2$ system, the ν_1 frequency decreased to the extent of ~7 cm^{-1}. This suggests that hydration water molecules at the equatorial plane of uranyl were substituted by Cl^- ions, which depressed the bonding strength of U=O.

The $CaCl_2$ system containing Np showed a specific Raman spectrum. Figure 1 shows the Raman spectrum of 0.01 M Np in 6.8 M $CaCl_2$. From electronic absorption spectrum obtained, it was suggested that Np(VI) and Np(V) coexist in the system. The Raman peaks shown in Fig. 1 are hence attributable to ν_1 vibrational modes of NpO_2^{2+} and NpO_2^+ complexes. Similar to the case of U, the Raman peak at ~835 cm^{-1} shifted by changing water content of the system. This may also suggest that the ligand exchange between hydrated water and Cl^- at the equatorial plane of neptunyl occurrs.

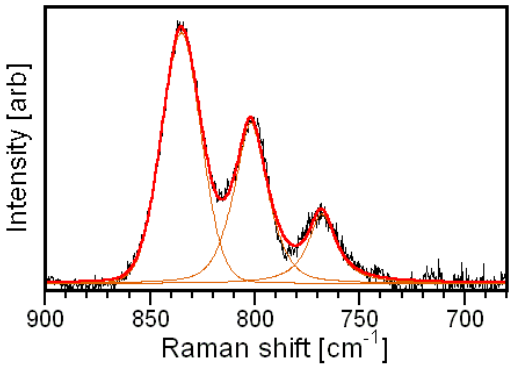

Fig. 1. Raman spectrum of 0.01 M Np in 6.8 M $CaCl_2$. The spectrum was decomposed into three Raman peaks by Gaussian/Lorentzian sum function.

[1] A. Uehara et al., NEA/NSC/DOC (2009) 15.
[2] A. Uehara et al., J. Appl. Electrochem., 42, 455 (2012).

Electrode Reaction of Actinide Ions in a Weak Acidic Solution

Yoshihiro Kitatsuji[1], Haruyoshi Otobe[1], Takaumi Kimura[1]
[1]Nuclear Science and Engineering Directorate, Japan Atomic Energy Agency

Abstract –Electrode reactions of U(VI) in weak acid solution are different from those in acid solution. Electrolysis of U(VI) can produce UO_2 fine crystal, not hydrolyzed U(IV). The formed UO_2 is easily deposited on an electrode and is electrode active.

Keywords – actinide ions, redox, weak acidic solution, aggregate

I. INTRODUCTION

Actinide (An) ions such as uranium, neptunium and plutonium exist as ionic species of trivalent to hexavalent in an aqueous solution. Most of studies concerning redox of actinide ions by electrochemical method have focused on acidic solution in which An ions are dissolving stably. However, redox behaviors of actinide ions in weak acid or neutral solution are expected to be different from that in an acid solution, because redox of AnO_2^+/An^{4+} is affected by H^+. Also hydrolysis has a great influence on the redox. In this paper, the authors report unique electrode reaction of actinide ions concerning an aggregation in a weak acidic solution.

II. EXPERIMENTAL

Voltammetry was carried out by using a microelectrode of Au of 25 μm in diameter. Controlled potential difference electrolysis was performed with an Au gauze electrode (80 mesh, 60 × 20 mm) as working electrode to bulk electrolysis. A Pt wire and a silver-silver chloride electrode with 1 M LiCl was employed as a counter electrode and a reference electrode, respectively.

Oxidation states of actinide ions in sample solutions after electrolysis were identified based on UV/VIS adsorption spectrometry. The aggregate produced in the electrolysis sample solution was analyzed by X-ray diffraction after filtration.

III. RESULTS AND DISCUSSION

Reduction of U(VI) ion in a solution of pH 2 to 5 was investigated by cyclic voltammetry (CV) with an Au microelectrode. Reduction currents of U(VI) to U(V) were observed at ca. −0.2 V clearly(see, Fig. 1, curve a). When CV measurements were repeated, oxidation peak current was observed at +0.2 V in a first cycle of CV for a solution of pH 4. In order to investigate this oxidation current, stripping voltammetry was applied. Clear adsorption current for oxidation of species produced by preelectrolysis at −0.3 V was observed. Similar adsorption behavior at carbon electrode had been reported by Duber previously[1], and they concluded that oxidation current was attributable to oxidation of U(V) adsorbed on the electrode.

U(V) ion was prepared from U(VI) by bulk electrolysis at −0.35 V. U(V) solution showed the peak of absorbance at 260 nm on UV/VIS spectrum. U(V) in a solution of pH 2.9 was stable for about 30 min. Then the peak at 260 nm became smaller, and the absorbance at all range of measurement was increased gradually. These results suggest the formation of aggregate. Only oxidation current of U(V) to U(VI) at −0.2 V was observed (curve b) by CV measurement immediately after preparation of U(V), but CV curve was changed after aggregation (curve c): large oxidation current peak was observed at +0.15 V and +0.3 V in a first cycle of CV measurement; oxidation current of U(V) was negligible; reduction current of U(VI) is about half amount of the initial solution (cf. curves a and c). The aggregate was prepared by electrolysis at −0.35 V in a solution of pH 2.9, and fluorite structure of UO_2 was determined by XRD analysis.

The authors conclude that U(IV) produced via disproportionation of U(V) aggregates to form UO_2. This fine UO_2 is easily deposited on electrode surface and is electrode active to oxidize.

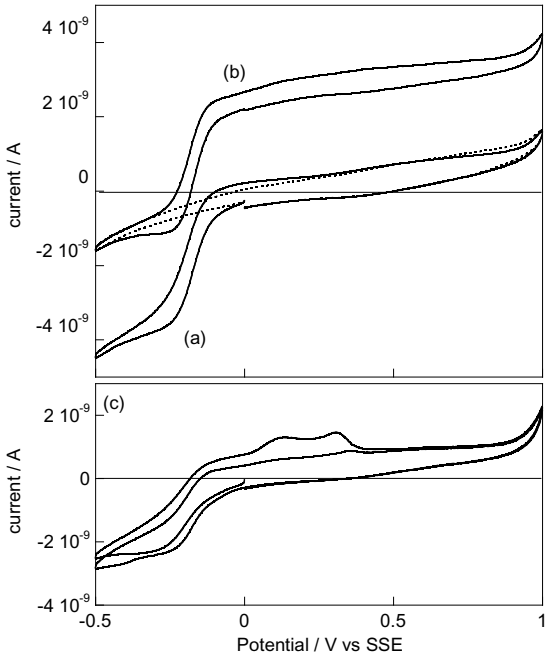

Fig 1. Cyclic voltammograms of 1mM U in a weak acid solution. (a) U(VI), (b) U(V) immediately after preparation, (c) U(V) solution after 60 min. broken line are background current.

REFERENCE

[1] R. E. Dueber, A. M. Bond, P. G. Dickens, J. Electrochem. Soc., 141(1994)311.

Biomineralization of uraninite and uranyl phosphate controlled by organic acids

Yoshinori Suzuki[1], Naofumi Kozai[2], Toshihiko Ohnuki[2]
[1] Graduate School of Bionics, Tokyo University of Technology, 1404-1 Katakura-cho, Hachioji, Tokyo 192-0982, Japan
[2] Advanced Research Center, Japan Atomic Energy Agency, Tokai, Ibaraki 319-1195, Japan

Abstract – Biomineralization of uraninite (UO_2) and uranyl phosphate minerals are both able to decrease the mobility of uranium in the environment. We examined biomineralization of UO_2 and uranyl phosphate by Shewanella putrefaciens in the basic medium containing lactate as an electron donor, β-glycerolphosphate as a phosphorous source, and uranyl nitrate in the absence and presence of weak or strong complexing organic acids (WCOA or SCOA) under an anaerobic condition. In the basic medium, only biomineralization of UO_2 was observed because of rapid reduction of U(VI). Biomineralization of UO_2 and uranyl phosphate occurred in the media with WCOA, however the no biomineralization was occurred in the presence of SCOA. It is thought that formation of stable U(VI)-, and U(IV)-organic complexes prevents the biomineralization. These finding suggest that coexisting organic acids control the biomineralization of UO_2 and uranyl phosphate minerals by microorganisms.

Keywords –biomineralization, U-organic complexes, Shewanella putrefaciens, effects of organic acids

I. INTRODUCTION

Uranium is a radionuclide found in high- and low-level radioactive wastes. Its safe geological disposal requires an understanding of the migration behavior of uranium in the environment. Biomineralization of uranium is one of the immobilization mechanisms. The formation of uraninite (UO_2) through bioreduction of U(VI) and of uranyl phosphate minerals by microbial phosphate release are well known biomineralization. These two mechanisms have been investigated individually. However, there is the possibility that the two types of biomineralization compete each other in the environment. In this study, we examined the biomineralization of UO_2 and uranyl phosphate by *Shewanella putrefaciens* under the conditions they compete. It has been reported that the presence of organic acids, which form complexes with uranium, affects the reductive mineralization of UO_2 [1]. Therefore we focused on the effects of weak and strong complexing organic acids (WCOA and SCOA) on the biomineralization of uranium.

II. EXPERIMENTAL

Shewanella putrefaciens, an iron-reducing bacterium, was incubated in the basic medium (pH 7.0), which contained 50 mM sodium lactate as an electron donor, 1 mM uranyl nitrate as an electron acceptor, and 0.44 mM β-glycerolphosphate as a phosphorous source, and mineral salts under an anaerobic condition at 30°C. To evaluate the effects of organic acids, 100 mM WCOA (acetic, or adipic acid), or SCOA (oxalic, tartaric, citric acid or EDTA) were added to the basic media and the cells were incubated in the same way. Aliquots of medium were periodically withdrawn. The uranium concentrations and UV-vis spectra of the aqueous phases were measured. The new solid phases formed in the media were analyzed by SEM-EDS.

III. RESULTS AND DISCUSSION

The time courses of the total aqueous uranium during the incubation are shown in Fig. 1. In the basic medium, uranium in the aqueous phases decreased rapidly and new solid phases were observed. In the basic media with WCOA, the decreasing rates of aqueous uranium were slower than that in the basic medium with no WCOA. New solid phases also formed in these media. No decrease of uranium in solution was observed the media with SOCA. The UV-Vis spectra of the medium with SOCA showed that U(VI) was reduced to U(IV) and formed aqueous complexes with SOCA. This indicates that the stable complex formation inhibits the precipitation of uranium.
SEM-EDS and UV-Vis analyses of the new solid phases indicated the solid phases in the basic medium were mainly UO_2, and those in the media with WOCA were mixture of UO_2 and uranyl phosphate. It was though that the addition of WCOA decreased the reduction rate of U(VI), and allowed U(VI) to react with inorganic phosphate released by biodegradation of β-glycerolphosphate. Uranyl phosphate was not formed in the absence of β-glycerolphosphate. These findings suggest that the biomineralization behavior of uranium is highly affected by organic acids and their complexing abilities with uranium.

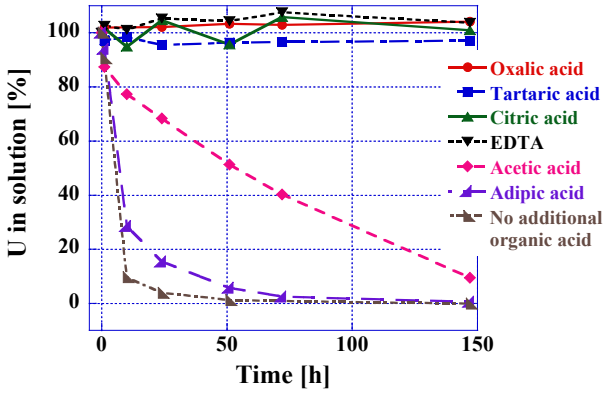

Fig. 1. Time course of aqueous uranium in the media with various organic acids during incubation with *S. putrefaciens*.

REFERENCES

[1] Y. Suzuki, K. Tanaka, N. Kozai, T. Ohnuki, Geomicrobiol. J., 2008, 27(3), 245-250.

Comparison of the spectroscopic characteristics of uranium species when U(III) in a LiCl-KCl molten salt is leached out with water and ionic liquid

Hee-Jung Im, Kyuseok Song
Nuclear Chemistry Research Division, Korea Atomic Energy Research Institute,
150 Deokjin-dong, Yuseong-gu, Deajeon 305-353, Republic of Korea

Abstract – U(III) in a LiCl-KCl molten salt was first dissolved into an appropriate ionic liquid and water, and identification and determination of the uranium (U) in the LiCl-KCl molten salt were performed using spectroscopic methods. The U(III) in LiCl-KCl molten salt showed the tendency of stable status in ionic liquid and unstable status in water. Based on the experimental data, a predictive theory of the factors involved in the process is discussed.

Keywords – Uranium species, LiCl-KCl eutectic, Molten salt, Ionic liquid, Spectroscopy

I. INTRODUCTION

As a type of spent nuclear fuel treatment, the pyrochemical process is well known for its non-proliferation of nuclear fuel cycles, separation of long-term radioactive nuclides during processing, the recovery of uranium for re-use as a nuclear fuel, and a significant volume-reduction of high-level wastes. After the complete pyrochemical processing is finished, a remaining small amount of salt waste, apart from the salt for recycling purposes, will be stored for the long term and is composed of some actinides and lanthanide species (mainly existing as 3+ ions) dissolved in molten salt. In this study, we investigate the behavior of U(III) dissolved in LiCl-KCl molten salt, especially when U(III) is leached out with ionic liquid compared to water, to obtain better understandable information for long-term waste salt storage. An ionic liquid system, which is similar to the environment of a slushy micelle system in a ground water migration, was considered as a medium for a convenient bench-scale experiment, and the results were compared to those from the water medium for U(III) behavior in different media.

II. EXPERIMENTAL

A U(III) in LiCl-KCl molten salt was prepared from the reaction of uranium metal with cadmium chloride in a LiCl-KCl mixture (44 wt.% LiCl) at 450 ^{o}C in an Ar-atmosphere glove box.

III. RESULTS AND DISCUSSION

Absorption spectra of the LiCl-KCl molten salt in an ionic liquid and UCl_3 in the LiCl-KCl molten salt in the ionic liquid are compared. The peaks at 460 nm and 553 nm are from U(III).

However, the absorption spectrum of UCl_3 in the LiCl-KCl molten salt with water was very different to the spectrum of UCl_3 in the LiCl-KCl molten salt in the ionic liquid. As it is well known that U(III) is easily oxidized into U(VI) during procedures, a characteristic peak of U(VI) was observed at 411 nm, and the color of the solution was changed from pale purple to yellow immediately after the solid was dissolved in water. Although at the preparation of samples, the U(III) was solidified on the LiCl-KCl molten salt from 450^{o}C to room temperature, the solidified U(III) was oxidized immediately in the presence of water.

The excitation spectrum of UCl_3 in a LiCl-KCl molten salt is shown in an ionic liquid by emission at 641 nm, and the spectrum was compared to an excitation spectrum of an ionic liquid only. There were specific peaks at 515 nm and 534 nm. The emission spectrum of UCl_3 in a LiCl-KCl molten salt in ionic liquid was also obtained at a 515 nm excitation, which was one of the positions obtained in the absorption spectra. Peaks were observed at 588 nm, 610 nm, and 640 nm.

Many experiments were undertaken to confirm luminescence peaks and to elucidate the exact phenomenon and mechanism.

IV. CONCLUSION

U(III) is unstable (oxidized) in an alkali fluoride molten salt or under general conditions, but is stable in LiCl-KCl molten salt. Moreover, the ionic liquid (1-hexyl-3-methyl-imidazolium chloride) used in this research did not cause an oxidation or reduction of U(III) as 1-ethyl-3-methyl-imidazolium chloride or water does. The behavior of U(III) in LiCl-KCl is dependent on the contact solvent (ionic liquid or water), and the results, including the actual assignment of each peak of the spectroscopic spectra, were conclusive.

Distribution of Neptunium in PUREX streams

Neetika Rawat, Aishwarya Kar, M.A. Mahajan, N.B. Khedekar, R.M. Sawant,
B. S. Tomar and K. L. Ramakumar
Radioanalytical Chemistry Division, Bhabha Atomic Research Centre, Trombay, Mumbai 400085

Abstract: *^{237}Np, is formed in abundance in nuclear reactors, however, the separation of neptunium from spent uranium fuel is difficult owing to the existence of its varied oxidation states in the dissolver solution. With a view to identify the stage in the PUREX plant, which can be used to tap neptunium, an exercise was undertaken to determine the distribution of neptunium in the different stages of the PUREX plant.*

Keywords: *^{237}Np, PUREX Streams,*

INTRODUCTION

^{237}Np, the long lived isotope of neptunium is the target isotope for production of ^{238}Pu by the neutron capture reaction. It is formed in abundance in nuclear reactors[1]. However, the separation of neptunium from spent uranium fuel is a difficult task owing to the existence of the element in varied oxidation states in the dissolver solution. With a view to identify the stage in the PUREX plant, which can be used to tap neptunium, an exercise was undertaken to determine the distribution of neptunium in the different stages of the PUREX plant.

^{237}Np is a pure alpha emitter with no gamma lines and hence its analysis requirescareful radiochemical separation from bulk uranium, plutonium and fission products before its estimation by alpha spectrometry. The alpha energies of plutonium isotopes are higher than that of ^{237}Np and hence traces of Pu in the separated neptunium fractions would have contribution at the alpha peak of ^{237}Np (Figure 1). Therefore, it was decided to measure the distribution ratios of Np in various streams of PUREX process using ^{239}Np tracer (β,γ emitter) from irradiated uranium target. The actual column conditions of different streams were simulated performing solvent extraction in lab scale for the distribution of Np.

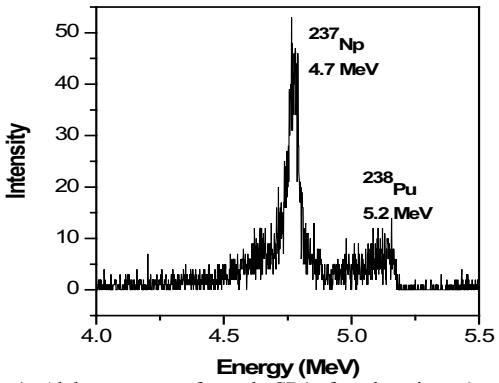

Figure 1. Alpha spectrum of sample CD1 after plutonium séparation

EXPERIMENTAL

The ^{239}Np tracer was obtained by irradiating natural Uranium (10 mg) in reactor. The irradiated U was dissolved in conc HNO_3 and then evaporated to dryness and made up to 20 ml using 3 M HNO_3. Aqueous feed solution was prepared by adding ^{237}Np, ^{239}Np tracer and U so as to maintain U and Np concentration 380 g/L and 10 mg/L respectively (acidity 3 M HNO_3). Distribution of Np (D_{Np}) in different streams was followed by counting the 278 keV gamma line in the gamma spectra using a HPGe detector. 4 ml of feed was equilibrated for 15 min with 19.6 ml of 30 % TBP in NPH (O/A = 4.9). Phases were separated by centrifugation. Suitable aliquots from the aqueous (HAW) and organic phase (HAP) were taken for assay of ^{239}Np. 16.4 ml from HAP was equilibrated with 4 ml of U(IV) ((28 g/l) in N_2H_4 (0.2 M) at 0.6 M acidity (O/A = 4.1). After phase separation, the organic and aqueous phases, labeled as 1BXU and 1BXP, respectively, were assayed for the activity of ^{239}Np. Subsequently 14 ml from 1BXU was equilibrated with 15.45 ml of 0.01 M HNO_3 (O/A = 0.906), and the aqueous and organic fractions, labeled as 1CP and 1CW, respectively, were counted. 14 ml of 1CP was concentrated to 2.5 ml termed as 1CPCON. To 2.0 ml of 1CPCON, U(IV) was added such that U(IV) concentration in final solution is 4.8 g/l and N_2H_4 is 0.2 M at 1.0 M acidity. 1CPCON was diluted to 3.58 mL, and was labeled as 2DCD. 1 ml of 2DCD was equilibrated with 2.3 ml of 30 % TBP (O/A = 2.3). The aqueous phase was labeled as 2DW. All the fractions were assayed for the activity of ^{239}Np.

RESULTS AND DISCUSSION

The complete experiment following the above procedure was carried out twice (Cycle 1 and Cycle 2). The D_{Np} values and percentage of Np in different steps, for both the cycle are given in table 1. D_{Np} values obtained for solvent extraction steps in both the cycles are in good agreement except for the step corresponding to HA column. D_{Np} in first cycle was found to decrease from 0.205 to 0.043 in the second cycle, which could be due to slow kinetics of change in oxidation state of neptunium. The decrease in D_{Np} values of Np from dissolver solution into TBP with the passage of time, indicates the reduction of Np(VI) to Np(V).

Table 1.D values and percentage of Np in different steps

Sample name	Cycle 1		Cycle 2	
	Distribution Coefficient, D	% Np	Distribution Coefficient, D	% Np
CD1		100		100
HAW	0.205	53	0.043	91
HAP		54		19
1BXP	0.266	26	0.26	9
1BXU		28		10
1CP	0.05	27	0.053	9.6
1CW		1.25		.4
1CPCON		27		9.6
2DCD		27		9.6
2DW	0.219	18	0.184	6.4
2DP		9		3.2

Reference

1. G.A.Burney and R.M.Harbour, Radiochemistry of neptunium, Nuclear Science Series NS-3060 (1974).

α-Radiation Effect on Solvent Extraction of Minor Actinide

Yumi Sugo[1], Yuji Sasaki[2], Mitsumasa Taguchi[1], Noriko S. Ishioka[1]
[1]Quantum Beam Science Directorate, Japan Atomic Energy Agency
[2]Nuclear Science and Engineering Directorate, Japan Atomic Energy Agency

Abstract – α-Radiation effect on the extraction of ^{241}Am was investigated using the solution of N,N,N',N'-tetraoctyldiglycolamide pre-irradiated with α-particles, in contrast to the irradiation using actinides as an α-particles emitter. ^{241}Am was extracted almost quantitatively from the aqueous phase into the organic one. The concentration in the organic phase nearly kept constant even after irradiation with α-rays.

Keywords – Solvent Extraction, Minor Actinide, Radiolysis

I. INTRODUCTION

A tridentate extractant, *N,N,N',N'*-tetraoctyl-diglycolamide (TODGA) has high extractability for actinides such as americium and curium from nitric acid into *n*-dodecane. α-Radiolysis study of the organic extractants using an actinide radionuclide has some experimental difficulties. For example, a long-term exposure to actinides is required, and the extractants are contaminated with the radionuclide. In the previous study [1], these issues were solved by irradiation with helium ions provided by an accelerator. It was also found that the radiation chemical yield for the degradation of TODGA in *n*-dodecane by helium ions corresponding to the α-particles was less than that by γ-rays. In this study, radiation effect on the extraction of ^{241}Am was investigated using the solution of TODGA pre-irradiated with α-particles, in contrast to the irradiation using actinides as an α-particles emitter.

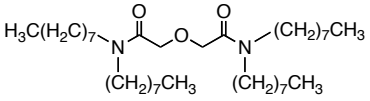

TODGA

II. EXPERIMENTAL

The organic solution of 0.1 M TODGA in *n*-dodecane pre-equilibrated with nitric acid was irradiated with helium ions provided by a tandem accelerator according to the previous report [1]. Incident energy of the ions was adjusted to 5 MeV corresponding to the typical energies of the α-rays emitted from actinide radionuclides. The absorbed dose rate was approximately 1-3 kGy min^{-1}.

The pre-irradiated solution was taken in an extraction tube with an equal volume of an aqueous 3.0 M nitric acid solution spiked with the radioactive tracer of ^{241}Am. The extraction tube was shaken mechanically for 30 min at 25±0.1°C. After centrifugation, the aliquots of both phases were taken and their α-activities were measured by liquid scintillation counter.

III. RESULTS AND DISCUSSION

The aqueous solutions containing ^{241}Am at radioactive concentration of 1.3 kBq ml^{-1} were used for the extraction using the organic solutions pre-irradiated with α-rays. After extraction, ^{241}Am concentration in the aqueous phase was less than 1 Bq ml^{-1}. This indicates that ^{241}Am is extracted almost quantitatively from the aqueous phase into the organic one. Figure 1 shows ^{241}Am concentration in the organic phase as a function of dose absorbed by the organic solution. The concentration in the organic phase nearly kept constant even after irradiation with α-rays. The absorbed dose had been estimated to be approximately 5 kGy per cycle in the actual process [2]. Consequently, it is suggested that the extractability of TODGA for minor actinides can be maintained after recycling on the order of dozens of cycles in the process.

In addition, we examined the α-radiation effect on the extraction of ^{241}Am using the organic solution containing complexing ^{241}Am as α-particles emitter at radioactive concentration of 8.4 MBq ml^{-1}. The result will be discussed in this presentation.

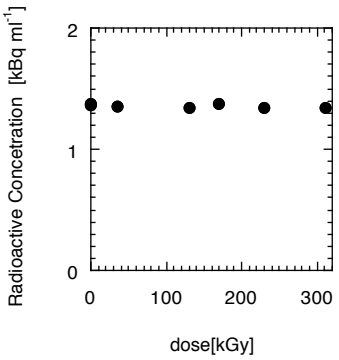

Fig. 1 ^{241}Am Concentration in the organic phase as a function of dose, obtained in the extraction using the solution of 0.1 M TODGA in *n*-dodecane pre-irradiated with α-particles.

REFERENCES

[1] Y. Sugo et al., *Radiat. Phys. Chem.* **78**, 1140 (2009).
[2] G. M. Gasparini et al., *Solv. Extr. Ion Exch.* **4**, 1233 (1986).

Retardation and Release Study of U(VI) on Phlogopite at Conditions Relevant to Uranium Contamination in Environment

Pan Duoqiang[1,2], Wang Zheming[2], Wu Wangsuo[1]
[1] Radiochemistry Laboratory, Lanzhou University, Lanzhou 730000, China
[2] Pacific Northwest National Laboratory, Richland, Washington 99352, United State

Hexavalent Uranium, which is fertile in mining tailings and wastewater from nuclear production activities, is a prominent radioactive contaminant and has dispersed into both sediments and water around the related uranium processing sites, posing a potential health and environmental risk to the biosphere [1]. The mobility of U(VI) in natural medium is significantly controlled by the sorption/desorption behavior which is influenced by U(VI) speciation, sorbent properties and coexisted organic/inorganic ligands [2,3]. Desorption of absorbed U(VI) from solid phase is actually considered to be potential secondary release sources to hydrosphere and the extent of desorption reversibility largely depends on the mechanisms involved in the sorption process [4]. As the sorption mechanism can vary by due to changes in sorption conditions, such as ligand complexation and change of pH or temperature, the uranium retardation and release rate in environmental media can be perturbed. Understanding the sorption mechanism and sorption reversibility of U(VI) is imperative to predict the future retention/migration behavior of U(VI) and to remediate contaminated soils and subsurface sediments. Many spectroscopic technologies that are capable of providing molecular-level information (FTIR, XPS, EXAFS, TRLIFS) have been employed to identify U(VI) species and local atomic structures of the surface complexes. Time resolved laser induced fluorescence (TRLIF) spectroscopy, particularly when performed at cryogenic temperatures, is one technique that offers high sensitivity and spectral resolution for the identification of U(VI) speciation in complex media at low U(VI) concentrations [5,6].

Here we applied a combination of batch sorption experiment and liquid helium temperature (LHeT) TRLIF spectroscopy to investigate sorption/desorption of U(VI) to phlogopite, which is a typical rock forming mineral in granite terrains. Effects of pH, humic acid (HA), background electrolyte and temperature were studied in detail by batch method. The sorption isotherms at different temperatures were simulated and analyzed by using Langmuir and Freundlich models. Roles of HA and temperature on sorption reversibility were investigated by sorption-desorption isotherms. The speciation of adsorbed U(VI) at low concentration were monitored and the sorption/desorption mechanism were explored with the aid of TRLIF spectroscopy. The results shows that the sorption of U(VI) on phlogopite is influenced obviously by pH while only slightly by ionic strength. Inner-sphere surface complexation and/or precipitation rather than ion exchange and outer-sphere complexation are the primary sorption mechanisms. HA makes little difference at low pH, while inhibits U(VI) sorption at high pH mainly because of formation of soluble binary complexes and repulsive interaction between both negative charged HA and solid surface. High temperature is advantageous for U(VI) sorption, Langmuir model fits the sorption data better than Freundlich model. The presence of HA switches U(VI) sorption reversibility by forming HA-bridge ternary complex.

Keywords: Uranium, Sorption/Desorption, Phlogopite, TRLIFS

[1] Chakraborty S., et al., *Environ. Sci.Technol*., 2010, 44(10): 3779-3785.
[2] Chang H.S., et al., *Environ. Sci.Technol*., 2006, 40(4): 1244-1249.
[3] Chisholm-Brause C.J., et al., *J. Colloid Interf. Sci*., 2001, 233(1): 38-49.
[4] Um W., et al., *Environ. Sci.Technol*., 2009, 43(12): 4280-4286.
[5] Wang Z., et al., *Geochim. Cosmochim. Acta*, 2005, 69(6): 1391-1403.
[6] Wang Z., et al., *Geochim. Cosmochim. Acta*, 2011, 75(10): 2965-2979.

APSORC'13 - 5th Asia-Pacific Symposium on Radiochemistry
Kanazawa, Japan, 22-27 September 2013

Application of Simplified Desorption Method to Sorption Study: (2) Sorption of Neptunium (V) on Montmorillonite-based Mixtures

Naofumi Kozai[1], Toshihiko Ohnuki[1]
[1]Japan Atomic Energy Agency, Tokai, Ibaraki, 319-1195 Japan

Abstract – To elucidate the sorption behaviors of radionuclides in multi-mineral systems and the mutual effects of minerals on the sorption, this paper carried out the sorption and desorption experiments of neptunium(V) on montmorillonite-based two-mineral mixtures. The Np sorbed on montmorillonite at pH from 4 to 8 was desorbed with 1M KCl solutions, indicating that the sorption was cation exchange. The Np sorbed on apatite and calcite was nondesorbable with 1M KCl solutions, which is in harmony with the knowledge that Np forms strong complexes with the phosphate groups of apatite and the carbonate groups of calcite. This study utilized these clear distinguishes of the desorption behaviors for examining the two-mineral systems. In montmorillonite-apatite mixtures, the sorption on the montmorillonite was decreased and Np was accumulated on the apatite. In montmorillonite-calcite mixtures, the sorption on the montmorillonite was decreased due to the interference by the calcium and carbonate ions dissolved from calcite while no accumulation of Np to calcite was observed.

Keywords – Neptunium, sorption, desorption, pH, montmorillonite, apatite, calcite

I. INTRODUCTION

Sorption is one of the key mechanisms to control the subsurface environmental behavior of the radionuclides. In most of the relevant experimental studies, the sorption experiments of radionuclides have been performed in a single mineral system, while most of the subsurface environment is a multi-component system. The knowledge on the mutual influence of minerals to understand the sorption in multi-component systems is limited. This paper investigated the sorption of neptunium(V) in two-mineral systems. Montmorillonite clay used as a major component mineral is found ubiquitously in the soil environment. As minor soil component minerals, apatite ($Ca_5(PO_4)_3OH$) and calcite ($CaCO_3$) were used. This paper applies a simplified desorption method to the sorption study and discuss the distribution of Np between minerals.

II. EXPERIMENTAL

This study used the same Na-montmorillonite as the one used in the former study [1]. The apatite used is fine powder of commercial calcium-phosphate having hydroxyapatite ($Ca_5(PO_4)_3OH$) like structure (Wako Pure Chemical Industries Co. Ltd.). Natural calcite ($CaCO_3$) was used after ground to particle sizes below 74 μm. These minerals were used singly or used as montmorillonite-based mixtures (montmorillonite 95-99 w%). A Np (V) nitrate stock solution was diluted with 0.01 M $NaClO_4$ to yield a working solution having a Np concentration of about $6x10^{-7}$ M.

The sorption and the desorption experiments were conducted in the same way as the method described elsewhere [1] except that a part of the sorption experiments were carried out for up to 60 d.

III. RESULTS AND DISCUSSION

When Na-montmorillonite was used alone, the fraction of the sorbed Np was roughly constant in the equilibrium pH range from 4 and 8. Most of the sorbed Np was desorbed by twice treatment with 1M KCl solutions. These results indicate that the sorption is electrostatic one between NpO_2^+ and the constant negative surface charge of the montmorillonite [2].

On the apatite and the calcite, all of the Np was sorbed in the examined equilibrium pH ranges that were limited from neutral to weak alkaline due to their partial dissolution. The Np sorbed on these two minerals was hardly desorbed by twice treatment with 1M KCl solutions. These results are consistent with the knowledge that Np forms strong complexes with the phosphate groups of apatite and carbonate groups of calcite [3, 4]. The subsequent experiments for the montmorillonite-based mixtures utilized these clear differences; that is, the Np desorbed with 1M KCl solutions was regarded as the Np sorbed on the montmorillonite fraction and the Np not desorbed with 1M KCl solutions was the one sorbed on the apatite and calcite.

The montmorillonite-apatite mixtures sorbed several times greater amount of Np than Na-montmorillonite itself, while that on the montmorillonite fraction in the mixture decreased. Above pH 7 almost all of the Np was sorbed on the mixture within 10 d and most of the Np was sorbed on the apatite fraction. Below pH 7 the sorption on the mixtures increased with time and needed a longer time (20 d) to reach equilibrium. This slow kinetics of the sorption did not occur when those minerals were used singly and suggests a possible Np sorption involving the phosphate ligands once dissolved at low pH. The sorption on the montmorillonite-calcite mixtures was less than that on Na-montmorillonite itself and no evidence of accumulation of Np to calcite was observed, suggesting that the calcium and carbonate ions dissolved from the calcite interfered with the sorption.

[1] Kozai N and Ohnuki T., APSORC13 Abstract.
[2] Kozai N et al., Radiochimica Acta, 75, 149-158 (1996).
[3] Moor R. C., Radiochim. Acta, ().
[4] Zavarin M. et al., Radiochim. Acta, 93, 9-102 (2005).

APSORC'13 - 5th Asia-Pacific Symposium on Radiochemistry
Kanazawa, Japan, 22-27 September 2013

Continuous measurement of radon exhalation rate of soil in Beijing

Lei Zhang[1, 2], Ke Sun[2], Qiuju Guo[2]
[1]Solid Dosimetric Detector and Method Laboratory, Beijing, 102205, China
[2]State Key Laboratory of Nuclear Physics and Technology, School of Physics, Peking University, Beijing 100871, China

Abstract – The continuous measurement of radon exhalation rate of soil is quite important for local radon level estimation. A continuous measurement system was developed and was applied to the measurement of the radon exhalation rate of soil in Beijing. The measurement results show that the average value of soil radon exhalation rate is 42.5 mBq•m^{-2}•s^{-1} in spring with a variation of 13.1~110 mBq•m^{-2}•s^{-1} and 20.8 mBq•m^{-2}•s^{-1} in summer with a variation of 1.1~112 mBq•m^{-2}•s^{-1}, which is quite constant with former surveys. The precipitation has an important influence on radon exhalation rate, normally the radon exhalation rate increases after a small rainfall, but it decreases to nearly zero shortly after a huge rainfall(with a precipitation rate of 238.5mm•h^{-1}). In May, the radon exhalation rate of soil in Beijing shows a clear periodic variation, higher around noon and lower around midnight.

Keywords – Radon; Soil; Exhalation Rate; Continuous Measurement; precipitation

APSORC'13 - 5th Asia-Pacific Symposium on Radiochemistry
Kanazawa, Japan, 22-27 September 2013

Dosimetric Evaluation of Thoron Exposure in Three Typical Rural Indoor Environments in China

Lei Zhang[1], Qiuju Guo[2], Shanqiang Wang[1]
[1]Solid Dosimetric Detector and Method Laboratory, Beijing, 102205, China
[2]State Key Laboratory of Nuclear Physics and Technology, School of Physics, Peking University, Beijing 100871, China

Abstract – The brick houses, the mud houses and the cave houses are the three typical rural residential houses in China, usually with naked surface from where thoron gas easily comes out. In order to evaluate the thoron exposure of those indoor environments, a series of field measurements was carried out by using portable measurement devices of both thoron progeny concentration and the size distribution of them. The dose conversion factors and annual effective doses of thoron exposure in those environments are calculated using dosimetric methods. Comparing with the results in urban indoor environment, it shows that the thoron progeny size distributions of rural indoor environments (AMAD: 76.5nm; GSD: 2.7) are much smaller than those of urban(AMAD: 115nm; GSD: 2.0), which make the dose conversion factors of thoron in rural environments(307.4nSv/(Bq•m^{-3}•h^{-1})) are much higher than those in urban indoor environments(113.4 nSv/(Bq•m^{-3}•h^{-1})). The annual average effective dose of thoron is influenced by dose conversion factor as well as thoron equilibrium equivalent concentration, and a quite high value of 10.12 mSv•a^{-1} in mud house in Yangjiang area is calculated by our survey.

Keywords – Thoron Progeny, Size Distribution, Dose Conversion Factor, Dose Evaluation

APSORC'13 - 5th Asia-Pacific Symposium on Radiochemistry
Kanazawa, Japan, 22-27 September 2013

Binary Technetium Phosphide Synthesis at Low Temperature Conditions

Bradley C. Childs[1], William M. Kerlin[1], Ken R. Czerwinski[1]
[1]University of Nevada Las Vegas, Las Vegas, Nevada 89154, USA

Abstract – Binary technetium phosphide exists through high temperature reactions that exceed 900 °C [1]. Recent phosphide studies have indicated that transition metal phosphide species such as molybdenum, ruthenium, and rhenium can be synthesized at temperatures that do not exceed 300 °C, and will provide a more reasonable synthesis technique. This process could allow for a technetium waste form application due to the high melting point and low solubility's that many transition metal phosphide species exhibit. Experimental methods include bench-top reactions that begin with a precursor produced from a transition metal chloride combined with either sodium hypophosphite (NaH_2PO_2) or ammonium hypophosphite ($NH_4H_2PO_2$).The second experimental method involves using hydrothermal and solvothermal experiments with phosphorus and various metal chloride species.

Keywords – Technetium, Phosphide, Synthesis

I. INTRODUCTION

Nearly 2 tons of ^{99}Tc ($T_{1/2}$ = 2.13x10^5 years, β^- = 280 keV) are produced in the United States each year. As spent fuel is being reprocessed, some of the technetium is present in the intermetallic epsilon phase (Mo, Tc, Ru, Rh, Pd), but majority of the technetium can be found in the high activity waste of reprocessing plants as pertechnetate (TcO_4^-) [2]. This becomes problematic due to the fact that TcO_4^- has a high mobility in the environment combined with its long half-life. Waste-form consideration must be given to those compounds that exhibit low solubility's that also allow for the waste to be stored for long periods of time without degrading. Technetium phosphide compounds that can be synthesized at low temperatures may provide a method and compound that will allow such a goal to be achieved.

A. Synthesis with NaH_2PO_2 or $NH_4H_2PO_2$

Hypophosphite ($H_2PO_2^-$) is a reducing agent that can also provide phosphorus when reacting with a metal chloride [3]. This compound is also thermodynamically unstable at temperatures above 200 °C. This provides the basis for a reaction between $RuCl_3$, $ReCl_3$, and $MoCl_3$ to react with the hypophosphite anion. A precursor will be made by dissolving one of the metal chlorides with NaH_2PO_2 or $NH_4H_2PO_2$ in distilled water [9] [10]. This mixture will then be heated to 60 – 80 °C. The resulting precursor would then be heated in static argon conditions at temperatures ranging between 200 °C and 300 °C. Based on results from the previous reactions, technetium chloride ($TcCl_4$, $TcCl_3$, and $TcCl_2$) will be used in place of other metal chlorides.

B. Phosphorus hydro-solvothermal synthesis

A 23 mL Teflon lined Parr 4749 autoclave was used to house reactions that involved reacting phosphorus with $RuCl_3$, $ReCl_3$, and $MoCl_3$ while using ethylenediamine as the solvent to create a reducing environment. The area for concern in this reaction involves over reducing the metal species before it gets a chance to react with the phosphorus. Therefore, water was also used as a solvent in separate experiments to avoid too much reduction. Afterwards, $TcCl_4$, $TcCl_3$, and $TcCl_2$ will be considered for the same reaction depending on the phosphorus chlorine products produced in comparison to the binary phosphide product.

Acknowledgement: Funding for this research was provided by a SISGR Grant from the U.S. Department of Energy, Office of Science, Office of Basic Energy Sciences, under Contract No. 47824B

REFERENCES

[1] K. Schwochau, Technetium: Chemistry and Radiopharmaceutical Applications, Wiley-VCH: Weinheim, Germany, 2000.
[2] M.C.A. Sandino and E. Östhols, eds., Chemical Thermodynamics of Technetium, Chemical Thermodynamics, 1999, **3**
[3] Greenwood, Norman N.; Earnshaw, Alan (1997). *Chemistry of the Elements* (2nd ed.). Butterworth–Heinemann.
[4] Q. Guan and W. Li, *Journal of Catalysis,* 271, (2010), 413-415.
[5] Q. Guan et al., *Catalysis Communications,* 14, (2011) 114-117.
[6] Y. Xie et al., *Journal of Solid State Chemistry*, 149, (2000), 88-91.

Dissolution behavior of ^{137}Cs absorbed on the green tea leaves

Yasuhisa Oya[1], Hiromichi Uchimura[1], Kensuke Toda[1], Takashi Ikka[2], Akio Morita[2], Kenji Okuno[1]
[1]Graduate School of Science, Shizuoka University
[2]Graduate School of Agriculture, Shizuoka University

Abstract – The green tea leaves was dipped in the ^{137}CsCl solution to elucidate the dissolution behavior of ^{137}Cs contaminated on the green tea leaves. It was found that the amount of ^{137}Cs dissolved into tea water was controlled by the temperature of water, and the activation energy of ^{137}Cs dissolution was estimated to be 0.045 eV, indicating that most of ^{137}Cs would exist as the adsorbed state. In addition, the dissolution behavior was controlled by the concentration of stable Cs dissolved in water, although no large correlation with pH was observed.

Keywords – ^{137}Cs, dissolution behavior, green tea leaves

I. INTRODUCTION

Shizuoka is the most common tea production region in Japan and more than 40% of tea leaves are produced in Shizuoka prefecture, Japan. In the accident of 2011 Fukushima Daiichi Nuclear Power Plant (FNPP), radiocesium species was felled in Shizuoka prefecture, Japan, which leads the shipping restriction of tea products. Recently, some of studies related to the distribution of fall-out radiocesium in Shizuoka were reported [1]. In addition, the dynamics of radiocesium in tea plant is also studied. It was reported that the higher radiocesium activity was found along Warashina area and southern slope of Udo Hills, where the most tasteful tea plant is produced. This distribution is controlled by the wind condition in the afternoon on March 15, 2011. Therefore, the weather is one of key parameter for the determination of radiocesium distribution profiles. But, tea plant is grown in the unique area for radiocesium deposition and it is quite difficult to get rid of fall out of radiocesium, when the nuclear power plant accident is happened. Most of tea leaves are not eaten with raw condition and, are processed and dried to brew green tea. So the extrability of radiocesium from tea leaves harvested after FNPP accident has been reported [2]. However, more detailed elucidation of dissolution behavior of radiocesium adsorbed on the green tea leaves under well-controlled condition is the next step to elucidate the fundamental behavior of radiocesium. In this study, the dissolution behaviors of ^{137}Cs to water from green tea leaves were studied as a function of water temperature, pH and cesium ion concentration in water.

II. EXPREMENTAL

The 6.0 g fresh green tea leaves were purchased and dipped in 39 ml of ^{137}CsCl solution with the ^{137}Cs concentration of 0.5 kBq/ml. These tea leaves were dried by infrared lamp for one night. Thereafter, the tea was brewed by 200 ml water. The activity of ^{137}Cs dissolved into water was measured by NaI (Tl) scintillation counter for 60 minutes.

III. RESULTS

It was found that the temperature dependence on ^{137}Cs dissolution rate was almost proportional to the water temperature. Fig. 1 shows the brewing time dependence on ^{137}Cs dissolution rate. Large dissolution rate was derived for the higher temperature sample. The dissolution behavior was assumed to be governed by the Arrhenius correlation and the activation energy was estimated to be 0.045 eV, indicating that most of ^{137}Cs would exist as the adsorbed state and no chemical interaction with tea leaves. To elucidate the key parameters to control the dissolution behavior, pH dependence on ^{137}Cs dissolution rate was also evaluated from the pH = 1 to 13 and showing that no large contributions of hydrogen ion and hydroxyl ion concentrations on ^{137}Cs dissolution. In addition, dependences for concentrations of K^+ and Cs^+ on ^{137}Cs dissolution were also evaluated. It was confirmed that the dissolution rate of ^{137}Cs in water was reduced almost half by the addition of the 1000 ppm Cs^+.

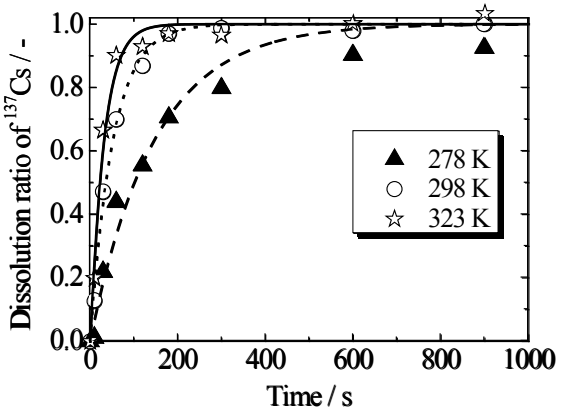

Fig. 1 Brewing time dependence on ^{137}Cs dissolution rate

REFERENCES

[1] T. Tsuboi, H. Wada, M. Yanaga, Radiat. Safety Manag. 11 (2012) 11-18.
[2] K. Tagami, S. Uchida, N. Ishii, J. Radioanal Nucl. Chem. 292 (2012) 243-247.

Characterization on the Radioactive Aerosols Dispersed during Plasma Arc Cutting of Radioactive Metal Piping

T. Shimada [1] and T. Tanaka [1]
[1] Nuclear Safety Research Center, Japan Atomic Energy Agency, Tokai-mura, Naka-gun, Ibaraki 319-1195, Japan

Abstract

In order to plan and execute the decommissioning of nuclear facilities safely and properly, it is necessary to understand the production and dispersion behaviors of radioactive aerosols which are dispersed during the cutting of components activated and/or contaminated. It will cause not only internal exposures of workers but public exposure resulting from discharge of those radioactive aerosols to the environment. It is also important for radiological safety assessment to figure out their behaviors. Therefore plasma arc cutting experiments were carried out to obtain particle size distribution and radionuclides concentrations.

Neutron induced-activated piping and surface contaminated piping were segmented along the outer surface by well-trained workers using air plasma arc cutting, of which current power was 100A, in the contamination control enclosure (4m length, 4m width, 4m height). The former was the stainless steel piping of primary reactor cooling system situated around the reactor pressure vessel of Japan Power Demonstration Reactor. It was 0.5m long, 318mm outer diameter, 17mm thickness. Values of specific radioactivity of ^{60}Co and ^{63}Ni in the base material were 64.4Bq/g to 170.9 Bq/g and 378.5Bq/g to 797.8Bq/g respectively. The tendency depended on the distance from the reactor core. The inner surface of the piping was grinded just in case even though its surface had been decontaminated by a chemical method after dismantling. The latter was the carbon steel piping of liquid waste treatment system of the advanced thermal reactor, FUGEN. It was 6.9m long, 60mm outer diameter, 5.5mm thickness. There was a great variability among the values of radioactive surface contamination density of inner surface of the piping, from 552.1Bq/cm^2 to 55,336Bq/cm^2 of ^{60}Co.

Air including aerosols was exhausted from the enclosure to the local ventilation system. Particle size distribution of the aerosols was obtained by sampling air though the nozzle at the center of the ventilation piping using ELPI (Electrical Low Pressure Impactor, Dekati Inc.) which could classify particles into 12 stages of 50% cutoff aerodynamic diameter, D50% ranging from 0.007 to 9.9μm. This instrument enables to measure particle size distribution and concentration of the aerosols in real-time by corona charger and electro-meters at each impactor stage. The radioactive quantity of ^{60}Co of aerosols collected on the impactor stage was measured by Ge semiconductor detector. That of ^{63}Ni was measured by liquid scintillation counter after dissolved by hydrochloric acid and separated by ion-exchange column.

Figure 1 shows the particle size distribution of specific radioactivity of ^{60}Co and ^{63}Ni of aerosols during cutting of activated piping. Those values were calculated by dividing the quantity of radionuclide at the each stage by the weight of aerosols collected at the stage. Specific radioactivity of both ^{60}Co and ^{63}Ni of 0.09μm indicated the highest value. Those of both ^{60}Co and ^{63}Ni of 0.15μm and 0.26μm indicated the similar values to those of base material of the piping. That of ^{60}Co larger than 0.26μm indicated the half value of the base material.

Figure 2 shows the particle size distribution of ^{60}Co specific radioactivity of aerosols during cutting of surface contaminated piping. Specific radioactivity of aerodynamic diameter of 0.05μm indicated the maximum value of approximately 2.7E+4 Bq/g which was fifty times as much as the average value of the aerosols. That of 9.9μm was approximately 100Bq/g which was the eighth part of the average value. Compared with the activated piping, the difference of specific radioactivity between maximum and minimum values were larger in contaminated piping. It is considered that contaminants on the inner surface were directly melted and vaporized by plasma arc and then concentrated into smaller particles

Those results indicated that the management for dispersion behavior of smaller particles is important for the radiation protection during dismantling activities.

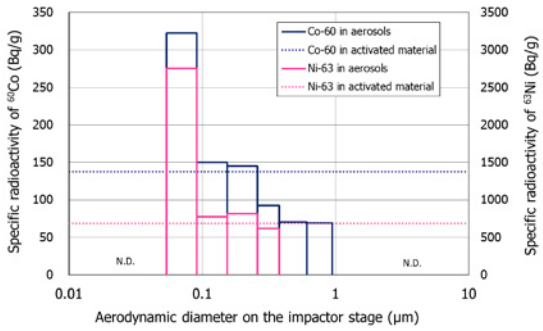

Figure 1 size distribution of specific radioactivity of activated piping

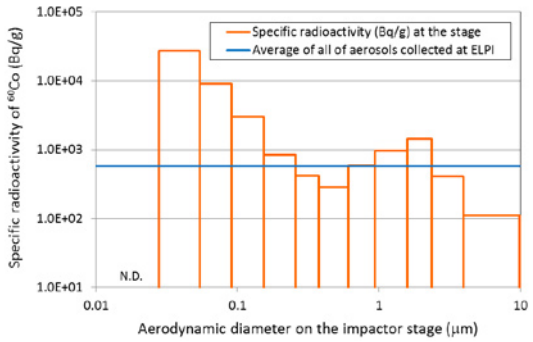

Figure 2 size distribution of specific radioactivity of surface contaminated piping

This work is a part of study funded by Japan Nuclear Energy Safety Organization.

A passive collection method for whole size fractions of suspended river materials

Takeshi Matsunaga[1], Takahiro Nakanishi[1], Mariko Atarashi-Andoh[1], Erina Takeuchi[1], Katsunori Tsuduki[1], Syusaku Nishimura[1], Jun Koarashi[1], Shigeyoshi Otosaka[1], Tsutomu Sato[2], Seiya Nagao[3]

[1] Nuclear Science and Engineering Directorate, Japan Atomic Energy Agency, Tokai-mura, Ibaraki 319-1195, Japan

[2] Division of Sustainable Resources Engineering, Graduate School of Engineering, Hokkaido University, Sapporo 060-8628, Japan

[3] Low Level Radioactivity Laboratory, Institute of Nature and Environmental Technology, Kanazawa University, Ishikawa 923-1224, Japan

Abstract – An innovative, yet simple method for the passive collection of radioactive materials in river water has been developed and validated. This method makes long-term, unmanned monitoring possible. In addition to regular radioactivity analyses, this method provides an opportunity for the characterization of suspended materials based on its ample collection quantities (more than several tens of grams). This method may also be applicable to sediment-bound chemicals.

Keywords – River, Radionuclides, Chemicals, Passive collection, Long-term monitoring, Suspended materials, Dissolved materials

I. INTRODUCTION

The migration behavior of atmospherically derived radionuclides and chemicals onto river catchments has been extensively studied thus far. Transport of these materials through rivers can be the most influential export process to downstream regions. These investigations, however, have often encountered essential difficulties; one of which is in sampling frequency. Rainfall events play an important role in fluvial transport of contaminants. However, it is difficult to carry out frequent manned observations for these stochastic events. Another difficulty is the ability to collect enough suspended material for characterization purposes such as chemical extractions and mineralogical analyses. The aforementioned analyses generally require several grams of suspended material. The concentration of such materials in river water typically ranges from a few mg l^{-1} to about 100 mg l^{-1}, meaning that ten to a thousand liters of water are required. Accordingly, handling such large amounts of water can be distressing. Here, we report an innovative, yet simple collection method for suspended and dissolved components in river water.

II. METHODS

A. Collection of suspended components

Two filter vessels (957 mm height, 350 mm width, 6SL-2S, Advantec Toyo Kaisha, Ltd.) were used sequentially with different nominal pore-sized filters, 100 μm and 0.5 μm. Each vessel contained six cartridge filters of wound type polypropylene (750 mm length). River water was led to the system naturally using a drop of the riverbed by hose from upstream. After an appropriate number of days of operation, the filters and the mud deposits on the bottom of the vessels were recovered. In the laboratory, the suspended material that was collected on the wound fibers was washed out with water in a bucket. The wash-water samples and the mud samples were concentrated via centrifugation. A composite of the mud sample was obtained and subjected to wet sieving, such that components of four sizes were obtained: 1) <2000 μm, 2) 500-2000 μm, 3) 75-500 μm, and 4) <75 μm, in principle. The first and second components were air-dried. The third and fourth components were freeze-dried to obtain final samples of suspended material.

B. Collection of dissolved components

The dissolved component, radiocesium in this study, was collected from part of the outlet water from the filter vessels. Namely, the outlet water was put through a series of two PVC columns (4 cm inner diameter, 20cm length), which contain Cs-specific adsorbent material (Anfezh).

III. RESULTS AND DISCUSSION

The effectiveness of this method was validated over a period of 15 months of field operation time since December 2011. The test site was a hilly, forested catchment of 0.62 km^2 containing a stream, located in the Northern area of Central Japan (Ibaraki Prefecture). The site was affected by fallout from the Fukushima nuclear accident. In this validation study, the aim was to obtain samples for radiocesium analyses. During the test period, ten sets of suspended material samples were successfully recovered. Intervals were changed from two to six weeks depending on the hydrological situation. Approximately 50-350 g of suspended material was recovered per collection period; variance depended on the length of the period and precipitation conditions. Adsorbent columns for dissolved radiocesium were added after November 2012. The collection efficiency of dissolved radiocesium was as high as 95 %. A consistent working method for collection of dissolved components and suspended components has therefore been established.

IV. CONCLUSION

A passive, yet simple collection method for radioactive materials in river water has been developed and validated. The method is advantageous as it: i) allows efficient recovery of whole size fractions of suspended material, ii) can be used in remote locations without electricity, iii) is suitable for unmanned operations over long periods of time.

Study of factors controlling organic pollution in Lake Kiba

Yuriko Kawano[1], Seiya Nagao[1], Shinya Ochiai[1], Masayoshi Yamamoto[1]
[1]Low Level Radioactivity Laboratory, Kanazawa Univ., Wake, Nomi, Ishikawa 923-1224, Japan

Abstract –
Lake Kiba is located in Ishikawa Prefecture and has been facing to high COD value, a simple indicator of organic pollution, of lake water. This study analyzed organic matter content in a sediment core with time scale and discussed factors controlling COD value. Sedimentation rate estimated from depth profile of $^{210}Pb_{ex}$ is divided into three periods such as present-1989, 1989-1959 and 1959-past. TOC flux at the present is five times higher than that of 1959. The TOC/TN molar ratio decreased from 15.7 to 12.8. These results suggest that accumulation of total organic matter increases but the contribution of terrestrial organic matter and phytoplankton relatively varies with time.
Keywords – ^{210}Pb, TOC, $\delta^{13}C$

I. INTRODUCTION

Lake as closed water area is likely to deposit pollutant because of its hydraulic characteristics. Therefore, it is not easy to improve water quality deteriorated. Chemical oxygen demand (COD) is used as a simple indicator of organic pollution in lake. The organic pollution is related to the direct load of organic matter from lake basin and the indirect load of organic matter produced by phytoplankton in lake. In order to facilitate water quality conservation, we evaluate concentration and characteristics of organic matter and its origin in lake.

This study was intended for Lake Kiba, because the lake ranked in the worst two of COD in Japanese lakes in 1990 and remains still high concentration level of COD (ca. 6 mg/l). The purpose of this study is to understand factors controlling variations in COD concentration of lake waters. We collected a sediment core sample and measured total organic carbon (TOC), total nitrogen (TN), carbon and nitrogen isotopic ratio ($\delta^{13}C$ and $\delta^{15}N$) to investigate variation of organic matter accumulation at the lake sediments because sedimentary organic matter recorded lake water environment during the period of past to present.

II. STUDY SITE AND MERHODS

Lake Kiba is located in Ishikawa Prefecture and has surface area of 1.44 km^2 with an average water depth of 2.2 m. Major inflow rivers are Hiyou River, Bou River and Yamashiro River. There are a number of drainage channels from paddy field. Outflow water from the lake is only Mae River.

A sediment core was collected in June 2012 with a HR-type corer at the center of lake. The collected core sample was cut into 1 cm interval at 0-10 cm depth in core and 2 cm interval below 10 cm depth. After the samples were freeze-dried, $^{210}Pb_{ex}$ was measured by gamma spectrometry. Sedimentation rate was estimated using constant rate of supply (CRS) model for the $^{210}Pb_{ex}$ profile. Total organic carbon (TOC) and total nitrogen (TN) were measured with an elemental analyzer after HCl treatment of sediment samples. $^{13}C/^{12}C$ and $^{15}N/^{14}N$ ratios were measured using mass spectrometer and expressed as $\delta^{13}C$ and $\delta^{15}N$, respectively.

III. RESULTS AND DISCUSSIONS

$^{210}Pb_{ex}$ activity in the sediment core gradually decreased from 0 to 8 cm depth in core, and was nearly constant from 8 to 14 cm, but rapidly decreased from 14 to 26.7 cm (Fig. 1a). The sedimentation rate is 0.15 g/cm^2/y at 0-8 cm depth and 0.05 g/cm^2/y at 14-26.7 cm depth. The changes of sedimentation rate occurred in 1959 and 1989. The sedimentation rate in recent years has been three times faster than in the past. This indicates that environmental change in the basin has occurred.

TOC flux ranges from 4.3 to 7.5 in the depth interval of 0-8 cm, 2.0 to 3.9 at 8-14 cm and 0.7 to 1.8 at 14-20 cm (Fig. 1b). This result shows increases in the accumulation of organic matter in the lake. The C/N molar ratio decreased from 15.7 to 12.8 towards the current, and $\delta^{13}C$ showed some variation (Fig. 1c). This result suggests ɔntribution of phytoplankton relatively increased rather an terrestrial organic matter during 1959-present.

These results suggest that organic matter supply from e lake basin and primary production in the lake increased ɔm 1959. This may be related to the changes in lake basin ıvironment and the increases of COD value in Lake Kiba.

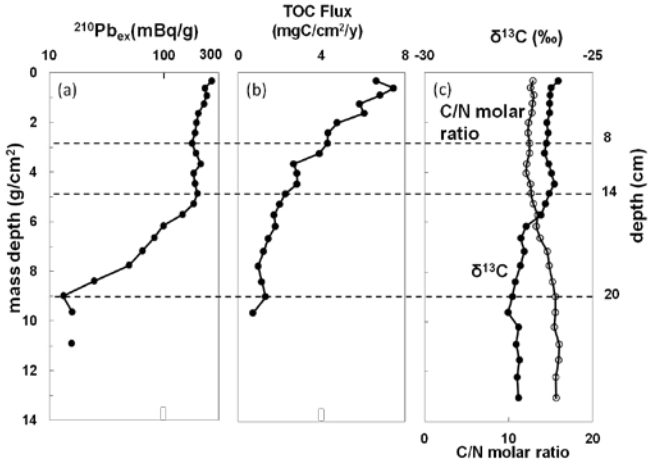

Figure1 The depth profile of $^{210}Pb_{ex}$ content (a), TOC flux (b) and C/N molar ratio and $\delta^{13}C$ (c).

Rapid monitoring particulate Radiocesium with nonwoven fabric cartridge filter and application to field monitoring

Hideki TSUJI[1], Yoshihiko KONDO[2], Shoji KAWASHIMA[2], Tetsuo YASUTAKA[1]
[1] National Institute of Advanced Industrial Science and Technology
[2] Japan Vilene Company. Ltd.

Abstract

A method for rapid monitoring particulate radiocesium using a nonwoven fabric cartridge filter was developed, which needs no further preprocessing before served to a detector. By a performance test, more than 98% of suspended solid (SS) was collected. This method showed the same radioactivity measurement accuracy as filtration by membrane filter and more rapid extraction capability of SS.

Keywords – radiocesium, nonwoven fabric filter, suspended solid

I. INTRODUCTION

The monitoring of dissolved and particulate radiocesium in environmental waters became important after the accident of TEPCO Fukushima Daiichi Nuclear Power Plant. Our research group has developed a monitoring method to investigate the radiocesium concentration in water by each existence form. Yasutaka et al. (2013) developed a method to absorb 90% of dissolved ^{137}Cs in 20 L water within 10 minutes using Prussian blue impregnated nonwoven fabric. Minami et al. (2013) set monitoring device onto paddy fields and more than 99% of dissolved ^{137}Cs in 400 L water was absorbed within 24 hours. In this study, a method for monitoring particulate radiocesium using nonwoven fabric cartridge filter was developed. The measurement accuracy and pre-concentration time was compared with a traditional method. Furthermore, environmental water in Fukushima Prefecture was monitored by this method.

II. MATERIALS AND METHODS

The radiocesium on SS was collected by the plain nonwoven fabric in the cartridge (SS-cartridge). This filter was made of polypropylene fibers with a pore size of 1 μm. The performance of the cartridges was examined using the simulated river water, which contains ^{137}Cs (4,340 Bq/kg-SS). The SS in water was set at 10 and 100 mg/L. Water samples were pumped through SS-cartridge at a rate of 2.5 L/min. The SS weight collected in the cartridge was calculated by the weight gain of SS-cartridge. The concentration of ^{137}Cs in SS –cartridge was measured by a Ge semiconductor detector. The geometric efficiency of SS-cartridge was calculated by dividing the detected ^{137}Cs radioactivity by the actual ^{137}Cs radioactivity in the cartridge, which is determined from the collected SS weight and the concentration of particulate ^{137}Cs. In addition, the maximum amount of SS weight in the SS-cartridge was determined by passing water with 1,000 mg/L of SS.

Next, this method was also applied to measure particulate ^{137}Cs concentration of environmental water in Fukushima Prefecture for testing field applicability. The river water of 20-100 L was pumped through the SS-cartridge. The detected SS concentrations and ^{137}Cs concentrations in SS-cartridge were compared with those filtrated with a 0.45 μm membrane filter in laboratory.

III. RESULTS

In the result of performance test, all SS in the water was collected in the cartridge for all experiments. The geometric efficiency of the cartridge was 0.71 on average (the S.D. was 0.07) and the recovery rates of ^{137}Cs, determined by dividing the detected ^{137}Cs by the geometric efficiency was calculated as Fig.1

This cartridge could hold 30 g SS under 0.2 MPa flow pressure. For the field performance test, concentrations of both SS and ^{137}Cs filtrated by two methods showed almost the same results in the samples from all locations except point E (Fig.2). In contrast to almost one day by the membrane filtration, only 10 min is needed for 20 L water filtration by this SS-cartridge method.

This study was supported by the budget (the development of systems and technology for advanced measurement and analysis) from Japan Science and Technology Agency.

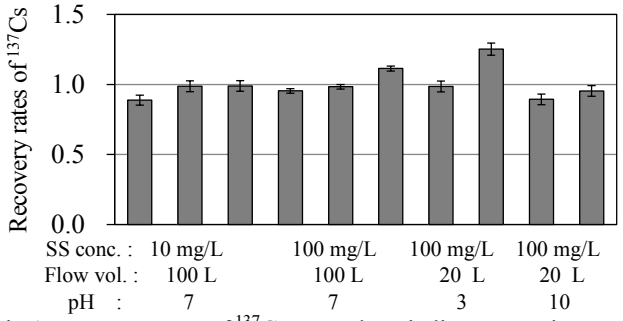

Fig.1 Recovery rates of ^{137}Cs. Error bars indicate counting error.

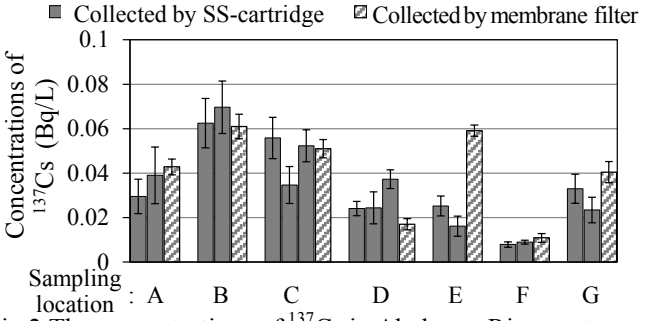

Fig.2 The concentrations of ^{137}Cs in Abukuma River water. Error bars indicate counting error.

[1] Yasutaka et al.(2013), *Appl. Chem.* (in Japanese), in press
[2] Minami et al.(2013), *Abstract of APSORC13*

In-situ measurement of ^{134}Cs and ^{137}Cs in seabed by underwater γ-spectrometry systems and application for the survey to the Fukushima Dai-ichi NPP accident

Hisaki KOFUJI
Japan Marine Science Foundation, Minato-Machi, Mutsu, Aomori, 035-0064 Japan

Abstract –

Underwater γ–spectrometry systems (Mooring and Towing system) with NaI(Tl) detector were applied to in-situ measurement of radiocesium in seabed derived from the Fukushima Dai-ichi Nuclear Power Planr(FDNPP) accident. Radiocesium concentration was calculated from towing system data with short integrated time (2–5 min) by the separating method of the γ–ray counts to 4 contributions (^{134}Cs+^{137}Cs, ^{40}K, U series and Th series nuclides) using 4 x 4 matrix. Concentration of ^{134}Cs+^{137}Cs in sediments located about 80 km north from the FDNPP was calculated to be 150–200 at muddy site and 5-25 Bq/kg-dry at sandy site, respectively.

Keywords – In-situ γ–ray measurement, Sea Sediment, ^{134}Cs, ^{137}Cs, Fukushima Dai-ichi NPP accident

I. INTRODUCTION

Large amount of radionuclide were released to environment by the FDNPP accident on March 11, 2011. In contrary to the gradual decrease of radiocesium concentrations in seawater after the FDNPP accident, high levels of radiocesium have remained in sea sediments around the FDNPP. We applied underwater γ-spectrometry systems to measurement of radiocesium in seabed derived from the FDNPP accident.

II. SYSTEM AND METHOD

Two underwater γ–spectrometry systems with 3" ϕ spherical NaI(Tl) detector were applied to in-situ measurement on seabed. Mooring system: log the temporal variation of radiation on seabed. Towing system: monitor the spatial distribution of radiation on seabed with underwater movie, depth, temperature, salinity in real time from a boat. Both of the systems are small (15–20 kg), it can be lifted and retrieved by human hand from a boat (Fig. 1).

These systems were operated at 2 sites in coastal area (37–38 m depth) located about 80 km north from the FDNPP on September 6–7, 2012. The sediments are muddy at St. A and sandy at St. B, respectively. For mooring system, it was taking down to the seabed and recover after 2 hours. For towing system, it was towed slowly (1 knot) during about 15 minutes on seabed, and next measured during 1–2 hours at one position. Surface sediments were also collected in each site and analyzed the density and water content.

γ–ray spectrum data were separated to 4 contributions (^{134}Cs+^{137}Cs, ^{40}K, U series and Th series nuclides) by 4 x 4 matrix. Parameters of the matrix were obtained from calculated γ–ray spectrum for radionuclides in sediment and seawater by Monte Calro simulation with EGS5 code [1].

III. RESULTS AND DISCUSSIONS

Radiocesium derived from the FDNPP accident was detected in sediment by both systems (Fig. 2) and the posture of towing system on seabed was stable during towing. These underwater γ–spectrometry systems were confirmed to be available to survey radiocesium contamination in seabed.

Radiocesium concentration could be calculated from short integrated time data (2–5 min) with small γ–ray counts by using 4 x 4 matrix. Assuming homogeneous distributions of ^{134}Cs and ^{137}Cs in 0–10 cm depth of sediment, the ^{134}Cs+^{137}Cs concentrations in sediment were calculated from data by towing system to be 150–200 Bq/kg-dry at muddy site (St. A) and 5–25 Bq/kg-dry at sandy site (St. B), respectively.

This work was performed with grant-in-aid from Watanabe Memorial Foundation for The Advancement of New Technology.

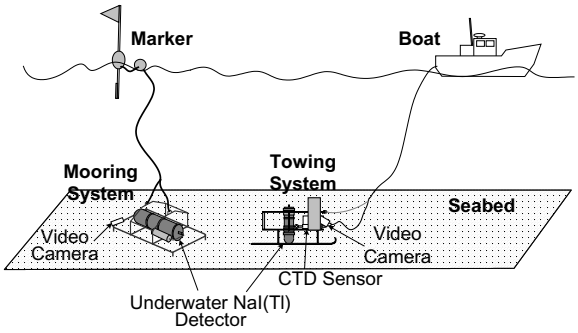

Fig. 1 Illustration of field operation of underwater gamma-ray spectrometry systems (mooring and towing system).

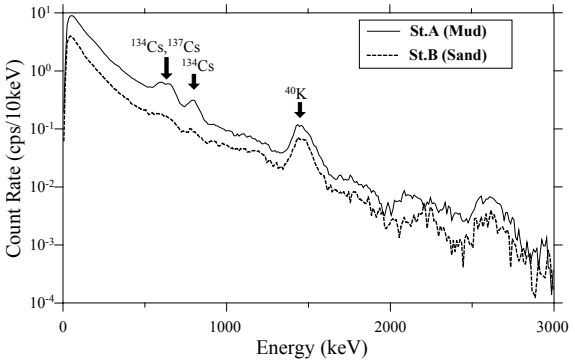

Fig. 2 γ–ray spectrum measured on seabed by towing system. (1h integrated data)

[1] Hirayama, H., et. al, 2005, The EGS5 Code System, SLAC-R-730 and KEK Report 2005-8

Radiocarbon dating of molluscan shells and its application

Yoshiki MIYATA[1, 2, 3], Hiroyuki Matsuzaki[2]

[1] The Low Level Radioactivity Laboratory (LLRL), Institute of Nature and Environmental Technology, Kanazawa University, Ishikawa 923-1224, Japan

[2] The College of Liberal Arts, International Christian University, 181-8585, Tokyo, Japan

[3] National Museum of Japanese History, 285-8502, Chiba, Japan

[4] Department of Nuclear Engineering and Management, School of Engineering (MALT), The University of Tokyo, 113-0032, Tokyo, Japan

Keywords – Radiocarbon dating; Marine reservoir effect; Molluscan shell; Marine reservoir correction value (ΔR); Sea Current

We investigated radiocarbon age differences among marine shells, terrestrial animal and marine fish bones, charred wood fragments and charred seeds from layer IV, at the Higashi michi no ue (3) archaeological site, Japan, which was occupied during the first half of the early Jomon period (3900-3750 cal BC) as shown in Table 1.

We attributed the differences to marine reservoir effects, which differed among these organisms because of differences in their habitats and diets. The ages of Corbicula japonica, Crassostrea gigas and Ruditapes philippinarum (molluscan shells) show 180 yrs, 270 yrs and 450 yrs older than the radiocarbon age of the charred wood fragments, which corresponded to the actual age of the excavated archaeological site, respectively (Fig.1). This shows the habitats of these molluscan shells change from fresh to oceanic water, so that the salinity of the habitats of these molluscan shells gradually increases into the level of the sea water.

According to the age of Ruditapes philippinarum, the marine reservoir correction value (ΔR) for the Tsugaru Warm Current, which flows around Shimokita peninsula, is 80 ± 41 ^{14}C years (N = 2). The radiocarbon ages were, in an increasing order, charred wood fragments, charred seeds ~ terrestrial animal bones (deer) < marine molluscan shells ~ marine fish bones < charred materials on potsherds. The different reservoir effects thus reflect difference in the diets or habitats of the shellfish, marine fish, and charred materials on potsherds found at the site.

This work was partly supported by a Grant-in-Aid for Young Scientists (B) No. 18700679 (Y.M.), Creative Scientific Research No.16GS0118 (T.N.) and Scientific Research (B) No.25282072 (Y.M.) of the Japan Society for the Promotion of Science.

Table 1. Radiocarbon ages of marine shells, charrd seeds, charred woods, animal bones, marinefishes and carbonized materials adhering to pottery excavated from the Higashi michi no ue (3) archaeological site.

Sample #	Lab code	Sample name (*Binomial name*)	^{14}C age (±σ) BP	R (±σ)*1 ^{14}C yr	ΔR (±σ)*2 ^{14}C yr
AOKH S8	MTC-7412	Japanese walnut (*Juglans mandshurica var. sieboldiana*)	4910 ± 30	-	-
AOKH C6	MTC-7410	Charred wood	5005 ± 35	-	-
AOKH B11	PLD-6043	(wild) boar (*Sus scrofa*)	4920 ± 30	-30 ± 38	-409 ± 36
AOKH K17	MTC-7444	Corbicula japonica*3 (*Ruditapes philippinarum*)	5210 ± 150	260 ± 152	-119 ± 151
AOKH K17	MTC-7565	Corbicula japonica*3 (*Ruditapes philippinarum*)	5140 ± 60	190 ± 64	-189 ± 63
AOKH K16	MTC-7443	Oyster (*Crassostrea gigas*)	5230 ± 60	280 ± 64	-99 ± 63
AOKH K15	MTC-7442	Japanese little neck*3 (*Ruditapes philippinarum*)	5380 ± 60	430 ± 64	51 ± 63
AOKH K15	MTC-7562	Japanese little neck*3 (*Ruditapes philippinarum*)	5430 ± 50	480 ± 55	101 ± 54
AOKH B13	PLD-6045	Japanese seabass (*Lateolabrax japonicus*)	5425 ± 25	475 ± 34	96 ± 32
AOKH 3	MTC-7408	Charred material from inner surface of potsherd	5505 ± 35	555 ± 42	176 ± 40

Measuremet errer is 1σ.

*1 R was subtracted from the average age of Japanese walnut and charred wood (4950±23 BP), excavated from the Higashi michi no ue (3) site.

*2 ΔR was subtracted form the marine model ^{14}C age (5329±20 BP), which corresponded to the age of the charred wood (4950±23 BP; 3766-3696 cal BC (68.2%)).

*3 Each same individuals of Corbicula japonica and Japanese little neck were measured twice.

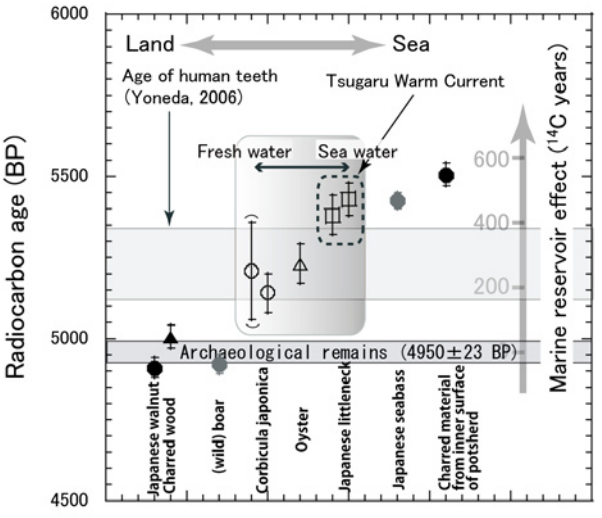

Fig. 1. Radiocarbon ages of archaeological remains from Higashi michi no ue (3) archaeological site.

Concentration of Uranium on TiO-PAN and NaTiO-PAN Composite Absorbers

Alois Motl, Ferdinand Šebesta, Jan John, Irena Špendlíková, Mojmír Němec
Czech Technical University in Prague, Department of Nuclear Chemistry, Brehova 7, 115 19 Prague, Czech Republic

Abstract

Inorganic ion exchangers have been extensively tested for use in separation and concentration of uranium from surface water. Except for separation of uranium from uranium-contaminated waste water (e.g. waste water from mining and milling of uranium, waste from nuclear fuel reprocessing) their main area of application has been foreseen to be their use for extraction of uranium from sea water which could partially cover future needs of uranium. Another perspective area of application is pre-concentration of uranium from natural waters followed by uranium determination via various specialized techniques such as TRLFS or AMS.

Possibilities of uranium extraction from sea water have been subject of several international conferences (e.g. Topical meetings on the Recovery of Uranium from Seawater in 1980's, ACS National Meetings 2012 etc.) and are critically evaluated in a review by Bitte [1] or recently by Kim [2]. In the Czech Republic uranium-selective inorganic ion exchangers might be applied for treatment of various wastes from uranium industry, namely underground water, uranium milling over-balance water, or acid waste water from underground uranium leaching and also like in other countries for determination of uranium isotopic composition focusing on anthropogenic and natural ^{236}U content.

Among the best performing inorganic ion exchangers for the above listed purposes hydrated titanium dioxide (abbreviated as TiO) and sodium titanate (abbreviated as NaTiO) can be listed. Properties of TiO and NaTiO were reviewed by Lehto [3]. From the point of view of ion-exchange, properties of hydrated titanium oxide and sodium titanate are very similar. The main disadvantage of these ion exchangers for industrial-scale application is their insufficient mechanical stability [1]. To improve this property, the sorption materials can be embedded into a binding matrix.

Modified polyacrylonitrile (PAN) has been proposed at the Czech Technical University in Prague as a universal binding matrix for finely divided inorganic absorbers. The general procedure for the preparation of the resulting inorganic-organic composite absorbers enables preparation of suitably grained composite absorbers [4]. The contents of active component may reach up to 90 % (w/w) in dry residue.

The aim of this study was to verify possibility of extraction of uranium with TiO-PAN and NaTiO-PAN composite absorbers, to compare properties of these two absorbers and to conclude whether they are prospective for uranium collection from surface and/or waste waters.

Hydrated titanium oxide (TiO) and sodium titanate (NaTiO) - the active components of the composite materials - were prepared from industrial intermediate from production of titanium white. Standard procedure was used to prepare the TiO-PAN and NaTiO-PAN composite absorbers [4]. In the experiments, distilled and tap water were used to compare the influence of the water hardness. pH of the effluent was also measured during the process.

The results showed that practical sorption capacity (10% break-through) from tap water containing 2.3 μg $U.mL^{-1}$ measured at flow rate of 100 $BV.h^{-1}$ was ~ 4.6 mg and ~ 1.5 mg of uranium per ml of swollen TiO-PAN and NaTiO-PAN absorber, respectively. The maximum flow rates are 60 $BV.h^{-1}$ and 60-100 $BV.h^{-1}$ for TiO-PAN and NaTiO-PAN absorbers, respectively, depending on the concentration of uranium (2.3 - 230 mg $U.L^{-1}$). Elution of uranium and regeneration of the absorber may be accomplished by 0.1 $mol.L^{-1}$ or stronger solutions of hydrochloric acid for both the absorbers.

Hence, TiO-PAN and NaTiO-PAN composite absorbers were proved to be applicable for extraction of uranium from aqueous solutions. With respect to the measured practical sorption capacity, TiO-PAN composite absorber is more suitable for the uranium collection from surface and/or waste water.

Keywords

Uranium extraction, TiO-PAN, NaTiO-PAN, composite absorber, fresh water

[1] Bitte J (1985) Advances in Uranium Ore Processing and Recovery from Non-Conventional Resources. IAEA-TC-491/18. IAEA, Vienna, 299

[2] Kim J, Tsouris C, Mayes RT, Oyola Y, Saito T, Janke CJ, Dai S, Schneider E, Sachde D (2013) Separ Sci Technol 48: 367-387

[3] Lehto J (1987) Sodium Titanate for Solidification of Radioactive Wastes - Preparation, Structure and Ion Properties. Academic Dissertation, University of Helsinki. Report Series in Radiochemistry 5/1987

[4] Šebesta F (1997) J Radioanal Nucl Chem 220: 77-88

USE OF RADON TO CHARACTERISE SURFACE WATER RECHARGE TO GROUNDWATER

N Hermanspahn,[1] M Close,[1] M Matthews,[1] L Burbery,[1] P Abraham,[1]
[1] Institute of Environmental Science and Research (ESR), Christchurch

Aims

Many groundwater systems in Canterbury and other parts of New Zealand gain a significant amount of recharge from rivers. This recharge provides significant storage of water within the groundwater system and it is used for many purposes, including domestic and stock water supply, irrigation and industrial use. There is significant uncertainty in the amounts of recharge from rivers, particularly large braided systems, as river flow gauging can only be carried out under low flow conditions and measurement errors are large.

Radon-222 is present in a dissolved state in groundwater from alluvial greywacke gravel aquifers in sufficient concentration to be easily detectable (10 – 50 Bq/L) while, in contrast, concentrations in surface water are close to zero (Gregory, 1980). This difference provides a means of distinguishing surface recharge water from groundwater. Surface water infiltrating into groundwater should initially contain negligible radon, but would start accumulating radon as it flows through the aquifer, reaching equilibrium in approximately 6 half-lives ($T_{1/2}$ = 3.82d). In addition to providing a tracer for surface water, this radon ingrowth also allows flow-rate estimation as the radon concentration increases with time at a known rate. The use of radon to estimate recharge of surface water into a groundwater system has been applied at a site in Switzerland (Hoehn & von Gunten, 1989).

The investigation of radon to estimate recharge from rivers to groundwater systems is presented using a relatively well-characterised reach of the Waimakiriri River in Canterbury to assess the potential for this method.

Methods

A reach from the Waimakariri River near McLeans Island just north of Christchurch, was selected as the study site. The river is known to lose water from this reach and there are a number of shallow wells close to the river that are suitable for sampling in this area. Two groups of wells were selected for sampling. The first group of wells was near the river and located at increasing distances from the river. Environment Canterbury had installed 22 wells in 2 arrays at Halketts and Crossbank to study river recharge to groundwater. These wells were sampled on 2-3 occasions. The second group of wells that were sampled were located remote from recent recharge from the river but screened in a similar groundwater environment. This group of wells provide an estimate of equilibrium radon concentrations and the likely variability within an alluvial gravel groundwater system.

Results

The results indicate that radon levels in the river are very low and concentrations increased with increasing distance from the river. These results are consistent with radon ingrowth processes and the site hydrology.

The eleven wells from the Crossbank array and eleven wells from the Halketts array were sampled, along with water from the Waimakariri River, at both high and low flows to determine any variation of radon concentrations with flow. There was no significant variation in radon concentration with flow in the Waimakariri River ranging from 50 to 250 m^3/s. The data were modelled using the "in-growth equation" for radon to determine values for the equilibrium radon value and groundwater velocity. The groundwater velocities were 350 and 390 m/day for the Halketts and Crossbank sites, respectively. These velocities are very high but possible near a large braided river.

Estimates of recharge to groundwater over a 20km reach using this information were similar to estimates derived from a water balance approach with the largest source of error being estimates of the effective porosity of the groundwater system.

References

Gregory, L.P. 1980. Radioactivity of potable waters: Country-wide survey in New Zealand. NRL report 1980/4. 19 p.

Hoehn, E.; von Gunten, H.R. 1989. Radon in Groundwater: A tool to assess infiltration from surface waters to aquifers. Water Resources Research 25: 1795-1803.

APSORC'13 - 5th Asia-Pacific Symposium on Radiochemistry
Kanazawa, Japan, 22-27 September 2013

Production and Utilization of Radioactive Astatine Isotopes in the $^{7}Li+^{nat}Pb$ Reaction

I. Nishinaka[1], A. Yokoyama[2], K. Washiyama[2], R. Amano[2], E. Maeda[2], N. Yamada[2], H. Makii[1], A. Toyoshima[1], S. Watanabe[1], N. S. Ishioka[1], K. Hashimoto[1]
[1]Japan Atomic Energy Agency (JAEA)
[2]Kanazawa University

Abstract – Production cross sections of astatine isotopes in 29-57 MeV $^{7}Li+^{nat}Pb$ reaction have been measured by α- and γ-ray spectrometry. Excitation functions of production cross sections have been compared with a statistical model calculation to study the reaction mechanism of the $^{7}Li+^{nat}Pb$ reaction. A chemical separation of astatine from an irradiated lead target has been studied with a dry-distillation method.

Keywords – Astatine, Cross section, Excitation function, Chemical separation, Dry-distillation

I. INTRODUCTION

An α radioactive nuclide ^{211}At with a half-life of 7.2 h is a prospective candidate for utilization in targeted alpha radiotherapy. In general, ^{211}At is produced through bombardment of a bismuth target with 28 MeV helium ions in the $^{209}Bi(\alpha,2n)^{211}At$ reaction [1]. However, the nuclear reactions using lithium ion beams, $^{6,7}Li+Pb$, Bi, provide the possible production routes of ^{211}At. Excitation functions have been extensively measured for the $^{6,7}Li+^{209}Bi$ to study the reaction mechanism involving complete fusion and breakup reaction for weekly bound nuclei $^{6,7}Li$ [2-4]. For $^{7}Li+^{nat}Pb$, however, only reports on production of astatine isotopes $^{207-210}At$ have been available [5]. Therefore, we have measured excitation functions of $^{207-211}At$ isotopes in the reaction of 29-57 MeV $^{7}Li+^{nat}Pb$. Besides, a chemical separation of carrier-free radioactive astatine isotopes from an irradiated lead target has been studied with a dry-distillation method.

II. EXPERIMENT

Lead targets with thickness of 0.78-1.47 mg/cm^2 were prepared with vacuum evaporation onto a backing sheet of aluminum. Each target was sandwiched between the backing and a cover sheet of 2.7 or 5.4 mg/cm^2 of aluminum. Six sets of the bismuth target, the backing and the cover sheet were irradiated with $^{7}Li^{3+}$ beams of 50 and 60 MeV from the 20 MV tandem accelerator at JAEA-Tokai. Activities of $^{207-210}At$ were determined by γ-ray spectrometry to obtain production cross sections of $^{207-210}At$. Details of irradiation and γ-ray spectrometry are described in [6].

The sample used for γ-ray spectrometry which consists of the lead target on the backing and the cover sheet was placed in a test tube with length of 18 cm. After sealing the test tube, a third of the portion from the bottom of the test tube was inserted into a furnace. Astatine was distilled at 650˚C for15-40 min. After cooling and opening the test tube and taking the sample from it, the test tube was rinsed with 1.8 ml ethanol, water, or diisopropyl ether. The solution is used for the preparation of a sample for α- and γ-ray spectrometry. The activities of astatine in the solution were measured to obtain production cross sections of ^{211}At and chemical yields in the dry-distillation method.

III. RESULTS

The obtained excitation functions of astatine isotopes in the $^{7}Li+^{nat}Pb$ were rather well reproduced with a statistical model calculation by the HIVAP code [7]; the calculation was independently carried out with the input parameters which systematically well reproduce a large number of experimental fusion-evaporation cross sections in the similar heavy-ion reactions without adjusting the input parameters to fit the present data [8]. Slightly large deviations of experimental data from the calculation are observed at higher incident energies, indicating the effect of breakup reaction of ^{7}Li.

In the α- and γ-spectrometry, only activities of astatine isotopes and their decaying daughters were observed in the samples prepared from the solution which obtained by the dry-distillation method. It shows that carrier free radioactive astatine isotopes were separated from lead targets with high radiochemical purity. Overall recovery yields of astatine in the dry-distillation method were approximately 65% for ethanol and water, and 25% for diisopropyl ether, implying chemical form of carrier free astatine. Using the ethanol solution of astatine, astatinated amino acid derivative was prepared in the high labeling yield, more than 97%, with electrophilic destannylation [9]. It indicates that the dry-distillation method provides carrier free astatine isotopes with high chemical purity.

[1] S, Lindergren, T. Bäch, H. J. Jensen, Appl. Radiat. Isot., 55 (2001) 157-160; S. Lindegren et al., J. Nucl. Med., 49 (2008) 1537-1545.
[2] H. Freiesleven et al., Phys. Rev.C, 10 (1974) 245-249.
[3] M. Dasgupta et al., Phys. Rev. C, 66 (2002) 04602-1-4; M. Dasgupta et al., Phys. Rev. C 70 (2004) 024606-1-20.
[4] Yu. E. Penionzhkevich et al., J. Phys. G, 36 (2009) 025104-1-12.
[5] K. Roy and S. Lahiri, Appl. Radiat. Isot., 55 (2008) 571-576; M. Maiti and S. Lahiri, Phys. Rev. C, 84 (2011) 067601-1-4.
[6] I. Nishinaka et al., JAEA-Review 2011-040 (2011) 50-51
[7] W. Reisdolf and M. Schädel, Z. Phys. A, 343 (1992) 47.
[8] K. Nishio, private communication.
[9] S. Watanabe et al., 7th Int. Sym. On Radiohalogens (7ISR), Sep18th (2012), Whistler, BC

APSORC'13 - 5th Asia-Pacific Symposium on Radiochemistry
Kanazawa, Japan, 22-27 September 2013

Production of actinium-225 from natural thorium irradiated with protons

Aleksandr N. Vasiliev[1], Valentina S. Ostapenko[1], Ramiz A. Aliev[1], Stepan N. Kalmykov[1], Elena V. Lapshina[2], Stanislav V. Ermolaev[2] and Boris L. Zhuikov[2]
[1]Chemisrtry Department, Lomonosov Moscow State University, Leninskie Gory, Moscow 119991, Russia
[2]Institute for Nuclear Research of Russian Academy of Sciences, 60th October Anniversary Prospect, 7a, Moscow 117312, Russia

New procedure for chemical separation and purification of ^{225}Ac from irradiated metallic Th targets for targeted radiotherapy of cancer is described.

Keywords – actinium-225, thorium, extraction chromatography

As a result of irradiation of natural thorium with high-energy protons various fission and activation products of ^{232}Th are formed [1, 2]. Among them ^{225}Ac is formed, which has characteristics that enable to use it in radiotherapy of cancer. There is a growing demand for this radionuclide, while current methods for producing actinium have significant limitations and cannot satisfy it completely. Production of actinium from ^{233}U is limited by its inaccessibility. Actinium-225 may be used either directly for preparation of radioimmunoconjugates or as a mother radionuclide in ^{213}Bi isotope generator. In addition the formation of ^{223}Ra should be noted, which is also a promising α-emitter for medicine.

The aim of this work is to develop the new method of chemical separation and purification of large quantities of ^{225}Ac from metallic Th irradiated with high-energy protons.

Radiochemical separation of Ac and Ra is a difficult task since a high activity of more than 80 other radionuclides have been observed in the gamma- and alpha-spectrum of Th-target after irradiation.

A developed method for chemical isolation of Ac is based on combination of liquid-liquid extraction and extraction chromatography.

Irradiated thorium is dissolved in a mixture of concentrated hydrochloric and nitric acids, or in concentrated nitric acid with the addition of catalytic amounts of hydrofluoric acid.

Tributylphosphate, trioktylphosphinoxide (TOPO) and di(2-ethylhexyl)orthophosphoric acid (HDEHP) are used in extraction experiments. The behavior of radionuclides, depending on the composition of the aqueous phase is studied.

For additional separation of remaining Th AG 1x8 (BioRad) anionite column and extraction chromatographic sorbent TEVA (Eichrom, mixture of trioctyl and tridecyl methyl ammonium chloride as extracting agent) are proposed. Sorption capacity of under experimental conditions (6 M HNO_3) for those sorbents is investigated.

Sorbents DGA Resin (Eichrom), Ln Resin (Eichrom), TRU Resin (Eichrom), TDi-2 (Karpov Institute) are taken for further chromatographic separations. The sorption behavior of radionuclides, depending on the parameters of the column and acidity of solution is given. It is shown that ^{225}Ac quantitatively adsorbed on Ln Resin and TDi-2 (di(2-ethylhexyl)orthophosphoric acid (HDEHP) as extracting agent) from dilute nitric acid (0.05 M HNO_3). Desorption is carried out with acid of higher concentration (3 M). Significant difference in the sorption behavior of ^{225}Ac for Ln Resin and TDi-2 is not observed. In 0.05 M HNO_3 most of the fission products (Cs, Ra, Ba, Ag, Pb), are not retained on the column and are eluted in the first few milliliters. After switching to 3 M HNO_3, actinium and rare earth elements (La, Nd and Ce) and ruthenium are eluted together in the fraction of 3 ml. On DGA Resin (N,N,N`,N` tetroctyldiglicolamide as extracting agent) Ac absorbed from 6 M nitric acid solution and desorbed with dilute nitric acid (0.01 M HNO_3). In this way it is possible to separate actinium fraction from ruthenium, this radionuclide makes some difficulties for the production of final preparation ^{225}Ac.

Actinium is eluted together with cerium and lanthanum. To separate Ac(III) from rare earth elements the eluted 3 ml fraction from Ln or DGA Resin (in 3 M HNO_3) is loaded onto extraction-chromatographic columns filled with TRU Resin (octylphenyl-N,N-di-isobutyl carbomoylphosphine oxide dissolved in TBP as extracting agent).

The possible scheme of separation of ^{225}Ac from the isotopes produced in irradiated thorium target is includes two sequential solvent extractions using HDEHP. After sorption on DGA Resin, for further separation the 3 M nitric acid can be passed through the sorbent TRU Resin. The procedure provides obtaining a pure Ac fraction, containing less than 0.2% ^{227}Ac and no other radionuclides; the chemical yield is 90% or more [3].

[1] S.V. Ermolaev, B.L. Zhuikov, V.M. Kokhanyuk, V.L. Matushko, S.N. Kalmykov, R.A. Aliev, I.G. Tananaev and B.F. Myasoedov. Production of actinium, thorium and radium isotopes from natural thorium irradiated with protons up to 141 MeV, Radiochim. Acta, 100, 1–7, 2012.

[2] B.L. Zhuikov, S.N. Kalmykov, S.V. Ermolaev, R.A. Aliev, V.M. Kokhanyuk, Produce of 225Ac and 223Ra from thorium irradiated with protons, Radiochemistry, 2011, 53, 1, p. 66-72.

[3] B.L. Zhuikov, S.N. Kalmykov, R.A. Aliev, S.V. Ermolaev, V.M. Kokhanyuk, V.M. Kokhanyuk, I.G. Tananaev and B.F. Myasoedov, A method of producing actinium-225 and radium isotopes and targets for its implementation (Options). Patent № 2373589, Russian Federation, 2009.

Development of ^{99}Mo-^{99m}Tc Domestic Production with High-Density MoO_3 Pellets by (n, γ) Reaction

K. Tsuchiya[*1], M. Tanase[*2], T. Shiina[*2], A. Ohta[*2], M. Kobayashi[*3], A. Yamamoto[*3], Y. Morikawa[*3], M. Kaminaga[*1], H. Kawamura[*1]

**1 : Japan Atomic Energy Agency, 4002 Narita, Oarai,Higashiibaraki, Ibaraki 311-1393, Japan*
**2 : Chiyoda Technol Corporation, 3681 Narita, Oarai, Higashiibaraki, Ibaraki 311-1313, Japan*
**3 : FUJIFILM RI Pharma Co. Ltd., 453-1 Shimo-okura, Matsuo, Sammu, Chiba 289-1592, Japan*

Keywords –(n, γ)^{99}Mo production, high-density MoO_3 pellets, solvent extraction, ^{99m}Tc solution, JMT

The renewed JMTR will start rerunning from the later half of JFY2013, and it is expected to contribute to many fields not only developments for nuclear materials, but also the other fields such as medical diagnosis medicine, science and technology for fusion reactor, etc. As one of effective applications of the JMTR, JAEA has a plan to produce ^{99}Mo by (n, γ) method ((n, γ)^{99}Mo production), a parent nuclide of ^{99m}Tc. ^{99m}Tc is most commonly used as a radiopharmaceutical in the field of nuclear medicine. In case of Japan up to now, the supplying of ^{99}Mo depends only on imports from foreign countries. Thus, the (n, γ)^{99}Mo production was selected from viewpoints of safety, nuclear proliferation resistance and waste management and the R&D for domestic production were started in JMTR. The main R&D items for (n, γ)^{99}Mo production are as follows;

(1) Fabrication development of irradiation target for the high-density MoO_3 pellets,

(2) Separation and concentration development of ^{99m}Tc by the solvent extraction from ^{99}Mo/^{99m}Tc solution, and

(3) Examination of ^{99m}Tc solution for a medicine.

In this study, the status of the R&D is presented for the (n, γ)^{99}Mo production. Molybdenum oxide (MoO_3) is the most commonly used chemical form as irradiation target for the (n, γ)^{99}Mo production. The MoO_3 pellet with high sintering density has been developed for large quantity (n, γ)^{99}Mo production, and the trail fabrication tests of MoO_3 pellets were carried out by the plasma sintering method. The solvent extraction method employs MEK to extract ^{99m}Tc from ^{99}Mo/^{99m}Tc solution. The extracted ^{99m}Tc content by the (n, γ)^{99}Mo production is less than that by the (n, *f*) methods and the concentration methods of ^{99m}Tc solution were developed in the ^{99m}Tc extraction devices. In the tests, rhenium (Re) was used instead of ^{99m}Tc because Re and Tc were homologous elements. The R&D will be carried out with foreign organizations using ^{99m}Tc based on the preliminary results with Re in the present work. It is important for medical use to determine detailed specifications of ^{99m}Tc solution. In the preliminary tests with practice solution using Re, chemical purities such as Mo, Al and MEK were measured in the solution and the content of impurities will satisfy the requirement of radiopharmaceuticals. In future, the solvent extraction demonstration tests will be carried out with the irradiated MoO_3 pellets in JMTR.

Preparation of ^{99}Mo–^{99m}Tc by using Spallation Neutron

Y. Hayashi*[1], N. Takahashi[1], K.Nakai[1], H. Ikeda[2], G. Horitsugi[2], T. Watabe[2], Y. Kanai[2], H. Watabe[2], E. Shimosegawa[2], Y. Miyake[2], J. Hatazawa[2], M. Fukuda[3], K. Hatanaka[3], K. Takamiya[4], S. Yamamoto[5],
Y. Kasamatsu[1] and A. Shinohara[1]

[1] Graduate School of Science, Osaka University
[2] Graduate School of Medicine, Osaka University
[3] Research Center for Nuclear Physics, Osaka University
[4] Kyoto University Research Reactor Institute
[5] Graduate School of Medicine, Nagoya University

Abstract – We developed the method for preparation of ^{99m}Tc used for diagnostic radiopharmaceuticals. We produced ^{99}Mo, the mother nuclide of ^{99m}Tc, by the ^{100}Mo(n,2n)^{99}Mo reaction using the spallation neutron which was produced by 400 MeV proton from a ring cyclotron. The ^{99m}Tc was extracted with methyl ethyl ketone and purified with an aluminum column. Furthermore, we demonstrated the bone scintigraphy by injecting ^{99m}Tc-MDP into the rats.

Keywords – ^{99m}Tc, ^{99}Mo, Spallation neutron, Methyl ethyl ketone (MEK), Aluminum column

I. INTRODUCTION

The ^{99m}Tc is one of most important radioisotopes used for diagnostic radiopharmaceuticals today. The most of those are made with the several nuclear reactors in the world. However, all those reactors using highly enriched ^{235}U fuel are aged more than 50 years, their deteriorations are anticipated and many alternative methods were explored for the production of ^{99m}Tc, as the ^{100}Mo(*p, 2n*)^{99m}Tc and ^{100}Mo(*p, d*)^{99}Mo reactions. In our previous work, we tested to produce ^{99m}Tc with spallation neutron by the ^{100}Mo(*n, 2n*)^{99}Mo reaction which has larger cross section than the proton induced reactions. The radioactivity of ^{99}Mo produced was 3MBq/(μA h g) and this result suggested that enough radioactivities of ^{99}Mo for the medical use can be obtained with this method. However, the specific activity of ^{99}Mo produced by an accelerator is very low, ^{99m}Tc cannot be separated by the conventional alumina and PZC columns. In this work, we separated ^{99m}Tc from macro amount of natural Mo by the solvent extraction with methyl ethyl ketone (MEK) and further purified it with the aluminum column. In addition we demonstrated the bone scintigraphy with the purified ^{99m}Tc as a preclinical test.

II. EXPERIMENTAL

We performed separation of ^{99m}Tc by the previously mentioned method using commercial ^{99m}Tc and macro amount of ^{nat}Mo and examined the purity of the ^{99m}Tc first. We prepared the Mo and ^{99m}Tc mixture by dissolving 40 g of $^{nat}MoO_3$ and 60 MBq of commercial ^{99m}Tc solution with 120 mL of 4 M sodium hydroxide solution. The ^{99m}Tc nuclide was extracted with 15 mL of MEK from macro amount of natural Mo. After the evaporation of the MEK solution under reduced pressure, the sample was dissolved with a few ml of saline. The solution was passed through the neutral aluminum column to remove the Mo species by adsorbing them on the column. Amount of impurities in the ^{99m}Tc solution were measured with ICP-MS and yield of ^{99m}Tc was determined by gamma-ray measurement using a germanium semiconductor detector. Furthermore, the purified ^{99m}Tc was labeled into MDP and injected into a rat. We determined the labeling efficiency of ^{99m}Tc-MDP using a silica-gel-coated thin layer chromatography plate. We took the bone scintigraphy of the rat using a gamma camera [1].

III. RESULTS & DISUCUSSION

As the results of measurement with ICP-MS, we found that only less than 10 ppb of Mo and Al coexist in the purified ^{99m}Tc solution. No other impurities were detected and this solution satisfied the demand of the United States Pharmacopeia (USP). The yield of ^{99m}Tc was 75-90% and the volume was only 5 mL. The labeling efficiency of the ^{99m}Tc-MDP was higher than 99%, well above the USP requirement (>90%).We obtained the bone scintigram which is not different from that obtained using commercial ^{99m}Tc as shown in Fig.1. Thus, it is thought that this separation technique is available for preparation of ^{99m}Tc. We have plan to separate ^{99m}Tc from ^{99}Mo produced by the ^{100}Mo(*n, 2n*)^{99}Mo reaction and to demonstrate the bone scintigraphy. In this presentation, we will also report the results of these experiments.

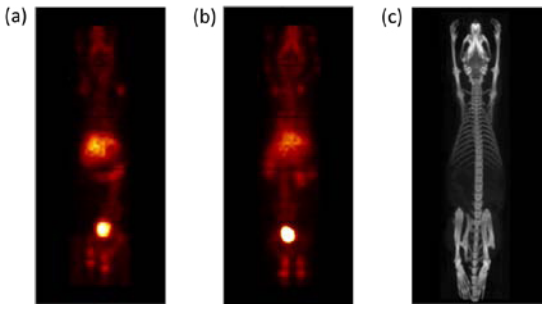

Fig.1 Bone scintigram by injecting with ^{99m}Tc-MDP into the rat (a: purified ^{99m}Tc, b: commercial ^{99m}Tc, c:CT image)

[1] S Yamamoto et al., Med Phys. 39. 581. 8. (2012)

Development of Automated Measurement System for Radioactive Intensities of Sealed Small Radiation Sources (Iodine-125 Seed Source) for Brachytherapy

M. Sakama,[1,*] H. Ikushima,[2] T. Saze,[3] Y. Nagano,[4] T. Yamada,[5] T. Ichiraku,[5] H. Takai,[5] Y. Kuwahara,[6] and S. Nakayama[7]

[1]*Department of Radiological Science (also Advanced Radio-Analytical Chemistry, Division of Biomedical Information Sciences, Institute of Health Biosciences, The University of Tokushima,Tokushima 770-8509, JAPAN*
[2]*Department of Radiation Therapy Technology, Division of Biomedical Information Sciences, Institute of Health Biosciences, The University of Tokushima,Tokushima 770-8509, JAPAN*
[3]*Otsuka Pharmaceutical Factory, Naruto,Tokushima 772-8601, JAPAN*
[4]*Department of Radiological Science, Division of Biomedical Information Sciences, Institute of Health Biosciences, The University of Tokushima,Tokushima 770-8509, JAPAN*
[5]*Dairyu Co. Ltd., Anan,Tokushima 774-0045, JAPAN*
[6]*Radioisotope Center, The University of Tokushima,Tokushima 770-8503, JAPAN*
[7]*Department of Nuclear Science, Institute of Socio-Arts and Sciences, The University of Tokushima,Tokushima 770-8502, JAPAN*

We have developed full automated measurement system for radioactive intensities of sealed small radiation sources (iodine-125 seed source) for brachytherapy in this work. Today, quality assurance (QA) of I-125 seed radioactive sources for brachytherapy following AAPM (American Association of Physicists in Medicine) Society's guideline is one of important subjects for hospitals that operate on patients for prostate cancer and medical companies that manufacture and sell these radioactive sources. In order to survey defective seed products into all the number of I-125 seed sources (there are usually fifteen seeds, one seed of dimensions is 0.8 mm ϕ $\times$ 4.5 mm length) within a cartridge, we have applied the method of single slit collimator with moving a radiation detector to measure each radioactive intensity of these I-125 seeds. As a result, it was found that our developed system in the present work has good performance of surveying the defective products manufactured with radioactive intensities out of about $\pm$ 15% error ($p < 0.05$).

I. INTRODUCTION

Today, there is no doubt about increasing in the patient population of prostate cancer year after year. Since the authorization from the Ministry of Health, Labor and Welfare in 2003, a brachytherapy using I-125 seeds has been one of most effective therapies of primary and middle stages of prostate cancer in Japan, and all the number of annual clinical operations in Japan has been probably reached to about 3,500 in 2012. In terms of safety management on quality assurance (QA) for the brachytherapy, such kinds of the guidelines stated from AAPM Society [1] and JASTRO (Japanese Society for Therapeutic Radiology and Oncology) have recommended that each radioactive intensity of I-125 seed sources should be appropriately surveyed before the therapy of prostate cancer. However, in fact, there are only a few facilities such as surveying the radioactive intensity of I-125 seed source in Japan. It should be seemed that additional works such as QA make radiologic workers in hospital bothered due to time consuming and also exposed due to operations of these radioactive sources using a dose meter like an ionization chamber. The purpose of this work is to develop full automated measurement system for radioactive intensities of I-125 seed source to comply with the demands of medical workers.

II. MATERIALS AND METHODS

The system has external dimensions of 600 mm width $\times$ 700 mm depth $\times$ 850 mm height and consists of a cartridge holder, NaI scintillation survey meter and drive mechanism, and a data analysis module. The survey meter is set behind a copper and stainless steel plate containing a slit (0.1 mm thickness). Radioactivity of the seeds within a cartridge is measured by the survey meter that is moved slowly (0.1 mm/sec) in front of the cartridge by the drive mechanism. The survey meter detects gamma rays passing through the slit in the plate. By keeping the seeds inside the cartridge, their individual activities can be measured while maintaining a sterile state.

FIG. 1. Photograph view of our developed system (BSQAS-2).

III. RESULTS

The system can automatically complete the activity measurement of all seeds contained inside 4 cartridges in less than 15 minutes, with about 15% of errors to detect miss-calibrated seed. This system enables us to survey the defective products manufactured with radioactive intensities out of about $\pm$ 15% error ($p < 0.05$).

IV. CONCLUSIONS

A full automatic measurement system of I-125 seed activity shows reliable precision and usability. Future development will include support for other source delivery methods parallel to efforts in reducing the size of the system.

[1] AAPM, MED. PHYS. **26**(10), 2054-2076 (1999).

* Corresponding author, electronic address: sakama@medsci.tokushima-u.ac.jp, *or,* minorusakama@tokushima-u.ac.jp

Extraction of astatine isotopes for development of radiopharmaceuticals

E. Maeda[1], A.Yokoyama[2], T. Taniguchi[1], K. Washiyama[3] I. Nishinaka[4]
[1]Grad. School Nat. Sci., Tech. Kanazawa Univ., [2]Inst. Sci. Eng., Kanazawa Univ.
[3]Sch. of Health Sci., College of Med., Pharma. Health Sci., Kanazawa Univ.
[4]ASRC, Japan Atomic Energy Agency

Abstruct—The ^{211}At isotope has gathered attention as a promising α-emitter for radionuclide therapy. We report the dependence of the distribution ratio of astatine on the concentration of HCl, and on the polarity of the organic solvent. The results will be useful for development of the ^{211}Rn-^{211}At generator.

Keywords—Astatine / radiopharmaceutical / Distribution ratio / Organic solvent

I. INTRODUCTION

Because of the short path length in tissues (<100 μm) and the high linear energy transfer (~100 keV/μm), α-particle therapy is expected to kill specific tumor cells efficiently with a low level of damage to surrounding tissues. There are approximately 100 radionuclides that decay with α-particle emission. Among them, an ^{211}At isotope with a proper half-life (7.2 h), has gathered attention as a promising α-emitter for radionuclide therapy. Because astatine isotopes are produced via a nuclear reaction, we have to separate astatine isotopes from irradiated targets with high purity. But, the chemical properties of astatine isotopes are not well known for that purpose. In order to research for preparation of astatine for a radiopharmaceuticals, we prepared for astatine isotopes by the reaction of ^{nat}Pb(^{7}Li, xn)$^{209-211}$At at the tandem accelerator of Japan Atomic Energy Agency– Tokai. We report dependence of the distribution ratio of astatine on the concentration of HCl, and on the polarity of the organic solvent as a part of the study.

II. EXPERIMENTS

1. Dependence of the concentration of HCl

A lead target (0.74 mg/cm^2) was irradiated with 50MeV ^{7}Li beam with a current of 120~200 nA using the tandem accelerator of JAEA-Tokai, so that we prepared for astatine isotopes by the reaction of ^{nat}Pb(^{7}Li, xn)$^{209-211}$At. We put on irradiated target into a test tube and heated up at 650 ℃ for about 20 minutes in a electric furnace. Then carrier-free astatine was separated from the lead target by dry distillation. After the dry distillation, we trapped astatine isotopes in 4 M HCl solution. We adjusted the concentration of HCl (1~8 M) and then extracted astatine isotopes by shaking with an equal volume of DIPE for 5 minutes. The γ-activity of each phase was measured by a HPGe detector, and the distribution ratio of astatine isotopes was calculated by the measurements.

2. Dependence of the polarity of organic solvent

Astatine isotopes are produced and distilled as in the previous section. Then astatine isotopes were trapped from test tube in 8 M HCl solution. They are extracted by shaking with equal volume of several different types of polarity of organic solvent for 5 minutes. The γ-activity of each two phase was measured by a HPGe detector and distribution ratio was calculated.

III. RESULTS

Dependence of the distribution ratio on the concentration of HCl was observed for DIPE as show in Fig. 1. Tends to increase in concentration of HCl, the higher the distribution ratio was observed.

The astatine isotopes were well extracted into DIPE and MIBK, but no significant extraction was observed in toluene and decane as show in Fig. 2. It is assumed that the extraction process of astatine is related to polarity of the organic solvent. These results in this study will be useful for development of the ^{211}Rn-^{211}At generator.

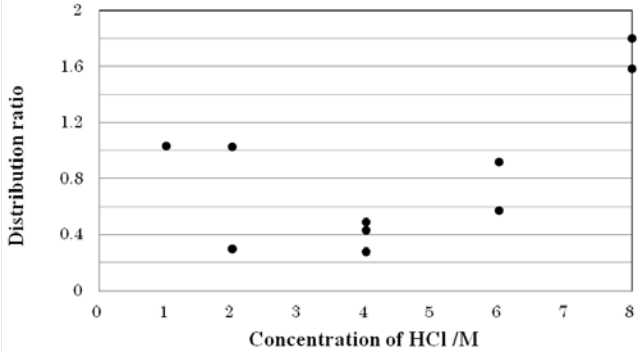

Fig. 1 Distribution ratios for several concentrations of HCl with DIPE.

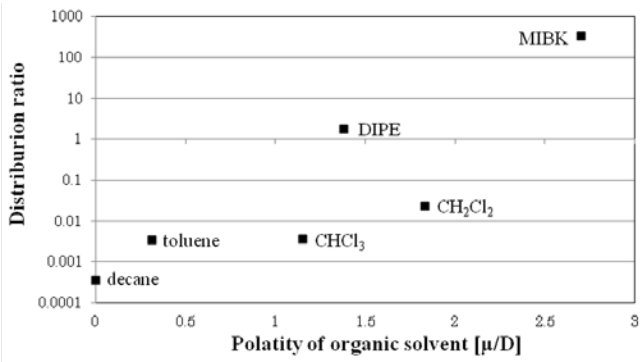

Fig. 2 Distribution ratio for different polarities of organic solvent with 8M HCl.

Lutetium-177 Complexation of DOTA and DTPA in the Presence of Competing Metals

Satoshi Watanabe[1], Kazuyuki Hashimoto[2], Noriko S Ishioka[1]
[1]Medical Radioisotope Application Group, Quantum Beam Science Directorate, Japan Atomic Energy Agency, Takasaki, Gunma 370-1292, Japan
[2] Medical Radioisotope Application Group, Quantum Beam Science Directorate, Japan Atomic Energy Agency, Tokai-mura, Ibaraki 319-1195, Japan

Abstract – ^{177}Lu complexation of DOTA and DTPA is investigated by the addition of Ca(II), Fe(II) and Zn(II). The ^{177}Lu complexation yield of DTPA was higher than that of DOTA in the presence of Ca(II), Fe(II) and Zn(II). Therefore, it was found that the ^{177}Lu complexation of DTPA was more advantageous compared with DOTA in the presence of competing metals, Ca, Fe and Zn.

Keywords – Lutetium-177, Complexation, DOTA, DTPA, Competing metals

I. INTRODUCTION

Lutetium-177 is considered to have potential for application in radioimmunotherapy, because it emits β-particles ($E_{\beta,max}$=498 keV) suitable to penetrate small tumors and its physical half-life of 6.734 days is long enough for ^{177}Lu-labeled antibodies to accumulate to tumor sites. In addition, real time imaging of biodistribution can be done by using the ^{177}Lu, because the energy of γ-rays (E_{γ}=113 keV and 208 keV) emitted from ^{177}Lu is particularly suitable for imaging by single photon emission computed tomography.

We have succeeded in the production of high purity no-carrier-added ^{177}Lu of capable of labeling antibodies using reversed-phase ion-pair liquid chromatography [1]. Usually, as chelating agents of the labeling antibodies, DOTA (1,4,7,10-tetraazacyclododecan-N,N',N'',N'''-tetraacetic acid) and DTPA (diethylenetriamine-N,N,N',N'', N ''-pentaacetic acid) are mainly used. Therefore, we carried out the labeling experiment of ^{177}Lu-DOTA-antibody by using the ^{177}Lu produced in our method in that study. It was found that metallic impurities such as Ca, Fe and Zn inhibited the complexation between ^{177}Lu and DOTA. However, the details of the inhibition by the metallic impurities have not been understandable. Therefore, in the present paper, the ^{177}Lu complexation of DOTA and DTPA is investigated by the addition of competing metals, Ca, Fe and Zn.

II. EXPERIMENTAL

The ^{177}Lu used in this experiment was produced by ^{176}Lu(n, γ)^{177}Lu process. For the experiment of ^{177}Lu complexation of DOTA and DTPA, to the mixture of 5 μL of the ^{177}Lu solution (5.0 x 10^{-5} M as Lu) and 5 μL solution of the competing metal (Ca(II), Fe(II) or Zn(II)) in a prescribed concentration, 0.875 μL of acetate buffer (3 M, pH=6.0) was added. After that, a 10 μL solution of DOTA or DTPA (5.0 x 10^{-5} M) was added. After incubating for 1.5 hours at 40°C, the complexation yield, which was defined as a percentage of the radioactivity of ^{177}Lu-DOTA or ^{177}Lu-DTPA to that of ^{177}Lu used for the complexation, was determined by thin layer chromatography on silica gel ITLC using aqueous ammonia : methanol : water (0.2 : 2 : 4) as a developing solvent. The unreactive ^{177}Lu remains at the origin point of a silica gel ITLC strip and the ^{177}Lu-DOTA or ^{177}Lu-DTPA moves to the solvent front.

III. RESULTS AND DISCUSSION

Figure 1(a) shows the results of ^{177}Lu complexation of DOTA and DTPA by the addition of Ca(II). The ^{177}Lu complexation yield of DOTA decreases with increasing [Ca(II)]/[Lu], while that of DTPA is constant. This result indicates that ^{177}Lu complexation of DOTA is more inhibited by Ca(II) than that of DTPA.

The results of ^{177}Lu complexation by the addition of Fe(II) and Zn(II) are shown in Figs.1(b) and 1(c). The ^{177}Lu complexation yield of both DOTA and DTPA decreases with increasing [Fe(II)]/[Lu] and [Zn(II)]/[Lu]. From comparison between DOTA and DTPA, the decrease of the complexation yield of DOTA was rather high compared with that of DTPA in both cases of Fe(II) and Zn(II). Therefore, the inhibition for the ^{177}Lu complexation of DOTA is higher than that of DTPA.

Consequently, the ^{177}Lu complexation of DOTA was more inhibited by Ca(II), Fe(II) and Zn(II) than that of DTPA. Therefore, it was found that the ^{177}Lu complexation of DTPA was rather advantageous compared with DOTA in the presence of competing metals, Ca, Fe and Zn.

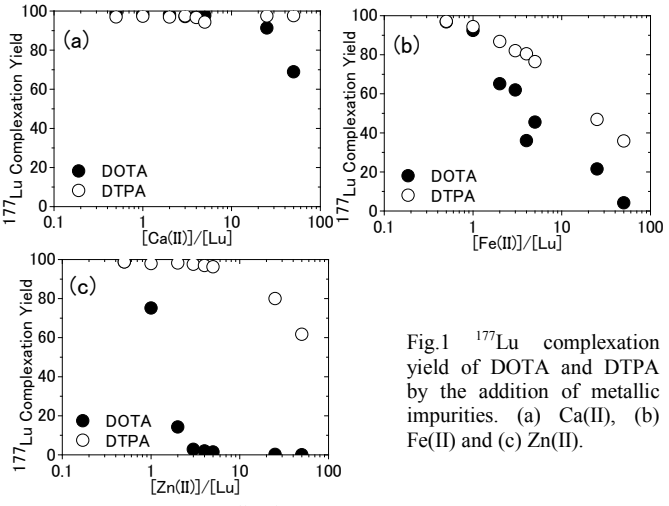

Fig.1 ^{177}Lu complexation yield of DOTA and DTPA by the addition of metallic impurities. (a) Ca(II), (b) Fe(II) and (c) Zn(II).

[1] Japanese patent application, 2010-223827.

APSORC'13 - 5th Asia-Pacific Symposium on Radiochemistry
Kanazawa, Japan, 22-27 September 2013

Hyperfine Fields at ^{140}Ce in He-Doped Fe

Y. Ohkubo[1], A. Taniguchi[1], Q. Xu[1], M. Tanigaki[1], K. Sato[1] and M. Tsuneyama[2]
[1]Research Reactor Institute, Kyoto University, Kumatori-cho, Sennan-gun, Osaka 590-0494, Japan
[2]Grauduate School of Science, Kyoto University, Kitashirakawa, Sakyo-ku, Kyoto 606-8502, Japan

Abstract – Room-temperature TDPAC spectra of ^{140}Ce in an Fe foil and two He-doped Fe foils, all annealed in vacuum at various temperatures were taken in order to see whether Ce and He form complexes in Fe as suggested in first-principles density functional theory calculations. The TDPAC results are presented.

Keywords – hyperfine fields, ^{140}Ce, He-doped Fe, TDPAC, ion implantation, ISOL

I. INTRODUCTION

The magnetic hyperfine fields at impurity elements in ferromagnetic metals are important quantities because they can be used to determine the magnetic moments of nuclear states having the same atomic number as the impurity elements and moreover, together with the electric field gradients, to test first principles calculations in condensed matter physics. Recently, we implanted ^{140}Cs in an Fe foil at room temperature with the help of KUR-ISOL and successfully observed an oscillation pattern due to a unique magnetic hyperfine interaction at ^{140}Ce arising from those ^{140}Cs in a TDPAC (time-differential perturbed angular correlation) spectrum, which is identical to the one seen in Fig. 1(b). From the known magnetic hyperfine field at ^{142}Ce in Fe, we have obtained the magnetic moment of the 2083-keV 4^+ state of ^{140}Ce [1]. This time, we have taken room-temperature TDPAC spectra of ^{140}Ce in an Fe foil (for short, ^{140}CeFe) and ^{140}Ce in two He-doped Fe foils, all annealed in vacuum at various temperatures in order to see whether Ce and He form complexes in Fe as suggested in first-principles density functional theory calculations [2].

II. EXPERIMENTAL PROCEDURES

Room-temperature implantations of 100-keV ^{140}Cs ions were performed at KUR-ISOL. Each of three Fe foils was 0.1-mm thick and of 99.995% purity, which had been annealed in H_2 atmosphere at 700°C for 2 h and then polished. 4-keV He irradiations were carried out at room temperature on two of the foils, one before ^{140}Cs implantation (^{140}CeHe-doped Fe) and the other after ^{140}Cs implantation (^{140}CeFe irradiated with He).

Before and after 0.5-h isochronous annealing in vacuum at various temperatures between 473-1073 K, the time dependences of the coincidence counts $N(\theta, t)$ of the 329-487 keV cascade γ rays for the three Fe samples were taken at room temperature with two measurement systems, each consisting of standard fast-slow electronic modules and four BaF_2 scintillation detectors. Here, θ and t denote the angle and the time interval, respectively, between the cascade γ rays. The directional anisotropy $A_{22}G_{22}(t)$ is obtained as follows:

$$A_{22}G_{22}(t) = 2\frac{N(180°,t) - N(90°,t)}{N(180°,t) + 2N(90°,t)}. \quad (1)$$

III. RESULTS

Figure 1 shows a part of the TDPAC spectra obtained for the three samples. Although the TDPAC spectra for the three samples before annealing are identical to the one shown in Fig. 1(b), there can be seen considerable differences among the samples, which may imply the existence of Ce and He complexes in He-doped Fe foils.

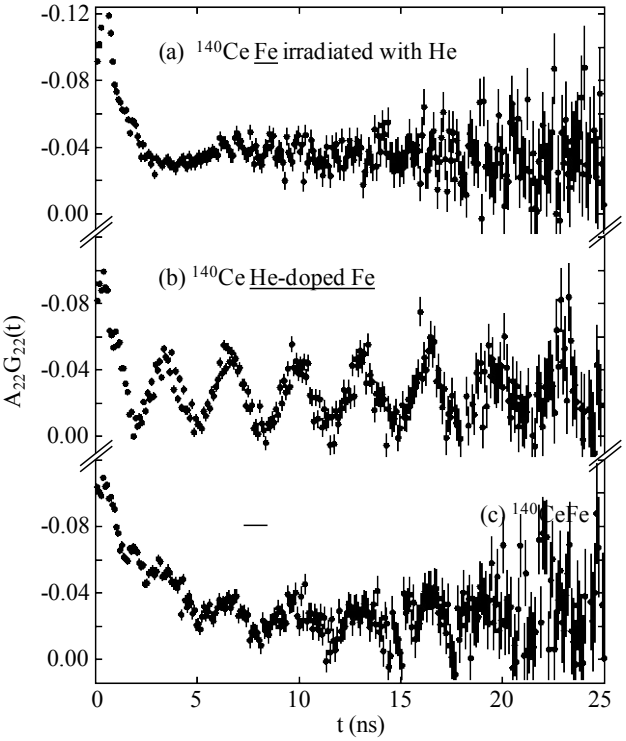

Fig. 1. Room-temperature TDPAC spectra of (a) ^{140}CeFe irradiated with He, (b) ^{140}CeHe-doped Fe, and (c) ^{140}CeFe, all annealed at 673 K in vacuum.

REFERENCES

[1] Y. Ohkubo, A. Taniguchi, Q. Xu, M. Tanigaki, N. Shimizu and T. Otsuka, Phys. Rev. C. **87**, 044324 (2013).
[2] W. Hao and W. T. Geng, Nucl. Instru. Meth. B **280**, 22 (2012).

APSORC'13 - 5th Asia-Pacific Symposium on Radiochemistry
Kanazawa, Japan, 22-27 September 2013

Mössbauer studies of lanthanum doped $Ni_{0.4}Cu_{0.2}Zn_{0.4}Fe_2O_4$ ferrites by Sol-Gel auto-combustion

Qing Lin[1,2], Chenglong Lei[1]*, Haifu Huang[3], Hui Zhang[1], Yun He[1]
[1]*College of Physics and Technology, Guangxi Normal University, Guilin 541004, China*
[2]*Department of Information Technology, Hainan Medical College, Haikou 571101, China*
[3]*Nanjing National Laboratory of Microstructures and Jiangsu Provincial Laboratory for NanoTechnology,,Department of Physics, Nanjing University, Nanjing 210093, China*
e-mail:hy@gxnu.edu.cn

Abstract:
In this literature, La^{3+} substituted $Ni_{0.4}Cu_{0.2}Zn_{0.4}Fe_{2-x}La_xO_4(0\leq x\leq 0.15)$ ferrites by using Sol-Gel auto-combustion route have been prepared. XRD of the powders calcined at 800℃/3h show only single phase cubic spinel ferrites and crystalline size decrease sharply, but at high temperature 950℃/3h that emerge extra phase $LaFeO_3$ when x≥0.05 and the crystalline sizes increase linearly. The Mössbauer spectrums at room temperature of samples at 800℃/3h vary from magnetic sextets to shrink magnetic sextet and collapse to relaxation doublet(x=0.1). This variation of magnetic order state confirms the Fe^{3+}-O^{2-}-Fe^{3+} super exchange interaction decrease due to La^{3+} substitutions. However, when that processed at 950℃/3h, The hyperfine magnetic field distribution probability moves to high magnetic field region. The magnetic order for all samples exhibits relaxation sextet magnetic spectra and does not change obviously up to substitution x=0.15. A broadening line width observed in Mössbauer spectra is interpreted as originating from various cation distributions. The super exchange interaction should have been enhanced and the Curie temperature increases.
Keywords: Rare earth, Sol-Gel, XRD, Mössbauer, NiCuZn ferrite, Hyperfine magnetic field

I. RESULTS AND DISCUSSION

We have successfully prepared ferrite system La^{3+} doped $Ni_{0.4}Cu_{0.2}Zn_{0.4}Fe_{2-x}La_xO_4(0\leq x\leq 0.15)$ by Sol-Gel auto-combustion method. The XRD patterns of ferrite powders calcined at 800℃ and 950℃are shown in Fig.1 and Fig.2, respectively.

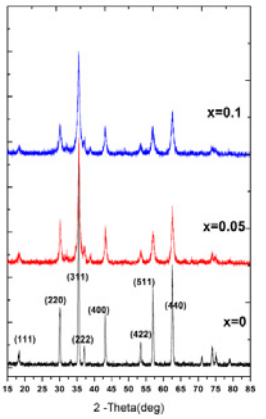

Fig.1 the XRD patterns of samples calcined at 80

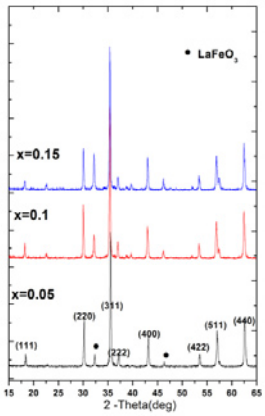

Fig.2 the XRD patterns of samples calceined at 950℃

Fig.3 and Fig.4 show the Mössbauer spectra (RT) of $Ni_{0.4}Cu_{0.2}Zn_{0.4}La_xFe_{2-x}O_4$ nano-crystalline ferrite powders measured at room temperatures , respectively.

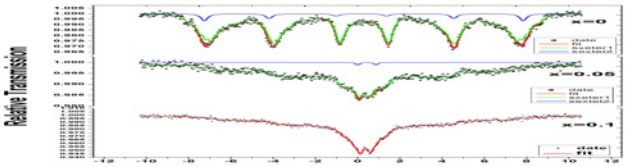

Fig.3 the mossbauer spectra at room temperature of $Ni_{0.4}Cu_{0.2}Zn_{0.4}La_xFe_{2-x}O_4$ (x=0,0.05,0.1) calcined at 800℃

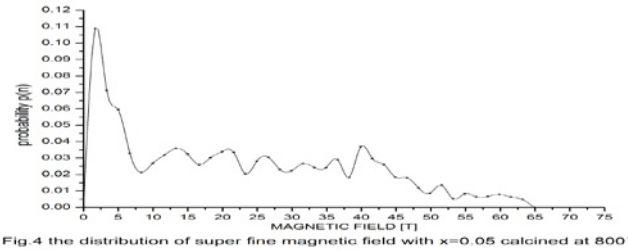

Fig.4 the distribution of super fine magnetic field with x=0.05 calcined at 800℃

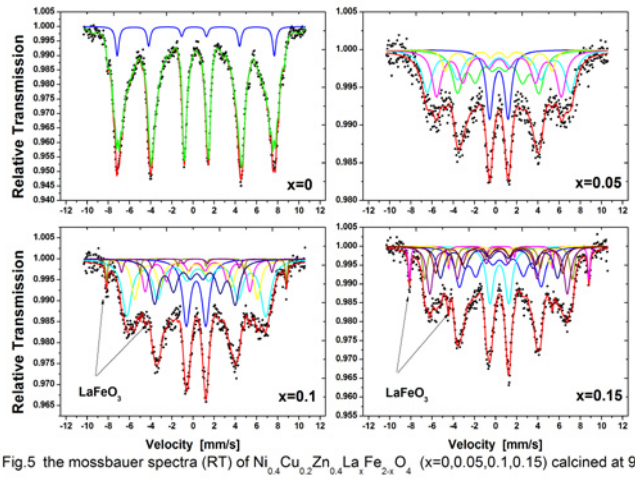

Fig.5 the mossbauer spectra (RT) of $Ni_{0.4}Cu_{0.2}Zn_{0.4}La_xFe_{2-x}O_4$ (x=0,0.05,0.1,0.15) calcined at 950℃

Fig.5 show the Mössbauer spectra of samples calcined at 950℃. The differences of Mössbauer spectra compared with the sample calcined at 800℃ confirm that the substitution of La^{3+} ions need more bond energy and affect the $(Fe^{3+})_A$-O^{2-}-$(Fe^{3+})_B$ super-exchange interaction so that the samples show ferromagnetism because of high sintering temperature.

[1] Gabal, M.A., et al., *Structural, magnetic and electrical properties of Ga-substituted NiCuZn nanocrystalline ferrite.* Ceramics International, 2010. 36(4): p. 1339-1346.、
[2] Roy, P.K., B.B. Nayak, and J. Bera, *Study on electro-magnetic properties of La substituted Ni–Cu–Zn ferrite synthesized by auto-combustion method.* Journal of Magnetism and Magnetic Materials, 2008. 320(6): p. 1128-1132.
[3] S.I.Moussa, R.R.Sheha, E.A.Saad, N.A.Tadros, Synthesis and characterization of magnetic nano-material for removal of Eu^{3+} ions from aqueous solutions, *Journal of Radioanalytical and Nuclear Chemistry*, 2013. 295: 929–935.

Analysis of corrosion products formed on anti-weather steel

Matashige OYABU[1], Ryo SATOH[1], Kiyoshi NOMURA[2]
[1]Math & Science Division, Kanazawa Institute of Technology,
Ohigigaoka 7-1, Nonoichi, Ishikawa, Japan 921-8501
[2]The University of Tokyo,
Hongo 7-3-1, Bunkyo-ku, Tokyo, Japan 113-8656

Abstract

Weathering steels (COR-TEN O) were corroded under the salty or acid rain condition in the laboratory. Corrosion products on weathering steel were analyzed by Mössbauer spectrometry and X-ray diffraction. The kind of products depended on the atmospheric condition. β-FeOOH, which disturbs the performance of weathering steel, was formed under the existence of chloride or fluoride ion. The formations of β-FeOOH, α-FeOOH, γ-FeOOH and γ -Fe2O3 were studied in various conditions.

I. INTRODUCTION

In recent years, use of weathering steel is increasing, and it became to be used to about 30% as steel materials for a bridge. Weathering steel is designed to protect the internal corrosion of steel by generating stable rust on the surface without painting. The paint is not needed, and so the cost of painting and maintenance can be reduced. The life may exceed 100 years under good atmosphere condition. The life of weathering steel depends on the environments largely. Especially it is difficult to use the steel under salty environment like coastal area. The stable rust on the surface might be composed of fine α-FeOOH, γ-FeOOH and magnetite. Those materials may form protection layer on the steel. However, β-FeOOH, which is not protective rust, may be generated under the existence of chloride ion. The formation on the surface and property of β-FeOOH should be studied to improve the performance of weathering steel. In this study, weathering steels were corroded under the different conditions and the corrosion products were analyzed by Mössbauer spectrometry and X-ray diffraction. With regard to β-FeOOH formation, pure material also was synthesized by hydrolysis of iron(III) solution and studied by X-ray diffraction.

II. EXPERIMENT

Corrosion test: The steel plate of COR-TEN O with 1mm thickness was used. It was cut to 80 mm x 60 mm. Corrosion tests were carried out based on JIS H8502 method. Each piece was sprayed with test solitions and kept in dry condition followed by wet condition. One cycle took 12 hours. The cycle was repeated 20 times finally. Test solutions used are 5% NaCl, acid rain (NaCl, HNO_3, H_2SO_4, pH3.5), acid rain "without NaCl", 5% NaF, and 5% ($NaF+Na_2SO_4$), respectively.

X-ray diffractions patterns were measured by Rigaku UltimaIV equipped with Cu target and monochromator, and were analyzed by Rietveld method to identify the crystalline products. Mössbauer spectra were measured at room temperature by using $^{57}Co(Cr)$ source and conventional instrument.

III. RESULT AND DISCUSSION

Mössbauer spectra and the hyperfine distributions were shown in Fig.1. By spraying 5% NaCl solution, strong paramagnetic doublet was observed. It perhaps is due to the β -FeOOH and γ -FeOOH contained in the rust products. With respect to acid rain, α -FeOOH, γ -FeOOH, and γ -Fe_2O_3 were identified. The large amount of sextet with 49T due to γ -Fe_2O_3 was produced under the condition of nitrate and sulfate solution. α -FeOOH exhibits the broad and collapsed sextet with 34T at RT. The α -FeOOH is considered to be poor crystalline or fine grains. Any corrosion product is composed from fine grains because the broadening sextets. Detailed discussion will be presented in the poster.

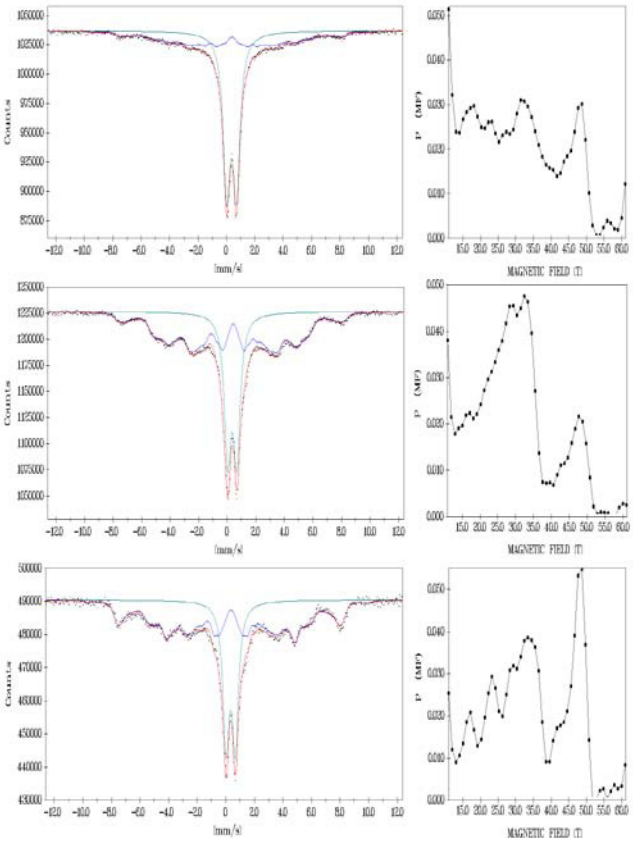

Figure 1 Mössbauer spectra of corrosion products using sprayed solution; (a) 5% NaCl (b) acid rain, and (c) nitrate and sulfate

Reference
1. "COR-TEN Catalog" published by Nippon Steel
2. Shuichi HARA, Zairyo-to-kankyo,57, 70-75(2008)

Study of the Spin-Crossover Phenomena in 1D Coordination Polymers, $[Fe^{II}(NH_2\text{-triazole})_3](C_nH_{2n+1}SO_3)_2$, by Fe-K edge XAFS and ^{57}Fe Mössbauer Spectroscopy

Hajime Kamebuchi[1], Akio Nakamoto[1], Masaya Enomoto[2], Toshihiko Yokoyama[3], Norimichi Kojima[1]

[1]Graduate School of Arts and Sciences, The University of Tokyo, Komaba 3-8-1, Meguro-ku, Tokyo 153-8902, Japan
[2]Department of Chemistry, Tokyo University of Science, Kagurazaka 1-3, Shinjuku-ku, Tokyo 162-8601, Japan
[3]Department of Materials Molecular Science, Institute for Molecular Science, Myodaiji-cho, Okazaki 444-8585, Japan

Abstract – The spin transition temperature of 1D spin-crossover system, $[Fe^{II}(NH_2\text{-trz})_3](C_nH_{2n+1}SO_3)_2{\cdot}xH_2O$ (NH_2-trz = 4-amino-1,2,4-triazole), was systematically controlled through the chemical pressure derived from the alkyl chain of counter-anion. We investigated the influence of the chemical pressure on the spin transition temperature and π-back donation from Fe^{II} ion to NH_2-trz ligand with increasing alkyl chain length by means of ^{57}Fe Mössbauer and XANES spectra.

Keywords – Spin-Crossover, ^{57}Fe Mössbauer, X-ray absorption

I. INTRODUCTION

When a transition metal ion with an electron configuration of d^4–d^7 is octahedrally coordinated by ligands, the ground state has a possibility to change the spin state between high-spin (HS) and low-spin (LS) states by external stimuli. Such the HS-LS transition is called spin-crossover phenomenon. In the past decades, one dimensional Fe^{II} coordination polymers bridged by 4-substituted-1,2,4-triazole (R-trz), whose general formula is $[Fe^{II}(R\text{-trz})_3](A)_2{\cdot}xH_2O$ (A = monovalent anion), have attracted much attention because of their potential applications to molecular electronics or molecular devices [1, 2]. The primary reasons for this are that their spin transition behavior occurs around room temperature with wide thermal hysteresis. Furthermore, their spin transition temperature ($T_{1/2}$) and hysteresis width ($\Delta T_{1/2}$) are controllable by various chemical and physical approaches [1, 3, 4]. This research aims at the control of the spin transition behavior through chemical pressure effect and the analysis of the ligand field by X-ray absorption (XAFS) and ^{57}Fe Mössbauer spectroscopy for $[Fe^{II}(NH_2\text{-trz})_3](C_nH_{2n+1}SO_3)_2{\cdot}\ xH_2O$ (n = 1 – 9).

II. RESULTS AND DISCUSSION

In $[Fe^{II}(NH_2\text{-trz})_3](C_nH_{2n+1}SO_3)_2{\cdot}xH_2O$, $T_{1/2}$ increases in the heating and cooling processes with increasing the alkyl chain length (n). In connection with this, there is a close relationship between $T_{1/2}$ and the nearest neighbor Fe-Fe distance (R(Fe-Fe)) estimated from EXAFS (extended X-ray absorption fine structure), which is shown in Figure 1. These are highly suggestive of the increase of intra-chain interaction with the alkyl chain length being attributed to the uniaxial chemical pressure effect induced by self-assembly interaction between alkyl chains, so-called "fastener effect".

In order to elucidate the effect of uniaxial chemical pressure on $T_{1/2}$, the ligand-field strength (Dq) and Racah parameter (B) in the HS state were estimated by analysing the pre-edge region in Fe-K edge XANES (X-ray absorption near edge structure) spectra based on the ligand field theory. It is clear from Figure 2 that the increase of Dq and the decrease of B were found with increasing n, which are closely consistent with the relationship between $T_{1/2}$ and the ^{57}Fe Mössbauer isomer shift (IS) at 200 K. Judging from these results, the following result is derived. The back donation from the 3d orbital of Fe^{II} ion to the π* orbital of NH_2-trz (d_π-p_π back bonding) is enhanced by the uniaxial chemical pressure due to the fastener effect between the alkyl chains of counter-anion, which induces the expansion of the 3d orbital and the decrease of B of Fe^{II} ion. Thus Dq/B increases with the alkyl chain length, which is the key parameter determining $T_{1/2}$ of spin crossover compounds.

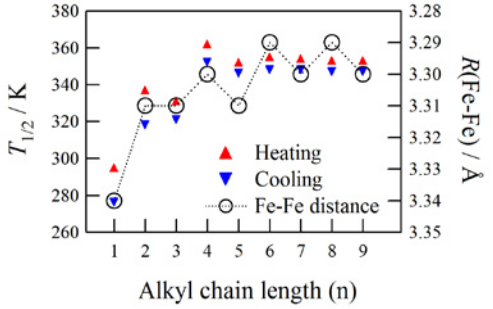

Figure 1. Correlation between spin transition temperature ($T_{1/2}$) and the nearest neighbor Fe-Fe distance (R(Fe-Fe)).

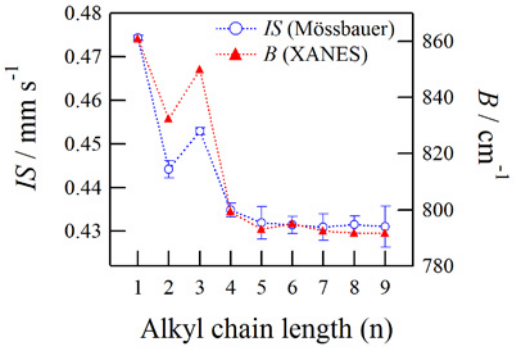

Figure 2. Correlation between ^{57}Fe Mössbauer Isomer Shift (IS) of the LS state and Racah parameter (B).

REFERENCES

[1] O. Kahn, C. J. Martinez, Science 279 (1998) 44.
[2] M. M. Dîrtu, F. Schmit, A. D. Naik, A. Rotaru, J. Marchand-Brynaert, Y. Garcia, Int. J. Mol. Sci. 12 (2011) 5339.
[3] V. A. Varnek, L. G. Lavrenova, J. Struct. Chem. 36 (1995) 104.
[4] P. Gütlich, V. Ksenofontov, A. B. Gaspar, Coord. Chem. Rev. 249 (2005) 1811.

Mössbauer Spectroscopic and Powder X-ray Diffraction Studies on Incorporation of Gaseous Organic Molecules into Intermolecular Nano-voids of Mixed-valence Trinuclear Iron Pentafluorobenzoate Complex

Yoichi Sakai[1], Satoru Onaka[1], Ryo Ogiso[1], Masashi Takahashi[2], Tadahiro Nakamoto[3], and Tsutomu Takayama[1]
[1]DaidoUniversity, Takiharu-cho, Nagoya 457-8530, Japan
[2]Toho University, Miyama, Funabashi 274-8510, Japan
[3]Toray Research Center, Sonoyama, Otsu 520-8567, Japan

Abstract – Incorporation of gaseous organic molecules into polycrystalline mixed-valence trinuclear iron (Fe^{3+},Fe^{3+},Fe^{2+}) pentafluorobenzoate complex $Fe_3O(C_6F_5COO)_6(C_5H_5N)_3$ with intermolecular nano-voids was studied by ^{57}Fe-Mössbauer spectroscopic and powder XRD measurements. Organic-molecule incorporation was mainly chased by using iron-valence fluctuation observed in a Mössbauer spectrum, and also researched supportively by a powder XRD technique.

Keywords –Intermolecular nano-void, Mixed-valence trinuclear iron complex, Valence fluctuation, ^{57}Fe-Mössbauer spectroscopy, powder XRD

I. INTRODUCTION

We have revealed that there is found a valence-detrapped (averaged) state of three iron ions for $Fe_3O(C_6F_5COO)_6(C_5H_5N)_3\cdot CH_2Cl_2$ (***1***) at room temperature in our Mössbauer study, while a valence-trapped (localized) state for $Fe_3O(C_6F_5COO)_6(C_5H_5N)_3$ (***2***) contrarily. In complex ***1***, dichloromethane is contained as a crystalline solvated molecule. Complexes of ***1*** and ***2*** are synthesized in our work both of which are a novel compound; complex ***2*** was prepared by heating of ***1*** under a reduced pressure. It was revealed previously from our single-crystal X-ray structure analysis that solvated CH_2Cl_2 molecules are arrayed in the intermolecular space of the complex ***1*** [2]. This finding led us into anticipating that gaseous organic molecules may be easily incorporated into such intermolecular nano-voids, since complex ***2*** was obtained by removing CH_2Cl_2 molecules of the complex ***1***. This expectation of ours was proved to be valid, which is reported elsewhere [2].

In the present work, the incorporation behaviors were examined by Mössbauer and powder X-ray Diffraction (XRD) techniques. Furthermore, the time constant of incorporation was also investigated.

II. EXPERIMENTAL

Complexes of ***1*** and ***2*** were prepared according to the procedures reported in our previous papers [1,2]. Organic-vapor exposure experiments were carried out as described in Ref. [2]; polycrystalline powder of ***2*** was placed in a small-sized vial and then this vial was placed in a large vial. An adequate amount of organic liquid was poured in the large vial, which then was tightly capped. All Mössbauer spectra and powder XRD patterns (Cu Kα) were recorded at room temperature in ordinary ways.

III. RESULTS AND DISCUSSION

Mössbauer spectra and powder XRD patterns at room temperature were shown in the left and right sides of Figure 1, respectively, where those for the following three samples are illustrated; a) polycrystalline powder of complex ***2***, b) polycrystalline powder of complex ***1***, and c) powder of ***2*** exposed to dichloromethane vapor at 20 ºC for 21 h. Mössbauer spectrum c) for complex ***2*** exposed to CH_2Cl_2 vapor shows that iron ions should be in the same valence-detrapping state as that of complex ***1***, implying a regain of solvated CH_2Cl_2 molecules to return to complex ***1*** from complex ***2***. Such regain and return were confirmed in the powder XRD patterns shown in Figure 1, where the patterns a) and c) could be ascribed to a hexagonal crystal form with a=1.35 and c=2.10 nm..

The re-absorption rate experiments suggested that benzene molecules were completely regained with a time constant of a few tens of seconds, surprisingly swift.

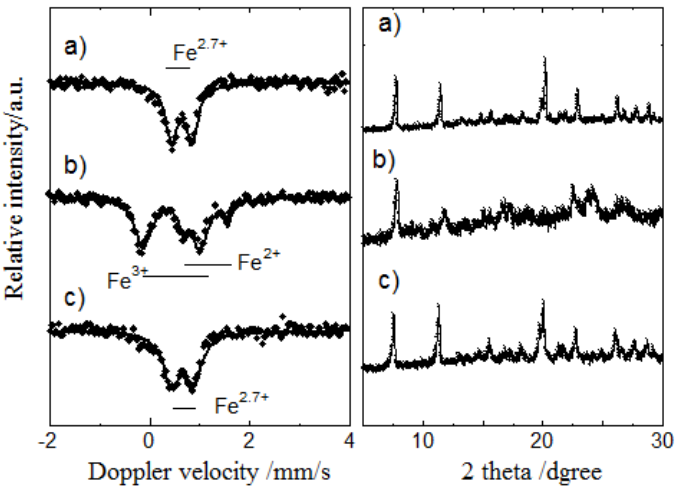

Figure 1. ^{57}Fe-Mössbauer spectra (left) and powder XRD patterns (right) at room temperature: a) $Fe_3O(C_6F_5COO)_6(C_5H_5N)_3\cdot CH_2Cl_2$, (***1***) b) $Fe_3O(C_6F_5COO)_6(C_5H_5N)_3$, (***2***) c) $Fe_3O(C_6F_5COO)_6(C_5H_5N)_3$ (***2***) exposed to CH_2Cl_2-vapor at 20 ºC for 21 h

[1] Y. Sakai et al., Hyperfine Interactions, **205** (2012) 1-5.
[2] S. Onaka et al., to be submitted to an international journal (2013).

Dynamic Perturbation to ^{111}Cd(←^{111}Ag) Doped in AgI Nanoparticles

W. Sato[1,2], R. Mizuuchi[2], N. Irioka[3], S. Komatsuda[2], S. Kawata[4], A. Taoka[1,2], and Y. Ohkubo[5]
[1]Institute of Science and Engineering, Kanazawa University, Kanazawa, Ishikawa 920-1192, Japan
[2]Graduate School of Natural Science and Technology, Kanazawa University, Kanazawa, Ishikawa 920-1192, Japan
[3]School of Chemistry, Kanazawa University, Kanazawa, Ishikawa 920-1192, Japan
[4]Department of Chemistry, Faculty of Science, Fukuoka University, Fukuoka, Fukuoka 814-0180, Japan
[5]Research Reactor Institute, Kyoto University, Kumatori, Osaka 590-0494, Japan

Abstract – Dynamic behavior of the extranuclear field relative to the ^{111}Cd(←^{111}Ag) probe doped in an ionic conductor silver iodide (AgI) was investigated by means of the time-differential perturbed angular correlation (TDPAC) technique. The room-temperature TDPAC spectrum for as-precipitated AgI powder shows no perturbation, reflecting the zinc blende crystal structure (γ-AgI); whereas in polymer-coated AgI nanoparticles, the ^{111}Cd(←^{111}Ag) probe is dynamically perturbed. This result signifies that Ag^+ ions in the latter sample can move around even at room temperature in the time scale of the present time window.

Keywords – Silver Iodide, Perturbed Angular Correlations, Dynamics, PVP, Nanoparticles, Superionic Conductivity

I. INTRODUCTION

It is well known that silver iodide (AgI) offers superionic conductivity as in its high-temperature α phase, and applications of this solid-state conductivity are desired in a wide field of industry. This conducting phenomenon, however, emerges at high temperature because of temperature-dependent crystal structures, which is indeed a barrier to the practical applications of this compound.

Recently, an epoch-making technique was reported to break through this situation: AgI powder coated by a poly-N-vinyl-2-pyrrolidone (PVP) can partially preserve the conducting α phase even at room temperature, recording the conductivity of 1.5×10^{-2} Ω^{-1} cm^{-1}[1]. The authors report that this achievement is due to successful control of the particle size as small as nanoscale. For a detailed understanding of ionic conductivity of this compound, it is of great importance to examine lattice-to-lattice hopping motion of Ag^+ ions on an atomic scale. For that purpose, in the present work, dynamic behavior of Ag^+ ions has been observed by means of the time-differential perturbed angular correlation (TDPAC) technique using the probe of ^{111}Cd(← ^{111}Ag) nuclei. Here, preliminary results of successful observation of room-temperature dynamic motion of Ag^+ ions are reported.

II. EXPERIMENTS

For the production of the TDPAC probe, Pd foil was irradiated by thermal neutrons in Kyoto University Reactor to produce ^{111}Pd. After radioequilibrium was achieved between ^{111}Pd and ^{111}Ag, the Pd foil was dissolved in HNO_3 aq. solution, and carrier-free ^{111}Ag was isolated by an anion exchange chromatography. The separated ^{111}Ag was incorporated together in AgI samples when the powder sample was synthesized by precipitation. In the present work, two different samples were prepared: PVP-free and PVP-coated. We confirmed by transmission electron microscope that microscopic particles with sizes of 10-100 nm were expectedly synthesized for ^{111}Ag-free PVP-coated AgI.

TDPAC measurements of the ^{111}Cd(← ^{111}Ag) probe were performed for both samples at various temperatures to observe temperature dependence of the spectra.

III. RESULTS

For the PVP-free AgI polycrystals, time variation was not seen in the TDPAC spectrum at room temperature, which suggests that the ^{111}Cd(←^{111}Ag) probe duly occupies tetrahedral lattice site of Ag^+ in zinc blende crystal structure as in γ phase. At high-temperature (> 419 K) α phase, the TDPAC spectra showed an exponential relaxation, signifying dynamic motion of the extranuclear field relative to the probe nucleus.

As regards the PVP-coated AgI nanoparticles, on the other hand, typical dynamic perturbation was observed even at room temperature as shown in Fig. 1. The directional anisotropy of the spectrum shows a relaxation in the time scale of 10^{-7} s, which corresponds to nuclear relaxation time by the dynamic perturbation arising from fast fluctuation of the extranuclear charge distribution, namely, hopping motion of Ag^+ ions. It is considered that PVP-coating has made it possible for the α phase to survive at room temperature, realizing superionic conductivity.

For the hopping rate of Ag^+ ions, it is essential to obtain the value of nuclear quadrupole frequency as they are still at their lattice site. Experiments for the data acquisition are now in progress.

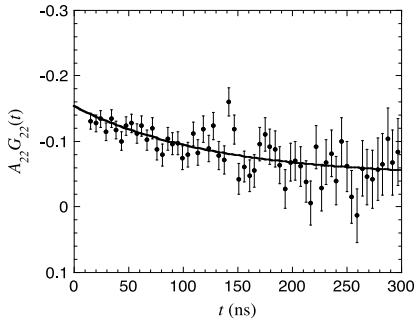

Fig. 1. TDPAC spectrum of ^{111}Cd(←^{111}Ag) in PVP-coated AgI at room temperature, where A_{22} stands for the angular correlation coefficient and $G_{22}(t)$ the time-differential perturbation factor as a function of the time interval of the cascade γ-ray emission, t.

[1] R. Makiura et al. Nature Mater. **8**, 476 (2009).

APSORC'13 - 5th Asia-Pacific Symposium on Radiochemistry
Kanazawa, Japan, 22-27 September 2013

A prototype of a simple collection system for the determination of ^{14}C

Tzu-Han Chuang, Tsuey-Lin Tsai, Hwa-Jou Wei, Lee-Chung Men

Chemistry Division, Institute of Nuclear Energy Research, Longtan, Taoyuan 32546, Taiwan, R.O.C.

Abstract

This study presents a simple and relatively cost-effective system for sampling ^{14}C in biological samples or the radwaste from nuclear power plants. The proposed system uses a CO_2 absorption technique to collect ^{14}C. This technique involves placing a sample in a quartz tube inside a furnace in a flowing stream of oxygen, and then heating the tube to a minimum temperature of 300^0C at heating rate of 14 °C/min. In the combustion zone, CuO catalytic oxidation ensures that any CO produced from the incomplete combustion of the sample carbon present in the gas stream is oxidized to form CO_2. This process uses dilute sulfuric acid (5%) for steam absorption. The proposed collection technique also provides a simple procedure for subsequent sample preparation and activity measurement using a liquid scintillation counting When combined with several counting vials, this trapping design can solve the overcapacity problem of carbon absorption for each collector. The following sample pretreatment also facilitates counting. This system achieves a minimum detectable activity level of 20 mBq/g for an l-g solid sample. This level of sensitivity is appropriate for the routine monitoring of radwaste at nuclear facilities.

Keywords: ^{14}C; CO_2 absorption; liquid scintillation counting; radwaste

Elemental analysis of Korean adult toenail using of instrumental neutron activation analysis

Sun-Ha Kim[1], Jong-Hwa Moon[1], Yong-Sam Chung[1], Ok-Hee Lee[2]
[1]Korea Atomic Energy Research Institute, Daedeok-daero 989-111, Yuseong-gu, Daejeon, 305-353, Korea
[2]Dept of Food Science and Nutrition, Yongin University, 470, Samga-dong, Cheoin-Gu, Yongin, 449-714, Korea

Abstract – The elemental contents in a toenail as a biological sample may depend on the dietary habit and health status. In this study, the inorganic elements in Korean adult toenail were determined by an instrumental neutron activation analysis (INAA). Toenail samples were collected from Korean adults, and the total number of samples was 50. The collected samples were pretreated and analyzed using INAA facilities at the HANARO research reactor. 15 elements, i.e., Al, As, Br, Ca, Cl, Co, Cr, Fe, Hg, K, Mn, Na, Se, V, and Zn in the toenail samples were determined and evaluated for the level of elemental concentration. Finally, correlation between 15 elements was examined. It is found that Mn-V, Na-Cl, Br-K, and Cr-Fe seem to be in close correlation.

Keywords–Instrumental Neutron Activation Analysis, Inorganic Elements, Toenail, Elemental Correlation

I. INTRODUCTION

The organic elements in a human organism such as serum, hair, nail, and internal organs are able to provide valuable information to estimate the health status of the human body. The elemental contents in a toenail as a biological sample may depend on the dietary habit and health status. In this study, the inorganic elements in a Korean adult toenail were determined using instrumental neutron activation analysis (INAA). For this purpose, the analytical condition for INAA was established, and 15 elements were determined. Finally, correlation between the elements was examined.

II. EXPERIMENTAL

The toenail samples were collected from Korean adults, and the total number of samples was 50. The collected samples were pretreated by cutting, cleaning, and homogenizing for INAA. The prepared samples were irradiated using NAA #1 or #2 irradiation holes at the HANARO research reactor. For the measurement of gamma-rays of the detectable nuclides, a HPGe detector coupled to a 16k-multichannel analyzer was used. The elemental concentration in the samples was determined by the absolute and/or relative method.

III. RESULTS

15 elements, i.e., Al, As, Br, Ca, Cl, Co, Cr, Fe, Hg, K, Mn, Na, Se, V, and Zn in the toenail samples were determined by INAA. The mean elemental concentration is shown in Fig. 1.

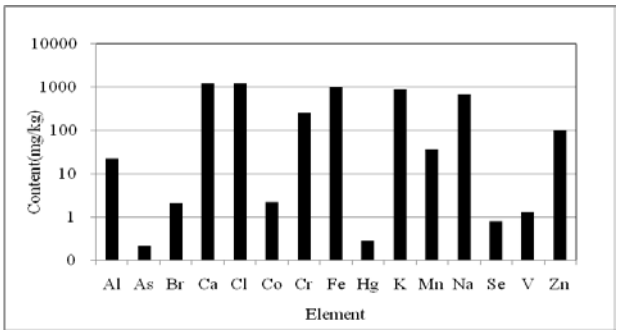

Fig. 1. Mean elemental concentrations in toenail samples

The correlation between the 15 elements was examined and Mn-V, Na-Cl, Br-K and Cr-Fe seem to be in close correlation. Fig. 2 shows the Cr-Fe correlation.

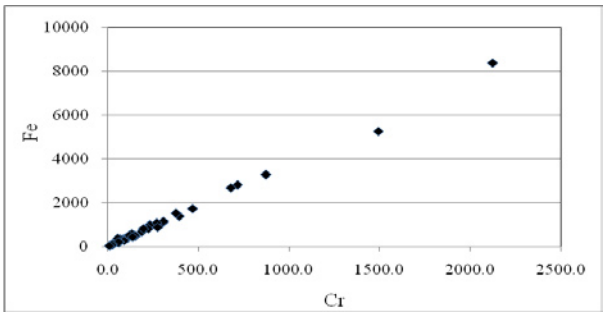

Fig. 2. Correlation between Cr and Fe in toenail samples

ACKNOWLEDGEMENT

This work was carried out under the Nuclear Research and Development Program of the Korean Ministry of Education, Science, and Technology.

REFERENCES

[1] Rita Mehra, Meenu Juneja: Fingernails as biological indices of metal exposure, Journal of Bioscience 2005, 30(2):253-257.
[2] World Health Organization (2006) Trace elements in human nutrition and health. Geneva, WHO, Belgium

Determination of Vanadium at ppb Levels in Relatively High-Salt Biological Materials without Chemical Separation and using Neutron Activation coupled to Compton Suppression Gamma-Ray Spectrometry

W. Zhang and A. Chatt

Trace Analysis Research Centre, Department of Chemistry, Dalhousie University, Halifax, NS, B3H 4J3, Canada

Abstract – APSORC'13 Abstract

Keywords – vanadium, INAA, Compton suppression, biological materials

I. INTRODUCTION

The toxicity of V has been known for some time. It is only recently that V has been recognized as an essential trace element. Its determination with high precision and accuracy in tissues, foods and other biological materials is needed. Techniques such as atomic absorption, X-ray fluorescence, and neutron activation analysis (NAA) can be used for this purpose. Vanadium can be determined by NAA through the interference-free 1434.2-keV gamma-ray of its short-lived (half-life of 3.74 min) nuclide ^{52}V produced *via* the ^{51}V(n,γ)^{52}V reaction. It has been reported that ^{52}V has sufficient sensitivity for its measurement down to nanogram levels [1]. However, it is seldom assayed in practice by instrumental NAA (INAA) in conjunction with conventional gamma-ray spectrometry (INAA-CONV), in particular for low V content in relatively high-salt biological materials, due to the Compton background interference from nuclides such as ^{28}Al, ^{38}Cl, ^{56}Mn, and ^{24}Na. Preconcentration NAA (PNAA) and radiochemical NAA (RNAA) methods are commonly used to separate V from the major and interfering elements [2-3]. Compton suppression spectrometry (CSS) counting technique can be alternatively used under such situations [4]. One of the objectives of the present work was to fully explore the advantages of INAA coupled to CSS (INAA-CSS) for the determination of low levels of V without any chemical separation in biological materials in general, nutritional materials in particular, containing varying amounts of sodium chloride.

II. EXPERIMENTAL

A total of 16 biological reference material (RM) and standard reference material (SRM) containing 1.4 to 1100 ppb V with low to high levels of sodium chloride were analyzed by INAA-CSS. Between 200 and 700 mg of these materials were irradiated in the Dalhousie University SLOWPOKE-2 Reactor facility at a neutron flux of 5×10^{11} cm^{-2} s^{-1} for 1 min, allowed to decay for 1 min, and counted for 10 min. The average sensitivity for V standard solutions under these conditions was 5025 counts μg^{-1} in the Compton suppression counting mode. The CSS used here consisted of a HPGe detector and a 10"x10" NaI(Tl) guard detector with a 3"x3" NaI(Tl) plug. The peak-to-Compton plateau ratio of this system was about 590:1.

III. RESULTS AND DISCUSSION

The application of CSS can reduce the Compton background under the 1434.2-keV peak, improve the statistical accuracy of the peak and lower the detection limit, if Cl and Na levels are not too high [4]. For example, the V content of Wheat Flour (NIST SRM 1567a) was determined by INAA-CSS as 9.0±2.9 ppb compared to the Information value of 11 ppb; the detection limit was 1.8 ppb by INAA-CSS relative to 8.6 ppb by INAA-CONV. In the case of Peach Leaves (NIST SRM 1547) our measured value of 355±17 ppb agreed well with the certified value of 370±30 ppb; the detection limit of 13 ppb by INAA-CSS was about 3 times lower than that of 34 ppb by INAA-CONV.

The overall background around the 1434.2-keV region was reduced by a factor of 5 to 10 for several biological RMs and SRMs in the Compton suppression counting mode compared to conventional counting. Consequently, the detection limits were lowered by factors of 3 to 5 in INAA-CSS compared to INAA-CONV making rapid and reliable V determinations possible above 1.5 ppb levels without any chemical separation. The agreement between the certified (information) and measured values for the RM and SRM analyzed in this work was generally within ±10%.

References

[1] A.J. Blotcky, F.G. Hamel, A, Stranik, A. Ebrahim, and R.B. Sharma, J. Radioanal. Nucl. Chem., Articles, 131(1989)319-329.
[2] A.J. Blotcky, W.C. Duckworth, and A. Ebrahim, J. Radioanal. Nucl. Chem., Aritcles, 134(1989)151-160.
[3] A.I. Kulathilake, A. Chatt, Trans. Am. Nucl. Soc., 65(1992)172.
[4] W. Zhang, Ph.D. Thesis, Dalhousie University, Halifax, NS, Canada, 1997.

Radiochemical neutron activation analysis of halogens (Cl, Br and I) in geological and cosmochemical samples

Mitsuru Ebihara[1] and Shun Sekimoto[2]
[1]Tokyo Metropolitan University
[2]Kyoto University Research Reactor Institute

I. INTRODUCTION

Accurate and reliable data of halogen abundance have been rarely reported for terrestrial samples, such as crustal rock and mantle material. Since halogens differ in volatility from element to element, their content and relative abundance are highly informative when discussing the petrogenesis of such samples. Among the halogens, iodine is the most informative element in discussion of the geochemical circulation of crustal materials (oceanic crust and continental crust) and mantle. Halogens are also important in meteorite samples, and in particular, iodine is of particular interest and of high importance in discussions of the cosmochemical behavior of its extinct nuclide ^{129}I (half-life of 15.7 million years) in the early solar system. However, the scarcity of halogen data for meteorite samples is more worrying.

There is a shortage of accurate and reliable data of halogens in meteorites, as well as in terrestrial rock samples, as can be witnessed in the data libraries, where only preferable, not certified values, and for some rocks, no values are listed. This deficit must be largely related to difficulties in determining trace amounts of halogens within these samples. To determine trace halogens in rock samples, either inductively coupled plasma mass spectrometry (ICP-MS) or neutron activation analysis (NAA) have commonly been utilized. Bromine and iodine are conventionally determined by ICP-MS after using pyrohydrolysis of rock powder, but neither fluorine nor chlorine can be reliably determined by this method. In principle, four halogens can be determined using NAA. However, only three halogens (chorine, bromine, and iodine) have been routinely determined by NAA with radiochemical purification.[1]

In this study, trace three halogens (chlorine, bromine, and iodine) were determined by radiochemical NAA (RNAA) for geological and cosmmochemical powder samples. Similar studies have been conducted for many years by a senior author of this paper and his colleagues with use of different types of reactors. Now that the Kyoto University reactor (KUR) is currently the only research reactor running in Japan, we initiated to perform RNAA of three halogens by using KUR. Our first goal was to present a modified radiochemical procedure for RNAA of three heavy halogens, which was to be more effective and convenient compared with the previous one. A part of our outcomes will be published soon.[2] In this paper, we demonstrated that RNAA data for bromine and iodine are more reliable and accurate than the data obtained by ICP-MS coupled with pyrohydrolysis preconcentration. Another goal was to apply our RNAA procedure to geological and cosmochemical samples for discussing geochemical and cosmochemical implications based on the analytical data for such samples. A part of the progress related to this goal is presented here.

II. EXPERIMENTAL

Both geological rocks (mantle xenoliths) and comochemical samples (Antarctic meteorites) were analyzed, along with several geological reference rock powders. Approximately 100 mg of each powder sample was weighed, inserted into a clean, small plastic vial. Chemical standard solutions of the three halogens were prepared for their quantifications. An appropriate amount of each solution was dropped onto a paper disk (17 mm ϕ), weighed, dried under a heat lamp and doubly sealed into polyethylene bags. Two rock samples, together with a set of three reference halogen samples, were irradiated for 10 min with a thermal neutron flux of 3.3 x10^{12} n/cm^2/s at Kyoto University Research Reactor Institute. After irradiation, the rock samples were cooled for a few minutes to enable the decay of ^{28}Al, and were then subjected to radiochemical separation of neutron-induced radionuclides of ^{38}Cl, ^{82}Br, and ^{128}I. We basically followed the radiochemical procedure for RNAA of three heavy halogens, as described by Ozaki and Ebihara,[3] and others cited within this paper. Chemical yields were determined by reactivation method.

III. RESULTS AND DISCUSSION

Our RNAA procedure was applied to several rock samples in powder. In addition, the Smithsonian Institution Allende meteorite powder sample, which has been repeatedly analyzed for many years, was also analyzed as a control sample. Our present data are consistent with the precious results. RNAA results of halogens for the Antarctic meteorite recovered from the Ice were compared with those for meteorites recovered from the bare ice field and a similar enrichment was observed for both of them, suggesting that halogens were added during the storage in Antarctic ice.

Reference: [1] Ebihara M. et al. (1997) JRNC, 216, 107-112. [2] Sekimoto S. and Ebihara M. (2013) Anal. Chem, in press. [3] Ozaki H. and Ebihara M. (2007) Ana. Chim. Acta, 583, 384.

Multielement analysis of KIGAM reference samples by INAA, ICP-AES and ICP-MS

Naoki Shirai[1], Meiramkhan Toktaganov[2], Hiroki Takahashi[1], Yuta Yokozuka[1], Shun Sekimoto[3], Mitsuru Ebihara[1]

[1]Tokyo Metropolitan University
[2]National Nuclear Center Republic of Kazakhstan Institute of Atomic Energy
[3]Kyoto University Research Reactor Institute

I. INTRODUCTION

Bulk chemical compositions of geochemical and cosmochemcial materials provide us the information of evolution processes and magmatism of planetary bodies. Instrumental neutron activation analysis (INAA), inductively coupled plasma mass spectrometry (ICP-MS) and X-ray fluorescence (XRF) have been used for the determination of bulk chemical compositions of these samples. For these analytical methods, reference materials are used as standard samples. Therefore, the quality of analytical data depends on accuracy and precision of such reference materials. Many kinds of reference materials having a wide range of chemical compositions were prepared and distributed by different institutions. Korean Institute of Geology, Mining and Materials (KIGAM) issued geological reference materials. However, the number of published values is very limited [1] and recommended values are not established. In this study, we aimed to determine chemical compositions for KIGAM reference materials by using three analytical methods.

II. EXPERIMENTAL

Eleven KIGAM reference materials (KB-1, KGB-1, KD-1, KT-1, KF-1, KF-2, KP-1, KP-2, KP-3, KG-1 and KG-2) were analyzed. In addition, JB-2 published by GSJ was analyzed as control sample. In INAA, samples were irradiated two times with different irradiation periods which are adjusted for half lives of nuclides usable for determining elements. Samples weighing about 0.04 g were irradiated for 10s at a neutron flux of 4.6 x 10^{12} $cm^{-2}s^{-1}$ at Kyoto University Research Reactor Institute (KURRI) and were immediately measured for their emitting gamma ray. The samples were reirradiated for 4 hrs at a neutron flux of 5.6 x 10^{12} $cm^{-2}s^{-1}$ at KURRI. After irradiation, samples were measured for gamma rays several times with different cooling intervals at KURRI and the RI Research Center of Tokyo Metropolitan University. ICP-AES and ICP-MS were used for determination of major and minor elements, and rare earth elements (REEs), Th and U, respectively. Samples were digested with HF, HNO_3 and $HClO_4$. Dissolved samples were dried and redissolved in HNO_3. By using a 10 % aliquot sample solution, REEs, Th and U abundances were determined by ICP-MS. Remaining sample solutions were used for determination of major and minor elements by using ICP-AES.

III. RESULTS AND DISCUSSION

About 40 elements were determined by INAA, ICP-MS and ICP-AES for each reference sample. Figure 1 shows CI-chondrite normalized REE abundance patterns for KB-1 and KGB-1. INAA and ICP-MS data are in good agreement with each other for comparable elements. REE abundances patterns for KB-1 and KGB-1 obtained by Sakamoto et al. [1] show small zigzag patterns in middle REEs, while our abundances patterns are smooth. CI-normalized REEs abundances patterns for KB-1 and KGB-1 are very close to each other and similar to those for continental crustal materials.

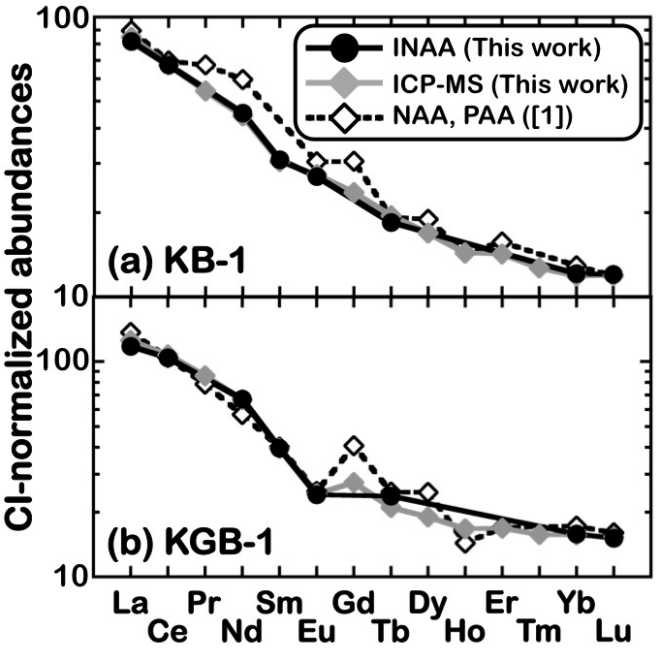

Fig. 1. CI-normalized REE abundances for KB-1 (a) and KGB-1 (b).

Reference: [1] Sakamoto K. et al. (1997) J. Radioanal. Nucl. Chem., 215 (1), 69-76.

Comparison of Calculated Results with NTD Measured Data for Establishment of Burned Core Model for Monte Carlo Simulation of HANARO Reactor

Dong-Keun Cho and Myong-Seop Kim
Korea Atomic Energy Research Institute, Dukjin-dong 150, Yuseong, Daejeon 305-353, Republic of Korea

Keywords – Monte Carlo Simulation, MCNP, Research Reactor

HANARO is a multipurpose research reactor operated for material testing, production of key radioisotopes, neutron activation analysis of nuclear-grade materials, and neutron radiography. To support various researches, HANARO has a very heterogeneous configuration with 25 vertical irradiation thimbles and seven horizontal beam tubes. Although the reactor core is predicted by HANARO core management system, called HANAFMS, equipped with WIMS and VENTURE, heterogeneity of the core and newly installed device for specific experiment makes the neutronic analysis difficult and sometimes doubtable. To resolve these limitations, MCNP has been utilized for neutron transport calculation in the HANARO reactor.

For HANARO, MCNP core model filled with fresh fuels has been used to support the experiments in addition to HANAFMS. And, the model has supplied acceptable analysis results for a design of experimental devices and facilities. However, it is definite that burned core model can provide better result than that obtained from the core model with fresh fuels. In this study, MCNP burned core model was established and then its viability was investigated through comparison of calculated result from the burned core model and measurement data from neutron transmutation doping (NTD) for producing silicon semiconductor.

Burned full-core model for MCNP simulation was established by using the data generated by WIMS and VENTURE codes. Brunup-dependent number density was calculated for each rod for each fuel assembly by WIMS to assign appropriate isotopic number density to each region of irradiated fuel of the core. The power and burnup of each region of fuel region were calculated by VENTURE for the equilibrium core of HANARO. Based on the burnup-dependent number density library calculated by WIMS, the number densities of major nuclides corresponding to the burnup of each region were assigned to each region of the irradiated fuel of MCNP model.

HANARO has two vertical holes in the heavy water reflector tank for the NTD- NTD1 and NTD2 holes having diameters of 22 and 18cm respectively. Because these two holes showed excellent conditions for NTD in the aspects of high thermal neutron flux and large hole size, and low fast neutron flux and gamma heating, commercial service for a 5 in., silicon ingot has been provided to produce silicon semiconductor at NTD hole. And measurement was also performed to check radial and axial uniformity of neutron irradiation in silicon ingots.

The actual irradiation geometry for silicon ingots as were used for the experiment were described almost exactly in the MCNP burned core model. Absolute and relative neutron flux distributions along radial and axial direction of the ingots for NTD were calculated by using MCNP burned core model. The neutron flux was averaged over each ring radially divided with the same thickness from the center of ingots. The reason why the calculated neutron fluxes were averaged azimuthally is to consider the rotation of the ingot during irradiation to obtain low RRG (radial resistivity gradient). Three axial positions of a silicon ingot - the top, bottom, and middle planes – were obtained as well. The longitudinal length of each plane was 2 cm.

Finally, these calculated data were compared with those from the measured data for silicon ingots for neutron transmutation doping carried out at NTD-1 and NTD-2 irradiation holes of HANARO research reactor.

1. M.S. Kim, et al., "Radial Uniformity of Neutron Irradiation in Silicon Ingots for Neutron Transmutation Doping at HANARO," *Nuclear Engineering and Technology*, **38**(1). 2006.

Neutron Activation Analysis of JCFA-1, JCu-1 and JZn-1

Shun Sekimoto[1], Yuta Homura[1], Ryo Okumura[1], Naoki Shirai[2]
[1]Kyoto University Research Reactor Institute
[2]Tokyo Metropolitan University

Abstract – We present NAA results of JCFA-1, JCu-1 and JZn-1 reference samples prepared by GSJ. Through NAA of those three reference samples, appropriate reference samples for quantification by INAA are discussed. We also report fundamental property of each irradiation port, such as neutron fluence rate, at Kyoto University Reactor after renewal of the reactor fuel.

Keywords – JCFA-1; JCu-1; JZn-1; Neutron activation analysis; Kyoto University Reactor; GSJ reference sample

I. INTRODUCTION

Geological Survey of Japan (GSJ) has prepared various kinds of geochemical reference materials [1]. In the most of igneous rock samples and sedimentary rock samples, their chemical compositions are presented as the certified values through compilation of a lot of data [2, 3]. In several reference samples, however, certified values have not been given yet, and provisional, recommended, or information values are given, and then multielement analysis by neutron activation analysis (NAA) has never been performed. In this work, the first NAA results of a coal fly ash reference sample (JCFA-1) and ore reference samples (JCu-1 and JZn-1), where certified values have never been given, are reported and compared to the literature data obtained by atomic absorption spectrometry (AAS), inductively coupled plasma-atomic emission spectrometry (ICP-AES), *etc.* [4, 5] Through NAA of the above three reference samples, we investigate appropriate reference monitor samples for quantification by INAA. The characteristics of the NAA systems using Kyoto University Reactor (KUR) after the furl conversion to low-enriched uranium intend to be presented.

II. EXPERIMENTAL

A. Sample preparation

Three reference samples analyzed in this work are JCFA-1 as coal fly ash, JCu-1 as copper ore, and JZn-1 as zinc ore, which were prepared by GSJ and were commercially distributed [4-5]. As reference monitor samples for quantifications by NAA, JA-1 (andesite), JB-1b (basalt), JG-1 (granite), and JP-1 (peridotite) are also prepared [2]. All the samples were in powder, and were not subjected to any additional treatment such as drying. Approximately 100 mg of each powder sample was weighed, doubly sealed into clean polyethylene bags.

B. Neutron irradiation

First, each sample was irradiated one by one for 10 s at pneumatic transport system No. 3 (Pn-3). After the 10 s irradiation, the outer bag of the sample was replaced by a new one and then the sample was immediately subjected to gamma-ray spectrometry for measurement of short half-life nuclides: ^{28}Al, ^{52}V, ^{49}Ca, ^{27}Mg, *etc.* Next the three reference samples together with all reference monitor samples were placed in one capsule and irradiated for 4 h at Pn-2. After 4 h irradiation, samples whose outer bags were also replaced in a similar manner as 10 s irradiation were subjected to gamma-ray spectrometry for measurements of long half-life nuclides: ^{59}Fe, ^{60}Co, *etc.*

C. Kyoto University Reactor

Kyoto University Reactor (KUR), a 5 MW research reactor in Japan, has worked as the central place to support the university researchers using NAA for their analytical studies. After four-year shutdown period for fuel conversion to low-enriched uranium fuel, KUR restarted in May 2010, and thereby a new inter-university research project using NAA system at KUR also restarted. During this renewal of the reactor fuel, the control system of the pneumatic irradiation system was refurbished to digital-control type. This improvement has been introduced elsewhere [6] and operated well after KUR restarted. To promote this inter-university research project successfully, fundamental properties of the irradiation sites, such as neutron fluence rate, cadmium ratio of gold, and temperature inner capsules during neutron irradiation at each pneumatic irradiation system used for NAA are shown in the presentation.

III. RESULTS AND DISCUSSION

Elemental contents of the three reference samples measured by NAA are reported. Among four reference monitor samples (JA-1, JB-1b, JG-1 and JP-1), inconsistencies in the activities of radionuclides produced by (n,γ) reaction per amounts of their corresponding elements was found in several elements determined. Through NAA of the three reference samples, we also investigate which reference sample is suitable or not for each element determined.

REFERENCES

[1] http://riodb02.ibase.aist.go.jp/geostand/welcome.html
[2] N. Imai et al., *Geochem. J.* **1995**, 29, 91-95
[3] N. Imai et al., *Geostand. Newslett.* **1996**, *20*, 165–216.
[4] S. Terashima et al., *Geostand. Newslett.* **1998**, *22*, 113-117.
[5] S. Terashima et al., *Geostand. Newslett.* **2003**, *27*, 259-271.
[6] K. Takamiya et al., *J. Radioanal. Nucl. Chem.* **2008**, 278, 719-721.

Prompt Gamma-ray Analysis of Chloride Concentration in Blended Cement Concretes

A. A. Naqvi[1*], M. Maslehuddin[2], O.S.B. Al-Amoudi[3], Khateeb-ur-Rehman[1] and M. Raashid[1]
[1]Department of Physics, [2]Center for Engineering Research, and [3]Department of Civil and Environmental Engineering
King Fahd University of Petroleum and Minerals, Dhahran, Saudi Arabia

Abstract – The chloride concentration in plain and blast furnace slag cement concrete has been measured using a D-D portable neutron generator.. The setup has been used to measure chloride concentration in specimens using chlorine prompt gamma-rays with different energies. Out of several chlorine gamma ray data, an optimum and a unique chlorine gamma-ray line has been chosen for the detection of chloride in all the blended cement concretes specimen including fly ash, blast furnace slag and superpozz cement concrete utilizing the portable neutron generator-based PGNAA setup

Keywords – *Chloride detection, blended concrete specimen, BGO detector , Portable D-D neutron generator based PGNAA setup, Monte Carlo simulations,*

I. INTRODUCTION

Industrial by-products, such as fly ash, silica fume and blast furnace slag, are added to concrete, as partial replacement of cement, to increase its denseness and impermeability. The increased impermeability of blended cement concretes decreases the rate of diffusion of chloride ions to the steel surface. Since reinforcement corrosion is predominantly attributed to the presence of chloride ions at the steel surface, a non-destructive technique is required to assess the level of chloride concentration in concrete. A portable neutron generator-based prompt Gamma-ray Neutron Activation setup has been designed by the authors to measure the chloride concentration in plain and blended concretes using a cylindrical 100 mm x 100 mm (diameter x height) BGO detector.

The setup has been used to measure chloride concentration in fly ash and blast furnace slag cement concrete specimens using chlorine prompt gamma-rays with different energies. An excellent agreement has been observed between the chlorine prompt gamma-ray experimental yield and the calculated values obtained through Monte Carlo simulations. The optimum choice of unique chlorine gamma-ray line for the detection of chloride in the blended cement concretes utilizing the portable neutron generator-based PGNAA setup data taken in present study and earlier [1,2] is presented.

[1] Naqvi, A. A., Zameer Kalakada, Faris A. Al-Matouq, M. Maslehuddin and O.S.B. Al-Amoudi. Prompt Gamma-Ray Analysis of Chlorine in Superpozz Cement Concrete .Nuclear Inst. and Methods in Physics Research, A Vol. 693 (November 2012), pp. 67-73

[2] Naqvi, A. A., Zameer Kalakada, Faris A. Al-Matouq, M. Maslehuddin and O.S.B. Al-Amoudi. Chlorine Detection in Fly Ash Concrete using a Portable Neutron Generator. Applied Radiation and Isotopes Vol70(2012) pp.1671-4.

Cold Neutron and Thermal Neutron PGAA facilities at The HANARO Research Reactor

G.M. Sun[1], E.J. Lee[1], B.G. Park[1], J.H. Moon[1]
[1]Neutron Utilization Technology Division, Korea Atomic Energy Research Institute, 305-353, Korea

A new cold neutron prompt gamma activation analysis facility has been developed at a cold neutron source of the HANARO research reactor and be prepared to open to users until the end of 2013.The performance tests were carried out and compared with an old thermal neutron facility. The neutron beam characteristics such as neutron flux, spatial distribution and energy spectrum were investigated and a background was also studied in detail. The measurements for the standard reference material provide the performance of the new facility and comparison with the old thermal neutron facility

Keywords –cold neutron, thermal neutron, prompt gamma activation analysis, HANARO

I. INTRODUCTION

Prompt gamma-ray activation analysis (PGAA) is based on the radiative neutron capture, which has been considered to be a complementary method to the conventional instrumental neutron activation analysis though in principle it can analyze almost elements in the elemental table. If a guided cold neutron beam with a relatively low background can provide a possibility that a PGAA itself becomes a complete elemental analysis tools. We operated a thermal neutron PGAA (SNU-KAERI PGAA) [1] on the horizontal ST1 beam line of the HANARO research reactor and newly developed a cold neutron PGAA (CN-PGAA) on the CG2B cold neutron guide from a cold neutron source. Figure 1 shows a SNU-KAERI PGAA facility, which was developed by a group from Seoul National University, has a neutron flux of $1x10^8$ n/cm^{2}s and detection limit for boron elemental of about 60 ng. Figure 2 shows a new CN-PGAA facility. Neutron guide after the end of the guide to a sample position is normally made of aluminum but Teflon chopper and The Teflon tube has a length of 100 cm and a double-layer structure and the space between double layers is introduced as material for the flight tube between disk chopper and is filled with 95% enriched $^6Li_2CO_3$ powder, whose thickness is 1 cm. Lithium layer catches neutrons scattered out from the path. Neutron beam is shaped with a ^{6}LiF beam cutter to have a reactangular shape of 2 cm x 2 cm. We investigated neutron characteristics such a neutron flux and its spatial distribution by using a gold foil activation method and neutron energy spectrum by using a time-of flight method. True integrated neutron flux a the sample position is a about $5x10^8$ n/cm^{2}s. The total beam characteristics of the CN-PGAA were compared with that of the SNU-KAERI PGAA and background was investigated in detail.

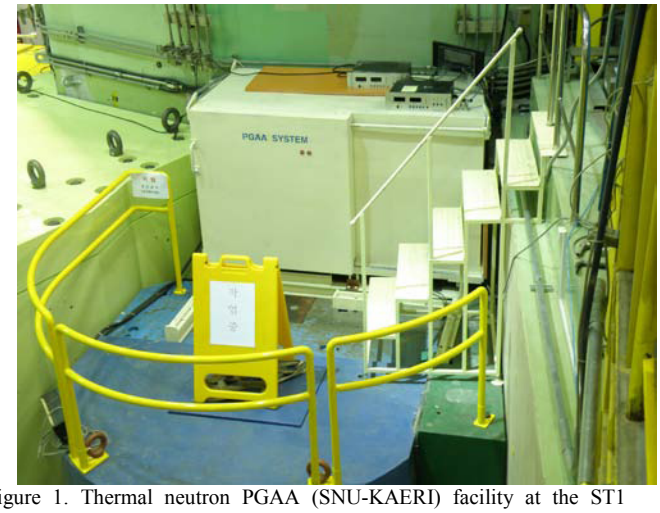

Figure 1. Thermal neutron PGAA (SNU-KAERI) facility at the ST1 horizontal beam line of the HANARO research reactor.

Figure 2. Cold Neutron Activation Station, where a cold neutron PGAA (CN-PGAA) was installed.

[1] S.H. Byun, G.M. Sun and H.D. Choi, "Development of a Prompt Gamma Activation Analysis Facility Using Diffracted Polychromatic Neutron Beam", Nuclear Instruments and Methods in Physics Research A, Vol. 487, (2002), pp. 521 ~ 529.
[2] G.M. Sun, "Development of HANARO Cold Neutron Activation Station", 2012 Asia-Pacific Winter Conference on plasma spectrochemistry, Jeju, Aug. 2012.

Exposing dogs to uranium contained in commercial diets

Camila Elias,[1] Elisabete A. De Nadai Fernandes,[1] Márcio A. Bacchi,[1] Peter Bode[2]
1. University of São Paulo, Nuclear Energy Center for Agriculture, P.O. Box 96, 13400-970 Piracicaba, SP, Brazil
2. Reactor Institute Delft, Delft University of Technology, Mekelweg 15, 2629 JB, Delft, The Netherlands

Abstract

The presence of uranium in dry dog food samples was investigated by instrumental neutron activation analysis (INAA). Some commercial brands showed uranium concentration as high as 4 mg kg^{-1}, which may lead to chronic exposure of dogs to a level about a thousand higher than the normal ingestion level for humans according to the US-EPA.

Keywords – Food safety, dog food, INAA

I. INTRODUCTION

Dry dog food is intended to be a complete and balanced diet and may be the unique source feeding the animal in all stages of life. Therefore, it is extremely important to choose a product capable of providing optimal nutrition, with all necessary substances at adequate levels and free of contaminants, for promoting long-term health.

The safety of dog diets has recently received increasing attention since the contamination with melamine caused the death of several animals and a major recall of pet food in the United States. In fact, the use of low quality ingredients in the pet food composition can introduce residues of pesticides, mycotoxins, hazard chemical elements and other toxic substances. Products derived from phosphate rocks, as dicalcium phosphate (DCP), normally used as feed additives to supplement phosphorus may have high concentrations of uranium [1].

Experiments with dogs, rabbits and rats have demonstrated that the animals are sensitive to both inhalation and oral exposure to uranium compounds. Uranium accumulates mainly in the bones, kidneys and liver, and presents both chemical and radiological toxicity.

The overexposure to uranium may cause pathological alterations to the kidneys, leading in extreme cases to renal failure. In this context, this work investigated the presence of uranium in several commercial brands of dry dog foods produced in Brazil.

II. EXPERIMENTAL

For this work, 61 dry dog food samples of 37 different commercial brands, including food for puppies and adults, were purchased in the local market of Piracicaba, SP, Brazil. After homogenization, a 300 g subsample of each dog food package of 1 kg was reduced in a knife mill for analysis by INAA. For analytical quality control, certified reference materials were used. Test portions of 200 mg were inserted in polyethylene vials and irradiated in the nuclear research reactor IEA-R1 of IPEN/CNEN at a thermal neutron flux of 7×10^{12} cm^{-2} s^{-1} for 4 h. Element concentrations and expanded uncertainties were calculated by the k_0-method, using the software package Quantu [2].

III. RESULTS AND DISCUSSION

A total of 14 samples out of 61 showed uranium concentrations above the detection limit of 0.2 mg kg^{-1}, with values ranging from 0.24 mg kg^{-1} to 3.61 mg kg^{-1}. Nine samples were for adult dogs and five for puppies. Two special foods, for intestinal and hypoallergenic treatments, respectively had uranium values of 1.05 mg kg^{-1} and 2.30 mg kg^{-1}. Some commercial brands from the same producers consistently presented higher uranium content.

Data were compared to values obtained in a previous study [3] as seen in Table 1. Two commercial brands were analyzed in both occasions. For one brand, uranium content was reduced from 3.15 mg kg^{-1} to 0.83 mg kg^{-1}, while for the other the content was similar, with 3.99 mg kg^{-1} in the first study and 3.61 mg kg^{-1} in the second.

Table 1. Uranium concentration (mg kg^{-1}) in dry dog foods compared with results published in previous work [3].

	This study	Previous work
Min	0.24	0.46
Max	3.61	3.99
Median	0.91	0.70
Average	1.49	1.36
Stdev (%)	81	85
N	14	13

No maximum regulatory limit was found for uranium in dog food, despite its nephrotoxic effects known already for a long time, causing renal diseases. According to US Environmental Protection Agency (EPA) [4], the average daily intake of uranium from food ranges from 0.07 µg to 1.1 µg for humans. The intake for a dog of 40 kg that consumes about 500 g of dry food per day would be as high as 2 mg of uranium, which can be considered a very high value compared to the range published by EPA.

REFERENCES

[1] Casacuberta N, Masquéa P, Garcia-Orellana J, Bruach J M, Anguita M, Gasa J, Villa M, Hurtado S, Garcia-Tenorio R (2009) J. Hazard. Mater. 170: 814-823.
[2] Bacchi M A, Fernandes E A N (2003) J. Radioanal. Nucl. Chem. 257: 577-582.
[3] Elias C, Fernandes E A N, Bacchi M A (2012) J. Radioanal. Nucl. Chem. 291: 245-250.
[4] United States Environmental Protection Agency (2010) Understanding radiation in your life, your world. http://www.epa.gov/radiation/radionuclides/uranium.html.

Authors Index

I

L

M

P

Q

R

S

T

U

V

W

X

Y

Z

Co-sponsorship

Ishikawa Prefecture　　Kanazawa City　　Kanazawa University

The Chemical Society of Japan
The Physical Society of Japan
Atomic Energy Society of Japan
The Geochemical Society of Japan
The Pharmaceutical Society of Japan
The Japan Society for Analytical Chemistry
The Japanese Society of Nuclear Medicine
Japanese Society of Radiation Chemistry
Japan Association of Solvent Extraction
The Rare Earth Society of Japan
Japan Atomic Energy Agency (JAEA)
Advanced Science Research Center, JAEA

IUPAC Sponsorship

IUPAC sponsorship implies that entry visas will be granted to all bona fide chemists provided application is made not less than three months in advance. If a visa is not granted one month before the meeting, IUPAC Secretariat should be notified without delay by the applicant.

IUPAC
(International Union of Pure and Applied Chemistry)

Exhibitors

Hitachi Aloka Medical, Ltd.

TRISKEM INTERNATIONAL

raytest Isotopenmessgeräte GmbH

Canberra Japan K.K.

Saint-Gobain K.K.

Sponsorship Company

Nuclear Safety Technology Center
Niki Glass Co. Ltd.
Nakayama Co. Ltd.
Tokyo Nuclear Services Co., Ltd.
Japan Environment Research CO., Ltd.
Hokuriku Nuclear Conference
Spectra-Physics KK

Chiyoda Technol Corporation
Ozushoukai. Inc.
ING Corporation
Fujimoto Science
Art Kagaku
Rikoh Kagaku
Marubuntsushou co. Ltd.

NKI GLASS CO.,LTD

LIST MODULE SERISE
A3XXX

A3200 QDC
A3300 TDC
A3400 ADC

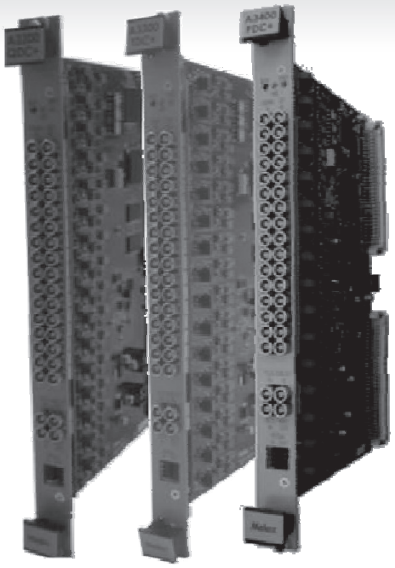

•A3XXX is multi-input modules of the VME standard.
• All modules are designed in the concept that it unified, and be superior in affinity.
•The 200MHz clock had built-in can provide a time stamp of minimum 5ns.
•Each board has 16 input and gates. They operate for independence.
•Can use common gate & VETO of the board unit.
•A3XXX can do the PHA measurement with the LIST measurement.
•Can synchronize with a clock of several A3XXX.
•A24/34,D16/D32/BLI Data transfer , MCST

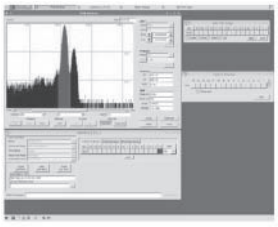

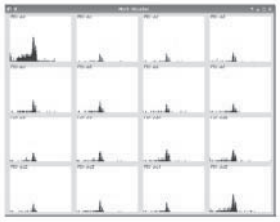

3000-E-C / SVP-511

Can give the control program for A3XXX on the basis of LINUX.
Can do control in the Ethernet by VME-PC based on the PowerPC in the latest system.
All the data are stored with a text on PC.
You can easily access your data.
The program is common to all A3XXX.
You do not have to change a program every purpose.

•This product is developed for the purpose of using it in Japan.
•When you plan use except Japan, The duty in accordance with the law of the countries concerned government produces you.

Please perform an inquiry of more information at the following.

NIKIGLASS CO.,LTD.
9-7 Mita 3-chome,Minato-ku,Tokyo 108-0073,JAPAN
Email to : sales@nikiglass.com

キャンベラジャパンの放射能測定システム

放射線計測の基礎から応用まで
広範で卓越した製品を提供しています。

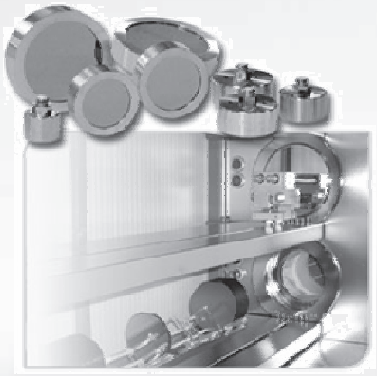

PIPS　荷電粒子検出器

5XLBシリーズ:
低バックグラウンド
α/β 自動計測システム

ゲルマニウム半導体検出器

iSolo®:
システムポータブルガスレスα/β計測システム

ガンマアナリスト:
統合型γ線スペクトロメータ

CANBERRA
キャンベラジャパン株式会社

放射能測定の世界的リーディングカンパニー

東 京 本 社　〒111-0053 東京都台東区浅草橋4-19-8 浅草橋ビル　TEL: 03-5835-5402　FAX:03-5835-5403
大 阪 営 業 所　〒532-0011 大阪市淀川区西中島5-14-5 ニッセイ新大阪南口ビル9F TEL: 06-4806-5662　FAX:06-4806-5663
URL:　http://www.canberra.com/jp/　E-mail : sales-jp@canberra.com

平成25年度　放射化物研修会　～放射化物の発生から、関連する安全規制まで～

平成24年４月に改正放射線障害防止法が施行され、２年間の経過措置を経て平成26年４月より放射化物を所持する事業所は放射化物保管設備又は保管廃棄設備に放射化物を保管することが義務付けられています。

平成24年３月に放射化物の安全規制に関する事務連絡が発出されましたが、対象となる事業所では必ずしもその内容について十分に理解されていないと思われます。

この状況を踏まえ、現場の作業者等を対象とした放射化物研修会を開催して放射化物を取り扱う上での基礎的知識及び具体的な取扱い方法等の習得を図り、放射化物の安全規制の推進に寄与することとしました。

大阪会場

10月13日(日) 10:30～16:20

大阪府私学教育文化会館

大阪市都島区網島町６－２０

受講料：１０，０００円

東京会場

10月19日(土) 10:30～16:20

渋谷アジアビル

渋谷区神南１－１２－１６

受講料：１０，０００円

内　容

＜午前の部＞

① 放射化物が発生するメカニズム、発生条件等について学術的見地から解説します。

② 具体的にどんな放射化物があるか、また、核種、数量及び線量の程度を紹介します。

＜講師：高エネルギー加速器研究機構放射線科学センター教授桝本氏を予定＞

(注)都合により講師、演題等に変更が生じる場合がありますので、予めご了承願います。

＜午後の部＞

① 法令上の位置づけ、安全規制に基づく取扱い方法について解説します。

② 記帳記録の方法について解説します。

＜講師：原子力規制庁放射線規制室職員を予定＞

① 放射化物保管設備、保管廃棄設備等の実例を紹介します。

② 受入れ・払出し記録、保管記録及び廃棄記録等の記載例について紹介します。

＜講師：横浜労災病院放射線取扱主任者渡辺氏を予定＞

＜送付先・問合せ先＞

FAX：０３－３８１４－４６１７　　E-MAIL：kcenter@nustec.or.jp　　TEL：03-3814-7100

郵送：〒112-8604　東京都文京区白山５丁目１番３－１０１　東京富山会館ビル

公益財団法人原子力安全技術センター　放射線安全事業部　安全業務部　研修センター

＜受講料振込先口座＞

三井住友銀行　　白山支店		普通預金	口座番号　　９６１０４４
口座名義	公益財団法人原子力安全技術センター　　ザイ）ゲンシリョクアンゼンギジュツセンター		

（注）受講料１万円をお振込み下さい。なお、振込手数料は受講者の負担となります。

平成25年度　放射化物研修会受講申込み書

以下のとおり、平成25年10月　　日(　　)開催の放射化物研修会(　　会場)への受講を申込みます。

受講者氏名（ふりがな）	住　　所	電話番号	MAIL ADDRESS

＊お申込みいただいたお名前等の個人情報は、受講確認及び今後の研修会等のご案内以外の目的には使用いたしません。

□　次回より案内状等の送付をご希望されない方は、□の中にチェックを入れて下さい。

HITACHI
Inspire the Next

ALOKA
illuminate the change

Survey Meters and Electronic Pocket Dosemeters

Hitachi Aloka Medical's measurement instrument is an optimal solution to help you check radioactive contamination, to know how much radiation there is and how much you are exposed by radiation.
We offer a whole variety of types to support what's necessary to measure.

Survey Meters

● Surface Contamination Measurement

for Beta TGS-146B

TCS-319H

TCS-316H

for Gamma(^{125}I) TCS-173C

for Alpha TCS-232B

for Alpha/Beta TCS-362

● Dose Rate Measurement

for Gamma(X)

ICS-331B

ICS-323C

TCS-171B

TCS-172B

PDR-111

for Neutron TPS-451C

Electronic Pocket Dosemeters

for Gamma(X) PDM-122

for X-ray PDM-127

for Neutron PDM-313

with Alarm

for Gamma(X) PDM-222

for X-ray PDM-227

for Gamma and Neutron ADM-353B

Hitachi Aloka Medical, Ltd.

www.hitachi-aloka.co.jp/english